

ADVANCES in ENVIRONMENTAL SCIENCES, DEVELOPMENT and CHEMISTRY

**Proceedings of the 2014 International Conference on Energy,
Environment, Development and Economics (EEDS 2014)**

**Proceedings of the 2014 International Conference on Geology and
Seismology (GESE 2014)**

**Proceedings of the 2014 International Conference on Maritime and
Naval Science and Engineering (MANASE 2014)**

**Proceedings of the 2014 International Conference on Water Resources,
Hydraulics & Hydrology (WHH 2014)**

**Proceedings of the 2014 International Conference on Chemistry and
Chemical Engineering (CCE 2014)**

Santorini Island, Greece

July 17-21, 2014

ADVANCES in ENVIRONMENTAL SCIENCES, DEVELOPMENT and CHEMISTRY

**Proceedings of the 2014 International Conference on Energy,
Environment, Development and Economics (EEDS 2014)**

**Proceedings of the 2014 International Conference on Geology and
Seismology (GESE 2014)**

**Proceedings of the 2014 International Conference on Maritime and
Naval Science and Engineering (MANASE 2014)**

**Proceedings of the 2014 International Conference on Water Resources,
Hydraulics & Hydrology (WHH 2014)**

**Proceedings of the 2014 International Conference on Chemistry and
Chemical Engineering (CCE 2014)**

**Santorini Island, Greece
July 17-21, 2014**

Copyright © 2014, by the editors

All the copyright of the present book belongs to the editors. All rights reserved. No part of this publication may be reproduced, stored in a retrieval system, or transmitted in any form or by any means, electronic, mechanical, photocopying, recording, or otherwise, without the prior written permission of the editors.

All papers of the present volume were peer reviewed by no less than two independent reviewers. Acceptance was granted when both reviewers' recommendations were positive.

ISBN: 978-1-61804-239-2

ADVANCES in ENVIRONMENTAL SCIENCES, DEVELOPMENT and CHEMISTRY

**Proceedings of the 2014 International Conference on Energy,
Environment, Development and Economics (EEDS 2014)**

**Proceedings of the 2014 International Conference on Geology and
Seismology (GESE 2014)**

**Proceedings of the 2014 International Conference on Maritime and
Naval Science and Engineering (MANASE 2014)**

**Proceedings of the 2014 International Conference on Water Resources,
Hydraulics & Hydrology (WHH 2014)**

**Proceedings of the 2014 International Conference on Chemistry and
Chemical Engineering (CCE 2014)**

Santorini Island, Greece

July 17-21, 2014

Organizing Committee

General Chairs (EDITORS)

- Prof. Nikos Mastorakis, Technical University of Sofia, Bulgaria
- Prof. Vladimir Sokolov, University of Karlsruhe, Germany
- Prof. Reinhard Neck, Klagenfurt University, Austria
- Prof. Rui Pedro Juliao, Universidade Nova De Lisboa, Portugal
- Prof. Jian Wang, Los Alamos National Laboratory, USA
- Prof. Efthimios Karymbalis, Harokopio University, Athens, Greece
- Prof. Levent Yilmaz, Istanbul Technical University, Turkey
- Prof. Ernst D. Schmitter, University of Applied Sciences, Germany
- Prof. Marc A. Rosen, University of Ontario, Canada
- Prof. Roy Perryman, University of East London, UK
- Prof. Ottavia Corbi, University of Naples Federico II, Italy
- Prof. Manijeh Razeghi, Northwestern University, USA
- Prof. Jun Zhang, Inner Mongolia University, P. R. China
- Prof. Samuel Lofland, Rowan University, USA

Associate Editors:

- Luís Loures
- Liandong Zhu

Senior Program Chair

- Prof. Shoji Arai, Kanazawa University,
Kanazawa, Ishikawa Prefecture,
Japan

Program Chairs

- Prof. Panos Pardalos,
Department of University of Florida,
USA
- Prof. Filippo Neri
Dipartimento di Informatica e Sistemistica
University of Naples "Federico II"
Naples, Italy
- Prof. Bharat Doshi,
John Hopkins University,
Mayrland, USA

Tutorials Chair

- Prof. Pradip Majumdar
Department of Mechanical Engineering
Northern Illinois University
DeKalb, Illinois, USA

Special Session Chair

- Prof. Essam Eldin Khalil,
ASME Fellow,
Cairo University, Cairo,
Egypt

Workshops Chair

- Prof. Hyung Hee Cho, ASME Fellow,
Yonsei University (and National
Academy of Engineering of Korea),
Korea

Local Organizing Chair

- Dr. Claudio Guarnaccia, University of Salerno, Italy

Publication Chair

- Prof. Marcin Kaminski,
Department of Structural Mechanics,
Al. Politechniki 6, 90-924 Lodz, Poland

Publicity Committee

- Prof. Kumar Tamma,
University of Minnesota,
Minneapolis, MN, USA
- Prof. Gang Yao,
University of Illinois at Urbana -
Champaign, USA

International Liaisons

- Prof. Quan Wen,
Department of Economics University of Washington,
Seattle, WA, USA
- Prof. Fotios Rigas,
School of Chemical Engineering,
National Technical University of Athens,
Greece.
- Prof. Vincenzo Niola
Departement of Mechanical Engineering for Energetics
University of Naples "Federico II"
Naples, Italy
- Prof. Christopher G. Provatidis,
National Technical University of Athens,
Zografou, Athens, Greece

Steering Committee

- Prof. Aida Bulucea, University of Craiova, Romania
- Prof. Zoran Bojkovic, Univ. of Belgrade, Serbia
- Prof. Ottavia Corbi, University of Naples Federico II, Italy
- Prof. Imre Rudas, Obuda University, Budapest, Hungary
- Prof. Metin Demiralp, Istanbul Technical University, Turkey
- Prof. Reinhard Neck, Klagenfurt University, Klagenfurt, Austria
- Prof. Ottavia Corbi, University of Naples Federico II, Italy

Program Committee

Prof. Bharat Doshi, John Hopkins University, Mayrland, USA
Prof. Gang Yao, University of Illinois at Urbana - Champaign, USA
Prof. Lu Peng, Luisian State University, Baton Rouge, LA, USA
Prof. Y. Baudoin, Royal Military Academy, Brussels, Belgium
Prof. F.Rigas, School of Chemical Engineering, National Technical University of Athens, Greece.
Prof. S. Sohrab, Northwestern University, IL, USA
Prof. A. Stamou, National Technical University of Athens, Greece
Prof. A. I. Zouboulis, Dept. of Chemistry, Aristotle University of Thessaloniki, Greece
Prof. Z. A. Vale, ISEP - Instituto Superior de Engenharia do Porto Rua Antonio Bernardino de Almeida, Portugal
Prof. M. Heiermann, Dr., Department of Technology Assessment and Substance Flow, Potsdam, Germany
Prof. I. Kazachkov, National Technical University of Ukraine (NTUU KPI), Kyiv, Ukraine
Prof. A. M.A. Kazim, UAE University, United Arab Emirates
Prof. A. Kurbatskiy, Novosibirsk State University, Department of Physics, Russia
Prof. S. Linderoth, Head of Research on Fuel Cells and Materials Chemistry at Riso National Laboratory. Denmark
Prof. P. Lunghi, Dipartimento di Ingegneria Industriale, University degli Studi di Perugia, Italy
Prof. J. Van Mierlo, Department of Electrotechnical Engineering and Energy Technology (ETEC) Vrije Universiteit Brussel, Belgium
Prof. Pavel Loskot, Swansea University, UK
Prof. N. Afgan, UNESCO Chair Holder, Instituto Superior Tecnico, Lisbon, Portugal
Prof. F. Akgun, Gebze Kocaeli, Turkey
Prof. Fernando Alvarez, Prof. of Economics, University of Chicago, USA
Prof. Mark J. Perry, Prof. of Finance and Business Economics, University of Michigan-Flit, USA
Prof. Biswa Nath Datta, IEEE Fellow, Distinguished Research Prof., Northern Illinois University, USA
Prof. Panos Pardalos, Distinguished Prof. Director, Center for Applied Optimization, University of Florida, USA
Prof. Gamal Elnagar, University of South Carolina Upstate, Spartanburg, SC, USA
Prof. Luis Tavares Rua, Cmte Guyubricht, 119. Conj. Jardim Costa do Sol. Atalaia, Brazil
Prof. Igor Kuzle, Faculty of electrical engineering and computing, Zagreb, Croatia
Prof. Maria do Rosario Alves Calado, University of Beira Interior, Portugal
Prof. Gheorghe-Daniel Andreescu, "Politehnica" University of Timisoara, Romania
Prof. Jiri Strouhal, University of Economics Prague, Czech Republic
Prof. Morris Adelman, Prof. of Economics, Emeritus, MIT, USA
Prof. Germano Lambert-Torres, Itajuba, MG, Brazil
Prof. Jiri Klima, Technical faculty of CZU in Prague, Czech Republic
Prof. Goricanec Darko, University of Maribor, Maribor, Slovenia
Prof. Ze Santos, Rua A, 119. Conj. Jardim Costa do Sol, Brazil
Prof. Ehab Bayoumi, Chalmers University of Technology, Goteborg, Sweden
Prof. Robert L. Bishop, Prof. of Economics, Emeritus, MIT, USA
Prof. Glenn Loury, Prof. of Economics, Brown University, USA
Prof. Patricia Jota, Av. Amazonas 7675, BH, MG, Brazil
Prof. S. Ozdogan, Marmara University, Goztepe Campus, Kuyubasi, Kadikoy, Istanbul, Turkey
Prof. Morris Adelman, Professor of Economics, Emeritus, MIT, USA
Prof. Robert L. Bishop, Professor of Economics, Emeritus, MIT, USA
Prof. Glenn Loury, Professor of Economics, Brown University, USA
Prof. Fernando Alvarez, Professor of Economics, University of Chicago, USA
Prof. Mark J. Perry, Professor of Finance and Business Economics, University of Michigan-Flit, USA
Prof. Quan Wen, Department of Economics University of Washington, Seattle, WA, USA
Prof. David E. Giles, Department of Economics, University of Victoria, Canada
Prof. Joao Ricardo Faria, University of Texas at El Paso, El Paso, Texas, USA
Prof. Jacob Engwerda, Tilburg University, The Netherlands
Prof. Thomas D. Crocker, University of Wyoming, 1000 E. University Ave. Laramie, USA

Prof. Jean-Marie Dufour, McGill University, Montreal, Quebec, Canada
Prof. Laura Gardini, Universita degli studi di Urbino Carlo Bo, Urbino PU, Italy
Prof. Junsen Zhang, The Chinese University of Hong Kong, Hong Kong
Prof. Reinhard Neck, Department of Economics, Klagenfurt University, Klagenfurt, Austria
Prof. Panos Pardalos, Department of University of Florida, USA
Prof. Shuliang Li, The University of Westminster, London, UK
Prof. Jiri Strouhal, University of Economics Prague, Czech Republic
Prof. Morris Adelman, Prof. of Economics, Emeritus, MIT, USA
Prof. Robert L. Bishop, Prof. of Economics, Emeritus, MIT, USA
Prof. Glenn Loury, Prof. of Economics, Brown University, USA
Prof. Fernando Alvarez, Prof. of Economics, University of Chicago, USA
Prof. Mark J. Perry, Prof. of Finance and Business Economics, University of Michigan-Flit, USA
Prof. Biswa Nath Datta, IEEE Fellow, Distinguished Research Prof., Northern Illinois University, USA
Prof. Gamal Elnagar, University of South Carolina Upstate, Spartanburg, SC, USA
Prof. Jiri Klima, Technical faculty of CZU in Prague, Czech Republic
Prof. Ze Santos, Rua A, 119. Conj. Jardim Costa do Sol, Brazil
Prof. Ehab Bayoumi, Chalmers University of Technology, Goteborg, Sweden
Prof. Maria do Rosario Alves Calado, University of Beira Interior, Portugal
Prof. Gheorghe-Daniel Andreescu, "Politehnica" University of Timisoara, Romania
Prof. Zhuo Li, Beijing University Of Technology, Beijing, China
Prof. Pradip Majumdar, Northern Illinois University, Dekalb, Illinois, USA
Prof. Ricardo Gouveia Rodrigues, University of Beira Interior, Portugal
Prof. Jiri Strouhal, University of Economics Prague, Czech Republic

Additional Reviewers

Santoso Wibowo	CQ University, Australia
Lesley Farmer	California State University Long Beach, CA, USA
Xiang Bai	Huazhong University of Science and Technology, China
Jon Burley	Michigan State University, MI, USA
Genqi Xu	Tianjin University, China
Zhong-Jie Han	Tianjin University, China
Kazuhiko Natori	Toho University, Japan
João Bastos	Instituto Superior de Engenharia do Porto, Portugal
José Carlos Metrôlho	Instituto Politecnico de Castelo Branco, Portugal
Hessam Ghasemnejad	Kingston University London, UK
Matthias Buyle	Artesis Hogeschool Antwerpen, Belgium
Minhui Yan	Shanghai Maritime University, China
Takuya Yamano	Kanagawa University, Japan
Yamagishi Hiromitsu	Ehime University, Japan
Francesco Zirilli	Sapienza Università di Roma, Italy
Sorinel Oprisan	College of Charleston, CA, USA
Ole Christian Boe	Norwegian Military Academy, Norway
Deolinda Rasteiro	Coimbra Institute of Engineering, Portugal
James Vance	The University of Virginia's College at Wise, VA, USA
Valeri Mladenov	Technical University of Sofia, Bulgaria
Angel F. Tenorio	Universidad Pablo de Olavide, Spain
Bazil Taha Ahmed	Universidad Autonoma de Madrid, Spain
Francesco Rotondo	Polytechnic of Bari University, Italy
Jose Flores	The University of South Dakota, SD, USA
Masaji Tanaka	Okayama University of Science, Japan
M. Javed Khan	Tuskegee University, AL, USA
Frederic Kuznik	National Institute of Applied Sciences, Lyon, France
Shinji Osada	Gifu University School of Medicine, Japan
Dmitrijs Serdjuks	Riga Technical University, Latvia
Philippe Dondon	Institut polytechnique de Bordeaux, France
Abelha Antonio	Universidade do Minho, Portugal
Konstantin Volkov	Kingston University London, UK
Manoj K. Jha	Morgan State University in Baltimore, USA
Eleazar Jimenez Serrano	Kyushu University, Japan
Imre Rudas	Obuda University, Budapest, Hungary
Andrey Dmitriev	Russian Academy of Sciences, Russia
Tetsuya Yoshida	Hokkaido University, Japan
Alejandro Fuentes-Penna	Universidad Autónoma del Estado de Hidalgo, Mexico
Stavros Ponis	National Technical University of Athens, Greece
Moran Wang	Tsinghua University, China
Kei Eguchi	Fukuoka Institute of Technology, Japan
Miguel Carriegos	Universidad de Leon, Spain
George Barreto	Pontificia Universidad Javeriana, Colombia
Tetsuya Shimamura	Saitama University, Japan

Table of Contents

Plenary Lecture 1: Floating Offshore Wind Turbines: The Technologies and the Economics <i>Paul D. Sclavounos</i>	17
Plenary Lecture 2: The Influence of a Magnetic Field in the Fuel of a Gasoline Engine <i>Charalampos Arapatsakos</i>	19
Embedding Sustainability Dynamics in Energy Conversion Chain on Electric Railway Vehicles with Traction Synchronous Motors <i>Cornelia A. Bulucea, Doru A. Nicola, Daniel C. Cismaru, Nikos E. Mastorakis, Carmen A. Bulucea, Constantin Brindusa</i>	21
Modelling of the Unsteady Flow-Sediment Interaction – Grain Size Approach <i>Srdjan R. Kolakovic, Ljubomir M. Budinski, Goran B. Jeftenic, Borislav T. Masic, Slobodan S. Kolakovic, Svetlana R. Vujovic</i>	29
Simulation Methodology with Control Approach for Water Distribution Networks <i>Diego Ricardo Diaz Vela</i>	37
The Market Value of in Use Industrial Machinery <i>Benedetto Manganelli, Pierluigi Morano, Francesco Tajani</i>	46
Insurance and Chain Bankruptcy Theory <i>Bijan Bidabad, Nikos Mastorakis</i>	51
Studies Regarding the Irrigation to the Hilly and Terraced Surfaces <i>B. Lepadatescu, A.-E. Dumitrascu, A. Nedelcu</i>	55
Development of Autonomous Energy Supply System Using a Sail Type Wind Turbine <i>A. Jakovics, S. Sakipova, K. Kussaiynov, Zh. Kambarova, Ye. Kussaiynov</i>	62
Assessing Pollution of Outdoor Insulators in the Cretan Power System <i>D. Pylarinos, K. Siderakis, I. Pellas, E. Thalassinakis</i>	67
Solar Powered LNG Regasification: Enhancing Power Generation and Water Desalination <i>Asad A. Salem, Emad Hudiab</i>	73
Credit Risk Evaluation and Analysis on Chinese Commercial Banks Using Logistic Model <i>Xiaorong Zou</i>	79
Development of Comsol 3D Model for Heat Collection under a Water Body <i>Hafiz M. K. U. Haq, Birgitta Martinkauppi, Erkki Hiltunen</i>	87
Fuel Consumption at Conditions of the Israel’s Highways Driving Cycle <i>M. Ben Chaim, E. Leybovitch</i>	92

Overview of the Most Developed Instances of Eco-Industrial Parks in Italy	95
<i>Sara Tessitore, Tiberio Daddi, Francesco Testa</i>	
Using Direct and Indirect Methods of Landscape Evaluation on Environmental Amenities' Valuation	104
<i>L. Loures, A. Loures, J. Nunes, T. Panagopoulos</i>	
Energy Efficiency and Sustainability of Low Energy Houses in Latvian Climate Conditions	109
<i>Andris Jakovics, Stanislavs Gendelis, Ansis Ozolins, Saule Sakipova</i>	
Thermal Behavior of a Simplistic Asphalt Pavement Model for Heat Pulses	115
<i>J. Birgitta Martinkauppi, Anne Mäkiranta, Jukka Kijärvi, Erkki Hiltunen</i>	
A Computational Study of a Prebiotic Synthesis of L-Leucine and L-Isoleucine	121
<i>N. Aylward</i>	
Examination of Deterioration on Diesel Engine when used as Fuel Mixture of Diesel-Vegetable Oil	130
<i>Charalampos Arapatsakos, Anastasios Karkanis, Ioannis Pantokratoras, Eirini Markidou</i>	
Assessing the Relation between Soil Edaphic Properties and Phosphorus Adsorption in Extremadura (Spain) Vertisols	136
<i>L. Loures, J. Nunes, A. López-Piñeiro, A. Loures, A. Navarro</i>	
New Tree Species for Agroforestry and Energy Purposes	142
<i>Andrea Vityi, Béla Marosvölgyi</i>	
Power-Information Models of Operation and Development of Megapolises Power Supply Systems	145
<i>Stepan A. Dmitriev, Sergey E. Kokin, Alexandra I. Khalyasmaa</i>	
Assessment of Water Quality of Artificial Water Bodies in Vojvodina (Serbia) using Factor and Cluster Analysis	151
<i>Srđan R. Kolaković, Svetlana R. Vujović, Slobodan S. Kolaković, Borislav T. Mašić, Goran B. Jeftenić, Ljubomir M. Budinski</i>	
Analysis of Multiannual Fluctuations and Long Term Trends of Hydrological Time Series	156
<i>O. Marusiak, J. Pekar</i>	
Log-Normality of the Tsunami Run-up Heights along the Eastern Coastal Line of Korean Peninsula	160
<i>Kim D., Cho H., Cho Y.-S.</i>	
Challenges for a Sustainable Ecosystem Management of Carpathian Forests	163
<i>Simona Frone, Dumitru Florin Frone</i>	

Effect of Secondary Pulp Mill Sludge Application as Soil Organic Amendment in Nitrate Leaching	169
<i>J. Rato Nunes, F. Cabral, A. López-Piñeiro, L. Loures, D. Becerra</i>	
Tisza River Modelling on the Common Interest Section of Hungary and Serbia	173
<i>Srdjan R. Kolakovic, Slobodan S. Kolaković, Goran B. Jeftenic, Borislav T. Masic, Svetlana R. Vujovic</i>	
Statistical Analysis of Low Flows in Eastern Slovakia	181
<i>M. Zeleňáková, P. Purcz, T. Soláková, D. Simonová</i>	
Svedberg's Number in Diffusion Processes	187
<i>Alfredo Constaín, Duvan Mesa, Carlos Peña-Guzmán, Paola Acevedo</i>	
Wet Scrubber for Cleaning of Syngas from Biomass Gasification	195
<i>Marek Balas, Martin Lisy, Zdenek Skala, Jiri Pospisil</i>	
The Effect of Regulatory Uncertainty on Water-Right Prices: The Case of the Loa Basin in the Antofagasta Region of Chile	202
<i>Oscar Cristi, Carlos Díaz, Gonzalo Edwards, Eric Edwards</i>	
Accounting Aspects of Risk Management and Improvement of the Entrepreneurial Venture Enterprise	209
<i>Nenad R. Lalić, Srdjan M. Lalić, Dragan Milovanović, Biljana Kovačević</i>	
The Comparison of Wood Chips and Cocoa Shells Combustion	217
<i>Michal Spilacek, Martin Lisy, Marek Balas, Zdenek Skala</i>	
Experimental Measurement of Load and Exhaust Gas Emissions on an Outboard Engine	221
<i>Anastasios Karkanis, Charalampos Arapatsakos, Christina Anastasiadou</i>	
The Impact of Salinity on Development the Most Important Copepoda Taxa in Baltic Sea	228
<i>Lidia Dzierzbicka-Głowacka, Maja Musialik, Anna Lemieszek</i>	
Geochemical Baseline Concentrations of Available Heavy Metals in Mediterranean Agricultural Soils: A Case Study in Calcareous Soils of Southwest Iberian Peninsula	235
<i>J. Rato Nunes, J. Ramos-Miras, A. Lopez-Piñeiro, L. Loures, C. Gil, J. Coelho, D. Peña</i>	
Thermochemical Characteristics of the Modern Gearboxes Housing Material	241
<i>Ion Silviu Boroza, Veronica Argeşanu, Inocenţiu Maniu, Raul Miklos Kulcsar, Mihaela Jula</i>	
Managing Value Chain Relationships in Cross-Level Organizations - Compare Cellar-Phone Manufacturing and Sport Shoemaking Supply Chain	247
<i>Chang Jang-Li, Lin Yu-Chuan</i>	
Transformation of Soil Texture Classifications by Ensemble Modeling	252
<i>Milan Cisty, Greta Dolakova, Jana Skalova, Peter Minaric</i>	

The Analysis of Stormwater Runoff and Overflow from the Novi Sad Catchment	258
<i>Srdjan R. Kolakovic, Matija B. Stipic, Goran B. Jeftenic, Borislav T. Masic, Filip M. Stipic, Slobodan S. Kolakovic, Svetlana R. Vujovic</i>	
Fate of Metribuzin Affected by De-Oiled Two Phase Olive Mill Waste Amendment in an Olive Grove Soil	265
<i>D. Peña, A. López-Piñeiro, A. Albarrán, D. Becerra, J. Sánchez-Llerena, J. Rato-Nunes</i>	
Assessment of Surface Water Quality for Sustainable Water Management in Samut Songkram Province, Thailand	270
<i>Tatsanawalai Utarasakul, Sivapan Choo-In, Chaisri Tharasawatpipat, Srisuwan Kasemsawat, Sathaporn Monprapussorn</i>	
The Effect of Roof Material on Rain Water Quality Parameters in Conditions of Slovak Republic	275
<i>Mohamed Ahmidat, Daniela Kaposztasova, Gabriel Markovic, Zuzana Vranayova</i>	
Socio-Hydrological Vulnerability: A New Science through Remote Sensing and GIS	281
<i>Mukesh Singh Boori, Vit Voženílek</i>	
Improvement of Power Management System in Electro-Solar Vehicle	286
<i>Hemza Saidi, Abdelhamid Mudoun</i>	
Novel Data-Mining Methodologies for Detecting Drug-Drug Interactions: A Review of Pharmacovigilance Literature	301
<i>I. Heba, A. Amany, S. E. Ahmed, S. Amr</i>	
Conversion of 2D Medical Scan Data into 3D Printed Models	315
<i>Eva Hnatkova, Petr Kratky, Zdenek Dvorak</i>	
Fault Throw and Sealing Thickness Relationship of Middle Cretaceous Muglad Basin, South Sudan	319
<i>Dorar Hamdoba Elshaikh, Zuhar Zahir Bin Tuan Harith</i>	
Environmental Impact of Masonry and RC Frame Structures	324
<i>A. Puskás, J. Virág, L. M. Moga, H. Szilágyi, M. Bindea, Sz. A. Köllő</i>	
Long-Term Water Balance Changes of the Pristine Bela River Basin	330
<i>D. Halmova, P. Miklanek, P. Pekarova</i>	
Short Term Effect of Different Management Practices on Rice Production and Agronomic Behavior in Mediterranean Conditions	336
<i>D. Becerra, J. Sánchez-Llerena, D. Peña, A. López-Piñeiro, A. Albarrán, J. Rato-Nunes, L. Loures</i>	

Engine Performance and Economic Impact Study of Gasoline-Like Tyre Pyrolysis Oil in Thailand	340
<i>C. Wongkhorsub, N. Chindaprasert, S. Peanprasit</i>	
Parameters of Insolvency Proceedings in Developed Countries and Their Dependence on Economic Performance	345
<i>Luboš Smrčka, Markéta Arltová, Jaroslav Schönfeld, Lee Louda</i>	
HVDC Transmission Corridor - Cost Benefit Analysis	353
<i>Udrea Oana, Gheorghe Lazaroiu, Ungureanu Gabriela</i>	
The Ability of Water Reservoir to Assure Required Water Supply under Changed Climate Conditions	359
<i>D. Halmova, M. Melo, P. Pekarova</i>	
Backstepping Control Based Three Phase Shunt Active Power Filter	364
<i>I. Ghadbane, M. T. Benchouia</i>	
The Role of Research and Development in the Central Region of Romania using Fuzzy Super FRM Model	371
<i>Moga Monika, Calefariu Gavrilă, Sârbu Flavius Aurelian</i>	
Oxidation of 2-Propanol at Low Temperature over Pt/γ-Al₂O₃ Catalyst	375
<i>F. Aghazadeh, D. Omidifar, A. Niaei, D. Salari</i>	
Significant Factors of Satisfaction of Bank Customers. Case Study from the Czech Republic	379
<i>J. Belás, A. Chochořáková, L. Gabčová</i>	
Solute Transfer in Layered Porous Media: An Approach Based on Differential Quadrature Method (DQ)	384
<i>Meysam Ghamariadyan, Abbas Ghaheri</i>	
Catastrophic Danube Flood Scenario between Kienstock and Nagymaros Using NLN Model	393
<i>V. Bacova Mitkova, P. Pekarova, J. Pekar</i>	
Renewable, Non-Renewable Energy Consumption, Economic Growth and CO₂ Emission: Evidence for Iran	399
<i>Soheila Khoshnevis Yazdi, Bahman Khanalizadeh, Nikos Mastorakis</i>	
The Assessment of the Effectiveness of Reforms in Various Countries	405
<i>Samson Davoyan, Tatevik Sahakyan</i>	
The Easiest and Least Expensive Way to Control Water Hammer in Irrigation and Drainage Network of Sivand Dam	417
<i>Reza Gharehkhani, Sayed Abbas Mousavi, Fatemeh Kazemi</i>	

Differences between Structural, Textural and Rheological Properties of two Cameroonian Mineral Clays Used as Cosmetic Mask	425
<i>Orléans Ngomo, Joseph Marie Sieliechi, Jean Bosco Tchatchueng, Richard Kamga, Aurel Tabacaru, Rodica Dinica, Mirela Praisler</i>	
Impact of Steering Committee Configuration and Decisions on Project Success in Pakistan	432
<i>Sabina S. Shirazi</i>	
Assessing Environmental Impacts of Aviation on Connected Cities via Environmental Vulnerability Studies and Fluid Dynamics: An Indian Case Study	438
<i>Gautham Ramchandran, Jethro Nagawkar, Karthik Ramaswamy, Sat Ghosh</i>	
Effects of Environmental Factors on Noise Emissions from Pig Housing	450
<i>M. Šítková, J. Brouček, P. Bartoš, I. Celjak, A. Dolan</i>	
Decrease the Scourge of Malnutrition in Sub-Saharan Africa through the Implementation of EU Financial Instruments	454
<i>Ionel Bostan, Carmen Năstase, Dana Drugus, Alunica Morariu, Ovidiu Bunget</i>	
Performance Measure of Switching Device (MOSFET) in Photo-voltaic System	460
<i>Kamala J., Janarthanan V., Santhosh K.</i>	
Novel Methods for Desulfurization of Petroleum Fractions	465
<i>H. Hosseini</i>	
New Land Use in Rural Marginal Areas. Renewable Energy vs Landscape Preservation	468
<i>Donatella Cialdea, Luigi Mastronardi</i>	
Economic Analysis of a Pumped Storage Project for Iran Generating System Based on a Dynamic Modeling	475
<i>A. R. Sohrabi</i>	
Authors Index	481

Plenary Lecture 1

Floating Offshore Wind Turbines: The Technologies and the Economics



Prof. Paul D. Sclavounos

Professor of Mechanical Engineering and Naval Architecture
Massachusetts Institute of Technology (MIT)

77 Massachusetts Avenue
Cambridge MA 02139-4307
USA

E-mail: pauls@mit.edu

Abstract: Wind is a vast, renewable and clean energy source that stands to be a key contributor to the world energy mix in the coming decades. The horizontal axis three-bladed wind turbine is a mature technology and onshore wind farms are cost competitive with coal fired power plants equipped with carbon sequestration technologies and in many parts of the world with natural gas fired power plants.

Offshore wind energy is the next frontier. Vast sea areas with higher and steadier wind speeds are available for the development of offshore wind farms that offer several advantages. Visual, noise and flicker impacts are mitigated when the wind turbines are sited at a distance from the coastline. A new generation of 6-10MW wind turbines with diameters exceeding 160m have been developed for the offshore environment. They can be fully assembled at a coastal facility and installed by a low cost float-out operation. Floater technologies are being developed for the support of multi-megawatt turbines in waters of moderate to large depth, drawing upon developments by the offshore oil & gas industry.

The state of development of the offshore wind energy sector will be discussed. The floating offshore wind turbine technology will be reviewed drawing upon research carried out at MIT since the turn of the 21st century. Floating wind turbine installations worldwide and planned future developments will be presented. The economics of floating offshore wind farms will be addressed along with the investment metrics that must be met for the development of large scale floating offshore wind power plants.

Brief Biography of the Speaker: Paul D. Sclavounos is Professor of Mechanical Engineering and Naval Architecture at the Massachusetts Institute of Technology. His research interests focus upon the marine hydrodynamics of ships, offshore platforms and floating wind turbines. The state-of-the-art computer programs SWAN and SML developed from his research have been widely adopted by the maritime, offshore oil & gas, and wind energy industries. His research

activities also include studies of the economics, valuation and risk management of assets in the crude oil, natural gas, shipping and wind energy sectors. He was the Georg Weinblum Memorial Lecturer in 2010-2011 and the Keynote Lecturer at the Offshore Mechanics and Arctic Engineering Conference in 2013. He is a member of the Board of the North American Committee of Det Norske Veritas since 1997, a member of the Advisory Committee of the US Navy Tempest program since 2006 and a member of the Advisory Board of the Norwegian Center for Offshore Wind Energy Technology since 2009. He has consulted widely for the US Government, shipping, offshore, yachting and energy industries.

<http://meche.mit.edu/people/?id=76>

Plenary Lecture 2

The Influence of a Magnetic Field in the Fuel of a Gasoline Engine



Professor Charalampos Arapatsakos

Department of Production and Management Engineering
Democritus University of Thrace
GREECE

E-mail: xarapat@pme.duth.gr

Abstract: This work examines the effect of magnetic field in a four stroke gasoline engine. The magnetic field that was created affected the fuel just before it enters to the engine. As a result there was a change in the combustion of the engine as well as variations in the exhaust gases. The engine was functioned without and under full load.

Brief Biography of the Speaker: Dr Charalampos Arapatsakos is a Greek citizen, who has been born in Athens. He has studied Mechanical Engineering. He is Professor on Democritus University of Thrace in Greece. Prof C. Arapatsakos has participated in many research programs about biofuels, gas emissions and antipollution technology. His research domains are mainly on biofuels and their use in internal combustion engines, the power variation from the use of biofuels, the gas emissions, mechanical damages, internal combustion engines, antipollution technology, renewable sources of energy, gas emissions, vehicle design, elements of machines, resistance of materials, technical mechanics, heat transmission.

Embedding sustainability dynamics in energy conversion chain on electric railway vehicles with traction synchronous motors

Cornelia A. Bulucea, Doru A. Nicola, Daniel C. Cismaru, Nikos E. Mastorakis, Carmen A. Bulucea, and Constantin Brindusa

Abstract—This paper addresses some aspects illustrating sustainable energy conversion processes during the operation of electric railway vehicles with traction synchronous motors. Increasing efforts are being expended to enhance the sustainability of transportation technologies and systems, and supporting transport systems' sustainability is a key way of thinking towards cleaner production. In line with this idea, this paper addresses the operation sustainability of electric railway vehicles with traction synchronous motors, highlighting the chain of interactions among the main electric equipment on an electrically driven railway system. The paper supports the findings that electric traction drive systems using traction synchronous motors powered by network-side converters and machine-side converters enhance the sustainable operation of railway trains.

Keywords—Electromagnetic torque, high speed electric train, railway vehicle, sustainability dynamics, synchronous motor

I. INTRODUCTION

In line with the framework of cleaner production, to address meaningfully many of the problems facing railway vehicles, conditions for the performance of sustainable transportation systems must be formulated [1-5]. Correspondingly, sustainability concepts can help understand the efficiencies of electrically driven systems and guide improvement efforts [1-5].

According to the term defined by United Nation Environmental Programme in 1990, cleaner production

Cornelia A. Bulucea is with the University of Craiova, Faculty of Electrical Engineering, Craiova 200440, Romania (e-mail: abulucea@gmail.com).

Doru A. Nicola is with the University of Craiova, Faculty of Electrical Engineering, Craiova 200440, Romania (e-mail: dorunicola@gmail.com).

Daniel C. Cismaru is with the University of Craiova, Faculty of Electrical Engineering, Craiova 200440, Romania (e-mail: dcismaru@gmail.com).

Nikos E. Mastorakis is with the Technical University of Sofia, Industrial Engineering Department, Sofia, Bulgaria & Military Institutions of University Education (ASEE), Hellenic Naval Academy, Piraeus 18539, Greece (e-mail: mastorakis4567@gmail.com).

Carmen A. Bulucea is with the University of Medicine and Pharmacy of Craiova, Craiova 200349, Romania (e-mail: carmen.bulucea@gmail.com).

Constantin Brindusa is with the University "Constantin Brancusi" of Targu-Jiu, Targu-Jiu, Romania (e-mail: rinstalctin@yahoo.com).

requires a new way of thinking about processes and products, and about how they can be made less harmful to humans and the environment [6-7]. Within the conceptual framework of cleaner production improvements of technology and changes in equipment design should suggest better choices in use of materials and energy in manufacturing and operation of industrial systems [5-7]. Improved control and automatization represent key concepts of cleaner production strategies [6-7]. Green products and systems are generally produced in a manner that consumes fewer natural resources or uses them in a more sustainable way, and they may involve high exergy efficiency in their manufacture and operation [4-5].

The sustainability of an electric transportation system is based on technical performance, safety, energy and exergy efficiency, mitigated environmental impact, economics and societal acceptance [1-3]. Costs should reflect value, which is doubtless associated with sustainability aspects [1-5]. Addressing the sustainability of traction and braking operation of the electric vehicles constitutes a challenge in electric transportation research.

II. STRUCTURE OF MAIN ELECTRIC CIRCUITS OF RAILWAY VEHICLES WITH TRACTION SYNCHRONOUS MOTORS

In order to be used as a traction motor on high speed trains (namely, the French TGV), the synchronous motor (being an electric motor with rotating field) is needing a variable frequency three-phase supply [8-14]. It results implicitly the necessity of the machine converter (MC) in the power circuit. The MC is a current inverter (CI) with a three-phase bridge (with 6 thyristor branches linked as a three-phase bridge) which operates being commutated by the counter-electromotive forces (CEMF) ($-e_0$) induced in the three-phase stator winding of the supplied synchronous motor [8-10].

One could notice that problems related to the natural commutation appear solely at very low speed, when the CEMF amplitude is small (and consequently, insufficient for ensuring the commutation). In such situation (from the starting regime up to 5-10% of the maximum speed v_{max}) the commutation adjustment is imposed. The devices for the assisting commutation are quite simple and don't have a hard weight (for instance, a weight of 70 kg for a 6000 kW locomotive). Moreover, by using the signals regarding the rotor position and speed at the inverter control, the synchronous motor will drive

(or pilot) the current inverter which is supplying it, this way being eliminated the risks of synchronism loss, whatever is the rotor speed. Hence, the traction synchronous motor is a self-piloted motor [8-14].

As a pattern, the operation of a self-piloted synchronous motor supplied by a current inverter source is similar to the DC motor with fixed armature and rotating inductor. According to this scenario, the speed regulation of the self-piloted synchronous motor will be ensured similarly to the DC motor with separate excitation [15-16]. Concretely, it is performed the change of voltage of the DC intermediary circuit with single phase bridges with phase regulation (mixed bridges or fully controlled bridges) in the case of the supply from a AC contact line, or there are utilized electronic DC drives (DC/DC converters) in the case of the supply from a DC contact line. In order to obtain high speeds there is performed the field weakening [8-14, 17-19].

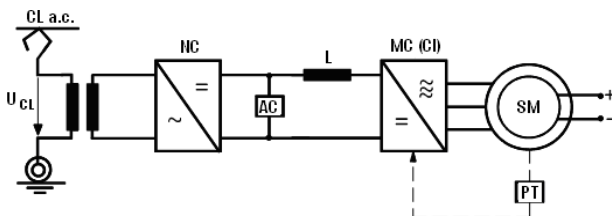


Fig.1 Power circuits' structure of electrical railway vehicle with traction synchronous motors supplied from AC contact line
 NC = network converter; AC = assisted commutation device;
 L = smoothing coil (with iron core); MC = machine converter;
 SM = synchronous motor; PT = position transducer

Unlike the electric railway vehicle with induction motors, during the electric power transmission on the vehicle with synchronous motors the amplitude regulation functions are completely separated from those of frequency regulation. Actually, the voltage variation is enabled as in classic traction with DC motors by the electronic DC drives (DC/DC converters) or by mixed single-phase half-controlled bridge rectifier by asymmetric type. Conversely, the frequency variation is provided by the current inverters (CI) through which the traction synchronous motors are powered.

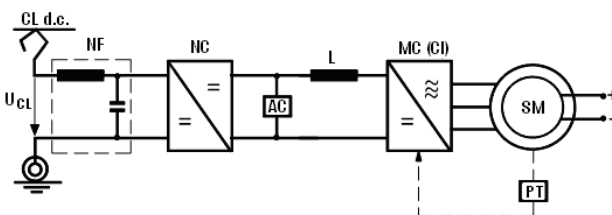


Fig.2 Power circuits' structure of electrical railway vehicle with traction synchronous motors supplied from DC contact line
 NF = network filter; NC = network converter; AC = assisted commutation device; L = smoothing coil (with iron core);
 MC = machine converter; SM = synchronous motor;
 PT = position transducer

Consequently, the electric trains with traction synchronous motors entail compulsory two conversion stages of the electric energy. Specifically, it is imposed the presence of the network

converter (NC) both when the railway electric vehicle is powered from an AC contact line (see Figure 1) and when the vehicle is supplied from a DC contact line (see Figure 2).

As a traction motor, the synchronous motor is operating in a self-piloted regime, the control pulses of the current inverter thyristors (synchronized with the induced voltages) being correlated with the rotor position due to the position transducer PT. In the operation at low speed, when the counter-electromotive forces can not anymore ensure the commutation of the current inverter thyristors it is carried out the "assisted commutation" performed by the auxiliary device AC.

In the case of electric locomotives and urban trains with traction synchronous motors supplied from an AC contact line, the network converter NC is encompassing a system of single-phase rectifiers (full or part controlled) connected in series (in order to improve the power factor). In contrast, when the electric railway vehicle is powered by a DC line, the network converter is a classic chopper (with operation in 1 or 2 quadrants).

Consequently, in both situations the structure of the network converters is similar to classic solutions with rectifiers and choppers. Conversely it is imposed to enhance the analysis of the system inverter – synchronous motor, underlining that its structure is identical for both supply types from the contact line.

In contrast with the case of electric locomotives and urban trains with traction induction motors, the utilization of synchronous motors as electric traction motor does not raise problems related to the electric braking safety. The electric braking might be easily accomplished, since when the contact line power is cut the traction synchronous motors, being excited now from the locomotives batteries will operate as synchronous generators, delivering the electric energy (converted to DC power by the converter bridge) on the electrical braking resistance conveniently sized.

For economic reasons, so far the synchronous motor has been used as traction motor only at high power (800 kW and 1.1 MW) on locomotives and electric trains TFV-A type.

III. ELECTROMAGNETIC TORQUE DEVELOPED BY SYNCHRONOUS MOTOR

Within the framework of cleaner production, the exergy concept, which is a measure of energy quality, can be used to enhance understanding and help improve the efficiencies of technical systems which convert energy and matter [1-5]. According to the laws of thermodynamics, energy is never destroyed during a process, although it can change from one form to another, but exergy can be destroyed. While energy is a measure of quantity only, exergy is a measure of quantity and quality or usefulness. Energy is often thought of as motion and exergy as work [1-5]. Thus, exergy has an important role to play in increasing efficiencies of energy systems and technologies, within energy optimization and engineering modeling studies.

Since exergy is a measure of the potential of a system to do work, the electromagnetic torque M developed by an electrical motor can be interpreted as the driving force of useful work, i.e. the electric motor output exergy [1-5].

The electromagnetic torque M (respectively, the electromagnetic power $P_M = M \cdot \Omega$ with $\Omega = \omega/p$) developed by any synchronous motor is determined by calculation on basis of the active powers' balance, as follows:

$$P_M = P_1 - p_{J1} = 3 \cdot U \cdot I \cdot \cos \varphi - 3 \cdot R_1 \cdot I^2 \quad (1)$$

$$M = \frac{P_M}{\Omega} = \frac{3 \cdot P}{\omega} \cdot (U \cdot I \cdot \cos \varphi - R_1 \cdot I^2) \quad (2)$$

For generalization, we consider the case of salient pole synchronous motor, referring to the classic phasor diagram depicted in Figure 3, where the components of the current \underline{I} and voltage \underline{U} on the axes d and q are:

$$I_d = I \cdot \sin \Psi; \quad I_q = I \cdot \cos \Psi \quad (3)$$

$$U_d = U \cdot \sin \theta; \quad U_q = U \cdot \cos \theta \quad (4)$$

If there is taken into consideration that $\varphi = \psi + \theta$, and the function $\cos(\psi + \theta)$ is trigonometrically developed as:

$$I \cdot \cos \varphi = I \cdot \cos \Psi \cdot \cos \theta - I \cdot \sin \Psi \cdot \sin \theta = I_q \cdot \cos \theta - I_d \cdot \sin \theta \quad (5)$$

and in the expression of active power ($U \cdot I \cdot \cos \varphi$) the components U_d and U_q are highlighted:

$$U \cdot I \cdot \cos \varphi = I_q \cdot (U \cos \theta) - I_d \cdot (U \sin \theta) = I_q \cdot U_q - I_d \cdot U_d \quad (6)$$

then the formula (2) for the calculation of electromagnetic torque M becomes:

$$M = \frac{3 \cdot P}{\omega} \cdot (I_q \cdot U_q - I_d \cdot U_d - R_1 \cdot I^2) \quad (7)$$

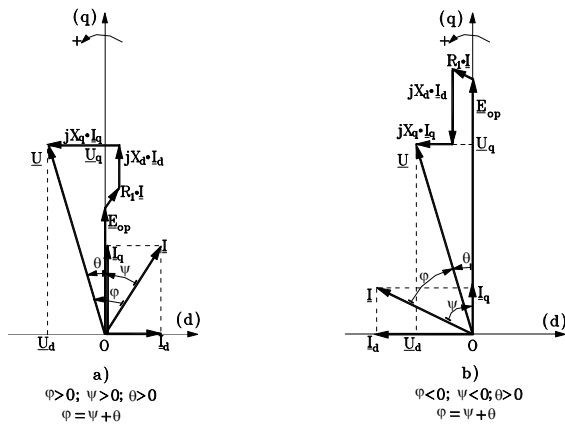


Fig.3 Blondel phasor diagram of synchronous motor with salient poles
a) under-excited operation (inductive current I); b) over-excited operation (capacitive current I)

Using again the phasor diagram (Fig.3.a), by projection of the phasors' contour on the axes d and q, the voltage equations in scalar form of components are obtained as:

$$U_d = -R_1 \cdot I_d + X_q \cdot I_q \quad (8)$$

$$U_q = E_{op} - R_1 \cdot I_q + X_d \cdot I_d$$

If further the term $I_q \cdot U_q - I_d \cdot U_d$ is evaluated as below:

$$I_q \cdot U_q - I_d \cdot U_d = E_{op} \cdot I_q + (X_d - X_q) \cdot I_d \cdot I_q + R_1 \cdot I^2 \quad (9)$$

then the expression of the electromagnetic torque M given by (7) will take the compact form:

$$M = \frac{3 \cdot P}{\omega} [E_{op} \cdot I_q + (X_d - X_q) \cdot I_d \cdot I_q] \quad (10)$$

At the non-salient synchronous motor, when $X_d = X_q = X_s$ the component caused by the magnetic anisotropy in the formula

(10) will not appear anymore. Actually, the final expression of the electromagnetic torque will depend on the type of the power supply of the synchronous motor (voltage source or current source).

A. Electromagnetic Torque Developed by the Synchronous Motor Supplied from a Three-Phase Sinusoidal Currents' Source

In the case of powering from a three source of sinusoidal currents the current phasor \underline{I} (through the reference stator winding) is specified by its magnitude $|\underline{I}| = I$ and initial phase (through the position angle) ψ to the axis q of the rotor. It means that implicitly there are specified the components I_d and I_q (3) of the stator current I .

In these supplying conditions the electromagnetic torque $M_I = M$ will be determined with relation (10) in which there are performed the substitutions specified by (3), obtaining the expression as follows:

$$M_I = \frac{3 \cdot P}{\omega} [E_{op} \cdot I \cdot \cos \Psi + (X_d - X_q) I^2 \cdot \sin \Psi \cdot \cos \Psi] \quad (11)$$

and the final form:

$$M_I = \frac{3 \cdot P}{\omega} \cdot [E_{op} \cdot I \cdot \cos \Psi + \frac{1}{2} I^2 (X_d - X_q) \cdot \sin 2\Psi] \quad (12)$$

On the whole, one could notice the presence of two components M_I' and M_I'' , so that based on relation (12) it can be written $M_I = M_I' + M_I''$.

The main component $M_I' = \frac{3 \cdot P}{\omega} E_{op} \cdot I \cdot \cos \Psi$ depends on the

excitation degree (namely, the magnitude of current I_e), while the secondary component $M_I'' = \frac{3 \cdot P}{\omega} \cdot \frac{I^2}{2} \cdot (X_d - X_q) \cdot \sin 2\Psi$ is determined

by the magnetic asymmetry of the rotor, being present (and non-zero) even in the absence of the synchronous motor excitation. At $I = \text{ct.}$, $f = \text{ct.}$ and excitation current $I_e = \text{ct.}$ (when $E_{op} = \text{ct.}$), the electromagnetic torque M_I depends solely on the load angle ψ .

For the salient pole synchronous motor, the characteristic $M_I = f(\psi)$ is represented in Figure 4 by a thick line.

In the case of non-salient pole motors, in which $X_d = X_q = X_s$ the secondary component will not appear ($M_I'' = 0$) and the load characteristic $M_I = f(\psi)$ is represented just by the main component with a cosine variation.

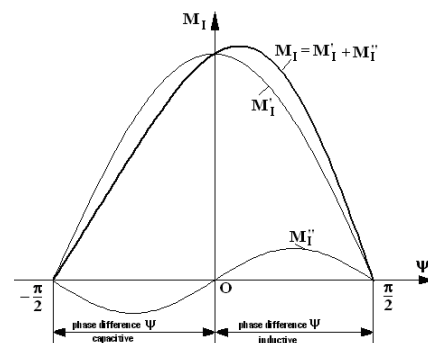


Fig.4 Characteristic representation $M_I = f(\psi)$ of synchronous motor with salient poles at powering from a three-phase source of sinusoidal currents

One could note that if in formula (12) of the torque M_I there are performed the substitutions:

$$E_{op} = \omega \cdot (w_1 \cdot k_{w1} \frac{\Phi_{om}}{\sqrt{2}}); \quad X_d = \omega \cdot L_d \quad \text{and} \quad X_q = \omega \cdot L_q \quad (13)$$

then the electromagnetic torque expression M_I (at the supply in current) becomes:

$$M_I = 3p \cdot (w_1 \cdot k_{w1} \frac{\Phi_{om}}{\sqrt{2}}) \cdot I \cos \Psi + \frac{3p}{2} \cdot I^2 (L_d - L_q) \cdot \sin 2\Psi \quad (14)$$

In relations (13) and (14) the physical significance of the new quantities are:

- w_1 = the number of turns, in series, on a stator phase of synchronous motor;
- k_{w1} = the winding factor of a stator phase;
- Φ_{om} = the maximum value of the main magnetic flux, depending on the magnitude of excitation current I_e , namely $\Phi_{om}=f(I_e)$;
- L_d = the longitudinal inductance of stator winding
- L_q = the transverse inductance of stator winding of synchronous motor.

Particularly, for $\psi=0$ (when $I_d=0$ and $I_q=I$), the expression (14) of the electromagnetic torque M_I becomes:

$$M_I = M'_I = 3p(w_1 \cdot k_{w1} \frac{\Phi_{om}}{\sqrt{2}}) \cdot I = K \cdot \Phi_{om} \cdot I \quad (15)$$

videlicet M_I will get a form that is mathematically identical to the electromagnetic torque $M=C_m \cdot \Phi \cdot I$ developed by a DC motor (with collector) with separated excitation.

In relation (15), with K has been denoted the constructive constant $K = 3p \cdot w_1 \cdot k_{w1} \frac{1}{\sqrt{2}}$ of synchronous motor.

Expression (14) highlights that at $I_e=ct.$, $I=ct.$ and $\psi=ct.$ the electromagnetic torque M_I is constant (and nonzero) and has the same magnitude regardless of the numerical value of the frequency f of the stator currents.

Precisely the existence of nonzero electromagnetic torque at the powering in current (by magnitude I phase shift $\psi=ct.$ related to the counter-electromotive forces E_{op}) led to the development of synchronous motor applications in electric traction.

On the electric locomotives and urban trains the synchronous motor is powered from a current inverter (thyristorised), with natural commutation, determined exactly by the counter-electromotive forces E_{op} (induced in the stator windings of the synchronous motor).

In order to ensure the phase shift ψ (of the current fundamental I leading the counter-electromotive forces E_{op}), the control of thyristors' conduction is based on the signals from a position transducer solidary with the rotor. Consequently the synchronous motor is piloting.

IV. SUSTAINABLE OPERATION OF SELF-PILOTED SYNCHRONOUS MOTOR (SPSM)

On the electric railway vehicles the most convenient source of three-phase currents (to powering the synchronous motor) is the current inverter with natural commutation. The reason of this choice is related to low price, high reliability and smallsize (due mainly to the absence of the auxiliary extinction circuits).

In this context one could remind that the synchronous motor operating is characterized by a three-phase system of induced counter-electromotive forces ($-e_{0A}, -e_{0B}, -e_{0C}$) which might ensure the commutation of the three-phase bridge thyristors, just

as the three-phase alternating voltage network ensured the commutation of rectifier bridge thyristors.

However, to ensure the natural commutation of the thyristorised bridge, the induced counter-electromotive forces must be sufficiently large values, even at low speed, which requires synchronous motor to run over-excited (from start up to rated speed). The over-excitation of synchronous motor will lead to winding currents I that are leading the voltage U (the phase shift φ being by capacitive type, like in Figure 3b), in this case the motor providing also through the terminals the reactive power necessary to the inverter bridge commutation.

In order to ensure the capacitive phase shift of the current, the control of bridge thyristor ignition will be based on signals from a rotor position transducer. This way is correlated the position of current phasor I to the axis d of the rotor.

On the opposite side (the DC side) the autonomous current inverter (CI) must be connected to a DC variable source. Usually, a variable DC source is made up of adjustable DC voltage source (of chopper type or single-phase rectifier bridge with phase adjustment) connected in series with a smoothing coil with iron core, with the inductance L_0 of large size.

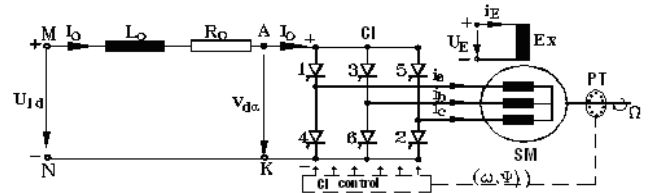


Fig.5 Self-piloted synchronous motor powered by a current inverter with natural commutation

SM = synchronous motor; Ex. = excitation winding; PT = position transducer
 IC = three-phase current inverter; L_0, R_0 = inductance and resistance of smoothing coil

Accordingly, the configuration of self-piloted synchronous motor powered from an autonomous current inverter is depicted in Figure 5. The representation entails the over-excited synchronous motor (SM), a three-phase thyristorised bridge (CI), a position transducer (PT) and a smoothing coil (with the parameters R_0 and L_0).

Since the supply is of current powered type, it results that the reversibility of assembly SM+CI can only be achieved by changing the sign (by reversing the polarity) of the average voltage V_{da} (on the DC side), therefore by controlling the passing of three-phase bridge (CI) in rectifier regime.

A. Detection of Rotor Position

In contradistinction to the thyristorised bridge connected to three-phase network (thereupon the firing pulses of thyristors were synchronized with the alternating voltages of the network), for the current case of thyristorised bridge (through that the self-piloted synchronous motor is powered) the generation of firing pulses of thyristors must be correlated with the rotor position. Specifically, in the case of a synchronous motor with $2p$ magnetic poles, the rotor position controller must generate $6 \cdot p$ „control orders” (at each complete rotation of the rotor) for the ignition of thyristors of bridge CI. It should be noted that „the control orders” of the thyristor ignition are given evolutionary (with time) as the rotor rotates.

As discussion at this point, one could highlight that, in such circumstances, it is necessary to provide a device that will help operation of the thyristorised bridge, since that needs to piloting of knowing angular position of the rotor. To this purpose, the traction synchronous motor shall be provided with:

- a toothed steel disc, solidary with the rotor, precisely positioned relative to inductor poles, and
- a set of sensors, set on the stator and precisely positioned relative to the stator core slots.

The successive passing of teeth and slots of the toothed disc under the position sensors shall allow finding at any time the exact rotor position. Depending on the rotor position as detected, further is established the control of the thyristors supplying phase stator windings so that the electromagnetic torque developed by the motor to be the maximum possible.

In principle, the stator sensors might be delayed in order to change the phase of control orders (of the ignition of thyristors) relative to the position of pole wheel. This way it is possible to control the phase angle ψ between the current and the induced counter-electromotive force on each phase. Nevertheless, on the modern traction synchronous motor the angle ψ is electronically controlled, by an electronic phase shift of signals generated by the position sensors. Usually, the device to detecting the rotor position is located inside the traction synchronous motor, being situated on the opposite side to the rotor shaft end.

B. Current Diagrams

Study of joint operation of current inverter and synchronous motor in self-piloted regime can be performed solely in the context of supply scheme from Figure 5. This is the easiest powering at variable frequency of synchronous motor [8-10].

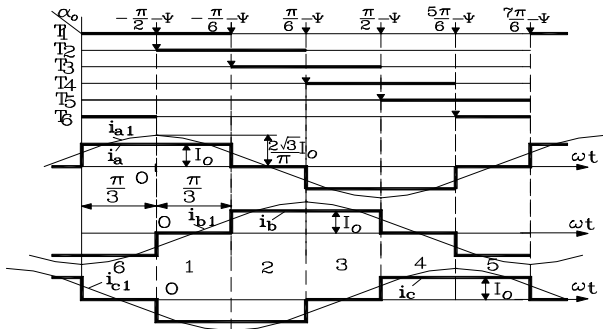


Fig.6 Conduction intervals of three-phase thyristor bridge and shapes of variation with time of currents i_a, i_b și i_c (and their fundamentals i_{a1}, i_{b1} și i_{c1})

The synchronous motor will be over-excited and the three-phase induced counter-electromotive forces ($-e_{0A}, -e_{0B}, -e_{0C}$) of frequency $f=\omega/2\pi$ will be able to drive the commutation of the current inverter thyristors at any speed $\Omega > \Omega_{min}$ without the risk of losing synchronism between rotor and rotating magnetic field. Specifically, at any speed “n” of the rotor of self-piloted synchronous motor (corresponding to the frequency $f=p \cdot n/60$ of stator currents) through the induced counter-electromotive forces the synchronous motor is piloting the converter which, from the DC current I_0 , is distributing (on each of the three phases of the stator) current pulses of amplitude $\pm I_0$, duration $T/3$ and a repetition frequency $f=1/T=\omega/2\pi$ which is proportional to the

angular mechanical speed of rotor rotation $\Omega=\omega/p$. The angular mechanical speed Ω of rotor is resulting from the fundamental equation of motion:

$$J \cdot \frac{d\Omega}{dt} = M - M_{ex} \tag{16}$$

Under the simplifying assumption of a DC current I_0 perfectly smooth (when $L_0 \rightarrow \infty$) and neglecting the commutation durations, the stator currents i_a, i_b și i_c (flowing through the phases of synchronous motor) will get the forms of variation with time depicted in Figure 6.

In these conditions the fundamentals of stator currents (denoted by i_{a1}, i_{b1} și i_{c1} in Figure 6) form a three-phase symmetrical current system (by direct sequence) with the frequency $f=\omega/2\pi$ and the effective I_1 value given by:

$$I_1 = \frac{\sqrt{6}}{\pi} \cdot I_0 \tag{17}$$

C. Synchronization of Commands

Operation of the self-piloted synchronous motor is based on ensuring the capacitive shift phase $\psi=ct.$ between the space phasor of stator currents and the axis q (like in Figure 3). Actually, this condition is verified 6 times during each time period T (by controlling the moments of thyristor ignition relative to the position $\alpha=\omega t+\alpha_0$ of the axis d of the rotor). For this purpose, a position transducer TP will provide the rotor positions (with respect to a reference direction of the stator) at which the bridge thyristors of the current inverter IC to be on.

Ideally, if harmonic variation of stator currents, their space phasor \underline{i}_{1dq} (in the rotor referential (d,q)) will be a fixed phasor, mathematically expressed by:

$$\underline{i}_{1dq} = \sqrt{2} I_1 \cdot e^{j(\frac{\pi}{2} + \psi)} \tag{18}$$

$$\text{with } I_1 = \frac{\sqrt{6}}{\pi} \cdot I_0$$

In the fixed stator referential the space phasor \underline{i}_{1dq} will match the expression \underline{i}_{1s} :

$$\underline{i}_{1s} = \frac{2}{3} (i_{a1} + a i_{b1} + a^2 i_{c1}) = i_{1dq} e^{j\alpha} = \frac{2\sqrt{3}}{\pi} I_0 \cdot e^{j(\frac{\pi}{2} + \psi + \alpha)} \tag{19}$$

$$\text{with } \alpha = \omega t + \alpha_0$$

If the reference stator axis will be overlapping the magnetic axis of phase „A”, and the temporal origin ($\omega t=0$) is chosen when the current i_{a1} (phase A) passes through a maximum (moment that is coinciding with thyristor ignition timing), the the space phasor \underline{i}_{1s} will be of the form:

$$\underline{i}_{1s} = \sqrt{2} \cdot I_1 \cdot e^{j\omega t} = \sqrt{2} \cdot \left(\frac{\sqrt{6}}{\pi} I_0 \right) \cdot e^{j\omega t} \tag{20}$$

From the expressions (19) and (20) follows that:

$$\frac{\pi}{2} + \psi + \alpha_0 = 0 \Rightarrow \alpha_0 = -\left(\frac{\pi}{2} + \psi \right) \tag{21}$$

That is the rotor position at the moment of ignition of thyristor T_2 . The other thyristors will be switched on their natural succession (at successive positions of the rotor evenly shifted by $\pi/3$ electric radians) as in Figure 6.

D. Considering the Current Fundamentals

When considering only the fundamentals of stator current, the space phasor \underline{i}_{1dq} (in the rotating referential d,q) is fixed and gets

the expression (in polar form) given by (18). From this relationship, identifying the equivalent algebraic form:

$$\dot{i}_{1dq} = \sqrt{2} \cdot I_1 \cdot e^{j(\frac{\pi}{2} + \psi)} = \sqrt{2} \cdot (I_{1d} + j \cdot I_{1q}) \quad (22)$$

there are obtained the effective values I_{1d} and I_{1q} of the orthogonal components:

$$I_{1d} = -I_1 \cdot \sin \psi = -\left(\frac{\sqrt{6}}{\pi} I_0\right) \sin \psi$$

$$I_{1q} = I_1 \cdot \cos \psi = \left(\frac{\sqrt{6}}{\pi} I_0\right) \cos \psi$$

If further in expression (10) of the electromagnetic torque M there are performed the substitutions $I_d=I_{1d}$ and $I_q=I_{1q}$, and, in addition there are used the substitutions (13), finally will result for $M=M_I$:

$$M_I = 3p \left[\frac{\sqrt{6}}{\pi} \cdot I_0 \cdot (K\Phi_{om}) \cdot \cos \psi - \frac{3}{\pi^2} \cdot I_0^2 \cdot (L_d - L_q) \cdot \sin 2\psi \right] \quad (23)$$

where the average value of current I_0 (which is established in the DC intermediary circuit, see Figure 5) is calculated from the relationship:

$$I_0 = \frac{U_{1d} - V_{d\alpha}}{R_0} \quad (24)$$

The sign „-“ between the components of the torque M_I (13) is caused by the over-excited operation (with the current fundamentals leading the counter-electromotive forces), that means with a capacitive shift (see Figure 3) of the self-piloted synchronous motor.

The sole problem of self-piloted synchronous motor is the starting regime. At low rotational speeds, under 5% of Ω_{max} , the counter-electromotive force ($-e_{op}$) becomes unable to ensure the commutation of the thyristors of the current inverter (CI). In this speed range it is applied the assisted commutation, realized by the device AC (see Figure 1 and Figure 2) through ingenious company solutions.

E. Considering the Non-Sinusoidal Currents

In very deed, the phase currents i_a, i_b, i_c are strongly distorted as against the ideal sinusoidal shape. Actually, under the simplifying assumptions adopted, each phase current (i_a, i_b or i_c from Figure 6) consists of „rectangular blocks” of amplitude $\pm I_0$ (and duration equal to $2\pi/3$) separated by intervals (by duration $\pi/3$) in which the currents are null.

Moreover, the fundamentals of phase currents (denoted by i_{a1}, i_{b1} and i_{c1} in Figure 6) have equal amplitudes (of magnitude $\frac{2\sqrt{3}}{\pi} I_0$) and they are shifted, one lagging another,

with the same angle of $2\pi/3$, forming a symmetrical three-phase system of sinusoidal currents, by direct succession. One could notice that by I_0 is denoted the DC intensity from the DC intermediary circuit.

In the fixed stator referential $\alpha\beta$, with the real axis $O\alpha$ overlapped to reference stator winding axis “A” and with the temporal origin ($\omega t=0$) chosen at the moment when its current is passing through a maximum (when $i_{a1} = \frac{2\sqrt{3}}{\pi} I_0$), the space

phasor \dot{i}_{1s} of stator current fundamentals, calculated with the formula:

$$\dot{i}_{1s}(\omega t) = \frac{2}{3} \cdot (i_{a1} + a \cdot i_{b1} + a^2 \cdot i_{c1}) = \sqrt{2} \left(\frac{\sqrt{6}}{\pi}\right) I_0 \cdot e^{j\omega t} \quad (25)$$

is a rotating phasor (with the angular speed $\omega=ct$) with the top-point describing the circle of radius equal to $\sqrt{2} \left(\frac{\sqrt{6}}{\pi}\right) \cdot I_0 = \frac{2 \cdot \sqrt{3}}{\pi} \cdot I_0$ (represented by dashed line in Figure 7).

In the same time interval, still in the fixed stator referential $\alpha\beta$, the space phasor \dot{i}_s (of non-sinusoidal currents) is completely different. For this reason, analytically it will proceed to an evaluation of this space phasor on each angular interval (by width $\pi/3$), in which the stator currents i_a, i_b and i_c remain constant. Thereby:

1. In the first interval $0 \leq \omega t \leq \pi/3$ when $i_a = +I_0, i_b = 0$ and $i_c = -I_0$ the space phasor \dot{i}_s is fixed (position „0” in Figure 7) and has the expression:

$$\dot{i}_s(\omega t) = \frac{2}{3} (i_a + a \cdot i_b + a^2 \cdot i_c) = \frac{2}{3} \cdot (I_0 - a^2 \cdot I_0) = \frac{2}{\sqrt{3}} \cdot I_0 \cdot e^{j\frac{\pi}{6}}; \quad 0 \leq \omega t < \frac{\pi}{3} \quad (26)$$

2. In the interval $(k+1)$ by width $\pi/3$, when ωt might be written as:

$$\omega t = k \cdot \frac{\pi}{3} + \omega t'; \quad 0 \leq \omega t' < \frac{\pi}{3}; \quad k=1, 2, 3 \dots \quad (27)$$

the space phasor \dot{i}_s remains fixed (in position „k”, $k=1,2,3 \dots$ in Figure 7) on whole duration $0 \leq \omega t' < \pi/3$.

Broadly speaking, for any ωt by type (27), the expression of space phasor \dot{i}_s can be written as:

$$\dot{i}_s(\omega t) = \frac{2}{\sqrt{3}} \cdot I_0 \cdot e^{j(\frac{\pi}{6} + k \cdot \frac{\pi}{3})} \quad \text{with } k = 0, 1, 2, 3 \dots \quad (28)$$

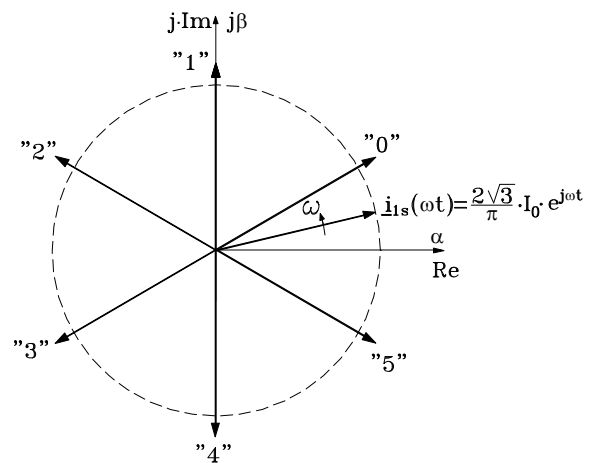


Fig.7 Rotating space phasor $\dot{i}_{1s}(\omega t)$ and the 6 fixed positions of non-sinusoidal current phasor $\dot{i}_s(\omega t)$ in the fixed stator referential

During each period $\omega T=2\pi$, the space phasor $\dot{i}_s(\omega t)$ of non-sinusoidal currents will successively scan all 6 fixed positions (denoted by “0”, “1”, “2”, “3”, “4”, “5” in Figure 7). At each position it will remain motionless for $t' = \frac{\pi}{3\omega} = \frac{\pi}{3} \left[\frac{T}{2\pi} \right] = \frac{T}{6}$, that

time being numerically equal to the duration between two successive commutations of the bridge, then instantly “jumps” to the next position.

Geometrically, over the duration of each period $\omega T=2\pi$, the “jumping” space phasor $\dot{i}_s(\omega t)$ performs a complete rotation, like the rotating phasor $\dot{i}_{1s}(\omega t)$ of current fundamentals. Accordingly, the virtual angular speed ω_{vir} (fictitious average) of rotation of

“jumping” phasor of non-sinusoidal currents $\omega_{vir} = \frac{2\pi}{T} = 2\pi f = \omega$ is

numerically equal to the rotation angular speed ω of the rotating phasor of stator current fundamentals. Consequently, this common value ω of angular speeds will be used at changing the referential of space phasors.

In the coordinates (d,q) rotating with angular speed ω , the space phasor \underline{i}_{1s} will become \underline{i}_{1dq} , while the space phasor \underline{i}_s will become \underline{i}_{dq} . At changing the referential, the relations among these phasors are as the form:

$$\underline{i}_{1dq} = \underline{i}_{1s} \cdot e^{-j\alpha}; \quad \alpha = \alpha_0 + \omega t \quad (29)$$

$$\underline{i}_{dq} = \underline{i}_s \cdot e^{-j\alpha}; \quad \alpha = \alpha_0 + \omega t \quad (30)$$

With expression (25) for \underline{i}_{1s} , the relation of phasor \underline{i}_{1dq} given by (29) gets the form:

$$\underline{i}_{1dq} = \sqrt{2} \cdot \left(\frac{\sqrt{6}}{\pi}\right) \cdot I_0 \cdot e^{j\omega t} \cdot e^{-j(\alpha_0 + \omega t)} = \frac{2\sqrt{3}}{\pi} I_0 \cdot e^{-j\alpha_0} \quad (31)$$

Absolutely similar, for any ωt as the form:

$\omega t = k \cdot \frac{\pi}{3} + \omega t'$ with $0 \leq \omega t' < \frac{\pi}{3}$ and $k = 0, 1, 2, 3, \dots$ when, in

fixed coordinates, the space phasor \underline{i}_s has the expression (28), it will result that, in synchronous rotating coordinates, the space phasor \underline{i}_{dq} (30) will be established by:

$$\underline{i}_{dq} = \frac{2}{\sqrt{3}} \cdot I_0 \cdot e^{j\left(\frac{\pi}{6} + k \cdot \frac{\pi}{3}\right)} \cdot e^{-j(\alpha_0 + k \cdot \frac{\pi}{3} + \omega t')} = \frac{2}{\sqrt{3}} \cdot I_0 \cdot e^{j\left(\frac{\pi}{6} - \alpha_0 - \omega t'\right)} \quad (32)$$

If the initial position α_0 it is chosen accordingly to relation (21), meaning $\alpha_0 = -\left(\frac{\pi}{2} + \psi\right)$, then in rotating coordinates (d,q), the

space phasors \underline{i}_{1dq} and \underline{i}_{dq} become:

$$\underline{i}_{1dq} = \frac{2\sqrt{3}}{\pi} \cdot I_0 \cdot e^{j\left(\frac{\pi}{2} + \psi\right)} = j \cdot \frac{2\sqrt{3}}{\pi} \cdot I_0 \cdot e^{j\psi} \quad (33)$$

respectively:

$$\underline{i}_{dq} = \frac{2}{\sqrt{3}} \cdot I_0 \cdot e^{j\left(\frac{\pi}{2} + \psi + \frac{\pi}{6} - \omega t'\right)} = j \cdot \frac{2}{\sqrt{3}} \cdot I_0 \cdot e^{j\left(\psi + \frac{\pi}{6} - \omega t'\right)} \quad (34)$$

Space phasors \underline{i}_{1dq} and \underline{i}_{dq} are geometrically represented in Figure 8, in the interval $0 \leq \omega t' < \frac{\pi}{3}$ (on the time duration

$0 \leq t < \frac{\pi}{3\omega} = \frac{\pi \cdot T}{3 \cdot 2\pi} = \frac{T}{6}$), meaning that exactly the duration $T/6$

between two successive commutations of the bridge.

Figure 8 emphasizes that during the time between two successive commutations $T/6$ the space phasor \underline{i}_{dq} rotates in opposite sense, with the angular speed $\omega = \omega t$, its extremity describing the arc between the points 1 and 2 corresponding to an angle at the centre of $\pi/3$ electrical radians.

Actually, at the moment $t'=0$, the phasor \underline{i}_{dq} starts from initial position 1 (corresponding to angle $\psi+30^\circ$) towards the final position 2 (corresponding to angle $\psi-30^\circ$), reached after $t'=T/6$. At each commutation of the bridge, the space phasor \underline{i}_{dq} instantly returns from position 2 to position 1, then the oscillation around the fixed phasor \underline{i}_{1dq} is repeated in an identical manner.

Accordingly, the electromagnetic torque M_I developed by the self-piloted synchronous motor will oscillate.

In order to evaluate the electromagnetic torque M_I , will first be established the effective values $I_d(t')$ and $I_q(t')$ of the orthogonal components of phasor \underline{i}_{dq} :

$$\underline{i}_{dq} = \sqrt{2} \cdot [I_d(t') + j \cdot I_q(t')] = j \cdot \frac{2}{\sqrt{3}} \cdot I_0 \cdot e^{j\left(\psi + \frac{\pi}{6} - \omega t'\right)} \quad (35)$$

then, by identifying follows immediately:

$$I_d(t') = -\sqrt{\frac{2}{3}} I_0 \sin\left(\psi + \frac{\pi}{6} - \omega t'\right) \quad (36)$$

$$I_q(t') = \sqrt{\frac{2}{3}} I_0 \cos\left(\psi + \frac{\pi}{6} - \omega t'\right)$$

If in expression (10) of the electromagnetic torque M there are performed the substitutions $I_d = I_d(t')$ and $I_q = I_q(t')$ specified by (36), and additionally there are used the substitutions (13), then the torque M_I will get the form:

$$M_I(t') = 3p \cdot \left[(K\Phi_{om}) \cdot \sqrt{\frac{2}{3}} I_0 \cos\left(\psi + \frac{\pi}{6} - \omega t'\right) - \frac{I_0^2}{3} (L_d - L_q) \sin 2\left(\psi + \frac{\pi}{6} - \omega t'\right) \right] \quad (37)$$

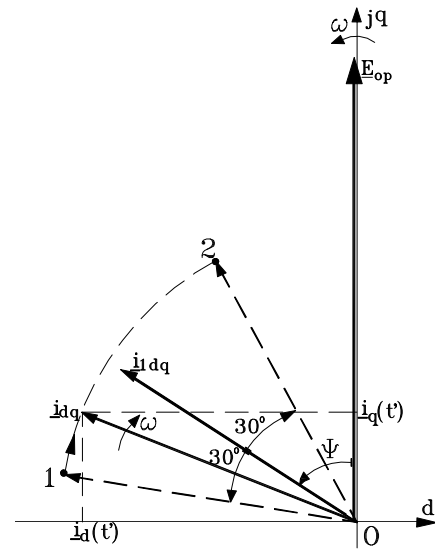


Fig.8. Oscillations of phasor \underline{i}_{dq} around \underline{i}_{1dq} in case of rectangular currents

This expression of the torque is valid on each interval $0 < \omega t' < \pi/3$ between two successive commutations of the bridge. Overall, the torque M_I results as irregular.

The non-uniformity of electromagnetic torque M_I is caused by the variation of the orthogonal components $I_d(t')$ and $I_q(t')$ accordingly to (36), this variation being determined by the oscillation of space phasor \underline{i}_{dq} around the fixed phasor \underline{i}_{1dq} . On each period T (of non-sinusoidal variation of currents) the electromagnetic torque M_I performs 6 pulsations of the type described by relationship (37).

In order to attenuate pulsations of electromagnetic torque one is searching for ways to limit the oscillation amplitude of phasor \underline{i}_{dq} (for instance between $\psi+15^\circ$ and $\psi-15^\circ$). For this goal, the stator winding of synchronous motor is divided in two distinct three-phase windings (spatially shifted with $\pi/6$ electrical radians), each being separately supplied from a current inverter. If the two inverters provide current pulses shifted from each other by $\pi/6$ electric radians, then it could be achieved a system with the pulsation index $q=2 \cdot 6=12$, consequently with a pulsation period of the electromagnetic torque equal to $T/12$. It results implicitly that the amplitude of torque pulsation will be less.

V. CONCLUSION

The sustainability dynamics in operation of electric railway vehicles has been addressed, highlighting the chain of interactions within the main electric equipment on an electrically driven railway system supplied from a d.c. or an a.c. contact line: the contact line-side converter, the machine-side converter and the traction synchronous motor.

The paper supports the findings that electric traction drive systems using synchronous motors fed by current inverters enhance the sustainable operation of railway trains. Electric traction drive systems using synchronous motors fed by current inverters provide high performance for high speed electric trains, in terms of both train dynamics and environmental issues, while advanced power current inverters ensure optimum traction and minimum energy use. Hence, the paper highlights that in order to synchronize the machine rotating field with the rotor (and avoiding the risk of losing the synchronism at any frequency value of stator currents) the synchronous motor will control the current inverter which is powering it, becoming this way a self-piloted synchronous motor. Actually, the position of direct axis of synchronous motor rotor will be evolutionary checked in time (through the position transducers) by 6-p times during each complete rotation (at any value of rotor speed), by the ignition control of the thyristor of the current inverter bridge that is supplying the motor.

The physical phenomena within the electric system composed by the contact line-side converter, the machine-side converter and the traction synchronous motor are complex and its overall behaviour suggests that cleaner production offers an appropriate framework for assessing the sustainability of an electric railway system. Hence, the paper emphasizes that at electrically driven railway systems with traction synchronous motors the functions of amplitude adjustment are completely separate from those of the frequency control. As sequel, the result is a simpler construction for both the power part and the control electronics of static converters.

REFERENCES

- [1] D.A. Nicola, M.A. Rosen, C.A. Bulucea, C. Brandusa, "Sustainable Energy Conversion in Electrically Driven Transportation Systems", *Proc. 6th WSEAS Int. Conf. on Engineering Education (EE'09)*, Rhodes, Greece, July 22-24, 2009, pp. 124-132.
- [2] D.A. Nicola, M.A. Rosen, C.A. Bulucea, C. Brandusa, "Some Sustainability Aspects of Energy Conversion in Urban Electric Trains", *Sustainability*, 2010, 2, 1389-1407.
- [3] C.A. Bulucea, D.A. Nicola, N.E. Mastorakis, M.A. Rosen, "Understanding Electric Industrial Ecosystems through Exergy", *Recent Researches in Energy and Environment: Proc. 6th IASME/WSEAS Int. Conf. on Energy and Environment*, Cambridge, UK, February 20-25, 2011, pp. 182-191.
- [4] D.A. Nicola, C.A. Bulucea, D.C. Cismaru, C. Brandusa, "Energy Saving in Electric Trains with Traction Induction Motors", *Proc. 4th IASME/WSEAS Int. Conf. on Energy & Environment*, Cambridge, UK, Feb. 24-26, 2009, pp. 226-232.
- [5] D.A. Nicola, M.A. Rosen, C.A. Bulucea, D.C. Cismaru, "Some Aspects of Sustainable Energy Conversion in Electric Railway Vehicles with Traction Induction Motors", *Recent Advances in Systems Science: Proc. 17th Int. Conf. on Systems*, Rhodes Island, Greece, July 16-19, 2013, pp. 44-53.
- [6] *INTRODUCTION TO CLEANER PRODUCTION (CP) CONCEPTS AND PRACTICE*, Prepared by the Institute of Environmental Engineering (APINI) Kaunas University of Technology, Lithuania, Sponsored by UNEP, Division of Technology, Industry, and Economics, Available at: <http://www.un.org/esa/sustdev/sdissues/technology/cleanerproduction.pdf>, accessed on 15 December, 2013.
- [7] United Nations, *The future we want*, United Nations Conference on Sustainable Development, Rio de Janeiro, Brazil, 20-22 June 2012, Available at: http://www.unep.fr/scp/pdf/Rio_The_Future_We_Want.pdf, accessed on 10 December, 2013.
- [8] D.A. Nicola, D.C. Cismaru, *Tractiune Electrica: Fenomene, Modele, Solutii (Electric Traction: Phenomena, Models, Solutions)*, SITECH Publishing House, Craiova, Romania, 2006.
- [9] D.C. Cismaru, D.A. Nicola, G. Manolea, *Locomotive electrice. Rame si trenuri electrice. Probleme specifice la viteze mari. Arhitectura electrice. Modele si scheme structurale. Control computerizat (Electric Locomotives. Electric Multiple Units and Electric Trains. Specific Problems at High Speed. Electrical Architecture. Models and Structural Diagrams. Computer Control)*, SITECH Publishing House, Craiova, Romania, 2009.
- [10] D.A. Nicola, *Tractiune electrica (Electric Traction)*, Universitaria Publishing House, Craiova, Romania, 2012.
- [11] R. Kaller, J.M. Allenbach, *Traction Electrique (Electrical Traction)*, Vol. 1-2, PPUR, Lausanne, 1995.
- [12] F. Perticaroli, *Sistemi elettrici per i trasporti: Trazione elettrica (Electrical Systems for Transportation: Electric Traction)*. Ed. Masson, Milano-Parigi-Barcellona, 1994.
- [13] A. Steimel, *Electric Traction. Motion Power and Energy Supply Basics and Practical Experience*, Oldenbourg Industrieverlag, München, 2008.
- [14] M. Georgescu, *Tractiunea electrică de mare viteză cu motoare sincrone (High Speed Electric Traction with Synchronous Motors)*, Publishing House Dacia, Cluj-Napoca, 2001.
- [15] J. Chatelain, *Machines électriques (Electrical Machines)*, PPUR, Lausanne, 1989.
- [16] U.A. Bakshi, M.V. Bakshi, *Electrical Drives and Controls*, Technical Publications Pune, First Edition, 2009, Available at: http://books.google.ro/books?id=RXRO2nTaDz4C&printsec=frontcover&dq=electrical++drives&hl=en&ei=-swoToC-AfCmsOK3kuGfCw&sa=X&oi=book_result&ct=result_esc=y#v=onepage&q&f=false, accessed on December 25, 2013.
- [17] H. Buhler, *Reglage de Systemes d'Electronique de Puissance*, Vol. I, PPUR, Lausanne, 1997.
- [18] M. Carpita, A. Monti, "Voltage Source Converters and Drives Simulation at System Level for Control Design Applications", *EPE Journal*, Vol. 5, No. 3/4, 1996, pp. 49-55.
- [19] N. Muntean, *Convertoare statice (Static Converters)*, Publishing House Politehnica, Timișoara, 1998.

Modelling of the unsteady flow-sediment interaction – grain size approach

Srdjan R. Kolakovic¹, Ljubomir M. Budinski², Goran B. Jeftenic³, Borislav T. Masic⁴, Slobodan S. Kolakovic⁵, Svetlana R. Vujovic⁶

Abstract- This paper presents a two-dimensional mathematical model of the unsteady flow-sediment interaction with sediment mixtures in natural watercourses, based on an enhanced MOBED2 modeling system. The hydrodynamic formulation is based on depth-averaged RANS equations. Bed and near-bed sediment processes are described using the active-layer and active-stratum approach, including bedload transport, bed-elevation changes, and the sediment exchange between the suspended material and the bed and near-bed material. This results in an essentially two-dimensional hydrodynamic formulation in the plane parallel to the bed's surface. Suspended-sediment transport is described by the depth-averaged form of the general three-dimensional advection-diffusion equation. The sediment mixture is represented through a suitable number of sediment size classes, and all sediment equations are re-formulated for sediment mixtures. Besides the modeling concept and associated numerical considerations, this paper presents the model's formulation, calibration and verification, based on two field-data sets collected at the Danube River experimental Bezdán-Moháč reach.

Keywords- 2-D unsteady flow-sediment interaction, modeling concepts, the Danube River Bezdán-Moháč field data, model's results

I. INTRODUCTION

In order to establish the set of the 1D, 2D and 3D mathematical models of water flow and sediment transport, during the period of 23 to 27 May 2011, corresponding measurements are carried out on the river Danube as part of an IPA project. For experimental river section, the location between city of Mohács on the Hungarian side, and the city of Bezdán on the Serbian side, is chosen. The flow measurements included bathymetry, velocity and discharge data, while the suspended sediment and bed material sampling were part of the sediment measurements.

Seven cross sections, distributed nearly evenly along the central part of selected river section (rkm 1438 ÷ rkm 1432), represents the measurements locations.

This work is supported by Ministry of Education and Science, Republic of Serbia (Grant No. TR 37003, TR 37018).

¹ PhD Srdjan R. Kolakovic, grad.civ.eng, Faculty of Technical Sciences, University of Novi Sad, Serbia, (e-mail: kolak@uns.ac.rs).

² PhD Ljubomir M. Budinski, grad.civ.eng, Faculty of Technical Sciences, University of Novi Sad, Serbia, (e-mail: ljubabu@gmail.com).

³ MsC Goran B. Jeftenic, grad.civ.eng, Faculty of Technical Sciences, University of Novi Sad, Serbia, (e-mail: goran.jeftenic@yahoo.com).

⁴ MsC Borislav T.Masic, grad.civ.eng, Faculty of Technical Sciences, University of Novi Sad, Serbia, (e-mail: boramasic@gmail.com).

⁵ MsC Slobodan S. Kolakovic, grad.civ.eng, Faculty of Technical Sciences, University of Novi Sad, Serbia, (e-mail: cole86grb@gmail.com).

⁶ MsC Svetlana R. Vujovic, grad.civ.eng, Faculty of Technical Sciences, University of Novi Sad, Serbia, (e-mail: svetlanavjvc@yahoo.com).

For flow discharge and velocity components the ADCP instrument in moving and stationary vessel is used, respectively. Utilizing the collected flow and sediment data, the 2-D mathematical model of water flow and sediment interaction, based on the depth-averaged equations transformed in to the curvilinear coordinate system using the non-orthogonal transformation, is applied. Numerical results are compared with corresponding field data. Analysis, which include velocity and free surface elevation comparison for the flow, and suspended sediment mixtures for the sediment data, shows very good agreement with the results obtained from the mathematical model.

II. MATHEMATICAL FORMULATION

A. Flow equations

The basic flow equations are the depth-averaged RANS equations, written herein in tensor notation:

The depth-averaged mass-conservation equation:

$$\frac{\partial h}{\partial t} + \frac{\partial (h \bar{u}_j)}{\partial x_j} = 0, \quad (1)$$

The depth-averaged momentum-conservation equations:

$$\begin{aligned} \frac{\partial \bar{u}_i}{\partial t} + \bar{u}_j \frac{\partial \bar{u}_i}{\partial x_j} = & -g \frac{\partial (Z_b + h)}{\partial x_i} + \frac{1}{\rho h} \frac{\partial}{\partial x_j} \left(\bar{\tau}_{ji} h \right) \\ & + \frac{\tau_{si} - \tau_{bi}}{\rho h} - \frac{1}{\rho h} \frac{\partial}{\partial x_j} \int \rho \left(u_j - \bar{u}_j \right) \left(u_i - \bar{u}_i \right) dz \quad i = 1, 2 \end{aligned} \quad (2)$$

where: t = time; $x_i = i$ - coordinate direction; $\bar{u}_i = i$ - direction component of the depth-averaged flow velocity; h is the flow depth; Z_b = the bed-surface elevation; ρ = the density of the water and suspended-sediment mixture; $\bar{\tau}_{ji} = i$ - direction component of the depth-averaged turbulent diffusion stress, and $\tau_{si}, \tau_{bi} = i$ -direction components of the free-surface and the bed shear stress, respectively.

The depth-averaged turbulent diffusion stress $\bar{\tau}_{ji}$ and the dispersion term τ_{ji}^{disp} are further expressed as $\bar{\tau}_{ji} + \tau_{ji}^{disp} = (\bar{v}_i + v^{disp}) \left(\partial \bar{u}_i / \partial x_j + \partial \bar{u}_j / \partial x_i \right)$, where \bar{v}_i

represents the Boussinesq eddy-viscosity coefficient (evaluated by using an appropriate turbulence model), and ν^{disp} represents the dispersion coefficient (evaluated by using the dispersion theory). The wind-shear stress at the water surface was neglected, since it has far less influence over the sediment processes than the bed shear stress. The bed-shear stress was expressed in the traditional manner: $\tau_{bi} = C_f \rho \tilde{u}_i \sqrt{\tilde{u}_1^2 + \tilde{u}_2^2}$, where C_f is the friction coefficient. More details can be found in Spasojevic and Holly (1990a, 1990b, 2007).

B. Sediment equations

As shown in Figure 1, the otherwise single and continuous domain of sediment-processes is divided herein into three subdomains: the suspended-sediment subdomain, the active-layer sediment subdomain, and the subsurface sediment subdomain (divided into so-called active stratum and other strata below). Governing sediment equations are then defined for each subdomain, including sediment exchange mechanisms between them. The sediment mixture is represented though a suitable number of sediment size classes $ks = 1, \dots, KS$, where KS represents the total number of size classes, allowing for the definition of, wherever appropriate, the governing-equations' terms as size-class specific.

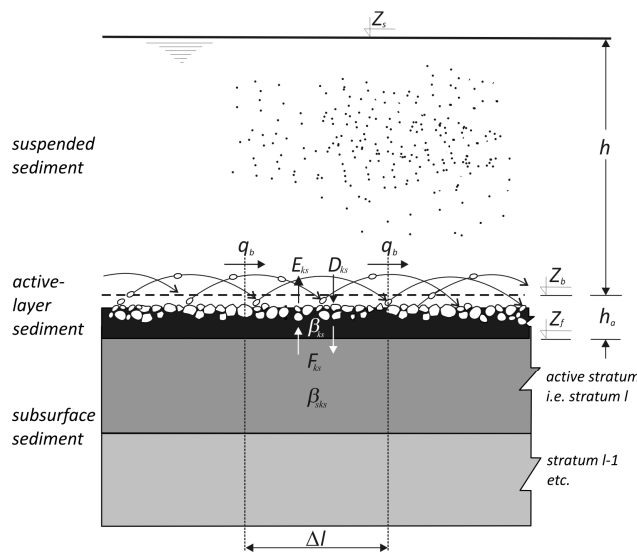


Figure 1. The Definition Sketch for Sediment Subdomains

C. Suspended solids

The governing equation for suspended sediment processes is obtained by depth-averaging the three-dimensional mass-conservation equation, written for size class ks of sediment particles. Then, the depth-averaged suspended-sediment mass-conservation equation, written for sediment size class ks , reads:

$$\frac{\partial \tilde{c}_{ks}}{\partial t} + \tilde{u}_j \frac{\partial \tilde{c}_{ks}}{\partial x_j} = -\frac{1}{h} \frac{\partial}{\partial x_j} (\tilde{q}_{jks} h) - \frac{1}{h} \frac{\partial}{\partial x_j} \int_h (c_{ks} - \tilde{c}_{ks}) (u_j - \tilde{u}_j) dz + \frac{E_{ks} - D_{ks}}{h}, \quad (3)$$

where: \tilde{c}_{ks} = depth-averaged volumetric concentration of the size class ks particles; \tilde{q}_{jks} - the depth-averaged suspended-sediment turbulent mass diffusion flux of the size class ks particles. The depth-averaged turbulent mass diffusion flux \tilde{q}_{jks} and the mass-dispersion term q_{sksj}^{disp} are expressed as $\tilde{q}_{sksj} + q_{sksj}^{disp} = (\epsilon_s + \epsilon^{disp}) \partial \tilde{c}_{ks} / \partial x_j$, where ϵ_s represents sediment mass-diffusivity coefficient and ϵ^{disp} represents the sediment mass dispersion coefficient.

D. Active layer sediment and subsurface sediment

Governing equations for bed and near-bed processes are based on the active-layer and active-stratum approach, used in conjunction with a modeling concept designed for the treatment of sediment mixtures, as introduced by Spasojevic and Holly (1990a, 1990b). Additional details can be found in Spasojevic and Holly (2007). The active layer (Figure 1) is assumed to comprise sediment moving as a bedload, as well as bed-surface and immediate subsurface sediment already agitated and ready to be set into motion.

The mass-conservation equation for size class ks of sediment in the active-layer control volume ΔV is written as follows:

$$\rho_s (1 - p_b) \frac{\partial (\beta_{ks} h_a)}{\partial t} + \frac{\partial q_{bksj}}{\partial x_j} + E_{ks} - D_{ks} - F_{ks} = 0, \quad (4)$$

where: β_{ks} = active-layer fraction of the size class ks , defined as a ratio of the mass of particles of the size class ks inside the active-layer control volume ΔV to the mass of all sediment particles contained in ΔV ; and q_{bksj} = the bedload flux component for the size class ks . As Figure 1 indicates, the only bedload particles changing the mass balance inside the active-layer control volume are the ones entering and leaving the volume. Other bedload particles start and end their trajectories inside the same active-layer control volume, remaining within the volume and not changing the mass balance within it. In order to enable use of a conventional bed-material porosity p_b , the active-layer thickness h_a in Eq. (4) is defined assuming that such bedload particles are positioned at the bed surface. Terms E_{ks} and D_{ks} represent an upward sediment entrainment flux and a downward sediment deposition flux, both for the size class ks , respectively, and correspond to the same terms in Eq. (3), but with the opposite signs. The entrainment and deposition fluxes are evaluated at some distance above the bed surface, and that location is

considered to be the bed or near-bed boundary of the suspended sediment subdomain. The term F_{ks} , called herein the active-layer floor source and again specific to the size class ks , represents the exchange of sediment particles between the active-layer and the active-stratum control volumes due to active-layer floor movement. The active-layer floor, which is at the same time an active-stratum ceiling, descends or rises whenever the bed elevation changes due to deposition or erosion occurring in the active-layer control volume.

The mass of a particular size class in the active-stratum control volume may change only due to active-layer floor movement, i.e. due to exchange of material between the active layer and active stratum, while the active-stratum floor elevation remains unchanged. This is expressed by a mass-conservation equation written for the size class ks in the active-stratum control volume:

$$\rho_s (1 - p_b) \frac{\partial}{\partial t} [\beta_{ks} (Z_b - h_a)] + F_{ks} = 0, \quad (5)$$

where: β_{ks} = active-stratum fraction of the size class ks ; and $(Z_b - h_a)$ = active-layer floor elevation, i.e. active-stratum ceiling.

Summation of Eqs. (4) for all size classes in the active-layer control volume and use of the basic constraint:

$$\sum_{ks=1}^{KS} \beta_{ks} = 1, \quad (6)$$

leads to the global mass-conservation equation for the active-layer control volume. A similar global mass-conservation equation (again invoking Eq. (6)) can be obtained for the active-stratum control volume. Summation of global mass-conservation equations for active-layer control volume and for active-stratum control volume gives the global mass-conservation equation for bed sediment:

$$\rho_s (1 - p_b) \frac{\partial Z_b}{\partial t} + \sum_{ks=1}^{KS} \left(\frac{\partial q_{bksj}}{\partial x_j} + E_{ks} - D_{ks} \right) = 0. \quad (7)$$

All active-layer sediment and subsurface sediment equations are essentially two-dimensional in the plane parallel to the bed surface.

E. Sediment exchange mechanisms

Sediment exchange between suspended sediment and active-layer sediment is defined by sediment entrainment E_{ks} and deposition D_{ks} terms in Eqs. (3), (4), and (7). Sediment exchange between active-layer and subsurface (active stratum) sediment is defined by the active-layer source term F_{ks} in Eq. (4).

Based on Eq. (3), the upward active-layer sediment entrainment (resuspension) flux E_{ks} and the downward suspended sediment deposition flux D_{ks} are modeled herein as a near-bed upward turbulent mass-diffusion flux, and a near-bed downward fall-velocity flux (Spasojevic and Holly, 1993):

$$E_{ks} = -\beta_{ks} \epsilon_s \frac{(c_{ks})_{a+\Delta a} - (c_{ks})_a}{\Delta a}, \quad (8)$$

and:

$$D_{ks} = w_{fks} (c_{ks})_{a+\Delta a}, \quad (9)$$

where $[(c_{ks})_{a+\Delta a} - (c_{ks})_a] / \Delta a$ represents the near-bed non-equilibrium concentration gradient, subscript 'a' denotes that the mass-diffusion flux (i.e. the near-bed concentration gradient) is evaluated at a near-bed point some distance a above the bed, β_{ks} reflects the availability of the size class ks in the active-layer control volume, $(c_{ks})_a$ is a near-bed active-layer sediment concentration, while $(c_{ks})_{a+\Delta a}$ represents a near-bed non-equilibrium concentration at distance $a + \Delta a$ above the bed surface, extrapolated from the suspended-sediment computations, and w_{fks} represents the particle fall velocity for the specific size class.

Following Spasojevic and Holly (1990a, 1990b), the active-layer source term F_{ks} is expressed by using Eq. (5). When the active-layer floor (active-stratum ceiling) descends, then:

$$F_{ks} = -\rho_s (1 - p_b) \frac{\partial}{\partial t} [\beta_{ks} (Z_b - h_a)],$$

gives the mass of the size class ks , formerly comprising size fraction β_{ks} of the active-stratum control volume, which becomes part of the active-layer elemental volume. When the active-layer floor (active-stratum ceiling) rises, then:

$$F_{ks} = -\rho_s (1 - p_b) \frac{\partial}{\partial t} [\beta_{ks} (Z_b - h_a)].$$

gives the mass of the particular size class, formerly comprising size fraction β_{ks} of the active-layer elemental volume, which becomes part of the active stratum control volume.

III. NUMERICAL SOLUTION

The governing flow equations, i.e. Eqs. (1) and (2), as well as the governing sediment equations, i.e. Eqs. (3), (4),

and (7), are transformed from Cartesian into general non-orthogonal curvilinear coordinates, following the rules of complete coordinate transformations.

A. Numerical solution approach

The flow equations, i.e. the continuity equation and two momentum-conservation equations, are solved in three consecutive steps (performed during each computational time step): advection, diffusion, and propagation. The hyperbolic-type flow advection-step equations describe the change of local acceleration components due to the sole action of advection terms in momentum-conservation equations. The elliptic-type flow diffusion-step equations describe the change of local acceleration components due to the action of diffusion terms in momentum-conservation equations, added to the action of advection terms. The flow propagation step combines the continuity equation and the propagation parts of momentum-conservation equations. The propagation parts of the momentum-conservation equations describe the change of local acceleration components due to the action of propagation terms (gravity and pressure) and the bed-shear stress term, added to the action of advection and diffusion terms. Once the depth is computed, propagation parts of the momentum equations yield the final local „advection-diffusion-propagation“ acceleration.

The size-class specific mass-conservation equation for suspended sediment is solved in two consecutive steps (again, performed during each computational time step): advection-source step and diffusion step. The hyperbolic-type, suspended-sediment, advection-source step equation describes the local change of the suspended-sediment concentration due to the action of advection terms and the entrainment-deposition terms. The elliptic-type suspended-sediment diffusion step equation describes the local change of suspended-sediment concentration due to the action of diffusion, added to the action of advection-source terms.

The numerical solution of hyperbolic-type equations is prone to numerical problems, such as numerical diffusion, oscillations or instability. To avoid (or minimize) these problems, the flow advection-step equations and the suspended-sediment advection-source step equation are solved by using a characteristics (trajectory) method with higher-order spatial interpolations (Hermite bicubic interpolation (Holly and Preissmann, 1977) for the sediment computations, and quadratic upstream interpolation (Leonard 1979, as described by Ferziger and Peric 2002) for the flow computations. The elliptic-type, flow, diffusion-step equations, the depth (or depth-increment) equation, and the suspended-sediment, diffusion-step equations are solved by using the implicit finite-difference scheme and ADI solution procedure, yielding a satisfactory and unconditionally stable numerical solution.

Due to the slow nature of the bedload movement, mass-conservation equations for the active-layer sediment (i.e. Eqs. (4)), and the global mass-conservation equation for the bed sediment (i.e. Eq. (7)), are discretized by integrating

them over the time step and control volume, i.e. using an upwind-like scheme for bedload flux derivatives.

B. Numerical coupling considerations

To satisfy the basic constraint (Eq. 6), all bed and near-bed sediment equations (i.e. Eqs. (4) and (7)), containing KS unknown active-layer size fractions β_{ks} and one unknown bed-surface level Z_b , are, for the same control volume, solved simultaneously by using the Newton-Raphson iterative procedure. More details can be found in Spasojevic and Holly (1990a, 1990b).

The bed and near-bed processes and suspended-sediment processes are strongly coupled through the sediment-exchange terms. Thus, numerical coupling for sediment computations is achieved through an iterative solution algorithm, with several iterations within each time step.

The sediment-processes feedback to the flow is modeled herein through changes in: bed elevations, the flow and the suspended-sediment mixture density (due to changes in suspended-sediment concentrations), and the bed friction coefficient (due to changes in bed surface size-fraction distribution). Since the sediment feedback has relatively minor effects during a single computational time step, the iterative coupling between the flow and sediment processes is typically restricted to a single iteration.

IV. ADCP, SEDIMENT AND BATHYMETRY DATA PROCESSING TO FIT MODELS NEEDS

In order to incorporate field measurements into to the mathematical model in sense of calibration and verification, collected raw data are therefore processed and used in adequate form. Bathymetry measurements, which are taken along the experimental river section on cross sections that are about 100.0 m apart, are handled using the GIS software and presented on the Figure 2a, while the selected region, provided for the detailed flow and sediment measurements, are presented on the Figure 2b. As can be seen from the Figure 2b, seven ranges are placed approximately at the distance of 950.0 m from each other, containing the seven measuring verticals, nearly evenly distributed along the cross section.

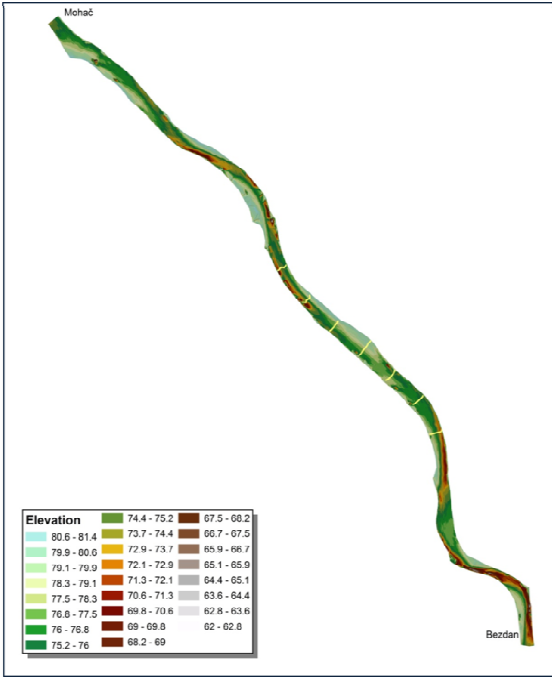


Figure 2a. Bathymetry of experimental section of the Danube river

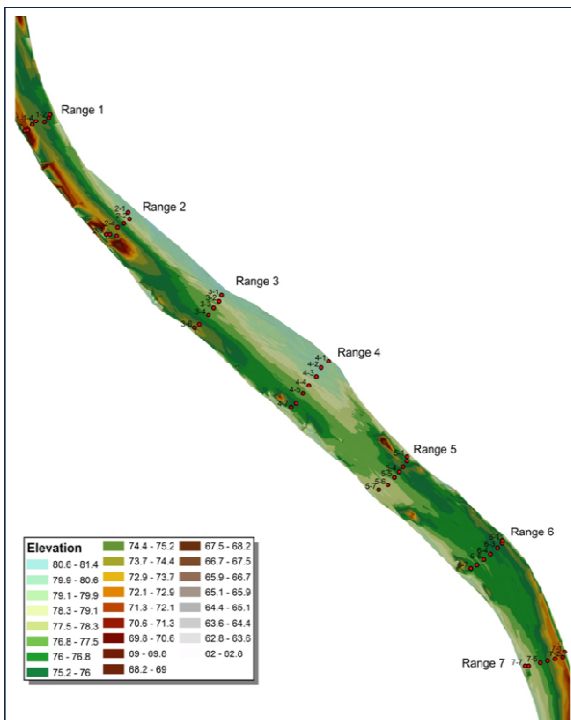


Figure 2b. Locations of measuring ranges and verticals

A. Flow measurements

As was indicated before, flow measurements included velocity components and flow discharge. For this part of measurements, the standard Acoustic Doppler Current Profiler (ADCP) is used. Having in mind that during the measuring period a possible flow variation may occur, the discharge is therefore measured in every range. Using the four time passing technique, which actually means that in

order to achieve better assessment of the volumetric flow rate, minimum 4 vessel passing is required, the discharge data are collected and then averaged applying the arithmetic mean. The results of this analysis are shown on the Table 1. Enforcing the same criteria regarding the accuracy of measuring methods, for velocity sampling the different approach is adopted. In order to eliminate all the negative influences during the acquiring period, like small and large scale turbulence, the stationary vessel with the minimum 10.0 min of sampling in every vertical is used. Applying the post-processing approach, for which the adequate ADCP software is used, acquired velocity data are then averaged along the each of the measuring verticals. As a result the time averaged velocity components, which include three Cartesian velocity components u (U_{east}), v (U_{north}) and w (U_{vert}), are obtained. As an example, vertical 6 is presented on the Figure 3.

Table 1. Discharge measurements

RANGE	PASS	DISCHARGE (m ³ /s)	Time		Average time	Average discharge by range (m ³ /s)	Average discharge (m ³ /s)
			h/min/sec				
1.00	0	1636.80	23.05.2011.	14:20:00	14:29:00	1647.90	1602.11
	1	1657.04		14:25:00			
	2	1649.87		14:30:00			
	3	1647.80		14:41:00			
2.00	0	1596.03	24.05.2011.	09:00:00	09:08:00	1601.07	
	1	1599.78		09:05:00			
	2	1596.04		09:11:00			
	3	1611.82		09:16:00			
3.00	0	1640.05	24.05.2011.	12:28:00	13:07:00	1650.46	
	1	1644.30		13:04:00			
	2	1656.02		13:10:00			
	3	1661.47		13:16:00			
4.00	0	1619.06	24.05.2011.	15:32:00	15:43:00	1619.47	
	1	1629.80		15:39:00			
	2	1631.07		15:47:00			
	3	1630.07		15:54:00			
5.00	0	1613.53	25.05.2011.	08:30:00	08:38:15	1605.93	
	1	1625.86		08:35:00			
	2	1625.72		08:41:00			
	3	1588.64		08:47:00			
6.00	0	1554.20	27.05.2011.	09:41:00	09:51:45	1591.02	
	1	1544.86		09:48:00			
	2	1563.95		09:56:00			
	3	1536.99		10:02:00			
7.00	0	1590.82	27.05.2011.	13:05:00	13:16:00	1539.92	
	1	1546.98		13:14:00			
	2	1534.82		13:20:00			
	3	1537.24		13:25:00			

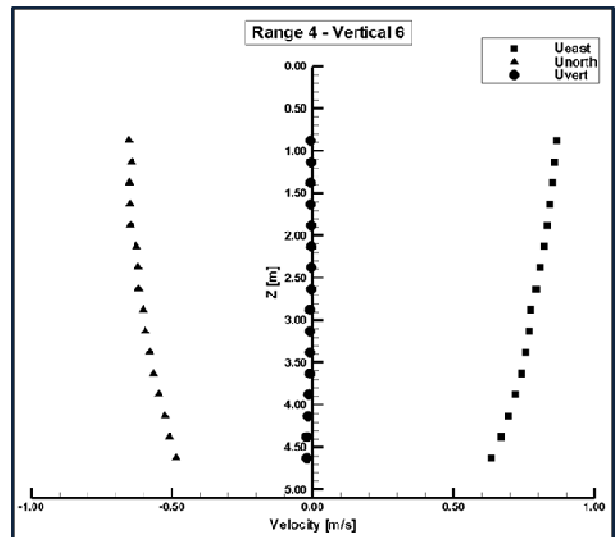


Figure 3. Velocity measurements – Vertical 6- Range 4

B. Sediment measurements

In contrast to the flow, sediment measurements are conducted only in 5 medium verticals along each range. The suspended sediment is collected in 5 levels, uniformly

spaced across the depth, while the bed material is sampled only at the bottom of measuring verticals. For both sediments the adequate sampler is used. To incorporate sediment data in previously described mathematical model, which is based on the sediment mixtures and interaction between water, suspend sediment and bed material, the acquired material is analyzed using the grain size approach. The results of that analysis for suspended sediment concentration are presented in Table 2 and Figure 4 (Range 4), while for the bed material they are shown on Table 3 and Figure 5 (Range 4).

Table 2. Grain size – suspended sediment

<i>suspended material sieve diameters (mm)</i>	<i>average size class grain diameter (mm)</i>
0.50	0.3535
0.25	0.1768
0.125	0.1118
0.10	0.0707
0.05	0.0316
0.02	0.0141
0.01	0.0070
0.005	0.0022
0.001	

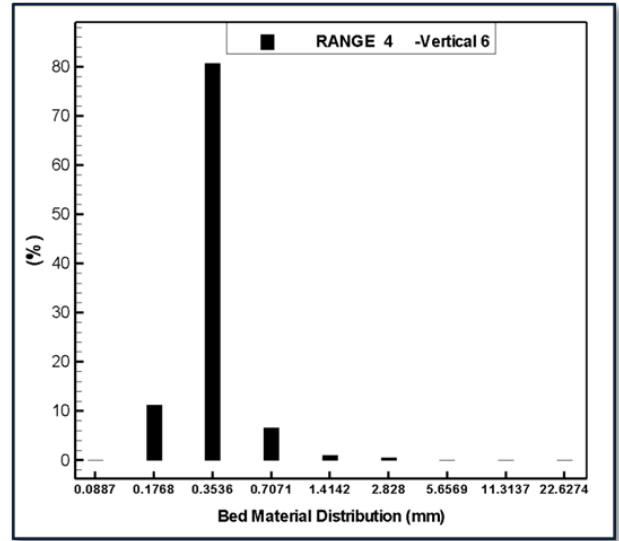


Figure 5. Bed material – Range 4

Table 2. Grain size – bed sediment

<i>bed material sieve diameters (mm)</i>	<i>average size class grain diameter (mm)</i>
32	22.6274
16	11.3137
8	5.6568
4	2.8284
2	1.4142
1	0.7071
0.5	0.3535
0.25	0.1768
0.125	0.0887
0.063	

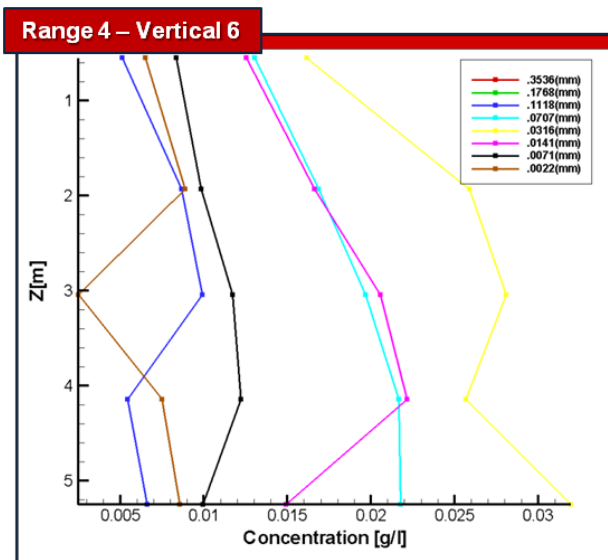


Figure 4. Suspended sediment – Range 4

V. CALIBRATION AND VALIDATION OF THE MODEL

Since the 2-D mathematical model of unsteady flow-sediment interaction with sediment mixtures was applied to the selected domain between the first and the seventh range (Figure 2b), as a first step numerical (computational) mesh is created. For this purpose three possible configurations of the computational mesh have been done, with cell dimension of 10x10 m, 10x20 m and 20x20 m in x and y direction, respectively. As a final configuration, the grid with cell dimension of 20x20 m has been chosen.

The hydrograph has been applied as an upstream boundary condition (Figure 6) and a water level graph as a downstream boundary condition (Figure 7b). For the flow simulation the following parameters are set : $\Delta t=50$ s, $\bar{v}_t = 0.00015 \text{ m}^2 \text{ s}^{-1}$, $n = 0.019 \text{ m}^{-1/3} \text{ s}$. As initial conditions, horizontal free surface level and zero velocity components are adopted.

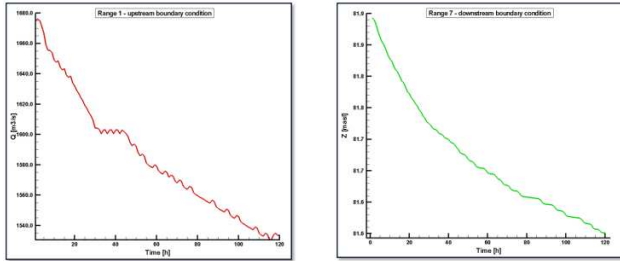


Figure 6. Hydrograph (the upstream boundary condition) and water level graph (the downstream boundary condition)

In the same manner, the sediment part of the model also requires definition of boundary and initial conditions. Specifying the upstream boundary condition in form of a depth averaged concentration for each size class (Table 2) of the suspended sediment is required, while the initial condition for both sediments (suspended sediment and bed material) includes averaged concentration/fraction of the size class k_s for each size class along the entire section. The simulation period of 5 days is adopted. Comparison of numerical results with the corresponding field data regarding the velocity computation, suspended sediment concentration and fraction of the size class k_s , which have been processed to fit the 2-D model (depth averaged), are presented in Figures 7, 8 and 9.

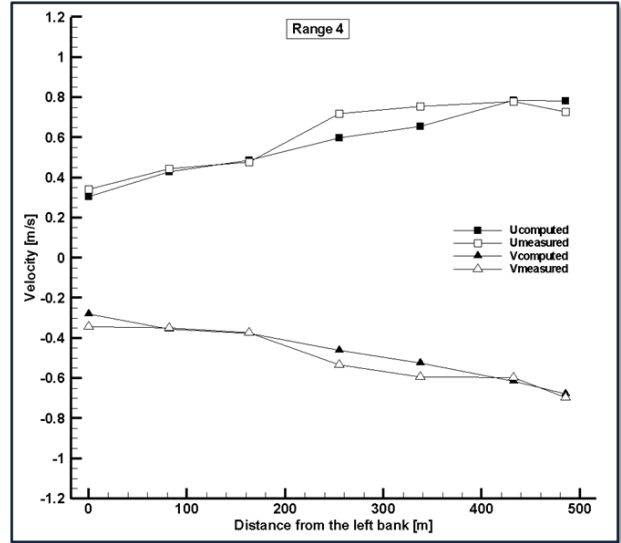


Figure 7b. Measured and computed depth-averaged velocity – Range 4

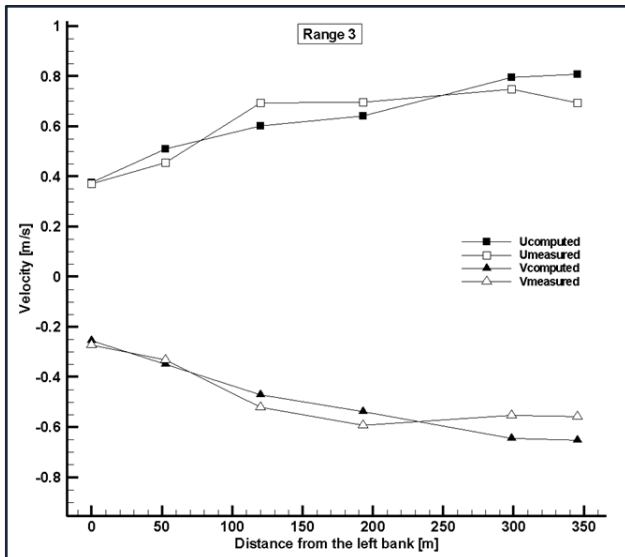


Figure 7a. Measured and computed depth-averaged velocity – Range 3

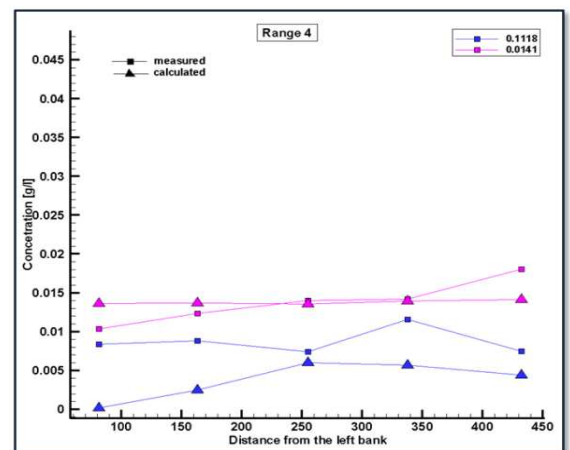
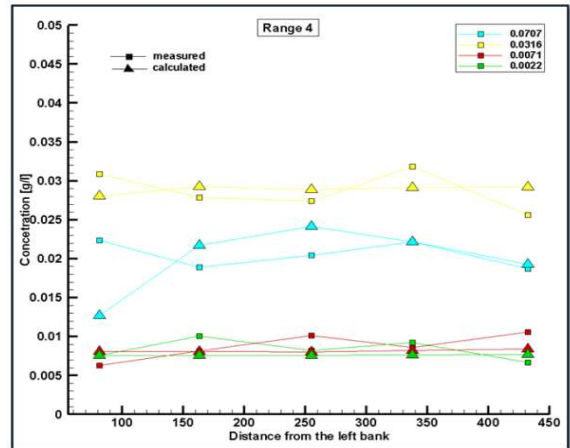


Figure 8a. Measured and computed concentration – Range 4

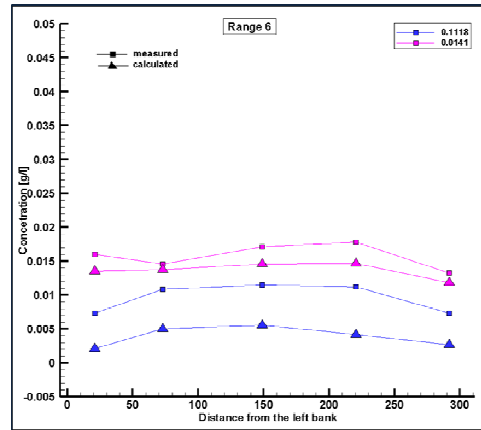
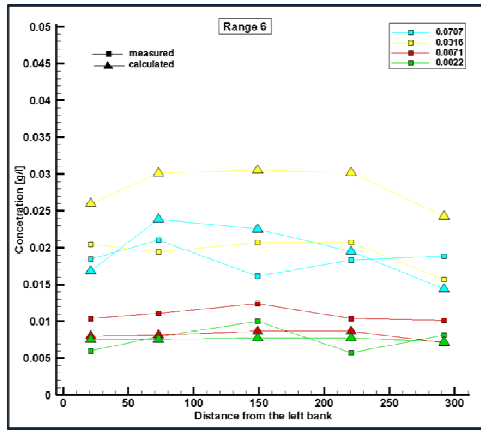


Figure 8b. Measured and computed concentration – Range 6

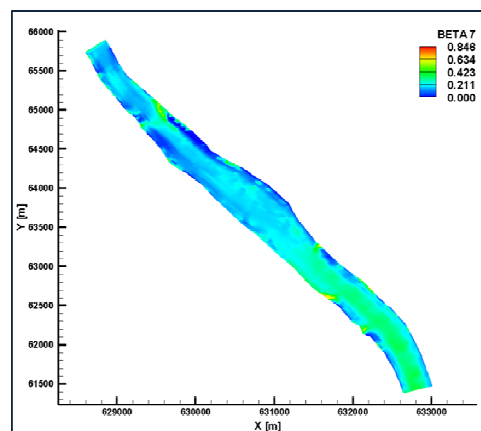
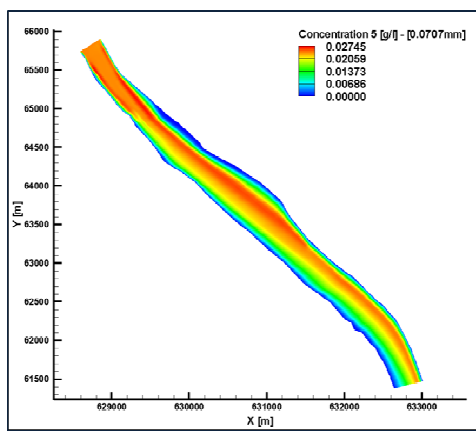


Figure 9. Computed concentration and fraction of the size class 5 and 7, respectively - plane view

VI. CONCLUSION

The presented paper addresses the calibration of 2-D mathematical model of unsteady flow-sediment interaction with sediment mixtures. For this purpose adequate field measurements of flow, suspended sediment and bed material on the river Danube have been used. Obtained field data are processed to fit models needs.

REFERENCES

This work is supported by Ministry of Education and Science, Republic of Serbia (Grant No. TR 37003, TR 37018).

REFERENCES

[1] Benqué, J.P., Cunge, J. A., Feuillet, A., Haguel, A., and Holly, F. M. Jr., (1982), "New Method for Computation of Tidal Currents," *Journal of the Waterways and Harbors Division, ASCE*, Vol. 108, No. WW3, Aug., pp. 396-417.
 [2] Benqué, J.P., Hauguel, A., and Viollet, P. L., (1983), "Numerical models in environmental fluid mechanics," *Engineering applications of computational hydraulics*, Vol. 2, Pitman Publishing Inc.
 [3] Duan, J.G., and Nanda, S.K., (2005), "Two-dimensional depth-averaged model simulation of suspended sediment concentration

distribution in a groyne field," *Journal of Hydrology* 327, pp. 426–437.
 [4] Ferziger, J.H. and Peric, M., (2002), *Computational Methods for Fluid Dynamics*, 3rd Edition, Springer, New York.
 [5] Holly, F. M., and Preissmann, A., (1977), "Accurate calculation of transport in two dimensions," *J. Hydr. Div., ASCE*, 103(11).
 [6] Leonard, B.P., (1979), "A Stable and Accurate Convective Modelling Procedure Based on Quadratic Upstream Interpolation", *Computer Methods in Applied Mechanics and Engineering*, Vol. 19, pp. 59-98.
 [7] Spasojević, M. and Holly, F.M. Jr., (1990a), "2-D bed evolution in natural watercourses - New simulation approach", *Journal of Waterway, Port, Coastal, and Ocean Engineering*, ASCE, Vol. 116, No. 4, July/August, pp. 425-443.
 [8] Spasojević, M. and Holly, F.M. Jr., (1990b), "MOBED2 - Numerical simulation of two-dimensional mobile-bed processes", *Iowa Institute of Hydraulic Research Technical Report No. 344*, The University of Iowa, Iowa City, Iowa, October.
 [9] Spasojević, M., Holly, F.M., (2007), "Two- and Three-Dimensional Numerical Simulation of Mobile-Bed Hydrodynamics and Sedimentation," Chapter 15 in *Sedimentation Engineering: Theories, Measurements, Modeling, and Practice*, ASCE Manuals and Reports of Engineering Practice No. 110, Garcia, M., ed, American Society of Civil Engineers.

Simulation Methodology with Control Approach for Water Distribution Networks

Diego Ricardo Diaz Vela, *Research Group, Aplicabilidad Tecnologica, Manuela Beltran University*

Abstract—This work presents and tests a simulation methodology for water distribution networks, developed as a simulation platform for dynamic pressure control purposes. The three model integration presented by Diaz y Quijano in 2012 is extended here as a general methodology including the Extended Period Simulation Global Gradient Algorithm proposed by Todini in 2000, the dynamic Pressure Reducing Valves model presented by Ulaniki in 1999 and the Stochastic Demand Model presented by Garcia in 1999. All these models are properly described and included in a general algorithm that solves all node pressure signals and pipe flow signals in a water distribution network under a dynamic scenario. This methodology is qualitatively tested in a simplified two variable tank network presented by Todini in 2000, showing satisfactory results.

Keywords—Distribution, EPS.GGA, Modeling, Network, Simulation, Water.

I. INTRODUCTION

WATER volume losses in Water Distribution Networks (WDN) represent a serious problem for provider companies. In some cases they could be near to 65% [1], [2]. The main cause of these losses is leakage in pipes, which is a pressure dependent variable. A strategy to reduce leakage in the WDN is to regulate pressure over the entire network using a control system [3]. This system has to maintain a certain pressure level for each node in the network under all the operation conditions (variable demand, disturbances, etc).

There are different approaches for the control problem in WDN. Most of them includes optimal control techniques such as: [4] who use the WATERNET solver, [5] who solve the system using Linear Theory Method (LTM) based on loop equations, [1] who assume steady state conditions, [6] that bases its formulation on LTM, [7] who use non-linear programming and LTM and [8] who support the solution of its model in EPANET. Other approaches consider hierarchical control [9], [10], robust control [11] that considers hydraulic models with non linear coupling, adaptive control [12] which includes modeling by identification, population dynamics based control [13], [14] and real-time control for wastewater systems [15].

Despite all these approaches contribute to the WDN control problem, many of them assume static conditions in their solvers (without dynamics) and present different tests with a maximum resolution of 1 hour. In order to develop a pressure control technique that considers the dynamics of the network in high resolution (in terms of seconds) it is necessary first

to proposed a preliminary stage where the WDN can be modeled and properly simulated (focus of this paper). Taking into account these items, it is important to have a simulation system capable of:

- 1) Dynamically¹ modelling the changes in the network.
- 2) Considering valves as time-varying actuators (not as static devices)².
- 3) Managing a great quantity of variables.

There are various software that provide a simulation platform for WDN like EPANET [16], [17], WaterGems [18] and MIKE [19]. All of them are based in the Global Gradient Algorithm (GGA) [20] to solve the hydraulic model. Despite this is a powerful algorithm, it decouples the steady-state analysis from the mass balance analysis at fixed times. This feature limits the application of the algorithm to networks with none variable storage devices (otherwise the system can reach a unsteady solution [20]). On the other hand, the valves included in many of these software are considered as static parameters, not as devices with variable setting (typically, valves are the actuators of pressure control systems, and have to be considered as variable devices).

In order to reduce the water volume losses in a WDN using pressure control systems, none of the simulation software presented above seems appropriate. In a water distribution network, the presence of variable storage devices induces considerable dynamical changes that the controller has to take into account to accomplish the control goal. Also, it is required the time-varying manipulation of valves parameters.

As the controller has to be designed and evaluated first in simulation, it is necessary the implementation of a specific control oriented WDN simulation methodology that includes variable tanks. In this paper, such simulation methodology is presented based on the integration of three different models: The Extended Period Simulation Global Gradient Algorithm (EPS-GGA) [20], the pressure reducing valve model developed by [3] and the stochastic network user demand model proposed by [21]. The integration of these three models and its extension to a general methodology are based on [22] where a specific two loops network with no variable storage devices was modeled with control purposes.

The remainder of this paper is organized as follows. Section II; Water Distribution Model, section III; Dynamic WDN Simulation Algorithm, section IV; Results and Discussion:

¹Here dynamical makes reference to changes caused by variations in demand and water storage. It is not consider instantaneous changes as the water-hammer phenomena.

²For pressure control purposes the valves in the system are consider actuators.

D. Diaz is with the Research Group Aplicabilidad Tecnologica, Manuela Beltran University, Bogota, Colombia e-mail: ricardo.diaz@docentes.umb.edu.co.

Manuscript received May 19, 2014; revised June.

Simulation Methodology Test, section V; Conclusion and section VI; Future Work.

II. METHODS: WATER DISTRIBUTION MODEL

The main purpose of a WDN is to deliver drinkable water from one or several main reservoirs to the final users who can be spread over different rural and urban area. Usually the reservoirs are located in high places and distribute water by gravity to the users located in lower areas. The water is distributed using a pipe network where each node is considered as a demand point that aggregates the user's demand near to it.

During distribution, water loses energy mainly because friction within the internal walls of the pipes and also loses mass caused by leakage. The energy loss can be interpreted as a pressure loss which is proportional to the flow in the pipe. Hence, the higher the nodal demands are, the higher flow and pressure losses in the pipes are.

The WDN considered here includes reservoirs (fixed storage devices), tanks (variable storage devices), pipes and pressure reducing valves³ (PRV). The simple nodes are considered as demand nodes that follow certain pattern according to the location and the activity developed for the population in the area.

The following subsections, the WDN model is described, followed by the valve type and model, and the nodal demand model. Finally all these models are integrated into a complete WDN model.

A. Water Distribution Network Model

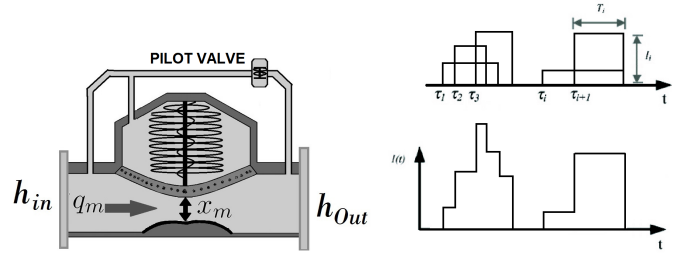
In order to model the dynamical behavior of the WDN, two main equations are used: energy balance and mass balance [20]. The energy balance equation defines the energy losses inside a pipe as pressure losses. The mass balance equation models the volume of water storage at each node depending on the inflow and outflow. Each equation is presented as follows:

1) *Energy Balance Equation*: The balance of energy in a WDN is associated to the pressure difference between two connected nodes. This connection is made by an ij pipe, where the flow inside is directed from node j to node i . The transported water loses energy mainly because friction within the internal walls of the pipe. The higher the flow the higher the pressure loss. According to [20] this pressure loss inside the pipe can be expressed as the pressure difference between ij nodes, as follows:

$$\frac{\partial H_{ij}}{\partial x} = \Delta H_{ij} = H_i - H_j = -K_{ij}|Q_{ij}|^{np-1}Q_{ij} \quad (1)$$

where ΔH_{ij} corresponds to the pressure difference between nodes i and j , Q_{ij} identifies the flow of the ij pipe, K_{ij} is the resistant coefficient of the ij pipe, and np is the flow exponent. The parameters K_{ij} and np depend on the equation

³This type of valve loses certain quantity of pressure according to a pilot screw reference. This characteristic is useful for the pressure control purposes wanted here.



(a) Scheme of a Pressure Reducing Valve (PRV). Sagittal cut. (b) Stochastic Demand Scheme.

Fig. 2. WDN subsystems.

selected to describe the friction inside the pipe. In [20], the empiric Hazen-Williams equation was used, but here the physics based Darcy-Weisbach equation is selected. This last equation depends only on physics parameters of pipes and water [23]. The calculation of the K_{ij} parameter is described in appendix A.

2) *Mass Balance Equation*: The second differential equation used to model the WDN corresponds to the mass balance [20]. This equation expresses the rate of storage water volume in a tank during a period, as the difference between inflow and outflow. It is defined as follows,

$$\frac{\partial V_i}{\partial t} = \sum_k^{ni} Q_{ik} + q_i \quad (2)$$

In this equation i represents the node where the tank is connected and k refers all other nodes connected to the tank node i . V_i corresponds to the volume of water storage in the tank, Q_{ik} represents the flow⁴ in the pipe that connects nodes i and k . The parameter ni is the number of nodes connected to the tank node i . Finally q_i corresponds to the flow demand in the node tank. Here, demand is a flow that leaves the node, then it is considered negative.

According to [20] the change in volume of Equation (2) can be expressed as a function of the transversal area of the tank and the change in high (denoted as $\Omega_i(H_i)$). Then Eq. 2 can be rewritten as follows:

$$\Omega_i(H_i) \frac{\partial H_i}{\partial t} = \sum_k^{ni} Q_{ik} + q_i \quad (3)$$

This last equation is particularly useful for modeling a consumption node⁵ or cylindrical tanks. For the first case it is only necessary to assume $\Omega_i = 0$. In the second case the Ω_i function is constant equal to the transversal area A_T .

B. Valve Model

A complete WDN model includes different kinds of components such as valves, pumps, etc. The simulation methodology presented here is intended to be used in a pressure control

⁴Flow that leaves the node is considered negative while flow that arrives to the node is considered positive.

⁵Consumption node is a node without tank.

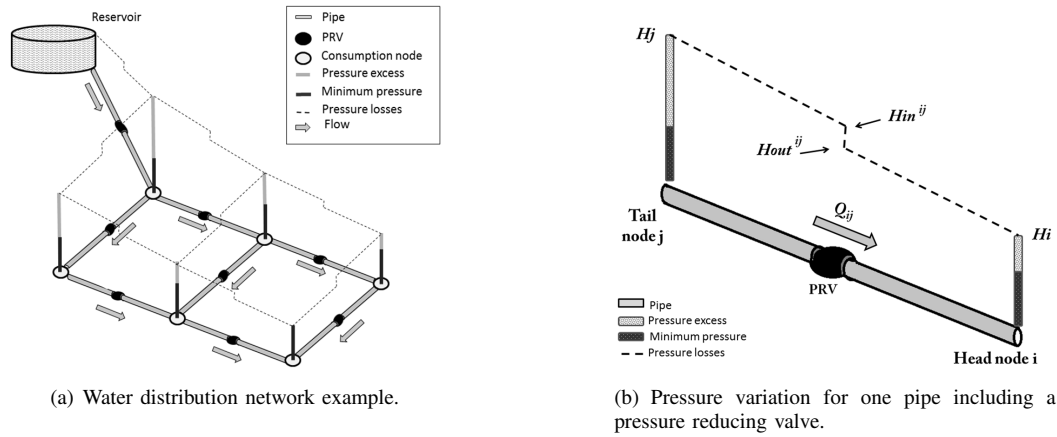


Fig. 1. Water Distribution System.

scheme where the pressure excess is reduced using Pressure Reducing Valves (PRV). For that reason, this model considers PRV as the only type of valve in the system.

The PRV dynamic proposed here is based on the behavioral model presented in [3]. The basic function of a PRV (Figure 2(a)) is to regulate output pressure h_{out} despite changes at the input pressure h_{in} , modifying the valve opening x_m according to a pilot screw reference. The pressure regulation responds to an exponential behavior and it is expressed here as follows,

$$\frac{\partial x_m}{\partial t} = \begin{cases} \alpha_{open}(x_m^{set} - x_m) & \frac{\partial x_m}{\partial t} \geq 0 \\ \alpha_{close}(x_m^{set} - x_m) & \frac{\partial x_m}{\partial t} < 0 \end{cases} \quad (4)$$

where x_m^{set} represents the desired opening associated to the desired output pressure h_{out}^{set} and x_m is the real opening associated to the real output pressure h_{out} . Here, the valve opening stop changing when the desired value and real value are the same. The valve responds at different speeds depending on the action (open or close) which are respectively associated to the servo-valve speed parameters α_{open} and α_{close} .

The main flow q_m depends on the pressure difference between input and output, and is expressed as follows,

$$q_m = C_v(x_m)\sqrt{h_{in} - h_{out}} \quad (5)$$

The bigger the difference between h_{in} and h_{out} , the bigger the flow. Note that h_{in} must be greater than h_{out} in order to obtain real values (the PRV is a passive device that only losses energy). Finally, the term $C_v(\cdot)$ is called the capacity function of the valve and it depends on the real opening x_m only. This function varies from valve to valve and depends on physical characteristics of each device.

1) Valve Opening Consideration: For simulation simplicity a main assumption is made in the valve model. The opening valve x_m is expressed here as a percentage of its maximum displacement X_m , then the PRV opening is manipulated through the variable γ as follows,

$$x_m = \gamma X_m \quad \forall \gamma : 0 \leq \gamma \leq 1 \quad (6)$$

It is important to remember that this simulation methodology is intended to be use in a pressure control scheme, then Equation

(6) allows the controller to use one single scale for all openings valves in the network despite their different sizes. Therefore, the complete valve model can be rewritten as,

$$\frac{\partial \gamma}{\partial t} = \begin{cases} \alpha_{open}(\gamma^{set} - \gamma) & \frac{\partial \gamma}{\partial t} \geq 0 \\ \alpha_{close}(\gamma^{set} - \gamma) & \frac{\partial \gamma}{\partial t} < 0 \end{cases} \quad (7)$$

$$q_m = C_v(\gamma X_m)\sqrt{h_{in} - h_{out}} \quad (8)$$

C. Users Demand Model

The users demand is modeled node by node, where all users located in the same area are aggregated as one and associated to a specific node. Depending on the location and the activity of the users it is possible to model certain behavior pattern for each demand node. Typically, this pattern is constructed in periods of 24 hours.

The simulation methodology proposed here considers the users demand q_i as a known flow that leaves the i node (see Equation (3)). Here the value of variable q_i responds to a stochastic model proposed in [21]. It is important to note that, despite the selection made here, others demand models can be included as well.

The stochastic approach incorporated in this methodology considers consumption as an aggregate signal of many demand events. Each event obeys to certain probabilistic distribution and it is characterized by 3 parameters: occurrence time τ_i , duration time T_i and intensity I_i (see Figure 2(b)). This demand model can be expressed for a j node in terms of volume as follows,

$$V_j = \sum_{i=1}^{C_j} T_i(\tau_i) I_i(\tau_i) \quad (9)$$

where C_j corresponds to the number of demand events for the j node. The variable T_i and I_i depend on the occurrence time τ_i and responds to exponential distribution and a Weibull distribution respectively. The occurrence time τ_i corresponds to a non-homogeneous poisson process with a rate of occurrence $\lambda_j(t)$ defined as follows,

$$\lambda_j(t) = C_j g(t) + \varepsilon(t) \quad (10)$$

where $g(t)$ is the unit time pattern during a entire day⁶, and $\varepsilon(t)$ is a random term with zero average and standard deviation σ_r . According to [21] the function $g(t)$ must satisfy,

$$\int_0^{24} g(t)dt = 1 \quad (11)$$

D. Integrated WDN Model

The integration of models introduced in section II-A, II-B and II-C is presented here. Basically, the complete model includes one mass equation for each node, one modified energy equation for each pipe, and one PRV dynamic equation for each valve. Also, there is one demand equation for each node according to the associated demand pattern.

1) *Modified Energy Equation:* As the PRV is a passive device that losses energy, it has to be included in the energy equation. According to this, PRV flow Equation (8) can be rewritten as follows,

$$h_{in} - h_{out} = \frac{q_m |q_m|}{[C_v(\gamma X_m)]^2} \quad (12)$$

This formulation is conveniently presented as a pressure difference between the input and output and can be associated to the pressure losses by the PRV. Then, it can be included in the ij pipe energy Equation (1) as follows,

$$\frac{\partial H_{ij}}{\partial x} = \Delta H_{ij} = H_i - H_j = -K_{ij} |Q_{ij}|^{np-1} Q_{ij} - \left(\frac{|Q_{ij}| Q_{ij}}{[C_v(\gamma_{ij} X_m^{ij})]^2} \right) \quad (13)$$

where pressure difference between ij nodes corresponds to the sum of the pressure losses caused by friction inside the pipe and the controlled pressure losses caused by the PRV. As the friction coefficient K_{ij} is calculated using the Darcy-Weisbach equation, then np parameter is 2.

There are two important physical considerations about the PRV model presented here. First, not all pipes in the network has installed a PRV and second a typically PRV does not work with reverse flow. Both cases are detailed next:

For the first case a P_{on}^{ij} parameter is included, where

$$P_{on}^{ij} = \begin{cases} 1, & \text{ij pipe with PRV.} \\ 0, & \text{ij pipe without PRV.} \end{cases} \quad (14)$$

For the second case, if $h_{in} - h_{out} < 0$ (reverse flow condition), the valve could operate in two forms depending on the valve type: it can block itself or bypass the water. The blocking case implies a disconnection of the ij pipe and a change of the network topology. The bypassing case just implies that the PRV has no effect on reverse flow. As a first approach, this work considers the bypassing case only⁷ using a B_{ij} parameter as follows,

$$B_{ij} = \begin{cases} 1, & Q_{ij} \geq 0 \\ 0, & Q_{ij} < 0 \end{cases} \quad (15)$$

It is important to note that the condition $Q_{ij} \geq 0$ implies that the PRV is installed in the same direction as the pipe (from node j to node i).

Finally, including the np value and the physical considerations Equation (13) can be rewritten as follows,

$$\frac{\partial H_{ij}}{\partial x} = \Delta H_{ij} = H_i - H_j = - \left(K_{ij} + \frac{P_{on}^{ij} B_{ij}}{[C_v(\gamma_{ij} X_m^{ij})]^2} \right) |Q_{ij}| Q_{ij} \quad (16)$$

Note that the PRV losses term in Equation(16) depends on the valve opening γ_{ij} which responds to a exponential behavior given by Equation(7).

2) *Complete WDN Model:* Summarizing, the complete model of Water Distribution System introduced in this work is given by:

$$\Delta H_{ij} = - \left(K_{ij} + \frac{P_{on}^{ij} B_{ij}}{[C_v(\gamma_{ij} X_m^{ij})]^2} \right) |Q_{ij}| Q_{ij} \quad (17)$$

$$B_{ij} = \begin{cases} 1 & Q_{ij} \geq 0 \\ 0 & Q_{ij} < 0 \end{cases} \quad (18)$$

$$P_{on}^{ij} = \begin{cases} 1, & \text{ij pipe with PRV.} \\ 0, & \text{ij pipe without PRV.} \end{cases} \quad (19)$$

$$\frac{\partial V_i}{\partial t} = \Omega_i(H_i) \frac{\partial H_i}{\partial t} = \sum_k^{ni} Q_{ik} + q_i \quad (20)$$

$$\Omega_i(H_i) = A_T^i \quad (21)$$

$$q_i = \text{Demand profile} \quad (22)$$

$$\frac{\partial \gamma_{ij}}{\partial t} = \begin{cases} \alpha_{open}^{ij} (\gamma_{ij}^{set} - \gamma_{ij}) & \frac{\partial \gamma_{ij}}{\partial t} \geq 0 \\ \alpha_{close}^{ij} (\gamma_{ij}^{set} - \gamma_{ij}) & \frac{\partial \gamma_{ij}}{\partial t} < 0 \end{cases} \quad (23)$$

Equation (17) represent a differential equation expressed as the pressure difference between two ij nodes. It represent the energy losses caused by internal friction inside the ij pipe and the controlled pressure losses caused by the installed ij PRV. There is one equation for each ij pipe. Equation (18) and (19) denote the configuration parameters for the ij pipes with a PRV installed. B_{ij} considers the reverse flow case. P_{on}^{ij} activates the PRV term in Equation (17). On the other hand, Equation (20) represents the mass balance for each i node expressed in terms of its pressure H_i . It also includes the demand flow q_i as a negative flow that leaves the node. Equation (22) models the flow demand for each i node. Finally, Equation (23) is a differential equation that models the exponential behavior of the PRV opening γ_{ij} , which modifies the pressure losses in Equation (17). There is one equation for each PRV.

III. DYNAMIC WDN SIMULATION ALGORITHM

The WDN model proposed in this work is intended to be simulated using the EPS-GGA algorithm proposed by Todini [20]. This algorithm is an improved version of the GGA

⁶Associated to the typical 24 hours simulation time.

⁷The blocking case where the network topology change is proposed as future work.

algorithm used in many water system simulation software like Epanet [16], [17]. The EPS GGA solves the unsteady condition generated by GGA in networks scenarios with variable storage devices (variable tanks) [20]. As those variable tanks induce notorious changes in network dynamic, it is necessary to have an algorithm capable of solving the WDN model under this circumstances. For this reason, the EPS-GGA algorithm is selected here as the simulation hydraulic engine.

It is important to note that the WDN model presented here and the EPS GGA, have some assumption with respect to inertial effects and rapid dynamic changes [20]. Despite this model is useful solving a time varying WDN scenario, it considers a slow-time varying conditions such as relative slow changes in demand and water storage accumulation. Hence, this model is not capable to solve water-hammer phenomena.

A. EPS-GGA consideration

In this work, the EPS GGA algorithm is implemented same as proposed in [20]. The only modification corresponds to the $n_T \times n_T$ time varying diagonal matrix A_{11}^t associated to the energy balance equation (17) as follows,

$$A_{11}^t(r, r) = \left(K_r + \frac{P_{on}^r B_r}{[C_v(\gamma_r X_m^r)]^2} \right) |Q_r| \quad (24)$$

where n_T corresponds to the number of pipes and $r = \{1, \dots, n_T\}$. In this formulation, each ij pipe is renamed as r . It is important to note that, different as [20], this matrix depends on the friction inside the pipe and pressure losses associated to the installed PRV which responds to an exponential behavior.

B. ALGORITHM DESCRIPTION

The simulation methodology introduced here is resumed in the algorithm description presented as follows.

Algorithm 1 Pressure Control Oriented WDN Algorithm

Require: Definition of simulation length T_s and delta time ΔT .

Require: Preset file with the physical description of the network and valves γ^{set} (if needed).

Require: Preset file with the demand profile q for all nodes.

- 1: $k = 1$
 - 2: $q_k \leftarrow$ Demand values for all nodes at iteration k loaded from file.
 - 3: $[H_k, Q_k] \leftarrow$ Initial values loaded from file.
 - 4: $\gamma_k \leftarrow$ Initial values loaded from file.
 - 5: **for** $k = 2$ **to** $round(T_s/\Delta T)$ **do**
 - 6: $q_k \leftarrow$ Demand values for all nodes at iteration k loaded from file.
 - 7: $[H_k, Q_k] \leftarrow EPS.GGA'(q_k, q_{k-1}, Q_{k-1}, H_{k-1}, \gamma_{k-1})$.
 - 8: $\gamma_k \leftarrow PRV_{opening}(\gamma_{k-1}, \gamma_k^{set}, \gamma_{k-1}^{set}, \alpha_{open}, \alpha_{close})$
 - 9: **end for**
-

The algorithm requires pre-computed information before it starts calculating network pressure H and flow Q . The physical description of the network such as location, tanks,

Node parameters	
i	Number of node.
$east_i$	East location coordinate (m).
$north_i$	North location coordinate (m).
elv_i	Node elevation (m).
tt_i	Type of node (0-Reservoir, 1-Var Tank, 2-No Tank).
A_T^i	Tank area (if needed)(m^2).
H_o^i	Initial pressure.
q_{max}^i	Maximum demand (m^3/s).
Pipe parameters	
r	Number of pipe.
j	Tail node.
i	Head node.
d_{ij}	Pipe diameter (m).
$A_{p_{ij}}$	Pipe transversal area (m^2).
l_{ij}	Pipe length (m).
ks_{ij}	Pipe roughness coefficient (m).
km_{ij}	Minor losses (m).
Q_o^{ij}	Initial Flow (m^3/s).
PRV_{on}^{ij}	Enable PRV (boolean).
α_{open}^{ij}	Opening PRV parameter.
α_{close}^{ij}	Closing PRV parameter.

TABLE I
REQUIRED PARAMETERS TO MODEL THE WDN.

pipes, valves, etc are preset in an external file (see table I). This information is saved in a preset file in order to initialize the algorithm. There is one set of parameters for each node and each pipe. The location parameters $east_i$, $north_i$ and elv_i are for 3D representation purposes only. For fixed reservoirs the parameter H_o^i corresponds to the fixed water level.

The demand profile for each node is also pre-computed, according to the demand model presented in section II-C and adjusted for the simulation length T_s and delta time ΔT .

Once all pre-computed information is available, the algorithm loads the initial values of demand q (Equation 22), PRV real opening γ , pressure H and flow Q corresponding to iteration $k = 1$. From iteration $k = 2$ onwards, the algorithm calculates iteratively H_k and Q_k solving the system expressed in Equations (17) to (20) using the modified *EPS GGA'* algorithm described in section III-A. For this calculation it is required all network physics parameters loaded from file and the values of pressure H_{k-1} , flow Q_{k-1} , demand q_k , q_{k-1} and valve opening γ_{k-1} , described in line 7 of algorithm description.

Next, the real PRV opening γ is calculated according to Equation (23), where the exponential dynamic behavior is described. The variable γ_k depends on the past value γ_{k-1} , the desired opening γ_k^{set} and γ_{k-1}^{set} , the physics parameters of the valve $\alpha_{open/close}$ and the valve capacity function $C(\cdot)$. This last function is assumed as a part of the $PRV_{opening}$ function described in line 8.

Finally, the iterative process from line 6 to 8 in the algorithm description is repeated $round(T_s/\delta T)$ times, solving all pressure level H and flows Q .

IV. RESULTS AND DISCUSSION: SIMULATION METHODOLOGY TEST

In order to test the simulation methodology developed here, three main simulation scenarios are proposed. All of this

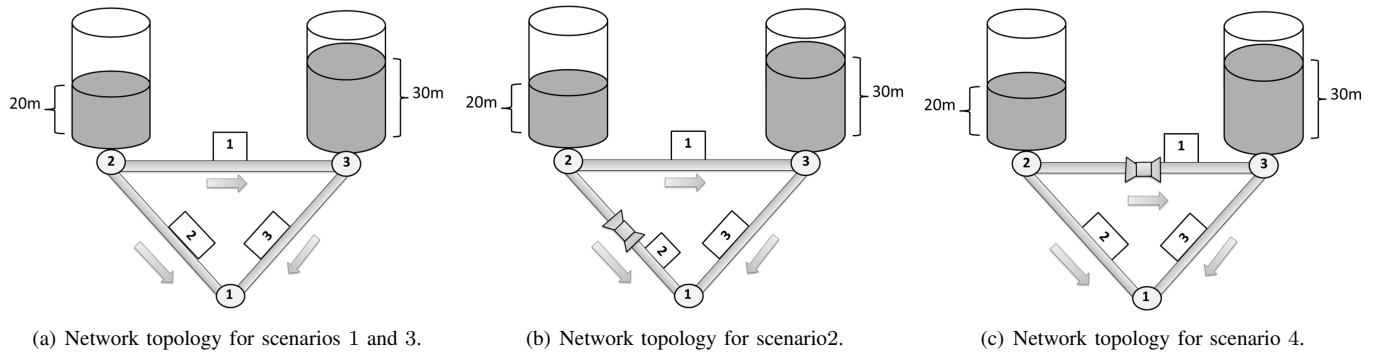


Fig. 3. Test Networks.

i	1	2	3	unit
$east_i$	50	0	100	m
$north_i$	0	86.6	86.6	m
elv_i	0	0	0	m
tt_i	0	1	1	
A_T^i	0	9.79	9.79	m^2
H_o^i	0	20	30	m
q_{max}^i	0	0	0	m^3/s

 TABLE II
 NODE PARAMETERS OF THE TEST NETWORK.

r	1	2	3	unit
j	2	2	3	
i	3	1	1	
d_{ij}	0.2	0.1	0.1	m
$A_{p_{ij}}$	31.4×10^{-3}	7.9×10^{-3}	7.9×10^{-3}	m^2
l_{ij}	100	100	100	m
ks_{ij}	1×10^{-4}	1×10^{-4}	1×10^{-4}	m
km_{ij}	0	0	0	m
Q_o^{ij}	150×10^{-3}	35×10^{-3}	45×10^{-3}	m^3/s
PRV_{on}^{ij}	0	0	0	
α_{open}^{ij}	0	0	0	
α_{close}^{ij}	0	0	0	

 TABLE III
 PIPE PARAMETERS OF THE TEST NETWORK.

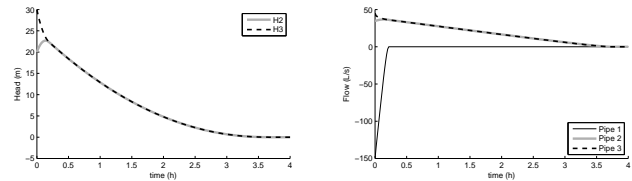
scenarios are based in the 2 variable tanks network proposed by Todini in [20] where the original EPS-GGA algorithm was presented. As this algorithm is relatively new and is also the core of the simulation engine used here, it is necessary to test it in a reference scenario for performance comparison.

The first scenario replies the results presented in [20] but using a Darcy-Weisbach resistant coefficient K_{ij} as presented in section II-A2. The second scenario is an extension of the first one and is intended to test a PRV inclusion in the same network. Same as second one, third scenario is an extension of the first scenario but including a stochastic demand scheme as presented in section II-C. Finally, the fourth scenario integrates the three presented models.

A. First Scenario: Two Variable Tank Test

This test replies the simulation scenario presented in [20] where two interconnected variable tanks are emptying through a third open node (see Figure 3(a)). The tanks 1 and 2 are set to a initial water level of $30m$ and $20m$ respectively. Qualitatively, it is expected an initial flow in pipe 1 from tank 1 to tank 2. After both tanks reach the same level, the flow in pipe 1 will stop and both tanks start to be emptied at the same rate through pipes 2 and 3. In this scenario all node demands are set to zero. The parameters of the test network are presented in Tables II and III. Pressure and flow results are presented in Figures 4(a) and 4(b).

Different as [20], the resistant coefficient K_{ij} is calculated here using the Darcy-Weisbach physic based equation. Despite this change, the flow and pressure results are very similar to the ones presented in [20] and are consistent with the expected qualitatively behavior. In both cases, during the first $15min$ the



(a) Pressure results.

(b) Flow results.

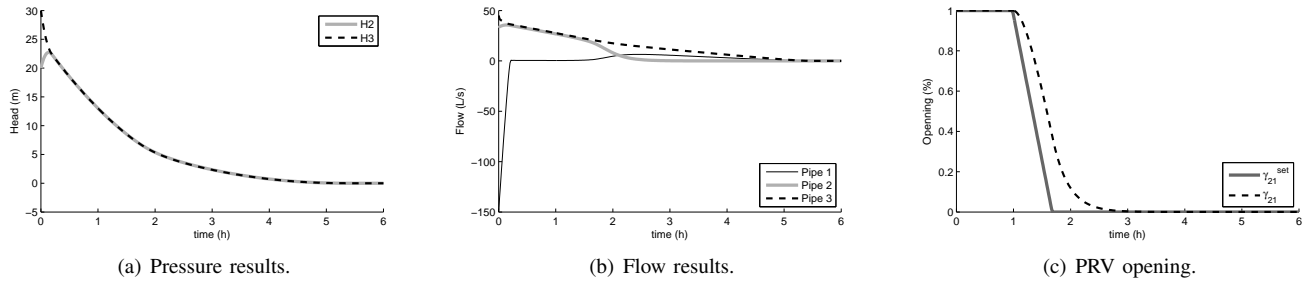
 Fig. 4. First Simulation Scenario. $\Delta t = 60s$

tank 3 supplies tank 2 trough pipe 1 (which has a negative flow according to the tail-nail definition). After this, tanks pressure level are equalized where tank 2 reach a maximum of $23m$ and flow 1 decrease to zero. Next, both tanks are emptied by pipes 2 and 3 at exponential rate during 4 hours approximately.

B. Second Scenario: PRV Test

The second simulation scenario is an extension of the first scenario including a PRV installed in the middle of pipe 2. In this case it is assumed a valve with a servo-speed constant $\alpha_{open/close} = 1 \times 10^{-3}$ and a maximum opening X_m of 70% of the pipe diameter⁸. Capacity function of the PRV is based in the one presented in [3] and assumed as $C_v(\gamma) = 0.45\gamma X_m$.

⁸A completely opened PRV does not have a pressure loss equal to zero. There is a bias losses and here are represented as a percentage of maximum open, which is less than the pipe diameter.


 Fig. 5. Second Simulation Scenario. $\Delta t = 60s$.

Pressure, flow and PRV results are respectively presented in Figures 5(a), 5(b) and 5(c).

Initially, the valve starts open at maximum, which means minimal pressure loss and opening signal $\gamma_{set} = 1$. After the first hour the reference opening signal decreases linearly to a minimal value $\gamma_{set} = 0.001$ and maintains during the rest of simulation. As is expected, the real opening signal γ shows the dynamic exponential response of the valve (see Figure 5(c)). The value $\gamma_{set} = 0.001$ corresponds to a maximum pressure loss, which means an almost closed valve. In this case, the flow through the pipe 2 should be minimum near to zero (as is presented in Figure 5(b)). When the real PRV opening γ reach its minimum (approximately at 3 hours), tank 2 is practically disconnected from node 1, and the system can only be emptied through pipe 3. At this point, tank 2 supplies tank 3 using the connection pipe 1 (which has now a positive flow according to the tail-nail definition). As is qualitatively expected, both tanks empty their content with the same pressure level, taking more time than first scenario (2 more hours).

C. Third Scenario: Demand Model Test

The third simulation scenario is based on the first scenario but including a flow demand profile in node 3. The demand profile is built using model of section II-C using parameters presented in table IV.

These parameters are based in real data taken from a residential area in Valencia-Spain, presented in [21] and properly scaled to the simulation network used here. The demand profile presents an increasing behavior from 15 mins to 1.3 hours approximately, then during 1 hour decreases until zero. The signal presents 4 notable peaks at 0.7 hour, 0.9 hour, 1.3 hour and 1.7 hour. The maximum demand peak reaches $50L/s$.

During the first 15 min the network has the same behavior as simulation scenario 1. After this, node 3 starts consuming according to the demand signal. As is expected, in order to maintain same level between the connected tanks, tank 2 supplies tank 3 through pipe 1 with a similar rate as demand profile. The flow peaks in pipe 1 occurs at the same time as the peaks in demand signal. As the total demand of the network is higher than scenario 1, the tanks empty their content 4 hour earlier.

D. Fourth Scenario: Integrated Model Test

The last simulation scenario integrates the 3 nodes network, the PRV model and the stochastic demand model. The topol-

Parameter	Value	Description
C_j	100	Average number of events.
α	0.4150	Average event length in hours.
λ	0.0136	Parameter of scale intensity in Weibull distribution for the events. (Lt/s)
β	2.3251	Parameter of form intensity in Weibull distribution for the events.
$Norm$	1×10^{-4}	Normalized factor in demand pattern $g(t)$.
A_1	-113.2367	Polynomial parameter of demand pattern $g(t)$. (h^{-1})
A_2	15.5405	Polynomial parameter of demand pattern $g(t)$. (h^{-2})
A_3	-0.4447	Polynomial parameter of demand pattern $g(t)$. (h^{-3})
C_o	326.8395	Polynomial parameter of demand pattern $g(t)$.
σ_r	0.6609	Standard deviation in demand pattern.

TABLE IV
PARAMETERS OF THE DEMAND MODEL BASED ON A RESIDENCE AREA IN VALENCIA, SPAIN [21].

ogy is presented in Figure 3(c) where a PRV and a demand profile are included in pipe 1 and node 3 respectively. In this case it is assumed a faster valve with a servo-speed constant $\alpha_{open/close} = 5 \times 10^{-3}$ and a maximum opening X_m of 70% of the pipe diameter. Capacity function of the PRV is based in the one presented in [3] and assumed as $C_v(\gamma) = 0.45\gamma X_m$. The demand profile has the same form as scenario 3 but with lower intensity ($23L/s$ maximum). The simulation results are presented in Figures 7(a) to 7(d).

During the first 15 mins, there is no demand in node 3 and the PRV remains completely open. Hence the pressure and flow results are practically the same as first scenario. From 15 mins to 45 mins, demand in node 3 increases causing a positive flow in pipe 1 maintaining both tanks at the same level. Therefore, the form of flow signal in pipe 1 is similar to the demand signal in node 3 (both have their peaks at same time). From 45 mins to 1.2 hours, the PRV closes rapidly (a very small opening value $\gamma_{23} = 0.001$). This causes decrease of flow 1 (near to zero) and the disconnection between nodes 2 and 3. Hence, both tanks empty their content at different rates (see Figure 7(a)). Tank 2 supplies only the sink node 1 and empty it content at exponential rate until 3.5 hours approximately. On the other hand, tank 3 supplies sink node 1 and satisfies it own demand, causing a faster emptying, delivering all water at 2.5 hours approximately.

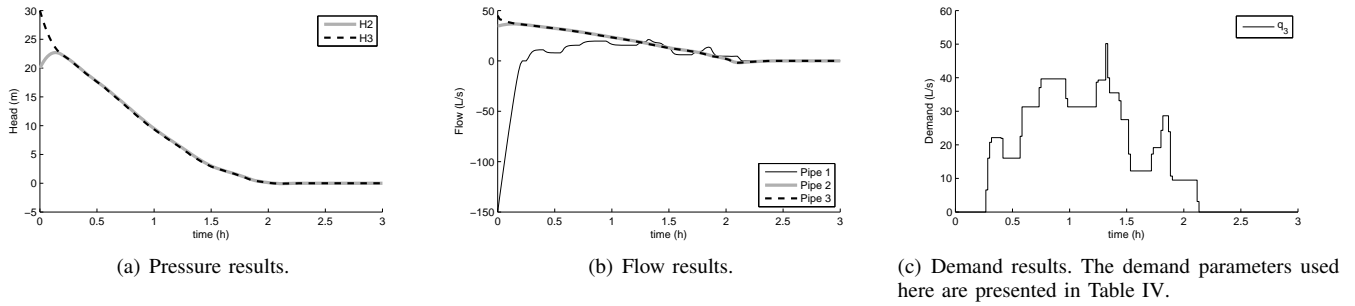


Fig. 6. Third Simulation Scenario. $\Delta t = 60s$.

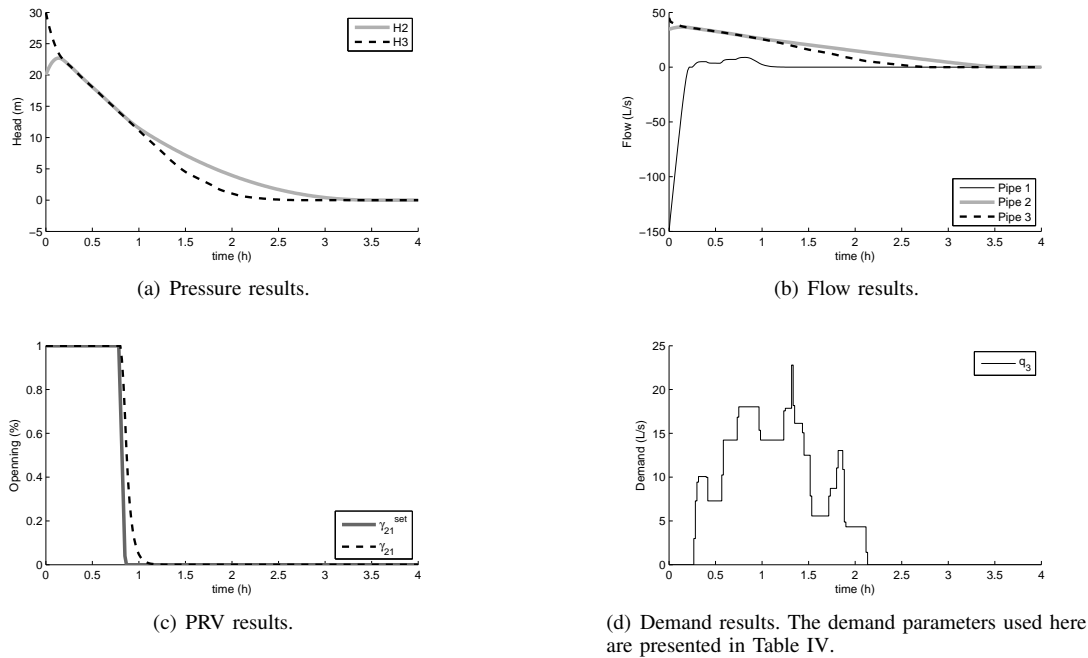


Fig. 7. Fourth Simulation Scenario. $\Delta t = 60s$.

V. CONCLUSION

A pressure control oriented simulation methodology for water distribution networks was introduced here based on the integration of three different models [22]: EPS-GGA water network model [20], PRV dynamic model [3] and a stochastic demand model presented in [21]. The complete model presented in Equations (17) to (23) was satisfactorily solved using the modified EPS-GGA algorithm [20] presented in section III-A.

The complete algorithm formulation of the methodology was presented in section III-B and tested in section IV. As a reference point, the qualitative results presented in [20] (where the EPS-GGA algorithm was first presented) were reproduced here. A simplified 2 variable tank network was successfully simulated despite both tanks were located relatively near. It is important to note, that this specific condition is not possible to simulate using other simulators like EPANET [17] [20]. Using the same network topology, the PRV and demand model were tested in other 3 new simulation scenarios,

showing a satisfactory performance.

The simulation methodology presented here proves to be capable of solving dynamic changes in water network. In light of the good result obtained, the methodology can be included under a pressure control scheme (phase two of this work). Despite the network used here is a very small one, the methodology presented is formulated to solve bigger scenarios including networks with i nodes, r pipes and m PRVs. It just changes the size of the input file and the processing time according to the network size.

The applications of this methodology are not restricted only to pressure control. It could be used to simulate different networks and scenarios for efficient urban planning, management and operation purposes. For example, the dynamic analysis of disconnection in some part of the network, caused by a programmed repair or an emergency situation (like a broken pipe).

As this simulation methodology is based in the relatively new algorithm EPS-GGA [20] and is tested in scenarios that

are not possible to simulate in others simulators [20], [17], it is necessary to compare its performance against real data for accuracy measurement purposes.

VI. FUTURE WORK

The simulation methodology presented here were intended as a first stage of a pressure control problem. Therefore, phase two will be developed including dynamic pressure control techniques in order to reduce volume water losses.

On the other hand, this work presents various ways of additional development. Different models could be added to expand the application scope such as chlorine concentration and water-hammer models. Also, many other devices could be included in the network, such as different types of valves (not only PRV) and pumping systems.

APPENDIX

RESISTANT COEFFICIENT K_{ij}

The resistant coefficient K_{ij} is associated to friction inside the ij pipe and calculated here using the Darcy-Weisbach equation as follows,

$$K_{ij} = \left(f_{ij} \frac{l_{ij}}{d_{ij}} + km_{ij} \right) \frac{1}{2gA_{p_{ij}}^2} \quad (25)$$

where l_{ij} , d_{ij} , $A_{r_{ij}}$ and ks_{ij} are respectively length, diameter, transversal area and absolute roughness coefficient of the ij pipe. The minor losses km_{ij} are associated with losses in accessories and connections of the respective pipe. The parameter f_{ij} corresponds to the Darcy coefficient and it is calculated depending on the type of flow (laminar or turbulent).

The laminar case correspond to a Reynolds number less than 2000 [23] calculated as follows,

$$Re_{ij} = \frac{|Vl_{ij}|d_{ij}}{\nu} \quad (26)$$

where ν is the kinematic viscosity of the water and Vl_{ij} is the velocity of the flow Q_{ij} calculated as $Vl_{ij} = \frac{Q_{ij}}{A_{p_{ij}}}$. For this case, the Darcy coefficient is calculated as follows and depends on the Reynolds number only [23],

$$f_{ij} = \frac{64}{Re_{ij}} \quad \text{if } Re_{ij} < 2000 \quad (27)$$

The turbulent case correspond to a Reynolds number calculated using equation (26) greater or equal than 2000. In this case the Darcy coefficient depends on the absolute roughness coefficient of the pipe material ks_{ij} , the diameter of the pipe d_{ij} and the Reynolds number [23], as follows,

$$\frac{1}{\sqrt{f_{ij}}} = -2 \log_{10} \left(\frac{ks_{ij}}{3.71d_{ij}} + \frac{2.51}{Re_{ij} \sqrt{f_{ij}}} \right) \quad \text{if } Re_{ij} \geq 2000 \quad (28)$$

This equation is not explicit for f_{ij} , then it needs numerical algorithms to find an approximate value of f_{ij} (knowing first the other variables).

REFERENCES

- [1] T. Tucciarelli, A. Criminisi, and D. Termini, "Leak analysis in pipeline systems by means of optimal valve regulation," *Journal of Hydraulic Engineering*, vol. Vol 125, pp. 277–285, March 1999.
- [2] E. Todini, "Design, expansion and rehabilitation of water distribution networks aimed at reducing water losses. where are we?" in *Proceedings of the 10th Annual Water Distribution Systems Analysis Conference WDSA2008*, K. V. Zyl, Ed. Kruger National Park, South Africa: ASCE, August 2008. [Online]. Available: [http://dx.doi.org/10.1061/41024\(340\)33](http://dx.doi.org/10.1061/41024(340)33)
- [3] B. Ulanicki, J. Rance, and P. Bounds, "Control of pressure management areas supplied by multiple prvs," in *Research Report Water Software Systems*. UK: De Montfort University, 1999.
- [4] G. Cembrano, G. Wells, J. Quevedo, R. Perez, and R. Argelaguet, "Optimal control of a water distribution network in a supervisory control system," *Control Engineering Practice*, vol. Vol 8, Iss 10, pp. 1177–1188, October 2000.
- [5] D. Savic and G. Walters, "Integration of a model for hydraulic analysis of water distribution networks with an evolution program for pressure regulation," *Microcomputers in Civil Engineering*, vol. Vol 11, pp. 87–97, 1996.
- [6] P. Jowitt and C. Xu, "Optimal valve control in water distribution networks," *Journal of Water Resources Planning and Management*, vol. Vol 116, no. N 4, pp. 455–472, July August 1990.
- [7] K. Vairavamoorthy and J. Lumbers, "Leakage reduction in water distribution systems: Optimal valve control," *Journal of Hydraulic Engineering*, vol. Vol 124, pp. 1146–1154, November 1998.
- [8] L. S. Araujo, H. Ramos, and S. T. Coelho, "Pressure control for leakage minimisation in water distribution systems management," *Water Resources Management*, vol. Vol 20, Iss 1, no. 1, pp. 133–149, 2006.
- [9] M. Marinaki and M. Papageorgiou, "Central flow control sewer networks," *Journal of Water Resources Planning and Management*, vol. Vol 123, no. 5, pp. 274–283, September October 1997.
- [10] M. Marinaki, M. Papageorgiou, and A. Messmer, "Multivariable regulator approach to sewer network flow control," *Journal of Environmental Engineering*, vol. 125, no. 3, pp. 267–276, March 1997.
- [11] I. Eker and T. Kara, "Operation and control of a water supply system," *ISA Transactions*, vol. Vol 42, Iss 3, pp. 461–473, September 2003.
- [12] D. Georges, "Decentralized adaptive control for a water distribution system," in *Control Applications, 1994., Proceedings of the Third IEEE Conference on*, Aug 1994, pp. 1411–1416 vol.2.
- [13] E. Ramirez-Llanos and N. Quijano, "E. coli bacterial foraging algorithm applied to pressure reducing valves control," in *American Control Conference*, Hyatt Regency Riverfront, St. Louis, MO, USA, June 2009, pp. 4488–4493.
- [14] E. R. Llanos and N. Quijano, "A population dynamics approach for the water distribution problem," *International Journal of Control*, vol. 83, no. 9, pp. 1947–1964, September 2010.
- [15] M. Schutzea, A. Campisanob, H. Colasc, W. Schillingd, and P. A. Vanrollegheme, "Real time control of urban wastewater systems where do we stand today?" *Journal of Hydrology*, vol. Vol 299, pp. 335–348, 2004.
- [16] E. P. Agency, "Epanet software," <http://www.epa.gov/nrmrl/wswrd/dw/epanet.html>, 2000, last Visit: 26th September 2013. [Online]. Available: <http://www.epa.gov/nrmrl/wswrd/dw/epanet.html>
- [17] R. Lewis, *Epanet 2 Users Manual*, W. Supply and W. R. D. N. R. M. R. Laboratory, Eds. United States Environmental Protection Agency, 2000.
- [18] B. Systems, "Watergems v8 user manual," 2006.
- [19] DHI, "Mike," 2008, last Visit: 26th September 2013. [Online]. Available: <http://www.mikebydhi.com/>
- [20] E. Todini, "Extending the global gradient algorithm to unsteady flow extended period simulations of water distribution systems," *Journal of Hydroinformatics*, vol. 13, no. 2, pp. 167–180, 2011.
- [21] V. J. Garcia, R. Garcia-bartual, E. Cabrera, F. Arregui, and J. Garcia-Serra, "Stochastic model to evaluate residential water demands," *Journal of Water Resources Planning and Management*, vol. 130, Iss 5, pp. 386–394, 2004.
- [22] D. Diaz and N. Quijano, *Magister Thesis: Asynchronous Distributed Pressure Controller for a Water Distribution Network*, Uniandes, Ed. Uniandes, March 2012.
- [23] J. Saldarriaga, *Hidraulica de Tuberias. Abastecimiento de Agua, Redes, Riegos*, AlfaOmega, Ed. Bogota, Colombia: Universidad de los Andes, 2007.

The market value of in use industrial machinery

Benedetto Manganelli, Pierluigi Morano and Francesco Tajani

Abstract— This paper proposes an estimation model of in use industrial machinery. The model is based on the cost approach (depreciated replacement cost). The model starts from the classification of the factors that contribute with different way to decrease the original value of the machinery. Value-time functions were constructed for the three main depreciation factors: age, income decay, obsolescence. Empirical formulas have been developed to estimate the market value of in use industrial machinery on the basis of quantitative and qualitative analysis of depreciation functions. The application of this procedure requires the preliminary typological classification of the machinery, the value of new machinery and the probable duration under new conditions.

Keywords— estimation model, use industrial machinery, depreciation factors.

I. INTRODUCTION

THIS work defines a procedure for estimating the depreciation of industrial machinery. This problem often arises in the case of companies undergoing liquidation where there is machinery that can be reused. The proposed model involves the use of very little input data, generally available, as well as the quantitative and qualitative analysis of the effects generated by the passing of time on the machinery.

The paper is structured as follows. In paragraph II, the possible degradation factors are classified into intrinsic and extrinsic, since they contribute and measure the decrease of the original value of the machinery. Paragraph III defines the algebraic expressions for the calculation of the reduction in value arising from intrinsic factors, while the expressions of the decrease generated by the extrinsic factors are discussed in section IV. In paragraph V, the various algebraic relations are summed to obtain the functions of depreciation. On the basis of a working hypothesis and depending on the type of machinery, a depreciation model for estimating the value of new machinery is discussed in paragraph VI. Paragraph VII briefly outlines the conclusions of the work.

II. DEPRECIATION FACTORS

In the indirect estimate, depreciation is usually quantified with coefficients applied to the value of new machinery. The evaluator determines an overall coefficient, or more

coefficients, through the evaluation of the effects of the passing of time and income decay factors on the machinery [2]. These factors can be classified into two groups: intrinsic, those directly related to the type of machinery and the function that it has; extrinsic, those derived from the boundary conditions, such as usage conditions and maintenance of the machinery, with market phenomena also leading to changes in value. Both the first and second result in deductions, sometimes added, to the value of a new piece.

A. Intrinsic Factors

The intrinsic factors generate reductions in value due to age and income decay. Depreciation due to age is the inevitable consequence of the fact that a piece of machinery, regardless of its economic benefits, in comparison with a corresponding new piece has a shorter efficiency life span. The reduction must therefore correspond to the difference in value between two pieces of machinery that have identical characteristics of productivity and equal operating costs, but a different useful life [3]. The reduction due to income decay is, however, the effect of the lesser utility of an asset already in use compared to the corresponding new piece of machinery, due to increasing operating costs, along with a more and more frequent need for extraordinary maintenance [4]. The reduction must also take into account the costs in the event of machinery failure and related slowdowns or stoppages required to carry out repairs[5, 6].

It is therefore evident that a more accurate and expensive maintenance produces, on the one hand, a growth of the deduction for income decay, while on the other, makes it possible to prolong the efficiency of the machine with the consequent reduction of the deduction due to age [7].

The way the machinery is used and the quality of maintenance are significantly influential on the sum of the two deductions. Thus, these variables can be considered in the calculation of the ordinary type of deduction for income decay. This also includes the assumption of income decay between the intrinsic factors of degradation.

It is important to take into account the possible future use of the piece of machinery when estimating its present value [8, 9]. It may be possible that the piece of machinery was conceived to be used exclusively at the site of the initial installation, or that it may be materially and economically convenient to transfer it to another site. In the first case, and when the company is undergoing liquidation, it is logical that the machinery has no value except that corresponding to its disposal [10]. The machine can even assume a negative value when the owner is forced to dispose of it (disassembly and transport) [11]. In the case of a change in management, it may be possible to reuse the machinery on site. In this case, the

This work must be attributed in equal parts to the three authors.

Benedetto Manganelli is with the Engineering School, University of Basilicata, Potenza, 85100, Italy (corresponding author to provide phone: 320-4238658; e-mail: benedetto.manganelli@unibas.it).

Pierluigi Morano and Francesco Tajani are with the Department of Sciences of Civil Engineering and Architecture, Polytechnic of Bari, 70126, Italy (e-mail: pierluigi.morano@poliba.it; francescotajani@yahoo.it).

possibility of physically moving the machine and the depreciated value of a new piece, obtained by applying the deductions for depreciation consequent to the different factors of degradation, plus the value of the economies resulting from savings of purchase and installation time of a new piece of machinery are irrelevant. Dismantling, transportation and assembly costs are not taken into account.

In the event of the machinery being reused within the same company, it can also occur, due to obsolescence caused by an incorrect technical organization and operation of the plant or following modifications and transformations of the production programs, that a further deduction must be made to the value of a new piece, due to the fact that the machinery does not produce as much as was paid for it, due to the changed organization and production conditions.

B. Extrinsic Factors

For the definition of the present value of a piece of machinery, the evaluator should also consider the depreciation generated by extrinsic factors [12,13]. The technological and functional obsolescence of the machinery can accelerate depreciation [14]. The corresponding deduction is due to being "outdated". This occurs whenever technological progress brings onto the market a new technical solution capable of ensuring a greater production and/or lower operating costs compared to the technical solution in use, thus the replacement of the piece of machinery being used with a new one becomes economically convenient. Extrinsic factors also include the usage status and degree of maintenance, lack of market demand for that particular type of machinery, any specifications and operations that do not comply with the legislation in terms of reliability, safety and accident prevention, due to changes in the laws or the introduction of new national provisions that are necessary for retrofitting. The disappearance and unavailability of the machinery manufacturer or spare parts, are other factors that may cause considerable un-usability of the machinery or the reduction of its residual life.

Another extrinsic factor stems from a particular behaviour of the application that can be called "suspicious buyer", always present and to an extent that is usually independent of the type of machinery. This factor, which has a reductive impact on the value, comes into play immediately after the commissioning of the new machinery and then quickly disappears. This factor can be identified in the distrust of those who must choose between buying a new piece of machinery or a piece that has been used little. The latter, which has almost identical characteristics to a new piece of machinery, is assigned a lower value caused by the depreciation measurement due to all the other degradation factors. The distrust of the buyer is partly offset by a greater appreciation of the machinery in the post-installation period, due to immediately having the machinery, which has already been tested and is fully operational. All the extrinsic factors as well as the intrinsic factors result in lowering coefficients of the value of a new piece of machinery. The magnitude of these coefficients should however be defined on a case by case basis.

III. DEDUCTIONS FROM THE INTRINSIC FACTORS

Compared to the effects of extrinsic factors, the effects of the intrinsic factors can be easily isolated and formally analysed. The forms of calculation of the individual corrections have already been expressed in analytical terms in current literature. Various authors proposed algebraic expressions with deductions for age and income decay [15, 16, 1]. The original formulation of the mathematical relationship for the estimation of the deduction for age is described without changes in the following paragraph. The deduction for income decay is developed with reference to a more general case. In fact, the value of the additional monthly maintenance costs of the machinery is assumed to increase over time.

A. Deduction due to age

The expression proposed for the measuring of the deduction due to age is Eq. 1.

$$\Delta C_1 = (C_o - C_v) \cdot \frac{(1+i)^n - 1}{(1+i)^v - 1},$$

(1)

where:

C_o = initial capital or new value of the machinery,

C_v = salvage value at the end of its useful life,

i = interest rate,

v = number of years of life in efficiency from purchase,

n = difference in years between the date of evaluation and the date of putting into operation of the machinery, assumed in normal operating mode (use and maintenance).

The value of n is to be considered equal to a virtual age of the machine when, instead of in normal use and maintenance, the machine is subject to interruptions, to methods of use and quality of maintenance that result in an extension or reduction of the normal life in efficiency. In these cases, the state of use of the machine does not reflect the actual operating time. The virtual age is then calculated as the difference between the duration that the machine would have had under normal operating conditions (v) and the number of years of probable useful life attributable to the used machine (u). Once the values of i , C_v , C_o and v , have been assigned to the analytical expression above, an exponential function of n is obtained.

B. Deduction due to income decay

This deduction is set equal to the sum of the largest annual spending on maintenance or the sum of the lower annual profits resulting from the use of the used machinery compared to an equivalent new piece. The sum should be referred to the probable years of efficiency of the used piece of machinery. In effect, the income decay is related to physical attrition and manifests itself, on the one hand, through the progressive increase of maintenance costs and, on the other, with the increasing reduction in the production capacity of the machinery. In relation to the expression of these variables, it is worth distinguishing: type *a*) machinery subject to normal wear and type *b*) machinery characterized by an accelerated physical attrition (in the case of machinery with components subject to rapid wear and frequent replacement).

Denoting with ΔX the amount of expenditure on the maintenance of a new piece of machinery (first year) and assuming for the subsequent years an exponential growth of ΔX , the amount of greater annual expenditure or lesser annual profit due to the use of used machinery can be calculated with the Eq. 2.

$$\Delta X \cdot [(1 + p)^{v-u}] - \Delta X \quad (2)$$

The deduction for income decay takes the form of Eq. 3.

$$\Delta C_2 = \Delta X \cdot [(1 + p)^{v-1} - 1] \cdot \frac{(1 + i)^u - 1}{i} \cdot \frac{1}{(1 + i)^u} \quad (3)$$

C. Sum of the deductions due to intrinsic factors

Trying to add up the deductions for age and income decay, the curves in Fig. 1 are obtained.

Fig. 1 shows that in cases where, due to physical attrition, the production capacity of the machinery is greatly reduced or in other words the use of the machinery involves a high and progressive increase of the maintenance costs, the k year life, even if the machinery has not yet reached the end of the term of efficiency, its value is null or equal to the residual value.

These observations lead to a calculation procedure of the depreciation generated by the intrinsic factors, alternative to those described above, but more rapid and simple. The procedure is based on the amount of deductions for age and income decay. In particular graphs, such as those described in Fig. 1, constructed on the basis of many different combinations of the values assigned to the variables in play, it is possible, with good approximation, to hypothesize a linear depreciation depending on the age of the piece of machinery. The depreciated value may then be defined by the Eq. 4.

$$V_n = C_o - \frac{C_o - C_v}{v^*} \cdot n, \quad (4)$$

where: n represents the actual age, expressed in years, of the machinery; if it is a piece of machinery subject to abnormal physical attrition (type a), v^* is a time to be taken as equal to the number of years of probable duration of the efficiency of a new piece of machinery ($v^* = v$); when the use of the machinery requires a considerable and progressive increase in the maintenance costs, or the machinery manifests an increasing reduction in production capacity (type b), the time to be allocated v^* is equal to the same v reduced by 10-15% ($v^* = 0.90$ to $0.85 v$).

IV. DEDUCTION DUE TO EXTRINSIC FACTORS

The deductions relating to the extrinsic factors, unlike what has been said for the deductions generated by intrinsic factors, are not easily schematized due to being associated to contingent situations and are therefore variable from case to case. Any attempt to give an analytical explanation is most of

the time neither possible nor justifiable. For factors such as the lack of demand or distrust of the buyer, the only way to quantify the effects is the attribution of empirical coefficients that represent the measurement. The amount of the deduction due to non-compliance of the technical characteristics and operating of the machinery in compliance with safety and reliability regulations can be assumed to be equal to the cost of restoring the machinery.

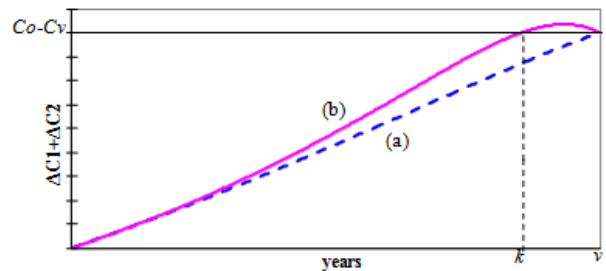


Fig. 1 sum of the deductions due to age, income decay

The deduction relating to a state of non-ordinary use and maintenance of the machinery can be calculated by assigning a different virtual age, more or less, than the actual operating time. Even the deduction for loss and/or unavailability of the manufacturer or spare parts, resulting in a reduction in the remaining life, can be translated into a correction of the real age of the piece of machinery.

A. Deduction due to being outdated

The analysis in this section completes and integrates many aspects of the estimation of the deduction due to being outdated already considered in the cited literature. The application of the function that describes this deduction, however, requires numerous data, which in practice are not always available. The analysis is developed by virtually replacing the outdated piece of machinery with a new one capable of offering a higher profit, then comparing the revenues and costs of replacing it. The hypothesis is therefore that within a plant there is a faulty piece or outdated piece of machinery A that could be replaced with a new one A' .

Below these symbols will be used:

$C'o$ = the cost of a new piece of machinery A' ;

C_o = the cost of a new piece of the faulty or outdated piece of machinery A ;

v' = the probable lifespan of the new piece of machinery A' under new conditions;

v = the probable service life of the old or outdated piece of machinery under new conditions;

$u = v-n$ further probable duration of the efficiency of the outdated piece of machinery from the moment of the estimate;

$C'v$ = the salvage value of the new piece of machinery A' in the year v' , the last of its useful life;

Cv = the salvage value of the old piece of machinery A in the year v , the last of its useful life.

In order for the comparison to be meaningful, the piece of machinery A' must not be new at the time of replacement, but old enough to be missing only u years after its decommissioning, where u is equal to the probable efficiency

of the machine to be replaced. This therefore, anticipates the purchase of a piece of machinery *A'* already in use with a virtual age *v'-u*. The cost of the replacement is a result of the difference between the cost of a new piece and the deductions due to age and income decay, calculated in terms of *v'* and *u* (Eq. 5).

$$C'_o - (\Delta C'_1 + \Delta C'_2). \tag{5}$$

In this relation, both the amount of any proceeds from the sale of the old piece of machinery *A* as well as the difference, at the end of year *u*, between the value of the disposal of the new piece of machinery and the same value of the outdated piece, both discounted to relevance. The formula is in Eq. 6.

$$[C_o - (\Delta C_1 + \Delta C_2 + Sp)] + \left[\frac{C'_v - C_v}{(1+i)^u} \right]. \tag{6}$$

$$\Delta C_3 = U \cdot \frac{(1+i)^u - 1}{i} \cdot \frac{1}{(1+i)^u} - \left[C'_o - (\Delta C'_1 + \Delta C'_2) - [C_o - (\Delta C_1 + \Delta C_2 + Sp)] + \left[\frac{C'_v - C_v}{(1+i)^u} \right] \right]. \tag{8}$$

In the case in which the development of this expression gives a positive result, the outdatedness of the machine is determined. The replacement is therefore convenient and the value of the outdated machinery is in Eq. 9.

$$V_n = C_o - (\Delta C_1 + \Delta C_2 + \Delta C_3). \tag{9}$$

In the simplified assumption in which the value of the new piece of machinery, capable of offering a higher profit than the machinery already in use is equal to the value of the outdated piece (*C=C'*) and the recovery value of the latter is equal to that of the new piece of machinery, in the case in which both pieces have no salvage value, the above expression is reduced as Eq. 10 shows.

$$\Delta C_3 = \frac{U \cdot \frac{(1+i)^u - 1}{i} \cdot \frac{1}{(1+i)^u} - Sp}{2}. \tag{10}$$

The proposed calculation has practical limits in its application due to the lack of data as well as a certain behaviour in the managing of companies, which hardly ever leads to taking initiatives for the replacement of obsolete machinery. The same system, however, makes it possible to measure the effect of the deduction due to being outdated on the current value of the machinery and then to have the data that is required for the estimation of its total depreciation. The most useful amount of *U* is related to the technological level of the machinery and with the event of being outdated due to technological and functional obsolescence, known or predictable. With reference to the technological level, the machinery may be classified as type *c*) machinery with

Sp represents the cost of the premature disposal of the outdated machinery and the losses associated with the stopping of production during the replacement phase. The replacement of the piece of machinery *A* with the new piece *A'* involves a lower expenditure and/or an increased revenue, therefore an annual profit *U* for the *u* years of remaining efficiency of the outdated piece. The present value of the annuity *U* is the benefit of the replacement (Eq. 7).

$$U \cdot \frac{(1+i)^u - 1}{i} \cdot \frac{1}{(1+i)^u}. \tag{7}$$

The accumulation of annuity *U* reduced by the costs that the replacement involves is the deduction due to being outdated. Eq. 8 synthesizes this difference.

mechanical components and type *d*) machinery with electronic components.

Type *c*) machinery includes traditional ones, with it being possible to recognise technological progress as a slow and discontinuous phenomenon. Type *d*) machinery includes those heavily influenced by rapid and continuous evolution of technology over time. In the first case, the value of *U*, obtained from the comparison of only two pieces of machinery (old and new) is constant over time. In the second case, the value of *U* that is derived from the comparison between the old machinery and the number of new pieces that over time replace it is assumed to increase over time.

V. SUM OF THE DEDUCTIONS DUE TO AGE, INCOME DECAY AND BEING OUTDATED

For the purposes of estimating the total depreciation, the classification of the machinery with respect to the technological level is combined with the classification made by the deduction from income decay and produces the following reference classes as represented in Table 1.

type	<u>physical attrition</u>	type	<u>obsolete machinery</u>	type	<u>technological level</u>	
a	normal	→	a-c	←	c	more mechanical component
		→	a-d			
b	<u>accelerated</u>	→	b-c	←	d	<u>more electronic components</u>
		→	b-d			

Table 1 Reference classes for machinery estimation

If the deduction due to being outdated is greater than the new value already corrected by age and income decay, then the machinery will not have any appreciation in the market rather than that corresponding to the decay value. This means that as

a result of the deduction due to being outdated, the machine has a value equal to the residual at a time (year k) still far from the end of the useful life. In year k , therefore, obsolete machinery is appreciated by the residual market value (positive or null). For both the extrinsic factors as well as the intrinsic ones, the observation of the total depreciation which also includes the intervened technical and/or functional obsolescence of the machinery makes it possible to define a model that approximates the function of depreciated value to the real data. For machinery with both mechanical and electronic components, if being outdated is known or predictable, the estimate of the depreciated value becomes as Eq. 11 shows.

$$V_n = C_o - \left[\frac{2 \cdot (C_o - C_v)}{v^*} \right] \cdot n - \left[\frac{(C_o - C_v)}{v^* \cdot (v^* + 1)} \right] \cdot n \cdot (n + 1), \quad (11)$$

where v' is:

- = v for type $a-c$ machinery,
- = 90-95% of v for type $a-d$ machinery,
- = 80-85% of v for type $b-c$ machinery,
- = 70-55% of v for type $b-d$ machinery.

The expression developed outlines a depreciation exposed to declining more rapidly during the first years of life.

VI. DEFINITION OF THE MODEL

The model proposed is intended to estimate the present value of the machinery as an expression of the depreciation to be applied to the value of a new piece.

The basic assumptions of the model are:

- 1) there is a need for used machinery,
- 2) the estimation comes at a time that is not located close to the initial operating of the machinery,
- 3) the machine is in use and maintained regularly.

The accuracy of the model is justified by the analysis carried out so far and will lead to errors that fall within the tolerances on the allocation of the dependent variables (C_o , C_v and v).

The value of a new piece of machinery depreciated by the intrinsic factors of age and income decay is described by Eq. 4.

In the event of supervening technical and functional obsolescence of the machinery, the value of a new piece depreciated by both age and income decay as well as technical and functional obsolescence is described by Eq. 11.

The depreciated replacement value derived from the formulas described above has always meant that n appears less than v^* . On the contrary, the same value is to be taken equal to the residual value of C_v . In relation to the average useful life of machinery, equipment and facilities, the data for the estimation can be deduced from tables B-1 and B-2 set out in the Publication 946, "How To depreciate Property", Department of the Treasury Contents - Internal Revenue Service (2012) which refer to the MARCS classification (Modified Accelerated Cost Recovery System). This system has been used in the U.S. since 1986 for the calculation of the depreciation of movable and immovable property [17].

VII. CONCLUSIONS

The simplified model for estimating the present value of industrial machinery in use proposed in this paper has its theoretical basis in the analysis of formal deductions of the value of new machinery. The interpretation and schematization of the results have led to the definition of value- time curves.

In addition to the simplicity of the application, the essential feature of the model is its flexibility when evaluating different types of machinery. Another advantage is related to the reduced number of variables that the model takes into consideration. Thus, the arbitrary judgment of the estimation is also reduced.

REFERENCES

- [1] B. Manganelli, *Il deprezzamento degli immobili urbani*, Franco Angeli, Milano, 2011.
- [2] F.C. Wong, W.B. Gan, "Total factor productivity growth in the Singapore manufacturing industries during the 1980's", *Journal of Asian Economics*, Vol. 5, No. 2, pp. 177-196, 1994.
- [3] A. Goto, K. Suzuki: "R & D Capital, Rate of Return on R & D Investment and Spillover of R & D in Japanese Manufacturing Industries", *The Review of Economics and Statistics*, Vol. 71, No. 4, pp. 555-564, 1989.
- [4] C.R. Hulten, F.C. Wykoff, "Issues in the measurement of economic depreciation introductory remarks", *Economic Inquiry*, Vol. 34, No. 1, pp. 10-23, 1996.
- [5] B. Manganelli, "Economic life prediction of concrete structure", *Advanced Materials Research*, Vols. 919-921, pp. 1447-1450, 2014.
- [6] R. Cooper, J. Haltiwanger, "The aggregate implications of machine replacement: theory and evidence", working paper No. 3552, National Bureau of Economic Research, 1990.
- [7] C.S. Tapiero, I. Venezia, "A Mean Variance Approach to the Optimal Machine Maintenance Problem", *The Journal of the Operational Research Society*, Vol. 30, No. 5, pp. 457-466, 1979.
- [8] S.E. Dreyfus, "A generalized equipment replacement study", *Journal of the Society for Industrial and Applied Mathematics*, Vol. 8, No. 3, pp. 425-435, 1960.
- [9] S.D. Oliner, "New evidence on the retirement and depreciation of machine tools", *Economic Inquiry*, Vol. 34, No. 1, pp. 57-77, 1996.
- [10] J.M. Malcomson, "Replacement and the rental value of capital equipment subject to obsolescence", *Journal of Economic Theory*, Vol. 10, No. 1, pp. 24-41, 1975.
- [11] B.C. Meyer, "Market Obsolescence and Strategic Replacement Models", *The Eng. Economist*, Vol. 38, No. 3, pp. 209-221, 1993.
- [12] C.R. Hulten, F.C. Wykoff, "Economic depreciation and the taxation of structures in United States Manufacturing Industries: an empirical analysis", *The Measurement of Capital*, pp. 83-120, University of Chicago Press, 1980.
- [13] D.W. Jorgenson, "Empirical Studies of Depreciation", *Economic Inquiry*, Vol. 34, No. 1, pp. 24-42, 1996.
- [14] D. Green, G.H. Sorter, "Accounting for obsolescence. A proposal", *The Accounting Review*, Vol. 34, No. 3, pp. 433-441, 1959.
- [15] N. Famularo, "Sulla determinazione dei coefficienti di vetustà", *Ingegneria*, No.8, Milano, 1925.
- [16] V. Bochi, *Estimo Industriale - Valutazione tecnica degli impianti industriali*, Ulrico Hoepli, Milano, 1947.
- [17] Information on <http://www.irs.gov/pub/irs-pdf/p946.pdf>.

Insurance and Chain Bankruptcy Theory

Bijan Bidabad, Nikos Mastorakis

Abstract—By economic analysis of insurance, the “chain bankruptcy” theory is put forward as a new theory. Through a mathematical-behavioral model we will show how insurance breaks the chain bankruptcy in the economy and make the business cycle oscillation range narrow.

Keywords—Insurance, Bankruptcy, Stabilizing the economy, Business cycles.

I. INTRODUCTION

ECONOMIC insurances which are often called commercial insurance, have a long history, going back to 6500 years ago. According to a found papyrus belonging to 65 centuries ago, in order to help and protect each others against accidents, ancient Egyptian lithographers used to pay a share to a fund. In 2250 B.C., Hammurabi, king of Babel legislated a law according to which transporters were responsible for the cargo they carried until delivery. In 588-640 B.C. in Greece, there were associations which established funds and received monthly fees to help and protect members against injury and damages. A similar organization has also been seen in ancient Rome². There are similar cases in middle ages which we will not go through³. Modern various⁴ economic insurances can be counted as follows:

1. Life insurances
2. Personal accidents insurances
3. Health insurances

4. Insurance for fire accidents and other hazards, such as explosion, theft, earthquake, flood and plane crash
5. Cargo insurances
6. Transportation vehicle (sea, air, road) insurances and its related civic responsibility
7. General (civic and professional) responsibility insurance
8. All risk insurances for contracting and installations and related civic responsibilities (engineering insurance)
9. Operation and cash in till insurances
10. Workers honesty insurances
11. Oil exploration and excavation and related industries insurances
12. Agricultural products insurances
13. Export insurances

In all kinds of above insurances upon the conditions written in their contracts and by taking fees from the insured, insurer will cover financial support mentioned in their policy, the following general rule is satisfied. Although these contracts are different in details, but generally they are similar.

The generality of insurance can be mathematically explained; suppose insurer receives A_i dollars from the i^{th} insured to insure asset B_i . Assume that the probability of losing the asset is equal to P . Accordingly, if the number of insured of this kind of asset is n , and $i=1\dots n$, the amount received by the insurer will be equal with:

$$A = \sum_{i=1}^n A_i \quad (1)$$

The mathematical expectation of the payments of insurer to insured in case of loss of the assets will be equal to:

$$B = \sum_{i=1}^n P B_i = P \sum_{i=1}^n B_i \quad (2)$$

If insurance fee is equal to the below ratio:

$$q = \frac{A_i}{B_i} \quad i = 1, \dots, n \quad (3)$$

By replacing the terms we can write:

$$\sum_{i=1}^n A_i = q \sum_{i=1}^n B_i \quad (4)$$

By replacing (1) and (2) in (4), we will have:

$$A = \frac{q}{P} B \quad (5)$$

That is to say, the received amount by insurer (A) is equal to the ratio of insurance fee (q) to the probability of loss of the

Bijan Bidabad is WSEAS Post Doctorate Researcher, (No. 2, 12th St., Mahestan Ave., Shahrak Gharb, Tehran, 14658, IRAN. (Tel.: +98-21-88360810, Mobile: +98-912-1090164, Fax: +98-21-88369336, email: bjjan@bidabad.com, web: <http://www.bidabad.com>)

Nikos Mastorakis, Technical University of Sofia, Bulgaria, Department of Industrial Engineering, Sofia, 1000, BULGARIA (email: mastor@tu-sofia.bg, web: <http://elfe.tu-sofia.bg/mastorakis>)

² - Salehi, Jan Ali Mahmoud (2002), Insurance Law, Bimeh Markazi Iran, Training and Publication Office, pp. 65-73.

³ - Before Islam, kinds of insurance have been prevailing in Arabia peninsula. The reason for not being mentioned in narrations may be because The Legislator did not want to go in detail of economic subjects except when necessary.

⁴ - There are two kinds of insurances called Co-insurance and Re-insurance which distribute the consequent accident risks subjected to the insurance policy. In co-insurance, two or more insuring companies jointly insure the asset. This kind of insurance is usually used for insuring large risks such as fire accidents or explosions in factories and in case of accident, each insurance company pays his share. Re-insurance is a kind of double insurance, and the first insurer insures the extra risk by another insurer. In other words, the first insurer insures a part of his obligations by another one. Another kind of insurance called Complimentary insurance which is different from double insurance covers other or extra risks for the insured.

asset (P) multiplied by the amount paid to insured (B) by insurance company. Insurer company profit will be:

$$\pi_I = A - \frac{q}{P} B \quad (6)$$

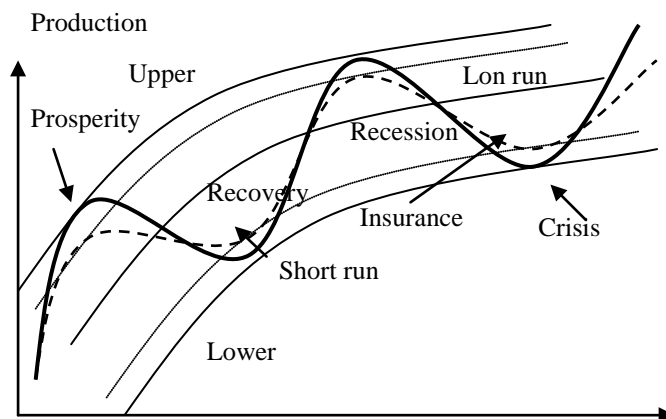
If $\pi_I = 0$, the relation (5) will satisfy and insurer practically will have no profit, which means her economic activity has no yield. Therefore, she should not enter the market. It is the same when $\pi_I < 0$, which means his income is less than his payments ($A < \frac{q}{P} B$). So, when

$$\pi_I > 0 \Rightarrow A > \frac{q}{P} B \Rightarrow \frac{A}{B} > \frac{q}{P}, \quad (7)$$

her activity is profitable. In other words, if the probability of accident is truly estimated, the rate of insurance should be higher than the occurrence of accident probability so that the ratio of income (A) of insurance company to her cost (B) is larger than one. In this case, the profit rate of the insurance company will be $\frac{q}{P} > 1$. This analysis means that the insurance

company is a commission-receiver agent and by rendering a service, obtains a percentage for risk coverage. This action is similar to levying tax on n firms to cover their risks. In spite of Reba, insurance acts against economic fluctuations. We can study this phenomenon in business cycle performance. In business cycles, fluctuations caused by periodical fluctuations and cycles which take 8-11 years to finish, turn the economy from recession to crisis and then to recovery and prosperity and again to recession and a new cycle. Business cycles are a lengthy subject in economics which we don't go into details now.

When economy is at prosperity stage, total production is at its maximum level and then tends to decline towards recession until finally reach to crisis. In this process, unemployment of factors of production exacerbates and reaches its maximum in crisis. Firms become bankrupt one after another until inventories empty and prices start to rise and increasing demand increases production and supply and a new recovery and then prosperity starts in the economy within 8-11 years. When the economy is in crisis, by decrease of prices, producers and intermediates start to bankrupt and since they cannot keep their financial obligations, social problems will be the consequences of this compulsory cycle in the economy. When the economy reaches its lowest in crisis stage, prisons will be filled with people who can not afford to pay their debts and obligations. Insurance practically will minimize this cycle and decreases its range. As it is seen in the figure below, the hachured curve has reduced production and income during recovery and prosperity, and instead, has decreased depression and crisis in the next steps. In other words, insurance has reduced the cycle range of short term oscillations and guided the growth trend towards long term economic trend and the economy has been more surrounded.



Long term and short term economic conditions during business cycles

II. CHAIN BANKRUPTCY THEORY

Let us start a new discussion about chain bankruptcy. Any firm at time t has some assets and liabilities. Its total assets (W_i) is equal to the value of all goods and physical capital and other acceptable items in firm's (C_i) portfolio plus its claims (F_i) from others. That is:

$$W_i = C_i + F_i \quad (8)$$

On the other side, debts (D_i) are equal to financial obligations of the firm. Altogether, in an economy with n firms, all claims will be equal to all obligations, or:

$$\sum_{i=1}^n F_i = \sum_{i=1}^n D_i \quad (9)$$

The net worth (asset) of each firm is equal to:

$$W_i^n = C_i + F_i - D_i \quad (10)$$

By summing up the above equation, and replacing from (9), the inventory in the economy will be equal to net worth of asset, or,

$$\sum_{i=1}^n W_i^n = \sum_{i=1}^n C_i \quad (11)$$

Now suppose n firms have transactions with each others and i^{th} firm buys C_i amount of goods from the $i-1^{th}$ firm and sells it to the firm $i+1^{th}$. If this process of purchase is based on credit, it will cause transmission of bankruptcy to other firms. As commodities are sold payable at maturity, i^{th} buyer promises to the $i-1^{th}$ seller to pay him the amount of D_i at maturity. On the other hand, he sells the good to $i+1^{th}$ buyer and receives a payable written document equal with F_i and the commodity goes from firm $i-1$ to firm i and then to firm $i+1$. These simple sequences will go on several times. To simplify the subject, let us suppose that the face value of the commodity C_i increases α percent in each transaction between firms and these firms have no other assets except this commodity and all their claims and obligations are related to this commodity which create their assets and liabilities. We can design the above chain as follows:

$$C_0 = (1+\alpha)C_0 \rightarrow C_1 = (1+\alpha)C_0 \rightarrow C_2 = (1+\alpha)C_1 \rightarrow \dots C_j = (1+\alpha)C_{j-1} \rightarrow \dots C_n = (1+\alpha)C_{n-1}$$

$$C_0 \rightarrow (1+\alpha)C_0 \rightarrow (1+\alpha)^2C_0 \rightarrow \dots (1+\alpha)^jC_0 \rightarrow \dots (1+\alpha)^n C_0$$

$$D_0 = 0 \rightarrow D_1 = C_0 \rightarrow D_2 = C_1 \rightarrow \dots D_i = C_{i-1} \rightarrow \dots D_n = C_{n-1}$$

$$F_0 = C_0 \rightarrow F_1 = (1+\alpha)C_0 \rightarrow F_2 = (1+\alpha)C_1 \rightarrow \dots F_j = (1+\alpha)C_{j-1} \rightarrow \dots F_n = (1+\alpha)C_{n-1} \quad (12)$$

$$\pi_0 = C_0 \rightarrow \pi_1 = \alpha C_0 \rightarrow \pi_2 = \alpha C_1 \dots \rightarrow \pi_j = \alpha C_{j-1} \rightarrow \dots \pi_n = \alpha C_{n-1}$$

The sale of firm zero to firm nth has been shown in the first row and each term shows the value of the commodity for firm j. This process is in the form of difference equation; therefore, the second row by replacing C_i in terms of C is essentially the solution for the first row. The third row shows the debt flow of the firms and the fourth row shows the firms' claims. The fifth row shows the profit of firms zero to firm nth. Total profit of the transactions in the economy will be equal to:

$$\pi = \sum_{i=0}^n \pi_i = C_0 + \sum_{i=1}^n \alpha(1+\alpha)^{i-1}C_0 = C_0 + \alpha C_0 \sum_{i=1}^n (1+\alpha)^{i-1} \quad (13)$$

Total debts created in the economy will be:

$$D = \sum_{i=0}^n D_i = \sum_{i=0}^n C_{i-1} = \sum_{i=0}^n (1+\alpha)^{i-1}C_0 = C_0 \sum_{i=0}^n (1+\alpha)^{i-1} \quad (14)$$

Total claims created in the economy will be:

$$F = \sum_{i=0}^n F_i = \sum_{i=0}^n (1+\alpha)^i C_0 = C_0 \sum_{i=0}^n (1+\alpha)^i \quad (15)$$

All above relations have a summation of a geometric progression term:

$$\sum_{i=0}^n (1+\alpha)^i = \frac{(1+\alpha)^{n+1} - 1}{\alpha} \quad (16)$$

Therefore, we have:

$$\pi = C_0(1+\alpha)^n \quad (17)$$

$$D = C_0 \left(\frac{(1+\alpha)^n - 1}{\alpha} \right) \quad (18)$$

$$F = C_0 \left(\frac{(1+\alpha)^{n+1} - 1}{\alpha} \right) \quad (19)$$

Again, we can find the trueness of the above relations by the below replacement:

$$\pi = F - D \quad (20)$$

Now suppose that the inventory of the last firm C_n is spoiled or damaged because of an accident. Therefore, his claims which were supposed to be created after selling goods to the next firm and could compensate its debts (D_n) and leave some profit π_n for the firm which is equal to α(1+α)ⁿ⁻¹ have been ruined. That is to say, his claims which are regarded as assets, becomes zero but his debts and obligations remain. Therefore:

$$F_n = 0 \quad (21)$$

$$\pi_n = -D_n \quad (22)$$

Now its losses are equal with its debts to firm n-1. The unfulfillment of his financial obligations in equations (12) will follow a reverse trend; that is equal to D_n of claims of the n-1th

firm (F_{n-1}) is not paid and the profit of the n-1th firm is also lost. By using equations (12) we can write:

$$F_n = (1+\alpha)D_n = (1+\alpha)(1+\alpha)C_{n-2} = (1+\alpha)F_{n-1} \quad (23)$$

Therefore:

$$F_{n-1} = \frac{1}{(1+\alpha)} F_n \quad (24)$$

That is to say, the claims of the firm n-1 from the firm n have been equal to zero, because of the accident for goods of the nth firm. The general form of the above equation applies to all firms:

$$F_{i-1} = \frac{1}{(1+\alpha)} F_i \quad (25)$$

Since this equation is recursive, when F_n = 0, all F₀, ..., F_{n-1} will be zero too. That means, in business of C, all merchants become bankrupt and since they cannot obtain their claims, they cannot pay their debts. Therefore, all merchants in relation with this commodity will be bankrupt. In this case, the losses of all merchants will be:

$$\pi_j = -D_j \quad (26)$$

which can be extracted from equations (12). The nominal loss to the economy will be:

$$\sum_{i=0}^n \pi_i = -\sum_{i=0}^n D_i = -C_0 \left(\frac{(1+\alpha)^n - 1}{\alpha} \right) \quad (27)$$

III. INSURANCE AND CHAIN OF BANKRUPTCY

Now suppose in each transaction of commodity C, its owner pays a percentage of it as insurance fee to insurance company. If insurance rate is q and the ith insured always pays qC_i to insurance company, by using equations (12) we can calculate insurance fees at any time. In the following sequence, Q_j is the insurance fee of the jth insured:

$$qC_0 \rightarrow qC_1 \rightarrow qC_2 \dots \rightarrow qC_j \rightarrow \dots qC_n \quad (28)$$

$$Q_0 = qC_0 \rightarrow Q_1 = q(1+\alpha)C_0 \rightarrow Q_2 = q(1+\alpha)^2C_0 \rightarrow \dots Q_j = q(1+\alpha)^jC_0 \rightarrow \dots Q_n = q(1+\alpha)^n C_0 \quad (29)$$

The total insurance fee paid will be:

$$Q = \sum_{i=0}^n Q_i = \sum_{i=0}^n qC_0(1+\alpha)^i = qF \quad (30)$$

Which means that the total insurance fee paid is equal to the insurance fee rate multiplied by total claims of merchants from each other for transacting commodity C. Assume there are one accident which ruins the commodity in n transactions, so the probability of this accident will be equal to:

$$P = \frac{1}{n} \quad (31)$$

Therefore, if the commodity is ruined in nth transaction, the insurance company has to pay D_n = C_{n-1} to nth merchant. The company can afford to pay this amount for her obligations and since F_{n-1} is not zero in this case, the recursive equation (25) for all claims of previous merchants will not become zero

and they obtain their profits. In this case, only the n^{th} merchant has no profit, but has even no loss, because insurance company has covered his loss by paying him D_n which is equal to the value of his lost commodity. The insurance company calculates the accident probability through equation (31) and thereof, insurance fee. In our sample, the insurance fee will be:

$$q = \frac{Q}{F} \quad (32)$$

And insurance cost for the j^{th} insured will be $Q_j = qC_0(1 + \alpha)^j$ and therefore, the income of the insurance company will be:

$$Q = qC_0 \left(\frac{(1 + \alpha)^{n+1} - 1}{\alpha} \right) \quad (33)$$

Mathematical expectation of insurance company cost from equation (31) will be:

$$E(B) = C_0 \left(\frac{(1 + \alpha)^{n+1} - 1}{n\alpha} \right) \quad (34)$$

Mathematical expectation of insurance company profit is as follows:

$$E(\pi_I) = Q - B = \left(q - \frac{1}{n} \right) C_0 \left[\frac{(1 + \alpha)^{n+1} - 1}{\alpha} \right] \quad (35)$$

If insurance fee rate is equal to one divided by the number of transactions, the insurance company profit will be equal to zero, but even in this case, the economy gets rid of bankruptcy. But since the insurance company has offered this service to the community, he has to obtain a profit:

$$q = \frac{Q}{F} > \frac{1}{n} \Rightarrow Q > \frac{F}{n} \quad (36)$$

That means, the total insurance fee received by the company should be more than the average claim of one transaction which is a clear result.

REFERENCES

- [1] Bidabad, Bijan, (2003) Religious-economic analysis of insurance and characteristics of Islamic government. Monetary and Banking Research Academy, Central Bank of Iran, 2003. <http://www.bidabad.com/doc/bimeh.pdf>
- [2] Bidabad, Bijan, (2003) Problems of macroeconomic policy making in Iran, collection of 40 articles of the author, <http://www.bidabad.com/doc/ketab-eghtesade-kalan.pdf>
- [3] Salehi, Jon Ali Mahmoud (2002), Insurance Law, Bimeh Markazi Iran, Training and Publication Management.

Studies regarding the irrigation to the hilly and terraced surfaces

B. Lepadatescu, A.-E. Dumitrascu, and A. Nedelcu

Abstract— In the paper is shown a solution to use irrigation for hilly and small terraced surfaces of upland areas, where the water is not available and the electricity grid is missing. The condition to use this solution of irrigation is to have a water source available. This water source can be a spring, an artesian well or a stream that must be near the surfaces on the hillside that need the water. Usually, the level of the water source must be above the site location of the homestead's water needs. If the location of household, garden, or livestock water supply is higher that the water source is necessary to use a solution to pump the water to this location. To pump the water without use electricity in hilly areas it is used a ram pump system which needs a minimum fall of the water. The paper presents a solution to irrigate hilly surfaces where the water source has not a fall to make working properly the ram pump.

Keywords— irrigation, ram pump, sustainable solution, hilly surfaces, zero pollution, renewable source.

I. INTRODUCTION

On the hilly and terraced surfaces due to topographical constraints, an irrigation system is very difficult to make and unavailable because the costs are very high. It is possible to find a solution to irrigate such lands the productivity of crops can increase by 2 times or higher. Most of the people have to depend on rain water due to the unavailability of irrigation facilities that decreases the productivity for the horticultural crops such as fruits, vegetables, flowers, tuber and rhizomatous crops and species. If they use water pump with electricity or fossil fuel the cost is high and the people from those lands cannot afford to pay and they cannot cultivate their primary means of food in time.

The solution that is proposed in the paper is to utilize kinetic energy of the flowing river to pump water uphill without using any other external sources of energy such as fuel or electricity. The proposed solution consists of a water wheel

B. Lepadatescu is associate professor at Department of Manufacturing Engineering, Faculty of Technological Engineering and Industrial Management, "Transilvania" University of Brasov, 29 Eroilor Street, 500036 Brasov, Romania (corresponding author: 40-268421318; fax: 40-268421318; e-mail: lepadatescu@unitbv.ro).

A.-E. Dumitrascu is lecturer at Department of Manufacturing Engineering, Faculty of Technological Engineering and Industrial Management, "Transilvania" University of Brasov, 29 Eroilor Street, 500036 Brasov, Romania (e-mail: dumitrascu_a@unitbv.ro).

A. Nedelcu is professor at Department of Manufacturing Engineering, Faculty of Technological Engineering and Industrial Management, "Transilvania" University of Brasov, 29 Eroilor Street, 500036 Brasov, Romania (e-mail: a.nedelcu@unitbv.ro).

which raises the water from a river at a height of 4-10 m and from there the water is conducted to a ram pump that will send some amount of water to a higher height uphill, from where it can be used for various crops and households for drinking water purpose.

To irrigate such hilly and terraced areas without the use of any outside source of energy which can supply homestead' water needs, or garden, orchard, was necessary to find a solution with simple construction, easy to install, which does not consume petrol, diesel or electricity, which can operate for 24 hours per day and maintenance free. This solution use the energy of a large amount of water falling a small height to lift a small amount of the water to a much greater height from where it can be used to a village or irrigation scheme on the hillside. When is obtained a fall of water, the ramp pump lift this water with a comparatively cheap and reliable means to a considerable heights.

The solution presented in the paper to use water from a river for the hilly and terraced surfaces is shown in Fig.1. To work the system is necessary to have a pump head or fall h needed to start the ram pump function. Because on the plain surfaces where the river is situated, to obtain this pump head is necessary to use a water wheel 1 which lifts the water from the river level to the height h that can be around 4-7 m. These values of pump head ensure a delivery head or elevation H till 7-10 times more than pump head h .

The diagram in Fig.1 shows the main components of a system which irrigate hilly and terraced surfaces. Water is taken from a river 10 with a water wheel 1 that transfers the water to a drive tank or intake tank 2 which ensure constant flow water to the ram pump 4, through the drive pipe 3. The ram pump lifts part of the water coming through the drive pipe to the delivery tank 7 on a higher level through the delivery pipe 6. The ram pump is protected by a pump house from accidental damage. From the delivery tank the water is conducted to the distribution system which consists for example of drinking water for the people 9 or for horticultural crops 9. Waste water is delivered out from pump house through the drain tile 5.

The main advantages of using this system of irrigation are:

- Use of a renewable energy source;
- Has a little environment impact by pumping only a small proportion of the available flow;
- Low maintenance requirement by his simplicity and reliability;

- Can be manufactured in the rural villages.

The main limitations of using this system of irrigation are:

- It is limited in hilly areas with a year-round water sources;
- It is pumped only a small fraction of the available

flow and therefore require source flows larger than actual water delivered;

- Are limited to small-scale applications.

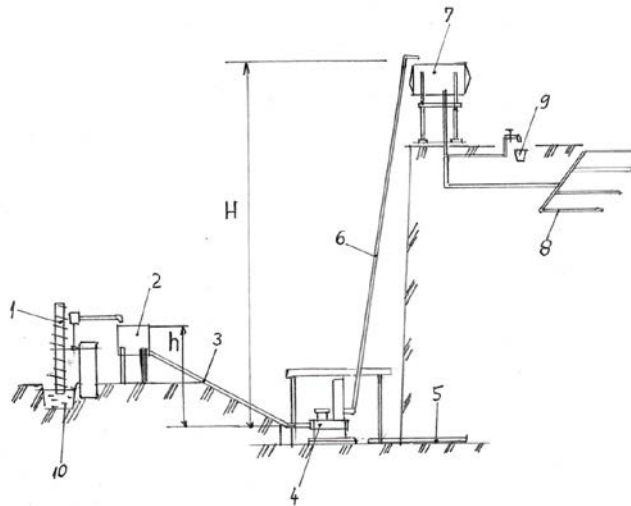


Fig. 1 Layout of the system to irrigate hilly and terraced areas

II. THE MAIN COMPONENT OF THE IRRIGATION SYSTEM

a. The water wheel

The water wheel 1 from Fig.1 is the first component of this system of irrigation. His role is to lift the water taken from the river to a considerable height h that is necessary to start the ram pump to work.

In Fig.2 is shown a constructive solution of a water mill

used to take the water from a river and to send further to a reservoir from where is conducted to the ram pump by drive pipe. The main elements of this water mill are (Fig.2): the primary reservoir (1), the pipe (2) from where the water is conducted to the main reservoir; the rotor axis (3); the screws (4) that permit setting of the water mill in a vertical plan; the counterweight (5); the concrete pillar (6) that supports all the construction; 24 collecting tubes (7); the rotor ring (8) where are mounted the collecting tubes.

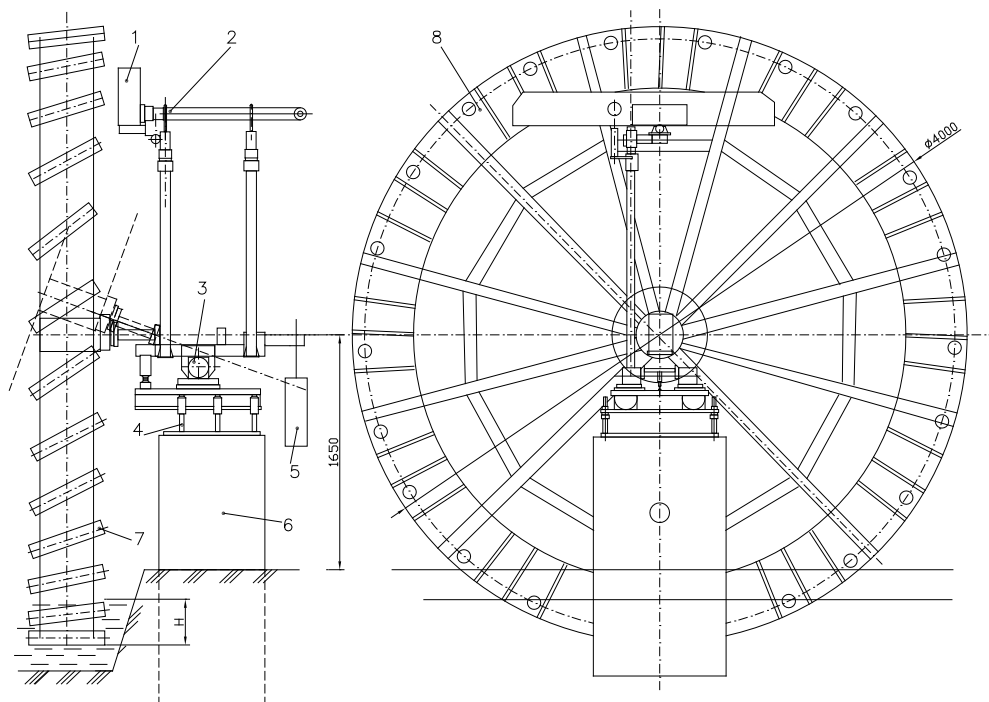


Fig. 2 The components of the water wheel

Water mill has a diameter of 4000 mm which allows lifting water from the river at a height of 3500 mm, where it is stored in a primary reservoir 1. From the primary tank (1), water is passed through the pipe 2 to the drive tank located at a distance of 2 m from the concrete pillar (6). Rotor ring (8) is made of two rings of steel sheet of thickness 0.5 mm and is connected to the main shaft (3) by means of profiled spokes. On the two rings of the rotor are fixed 24 tube collectors, made by polypropylene, with a length of 500 mm and diameter of 75 mm. The impeller is submerged in river water at a depth of 200 mm. This allows complete filling tube collector with water from the river. Turbine construction allows adjustment of horizontal and vertical plan to a range of 150 mm which allows being adapted at specific conditions of the installation in the site near to the river.

In the period between harvest crops and starting a new season in agriculture, the turbine is decommissioned by tilting it 20 degrees. In this mode extends the life of the plant and reduce costs maintenance. Keeping the turbine in this inclined position is realized by a lock system.

Turbine works without interruption throughout the period between the start of the season in farming and till harvesting period ends. During this time water is stored in the drive tank, and then distributed through the drive pipe to the ram pump and further to the delivery tank from where water is used.

To calculate the turbine parameters it is used Fig.3. This figure shows schematically the position of the collector tube fixed on the rotor in the time when its upper end comes out from the water.

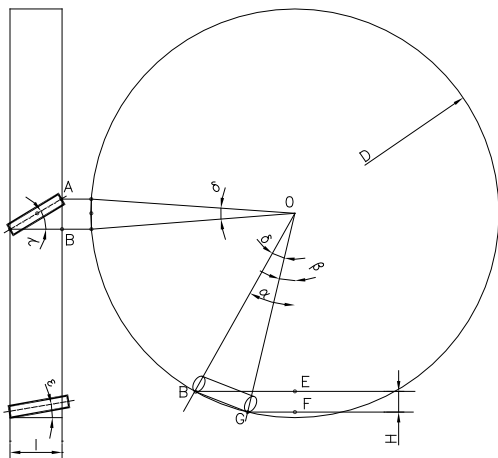


Fig. 3 Sketch used to calculate the water wheel parameters

b. The components calculus

At this point the collector tube is almost full with water and continue lifting movement once the rotation of the rotor. Water collection tube is mounted on the rotor's circumference at an angle γ . Using triangle VAB we can calculate the connection between the angle of tube collector and rotor construction elements:

So the angle δ is given by:

$$\delta = 2\arcsin \frac{l \sin \gamma}{2} \tag{1}$$

Equation 1 shows the relationship between the tube collector mounting angle and rotor construction elements.

Using ODE triangle is calculated the relationship between the constructive elements of the rotor and the exit angle of the tube collector from the water. So:

$$\alpha = \arccos \left(1 - \frac{2H}{D} \right) \tag{2}$$

After some calculations we have:

$$EF = \frac{D}{2} [\cos(\alpha - \delta) - 1] + H \tag{3}$$

Due to tube collector mounting angle, water can never fill its entire cavity. To calculate the amount of water that is transported by one collector tube it is used Fig.4.

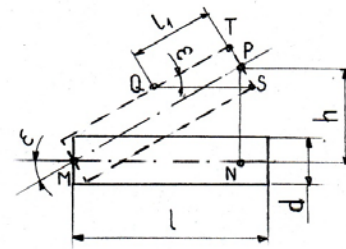


Fig. 4 Calculation of the amount of water carried by the tube collector

Using triangle MNP we have:

$$\epsilon = \arcsin \frac{EF}{l} = \arcsin \frac{D[\cos(\alpha - \delta) - 1] + 2H}{2l} \tag{4}$$

$$V_{tube} = \frac{\pi d^2}{4} l \tag{5}$$

$$V_1 = \text{volume of the cylinder with height } l_1, V_1 = \frac{\pi d^2}{4} l_1$$

Using triangle TSQ, we have: $l_1 = \frac{d}{\tan \epsilon}$ But:

$$V_1 = \frac{\pi d^2}{4 \tan \epsilon} \tag{6}$$

V_2 is the volume of the water that is transported by one collector tube and can be calculated with relation $V_2 = V_{tube} - \frac{V_1}{2}$. Using relation (5) and (6) we obtain:

$$V_2 = \frac{\pi d^2}{4} \left(l - \frac{d}{2 \tan \epsilon} \right) \tag{7}$$

But, $\tan \epsilon = \frac{\sin \epsilon}{\sqrt{1 - \sin^2 \epsilon}}$. Using relation (4) equation (7)

becomes:

$$V_2 = \frac{\pi d^2}{4} \left(l - \frac{d \sqrt{4l^2 - [D[\cos(\alpha - \delta) - 1] + 2H]^2}}{2[D[\cos(\alpha - \delta) - 1] + 2H]} \right) \tag{8}$$

Equation (8) gives the amount of water that is taken from the river by one tube collector. Since the rotor has 12 tube collectors, this value must be multiplied by 12 to determine the amount of water that comes to one rotation of the rotor.

Below is calculation of water volume that is taken from the river for the next elements of the rotor:

$l = 500 \text{ mm}$; $D = 3900 \text{ mm}$; $H = 200 \text{ mm}$; $\gamma = 45^\circ$; $d = 75 \text{ mm}$.

First we must calculate value of angle α with relation (2):

$$\alpha = \arccos\left(1 - \frac{2H}{D}\right) = \arccos\left(1 - \frac{2 \cdot 200}{3900}\right) = 26^\circ 10'$$

Next we must calculate value of angle δ with relation (1):

$$\delta = 2 \arcsin \frac{l \sin \gamma}{D} = 2 \arcsin \frac{500 \cdot 0,70711}{3900} = 10^\circ 20'$$

So, the amount of water that will be transported during one rotation of the rotor will be: $1.57 \cdot 24 = 37.68 \text{ l}$.

An important factor for plant efficiency is the speed of the water of the river. As the speed of the water is higher the amount of water extracted by the rotor will be higher and therefore higher plant efficiency.

Number of revolutions of the rotor in a minute n_{min} is given by:

$$n_{min} = \frac{v_w}{\pi \cdot D} \quad (9)$$

where v_w is the velocity of river water, and D is the diameter of the tube collector disposed on the circumference of the rotor.

Volume of water extracted from the river in one minute V_{min} is given by:

$$V_{min} = n_{min} \cdot V_2 \quad (10)$$

where V_2 is the volume of water extracted from the river by the rotor in one rotation given by equation (8).

Relation (10) can be written:

$$V_{min} = C \cdot v_w \quad (11)$$

where C is a coefficient given by: $C = \frac{V_2}{\pi \cdot D}$.

Coefficient C was calculated for the following angles γ of mounting tube collectors on the rotor circumference, and volume of water V_2 extracted from the river water at one rotation (Table 1).

Using C coefficient values (Table 1) we can calculate the volume of water extracted from the river in one minute V_{min} , depending on the speed of river v_w for different mounting angles γ of the collector tubes on the rotor circumference (Tables 2-7).

Table 1. Coefficient C depending on the angle γ and the water volume V_2 .

γ	15°	20°	25°	30°	45°	60°
V_2	14.64	24.20	27.12	36.24	37.68	40.08
C	1.196	1.979	2.215	2.959	3.077	3.273

Table 2. The volume of water extracted from the river for different parameters: $\gamma = 15^\circ$, $C = 1.196$

v_w [m/s]	0.3	0.4	0.5	0.6	0.7	0.8	0.9	1.0
(m/min)	(18)	(24)	(30)	(36)	(42)	(48)	(54)	(60)
V_{min} [l]	21.53	28.70	35.88	43.06	50.23	57.41	64.59	71.76

Table 3. The volume of water extracted from the river for different parameters: $\gamma = 20^\circ$, $C = 1.979$

v_w [m/s]	0.3	0.4	0.5	0.6	0.7	0.8	0.9	1.0
(m/min)	(18)	(24)	(30)	(36)	(42)	(48)	(54)	(60)
V_{min} [l]	35.62	47.50	59.37	71.24	83.12	95.00	106.87	118.74

Table 4. The volume of water extracted from the river for different parameters: $\gamma = 25^\circ$, $C = 2.215$

v_w [m/s]	0.3	0.4	0.5	0.6	0.7	0.8	0.9	1.0
(m/min)	(18)	(24)	(30)	(36)	(42)	(48)	(54)	(60)
V_{min} [l]	39.88	53.16	66.45	79.74	93.03	106.32	119.61	132.90

Table 5. The volume of water extracted from the river for different parameters: $\gamma = 30^\circ$, $C = 2.959$

v_w [m/s]	0.3	0.4	0.5	0.6	0.7	0.8	0.9	1.0
(m/min)	(18)	(24)	(30)	(36)	(42)	(48)	(54)	(60)
V_{min} [l]	53.26	71.02	88.77	106.52	124.28	142.03	159.79	177.54

Table 6. The volume of water extracted from the river for different parameters: $\gamma = 45^\circ$, $C = 3.077$

v_w [m/s]	0.3	0.4	0.5	0.6	0.7	0.8	0.9	1.0
(m/min)	(18)	(24)	(30)	(36)	(42)	(48)	(54)	(60)
V_{min} [l]	55.39	73.85	92.31	110.77	129.23	147.70	166.16	184.62

Table 7. The volume of water extracted from the river for different parameters: $\gamma = 60^\circ$, $C = 3.273$

v_w [m/s]	0.3	0.4	0.5	0.6	0.7	0.8	0.9	1.0
(m/min)	(18)	(24)	(30)	(36)	(42)	(48)	(54)	(60)
V_{min} [l]	58.91	78.55	98.19	117.83	137.47	157.10	176.74	196.38

III. THE RAM PUMP

As is shown in Fig.1 [16], the second main component of this irrigation system is the ram pump (Fig.5). Ramp pump is useful where the water source flows constantly and the usable fall from the water source to the pump location is at least 2 m. In our case this distance is 3, 5 m. The operational principle of ram pump is based on water hammer, effect in the ram to transmit water from lower elevation to a much higher elevation. It has only two moving parts that dictates the whole operation. These are waste valve *B* and the check or discharge valve *C*.

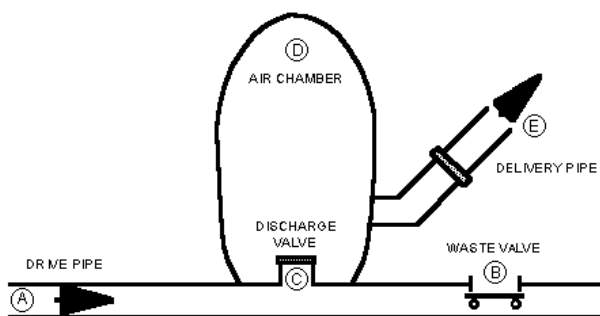


Fig. 5 Schematic illustration of a ram pump

There is an optimum configuration for the ram pump set up. It is a 5 to 1 ratio, where the drive pipe length is five times longer than the vertical fall from the water source to the ram pump. Ideally the drive pipe should have a length of at least 100 times its own diameter. The drive pipe *A* must generally be straight; any bends will not only cause losses of efficiency, but will result in strong fluctuating sideways forces on the pipe which can cause it to break loose. The length of the delivery pipe *E* is not considered in the equation because friction less are normally small due to low flow rates.

The ram pump body requires to be firmly bolted to a concrete foundation, as the beats of its action apply a significant shock load. The ram pump should be located so that the waste valve is always located above flood water level, as device will cease to function if the waste valve becomes submerged.

Its operation is based on converting the velocity energy in flowing water into elevation lift. Water flows from the source through the drive pipe which is the drive tank (Fig.1) and escapes through the waste valve until it builds enough pressure to suddenly close the waste valve. Water then surges through the interior check valve inside the pump body into the air chamber *D*, compressing air trapped in the chamber. When the pressurized water reaches equilibrium with the trapped air, it rebounds, causing the check valve to close. Pressurized water then escapes from the air chamber through a check valve and up the delivery pipe *E* to its destination. The closing of the check valve causes a slight vacuum, allowing the waste valve to open again, initiating a new cycle.

The process occurs over and over again until something happens to stop the cycle. Ram pumps can cycle anywhere from 25 to 300 times per minute. The frequency of the cycle is adjustable by changing the length of the stroke of the waste valve. A longer stroke produces a lower frequency. This means more of the supply flows to and through the pump and more is pumped up the delivery pipe. The stroke is adjusted to restrict the amount of water used to the amount available, or if supply is unlimited, to regulate the amount delivered to match the amount needed.

The ram pump utilizes the inertial energy to pump water to a height greater than the source of the water. It runs all the time, requires no fuel, and needs only minor adjustment and cleaning for maintenance after the initial setup. The ram pump uses much more water than it pumps; it uses the energy of a lot of water to move a portion of it, about 10-15%. Because it is somewhat more involved to set up than a powered pump, a ram pump is generally used only where electricity is to expensive or not available.

The cycle repeats between 20 and 100 times per minute, depending upon the flow rate. If properly installed, a ram pump will operate continuously with a minimum of attention as long as the flowing water supply is continuous and excess water is drained away from the pump.

The location of the water source in relation to the desired point of water use determines how the ram pump will be installed. The length of drive pipe should be at least 5 times the vertical fall to ensure proper operation. The length of delivery pipe is not usually considered important because friction losses in the delivery pipe are normally small due to low flow rates. For very long delivery pipes or high flow rates, friction losses will have an impact on the performance of the hydraulic ram pump.

The relationship between vertical fall (*F*) and length of drive pipe is given in Table 8.

Table 8. Relation between vertical fall and length of drive pipe.

Vertical Fall [m]	Length of drive pipe [m]
0.9-4.5	5.4-27
4.8-7.5	19.2-30
7.8-15	23.4-45

A ram pump system is designed to deliver the desired pumping flow rate for a given elevation lift. The range of available flow rates and elevation lifts is related to the flow quantity and velocity from the water source through the drive pipe. The mathematical relationship for pumping flow rate is based upon the flow rate through the drive pipe, the vertical fall from the source through the drive pipe, and the vertical elevation lift from the pump to the point of use.

To calculate water delivered by ram pump *D* [l/day] to the delivery pipe is used equation (12), [5]:

$$D = (S \times F \times E)/L \quad (12)$$

where: S is the quantity of water supplied in liters per minute, F is the vertical fall [m], E is the efficiency of the ram pump installation (usually 0.6), L is the delivery head [m].

More water can be obtained by installing two or more ram pumps in parallel in tandem if is needed. Each ram pump must have its own drive pipe, but all can pump through a common delivery pipe. In Table 9 is shown the delivery liters per day for different working fall and different delivery head [12].

Table 9. Ram pump performance data for a supply of 1 liter/minute.

Working fall[m]	Delivery head (vertical elevation) during one day											
	5	7.5	10	15	20	30	40	50	60	80	100	125
1.0	144	77	65	33	29	19.5	12.5					
1.5		135	96.5	70	54	36	19	15				
2.0		220	156	105	79	53	33	25	19.5	12.5		
2.5		280	200	125	100	66	40.5	32.5	24	15.5	12	
3.0			260	180	130	87	65	51	40	27	17.5	12
3.5				215	150	100	75	60	46	31.5	20	14
4.0				255	173	115	86	69	53	36	23	16
5.0				310	236	155	118	94	71.5	50	36	23
6.0					282	185	140	112	93.5	64.5	47.5	34.5
7.0						216	163	130	109	82	60	48
8.0							187	149	125	94	69	55
9.0							212	168	140	105	84	62
10.0							245	187	156	117	93	69
12.0							295	225	187	140	113	83
14.0								265	218	167	132	97
16.0									250	187	150	110
18.0									280	210	169	124
20.0										237	188	140

IV. CONCLUSIONS

The present paper is centered towards the development of a hydraulic ram pump that would conveniently alleviate the problem of water supply to the mass populace. Ideally, different combinations of the supply and delivery heads and flows, stroke length and weight of the impulse valve, length to diameter ratio of the drive pipe, volume of the air chamber and size of the sniffer valve, were tried to come up with an optimum size of a ram pump presented in the paper.

This solution presented in the paper can save hours of back-breaking work carrying water and cash where expensive water pumps are replaced. As long as is free water and we have or can create at least two meters drop, the installation is best suited option compared to fuel, wind or solar operated pumps.

The benefits of working with this installation are:

- It puts an end to children and women carrying heavy water jugs to and from the spring;
- Its time saving;
- It improves general health of the villages;
- It makes laundry washing near the houses possible;
- Fishponds become possible, as well as vegetable growing, and animal husbandry.

Some of the advantages of installing this system of obtaining water are listed below:

- Zero pollution;
- Operates 24 hours a day, 7 days a week without

supervision;

- Pumps 20+ more its own falls with the record of 200 meters up without a motor;
- No fuel or electricity cost;
- Low maintenance and repair cost;
- Repairs are done locally;
- Installation is up to 80% cheaper than other water system models;
- Local manufacturing and training generates employment.

REFERENCES

- [1] F. D. Graham, *Audels Pumps, Hydraulics and Air Compressors*. Theo. Audel & Co. 49 West 23 rd St, N.Y., 1998.
- [2] D. S. Harrison, Dalton S, *Hydraulic ram pumps*, Fact Sheet No.AE 19, Extension division, Agricultural Engineering, University of Florida, 1990.
- [3] H. Matson, *The Hydraulic Ram*, Cir.No.246, College of Agriculture, University of Kentucky, 1992.
- [4] C. Privette, *Hydraulic Ram*, Irrigation Fact Sheet No.4, Agricultural Engineering Department, Clemson University, 1989.
- [5] T. D. Jeffery, and T. H. Thomas, "Hydraulic ram pumps; a guide to ram pump water supply systems," *IT Publications*, 1992.
- [6] H.W. Iversen, "An Analysis of the Hydraulic Ram," *Journal of Fluids Engineering, Transactions of the American Society of Mechanical Engineers*, 1995.
- [7] E.W. Kindel, *A Hydraulic Ram for Village Use*, Volunteers in Technical Assistance, Arlington, USA, 1985.
- [8] Hofkes and Visscher, *Renewable Energy Sources for Rural Water Supply in Developing Countries*, International Reference Centre for Community Water Supply and Sanitation. The Hague, The Netherlands, 1996.

- [9] S. B. Watt, *A Manual on the Hydraulic Ram for Pumping Water*, ITDG Publishing, 1985.
- [10] J. Krol, "Automatic hydraulic Pump," *PROC. I. MECH.E.*, 1975.
- [11] N.G. Calvert, *Hydraulic Ram, The Engineer*, 1997.
- [12] F. Molyneux, *The Hydraulic ram for Rival Water Supply*, Fluid Handling, 1990.
- [13] W.W. Thierheimer, N.Tane., D.C. Thierheimer., "Study of using diaphragm like elastic elements in development of ABS controller," *Annals of DAAAM for 2009 & Proceedings of 20th DAAAM World Symposium*, 25-28 November 2009, Vienna, Austria.
- [14] S. B. Watt, *Manual on the Hydraulic for pumping water*, Intermediate technology publication, London, 1995.
- [15] *Designing a Hydraulic ram pump. Water for the world*, Technical note no.RWS.4.D.5
- [16] W.W. Thierheimer, N.Tane, R.Gruia, L.Gaceu, D. Thierheimer, D. Ola, M. Cliniciu, V. Cojocaru, "Reducing Environmental Loppution from Mobile Sources," *In Environmental Engineering and Management Journal*, December 2010, Vol.9, No.12, Iasi, Romania.
- [17] T. Tefery, "Hydraulic Ram pump," *Journal of the Ethiopian Society of Mechanical Engineers*, Vol. II, No.1, July, 1998.
- [18] [16] D. Gregory, S. Jennings, *Hydraulic ram pumps*, North Carolina Cooperative Extension Service, March 1996.
- [19] R. K. Linsley, M. A. Kohler, J. Paulus, *Hydrology for engineers*, McGraw-Hill, London, 1984.
- [20] A.M. Michael, *Irrigation theory and practices*, Vikas Publishing House, New Delhi, 1978.

Engineering and Management. Professional experience was performed within the innovative manufacturing engineering, CAD/CAPP/CAM systems, Reverse Engineering. Also is member of Manufacturing Romanian Association and Center for Scientific Research of "Technological Development System" (CCSDeTInfo) of the Transilvania University of Brasov, NURC recognized center, member of Scientific Research Center "Advanced Technologies and Manufacturing Systems". He published over the 200 scientific papers and he participated as project manager or member in international and national grants.

B. Lepadatescu is associate professor at „Manufacturing Engineering” Department, Faculty of Technological Engineering and Industrial Management, Transilvania University of Brasov. He received a Ph.D. degree in Industrial Engineering from Transilvania University of Brasov in 1999 and a M.Sc. in Quality Engineering, with 40 years experiences in the fields of renewable resources valorization, reliability engineering, industrial project management, manufacturing, quality and environment management system implementation. He published over the 130 papers in prestigious international and national journals, and at international conferences in the field of design and manufacturing engineering, from which 19 papers in the field of renewable energies.

He finished over 40 research contracts with prestigious industrial factories from Romania, as researcher engineer in the field of manufacturing technologies. He is member of the Center for Scientific Research of "Technological Development System" (CCSDeTInfo) of the Transilvania University of Brasov, member of Scientific Research Center "Advanced Technologies and Manufacturing Systems".

From the research activities in the field of renewable sources of energy we can note some of them as :

- Design and execution of a horizontal axis wind turbine for extracting water from the river Danube ;
- Design and execution of a vertical axis wind turbine 1000 W ;
- Design and execution of an installation to extract water from the river using only the energy of river water, used in irrigation.

Also, he obtained the Winner of Excellences Prize for scientific research and international recognition offered by "Transilvania" University in 2010

A.E. Dumitrascu is currently an senior lecturer and quality management responsible of „Manufacturing Engineering” Department, Faculty of Technological Engineering and Industrial Management. She received a Ph.D. degree in Industrial Engineering from Transilvania University of Brasov in 2005 and a M.Sc. in Quality Engineering, with 14 years experiences in the fields of renewable resources valorization, reliability engineering, industrial probability and statistics, industrial project management, manufacturing, quality and environment management system implementation. Member of the Center for Scientific Research of "Technological Development System" (CCSDeTInfo) of the Transilvania University of Brasov, NURC recognized center, member of Scientific Research Center "Advanced Technologies and Manufacturing Systems". The scientific activities consists of publication as author and coauthor of 146 scientific papers (128 scientific articles, 11 books), 7 research grants - one as project manager, and co-organizer of several international conferences.

A. Nedelcu is Head of Department for Continuing Education, "Transilvania" University of Brasov, Ph.D. supervisor in the domain of Industrial

Development of autonomous energy supply system using a sail type wind turbine

A. Jakovics, S. Sakipova, K. Kussaiynov, Zh. Kambarova, Ye. Kussaiynov

Abstract— The paper discusses the problem of creating autonomous power supply system based on renewable resources according to climatic conditions. The authors studied the characteristics of climate and wind energy potential in Kazakhstan and Latvia and considered the possibilities of creation of a device to convert wind energy at low speed wind. A model of a wind turbine, working effectively at low wind speeds, was developed. Initial tests of a sail type wind turbine model with dynamically changeable blade shape were made at a wind tunnel. The results of experimental study of aerodynamic characteristics of wind turbine models are presented. The dependencies of the drag force and traction force at various speeds and directions of airflow were obtained.

Keywords— renewable resource, wind energy potential, sail type wind turbine, changeable blade shape, drag force, traction force.

I. INTRODUCTION

High level of development and technology concepts in the field of alternative energy systems make it possible to provide energy for the normal functioning of human life and activities from renewable energy sources (RES). And most accessible ones and promising are technologies and devices for converting wind energy.

In recent years the power growth rate of wind-driven power plants (WDPP) in the world has averaged 26%, which is much higher than the power growth rate of all other types of power plants. Experts claim that every five years, this figure will be doubled, and by 2020 to 18-20% of the entire energy in the world will be produced by the wind [1]. However, currently generated by WDPP energy provides only 2.5% of global electricity consumption in the world.

This research is done with financial support of ESF, project realized by University of Latvia, No. 2013/0027/1DP/1.1.1.2.0/13/APIA/VIAA/007 and by Kazakhstan Republic Ministry of Education and Science, project no. 523, realized by E.A.Buketov Karaganda State University.

Andris Jakovics is professor of University of Latvia, Head of Laboratory for mathematical modelling of technological and environmental processes at Faculty of Physics and Mathematics, University of Latvia, manager of ESF project.

Saule Sakipova is associate professor of E.A.Buketov Karaganda State University, Kazakhstan; visiting researcher of ESF project, mob.phone: +371-224-170-81; +7-777-999-3037, fax: +371-337-81; (e-mail: sesaule@mail.ru)

Kappas Kussaiynov is professor, Head of Engineering Thermophysics Chair, E.A.Buketov Karaganda State University, manager of project no.523.

Zhanar Kambarova is PhD, senior lecturer of the E.A.Buketov Karaganda State University, senior researcher of project no.523.

Yerlan Kussaiynov is Master program student, Kazakhstan, researcher of project no.523.

It is known that every produced by wind GW of energy reduces 780 kg of CO₂ emissions discharged into the atmosphere [2]. In addition, unlike fossil fuels, wind energy is virtually inexhaustible and available everywhere.

Indeed, energy production using wind power cannot be regular. However, it is easier to predict weather conditions than a sudden blackout of thermal power plants. Alterability and inconstancy of wind don't bring any negative consequences for the environment, and are much "safer" than the radiation leak under depressurization of power generating units at nuclear power plants or nitrogen oxide emissions from coal combustion.

As a member of the European Union, Latvia has an obligation to implement 23% RES of the total energy consumption by 2020 [3]. And in Kazakhstan national objectives were posed; according to them, in 2024 it is planned to produce 5 TWh of energy from renewable energy sources [4]. This tendency to use RES is caused by rise in prices for traditional energy sources such as oil, coal and gas. Moreover, besides environmental safety and reduction of pollutant emissions into the environment, wind power engineering potential is based on socio-economic factors such as development of new technologies, providing employment, increase in taxes, etc.

Electrical energy supplying Enefit company reported that in Latvia the amount of energy produced by the wind, almost doubled to 72 GW in 2012 [5]. These facts indicate that the energy consumption in cities and large enterprises increasingly use RES, including wind power. At the same time detached small household buildings and homes outlying the central power transmission lines are neglected. Today, Kazakhstan has about 200000 farms, of which 90 % have no access to centralized power supply [6]. Actually, at long range electrical power networks maintenance, electric power losses of electricity amount to almost 30%. This makes centralized power supply to remote consumers unprofitable.

President of the Republic of Kazakhstan N. Nazarbayev in the "National programme for the development of wind power engineering in Kazakhstan until 2015 with a view to 2024" notes that the potential of renewable energy sources in Kazakhstan is not still adequately used [7]. He emphasizes that the development of renewable energy sources "would be particularly effective for power generation at the local level, as well as for small distributed loads."

Thus, the development and creation of small wind-driven power plants operating at low wind speeds and adapted to the climatic conditions, are relevant both in Latvia and Kazakhstan.

II. ANALYSIS OF DATA ON WIND ENERGY POTENTIAL IN LATVIA AND KAZAKHSTAN

The proportion of wind power engineering in total energy consumption in Kazakhstan, as well as in Latvia is less than 1%. Introduction of technologies for converting wind energy still remains a problem, since, despite the different geographical location, in most parts of these countries there are areas with values of an average annual wind speed of about (3-4) m/s. Latvia has a high potential of wind energy only along the coast of the Baltic Sea. Areas with the greatest wind speeds are only in the coastal zone of the Baltic Sea and in the northern part of the eastern coast of the Gulf of Riga, Fig.1. Wind speed in these areas reaches 5.1-6.8 m/s and more [8, 9]. Width of the area with strong winds on the coast of the Baltic Sea is 15-20 km, and in the area of the Gulf of Riga is about 10-15km.

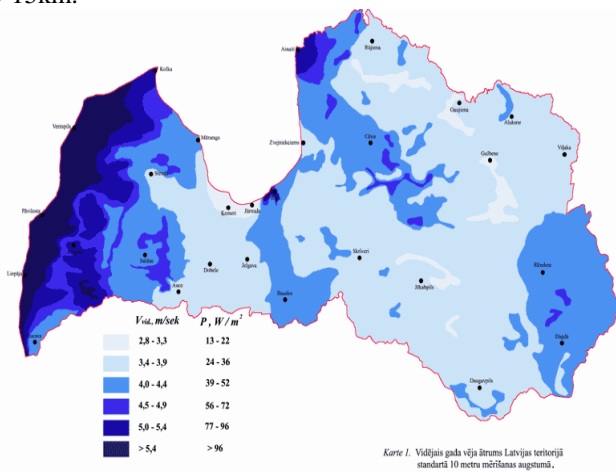


Fig. 1 Map of Latvia winds [8].

This picture of wind potential is confirmed by regular wind speed measurements performed by the office workers of the Latvian Center for Environment, Geology and Meteorology at the meteorological station located near the international airport of Riga [9]. Figure 2 shows an example of wind speed data obtained on-line.

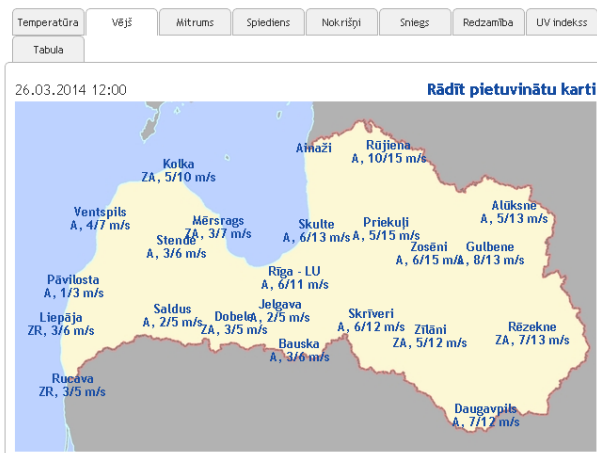


Fig. 2 Example of on-line data on wind speed.

More accurate wind speed values in Riga can be obtained from the results of automated measurements

performed continuously at a weather station based in Botanical Garden of the University of Latvia, Fig.3, 4.

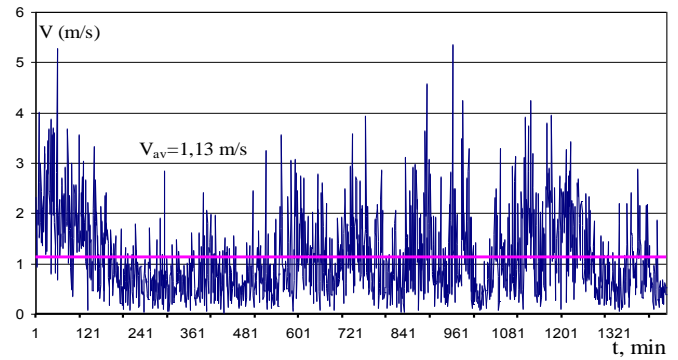


Fig. 3 Diagram of every minute change of wind speed during a day, 12.02.2014.

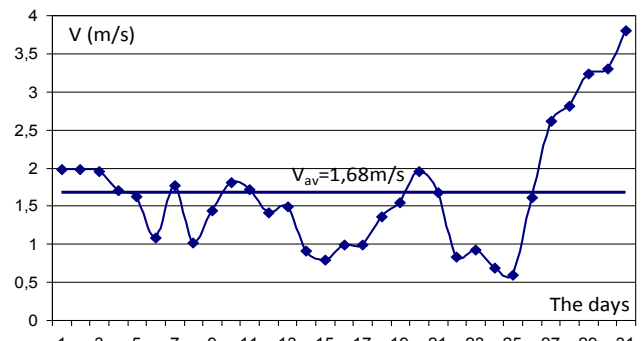


Fig. 4 Diagram of daily change of wind speed in January 2013, Riga.

Data analysis showed that in Latvia in 2013, the value of an average annual wind speed is $V=2,37$ m/s. Measurements show that in the central part of Latvia, an average wind speed is (3-4) m/s; in Riga the wind speed is even smaller and varies from 1.9m/s to 2.8m/s.

A similar picture of the wind potential can also be seen on the map of winds in Kazakhstan, Figure 5. Due to its geographical position, the Republic of Kazakhstan is in a wind zone of the northern hemisphere and in some regions of Kazakhstan there are sufficiently strong air currents [10, 11].

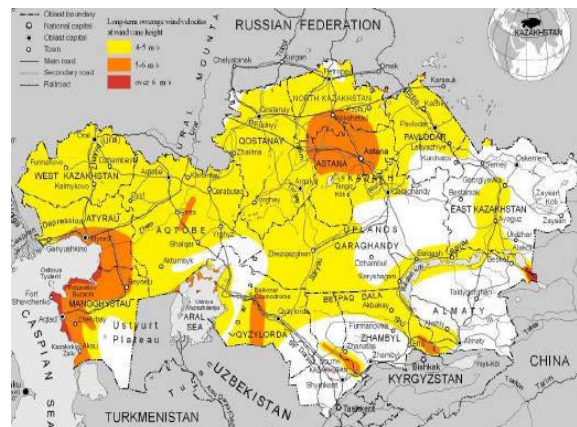


Fig. 5 Map of winds in Kazakhstan [4]

For example, according to the data of weather stations in Karaganda region in 2013, in the central part of Kazakhstan the average annual wind speed measured at a height of 10m, is equal to 3.8 m/s, and in Karaganda city it is less, Fig. 6.

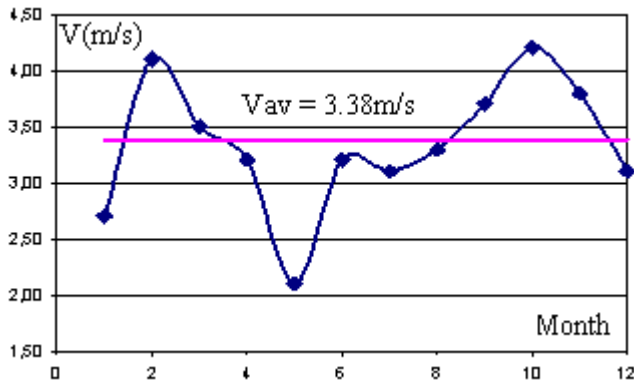


Fig.6. Diagram of the monthly change in the average wind speed in Karaganda city, 2013.

Use of manufactured in production scale small or medium power WDPP are economically unprofitable, since at these wind speeds, they do not work. But during its running time, an adequate wind turbine produces energy, which costs almost 80 times more than it is spent on its production. For this purpose, it is necessary to take into account specific features of the climate in the area, in this case, the wind speed and its direction. In fact, the owner of an autonomous power plant becomes quite independent of traditional energy producers.

III. DEVELOPMENT OF SAIL TYPE WIND TURBINE. EXPERIMENTAL CONDITIONS.

When choosing a wind turbine for energy supplying autonomous system, priorities are determined by many factors that depend on the demands of a particular customer, the quality and price of products. Known various methods and devices of convert wind energy into electrical energy are given in [6, 12, 13]. Efficiency of the use of wind turbines at small wind speeds was described in [6]. Wind turbine analogs designed for operation at low average wind speeds, are given in [14-19]. Articles of Bychkov N.M., N. Murakami (Japan) [11, 15], Nobuhiro M. [17] were shown a wind turbines for small wind speeds based on the Magnus effect. Characteristics analysis of various WDPP showed that sail type wind turbines are suitable for low wind speeds. The advantage of sail type wind turbines is that they can generate electrical energy at low wind, less than 3m/s. Previously authors of this paper also were engaged in the development of wind turbines using the Magnus effect and oriented for low wind speeds also, the results are given in [18,19].

The closest analogue for given sail type turbine is described in works [20, 21]. But weakness of this design is the absence the dynamically changeable surface shape of the blades, which does not allow to optimize the aerodynamic characteristics of a wind turbine in the work process. Moreover, the change of wind direction to the opposite

direction leads to a change in the rotation axis of the wind turbine that is inconvenient in practice.

Now the authors for the first time are developing sailing wind turbine type with dynamically changeable blade shape. The dependence of the traction force and lift force were studied for the wind turbine prototype with five a triangular shaped sailing blades. In [22] studies are the results of real testing experiments for a wind turbine with six blades and 1.6 meters diameter.

For sample studies, a sail type wind turbine model was designed to be used in creating an autonomous wind power system. The model consists of a wind wheel made of metal frame rods with six sail blades of triangular shape fixed on them. The sail blades are made of lightweight and durable material, one end of the blade is attached to the top of the frame by strong thread. The diameter of the sail wheel is 0,4m. The model is fixedly attached to the mount by support rods.

This model of wind turbine differs from known analogues in that as load bearing elements, triangular blades of dynamically variable surface shape with a movable end are used. It provides continuous rotation of the wind wheel during a rapid change in the direction of airflow. To supply with electrical power, the model of sail wind turbine is coupled to a low power generator through a sheave and a belt drive. Initial tests of the model of a sail type wind turbine were carried out at T-I-M wind tunnel with an open test section in the laboratory of E.A.Buketov Karaganda State University (Fig.7).

Main characteristics of the working part of the wind tunnel are follows: the diameter is 500mm; the length is 500mm; turbulence level is 3%; the range of variation of airflow speed is (1 ÷ 25) m/s. Rotational speed of the sail type wind turbine is 50-100 rev/min, the minimum threshold of airflow operating speed is 3 m/s. Measurement errors of airflow speed in the test section using a built-in sensor do not exceed 3-5%.



Fig. 7 The model of a sail type wind turbine in the test section of the T-I-M wind tunnel

The traction force was measured using a spring dynamometer, which was rigidly attached to the sheave of the

wind turbine model. The model of the wind turbine in the test section is fixed to the cubic frame of an aerodynamic balance using thin metal braces to minimize the resistance of auxiliary elements. Aerodynamic characteristics of the wind turbine model at various speeds and directions of airflow were measured using a three-component aerodynamic balance.

IV. DISCUSSION OF THE EXPERIMENTAL RESULTS

As a result of the experiments we obtained dependences of changes in the drag force, lifting force and traction force at various air flow rates and different angles of attack.

The dimensionless drag coefficient C_x , traction force coefficient C_M and Re is similarity criterion - Reynolds numbers were calculated from measurements by next formulas:

$$C_x = \frac{2F_x}{\rho u^2 \cdot S} \tag{1}$$

$$C_M = \frac{2M}{\rho u^2 \cdot S \cdot l} \tag{2}$$

$$Re = \frac{u \cdot L}{\nu} \tag{3}$$

where F_x is the drag force, M is the thrust moment, ρ, ν are the air density and viscosity, u is the flow rate, S is the characteristic area of midship section, l is the length of the lever arm, L is the characteristic size of the wind turbine model.

Figure 8 shows the dependence of the drag coefficient on the Reynolds number. A sharp fall of the drag coefficient is observed up to the Reynolds value that is equal to $1,5 \cdot 10^4$, at further increase in the flow rate this decrease becomes less intense, and then virtually remains constant.

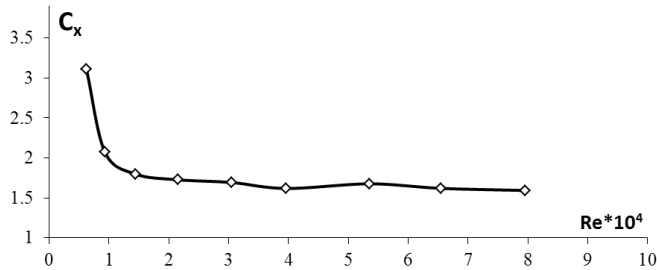


Fig. 8 Dependence of the drag coefficient of the wind turbine model on the Reynolds number

Figure 9 shows the variation of the drag coefficient C_x of the wind turbine model by changing the dimensionless attack angle β of flow at two different airflow rates: of 3m/s and 5 m/s. It is evident that the types of dependences of drag force on the dimensionless angle of attack for these rates are practically the same.

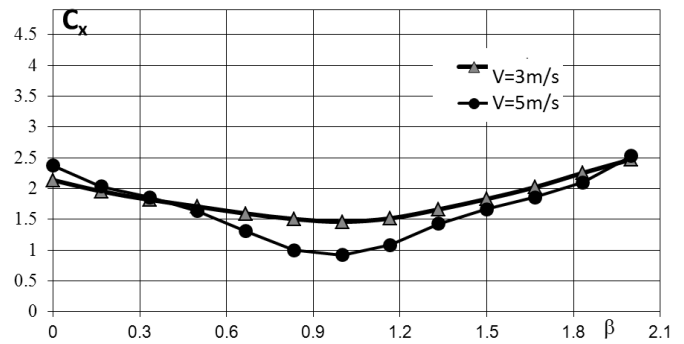


Fig. 9 The dependence of the drag coefficient of the wind turbine model on the dimensionless angle of attack

It can be seen that when the attack angle of airflow increases up to 90° , the drag force coefficient diminishes and then rises. This is due to the fact that when the attack angle of the wind flow increases up to 90° , the square of midship section of the wind wheel decreases, and at further increase in angle of attack up to 180° it grows.

Figure 10 shows the dependencies of the traction force coefficient C_M of the wind turbine model on the Reynolds number at various attack angles of airflow. The highest value of the coefficient of traction force of a model are observed in the forward direction of the wind flow. For various angles of attack of the flow when Reynolds number increases, the traction force coefficient gradually rises.

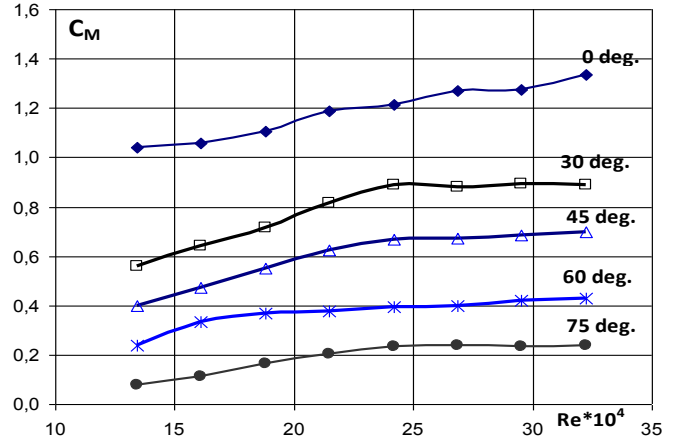


Fig. 10 Dependences of traction force coefficient of the wind turbine model on Reynolds number at various angles of attack of wind flow

Figure 11 presents dependencies of the traction force coefficient C_M of the wind turbine model on the Reynolds number when the direction of the airflow is reversed. The graphs show that the thrust moment varies virtually in the same way. The experiments showed that the designed model of the sail type wind turbine has optimum aerodynamic characteristics due to a self-regulating surface shape of blades. The wind turbine in the air flow acts as self-organized device, efficiently converting wind energy into the energy of rotational motion.

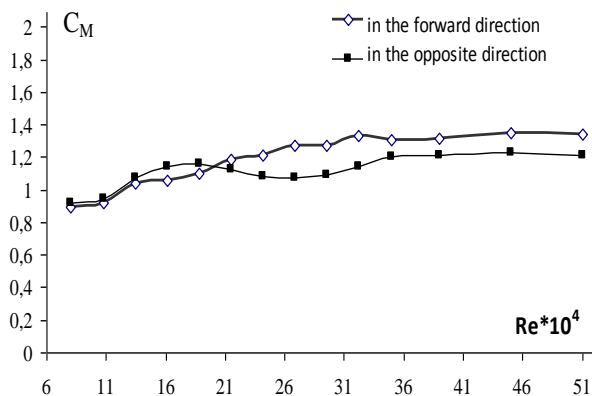


Fig. 11 Dependence of the traction force coefficient of the wind turbine model on Reynolds number at different flow directions.

The design flexibility with dynamically variable surface shape of blades provides the minimum aerodynamic resistance, and increases the utilization ratio of the wind. The comparison of experimental data on changes in drag forces another wind turbine is showing qualitative agreement. The wind turbine maintains operability in a wide range of changes of wind direction that is a positive factor in operation. It was experimentally found that even when the direction of the airflow is reversed, the wind turbine continues to rotate in the previous direction. All experimental measurements were repeated under the same conditions 5-7 times for credibility.

Sail type WDPP matches a wind direction and practically does not originate noise and vibration [13, 22]. Power generated by a sail type wind turbine is proportional to the third power of wind speed, i.e. when wind speed doubles, the power is increased by eight times.

V. CONCLUSION

A pilot model of a sail type wind turbine with dynamically changeable surface shape of the blades was designed and developed.

The dependences of the thrust moment of the laboratory model and that of the drag force on the airflow rate at different angles of attack were studied by experiments. As the result of research we developed a measuring technique of aerodynamic characteristics of a sail type wind turbine. It was demonstrated that due to the self-regulated surface shape of blades of a sail type wind turbine, the latter can efficiently convert the energy of airflow even when the direction of airflow is reversed.

The results obtained will be used for engineering calculations in the development of sail type WDPP, adapted to specific climatic conditions, i.e. operating at low wind speeds and generating a targeted amount of electricity.

REFERENCES

[1] A. S. Vorobyev, On the current state of wind power engineering in the world. *Proc. of the Russian Scientific Technic. Conf. "High Tech in the instrument engineering and machine building and development of innovation activities in a higher educational establishment."* Moscow, 2011, vol.1, pp. 109-110.

[2] D. Glickson, (2014, January) New Test Facility to Improve Wind Turbines Renewable Energy News & Information. <http://www.renewableenergyworld.com/>

[3] C. Ender, International development of wind energy use – Status 31.12.2008. *DEWI Magazine*, 2009, no. 35, pp. 28–33.

[4] M.M.Kenisarin, K.M.Kenisarina, *Development of wind power engineering in the world and the prospects of its development in the CIS and Baltic countries*. <http://www.bib.convdocs.org>

[5] EBRR Renewable Development Initiative - Latvia. <http://www.ebrdrenewables.com/sites/renew/countries/>

[6] R.S. Abdrakhmanov, F.V. Yakimov, The effectiveness of using wind energy sources with reduced wind speeds. *Izvestiya RAN Energy*. Moscow, 2001, no. 5, pp. 54-57.

[7] N.A. Nazarbayev, *National program for development of wind energy in Kazakhstan until 2015 with a view to 2024*. <http://www.windenergy.kz/files/121379>

[8] Sustainable Energy Roadmaps <http://www.worldwatch.org/>

[9] Operative information of Latvian Center for Environment, Geology and Meteorology <http://www.meteo.lv/meteorologijas-operativa-informacija/?nid=459&pid=100>

[10] G.Doroshin, About perspectives of wind power development in the Republic of Kazakhstan <http://carnegieendowment.org/files/Presentation - Rus.pdf>

[11] A. Orlov, Prospects for the use of wind power engineering in Kazakhstan. *Proc. 8th Rep. Conf. "Seifullin readings."* Astana, 2012, vol. 1, pp.16-17.

[12] Ya.I. Shefter, *The use of wind energy*. Moscow: Energoatomizdat. 1983, 200 p.

[13] O.G. Denisenko, G.A. Kozlovsky, L.P. Fedossenko, A.I. Osadchiy, *Transformation and use of wind energy*. Kiev: Technique, 1992, 176 p.

[14] N.M. Bychkov, Magnus wind turbine. The calculated characteristics of wind wheel. *Thermophysics and Aeromechanics*, Novosibirsk, 2008, vol.15, no. 2, pp.583-596.

[15] N.M. Bychkov, A.M. Sorokin, N. Murakami, "Wind turbine", Russian Patent no. 2118699, September 10, 2009.

[16] N. Nobuhiro, Ito Dzun, "Wind power Magnus", Russian Patent no. 2330988, March 27, 2008.

[17] K. Kusaiynov, S.E. Sakipova, L.N. Nikitina, Aerodynamics of the transversally streamlined rotated barrel. *Proc.12th Int. Conf. ICMAR "Methods of aerophysical research"*, Novosibirsk, 2004, vol. 4, pp. 195-198.

[18] K. Kusaiynov, S.E. Sakipova et al., Experimental research of aerodynamics of the system of the revolved cylinders in a turbulent stream. *Proc. 7th International Symposium Turbulence, "Heat and Mass Transfer"*, Italy, Palermo, 2012, pp. 577 - 580.

[19] B.V. Voitsekhovskii, Promising energy sources and their comparison. *J. of Applied Mechanics and Theoretical Physics*, 1980, no. 5, pp. 118-125.

[20] B.V. Voitsekhovskii, F.F. Voitsekhovskaya, M.B. Voitsekhovskiy, *Micro modular wind energy*. Novosibirsk: Publ. Institute of Hydrodynamics, 1995, 71 p.

[21] S.E. Sakipova, Zh.T. Kamarova, M.M. Turgunov et al. Development of sail type wind turbine for small wind speeds. *Eurasian Physical Technical Journal*, Karaganda, 2013, vol. 10, no. 2(20), pp.20-25.

[22] N.A. Lavrentiev, G.V. Volobueva, et al, Wind energy resources and conditions for construction of wind-driven power plants in Eastern Baltic and the Black Sea area of Europe — Minsk, 2010. — 455 p.

Assessing Pollution of Outdoor Insulators in the Cretan Power System

D. Pylarinos, K. Siderakis, I. Pellas, E. Thalassinakis

Abstract—Insulators are key components of power systems as a single insulator fault may lead to an excessive outage. Insulators' performance is strongly linked with local conditions and especially with the experienced pollution. Therefore pollution mapping is an important procedure for power utilities that can be used for insulator maintenance, selection and replacement. For this purpose, several approaches can be followed considering the severity of the problem and also the available time and funds. These include the consideration of geographical and environmental data, human expertise/experience, fault analysis and specially designed measurements such as ESDD, NSDD and DDDG. In this paper, the experience from pollution mapping in the Mediterranean Island of Crete, is presented. The Cretan power network bears a significant interest due to its unique characteristics which are also briefly described. Results and future research perspectives are discussed and conclusions are drawn.

Keywords—insulator, lab, field, high voltage, monitoring

I. INTRODUCTION

HIGH voltage insulators are important components of power systems and their performance strongly reflects to the system's performance and reliability [1]. A single insulator fault may result to excessive outages and therefore insulator research is of significant importance for power utilities. One of the main factors affecting insulators' performance is the experienced pollution, which is highly localized [2-3]. Deposited pollutants allow leakage current to flow on the surface, which in turn may cause the formation of dry bands, discharges and may even result to a complete flashover [1-3]. To suppress the problem several remedies can be employed, such as extending the creepage distance, using specially designed profiles and using hydrophobic materials to manufacture insulators or to coat their surface [1-7].

Assessing a Site's Pollution Severity (SPS) class is a

This work was supported in part by the POLYDIAGNO research project (project code 11SYN-7-1503) which is co-funded by the European Union and Greek National Funds.

D. Pylarinos is a researcher/consultant for the Hellenic Electricity Distribution Network Operator S.A. (dpylarinos@yahoo.com).

K. Siderakis is an Assistant Professor at the Technological Educational Institute of Crete (ksiderakis@staff.teicrete.gr)

J. Pellas is the Head Engineer of the Transmission Lines Department in the Islands Network Operations Department, Hellenic Electricity Distribution Network Operator S.A., Greece (i.pellas@deddie.gr)

E. Thalassinakis is the Assistant Director of the Islands Network Operations Department, Hellenic Electricity Distribution Network Operator S.A., Greece (e.thalassinakis@deddie.gr)

complex task which is strongly related to available funds and time [3]. Depending on the case, some or all of the following may be employed: laboratory tests, field tests, pollution measurements, past experience, fault analysis, weather and geographical data [3]. The distance from pollution sources is mostly considered when referring to geographical data with the addition of altitude when it is high enough to bring about extreme conditions (icing, snow) [8].

The Greek island of Crete is located in the Mediterranean Sea and its power system suffers mainly from severe marine pollution due to local weather conditions and its coastal development [9]. The Greek utility (now the Hellenic Electricity Distribution Network Operator S.A., a former part of the Public Power Corporation S.A.) has issued several different remedies to cope with the problem over the years [10-12]. Further, significant efforts have been made towards mapping the island's pollution and its impact on outdoor insulators. In this paper, the different data related to the assessment of the experienced pollution are presented. The island's morphology, the climate, the network's geography, the recorded faults on different parts of the network and finally the results from pollution measurements conducted in different locations throughout the island's network are presented.

II. LOCAL CONDITIONS & POWER NETWORK

A. Island's morphology and location

Crete is a Greek island located in the Mediterranean Sea, at the Southern end of Europe as shown in Figure 1a. Crete has a rather elongated shape (it is 260 km long and 15-60 km wide) and has a coastline of 1046 km, mostly rocky. Three large mountain formations cover the center part of the island from east to west as shown in Figure 1b. The development of the island is mostly coastal with the four largest cities (Iraklion, Rethimnon, Chania, Ierapetra, Agios Nikolaos with a descending order) being located next to the coast as shown in Figure 1b.

B. Weather and Climate

Crete's climate is characterized by prolonged periods of dry and then wet weather. The dry period usually starts in April and lasts until the end of October. Although the amount of rainfall is significant, most occurs only between November and March. Crete also experiences strong winds mainly of north-northwest direction. Wind reaches its strongest during the summer. Strong winds combined with the rocky coasts result

to increased salt deposition on outdoor insulators. Further, towards the end of August increased precipitation (and relative humidity) is observed [9-11]. As a result of the above, pollution builds up during the dry period and results to an increased risk when wetting occurs. In addition, a significantly diverse behavior is observed between the eastern and the western part of the island. Strongest winds are recorded on the east side of the island whereas the west part receives almost twice the rainfall compared to the east [9-11].

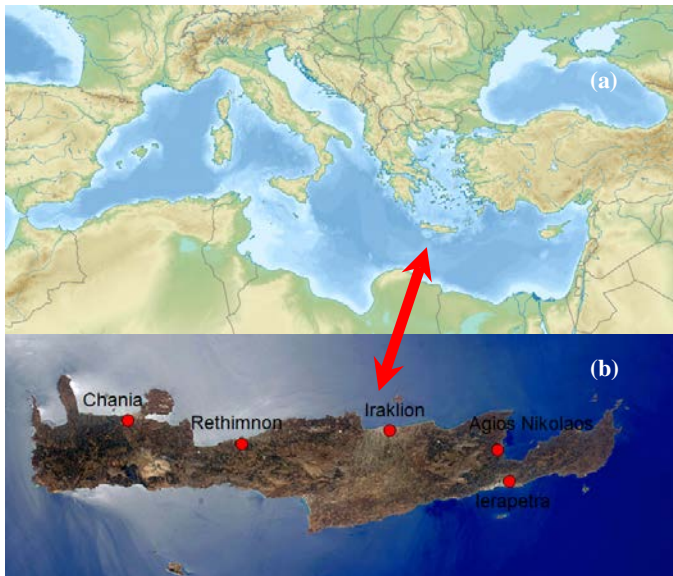


Fig. 1. (a) Crete located in the Mediterranean Sea (b) the island of Crete

C. Network Development and Past Experience

The location of all 150 kV towers of the transmission system, and thus the route of the transmission lines, is shown in Figure 2.



Fig. 2. The location of the 150 kV Transmission Towers

As it can be seen from this figure, the network is mainly coastal, which exaggerates the marine influence. In fact, pollution was responsible for a large percentage of faults that was gradually diminished as more maintenance experience was gained and further reduced as more Transmission Lines were equipped with composite insulators [9, 13]. Historically, pollution problems were recorded as soon as the first transmission line (from Iraklion to Chania) was constructed in the early 60's. The voltage level was then only 66 kV, wooden poles were used and pollution resulted to the burning of the upper parts of several poles [11]. The 150 kV Transmission

Lines were gradually installed from 1976 to 1979 and pretty soon the first problems were recorded at the eastern part of the island. It should be noted that from 1978 until 1993 the faults per km where ten times more in the east compared to the west, even though the eastern side was overinsulated and was also washed clean occasionally [9, 14]. Limited installation of composite insulators started in the 90's in order to monitor their performance and as results we encouraging, extended installation started after 2000. As shown in Figure 3, composite insulators was only the 3% of installed insulators in 2000 and their percentage reached 52% in 2010 [13] and keeps increasing.

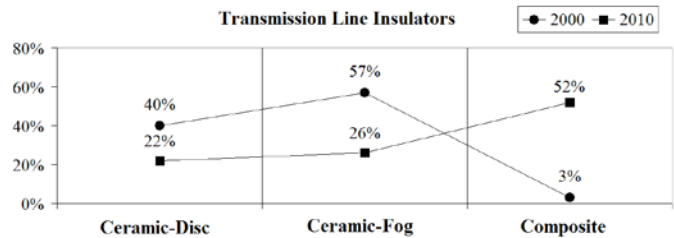


Fig. 3. Transmission line insulator percentage from 2000 to 2010

The total number of faults per 100 km for the years 1980-2010 is shown in Figure 4. The Cretan network has expanded about 36,000 km over these 30 years and therefore the faults per 100 km have been considered in this Figure. As shown in Figure 4 the number of faults per 100 km shows a significant decrease from a decade to next which can be largely attributed to pollution maintenance procedures. For example, from 1978 to 1981 sponge washing was applied. Then, from 1982 to 1985 no washing was applied which led to the increased number of faults in 1985, when pollution was combined with suitable weather conditions [9-11]. As a reaction, washing using pressurized water was introduced as a pollution maintenance procedure, which prevented similar “breakouts” in the following years [9-11]. The gradual installation of composite insulators in the 00's led to a significant decrease in the total number of faults as shown in Figure 4. It should be noted that no flashover has been recorded on any SIR composite insulator in the Cretan power system since their installation.

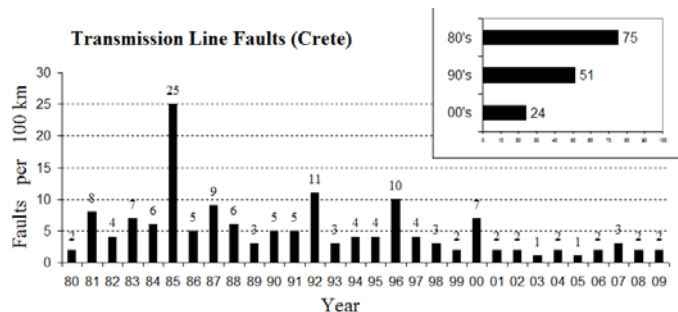


Fig. 4. Transmission Line faults (1980-2010) per 100 km

III. POLLUTION MEASUREMENTS

A. Introduction, Set-Up and Location

Three basic procedures have been standardized in order to

measure pollution: the Equivalent Salt Deposit Density (ESDD), the Non-Soluble Deposit Density (NSDD) and the Directional Dust Deposit Gauge (DDDG) [3]. ESDD relies on collecting the pollution deposited on the surface of off-line insulators in certain intervals, diluting it in water and measuring the conductivity and temperature of the solution in order to define the equivalent amount of salt in mg per cm² of the insulator's surface. To acquire the NSDD measurement the solution is filtered, the filter is dried and weighted to calculate the weight of non-soluble deposits. The DDDG measurement relies on the installation of special kits of cylindrical design that collect pollution from four directions (East, West, South, North).

Each procedure has its pros and cons. ESDD is considered a low cost technique that considers the insulator's profile and can be conducted on site but requires frequent mounting and unmounting of insulators. NSDD is especially needed when non-soluble deposits are present (e.g. sand) but requires special equipment (a drying oven, a dessicator, a laboratory weighing scale) and therefore may be costly and can not be conducted on site. DDDG is an easily implemented procedure which is considered as an easy alternative for large area mapping but has the disadvantage of not considering the insulator's profile which is strongly related to the amount of deposits that actually stays on the insulator's surface and also to the cleaning effect of rainfalls. In fact, it should be mentioned that some 400 kV insulators were installed in one Transmission Line of the Cretan network when the line was first upgraded from 66 kV to 150 kV, but their performance was rather poor [9, 11]. Indeed a 55% of them was damaged (and replaced) due to flashovers from 1985 to 1994 [11]. At the same time, only 0.7% of the 150 kV insulators installed at the same line had to be replaced. This was largely attributed to the difference of their profile, as the 400 kV insulators exposed only 36% of their surface to the cleaning effect of rain whereas the 150 kV insulators exposed the 53% [11]. Therefore, it became obvious to PPC engineers that what mattered was not merely the amount of salt that is carried from the sea, but the actual amount that stays on the insulators' surface.

Considering the above, it was decided that ESDD measurements were conducted on various locations throughout the island. A number of 35 towers of 150 kV lines were selected considering past network experience, as shown in Figure 5. Most selected towers belong to eastern coastal lines and especially the line connecting Iraklion (starting at the Linoperamata Substation) with Ierapetra, due to the experienced problems recorded on this line and also considering the line's importance. Further, multiple towers were selected near the larger cities as these were areas also exposed to other pollution types (industrial, domestic etc). Strings of insulators were hanged from the metal structure of towers as shown in Figure 6. These dead strings were hanged from a lower height compared to live ones in order to be easily and safely accessible by the crew.

Although small intervals are proposed for ESDD measurements, this was not practical in this case due to the number of the measuring points and also considering local weather conditions. In fact, conducting multiple measurements during the dry period would be redundant as pollution kept concentrating on the insulators' surface whereas further measurements after the rainfall period starts would result to lesser pollution due to the cleaning effect. Therefore, and also considering the man hours needed, it was decided that a single measurement was conducted yearly at each tower in the months September and/or October (at the end of the dry period and before rainfalls start). To cut costs, measurements were conducted on site by the line crew with the opportunity of other works in the area. To make sure that a credible measurement was taken, the procedure was repeated for three years in a row to minimize the risk of a local rain before the measurement. The maximum of the 3 measurements was then considered as the ESDD value for the location.



Fig. 5. The location of the ESDD measurement spots



Fig. 6 Offline installation of an insulator string for ESDD measurements

In order to calculate the area of the insulators' surface, computer aided design was implemented using Autocad as shown in Figure 7. Further, as both fog and disc profile insulators were used to conduct measurements a correction factor should be applied in order to correlate measurements as proposed in [15]. However, the exact value of the correction factor is not specified, as a value in the range of (0.8 ± 0.3) is proposed. In order to follow the worst case scenario the maximum value of 1.1 was selected in this paper. However,

further research is needed for the exact determination of this factor. PPC (and now HEDNO) have constructed and operate an outdoor High Voltage Test Station in Iraklion Crete [16], where a series of comparative measurements have been scheduled in order to define this factor with further accuracy.

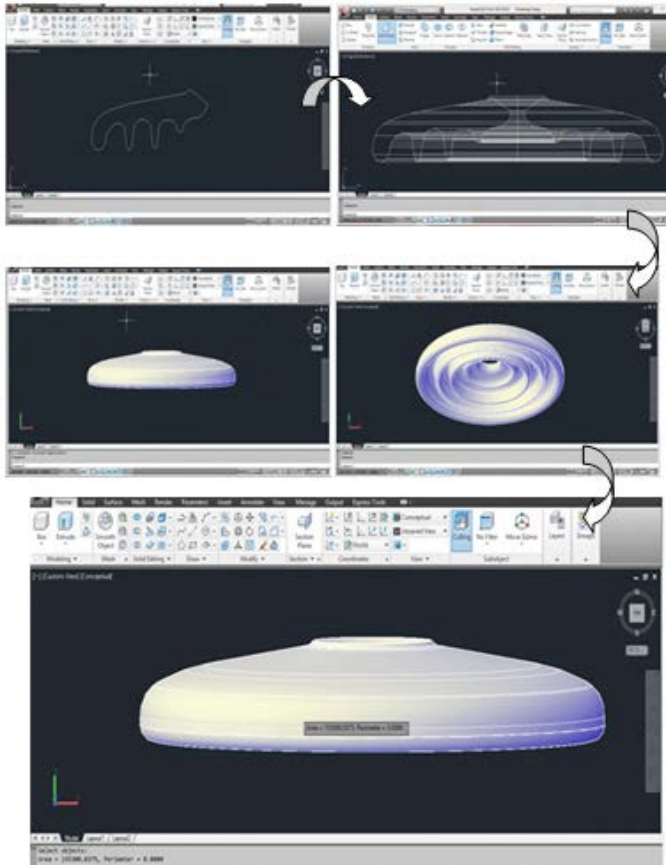


Fig. 7. Calculating an insulator’s surface area using Autocad

B. Results

In order to classify a Site’s Pollution Severity (SPS) to the three basic classes (light, medium, heavy), slightly different ranges of ESDD measurements have been proposed by IEC [3], IEEE [17] and CIGRE [18]. The IEC values are given through an ESDD-NSDD diagram and have relatively large cross-areas, therefore the more specific IEEE [17] and CIGRE [18] values shown in Table I are used in this paper. Results are shown in Figures 8a and 8b for IEEE and CIGRE limits respectively. It should be noted that further splitting up of the three basic classes (e.g. using a “very light” [3] or a “very heavy” SPS class [18]) has been avoided, in order to produce easily comparable results. Further, IEC [3] has suggested that the distance from the sea (or other pollution sources) could be considered as an indication, especially when there are no other measurements. Since the actual distance can not be conducted from the images and the size of the marker icon may be misleading, the minimum distance of each tower from the sea is presented in Figure 8c. Further, the altitude for each tower is shown in Figure 8d.

Coastal towers of low altitude are mainly selected. As shown in Figure 8, 27 of 35 towers have a distance of less than

5 km from the sea and 28 of 35 have an altitude of less than 200 m.

Table I. SPS and ESDD values

SPS	ESDD value (mg/cm ²) (IEEE) [17]	ESDD value (mg/cm ²) (CIGRE) [18]
light	<0.06	<0.06
medium	0.06-0.10	0.06-0.12
heavy	>0.10	>0.12

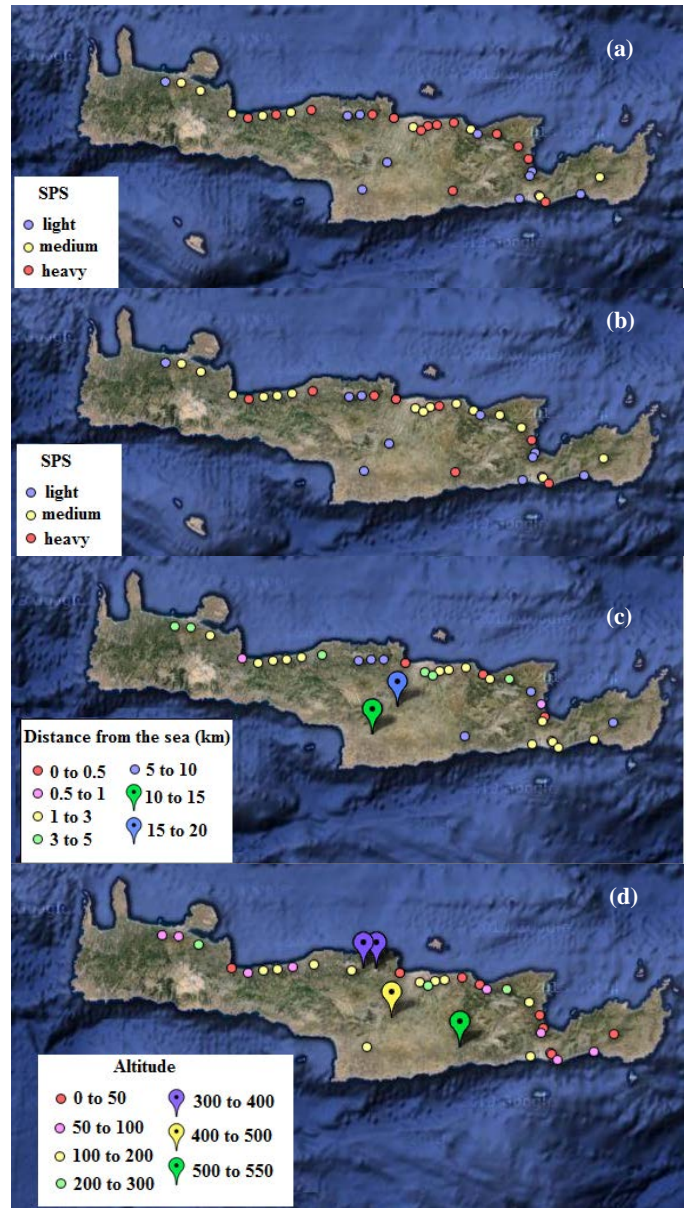


Fig 8. (a) SPS classes according to IEEE (b) SPS classes according to CIGRE (c) the minimum distance from the sea for each tower (d) the altitude of each tower

As shown in Figure 8 some locations changes classes when moving from IEEE to CIGRE limits. This shows that a more tolerant approach as the one proposed by IEC [3] is probably closer to reality, even though a strict definition is usually preferred by utility engineers. Further, it shows that added

measurements such as NSDD and DDDG could prove helpful in providing a more accurate classification. In addition it should be noted that the highest tower (529 m) also shows increased pollution severity (falls in the “heavy” SPS class) even though it is in a relatively long distance from the sea (6.7 km). Although additional research is required to define the impact of lower altitude variations on pollution deposition, nevertheless this result may be an indication of the multivariate procedure behind SPS definition.

An added strong conclusion is best portrayed in Figure 8b. As shown the proximity to pollution sources, mainly the coast and large cities, is proven to be a key factor for heavier pollution. However, rainfall patterns and wind direction is also to be considered. As shown in Figure 8b, heavy pollution has been recorded next to Iraklion, Rethimnon, Agios Nikolaos and Ierapetra. However, not near Chania even though Chania is larger than Agios Nikolaos and Ierapetra. This verifies the different conditions experienced on the west part of the island as described earlier in this paper. Further, the measurements conducted on coastal towers located in the south part of the island shows a lighter pollution image which should be largely attributed to the direction of the experienced winds which is mostly north-west.

IV. CONCLUSION

Assessing the pollution of outdoor high voltage insulators is an important piece of information for power utilities. Several approaches can be followed to map the experienced pollution depending on the available time and funds. Crete is a Greek island located in the Mediterranean which offers a valuable case study for pollution of outdoor insulators due to its location, shape, climate and power network design. Marine pollution is the dominant pollution form experienced by the island’s power network. The Greek power utility has employed several remedies to cope with the problem and has also participated in several research schemes that investigate the phenomenon’s various different aspects, including pollution mapping. Various factors are considered and presented in this paper: the island’s morphology and location, the experienced weather and climate, the network’s development, past fault and maintenance experience as well as pollution measurements conducted on 35 different spots throughout the island. The island’s pollution profile is portrayed through the use of descriptive maps. The overall conclusion is that pollution mapping is a rather complex procedure and even though the distance from the sea is a strong indication, additional data such as the distance from other pollution sources as well as wind strength, wind direction and rainfall patterns should also be considered.

V. FUTURE WORK

As mentioned in paragraph III, the exact definition of a correlation factor should be established in order to define SPS classes when ESDD measurements are conducted on fog profile insulators (instead of the reference disc profile). In this paper, we have followed the worst case scenario described in

[15] by setting the correlation factor equal to 1.1. However, further research should be conducting toward this direction in order for the correlation factor to be more accurately defined. Therefore, a specially designed arc has been installed in TALOS High Voltage Test Station where parallel ESDD measurements can be conducted on different insulators and the first series of measurements will be initiated in 2014. Further, setting up and initiating a series of NSDD and DDDG measurements is also a goal set for 2014.

ACKNOWLEDGMENT

This work was partially supported by the POLYDIAGNO research project (project code 11SYN-7-1503), which is implemented through the Operational Program “Competitiveness and Entrepreneurship”, Action “Cooperation 2011” and is co-financed by the European Union (European Regional Development Fund) and Greek national funds (National Strategic Reference Framework 2007 - 2013).

REFERENCES

- [1] J. S. T. Looms, *Insulators for High Voltages*, IET, 1988
- [2] CIGRE WG 33-04, TF 01: *A review of current knowledge: polluted insulators*, CIGRE, 1998
- [3] IEC/TS 60815, *Selection and dimensioning of high-voltage insulators intended for use in polluted conditions*, International Electrotechnical Commission, 2008
- [4] R. Hackam, Outdoor HV composite polymeric insulators, *IEEE Transactions on Dielectrics and Electrical Insulation*, Vol. 6, No. 5, pp. 577-585, Oct. 1999
- [5] E. A. Cherney, R. S. Gorur, “RTV silicone rubber coatings for outdoor insulators”, *IEEE Transactions on Dielectrics and Electrical Insulation*, Vol. 6, No. 5, pp. 605-611, Oct. 1999
- [6] K. Siderakis, D. Pylarinos, “Room temperature vulcanized Silicone Rubber coatings, Application in high voltage substations”, in: *Concise Encyclopedia of High Performance Silicones*, John Wiley & Sons Inc, USA, 2014
- [7] E. A. Cherney, A. El-Hag, R. S. Gorur, L. Meyer, I. Ramirez, M. Marzinotto, J. George, “RTV silicone rubber pre-coated ceramic insulators for transmission lines”, *IEEE Transactions on Dielectrics and Electrical Insulation*, Vol. 20, No. 1, pp. 237-244, Feb. 2013
- [8] M. Farzaneh, W. A. Chisholm, *Insulators for icing and polluted environments*, John Wiley & Sons Inc, USA, 2009
- [9] J. Stefanakis, E. Thalassinakis, K. Siderakis, D. Agoris, E. Dialynas, “Fighting Pollution in the Cretan Transmission System. 25 Years Experience”, presented at the Contamination Issues on High Voltage Installations conference, Iraklion, Crete 2001 (available at: http://talos-ts.com/files/2001_CIHVI.pdf)
- [10] S. Gubanski, “Greek power company evaluates alternatives to combat pollution in transmission system on Crete”, *INMR*, Vol. 10, No. 4, Page 30, 2002
- [11] E. Thalassinakis, J. Stefanakis, K. Siderakis, D. Agoris, “Measures and techniques against pollution in the Cretan transmission system”, presented at the 2nd IASTED European Conference on Power and Energy Systems (EuroPES), Crete, Greece, June 25-28, 2002 (available at: http://talos-ts.com/files/2002_IASTED-2.pdf)
- [12] K. Siderakis, D. Pylarinos, E. Thalassinakis, E. Pyrgioti, I. Vitellas, “Pollution maintenance techniques in coastal high voltage installations”, *Engineering, Technology & Applied Science Research*, Vol. 1, No. 1, pp. 1-7, 2011
- [13] Public Power Corporation/ Islands Network Operations Department, 2010 Internal Report, 2010
- [14] K. Siderakis, J. Stefanakis, E. Thalassinakis, D. Agoris, E. Dialynas, “Coastal Contamination of the High Voltage Insulators in the Cretan Power System”, presented at the 2nd Mediterranean Conference on Power Generation, Transmission, Distribution and Energy Conversion, IEE Conference Med Power 2000, Herzlia, Israel, November 13-15, 2000 (available at: http://talos-ts.com/files/2000_MEDPOWER.pdf)

- [15] CIGRE WG C4.303, Outdoor insulation in polluted conditions: guidelines for selection and dimensioning, CIGRE, 2008
- [16] TALOS High Voltage Test Station, www.talos-ts.com
- [17] IEEE Std 1313.2-1999, *IEEE Guide for the Application of Insulation Coordination*, The Institute of Electrical and Electronics Engineers, 1999
- [18] CIGRE WG B2.03, Guide for the establishment of naturally insulator testing stations, CIGRE, 2007

Dionisios Pylarinos received a Diploma degree in Electrical and Computer Engineering in 2007 and the Ph.D. degree in the same field in 2012 from the University of Patras, Greece. He is a researcher/consultant for the Public Power Corporation Greece and the Hellenic Electricity Distribution Network Operator, Greece since 2008, in the field of HV insulator testing and monitoring and he is a part of the team behind Talos High Voltage Test Station. He is a member of the Technical Chamber of Greece and of the Greek National CIGRE Committee. His research interests include outdoor insulation, electrical discharges, leakage current, signal processing and pattern recognition.

Kiriakos Siderakis was born in Iraklion in 1976. He received a Diploma degree in Electrical and Computer Engineering in 2000 and the Ph.D. degree in 2006 from the University of Patras, Greece. Presently, he is an Assistant Professor at the Department of Electrical Engineering, at the Technological Educational Institute of Crete. His research interests include outdoor insulation, electrical discharges, high voltage measurements and high voltage equipment diagnostics and reliability. He is a member of the Greek CIGRE and of the Technical Chamber of Greece.

Ioannis Pellas was born in Ptolemaida in 1956. He received a degree in Engineering from the Technological Educational Institute of Crete in 1978 and joined the Public Power Corporation in 1981, where he is now the Head Engineer of the Transmission Lines Department of the Islands Network Operations Department of the Hellenic Electricity Distribution Network Operator S.A., a former part of PPC.

Emmanuel Thalassinakis received the Diploma in Electrical and Mechanical Engineering and also the Ph.D. degree from the National Technical University of Athens. After working for the Ministry of the Environment, in 1991 he joined the Public Power Corporation (PPC). He is the Assistant Director of the Islands Network Operations Department of the Hellenic Electricity Distribution Network Operator S.A., a former part of PPC.

Solar Powered LNG Regasification: Enhancing Power Generation and Water Desalination

Asad A. Salem¹, and Emad Hudiab²

¹ Professor of Engineering, Marshall University, Huntington, WV, USA (salema@marshall.edu)

² Project Engineer, SGS North America, Houston, TX, USA (emad_me2006@hotmail.com)

Abstract- This paper has proposed a solar energy powered Liquefied Natural Gas (LNG) regasification system that incorporates a water desalination process utilizing the cold energy available in the LNG. The solar energy is utilized in an air humidification unit, where hot and saturated air is produced. This saturated and hot air is employed by a LNG regasification unit which converts LNG to natural gas (NG). During the regasification process, the hot and saturated air is cooled below the Dew-point temperature producing a sizable amount of fresh water. The proposed system is tested under various conditions of temperatures and relative humidity. The results show that there is a substantial increase in the efficiency of the gas turbines (GT) which translated to the efficiency of the power plant as a result of cooling the air that is fed to the GT. A model of the proposed regasification system in a capacity of 28 million cubic meter/day (MCMD) (19120 ton/day) is considered, the expected fresh water production for this proposed model is around 6.5 million liter per day, the produced cold dry air of this proposed regasification technique would enhance the power output of the attached gas turbines by 5-20%. The proposed system is a mix of various technologies and a proposal for the better utilization of energy to generate power.

Keywords- LNG; Regasification; Solar Energy; Desalination

I. INTRODUCTION

Liquefied Natural Gas (LNG) is a natural gas that has been cooled to a temperature of $-161\text{ }^{\circ}\text{C}$ where it turns to liquid. Liquefaction reduces the volume of the natural gas (NG) by 600 times which makes it more practical to be shipped and transported through specially designed vessels. The shipped gas is received via either onshore or offshore receiving terminals [2].

Onshore and offshore LNG receiving terminals have been built around the world responding to the increased demand on the imported LNG to these receiving terminals.

The demand on natural gas is expected to keep growing for the coming decades as it is illustrated in figure 1. Rising demand on LNG creates incentives for new importing facilities, given that the existing facilities (even considering planned expansion) are not expected to give enough capacity to handle the eventual volumes of imported LNG [1].

At those terminals the LNG vessels are connected to the receiving terminals as part of a complete chain of processes of handling the

LNG to be vaporized into NG which is used to be conveyed through the NG pipelines to the final destination in the NG fueled electric power plants any others [2].

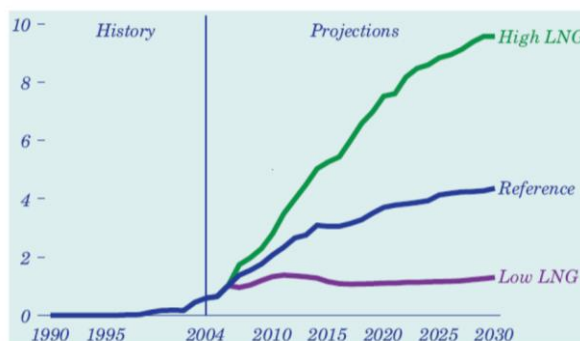


Figure 1: LNG Import Demand (US EIA) [1]

The LNG regasification process can be conducted through adapting several types of vaporizers; each type of vaporizers has its own advantages and disadvantages.

The traditional type of vaporizers is the gas fired vaporizers, or what is commonly called submerged combustion vaporizers SCV (refer to figure 2), SCV is commonly used in US and it is industry proofed with efficient heat transfer, while its main disadvantages are the high operation cost, as 1.5 to 2 % of the vaporized LNG will be fired to serve the regasification process, and the SCV results in acid water that is required to be treated, moreover; the air emission is another environmental impact of SCV such as CO_2 , CO , and NO_x [3] [6].

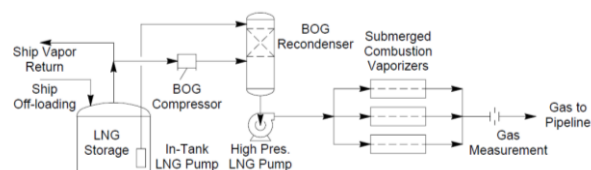


Figure 2: Schematic of SCV [6]

The other common technique in LNG vaporization is the falling film, open rack (ORV), sea-water vaporizers; in which the LNG is introduced through manifold to bank of vertical panels constructed of special extruded fins, on which the heat transfer between the sea water and the LNG is taking place and the natural

gas will be collected through a manifold connected to the NG pipeline [3]. The main advantage of open rack type (ORV) is the low emissions and better economy compared to SCV, but it has restrictions and impact on the seawater quality, and using the seawater results in higher corrosion rate for the pipes and the heat exchangers that requires more frequent preventive maintenance and applying anti-corrosive measures, figure 3 illustrates the schematic of the ORV [7].

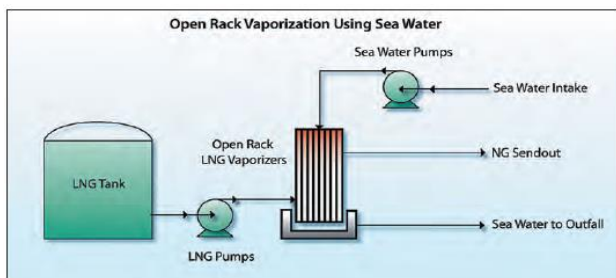


Figure 3: ORV schematics [7]

The recent trend in the LNG regasification is using the atmospheric heat exchangers as a competitive replacement for both SCV and ORV, but in general the LNG industry is very slow in accepting new technologies due to large investment cost and the risk implied in such change [5], in this regard Mustang Engineering LP developed a vaporizer using the atmospheric heat exchangers called SAV (Smart Air Vaporizer), in which the vaporizer relies on air instead of either gas or seawater, better process economy, higher versatility as it can be mounted onshore, offshore, or on board of LNG carriers (vessels), environmental friendly but requires supplemental heat source [4]. Figure 4 shows a schematics of the SAV provided by Mustang Engineering [6]

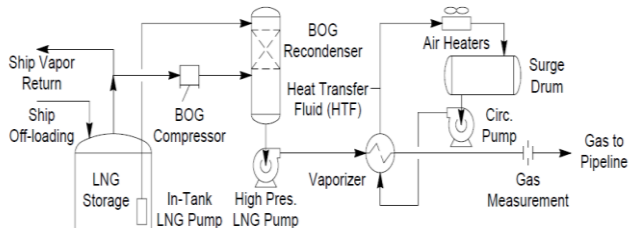


Figure 4: SAV provided by Mustang Engineering [6]

II. METHODOLOGY

The objective of this proposed work is to develop a LNG regasification plant that is powered by a renewable energy source and to utilize the synergy of the LNG to enhance the efficiency of power generation systems and to couple the regasification plant with water desalination system. Concentrated solar energy will be used to heat ambient air, this heated ambient air is, then, introduced to a humidification process. Though this humidification process the heated ambient air will reach saturation and will be exposed to LNG via a heat exchanger. During this exchange of energy the evaporation of the LNG will

take place and the saturated hot air is cooled below the dew point where fresh water is produced as a result of this energy exchange. The evaporated NG will go through additional heating, and then introduced to gas turbines along with cold dry air for combustion. The introduction of dry cold air enhances the efficiency of the gas turbines. This new process produces fresh water, enhance the efficiencies of gas turbines and reduces the carbon footprint of such technologies. Hence, improving the economics of the LNG regasification systems and produce useful by-products that can be utilized to enhance the performance of power generation systems or in many other applications and subsequent downstream processes of the NG power stations.

The basic layout of the proposed LNG regasification system is divided into two main sub-cycles or systems as it is illustrated in figure 5; the LNG regasification sub-cycle and the air sub-cycle.

In the LNG sub-cycle, the LNG is pumped from the storage tank (or the vessel) to the regasification heat exchangers; in which the LNG will turn into NG and heated through the hot humid air blown through the air sub-cycle, the natural gas can be conveyed through the NG pipeline to the attached gas turbines in the power stations.

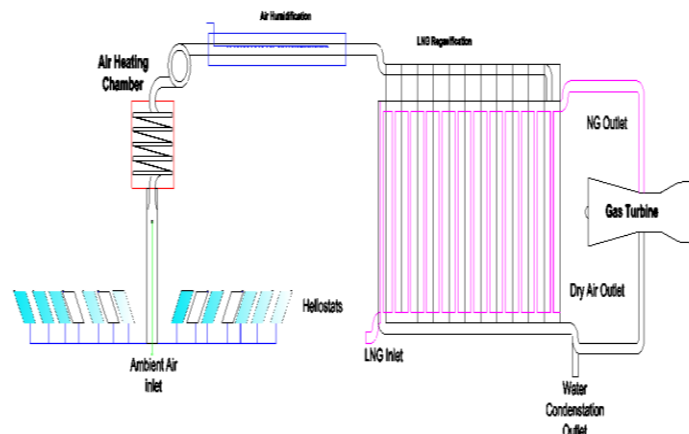


Figure 5: A Schematic of the Proposed LNG Regasification Plant

While on the air sub-cycle; the available humid air is being heated and humidified relying on the available solar energy collectors, the saturated humid air at high temperature is blown through the vaporization heat exchangers, which will transfer the heat toward the cold LNG sub-cycle, the outcome of air sub-cycle will be a cold dry air and cold water both at the temperature of outgoing NG of LNG sub-cycle.

III. PROPOSED REGASIFICATION PLANT

The solar irradiance is collected and concentrated through the heliostats (solar tracking mirrors), which is arranged in a clusters

to focus the solar incident into the air heating chamber (receiver); which is filled up with a heating media (molten salt) that is including the submerged air heating pipeline; in which the ambient air is heated up and conveyed using a suction fan (attached to the gas turbines) toward the humidification unit, in this unit the sea water is misted and introduced to the hot air pathway which leaves the humidifier saturated at 85 °C, this saturated hot humid air is acting as the heating source in the regasification heat exchangers that are designed to accommodate a counter flow for the sub-cooled LNG and the heating air, the process takes place on a massive heat transfer area which requires a smarter design for the flow and the heat exchanger geometry to come up with an efficient feasible regasification process.

The outgoing NG and the dry cold air would operate the connected gas turbines in the attached power generation stations, while the cold water which is the third by-product of this regasification process is potable fresh water that can be utilized in cooling applications as well.

The plant is designed based on the coldest climate along the year (the biggest estimated solar mirrors field) so the production will exceed the expected send-out rate during the summer and maintain the design send-out rates during the cold winter. Production fluctuation can be managed through an optimum plant operation scheme, in which the annual shutdown and periodic maintenance will be scheduled during the low production season (cloudy winter), and that would give a better chance for more focus on production during the peak summer season (higher demand on electricity, and air conditioning). The additional solar energy collected through the oversized solar field can be stored in terms of molten salt in a form of latent heat required for phase change (melting the salt), and that can accommodate the energy requirement for overnight operation.

IV. BASIC CONSIDERATIONS

- A. The LNG send-out rate is 28 MCMD.
- B. The LNG regasification is assumed to run under constant 1 atm pressure for simplicity, the LNG is assumed to consist solely of methane, and the regasification process is assumed to take place under constant pressure (1 atm).
- C. All the air, solar, and climate specific data have been adapted for Houston, Texas as the location in which the model is to be operated.

V. THE LNG –NG SUB-CYCLE

The LNG is pumped from the source toward the regasification heat exchangers, in which the LNG is heated from ($T_1 = -182\text{ °C}$) to the boiling point ($T_b = -162\text{ °C}$), on which the boiling process would take, then the gas is heated up to ($T_2 = 5$). The heating requirement for such process is served through the hot humid air provided by the air-solar sub-cycle, for the sake of simplicity; the

targeted send-out rate of the gas has been converted into mass flow which is equal to 221.3 Kg/s, and the total heating requirement is calculated based on the enthalpies of the LNG and NG in equation (1) and found around 208 MW.

$$Q_{LNG\ vap} = m'_{LNG}(h_2 - h_1) \tag{1}$$

Where:

$Q_{LNG\ vap}$: LNG required thermal power KW.

m'_{LNG} : LNG send-out mass flow rate Kg/s.

h_2 : NG Specific Enthalpy ($T_2 = 5^\circ\text{ C}$) KJ/Kg.

h_1 : NG Specific Enthalpy ($T_1 = -182^\circ\text{ C}$) KJ/Kg.

$$m'_{Humid\ Air} = Q_{LNG\ vap}/\Delta h_{Humid\ Air} \tag{2}$$

Where:

$m'_{Humid\ Air}$: Required saturated humid air mass-flow rate required for vaporization process in Kg/S.

$Q_{LNG\ vap}$: LNG Regasification required Thermal Power KW.

$$\Delta h_{Humid\ Air} = C_{p\ da}\Delta T_a + X_s(C_{p\ w}\Delta T_a + h_{we}) \tag{2.1}$$

Where:

$\Delta h_{Humid\ Air}$: Specific enthalpy change in humid water to reach saturation over the ΔT_a .

$C_{p\ da}$: Specific heat of dry air KJ/Kg. °K.

ΔT_a : Change of air temperature during the LNG vaporization process °C.

X_s : Absolute humidity at saturation level Kg_{vap}/Kg_{air}

$C_{p\ w}$: Specific heat of water vapor in KJ/Kg. °K.

h_{we} : Latent heat of vaporization of water which is assumed here 2504 KJ/Kg

Though and optimization process and based on equations (1) and (2), the required air mass-flow rate of the targeted saturated humid air ($T = 85\text{ °C}$) is 90 Kg/s is required in this process; and 76 kg/s of water can be extracted from a total flow of saturated humid air of about 90 Kg/s.

It has been a challenge to accurately estimate the enthalpy of the ambient air along the year in Houston. We have employed an extended experimental data and equation (2) with slight modification, as X_s has been located for each average monthly temperature from the humid air table in chapter 6 of reference [14], then calculating the ($X_{ambient\ air} = RH\% \times X_s$) and plug it in the equation above to find the enthalpy of ambient air (h_i) as per table 1.

Table 1: Estimated air mass-flow rate, humid air heating requirements, and solar collectors estimated area

Month	h_w (KJ/Kg)	h_a (KJ/Kg)	X_s (Kg/Kg)	h_i (KJ/Kg)	Power (MW)	Collecte (Km ²)
Feb	35.3	12.6	0.0094	12.85	206.9	1.50
April	58.7	20.2	0.0514	20.86	206.1	1.34
June	84.64	27.0	0.0226	28.49	205.5	1.17
Aug	89.49	28.1	0.0241	29.72	205.3	1.15
Oct	61.42	20.2	0.0160	20.91	206.1	1.15
Dec	34.05	11.8	0.0088	12.03	207.0	1.99

VI. AIR FLOW FAN REQUIRED POWER

Fan selection starts with a basic knowledge of system operating conditions: air properties (moisture content, temperature, density, contaminant level, etc.), airflow rate, pressure, and system layout. This condition determines which type of fan—centrifugal or axial—is required to meet service needs [15].

The air flow rate required for the regasification process effect the energy consumption of this proposed system, the mass flow rate estimated for the targeted regasification rate is around 90 kg/s, the power consumed by the fan to deliver such mass flow rate can be briefly estimated using the following equation:

$$P_{Air\ fan} = \frac{(P_t \times V'_{air})}{(\mu_f \times \mu_b \times \mu_m)} \quad (3)$$

Where:

- $P_{Air\ fan}$: Power required by fan (W).
- P_t : Total pressure (Pa)
- V'_{air} : Humid air volumetric flow-rate (m^3/s).
- μ_f : Fan efficiency (%).
- μ_b : Belt efficiency (%).
- μ_m : Motor efficiency (%).

In a counter-flow heat exchanger in which the LNG is being heated through the counter-flow of the humid air blown around the heat exchange surfaces, and assuming full flow condition and overall heat transfer coefficient of is estimated to be around 21 ($W/m^2.K$) under atmospheric pressure; the estimated required area for vaporization and heating of LNG (refer to equation 4) is about 75000 m^2 (using the logarithmic mean temperature difference - LMTD [12]; which indicates a sizable heat exchanger (10 x 6x 6 meter plate heat exchanger) is required for such process. The ambient air (which varies along the year) of the selected site (Houston is adapted here) is pumped through the heat exchanger in which the molten salt heats up the air up to 85 °C passing through the attached humidifier to reach the saturation state, before being pumped through the regasification heat exchanger of the LNG-NG sub-cycle, the

heat requirement for the air to reach the targeted temperature and humidity is served through the proposed solar system which varies according to the average monthly temperature and humidity, the required average heating requirement is calculated using equation (2), in which the heating requirement is calculated as the difference in the enthalpies of both humid air (at the ambient average monthly temperature) and the enthalpy of saturated air at 85 °C.

The required area of the solar collectors will vary according to the monthly fluctuation in the temperature and humidity of the ambient air in Houston along the year, table 4 summarizes the heating requirement and the area of the solar collectors to serve the air heating (required for regasification process) in each month along the year in Houston based on equation 4.

$$A_{solar} = \frac{Q_{LNG\ vap}}{Q_{solar\ Irradince}} \quad (4)$$

Where:

A_{solar} : Required area of solar collecting mirrors to produce $Q_{LNG\ vap}$ in m^2 .

$Q_{solar\ Irrad.}$: Average sun irradiance power KW/m^2 , (estimated based on reported irradiance) [10].

The heating requirements for the regasification is served through the solar collecting mirrors (Heliostats) concentrating the solar irradiance into the heating chamber in which the heating media will be utilized to heat up the air being pumped through, and then through the humidifiers where a sea water will be misted in the air pathway to reach the saturation at 85 °C, which in turn is utilized in LNG regasification heat exchangers.

The heating chamber includes the air heating pipeline which is submerged in the molten salt which acts as the heating and thermal storage media as per the schematic shown in figure 6.

The molten salt used in CSP (concentrating solar power) proved to be a sufficient heating media that may reach up to 565 °C, and may store the heat after sunset up to 6 hours (the molten salt consists of 60% Sodium Nitrate and 40% Potassium Nitrate), the primary advantages of molten nitrate salt as the heat transfer fluid for a solar power tower plant include a lower operating pressure and better heat transfer properties. This translates into a smaller, more efficient, and lower cost receiver and support tower [17]. The hot humid air (which is acting as the heating media to vaporize the LNG) can be further heated. But, it has been noticed that higher temperatures would result in higher moisture content capabilities under saturation condition. That results also in lower requirements for air mass-flow and higher heating energy requirements to accommodate high latent heat of water vaporization, so among other scenarios of humid air temperatures in the range of 85-90 °C would form the optimum operation temperature as it can be noticed in figure 7.

While the increase in temperature results in raising the required heating energy; the expected condensate flow rate will not be improved in the same manner, notice the major increase in heating demand versus the minor increase in water condensation rate as we increase the operating temperature.

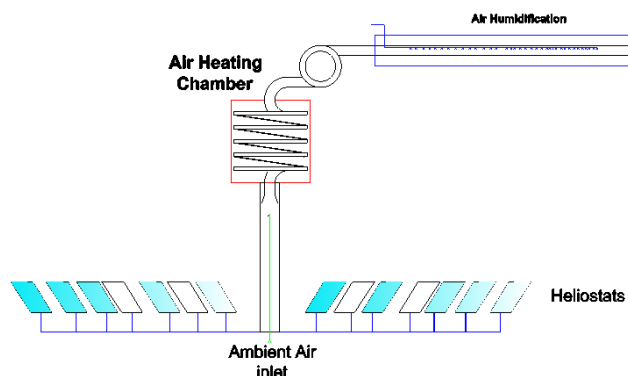


Figure – 6: Heating and humidifying air using CSP Tower.

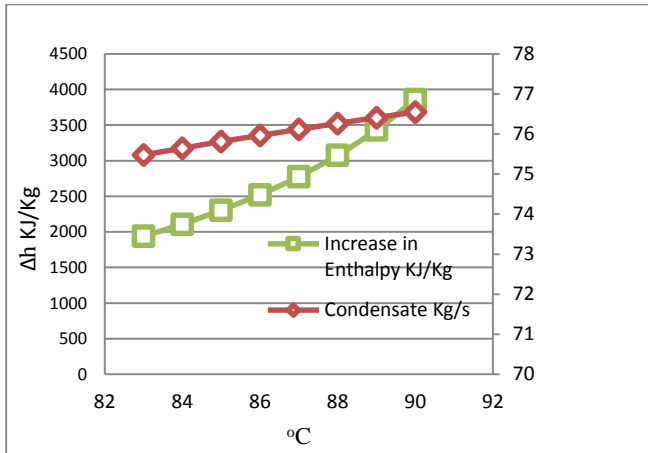


Figure 7: Effect of increasing temperature on the increase of specific enthalpy required for regasification and the expected increase in condensate flow.

VII. THE ENHANCEMENT EFFECT ON GAS TURBINE PERFORMANCE

In addition to the fresh water the proposed system will result in a sensible flow rate of cold dry dense air, which can be connected to the attached gas turbine air-intake.

The effect of intake air temperature and humidity is affecting the performance of the gas turbine, as the air is cooled and the humidity is reduced the performance of the gas turbine is improved proportionally [16], figures 8 and 9 shows the trend of the turbine performance versus the air temperature and humidity respectively. In figure 9 it is noticeable that the output line is improved as we reduce the temperature, so if we consider the ambient condition in Houston on November is 16 °C, so using the 5 °C by-product cold air of the proposed regasification system would improve the output power with almost 5%, and by about 15-25% during summer while the absolute dry air would be more dense and as per figure 9; the power output would be improved as well.

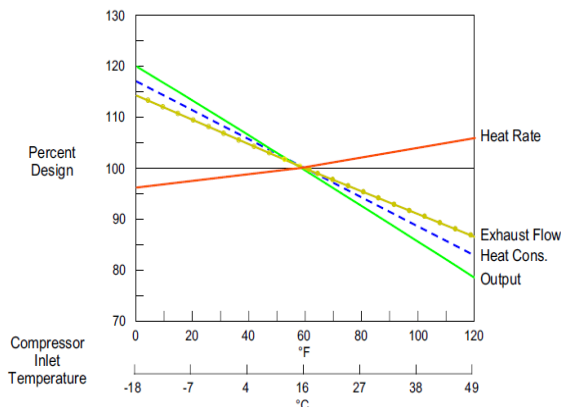


Figure 8: Effect of intake air temperature on Gas Turbine (GE MS7001) Output [17]

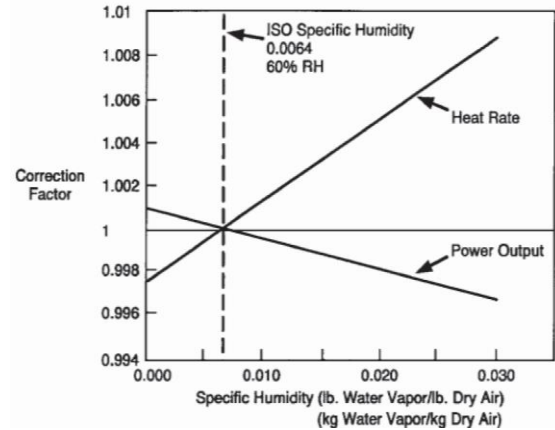


Figure 9: Effect of intake air humidity on Gas Turbine Output [17]

The proposed model is powered by solar energy collected by concentrating mirrors which reflect high intensity solar energy into a heating chamber in which the heat is stored in form of molten salt that is used to heat up and humidify the ambient air to the targeted temperature and humidity. Table 2 summarizes the average values of the proposed model parameters.

The proposed regasification plant is designed on the least solar heating capabilities of December in Houston, which requires around 2 Km² solar collection areas, of course this will not eliminate the fluctuation in regasification send-out rate along the year, but that can be optimized through adapting smart operation schemes in which the annual shutdown of the plant will be conducted in the least production month, while the shortage of production will be compensated within the expected excess production during the peak production season in summer.

Table 2: The Proposed Model Annual Average Parameters

LNG out R <i>MCMD</i>	LNG out R <i>Kg/S</i>	Humid Hot air mass flow <i>Kg/S</i>	Condensate flow rate <i>Kg/S</i>	Dry Air flow rate <i>Kg/S</i>
28	221.3	90.25	75.81	14.44
Avg. requi Solar Pow (<i>MW</i>)	Avg. Sola Collection Area (<i>Km</i>	Avg. Solar Irradiance (<i>KW / m² / da</i>	Avg. Relati Humidity (%)	Avg. Tempera e (<i>°C</i>)
206.14	1.40	3.66	74.75	20

VIII. CONCLUSIONS AND DISCUSSION

Implementing the proposed LNG regasification technology relying on solar energy as the power source will provide the industry with a sustainable environmental friendly solution; this

proposed technique is expected to come up with the following advantages:

1. An efficient and productive LNG regasification technique, that will cut on the cost of the LNG regasification process, using solar power tower in which the solar power will be collected through mirrors and will be used to heat up an intermediate heating liquid (molten salt) which will heat up the humid air, which in turn will be blown through the heat exchangers of the LNG receiving terminals to vaporize the LNG.
2. As an added value to the NG power plants efficiency, the air resulting from the LNG regasification process will be cold dens dry air, which can improve the combustion of the attached gas turbines of the relevant power plants.
3. One of the expected valuable by-products in this proposed LNG regasification technique is the fresh water which will be as condensate resulting from the vaporization heat exchangers, for this plant it is expected to produce around 270 m^3 /hour of plant operation; this chilled water can serve as fresh water source and for cooling applications.
4. The efficiency of collecting solar power through the floating mirrors is expected to be higher as the issue of dust accumulation on the mirrors will be minimized compared to the conventional onshore solar concentrating mirrors in case the plant is erected offshore, but of course the cost element should be considered.
5. Relying on renewable resources such as solar may not be reliable everywhere and along the year due to the fluctuation of the availability of these resources, but for a climate like Houston it is promising and feasible technique.
6. Costly investment is needed to realize the proposed renewable powered LNG Regasification process compared to the conventional systems, but the expected pay back and low maintenance of the proposed system may make it the optimum choice for some areas which has a warmer and humid conditions such as in the USA, India, South East Asia, Southern Europe, the Middle East, and others where the LNG is used widely in power generation and there is an increasing demand for fresh water as well.

REFERENCES

- [1] Michelle M Foss, "Offshore LNG Receiving Terminals", CEE, Bureau of Economic Geology, Jackson Scholl of Geosciences, University of Texas, Austin. November, 07, 2006.
- [2] Michelle M Foss, "Introduction to LNG", CEE, Bureau of Economic Geology, Jackson School of Geosciences, University of Texas, Austin.
- [3] Pelto, P.J.; Baker, E.G.; Holter, G.M.; Powers, T.B., "An Overview Study of LNG release Prevention and Control Systems", Pacific Northwest Lab operated for US Department of Energy by Bettelle Memorial Institute, under contract DE-AC-06-76-RLP -1830. March 1982.
- [4] Mustang Engineering LP," LNG Smart Air Vaporization (SAV)" presented to LNG Interagency Working Group, Hercules, California, December, 07, 2006.
- [5] Tom Dendy, "Utilization of Atmospheric Heat Exchangers in LNG vaporization processes: a comparison of systems and methods", SPX Corporation, Houston, Texas.
- [6] Kyle T. Cuellar, " Economical Options for Recovering NGL/PGL at LNG Receiving Terminals", Ortloff Engineers Limited, Houston- TX, Presented to "86th Annual Convention of the Gas Processor Association" on March , 13 , 2007, San Antonio, Texas.
- [7] Brian Eisentrout, Steve Wintercorn, and Barbara Weber, "A Study on Six LNG Regasification Systems", LNG Journal, July/August 2006, pages (21-22).
- [8] The International Group of Liquefied Natural Gas Importers - GIIGNL, "Basic Properties of LNG " – LNG Information Paper No. 1, Web address: <http://www.giignl.org>.
- [9] U. Setzmann and W. Wagner, "A New Equation of State and Tables of Thermodynamic Properties for Methane Covering the Range from Melting Line to 625 K at Pressures up to 1000 MPa", Institute for Thermo and Fluid-dynamic – Republic of Germany, received on June 1990.
- [10]The solar and weather publication of NREL: WBAN No. 12960, Weather Station Type: Secondary, Latitude: 29.98 ° north, Longitude: 95.37 ° west. <http://rredc.nrel.gov/solar/pubs/redbook/PDFs/CA.PDF>
- [11]Zoran K. Morvay, D.D. Gvozdenac, "Applied Industrial Energy and Environmental Management, Part III – Toolbox: Thermodynamic and Transport Properties of Moist Air." © John Wiley & Sons, Ltd.
- [12]Leinhard John H V and Leinhard John H IV, " A HEAT TRANSFER TEXTBOOK", 3rd Edition, published by J. H. Leinhard V, Cambridge, Massachusetts, USA.
- [13]Cong Den, Joseph Cho, Jay Yang, "COST-EFFECTIVE LNG REGASIFICATION WITH MULTI-TEMPERATURE LEVEL (MTL) AIR HEATERS ",SK Engineering & Construction Co. Ltd. Houston, Texas USA. www.skec.com
- [14]ASHRAE Fundamentals Handbook (SI) – Chapter 6: PSYCHROMETRICS, ©2001 by the American Society of Heating, Refrigerating and Air-Conditioning Engineers, Inc.
- [15]Gary Benson and others, "Improving Fan System performance: A source book for Industry", developed by US Department of Energy – DOE Industrial Technologies Program and the Air Movement and Control Association International Inc. (AMCA) - DOE/GO-102003-1294 April 2003
- [16]Salem, A; R. G. Mathews , and A. K. Mathew, "LNG Energy Conversion Power Plant", USCUDAR 12, pp 113-118, ISBN:978-1-61804-132-4
- [17]Frank J. Brooks," GE Gas Turbine Performance Characteristics", GE Power Systems, Schenectady, NY, GER- 3567H.
- [18]Craig E. Tyner, J. Sutherland, and W. R. Gould,"Solar Two: A Molten Salt Solar Power Demonstration", consortium of Sandia National Laboratory, Southern California Edison Company – SCE, and sponsored by DOE, under contract No.DE-AC0494ALd3500.

Credit Risk Evaluation And Analysis On Chinese Commercial Banks Using Logistic Model

Xiaorong Zou

Leonardo Investment Ltd, United Kingdom

(Email: xiaorongzouuk@126.com)

Abstract—With high loan demand of manufacturing enterprises, the management efficiency is vulnerable to be disturbed by macroeconomic risks. Therefore, the breach of contract will result in the huge fluctuation in domestic financial industry. In this paper, Logistic model was used to evaluate credit risks of commercial banks and manufacturing enterprises. Firstly, according to the status quo of depressive manufacturing industry impacted by macroeconomic form, further resulting the declining of bank credit assets quality, some empirical data of manufacturing listed companies are selected specially, and the data of selected index shall be published for transparency. Secondly, data analysis was processed by not only the conventional financial index, but also non-financial index, such as ownership structure, board structure and enterprise scale. Finally, to clear and distinct the extracted variable factors, to better explain and elaborate on the actual economic issues, the indexes are divided into financial index and non-financial index, the financial index is further divided into four types, with each type being factor analyzed separately. Combined with the macroeconomic trend, and according to the results obtained from model, the possible fluctuations resulted by the default of manufacturing enterprises have been made the summary analysis.

Keywords: Credit Risk Evaluation, Chinese Commercial Banks, Logistic Model.

I. INTRODUCTION

With financing difficulty of manufacturing enterprise loan, manufacturing enterprises urgently need large scale funds for recruitment, expanding production, product research and development, improving their competitiveness and getting bigger and more prosperous [1]; however, due to banks are in lack of a full set of reasonable and effective method and basis for manufacturing enterprises to measure and manage the credit risks, as well as determining the loan financing of manufacturing enterprises, the credit decision and loan commitment can't be offered promptly for all the time[2]. Meantime, with high loan demand of manufacturing enterprises, the management efficiency is vulnerable to be disturbed by macroeconomic risks; therefore, the breach of contract will result in the huge fluctuation in domestic financial industry.

Logistic regression model is the most commonly used in the banking industry due to its desirable features. To improve the prediction accuracy of logistic regression, logistic regression with random coefficients is proposed. The proposed model can improve prediction accuracy of logistic regression without sacrificing desirable features [3]. In [4], a brute force logistic regression modeling approach is proposed and used to develop predictive credit scoring model for corporate entities. The modeling is based on 5 years of data from end-of-year financial statements of Serbian corporate entities, as well as,

default event data. To the best of our knowledge, so far no relevant research about predictive power of financial ratios derived from Serbian financial statements has been published. The primary objective of this study is to determine network-level project sections for effective sustainable pavement management using logistic regression analysis. A huge volume of inventory data documented from pavement management information systems was used to develop the logistic regression model for selecting candidate sections [5]. In order to explain Enterprise risk management applications with profitability, leverage and company size a Logistic Regression model was established. As a result of the analysis it was determined that about half of the financial sector companies within the Istanbul Stock Exchange employed a chief risk officer, which means a culture of risk management has been founded within these companies [6]. The goal is to characterize future trends in the generation of obsolete computers in the U.S. Starting from historical sales data on new computers and assuming a plausible first lifespan distribution, they extrapolate the historical sales trend to the future using a logistic model. The approach is to use a bounding analysis which characterizes a range based on plausible upper and lower bounds on the future carrying capacity. This analysis does not address how long obsolete computers are stored nor the distribution of obsolete computers to reuse, recycling, landfill options [7]. In [8], they provided a random effects logistic regression model to predict the default of funded the small and medium enterprises based on both financial and non-financial factors. Advantage of such a random effects model lies in the ability of accommodating not only the individual characteristics of each SME but also the uncertainty that cannot be explained by such individual factors.

In relevant literature about the management of commercial banks credit risks, the research samples are mostly involved in scattered industries, and short of the separate research on certain industry. This paper is based on the status quo of depressive manufacturing industry impacted by macroeconomic form, further resulting the declining of bank credit assets quality, some empirical data of manufacturing listed companies are selected specially, and the data of selected index shall be published for transparency. Therefore, this paper has some innovation in studying samples and data. In this context, this paper shall carry out analysis and comparison on various credit measure models of commercial banks, furthermore select credit evaluation model which is more suit our manufacturing listed companies, and perform empirical research, try efforts to employ Logistic model to analysis the credit risks of manufacturing enterprises and establish credit risk assessment methods suit for our commercial banks [9]. Meanwhile, this paper puts forth some result outlook and

suggestion for future, which have important practical significance on resolving the financing difficulty of our manufacturing enterprises as well as improving the credit assets quality of our commercial banks[10]. This paper is also equipped with favorable guiding significance on practical economic operation, structuring a set of credit risk assessment model consist with the industry characteristics of manufacturing enterprises which take the largest proportion of listed companies, and also provides with technical support for commercial banks to perform strategic credit asset management. Its practical value is embodied in the following two aspects: improving the competitiveness of commercial banks and perfecting important references of stock market. The analysis on significant variable factors which influence credit risks can make banks profound and clear understanding on credit risks, and force banks to improve their own credit risk assessment and management level, to avoid loss resulted from credit crisis.

II. BRIEF INTRODUCTION FOR LOGISTIC MODEL

A. Logistic-model

Usually, we can employ linear and nonlinear probability model to carry out measurement and assessment on credit risks. When linear probability model being employed to carried out the risk measurement and assessment, the independent variable is too large of small, there are some defects: the obtained probability may exceed [0, 1] interval, therefore the obtained model result doesn't make sense. As a nonlinear probability model, Logistic model overcome the defects of linear probability model based on the following points: (1) this model doesn't require the hypothesis that independent variable conforms to joint normal distribution, and independent may be continuous, discrete, even dummy variable.(2) this model takes the form of nonlinear to ensure the obtained probability value meaningful. (3) Dependent variable is binary variable, this model can only take 0 and 1 to represent event occurrence or not. Therefore, the event occurrence probability can revert to the probability problem of dependent variable based on the value of 1, the result can be more direct, and the theory explanation can be more convenient. In this model, a dummy variable problem can be employed to predict default probability. Dummy variable, refers to the variable represent the attribute factors which are based on the value of 0 and 1. Dummy variable usually takes various types and levels, the value of 1 and 0 exhibit some certain status or attribute exist or not. In this paper, if enterprise defaults, the dummy variable shall take the value of 1, on the opposite, if the enterprise credit status is favorable and the dummy variable takes the value of 0. When Logistic model is taken for calculation, default probability or probability shall increase with the increasing of dummy variable takes the value of 1.

In this paper, some financial index, ownership structure, board structure, enterprise scale and other non-financial index are selected, and financial index are further subdivided. By selecting some sample data of manufacturing enterprises and carrying out factor analysis on each type of index, the variable factors with great significance can be selected, and Logistic model can be established to further predict the probability of

enterprise defaulting, analyze and explain the influence of important variable factors which impact on enterprise credit situation to the probability of enterprise defaulting.

The function expression of Logistic model as follows:

$$p = \frac{1}{1 + e^{[-\beta_0 - \beta_1 x_1 - \dots - \beta_i x_i]}} \quad i=1, \dots, K$$

In the expression, β_0 is the model intercept term, $x_i = (x_{1i}, x_{2i}, \dots, x_{Ki})^T$ is $K \times 1$ column vector, indicating each variable factors elected by model; $\beta_i = (\beta_{1i}, \beta_{2i}, \dots, \beta_{Ki})$ is $1 \times K$ column vector, indicating the determination coefficient of each variable factors.

Logit transform can be employed the above nonlinear into linear function:

$$\ln \left[\frac{p_i}{1 - p_i} \right] = \beta_0 + \sum_{m=1}^K \beta_{mi} x_{mi}$$

Based on the following reasons, this model is selected to carry out the measurement and assessment on manufacturing enterprise credit risks:

(1) If assumption condition is relaxed to better fits with the practical situation. For OLS regression model, the independent homo-distributivity and homoscedasticity is assumed, but as for Logistic regression model, such assumption shall not be required. The assumption condition of independent distribution is not required, the independent variable may be continuous, scattered or dummy variable. In this model, there is nonlinear relationship between the independent and dependent variable, and no assumption condition of their multivariate normal distribution is required. However, the prediction accuracy and explanatory of this model shall be strengthened by the multivariate normal distribution of variables; meantime, the stability of predicted results can be further improved.

(2) The requirement of data can be easily satisfied. Compared with other credit risk assessment models, Logistic model collecting data is not difficult, which only need the relevant data on manufacturing enterprises loan internal banks in previous years and annual report data of enterprise.

(3) At present, our credit rating agency still needs improving, but Logistic model doesn't depend on the external rating any longer, therefore, the situation of model result being influenced by the imperfect rating shall not occur. When employing this method, we shall firstly suppose whether the manufacturing enterprise loan default or not shall conforms to Logistic distribution. Some financial index and non-financial index can be selected to structure proper Logistic model, furthermore to response the enterprise crises and the probability of default. When utilizing this model, the critical point shall be set and determined by bank risk appetite. Whether they belong to default group shall be determined by their own circumstance. Enterprise's credit performance situation to their debt shall be divided into default and implementation. Therefore, in making measurement and assessment on the credit risks of manufacturing enterprises, the distribution characteristics of Logistic model fit with the estimation of enterprise default probability.

(4) The strong expansibility and practicability. On the basis of certain data, this model can give direct predict on the default probability of enterprising enterprises in the next period, and the structuring and operation of this model shall be much easier. Compared with other credit risk measurement and assessment models, this model has the following advantages: flexible data processing and easy operation.

B. Collecting index data

In empirical study, the proposed classification standard shall be whether the enterprises default or not, meantime, we shall determine whether enterprises shall default according to the stock of listed companies is ST stock or not: if the listed company hold ST stock, it shall default; otherwise, the listed company holds favorable reputation. In employing Logistic model to carry out empirical analysis on our manufacturing enterprises credit risks, limited to data collection and treatment difficulty, this paper only select randomly 50 sample enterprises from the most typical manufacturing listed companies, of which, the default enterprise covers 20, the enterprises with favorable reputation covers 30. Except the sample individuals with abnormal and incomplete data, the annual report data at the end of 2011 of the above 50 enterprises are selected, and all data are originated from www.Cninfo.com.cn. We have made a simple analysis and treatment on those data, with the treated index data attached as Addendum 1.

III. FACTORS AND RESULTS ANALYSIS

Factor analysis refers to research on the basic structure of observed data by researching the internal correlativity among variables. The basic thought is to realize dimensionality reduction by finding common factors. In the circumstance of lacking apriori information and major influence factor, this paper mainly depends on factor analysis, and completely depends on the original observed data, employ SPSS statistical software for analysis and furthermore find the variable factor which influence the index variable, figure up the linear expression among each variable factor and index variables.

This paper firstly takes KMO and Bartlett examination to analyze each type index variable suit for factor analysis, and then extract the variable factors with above 70% of total variance cumulative explain degree by observing Total Variance Explained, name each variable factor according to the influence degree of each variable factor influenced by index variable obtained by rotating component matrix, and last the linear expression of each variable factor about the index variables by component scoring coefficient matrix. This paper lists chart analysis process of factor analyzing profitability index variables by employing SPSS statistical software.

A. Profitability index

Profitability index reflects the company's profitability. This paper mainly expounds analysis from the following three ratios:

(1) Return on net assets reflects the amount of owners' profit for each yuan investment. This higher the ratio, usually the better. The formula is expressed as follow:

$$\text{Return on equity} = \frac{\text{the total profit in this year}}{(\text{the total owners' equity in last year} + \text{the total owners' equity last year in this year})/2} \times 100\%$$

(2)Return on total assets is used to measure the all companies' ability to use assets for profit, which refers the ratio of total profit and total assets. The formula is expressed as follow:

$$\text{Return on total assets} = \frac{\text{gross profit in this year}}{\text{total assets in this year}} \times 100\%$$

(3)Sales net interest rate, also known as the sales net profit margin, is the ratio of net profit and sales revenue. This ratio reflects the amount of net profit brought by each yuan sales revenue, and the profitability of sales revenue. The formula is expressed as follow:

$$\text{sales net profit margin} = \frac{\text{net profit}}{\text{sales revenue}} \times 100\%$$

The above three profitability index values, the greater values show that company's profitability is stronger, and company profit level is higher. We analyze whether profitability index variables suit for factor analysis. It is known from KMO and Bartlett test results in the Table2:KOM value of 0.599,between 0.5 and 0.7, so the correlation between variables is normal ,which suits for factor analysis in Table 1; At the same time, we get the result that Bartlett test P value is 0.000, less than the significance level of 0.05. Therefore we can reject the Bartlett test null hypothesis, regard the profitability index variables suitable for factor analysis.

Table1 KOM and Bartlett Test

Kaiser-Meyer-Olkin Measurement of sampling sufficient degree		.59
Bartlett's degree of sphericity test	Approximate chi-square	44.429
	Df	3
	Sig	.000

Table 2 is total variance explained. "Components" listed in the table corresponds to the root factor number with different characteristics. In "Initial eigenvalue" column, "total" refers to eigenvalue of correlation coefficient matrix R of raw data value; the "total" in "Extract the square and load" Column, "total" shall be the load total square corresponding to the selected factors; the "total" in "Rotate the square and load" Column, "total" shall be the load total square corresponding to the rotated factors; The three "variance %" columns are the proportion of the population variance, the "cumulate" columns are the cumulative percentage of total variance.Data in the table shows that the cumulative explain degree of the first two factors for the population variance reached 90.442%, which exceeds 70% of our required and the explain effect is better.

Table2 The Total Variance Explained

components	Initial Eigenvalue			Extract the square and loading			Rotate the square and loading		
	Total	Variance %	Accumulate %	Total	Variance %	Accumulate %	Total	Variance %	Accumulate %
1	1.756	58.540	58.540	1.756	58.540	58.540	1.698	56.569	56.592
2	.957	31.903	90.442	.957	31.903	90.442	1.016	33.851	90.442
3	.287	9.558	100.00						

B. Extraction method by principal component analysis.

Table3 refers to the component matrix by employing Varimax. The data in the table shows that after rotation, factor 1 are greatly influenced by rate of return on net assets and total assets, entitled asset income factor (X1). Factor 2 is greatly influenced by sales net interest rate, entitled sales income factor (marked X2).

Table3 Rotating component matrix

ICA	component	
	1	2
Return on equity	0.929	-0.011
Return on total assets	0.910	0.159
Sale Net Margin Method	0.74	0.995

C. 3.3 Extraction method: principal component analysis (pca).

Table4 Component score coefficient matrix

PCA	component	
	1	2
Return on equity	0.563	-0.126
Return on total assets	0.530	0.048
Sale Net Margin Method	-0.078	0.996

Rotating method: Kaiser standardized orthogonal rotation method a. rotation convergence after three iterations. Table4 is the component score coefficient matrix. It is known from the data in the table, X1=0.563* return on equity+0.530* return on total assets-0.078* net profit margin on sales; X2=-0.126* return on equity+0.048*return on total assets+0.996* net profit margin on sales.

Extraction method: principal component analysis. Rotating method: Kaiser standardized orthogonal rotation method. Components score.

D. Solvency index

Solvency index is used to measure enterprise's ability to repay debt. This paper shall expound analysis from the following four ratios:

(1)Current ratio reflects the company's amount of liquid assets as the guarantee of repayment for each yuan current liabilities. The formula is expressed as follow:

$$\text{current ratio} = \frac{\text{current assets}}{\text{current liabilities}} \times 100\%$$

Enterprise short-term liquidity strengthens with the increasing of the ratio. The higher the ratio, shows that the possibility of enterprise failing to repay short-term debt, and the occurrence of financial risk is smaller; however, too high rate shows that the enterprise takes up too much liquid assets, which may weaken the profitability of enterprise capital. The suitable ratio is usually 2.

Quick ratio refers to the ratio of the part with strongest cashability in current assets and the current liabilities. The ratio deducts index factor which cannot be converted into cash immediately in the current assets such as the inventory and prepaid expenses. The formula is expressed as follow:

$$\text{Quick ratio} = \frac{\text{monetary capital} + \text{temporary investment} + \text{bill receivable} + \text{accounts receivable in a year}}{\text{current liabilities}} \times 100\%$$

The higher the ratio, the enterprise's future debt paying ability is more guaranteed; however, the too high ratio shows that the enterprise takes up too much monetary funds, which may make the enterprise capital profitability reduce. The suitable ratio is usually 1.

(3) Asset-liability ratio is also called financial leverage coefficient, which measures the proportion of the funds provided by creditors in the total enterprise assets, or the creditors' rights' guarantee degree subject to the enterprise total assets. The formula is expressed as follow:

$$\text{Asset-liability ratio} = \frac{\text{the total liabilities in last year} + \text{the total liabilities in this year}}{\text{the total assets in last year} + \text{the total assets in this year}}$$

The role of financial leverage has two sides: When business operation management is favorable, the positive role of financial leverage multiplies the enterprise operation profit; conversely, when business operation management is poor, not only the liquidity need of enterprise cannot rely on the existing funds for guarantee, the negative effect of leverage will further deteriorate enterprise debt paying ability. The smaller this ratio,

the enterprise long-term debt paying ability is stronger. The ratio is usually not higher than 70%.

E. Cash flow liability ratio.

Cash flow liability ratio, reflects the ratio of net operating cash flow to current liabilities in a certain period. It reflects the enterprise's ability to repay short-term debt ability at current from the perspective of cash flow. The formula is expressed as follow:

$$\text{Cash flow liability ratio} = \frac{\text{Annual net cash flow from operating}}{\text{The total annual current liabilities}}$$

The higher the ratio, the more is the net cash flow produced by enterprise business operation activities, the stronger is the due short-term solvency ability. However, the excessive high ratio shows that the enterprise takes too much idle of current liabilities, thereby weakening the profit ability of enterprise current capital. Generally the ratio is greater than 1, which means enterprise payment of current liabilities is more reliable guaranteed. We carry out KMO and Bartlett inspection on solvency index variables, the correlation between variables is normal for factor analysis. At the same time, we extract the first two factors with more than 70% of the interpretation degree of population variance accumulation: After rotating, factor 1 are greatly influenced by quick ratio and flow ratio, entitled short-term solvency factor (X3) and $X3 = 0.465 * \text{current ratio} + 0.454 * \text{quick ratio} - 0.047 * \text{asset-liability ratio} - 0.153 * \text{Cash flow ratio}$; factor 2 is greatly affected by asset-liability ratio, entitled long-term solvency factor (X4) and $X4 = 0.074 * \text{current ratio} - 0.082 * \text{quick ratio} + 0.884 * \text{asset-liability ratio} + 0.021 * \text{Cash flow ratio}$.

F. Operation ability index

Operation ability index is the measurement and reflection of the enterprise in the operation and management efficiency. This paper is expounded from the following four ratios: (1) current asset turnover ratio reflects the amount of main business net income obtained by each yuan total liquid assets value at a certain period, which is an important index to evaluate enterprise asset utilization ratio. The formula is expressed as follow:

$$\text{current asset turnover ratio} = \frac{\text{Main business net income}}{(\text{the total current assets in this year} + \text{the total current assets in last year}) / 2}$$

Generally the higher the ratio is, the speed of current assets turnover is faster, the utilization of current assets is better and more savings. To a certain extent, enterprise profitability shall be strengthened with the increasing of liquid assets investment; conversely, the slow speed of current assets turnover needs more cash flow up to guarantee, which may result in waste of enterprise liquidity, and the deterioration of corporate profitability.

(2)Accounts receivable turnover ratio reflects the speed ration of enterprise's accounts receivable turnover. It shows the average times of company accounts receivable converting into cash in a certain period of time. The formula is expressed as follow:

$$\text{Accounts receivable turnover} = \frac{\text{Main business net income}}{(\text{the total amount of accounts receivable in this year} + \text{the total amount of accounts receivable in last year}) / 2}$$

Usually, the higher the accounts receivable turnover ratio is, the better, which indicates that the rapid speed of company bill-collecting, the short average bill-collecting time limit, the less loss on bad debt, quick liquidity and the strong debt solvency.

(3)Inventory turnover ratio is used to measure a comprehensive ratio of inventory fit efficiency each link in the enterprise production and management. The formula is expressed as follow:

$$\text{Inventory turnover ratio} = \frac{\text{Main business cost}}{(\text{the inventory balance in this year} + \text{the inventory balance in last year}) / 2}$$

Usually, the higher Inventory turnover is higher, the better, which indicates the favorable stock liquidity, and operation management with high efficiency, and a better sales market.

(4) Total asset turnover ratio is used to measure the use efficiency of enterprise total assets. The formula is expressed as follow:

$$\text{Total assets turnover ratio} = \frac{\text{Main business income}}{\text{total assets in this year} + \text{total assets in last year}} / 2$$

The ratio will be affected by any link in the asset management. Generally speaking, the higher the ratio is, the better. We carry out KMO and Bartlett test on operating capacity index variables, the correlation between variables is found weak which is suitable for factor analysis. At the same time, we extract the first two factors with the interpretation degree of population variance accumulation of more than 70%: After rotating, factor 1 is greatly influenced by quick ratio and flow ratio, entitled asset turnover factor (marked X5) and $5 = 0.442 * \text{current asset turnover} + 0.119 * \text{turnover of account receivable} - 0.177 * \text{inventory turnover ratio} + 0.471 * \text{total assets turnover}$; Factor 2 is greatly influenced by inventory turnover, entitled inventory turnover factor (marked X6) and $X6 = -0.087 * \text{current asset turnover} - 0.213 * \text{turnover of account receivable} + 0.996 * \text{inventory turnover ratio} - 0.036 * \text{total assets turnover}$.

G. Development capacity index

Development capacity index is used to measure the growth and development trend of the company's business in a certain period of time. This paper is mainly expounded from the following four ratios:

(1) Total assets growth rate is used to measure the development and growth speed of enterprise overall management level. Usually the higher the ratio is, the better, which indicates the rapid growth of the enterprise total assets, and the rapid development of enterprise strength.

(2) Main business revenue growth reflects the growth and development of the company's main business revenue. The ratio reflects the future development prospect of the enterprise: If the enterprise is in growth period, the ratio value is usually higher; If the enterprise in the mature period, the rate may be low, and the continuous favorable profit-level of the enterprise mainly depends on the powerful market share it occupied; If the enterprise is in recession, the ratio may even be negative, which is usually a dangerous signal.

(3) Main business profit growth reflects the expansion situation of corporate profitability, manifesting the enterprise's long-term profitability trend.

(4) Growth rate of earnings per share measures the growth degree of each common share profit.

We carry out KMO and Bartlett test on development capacity index variables, the correlation between variables is found normal which is suitable for factor analysis. At the same time, we extract the first two factors with the interpretation degree of population variance accumulation of more than 70%: After rotating, factor 1 is greatly influenced by operating profit growth and growth rate of earnings per share, named earnings growth factor (marked X7) and $X7 = -0.266^*$ growth rate of total assets $+0.171^*$ increase rate of business revenue $+0.510^*$ growth rate of operating profit $+0.626^*$ EPSG; Factor 2 are greatly influenced by growth rate of total assets, named asset growth factor (marked X8) and $X8 = 0.859^*$ growth rate of total assets $+0.312^*$ increase rate of business revenue -0.011^* growth rate of operating profit -0.242^* EPSG.

H. Non-financial index

The share proportion of the first biggest shareholder is the proportion of the share amount of the first largest shareholder in the total amount of enterprise stocks. The share proportion of the top 10 shareholders is the proportion of the share amounts of the top 10 shareholders in the total amount of enterprise stocks. The board size shall take the logarithmic value of the total number of the board. The proportion of independent directors is the proportion of the number of independent directors in the total number of all board directors. The number of staff shall take the logarithmic value of the total number of employees.

We carry out KMO and Bartlett test on non-financial index variables, and the correlation between variables is found normal which is suitable for factor analysis. At the same time, we extract the first two factors with the interpretation degree of population variance accumulation of more than 70%: After rotating, factor 1 is greatly influenced by the shareholding ratio of the first largest shareholder and the shareholding ratio of the top 10 shareholders, named shareholder shareholding ratio factor (marked X9) and $X9 = 0.446^*$ the shareholding ratio of the first largest shareholder $+0.447^*$ the shareholding ratio of the top 10 shareholders -0.073^* Theboard of directors logarithmic scale $+0.286^*$ the proportion of independent directors $+0.217^*$ the logarithmic of the employees number; Factor 2 is greatly influenced by the board scale logarithmic and the logarithmic of the employees number, named scale factor (marked X10) and $X10 = 0.216^*$ the shareholding ratio of the first largest shareholder $+0.116^*$ the shareholding ratio of the top 10 shareholders $+0.561^*$ the board scale logarithmic -0.238^* the proportion of independent directors $+0.660^*$ the logarithmic of the employees number.

I. Building model

This paper employs SPSS statistical software for analysis, resorts to entering method (Enter), namely all variable factors (X1 - X10) are input into the equation at one time. The model analysis results obtained by regression analysis can see Table6:

Table5 The variables in equation

	B	S.E.	Wald	df	Sig.	Exp(B)
X1	1.224	1.334	8.983	1	0.008	0.294
X2	0.339	0.245	4.135	1	0.032	0.713
X3	0.061	0.036	6.972	1	0.019	0.941
X4	1.135	0.883	7.067	1	0.018	0.321
X5	0.413	0.327	6.476	1	0.022	0.662
X6	0.742	0.609	8.087	1	0.015	0.476
X7	0.018	0.109	5.763	1	0.025	0.982
X8	1.027	0.903	8.546	1	0.011	0.358
X9	0.863	0.624	6.134	1	0.023	2.307
X10	0.535	0.509	9.087	1	0.006	1.707
	0.924	1.012	5.070	1	0.027	2.519

a. Input the following variables into step 1: X1, X2, X3, X4, X5, X6, X7, by 8, X9, X10. X1 is assets benefit factor, X2 is sales benefit factor, X3 is short-term solvency factor, X4 is long-term solvency factor, X5 is asset turnover factor, X6 is inventory turnover factor, X7 is earnings growth factor, by 8 is asset growth factor, X9 is shareholding ratio factor for shareholders, X10 is scale factor. In this paper, to determine whether the independent variables should be included into the regression model is to consider the significance of each independent variable in the regression equation, mainly take consideration of Wald statistic. It can be seen from Table6, Wald statistics of each variable coefficient in the model corresponding to the P values are less than the significance level of 0.05, therefore we can regard that each variable coefficient in the regression model is more significant, with statistical significance.

Obviously, we can know from the final mathematical expression of the model: Given a certain enterprise, put the index data after analyzing and processing into the model can determine the default probability. If the result is close to 1, the default possibility is greater; conversely, if the result is close to 0, the possibility of keeping favorable credit condition is greater.

IV. MODEL TESTING

A. Goodness of fit test

There are many independent variables, continuous variables, and large sampling amount of independent variable combinations, therefore Hosmer and Lemeshow test method is suitable for adoption.

It is known from Table6, Hosmer and Lemeshow statistic is 5.147, degree of freedom is 8, $P = 0.858$, therefore we can regard model's imitative effect to sampling data is favorable.

Table 6 Hosmer and Lemeshow Test

Step No.	Chi-square	f	Sig
1	5.147	8	0.858

B. Prediction accuracy test

This test randomly select 10 enterprises, 4 default enterprises and 6 enterprises with favorable reputation separately, from typical manufacturing listed companies, and select annual report data at the end of 2011 which are originated from www. Cninfo.com.cn. The data after being analyzed and processed shall be tested by model. If the result is closer to 1, it shall be judged to be default enterprise; otherwise, if the result is more close to 0, then it shall be judged as enterprises with good credit. The sample data after being analyzed and processed can refers to Addendum 2.

Table7 shows that the prediction of Logistic regression model on the default of test sample. It can be seen that, in view of the manufacturing enterprise credit risk, the regression model discriminant accuracy is higher, reached 80.00% (8/10); Among them, the discriminant accuracy rate of the default enterprise is 75.00% (3/4), the discriminant accuracy rate of enterprise with favorable reputation is 83.33% (5/6). The discriminant effect of a practical problem model is well.

Table7 Prediction Accuracy test

Observed		Predicted		
		Whether default or not		Percentage of correction
		No default	Default	
Whether default or not	No default	5	1	83.33
	Default	1	1	75.00
Total percentage				80.00

V. DISCUSSION AND CONCLUSION

Through the observation of the flow coefficient of the Logistic regression model, we can draw the following conclusions: (1) in this paper, assets benefit factor is mainly affected by two financial indexes: return on net assets and return on total assets. In this paper, the sales revenue factor is mainly influenced by the sales net interest rate –a financial index. These two factors reflect the capability of enterprise profit; the greater value shows that the strong enterprise profiting ability, the enterprise has more sufficient profits funds and assets as guarantee, and the smaller default probability.

In this paper, the short-term solvency factor is mainly affected by two financial indexes: current ratio and quick ratio. The long-term solvency factor in this paper is mainly influenced by asset-liability ratio, a financial index. These two factors is used to reflect the enterprise capital and assets to repay debt the ability before the debt due, the greater numerical value, shows that the enterprise has more sufficient short-term

financing and long-term assets to repay debt, the production and business operation is more assured, and the smaller the default probability.

(3) In this paper, assets turnover factor is mainly affected by two financial indexes: current assets turnover and total assets turnover. The inventory turnover factor in this paper is mainly affected by inventory turnover -a financial index. These two factors reflect the operation efficiency of enterprise funds, assets and inventory. The larger value shows that the enterprise c funds, assets and inventory operation efficiency is good, with enough available short-term funding, long-term assets and inventory pledge to guarantee their own solvency, and the smaller default probability.

In this paper, earnings growth factor is mainly affected by two financial indexes: operating profit growth rate and earnings growth rate per share. In this paper, assets growth factor is mainly affected by the financial index- growth rate of total assets. These two factors is used to reflect the enterprise growth and the development trend, the bigger numerical value, shows the greater enterprise management, the rising trend of enterprise's profit, income and assets, and the stronger the enterprise insolvency strength, and the smaller the default probability.

In this paper, the shareholder shareholding ratio factor mainly be affected by the following two non-financial index: the shareholding ratio of the first biggest shareholder holds, and the shareholding ratio of the top 10 shareholders. This factor reflects the enterprise holdings of major shareholders, the larger value shows that the more concentrated enterprise equity, even the possibility of the single-large shareholder, thus enterprise may have poor management decision, the phenomenon of minority shareholders abusing power for personal gains, the default probability will therefore increase.

In this paper, the scale factor is mainly influenced by the two following nonfinancial indexes: board logarithmic scale and staff logarithmic scale. The factor reflects the overall size and structure of the enterprise, the bigger value mirrors the redundant personnel structure, the inflexible governance mechanism, the low enterprise management efficiency, and less market competitiveness, furthermore the increasing default probability.

Through the empirical analysis and prediction, the prediction accuracy is found low, which may have the following reasons.(1) The financial management of many manufacturing enterprises is not standard, and external audit for manufacturing enterprise is not mature, therefore its financial statements may be whitewashed, accounting information may is be fabricated and in lack of authenticity.(2) Macroeconomic situation shall affect the business operation condition of manufacturing enterprises, the macroeconomic fluctuation shall dramatically improve or deteriorate manufacturing companies, referring as the lack of data stationarity reflected in the financial statements, and furthermore resulting in certain deviation on estimated results.(3) Due to the limitation of calculation amount, the selected sample in this paper is limited, and the analysis is only performed on the financial data and non-financial data analysis extracted from this paper without consideration of the

commercial bank's credit risk management on manufacturing enterprises and other aspects, which also affect the accuracy of prediction.(4)This paper only uses factor analysis to find out variable factor with significant impact, but multicollinearity among variables factor may exist, which may affect the prediction precision of this model. The author has taken consideration of the problem, however, in consideration of the interpretation of the number of variables of practical economic problems and explanation power, after repeated consideration, the author finally abandoned to structure the model by using stepwise regression method.

REFERENCE

- [1] Kim, H., & Gu, Z. (2009). Financial features of dividend-paying firms in the hospitality industry: A logistic regression analysis. *International Journal of Hospitality Management*, 28(3), 359-366.
- [2] Sohn, S. Y., & Kim, H. S. (2007). Random effects logistic regression model for default prediction of technology credit guarantee fund. *European Journal of Operational Research*, 183(1), 472-478.
- [3] Dong, G., Lai, K. K., & Yen, J. (2010). Credit scorecard based on logistic regression with random coefficients. *Procedia Computer Science*, 1(1), 2463-2468.
- [4] Nikolic, N., Zarkic-Joksimovic, N., Stojanovski, D., & Joksimovic, I. (2013). The application of brute force logistic regression to corporate credit scoring models: Evidence from Serbian financial statements. *Expert Systems with Applications*, 40(15), 5932-5944.
- [5] Kim, D. Y., Kim, M. Y., Chi, S., Arellano, M., & Murphy, M. R. (2013). A Logistic Regression Model to Select and Prioritize Network-Level Project Sections for Sustainable Pavement Management in Texas. In *Transportation Research Board 92nd Annual Meeting* (No. 13-3110).
- [6] Önder, Ş., & Ergin, H. (2012). Determiners of enterprise risk management applications in Turkey: An empirical study with logistic regression model on the companies included in ISE (Istanbul Stock Exchange). *Business & Economic Horizons*, 7(1).
- [7] Yang, Y., & Williams, E. (2009). Logistic model-based forecast of sales and generation of obsolete computers in the US. *Technological Forecasting and Social Change*, 76(8), 1105-1114.
- [8] Sohn, S. Y., & Kim, H. S. (2007). Random effects logistic regression model for default prediction of technology credit guarantee fund. *European Journal of Operational Research*, 183(1), 472-478.
- [9] Nie, G., Rowe, W., Zhang, L., Tian, Y., & Shi, Y. (2011). Credit card churn forecasting by logistic regression and decision tree. *Expert Systems with Applications*, 38(12), 15273-15285.
- [10] Blanco, A., Pino-Mejías, R., Lara, J., & Rayo, S. (2013). Credit scoring models for the microfinance industry using neural networks: Evidence from Peru. *Expert Systems with Applications*, 40(1), 356-364.

Development of Comsol 3D model for heat collection under a water body

Hafiz M K U Haq, Birgitta Martinkauppi, and Erkki Hiltunen

Abstract— Pipe flow is modeled to study the heat transfer for a low energy network in which energy is collected from a sediment layer located under water body. These results can be used to predict the behavior of a system as well as effects of different heat carrier fluids. The accuracy of these predictions depend on the analysis and modeling technique used for the system and most importantly the difference between the actual measurements and the simulated results. This study implements numerical 3D modeling using COMSOL on a special pipe that has been used as a heat collector for a heating system and it compares the simulated results with the actual measurements.

Keywords— Heat transfer, Heat collector, Sediment energy, Pipe flow.

I. INTRODUCTION

A sediment layer exists typically under water body like river, lake or seabed. The sediment layer has heat energy which is mainly from the sun and a small part is geothermal energy. During winter, some of the heat energy is conveyed back to the sea water from the sediment and keeps the bottom layer warm. Typically, water is densest around +4 degC which limits heat conduction back to the water. To utilize this energy, a low energy network has been installed. As a part of this system, twelve heat collector pipes has been installed and spread in the sediment layer locating 3-5 meters below sea at Liito-oravankatu Street, Suvilahti (Vaasa) [2]. The temperature distribution analyses of these pipes with respect to the distance from the sea shore are an important factor in order to understand the heat transfer process and the prediction of the system on the time scale. This paper presents the simulated results of the temperature distribution along the size of the pipe and compares with the measured data taken by a method of Distributed Temperature Sensing (DTS). Typically, water is denser at the bottom called stratified layer around +4 degC which limits heat conduction back to the water.

The rest of the text is organized in sections. The second section provides the background of the study including the material of the pipe, geometry of the pipe, fluid properties flowing inside the pipe and COMSOL software. The next section describes the method of implementation and variables used for the simulation. The results and discussion are given followed by the comparison of simulated and measured data.

II. BAKGROUND

The Geological survey of Finland has measured earlier the temperature of the seabed sediment which stayed stable at +8-9 degC at the depth of 3-4 meters [5]. Fig. 1 presents the temperature profile of the sediment in Suvilahti area in Vaasa from year 2006. To exploit the sediment energy, low energy network system has been installed and the energy is used in 42 houses [2]. Later on, Geoenergy group (University of Vaasa) has monitored sediment temperatures using DTS measurements. The cable for DTS measurements was installed with the construction of the network.

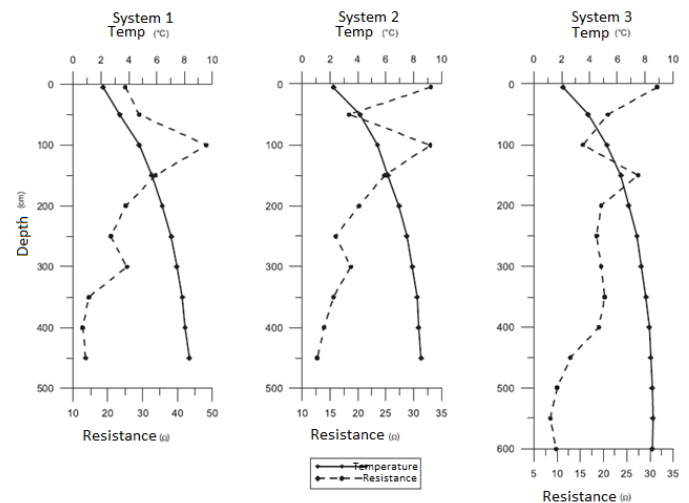


Fig.1 Temperature and resistance of the sediment (GTK Länsi-Suomenyksikkö: Valpola 2006)

The heat collector pipes are placed under the sediment layer to collect heat from the surrounding and enable the carrier fluid to increase the temperature by heat transfer. This fluid goes back to the storage tank of the heating system. The length of this pipe is equally important as compared to sediment temperature for heat exchange. In the heat collection well at Liito-oravankatu Street, the energy network is composed of 12 PE-pipes with a length of 300 meters. The flowing fluid is called Altia's Naturet maalämpönesteet (geothermal fluid) a mixture of ethanol and water with 1:1 ratio. The geometric model of the PE-Pipe is given in Fig. 2.

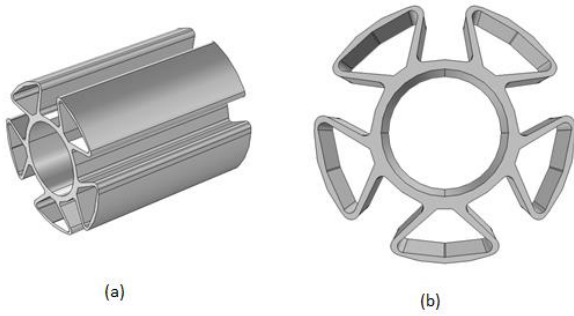


Fig. 2 Geometric model of the PE-Pipe created using COMSOL:
a) 3D view and b) Front view

PE-Pipe named Refla energy pipe has five outer pipes each with area of 360 mm^2 to supply fluid (see Fig. 2b). The inner pipe is for returning fluid output and has an area of 1194.6 mm^2 . Cooler water is provided on the input pipes which flows across the length of the pipe and return back from the output pipe with the temperature change depending on sediment to pipe energy exchange. This warmer water is used in the heating system. The temperature difference between the inlet and outlet fluid is an important factor which reflects in the efficiency of the heating system.

COMSOL software is utilized to present the evaluation of the 3D modeling of pipe flow under the sediment layer. The 3D problem is solved using the average temperature of the sediment over months. The temperature distribution has been calculated using the thermal properties of the pipe and fluid.

III. METHODOLOGY

The focus of this study is to simulate the 3D model of the pipe and to evaluate the temperature distribution during pipe flow. COMSOL provides multiphysics functionality of the pipe flow:

$$F - f \frac{\rho}{2d} |u|u - \nabla P = 0 \quad (1)$$

$$\nabla \cdot (A\rho u) = 0 \quad (2)$$

where, $A \text{ (m}^2\text{)}$ is the cross sectional area of the pipe, $\rho \text{ (Kg/m}^3\text{)}$ is the density of the pipe, $u \text{ (m/s)}$ is the fluid velocity flowing inside the pipe, $P \text{ (N/m}^2\text{)}$ is the pressure, d is the hydraulic diameter of the pipe, f is the Darcy friction factor and $F \text{ (N/m}^3\text{)}$ is the volumetric force.

The variation in the density is negligible in (1) and the model is not pressure driven. The common practice of modeling dictates to exclude the gravity from the equation. Now, F represents the pressure variable as the reduced pressure. These assumptions significantly simplify the complexity of the equation [1]. The most important parameter in (1) is Darcy friction factor which describes the friction loss in the pipe flow.

Friction factor is a function of Reynolds number. Friction factor is directly proportional to the surface roughness of the pipe and inversely proportional to the hydraulic diameter of the pipe. Reynolds number basically predicts the pattern of the

fluid flow. The pattern of the fluid can be laminar, turbulent or in transition phase. In the transition region, fluid undergoes a shift from laminar to turbulent region. To solve the Darcy friction factor in all of these regions of the flow, a Churchill expression has been used [1].

$$f = 8 \left[\left(\frac{8}{R_e} \right)^{12} + (A + B)^{-1.5} \right]^{1/12} \quad (3)$$

$$A = \left[-2.457 \ln \left(\left(\frac{7}{R_e} \right)^{0.9} + 0.27 \left(\frac{e}{d} \right) \right) \right]^{16} \quad (4)$$

$$B = \left(\frac{37530}{R_e} \right)^{16} \quad (5)$$

The importance of the Reynolds number described in (1) - (3). Reynolds number depend the properties of the fluid flowing inside the pipe. Dynamic viscosity and the hydraulic diameter of the pipe are important factors in order to understand the region of the fluid flow. Reynolds number usually defines as:

$$R_e = \frac{\rho v D_H}{\mu} \quad (6)$$

where, $\rho \text{ (Kg/m}^3\text{)}$ is the density, $v \text{ (m}^2\text{/s)}$ is kinematic viscosity of the fluid, $D_H \text{ (m)}$ is the hydraulic diameter of the pipe and $\mu \text{ (Kg/(m.s) = (Pa.s))}$ is the dynamic viscosity of the fluid.

Heat transfer from sediment layer to the pipe depends on two constraints, the wall (pipe) heat transfer and the thermal conductivity of the sediment. Wall heat transfer further depends on the temperature gradient and the coefficient of the heat transfer.

$$Q_{wall} = hZ(T_{ext} - T) \quad (7)$$

$$\rho A c_p u \cdot \nabla T = \nabla \cdot A k \nabla T + f \frac{\rho}{2d_h} |u|^3 + Q_{wall} \quad (8)$$

where, h is the coefficient of heat transfer, T_{ext} is the temperature of the sediment and Q_{wall} is the heat transfer between the pipe wall and the sediment layer. In case of several walls, the heat transfer coefficient will automatically be calculated considering the wall resistance and the external film resistance [1]. In this model, the thickness of the inner and outer wall is 4 mm and 3 mm respectively. The thermal conductivity of the pipe is 0.45 (W/mK) [4].

The measured temperature profile of the sediment calculated by the Geoenergy research group provides the detail information characterized in months for 300 meters of length

of the pipe from the sea shore. It is evident that the temperature of the sediment is higher than +8 degC for the months of August, September and October. On the other hand, from November till February, the temperature of the sediment is measured to be less than +6 degC (Geoenergy Group). In simulation, the important parameter is the average temperature of the sediment with respect to the length of the pipe round the year rather than individual months. But despite of this fact it has been noticed that the sediment temperature maintained to +9 degC [5].

Table I. Thermal properties of the pipe and fluid

Thermal Properties of the Fluid		Thermal Properties of the Pipe	
Density (kg/m ³)	960	Thermal conductivity (W/mK)	0.45
Dynamic viscosity (10 ⁻³ Pa*s)	2.12	Heat capacity (J/kgK)	2000
Heat capacity (kJ/kgC)	3.25	Density (kg/m ³)	950
Thermal conductivity (W/mK)	0.29		

Table I presents the average thermal properties of the pipe and fluid flow. The density of the fluid has been taken from the online documentation of Altia company website for Naturet-maalämpönesteet (Naturet -17 degC) at 20 degC temperature. Dynamic viscosity, heat capacity and thermal conductivity of the fluid are the average of seven values at temperatures (-30 – +30 degC) [3]. Thermal properties should be taken as an average value for the corresponding temperatures, the reason for this, is the consideration of fluctuation of the sediment temperature round the year and the steady state assumption. It should be clear that in winter, sea surface is frozen and the sediment temperature at this time is as low as -4 degC (Geoenergy group). In this case, the thermal properties of the fluid changes which will cause an alteration in the heat transfer process. So to avoid these conditions, average values have been taken into account.

IV. RESULTS AND DISCUSSION

The velocity of the fluid and the temperature distribution of fluid flow are shown in Figs. 3 and 4 respectively. To visualize the temperature distribution, a cross section of 1 meter pipe has been considered. The reason is that the length of pipe is approximately 300 m and the distance between the inlet and the outlet pipes are 3 mm. The pipe flow model in COMSOL provides a platform to study both the steady state simulation and the transient (Time – dependent) state simulation. This paper only focuses on the steady state process of the pipe flow to generate the temperature distribution across the pipe length.

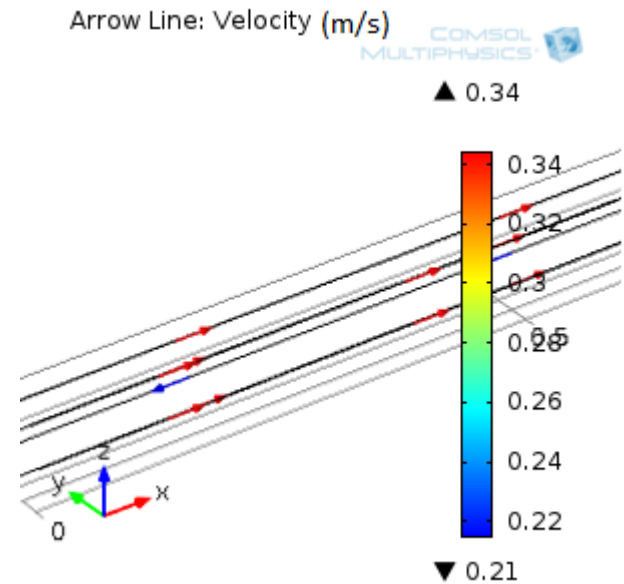


Fig. 3 Velocity of the fluid

In this case, the pipe is considered to be under the sediment layer and a cross section of only 1 meter. The maximum temperature is shown by the red color at the outlet in Fig. 4 and the rest of the pipe flow undergoes heat transfer process. It should be noted that the heat exchange process depend not only on the temperature of the sediment layer but also on the fluid velocity. The sediment temperature is considered to be +9 degC [5]. The volumetric flow rate is considered to be 0.0567 (l/s). The inlet temperature is +5 degC.

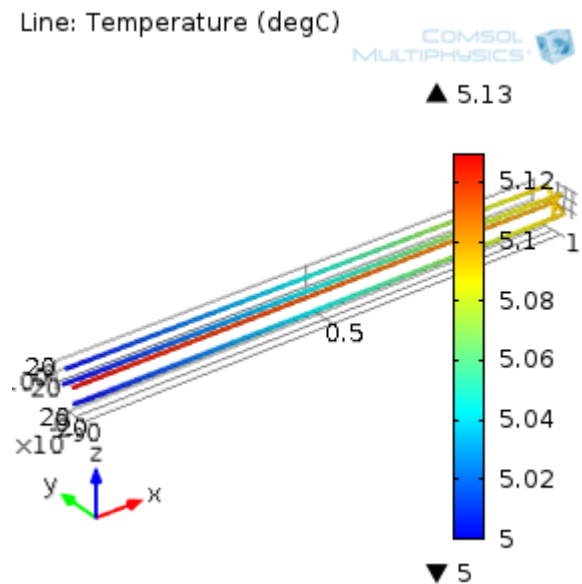


Fig. 4 Temperature distribution of fluid flow

The temperature profile for 300 meter pipe is shown in Figs. 5 and 6. Since the distance between incoming and outgoing fluid is very small, it is not possible to see the 3D distribution. The incoming and outgoing fluid profile has been presented in

Figs. 5 and 6. At the beginning, there is a slight increase in the temperature for first 10 meters of pipe length, but then it rapidly increases until 100 meters. It can be seen that there is an abundant rise of temperature from almost 20 meters to 100 meters. After that point, the heat exchange process is fairly slow maintaining equilibrium until 300 meters. In Fig. 6, the outgoing fluid has an exponential slow increase in the temperature profile across the length of the pipe.

In a similar way, a model has been derived with 12 heat collector pipes of a cross section of 10 meters. The temperature profile of the fluid flow is shown in Fig. 7. The inlet temperature is kept at +5 degC which is exchanged over +7 degC at the outlet. The transfer process is at peak at the 10 meter length of the pipe as it shows the red color at that point. There is a slight temperature increase after 10 meters.

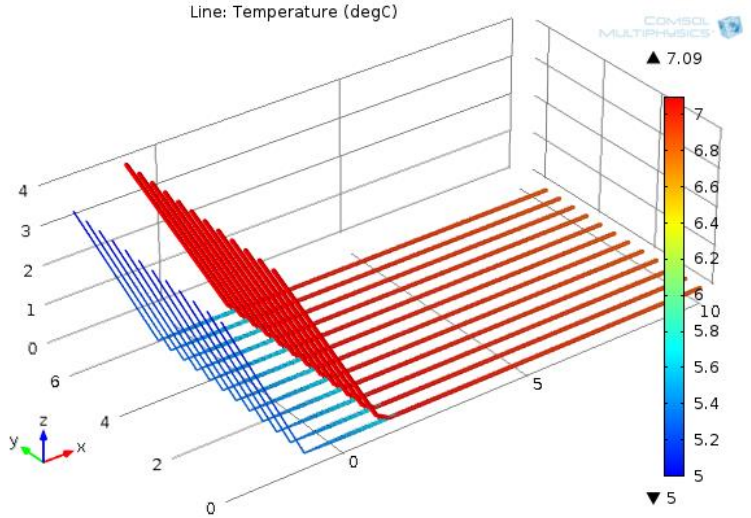


Fig.7 Temperature distribution of fluid flow model similar to Liito-oravankatu site

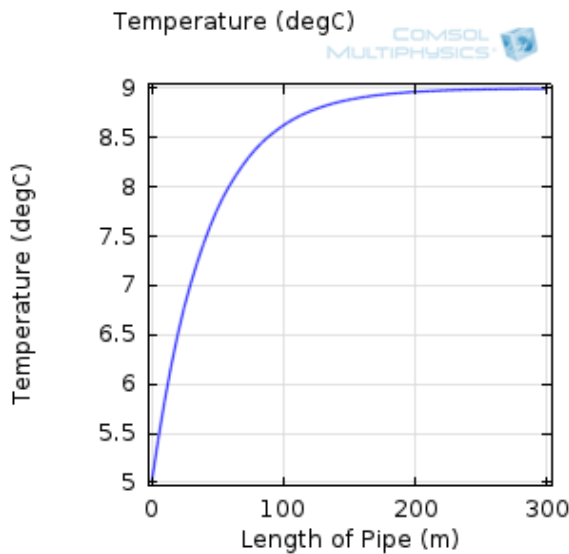


Fig. 5 Temperature of incoming fluid

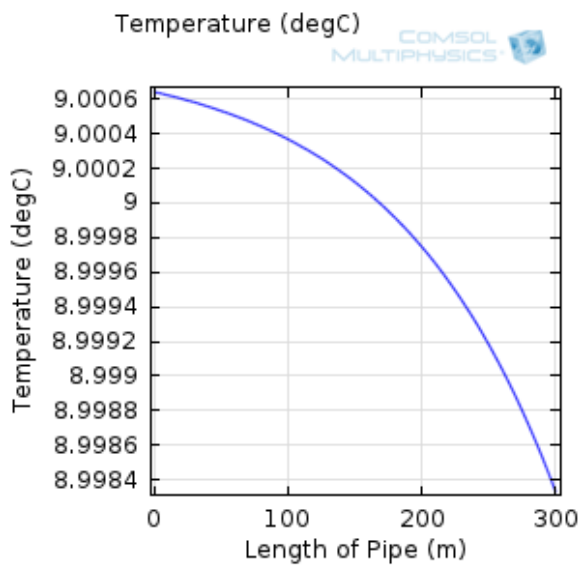


Fig. 6 Temperature of outgoing fluid

V. COMPARISON

A comparison has been made in this section between the simulated result and the measured value of the outlet temperature. But before doing so, the input parameters of the system must be changed in order to present the actual values rather than the average results. For this, the temperature profile of the sediment will be taken into consideration for the alternating months of 2009 (Geoenergy research group).

The unmarked line in Fig. 8 represents the measured temperature value of the fluid in Liito-oravankatu in a period from January 2009 to November 2009. The corresponding marked line indicates the simulated temperature of the fluid using COMSOL. The input surrounding temperature is the measured value of the sediment temperature taken by Geoenergy group from January 2009 to November 2009. The difference between the measured and the calculated values indicate the error caused by the simulation platform.

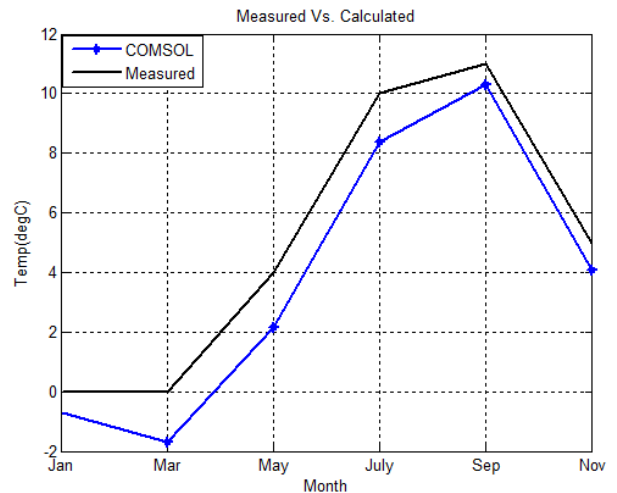


Fig. 8 Temperature distribution (measured Vs. Calculated)

REFERENCES

- [1] COMSOL Pipe Flow Module (Model Library Manual). Version 4.4 2012.
- [2] Hiltunen, E, Martinkauppi, B, Zhu, L, Makiranta, A, Lieskoski, M and Rintaluoma, J. Renewable carbon-free heat production from urban and rural water areas. Manuscript to be submitted.
- [3] Kemppainen, Joni. Lämpökaivojen Käyttö rakennuksen lämmityksessä 2012. Available at: <URL: http://www.theseus.fi/bitstream/handle/10024/51580/Kemppainen_Joni.pdf?sequence=1>.
- [4] Lienhard, John H. A Heat Transfer Text Book. Phlogiston Press 2008. Available at: <URL: <http://web.mit.edu/lienhard/www/ahtt.html>>.
- [5] Martinkauppi, Ilkka. Sedimentilämpömittaukset Pohjanmaalla ja Etelä-Pohjanmaalla 2010. Available at: <URL: http://www.geoenergia.fi/pdf/I_Martinkauppi.pdf>.
- [6] Stober, Ingrid and Bucher, Kurt. Geothermal Energy 2013. Page (70). ISBN 978-3-642-13352-7.
- [7] Valpola, Samu. Sedimentin lämpötilamittaukset Vaasan Suvilahden edustalla 2006. (Available in Finnish) Arkistoraportti P31.4.053. GTK Länsi-Suomenyksikkö.

Figs. 9 and 10 show the temperature response of the flow when using different carrier fluids [6]. In Fig. 9 Naturet (fluid) has been used to calculate the resulting fluid temperature in degC. While, in Fig. 10, different fluids (including: Ethylene glycol, Propylene glycol, Calcium chloride, Methanol and Water) has been used to compare the temperature response. A minimal difference in the temperature can be seen throughout the year by using different carrier fluid for heat transfer.

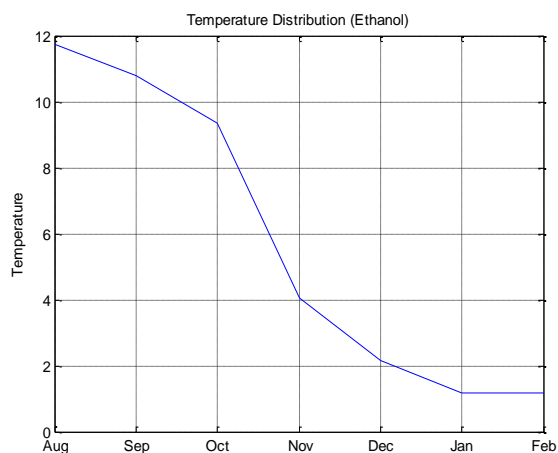


Fig. 9 Temperature in degree Celsius using Naturet

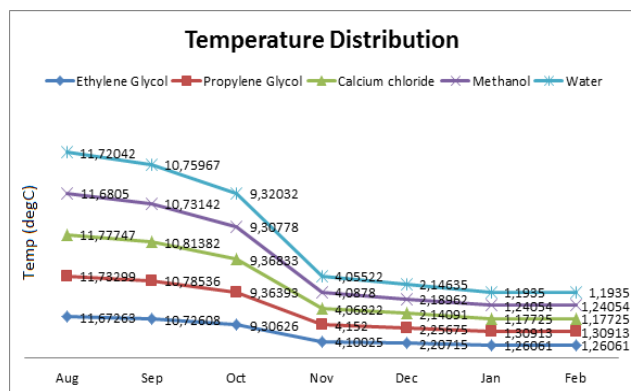


Fig. 10 Temperature in Celsius using multi fluids

VI. CONCLUSION

An acceptable model of the pipe flow considering all the parameters of the pipe including geometry, material of the fluid and the pipe, thermal properties of the fluid and the pipe and the temperature profile of the sediment has been presented in this paper. An approximate value of the fluid coming out from the outlet has been obtained by simulation and compared to the measured value. The results indicate a good match between simulation values and real measurement. Simulation has been done using multi fluids having different thermal properties and the results have been presented which indicates a minimal difference in the temperature distribution. It is possible to change the configuration of the pipe in reference to Fig. 7, since COMSOL allows creating and simulating all kinds of possible fluid flow geometry.

Fuel Consumption at Conditions of the Israel's Highways Driving Cycle

M. Ben Chaim, E. Leybovitch

Abstract— Known that the fuel consumption of different Vehicles models defined on the basis of driving cycles, which are set by UN ECE and based on European roads. They are not suitable for Israel, due to the fact that the density of traffic on Israel roads is almost 3-3.5 times higher than in Europe. Therefore, in order to calculate fuel consumption, used driving cycles of Israel. At the Israel's Highways driving cycle fuel consumption has two significant components: fuel consumption at average speed and during accelerations, and therefore, in the model, it is determined separately for two different operating modes: average speed and accelerations. Unlike previously developed models, which determine fuel consumption based on specific fuel consumption, ours determines fuel consumption based on the efficiency of the engine, which makes the model more adequate since it incorporates engine mode changes. Was compared the results of fuel consumptions for few modern automobiles for EUDC driving cycle and for Israel's Highways driving cycle. We found, that fuel consumptions for Israel's Highways more on 5-7%, then fuel consumptions on Europe's countries Highways. This indicates that the traffic conditions on the Israel's Highways difficult, then the traffic conditions on the Europe's countries roads.

This work was supported in part by the Israel's Ministry of Environment under Grant.

Keywords— vehicle, fuel consumption, driving cycle

I. INTRODUCTION

REDUCING the transportation sector energy consumption is an important part of reducing overall energy consumption. It requires development of new, more fuel efficient vehicle models and more efficient operating of existing vehicles. This makes the development of fuel consumption estimation methods very important. The most simple and conveniently implemented method is based on utilization of mathematical models, and therefore, the development of such models is highly desirable.

Vehicle fuel economy test cycles are based on the UN ECE regulations [1, 2], and therefore models for estimating fuel consumption should also be based on these regulations.

Mathematical models for estimating fuel efficiency are widely represented in literature. For example, in [2, 3] it is

M. Ben Chaim is with the Department of Mechanical Engineering and Mechatronics, Ariel University, Ariel 40700, Israel (corresponding author to provide phone: +972-54-3394745; fax: +972-3-9076652; e-mail: michailbc@ariel.ac.il).

E. Leybovitch, is with the Department of Mechanical Engineering and Mechatronics, Ariel University, Ariel 40700, Israel (e-mail: elyas33@gmail.com).

proposed to evaluate fuel consumption measured in liters per 100 km, on the basis of hourly fuel consumption and engine power. In [4] it is proposed to calculate fuel consumption based on regression models dependent on speed and acceleration. Both of these models do not incorporate important constructive parameters and operating conditions that significantly affect fuel consumption, which makes these models insufficiently adequate and exact. Unlike previously developed models, ours determines fuel consumption based on the efficiency of the engine, which makes the model more adequate since it incorporates engine mode changes. The efficiency of the engine is expressed as a function of the speed mode of the engine and of the degree of power utilization of the engine.

The purpose of this paper is the development of a fuel consumption estimation method for the extra-urban driving cycle. The extra-urban cycle fuel consumption has two significant components: fuel consumption at average speed and during accelerations, and therefore, in the model, it is determined separately for two different operating modes: average speed and accelerations. In the model the efficiency of the engine is calculated based on the speed mode of the engine and the degree of power utilization of the engine.

II. EQUATION FOR ESTIMATING FUEL CONSUMPTION

The formula for calculating fuel consumption is based on the UN ECE regulations.

As in [2, 3], we divide the energy expenditure into three parts, the first one being the energy required for overcoming the resistance of the air, the second – the energy required for overcoming the resistance of the road, and the third – the energy required for overcoming the resistance of the inertia of the weight of the vehicle during accelerations.

As stated above, the automobile engine operates in two main modes, the first of which is movement at average speed, and the second – series of accelerations. The equation for estimating fuel consumption must take this into account.

In the formula the energy expenditure is expressed as a sum:

$$E_s = E_1 + E_2,$$

where:

E_1 is the energy required to overcome the forces of resistance at average speed on the 100 km interval, J,

E_2 is the kinetic energy required for episodic accelerations on the 100 km interval, J.

Fuel consumption per 100 kilometers has the form:

$$Q_{S(e)} = \frac{E_s}{\eta_T H_L}, [l/100km],$$

where H_L is the calorific value of one liter of fuel.

The total energy required for driving 100 kilometers, taking into account the accelerations, is:

$$E_S = \frac{1}{\eta_{P,n}} \left(m_a \cdot g \cdot f_r + \frac{\rho}{2} \cdot C_D \cdot A_f \cdot V_a^2 \right) \cdot S + \sum_{i=1}^k \frac{q_i}{\eta_{(P,n)}} m_a a_i \gamma_{mi} S_i \quad [J/100 km],$$

where

η_T is the efficiency of the transmission,

ρ_f is the fuel density, kg/l,

V_a is the average speed of the vehicle, m/sec ,

m_a is car mass, kg ,

c_r is the rolling resistance coefficient,

c_D is the coefficient of aerodynamic resistance of the car,

A_f is the characteristic area of the car, m^2 ,

S is the car mileage, which equals 100000 m, i.e. 100 km,

ρ is air density, $N \cdot s^2 / m^4$,

g is the acceleration of gravity m / s^2 ,

γ_{mi} is the mass factor of the vehicle,

a_i is the acceleration of the vehicle, m / s^2 ,

S_i is the acceleration distance of the vehicle, m.

k is the number of acceleration intervals ,

q_i is the number of accelerations in each acceleration interval.

$\eta_{P,n}$ is the efficiency of the engine, which depends on the coefficient of the degree of power utilization μ_P and the coefficient of the engine speed mode μ_n in the following way:

$$\eta_{P,n} = \eta_e \mu_P \mu_n.$$

Here η_e is engine's peak efficiency.

In order to obtain functions μ_P and μ_n , the dependences $\mu_P = f(P/P_e)$ and $\mu_n = f(n/n_p)$ were analyzed for a number of modern gasoline and diesel engines, information about which is available in the literature [5, 6, 7, 8, 9]. As a result of the data analysis the following formulas were derived:

a formula for calculating μ_P for diesel engines the form:

$$\mu_P = 0.5968 - 0.1666s + 2.4968s^2 - 2.1128s^3 ,$$

a formula for calculating μ_P for gasoline engines has the form:

$$\mu_P = 0.234 + 1.0592s + 0.8149s^2 - 1.2121s^3 ,$$

and a formula for calculating μ_n for diesel and gasoline engines has the form:

$$\mu_n = 0.7107 + 0.9963 \left(\frac{n}{n_p} \right) - 1.0582 \left(\frac{n}{n_p} \right)^2 + 0.3124 \left(\frac{n}{n_p} \right)^3 ,$$

where s is the ratio of the engine power required for the given mode of motion and the engine power by the performance characteristics of the engine, corresponding to vehicle speed.

According to the definition

$$s = \frac{P}{P_e} = \frac{(m_a g c_r + 0.5 c_D A_f V_a^2 + m_a a \gamma_m) V_a}{P_e}$$

Here the numerator is the engine power required for the given mode of motion, and the denominator is the engine power by the performance characteristics of the engine for the corresponding vehicle speed. It is a function of engine speed and maximum engine power and is determined by the empirical formula [3]

$$P_e = 10^3 P_{max} \left[a \left(\frac{n}{n_p} \right) + b \left(\frac{n}{n_p} \right)^2 - c \left(\frac{n}{n_p} \right)^3 \right] ,$$

where

P_{max} is the engine's maximum power, kW,

a, b, c are the polynomial coefficients, different for different types of engines [3],

n_p is the engine speed at maximum power of engine, min^{-1} ,

n is the engine speed at average speed of vehicle, min^{-1} .

The formula for determining it has the following form

$$n = \frac{9.55 V_a \xi_{ax} \xi_n}{r_d} ,$$

where

r_d is the rolling radius of the tire, m,

ξ_{ax} is the finale drive gear ratio,

ξ_n is gear ratio in the gearbox.

III. ESTIMATING OF FUEL CONSUMPTION FOR ISRAEL'S HIGHWAYS DRIVING CYCLE

In these calculations it was used the parameters of Israel's Highways driving cycle (Table I, Fig. 1):

Table 1. Parameters for Israel’s Highways driving cycle

Characteristics	unit	value
Distance	km	6,270
Duration	sec	400
Average Speed	km/h	56.4
Maximum Speed	km/h	105

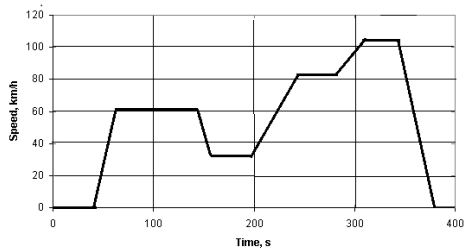


Fig. 1. Scheme of Israel’s Highways driving cycle

As a result of calculation, the following table (Table 2) was obtained. In parallel, in order to compare calculated fuel consumption for EUDC driving cycle [5].

Table 2. Fuel consumption rates of different Driving Cycle

Vehicle	EUDC driving cycle	Israel’s Highways driving cycle
Volkswagen Polo Sedan	4.9	5.2
Toyota Yaris	4.8	5.1
Toyota Sienna AWD	11.2	11.7
Toyota Camry AWD3.5	7.3	7.8
Hyundai Genesis Coupé 2.0 T	7.5	8.3

IV. CONCLUSION

We compared the results of our calculations via the formula for few modern automobiles for EUDC driving cycle [5] and for Israel’s Highways driving cycle. The discrepancy between

driving cycles 5-7 %, which indicates that the Traffic condition on Israel’s Highways hard, then Traffic condition on Europe’s countries Highways. The vehicle-specific parameters that we used were the type of engine, automobile mass, maximum power and engine speed at maximum power.

REFERENCES

- [1] United Nations Economic Commission for Europe (UNECE), *Vehicle Regulations*, from accessed on 2011-08-01.
- [2] Guzzella, L. and Sciarretta, A. *Vehicle propulsion systems*, Springer Verlag, Berlin, 2007.
- [3] Gaevsky, V., Ivanov, A. (2007). Theory of Ground Vehicles. MADI, Moscow (in Russian).
- [4] Widodo, S., Hasegawa, T., Tsugawa, S.(2000) Vehicle fuel consumption and emission estimation in environment-adaptive driving with or without inter-vehicle communications: Intelligent Vehicles Symposium, 2000. IV. 2000. Proceedings of the IEEE, pp.382 – 386.
- [5] M. Ben Chaim, E. Shmerling (2013) A Model o Vehicle Fuel Consumption at Conditions of the EUDC. International Journal of Mechanics, V.7, 2013, pp. 10-17.
- [6] Bosch, (2004) Gasoline Engine Management.
- [7] Stone, R. (1985) Introduction to Internal Combustion Engines, Macmillan.
- [8] Jimenez-Palacios, J. Understanding and Quantifying Motor Vehicle Emissions and Vehicle Specific Power and TILDAS Remote Sensing. Ph.D. thesis, Massachusetts Institute of Technology, February 1999.
- [9] J.B.Heywood (1988) Internal Combustion Engine Fundamental. McGraw-Hill, Inc., New York

Overview of the most developed instances of Eco-Industrial Parks in Italy

Sara Tessitore, Tiberio Daddi, Francesco Testa

Abstract—The literature presents a gap related to Italian experiences with Eco-Industrial parks (EIPs). Although this approach is distributed throughout many regions of Italy, particularly in the northern and central regions. This paper describes the dissemination of EIPs in Italy and the “Key Elements” of this model in Italian experiences. The study introduces 5 of most important Italian case studies of EIPs and describes the environmental infrastructure and services implemented in those cases. The research compares the main international features of EIPs with the characteristics of these 5 case studies and highlights the differences and similarities between Italian and international EIPs.

Keywords—Eco industrial park, industrial ecology, case study, sustainable development, case study, Italy.

I. INTRODUCTION

INDUSTRIAL ecology is a new approach to more sustainable production that supports companies in implementing sustainable development strategies. The concept of industrial ecology evolved from environmental management paradigms and springs from interests in integrating notions [1] of sustainability with environmental and economic systems [2]. Industrial ecology can be applied to eco-industry development at three levels. The boundaries can be defined at the micro-level (firms), the “meso level” (eco-industrial parks), and the macro-level (regional and wider global networks of manufacturing activity centers) [3].

This article focuses on the concept of eco-industrial parks (EIPs). The research investigates the spread of EIPs in Italy and their distinctive features. An industrial park is defined as “a large tract of land, sub-divided and developed for the use of several firms simultaneously, distinguished by its shareable infrastructure and close proximity of firms” [4]. Other definitions of EIPs were introduced in other studies. Cotè [5] was the first author to cite the issue of economic and natural resource conservation. This author defined the eco-industrial

park (EIP) as “an industrial system which conserves natural and economic resources; reduces production, material, energy, insurance and treatment costs and liabilities; improves operating efficiency, quality, worker health and public image; and provides opportunities for income generation from the use and sale of wasted materials”. This concept affects worker health as well, which is not included in the other definition of the EIP. The definition of an EIP was discussed during the 1990s by authors such as Lowe [6] and Ayres [7]. The interest in the development of EIPs is relevant especially in the USA. The USEPA (United States Environmental Protection Agency) defined EIPs as A community of manufacturing and service businesses seeking enhanced environmental and economic performance by collaborating in the management of environmental and reuse issues. By working together the community of businesses seeks a collective benefit that is greater than the sum of the individual benefits each company would realise if it optimised its individual performance only. In the most recent years the concept of the EIP has been globally popularized and has attracted interest in less developed, industrializing, as well as developed countries [8]. From the 1990s onwards, a number of local and regional projects were initiated to plan and actively develop EIPs. As Heeres [9] states: “attention for eco-industrial park (EIP) development projects has grown enormously among national and regional governments and industries in many countries. It is believed that a well planned, functioning EIP has the potential to both benefit the economy and substantially relieve environmental pressure in and near the location of its development”.

II. INTERNATIONAL EXPERIENCES OF EIPs

The EIP approach has been developed at the international level and the experiences of EIPs have disseminated in many industrial areas that have adopted industrial ecology solutions. Many national institutions supported the dissemination of EIPs by programmes and policies. In the USA the dissemination of EIPs was encouraged by the federal government through the President's Council for Sustainable Development, which identified and promoted four demonstration sites [10] [11]. EIPs have been similarly encouraged in Europe, particularly in the Netherlands [12], Denmark [13] and Finland [14]. Experiences with EIPs have increased and the literature has been enriched by many case studies.

Some studies describe the International EIPs and the most

Sara Tessitore, Istituto di Management Scuola Superiore Sant'Anna, Piazza Martiri della Libertà, 33, 56127, Pisa Italy, phone.+39 050.88 3973, fax +39 050.88 3936. s.tessitore@sssup.it

Tiberio Daddi, Istituto di Management Scuola Superiore Sant'Anna, Piazza Martiri della Libertà, 33, 56127, Pisa Italy.

Francesco Testa, Istituto di Management Scuola Superiore Sant'Anna, Piazza Martiri della Libertà, 33, 56127, Pisa Italy.

famous experience in Europe and in other countries. Looking at the European experiences we note Kalundborg as one of the most interesting case studies of EIPs. Kalundborg Park in Denmark was developed in the 1960s. The industrial district at Kalundborg is labeled as an “industrial ecosystem” or “industrial symbiosis” because of the many links between the firms [10]; [13]; [15].

This approach was developed in Canada [16] and Australia [17]. We also found EIPs in Germany, the UK and other countries, especially in Northern Europe [18].

Examples of EIPs in Asia are mainly concentrated in China and Korea [19]; [20], but the development of EIPs is attracting interest in India [21], the Philippines, Thailand and Sri Lanka [22] as well.

There are many studies that describe the EIP experiences of China, where there are now over 100 EIP projects [23]. The SEPA (State Environmental Protection Agency of China) categorized industrial parks in China into three groups in this new regulation, namely the sector-integrated group, the venous group, and the sector-specific group, each with slightly different criteria and indicators. The sector-integrated group refers to those parks with multiple industrial sectors, the venous industrial grouping particularly refers to those resource recovery parks where environmental technology companies and firms making “green products” coexist and the sector-specific group refers to parks with primarily one main sector [24]; [25]. One of the most important Chinese case studies is that of the Tianjin Economic-Technological Development Area (TEDA). The emergence of an environmental institution in TEDA is used as a backdrop to assess how TEDA has transformed itself into one of the top three national eco-industrial parks in China. Following two years of field research, a network of 81 symbiotic inter-company relationships formed in TEDA during the past 16 years. These relationships involve utilities, automobiles, electronics, biotechnology, food and beverage, and resource recovery clusters [26]. Another famous Chinese EIP is Guigang. The Guigang Group (GG), which operates one of China's largest sugar refineries, has been developing and implementing an internal and external industrial symbiosis strategy for more than four decades. The GG first invested in developing its own collection of downstream companies to utilize nearly all by-products of sugar production. This strategy has generated new revenues and reduced environmental emissions and disposal costs, while simultaneously improving the quality of sugar [27].

Singapore's Jurong Island is developing three EIP projects in the form of mini ecological parks and alternative fuel infrastructures, created through long range planning [28]. The first Korean EIP is the Daedok Technovalley (DTV) Development Project. The Korean EIP focused on symbiotic industrial network construction, energy and material flow planning, externally and internally built environmental design and cultural identity creation [29]. The experience of Ulsan city is also notable. The Ulsan industrial complex has been

continuously evolving from conventional industrial complexes to eco-industrial parks by spontaneous industrial symbiosis.

A project by the Technology Development Foundation of Turkey to disseminate cleaner production and EIPs also began in Turkey in 2009 [30].

The Queensland State Government in Australia developed the first eco-industrial park in 1994, Synergy Park, a site 22 km west of Brisbane. The park aims to support several key scale economies. The first is the central warehouse, which will allow for shared logistics and the controlled movement of vehicles. The second is the sophisticated logistics management system. The third level of economy arises from the energy supply infrastructure (a co-generation plan for the park's business). The EIPs in Australia are built on “the importance of an industrial catalyst, a synergy trust, coordination of key industries and utilizing players, the need for strategic planning that has foresight and flexibility and developing community oriented development” [17].

Another important case study is the idea of the West Midlands Industrial Symbiosis programme (WISP). West Midlands, which is located some 200 km Northwest of London and covers the areas around Birmingham. One plan has already become operational, providing economic, environmental and social benefits. This consists of the conversion of 5000 t/year of waste edible oils into bio-diesel [18].

Many other studies [31] describe some EIP case studies in the Netherlands and Canada, analyzing their key elements (Material/energy networks, Process integration) and management.

The following table summarizes some of most famous EIPs at the international level.

Table I: Case studies of International EIPs

Table I: International EIPs case studies

EIPs	Country	Industrial Sector	Dimension (ha)	N. of companies	Reference
Devens	USA	mixed	1780	not available	Mirata, 2004
Kalundborg	Denmark	mixed	not available	not available	Many authors
West Midlands industrial symbiosis programme (WISP)	UK	mixed	not available	20	Mirata, 2004
Guigang / Guitang group	China	sugar	not available	not available	Zhu et al 2007
Synergy Park	Australia	food and beverage	37	not available	Roberts, 2004
Burnside Industrial Park	Canada	many	760	1300	Janet et al. 2004
Ulsan industrial parks	Korea	petrochemical, nonferrous metal, ship building and automobile industries	5544	700	Park et al. 2008

Despite the national Italian law issued in 1998 mandating the spread and application of EIPs and despite Regional Governments who are actively applying EIP concepts in their local policies, there is currently no literature related to Italian EIPs. There are just a few surveys and studies that cite Italian EIPs, and often the ones mentioned are not the country's most important ones. For instance a recent survey of EIPs in the USA and Europe [34] investigated 53 EIPs and only 3 are Italian case studies. Coté and Cohen-Rosenthal [35], cited the EIP experiences in Emilia-Romagna without providing data or technical information on the EIPs developed there. The Turin Environment Park is mentioned in an article by Gibbs in 2003 [36] and the experience of Montagna-Energia Valle di Non [37].

III. INTERNATIONAL CHARACTERISTICS OF EIPs

There are many studies identifying the main features of EIPs. Many authors focus on industrial symbiosis and others on landscape ecology or networking. From our review of the literature we have selected the "key elements" of the EIP concept. The initial characteristics of EIPs were essentially the industrial symbiosis initiatives and the "by-product exchange". These aspects characterized the first EIP experiences. The by-products exchange is influenced by geographic proximity of firms and especially since transport costs will eventually limit the spatial boundaries over which certain by-product exchanges remain economically viable [38]. In a preview publication Chertow [38] suggested three criteria to develop EIPs: building on existing types of material and energy exchange, building on pre-existing organisational relationships and networks and the anchor tenant model. Another authors [39] build their EIP conceptual framework on the model of natural ecosystems. They argue that increased diversity (of the actors involved) enhances connection and opens up new possibilities for cooperation, although increasing the number of actors can also lead to conflicting interests, thereby acting as a decisive factor in preventing the development of an EIP. In recent years Chertow [40] identified many types of collaborative arrangements for businesses that can lead to the development of industrial symbiosis. In addition to by-product

exchanges there are other typical approaches to EIP development such as the sharing of utilities and joint service provision. Utility sharing includes shared access to public goods and services. An example of utility-sharing initiatives is the collective use of a geothermal exchange system in the Phillips Eco-Enterprise Center in Minneapolis, Minnesota, which improved energy efficiency by 35% in its office building facility [41]. "Joint service provision" provides for the creation of common services for firms. These tools create economies of scale and benefit sources of both urbanization and localization of economies [42]; [43]. "Policy programs from governmental agencies are usually referred to as a major conditioning factor. The Chinese policy on circular economy is one of the central factors of influence on Chinese industrial symbiosis development [44]; [45]. In the United Kingdom the influence of public policies is also evident, as a result of the NISP and of waste management policies [18]. The importance of a comprehensive legal framework in order to move towards a recycling-based society is confirmed by Japan's experience in which the Government implemented a programme that involves societal actors in shaping the initiatives [46]. Tudor [47] defined the three main elements of EIPs as IE (industrial ecology), biological ecology, and the spatial perspectives provided by landscape ecology. IE relates to industrial and ecological systems that are based on optimal circulation of materials and energy. Regarding biological ecology, EIPs seek to mimic natural ecosystems where 'waste' products from one process are incorporated into another process, just as carbon dioxide and oxygen in the processes of photosynthesis and respiration [47]. Landscape ecology aims to reduce the 'negative' ecological effects of urban and industrial development. In a survey of European and USA EIPs [34] the key features of IE and EIPs were investigated: the cycling of materials and energy as industrial symbiosis initiatives, or closed cycle, networking and cluster building concerning networking among firms, sustainable development and collaboration with local stakeholders.

The following table summarizes the key elements of the most cited EIPs in the international literature.

Table II: Case studies of International EIPs

Table 2 Key elements of EIP emerged from literature framework

Key Elements	Tudor et al, 2007	Gibbs and Deutz 2007	Chertow et al, 2008	Boons et al. 2011
By products and energy exchanges	X	X	X	X
Sharing service			X	X
Landscape ecology	X			X
Common infrastructures			X	X
Networking		X	X	
Involvement of local stakeholder		X		X

IV. GOALS AND METHOD

During our review we noted a gap in the literature. There are very few articles that describe Italian case studies of Eco-Industrial Parks.

However, in Italy there is a strong interest in EIPs and many policy makers are stimulating the establishment of them or the

reconversion of existing industrial areas into areas based on the key concepts of industrial symbiosis.

To achieve this objective we will use the following method: First we will describe the main drivers of the dissemination of EIPs in Italy. Then we will focus on the description of the characteristics of five of the most important experiences developed in Italy. Finally, in the discussion section we will compare the key aspects of international EIPs identified in the literature review with the distinctive features identified in the Italian cases.

The main source of information on the Italian case studies is a report issued by the regional government of Emilia-Romagna, issued in 2010 [49]. It describes 14 highly developed experience examples of EIPs. We selected the five case studies presented in this paper from these, according to the following criteria: maturity and degree of development of the EIP, geographical distribution, and relevance of the experiences in terms of results achieved.

V. RESULTS: DRIVERS OF THE DISSEMINATION OF EIPs IN ITALY

Italy is witnessing a growing interest in EIPs among policy makers on all administrative levels. Usually, four "visions" can be identified, which have emerged gradually in the Italian experience.

The "technocratic vision" considers the EIPs to be a result of production and location choices made by the companies. These choices are linked to the advantages of building industrial plants close together and to the synergies obtained from a mere "technical" point of view. For example, businesses may find it convenient to combine and share the management of some environmental facilities. This view explains the development of the EIPs as a result of the enterprises' (usually SMEs) need to share the management of the most significant environmental aspects (waste water treatment, power generation, waste collection) through the construction of common structures and facilities [34]. Their aim is to increase environmental efficiency, as well as economic efficiency through cost savings, thanks to the sharing of collective facilities or structures in the area, obtaining advantages from geographic proximity [51].

The "managerial vision" is more directly based on the opportunity to stimulate and promote management and organizational coordination among the environmentally relevant business activities undertaken by the already established enterprises or businesses that are going to settle in an area. In this case, scale economies are improved not only in technical terms but they also achieve benefits linked to more "intangible" variables such as the management and organisation of environmental issues. The objective is to optimize and prevent environmental impact related to the productive activities located in the area by focusing on aspects that can facilitate proper and effective management [52].

The "governance vision" exceeds the boundaries of technical and management efficiency of enterprises and sees the development of EIPs as the response to a problem of "governance". The systemic approach of EIPs can indeed be

seen as a policy trend, and as an opportunity for institutions to promote local development geared towards sustainability. This vision treats the EIP as a lever for local policies and as a technical and managerial solution for the local production system [50]. Many Italian experiences have shown that over time the role of institutions can be crucial in stimulating and strengthening the development and functioning of EIPs.

Taking the categorization of the literature studies presented in the previous section into account, we may note that the effects of the policies of the three groups of drivers described above are more oriented toward the Command and Control approach than toward voluntary tools [53].

In contrast, in the Italian experience we observe another kind of driver that follows more "holistic" methods, and which are linked to voluntary policy tools. In this case, the process leading to the creation of an EIP is no longer just a matter of technical drafting and territorial planning of the area. It becomes a decision-making process, in which enterprises are involved, along with their representatives, local institutions and even the social partners in the territory. Right from the planning stage, the common goal is to coordinate the choice of location and the technical and managerial solutions that are most effective from an environmental point of view. To sum up, the "holistic" vision is able to increase the benefits for the different stakeholders, provided that they are capable of operating within the framework of a true "industrial policy for the territorial production systems" which is voluntarily oriented towards sustainability.

VI. RESULTS: ITALIAN EIPs KEY EXPERIENCES

The study published by the Regional Government of Emilia-Romagna in 2010 (ERVET and Emilia Romagna Region, 2010) defined 84 experiences in which there was an attempt to experiment with the EIP approach and an interest in carrying out localized solutions that favour sustainable development. These 84 experiences are located in only 5 Italian regions (Emilia-Romagna, Friuli-Venezia Giulia, Liguria, Marche, Piedmont and Tuscany) and are distributed as follows:

- 30 in Emilia-Romagna
- 21 in Friuli-Venezia Giulia
- 15 in Liguria
- 7 in Marche
- 1 in Piedmont
- 9 in Tuscany

The study selected 14 case studies whose characteristics were most strongly linked to the EIP approach, namely the productive areas that had adopted managerial and infrastructural solutions inspired by the concept of industrial ecology and also had a management body, which is a fundamental element of Italian EIPs.

This paper will present the following EIPs:

- 1) Macrolotto of Prato (Tuscany),
- 2) Industrial Area of Ponterosso (Friuli-Venezia Giulia),
- 3) Industrial Area of Ponte Rizzoli (Emilia-Romagna),

- 4) Industrial Area of Padova (Veneto),
- 5) Industrial Area of Ancona (Marche).

“Macrolotto di Prato” is located in Prato, Tuscany, which is one of the most important productive districts of Italy and specialize in textiles. Macrolotto is the first EIP in Italy and it is the most advanced in eco-innovation technologies and services.

Macrolotto is an industrial area of 150 hectares. There are about 380 companies in the district with over 3,000 employees. The environmental initiative originates from the need to provide this industrial area with centralized environmental services (such as recycling the waste water for production use and for firefighting, reducing the use of private vehicles for employee transportation, etc.). The nonprofit consortium CONSER managed the common environmental services introduced in the Macrolotto productive area.

The following centralized environmental infrastructures and services are present in Macrolotto:

- 1) Management and maintenance of the centralized waste water recycling plant and of the industrial aqueduct, and the provision of a centralized firefighting service;
- 2) Promotion and provision of centralized services for the industrial area that can create scaled economies to reduce production costs while also respecting the surrounding environment and society;
- 3) Training and environmental education initiatives;
- 4) Mobility management (carpooling, car sharing and freight);
- 5) Other centralized services for workers (laundry, pharmacy, post office, nursery).

In 1975, following the depletion of ground water resources due to the presence of textile companies with a high demand for water, the town of Prato pushed the industrial area to build an industrial aqueduct fed by wastewater from the treatment plant which was under construction at the time. However, the water could not be used and therefore it was necessary to build a refining and pumping station as well as 12 km of water pipes. Planning began in 1985 to define a design that, after the usual treatment, reduces the suspended solids using sand and anthracite filters. The process also removes color through an activated charcoal treatment. An economic calculation showed that the centralized solution was cheaper for the companies than paying a water supplier.

The system began operating in 1990 and currently the plant in Prato is able to provide 5 million cubic meters of water per year, which is why other companies outside the Macrolotto area that have a high demand for water have joined the system. The Industrial Area of Ponterosso is located in the Municipality of San Vito al Tagliamento, near Pordenone, in the lowlands of Friuli. There are 120 companies (with a total of approximately 3,150 employees) which are very diversified both in products and in size. The sectors range from chemicals to food products, from glass to machinery and components, and from woodworking to services.

The area has a double collecting system where wastewater goes into a sewage treatment plant for the exclusive use of the industrial zone. This EIP is managed by the Consortium for the Industrial Area of Ponterosso.

From the energy supply standpoint, the Consortium operates combined production plants, and self production of electricity and heat distribution plants.

The Consortium provided the industrial area with a railway that is linked with the national network, offering each company the opportunity to have terminals in their area and manage the distribution of goods as an alternative to road transport.

Among the consulting services offered indirectly through an agreement with third parties, there are also services that can lead the company to greater environmental sustainability, such as advice on quality, environment and safety. The environmental monitoring system managed by the Consorzio Ponterosso that periodically monitors some indicators. The Ponterosso area is equipped with other services and infrastructure for all companies operating in this EIP including the following:

- 1) Rail access
- 2) Natural gas pipeline
- 3) Street management
- 4) Cafeteria for workers
- 5) Other services for workers

“APEA Ponte Rizzoli” is an industrial zone of about 105 hectares and approximately 170 companies in the region of Emilia-Romagna.

The area is characterized by the predominance of production activities in the sectors of manufacturing and business services. The Province of Bologna has implemented a pilot project to promote the Environmentally Equipped Areas, involving the production area of Ponte Rizzoli as a pilot project.

The plan to design the area and its services and infrastructure was the result of a survey conducted in 2004. The companies suggested creating a plan for energy production and waste management. The design of APEA Ponte Rizzoli includes three projects:

- 1) Heating plant and cogeneration plant powered by methane and biomass;
- 2) Network for rainwater recovery;
- 3) Bicycle paths for productive area employees.

The area will be also equipped with many services for workers such as a cafeteria, parking and others.

This project is not yet concluded but the local institutions are working to create all of the infrastructure and services for the companies provided for in the plan.

The Industrial Area of Padova is located in Friuli-Venezia Giulia. It is composed of 1,500 companies operating in different manufacturing fields. The area is one of the biggest in northern Italy and starting from 1956 has been managed by a consortium of local public institutions (Municipality, Province and Chamber of Commerce). The area is served by a railway with 7 km of tracks, 2 toll booths, 5 service centers with post

offices, hotels, restaurants, banks, professional offices, business services, and a fiber optic ring of 30 km. 18% of its territory is dedicated to green areas. The main infrastructures in this area relate to mobility management since approximately 50,000 people (workers, suppliers, consultants and other stakeholders) travel to the productive area every day. Mobility management was the main problem presented by the industrial area for the workers and the local community. The consortium invested in this problem and organized services and infrastructures to reduce the pressures connected with road traffic. There is a mobility manager that identifies some solutions and improvements. The area also invested in training activities on sustainability and planned for the new plant to increase energy production from renewable energy sources.

The productive area of Ancona is the first EIP in the Marche region. This area began to develop in the 1980s and is located around Ancona's harbor. The area is composed of about 90 companies operating in various sectors (industry, services, craftsmen) linked to maritime activities such as shipbuilding, mechanical repairs, electrical systems, nautical decor, food supplies, logistics, shipping agencies, seafood processing, etc. ZIPA manages the productive area and four other productive areas in the Marche. The shared services relate to training activities, consulting and company support of infrastructure for water discharge and waste. ZIPA aims to develop "area management" based on a high level of company involvement in the improvement of environmental performance.

VII. DISCUSSION: A CROSS COMPARISON OF THE CHARACTERISTICS OF ITALIAN EIPs AND INTERNATIONAL EIPs

The development of EIPs in Italy was mandated in the national Legislative Decree 112/1998, which introduced the APEA production model. The APEA model is linked to the EIP concept. The law has decreed that every region has the job of regulating the criteria and the system requirements of EIPs (APEA).

The fundamental elements of Italian EIPs (APEA) are the presence of unified area management (management body) and of common environmental services and infrastructure for the companies that operate the EIPs.

Italian EIPs were characterized by the presence of a management body, which exists in all 5 cases examined above. The "management body" is an organism (a public-private company or consortium) that coordinates the development of the productive area and promotes the adoption and implementation of services and infrastructure to reduce the environmental impact of companies that operate within EIPs. The management body of an EIP has numerous abilities. It can coordinate the management of environmental aspects such as waste and water resources, organize services such as transportation, as well as education and communication initiatives. They can also create infrastructure and develop relationships and transactions with local stakeholders. The latter task is another element that stands out about Italian EIPs (APEA). The collaboration between companies and institutions is considered a very relevant element to the adoption of managerial and infrastructural solutions that foster

the creation of EIPs. Much of the collaboration therefore begins with participation in decision-making processes related to the adoption of widely shared solutions that allow companies to implement more sustainable production methods. The presence of shared services and infrastructure is provided for in the national regulation and is therefore an essential criteria for all EIPs (APEA) developed in Italy. This relates to various types of services such as transportation, waste collection, lighting, etc. The legislations of many regions address the infrastructure of purifying areas, energy production plants, and rain water collection systems, which are strongly encouraged through funding and incentives. Objectives of the analysis of Italian EIPs and the key elements of international EIPs is to reveal how much these aspects are present in the Italian experience and to discover similarities and differences in the implementation of the methodologies and instruments for more sustainable production.

Already in the legislation's definition of APEA, some similarities and differences emerge with respect to the experiences of the EIPs cited in numerous international studies. The APEA concept recalls the definition of EIP given by USEPA, "A community of manufacturing and service businesses seeking enhanced environmental and economic performance by collaborating in the management of environmental and reuse issues". Also in much regional legislation the APEAs are described as a sustainable approach to production, whose goal is both improvement of environmental performance of businesses and increasing their competitiveness.

In summary, Italian EIPs (APEA) have three main characteristics: the management body, the shared environmental services and infrastructure and the tight collaboration between public and private entities. The shared services and infrastructures and the collaboration between the various stakeholders emerge as essential characteristics of international EIPs, as shown in the literature analysis, in contrast with the management body that results as an essential Italian aspect. Reference is made to a coordinating entity in the EIP in only a few other case studies, such as the British case study of WISP, described by Mirata (2004). This aspect, particularly because it is rarely cited in the international literature on EIPs was not a part of the comparative analysis. The comparative analysis focused on the 6 characteristics which emerged from the articles that were analyzed. The characteristics defined in table 2 were searched for in the 5 case studies described, which are representative of the national EIP scenario. Each of these Key Elements was verified to have been implemented in the case studies and the level of implementation was distinguished as one of the following:

- (-) not implemented
- (+) poorly implemented
- (++) implemented
- (+++ strongly implemented

Table III Comparative analysis of the Key elements of the international concept of the EIP and Italian EIP features

Table 3 Comparative analysis between Key elements of International concept of EIP and Italian EIP features

Italian EIPs	Exchange of materials and Energy (Industrial symbiosis)	Sharing service	Landscape ecology	Common infrastructures	Networking	Involvement of local stakeholder
Macrolotto of Prato	-	+++	++	+++	+++	++
Ponterosso	-	+++	++	+++	++	+++
APEA Ponte Rizzoli	-	++	++	++	+	+++
I.Z. of Padova	-	+++	+++	++	++	+++
Productive area of Ancona	-	++	++	+	+++	+++

Table 3 clearly shows the substantial differences between Italian EIPs and the international approach, highlighting for example the minimal attention to the solutions related to industrial symbiosis. Today, experimentation with symbiosis initiatives at the area level has been applied minimally in this country, while there is instead a strong presence of shared infrastructures. The aspect of shared services and infrastructure is strongly developed in Italian EIPs, both because it is encouraged and outlined in the APEA legislation and because many national experiences exist that were economically and environmentally significant. The most notable case is certainly that of the industrial aqueduct of Macrolotto di Prato, which resulted in a significant reduction of industrial impact on local water resources. In fact, that installation made it possible to re-use 5 million MC of purified water per year in the productive processes of the Macrolotto companies. Shared services were one of the strong points of Italian EIPs and were present in all 5 case studies. Instances of shared services are numerous and are not limited to the environmental services of waste collection, transportation, energy supply, etc., but also include services for workers such as cafeterias and childcare.

Attention to "Landscape ecology" is present in all 5 case studies presented, although initiatives for landscape improvement are all fairly recent. Only Padova's Industrial Zone is strongly engaged in this aspect, inasmuch as the company is located near a park where it has launched numerous projects and initiatives for the protection of the landscape, bio-monitoring of the area and educational projects on subjects such as renewable energy sources and sustainable development.

Networking among companies is mainly characterized by 4 of the 5 experiences examined. In the APEA of Ponte Rizzoli this aspect is minimally implemented because the EIP is still in the startup phase in which few companies are located there and they have not yet activated the mechanisms of cooperation. The networking is manifested in different ways among the various cases considered, including through information exchange, the organization of and participation in projects and initiatives for the development of the EIP and improvements in sustainability.

The involvement of the stakeholders, namely public institutions, sector organizations, etc., has a high level of development in 4 of the case studies. Only Macrolotto limits stakeholder involvement mainly to private entities, reducing interactions with public institutions.

Also, the involvement of the stakeholders, like networking, is

implemented in different ways across the Italian case studies. For example, in the Ancona area, there is strong participation in the decision making path, especially in defining the development plans and initiatives for the EIP. On the other hand, Padova's IZ collaborates with organisations and foundations for the execution of educational projects.

The 5 Italian case studies can therefore be considered partly different from the many examples of international EIPs, both with regard to the limited spread of industrial symbiosis initiatives and for the presence of the management body that was rarely found in the international EIP scenarios. These differences are emphasized when one compares Italian experiences with those of Asian countries, such as the EIP of Guiyang City and Lubei or the Korean case of Ulsan Industrial Park, in which the principle element mainly consists of the presence of technological solutions that allow for the exchange of materials and energy between the various businesses. Italian examples of EIPs are therefore shown to be more similar to some European and American cases, such as the case study of Humber in the UK which refers to the presence of a management body, as well as the case of Denves in the USA, where there is coordination between enterprises, sector organizations, institutions and representatives of the local community.

VIII. CONCLUSION

This paper gives a contribute in the bridging the gap linked with the experiences on Italian EIPs. From our overview emerges clearly that Italy is not a Country without interesting case studies to describe even if these are partially different by the cases identified at international level. Some peculiarities can be pointed out.

Firstly, as aforementioned, the initiative of industrial symbiosis declined in its form of by-products and energy exchange are not so disseminated. One of the reason can be identified in the fragmentation and the characteristics of the Italian industrial sector. In our Country the industrial areas are mainly composed by small and micro enterprises. The large presence of these kind of firms reduce the possibility to have relevant quantity of by-products and energy to recover from one hand and on the other hand increase the difficulty to manage in an integrated way the industrial area due to the necessity to coordinate too many subjects.

Secondly, Italy has chosen a policy approach based on national legislation to stimulate the diffusion of industrial ecology concepts among the industrial areas. Among the different approach adopted in other Countries this seems as an Italian peculiarity.

Thirdly, the Italian EIPs are based on a strong presence of the manager of the industrial area as a subject capable to involve private and public actors to pursue the common objective of the sustainable development of the industrial areas. In the carrying out this phase at the beginning we can assist to some tensions among stakeholders. For example the industrial associations can identify the Management Body of the area as a hypothetical competitor in the providing of environmental service and assistance to the tenant companies. In any case after this initial phase the fact to have on board of the initiative

both private as well as public actors can give an added value to its effectiveness.

According to the results described in this paper possible future research topics can be identified. One of these is the focus on the role and power assigned to the Management bodies of the different Countries. Which functions? How they get financial resources for its functioning? Do they benefit from the economic synergies realized in the area or are they funded by public resources?

A second research aim could investigate the environmental performance of the Italian industrial areas comparing them with the performance of areas of other Countries where industrial symbiosis initiatives are wider adopted. Strictly referred to this, the measurement of the environmental performance of the industrial area as a whole instead of the effectiveness of a singular initiative in our opinion can be considered a further topic to be investigated by scholars in this field.

REFERENCES

- [1] J. Ehrenfeld, N. Gertler, "Industrial Ecology in Practice: The Evolution of Interdependence at Kalundborg", *Journal of Industrial Ecology*, Vol. 1, pp. 67–79, January 199
- [2] B. R. Allenby. "Achieving sustainable development through industrial ecology". *International Environmental Affairs* Vol. 4, pp. 56-68, 1992
- [3] B.H. Roberts, E. Greenhalgh "Planning for eco-industrial parks to facilitate industrial ecologies in SE Queensland". In: *Shaping the sustainable millennium conference*, A. Shenablah, B. Byjacharya, ed. Brisbane, Brisbane: Queensland University of Technology; 2000.
- [4] M.T. Peddle, "Planned industrial and commercial developments in the United States: a review of the history, literature and empirical evidence regarding industrial parks", *Economic Development Quarterly*, Vol 7 (1), pp. 107–124, 1993
- [5] R.P. Cote', J. Hall "Industrial parks as ecosystems". *Journal of Cleaner Production*, Vol.3, pp.41–6,1995
- [6] E. Lowe, S. Moran, D. Holmes "A fieldbook for the development of eco-industrial parks". Report for the U.S. Environmental Protection Agency. Oakland (CA): Indigo Development International, 1995.
- [7] R.U. Ayres, "Industrial metabolism: theory and policy. In: Richards DJ, Allenby BR, Frosch RA, ed. *The greening of industrial ecosystems*". Washington: National Academy of Science, 1995
- [8] Y. Geng, R. Coté, "Applying industrial ecology in rapidly industrializing countries", *International Journal of Sustainable Development and World Ecology* Vol.11, pp. 69–85, 2004
- [9] R.R. Heeres, W.J.V. Vermeulen, F.B.de Walle, "Eco-industrial park initiatives in the USA and the Netherlands: first lessons". *Journal of Cleaner Production*, Vol. 12, pp. 985-95, 2004.
- [10] L. Evans, "Lessons from Kalundborg", *Business and the Environment* Vol. 6, 1995.
- [11] E. Cohen-Rosenthal "What is eco-industrial development?. In: *Eco-industrial strategies: unleashing synergy between economic development and the environment*. E. Cohen-Rosenthal, J. Musnikow , ed. Sheffield:Greenleaf; 2003, pp. 14-29.
- [12] J.A.M. Eilering, W.J.V. Vermeulen, "Eco-industrial parks: toward industrial symbiosis and utility sharing in practice". *Industrial Ecology*, Vol.1,pp.245-70, 2004
- [13] J.R. Ehrenfeld, "Industrial ecology: A strategic framework for product policy and other sustainable practices". In *Green goods*, E. Ryden and J. Strahl ed. Stockholm: Kretslopp delegation, 1995.
- [14] J. Korhonen, J. Snäkin, "Analysis the evolution of industrial ecosystem: concepts and application, *Ecological Economics*, Vol. 52, pp.169–186,2005
- [15] A. Garner, C.A. Keoleian, "Industrial ecology: an introduction", *Pollution, Prevention and Industrial Ecology*, pp.1–32,1995.
- [16] G.J.Venta, M. Nisbet, "Opportunities for industrial ecological parks in Canada. Case Study of Sarnia–Lambton IndustrialComplex". Environment Canada, Ottawa,1997.
- [17] B.H. Roberts,"The application of industrial ecology principles and planning guidelines for the development of eco-industrial parks: an Australian case study", *Journal of Cleaner Production* Vol. 12, pp. 997–1010, 2004.
- [18] M. Mirata "Experiences from early stages of a national industrial symbiosis programme in the UK: determinants and coordination challenges". *Journal of Cleaner Production* Vol.12, pp. 967-83, 2004.
- [19] Y. Genga, R. Cote'b "Applying industrial ecology in rapidly industrializing Asian countries", *International Journal of Sustainable Development & World Ecology*, Vol.11, 2004
- [20] Q.Zhu, R. Cote', "Integrating green supply chain management into an embryonic eco-industrial development: a case study of the Guitang Group". *Journal of Cleaner Production*, Vol.12, pp. 1025–1035, 2004.
- [21] R. Patel, B. Modi, S. Patwari, R. Gopichandran, "M. Wilderer..Aspect of e eco-industrial networking exercise at the Naroda industrial estate". Proceedings of *International Con. on Industrial Park Management: New Strategies for Industrial Development*. Manila, Philippines,2001.
- [22] Lowe E. "Eco-industrial development in Asian developing countries" (Book style with paper title and editor) In: *Eco-industrial strategies: unleashing synergy between economic development and the environment*. Cohen-Rosenthal E, Musnikow J, ed. Sheffield: Greenleaf; 2003, pp. 341-52.
- [23] SEPA (State Environmental Protection Agency). "National environmental protection plan". Beijing , China : SEPA, 2007.
- [24] Festel,G. and Geng, Y.,," Chemical Industry parks in China". In: *The Chemical and Pharmaceutical Industry in China*.,Springer Verlag,ed. Berlin, 2005.
- [25] Q. Zhu, E. A. Lowe, Y. Wei, D. Barnes, "Industrial Symbiosis in China: A Case Study of the Guitang Group", *Journal of Industrial Ecology*. Vol. 11, Issue 1, pages 31–42, January 2007
- [26] H.Shia, M. Chertowa, Y. Song, "Developing country experience with eco-industrial parks: a case study of the Tianjin Economic-Technological Development Area in China", *Journal of Cleaner Production*, Vol. 18, pp. 191–199, 2010.
- [27] L. Zhang, Z. Yuan, J.Bi , B. Zhang, B. Liu, Eco-industrial parks: national pilot practices in China, *Journal of Cleaner Production*, Vol. 18, pp. 504– 509, 2010.
- [28] P.P.J. Yang, O.B. Lay. "Applying ecosystem concepts to the planning of industrial areas: a case study of Singapore's Jurong Island". *Jpurnal of Cleaner Production*, Vol.12,pp.1011–23, 2004.
- [29] O. Deog-Seong, K. Kyung-Bae, J.Sook-Young, "Eco-Industrial Park Design: a Daedeok Technovalley case study", *Habitat International* Vol. 29, pp. 269–284, 2005.
- [30] F. Ulutas, E. Alkaya, M.e Bogurcu, N. Goksel, N. Demirer, "Determination of the framework conditions and research–development needs for the dissemination of cleaner (sustainable) production applications in Turkey", *International Journal of Sustainable Development & World Ecology*, Vol. 19, pp. 203-209, 2012
- [31] A.J.D Lamberta, F.A. Boons, "Eco-industrial parks: stimulating sustainable development in mixed industrial parks", *Technovation*, Vol. 22, pp. 471–484, 2002.
- [32] J.A.M. Eilering, W.J.V. Vermeulen, "Eco-industrial parks: toward industrial symbiosis and utility sharing in practice" *Progress in Industrial Ecology*, Vol. 1, pp. 245-270, 2004.
- [33] H.S. Parka, E. R. Renea, S.M. Choia, A. S.F. Chiub, "Strategies for sustainable development of industrial park in Ulsan, South Korea— From spontaneous evolution to systematic expansion of industrial symbiosis", *Journal of Environmental Management*, Vol. 87, pp.1–13, 2008.
- [34] D. Gibbs, P. Deutz, "Reflections on implementing industrial ecology through eco-industrial park development", *Journal of Cleaner Production*, Vol. 15, pp. 1683–1695, 2007.
- [35] R. Cote, E. Cohen-Rosenthal "Eco-industrial development: about eco industrial parks", 1997. Available: www.cfe.cornell.edu/wei/eid.html
- [36] D. Gibbs "Trust and Networking in Inter-firm Relations: the Case of Eco-industrial Development". *Local Economy*. Vol. 18, pp. 222-236, 2007.

- [37] E. M. Lovelady, M. M. El-Halwag "Design and integration of eco-industrial parks for managing water resources". *Environmental Progress & Sustainable Energy*, Vol. 28, pp. 265–272, 2009.
- [38] M. R. Chertow, "Industrial symbiosis: literature and taxonomy", *Annual Review of Energy and Environment*, Vol. 25, pp. 313–337, 2000.
- [39] J-P. A. Snäkin, J. Korhonen "Industrial ecology in the North Karelia Region in Finland — Scenarios for heating energy supply" *International Journal of Sustainable Development & World Ecology*, Vol. 9, pp.9-21, 2002.
- [40] M. R. Chertow, W.S. Ashton, J.C. Espinosa, "Industrial Symbiosis in Puerto Rico: Environmentally Related Agglomeration Economies", *Regional Studies*, Vol. 42, pp. 1299 — 1312, 2008.
- [41] M. Krause and C. Brinkema, "The Green Institute Phillips Eco-Enterprise Center in Minneapolis, Minnesota", (Book style with paper title and editor) in *Eco-Industrial Strategies*, E.Cohen-Rosenthal and J.Musnikov ed. Greenleaf, Sheffield, 2003, pp. 276–287.
- [42] P.McCann "Urban and Regional Economics". Oxford University Press, Oxford, 2001.
- [43] J. B. Parr, "Missing elements in the analysis of agglomeration economies", *International Regional Science Review*, Vol. 25, pp. 151–168, 2002.
- [44] Y. Geng, B. Doberstein, "Developing the circular economy in China : challenges and opportunities for achieving leapfrog development". *International Journal of Sustainable Development and World Ecology*, Vol. 3, pp. 231-239, 2008.
- [45] Y. Geng, B. Mitchell, Q.H. Zhu, "Teaching industrial ecology at Dalian university of technology: toward improving the overall eco-efficiency". *Journal of Industrial Ecology*, Vol.13, pp. 978-989, 2009.
- [46] R. Van Berkel, T. Fujita, S. Hashimoto, Y. Geng, "Industrial and urban symbiosis in Japan: analysis of the eco-town program 1997-2006", *Journal of Environmental Management*, Vol. 90, pp. 1544-1556, 2009b
- [47] T. Tudor, E. Adam, M. Bates, "Drivers and limitations for the successful development and functioning of EIPs (eco-industrial parks): A literature review" *Ecological Economics*, Vol. 61 pp.199 – 207, 2007.
- [48] F. A. A. Boons, L. W. Baas, "Types of industrial ecology: the problem of Coordination". *Journal of Cleaner Production*, Vol. 5, pp. 79-86, 1997.
- [49] ERVET, Regione Emilia Romagna "Le aree produttive ecologicamente attrezzate in Italia: stato dell'arte e prospettive". Edizione sostenibile, Bologna, 2010.
- [50] D.Gibbs, Deutz Pauline. Implementing industrial ecology? Planning for eco industrial parks in the USA. *J Geoforum*, Vol.36, pp. 452–64, 2005.
- [51] M.R.Chertow, "Dynamics of geographically based industrial ecosystem", (Book style with paper title and editor) In: *The Dynamics of Regions and Networks in Industrial Ecosystems*, M. Ruth, B. Davidsdottir ed., Cheltenham, 2009.
- [52] L. Sokka, S. Pakarinen, M. Melanen, Industrial symbiosis contributing to more sustainable energy use – an example from the forest industry in Kymenlaakso, Finland, *Journal of Cleaner Production*, Vol.19, pp. 285-293, 2011.
- [53] P. Gallo, P. Carletti "Principles and Guidelines for a Sustainable Environmental Development." In: *Proceedings of PLEA 17th International Conf. on Passive and Low Energy Architecture*, James & James ed., London. 2000.

Sara Tessitore is graduated at University of Pisa in 2005 attended the Master in Environmental Management and Control at Sant'Anna School of Advanced Studies in 2006 Starting from 2009 is a PhD student in Management, Innovation, Sustainability and Healthcare.

Since 2007 she collaborates with the "Istituto di Management - Scuola Superiore Sant'Anna" on National and European projects on sustainability. She specializes in the environmental management tools and policies to improve the performance of companies especially small and medium.

Tiberio Daddi is Assistant Professor -at the Institute of Management, Sustainability Management area, and senior consultant in Environmental and H&S management in ERGO srl (a spin-off company of Sant'Anna School)

He is graduated in environmental economics at the University of Florence in 2001 and had an M.Sc. in *Environmental Management and Audit* in 2002.

Since 2002 he's research officer at S. Anna School of Advanced Studies with participation in many European and national projects related to the environmental management issues in industrial enterprises and territorial areas (clusters).

He worked in projects promoted by European Commission - DG Environment, DG Enterprise, DG Research). Since 2010 he is in chief of a VII Framework Programme project promoted by DG Research (BAT4MED) dealing with the impact of introduction of the EU Integrated Pollution Prevention and Control approach to the participating Mediterranean Partner Countries (Tunisia, Morocco, Egypt) and the implementation of Best Available Techniques).

Francesco Testa is Assistant Professor -at the Institute of Management, Sustainability Management area, and senior consultant in Environmental and H&S management in ERGO srl (a spin-off company of Sant'Anna School).

He has specialized in the economics and management of innovative environmental policy instruments and their relationship with the economy fundamentals and competitiveness.

He is lecturer in Environmental Management at the international PhD in Management (Innovation, Sustainability and Healthcare), at the Master of environmental Management and Audit –efficient management of resources held at Sant'Anna School and in the ordinary course at SSSA. He has been working on many pilot projects promoted by EC in the field of environmental management, impact assessment of IPPs and analysis of the relationship between environmental management and competitiveness. He has distinctive competences in the field of environmental product policies, GPP and SCP and environmental management having published several papers in International journals

Using direct and indirect methods of landscape evaluation on environmental amenities' valuation

L. Loures, A. Loures, J. Nunes and T. Panagopoulos

Abstract— The aesthetic component is increasingly recognized as an indispensable attribute for a better understanding of the landscape. In this sense, one of the objectives of this research is to analyze the aesthetic quality and economic valuation of river landscape of the Guadiana River, through the application of direct and indirect methods of landscape analysis, supported by the collection of public perception throughout the application of public participation questionnaires. In this sense it will be possible to measure the quality and the aesthetic value of this landscape not only by specialists but also by those for whom landscape constitutes a quotidian element.

Considering the performed analysis regarding landscape quality, fragility and absorption capability developed according to the six identified landscape subunits, it was found that the subunits Touristic Complex|Golf and Woodlands were the ones which have a higher visual quality, that the Agricultural|Production subunit was the one with the higher level of visual fragility, and that the subunit Touristic Complex|Golf was the one with the higher visual absorption capacity. Still considering the performed aesthetic analysis it is possible to verify that, according to the collected data, users prefer landscape units associated to golf and marsh, and that the presence of water is one of the most relevant factors in their preference. With regard to the economic assessment it was found that each user spent approximately 50 Euros, value that they would be willing to spend again in order to re-visit the study area. The performed analysis concludes that the used methods suit the proposed analysis and noted that even through the application of hypothetical approaches it is possible to capture and quantify the value of existence, management and maintenance of a particular environmental amenity.

Keywords— Aesthetic Analysis, Baixo Guadiana, Riverscapes, Public Participation, Economic Valuation.

This work was supported in part by the Centre for Spatial and Organizational Dynamics (CIEO) and from the Foundation for Science and Technology (FCT).

Luís Loures is with the Research at the Centre for Spatial and Organizational Dynamics and with the Polytechnic Institute of Portalegre, C3I, Portugal (corresponding author phone: 00351 965193379; e-mail: lloures@gmail.com).

Ana Loures is with the Polytechnic Institute of Portalegre - C3I, Portugal.

José Nunes is with the Polytechnic Institute of Portalegre, C3I and the UIQA – Research Center of Environmental Chemistry, Superior Institute of Agronomy, Portugal

Thomas Panagopoulos is with the Centre for Spatial and Organizational Organizational Dynamics Dynamics

I. INTRODUCTION

LANDSCAPE is something more than what is seen. Observer's knowledge, and the processes that led to its formation are becoming ever more important in landscape assessment and definition [1]. Thus, the analysis of the evolution of the term landscape represents a crucial starting point in studies in which it is the central element.

The concept has acquired multiple definitions according to the spectrum analysis and the knowledge area that analyzes it. According to Telles [2], one could say that "landscape is everything", because although, over the years, some authors have presented various types and concepts of landscape, they are merely definitions of analytical value, based on a whole in which the human being is an integral part, comprising a specific identity.

This research intends to carry out the Aesthetics and Economic Assessment of the Lower Guadiana river landscape, as well as to compare the application of direct and indirect methods of landscape assessment to this area. It also noted a set of secondary objectives, such as: assessing the parameters of aesthetic appreciation of the landscape, with greater significance and prevalence relative to the intervention area considering the different landscape subunits identified in the study area; identify patterns of public preference; verify the relationship between the different techniques for evaluating the quality of the landscape; and assess the value that people attach to the river.

II. LANDSCAPE ASSESSMENT METHODS

Panagopoulos [3] proposed the subdivision of the methods of landscape evaluation in direct and indirect methods. This subdivision was used as a starting point in this study, taking into account not only the overall objectives of the research, but also the ideas according to which the methods to carry out the evaluation of the aesthetic qualities of the landscape should be based on mixed methods of evaluation, such as specialist or behavioral type analyzes.

A. Direct Methods of Landscape Assessment

The methodologies for direct landscape evaluation consist in analyzing and describing a set of landscape features, combined in a certain way in order to obtain a total value, which represents the total scenic quality, obtained by sum of the parts [4]. Regardless of the skills and knowledge of each observer, it is accepted that the quality of the landscape derives from an interaction between their biophysical characteristics, the perceptive processes and the experiences and knowledge of the observer [5, 6].

- Visual Quality Assessment (VQA) and Landscape Visual Fragility (LVF)

Once introduced the issues inherent in the landscape analysis is important to define what is meant both by QVP and FVP. Generally, while the quality of a landscape is based on the capacity that it has or not to be impaired or destroyed *ie* landscape inherent ability to retain its essence and structure [7], fragility is the degree of susceptibility inherent to a certain landscape to transformation as a result of an amendment to the original, and therefore the expression of the degree of deterioration that the landscape would experience before the incidence of other use [7]. In this sense, unlike quality, fragility depends directly on the type of activity that you think will develop in a given landscape [6, 7, 8]. For example, Ayala *et al.* [7] defines as relevant for the analysis of VQA: vegetation, land use, slope, physiography, size and shape of the visual basin, and distance to roads, paths, and urban centers. Regarding the analysis of the LVF, the same author considers the physical geography, vegetation and land use, the presence of water, and the degree of humanization.

- Visual Absorption Capability – VAC

The VAC is considered by Canter [6], as the last component of visual management systems, to allow the definition of the magnitude of visual impacts on the landscape and | or the ability that a particular landscape has to absorb them. According Vargues [9] the method of determining the VAC is used to calculate the magnitude of the impact that a project or specific activity can have on a given landscape, through the relationship of physical factors, perceptive factors, variables significantly inherent the existing visual quality (shape, line, color and texture) and the proposed activity (scale, setting, duration, frequency, etc.) and whose analysis is highly subjective and dependent on the observer., which according to Burley [8], must consider the following factors: slope; vegetation; and the observer distance, for which considers three categories of space inherent in different planes - the foreground, middle ground and background - is that when the distance from the observer increases, so does the ability of visual absorption.

- Models of Psychophysical Preference

Psychophysical preference models constitute a typology of landscape evaluation used quite often [3], whose main

advantage is the ability to allow the creation of new standards and protocols able to estimate objectively the public perception inherent aesthetic quality of the landscape.

In this approach, public preference, obtained through processes associated with direct and indirect participation surveys is combined with the characteristics of the landscape in order to obtain balanced information between the two components, with the weights of each factor and the compose variable and generally estimated through assessments of public preference.

B. Indirect Methods of Landscape Assessment

According Mazure and Burley [10], integrated landscape assessments, considering aesthetic, economic and ecological variables, showed that the values are not independent and that there is a direct relationship between the different components and co-analysis. Considering these principles, several economists have focused on the development of methodologies for indirect assessment of the landscape, in which the demand and use value are used to assess the quality of the landscape, giving it an economic value to produce relevant information for the development of effective management policies. Among existing methods of economic valuation two deserve special mention, the "travel-cost" and contingent valuation methods.

- "Travel Cost" Method

According Leite and Jacoski [11] the travel cost method - is one of the most used indirect methods of landscape assessment that can be used to appraise the activities of recreation and leisure. This method, may be defined according to Oesten [12], as a evaluation form whereby the value of an indirect benefit is attributed based on the average cost spent by a given set of individuals to reach a particular good or service without defined market cost.

However, this method works with some assumptions [13] which may be considered limitations of the method: (i) it is considered that each person is traveling alone, even if it was a group journey; (ii) regardless of the reasons or goals that led the person to move to a particular location can be varied, it is considered that the visit or travel to the amenity in question was the sole reason for the trip, even if there were others. Regardless of the limitations that are inherent in the direct application of the method, it allows us to estimate a demand curve for a particular environmental/ recreational amenity, where the number of visits is a function not only of travel costs, but also of other socio-economic variables [11, 14], thus defining the possible added value to the enjoyment of the natural resource | amenity.

- Contingent Valuation Techniques

The contingent valuation techniques consist of interviews with certain individuals in order to assess the valuation of specific property using a hypothetical market [15]. In general, the use of contingent valuation relates to the use of

questionnaires for public participation to a particular sample of the population of users of a given amenity or environmental resource, aiming to collect information on the use value, the option value and the value of existence, which refer to the possibility of passive using the amenity [15]. Use value, option value and existence value mean the inherent willingness of each individual to pay to use a particular amenity in the present, to pay for the possibility to use it in the future, or even to pay simply to ensure its existence [16].

Once presented both direct and indirect methods of landscape evaluation, it appears that public participation and involvement constitute key elements in most of the above described and analyzed methodologies. It is therefore important to address, albeit in a perspective more or less applied to the purposes of this study, the concepts and techniques inherent in the public participation process and the forms that it can get taking into account the specificities of the methods of landscape evaluation to use.

III. MATERIALS AND METHODS

The methodology developed in this study was based on the following steps: the choice of topic and study area; research questions and methodological framework definition; and description of the guiding objectives of the investigation.

Considering this framework we started by the preparation of the visual landscape analysis map, starting by the definition of a visual basin and then the different landscape subunits.

In this sense, and since the processes are relatively dependent on the observer, it was considered of particular relevance to reduce this subjectivity by introducing multiple analyzes, as is the case of travel cost methods crossed with psychophysical preference models, using a predefined questionnaire. The data obtained from this questionnaire was entered into Microsoft Office Excel 2013, which averages were calculated from the values assigned to each of the landscape subunits for each factor, in order to obtain data regarding public opinion considering VQA and LVF for each of the considered subunits.

In regard to public interest assessment a specific questionnaire consisting of ten questions was developed, nine of which were closed response, where respondents were asked to choose among options previously established, in order to limit the variability of response and decrease complexity - as a way to gauge the opinion of people who visit the landscapes of the Lower Guadiana both regarding aesthetic and economic valuation of this landscape. Since the questionnaires were supposed to be delivered during a boat trip they were developed considering a process of direct interview. In this regard 250 questionnaires were delivered at the entrance of the boat, where a brief presentation of the research objectives was developed. The questionnaires were collected at the end of the boat trip. The information was then inserted into Microsoft Office Excel 2013 in order to organize them, and later in

Statistical Package for Social Sciences (SPSS). The answers to the open questions before inserted into the database were classified. Although the analysis of the questionnaire was essentially based on descriptive statistics some inferential statistics were also developed (chi-square test) in order to assess whether or not, according to public preference there is a significant relationship between the landscape subunits (statistical analysis used by Burley *et al.* [17] and by Loures [18]).

IV. STUDY AREA

The study area is located on the right bank of the river Guadiana, covering the municipalities of Vila Real de Santo António, Castro Marim and Alcoutim - area known as Baixo Guadiana (Figure 1). The climate of this region is temperate Mediterranean, with mild and short winters and long, hot and dry summers, with very high insolation. Relative air humidity values are considerably high, especially in the winter months, due to the proximity of the river and the sea [19].



Fig. 1 Study Area – Algarve, Portugal

The study area presents significant differences between its three geographic units (coastline, barrocal and mountain areas) noted not only in physiographic terms, but also in terms of population density, services, routes, tourism (the main driver of the local economy) etc.

V. AESTHETIC ANALYSIS

The visual basin of the study area was measured over ArcGIC 3D Analyst 9.2, which produced a digital terrain model (DTM) from digitized contour lines. However, over the several trips made to identify that, mainly due to vegetation and construction, the area actually visible from the river was smaller than that calculated by the MDT. In this sense, the visible area was adjusted manually in situ on an ortofotomapa, considering the area, which could actually see.

After defining the visual basin the different landscape subunits present in the study area, were identified according to a relative homogeneity criteria, defined by d'Abreu *et al.* [20]. At this level, it should be noted that the delimitation obeys to the establishment of an internal coherence, according to which they might be easily identified and characterized. Thus, 6

landscape subunits were identified: Salinas; Wetlands and Marshland; Agricultural and Production areas; uncultivated areas; Golf and Touristic Complex; and Urban Areas.

For each of the identified landscape subunits, in accordance with the objectives of the study, VQA, LVF and VAC were analyzed, using, as mentioned, the collaboration of specialists from related areas, and the visitors who completed the questionnaire during a boat trip along the Guadiana. Along the route several stops were made at strategic observation points - marked in Figure 2 – in order to allow a better analysis of the the aforementioned landscape subunits.

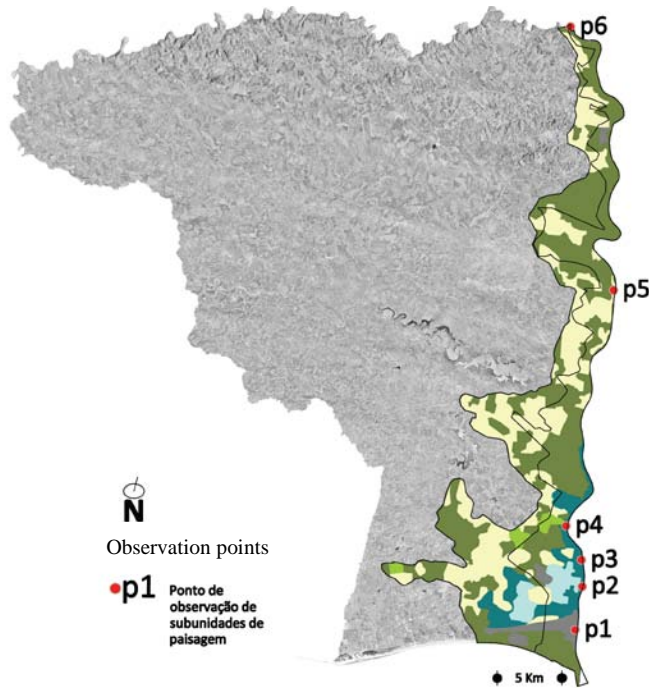


Figure 2 – Visual basin, Landscape subunits and Observation points.

VI. RESULTS

Questionnaires were completed between March and May 2011, during which 250 questionnaires were delivered. Of these, 148 were returned resulting in a response rate equal to 59.20%. Of the respondents, 56.80% were women, 24.30% men and 18.90% of the people did not respond. The most represented age group was over 65 years, with 47.30%; 39.20% were aged between 46 and 65; 6.80% were aged between 30 and 45 years, and 6.80% of people did not respond. With regard to education, 55.40% of respondents had primary education, 32.40% had secondary level, 4.10% were degree holders, 2.70% were postgraduates, and the remaining 5.40% did not answer the question.

With regard to the descriptive analysis of the data considering public preference of 12 images concerning the 6 identified landscape subunits, it was found that the subunit Touristic Complex and Golf, was one that got a higher value, with an average of 9.70, where the Touristic Complex and Golf 1 scored 10.22 image and Touristic Complex and Golf 2

scored 9.18. In the opposite situation lies the subunit Urban areas that scored 3.12; 2.40 for Urban area image 1 and 3.83 for Urban area image 2.

When asked about the quality of the landscape, considering the assigned range - 1- Very Low, 2- low, 3- Average, 4- High, and 5 Very High - responses were described by frequency analysis, average and trend. The trend was 3 and the average was 3.75 - which, according to the selected classes, rank as "High". When crossing this data with the characteristics of the sample population (age, gender, education and residence) one could see that the average of 3.75, can be due to the fact that a high percentage of individuals - 70 - have considered the quality of the landscape "High" or "Very High".

With regard to the most relevant landscape parameters considering landscape quality, 23.60% of respondents felt that the "presence of water" is the most significant parameter in the quality of this landscape, on the other hand, the mystery was considered the least important factor, which have been selected by only 2% of respondents.

When asked about the influence of the urban construction in the degradation of the landscape, most of the respondents (77%) considered that urban construction influences negatively the overall landscape quality.

The majority of respondents (86.50%) used the bus to get to the study area, explained that a high percentage of participants were on group visits. As for distance most of the respondents (54.10%) ran between 50 and 300km, with only a small percentage of people - 4.10% - traveling less than 10km to reach the study area. It was also found that the majority of respondents (39.20%) took between 1 and 3 hours to arrive the boarding area, while 6.80% of respondents took less than 15 minutes to get there. To visit the study area most of the respondents (36.50%) spent less than 50 € however 4 people (2.70%) spent more than 500 € When asked if they would be willing to pay to visit the study area, 77.03% of respondents were willing to pay in order to maintain this landscape as it is, so that they could revisit it in the future.

VII. CONCLUSION

Taking into account the objectives of this research and the premise used as a starting point, whereby the application of direct and indirect methods of landscape evaluation allows to measure not only the aesthetic and visual qualities of a particular environmental amenity, but also its possible to attribute market value to certain unmeasurable environmental amenities, the developed analysis of the public participation questionnaire allowed us to infer some relevant data, namely that:

- Even if Portugal does not have a great tradition in terms of public participation, the results exceeded the reference values for the typology of questionnaire used, according to Hill and Hill [21], since of 250 questionnaires delivered, 148 have been returned, duly completed, which shows a response rate of 59.2%;

- The results obtained for the subunit agricultural and production areas, corroborate with the conclusions drawn by Panagopoulos [3] according to which the organization of

agricultural production landscapes tend to be associated with a low aesthetic quality;

- Although marshes are considered one of the most productive ecosystems in environmental and ecological perspective, it appears that regarding landscape visual quality, this landscape subunit is characterized by low values, when compared to other landscape subunits considered in the present study;

- Though the subunit Touristic Complex and Golf has obtained the highest result considering respondent's preference, the fact that the "Presence of Water" parameter have been considered as the most relevant to landscape quality might have had influenced the results, considering the presence of water in these images;

- While about half of the respondents agree that the construction along the banks of the river contributes to the degradation of the landscape quality, it appears that the touristic complex and golf subunit, which correspond to the various buildings associated with tourism developments, was the one that obtained a higher preference;

- Although it is considered important that each visitor has spent on average about 50 Euros to visit this landscape, it should be noted that this value may be oversized considering the assumptions made by Selig and Spathelf [13], according to which the money spent in certain trips, cannot be exclusively attributed to a specific component of the trip; and

- The importance of this landscape at regional, national and international level, is supported by the analysis of the residence areas of each of the respondents | Boat users, since approximately 70% had to travel more than 50 kilometers to visit this landscape.

More over, it can be concluded that the application of public participation questionnaires increases the sense of social responsibility of the population, playing a key role to sustainable development and to future landscape planning, since it allows the acquisition of relevant information not only regarding landscape features but also considering public preference on landscape characteristics. For example, it was found that though tourist complexes associated with golf practice are generally a target of criticism, both from aesthetic an environmental standpoints, the representative images of this landscape subunit were the ones to which most respondents attributed a greater aesthetic quality, factor that might be an aspect of attractiveness to an increasingly desertified area. Alongside the data obtained indicate that the study area is worthy of special attention from political power, since it can contribute to an effective improvement of quality of life.

ACKNOWLEDGMENT

The authors would like to acknowledge financial support given by the Centre for Spatial and Organizational Dynamics (CIEO) and from the Foundation for Science and Technology (FCT).

REFERENCES

- [1] L. Loures (2005), *A Revitalização das Aldeias do Algarve*. Trabalho Final de Curso. Universidade do Algarve, Faro.
- [2] G. Telles (2004), *A paisagem é tudo. Pessoas e Lugares*. Available: <http://www.leader.pt/pt.lugares/jornalp116.pdf>.
- [3] T. Panagopoulos (2009), Linking forestry, sustainability and aesthetics. *Ecological Economics*. Vol.68, p.2485–2489.
- [4] L. Arthur, T. Daniel and R. Boster (1977), Scenic assessment: An overview. *Landscape Planning* 4, 109–129.
- [5] K. Hanna (1999), *GIS for Landscape Architects*. ESRI Press, New York.
- [6] L. Canter (1996), *Environmental Impact Assessment*. McGraw-Hill International Editions, Singapore.
- [7] R. Ayala, J. Ramirez and S. Camargo (2003), *Valoración de la calidad y fragilidad visual del paisaje en el Valle de Zapotitlán de las salinas, Puebla (México)*. Faculdade de Geografia e Historia da Universidade de Madrid, Madrid.
- [8] J. Burley (2001), *Environmental Design for Reclaiming Surface Mines*. The Edwin Mellen Press, New York.
- [9] P. Vargues (2006), *Avaliação de Impacte Visual do campo de golfe da quinta da Ombria – Querença – Loulé*. Trabalho de Final de Curso. Universidade do Algarve, Faro.
- [10] A. Mazure and J. Burley (2005), An aesthetic, economic, and ecological equation/theories for predicting environmental quality: including a GIS-based remote access application. Em: E. Lange and D. Miller (Eds.), *Our Shared Landscape: Integrating Ecological, Socio-economic and Aesthetics Aspects in Landscape Planning and Management*. InAscona, Switzerland, pp. 68–69.
- [11] D. Leite and C. Jacoski (2010), *Comportamento do usuário na valoração contingente e custo de viagem - O parque das palmeiras em Chapecô, SC, Brasil*. Revista Ambiente & Água, vol.5, n.2, p.226-235.
- [12] G. Oesten (1994), *Zur Wertschätzung der Infrastrukturleistungen des Pfälzerwaldes*, Trippstadt: Mitteilungen aus der Forstlichen Versuchsanstalt Rheinland-Pfalz, 156 p.
- [13] I. Selig and P. Spathelf (1999), *Benefícios indiretos da floresta*. Revista de Ciência Florestal, vol.9, n. 2, p. 137-146.
- [14] H. Varian 1999. *Microeconomia – Princípios Básicos*. Ed. Campus, Rio de Janeiro.
- [15] A. Barbisan, R. Kalil, A. Pandolfo, R. Lublo, L. Pandolfo, E. Brandli and M. Martins (2007), *Aplicação da Técnica de Valoração Econômica de Ações de Requalificação do Meio Ambiente em Área Degradada*. Em: RA'E GA - Curitiba, vol. 14: 129-147. Edição da Universidade Federal do Paraná.
- [16] C. Faria and J. Nogueira (2010), *Método de valoração contingente: aspectos teóricos e testes empíricos*. Available: www.unb.br/face/eco/nepama2k/NEPAMA004.doc.
- [17] J. Burley, V. Singhal, C. Burley, D. Fasser, C. Churchward, D. Hellekson and I. Raharizafy (2009), Citation analysis of transportation research literature: a multi-dimensional map of the roadside universe. *Landscape Research*, 34(4):481-495
- [18] L. Loures (2011), *Planning and Design in Postindustrial Land Transformation: East Bank Arade River, Lagoa – Case Study*. Ph.D Dissertation, Universidade do Algarve, Faculdade de Ciências e Tecnologia: Faro, Portugal.
- [19] J. Faria, S. Godinho, M. Almeida and M. Machado (1981), *Estudo Hidroclimatológico da Região do Algarve: O Clima de Portugal*. Fascículo XXVII, Lisboa.
- [20] A. Abreu, T. Correia and R. Oliveira (2004), *Contributos para a identificação e caracterização da paisagem em Portugal Continental - Colecção Estudos 10*, Lisboa, Universidade de Évora, Direcção Geral do Ordenamento do Território e Desenvolvimento Urbano.
- [21] M. Hill and A. Hill (2008), *Investigação por questionário*. Edições Sílabo, Lisboa.

Energy Efficiency and Sustainability of Low Energy Houses in Latvian Climate Conditions

Andris Jakovics, Stanislavs Gendelis, Ansis Ozolins and Saule Sakipova

Abstract—Five experimental test buildings (stands) have been built for the first time in Riga, Latvia (see Figure 1). They are identical except external walls for which different mainly regional building materials are used. However, projected heat transmittance (U -value) of the other walls, floor and ceiling is the same for each test building. Initial moisture influences the relative humidity of indoor air, which can be higher at initial time period when buildings have just been built. As a result the U -values are also very different and cause different heating/cooling energy consumption. Measurements show that critical situation is observed for two test houses where initial moisture is high and the drying process of external walls is slowly. One external wall consists from aerated concrete and insulation layer on the outer side. The second external wall is created from one aerated clay block with insulation filling. Results show that the heat demand in cold period for this two test houses are significantly higher than another 3 test stands. Moreover, overheating risks for two “critical” test houses are significantly lower in summer. However, the situation is not normal in that case. Both summer and heating seasons have been analysed and differences between five test houses are discussed in details.

Keywords—energy efficiency; low energy buildings; building materials; in-situ measurements; heating/cooling consumption.

I. INTRODUCTION

As the energy efficiency (EE) requirements in the context of building design and engineering performance become more rigorous, increasing attention must be paid to ensure the required indoor environment quality (IEQ). The task of a building’s design and construction is to ensure that with the minimum energy expenditure yields as consistent IEQ at varying outdoor air conditions as possible. The choice of building’s design affects the initial investment and exploitation costs as well as the long-term impact on human health, which is determined by the selected design characteristics (e.g., thermal inertia, hygroscopic qualities, etc.) and their impact on the ability to achieve the desired EE and IEQ performance. This article presents the implementation phase and first year’s results of the test buildings monitoring project.

Andris Jakovics is an associate professor at University of Latvia and the head of Laboratory for mathematical modelling of technological and environmental processes at Faculty of Physics and Mathematics, University of Latvia (8 Zellu Str., Riga LV-1002, Latvia; phone: +37129155711; e-mail: andris.jakovics@lu.lv; www.modlab.lv).

Stanislavs Gendelis is a senior researcher, Ansis Ozolins is a scientific assistant and Saule Sakipova is a visiting researcher at Faculty of Physics and Mathematics, University of Latvia.

This research is done with financial support of ESF, project realized by University of Latvia, No. 2013/0027/1DP/1.1.1.2.0/13/APIA/VIAA/007.



Fig. 1. Experimental test buildings.

The choice of building material for the five different walls of experimental constructions was determined by the target to find the best possible application of materials produced from the local resources, and high-quality insulation materials. The expected outdoor and indoor air parameters and energy consumption monitoring data will provide an opportunity to analyse the buildings in which five different construction materials have been used. Similar studies were performed on a variety of building design solutions and material effect on energy consumption and indoor climate also in other countries, e.g. in Finland, Spain [1, 2].

II. DESCRIPTION OF THE TESTING GROUND

In the framework of the project 5 test stands are built with different exterior materials, identical in terms of design, geographic location and engineering solutions. More detailed information about project is summarized in [3].

The building design provides solutions for reduction or elimination of thermal bridges. For all types of exterior wall constructions the U -value equals $0.16 \text{ W}/(\text{m}^2\text{K})$, calculated according to the standard EN ISO 6946. Constant air exchange rate of $0.4 \dots 0.5 \text{ h}^{-1}$ is provided by the air-air heat pump, which is used also for heating and cooling.

The experimental constructions are localized in the urban environment, under natural conditions in Riga, Latvia, characterized by cold, maritime climate (duration of the average heating period of 203 days, the average outdoor air temperature during the heating period is 0.0°C , the coldest five-day average temperature -20.7°C , the average annual air temperature 6.2°C , the daily average relative humidity is 79% [4]). The selected location is the University’s Botanical garden territory, all five stands are placed on equal relation to the sun and the surrounding shading objects (such as trees).

The experimental constructions are designed in order to minimize differences in output data of energy consumption and indoor climate measurement data analysis and interpretation. Each experimental stand imitates a free-standing building with an interior room (9 m² floor area, ceiling height of 3 m) with a window on the south façade and a front door on the north façade – see Fig. 2. Each building is placed on pillars and has no contact with the ground. To prevent the thermal bridges, window and door installations have been taken out to the insulation layer.

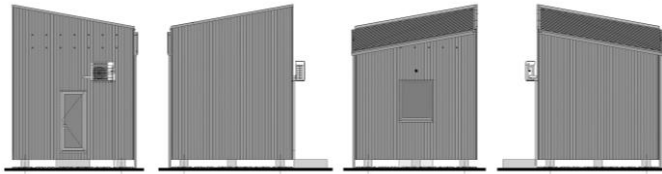


Fig. 2. The facades of one experimental building

The basic materials used for the ventilated facade exterior wall construction are (see Figure 3):

- 1) perforated ceramic blocks (440 mm) with flexible stone wool insulation outside (type CER);
- 2) aerated concrete blocks (375 mm) with flexible stone wool layer outside (type AER);
- 3) modular plywood panels with flexible stone wool filling (200 mm) and fibrolite (70 mm) inside (type PLY);
- 4) perforated ceramic blocks (500 mm) filled with insulating granules (type EXP);
- 5) laminated beams (200 mm) with flexible stone wool insulation layer and wood paneling inside (type LOG).

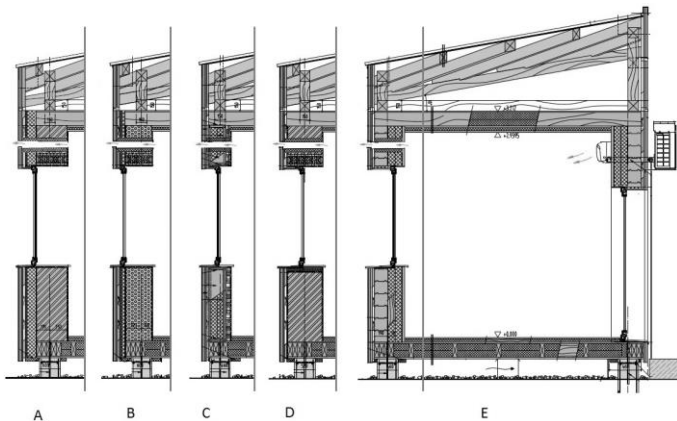


Fig. 3. Cross-section of different types of test buildings.

To provide the same set temperature and air exchange rate, every building is equipped with an air-air heat pump (heating/cooling capacity 3.6/2.8 kW; outdoor air supply 24/32 m³/h). Air conditioning equipment is installed above the door. Air leakage from the building exists through natural ventilation ducts fitted with a gravity louver, the channel which is located above a window.

III. MEASUREMENT DATA ACQUISITION SYSTEM

All the test stands are equipped with the same set of sensors. 40 different sensors include:

- 1) temperature and humidity (T/H) sensors,

- 2) air velocity flow sensors,
- 3) solar radiation sensor,
- 4) energy meter,
- 5) differential pressure sensor,
- 6) heat flow sensor,
- 7) atmospheric pressure sensor.

The locations of main air T/H sensors are shown in Fig. 4 as black dots. The data logger is collecting all sensor data including data from the electric energy meter. To collect meteorological data a weather station is installed on the top of a test stand with the separate data logger. Details of the developed measuring system can be found in publication [5].

The webserver and the FTP server are installed in each data logger providing remote access to the stored data for each sensor and to the software's parameters. All measurements are performed every minute and saved to the logger memory. The measurement data file from loggers is sent to the main FTP server once a day, where the data is collected and post-processed for detailed analysis. Measurements can be displayed directly using Web access to the logger memory, and using data from the user FTP server.

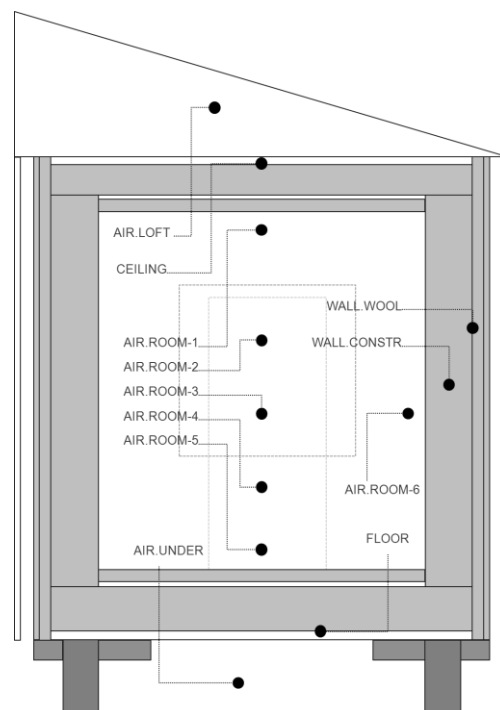


Fig. 4. The location of T/H sensors in a test building.

IV. AIR EXCHANGE RATE MEASUREMENTS

The main aim of the project is to determine and analyse energy consumption for all test buildings, therefore it is very important to evaluate all the heat losses. One of them is convection heat losses through ventilation opening and construction joints, which can be characterized by the air exchange rate in the room. Tracer gas method [6, 7] and special measuring system *Lumasense* [8] including multipoint sampler/doser *Innova 1303* and photoacoustic gas monitor *Innova 1412* are used for this purpose (Fig. 5).

Experimental studies of actual air change were made in all the test buildings after airtight sealing and with ventilation system running in standard mode. Measurements were carried out at least for 24 hours for every building. Obtained results (Table 1) show that the actual air exchange rate with switched on ventilation system in all test buildings is within the range of 0.43...0.50 (1/h). An additional measurement was carried out with switched off ventilation system and sealed ventilation opening; this study shows that air change in this case is very close to zero (see [9]). The general finding of this experiment is test buildings are very air-tight and the actual air exchange rates n with switched on ventilation system are very close, which means that more than 90% of actual air exchange is a result of mechanical ventilation system operation.



Fig. 5. System used for tracer gas air exchange measurements.

Table 4. Air exchange rate n (1/h) for test building under actual operating conditions.

Test building	Air exchange rate n (1/h)
LOG (log house / internal insulation)	0.45±0.03
EXP (polystyrene filled ceramic blocks)	0.48±0.02
AER (aerated concrete / external insulation)	0.50±0.03
CER (ceramic blocks / external insulation)	0.43±0.04
PLY (plywood boards / mineral wool filling)	0.44±0.01

V. U-VALUE MEASUREMENTS

The measurements of heat transmittance or U -value (W/m^2K) are made for constructions in all different test buildings just after test buildings are built and after one year of operation. Measurements are carried out using long-term monitoring of heat flux density and temperature difference (Fig. 6).

Obtained results for all test buildings are visualized in Fig. 7. The variation in determined U -values is mainly caused by different humidity conditions of a building structure (see next chapter). The resulting range is a result of several measurement cycles (up to 5 for any construction); the greatest deviations is obtained for AER, EXP and CER building in year 2013, but still remain high only for AER building in year

2014. This building's type differs from other masonry structures with porous structure of the blocks, which means slower drying; this effect is clearly seen from Fig. 7 – measured U -values measured in year 2014 are decreased.

Comparing experimental results with the calculated (designed) it is seen, that walls in PLY building, as well floors and ceilings in all buildings are very close. Measured U -value for wall in LOG building is lower than calculated value; this can be explained by low moisture content in timber constructions just after manufacturing, which slightly increases in year 2014 (see Fig. 7).

Very high values of heat transmittance obtained for EXP building can be explained by mistakes in manufacturing process of ceramic blocks, resulting in the highest volume of ceramics and the highest thermal conductivity value.

Based on the experimental result obtained, it is estimated that the U -values for all the masonry constructions (especially for aerated concrete) in the first year of operation are very closely linked with the moisture content in structures. In the second year heat transmittance decreases, this means also reduction in conduction heat losses from the buildings.



Fig. 6. Heat flux density and temperature measurements.

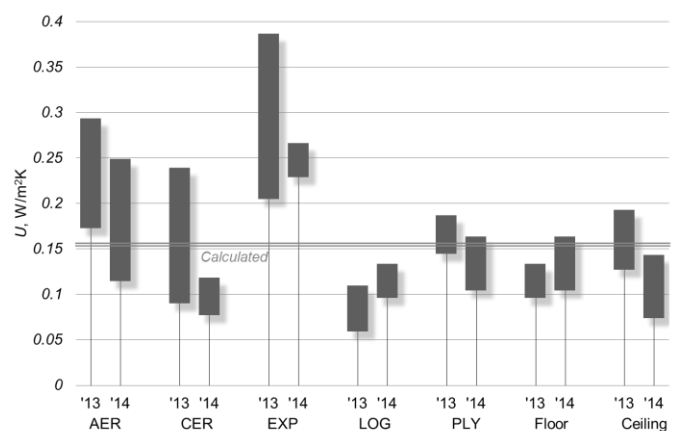


Fig. 7. Measured U -values of different constructions for all test buildings in years 2013 and 2014.

VI. AIR HUMIDITY MEASUREMENTS

Temperature and air humidity in different places of test buildings (in the air as well as in the building structures) are controlled by several sensors (Fig. 4). Characteristic values of air humidity in all buildings (data from sensor located in the middle of a room) for all monitored period are displayed in Fig. 8. The highest values are observed for AER type building built from aerated concrete, ever after one year operation under set ventilation conditions (measured air exchange rate 0.5 (1/h), see Table 4) the air humidity is highest in comparison with other types of buildings. It should be noted that this difference decreases in time and after another heating season it may be very close to another buildings, it is due to relatively slow drying of construction. From this picture it is seen that the relative air humidity in the summer is higher than in winter.

As the test buildings are well ventilated, the measured air humidity depends mainly on moisture content in building structures. However, humidity measurements in the structures or near its surfaces are also very important, e.g. data from humidity sensors located under the window sill (Fig. 9) and between mineral wool layer and main material (Figs. 10, 11) allows to better understanding of drying processes and moisture transport in building constructions [10]. As is seen from the graphs on Fig. 9, the relative air humidity in AER and EXP buildings are very high and can reach even 100% in the autumns near under the windows sill. Measured relative humidity near mineral wool layer for CER, LOG and PLY buildings (Fig. 11) is very high throughout the year (more than 65%); and it is 100% even after one year of exploitation for AER building, but it should decrease in the next years.

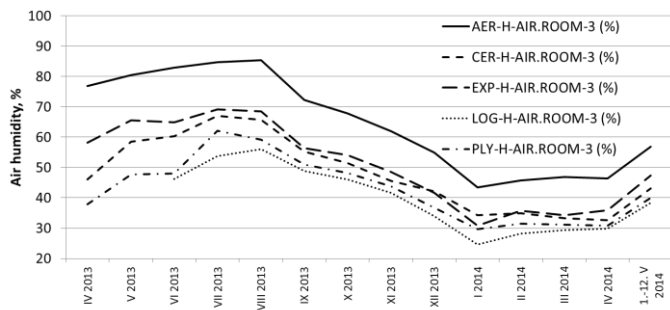


Fig. 8. Measured relative air humidity in the middle of the room.

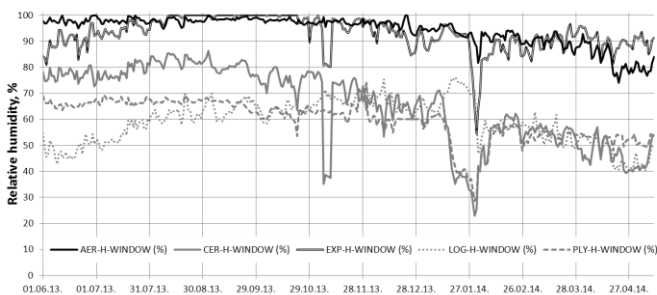


Fig. 9. Measured relative air humidity under the window sill.

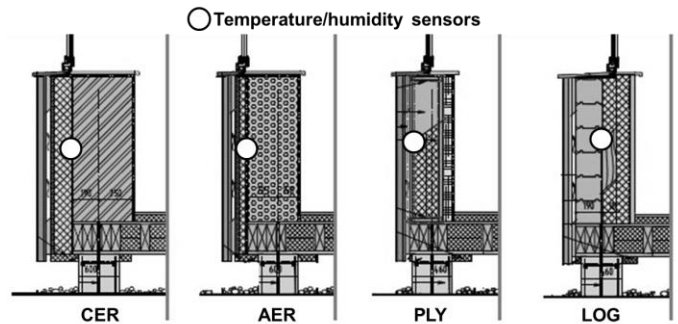


Fig. 10. Location of temperature and humidity sensors between a layer of mineral wool and ceramics blocks (CER), aerated concrete blocks (AER),plywood (PLY) and timber (LOG).

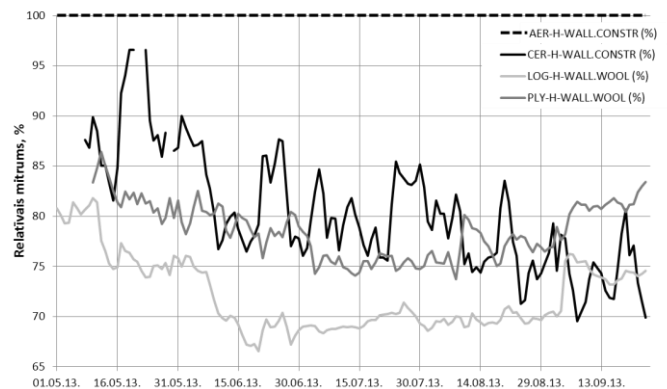


Fig. 11. Measured relative air humidity for sensors shown on Fig. 10.

The moisture has a significant negative influence on building structures, not only in terms of increasing of thermal transmittance, but also on condensation and mould growing. More information about mathematical modelling and analysis of condensation risk and mould growth in test building is summarised in [11].

VII. ENERGY CONSUMPTION MEASUREMENTS

After one year project running, there is collected huge amount of data from all types of sensors. The most interesting and representative results it is possible to get by analyzing the heating and cooling energy consumption for different test buildings.

In the beginning of heating season, couple of months after the test buildings are built, energy consumption in buildings AER and EXP was higher than in another three buildings with practically the same consumption. Graphs in Fig. 12 show the increasing of difference in heating energy consumption for all test buildings in the beginning of heating season in year 2013. Comparing the energy consumption, the difference between AER and CER buildings is 134%; it means one-third more heating energy consumption. The main reason is the increased conduction heat losses (see chapter V) through walls in AER building due to higher moisture content. Increasing of U-value for walls also in EXP building has an effect on heating energy consumption, which is 25% higher.

Comparing the cooling energy consumption in several summer days (Fig. 13) it is seen, than the same buildings which consumed more heating energy (AER and EXP), now look very energy efficient. It can be explained by two factors:

- highest thermal transmittance for those buildings (see Fig. 7), which means more intense heat transmittance form the room and
- drying of relatively humid structures (see Fig. 9), which requires an additional energy for evaporation.

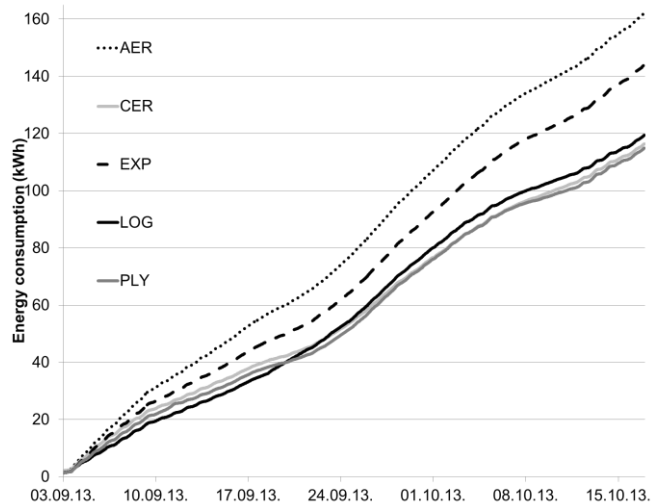


Fig. 12. Heating energy consumption in different test buildings (indoor temperature $T_{in}=19^{\circ}\text{C}$, air exchange rate $n=0.45$ (1/h)).

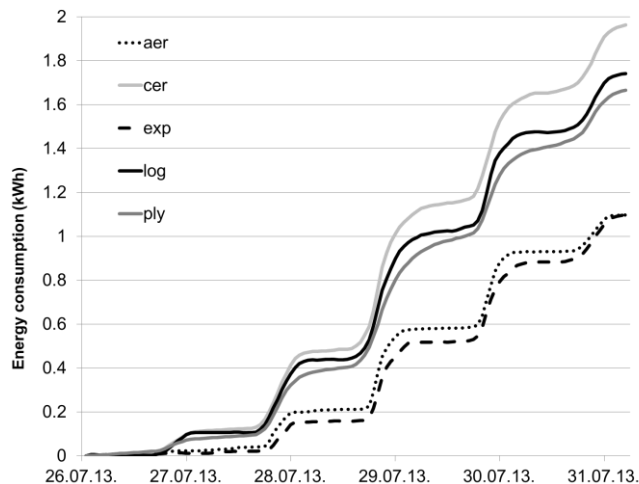


Fig. 13. Cooling energy consumption in different test buildings (indoor temperature $T_{in}=24^{\circ}\text{C}$, air exchange rate $n=0.45$ (1/h)).

The role of a heat capacity is very important to reduce peaks of temperature fluctuation, especially in summer days when a solar radiation influences the indoor temperature very significantly. The effect of rapidly increasing of indoor temperature during direct solar radiation called also “overheating”; an example of this process is shown in Fig. 14, where temperature in the test buildings are not controlled, but only ventilation system is on. As it is seen, the maximum temperature inside LOG building is 5°C higher than in AER building.

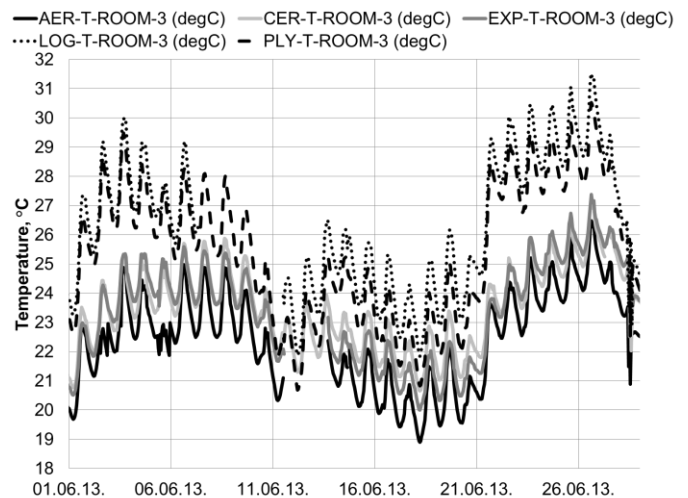


Fig. 14. Overheating of light-weight test buildings (LOG and PLY) without cooling.

VIII. CONCLUSION

Long-term monitoring of various physical parameters in 5 different low energy test buildings in Latvian climate show, that:

- Calculated and measured heat transmittance for building structures may vary mainly due to different moisture content. Therefore, heating energy consumption for such buildings differs up to 34%.
- After one year of operation, wet constructions dry out and room’s air humidity decreases; it means decreasing in heating energy consumption for the next heating seasons.
- Thermal mass of a building structure is very important factor, which affects increasing of indoor temperature in buildings without cooling systems in summer time.

More information about actual research results in the test buildings is possible to find of project’s web site [12].

REFERENCES

- [1] J. Vinha. *Hygrothermal performance of timber-framed external walls in Finnish climatic conditions: A method for determining the sufficient water vapour resistance of the interior lining of a wall*. PhD thesis, University of Tampere, Tampere, 2007.
- [2] Cabeza F.L., Castell A., Medrano M., Martorell I., Perez G., Fernandez I. Experimental study on the performance of insulation materials in Mediterranean construction. *Energy and Buildings*. Vol. 42, Issue 5, 2010, pp. 630-636.
- [3] Dimdiņa, I., Jakovičs, A., Gendelis, S., Kļaviņš J. Testing of Energy-Efficient Building Envelope Materials in Natural Conditions. In: *Proceedings of World Sustainable Energy Days 2013*, Wels, Austria.
- [4] Regulations regarding the Latvian Building Code LBN 003-01 “*Construction Climatology*”. 2001. Latvian Cabinet of Ministers, Riga.
- [5] Greitans, M., Grunde, U., Jakovics, A., Gendelis, S. Web-based real-time data acquisition system as tool for energy efficiency monitoring. In: *21st Telecommunications Forum (TELFOR)*, Belgrade, Serbia, November, 26-28, 2013.
- [6] Laussmann D. and Helm D. *Air Change Measurements Using Tracer Gases: Methods and Results. Significance of air change for indoor air quality, Chemistry, Emission Control, Radioactive Pollution and Indoor Air Quality*, Dr. Nicolas Mazzeo (Ed.), ISBN: 978-953-307-316-3, InTech, DOI: 10.5772/18600.

- [7] ISO 12569. *Thermal performance of buildings and materials -- Determination of specific airflow rate in buildings -- Tracer gas dilution method*. ISO Standard 12569:2012. Geneva: International Organization for Standardization.
- [8] Lumasense. (15.04.2014.) Ventilation and Air-exchange Measurements [Online]. Available: www.lumasenseinc.com/EN/products/gas-monitoring/ventilation-measurement
- [9] Gendelis S., Jakovičs A., Nitijevskis A., Ratnieks J. Comparison of different air tightness and air exchange rate measurements in very small test buildings. In: *34th AIVC conference: Energy conservation Technologies for mitigation and adaptation in the built environment – Athens, September 2013*, p. 142 – 143.
- [10] A. Ozolinš, A. Jakovičs, J. Ratnieks, S. Gendelis. Numerical Modelling of Humidity and Temperature Conditions in Buildings with Different Boundary Structures. *Proceedings of the 11th REHVA World Congress & 8th International Conference on IAQVEC - CLIMA 2013 "Energy efficient, smart and healthy buildings"*, Prague, Czech Republic, June 16–19, 2013, 10 p.
- [11] A. Ozolinš, A. Jakovičs. Risk of Condensate Formation and Mould Growth in Buildings under Latvian Climate Conditions. *Latvian journal of physics and technical sciences – 2013, Nr. 5, p. 44 - 53*. DOI: 10.2478/lpts-2013-0032.
- [12] University of Latvia (19.05.2014). Project on buildings' energy efficiency monitoring in Latvian Climate [online] Available: <http://www.eem.lv>

Thermal behavior of a simplistic asphalt pavement model for heat pulses

J. Birgitta Martinkauppi, Anne Mäkiranta, Jukka Kiijärvi, and Erkki Hiltunen

Abstract—Asphalt pavements are very common in urban areas which make them a potential source for heat energy collection. In this paper, the heat conduction through asphalt, gravel, and sand layer is thus studied in laboratory experiment in which the temperature was measured with distributed temperature sensing method. The results indicate differences in thermal behavior of between materials as well as heat energy storing in the lowest layer. A real temperature measurement system for an asphalt pavement was constructed due to this and is shortly reviewed here.

Keywords—Asphalt, thermal behavior, heat energy, heat transfer.

I. INTRODUCTION

Urban energy means accumulation of energy already existing in urban, built and constructed areas. One of its approaches is asphalt energy in which the heat energy is collected under asphalt layer. Asphalt heat energy collection is an exciting approach since asphalt pavements cover large areas in cities and roads thus making a huge reservoir already available for use. Different aspects of asphalt and heat have been already studied in many publications and even patents have been issued – first patent is already from 1979 (Wendel 1979 [11]). One of the aspects is the effect of heat on the asphalt structure like cracking (Roque et al. 2004 [7]) or healing (Carpenter and Shen [3]) or thermal behavior (Xu and Solaimanian 2010 [12]). Other aspects are the possible use of asphalt as latent heat storage (Morcos 1990 [5]) or as a source of heat energy.

Asphalt solar collectors has been suggested not only to collect heat but also to prevent so called heat island effect and structural damage of pavement due to thermal cycles with temperature as high as 70°C (Bobes-Jesus et al. 2013[2]). The heat island effect depicts the phenomenon where the asphalt heats up the air above causing an increase in the need of air conditioning and a decline in air quality (Allen et al. 2003 [1], Bobes-Jesus et al. 2013 [2]). An asphalt solar collector is made by installing pipes inside the asphalt. Fluid circulation inside the pipes causes heat to be transferred from warmer pavement

to cooler fluid thus lowering the temperature of the pavement. Heat is extracted from the fluid using low temperature geothermal heat pumps. Typical applications of collector systems are snow-melting systems (see e.g. Morita et al. 2000 [6]) and thermal uses in near-by buildings.

The solar collector approach requires embedment of pipes which make utilization of already existing pavements difficult and expensive. Vertical pipes might be thus a better option for heat collection since they can be constructed on existing pavement and are able to collect heat from deeper layer. To test this, a laboratory set-up with sand, gravel and asphalt layers was made and subjected to heating. The purpose of the set-up is to provide some understanding of behavior of different materials under heating as well as to be a preliminary test for pavement temperature measurements. The heating was applied in four occasions on the set-up while measuring the temperature of layers. Since the results were promising, a temperature measurement system has been constructed on the pavement with five wells of different depths.

In this paper, the selected temperature measurement method, laboratory set-up and constructed pavement temperature measurement system is described in Chapter 2. Measurements are described in Chapter 3. Chapter 4 provides an analysis of data from the laboratory measurement. Conclusions are drawn in Chapter 5.

II. MEASUREMENT ARRANGEMENTS

A. Temperature measurement

Distributed temperature sensing (DTS) was selected for temperature measurement. It uses optical fiber as a sensor element and this provides possibility to collect temperature data from whole fiber cable. This is advantageous since several other temperature measurement methods provide only data values at a certain measurement point. DTS has been showed to be feasible for monitoring soil moisture on an experiment with a sand filled tub (Sayde et al. 2010 [8])

DTS is based on emitting short pulses of laser and then detecting backscattered light (Ukil et al. 2012 [10], LIOS Technology, 2012 [4]). Part of backscattered light depends on temperature and based on this, the temperature for points of fiber cable is calculated by the DTS device. The measurement device used was Oryx DTS device (Oryx 2014 [9]). The manufacturer data sheet gives the accuracy of an Oryx DTS

All authors are with the Faculty of Technology, University of Vaasa, Wolffintie 34, 65200 Vaasa, Finland (phone: +358 29 449 8000; fax: +358 (6) 324 8208; e-mail: {Birgitta.Martinkauppi, Anne.Makiranta, Jukka.Kiijarvi, Erkki.Hiltunen}@uva.fi).

device to be ± 0.5 °C. The Oryx DTS device was configured for 1 m spatial resolution which indicates that the position of measurement point can be located within 1 m accuracy. The operation mode was set to two channel measurements, with 5 minute measurement time for each channel. These settings produce data 6 measurements per hours.

The optical fiber used had bare fiber diameter of 50 μm , diameter of 125 μm with cladding and diameter of 250 μm with acrylate primary coating. Its product details are multimode, Ultra-Fox Plus. To monitor the room temperature during measurements, a different sensor, a PT100 platinum resistance temperature sensor, was employed and its accuracy given is ± 0.25 °C.

B. Laboratory set-up

The measurement set-up was built in Technobothnia Research Centre, Vaasa. The room temperature was kept around +20 °C. Fig. 1 displays the experimental arrangement: under a 60 W heating lamp there were three layers of material: asphalt, gravel and sand. Thickness of the asphalt layer was 5 cm while other layers were 10 cm thick. The set-up was made inside a plastic tub (size 80 liters).

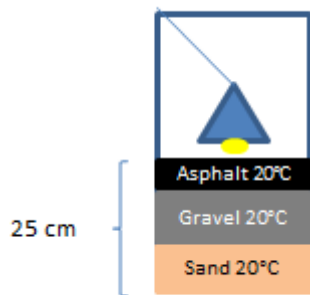


Fig. 1 Experimental laboratory set-up for asphalt measurements.

The cable with optical fibers inside needed to be first centralized in the tub vertically. The optical fiber cable was thus wrapped around a round frame made from metal net (Fig. 2) which was adjusted to middle.



Fig. 2 The cable was wrapped around a metal frame which was positioned inside the plastic tub.

The length of the cable is 525 m and it consists of two optical fibers joined at the end of the cable thus the length of optical fiber is 1050 m. However, only a 70 m of cable was possible to wrap around the metal net up to the height of 0.5 m. This means that wrapping 1.4 m cable produce a 1 cm rise. The simple schematic for cable is shown in Fig. 3; note that parts of the cable were not inside the tub since the cable was not cut. In the Table I, the ranges of the cable are shown with corresponding material layer.

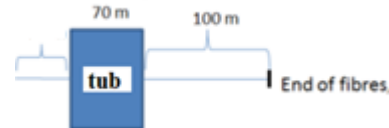


Fig. 3 Schematic for cable arrangement.

Table I. Cable position, material and height of layer (if applicable)

Cable position [m]	Material /element	Height of layer [m]
355-369	sand	0.10
369-383	gravel	0.10
383-390	asphalt	0.05
390-408	air	0.13
408-409	60 W lamp bulb	-

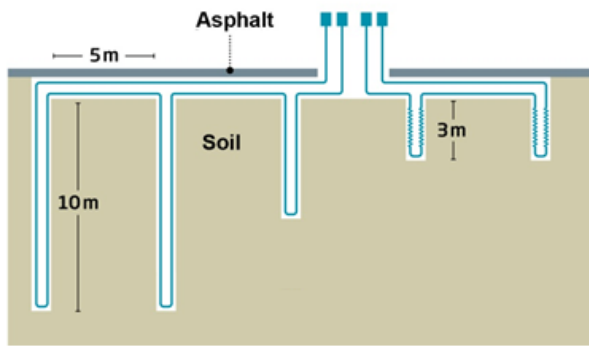
Cellular plastic (Nomalen 30, PE 30kg/m³) was used as an insulation element around the metal net. Thermal conductivity of Nomalen 30 is 0,038 W/(m•K) and thickness is 15 mm. (NMC Cellfoam Oy 2013.) The bottom was also insulated. After adding insulation, sand, gravel and asphalt layer was added to the tub. The asphalt layer consisted of disc with diameter of 0.10 m and height of 0.05 m. Fig. 4 shows the final set-up which was used in measurements.



Fig. 4 The set-up for measurements.

C. Pavement set-up

Five holes were drilled to the pavement; a diagram is shown in Fig. 5 (a). Depths of the holes are the following: two holes with 10 m depth, one hole with 5 m depth and two holes with 3 m depth. The optical measurement cable was installed in each hole as displayed in Fig. 5 (b), and later the cables were connected together. For 3 m holes, the installed cable is wrapped around a pipe. No wrappings were done for other holes. The holes will be covered later with asphalt layer.



(a)



(b)

Fig. 5 (a) this basic diagram indicates drilled holes in the asphalt pavement. (b) Installing cable to a 10 m hole.

III. MEASUREMENTS

A. Measurement at laboratory

The dry asphalt tub was subjected to measurement for a 4 day period. The asphalt layer was heated with a 60 W lamp bulb (see Fig. 4). The duration of heating is shown in Table II.

Table II. Date, time and duration of asphalt heating experiment

Date	Time	Duration
15.1.2013	8:16-13:26	5 h 10 min
16.1.2013	8:11-15:13	7 h 2 min
17.1.2013	8:25-15:31	7 h 6 min
18.1.2013	7:50-15:15	7 h 22 min

B. Measurement at pavement

The Oryx DTS device was used to collect the data from the installed cables. The measurement set-up is shown in Fig. 6 (a) and preliminary result is displayed for a hole in Fig. 6 (b). The central peak is measured from the hole and it indicates that a layer under pavement reaches +8 °C at the depth of 10 m. The side peaks are data from parts of the cable buried near the surface.

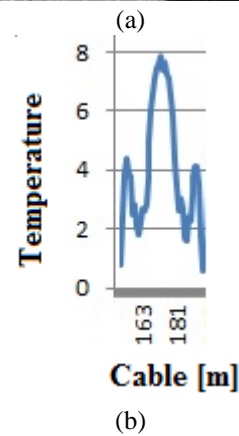
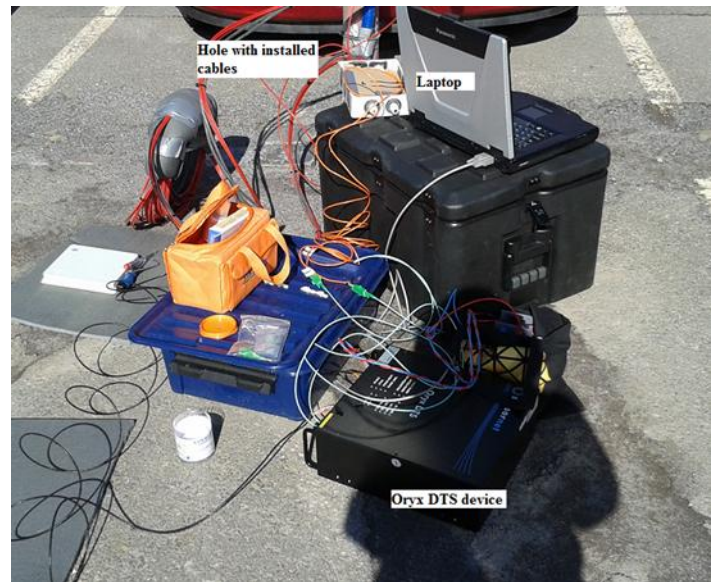


Fig. 6 (a) Set-up for asphalt temperature measurement. (b) Preliminary results for a hole measured in April. X-axis indicates the distance of cable from the beginning while the y-axis shows temperature in Celsius degrees.

IV. ANALYSIS OF LABORATORY MEASUREMENTS

A. Period of heating

The temperature of material layers in the tub was measure before heating and the results are shown in Fig. 7 (a). Some temperature variations exist but they are relatively minor and all layers are approximately in the same temperature. Fig. 7 (b) displays the situation 4 minutes after starting the heat: the asphalt layer starts warming up and thermal gradient has formed across it. The heat is beginning to conduct to the lower layers. After the heating, the surface of asphalt layer has almost reached the temperature of +44 °C as shown in Fig. 7 (c). Even the lowest layer, sand, is now slowly starting to warm up. The air gap between asphalt and lamp is also getting warmer partly due to heat energy reflected from the asphalt surface.

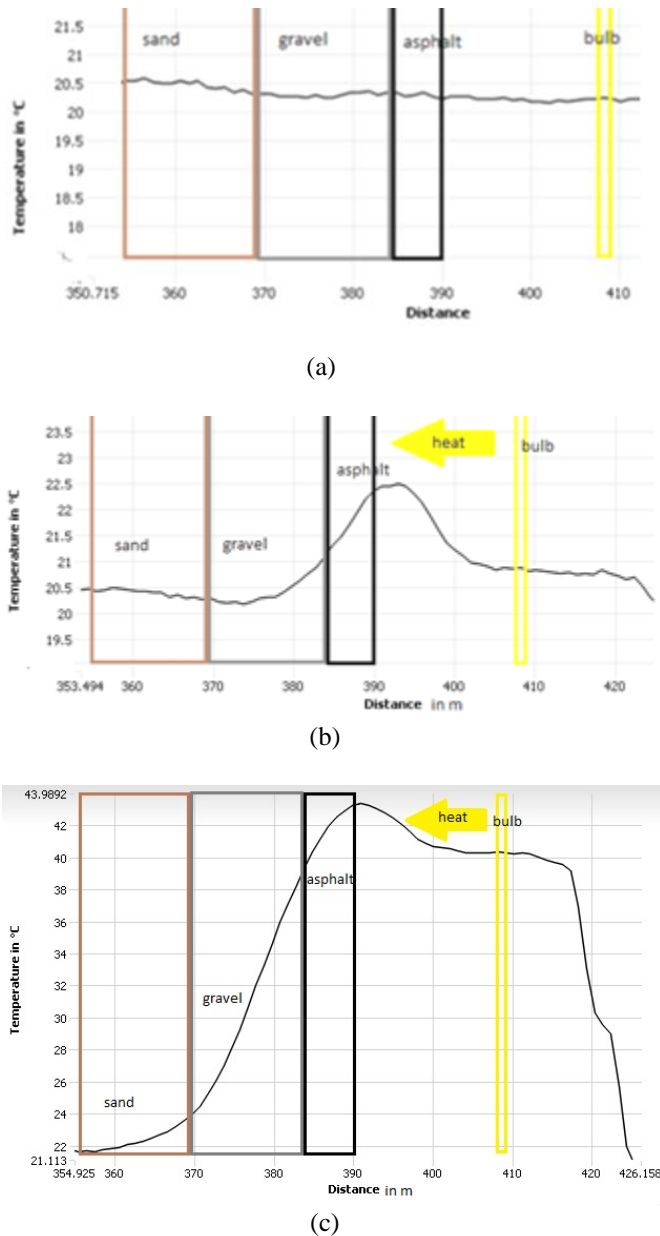


Fig. 7 a) The temperatures of sand, gravel and asphalt layers are approximately at the room temperature before the heating starts (time stamp of data: 15.1.2013, 8:00; room temperature 20.06 °C). (b) Four minutes after heating starts, warming of asphalt layer surface is clearly observed and thermal gradient is formed (time stamp of data: 15.1.2013, 8:20; room temperature 20.25 °C). (c) The sand layer is also warmer after the heating period of 5 hours and 4 minutes (time stamp of data: 15.1.2013, 13:20; room temperature 20.57 °C).

B. Cooling and heating cycles

The asphalt layer was subjected to heating in four occasions. After heating, the material layers were allowed to cool down towards the room temperature. The temperatures were measured with 10 minutes interval with DTS-method during

these times. These heat-cooling-cycles are displayed for asphalt layer in Fig. 8, gravel layer in Fig. 9, sand in Fig. 10. In each figure, the measurements have been made from several cable positions and the rounded value of cable positions from the beginning of the cable are indicated on the right side of the figures.

The thermal behavior seems to depend on position of the material at a layer during heating while be independent during cooling. The structure of material has naturally an effect: temperature variations in coarse gravel layer are larger than the two other layers. The asphalt layer as well as gravel layer reaches the prevailing room temperature during cooling time (Figs. 8-9). However, the sand layer seems to store some of the heat energy as its temperature remains higher (Fig. 10).

V. CONCLUSION

Asphalt pavements cover large areas in cities, thus making them an interesting possibility for heat energy collection. Studies have been so far concentrated on so called asphalt heat collector in which pipes are installed horizontally under the road or pavement. The horizontal heat collection from an asphalt pavement would be, however, easier to install in already existing pavements since they would require only small construction area. A laboratory set-up as well as real pavement DTS measurement system has been thus made as preliminary tests.

Heat conduction through three layers, asphalt, gravel and sand, is studied in a laboratory experiment. The layers were subjected to four heating-cooling cycles while measured the temperatures via DTS-method. The results indicate that while the upmost layer, asphalt, cools down relatively fast to the prevailing temperature, the lowest layer, sand, seems to store some of the heat energy. Thermal behavior for material inside a layer seemed to be dependent on their height positions during heating period while this was not observed during cooling period. The material content of a layer has naturally has effect on results. Coarse gravel had highest variation in its heat profile.

Since the results of laboratory experiments were very promising, a DTS measurement system was constructed on an asphalt pavement with 5 holes. Some preliminary data indicate that the system is suitable for measurements.

VI. FUTURE WORK

The future works will include an evaluation of different methods for calculating rate of temperature change as well as analysis measurement data of real, constructed pavement temperature measurement systems.

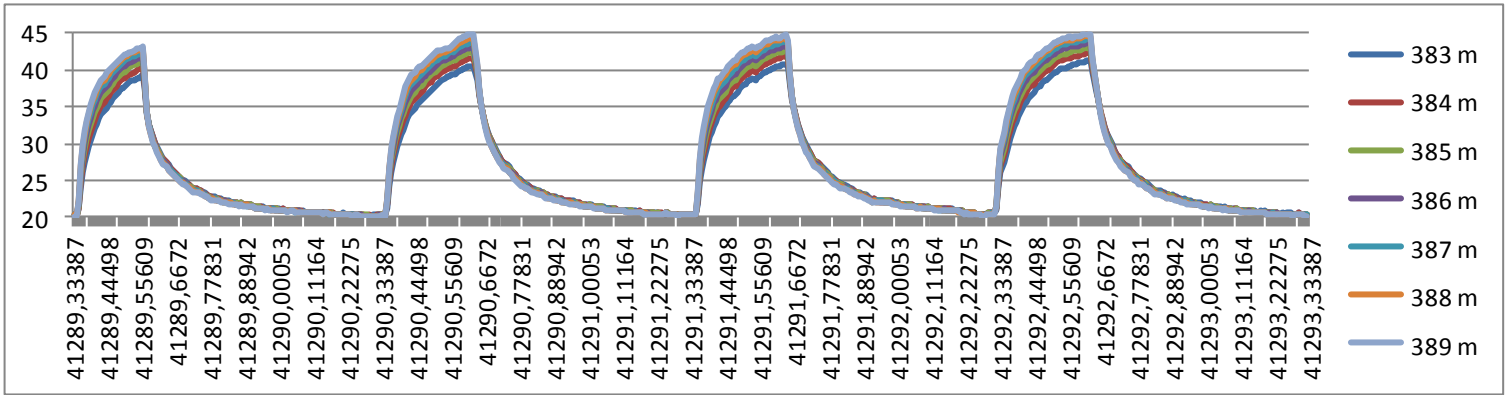


Figure 8. Heating-cooling cycles for asphalt.

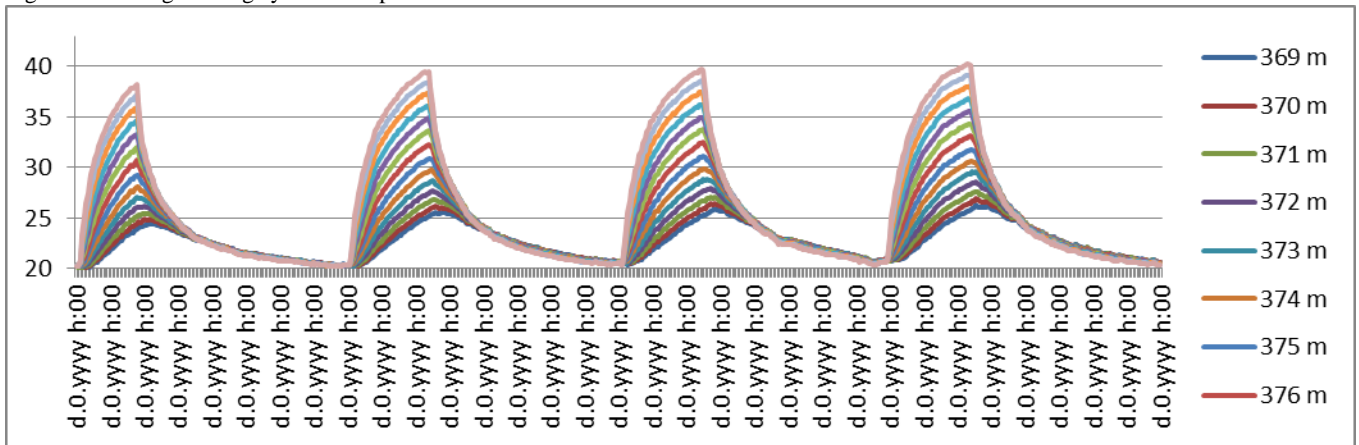


Figure 9. Heating-cooling cycles for gravel.

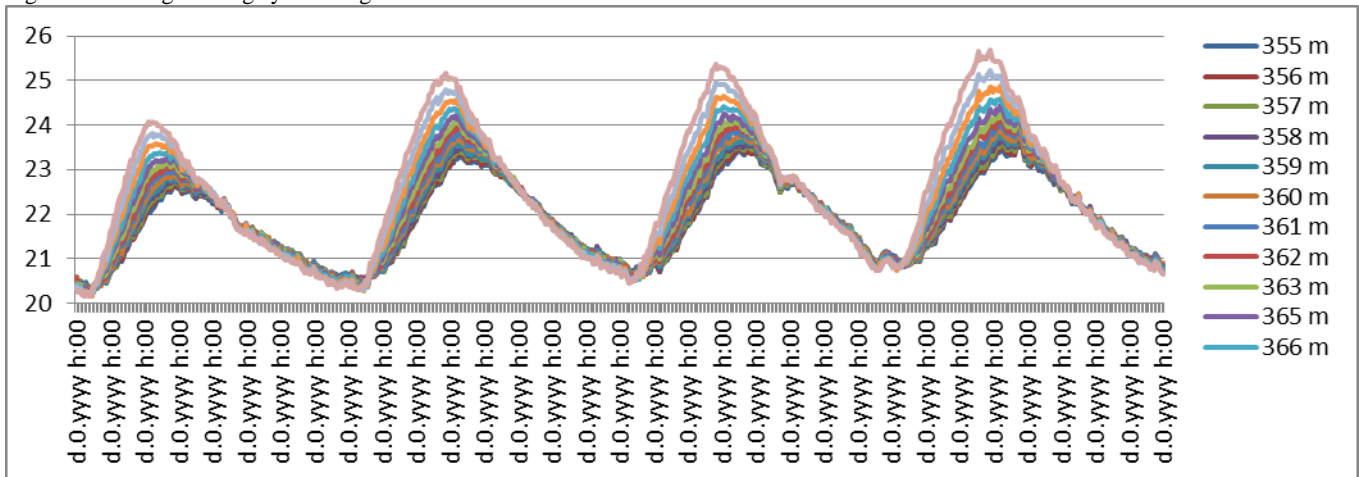


Figure 10. Heating-cooling cycles for sand.

REFERENCES

- [1] A. Allen, D. Milenic, and P. Sikora, "Shallow gravel aquifers and the urban 'heat island' effect: a source of low enthalpy geothermal energy," *Geothermics*, vol. 32(4), pp. 569-578, 2003.
- [2] V. Bobes-Jesus, P. Pascual-Muñoz, D. Castro-Fresno, and J. Rodriguez-Hernandez, J., "Asphalt solar collectors: A literature review," *Applied Energy*, vol. 102, pp. 962-970, 2013.
- [3] S.H. Carpenter and S. Shen, "Dissipated energy approach to study hot-mix asphalt healing in fatigue," *Transportation Research Record: Journal of the Transportation Research Board*, vol. 1970(1), pp. 178-185, 2006.
- [4] LIOS Technology, Distributed Temperature Sensing. Available: <http://www.lios-tech.com/Menu/Technology/Distributed+Temperature+Sensing>
- [5] V. H. Morcos, "Investigation of a latent heat thermal energy storage system," *Solar & wind technology*, vol. 7(2), pp. 197-202, 1990.
- [6] K. Morita and M. Tago, "Operational characteristics of the Gaia snow-melting system in Ninohe, Iwate, Japan," presented at World Geothermal Congress, pp. 3511-3516, 2000
- [7] R. Roque, B. Birgisson, C. Drakos, and B. Dietrich, "Development and field evaluation of energy-based criteria for top-down cracking performance of hot mix asphalt," *Journal of the association of asphalt paving technologists: from the proceedings of the technical sessions*, vol. 73, pp. 229-260, 2004.
- [8] C. Sayde, C. Gregory, M. Gil-Rodriguez, N. Tuffillaro, S. Tyler, N. van de Giesen, M. English, R. Cuenca, and J.S. Selker, "Feasibility of soil moisture monitoring with heated fiber optics", *Water Resources Research*, vol. 46(6), 2010.
- [9] Sensornet, Oryx . Available: <http://www.sensornet.co.uk/technology/distributed-temperature-sensing/oryx-dts-sensors.html>
- [10] A. Ukil, H. Braendle, and P. Krippner, "Distributed Temperature Sensing: Review of Technology and Applications," *IEEE Sensors Journal*, vol 12(5), pp. 885-892, 2012.
- [11] I.L. Wendel, "Paving and solar energy system and method," U.S. Patent 4 132 074, 1979.
- [12] Q. Xu and M. Solaimanian, "Modeling temperature distribution and thermal property of asphalt concrete for laboratory testing applications", *Construction and Building Materials*, vol. 24(4), pp. 487-497, 2010.

A Computational Study of a Prebiotic Synthesis of L-Leucine and L-Isoleucine

N. Aylward

Queensland University of Technology, Brisbane, Australia
n.aylward@alumni.qut.edu.au

Abstract: - The magnesium ion metalloporphyrin complex is shown to bind the ligand pent-1,3-diyne in a weak van der Waals complex on the metal site. Photochemical excitation allows the formation of cyclic adducts which may become partially hydrogenated. Subsequent reaction of the adducts with ammonia gives amines that easily transform to aziridine derivatives, and ultimately imines bound to the catalyst. When carbon monoxide is also bound to the complex as a high energy compound whose particular structure has been dictated by the magnetic vector of the exciting radiation, reaction occurs to give substituted aziridine-2-ones that may easily hydrolyse to the zwitterionic form of the amino acids L-leucine and L-isoleucine.

The reactions have been shown to be feasible from the overall enthalpy changes in the ZKE approximation at the HF and MP2/6-31G* level, and with acceptable activation energies.

Key-Words: -Prebiotic photochemical synthesis, L-leucine, L-isoleucine, L-norleucine.

1 Introduction

The amino acids L-leucine (Leu,L) and L-isoleucine (Ile,I), are essential amino acids [1], that occur naturally as the L-isomer [2] and are present in many proteins such as haemoglobin, elastin, wool keratin, myosin and ovalbumin [2]. N-Methylleucine occurs naturally in seeds of *Cycas circinalis* and *Phaseolus vulgaris* [3]. Norleucine, α -aminocaproic acid also has a natural occurrence in an ergot alkaloid [4]. Isoleucine contains two asymmetric carbon atoms and therefore exists in two racemic forms, DL-isoleucine and DL-alloisoleucine giving four optical isomers. The configuration of normal L-isoleucine is 2S, 3S [1]. L-leucine is regarded as hydrophobic [5] with α -COOH pKa, 2.36 and an α -NH₂ pKa 9.60 [1], for isoleucine the corresponding values are 2.4 and 9.7 [6]. The biosynthesis of leucine is from α -ketovaleric acid [1] and isoleucine from α -ketobutyric acid [1]. The

metabolism of L-leucine yields acetyl-CoA in the tricarboxylate cycle [1]. The metabolism of isoleucine leads to succinyl-CoA [1].

From a prebiotic perspective [7] it is desirable if the reactant molecules formed spontaneously from a supposed prebiotic atmosphere to be inevitably present. It has often been held that the atmosphere of the Earth was originally mildly reducing [1,8] implying the presence of concentrations of carbon monoxide, ammonia, water and hydrogen. It is also supposed that methylidyne, CH₃-(C \equiv C)₂-H, that has been found in interstellar space [9] was also present, possibly formed from the free radical mediated condensation of acetylene and allylene or by ionic species [10]. It has also been demonstrated that porphyrin may act as a catalyst for the formation of sugars [11], polyenes [12], and amino acids [13-15].

This paper proposes a model for the catalytic photochemically activated formation of L-leucine and L-isoleucine from methylidyne, ammonia, carbon monoxide, hydrogen, and the catalyst magnesium porphyrin, whilst seeking to explain the meager occurrence of norleucine and ψ -leucine [2].

The reactions described have been deduced as kinetically and thermodynamically viable, but photochemical excitation is required.

2 Problem Formulation

This proposed computational study of a plausible synthesis of L-leucine and L-isoleucine involves the calculation of the enthalpy changes for reaction intermediates in the ZKE approximation and the calculation of activation energies at the HF level. These activation energies may all be accessible as the catalyst may absorb appreciable photochemical activation (0.21 h). The computations tabulated in this paper used the GAUSSIAN03 [16] commercial package. The standard calculations at the HF and MP2 levels including zero-point energy corrections at the Hartree-Fock level, [17], together with scaling [18], using the same basis set, 6-31G*. are as previously published [7]. Enthalpy changes at the MP2 level not including scaled zero point energies are designated as $\Delta H_{(MP2)}$. The charge transfer complexes are less stable when calculated at the

HartreeFock level [17], and activation energies calculated at the HF level without scaling are less accurate..

If the combined energy of the products is less than the combined energy of the reactants it may show that the reaction is also likely to be spontaneous at higher temperatures. This paper uses the atomic unit of energy, the hartree [16].

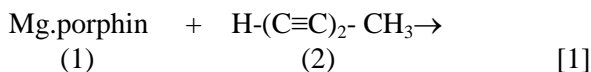
1h = 627.5095 kcal.mol⁻¹. 1h = 4.3597482 x 10⁻¹⁸ J

Charges are in units of the electronic charge.

3 Problem Solution

3.1 Total Energies (hartrees)

Methyl diacetylene may chelate with the magnesium ion of magnesiumporphin, which is here taken as a possible catalyst, to form an in-plane charge transfer complex where the charge on the ligand is positive, 0.06. and the charge on the porphin molecule is negative. The enthalpy of formation of the van der Waals complex is small but it appears stable.



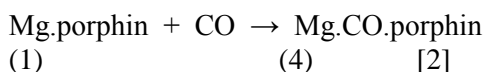
$$\Delta H = -0.02556 \text{ h}$$

The adduct has formal charges of -0.59, 0.22, 0.19, -0.23 and -0.50 on the carbons C1-C4, respectively.

This is the first reactant required in the synthesis.

3.2 The asymmetric induction of chirality

Mg.porphin also forms a stable complex with carbon monoxide in which the carbon monoxide is bonded to the magnesium ion, as shown,



$$\Delta H_{(\text{HF})} = -0.00919 \text{ h}$$

This is the low energy complex [11]. When this complex is photochemically activated, an in-plane electronic transition occurs in which the HOMO may be excited to the LUMO [11]. If the magnetic vector of the radiation is directed perpendicularly upward from the ring when viewed from above, the energy levels of the HOMO and LUMO are each split according to the Zeeman effect [19] and the adduct may dissociate, and rise in height above the ring. The first excitation energy

(0.21 h) is greater than the activation energy (0.19668h) and much greater than the bonding energy (-0.02164 h) [11]. The system of conjugated bonds in porphin has been approximated to the particle on a ring quantum mechanical problem [20]. In this model the molecule is described as a cyclic system [21] where the removal of the degeneracy of the orbitals by the magnetic field allows the contributing mesomeric forms [22] to have different energies, as shown in Fig.1.

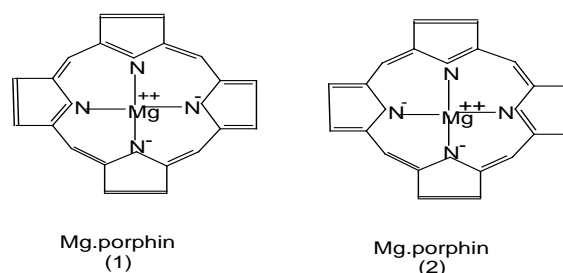


Fig.1. Mesomeric forms of Mg.porphin in the presence of a magnetic field pointing perpendicularly upwards from the ring towards the observer.

Four transitions may occur[19] of which two are allowed by the selection rules [23]. As the molecule is normally diamagnetic [24] the highest energy HOMO orbital should correspond to that shown as Fig.1(1). It is postulated that the CO group is able to move through a transition state to the porphin ring where it forms an excited, but stable bridged aziridine-2-one ring [11,25-26] at a pyrrole unit with this isomer, as shown, Fig.2(1)

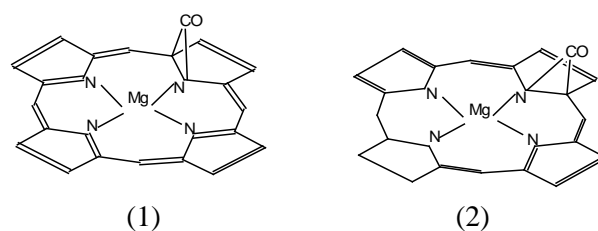
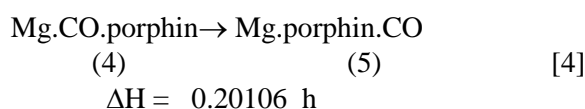
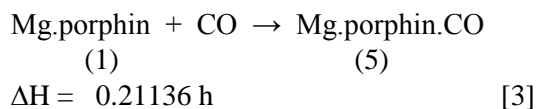


Fig.2. Isomers of Mg.porphin.CO

This is a higher energy charge transfer complex, where a high proportion of the photochemical energy has been conserved as chemical energy. If the magnetic field reverses the positively charged adduct is compressed down on the ring and less liable to reaction. If the unfavourable complex Fig.2(2) is formed from atmospherically activated carbon monoxide, then further excitation may lift the adduct from the periphery of the ring and convert it to the more favourable orientation for asymmetric induction. The activation energy

required to convert the forms Fig.2(1) to Fig.2(2) is < 0.11 h.

This is also involved in the proposed synthesis, as shown later. The formation requires photochemical activation,. The enthalpy of formation is positive.



These are the reactants that will be used in the synthesis of the amino acids, leucine and isoleucine.

The total energies and zero point energies for the HF and MP2/6-31G* equilibrium geometries for some of these stable molecules are given in Table 1.

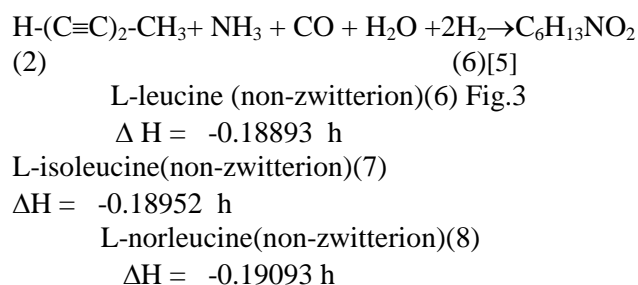
Table 1
MP2 /6-31G* total energies and zero point energies (hartrees) for the respective equilibrium geometries

Molecule hartreehartree	MP2	ZPE (HF)
Mg.porphin (1)	-1185.12250	0.29262
Methyl diacetylene(2)	-192.16934	0.06934
Mg.H-(C≡C) ₂ -CH ₃ .porphin(3)	-1377.31505	0.35932
Mg.CO.porphin (4)	-1298.13452	0.29942
Mg.porphin.CO(5)	-1297.93784	0.30434
L-leucine (non-zwitterion)(6)	-440.26501	0.20796
L-isoleucine (non-zwitterion)(7)	-440.26559	0.20794
L-norleucine (non-zwitterion)(8)	-440.26648	0.20817
Mg-1, 2-amino pent-1,3-diyn-1yl.porphin(9)	-1433.62989	0.40324
Mg.1,3-amino pent-1-yne-3-ene-1-yl.porphin (10)	-1433.69366	0.40245
Mg.1,2-methyl bicycle[1.1.0] but-1-dehydro-1-en-4yl.porphin (11)	-1377.22809	0.35678
Mg.1,(2-didehydro-3-dehydro 3-methyl cyclopropenyliden-1yl) methan-1yl.porphin (12)	-1377.216150.35551	
Mg.1,2-didehydro-3-dehydroethyliden-1yl cyclopropan-1yl.porphin(13)	-1377.21941	0.35513
Mg.1,(2-dehydro-2-methyl cyclopropenyliden-1yl) methan-1yl.porphin(14)	-1378.43219	0.38281
Mg.1,3-methenyl butyn-1-yl.porphin (15)	-1374.59087	0.38431
Mg.1,2-amino 3-methenyl butyn-1-yl.porphin (16)	-1434.86584	0.42952

Mg.1,3-(1-methenyl ethyl) 1H aziridin-2yl.porphin(17)	-1434.86399	0.42924
Mg.1,3-methenyl butanimin-1yl.porphin(18)	-1434.94414	0.42832
3-methenyl butanimine (19)	-249.78846	0.14028
Mg.1,3-methenyl butanimin-1-yl.porphin.CO(20)	-1547.93017	0.43879
Mg.1,(2-methenyl propyl) aziridine-3-one-1-yl.porphin(21)	-1547.94954	0.43870
CO	-113.02122	0.00556
H ₂ O	-76.19685	0.02298
NH ₃	-56.35421	0.03700
H ₂	-1.14414	0.01059

3.3 The overall stoichiometry for the formation of L-leucine, L-isoleucine and L-norleucine.

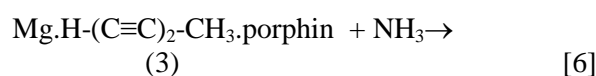
Although Mg.porphin is here taken as the catalyst for the reaction, the overall stoichiometry to form the amino acids, L-leucine, L-isoleucine and L-norleucine are as follows,

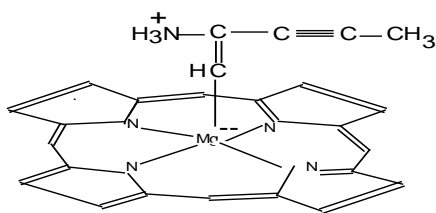


The enthalpy changes are negative indicating that this may be the energetically favourable route to the initial formation of the amino acids. The intermediates by which these stoichiometric reactions may have occurred are as follows:

3.4 The formation of Mg-1, 2-amino pent-1,3-diyn-1yl.porphin.

The first reaction in this synthesis is probably not the reaction of Mg-1,methyldiacetylene.porphin with ammonia, as shown,





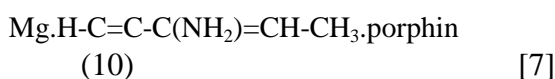
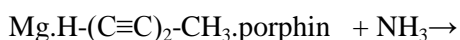
Mg-1, 2-amino pent-1,3-diyne-1yl.porphin.(9)

Although this is the rate determining step in the prebiotic synthesis of most of the amino acids[13-15] this enthalpy change is the largest encountered and implies a large activation energy and the formation of a high energy compound.

$$\Delta H = 0.04553 \text{ h}$$

The activation energies for the forward and reverse reactions were calculated as 0.041 h and 0.001 h, respectively at MP2 accuracy.

There is also a more favourable enthalpy change for the addition of ammonia across the triple bond of the adduct than addition to C2 of the adduct and subsequent reaction to form a cyclic aziridine as shown later,



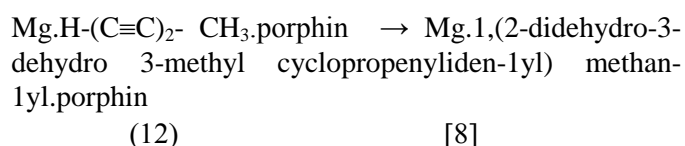
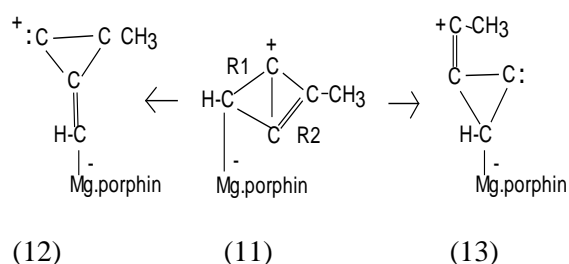
$$\Delta H = -0.01894 \text{ h}$$

These initial calculations are not favourable for the formation of substantial concentrations of norleucine, 2-amino hexanoic acid, compared to the other isomers. Similarly, the isomer, ψ -leucine, 2-amino-3,3-dimethyl butyric acid, cannot form as there is not any possible alkyne hydrocarbon to react with the catalyst.

3.5 The formation of cyclic isomers of Mg-1,methyl diacetylene.porphin.

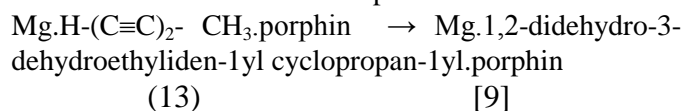
Here, it is postulated that the formation of the amino acids L-leucine and L-isoleucine was initiated by photochemical excitation of the adduct Mg-1,methyldiacetylene.porphin. to form a bicyclic high energy product (11). The activation energy was calculated as 0.085 h. This may dissociate into two products of almost identical energy with both being inter-convertible via the marginally more stable molecule, Mg.1,2-methyl bicycle[1.1.0] but-1-dehydro-1-en-4yl.porphin (11). The following structures depict these molecules with a stereochemistry determined by the presence of the magnetic field pointing upwards from the porphin ring such that the positive charges of the adduct tended to move counterclockwise whilst the negative charges moved clockwise. For Mg.1,(2-

didehydro-3-methyl cyclopropenyliden-1yl) methan-1yl.porphin the adduct retains a positive charge of 0.08 with the only positively charged carbon atom of the adduct (C diradical) being 0.018. For Mg.1,(2-didehydro-3-dehydroethyliden-1yl) cyclopropan-1yl.porphin the adduct has a charge of 0.08 with the only positively charged carbon atom of the adduct (C radical) being 0.057. For each the only carbon atoms with positive charges, 0.018 and 0.057, respectively, move counterclockwise when viewed from above, giving rise to the structures shown.



$$\Delta H = 0.09551 \text{ h}$$

The activation energy to dissociate the bicyclic complex is 0.041 h and to form the complex 0.002 h.

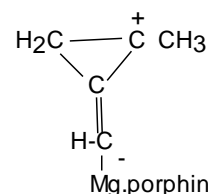
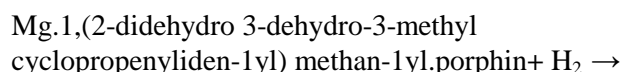


$$\Delta H = 0.09191 \text{ h}$$

The activation energy to dissociate the bicyclic complex is 0.051 h and to form the complex 0.020 h.

3.6 The formation L-leucine from Mg.1,(2-didehydro-2-methyl cyclopropenyliden-1yl) methan-1yl.porphin

The Mg.1,(2-didehydro 3-dehydro 3-methyl cyclopropenyliden-1yl) methan-1yl.porphin is a high energy diradical which would be much stabilized by atmospheric hydrogenation.



Mg.1,(2-dehydro-2-methyl cyclopropenyliden-1yl) methan-1yl.porphin(14)[10]

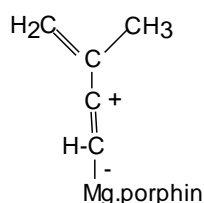
$$\Delta H = -0.05703 \text{ h}$$

The activation energy to form the carbon-hydrogen bond was found to be, 0.036 h, whilst the energy to restore the hydrogen-hydrogen bond was 0.091 h.

3.7 The formation of Mg.1,3-methenyl but-1-yl.porphin

With only moderate activation energy the Mg.1,(2-dehydro-2-methyl cyclopropenyliden-1yl) methan-1yl.porphin may isomerise to give Mg.1,3-methenyl butyn-1-yl.porphin

Mg.1,(2-dehydro-2-methyl cyclopropenyliden-1yl) methan-1yl.porphin(14)→



Mg.1,3-methenyl butyn-1-yl.porphin (15)
[11]

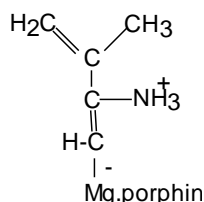
$$\Delta H = -0.09354 \text{ h}$$

The activation energy to open the ring was calculated as 0.024 h, whilst that to close it was 0.103 h.

3.8 The formation of Mg.1,2-amino 3-methenyl butyn-1-yl.porphin

The Mg.1,3-methenyl butyn-1-yl.porphin may react with ammonia gas at the positively charged C2 of the adduct. This is the rate determining step in the synthesis.

Mg.1,3-methenyl butyn-1-yl.porphin +NH₃→



Mg.1,2-amino 3-methenyl butyn-1-yl.porphin (16)
[12]

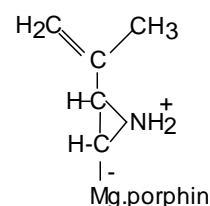
$$\Delta H = 0.02275 \text{ h}$$

The activation energy to add the ammonia was calculated as 0.028 h and 0.036 for the reverse reaction.

3.9 The formation of Mg.1,3-(1-methenyl ethyl) 1H aziridin-2yl.porphin

The Mg.1,2-amino 3-methenyl butyn-1-yl.porphin may cyclise to an aziridine derivative during being activated to transfer a hydrogen atom. The enthalpy change is marginal.

Mg.1,2-amino 3-methenyl butyn-1-yl.porphin →



Mg.1,3-(1-methenyl ethyl) 1H aziridin-2yl.porphin
(17) [13]

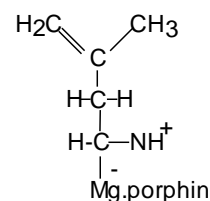
$$\Delta H = 0.00161 \text{ h}$$

The activation energy to form the ring was calculated as 0.099 h, whilst that to close it was 0.093 h.

3.10 The formation of Mg.1,3-methenyl butanimin-1yl.porphin

With only moderate activation energy a second hydrogen may be transferred from the protonated imino group to form the second carbon-hydrogen bond and opening the aziridine ring, as shown.

Mg.1,3-(1-methenyl ethyl) 1H aziridin-2yl.porphin
→

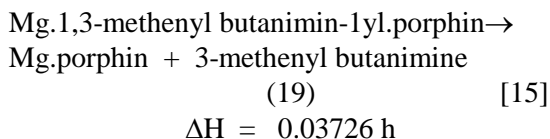


Mg.1,3-methenyl butanimin-1yl.porphin
(18) [14]

$$\Delta H = -0.08097 \text{ h}$$

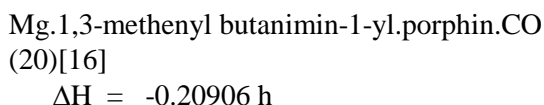
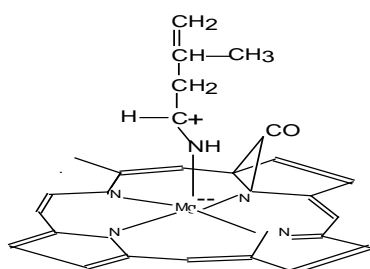
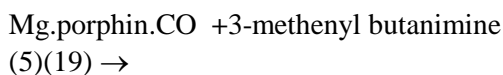
The activation energy to open the ring was calculated as 0.109 h, whilst that to close it was 0.205 h.

At the transition state the metal bonding changes from Mg-C to Mg-N. The imine is expected to dissociate to a minor extent with a small vapour pressure, but this requires a small activation energy according to the equation,



3.11 The formation of Mg.1,3-methenyl butanimin-1-yl.porphin.CO

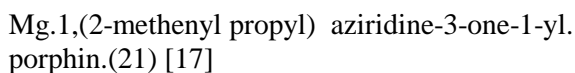
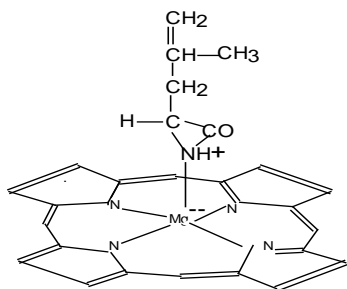
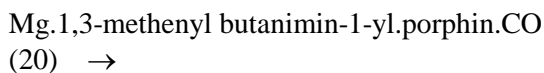
For the correct formation of the L-isomer the 3-methenylbutanimine needs to chelate to the magnesium ion on a Mg.porphin which has already obtained the correct orientation of a bound carbon monoxide molecule [11], as shown,



The enthalpy change is favourable and the activation energy to form van der Waals complexes is usually not significant if they are spontaneous.

3.12 The formation of Mg.1,(2-methenyl propyl) aziridine-3-one-1-yl.porphin.

The Mg.1,3-methenyl butanimin-1-yl.porphin.CO may easily rearrange to form Mg.1,(2-methenyl propyl) aziridine-3-one-1-yl.porphin.



The enthalpy change is favourable.

$$\Delta H = -0.01946 \text{ h}$$

The activation energy to form the aziridine was 0.093 h and the ring dissociation activation energy of 0.147 h.

3.13 The formation L-leucine.

Hydrolysis and hydrogenation in the reducing environment of the complex, is here depicted as releasing from the catalyst the non-zwitterionic form of L-leucine. Fig.3. Further formation of the zwitterions may occur.

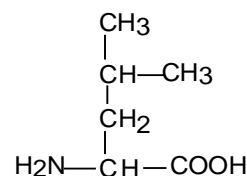
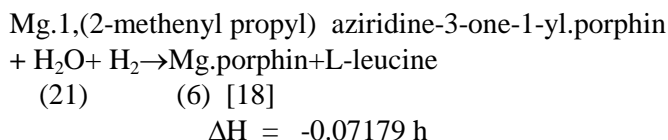
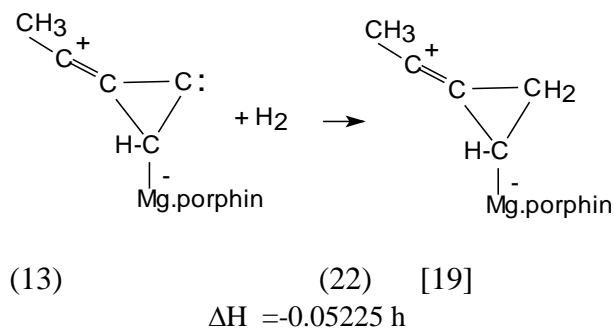
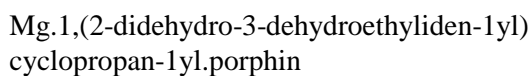


Fig.3 L-leucine (non zwitterion) (6)

4. The formation of L-isoleucine.

The proposed synthesis of L-isoleucine starts with the hydrogenation of the other cyclic high energy compound from the photolysis of Mg.H-(C≡C)₂-CH₃.porphin, Mg.1,(2-didehydro-3-ethyliden-1yl) cyclopropan-1yl.porphin to give Mg.1,2-ethylidenyl cyclopropan-1yl.porphin, and proceeds in an identical manner.



The activation energy for the addition was calculated as 0.089 h and 0.121 h for the reverse reaction.

The total energies and zero point energies for the HF and MP2/6-31G* equilibrium geometries for some of these stable molecules are given in Table 2.

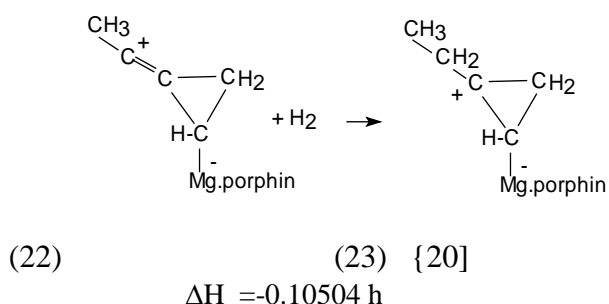
Table 2
MP2 /6-31G* total energies and zero point energies (hartrees) for the respective equilibrium geometries

Molecule	MP2	ZPE (HF)
Mg.1(2-dehydroethylidenyl cyclopropan-1-yl.porphin(22)		-1378.42926
0.38084		
Mg.1,2-dehydro 2-ethyl cyclopropan-1-yl.porphin(23)		
-1379.69479	0.40982	
Mg.1,2-amino 2-ethyl cyclopropan-1-yl.porphin(24)		
-1436.02905	0.45425	
Mg.1,3-ethyl 3-methyl 1H aziridin-2-yl.porphin(25)		
-1436.06973	0.45377	
Mg.1, 2-methyl butanimin-1-yl.porphin(26)		
-1436.15250	0.45396	
2-methyl butanimine(27)	-250.98865	0.16548
Mg.1,2-methyl butanimin-1-yl.porphin.CO (28)		
	-1549.14088	0.46451
Mg.1,2-(1-methyl propyl) aziridine-3-one-1-yl.porphin (29)		
	-1549.15132	
0.46429		

4.1. The formation of Mg,1,2-dehydro 2-ethyl cyclopropan-1-yl.porphin

The Mg.1(2-dehydroethylidenyl cyclopropan-1-yl.porphin may undergo a further highly favourable hydrogenation to give Mg,1,2-ethyl 2-dehydro cyclopropan-1-yl.porphin.

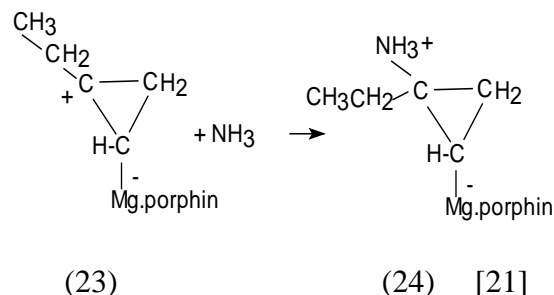
Mg.1(2-ethylidenyl cyclopropan-1-yl.porphin



The activation energy for the addition was calculated as 0.044 h and 0.176h for the reverse reaction

4.2. The formation of Mg,1,2-amino 2-ethyl cyclopropan-1-yl.porphin

The Mg.1, 2-dehydro 2-ethylcyclopropan-1-yl.porphin may add ammonia to give Mg,1,2-amino 2-ethyl cyclopropan-1-yl.porphin.



This is the rate determining step where the enthalpy change is comparable to that found for the formation of other amino acids [11-15] and less than that for the formation of norleucine.

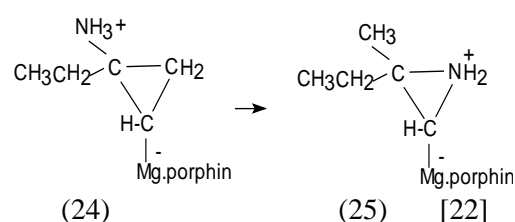
$$\Delta H = 0.02657 \text{ h}$$

Also, the activation for the addition is lower, 0.019 h, and for the dissociation, 0.013 h.

4.3 The formation of Mg,1,3-(2-ethyl 2-methyl) 1H aziridin-2-yl.porphin

The Mg,1,2-amino 2-ethyl cyclopropan-1-yl.porphin may cyclise to an aziridine derivative, Mg,1,3-ethyl 3-methyl 1H aziridin-2-yl.porphin, during being activated to transfer a hydrogen atom. The enthalpy change is favourable.

Mg,1,2-amino 2-ethyl cyclopropan-1-yl.porphin

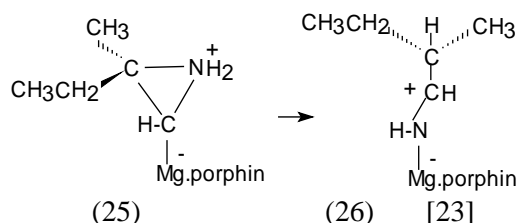


$$\Delta H = 0.04110 \text{ h}$$

To determine the activation energy to form an aziridine, the potential energy surface studied involved the stretching of the CH-CH₂ bond of the cyclopropane ring and the stretching of the CH₂-H(NH₂) bond. The activation for the cyclisation was , 0.121 h, and for the reverse reaction, 0.087 h.

4.4 The formation of Mg,1, 2-methyl butanimin-1-yl.porphin

With only moderate activation energy a second hydrogen may be transferred from the protonated imino group to form the second carbon-hydrogen bond and opening the aziridine ring, as shown to give Mg.1,2-methyl butanimin-1-yl.porphin

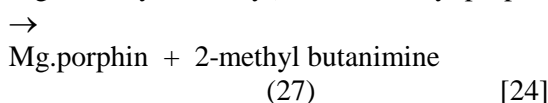


$$\Delta H = -0.08261 \text{ h}$$

The activation for the ring opening was, 0.087 h, and for the reverse reaction, 0.136 h.

At the transition state the metal bonding changes from Mg-C to Mg-N. The imine is expected to dissociate to a minor extent with a small vapour pressure, but this requires a small activation energy according to the equation,

Mg.1,2-ethyl 2-methyl) butanimin-1-yl.porphin

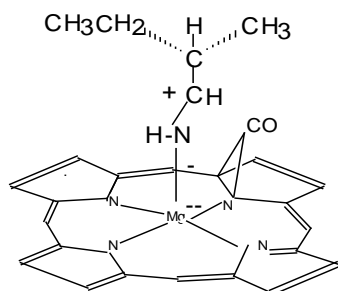


$$\Delta H = 0.04504 \text{ h}$$

4.5 The formation of Mg.1,2-methyl butanimin-1-yl.porphin.CO

For the correct formation of the L-isomer the 2-methylbutanimine needs to chelate to the magnesium ion on a Mg.porphin which has already obtained the correct orientation of a bound carbon monoxide molecule [11], as shown,

Mg.porphin.CO + 2-methyl butanimine
(5)(27) \rightarrow



Mg.1,2-methyl butanimin-1-yl.porphin.CO
(28)[25]

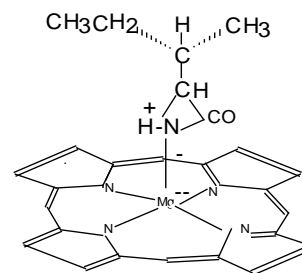
$$\Delta H = -0.21912 \text{ h}$$

4.6 The formation of Mg.1,2-(1-methyl propyl) aziridine-3-one-1-yl.porphin.

The Mg.1,2-methyl butanimin-1-yl.porphin.CO may easily rearrange to form Mg.1,2-(1-methyl propyl) aziridine-3-one-1-yl.porphin with an activation energy of 0.105 h and a ring dissociation energy of 0.100 h. The enthalpy change is marginal.

$$\Delta H = 0.01073 \text{ h}$$

Mg.1,3-methenyl butanimin-1-yl.porphin.CO
(28) \rightarrow



Mg.1,2-(1-methyl propyl) aziridine-3-one-1-yl.porphin
(29) [26]

4.7 The formation L-isoleucine.

Hydrolysis and hydrogenation in the reducing environment of the complex, is here depicted as releasing from the catalyst the non-zwitterionic form of L-isoleucine. Fig.4. Further formation of the zwitterions may occur.

Mg.1,2-(1-methyl propyl) aziridine-3-one-1-yl.porphin
+ H₂O \rightarrow Mg.porphin + L-isoleucine
(29) (7) [27]

$$\Delta H = -0.02800 \text{ h}$$

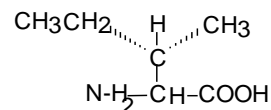


Fig.4 L-isoleucine (non zwitterion) (7)

5. Conclusion

This paper suggests that a simple interstellar molecule, methyl diacetylene, may have been induced to isomerise in a surface catalysed photochemically activated reaction where the magnetic field of the radiation induced the stereochemistry. The enthalpy changes and activation energies do appear attainable with this catalyst to produce over time some concentrations of L-leucine and L-isoleucine.

Further work at a higher accuracy may alter the values given here.

6 Acknowledgements

Appreciation is expressed for the advice and support given to this project by Professor Curt Wentrup of the University of Queensland.

Appreciation is also expressed to APAC for facilities at the ANU and QMAS facilities at UQ, and the assistance of Mr.D.Green and H.Hartig.

References

- [1] A.L.Lehninger, *Biochemistry*,Worth, New York, 1975,pp.703,567,571,577,704,705.
- [2]E.H.Rodd.(ed), *Chemistry of Carbon Compounds*, Elsevier, Amsterdam,Vol.1B, 1952, pp.830,1338.
- [3] C.J.Li,D.M.Brawson,T.J.Mabry,C.Perera,E.A.Bell, Non protein amino acids from seeds of *Cycascircinalis* and *Phaseolus vulgaris*,*Phytochemistry*,42,2,1996.pp443-445.
- [4] L.Cvak,A.Jegorov,P.Sedmera,J.Cejka,B.Kratochvil,S.Pa khomova, *Amino Acids*,20,2,2005.pp145-150.
- [5] E.E.Conn and P.K.Stumpf, *Outlines of Biochemistry*, John Wiley Inc.1972,pp71
- [6] C.R.Cantor and P.R.Schimmel, *Biophysical Chemistry*,Part 1, W.H.Freeman, San Francesco,1980.p.49.
- [7] N.Aylward, and N.R.Bofinger, "Possible origin for porphyrin derivatives in prebiotic chemistry - a computational study,"*Orig.LifeEvol. Biosph.*vol.35(4), ,2005, pp345-368
- [8]. S.L.Miller and L.E.Orgel, *The Origins of Life on Earth*, Prentice-Hall Inc.,Englewood Cliffs, N.J. ,1975.
- [9]R.B.Loren,A.Wootten,L.G.Mundy,The detection of interstellar methyl diacetylene,*Astrophysical Journal*,Part2,,286,1984,pp.23-26.
- [10] T.Oka, The infrared spectrum of H^{3+} in laboratory and space plasmas,*Rev.Mod.Phys.*64,1992,pp.1141-1149
- [11] N.N.Aylward, and N.R.Bofinger, Carbon monoxide clusters in the formation of D-sugars and L-amino-acids in prebiotic molecular evolution on Earth, in G.Palyi, C.Zucchi, L.Cagliotti, (eds.), *Progress in Biological Chirality*, Elsevier,Oxford (GB), 2004, ch2,pp.429,
- [12] N.N. Aylward, The synthesis of terpenes in prebiotic molecular evolution on Earth,in *WSEAS New Aspects of Biomedical Electronics and Biomedical Informatics*. Eds. C.A.Long, P.Anninos, T.Pharm, G.Anastassopoulos, N.E.Mastorakis,2008, pp.202-207
- [13] N. Aylward, A Prebiotic Surface Catalysed Synthesis of Alkyl Imines, in *WSEAS Int. Conf. on Biomedical Electronics and Biomedical Informatics*. Moscow, Russia, August 20-22, 2009, pp.52-59.
- [14] N.N. Aylward, "A computational study of a prebiotic synthesis of L-histidine," in *WSEAS Proceedings of the 15 th. International Conference on Computers.*, Eds. N.Mastorakis et.al.Corfu Island, pp.166-171,2011.
- [15] N. Aylward,) A Computational Study of a Prebiotic Synthesis of L-Tryptophan,in *WSEAS Proceedings of the 7th European Computing Conference (ECC '13)*, Eds.N. M Preradovic, F. Moya, M.Roushdy, A.M. Salem.Croatia, 2013, pp.105-111.
- [16] *Gaussian03, Users Reference*,GaussianInc.,Carnegie Office Park, Bldg.6., Pittsburgh, PA 15106, USA,2003.
- [17] W.J.Hehre, L.Random, P.V.R. Schleyer, and J.A.Pople, *Ab Initio Molecular Orbital Theory*, Wiley, New York.,1986.
- [18].J.A.Pople, H.B.Schlegel, R.Krishnan, D.J. DeFrees, J.S. Binkley, M.J. Frisch, R.A.Whiteside, R.J.Hout and W.J.Hehre, "Molecular orbital studies of vibrational frequencies,"*Int.J.Quantum Chem. Symp.* vol.S15.,1981, pp.269-278
- [19] P.W.Atkins, *MolecularQuantumChemistry*, ClarendonPress, Oxford,1970.
- [20] W.T.Simpson, On the theory of the π -electron system in porphyrins,,*J.Chem.Phys.*,17, 1949,pp. 1218-1221
- [21] J.R.Platt, Classification of cata-condensed hydrocarbons, *J.Chem.Phys.*17, 1949,pp.484-495
- [22]H.G.Longuet-Higgins,C.W.Rector,andJ.R.Platt, Molecular orbital calculations on porphine and tetrahydroporphine,*J.Chem.Phys.*18(9), 1950,pp.1174-1181
- [23] J.M.Anderson,*Introduction to Quantum Chemistry*,W.A.Benjamin.Inc.N.Y.1969.
- [24] J.A.Pople,W.G.Schneider and H.J.Bernstein, *High-resolution Nuclear magnetic resonance*, McGraw-Hill Book Company, 1959.
- [25]. J.P.Collman, L.S.Hegedus, J.R.Norton, R.G. Finke, "*Principles and Applications of Organotransition Metal Chemistry*", University Science Books, Mill Valey, California.,1987.
- [26] D.Mansuy,J.P.Battioni, D.Dupree,E.Santoni, *J.Am.Chem.Soc.*104, 1982, pp.6159-6161

Examination of deterioration on Diesel engine when used as fuel mixture of diesel-vegetable oil

Charalampos Arapatsakos, Anastasios Karkanis, Ioannis Pantokratoras, Eirini Markidou

Abstract—This paper examines, the effects when mixtures diesel-30%vegetable oil used as fuel in a four stroke diesel engine. To this end, the engine functioned, with diesel and with mixture diesel-30% vegetable oil (B30) as fuels. The engine was functioned for 60h with diesel fuel and 60h with B30 us fuel. The top surface of the piston was examined and compared by photographic method after removing its injector. The analyses did not present important structural changes in the surface of piston when B30 used as fuel.

Key- Words—Gas emissions, Vegetable oil as fuel, Biofuels

I. INTRODUCTION

The concept of using biofuels in diesel engines originated with the demonstration of the first diesel engine by its inventor, Rudolf Diesel, at the World Exhibition in Paris in 1900, using peanut oil as the fuel. However, due to the advert of cheap petroleum diesel, research and development activities on vegetable-oil fuels were not seriously pursued. In the 1930s and 1940s vegetable oils were used as diesel fuel from time to time, but usually only in emergency situations. Recently, these fuels received attention, because of the increase of petroleum fuel prices, limited resources of fossil oil and environmental concerns there has been a renewed focus on vegetable oils and animal fat to make biodiesel fuels [1,2]. Biofuels are liquid or gaseous fuels for the transport sector that are predominantly produced from biomass. Biofuels are generally considered as offering many priorities, including sustainability, reduction of greenhouse gas emissions, regional development, social structure and agriculture, security of supply and are applicable as motor fuels, without or with slight engine modifications. Several biofuels, including bioethanol, biomethanol, biodiesel and biohydrogen, appear to be attractive options for the future of the transport sector. The production of biofuels is expected to rise steadily in the next few decades. In developed countries there is a growing trend towards employing modern technologies and efficient bioenergy conversion using range of biofuels, which are becoming cost-wise competitive with fossil fuels.

This work developed in the Laboratory of Thermodynamics and Thermic machines of Democritus University of Thrace-Greece, under the supervision of Prof. Charalampos Arapatsakos.

Dr C. Arapatsakos is Professor on Democritus University of Thrace-Greece. Tel. 00302541079362, Fax. 00302541079362, email: xarapat@pme.duth.gr

At present several countries such Brasil, the United States, Germany, Australia, Italy and Austria are already using biofuels such as bioethanol and biodiesel. It is expected that this trend will continue to grow and more countries will use biofuels [1,3]. Bioethanol is an alternative fuel based on alcohol produced by the fermentation and distillation of raw materials with high sugar and starch contents. Besides these raw materials, ethanol can be obtained from lignocelluloses biomass from trees and some annual plants. Ethanol can be produced from any organic matter of biological origin with considerable amounts of sugar and/or materials that can be converted into sugar such as starch or cellulose. Alternative fuels produce less pollution than gasoline or diesel. The transportation fuels that are made from biomass through biochemical or thermochemical processes are known as biofuels. Examples of well known alternative fuels and particularly biofuels include biodiesel, ethanol and methanol[4]. Biodiesel is an alternative fuel made from soybean, canola or other vegetable oils, such as animal fats and recycled grease. It contains no petroleum, but it can be blended at any level with petroleum diesel to get different blends like B2 (2 percent biodiesel and 98 percent conventional diesel) or B20 (20 percent biodiesel) or it can be used as 100 percent biodiesel (B100). Most diesel powered vehicles can use biodiesel without conversion or alteration of the engine. The use of biodiesel in a conventional diesel engine results in substantial reductions of unburned hydrocarbons, carbon monoxide and particulate matter compare to emissions from diesel fuel. Additionally, biodiesel exhaust has a less harmful impact on human health than petroleum diesel fuel[4]. The major issue is how a four-stroke diesel engine behaves on the side of, deterioration, solid deposits and function, when it used as fuel diesel-30% vegetable oil.

II. INSTRUMENTATION AND EXPERIMENTAL RESULTS

In the experiment stage has been used directly vegetable oil (soy oil) oil in the mixture of diesel in to a four – stroke diesel engine. Specifically it has been used diesel, mixture of diesel-30% vegetable oil (B30) in a four-stroke diesel engine with volume 377cc, and power 8.2hp/3000rpm, was connected with a pump of water centrifugal in real conditions (figure 1, figure 2).

The engine injector spray was removed and the piston inside the fuel pump was examined. The surface of the pump piston was examined by using an Electronic Video Bore scope (EVB) model 961 P6 Beta. With this EVB it was able to have a clear picture of the top surface of the piston and compare the deposits from the fuels combustion. The pictures were taken in five positions per centimeter. There are three sets of pictures, first set: The initial state of the piston, second set: After 60hours used only diesel us fuel, and third set: After 60hours used as fuel mixture diesel- 30% vegetable oil.

Experimental measurements

During the experiments, it has been measurement CO, HC, NO and Smoke emissions[5,6,7,8,9]:

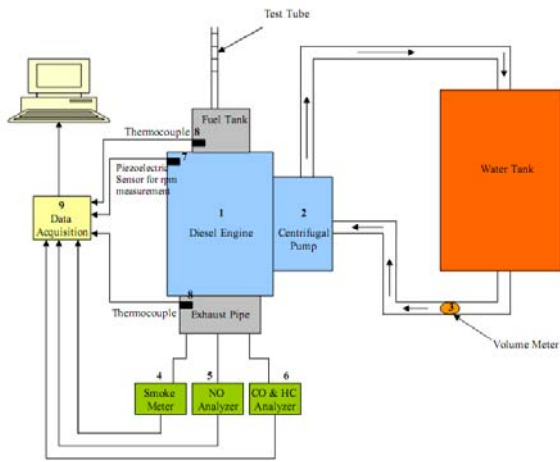


Figure 1. Experimental layout



Figure 2. Experimental layout

Experimental results

The experimental results are shown at the following figures:

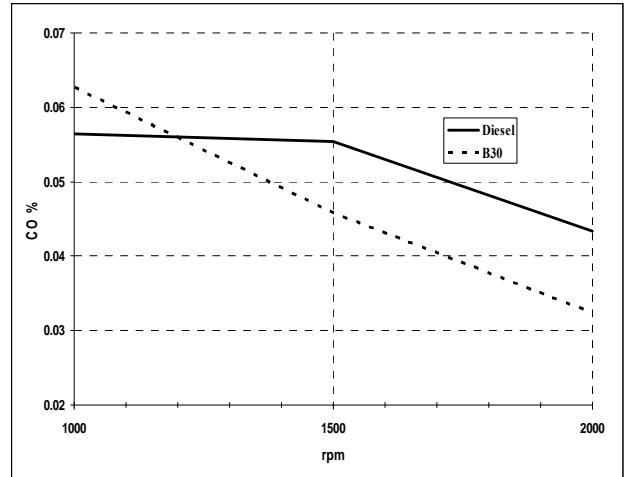


Figure 3. The CO variation on different rpm regarding to the vegetable oil mixtures

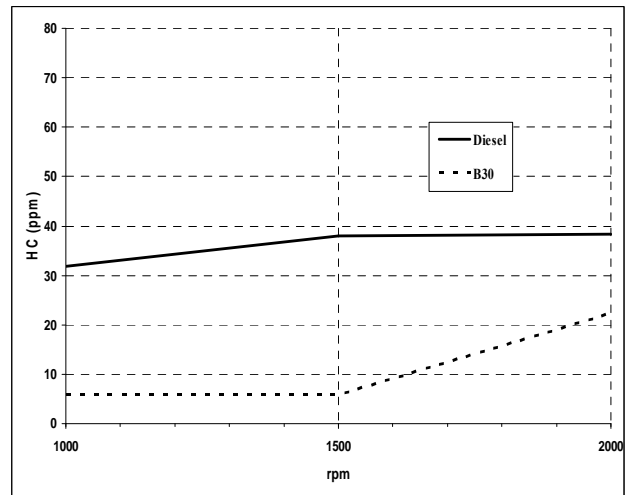


Figure 4. The HC variation on different rpm regarding to the vegetable oil mixtures

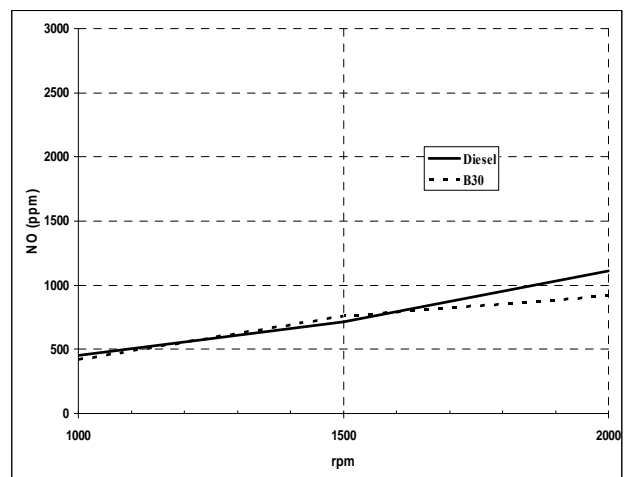


Figure 5. The NO variation on different rpm regarding to the vegetable oil mixtures

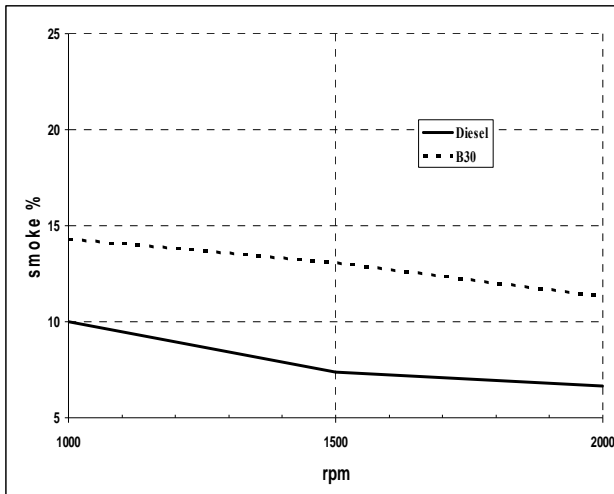


Figure 6. The smoke variation on different rpm regarding to the vegetable oil mixtures

Electronic Video Bore scope (EVB) photos were taken before the study began and after the engine function for 60h with diesel fuel and 60h with mixture diesel-30% vegetable oil as fuel. The photos in figures 7, 8, 9, 10, 11 show the initial situation and the deposits on the face of the piston:



Figure 7. The Electronic Video Bore scope (EVB) photo - initial situation



Figure 8. The Electronic Video Bore scope (EVB) photo - initial situation



Figure 9. The Electronic Video Bore scope (EVB) photo - initial situation



Figure 10. The Electronic Video Bore scope (EVB) photo - initial situation



Figure 11. The Electronic Video Bore scope (EVB) photo - initial situation

The following Electronic Video Bore scope (EVB) photos (figure 12, 13, 14, 15, 16) has been taken after 60h used as fuel only diesel. There are deposits on the surface of the piston in several places compared to the initial state of piston, but they are normal:



Figure 12. The Electronic Video Bore scope (EVB) photo – used as fuel only diesel



Figure 13. The Electronic Video Bore scope (EVB) photo – used as fuel only diesel



Figure 14. The Electronic Video Bore scope (EVB) photo – used as fuel only diesel



Figure 15. The Electronic Video Bore scope (EVB) photo – used as fuel only diesel



Figure 16. The Electronic Video Bore scope (EVB) photo – used as fuel only diesel

The following Electronic Video Bore scope (EVB) photos (figure 17, 18, 19, 20, 21) shows the piston's surface after 60h used as fuel mixture diesel-30% vegetable oil:



Figure 17. The Electronic Video Bore scope (EVB) photo – used as fuel mixture diesel-30% vegetable oil



Figure 18. The Electronic Video Bore scope (EVB) photo – used as fuel mixture diesel-30% vegetable oil



Figure 19. The Electronic Video Bore scope (EVB) photo – used as fuel mixture diesel-30% vegetable oil



Figure 20. The Electronic Video Bore scope (EVB) photo – used as fuel mixture diesel-30% vegetable oil



Figure 21. The Electronic Video Bore scope (EVB) photo – used as fuel mixture diesel-30% vegetable oil

The deposits in the piston's surface they are not more from the previous case where used only diesel fuel.

III. CONCLUSION

The use of mixture of diesel- vegetable oil has the following impacts[9]:

- Differentiation in the gas emissions
- No change in the behaviour of operation of engine
- No deterioration of engine
- The deposits in the surface of piston of engine they were not important.

REFERENCES

- [1] N.N.A.N Yusuf, S.K. Kamarudin, Z. Yaakub (2010), Overview on the current trends in biodiesel production.
- [2] Fangrui Ma, Milford A. Hanna (1999), Biodiesel production: a review.
- [3] Ayhan Demirbas (2007), Importance of biodiesel as transportation fuel
- [4] C. Arapatsakos, A. Karkanis, D. Christoforidis, M. Moschou, I. Pantokratoras, Comparison between Cotton oil and Sunflower oil fuel mixtures, "WSEAS International Conference on Heat Transfer, Thermal Engineering and Environment, Florence – Italy 2011.
- [4] C. Arapatsakos, D. Christoforidis, A. Karkanis, G.Sarantitis, D. Giannopoulos, "The Exhaust Gas Emissions Quality When Used as Fuel Mixtures of Diesel-Maize Oil", Proceedings of 2nd WSEAS/IASME International Conference on Renewable Energy Sources(RES'08), Corfu, 2008
- [6] C. Arapatsakos, D. Christoforidis, A. Karkanis, K. Mitroulas, "Soy Oil as Fuel and Its Environmental Impact", Proceedings of the 6th International Conference on Heat Transfer, Thermal Engineering and Environment(THE' 08) Rodos 2008.
- [7] C. Arapatsakos, D. Christoforidis, A. Karkanis, K. Mitroulas, "Soy Oil as Fuel in a Four Stroke Engine", WSEAS transactions on environment and development 2008.

[8] C. Arapatsakos, A. Karkanis, D. Christoforidis, M. Moschou, Blends of diesel-maize oil and diesel-soy oil in a four stroke diesel engine, WSEAS 5th International Conference of Urban Planning and Transportation Conference, Cambridge 2012

[9] C. Arapatsakos, A. Karkanis, M. Moschou, I. Pantokratoras "The Effect of Fuel Gases in Air", WSEAS International Conference of Urban Planning and Transportation. Corfu 2011.

Assessing the relation between Soil Edaphic Properties and Phosphorus Adsorption in Extremadura (Spain) Vertisols

L. Loures, J. Nunes, A. López-Piñeiro, A. Loures and A. Navarro

Abstract— Agricultural landscapes are continuously changing as a result of complex and interacting natural processes coupled with planned and unplanned actions by man. The Extremadura region, located in southwestern Spain, in which Vertisols represent an important resource for rain-fed agriculture, is no exception. Phosphorus (P) is the major limiting plant nutrient, and, its availability is a critical factor in the agricultural use of these soils. The sorption and their prediction by soil properties is important for understanding fertilizer-P behavior in soils over time, and it serves as a guide for determining the amount of P available to plants and the effectiveness of P fertilizers. Previous studies have revealed that both Fe and Al extracted by dithionite-citrate-bicarbonate (Fe-Al-CBD) are the parameters that best predict the maximum sorption in soils of Mediterranean climate. By contrast, other researchers conclude that the Fe and Al extracted with oxalate correlated, and therefore better predict, the maximum adsorption of phosphorus that the Fe-Al-CBD and CBD. This paper intends to examine phosphorus adsorption in surface samples from Extremadura Vertisols, comparing the results obtained by applying the Langmuir equation for uniform surfaces and uneven surfaces and to characterize the soil properties that best correlate with the adsorption of phosphorus, establishing the regression equations that allow an accurate prediction of the same. Considering this, Phosphate sorption was investigated in surface-samples of nineteen Vertisols in Extremadura (Spain) by uniform-surface and two-surface Langmuir equations. The obtained equations could offer a rapid estimation of P-sorption in Vertisols.

Keywords— Adsorption Capability, Extremadura, Phosphorus, Soil Properties, Vertisols

I. INTRODUCTION

AGRICULTURAL landscapes are continuously changing as a result of complex and interacting natural processes coupled with planned and unplanned actions by man [1, 2, 3, 4 and 5]. However, this on-going transformation has raised

Luís Loures is with the Centre for Spatial and Organizational Dynamics and the C3I, Polytechnic Institute of Portalegre, Portugal (corresponding author phone: 00351 965193379; e-mail: lcloures@gmail.com).

José Nunes is with the Polytechnic Institute of Portalegre, Department of Agriculture and Natural Resources and the UIQA – Research Center of Environmental Chemistry. Superior Institute of Agronomy, Portugal

António López-Piñeiro is with the Department of Edaphology and Agricultural Chemistry. Extremadura University, Spain.

Ana Loures is with the C3I's – Interdisciplinary Center for Research and Innovation. Polytechnic Institute of Portalegre, Portugal.

Arturo Navarro is with the Department of Edaphology and Agricultural Chemistry. Extremadura University, Spain.

global concerns as is the need to rethink rain-fed agricultural practices in order to protect the environment, and the Extremadura region (fig 1), located in southwestern Spain, in which Vertisols represent an important resource for rain-fed agriculture, is no exception.



Fig 1 – Geographic location of the Spanish Extremadura – adapted from Google images

Vertisols are traditionally seen as one of the most fertile soils of Extremadura in Spain and an important feature of rain-fed agriculture. Vertisols are soils rich in clay, generally found in Spain, in the provinces of Andalusia and Extremadura. In the first region there are typically darker Vertisols (Chroma <2) and in the second one they have a more brown color (Chroma > 2). The color contrast is due to the organic matter content, which is always very low. The reasons for this darker tone are the complexation of colloids and organic smectites and the presence of finely divided oxide of manganese. The brown color is due to the low levels of montmorillonite, the high content of well drained iron oxyhydroxides or to a combination of all these characteristics. Vertisols are difficult soils to manage due to its high clay content, but have high natural fertility and appear especially in regions of smooth topography. They are therefore able to withstand the changes in a culture system based on the requirements of the market

[6].

These characteristics correspond to the main edaphic ones, one can find in the Vertisols in the region of Spanish Extremadura, as reported by several authors [7, 8, 9, 10, 11, 12 and 13]. Vertisols are soils which after the 18 cm surface had been mixed, have 30% or more clay in all horizons to a depth of at least 50 cm, that in some periods, of most years (except when watered, open slits, from the surface, at least 1 cm wide, to a depth of 50 cm. These soils are very rich in terms of nutrients, in neutral to slightly alkaline pH and possess a high water retention capacity. They present generally high chemical fertility, but are very heavy and have poor aeration.

These soils are characterized by having a high plasticity, being hard and very difficult to work when dry. Despite their high water retention capacity, they present a water loss greater than would be predictable on the basis of the potential evaporation zone where they are implanted. This is due to the formation of cracks which increase greatly the surface through which water may be lost (fig.2).

Among the most common in the Spanish Extremadura Vertisols, we have the following: Luvic Vertisol - it is said that a soil possesses luvic characteristics when B has a horizon with a cation exchange capacity greater than 24 cmol (+) 1 kg of clay in its entire thickness and degree of saturation with bases (method of ammonium acetate) of 50% or more on the whole horizon, to a depth of 100 cm from the ground surface. Calcic Vertisol - These are Vertisols with calcic horizon or concentrations of white limestone powder depth less than 125 cm.



Fig 2 – Appearance of dried Vertisols Source: Vertisol atlas nacional de espanha.

In this type of soil, phosphorus is the main limiting factor of crop nutrition, and its availability is a critical issue in the agricultural use of these soils [14]. The adsorption exerted by different components of the soil in the edaphic P is of vital

importance, since it can serve as a guide for determining the amount of available P in the short and long term for plants and can even lead to more effective fertilization with this element [15, 16].

In this sense, the Langmuir adsorption isotherms are converted into important tools for estimating the availability of phosphorus and to adjust the concentration of phosphorus in the soil solution, to determine the amount of phosphorus adsorbed per unit mass, as well as the constant related to the adsorption energy [17].

Previous studies [18, 19] have revealed that both Fe and Al extracted by dithionite-citrate-bicarbonate (Fe-Al-CBD) are the parameters that best predict the maximum sorption in soils of Mediterranean climate. By contrast, other researchers conclude that the Fe and Al extracted with oxalate correlated, and therefore better predict, the maximum adsorption of phosphorus that the Fe-Al-CBD and CBD [17, 20].

This paper intends to examine phosphorus adsorption in surface samples from Extremadura Vertisols, comparing the results obtained by applying the Langmuir equation for uniform surfaces and uneven surfaces and to characterize the soil properties that best correlate with the adsorption of phosphorus, establishing the regression equations that allow an accurate prediction of the same.

1.1 General characteristics from typical Vertisols

Typical Vertisols present some distinctive characteristics from other soil typologies, which go beyond the ones mentioned before. In general this soil has a clay content of approximately 45%, normal values for the region of Extremadura [6 and 21]. The higher clay content appears in upper horizons, where the relationship between Limo and clay is also the lowest. The pH is alkaline and increases with depth, reaching its maximum in the Btk horizon, coinciding with the maximum concentration in carbonates. The cation exchange capacity decreases with depth and the exchangeable cations shows an uneven distribution over the profile. The Mg and Na are mainly in the middle of the soil section, reaching a peak on the horizon Ctk. The Ca / Mg ratio is around 3.5 in the top soil and progressively lowered until it reaches the horizon C about 0.2. The Na percentage in the soil exchange complex is between 8 and 10% in the Ctk and Cc horizons, however, the electrical conductivity indicates that there is no problem of soil salinity [6].

II. MATERIALS AND METHODS

For this study 19 topsoil samples (0-30 cm) were collected, in the province of Badajoz (Extremadura, Spain). These soils were classified as Vertisol by FAO (Cromoxeret Entice, y Pelloxeret Cromoxeret Typical). Table 1/3 is a statistical summary of the main parameters. None of the selected soils were subjected to fertilization during the year preceding the samples collection. The climate of the area is characterized by having an annual rainfall ranging from 487 to 512 mm and an

annual medium temperature oscillating between 15.6 and 16.1°C.

constant related to adsorption energy; MAP is the Langmuir maximum adsorption (mg kg⁻¹) and C is the final

Table 1: Statistic summary for the analysis performed during the study

	Clay g kg ⁻¹	O.C. g kg ⁻¹	pH	CEC. Cmol _c kg ⁻¹	C.C.A. g kg ⁻¹	Fe-CDB g kg ⁻¹	FeO g kg ⁻¹	Al-CDB g kg ⁻¹	AlO g kg ⁻¹	AST m ² g ⁻¹
Average	429	9.88	7.68	46.89	13.05	5.95	1.17	0.73	0.11	211
STD. Desv	83.6	3.29	0.42	10.75	13.41	5.56	0.49	0.28	0.04	86.4
Variance	6995	10.84	0.18	115.76	179.94	30.96	0.24	0.08	0.00	7465
Minimum	305	5.60	6.60	27.00	2.00	1.42	0.56	0.29	0.01	103
Maximum	610	17.80	8.20	68.00	52.00	22.42	2.20	1.30	0.19	423

OC= Organic Carbon; C.E.C.= Cation Exchange Capacity; CDB= extracted with Citrato-Ditionito-Bicarbonato; O= Extracted with Oxalato; AST= Total Surface Area

2.1 Soil analysis

Particle size analysis: The particle size was determined using the Robinson pipette. Prior were eliminated the organic matter content and the free sesquioxides.

pH: It was determined in a mixture of soil-water with a 1:1 ratio using a combined electrode. Organic carbon: It was determined by oxidation with dichromate according to Nelson, and Sommers [22].

Cation exchange capacity: was determined by saturating the soil with NH₄OAC 1N at pH 7, then washed this soil with ethanol. The ammoniacal nitrogen was extracted by NaOAC and determined by the Kjeldahl method.

Active calcium carbonate (ACC) was determined by the method of Drouineau [23]. Total surface area, was determined using ethylene glycol monoethyl ether following the recommendations of Carter, Heilman and Gonzalez [24].

Fe and Al extractable with oxalate, were obtained by extraction with 0.2 M ammonium oxalate at pH 3 [25].

Fe and Al extractable with citrate-bicarbonate-dithionite were determinate according to the methodology proposed by Mehra and Jackson [26].

2.2 Adsorption isotherms

The sorption isotherms were obtained by shaking the samples for 240 hours at a constant temperature of 25° C with a solution of 0.01 M CaCl₂ containing different levels of KH₂PO₄, at a 1:10 ratio. The initial concentrations of P in the solutions were 25, 50, 100, 200, 300, 400 and 500 mgP L⁻¹. Three drops of toluene were added to inhibit microbial activity. After shaking the samples, they were centrifuged at 6500 g for 15 minutes and then the phosphorus was determined from the supernatant by the method of [27]. The amount of phosphorus adsorbed was calculated by the difference between initial and final amounts of P in solution. The Langmuir equation [28] was used to determine the adsorption parameters according to the following equation:

$$K \cdot \text{MAP} \cdot C = P_a / (1 + K \cdot C)$$

Where P_a is the amount of P adsorbed (mg kg⁻¹), K is a

concentration of P in balance solution (mg L⁻¹), MAP and K were determined in the graphic representation of C/P_a over C, being the slope equal to 1/MAP and the point of intersection with the Y-axis equal to 1/(MAP.K).

The equation presented above assumes that P is adsorbed on a uniform surface. However and due to the heterogeneous nature of the P adsorption systems, it is expected that more than one parameter acts in the adsorption process. Thus if we assume that P is adsorbed on two different surfaces with different energies, the Langmuir equation that better describe this phenomenon is the equation for two surfaces [17, 29, 30] as the one presented here:

$$P_a = [K' \cdot \text{MAP}' \cdot C / (1 + K' \cdot C)] + [K'' \cdot \text{MAP}'' \cdot C / (1 + K'' \cdot C)]$$

Where k' e K'' are the energies for the adsorption sites of high and low energy, respectively. The maximum adsorption of P is represented by MAP' e MAP'' for sites with high and low energy, respectively, and MAPT is the maximum adsorption of phosphorus (MAP' + MAP'').

The adsorption parameters derived from the Langmuir equation for heterogeneous surfaces were obtained in the graphic representation of P_a/P_a over C according to [31].

III. RESULTS AND DISCUSSION

Fig. 4 shows an example of the Langmuir isotherm for a selection of three soils, which have low, medium and high phosphorus adsorption (P_a is the amount of phosphorus adsorbed per weight unit and C is the concentration of P in the existing solution).

As show in Table 1 MAP differ widely, presenting levels which vary between 150 and 2566 mg P kg⁻¹, with an average value of 1115 mg P kg⁻¹, indicating important differences in the behavior of soils with respect to P adsorption. Most of our soils have a high adsorption capacity of P in comparison with the results found by [18] regarding Vertisols.

However, the results obtained in this study are similar to those obtained by [17] in Alfisols and Vertisols. Observing Table 2 it's also possible to note that the adsorption energy (K) provides a wide range, although lower than that offered by the maximum adsorption capacity.

The graphic representation of C/Pa over C (figure 3) shows that the relationship is curvilinear. This fact is in line with the results found by other researchers [17, 32, 33, 34].

This result shows that in a heterogeneous system, as the soil, phosphate is adsorbed on two different surfaces and with different energies of adsorption and, in consequence, the Langmuir equation for two surfaces (heterogeneous surfaces), describe better the P adsorption than the Langmuir equation for uniform surfaces. In figure 1, can be observed the existence of a first line segment with stronger inclination, for every presented sample this line portion correspond to a maximum adsorption capacity of P very small, but in which the retention is made with a very high energy, followed by another line segment, with a smoother slope, which would correspond to a large amount of P adsorbed, with a much smaller energy level much lower.

Because of this, when considering two simple linear regressions, one for each segment of the line, it's possible to obtain a best model for the adsorption of P (Table 2/4) and a better regression coefficient.

Fig 3 - Langmuir adsorption isotherms for three different soils

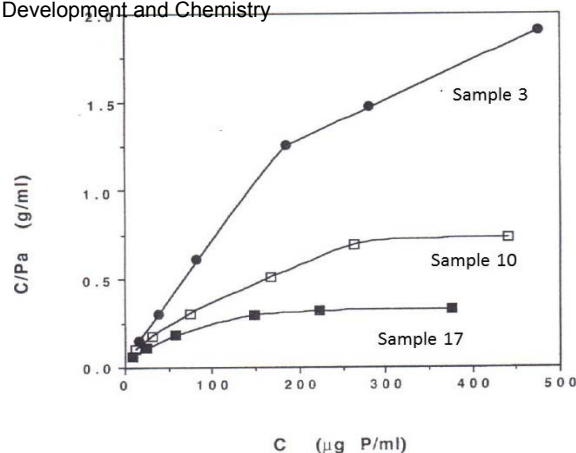
These results also prove that in all the analyzed samples, the estimated values of MAPT considering the Langmuir equation for distinct adsorption surfaces were higher than the values of MAP obtained from the Langmuir equation for uniform surfaces.

The levels of MAPT vary between 410 and 15 406 mg P kg⁻¹, with an average value of 4295 mg P kg⁻¹, consequently, a significant underestimation (about 4 times less) of P adsorption was observed when the traditional Langmuir equation was used, since in this case the values of MAP vary between 150 and 2566 mg P kg⁻¹, with an average value of 1115 mg P kg⁻¹. In all soils analysed, the MAP'' levels are higher than those corresponding to MAP' with mean values of 3674 mg P kg⁻¹ and 495 mg P kg⁻¹ respectively, indicating that most of P was adsorbed on sites of low energy and therefore can consider itself as easily available to plants.

The results obtained in the simple correlation analysis between the different edaphic properties and adsorption parameters are presented in Table 3/5.

It is possible to verify that the property that shows higher correlation with MAP is AST followed by Fe-CBD. The close relationship between MAP and Fe-CBD corroborate the results obtained by [18, 35, 36] among other authors, which conclude that Fe-CBD is a very important property in the characterization of P adsorption produced in Mediterranean region. The edaphoclimatic conditions in Mediterranean soils favor the formation of iron crystalline oxide, closely related with the iron extracted with the citrate-dithionite-bicarbonate [37, 38, 39].

The correlation between the amount of clay ($r = 0.508^{**}$) and MAP is low, although statistically significant. Similar correlation coefficient ($r = 0.502^{**}$) is obtained by relating the pH with MAP, demonstrating that P adsorption tends to



increase when increasing the pH value in soil where the Ca is the dominant cation in the exchange complex. Similar results were obtained by [40].

Also active calcium carbonate provides a positive and significant correlation ($r = 0.471^{*}$) with MAP, putting in evidence the importance of CaCO₃ in the adsorption of P in Mediterranean soils. In contrast, the correlation between organic carbon and MAP ($r = 0.240$) was not statistically significant. Similar results were obtained by [41, 42] among other investigators. On the other hand [36], working in organic soils and [16] working in different kind of soils from eastern India found that the organic carbon and MAP are significantly and negatively correlated.

When comparing the adsorption parameters derived from the application of the Langmuir equation for two surfaces, it is noted that AST is most strongly correlated with MAP'' and MAPT then with MAP' and MAP. The active calcium carbonate gives the best correlation coefficient with MAP', whereas the Fe-CBD do the same thing with MAP'', indicating that ACC was the main adsorbent of P in high energy places while at low energy was the Fe-CBD.

Considering the objective of finding equations that can predict more accurately the maximum adsorption of phosphorus from properties routinely analyzed in the laboratory, a series of multiple regression analyzes were carried out. From the different combinations tested, the equation that best predicts MAP is:

$$\text{MAP} = -509 + 72.25 \text{ X1} + 21.60 \text{ X2} + 20.20 \text{ X3} + 20.20, R = 0.850$$

Where X1 is Fe-CBD, clay content is X2 and X3 is CCA. These three variables represent and predict more than 80% of P maximum adsorption.

The equation that best predicts MAPT were the one that included in the multiple regression analysis the variables AST (X1) and Fe-CBD (X2), being as follows:

$$\text{MAPT} = -3809 + 25.40 \text{ X1} + 386 \text{ X2}, R = 0.954$$

These variables explain more than 91% of the MAPT variation. The results suggest that for the soil considered in this study, the maximum adsorption of P can be quickly and accurately estimated by the inclusion of CBD and Fe-AST in a multiple regression analysis.

Table 2 – Parameters of sorption derived from Langmuir's equation for uniform surfaces and two surfaces

Sample n ^o	Uniform surface			Heterogeneous surfaces						
	MAP mg kg ⁻¹	K 103 L kg ⁻¹	r	MAP' ^o mg kg ⁻¹	K 103 L kg ⁻¹	r	MAP'' ^o mg kg ⁻¹	K 103 mg kg ⁻¹	r	MAPT mg kg ⁻¹
1	721	12.1	0.960	405	52.7	0.990	871	2.5	0.997	1276
2	450	16.7	0.980	291	76.5	0.901	467	2.8	1.000	757
3	260	14.6	0.965	152	116.0	0.960	299	2.6	0.999	451
4	1504	10.6	0.973	803	36.9	0.933	1268	4.3	0.983	2071
5	1456	5.0	0.882	384	51.7	0.941	4227	0.8	0.989	4612
6	1585	5.2	0.860	356	101.0	0.933	3268	1.2	0.971	3624
7	2566	3.8	0.818	571	43.1	0.832	12801	0.5	0.985	13372
8	1010	7.8	0.958	390	47.2	0.953	1301	2.4	0.954	1691
9	860	11.8	0.987	436	45.6	0.977	591	6.1	0.996	1026
10	658	8.9	0.935	395	30.4	0.938	4430	0.3	1.000	4825
11	1749	8.1	0.990	817	20.8	0.978	1074	5.6	0.976	1891
12	885	9.3	0.980	398	41.7	0.989	761	4.2	0.999	1158
13	1854	5.1	0.888	606	29.5	0.978	6850	0.6	0.961	7456
14	810	10.9	0.965	468	39.8	0.891	720	3.5	0.937	1188
15	298	23.6	0.982	194	266.0	0.969	216	5.1	0.996	410
16	150	13.9	0.958	264	82.9	0.955	504	2.4	0.990	806
17	1455	6.9	0.871	603	37.2	0.941	14803	0.2	0.995	15406
18	1394	6.0	0.917	641	22.6	0.971	3243	1.0	0.982	3884
19	1511	5.2	0.880	627	22.5	0.968	6258	0.5	0.917	7155

IV. CONCLUSIONS

Table 3 – Simple linear correlation coefficients between P sorption parameters and relevant soil properties

	MAP ^c	MAP' ^d	MAP'' ^e	MAPT
pH	0.502**	0.351NS	0.406**	0.415**
Clay	0.508**	0.433*	0.207NS	0.221NS
C.O. ^a	0.240NS	0.163NS	0.165NS	0.170NS
CCA ^b	0.417*	0.592**	-0.040NS	-0.026NS
Fe-CDB	0.628**	0.295NS	0.900***	0.897***
Al-CDB	0.617**	0.352*	0.629**	0.633**
Fe _o	0.217NS	0.421*	0.065NS	0.082N
Al _o	0.048NS	0.199NS	-0.124NS	-0.111NS
AST	0.708***	0.451**	0.897***	0.900***

^aOrganic carbon; ^bActive CaCO₃ equivalent; ^cP maximum sorption; ^dP maximum sorption in high energy places; ^eP maximum adsorption in low energy places; CDB= Extracted with citrate-bicarbonate dithionite; o= Extracted with com oxalate; *, **, *** significant at 0.05, 0.01 y 0.001 probability levels respectively; NS= not significant.

The results puts in evidence that for the Vertisols studied in this work, the Langmuir equation for two surfaces better describes the adsorption of P than the Langmuir equation for uniform surfaces. It's possible to notice that the traditional Langmuir equation underestimates (4 times lower) the levels of P adsorption when compared with Langmuir adsorption equation applied to two distinct surfaces.

The inclusion of soil properties routinely analyzed in the laboratory, such as the content of clay, Fe-CBD and CCA explains 80% of maximum adsorption variation of P (MAP). Finally, the inclusion of Fe-CBD and AST in multiple regression analysis explain 90% of the P maximum adsorption variation (MAPT).

ACKNOWLEDGMENTS

The authors would like to acknowledge financial support given by the Centre for Spatial and Organizational Dynamics (CIEO) and from the Foundation for Science and Technology (FCT).

REFERENCES

- [1] L. Loures, and T. Panagopoulos. From derelict industrial areas towards multifunctional landscapes and urban renaissance. WSEAS Transactions on Environment and Development, 2007, Vol. 3 (10) 181-188.
- [2] L. Loures, J. Nunes and T. Panagopoulos. Learning by Experience: Using Case Study Research towards the Definition of a Postindustrial Redevelopment Approach. International Conference on Urban Rehabilitation and Sustainability (URES '10), Alg. PT, 2010, pp. 159-164.
- [3] L. Loures, J. Burley, and T. Panagopoulos. Postindustrial landscape redevelopment: addressing the past, envisioning the future. International Journal of Energy and Environment, 2011, 5(5): 714-724.
- [4] L. Loures, R. Santos, and T. Panagopoulos. Urban parks and sustainable city planning - The case of Portimão, Portugal. WSEAS Transactions on Environment and Development, 2007, Vol. 3(10) 171-180.
- [5] L. Loures, T. Heuer, D. Horta, S. Silva, and R. Santos. Multifunctional clusters in Post-industrial Landscapes: rising from what's left. WSEAS Transactions on Environment and Development, 2008, Vol. 4(8) 619-628.
- [6] J. Gallardo and A. Saldaña. Génesis; Clasificación y Problemas Agronómicos de los Barros: Tierra de Barros, Extremadura. Anales de Geografía de la Universidad Computense 12: 265-275. Ed. Univ. Complutense, 1992.
- [7] J. Cardoso. Os solos de Portugal: sua classificação, caracterização e génesis. Ed Ministério da Economia. Secretaria de Estado da Agricultura. Direcção Geral dos Serviços Agrícolas, 1969.
- [8] Food and Agriculture Organization. Guidelines for soil description. 81 p. Ed FAO, Rome, 2009.
- [9] D. Fanning, M. Fanning. Soil: morphology, genesis and classification. New York: John Wiley & Sons, 1989.
- [10] P. Sousa. Modernização do regadio em Portugal. Que opções?. *Gazeta das Aldeias*, 1998, 3065: 25-28.
- [11] J. Porta, M. López-Acevedo and C. Roquero. Edafología para la agricultura y el medio ambiente. Mundi-Prensa (Eds). p. 225-241. Madrid, 1994.
- [12] G. Navarro and A. Piñeiro. Mapa De Suelos De La Provincia De Caceres. Escala 1:300.000. Ed. Universidad da Extremadura, 2002, 119 p.

- [13] J. Nunes. Los Suelos del Perimetro Regable del Caia : Tipos, Fertilidad e Impact del Riego en Sus Propiedades Químicas. Ph.D. UNEX, Espanha, 2003, 878 p.
- [14] A. Lopez-Piñeiro. Caracterización de la dinámica de macronutrientes en Vertisoles de la Provincia de Badajoz. Ph.D. diss. UNEX Spain, 1990.
- [15] M. Probert,. The sorption of phosphorus by soils. *In soil: an Australian viewpoint*. Division of soils. CSIRO: Melbourne/Ac. Press. London, 1983.
- [16] S. Pal. Phosphorus sorption-desorption characteristics of soils under different land use patterns of eastern India. *Archives of Agronomy and Soil Science*, 2011, 57 (4): 365-376.
- [17] B. Yerima, L. Hossner, L. Wilding, and F. Calhoun. Forms of phosphorus and phosphorus sorption in northern Cameroon Vertisols and associated Alfisols. *In* L. P. Wilding and R. Puentes (eds). *Vertisols: Their distribution, properties, classification and management*. Technical monograph No. 18. Soil Management Support Service. Texas A & M University Printing Center College Station, TX, 1988.
- [18] P. Solis, and J. Torrent. Phosphate sorption by calcareous Vertisols and Inceptisols of Spain. *Soil Sci. Soc. Am. J.*, 1989, 53:456-459.
- [19] F. Peña, and J. Torrent. Predicting phosphate sorption in soils of mediterranean regions. *Fertilizer Research.*, 1990, 23:173-179.
- [20] G. Yuan, and L. Lavkulich. Phosphate sorption in relation to extractable iron and aluminum in spodosols. *Soil Sci. Soc Am. J.*, 1994, 58:343-346.
- [21] G. Navarro and A. Piñeiro. Nivel de Fertilidad de los vertisoles de la provincia de Badajoz (España). I. Características generales de la capa arable. *An. Edaf y Agrobiol.*, 1987, 46: 1303-1318.
- [22] D. Nelson, and L. Sommers. Total carbon, organic carbon and organic matter. p. 539-580. *In*: A.L. Page et al. (eds.) *Methods of soil analysis. Part 2*. 2nd ed. Agron. Monogr. 9. ASA and SSSA, Madison, WI, 1982.
- [23] G. Drouineau. Dosage rapide du calcaire actif du sol: Nouvelles données sur la repartition et la nature des fractions calcaires. *Ann. Agron.*, 1942, 12:441-450.
- [24] D. Carter, M. Heilman and C. Gonzalez. Ethylene glycol monoethyl ether for determining surface area of silicate minerals. *Soil Sci. Soc. Am. Proc.*, 1965, 28:632-635.
- [25] U. Schwertmann. Differenzierung der Eisenoxide des Bodens Durch Extraktion mit Ammoniumoxalat-Lösung. *Z. Pflanzenernähr. Düng. Bodenkd.*, 1964, 105:194-202.
- [26] O. Mehra, and M. Jackson. Iron oxide removal from soils and clays by a dithionite-citrate system buffered with sodium bicarbonate. *Clays Clay Miner.*, 1960, 7:317-327.
- [27] J. Murphy, and J. Riley. A modified single solution method for determination of phosphate in natural waters. *Anal. Chimi. Acta*, 1962, 27:31-36.
- [28] N. Barrow. The description of phosphate adsorption curves. *J. Soil Sci.*, 1978, 29:447-462.
- [29] G. Mattingly. Labile phosphate in soils. *Soil Sci.*, 1975, 119:369-375.
- [30] J. Mead. A comparison of the Langmuir, Freundlich and Temkin equations to describe phosphate adsorption properties of soils. *Aust. J. Soil Res.*, 1981, 19:333-342.
- [31] G. Sposito. On the use of the Langmuir equation in the interpretation of "adsorption" phenomena:II. The "two-surface" Langmuir equation. *Soil Sci. Soc. Am. J.*, 1982, 46:1147-1152.
- [32] B. Bache and E. Williams. A phosphate sorption index for soils. *J. Soil. Sci.*, 1971, 22:289-306.
- [33] I. Holford, R. Wedderburn and G. Mattingly. A Langmuir two surface equation as a model for phosphate adsorption by soils. *J. Soil Sci.*, 1974, 25:242-255
- [34] Q. Wang and Y. Li. Phosphorus adsorption and desorption behavior on sediments of different origins. *J. Soils Sediments*, 2010, 10:1159-1173
- [35] C. Borrero, F. Peña and J. Torrent. Phosphate sorption by calcium carbonate in some soils of the mediterranean part of Spain. *Geoderma.*, 1988, 42:261-269.
- [36] L. Janardhanan and S. Daroub. Phosphorus Sorption in Organic Soils in South Florida. *Soil Sci. Soc. Am. Journal*, 2010, 74(5):1597-1606.
- [37] U. Schwertmann. Some properties of soil and Synthetic iron oxides. p. 203-250. *In* J. W. Stucki et al. (eds.) *Iron in soils and clay minerals*. NATO Adv. Inst., Bad Windsheim, GE. Reidel Publ. Co., NL, 1988.
- [38] E. Afif, A. Matar and J. Torrent. Availability of phosphate applied to calcareous soils of West Asia and N.Africa. *Soil Sci. Soc. Am. J.*, 1993, 57:756-770.
- [39] A. Mehmood, A. Mohammad, R. Hayat and M. Memon. Phosphorus Adsorption Parameters in Relation to Soil Characteristics. *J. Chem. Soc. Pak.*, 2010, 32:129-139
- [40] D. Curtin, J. Syers and N. Bolan. Phosphate sorption to exchangeable cation composition and pH. *Aust. J. Soil Res.*, 1992, 31:137-149.
- [41] E. Udo and F. Uzu. Characterization of phosphorus adsorption by some Nigerian soils. *Soil Sci. Am. Proc.*, 1972, 36:879-883.
- [42] Y. Soon. Solubility and retention of phosphate in soils of the northwestern Canadian prairie. *Can. J. Soil Sci.*, 1991, 71:453-463.

New tree species for agroforestry and energy purposes

Andrea Vityi, Béla Marosvölgyi

Abstract—Bibliographic data and the results of present domestic experiments show that Paulownia species can be grown easily, have high biomass production, favourable energetic parameters and modest requirements as to site quality. Establishment of Paulownia plantations may support the aim to meet the growing needs for site-remediation and biomass for energy purposes. This paper gives an overlook on the relevant research activity and results of the University of West Hungary. The use of the selected species can reasonably be recommended for these purposes, since the plantations - grown from self-developed propagating material, managed and tested according to the formulated methods - have a high production of biomass and thus confirmed as suitable for energy purposes. The use of Paulownia for agroforestry purposes may also be a prospective way of multifunctional land use while providing beneficial ecosystem services.

Keywords— energy, biomass, Paulownia, agroforestry.

I. INTRODUCTION

THE empress tree (*Paulownia tomentosa*) is one of the world's most multifaceted tree species. It originates from China and are also grown throughout Asia, USA, Australia and Europe. (AFBI, 2008)

Its wide spectrum of utilization ranges from industrial use (furniture, timber, pulp and paper, energy), to medical and hive products, or decoration (eg. ornamental trees and wood carvings).

In recent years the awareness and business interest for Paulownia is growing fast in Central-Eastern Europe, while there is a lack of research activities in the subject of cultivation, utilization, and adoption of the best practices in these countries. However it is of utmost importance to take the local conditions into consideration when adopting new species and technologies.

As no preliminary research activity can be recognized on this subject in Hungary, NyME KKK together with external partners (cooperative and farmers) started a research program on energy and agroforestry use of Paulownia.

A. Vityi is with the University of West Hungary Institute of Forestry and Environmental Techniques, and UWH Cooperational Research Centre Nonprofit Ltd., Bajcsy-Zs. u. 4. Sopron, H-9400, Hungary (e-mail: and@emk.nyme.hu)

B. Marosvölgyi is with the University of West Hungary Cooperational Research Centre Nonprofit Ltd., Bajcsy-Zs. u. 4. Sopron, H-9400, Hungary (e-mail: marosvolgyib@asys.hu)

II. MATERIAL AND METHOD

According to the literature, Paulownia can be multiplied from seeds, cuttings or by micropropagation. (Al-Tinawi, I. A. et al., 2010, Lobona, S., 2008) (Gyuleva, V., 2008) In favourable conditions a 10 year-old tree may reach 30-40 cm in diameter, 10-12 m in height and provide 0,2-0,6 m³ volume production. (Yang, 2004)

In the first stage of our experiments we used selected mother plants and developed a special method of propagation from seeds. The method is based on a special substrate composition and strict planting protocol. In spring seedlings with 4-6 leaves were relocated into planting containers where they grew until planting out in autumn. (Image 1)



Image 1 Selected Paulownia seedlings in spring 2006.
(Picture made by the Authors)

The first experimental bioenergy plantations were established from this selected material in autumn 2006. Planting and research activities were coordinated by the Eco-energetic Research Division of NyME KKK.

Plantations were located in various parts of the country with different climate conditions. Also different planting structures and cutting rotation systems were applied in order to examine the growing and other relevant parameters of the plants.

In order to scan the usability of the trees in energetic processes we studied the international literature available on Paulownia, then made tests with the samples originated from our own plantations on bulk density, moisture content, ash content, and heating value, which are basic parameters concerning energetic utilization.

III. RESULTS AND CONCLUSIONS

A. Experiences on propagation, planting and plant management

By the use of specifically selected Paulownia plants and self-developed propagation method we managed to realize 80% plant survival. Further experimental plantations based on the selected material are planned to be established for extended research purposes in the next years.

B. Experimental results of biomass production

According to the results of the crop yield survey the biomass production of the experimental plantation was definitely high (55 t/ha).



Image 2 The 6-year-old experimental plantation with one-/two-year cutting rotation (2012 October). Seedlings were planted in double-rows taking the needs of harvesting technology into account. (Source: Vityi-Marosvölgyi,2012)

It has to be underlined that the given high yield volume is only valid under the specific parameters of the experimental system (applied planting structure, site conditions, selected material, cutting rotation, site management, etc.). Furthermore, given the dimensions of the test parcel, we had to calculate with border-effect which surely had significant benefits for the biomass production volume.



Image 3 Cross-sectional view of a 4-year tree form a Hungarian bioenergy test plantation with selected Paulownia tomentosa (replanting system) (Source: Vityi-Marosvölgyi,2011)



Image 4 Energy-wood from a Hungarian Paulownia tomentosa experimental site (from one stem) (Source: Vityi-Marosvölgyi, 2011)

C. Results of the energetic analyses of the biomass from the Paulownia experimental site

Having studied the literature we found that the available data on certain energetic parameters of Paulownia-biomass varied, but basically were comparable with the results of our measurements.(Table 1) (Source: Vityi-Marosvölgyi,2012)

The good test results of the woody biomass from the experimental sites - whether in annual cutting rotation or in multi-year rotation system - show that Paulownia may definitely be suitable for energy purposes.

	Mechanical and combustion parameters of the one-year-old shoot of selected <i>Paulownia tomentosa</i> variety			Bibliographical data on the mechanical and combustion parameters of <i>Paulownia</i> species		
	wood	bark	mean*	wood	bark	mean
Bulk density (g/cm ³ , air-dry)	0,35					0,22-0,30
Moisture content (m/m%, air-dry)	11,80	10,90	11,61			7,74-10,00
Ash content (m/m%)	0,92	3,05	1,37			0,5-5,28
Heating value (MJ/kg, air-dry)	16,66	17,40	16,82			16,58-18,83
Fűtőérték (MJ/kg, absolute dry)	18,92	19,67	19,10			
*based on bark-rate of 21% measured from one-year-old shoot samples						

Table 1 Results of the University of West Hungary Cooperational Research Centre's tests compared with the data available in the literature on the energetic parameters of *Paulownia*

D. The Use of *Paulownia* in agroforestry systems

Agroforestry is the practice of deliberately combining woody vegetation (trees and/or shrubs) with crop and/or livestock systems.

Agroforestry practices help farmers to diversify farm income, while benefiting from the resulting ecological and economical interactions e.g. improve soil and water quality, reduce erosion, pollution, or damage due to extreme weather, enhance resource efficiency, biodiversity, and the resiliency of the production system. Agroforestry systems manifest in several practices: forest buffers, windbreaks, silvopasture, alley cropping, forest farming, etc.

Based on the positive bibliographic data on the use of *Paulownia* in alley-cropping and the favorable results of NyME KKK's field tests we decided to extend the examinations to the use of *Paulownia* for agroforestry purposes.

Agroforestry experiments with *Paulownia* started in 2012. The initial step was the plantation of the first and so far only experimental *Paulownia* intercropping system in Hungary. In the next years NyME KKK plan to make investigations on crucial parameters of sustainable management of the *Paulownia*-intercrop systems. This activity will also be a contribution to EU FP7 project called „AGFORWARD”. This is a four-year pan-european project, with the goal of promoting appropriate agroforestry practices that advance sustainable rural development.

REFERENCES

- [1]. Al-Tinawi, I. A. et al.(2010): Development of In vitro Propagation System for *Paulownia tomentosa* L. Using Tissue Culture Techniques. *Jordan Journal of Agricultural Sciences*, 6 (4), 2010
- [2]. Gyuleva, V. (2008): Project “Establishment of geographical plantations of *Paulownia elongata* hybrids in Bulgaria” – contract No 37 with State Agency of Forests (2007–2010). *Bulgarian Academy of Sciences - News*. No 12 (64), Year VI, 2008.
- [3]. Lobna, S. Taha (2008): A Micropropagation Protocol of *Paulownia kowakamii* through *in vitro* culture technique. *Australian Journal of Basic and Applied Sciences*, 2(3): 594-600
- [4]. Muthuri, C. W. et al. (2005): Tree and crop productivity in *Grevillea*, *Alnus* and *Paulownia*-based agroforestry systems in semi-arid Kenya. *Forest Ecology and Management*, 212: 23-39.
- [5]. Vityi, A. – Marosvölgyi, B. (2011.): Hazai eredetű császárfa mint energianövény. *Környezeti Kutatások. Környezeti Erőforrás-gazdálkodási és védelmi Kooperációs Kutatási Központ Nonprofit Kft., Ökoenergetikai Kutatási Főirány, Sopron.*
- [6]. Vityi, A. – Marosvölgyi, B. (2012.): A fajszi kísérleti *Paulownia* ültetvények újabb kutatási eredményei. *Környezeti Erőforrás-gazdálkodási és védelmi Kooperációs Kutatási Központ Nonprofit Kft., Ökoenergetikai Kutatási Főirány, Sopron.*
- [7]. Woods, V.B. (2008): *Paulownia* as a novel biomass crop for Northern Ireland? A review of current knowledge. Occasional publication No. 7. Agri-Food and Biosciences Institute, Hillsborough, 2008.
- [8]. Yang, X. (2004): *Paulownia* Agroforestry Systems in China. Poster. Preceedings of the International Ecoagriculture Conference and Practitioners' Fair. vol. 2: 21-22. Conference abstracts. Nairobi, 2004.

Power-information models of operation and development of megapolises power supply systems

Stepan A. Dmitriev, Sergey E. Kokin and Alexandra I. Khalyasmaa

Abstract— The article is concerned with development of distribution network facility control model based on reliable status information of its objects. General provisions of power-information models of operation and development of megapolises power supply systems are considered. Basic results are presented.

Keywords— power-information model, genetic algorithms, indicative analysis, fuzzy logic, optimal development.

I. INTRODUCTION

Modernization of electric power industry in Russian Federation led to financial capability of power grid companies, herewith monetary resources for power energy transport and rate for grid connection are the basic sources of fiscal sustainability [1]. Fiscal responsibility of power grid companies for their own electrical grids results in increase in energy saving importance [2], reduction of excessive power energy losses [3] and quality improvement of measurement systems of electric power metering.

In recent years there exists a growing demand for electric energy of low power generating units [4] in power supply systems (PSS) at medium and low nominal voltage classes including facilities based of renewable energy sources in the form of distributed energy resources complex. Appearance of distributed energy generation sources, energy accumulation units, modern digital devices for control and measurement of energy systems operating parameters results in quality changes both in PSS and PSS control systems [5]-[10]. Medium voltage radial distribution networks with simple control are replaced by networks with two-way power supply [11]. Due to complication of electric power transmission and distribution processes modernization of network control system is required.

Creation of new generation networks provides for reorganization of networks control system. Creation of effective control system of megapolise PSS, determination of its correct structure, generation of subdivisions functions and mechanisms of their interaction is a complicated problem. Reliability of consumers power supply depends on organization level of technical administration system.

For new generation networks organization of breakthrough

communication is required for monitoring of PSS objects status and topological connectivity, network operating parameters etc. Nowadays there is no comprehensive tool for complex solution of analogous problems. Therefore, development of integral system, entitled “power-information model” (PIM), is required.

It should be mentioned that for transition to a new conception PSS control system should comprise the elements which on addition to the system will not result in increase in breakdown rate, connected with control system failures. Due to emergence the set of separate PSS elements properties can't describe behavior of the whole system [12]. New properties should be identified and used during PSS control. Herewith maintaining the required reliability level of power supply with consideration of main equipment, RPEA and communication channels failures remains the main criterion of accepted decisions

II. BASIC OBJECTIVES OF POWER-INFORMATION MODELS

Creation and implementation of power-information models of PSS development and operation allows the following problems solving [12]-[19]:

- Essential improvement of accuracy, validity and promptness of estimates concerning current and expected states and operation modes of PSS due to creation of adaptive information model;
- Analysis of existing and further power distribution by electric power grid for minimization of energy losses and formulation of recommendations concerning determination of PS equipment operation modes;
 - Functionality state assessment of PSS separate subsystems and PSS as a whole;
 - Impact assessment of most probable equipment failures on PSS operation;
 - Determination of PSS “bottle necks” during connection of new consumers and taking equipment out of service for repair.

PSS of big cities develops at a faster pace in comparison with other power facilities due to the fact that advanced technologies are applied. Megapolise is the biggest urban settlement which occurs as a result of integration of main city and surrounding settlements. As a result of infrastructures integration large and complicated engineering systems

providing guaranteed heat and electric power supply to consumers and all subsystems operation are formed. Megapolise PSS becomes commensurable with electric power systems (EPS) of middle size. Herewith PSS takes on the properties present in EPS of middle and large size.

Due to the necessity of integrated power grid monitoring the model which can be adjusted to assigned problem was created. The present model should be based on multidimensional, hierarchical communication system which comprises subsystems and elements connected by a number of functional relations. Just these relations allow assessment of subsystems and systems functional state, which is described by the following parameters: electrical equipment performance, electrical mode, power supply reliability, energy efficiency, ecological compatibility, financial capability etc.

III. OBJECT-ORIENTED GRAPH MODEL

EPS consists of stations, substations and OHL. Integrated system can be divided into subsystems by territorial, operational or other principles. Each subsystem is an object with individual properties. Practically power energy transfer and distribution system is the universal set described by information graph comprising a number of substations (SS), power stations (PS) and OHL. Herewith each element of the universe is a set of elementary objects, integrated in topologically and informationally connected structure.

On electrical system level PSS topological model can be represented as a set of system communications and nodes. It should be mentioned that generally in graph interpretation such objects as SS, PS are presented by nodes (graph nodes) whereas communications, providing engineering, topological and galvanic connectivity are presented by graph edges. However in some cases, for example during analysis of structural reliability with failures of short current type such elements as OHL can be presented as graph nodes and in other cases (electrical mode analysis) OHL are presented as graph edges. Consequently informational graph should be adaptive to particular problem.

Each EPS (S or PS) object in its turn is presented by complicated subsystem with its internal structure which can be also presented by informational graph. System model is multiple-level due to PS classification by voltage levels. It should be mentioned that a number of objects can be included in subsystems of different hierarchical levels. For example OHL can be referred to electric power grids level and SS and PS level at the same time. Power lines are “entry points” for SS.

At SS and PS distribution units (DU) level power equipment is considered as a set of elementary objects, while during analysis of equipment performance each object is presented as a complicated subsystem. Consequently communication model should provide transition from the high formalized level of objects presentation worst provided by information to the low level when technical equipment is presented as an integrated elementary object. All electrical

system levels are interrelated by topology, functions etc. For example object state at DU level has an impact on elements connectivity at EPS level. In addition to topological multiple-level and multicoupling communication interrelation should be mentioned.

For most practical problems information about graph structure and objects which form informational system is required. It is understood that each PS object is presented by graph node and a set of graph nodes of the network. It means that electrical system model should be defined by the following three parameters:

$$ES = (V, E, Obj), \quad (1)$$

where V is nodes set, E is edges set, Obj is objects set.

Introduction of Obj parameter allows setting arbitrary parameters of PS graph nodes and presenting power energy transfer system as the objects' structural organization. PIM development is performed in accordance with international standard – Common Information Model (CIM) and consequently PIM is compatible with a number of existing complexes. Objective and topological levels of PSS model are implemented.

Structural organization is based on object-oriented principle of PS model building [12]. Each elementary object of the network $Obj = (Class, Param)$ has a set of individual standard data, properties and features, which describes the purpose, operational characteristics and operation mode in different conditions. Objects register structure is hierarchical. Register contains complete description of power grid structure and properties.

$$RO = SES \cup RES \cup PS \cup Trans \cup QS \cup QR \cup Obj. \quad (2)$$

A set of registration entries corresponds to RO, where SES is a set of SES; RES is a set of RES; PS is a set of PS; $Trans$ – is a set of transformers; QS – is a set of breakers; QR – is a set of disconnecting devices; Obj – other objects. System is presented as a set of subsystems. PSS segments classification and system consideration as a set of interrelated components allowed reducing calculation amount and making mathematical-communication model closer to real industrial system.

System model is multiple-level due to PS classification by voltage levels. System is multiple-level by topology and communication. It should be mentioned that each PSS fragment belongs to a definite level and layer which correspond to special voltage type and a set of available information. Level of PS segments significance corresponds to a set of available information and its actuality. Basic characteristics of subsystems are interrelated. Due to PSS multiple-level property multiple-level control system is defined (communicational multiple-level PSS). Developed object-oriented graph structure allowed solving a number of practical problems of PSS control:

A. Determination of optimal disconnection points in meshed systems

Determination of optimal disconnection points in 10-20 kV meshed systems in megapolises for reduction of total losses in active power and energy is an actual problem, which defines operation efficiency.

In accordance with analysis of energy saving systems operation 6-35 kV power grids appeared to be the most popular grids. Herewith 10-20 kV grids have maximum length. In the context of reliability grids mentioned above are meshed, but all electric circuits comprise special disconnection point for costs reasons. It is made to prevent balanced currents leakage in circuit which leads to additional losses and deterioration of PS technical and economic performance.

By means of power-information model PSS structure was studied and a method for selection of activation function for active power losses analysis was developed on the base of artificial neural network. Network mentioned above provides rather fast assessment of power and energy losses in urban power grid and possibility of losses prediction being a crucial engineering and economical factor [20].

Solution of two problems and their further combination were performed in the present article. On the first stage steady mode calculation at given grid parameters and measurement equipment readings is performed. On the second stage invocation to goal function value, defined on the first stage, is implemented by means of designed genetic algorithm (GA). GA doesn't guarantee solving for the optimum, but usually it allows obtaining "rather quick and good" problem solution.

Just an integration of two problems mentioned above involves the main difficulty and scientific novelty of problem solution concerning finding the optimal points of circuits' disconnection.

Optimal mode is a mode which provides minimum total energy losses.

$$F = \sum \Delta W_{ij}^p \rightarrow \min, \quad (3)$$

where ΔW_{ij}^p – power losses at ij circuit network.

Algorithm of finding the optimal points of power system disconnection by electric energy (EE) losses value is based on GA. In general algorithms structure can be presented as follows [21]:

Step 1 – creation of initial population. It is performed by means of random generation method within the range of permissible values. Number of chromosomes participating in population and genes in chromosome is set in program.

Step 2 – fitness function value is calculated for initial population chromosomes. The present value is equal to goal function value or in other words it is equal to total losses of circuit active power. Herewith at each generation for each chromosome calculation of power grids steady mode is performed by Newton method.

Program based on GA refers to program module of power distribution calculation. Chromosome is presented by 1 and 0,

zero means disconnection. If zero value is met in chromosome program takes away L index in initial program data before the corresponding string and launches power distribution calculation. Then program stores PE losses value and saves it in data base. If solution is not found or at last iteration (10 iterations are used) required accuracy is not maintained penalty function is applied. Penalty function excludes the present chromosome from population. Herewith chromosome information is entered in data base.

Step 3 – check of algorithm stop condition.

In this case an algorithm stop criterion is a stop of achieved value improvement. Algorithm is stopped after generation of predetermined number of generations. If stop condition is met transition to the final stage of "best" chromosome determination is performed, otherwise selection is performed on the next step.

Step 4 – population life cycle is implemented in the form of genetic operators set.

– parents' selection. Chromosomes selection for new population formation is performed by roulette-wheel selection method;

– obtaining new solutions by chromosomes crossing method. Arithmetic crossover is applied for real variables with probability;

– mutation operator with predetermined probability is applied for one randomly chosen gene in each chromosome in accordance with uniform mutation operator.

Step 5 – new population creation. When genetic operators are applied to chromosomes of temporary parental population obtained chromosomes will be included in new population. Consequently these chromosomes gain the current population status for GA iteration under consideration. When Step 5 is finished program returns to Step 2.

Step 6 – determination of "best" chromosome. When algorithm stop condition is met algorithm output or in other words desired solution is presented.

PSS network fragment of Yekaterinburg city (Russian Federation) was considered for developed approach approbation. Network fragment consists of 48 nodes and 35 edges [21]. There are 16 points for potential circuit disconnection. It means that if the problem is solved by enumerative technique, there exist 65536 combinations of optimal disconnection points' arrangement.

Electric energy losses value in obtained scheme (Fig. 1a) is less than losses value in meshed scheme (Fig. 1b). Arguably, rather good solution was obtained in relation to meshed scheme, taken as an initial variant for consideration. EE losses value ΔW decreased on 106 260 kW-h. In order to further decrease EE losses it is required either to expand initial population or to change algorithm stop criterion upward, it means increasing considered variants number during optimal solution search. It can be achieved by changing parameters of main GA operators' application probability [21].

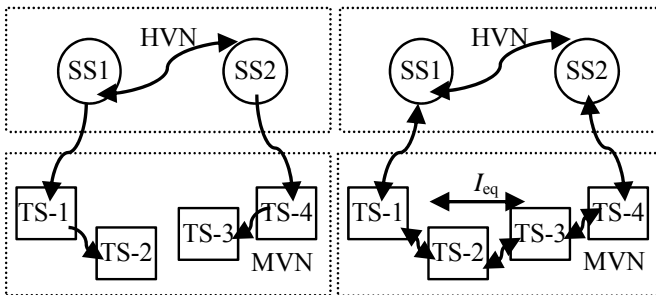


Fig. 1 principal variants of medium voltage distribution networks operation

It should be mentioned that if population is small and stop criterion is less than 1000 it may be a problem to obtain solution with goal function value exceeding value for solution with smaller GA application probability when changing probability parameters of main operators' application. It results from the fact that chromosomes in initial population are randomly created and during problem solving algorithm is not able to consider all possible genes combinations.

Efficiency of the offered GA is proved by power distribution calculation and comparison of EE losses before and after GA application. Optimization of disconnection points arrangement in network allowed reducing losses on 27,7%. GA for optimal solution search doesn't impose demands on goal function continuity and derivability, doesn't require derivation and provides global minimum search if there are several minimums in the problem.

B. Assessment of power grid objects' functional status

Problem of PSS objects state assessment was solved on the base of indicative analysis. Undertaken studies show that the present assessment method is the most acceptable under conditions of incomplete and unreliable initial information. Criterion factor of PSS performance is the key indicator. Its value gives a reasonable indication of functional status level in engineering, operational, financial or any other field.

In accordance with approach mentioned above PSS diagnostics is performed on the base of a set of performance indicators. The present indicators signal about failures rate increase, quantitatively assess the level of normal operation threats and form complex of special purpose-program measures for situation stabilization. Indicator function is defined by communication characteristic between the problem and its purpose.

For PSS objects performance assessment strict states classification with separation according to failure rates by each indicator, indicative block and generalized state as a whole is required. States analysis is performed by means of indicator or indicators group comparison with the corresponding threshold values. For performance evaluation the following states classification is used: normal, pre-emergency, emergency. x_{ij} indicator ownership is defined by (L-R) linear characteristic fuzzy membership functions of $\mu_k(x)$ class [13], [19]. States borders are located at the

intersection of $\mu_k(x)$ characteristic membership functions.

Generalized estimation is performed on the base of states indicators in different fields (by M indicative blocks):

- engineering - is used for assessment of engineering and technological differentiation of power system objects;
- operational - characterizes objects status by performance criteria;
- financial and economic– reflects cost factors of power system objects;
- ecological - characterizes impact on ecological situation;
- energy saving and efficiency - is used for estimation of power energy transfer value and cost;
- expert analysis - provides value judgment of skilled professionals;
- diagnostics - characterizes equipment status on the base of technical diagnostics [22].

The structure of each indicative block includes the indicators characterizing the object state in different areas. For example the object power transformer has the following indicators: transformers deterioration, transformers loading indicator, indicator of short circuits, indicator of the average lifetime of transformers, transformers failure indicator, indicator of the effectiveness of the transformer cooling system, environmental impacts indicator, indicator of energy saving, expert estimation indicator and technical diagnostics indicator.

Boundary values of performance states are defined for normalized indicators values: "0" – corresponds to normal performance state; "1" – corresponds to transition to emergency stage, connected with of permissible value violation.

State assessment algorithm of PSS objects is shown in Fig. 2

State assessment is performed sequentially from elementary to complex network object (increasing the level of the hierarchy L).

For example SS state assessment algorithm is as follows: state assessment of elementary object (circuit breakers, bus sections, disconnectors etc.) on all indicative blocks M by calculation of the weighted average of indicators; state assessment of complex object K (switchgear etc.) consisting of the set of elementary objects (elementary objects level is $L-1$) on all indicative blocks N by calculation of the weighted average of indicators.

Problem of generalized assessment of essential dispersion in case of multiple accounting of different indicators was solved by means of application of weighted average numerical assessment with the use of different scale: proportional $\{1, 2, 3, \dots\}$ or Saaty scale $\{1, 3, 5, 7, 9, \dots\}$.

The factor space based on Bayes' method is analyzed for determining the point scale. The result of this analysis is given in [18]. It should be noted that the appearance or vice versa of only one indicator does not significantly affect on the object operation.

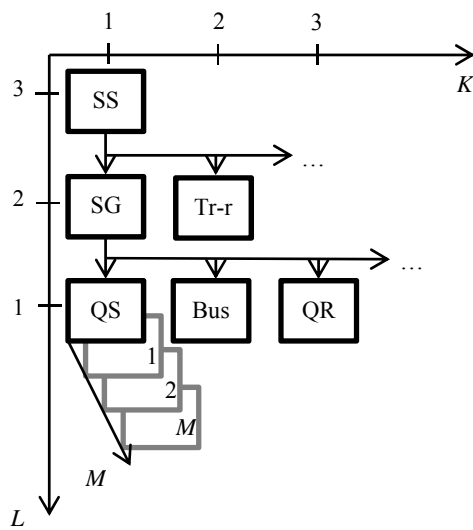


Fig. 2 state assessment algorithm of PSS objects

Indicative analysis method allows assessment of each PSS object. Numerical value of assessment is not only qualitative but also quantitative characteristic of PSS object performance. It describes object status in the context of interaction of different spheres of influence, performance aspects and indicative blocks and can be considered as a universal method. The presence of retrospective information about PSS object state allows determining its further state by extrapolation of accumulated experience. In this case it is possible to determine consequences of injectable impact on PSS. Thereafter for formation of required impacts on system for its maintaining it is sufficient to range objects from higher hierarchical level to elementary PSS objects.

C. Determination of probability-optimal solutions of modernization problem

Required level of PSS performance can be obtained by a number of tools and methods. It should be mentioned that transitions to new advanced state have different efficiency parameters, which can be expressed by implementation costs.

Solution of technical re-equipment problem is connected with assessment of probability solutions of \mathbf{R} modernization. A set of probability solutions by a definite plan \mathbf{i} can be described as:

$$R_i = \{r_{ih}, h = 1, 2, \dots, H\}, i = 1, 2, \dots, N, \quad (4)$$

where N – is a number of conceptual approaches (plans) of PSS objects construction or re-equipment; H – is a number of approaches implementation by certain modernization plan.

A set of engineering and technological constraints is imposed to solution of electric power objects' modernization, reconstruction and construction problem. Constraints can be expressed by NO set:

$$NO_i = \{no_{ik}, k = 1, 2, \dots, K\}, i = 1, 2, \dots, I, \quad (5)$$

where K – is a number of constraints. In this case a set of

possible solutions VR can be expressed as: $VR = R \setminus NO$.

The presence of nonvacuous set VR_i of possible solutions vr_{ij} is a condition of probability-optimal solutions existence

$$VR_i = \bigcap_{j=1}^J vr_{ij} \neq \emptyset, VR_i = \{vr_{ij}, j = 1, 2, \dots, J\}, \quad (6)$$

where J – is a number of possible realizable solutions.

The presence of nonvacuous set VR of possibility-optimal solutions VR_i of system development is a sufficient condition for complete satisfying of all criteria.

$$VR = \bigcap_{i=1}^I VR_i \neq \emptyset. \quad (7)$$

Problem is complicated by the fact that elements of probability-optimal solutions VR_i form a set of probability-optimal plans P . All probability-optimal plans P_g are subject to further comparison, and optimal plan is defined by efficiency indicator of all probability-optimal plans' implementation. Optimum determination is a multi-objective problem and it reduces to choice between probability-optimal variants by one criterion or criteria group. As the final result it is required to choose such solution which would have a maximum effect in the long term.

It should be mentioned that complete set of solutions forms a complete graph. Determination of optimal solution is performed from a set of solutions, being spanning trees of complete problem solving graph, by means of ranging by total implementation costs value with consideration of stage-by-stage approach and indicators values of PSS functional state in the long term [13], [23].

Designed system of modernization solutions efficiency' assessment allows development of high-priority measures complex and giving recommendation for their implementation with consideration of existing constraints [14], [15].

IV. CONCLUSION

Basic results of the present investigation can be summarized as follows:

Object-oriented approach based on graph implementation is offered for creation of power-information model. Just this approach provides flexibility, possibility of scaling and transformation of fully-connected structure of city PSS with consideration of its topological variety, PS multiple-level hierarchical representation and basic structure invariance for operation modes' modeling.

Genetic algorithm for solution of optimization problem of disconnection points search in complex distribution networks for minimization of power energy losses was offered.

Concept of power system functional state was introduced. This concept reflects engineering, economical, ecological and other characteristics of power systems. Indicative analysis methodology was offered for assessment of PSS functional state. Approaches for indicators determination and grouping in the context of problems of big cities PSS development and reconstruction were designed.

Possibility of indicative analysis results' application for

formation of complete set of engineering measures for PSS objects maintaining in normal mode and also elimination of pre-emergency modes by objects state ranging under conditions of limited financing was shown. Necessity of combinatorial problem solution of PSS optimal development search, investments calculation and their efficiency analysis on each stage was justified.

Efficiency assessment technique for accepted solutions for power grid complex elements' repair and reconstruction was developed. This technique allows formation of high-priority measures with consideration of financial, engineering and other constraints.

Presented models, based on combination of different approaches, offer opportunities for other crucial problems solution: determination of optimal arrangements of generating units with consideration of variety of schemes and modes, detection of energy saving potential etc.

REFERENCES

- [1] S. A. Dmitriev, S. E. Kokin, S. A. Lysak, O. B. Moshinskiy, N. N. Pyzhyanova, "Methodological approaches to concept formation of power grids development in big cities (Translation Journals style)," *Power industry problems*, Kazan: KSPEU, vol. 11-12/1, 2008, pp. 89-93.
- [2] S. E. Kokin, A. V. Pazderin, E. N. Adarichev, "Ways of decreasing maximum and equalizing curve of big cities' power demand (Published Conference Proceedings style)," in *Proc. The First International Conference on Sustainable Power Generation and Supply*, Nanjing, China, April 6-7, 2009, pp. 315-319.
- [3] A. V. Pazderin, V. O. Samoylenko, "Localization of non-technical energy losses based on the energy flow problem solution controllers (Published Conference Proceedings style)," in *Proc. The 6th IASTED Asian Conference on Power and Energy Systems*, AsiaPES, 2013, pp. 100-103.
- [4] S. A. Eroshenko, A. I. Khalyasmaa, S. A. Dmitriev, A. V. Pazderin, A. A. Karpenko, "Distributed generation siting and sizing with implementation feasibility analysis (Published Conference Proceedings style)," in *Proc of 2013 International Conference on Power, Energy and Control*, ICPEC 2013, pp. 717-721.
- [5] Pavlos S. Georgilakis, Peter G. Vernados, "Flexible AC transmission system controllers: an evaluation," *Trans Tech Publications*, Switzerland, vol. 670 2011, pp. 399-406.
- [6] *European Commission, Directorate General for Research, Directorate Energy*, "Strategic research agenda for Europe's electricity networks of the future," European Technology Platform Smart Grid, 2007.
- [7] *Office of the National Coordinator for Smart Grid Interoperability, National Institute of Standard and Technology, U.S. Department of Commerce* "NIST Framework and roadmap for smart grid interoperability standard, release 1.0," NIST Special Publication 1108, Jan. 2010.
- [8] *Electric Power Research Institute*, "Intelligrid," 2010. [Online]. Available: <http://intelligrid.epri.com>.
- [9] *European Commission*, "European Smart Grid technology platform - vision and strategy for European electricity networks of the future," 2010. [Online]. Available: <http://www.smartgrids.eu/web/node/28/default.asp>.
- [10] *National Institute of Standard and Technology*, "NIST and the Smart Grid," 2010. [Online]. Available: <http://www.nist.gov/smartgrid/nistandsmartgrid.cfm>.
- [11] S. E. Kokin, "Polygon scheme with a replacement switch controllers (Published Conference Proceedings style)," in *Proc. Third International Conference "Electric Utility Deregulation and Restructuring and Power Technologies"*, DRPT 2008, Nangin: IEEE, pp. 1538-1541.
- [12] S. A. Dmitriev, S. E. Kokin, A. I. Khalyasmaa, "Evaluation model for urban power supply systems," *Advanced Materials Research*, vol. 468-471, 2012, pp. 1642-1648.
- [13] S. A. Dmitriev, S. E. Kokin, "Working out the policy of technical modernization of big cities' power supply on the basis of network condition assessment model (Published Conference Proceedings style)," in *Proc. 9th International Conference on Environment and Electrical Engineering*, EEEIC, 2010, pp. 235-238.
- [14] S. A. Dmitriev, A. I. Khalyasmaa, S. E. Kokin, "Substation equipment state assessment using indicative analysis (Published Conference Proceedings style)," in *Proc. of the 6th IASTED Asian Conference on Power and Energy Systems*, AsiaPES, 2013, pp. 240-245.
- [15] A. I. Khalyasmaa, S. A. Dmitriev, S. E. Kokin, "Methods of failure analysis of 35-110 kV overhead transmission lines," *Advanced Materials Research*, 2013, vol. 732-733, pp. 677-681.
- [16] A. I. Khalyasmaa, S. A. Dmitriev, S. E. Kokin, "Membership functions for the formation of the electrical equipment state assessment for power stations and substations," *Advanced Materials Research*, 2013, vol. 806-806, pp. 663-666.
- [17] A. I. Khalyasmaa, S. A. Dmitriev, S. A. Eroshenko, "Technical feasibility of distributed generation network connection," *Advanced Materials Research*, 2013, vol. 860-863, pp. 2131-2136.
- [18] Khalyasmaa, A. I., S. A. Dmitriev, S. E. Kokin, "Assessment of power transformers technical state based on technical diagnostics," *Applied Mechanics and Materials*, 2014, vol. 492, pp. 218-222.
- [19] A. I. Khalyasmaa, S. A. Dmitriev, "Power equipment technical state assessment principles," *Applied Mechanics and Materials*, 2014, vol. 492, pp. 531-535.
- [20] D. A. Pavluchenko, V. Z. Manusov, "Electrical network optimization by genetic algorithm," *European Transactions on Electrical Power*, 2006, vol. 16, issue 6, pp. 569-576.
- [21] S. E. Kokin, S. A. Dmitriev, A. I. Khalyasmaa, "Determining Optimal Breakpoints in Urban Power Networks with Genetic Algorithm (Published Conference Proceedings style)," in *Proc. International Conference on Renewable Energies and Power Quality (ICRE PQ'12)*, Santiago de Compostela, Spain, 2012, pp. 262-264.
- [22] D. A. Glushkov, A. I. Khalyasmaa, "Discharge criterion along the surface of solid dielectric SF6 under high pressure," *Applied Mechanics and Materials*, 2014, vol. 548-549, 2014, pp. 21-24.
- [23] V. A. Popov, O. V. Panchenko, "The enterprise structuring with using of the assignment problem models on the bipartite graphs," *Radioelectronic and Computer Systems*, vol. 1(53), 2012, pp. 176-184.

Assessment of water quality of artificial water bodies in Vojvodina (Serbia) using factor and cluster analysis

Srdan R. Kolaković¹, Svetlana R. Vujović², Slobodan S. Kolaković³, Borislav T. Mašić⁴, Goran B. Jeftenić⁵, Ljubomir M. Budinski⁶

Abstract—Multivariate statistical techniques, such as factor analysis (FA)/principal component analysis (PCA) and cluster analysis (CA), were applied to the evaluation of variations and the interpretation of water quality data of artificial water bodies in Vojvodina (Serbia). Factor analysis is applied to physicochemical parameters of artificial water bodies with the aim classification and data summation as well as segmentation of heterogeneous data sets into smaller homogeneous subsets. CA showed similarities and dissimilarities among the sampling sites and explained the observed clustering in terms of affected conditions.

Keywords—Artificial water bodies, Cluster analysis, Factor analysis, water quality,

I. INTRODUCTION

River water pollution is mainly the result of anthropogenic activities that occur within the river basin. In order for a river to be properly managed, these activities need to be identified and functionally related to the water pollution parameters [1]. It is well known that environmental data are usually characterized by high variability, because of a variety of natural and anthropogenic influences. The best approach to avoid misinterpretation of environmental monitoring data is the application of multivariate statistical (chemometric) methods for environmental data classification and modeling [2].

This paper illustrates the utility of Factor analysis/Principal component analyses (FA/PCA) and Cluster analysis (CA) techniques for analysis and interpretation of water quality data sets and identification of pollution sources/factors with a view

to get better information about the water quality and design of monitoring network for effective management of water resources. The analysis of water quality is based on the data of the Republic Hydrometeorological Service of the Republic of Serbia published in the Hydrology Almanac – Water quality for the period 2008- 2011.

II. STUDY AREA

The Autonomous Province of Vojvodina covers an area of 21 506 km², it is located in the Pannonian Plain, where the natural landscape consists mainly of low-lying flat land, except for Srem which is dominated by the Fruška Gora Mountain (the highest peak 539 m) and the southern-east part of the province dominated by the Vrsacka Mountains (the highest peak 641 m). Vojvodina is intersected by three navigable rivers: Danube, Sava and Tisa, dividing its territory into three geographic-historic areas: Backa, Banat and Srem. With a population of about 2 million, Vojvodina accounts for 27% of the total population in Serbia. The capital of the province is Novi Sad located on the left bank of the Danube river (rkm 1255) with over 300 000 inhabitants. Canals of the Danube-Tisa-Danube Hydrosystem run through almost all settlements in the Province, or in close proximity. The navigable canal network in Vojvodina forms an integral part of unique hydro-engineering system Danube-Tisa-Danube covering Backa and Banat District and connecting the Danube and Tisa rivers. The entire length of main canals of the Hydrosystem DTD (DTD Hs), together with the parts of nature water course, that while having regulative works have lost the character of natural rivers, is 930 km., where 421 km are in Backa, and 509 km. are in Banat. Regarding its height, the DTD Hs is divided into pools. A pool is made of one or greater number of canals limited by gates, ship-locks and pumping stations, and there is, concerning water flow and water level (in compliance with technical capacities and adequate rule books), controlled water regime. The Bajski Canal is meander of the Danube river that extends from Baja in Hungary to Bezdan in Serbia, with total length of 44,8 km. It rises at the Sugavica Canal near Hungarian town Baja, and flows into Vrbas-Bezdan Canal at the kilometer 77+460 [3]. The Jegricka had been a natural stream in the central part of the Vojvodina Province which was made part of the canal network of the multi-purpose Danube-

¹ PhD Srdjan R. Kolakovic, grad.civ.eng, Faculty of Technical Sciences, University of Novi Sad, Serbia, (e-mail: kolak@uns.ac.rs).

² MsC Svetlana R. Vujovic, grad.civ.eng, Faculty of Technical Sciences, University of Novi Sad, Serbia, (e-mail: vujovics@uns.ac.rs).

³ MsC Slobodan S. Kolakovic, grad.civ.eng, Faculty of Technical Sciences, University of Novi Sad, Serbia, (e-mail: cole86grb@gmail.com)

⁴ MsC Borislav T.Masic, grad.civ.eng, Faculty of Technical Sciences, University of Novi Sad, Serbia, (e-mail: boramasic@gmail.com).

⁵ MsC Goran B. Jeftenic, grad.civ.eng, Faculty of Technical Sciences, University of Novi Sad, Serbia, (e-mail: goran.jeftenic@yahoo.com).

⁶ PhD Ljubomir M. Budinski, grad.civ.eng, Faculty of Technical Sciences, University of Novi Sad, Serbia, (e-mail: ljubabu@gmail.com).

Tisza-Danube Hydro System. The Jegrička runs for a greater part through agricultural land, flowing through or near several urban areas. Due to such geography, the stream is exposed to a number of point and non-point pollution sources which directly affect the quality of water and sediments on river bottom [4]. The Navigable Begej or Begej Canal springs in the Craiova Mountains (Pojana Ruske) under the peak of Mt Padešin the neighbouring Romania, at the absolute altitude of 1,135 mANV. The length of the stream, including the unified section of the stream from Klek to the mouth, is 233 km [5].

The analysis of water quality is based on the data of the Republic Hydrometeorological Service of the Republic of Serbia. Data sets consists of annually average values of water quality variables measured during period 2008-2011. [6] in a quality monitoring network (Figure 1):

- **Canal DTD:** Sombor (1), Mali Stapar (2), Vrbas 1 (3), Vrbas 2 (4), Srpski Miletić (5), Savino Selo (6), Bačko Gradište (7), Novi Sad (8), Bač (9), Bački Petrovac (10), Melenci (11), Vljakovac (12), Kajtasovo (13);
- **Jegrička:** Žabalj (14);
- **Kikindski Kanal:** Novo Miloševo (15);
- **Canal Nadel:** Uzdin (16), Starčevo (17);
- **Bajski Canal:** Bački Breg (18);
- **Navigable Begej:** Srpski Itebej (19), Klek (20), Stajićevo (21).



Fig. 1 Study area – monitoring stations

III. FACTOR AND CLUSTER ANALYSIS

Factor analysis, a multivariate statistical method, yields the general relationship between measured chemical variables by showing multivariate patterns that may be help to classify the

original data [7]. Factor analysis integrates a large number of variables into several significant factors that explain the correlations among the observed variables [8]. FA can be expressed as [9]:

$$F_i = a_1x_{1j} + a_2x_{2j} + \dots + a_mx_m$$

Where : Fi = factor

a = loading

x = measured value of variable

i = factor number

j = sample number

m = total number of variables

There are three stages in factor analysis [10] – [11].

- For all the variables a correlation matrix is generated
- Factors are extracted from the correlation matrix based on the correlation coefficients of the variables
- To maximize the relationship between some of the factors and variables, the factors are rotated.

Cluster analysis is an exploratory data analysis tool for solving classification problems [12]. A good outcome of cluster analysis will result in a number of clusters where the observations within a cluster are as similar as possible while the differences between the clusters are as large as possible [13]. The Euclidean distance usually gives the similarity between two samples and a ‘distance’ can be represented by the ‘difference’ between analytical values from both the samples. Hierarchical agglomerative CA was performed on the normalized data set by means of the Ward’s method, using Euclidean distances as a measure of similarity [14]. The similarities–dissimilarities were quantified through Euclidean distance measurements; the distance between two objects (monitoring point locations), i and j, is given as:

$$d_{i,j}^2 = \sum_{k=1}^m (z_{i,k} - z_{j,k})^2 \quad (1)$$

Where d_{ij} denotes the Euclidean distance, $z_{i,k}$ and $z_{j,k}$ are the values of variable k for object i and j, respectively, and m is the number of variables. Hierarchical agglomerative cluster analysis (HACA) was used to investigate the grouping of sampling points. HACA is a common method to classify variables or cases (observations/samples) into classes (clusters) with high homogeneity level within the class and high heterogeneity level between classes with respect to a predetermined selection criterion. HACA starts with each point in separate clusters and iteratively agglomerates the closest pair of clusters in each iteration until all points belong to a single cluster. The final hierarchical cluster structure is called a dendrogram, a tree like structure that shows which clusters are agglomerated at each level. The dendrogram provides a visual summary of the clustering processes, presenting a picture of the groups and their proximity, with a dramatic reduction in dimensionality of the original data [1]-[12]-[15]-[16]-[17].

IV. RESULTS AND DISCUSSION

The selected parameters for the estimation of surface water quality characteristics were: Temperature (T), suspended solids (SS), dissolved oxygen (DO), total hardness (TH), pH, electrical conductivity (EC), ammonium nitrogen ($\text{NH}_4\text{-N}$), nitrate nitrogen ($\text{NO}_3\text{-N}$), total phosphorous (TP), (Ca^{2+}), magnesium (Mg^{2+}), biochemical oxygen demand (BOD_5), surface-active substances (SAS). Water quality data (mean value) are presented at Table 1.

Calculated eigenvalues, percent total variance, factor loadings and cumulative variance are given in Table 2. The factor analysis generated four significant factors which explained 82.61 % of the variance in the data set.

First factor F1 explained 33.21 % of the total variance and had strong positive loadings on $\text{NH}_4\text{-N}$, BOD_5 and SAS, moderate positive loading on TP, strong negative loading on dissolved oxygen and moderate negative loading on pH. First factor represents influence of point sources pollution on water quality.

Second factor F2 explained 33 % of the total variance and had strong positive loadings on TH, EC, Ca^{2+} i Mg^{2+} , moderate positive loadings on pH and TP. Second factor represents hydro chemical component of water quality.

Third factor F3 explained 16.42 % of the total variance and had strong positive loadings on SS and $\text{NO}_3\text{-N}$, moderate negative loading on pH. Third factor represents explained influence of coastal erosion and surface runoff.

The correlation matrix of variables was generated and factors extracted by the Centroid method, rotated by Varimax rotation. Only factors with eigenvalue greater than one were

selected for this analysis. Factor loadings can be classified as “strong,” “moderate,” and “weak,” corresponding to absolute loading values of >0.75 , $0.75\text{--}0.50$, and $0.50\text{--}0.30$, respectively [18]-[19].

Table 2. Rotated factor loadings, communalities, eigenvalues and percentage of variance for water quality parameters

Variable	F1	F2	F3
T	-0.066296	0.401567	-0.609853
SS	0.391267	0.158375	0.796834
DO	-0.862549	-0.078248	-0.327730
TH	0.065859	0.976044	-0.023214
pH	-0.620678	0.518190	-0.330159
EC	0.160222	0.907066	0.185464
$\text{NH}_4\text{-N}$	0.939458	0.195539	-0.067892
$\text{NO}_3\text{-N}$	-0.316381	0.032106	0.760485
TP	0.702878	0.512011	0.460249
Ca^{2+}	-0.065029	0.820731	-0.224438
Mg^{2+}	0.126879	0.944945	0.068610
BOD_5	0.861765	0.293105	-0.165042
SAS	0.872871	-0.310080	0.018783
Eigenvalue	4.318312	4.286415	2.135658
Total variance (%)	33.217786	32.972420	16.428138
Cumulative (%)	33.217786	66.190206	82.618344

Table 1. Water quality data of artificial water bodies in Vojvodina (mean value)

	T (°C)	SM (mg/l)	Ras. O ₂ (mgO ₂ /l)	UT (mg/l)	pH	EP (µS/cm)	$\text{NH}_4\text{-N}$ (mg/l)	$\text{NO}_3\text{-N}$ (mg/l)	TP (mg/l)	Ca^{2+} (mg/l)	Mg^{2+} (mg/l)	BPK ₅ (mg/l)	PAM (mg/l)
Sombor	15.90	12.19	8.80	281.62	8.07	605.42	0.04	0.66	0.07	66.50	28.18	3.13	0.02
Mali Stapar	15.94	12.12	10.22	278.93	8.16	653.37	0.04	0.68	0.06	62.26	30.15	3.09	0.01
Vrbas 1	17.02	12.23	10.58	269.60	8.32	708.06	0.03	0.44	0.06	53.75	33.04	3.05	0.04
Vrbas 2	16.44	34.01	2.73	316.36	7.76	911.88	7.58	0.37	1.18	63.89	38.42	31.07	0.15
Srpski Miletic	15.53	20.16	10.31	217.79	8.11	527.29	0.06	1.18	0.15	56.36	18.95	3.62	0.02
Savino Selo	16.13	17.86	10.10	224.97	8.06	556.89	0.08	1.00	0.14	56.27	20.67	3.78	0.02
Bačko Gradište	14.86	31.46	10.96	247.25	8.34	657.35	0.40	0.75	0.26	53.25	27.78	7.78	0.04
Novi Sad	15.64	15.18	9.51	235.22	8.08	577.29	0.12	0.53	0.12	52.53	25.38	3.82	0.03
Bač	16.32	16.74	8.40	225.80	7.84	547.74	0.17	0.52	0.14	53.67	22.44	4.24	0.03
Bački Petrovac	16.21	15.13	8.90	248.38	7.97	596.41	0.09	0.40	0.13	55.68	26.63	3.98	0.03
Melenci	15.44	22.93	7.78	210.62	7.89	663.74	0.17	0.99	0.19	53.63	18.70	2.20	0.02
Vlajkovac	15.41	36.09	8.25	166.39	7.88	480.77	0.21	1.08	0.21	39.10	15.88	2.15	0.04
Kajtasovo	15.64	32.34	9.93	171.32	8.03	467.58	0.14	0.99	0.17	45.22	13.40	3.12	0.02
Žabalj	15.03	28.27	9.50	248.89	8.26	875.40	0.36	0.25	0.19	49.41	30.66	4.59	0.03
Novo Miloševo	15.65	27.22	7.06	231.48	7.82	782.67	0.47	0.95	0.34	56.85	21.74	3.43	0.04
Uzdin	15.96	15.94	11.18	187.06	8.25	667.94	0.04	0.44	0.07	41.71	20.19	2.54	0.02
Starčevo	15.18	42.06	5.88	434.51	8.06	1271.03	0.94	1.13	1.32	66.30	65.49	5.06	0.03
Bački Breg	14.81	11.59	9.00	267.34	8.07	570.14	0.06	0.41	0.07	64.62	25.67	3.23	0.02
Srpski Itebej	14.06	24.69	5.74	113.63	7.39	308.18	1.96	0.45	0.45	30.33	9.22	5.87	0.20
Klek	14.22	28.30	7.73	174.57	7.76	517.32	0.52	0.93	0.27	45.15	15.08	2.79	0.04
Stajicevo	15.14	27.14	5.73	168.80	7.60	515.12	0.79	0.84	0.41	44.74	13.93	5.27	0.05

From the results of factor analysis, it appears that such type of analysis has identified the sources of water quality variations in the study area. This shows the importance of such technique for water quality management agencies [20]. Cluster analysis was performed to detect similarity group between the monitoring stations.

On basis of cluster analysis in relation to the first factor, as shown in Figure 2., monitoring stations are divided as follows:

- Cluster I: monitoring station (4)
- Cluster II: monitoring stations (7,19,21,17)
- Cluster III: all others monitoring stations

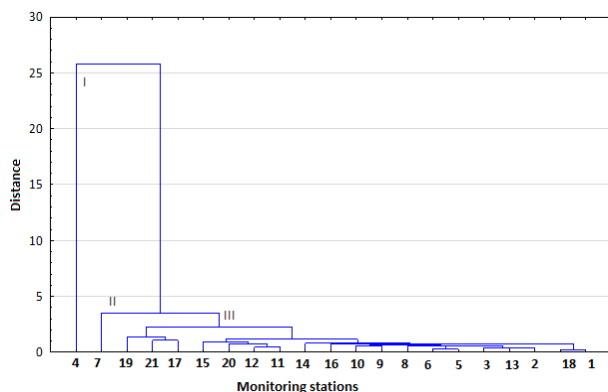


Fig. 2 Cluster analysis dendrogram of monitoring stations in relation to the first factor F1

On basis of cluster analysis in relation to the second factor, as shown in Figure 3., monitoring stations are divided as follows:

- Cluster I: monitoring station 17
- Cluster II: all others monitoring stations

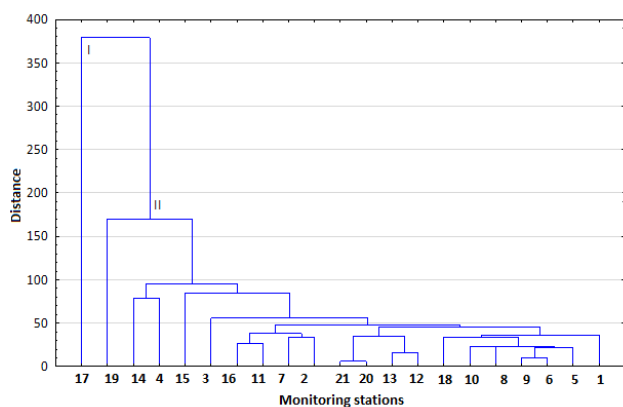


Fig. 3 Cluster analysis dendrogram of monitoring stations in relation to the second factor F2

On basis of cluster analysis in relation to the third factor, as shown in Figure 4., monitoring stations are divided as follows:

- Cluster I: monitoring station 17
- Cluster II: all others monitoring stations

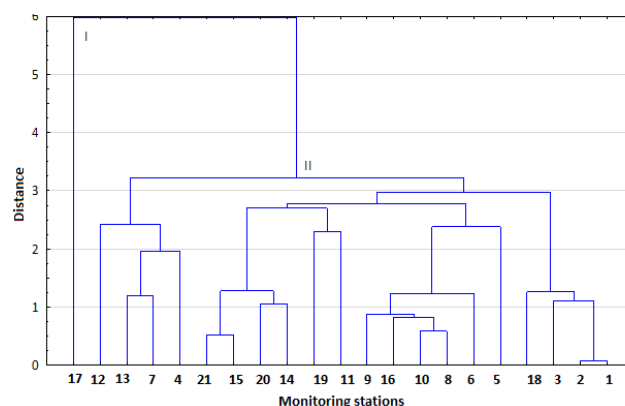


Fig. 4 Cluster analysis dendrogram of monitoring stations in relation to the third factor F3

CA could be useful tool in designing optimal sampling strategy, which could reduce the number of monitoring stations. The number of the monitoring sites could be optimized in such a way that for rapid quality assessment studies only representative sites from each cluster (not all monitoring sites) can be used. This reduces the number of analysis and the cost of the risk assessment procedure [21].

V. CONCLUSION

The application of FA and CA on the available data indicated that the water quality variations are mainly due anthropogenic (point and non point sources of pollution) and natural processes (erosion and runoff). From the results of factor analysis, it appears that such type of analysis has identified the sources of water quality variations in the study area. CA could be useful tool in designing optimal sampling strategy that could reduces the number of analysis and the cost of the risk assessment procedure.

ACKNOWLEDGMENT

This work has been produced with financial assistance of Ministry of Education, Science and Technological Development (TR 37018; TR 37003).

REFERENCES

- [1] H. Juahir, S. M. Zain, A. Z. Aris, M. K. Yusoff, M. B. Mokhtar, "Spatial assessment of Langat river water quality using chemometrics", *J. Environ. Monit.*, 2010, 12, 287–295.
- [2] V. Simeonov, J. W. Einax, I. Stanimirova and J. Kraft, "Environmetric modeling and interpretation of river water monitoring data", *Anal Bioanal Chem* (2002) 374, pp. 898–905, DOI 10.1007/s00216-002-1559-5.

- [3] B. Miljanović, S. Pogrmic, Š. Šipoš, N. Pankov, I. Mijić, Bajčetić R. Ecological-touristic potential of Bajski Canal, Conference Book, 22nd World Canals Conference, Novi Sad, Art print, Novi Sad, p. 80, 2009.
- [4] R. Savić, L. Maksimović, S. Cimpeanu, D. Bucur, G. Ondrašek, J. Vasin, M. Harja and S.o Milić, "Hazardous and harmful substances in sediments of the Jegricka stream", *Journal of Food, Agriculture & Environment*, Vol.11 (1), January 2013, 1152- 1156.
- [5] TICAD Tisa Catchment Area Development, NATIONAL STUDY Serbia 1st Draft, October 2010, Novi Sad
- [6] Hydrology Almanac – Water quality for the period 2008-2011. Republic Hidrometeorological Service of Serbia, Belgrade. 6
- [7] C.W. Liu, Kao-Hung Lin, Y.M. Kuo, „Application of factor analysis in the assessment of groundwater quality in a blackfoot disease area in Taiwan”, *The Science of the Total Environment* 313(2003)77–89.
- [8] H. B. Chu, W. X. Lu1, and L. Zhang, "Application of Artificial Neural Network in Environmental Water Quality Assessment", *J. Agr. Sci. Tech. (2013) Vol. 15: 343-356*.
- [9] A. Mahmood, W. Muqbool, M.W. Mumtaz and F. Ahmad, "Application of Multivariate Statistical Techniques for the Characterization of GroundWater Quality of Lahore", *Gujranwala and Sialkot (Pakistan), Pak. J. Anal. Environ. Chem. Vol. 12, No. 1 & 2 (2011) 102-112*.
- [10] H. Boyacioglu and H. Boyacioglu, "Surface Water Quality Assessment by Environmetric Methods", *Environ Monit Assess (2007) 131*, pp 71–376 DOI 10.1007/s10661-006-9482-4 M. J.
- [11] B. Alam, A. A. M. Ahmed and E. Ali1, "Evaluation of Surface Water Quality of Surma River Using Factor Analysis", *Proc. Of International Conference on Environmental Aspects of Bangladesh (ICEAB10), Japan*, pp. 186-188, Sept. 2010.
- [12] E. A. M. Salah, A.M. Turki, E.M. Al-Othman, "Assessment of Water Quality of Euphrates River Using Cluster Analysis", *Journal of Environmental Protection*, 2012, 3, 1629-1633.
- [13] M. Templ, P. Filzmoser and C. Reimann, "Cluster analysis applied to regional geochemical data, problems and possibilities", *Applied Geochemistry*, 23 (8) (2008), pp. 2198–2213.
- [14] K. P. Singh, A. Malik, D. Mohan and S. Sinha, "Multivariate statistical techniques for the evaluation of spatial and temporal variations in water quality of Gomti River (India)—a case study", *Water Research* 38 (2004) 3980–3992.
- [15] T. Kowalkowski, R. Zbytniewski, J. Szpejna and B. Buszewski, "Application of chemometrics in river water classification", *Water Research* 40 (2006) 744-752.
- [16] A. Mustapha and A.Z. Aris, "Spatial Aspect of Surface Water Quality Using Chemometric Analysis, *Journal of Applied Sciences in Environmental Sanitation*", 2011, 6 (4):411-426.
- [17] S. Adaekalavan, C. Chandrasekar, "Towards new estimating incremental dimensional algorithm (EIDA)", *Journal of Theoretical and Applied Information Technology*, ISSN: 1992-8645, 2013. Vol. 51 No.2, pp. 222-227.
- [18] C. W Liu, K. H. Lin and Y. M Kuo, "Application of factor analysis in the assessment of groundwater quality in a blackfoot disease area in Taiwan", *The Science of the Total Environment*, 313, 2003, pp. 77–89., doi: 10.1016/S0048-9697(02)00683-6.
- [19] S. M. Ahmed, M. Hussain and W. Abderrahman, "Using multivariate factor analysis to assess surface/logged water quality and source of contamination at a large irrigation project at Al-Fadhli, Easter Province. Saudi Arabia", *Bull Eng Geol Env*, 64, pp. 315-232, 2005.
- [20] S. M. Al-Rawi and A. S. Shihab, "Application of Factor Analysis as a Tool for Water Quality Management of Tigris River within Mosul City", *Raf. Jour. Sci.*, Vol. 16, No. 1 Geology, Special Issue, pp.56-64, 2005.
- [21] V. Simeonova, J.A. Stratib, C. Samarac, G. Zachariadisb, D. Voutsac, A. Anthemidis, M. Sofonioub, and T. Kouimtzi, "Assessment of the surface water quality in Northern Greece", *Water Research* 37, pp. 4119–4124, 2003.

Analysis of multiannual fluctuations and long term trends of hydrological time series

O. Marusiak, J. Pekar

Abstract—The aim of the paper is an identification of the long- and short-term variability and trends in the discharge time series of the selected Slovak rivers, as well as in the precipitation series. A better understanding of the flow fluctuations is important for flood control and water availability planning, river transport, etc. The following monthly discharge time series were used: the Danube River (133 years, i.e., 1596 measurements), the Hron and Ipe rivers (78 years, 936 measurements), and the Vah River (88 years, 1056 measurements). The monthly discharge time series were decomposed into IMF components by the modified EMD (Empirical Mode Decomposition) method CEEMDAN (Complete and Ensemble Empirical Mode Decomposition with Adaptive Noise). This method, for example, eliminates the mode mixing problem of dramatically different periods into a single component which may occur in the EMD method. It was shown that correlations between the IMF components of these series indicate that part of the variance can probably be explained by the same climatic phenomena.

Keywords— Complete and Ensemble Empirical Mode Decomposition, discharge time series, long-term hydrological variability, white noise, residuals.

I. INTRODUCTION

HYDROLOGICAL and climatic time series fluctuate according to various multi-day to year and longer periods. These periods result from various non-linear interactions of temperature, precipitation, year seasons, solar activity, lunar movements, or global climate phenomena such as SO - Southern Oscillation, NAO - North Atlantic Oscillation, or AO - Arctic Oscillation [1]. Increasing attention is given to the examination of these phenomena in the world, with prolonging data more accessible. Various methods are used to examine the phenomena. Most of them assume that the data are both, stationary and linear. When observing natural phenomena, non-stationarity or non-linearity of data often occurs. In the paper we used the method CEEMDAN, which is also suitable for the investigation of nonlinear and non-stationary data that we provide in this work. CEEMDAN method was proposed by Torres [2], method based on Empirical Mode Decomposition EMD was proposed by Huang [3]. EMD was designed to investigate the nonlinear and non-stationary data and applied in the paper of Huang [3],

This work was supported by the Science and Technology Assistance Agency (Slovakia) under contract no. APVV-0015-10.

O. Marusiak is with the Faculty of Mathematics, Physics and Informatics, Comenius University, Bratislava, Slovakia.

J. Pekar is with the Faculty of Mathematics, Physics and Informatics, Comenius University, Bratislava, Slovakia (e-mail: pekar@fmph.uniba.sk).

for example, to the water level of the oceans in the equatorial region. This method was since successfully applied to various climatic phenomena. For example, Salisbury and Wimbush [4] addressed the prediction of ENSO SOI index, Franzke and Woollings [5] focused on the predictability of North Atlantic climate and Huang et al [6] analyzed the flow of two selected rivers in France [7].

II. DATA

In this study, we analyzed the average monthly discharge time series of:

- the Danube River from Bratislava water gauge (1876–2008, 1596 measurements), [8]–[10];
- the Hron River from the station Brehy (1931–2008, 936 measurements);
- the Vah River, Liptovsky Mikulas water gauge (1921–2008, 1056 measurements);
- the Ipe River from Holisa measuring station (1931–2008, 936 measurements), Fig. 1 and total monthly precipitation series, average on Slovak territory, (1881–2010).

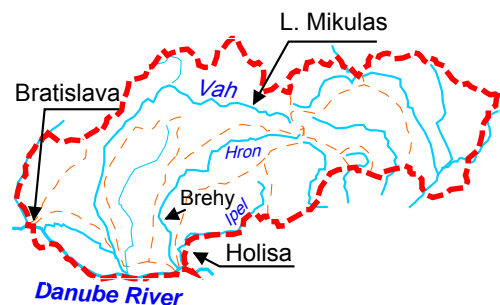


Fig. 1 Location of the selected rivers in Slovakia

Danube is the second largest (after the Volga River), and longest river of Europe. It is the largest river in European Union. It begins in the Black Forest in Germany and flows through the Central Europe into the Black Sea. In average, the long-term annual discharge of Danube in its mouth is $6500 \text{ m}^3 \text{ s}^{-1}$, at Budapest $2350 \text{ m}^3 \text{ s}^{-1}$, at Bratislava $2025 \text{ m}^3 \text{ s}^{-1}$, and at Vienna $1900 \text{ m}^3 \text{ s}^{-1}$.

Hron River flows from Horehronské podolie, between the Low Tatras mountains and Spissky karst. Hron River has a mountainous character. The area of the Hron River basin takes 11 % of Slovakian land. The average annual long-term discharge of Hron River is $47 \text{ m}^3 \text{ s}^{-1}$ at Brehy gauge [1].

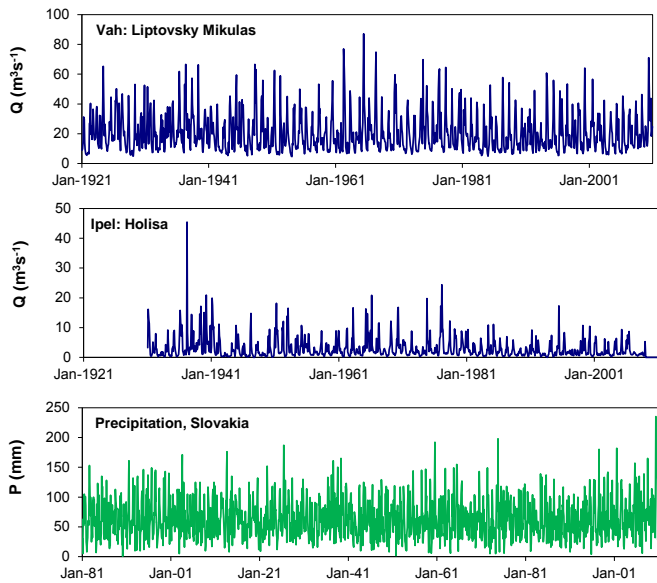


Fig. 2d. Examples of the mean monthly discharge time series of the Vah and Ipel rivers, period 1921–2008. Average monthly precipitation on territory of Slovakia, period 1881–2011.

The Vah River is the longest river in Slovakia, it is created by Biely and Cierny Vahs confluence. Biely Vah flows from the hillside of Krivan in High Tatras, Cierny Vah originates under Kralova hill in Low Tatras. The long-term average annual flow of Vah River is $20.4 \text{ m}^3\text{s}^{-1}$ at Liptovský Mikulas gauge (Fig. 2a).

The Ipel River is 232.5 km long, it flows from Veporskevrchy. The long-term average annual flow of the Ipel River is $3.03 \text{ m}^3\text{s}^{-1}$ in Holisa (Fig. 2b).

Long-term average annual precipitation on territory of Slovakia during the period 1881–2011 is 760 mm (Fig. 2c).

III. METHODS

A. The Empirical Mode Decomposition EMD

The empirical mode decomposition (EMD) is a relatively new method introduced by Huang [3], which decomposes a time series of flow rates to the sum of the various components - Intrinsic Mode Function (IMF) with varying amplitude and phase. IMF components must meet the following conditions:

1. After successive extremes, the IMF must pass through the zero point only once, i.e. number of extremes and the number of zero crossing points in a range must be equal or at most differ by one (this number may differ from that in the original time series);

2. At any point, the mean value of the upper envelope, defined from local maxima and the lower envelope, defined from the local minima is equal to zero.

Under this definition of IMF every time series – therefore also those of the discharges – can be decomposed by the following procedure:

1. We identify all local maxima (minima) of flows, which we combine with cubic spline as an upper envelope $e_{max}(t)$ (lower envelope $e_{min}(t)$).
2. We calculate an average between the envelopes as $m_1(t) = \frac{e_{max}(t) + e_{min}(t)}{2}$
3. The first component is estimated as $h_1(t) = x(t) - m_1(t)$

Ideally a h_1 series satisfies the conditions of the IMF. If it does not comply, we take the $h_1(t)$ as a new series and repeat the procedure again. We get $h_{11}(t) = h_1(t) - m_{11}(t)$, where $m_{11}(t)$ is the average of the envelopes for a h_1 series. This procedure we iteratively repeat k -times, until the h_{1k} series does not meet IMF conditions, i.e. until $h_{1k}(t) = h_{1(k-1)}(t) - m_{1k}(t)$. Then $c_1(t) = h_{1k}(t)$ is called the first IMF component from the original time series flow.

In fact, the problem is how to determine after how many iterations of the series $h_{1k}(t)$ we get IMF. To determine which range $h_{1k}(t)$ can be considered as the IMF, stopping criterion were introduced. More information can be found in the paper written by Huang [3]. The first IMF component should contain the shortest period of the original time series. Then we compute a number of residues r_1 as $r_1(t) = x(t) - c_1(t)$. As the time series r_1 still contains longer periods of the original time series, we repeat the above mentioned procedure on the series r_1 until the series $r_l(t)$ is a monotonic function, or will contain one local extremum at the most. Thus it will be no longer possible to extract further IMF component from the $r_l(t)$. At the end we should get $l-1$ IMF components and one series of residuals $r_l(t)$. If the original time series of the flows contains trend, the series $r_l(t)$ should be this trend. We can get the original time series as

$$x(t) = \sum_{i=1}^{l-1} c_i(t) + r_l(t) \quad (1)$$

Such problems like mixing extremely different periods into one IMF component, may occur during the EMD decomposition. This component then ceases to give physical sense. For more information see [7],[2], [12].

B. CEEMDAN method

To eliminate the problems mentioned above, Torres [2] proposed the new method CEEMDAN (Complete Ensemble Empirical Mode Decomposition with Adaptive Noise). In this method we add different realizations of white noise to the original time series in order to get a set of series $x_i(t) = x(t) + w_i(t)$, where $w_i(t)$ are different realizations of the white noise. White noise is a random process with a constant power spectral density (PSD). Each series of $x_i(t)$ is decomposed using the method EMD independently of other realizations of series $x_i(t)$. Obtained from the first series of components $x_i(t)$ we calculate the first component series $x(t)$ as $\tilde{c}^1(t) = \frac{1}{I} \sum_{i=1}^I c_i^1(t)$. The first series of residuals are calculated following $r^1(t) = x(t) - \tilde{c}^1(t)$. In the next step, we calculate $\tilde{c}^2(t)$ as the average of the individual series of the implementation of the series $r^1(t)$ together with the first component of the white noise EMD decomposition $w_i(t)$.

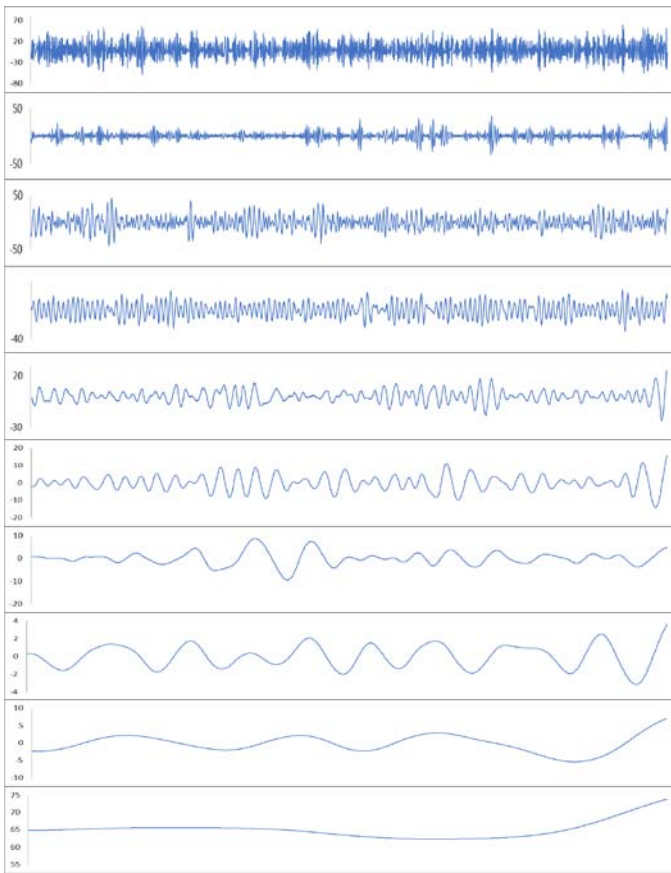


Fig. 3. IMF components for the Slovak precipitation series, IMF1 to IMF10 (from top to bottom), and the last component are residuals.

Thus, we proceed with other components until we reach the stopping criteria[2],[11].

For all the data we have chosen 500 realizations and a standard deviation of white noise as 0.3, based on the work of [2],[7]. Calculations are carried out using EMD toolbox for Matlab software available on <http://perso.ens-lyon.fr/patrick.flandrin/emd.html> and <http://rcada.ncu.edu.tw>.

IV. SOME COMMON MISTAKES

After the CEEMDAN method decomposition for the flow of the Danube River we identified an upward trend (as well as in the case of precipitation series during the last 10-years, see Fig. 3). For the flow of the Vah, Hron and Ipel rivers we discovered a decreasing trend over the observed time period.

This trend can be viewed in Figs. 4a-4d, where the full line represents residuals from CEEMDAN decomposition, the dashed line represents longer-term calculated from inter-annual IMF components plus residuals and the dotted line represents longer-term trend of moving average with 48 months period.

The average period of individual components was calculated as average distance between two local maximums in pertaining with IMF component according to Franzke [8]. The results are in Table I. The periods to the fourth IMF component are shorter than a year. We observe about a year

long period for fourth IMF component for all four time series.

After the decomposition of given time series by CEEMDAN method, we can observe a higher rate of correlation in comparison to the original time series.

Correlations between the original time series and each IMF component are in Table II. We observe higher relation with one year long and longer periods. From the results of correlation and the length of periods among these components we can anticipate that the flow time series are influenced more by various short term climate occurrences and from the year period similar climate influences have more affect. The most correlated IMF component among the flow of rivers was the sixth one, which corresponds to 44–46.8 month long period, which represents approximately 3.66–3.9 year long period. The significance of individual IMF components was observed by Huang [3]. Here we tested with a 99 % probability whether the given component differs from white noise. Insignificant IMF components are highlighted in italic in Table I and III for every river.

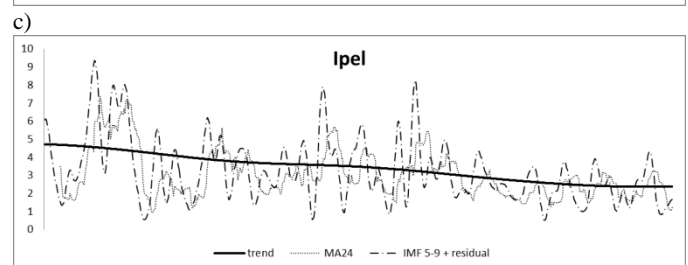
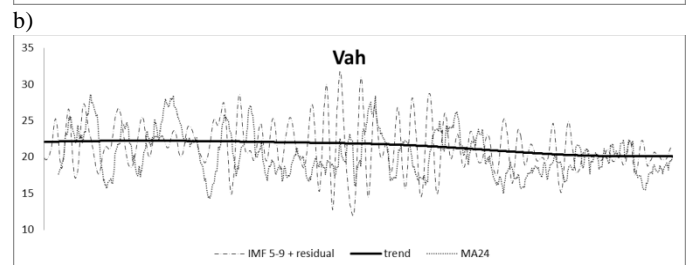
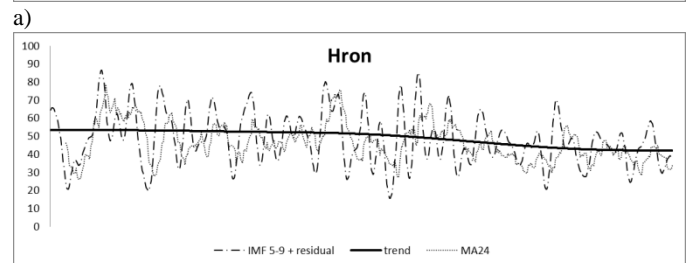
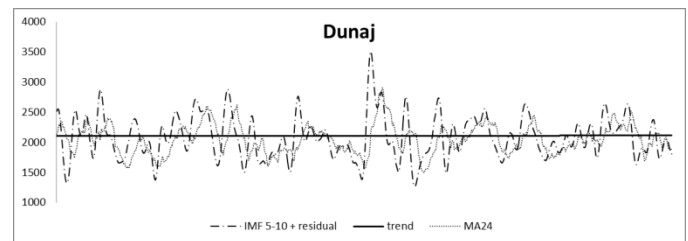


Fig. 4a)-d) Long-term flows of the a) Danube (Dunaj); b) Hron; c) Vah and d) Ipel Rivers. Full bold line is trend, dashed line is calculated from inter-annual IMF components and dotted line is moving average with period of 48 months

Table I. Monthly average periods, non-significant components are highlighted in italic.

	IMF1	IMF2	IMF3	IMF4	IMF5	IMF6	IMF7	IMF8	IMF9	IMF10
Dunaj	2.91	4.74	7.67	12.09	22.80	45.60	88.67	199.50	<i>266.00</i>	<i>532.00</i>
Hron	3.26	4.98	6.93	12.16	22.83	46.80	93.60	<i>156.00</i>	<i>312.00</i>	
Váh	3.28	5.18	6.44	12	23.47	<i>44</i>	<i>81.23</i>	<i>176</i>	<i>352</i>	
Ipel	3.19	4.83	<i>6.92</i>	12	23.31	45.33	102	<i>163.2</i>	408	

Table II. The correlation between individual IMF components

	original data	IMF1	IMF2	IMF3	IMF4	IMF5	IMF6	IMF7	IMF8	IMF9
Dunaj - Hron	0.44	0.28	0.07	0.43	0.47	0.41	0.71	0.32	0.45	-0.55
Hron - Ipel	0.31	0.10	0.02	0.11	0.16	0.14	0.37	0.06	-0.03	-0.03
Dunaj - Ipel	0.04	0.09	0.01	0.09	0.20	0.21	0.29	0.35	0.03	0.09
Vah - Hron	0.63	0.54	0.45	0.60	0.62	0.73	0.67	0.69	0.72	0.90
Vah - Ipel	0.11	0.13	-0.02	0.17	0.28	0.14	0.21	0.05	0.04	-0.01
Vah - Dunaj	0.62	0.29	0.25	0.64	0.85	0.46	0.71	0.38	0.35	-0.45

Table III. Variance of the decomposition components of the original time series of flows, non-significant components are highlighted in italic

	IMF1	IMF2	IMF3	IMF4	IMF5	IMF6	IMF7	IMF8	IMF9	IMF10
Dunaj	28.61%	2.52%	27.23%	18.71%	8.89%	6.81%	4.02%	2.56%	<i>0.39%</i>	<i>0.26%</i>
Hron	40.45%	4.74%	20.30%	15.97%	8.10%	6.44%	2.32%	<i>1.14%</i>	<i>0.54%</i>	
Váh	34.89%	3.10%	22.34%	24.67%	8.86%	<i>2.53%</i>	<i>1.81%</i>	<i>0.73%</i>	<i>1.08%</i>	
Ipel	41.86%	11.3%	<i>14.33%</i>	11.55%	6.53%	6.09%	5.78%	<i>1.03%</i>	1.53%	

For every IMF component we calculated the variation for the given time series and compared to overall variation cleaned from trend (residuals). These results are given in table III. The sixth component, the most correlated, explains approximately 6-7 % of variation of the Danube, Hron and Ipel rivers, 2.5 % for the Vah River. However, this component for the Vah River was not significant.

V. CONCLUSION

In the paper we applied the CEEMDAN method to decomposed discharge time series of four Slovak rivers: Vah, Hron, Ipel, and Danube Rivers. From the results of the decomposition we can assume the same climatic impact on discharge time series of these rivers for annual and multi-annual periods. This impact is based on the degree of correlation and the length of the period between these components. Inter-annual and multi-annual influences explain in the case of the Danube River about 41 % of variance flow. For the Hron River it is 32 %, for the Vah River 33.5 %, and for the Ipel River 31.7%. Thus, for the long range forecast we can potentially predict 32% to 41% variance of the monthly discharge of selected rivers via annual and inter-annual influence. For every discharge time series of the considered rivers it was shown that most of the variance comes from intra-annual influence, for flow of the Danube river 58% from the total variation, 66 % for Hron, 60 % for Vah and 53 % for Ipel River.

For the discharge of the Danube River and precipitation totals we identified an upward trend. It is in the agreement

with [13]. For the flow of the rivers Hron, Vah and Ipel we identified downward trend over a given period time. For further research in this area it would be useful to concentrate on daily data and eventually on other hydrological and climatic time series (e.g. other river discharge, temperature, wind speed, and SO, AO, or NAO phenomena).

REFERENCES

- [1] P. Pekarova, and J. Szolgay (eds). "Assessment of climate change impact on selected components of the hydrosphere and biosphere in Slovakia". Bratislava, Veda, 81–104. 2005.
- [2] M. E. Torres, M. A. Colominas, G. Schlotthauer, and P. Flandrin. "A complete Ensemble Empirical Mode decomposition with adaptive noise." IEEE Int. Conf. on Acoust. Speech and Signal Proc. ICASSP-11, Prague. 4144–4147, 2011.
- [3] N. E. Huang, Z. Shen, S. R. Long, M. C. Wu, H. H. Shih, Q. Zheng, N. C. Yen, C. C. Tung, and H. H. Liu. "The Empirical Mode Decomposition and the Hilbert Spectrum for Nonlinear and Nonstationary Time Series Analysis", Proc. R. Soc. Lond. A. 903–995, 1998.
- [4] J. I. Salisburry, and M. Wimbush. "Using modern time series analysis techniques to predict ENSO events from the SOI time series." *Nonlinear Process in Geophysics*. Vol. 9, 341–345, 2002.
- [5] C. Franzke, and T. Woollings. "On the Persistence and Predictability Properties of North Atlantic Climate Variability." *J. Climate*, 24, 466–472, 2011.
- [6] N. E. Huang, M. L. Wu, S. R. Long, S. S. P. Shen, W. Qu, P. Gloersen, and K. L. Fan. "A confidence limit for the empirical mode decomposition and Hilbert spectral analysis." Proc. R. Soc. London, 459 (2037), 2003.
- [7] Y. Huang, F. G. Schmitt, Z. Lu, and Y. Liu. "Analysis of daily river flow fluctuations using Empirical Mode Decomposition and arbitrary order Hilbert spectral analysis." *J. of Hydrol.* Vol. 373, Issues 1–2, 103–111, June 2009.
- [8] D. Halmova, P. Pekarova, and I. Meszaros. "Identification of the low flow change in selected gauging stations on the Danube River." *Acta Hydrologica Slovaca*, ISSN - 1335-6291, vol. 12, 2, pp. 286–295, 2011.
- [9] P. Pekarova, P. Miklanek, and E. Balogh. "Flood regime analysis of the Danube in 1876–2005." In: Proc. XIX. Poster day (Ed. A. Celkova), ISBN - 978-80-89139-26-2, Bratislava: ÚH SAV, 628–635. 2011.
- [10] B. Pramuk, P. Pekarova, and D. Halmova. "Identification of flood flows changes of the Danube River in Bratislava station in period 1876–1943 and 1944–2010." *Acta Hydrologica Slovaca*, ISSN - 1335-6291, vol. 14, 2, 327–336, 2013.
- [11] A. Antico, G. Schlotthauer, and M. E. Torres. "Analysis of hydroclimatic variability and trends using a novel empirical mode decomposition: Application to the Paraná River Basin." *Journal of Geophysical Research: Atmosphere*, 119, 3, 1218–1233, 2014.
- [12] Z. Wu, and N. E. Huang. "Ensemble Empirical Mode Decomposition: A Noise-assisted Data Analysis Method." *Adv. Adapt. Data Anal.* Vol. 1, 1–41, 2009.
- [13] M. Zelenakova, P. Purcz, I. Gargar, H. Hlavata. "Research of Monthly Precipitation Trends in Libya and Slovakia." In: Recent advances in environmental science and geoscience, Proc. of the 2014 International Conference on Environmental Science and Geoscience (ESG '14), ISBN: 978-1-61804-224-8, pp. 46–50, 2014.

Log-normality of the Tsunami Run-up Heights along the Eastern Coastal Line of Korean Peninsula

Kim, D., Cho, H., and Cho, Y.-S.

Abstract—While tsunami is one of the most dangerous disasters threatening the survival of human being, the analysis of tsunami often requires the numerical simulation which needs tremendous amount of input data such as the ones related to sea bathymetry, terrain, and undersea earthquakes. To overcome this problem, the statistical approaches are often used. In this study, the method of L-moment ratio diagram was used to identify the best-fit distribution of the tsunami runup height along the eastern coastline of Korean Peninsula, which can subsequently be used as the reference distribution to analyze the risk due to tsunami attack. The result of the analysis indicates the generalized Pareto (GPA) distribution is the best-fit distribution representing the tsunami runup heights regardless of the characteristics of the undersea earthquakes. This is particularly because the tsunami runup height is influenced not only by the characteristics of the undersea earthquakes but also highly by the bathymetry and the terrain of the area near the tsunami attack. Further analysis was performed to figure out why the tsunami runup height does not have the ideal theoretical form, which is the log-normal distribution. Result of the investigation indicates that the log-normality of the tsunami runup heights can be preserved when the length of the coastal line is not long such that the homogeneity of the length of the wave propagation paths reaching at different locations of the coastal line is preserved. This subsequently secures the principle of the central limit theorem making the distribution of the tsunami runup heights follow the log-normal distribution. As the length of the coastal line increases, the deviation of the tsunami runup height distribution from the log-normality increased.

Keywords— tsunami, log-normal distribution, central limit theorem, generalized Pareto distribution

The research of the first author (Prof. Dongkyun Kim) was financially supported by the National Research Foundation of Korea funded by the Ministry of Science, ICT and Future Planning (Grant No. 2013R1A1A1011676). The research of the corresponding author (Prof. Yong-Sik Cho) was financially supported by the National Research Foundation of Korea (Grant No. 2010-0022337).

Professor Dongkyun Kim is with the Department of Civil Engineering, Hongik University, 94 Wausan-ro Mapo-gu, Seoul, 121-791, Korea (e-mail: kim.dongkyun@hongik.ac.kr).

Ms. Hyerin Cho is with Department of Civil Engineering, Hanyang University, 222 Wangsimni-ro, Seongdong-gu, Seoul 133-791, Korea

Professor Yong-Sik Cho is with Department of Civil Engineering, Hanyang University, 222 Wangsimni-ro, Seongdong-gu, Seoul 133-791, Korea

I. INTRODUCTION

Tsunami is extremely disastrous. The Sumatra-Andaman tsunami of 2004 caused the casualty of approximately 230,000 people. The tsunami caused in the North Pacific Coast near Japan in 2011 took the lives of 20,000 people. However, the occurrence of tsunami is as scarce as its impact is calamitous placing a major obstruction for the intensive analysis based on observation. For this reason, significant portion of the studies related to tsunami relies on numerical simulation, which requires extensive amount of input data for model development and execution such as sea bathymetry, terrain, and undersea earthquakes.

On the other hand, there has been also a good amount of efforts investigating the tsunami from statistical view points, which does not require as much extensive information about tsunami as the numerical simulations. In the statistical approaches, the spatial or temporal distribution of tsunami heights is modeled with a statistical distribution, which can be used to assess the risk of tsunami for a given region.

Most of these studies suggest that the log-normal distribution generally fits the tsunami heights observed along a given coastal line even though the level of fit varies depending on how well the field condition meets the theoretical assumptions of tsunami propagation. (Van Dorn, 1965; Kajiwara, 1983; Go, 1987; Go, 1997; Choi et al., 2006) The fundamental basis of the log-normality of the tsunami heights is that the tsunami propagation can be considered as a random process in which the central limit theorem can be applied. This is because the bathymetry along many tsunami propagation paths, which exerts a substantial influence on the tsunami heights, can be considered as a random variable. Choi et al. (2002) verified that the tsunami wave heights converges from uniformity into the log-normality along with the propagation of the wave. Choi et al. (2012) showed that the tsunami runup heights observed in the Sanriku area, Japan for the 1896, 1933, 2011 Japanese Tsunamis have the log-normality.

This study firstly shows that the best-fit distribution of tsunami height of the study area is not the log-normal distribution but the generalized Pareto distribution. Then, this study performed a further analysis to identify the reason of this finding, especially focusing on the log-normality of the tsunami height distribution. This study particularly focuses on identifying and verifying the reason of this discrepancy based

on the extensive numerical simulations performed along the Eastern Coast of Korean Peninsula.

II. METHODOLOGY

The study area is shown in Fig. 1 along with the locations of the 4 most probable undersea earthquakes according to the suggestion of Korean Peninsula Energy Development Organization (1999). The tsunami propagations corresponding to these 4 undersea earthquakes were numerically simulated to obtain the tsunami heights along the Eastern Coast of Korean Peninsula. The tsunami simulation model of Cho et al. (2007) was used in this study to acquire the tsunami heights. The accuracy of the computational algorithm adopted in the model was verified through the study performed on the same study area. (Sohn et al., 2009)

The best-fit probability distribution representing the tsunami heights along the coastline was determined using the L-moment ratio diagram method. In the L-moment ratio diagram method, the 3rd and 4th L-moment ratio, or the ratio of the 3rd and 4th L-moment to the 2nd L-moment of the sample data is compared to those of the model probability distribution. In this study, the following model distributions were chosen as the candidate distribution to fit the sample tsunami heights along the east coast of Korean Peninsula: generalized logistic distribution (GLO); generalized extreme value distribution (GEV); generalized Pareto distribution (GPA); 3-parameter log-normal distribution (LN3); and Pearson type III distribution (PA3). All these distributions have been widely applied in modeling the extremes of the hydrologic time series.

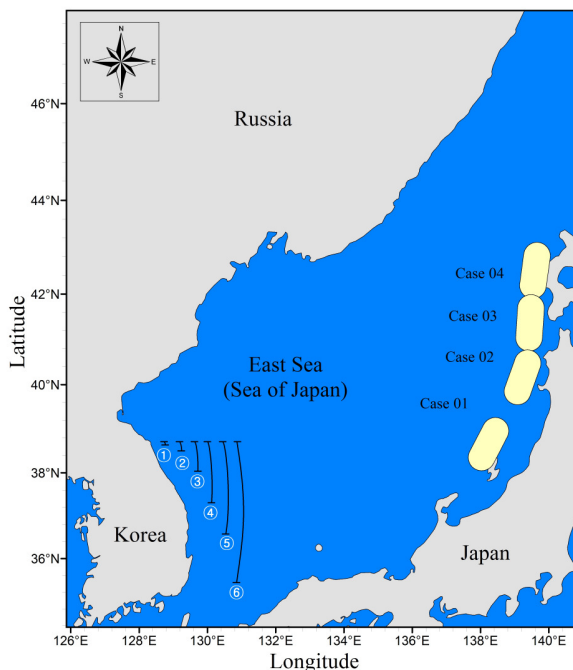


Fig. 1. Study area and the location of the 4 virtual undersea earthquakes used for the simulation of this study. The size of the sub-segments of the coast line over which tsunami height distribution was analyzed is shown together.

III. RESULT

Fig. 2 shows the L-moment ratio diagram which identifies the type of the best-fit distribution representing the tsunami heights for the 4 most probable tsunami event shown in Fig. 1. In this diagram, the candidate model probability distributions considered in this study are represented as curvilinear lines, and the pair of the sample 3rd and 4th L-moment ratio value is represented as a numbered point. The number of each point represents the undersea earthquake identification number. The tsunami run-up heights corresponding to all 4 undersea earthquakes were best represented by generalized Pareto distribution. This finding suggests that, regardless of the characteristics of the causative undersea earthquake, the tsunami heights over a given coastline may have the similar probability density. This is particularly because the relative magnitude of the tsunami height is not only governed by the characteristics of the causative undersea earthquake, but also highly governed by the bathymetry and the terrain of the area near tsunami attack. Therefore, it can be concluded that the probability density of tsunami heights over a given coastline is likely to remain similar even if the causative undersea earthquake is different.

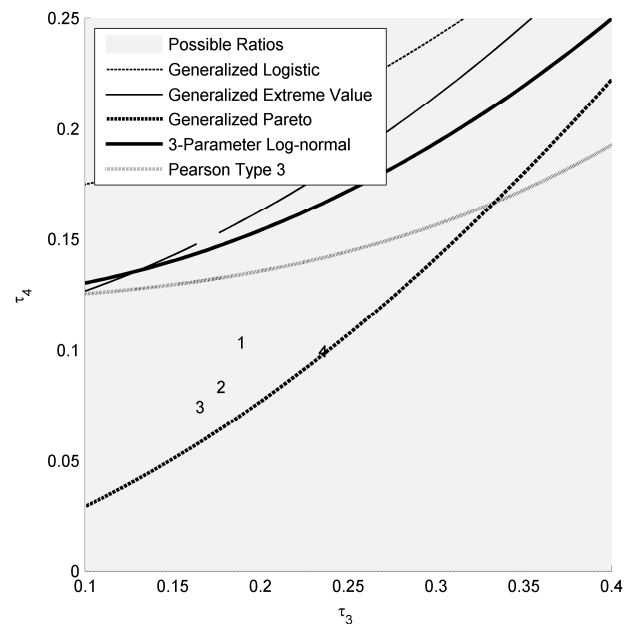


Fig. 2. L-moment ratio diagram along with the numbered points representing the 3rd and 4th L-moment ratio of the simulated tsunami heights. Number represents the undersea earthquake identification number

This study also investigated the reason why the tsunami heights along the east coast of Korean Peninsula do not follow the log-normal distribution but generalized Pareto distribution. This study assumed that the reason is because a fundamental assumption of the central limit theorem is not preserved. In other words, the length of the east coastal line of Korean Peninsula over which tsunami heights were observed is too long to assume the uniformity of the length of each wave propagation path. To verify this assumption, we subsequently shortened the

length of the coastline of tsunami height observation and see how the L-moment diagram behaves. Fig. 3 shows the L-moment diagram when the length of the coast line of tsunami observation was divided into the sub-segments with the length of 10 km, 30 km, 100 km, 200 km, and 300 km. It can be seen that the distribution of the tsunami height converges to log-normality as the length of coastal line of the tsunami height observation approaches to the characteristic length scale ranging between 100 km and 300 km.

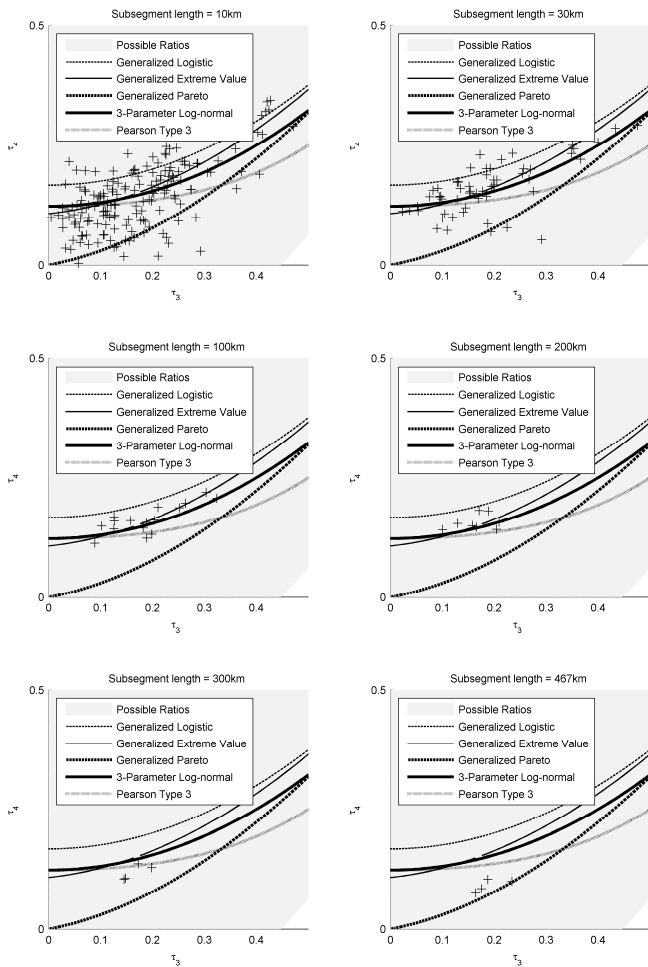


Fig. 3. Variation of the L-moment ratio along with the variation of the coast line sub-segment length

IV. CONCLUSION

The major findings of this study are as follow:

(1) For a given coastal area, the best-fit distribution is likely to remain similar regardless of the causative undersea earthquake. This is particularly because the relative magnitude of the tsunami height is influenced not only by the characteristics of the undersea earthquakes but also highly by the bathymetry and the terrain of the area near the tsunami attack.

(2) Tsunami wave propagation can generally be modeled as a random process, thus the tsunami heights along a given coastal area have the log-normality in general. However, the deviation from the log-normality increases as the length of the coastal line increases. This study identified the characteristic coastal line length ranging between 100km and 300km as the limit within which the log-normality of the tsunami height can be preserved.

ACKNOWLEDGMENT

The research of the first author (Prof. Dongkyun Kim) was financially supported by the National Research Foundation of Korea funded by the Ministry of Science, ICT and Future Planning (Grant No. 2013R1A1A1011676). The research of the corresponding author (Prof. Yong-Sik Cho) was financially supported by the National Research Foundation of Korea (Grant No. 2010-0022337).

REFERENCES

- [1] Y.-S. Cho, D.-H. Sohn and S.-O. Lee, 2007. "Practical modified scheme of linear shallow-water equations for distant propagation of tsunamis" *Ocean Engineering*, 34 (11-12), 1769-1777.
- [2] B. H. Choi, S. J. Hong, and E. Pelinovsky, 2006. "Distribution of runup heights of the December 26, 2004 tsunami in the Indian Ocean" *Geophysical Research Letters*, 33(L13601), 1-4.
- [3] B.H. Choi, E. Pelinovsky, I. Ryabov and S.J. Hong, 2002. "Distribution functions of tsunami wave heights" *Natural Hazards*, 25 (1), 1-21.
- [4] Ch.N. Go, 1987. "Statistical properties of tsunami runup heights at the coast of Kuril Island and Japan" *Institute of Marine Geology and Geophysics, Sakhalin*, Preprint.
- [5] Ch.N. Go, 1997. "Statistical distribution of the tsunami heights along the coast. Tsunami and accompanied phenomena" *Sakhalin*, 73-79.
- [6] K. Kajiura, 1983. "Some statistics related to observed tsunami heights along the coast of Japan", in: Iida, K., and Iwasaki, T. (Eds.), *Tsunamis: Their science and engineering*. Terra Scientific, Tokyo, Japan, 131-145.
- [7] Y. C. Kim, M. Choi, and Y.-S. Cho, 2012. "Tsunami Hazard Area Predicted by Probability Distribution Tendency" *Journal of Coastal Research*, 28(5), 1020-1031.
- [8] Korean Peninsula Energy Development Organization, 1999. "Estimation of Tsunami Height for KEDO LWR Project" *Korea Power Engineering Company, Inc., Korea*.
- [9] D.-H. Sohn, T. Ha and Y.-S. Cho, 2009. "Distant tsunami simulation with corrected dispersion effects" *Coastal Engineering Journal*, 51 (2), 123-141.
- [10] W.G. Van Dorn, 1965. "Tsunamis", in: Chow, V.T. (Eds.), *Advances in hydroscience*.

Challenges for a sustainable ecosystem management of Carpathian forests

Simona Frone, Dumitru Florin Frone

Abstract— Our paper aims to increase the awareness on the environmental, economic and social importance and value of the forests in the Carpathian mountains, a natural heritage that may be a reliable factor of sustainable economic development in Romania. To enhance the theoretical and methodological background, we employ a comparative analysis between the main trends and approaches in modern sustainable forest management. We also highlight some of main challenges raised by maintaining and developing the main ecosystem services (ES), a most important concept at the base of a practical sustainable ecosystem management (SEM) of forests. In order to demonstrate the potential of a sustainable ecosystem management of the forests captured in the protected areas of the Carpathians, we presented some outstanding outcomes of a recent case-study. The main objective was to demonstrate the importance of ecosystem services provided in and around these protected areas, for the sustainable local as well as national economic development.

Keywords—ecosystem approach, ecosystem services, protected areas, sustainable ecosystem management

I. INTRODUCTION

Sustainable economic development strategies increasingly recognize the capital values of forests in national policies and programmes that modify forest stocks, qualities and distributions.

Forests are now widely acknowledged as both productive capital stocks and as components of public infrastructural systems. As ecological analogues of industrial capacity and physical infrastructure, forests are entering the central equations of macro-economic growth.

Although the concept of 'forest as infrastructure' is not yet widely supported, the absence of forests clearly requires constructed infrastructure at the expense of other potential uses of scarce capital. Forests provide infrastructural services without which development opportunities decline. They stabilize streamflow and microclimates, protect land and earth structures such as roads and canals, drain and shade the land, and purify the atmosphere.

Simona Frone is a Senior researcher at the Institute of National Economy, Romanian Academy, 13, Calea 13 Septembrie, 050711, Bucharest, Romania (+40745-078695; frone.simona@gmail.com)

D.F. Frone is an Associate professor at the University of Agricultural Sciences and Veterinary Medicine, Bucharest 59 Marasti, 011464, Bucharest, Romania (e-mail: ffrone@hotmail.com).

The economic and social consequences of changes in forests ecosystems are difficult to predict. Changes in the dynamics of river basins, ecological regions or wildlife systems, for example, may reduce or increase different aspects of human well-being; without sufficient knowledge, the unpredictability of the consequences tends to rise with the extent of change.

In recent years, forests have become more widely recognized as homes of cultures. International concern and appreciation for the value of traditional cultures and their knowledge of nature have contributed to the preservation of forest regimes and increased attention to the needs of forest dwelling communities as a matter of national interest [1].

II. MATERIALS AND METHODS

In the last two decades, there have been important theoretical and methodological developments in the field of forest management, driven by the urgent need to acknowledge the most important issues of sustainable development, environmental protection and valuation, biodiversity conservation and climate change mitigation. The trends in the area have focused in two main approaches [2]:

- i. Sustainable Forest Management (SFM) is considered an approach that balances environmental, socio-cultural and economic objectives of management in line with the „Forest Principles” adopted at the United Nations Conference on Environment and Development, in 1992 [3];
- ii. The Ecosystem Approach (EA) was developed mainly due to increasing efforts in environmental conservation. This is a holistic approach for the conservation and the sustainable use of biological diversity and its components, in all types of ecosystem.

Both these approaches, as important concepts in environmental management, aim at promoting the best environmentally, socially and economically sustainable forest management, and to generate benefits for both present and future generations.

If forests are to be considered an important natural heritage, it is useful to acknowledge the importance and features of both these environmental management approaches, within a sustainable heritage management strategy, for instance. There are many features, principles and concepts common to both SFM and EA (Table I).

Table I Main concepts and principles of forest management in SFM and EA

Concepts and principles	SFM approach	EA approach
Sharing and use of local knowledge and other information sources	x	x
Adaptive management and social learning (precautionary principle)		x
Intergenerational equity	x	x
Appropriate scale		x
Conservation of the ecosystem structure and functioning (the ecological balance)	x	x
Sustainable use of productive functions	x	x
Multiple use and values	x	x
Equitable benefit sharing	x	
Integrated management (considering impacts on other ecosystems)	x	x
Intersectoral collaboration	x	x

Source: Authors' synthesis, based on references.

However, the two approaches also have some few conceptual differences, since the Forest Principles were developed at a sectoral level, while the ecosystem approach started from an ecological point of view, with a focus on conservation issues. Therefore, the SFM did not pay enough attention to some important management principles, such as the precautionary principle and the adaptive management, or the appropriate scale.

An important difference is also the fact that the EA approach is applicable to all the types of ecosystems, while SFM was mainly designed to deal with the forest ecosystem. An ecosystem (e.g. forest, wetland, marine area) is a natural unit of living things (animals, plants and micro-organisms) and their physical environment, e.g. forest.

There is agreement on the fact that it is possible to integrate the SFM and the EA approaches, this leading to synergies in policy processes at international and national levels. For instance, the Fourth Ministerial Conference on the Protection of Forests in Europe, held in Vienna in May, 2003, recognized the essential benefits that forests provide. The signatory countries committed to promote incentives that have positive impacts on sustainable forestry, and also to the removal of incentives that have negative impacts.

At the Fifth Ministerial Conference, held in Warsaw in 2007, signatory countries and the European Community recognized the vital role that sustainable management of forests plays in protecting water quality, and committed themselves to implement tools for securing water-related services provided by forests.

They also agreed to: facilitate the implementation of measures, including payments for ecosystem services, to diversify the financial basis for sustainable forest management; enhance the protective role of forests for water and soil as well as mitigating local water-related natural disasters; assess forestation programmes for their effects on quality and quantity of water resources, flood alleviation and soil maintenance; develop and improve policies for forest and water resource management contributing to the maintenance of sustainable ecosystems; assess the economic value of forest services related to quality and quantity of water resources and flood alleviation.

Another important concept is that of ecosystems services (ES), related to a flow of resources or service from the natural environment that directly or indirectly benefit people. More, the Ecosystem Approach was further developed for practical implementation reasons, into the increasingly important Ecosystem Services Approach. As we shall further analyse, the Ecosystem Services Approach (ESA) provides a framework for considering whole ecosystems in decision making and for valuing the services they provide.

The Ecosystem Services Approach (ESA) explicitly recognizes that ecosystems (e.g. forests, wetlands) and the biological diversity contained within them contribute to individual and social wellbeing. Importantly it recognizes that this contribution extends beyond the provision of goods such as timber and fish to the natural regulating functions such as carbon sequestration [4].

Therefore, the economic valuation of ES is focused on the „final benefits” or „outcomes” realised by society from the services an ecosystems provide, not the services and functions that contribute to those outcomes. In order to avoid double counting, the benefits generated by supporting services, while fundamental to the provision of final benefits, are not valued independently as they are intermediate benefits which contribute to the provision of a range of final benefits. Their value is captured in the valuation of the final outcomes associated with the other ecosystems services they support (see Figure 1).

A research study [5] on the UN-sponsored Millennium Ecosystem Assessment [6] (hereafter MA), assessed the state of the world's ecosystems and examined 24 essential ecosystem services in the context of “benefits people obtain from ecosystems.” It found that over the past 50 years, only four of these services have shown improvement whereas fifteen have shown serious decline, with the remainder under stress in some parts of the world.

Therefore, we should acknowledge that ecosystems provide a wealth of services that are fundamental for proper environmental functioning and economic and social development. While the demand for these services, including provision of clean freshwater is continually increasing, the capacity of ecosystems to provide such services is hampered by their ever-growing degradation.

The main ecosystem services (ES) may be classified into four types (MA), which also apply to forest ecosystems as follows (see Figure 1):

Provisioning: Provisioning ecosystem services relate to the tangible products, such as timber, non timber forest products (NTFPs), ornamental and pharmaceuticals products provided by ecosystems. Thus, provisioning services are useful physical products of the forest such as food, wood, fibre and fuel;

Regulating: These are the ‘preventative’ benefits of forests: their role in erosion control, flood prevention, climate regulation, carbon sequestration and water purification. Regulating ecosystem services refer to an ecosystems natural processes (such as carbon sequestration and water regulation) that contribute to social wellbeing;

Cultural: Forests are sources of aesthetic and spiritual regeneration as well as providing recreation and education, which supplies services for the tourism industry. Cultural ecosystem services relate to the non-material benefits obtained from ecosystems, for example, through tourism and educational use;

Supporting: This describes the role of ecosystems as a ‘nursery’ for other environmental benefits, such as nutrition cycling and soil formation. The biodiversity services such as species and habitat conservation fall into this category. As suggested, supporting ecosystem services are necessary for the production of all other ecosystem services (e.g. soil formation or nutrient cycling). They differ from the other services in that their impacts on people are either indirect (via provisioning, regulating or cultural services) or occur over a very long time.

Ecosystem services (features and outcomes)		Link to well-being benefits				Economic sectors supported
		A	B	C	D	
S U P P O R T I N G	PROVISIONING (Food, Fuel, Freshwater, Fiber, Natural Medicines, Ornaments)	***	**	***	*	House holds Forestry, Industry, Energy, Tourism
	REGULATING (Climate Regulation, Flood Regulation, Disease Regulation, Water Purification)	***	***	***	*	All
	CULTURAL (Aesthetic, Recreational, Educational)	*	*	**	**	Tourism, House holds

Legend:

A=Basic material for life; B=Security; C=Health; D= Good social relations
*=Weak; **=Medium ; ***=Strong

Source: Own contribution based on [6]

Figure 1 - Potential ecosystem services of forests and links to human well-being and economic sectors

Most ecosystem services are not traded on markets and do not have a price, but this does not mean they have no economic value. In recent years, innovative financing mechanisms, and especially payments for ecosystems services (PES) have been recognised as crucial for addressing some of the failures in environmental management. Payments for ecosystem services (ES) are financing mechanism that rewards stakeholders who conserve natural resources by providing payments for valuable goods and services resulting from their conservation activities .

Also, the Millennium Ecosystem Assessment (MA, 2005) has emphasized that Protected Areas (PAs) provide critical ES that support human prosperity and survival, like clean water, flood and storm mitigation, fish stock replenishment, and carbon sequestration. Theoretically, healthy and bio-diverse

ecosystems generate greater amounts, higher quality, and more stable flows of ES over time.

This is why the new concept of Sustainable Ecosystem Management (SEM) was developed. Under SEM, funding and capacity are available to meet basic to optimal protection needs. SEM is understood as an advanced management approach in which protected area management functions are more aligned with human, financial, institutional, and informational resources.

In SEM, protected "sustainable conservation goals and objectives are linked to ecosystems conservation programs and are realistically linked to funding. As a result, ecosystem health improves and their benefits, in terms of increased productivity and equity, expand. By and large, the benefits of SEM outweigh its costs. Under a SEM scenario, the focus is on long-term gains (10-20 years), while the costs of impacts are internalized. Degradation of ES is avoided, thereby generating potential for a long-term flow of ecosystem goods and services [7].

As a first theoretical conclusion, which will be supported below by the case-study [7], the most effective and recommended forest management approach is a Sustainable Ecosystem Management (SEM). As compared to the business as usual (BAU) practices, SEM practices tend to support ecosystem sustainability, not for ideological reasons mainly (as in the SFM or EA), but, rather, as a practical, cost-effective way to realize long-run socio-economic and environmental benefits.

III. RESULTS AND DISCUSSION

As stated in another recent study [8], the Romanian forest management system was known for its performance during the communist period, all the forest belonging to the state and being managed following sustainability principles.

At present, after 20 years of structural changes triggered by an extended process of restitution, a more stable system is now in place with almost all the forests (6.0 million ha out of 6.3 million ha) being administrated by National Forest Administration Romsilva or by private forest districts. Forest management is based inter-alia on biodiversity conservation principles [9], creating the opportunity to develop a protected areas (PA) network covering 23% of the total territory of Romania and almost 30% of the forests in the country.

Therefore, further we shall also briefly present some outcomes of an Ecosystem Services Approach applied in the case of the Carpathian Network of Protected Areas (CNPA), highlighting mainly the importance of their forest ecosystems. The pilot protected areas selected for study by the *GEF/UNDP Project: Improving the Financial Sustainability of the Carpathian System of Protected Areas* were Apuseni National Park (ANP), Retezat National Park (ReNP), Piatra Craiului National Park (PCNP), Vanatori-Neamt Natural Park (VNP) and Maramures Mountains Natural Park (MNP).

Ecosystems within Romania's PAs provide ecosystem services (ES) such as water provision and regulation, soil fertility, pollination, pest control, growth and reproduction of food species, storm mitigation, climate regulation and waste

assimilation, which directly and indirectly provide inputs into the production of key sectors in Romania's economy. The sectors studied were: tourism and recreation; forestry and hunting; agriculture; water resources; and disaster risk management. The main results and recommendations of the *GEF/UNDP Project* research project are published in [7].

The Carpathian Mountains, which extend over an area of 210,000 km² in Central and Eastern Europe, are included in the WWF Global 200 Ecoregion list and host Europe's most extensive tracts of montane forest, the largest remaining natural mountain beech and beech/fir forest ecosystems, and the largest area of virgin forest left in Europe. Romania holds 54% of the Carpathian mountain range [7]. The Carpathian Network of Protected Areas (CNPA) is comprised of 285 protected areas that cover 31,978 km².

However this network of Protected Areas (PAs) is considered to be insufficient in terms of scale, connectivity and management to prevent the irreversible loss of biodiversity in the Carpathian ecoregion. PAs of the Carpathian mountains face a range of pressures: overexploitation of forest resources through logging and poaching; habitat degradation and fragmentation caused by the construction of roads, houses and tourism infrastructure that is not properly planned and developed [7]. Due to the fact that forest cover areas of more than 50% of the selected 5 PA in their study (Table II) it may be stated that most of the ES are forest ecosystem services.

Table II Forest coverage of the pilot protected areas PA in the Carpathian Mountains of Romania

PROTECTED AREAS	Total PA surface	Forest coverage type			
		Forest cover		Strictly protected forest	
		ha	%	ha	%
Piatra Craiului National Park (ANP)	14773	10170.8	68.85	3753.68	25.4
Retezat National Park (ReNP)	38138	19254	50.49	884.9	2.3
Apuseni Natural Park (ANP)	75784	48795.5	64.39	11467	23.8
Vânători Neam Natural Park (VNNP)	30818	26322	85.41	11417	37.0
Munții Maramureșului Natural Park (MNP)	148850	72000	48.37	8850	5.9

Source: Own computations and primary data from Table 0-1, p.113 [7]

In our opinion, based on the main recent studies and case-studies in the field [7,8], there are quite important challenges to be signalled in the management of the most important Romanian forest ecosystems, in the protected areas.

For instance, [7,8] claim that, although in theory, forest ecosystems within the PAs are managed, in Romania, according to the forest and parks management plans (MP), in reality these plans are not always fully enforced due to a range of factors : i) not all PA MPs are approved; ii) there is no compensation for harvesting restrictions within private forests and owners therefore have no incentive to limit harvesting; iii) in some of the PAs there may be the need to extend the area of protected forests, but in the absence of a comprehensive biodiversity inventory and monitoring system, and with

resistance from forest administrators and owners, these forests continue to be harvested for wood, which may entail a number of negative effects on the provision of important ES; iv) while there is a good legal framework in place, enforcement of the law is weak and in many cases over cutting and illegal logging is evident.

Thus, a very important challenge is keeping the balance of the forest ecosystems by avoiding the excessive and illegal wood harvesting. The Carpathian forest ecosystems provide important quantities of economically attractive wood species such as beech, spruce and oak. Based on official statistics, 59% of the annual increment is harvested. Forest harvesting is a complex activity with potential impacts on biodiversity and the ES provided by PAs such as carbon sequestration, air quality, water and soil erosion regulation, nutrient retention, landscape, and the production of NTFP. Therefore, sustainable forest harvesting is crucial for effective provision of PAs ecosystem services [7].

No statistics are available on the extent of illegal logging, and while this is occurring in almost all areas it is not considered to be significant. However, illegal clear cutting in some parts of the Carpathians has created problems in the past, and remains a potential threat. For example, the floods and landslide in Maramures in 2006 -2010 can be linked to clear cutting that occurred in Borsa and Viseu forests in 2001-2005. Furthermore, clear cutting in private forests in Arges County and around Piatra Craiului National Park have had significant negative effects on the quality and effectiveness of ecosystems and its landscape [7].

Another conclusion of the cited study and a challenge of SEM is that, with the present limited levels of stricted protected forest areas (Table II), the potential threat to biodiversity (which is not yet properly assessed due to ongoing lack of funding for proper identification and monitoring of flora and fauna) will lead to continuous degradation of potentially valuable ecosystems, hindering the development of recreation, tourism and educational activities.

Futhermore, the study [7] showed that Carpathian PAs are underfunded. For example, the 5 pilot Romanian PAs selected for study received around €50,000 in funding in 2010, while €1,600,000 is considered to be necessary to meet basic needs and around €2,550.000 to optimally manage the sites [10].

As for the multiple functions and benefits of the forests of these PA, there are quite many issues to be raised, analysed and assessed, by employing an ESA approach. This case-study [7] has set out the economic and social arguments for the Romanian CNPAs, aiming to generate evidence of how a sustainably managed CNPAs supports productivity in key sectors such as tourism, forestry and industry, using key indicators such as employment, tax revenue, foreign exchange earnings and equity aspects. The study also seeked to demonstrate the costs associated with unsustainable management.

The analysis covered an assessment of how ecosystem services provided by the pilot PAs contribute to tourism and recreation benefits, primary wood production associated with the active management of forests, NTFP (non-timber forest

products) values and hunting carried out in and around the PAs, carbon sequestration, food provision (milk) related to PA pastures, and water provision to the bottled water industry and for urban supply in the case of the water resources sector. The analysis of disaster mitigation was focused on the damage costs avoided as a result of the erosion and water flow regulation services provided by the PAs.

First, the **forestry** sector is very dependent on the forest ecosystems, and the value of forest provisioning ES (timber, non-timber forest products (NTFP) and hunting) for the pilot PAs was estimated at around €0.1 million per year (2010). [7] claim that, although under a business-as-usual scenario (BAU) forestry activities may add some €2.8 million over the next 25 years to Romania's economy, this revenue will disappear after 30 years as the capacity of PAs to generate economically valuable wood and NTFP is eroded (without taking into consideration the considerable losses in other forest ecosystem services such as carbon sequestration, water and soil erosion regulation and landscape provision and tourism). On the other hand, SEM implies a decrease in forest wood, NTFP and hunting values in the short term, but in the long run, the value of PAs under the SEM scenario will recover, and is projected to generate a higher Net Present Value (NPV) beyond a 25 year horizon. In addition other ecosystem services generated and/or maintained by sustainable forestry (e.g. carbon sequestration, water and soil erosion regulation, landscape) are ensured. Carbon sequestration functions of the forest under SEM could generate an additional €3 million (cumulative value over 25 years).

Since the analysis of provisioning forest ecosystem service values for each of the PAs and the economic links between ecosystem services of protected areas on the one hand and the practices and results of the forestry sector were highlighted in detail by the paper of [8], we shall briefly cite here other outcomes of the [7] study, in order to point out to the importance of the regulating and provisioning services of the forest ecosystems in the Carpathian region.

The ecosystems of the pilot PAs provide a number of key regulating services including soil loss prevention and the regulation of water flow and quality.

- As regarding **water resources**, water quality and quantity is very important to the many brands of mineral water sourced from the Carpathian mountains. The estimated total cumulative value to the economy of SEM relative to BAU of clean water provision, based on water treatment cost avoided, is estimated at 35.4 million (over 25 years). Private water bottling companies are the main beneficiary and are identified as potential partners in Payment for Ecosystem Services (PES) schemes. Around 70% of the watershed areas in the PAs are forested and soil erosion is currently well regulated, as a result there is not a significant monetary difference between the BAU and SEM scenario. However, it is important to note that the benefits provided by the ecosystem services could be lost through increased pressures on the sites [7].

- Romania also has a long history of **natural disasters** (floods and landslides). The potential economic loss associated with these events is estimated at 6% of the GDP accounting for approximately \$2,300 million a year, with an annual probability of occurrence of 0.5 %. The quality and quantity of ecosystems significantly impacts the frequency and severity of natural disasters and the growing emphasis on PAs could play a central role in risk reduction under sustainable forest ecosystem management. If the upstream protection functions of the ecosystems of 3 pilot PAs serve to minimize the impact of floods by just 25% below what it would have been in the absence of the protective functions, then the ecosystems' value of flood control in terms of avoided damage costs equates to an average of €0.4 million a year – 9 million a year based on a damage cost avoided and preventative expenditure approach respectively. When applying the damage cost avoided and preventative expenditure values as upper and lower value limits for the ecosystems of the 5 pilot PAs over the next 25 years, the water retention regulating services within the PAs in terms of mitigating natural disasters (flood control), is valued at between €27 million and €182 million (under BAU) and €44 million and €182 million under SEM.
- However, the key sector benefiting from PAs is shown to be the **tourism sector** which if sustainably managed has the potential to generate an additional €2,626 million over the next 25 years (94% of the total additional value of SEM). It is important to note that this value depends on the continued provision of healthy PAs ecosystems that contribute to the tourism experience and for which tourists are prepared to pay. The significant consumer surplus estimated for tourism and recreational experiences within PAs in Romania suggests that mechanisms, such as entrance fees, would be successful, and can also be used to control demand and minimize impacts on the site. Currently entrance fees are very low or non-existent, so there is therefore the scope to introduce and increase entrance fees, particularly at sites where the tourism potential is high. However, realizing the full tourism potential (benefits) is dependent on the prior investment in tourism and recreational facilities [7].

The results of the study [7] summarized in the indicator of cumulative benefit of SEM for all five PAs is the more than impressive amount of €2,794 million (i.e. the total benefit of SEM relative to BAU over 25 years). This can be viewed either as the benefit of implementing a sustainable ecosystem management SEM or the cost to the economy of continuing with the business-as-usual BAU practices.

IV. CONCLUSIONS

As stated also by H.R.H. Prince Charles [11]: „the Romanian Carpathians are a priceless natural treasure in a continent that has long since destroyed most of its

wildernesses. What you still possess here in Romania has become extremely rare. Many European countries have little or no primary forest left...The great Carpathian forests and landscapes help to define Romania and to lose them would, in my humble opinion, be a tragedy”.

Our paper aimed to increase the awareness on the environmental, economic and social importance and value of the forests of the Carpathian mountains, as a natural heritage that may be managed as a reliable factor of sustainable economic development in Romania. But we also had to highlight some of the main issues raised by the current management practices.

In order to demonstrate the potential of a sustainable forest ecosystem management of the natural heritage captured in the protected areas of the Carpathians, we presented some outstanding outcomes of a recent study by [7]. Their case-study seeks to demonstrate that PAs are an important and productive asset providing a significant flow of economically valuable goods and services. Economic studies drawing out the significance of these services in monetary terms and their contribution to local, regional and national economies can be a powerful way of demonstrating the significance of PAs to decision makers.

For instance, [7] consider as an important challenge the poor financing of the Carpathian network of PA, which triggers the need for a better assessment of ecosystem services values and a better way to communicate these findings to decision makers, to support their decisions in terms of forest management and biodiversity conservation funding.

Since the presented study is quite a new and pioneering approach for Romania, using some research outcomes from previous European studies, our further research will be dedicated to the development and implementing of the best suited methods of assessing the regulating forest ecosystem services (especially the flood and soil erosion regulation).

Considering the presented issues and taking into account the high production and protection value of Romanian forests and the public goods or services provided by forest ecosystems, as well as the changes in forest ownership, we believe there is still a strong need for a public awareness campaign on the need for sustainable management and conservation of forest resources.

REFERENCES

- [1] Food and Agriculture Organization of the United States, “State of the World’s Forests”, FAO Rome, 2012
- [2] Wilkie M.L., Holmgren, P. and F.Castaneda, „Sustainable forest management and the ecosystem approach: two concepts, one goal.” Forest Management Working Papers, Working Paper FM 25, Forest Resources Development Service, Forest Resources Division, FAO, Rome, 2003
- [3] United Nations General Assembly, 1992. Report of the United Nations Conference on Environment and Development (Rio de Janeiro, 3-14 June 1992) Annex III, A/CONF.151/26 (Vol.III)
- [4] TEEB, „TEEB – The Economics of Ecosystems and Biodiversity for National and International Policy Makers –Summary: Responding to the Value of Nature 2009.
- [5] Vihervaara et al., „Trends in Ecosystem Service Research: Early Steps and Current Drivers”*Ambio*. Jun 2010; 39(4): 314–324.
- [6] MA Millennium Ecosystem Assessment (2005): Ecosystems and Human Well-being: Synthesis, UNDP 2005
- [7] Bann C., Popa B.,”An assessment of the Contribution of Ecosystems in Protected Areas to Sector Growth and Human Well Being in Romania” UNDP, Bucharest, 2012
- [8] Popa et al, 2013.THE VALUE OF FOREST ECOSYSTEM SERVICES IN ROMANIAN PROTECTED AREAS – A COMPARATIVE ANALYSIS OF MANAGEMENT SCENARIOS, Bulletin of the *Transilvania* University of Braşov Series II: Forestry • Wood Industry • Agricultural Food Engineering • Vol. 6 (55) No.2 - 2013
- [9] Stancioiu P.T., Abrudan I.V., Dutca I., 2010. The Natura 2000 ecological network and forests in Romania: implications on management and administration. In: *International Forestry Review* 12(I): 106-113
- [10] UNDP, 2011. The Economic Value of PAs in Montenegro, final draft, UNDP GEF project Montenegro, 4279: Catalysing
- [11] Speech by His Royal Highness Prince Charles at the launch of Wild Carpathia 3 in Bucharest, on 30 October 2013, available at <https://www.gov.uk/government/news/romania-is-losing-three-hectares-of-virgin-forest-per-hour>

Effect of Secondary Pulp Mill Sludge Application as Soil Organic Amendment in Nitrate Leaching

J. Rato Nunes, F. Cabral, A. López-Piñeiro, L. Loures, and D. Becerra

Abstract— The pollution of groundwater with nitrates is nowadays one of the biggest environmental concerns of humanity. Indeed, when the level of nitrate nitrogen in water exceeds certain limits, there may be negative consequences for the environment and for human health, being of great importance to conduct studies that can contribute to the clarification of the factors influencing nitrate leaching.

This study was conducted under greenhouse conditions with the main goal of evaluate the potential effect of Secondary Pulp-Mill Sludge (SPS) application in nitrate leaching. Two representative Mediterranean agricultural soils, a Cambic Arenosol (cmAR) and a Cromic Cambisol (crCM) were used. Treatments included four sludge rates ranging from 0 to 40 g kg⁻¹ (equivalent of 0, 38, 88 and 120 Mg ha⁻¹). Sludge application significantly increased nitrate leaching. In what potassium concern, the SPS application decrease the potassium leaching in the Cambic Arenosol and have no effect on the potassium leaching in the Cromic cambisol.

Keywords—Soil amendment, Pulp mill, Nitrate leaching, groundwater pollution.

I. INTRODUCTION

ALL the existing pulp factories in Portugal already have a secondary treatment of their liquid effluent, leading to the production of huge quantities of cellulosic secondary sludge (Secondary Pulp-Mill Sludge) [1]. In Portugal alone the production of this kind of organic residue are estimate in more than 100.000 Mg per year [2], therefore it becomes urgent to find a technical and economically solution for the disposal of this potentially pollutant organic waste [3].

For this kind of organic material, with high content of easily biodegradable organic matter and alkalizing power, one of the most promising and viable alternatives is its use as a

J. M. Rato Nunes is with the Polytechnic Institute of Portalegre, C3I and the UIQA – Research Center of Environmental Chemistry. Superior Institute of Agronomy, Portugal. (corresponding author e-mail: ratonunes@esaivas.pt).

F. Cabral is with UIQA – Research Center of Environmental Chemistry. Superior Institute of Agronomy, Portugal. (corresponding author e-mail: fmcabral@isa.ulisboa.pt)

A. Lopez-Piñeiro is with UIQA – Research Center of Environmental Chemistry. Superior Institute of Agronomy, Portugal and UIQA – Research Center of Environmental Chemistry. Superior Institute of Agronomy, Portugal. (corresponding author e-mail: pinero@unex.es)

L. Loures is with the Research at the Centre for Spatial and Organizational Dynamics and with the Polytechnic Institute of Portalegre, C3I.

D. Becerra is with Área de Producción Vegetal, Escuela de Ingenierías Agrarias, Universidad de Extremadura.

agricultural fertilizer [4], mainly in acidic soils, the ones, as

referred by Santos [5], are dominant in Portugal and in all the Mediterranean basis.

However, this can't be considered as free of any inconvenient. In fact, this residue has a high level of nitrogen [3, 6]. Therefore during the mineralization process, the amounts of nitrogen liberated in to the soil are considerable and if there aren't any crops or natural vegetation that could use this nutrient, the risk or nitrate leaching are very high [7] and may be considered as one of the mail environmental risks of SPS use as agricultural fertilizer [8].

It was with the aim of contributing to the clarification of this issue, still surrounded by much controversy, that the authors conducted several tests, whose results are now presented.

II. MATERIAL AND METHODS

A. Soil

Two soils with different characteristics were used in the assay. Soil 1, from the region of Pegões (Portugal) is classified as Cambic Arenosol; soil 2, from the region of Castelo Branco (Portugal), is classified as Cromic Cambisol. The most important aspects of both soils composition is given in Table 1. Lease submits your manuscript electronically for review as e-mail attachments.

Table 1: Main Chemical Characteristics of the soils use in the trial

Characteristics		Soil 1	Soil 2
Organic matter	%	1,28	0,53
pH (água)		6,40	5,00
Total Nitrogen	mg.kg ⁻¹	421,62	387,37
Nitric Nitrogen	mg.kg ⁻¹	15,81	24,05
Ammonium Nitrogen	mg.kg ⁻¹	7,21	4,56
Phosphorus	mg.kg ⁻¹	25,00	18,00
Potassium	mg.kg ⁻¹	55,00	104,00
ECC	cmol(+)kg ⁻¹	3,73	9,09
BSR	%	65,14	18,26

B. Secondary Pulp Mill Sludge

The secondary pulp mill sludge used in the assay was obtain in Portucel production center located in Setúbal (Portugal). The most important aspects of its chemical composition are in Table 2.

Table 2: Main Chemical Characteristics of the soils use in the trial

Characteristics		SPS
humidity	%	84,17
organic matter	%	48,68
potassium	%	0,09
phosphorus	%	1,53
sodium	%	0,60
calcium	%	2,56
magnesium	%	0,26
total nitrogen	%	2,67
iron	mg.kg ⁻¹	3053,00
copper	mg.kg ⁻¹	22,75
manganese	mg.kg ⁻¹	4028,75
zinc	mg.kg ⁻¹	58,50
C / C		10,42
C / P		40,94

C. Experimental Design

Each of the four different amounts of SPS (0, 40, 80, 120 Mg ha⁻¹) were added to the two different soil types, leading to a total of 8 treatments. For each treatment we made 3 repetitions, leading to a total of 24 experimental units. The experimental design was a randomized block design, in which different types of soil were the blocks.

Statistical analyses of the results were made using the SPSS software, version 19. The multiple comparison of means were performed with the Scheffe test (significance level of 95%).

D. Procedures

The trial was carried out in pots with a Double wall made from white polyethylene, chemically inert. The pots are generally know as "Kick-Brauckman pots". These have 20 cm diameter in the upper part and 25 cm depth. These pots have a single orifice at its basal part to which a drainage system was adapted to collect all the drained water.

The pots were filled with 9 kg of the mixture of SPS and soil and then we sow 25 plants in each pot of wheat (*Triticum aestivum* L.) cv. Almansor.

The trial was conducted outdoors from 20th October to the 14th June, during this period the fluids drained internally by vessels were collected and were analyzed immediately.

Table 3: Amounts of Drained collected (L vaso-1)

	Soil 1				Soil 2			
	0 tha ⁻¹	40 tha ⁻¹	80 tha ⁻¹	120 tha ⁻¹	0 tha ⁻¹	40 tha ⁻¹	80 tha ⁻¹	120 tha ⁻¹
Before second fertilization	2,01b	2,00b	1,82ab	1,63a	2,68b	2,32ba	2,17ba	1,84a
After second fertilization	0,92a	1,18a	1,30a	0,99a	0,92a	0,31a	0,31a	1,08a
TOTAL	2,93a	3,18a	3,18a	2,62a	3,60a	2,63a	2,48a	2,92a

Note: for each soil, in each line, values followed by the same letter don't differ significantly between them self (P>0,95).

We fertilized, according to the bibliography) each pot with the normal amount of nutrients used in this kind of trials using potted wheat, more precisely 1.00 g K₂O Vase-1; 1.50 g P₂O₅ Vase-1; 1.25 g N Vase-1 (0.75 g at sowing and 0.25 g when

the plants had 4 leaf).

When it stopped raining, we irrigated the crop with small amounts of water in order to keep the crop until the end of its cycle. There was no longer any collection drained.

E. Analyses

We measure the amount of drained water, collected every times that it rains and in each of these fractions we analyzed the amount of total nitrogen, nitrate nitrogen and ammonium nitrogen (determined in a segmented flow auto-analyzer). Potassium were determinate by Egner-Riehm method using atomic absorption spectrophotometry for measurement.

III. RESULTS AND DISCUSSION

When starting the discussion of the results there are two points that should be emphasized. The first point concerns the fact that the SPS used in this trial have a particular composition which may differ markedly in composition of the SPS that the farmer will apply, thus making it imperative to examine the product before used. The second point concerns the precipitation occurred, which is obviously different between different years and which will, according to the authors consulted, have a remarkable influence the amount of leached nutrients.

A. Volume Drained

The water volume drained from the soil is given in Table 3. As we can see in the results the volume of drained collected in both soils, are independent from the amount of SPS applied.

However it appears that, prior to topdressing fertilization, the volume of drainage water collected was lower for higher doses of SPS applied. This result, with no statistical significance, could be due to the absorption capacity of this residue.

Comparing the results obtained in the two different soils we can notice that no significant differences can be observed with respect to the volume of collected drained. However soil 1 presents average values of drained water 6% higher than the soil 2, which can be explained by the lighter texture with higher permeability of the first one of these soils.

B. Nitrogen

We chose to jointly discuss the results relating to the losses in the nitrate and the ammonium forms of nitrogen, since their relationship is so evident (Table 4).

By analyzing in both soils the total nitrogen leached (obtained adding the nitrate and ammonium nitrogen leached) we found that this increases significantly with the application of SPS. According to Costa [9] this increase is mainly due to the increase in nitrate losses, since the losses of ammonium remained virtually constant between the various modalities in study (amounts of SPS applied).

It is noteworthy that the proportion of nitrate in total nitrogen leached (Figure 1) is substantially higher than the proportion of ammonium. This result is due to the fact that ammonium suffers a much greater physical retention in the soil colloids when compared with nitrates. For these last ones the physical retention in soils is nearly null [10].

in soil 2 in the treatment with no SPS application. In this treatment the amounts of nitrogen leached from the soil are substantially lower than the ones obtain in all the other treatments. This result, in our opinion, was due to the characteristics of this soil, which presenting very unfavorable conditions to nitrification, namely acid pH and low concentration of exchangeable bases, what could lead to some difficulties in the nitrification process and therefore the amounts of nitrate formed are lower than in the treatments. Because the nitrate is the main chemical form of nitrogen leached, this could explain why in this treatment the amount of nitrogen leached was significantly lower when comparing with the other treatments.

Table 4: Amounts of nitrogen leached from the soils – Total Nitrogen, nitrate and ammonium (mg Vaso-1)

	Soil 1				Soil 2			
	0 tha ⁻¹	40 tha ⁻¹	80 tha ⁻¹	120 tha ⁻¹	0 tha ⁻¹	40 tha ⁻¹	80 tha ⁻¹	120 tha ⁻¹
Nitrate								
Leaching BT	1,70 a	11,73 b	18,19 c	25,52 d	0,16 a	24,29 b	63,75 c	65,19 c
Leaching AT	2,81 a	6,04 a	9,70 a	31,22 a	0,18 a	0,09 a	0,14 a	28,30 b
TOTAL	4,51 a	17,77 b	27,89 b	56,74 c	0,34 a	24,38 b	63,89 c	93,49 d
Ammonium								
Leaching BT	0,45 c	0,37 b	0,29 a	0,25 a	1,64 b	0,43 a	0,45 a	0,28 a
Leaching AT	0,46 a	0,45 a	0,57 a	0,50 a	0,32 a	0,21 a	0,16 a	0,60 a
TOTAL	0,91 a	0,82 a	0,86 a	0,75 a	1,96 b	0,64 a	0,61 a	0,88 a
Mineral Nitrogen								
Leaching BT	2,16 a	12,10 b	18,47 b	25,77 c	1,80 a	24,71 b	64,20 c	65,47 c
Leaching AT	3,27 a	6,49 a	10,27 a	31,73 b	0,50 a	0,30 a	0,30 a	28,90 b
TOTAL	5,43 a	18,69 b	28,74 b	57,50 c	2,30 a	25,01 b	64,50 c	94,37 c

Note: for each soil, in each line, values followed by the same letter don't differ significantly between them self ($P > 0,95$).

Legend: BT – Before topdressing
AT – After topdressing

When compare the nitrogen leaching in the two different types of soils, we can notice that the total nitrogen lost from soil 2 is significantly higher than the total nitrogen lost from soil 1. This result can be due to the fact that the latter leaching of nitrate (after topdressing) was significantly lower in soil 1. One possible explanation for this result, unexpected for us, can be the fact that soil 1 texture could lead to a rapid water infiltration, and therefore the contact time between soil moisture and soil particles wasn't enough to allow an efficient washing of this nutrient, as described by other authors when refers to internal drainage preferential flow.

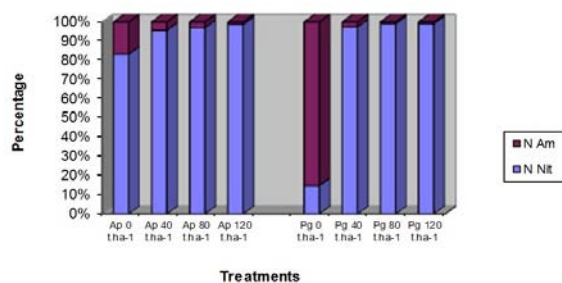


Figure 1 - Ratio of nitrate and ammonium leached in the total nitrogen lost from the soil

One result that we considered important is the one obtained

C. Potassium

The potassium leaching (Table 5) has a distinct pattern in the two analyzed soils. Thus, while in the soil 1, potassium losses decrease as the amount of SPS applied increased, with significant differences between the first and the others treatments, in soil 2 the results obtained for the various dosages of SPS were very close, and did not differ significantly from each other.

Comparing the two soils in study, it appears that the soil 1, originally poorer in this nutrient, drains significantly more potassium than soil 2 (over 230%). This result is due to the fact that the soil 2 have a higher cation exchange capacity and therefore could retain a larger amount of this cation in their colloidal surfaces. Note that this result, which we expected according to the soils characteristics, is the opposite of what was found in relation to ammonium ion. This explanation is now more in line with existing knowledge.

When comparing the results obtained before and after topdressing fertilization we could conclude that most of the potassium is leached after this agronomic operation, and approximately the same proportion in both soils (76% in soil 1 and 70 % in soil 2). The explanation for this result lies in the fact that we have added significant quantities of ammonium ion during topdressing operation, which, exchanging with

potassium previously adsorbed on colloidal surfaces, causes a noticeably increase in potassium concentration in soil solution and consequently in the amount of this nutrient leached.

Table 5: Amount of Potassium leached from the soil (mg Vaso-1)

	Soil 1				Soil 2			
	0 tha ⁻¹	40 tha ⁻¹	80 tha ⁻¹	120 tha ⁻¹	0 tha ⁻¹	40 tha ⁻¹	80 tha ⁻¹	120 tha ⁻¹
Before Topdressing	2,13 b	1,68 a	1,20 a	1,14 a	2,10 b	0,18 a	0,22 a	0,53 a
After Topdressing	12,36 b	5,14 a	3,89 a	2,37 a	0,92 a	1,12 a	3,53 a	0,81 a
TOTAL	14,49 b	6,82 a	5,09 a	3,51 a	3,02 a	1,30 a	3,75 a	1,34 a

Nota: Para cada um dos solos, numa dada linha, os valores seguidos da mesma letra não diferem significativamente entre si (P>0,95).

IV. CONCLUSIONS

The water volume leached were, in both analyzed soils independent from the amount of SPS applied.

The increase in the SPS doses applied to the soil, increases the amount of mineral nitrogen leached.

From the total amount of mineral nitrogen leached, 90 to 95% were nitrates and only 5 to 10% was ammonium.

The increase amounts of SPS applied in soil 1 leads to a significant decrease in the potassium leached. In soil 2, on the other hand, the application of successively larger quantities of SPS doesn't show any significant effect on the amounts of potassium leached over time.

REFERENCES

- [1] J. Santos and L. Falcão (1992) - Interesse fertilizante das lamas celulósicas. In Proceedings do Seminário "O Controle da Poluição nas Indústrias Agrárias: Benefícios Ambientais e Económicos" Lisboa.
- [2] APA - Agência Portuguesa do Ambiente (2012) - Anuário do Ambiente
- [3] J. Nunes (1996) - Interesse Fertilizante e impacte ambiental da aplicação de lamas celulósicas secundárias. Dissertação do Mestrado em Nutrição Vegetal, Fertilidade dos Solos e Fertilização. Univ. Téc. de Lisboa - Instituto Superior de Agronomia. Lisboa.
- [4] L. Falcão, F. Pinto, M. Alves and M. Rafael (1986) - Lamas celulósicas. Estudo da possibilidade do seu aproveitamento como fertilizante. In Proceedings do 1º Encontro nacional Sobre a Qualidade do Ambiente.
- [5] J. Santos (2013) - Fertilizantes – Aspectos práticos da sua utilização. Publicações Europa-América, Lisboa.
- [6] A. Varennes (2003). Produtividade do solo e ambiente. Escolar editor. Lisboa.
- [7] T. Addiscott and R. Wagenet (1985) - Concepts of solute leaching in soils: A review of modelling approaches. J. of Soil Sci.,36, pp 411-424.
- [8] F. Cabral, E. Vasconcelos and J. Santos (1990) - Utilization of pulp-mill sludges as fertilizers to wheat crop (*Triticum aestivum* L.). In Proceedings of I Congress of European Society of Agronomy, session 1, Paris, pp. 39.
- [9] I. Costa (1993) - A influência das lamas celulósicas na lixiviação de nitratos do solo. Trabalho realizado como relatório do trabalho final do curso de Engenharia Agronómica. Inst. Sup. Agron.. Lisboa.
- [10] L. Zibilske (1987) - Dynamics of nitrogen and carbon in soil during papermill sludge decomposition. Soil Science, 143(1), pp. 26-33.

Tisza River Modelling on the common interest section of Hungary and Serbia

Srdjan R. Kolakovic¹, Slobodan S. Kolakovic², Goran B. Jeftenic³, Borislav T. Masic⁴, Svetlana R. Vujovic⁵

Abstract—This work describes the methodologies used in performing the one-dimensional flow calculations within HEC-RAS. With HEC-RAS we perform one-dimensional water surface profile calculations for steady gradually varied flow in natural or constructed channels. Subcritical, supercritical, and mixed flow regime water surface profiles were calculated. We also used equations for basic profile calculations; cross section subdivision for conveyance calculations; composite Manning's n for the main channel; velocity weighting coefficient alpha; friction loss evaluation; contraction and expansion losses; computational procedure; critical depth determination. This produced a prognostic-simulation model that links the whole catchment area of the Tisza river from Ukrainian borders to Tisa river inflow into the Danube in Serbia provides an integrated approach to the problems of water control. The model enables integrated management of river systems in both countries and the regulation of the impact of high water.

Keywords—hydraulic calculation; Tisza river model;

I. INTRODUCTION

BECAUSE of its returning and gradually increasing, and sometimes extremely high floods as well as of recurring and lasting low water periods the River Tisza is considered to be the most variegated river in this part of Europe. Characteristics of the river decisively originate from the shape of the catchment system, from the relation between the water output of tributaries and that of the main stream, from the considerable amount of drift and stream deposit, from the slight slope on the long lowland section of the river, from the extreme climate and from the regulation of both low and high water bed.

The effects of human interventions can be demonstrated along each stream kilometre of the Tisza as well as on each

square kilometre of its catchment system. The run-off conditions of flood waves have changed across the full water level range. The river, practically from its region of source down to the mouth flows between embankments. On the catchment area of the River Tisza there are a number of head works, both public and industrial or agricultural with different purposes. Total joint capacity of these head works exceeds the water output of the river in the Tisza Valley at the time when conditions of low water are prevailing. River Tisza, with its catchment area of 157.200 square km is considered to be the most important tributary of the water system of the River Danube. Approximately 30 percent of the total catchment area of the River Tisza lies on the territory of Hungary while the further 70 percent is to be found on the territory of Slovakia, Ukraine, Romania and the Serbia [7].

Most of the river basin area is covered by impermeable (magmatic, metamorphous) rocks, and by semi-permeable (tufaceous, foliated, marly) layers as well as soils of different permeability over these formations [7].

Vegetation cover has an important role in the soil protection. Considerations on the role of forests on the catchment area are rather different. According to certain professionals the forests are not able to significantly reduce the run-off of waters deriving from rainfalls of extremely high intensity. Differences in some percentage of forest covered areas have no significant affect on to the run-off. However, the reduction of forest covered area up to more ten percents results in considerably increased collection of water and erosion [3]. At the beginning of 1900s 5 to 8 percent of the flood plain was covered by forest, while this proportion reaches up to 40 to 60 percent today. This difference, however, considerably decreases the water discharge ability of the river in case of high-waters [7].

II. METHODOLOGY

A. Climate conditions of the catchment system

In the formation of climate conditions on the catchment area of the River Tisza there are four air mass groups playing a decisive role. The arctic continental air having lower moisture content, but delivers air waves being cooler by 10 to 15 °C. Air waves arriving from the northern section of the moderate belt, i.e. from the Atlantic Ocean deliver milder air in winter and cooler in summertime as compared to that of the Carpathian Basin, however, with higher humidity in both cases. Air masses from inside the Eurasian continent deliver rather cold

This work was supported by IPA Cross-border Co-operation Programme (ID: HUSRB/0901/121/060) and Ministry of Education and Science, Republic of Serbia (Grant No. TR 37003, TR 37018).

¹ PhD Srdjan R. Kolakovic, grad.civ.eng, Faculty of Technical Sciences, University of Novi Sad, Serbia, (e-mail: kolak@uns.ac.rs).

² MsC Slobodan S. Kolakovic, grad.civ.eng, Faculty of Technical Sciences, University of Novi Sad, Serbia, (e-mail: cole86grb@gmail.com).

³ MsC Goran B. Jeftenic, grad.civ.eng, Faculty of Technical Sciences, University of Novi Sad, Serbia, (e-mail: goran.jeftenic@yahoo.com).

⁴ MsC Borislav T. Masic, grad.civ.eng, Faculty of Technical Sciences, University of Novi Sad, Serbia, (e-mail: boramasic@gmail.com).

⁵ MsC Svetlana R. Vujovic, grad.civ.eng, Faculty of Technical Sciences, University of Novi Sad, Serbia, (e-mail: svetlanavjvc@yahoo.com).

and dry air in winter period and that of slightly warming character in summertime. The fourth group of air masses is constituted by warm zone air, i.e. the one arriving through the Mediterranean Sea. Arrival of these air waves is accompanied by warming up and regularly by rainfalls.

The average temperature on the catchment area of the River Tisza varies between 1 °C and 11 °C, depending on regional location and altitude. Extreme values of the temperature reached -36 °C and +41 °C. The extent of evaporation is in close relation with the temperature of the air. On the Great Hungarian Plain the maximum annual value of evaporation exceeds 700 mm. The value of aridity factor, i.e. the quotient of annual evaporation and precipitation, exceeds 2 in extremely droughty years [7].

B. Remarkable floods on the River Tisza

In the Figure 1 we demonstrated the height of significant flood waves culminating over 800 cm that were measured at four water gauges on the River Tisza with the indication of the year, the number of years elapsing between them as well as the time differences of breaking the records [1].

At the section at Vásárosnamény, there was the longest period lasting for 15 years between 1947 and 1962, when there was no flood wave over 800 cm. This was characteristic between 1941 and 1964 (23 years) at Tokaj, between 1895 and 1915 (20 years) at Szolnok, while between 1941 and 1962 (21 years) at Szeged. During the past couple of years there were flood waves over 800 cm relatively frequently. However, at the section at Tokaj, Szolnok and Szeged, there were no such hydro-meteorological conditions between 1981 and 1998 (in case of Szeged between 1981 and 1999) which should have

provided conditions for development of flood waves exceeding 800 cm. The flood wave in the year 1855 was an important station in the history of floods in the Tisza Valley as well as in that of flood prevention arrangements; its extraordinary dimensions have applied pressure on the government for taking measures considering the matter of regulations. This event may be considered as the last flood before the regulation works; and following this the flood levels have considerably increased as a result of raising embankments and decreasing the area of the flood plain. Between the years 1998 and 2010, there were six disastrous flood waves following each other that stand without reference in the history of floods on the River Tisza and, have unavoidably arisen the reconsideration of flood prevention measures both in domestic and international relation.

C. Hydrological, hydraulic and statistical surveys

Because of its returning and gradually increasing, and sometimes extremely high floods as well as recurring and lasting low waters the River Tisza is considered to be the most variegated river of our country. Characteristics of the river decisively originate from the shape of the drainage system, from the relation of water output of tributaries to the main stream, from the considerable amount of drift, from the small slope on the long lowland section and from the regulation of both low and high water bed. Current length of the River Tisza is 945.8 km; its catchment area covers 157.200 square km. According to the measurements of past decades the maximum water discharge of the river at the Tivadar section (705,7 stream-km) exceeds the value of 4.000 m³/sec, in the middle section, between Kisköre and Szolnok it is between 2.600 and

Vásárosnamény				Tokaj				Szolnok				Szeged			
Year	Culmination	Differences in years	Difference of years in record breaking	Year	Culmination	Differences in years	Difference of years in record breaking	Year	Culmination	Differences in years	Difference of years in record breaking	Year	Culmination	Differences in years	Difference of years in record breaking
1888	900			1888	872			1888	818			1888	847		
1895	840	7		1895	815	7		1895	827	7	7	1889	805	1	
1915	830	10		1915	825	20		1915	808	20		1895	884	6	7
1919	850	4		1919	860	4		1919	884	4	24	1913	802	8	
1932	848	13		1924	802	5		1924	846	5		1919	916	6	20
1940	802	8		1932	856	8		1932	894	8	13	1924	872	5	
1947	885	7		1940	818	8		1940	880	8		1932	923	8	13
1962	816	15		1941	800	1		1941	856	0		1940	847	8	
1964	850	2		1964	857	23		1953	801	12		1941	855	1	
1968	800	4		1967	831	3		1962	836	9		1962	820	21	
1970	912	2	82	1970	858	3		1964	853	2		1970	960	8	38
1974	848	4		1979	880	9	91	1966	855	2		1974	804	4	
1978	870	4		1980	837	1		1967	881	1		1979	842	5	
1979	853	1		1981	805	1		1970	909	3	38	1981	873	2	
1981	834	2		1998	872	17		1974	840	0		1999	817	18	
1985	831	4		1999	894	1	20	1977	880	3		2000	930	1	
1993	876	8		2000	928	1	1	1979	904	2					
1995	843	2		2001	847	1		1980	873	1					
1998	923	3	28					1981	885	1					
1999	830	1						1998	897	17					
2000	882	1						1999	974	1	29				
2001	941	1	3					2000	1041	1	1				

Fig. 1 Significant floods in the Tisza Valley

2.900 m³/sec, while in the lower section, i.e. at Szeged (173,6 stream-km) it is over 4.000 m³/sec. Before the regulation works the River Tisza was a strongly meandering stream with a small slope [1].

In the course of years between 1998 and 2001 such flood waves subsided on the River Tisza which have never been experienced before. The values of culminations have exceeded the previous maximum values by 130 to 140 cm. These new flood waves of critical height resulted in the reconsideration of flood prevention alongside the River Tisza.

D. Hydro-meteorological factors

The coincidence in time of flood waves of the River Tisza and those of tributaries basically determine the values of culminating water levels.

The Figure 2 represents the time series of flood waves in the sections at Vásárosnamény and Szolnok related to the years 1888 and 2000. In the illustration the different water mass and water level difference can be very well observed in the two sections between the flood waves in 1888 and 2000.

of the flood wave in March, 2001, the snow cover of 2 cubic km on the catchment area played a important role, however, the flood wave was the result of heavy rainfalls. In 2001, similar to the autumn flood wave in 1998, the heavy rainfall (124.5 mm between 3rd and 5th March) was the generator of the fierce flooding. These two flood waves resulted in a high, but not authoritative water level increase on the middle section of the River Tisza.

E. Water discharge ability of the bed

We can best and most accurate demonstrate the water discharge ability of the bed by analysing of water outputs. Figure 3 demonstrates the water output measurements on the occasions of floods with outstanding dimensions in the years 1895, 1932, 1970, 1979, 1999 and 2000.

There is a considerable difference to be observed among the loop curves drawn up on the base of measurement results, but there can also be similarities explored sometimes. The maximums of water discharge measures in 1895 ($H_{\max} = 827$ cm) and in 1932 ($H_{\max} = 894$ cm) were similar and exceeded

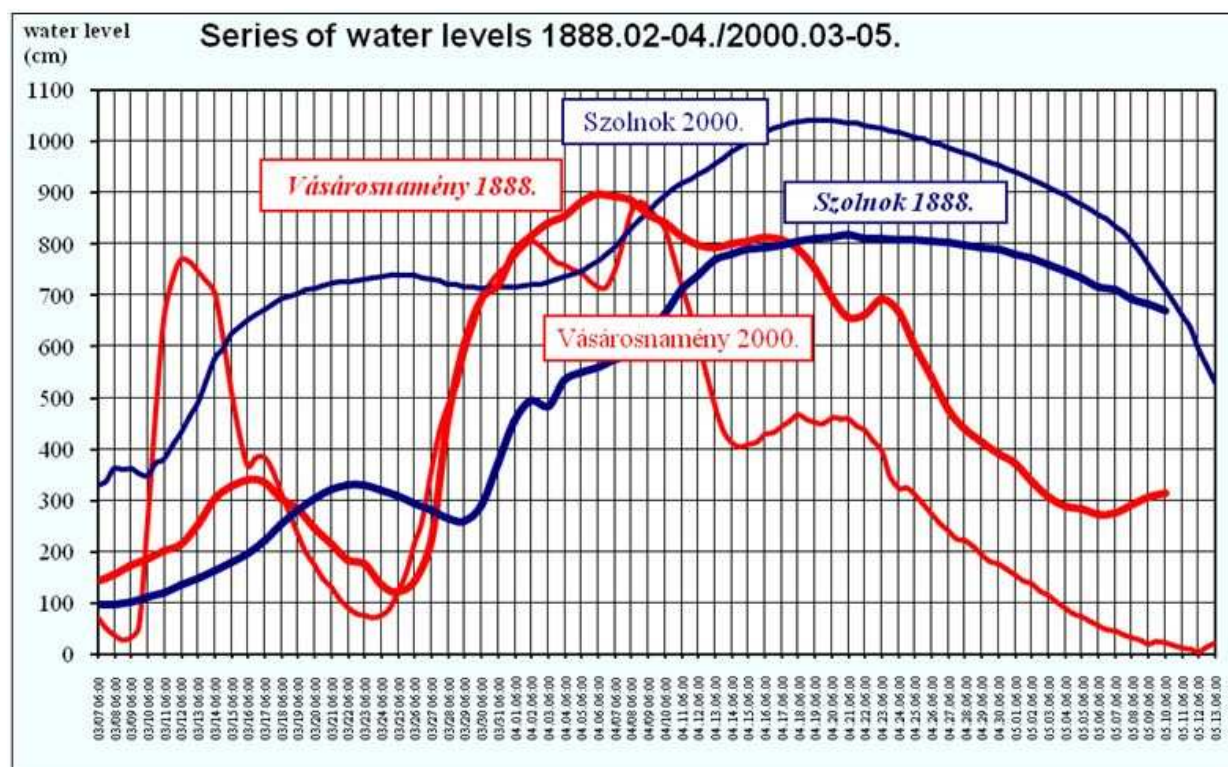


Fig. 2 Water level curves of flood waves in 1888 and 2000

In 1999 and 2000, there were long lasting flood waves exceeding the authoritative level on the Middle-Tisza section. However, in 1998 and 2001, there were extremely high flood waves on the Upper-Tisza. The autumn flood wave in 1998 was exclusively generated by the heavy rainfalls. In the periods between 25th and 31st October and 1st and 5th November, 1998 there was a rainfall with 136.9 mm on the entire catchment area of the Upper-Tisza. In the development

the value of 3.100 m³/sec. (In 1932, it was possible to measure only close to the maximum water level.) The maximum water level was less by 140 m³/sec in 1932 than in 1895; despite of it the culmination of water level occurred higher by 67 centimetres. Between 1895 and 1932, there were 37 years elapsing. During this period of close to four decades new, short embankments were built to regulate the overbank. The increase of water levels can be explained by the change of

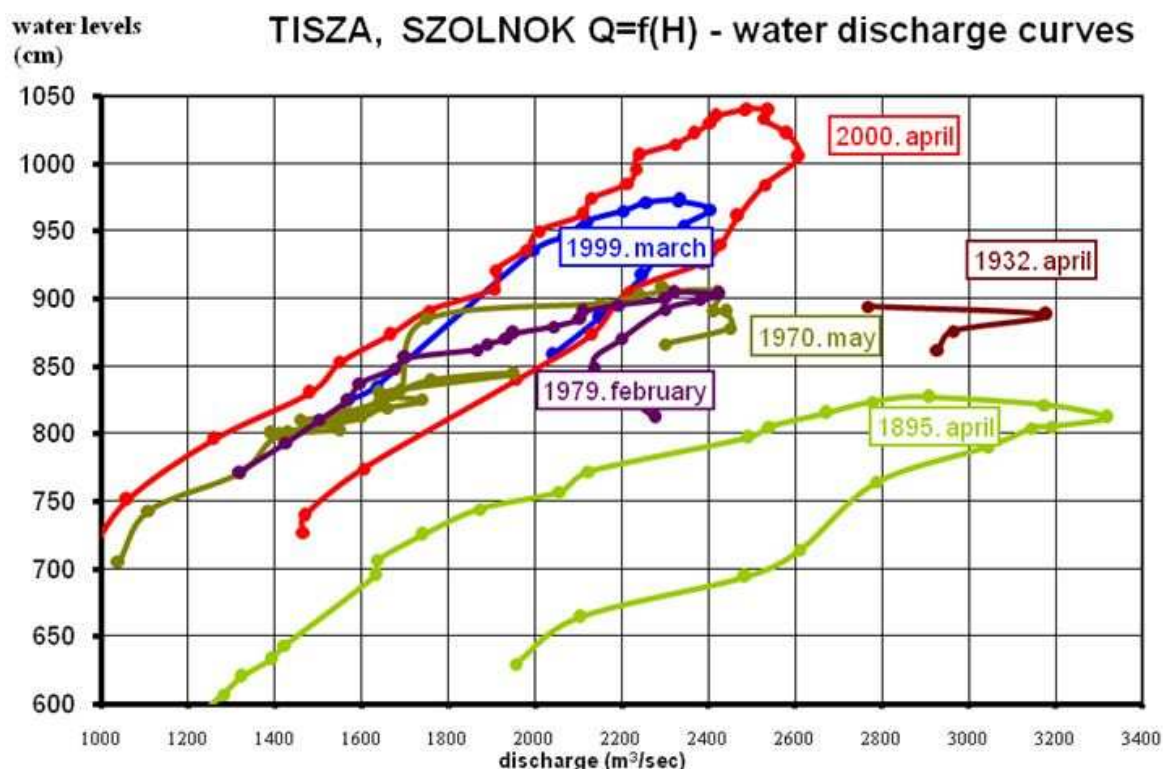


Fig. 3 Water discharge curves on the River Tisza at the Szolnok section (334,6 stream-km)

water discharge ability of the bed. In the course of the flood wave in 1919, unfortunately, there was no opportunity to accomplish water output measurements.

The measurement results obtained in 1970 ($H_{\max} = 909$ cm) and in 1979 ($H_{\max} = 904$ cm) were very resembling to each other considering both water levels and water output. To the culminations that slightly exceeded the 900 cm there were water outputs belonging over $2.400 \text{ m}^3/\text{sec}$. Between 1932 and 1970, there were 38 years elapsing. (Almost exactly as many years as between 1895 and 1932.) However, the culminating water levels in 1970 and 1979 that slightly exceeded the values of 1932 occurred at water outputs that were less by 400 to $500 \text{ m}^3/\text{sec}$.

In the course of flood waves of the past years considerably higher maximum water levels developed. In 1999 ($H_{\max} = 974$ cm) there were resemble water outputs measured to those of 1970 and 1979, however, at a water level being higher by 65 cm. In the course of the flood wave in 2000 ($H_{\max} = 1041$ cm) the maximum water output was $2.600 \text{ m}^3/\text{sec}$. The steepness of (water output) loop curves gradually increases with the progress of decades. It has to be mentioned that for 1 cm increase of water level in the range over 800 cm it is only a water output of $3,5 \text{ m}^3/\text{sec}$ enough in the river section at Szolnok.

Effects of flood reduction and the improvement of water discharge ability at high water have been based by scientific surveys.

Within surveys the numerical hydraulic calculations constituted a part of overriding importance including also 1D and 2D hydrodynamic model running.

III. RESULTS AND DISCUSSION

In this paper we shortly summarize our 1D hydrodynamic modelling activities serving as a base for further planning. The modelling has been accomplished by applying the HEC-RAS software [4].

A. The stream network of the 1D model

In its current structure, the database of the model includes the 403 km long river section between Kisköre and Titel, as well as the 7 tributaries mouting into the main stream, reaches is 13. The total length of streams involved into calculations exceeds 762 km (Figure 4.). We have approached the stream system of the River Tisza and its tributaries by more than 1.200 cross sections. We installed 62 bridges, inline structures 1, lateral structures 5 and 12 storage areas (flood reducing structures) into the model [1].

The HEC-RAS model applied for the detailed description of the entire river system provides an opportunity for taking into consideration the hydraulic engineering structures, as well like bridges, barrages, culverts, overflow weirs, floodgates, bottom stages, bottom sills, side overflows and gates, static reservoirs, pump head stations and water intakes [5].

B. Roughness (smoothness) coefficient

For calculation of the water discharge capacity of the main bed as well as for taking the flood plain cultivation branches into consideration we used the roughness (smoothness) factors given in the Figure 5. in the course of calibration of the model [7].



Fig. 4 Stream network of the River Tisza in the mode, from Kiskore to Titel

Serial No.	Type	n (s/m ^{1/3})		k (m ^{1/3} /s)	
		min	max	min	max
0	Main bed	0.060	0.017	16.67	58.8
1	Grazing ground	0.050	0.025	20.00	40.0
2	Plough-land	0.050	0.020	20.00	50.0
3	Sparse thicket	0.080	0.035	12.5	28.6
4	Dense thicket	0.160	0.040	6.25	25.0
5	Forest without undergrowth	0.120	0.030	8.33	33.3
6	Forest with undergrowth	0.200	0.080	5.00	12.5
7	Rough pebbles	0.070	0.030	14.3	33.3

Fig. 5 Roughness / smoothness coefficients

After having determined the value ranges of basic data and smoothness factors we agreed in the following calibration procedure, or convention, respectively [1]:

We determined the longitudinal variation of the smoothness factor in the main bed for such flood waves which advanced toward but did not exceed the first prevention grade (the river is still in the main bed). Through appropriate selection of the smoothness factor we were able to model the main bed water levels with sufficient accuracy in the region of the first prevention grade. At the same time, we accepted that this convention results in greater failure in the range of low waters.

Crosswise on the flood plain we determined zones of same smoothness and assigned the mean values of above smoothness categories to them. When determining these flood

plain zones, based upon a good engineering estimation, we took into consideration also the roughness conditions of the sections between the two adjacent zones, i.e. the width of individual zones was taken as an average width related to the certain sections.

After this we completed the high water calibration of the model in a manner that we changed the smoothness factors assigned to the flood plain zones, related to a certain section of the Tisza, while paying attention for remaining within the smoothness ranges given in the above table. (Figure 6).

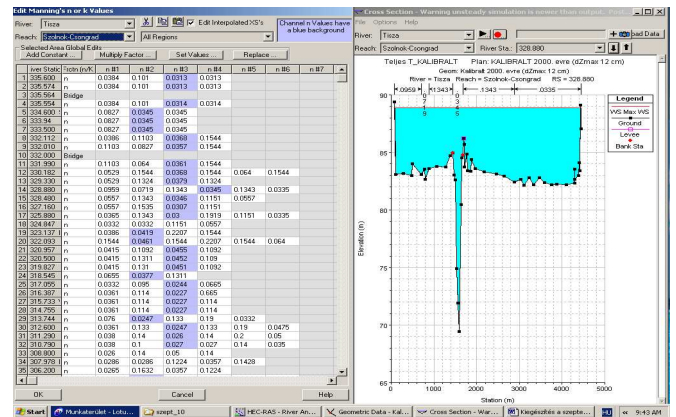


Fig. 6 Detailed demonstration of roughness factors in the cross section

In the course of flood waves the depth of the main bed reaches 24 to 26 m at many places, especially in river bends. In case of such water depths it is necessary to divide the water movement, i.e. to create also vertical layers. As soon as the water reaches the height of the bank edge, the branches of trees protruding into the water are decreasing the movement or flow rate of the water. In the case of meandering rivers with flood plain the flow conditions are modified vertically to a great extent by the coinciding waters passing along the main bed and on the flood plain (Figure 7).

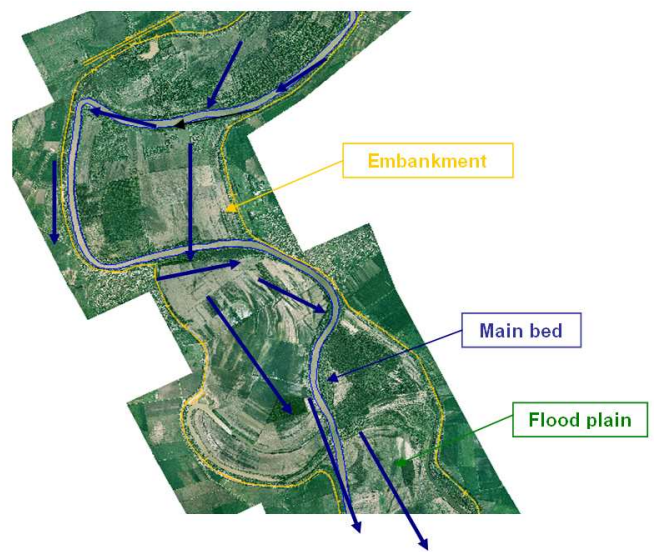


Fig. 7 Bird's eye view on the bed of the River Tisza

The results of water discharge measurements in the course of flood waves have proven the need of vertical modification of the roughness factor. The results of measurements and calculations related to the main bed and the flood plain at the Szolnok section of the Tisza are demonstrated in Figure 8. On the base of measurements accomplished in the course of 1998 and 2001 the roughness factors varied between 0,026 and 0,032 in the main bed. The shape of curves drawn up according to individual flood waves deviate from each other. In 1998, the value of the roughness coefficient increased with the increase of water level; however, it gradually decreased in the year 1999. In the course of the flood wave in 2000 we experienced an increase in the range between 350 and 750 cm, a decrease in that of 750 and 950 cm, then again an increase of the roughness factor in the range between 950 and 1040 cm [1].

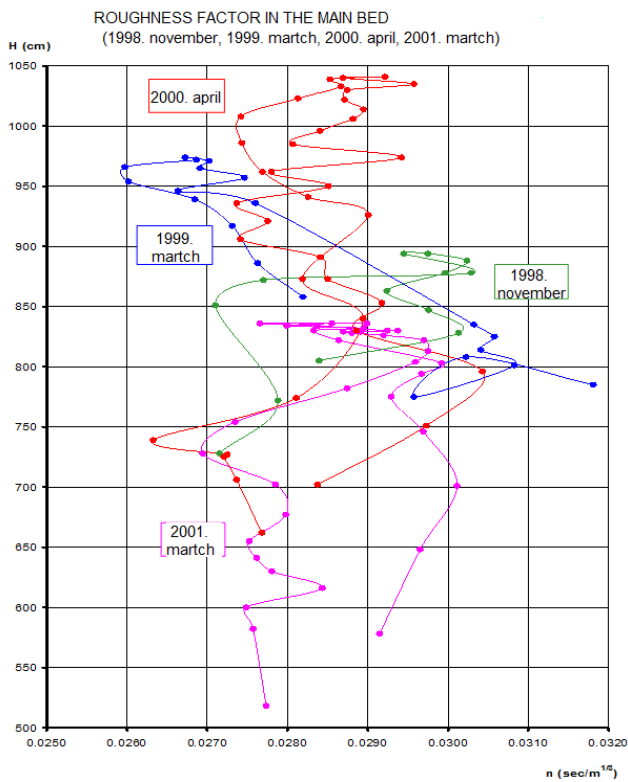


Fig. 8 Development of the roughness factor in the main bed of the River Tisza

C. Hydrological basic data and limiting conditions

The hydrological database for the first part of calculations included the values of hourly water levels (Z), the water outputs (Q) of flood waves 2006 [10]. Over the above mentioned data, we developed also almost 50 time series of 1 hourly water levels having measured at standard measuring posts and at those of dam keepers for the calibration and verification of the model. It has been emphasized on more forums that the fundamental aim of regulations of flood plains consists in the possible restoration of water discharge ability of the River Tisza prior to the year 1970 [2,3]. On the river section between Kisköre and the southern confines of the country, within the framework of transformation of land use on

flood plains we plan to clean out the high water run-off stripe, the so called hydraulic corridor, the demolition of summer dikes, the formation of hollow-chamfers that follow the track of drift line and improve the water discharge performance[6].

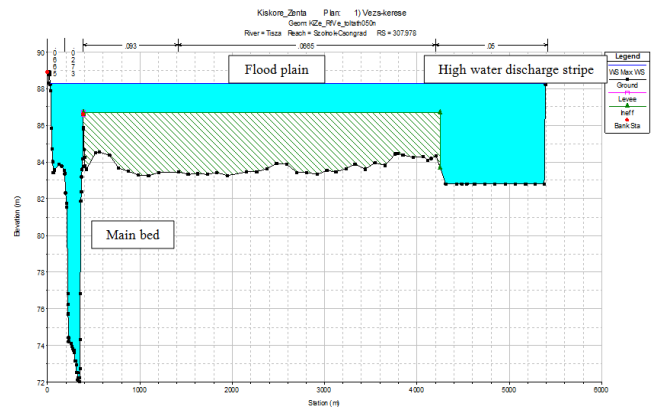


Fig. 9 Regulation of the flood plain

An important part of the analyses is the comparison between the authoritative flood levels with those developing as an effect of intended interventions.

IV. CONCLUSIONS

The calculations performed with flood plain interventions demonstrate very well, that there will still be a river section (between the 278 and 302 stream-km) where the envelope of maximum water levels is above the authoritative flood levels even after the accomplishment of planned interventions [1]. The natural decrease of water discharge ability is considerable in the bed of the River Tisza as well as on the flood plain related with it. The interventions on short sections may mitigate the local problems only for a short time. Following the survey in connection with interventions on flood plains we accomplished the examinations related to reservoirs, or groups of reservoirs with and without flood plain interventions. Within framework of the first cycle of the “Update of the Vásárhelyi Plan” program there are 6 reservoirs designated. We performed the survey of reservoirs both for the authoritative historical flood waves and for the synthetic, so called generated flood waves, too. The number of model runs exceeded the 300 [1]. What has been done in the survey with and without flood plain interventions (related to the authoritative conditions of the past) of the 6 reservoirs designated for the first phase of the development is shown below [1,6]:

We accomplished the survey related to the flood plain interventions and their possible effect on reservoirs with flood waves of different character. In this paper we introduce only those runs that were accomplished for the flood waves of the years 2000 and 2006. According to this, the flood plain interventions and the flood decreasing effect of reservoirs have demonstrated differences.

In the case of the flood wave of the year 2000 the maximum decrease of water level would be close to 160 cm as a result of flood plain interventions and the effect of opening the reservoirs. The results of the modelling have been shown in the Figures 10 and 11.

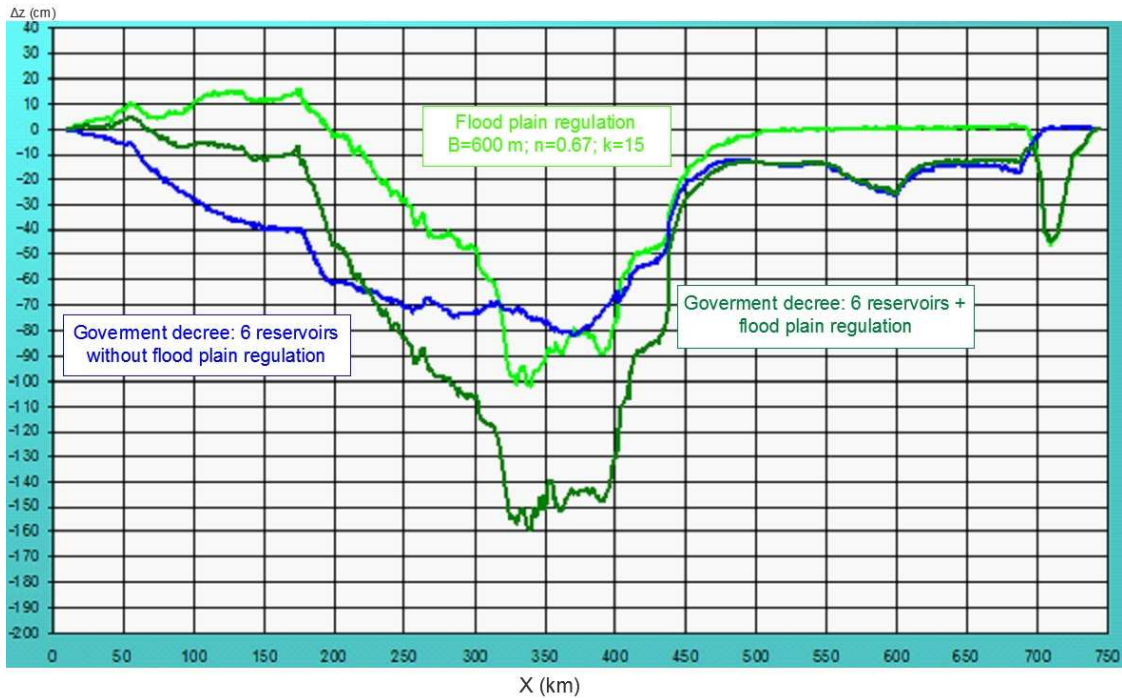


Fig. 10 Effect of the 6 reservoirs, designated in the government decree, with and without flood plain regulation in case of the flood wave in the year 2000

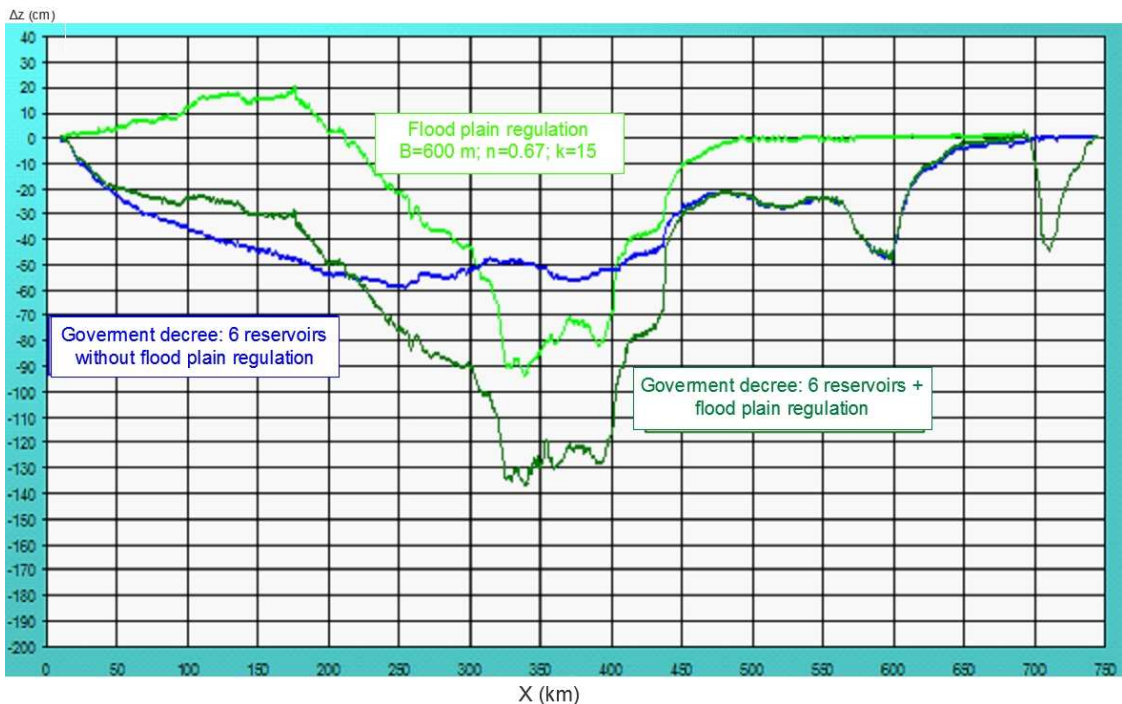


Fig. 11 Effect of the 6 reservoirs, designated in the government decree, with and without flood plain regulation in case of the flood wave in the year 2006

In the case of the flood wave of 2000 the degree of water level decrease would reach 160 cm as a result of joint effect of reservoirs and the flood plain regulations. With putting the flood time reservoirs into operation we can compensate the water level increasing effect of flood plain regulations on the lower section of the Tisza, below Algyó.

Improvement of flood prevention safety along the Tisza Valley can unanimously be determined in the reduction of flood levels which can be performed by increase and opening

of flood plains on areas where the geomorphologic, economic and socio-geographical conditions as well as the infrastructure make it possible. Also through the improvement of water discharge ability of the high water bed and through the realization of a flood level reduction reservoir system on the Hungarian flood plain in case the flood level reduction of disastrous floods should be accompanied with the reactivation of the inundation area by controlled water discharge.

The relation between the water discharge ability of the high water bed and the flood level, especially the culmination, is rather complicated in the case of the River Tisza. Further on, it is of decisive importance that flow related conclusions and the calculations of water discharge lead to reliable results only in case of advancing from below to upwards and by taking the storage process into consideration. For this reason the interventions have been exposed to thorough hydraulic, fluid mechanical examinations constituting the fundamentals of selection of most pressing and effective interventions. The task of the program is to promote the society controlled restoration of the relation between the river and its inundation area. At the same time it makes a proposal for land use and infrastructural developments which are supporting the improvement of living conditions of residents in the sub-regions [2,5].

ACKNOWLEDGMENT

This work is supported by IPA Cross-border Co-operation Programme (ID: HUSRB/0901/121/060) and Ministry of Education and Science, Republic of Serbia (Grant No. TR 37003, TR 37018).

REFERENCES

- [1] Directorate for Environmental Protection and Water Management of Lower Tisza District, *Tisza River Modelling on the common interest section of Hungary and Serbia and developing of the measuring equipment*, Project ID: HUSRB/0901/121/060, Hungary, 2010-2012.
- [2] Sr. Kolaković, *Some Operational Aspects of the Defence System against External and Inland Waters in Vojvodina*, Monograph, Novi Sad University, Faculty of Technical Sciences, Serbia, 2003.
- [3] S. Kovács, *Improvement of the flow carrying capacity of the flood-channel*, Dutch-Hungarian workshop, Szolnok, Hungary, 2003.
- [4] S. Kovács, *Experiences in Application of HEC-RAS Model under Circumstances of Flood Waves*, NATO Advanced Research Workshop, Ostrov u Tise, Czech Republic, 2004.
- [5] S. Kovács, *Modelling the River Tisza by using one-dimension hydro-dynamic model*, Third International Symposium on Flood Defence, Nijmegen, The Netherlands, 2005.
- [6] S. Kovács, *Forecast and hydraulic models in relation with the planned Tisza reservoirs*, XXIII Conference of Danubian Countries on the Hydrological Forecasting and Hydrological Bases of Water Management, Beograd, 2006.
- [7] S. Kovács, *A Tisza lefolyásviszonyainak elemzése (Analysis of the Tisza river runoff relationship)*, Mérnök Kamara Újság, Budapest 4, 2007.
- [8] R. K. Price, Z. Vojinović, *Urban Flood Disaster Management*, Urban Water Journal, 5 (3), 259-275, 2008.
- [9] Lj. Savić, *Principles of Hydraulic Engineering Design*. Beograd University, Faculty of Civil Engineering in Beograd, Serbia, 2003.
- [10] 2006. március - május havi árhullám levonulása a Közép-Tiszán (The passing of flood wave in 2006th March to May on the medium section of Tisza river), XXV. MHT Vándorgyűlés 2007, Tata, Hungary.

Statistical Analysis of Low Flows in Eastern Slovakia

M. Zeleňáková, P. Purcz, T. Soľáková, and D. Simonová

Abstract—The article presents a statistical analysis of low flow in water streams in Eastern Slovakia. The main objective was to identify low flow trends in the selected 63 river stations in Eastern Slovakia in time period 1975-2012. The Mann-Kendall non-parametric test was used to detect trends in hydrological time series. Statistically significant trends have been determined from the trend lines in each month of hydrological year for the whole territory of Eastern Slovakia. Statistical tests can detect the existence of trends in hydrological time series. Non-parametric Mann-Kendall test has wide application in testing of hydro-meteorological characteristics. The results confirmed the rising incidence trends of decreasing of low flows in the streams in Eastern Slovakia in river catchments Poprad, Hornád, Bodva a Bodrog.

Keywords—Hydrological drought, low flow, Mann-Kendall test, trend analysis.

I. INTRODUCTION

THE sustainable use of water is a priority question for water scarce regions and for agriculture in particular. Imbalances between availability and demand, degradation of surface and groundwater quality, inter-sectorial competition, inter-regional and international conflicts, all bring water issues to the foreground. In fact, developments in controlling and diverting surface waters, exploring groundwater, and in using the resources for a variety of purposes have been undertaken without sufficient care being given to conserving the natural resource, avoiding wastes and misuse, and preserving the quality of the resource. Thus, nowadays, water is becoming scarce not only in arid and drought prone areas, but also in regions where rainfall is relatively abundant. Scarcity is now viewed under the perspective of the quantities available for economic and social uses, as well as in relation to water requirements for natural and man-made ecosystems. The concept of scarcity also embraces the quality of water because degraded water resources are unavailable or at best only marginally available for use in human and natural systems [1].

This work has been supported by the Slovak Research and Development Agency SK-PT-0001-12.

M. Zeleňáková is with the Technical University of Košice, Institute of Environmental Engineering, Vysokoškolská 4, 042 00 Košice, Slovakia (corresponding author to provide phone: +421-55-602 4270; e-mail: martina.zelenakova@tuke.sk).

P. Purcz and T. Soľáková are with the same university (e-mail: pavol.purcz@tuke.sk; tanik@post.sk). P. Purcz is assistant lecturer and T. Soľáková PhD student in external form

H. Hlavatá is with the Slovak Hydrometeorological Institute, Ďumbierská 26, 042 00 Košice, Slovakia (e-mail: helena.hlavata@shmu.sk).

Owing to the rise in water demand and looming climate change, recent years have witnessed much focus on global drought scenarios. As a natural hazard, drought is best characterized by multiple climatological and hydrological parameters. An understanding of the relationships between these two sets of parameters is necessary to develop measures for mitigating the impacts of droughts [2].

Hydrological drought is a phenomenon which rise with existence of occurrence of no- precipitation period coupled with extreme temperatures [3]. The genesis of hydrological extremes also affects the morphological conditions of origin, climatic factors, geological and hydrogeological conditions and anthropogenic activities [4], [5], [6]. This type of drought is defined by long-term decrease in levels of surface water bodies (e.g. rivers, lakes, reservoirs and other) and drops in groundwater levels [7]. Low water content is proof of this type of drought [8].

The task of this paper is to identify statistically significant trends in stream flow characteristics of low water content in the eastern Slovakia, which could be used in the evaluation of hydrological drought. Methodology for evaluating hydrological drought is based on statistical analysis of observed low stream flows at gaging stations. Mann-Kendall statistical test identifies the frequency of low stream flow trends. Obtained results from the statistically significant trends in the stream flows can be the basement for the regionalization of the eastern Slovakia territory from the point of hydrological drought risk.

II. MATERIAL AND METHODS

A. Study area

Study area is situated in the eastern Slovakia. There are located 63 gaging/river stations in four river basins – Hornád, Poprad, Bodva and Bodrog.

The morphological type of Poprad river basin and is dominated by rolling hills and higher uplands as terrain in the Hornád valley which downstream is situated in lower uplands. The morphological type of the Bodrog river basin relief is hilly in the northern part and flat in the southern part. Bodva basin is predominantly flat.

These river basins have varied climatic conditions. Precipitations are highly differentiated. The highest annual totals are mainly in the northern and eastern border mountains (Poprad and upper part of Bodrog and Hornad) where rainfall

totals are about 1000 mm. Decrease in total precipitation is quite marked directly to the south, where annual totals fall to below 800 mm (Bodva and lower part of Bodrog and Hornad). These territories rank among the driest in the eastern region (550 mm rainfall per year) [9], [10].

B. Data

The first step in the evaluation was to obtain values of the monthly low flow for selected gaging stations. Hydrological data were provided by Slovak Hydrometeorological Institute Regional Centre Košice, at monthly intervals during years 1975-2012.

C. Statistical analysis

A statistical hypothesis is an assumption about the distribution of a random variable generally. A statistical test of the hypothesis is a procedure which is used to find out whether we may “not reject” (“accept”) the hypothesis, that is, act as though it is true, or whether we should “reject” it, that is, act as though it is false.

The Mann-Kendall test is a non-parametric statistical test. That means that we needn't make any assumptions about distribution of the random variable. This statistical test has a variety of applications for trend analysis [11], [12], [13], [14], [14]. Its results are relevant so long as $40 \leq n$ (n – range of the file). Only in this case can the Mann-Kendall statistic have a Normal distribution [15], [16], [17], [18], [19]. The data must be ordered chronologically in terms of one or more criteria. This test is based on the calculation of a special statistical value S . Comparing each of the couples y_i, y_j , ($i > j$) of the random value Y , it is possible to determine if $y_i > y_j$ or $y_i < y_j$. Let's define the number of the first type as P and of the second type as M . Now S can be defined as [15], [16], [17], [18]:

$$S = P - M$$

The next Mann-Kendall statistic Z has a Normal distribution, where:

$$Z = (S - 1)/\sigma_s/2 \quad \text{if } S > 0$$

$$Z = 0 \quad \text{if } S = 0$$

$$Z = (S + 1)/\sigma_s/2 \quad \text{if } S < 0$$

The deviation σ_s is defined as:

$$\sigma_s = n(n - 1)(2n + 5)/18,$$

where n is the number of samples.

The hypothesis H_0 : no trend “not reject”, if $Z < Z\alpha/2$ or “reject” if

$Z > Z\alpha/2$. The value α is called the significance level; we choose $\alpha = 0.5$ and $Z\alpha/2$ is a table value for Normal distribution, so it depends on the number of samples. Moreover, the value of Z gives further information about any increasing or decreasing of the trend, but not its magnitude exactly [15], [16], [17], [18].

All calculations, both of the basic characteristics of the entry data and of the testing of the samples were done using VisualBasic on the Microsoft Excel platform.

III. RESULTS AND DISCUSSION

The statistical analysis of monthly low flows for river station in assessed basins was done as a first step. Figures 1 to 4 present course of low flows in m^3/s per each month of hydrological year (IX–X) in river basins Poprad, Hornád, Bodva and Bodrog.

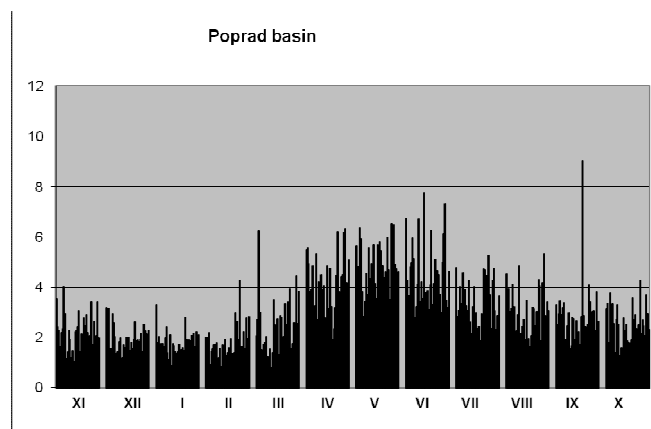


Fig. 1. Statistical analysis of low flows in Poprad basin

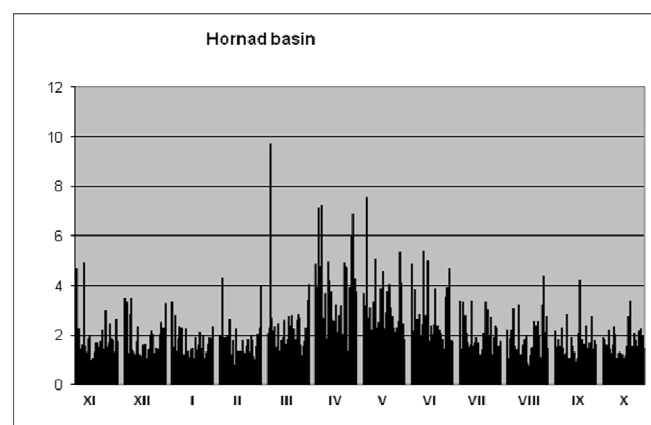


Fig. 2. Statistical analysis of low flows in Hornád basin

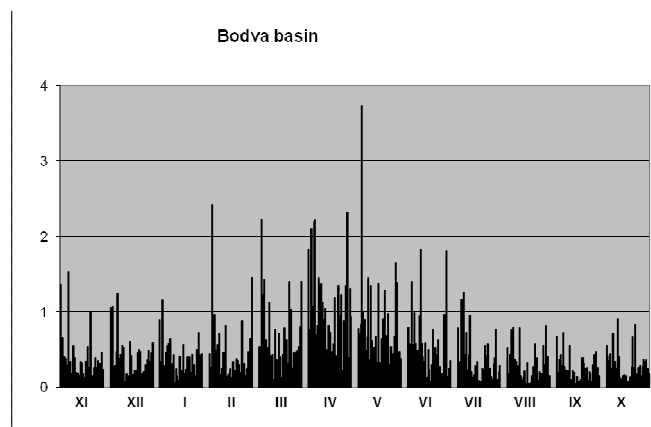


Fig. 3. Statistical analysis of low flows in Bodva basin

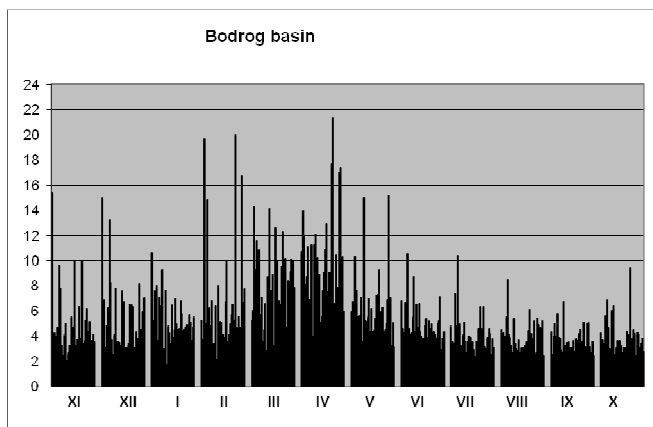


Fig. 4. Statistical analysis of low flows in Bodrog basin

Poprad basin (Figure 1) appears to be relatively most stable in all four river basins observed with the fewest number of extremely high values. Period of increased minimum flows is most visible in the period March to June. In July and August, they are visibly smaller values and generally more stabilized and this trend is also reflected in the other autumn and winter months.

Bodrog basin (Figure 2) shows a little different course when the lowest value of the minimum flow rate is located between July and October. In recent months, in addition to increased minimum flows can also be seen by their relatively high unsteadiness and frequent changes extremes of higher and lower values.

Both basins, Hornad and Bodva show similar values of minimum flows over time (Figure 3–4). Increased but also more unstable flow values we can observe especially from March to June. In this period were also observed individually extremely high values.

In all four histograms (Figure 1–4) is clearly obvious fact that in the middle of the observation period (between year 1975-2012) for all month seasonal stages we see lower levels of minimum flows as from the beginning or from the end of this period, respectively, it means a period around 1990.

In the following monthly low flows in each river station were tested by non-parametric Mann-Kendall statistical test. Tables I.–IV. present statistically significant trends positive or negative in the months during the hydrological year for river basins in the eastern Slovakia.

TABLE I. STATISTICALLY SIGNIFICANT TRENDS IN RIVER STATIONS IN RIVER BASIN POPRAD

	November	December	January	February	March	April	May	June	July	August	September	October
1	0,000963	-0,00531	0,002	0,0044	0,007	0,003273	0,024	-0,0262	-0,02348	-0,01862	-0,0165	-0,01115
2	-0,00353	-0,00307	-0,00096	-0,00042	0,00125	0,006	0,018643	-0,0107	-0,00815	-0,014	-0,01246	-0,00595
3	0,006071	0,00287	0,002067	0,004731	0,007067	0,005552	0,006905	0,0074	0,0075	0,003941	0,0014	0,004455
4	0	0,034786	0,094	0,183118	0,163174	-0,09695	-0,05929	-0,04973	-0,06889	-0,005	-0,01	0,024444
5	-0,0004	-0,00333	-0,00185	0,000136	0,001214	0,007353	0,010111	-0,01075	-0,01212	-0,0102	-0,0065	-0,00183
6	0,0017	0,0004	0,001	0,001867	0,001357	-0,00421	-0,00324	-0,00783	-0,00473	-0,00184	-0,001	-0,0021
7	0,004846	0,001167	0	0,00025	0,002	0,0046	0,00325	0,005259	0,005308	0,005846	0,00324	0,004143
8	0,001	0,001083	0,000611	0,000957	0,002895	0,004875	0,003556	0,001211	0,001364	0,000636	0,001286	0,002857
9	0,007136	0,004929	0,0045	0,004667	0,005143	0,0118	0,011679	0,002105	0,00425	0,010353	0,007167	0,007222
10	0,005333	-0,02113	-0,014	-0,00073	-0,0038	-0,0207	0,003444	-0,0484	-0,05565	-0,0411	-0,03876	-0,01721
11	0,003294	0,002286	0,002867	0,0042	0,005	0,002792	0,00225	0,001882	0,0021	0,002214	0,000923	0,000913
12	0,005464	-0,02744	-0,017	0,005767	-0,0176	-0,02	-0,01818	-0,06883	-0,05221	-0,03137	-0,02232	-0,00117

TABLE II. STATISTICALLY SIGNIFICANT TRENDS IN RIVER STATIONS IN RIVER BASIN HORNÁD

	November	December	January	February	March	April	May	June	July	August	September	October
1	0,0068	0,006429	0,003417	0,004391	0,001714	0,0062	0,0015	0,000654	0,004154	0,009556	0,007667	0,009
2	0,004938	0,005278	0,000818	0,002143	-0,00171	-0,0125	-0,01524	-0,0102	0,001313	0,006571	0,011	0,0056
3	0,006	0,00355	0,002133	0,00225	0,001576	0,000385	-0,001	-0,00178	0,003333	0,006913	0,005429	0,0069
4	0,007471	0,003125	0,002857	0,003381	0	-0,01867	-0,02489	-0,01733	-0,0025	0,008621	0,0116	0,007071
5	0,005481	0,00575	0,005667	0,0045	0,002857	0,008	0,00163	0,006818	0,008	0,007414	0,005692	0,006429

6	0,011625	-0,0036	-0,00133	-0,00925	-0,01968	-0,04792	-0,07316	-0,04033	-0,02208	0,029913	0,0302	0,019565
7	0,001222	0,00205	0,0005	0,003818	0,004591	-0,0019	-0,00321	-0,01107	0	0,00175	0,000167	0,004889
8	0,016417	0,013682	0,009667	0,007	0,006438	0,001852	-0,02683	-0,01161	-0,005	0,003	0,008105	0,019375
9	-0,00671	-0,01742	-0,01388	-0,01506	-0,02374	-0,0969	-0,083	-0,06379	-0,04388	-0,02	-0,00782	-0,00655
10	0,001375	0,001235	0,000833	0,001526	0,000667	0,001769	0,000462	0,000517	0,00044	0,000333	0,000667	0,00075
11	-0,024	-0,01586	-0,02009	-0,035	-0,05836	-0,06627	-0,11546	-0,05271	-0,02947	0,0038	-0,0325	-0,00886
12	0,001952	0,002133	0,00125	0,001647	0,001846	0,003714	0,0012	0,001941	0,002313	0,002438	0,001091	0,001846
13	0,000625	0	-0,00227	-0,00113	0,000364	0,00288	-0,00058	-0,00346	-0,00162	0,002438	0,0004	0,001
14	0,01475	0,013833	0,012692	0,018519	0,013692	0,010607	-0,0065	-0,009	0,0004	0,004667	0,005071	0,013143
15	-0,00275	-0,005	-0,008	-0,0088	-0,01632	-0,04077	-0,03556	-0,05068	-0,02571	-0,01345	-0,00809	-0,00905
16	0,005286	0,001	0,000833	-0,00048	-0,00167	-0,00429	-0,00618	-0,00638	-0,0025	0	-0,00011	0,0022
17	0,005913	0,004444	-0,00144	-0,002	-0,00905	-0,00194	-0,005	-0,00845	-0,00244	0,0017	0,005333	0,003083
18	-0,00962	-0,02586	-0,03575	-0,03252	-0,0732	-0,06916	-0,0762	-0,09379	-0,0568	-0,028	-0,022	-0,02041
19	0,000947	0,000364	0,0004	0,00145	0,001158	0,0026	-0,0003	-0,00014	-0,00044	-0,00052	-0,00015	0,000313
20	0,006043	0,003167	0,000125	0,0098	-0,00235	-0,0072	-0,00513	-0,004	-0,00258	-0,00182	-0,00015	0,002556
21	-0,0117	-0,02864	-0,096	-0,0175	-0,08044	-0,22334	-0,22958	-0,20889	-0,09083	-0,022	-0,0269	-0,01273

TABLE III. STATISTICALLY SIGNIFICANT TRENDS IN RIVER STATIONS IN RIVER BASIN BODVA

	November	December	January	February	March	April	May	June	July	August	September	October
1	-0,001	0,001	0,00225	-0,00114	-0,00422	-0,00031	-0,00252	-0,00275	-0,0043	-0,00275	-0,00215	-0,0003
2	-0,00207	0,0004	0,002333	-0,00232	-0,00653	-0,01508	-0,01167	-0,01231	-0,00546	-0,00492	-0,00213	-0,00112
3	0,002348	0,004	0,001778	0,001769	0,000667	-0,00207	-0,001	-0,0022	-0,00075	-0,00037	0,001	0,001308
4	-0,00588	-0,006	-0,00678	-0,01	-0,01945	-0,02767	-0,03479	-0,02431	-0,01525	-0,0105	-0,00985	-0,00936
5	-0,0016	-0,00113	-0,00043	-0,00073	-0,00383	-0,01067	-0,0084	-0,00762	-0,00442	-0,00271	-0,00171	-0,002

TABLE IV. STATISTICALLY SIGNIFICANT TRENDS IN RIVER STATIONS IN RIVER BASIN BODROG

	November	December	January	February	March	April	May	June	July	August	September	October
1	0,000556	-0,00244	0,002519	0,000269	0,001591	-0,00085	-0,00207	-0,001	-0,0035	-0,00153	-0,00064	0,00085
2	0,003333	0,003091	0,002733	0,007824	0,006313	0,005273	0,00105	0,001353	0,000304	-0,00194	-0,0015	0,000688
3	-0,003	-0,011	-0,00276	-0,00275	-0,00643	-0,00627	-0,01154	-0,012	-0,01617	-0,01389	-0,00538	-0,00513
4	0,001154	-0,00086	0,009261	0,001935	0,00675	0,009714	-0,00496	-0,0022	-0,0035	-0,00439	-0,00168	0,001
5	0,0059	0,003118	0,0066	-0,002	-0,00634	0,001357	-0,00964	0,001222	-0,00069	0,007571	0,006714	0,006857
6	0	0,001308	0,0009	-0,0018	0,00025	0,003895	0,000931	0	-0,00067	-0,00032	-8E-05	-0,00074
7	0,008731	0,008667	0,009471	0,010556	0,01515	0,015214	0,0129	0,010826	0,010083	0,009875	0,008917	0,01052
8	0,033533	0,049143	0,05	-0,01636	-0,02279	0,0295	-0,00425	0,005238	-0,00371	-0,00245	0,009346	0,015333
9	-0,02622	-0,02	-0,01283	-0,02958	0,000429	-0,073	-0,08838	-0,06538	-0,04983	-0,04973	-0,02118	-0,03038
10	0,000667	0,000538	0,002	0,002348	0,00248	0,0025	0,000286	-0,00025	0,000393	0,000667	0,0007	0,000917
11	-0,0448	-0,01923	-0,10667	0,160944	0,126667	-0,02381	-0,02	-0,06	-0,05275	0,099217	-0,119	-0,09382
12	0,00325	0,003148	0,0058	0,0098	0,009556	0,014889	0,004714	-0,00253	-0,00027	-0,00124	-8,3E-05	0,0015
13	-0,04106	-0,072	-0,12375	-0,06846	-0,05954	-0,02333	-0,05844	-0,10457	-0,11763	-0,1076	-0,08422	-0,03645

14	0,002353	-4,5E-05	0,001828	0,001	0,000808	-0,00355	-0,00036	-0,00213	-0,00173	-0,00212	-0,002	-0,00106
15	0,000267	0,000909	0,003053	0,00045	0,00325	0,0044	0,004235	0,001111	0,000381	0,000909	0,000375	0,000478
16	-0,05736	0,035	-0,09257	0,097647	0,1155	0,075	-0,08	-0,15586	-0,12577	-0,02412	-0,166	-0,1944
17	-0,06087	-0,03443	-0,1536	-0,23342	-0,28846	-0,20857	-0,32367	-0,25894	-0,23133	-0,18873	-0,162	-0,0825
18	0,010185	0,017	0,020222	0,024048	0,014077	0,01095	-0,012	-0,0006	0,000875	0,005167	0,003429	0,006381
19	-0,015	-0,03557	-0,02985	-0,01058	-0,04065	-0,07129	-0,0895	-0,06303	-0,04913	-0,036	-0,03863	-0,02858
20	0,002136	-0,00268	0,001667	0,007714	0,003333	0,01715	0,000217	0,000929	-9,5E-05	0,0008	0,002	0,002167
21	0,002625	-0,00287	0,002938	0,00775	0,010645	0,010667	0,0023	-0,00429	-0,00213	-0,00085	-0,00032	-0,00067
22	-0,00382	-0,02127	-0,0085	-0,00933	-0,02067	-0,0047	-0,01935	-0,01648	-0,02086	-0,0105	-0,01088	-0,011
23	0,004286	0,004536	0,0025	0,010895	0,007706	0,0071	0,000556	-0,00043	-0,00074	0,000125	0,002571	0,002571
24	0,07469	0,075	0,028778	0,154833	0,036125	0,037778	-0,0172	0,031667	0,055889	0,078263	0,060444	0,079167
25	-0,20111	-0,32917	-0,60675	-0,47063	-0,47232	-0,71053	-0,63209	-0,598	-0,53526	-0,309	-0,325	-0,29558

Trends of low flows in each station were proved by non-parametric Mann-Kendall test. Trend was statistically significant when paid condition $Z > Z \alpha / 2$, and was accepted hypothesis H1: there is a trend of minimal flows. These statistically significant trends in individual months was associated with the size of which was directly calculated from the values of minimum monthly flow for each month in the station for a 32 year period. The results are documented in Tables I.–IV.. Months in which there is a decrease in water content are shown minus. Bold numbers represent statistically significant trends.

IV. CONCLUSION

Changes in the magnitude and frequency of droughts will have extensive impacts on water management, agriculture and aquatic ecosystems. With the projected global temperature increase, scientists generally agree that the global hydrological cycle will intensify and suggest that extremes will become or have already become more common [20], [21]. An important function in engineering hydrology is performed by trend analysis of low flows. In this study, statistical analysis and specifically trends in low flow characteristics were analyzed for streams in eastern Slovakia by using data at selected gaging stations. Low flow is defined as the smallest untouched flow volume in time. There are many statistical methods for data evaluation. The most of useful is the non-parametric Mann-Kendall test. This analysis was carried out for statistical data from 63 gaging stations lying in the eastern part of Slovakia. These data were obtained from the Slovakian Hydrometeorological Institute, regional centre Košice, at monthly intervals during the years 1975–2012. Because the minimal flow data are not comparable for the individual stations, normally it is only possible to do the statistical analysis for gaging station separately. In case it becomes necessary to evaluate the data from a group of stations, the problem of aggregation of data files must be dealt with, which was the aim of this paper. Results prove mainly decreasing trend in low flows in studied area.

ACKNOWLEDGMENT

The contribution is written thanks to support of project VEGA 1/0609/14.

REFERENCES

- [1] L.S. Pereira, I. Cordery and I. Iacovides, 2002. "Coping with Water Scarcity." UNESCO IHP VI, Technical Documents in Hydrology No. 58, UNESCO, Paris, 267 p. 2002, Available: <http://unesdoc.unesco.org/images/0012/001278/127846e.pdf>
- [2] K. Mishra, and P. Singh, "A review of drought concepts," *J. Hydrol.* Vol. 263, pp. 203–212, 2010.
- [3] D. A. Wilhite, "Drought: A Global Assessment," Volume 1 and 2. Routledge, New York, 2000.
- [4] G. Markovič, D. Káposztásová, and Z. Vranayová. "The analysis of the possible use of harvested rainwater in real conditions at the university campus of Kosice," In: *Recent Advances in Environmental Science and Geoscience: Proceeding of the 2014 International Conference on Environmental Science and Geoscience (ESG'14)*: March 15-17, 2014, Venice, Italy, Sofia: EUROPMENT, p. 82–88, 2014.
- [5] J. Korytárová, M. Šlezinger, and H. Uhmánová, "Determination of Potential Damage to Representatives of Real Estate Property in Areas Afflicted by Flooding," *J.Hydrol.Hydromech.* Vol. 55, pp. 282-285, 2007.
- [6] P. Pelikán, and M. Šlezinger, "Methodology for the establishment of physical and geometric properties of a drainage basin," *Acta univ. agric. et silvic. Mendel. Brunen.* Vol.59, pp. 265–270, 2011.
- [7] B. Demeterová, and P. Škoda, "Low flow in selected streams of Slovakia (in Slovak)," *J.Hydrol.Hydromech.* vol. 57, pp. 55-59, 2008.
- [8] J. Szolgay, M. Dzubák, and K. Hlavčová, "Hydrology. Runoff process and hydrology of surface water (in Slovak)," Slovak Technical University, Bratislava, 1994.
- [9] M. Zeleňáková, "Preliminary flood risk assessment in the Hornád watershed," In: *River Basin Management 5*. Southampton: Wessex Institute of Technology, p. 15-24, 2009.
- [10] M. Zeleňáková, P. Purcz, I. Gargar and H. Hlavatá, "Research of monthly precipitation trends in Libya and Slovakia," In: *Recent Advances in Environmental Science and Geoscience : Proceeding of the 2014 International Conference on Environmental Science and Geoscience (ESG'14)* : March 15-17, 2014, Venice, Italy. Sofia: EUROPMENT, p. 46-50, 2014.
- [11] D. H. Burn, and M. A. H. Elnur, "Detection of hydrologic trends and variability," *J. Hydrol.* Vol. 255, pp. 107–122, 2002.
- [12] R. M. Hirsch, R. B. Alexander, and R. A. Smith, "Selection of methods for the detection and estimation of trends in water quality," *Water Resour. Res.*, vol. 27, pp. 803-813, 1991.
- [13] D. P. Lettenmaier, E. F. Wood, and J. R. Wallis, "Hydro-climatological trends in the continental United States 1948–88," *J. of Climate*, Vol. 7, pp. 586–607, 1994.

- [14] E. M. Douglas, R. M. Vogel, and C. N. Kroll, "Trends in floods and lowflows in the United States: impact of spatial correlation," *J. Hydrol.* Vol. 255, pp. 107–122, 2002.
- [15] J. F. Santos, I. Pulido-Calvo, and M. M. Portela, "Spatial and temporal variability of droughts in Portugal," *Water Resour. Res.*, Vol. 46, W03503, 2010.
- [16] B. Önöz, and M. Bayazit, "The Power of Statistical Tests for Trend Detection," *Turkish J. Eng. Env. Sci.* Vol. 27, pp. 247–251, 2003
- [17] M. G. Kendall, "Rank Correlation Measures," Charles Griffin, London, 1975.
- [18] H. B. Mann, "Non-parametric tests against trend," *Econometrica*, Vol. 13, pp. 245-259, 1945.
- [19] P. K. Sen, "Estimates of the regression coefficient based on Kendall's tau," *Journal of the American Statistical Association* Vol. 63, pp. 1379–1389, 1968.
- [20] K. Stahl, H. Hisdal, J. Hannaford, L. Tallaksen, H. Van Lanen, E. Sauquet, S. Demuth, M. Fendekova, and J. Jordar, "Streamflow trends in Europe: evidence from a dataset of near-natural catchments," *Hydrol. Earth Syst. Sci.* Vol. 14, pp. 2367–2382, 2010.
- [21] H. Hisdal, and L. M. Tallaksen, "Impact of Droughts in Europe," Drought Event Definition. Technical Report No. 6. 2000.



Martina Zelenáková is assistant professor at Institute of Environmental Engineering at Civil Engineering Faculty, Technical University of Košice. She is oriented on the field of water management and environmental risks in her scientific-research work. She publishes results of her work in journals and scientific proceedings from Slovak and abroad conferences.

Pavol Purcz is assistant professor at Institute of Construction Technology and Management at Civil Engineering Faculty, Technical University of Košice. He teaches mathematics and is interested in the field of mathematical statistic.

Tatiana Soľáková is PhD student at Institute of Environmental Engineering at Civil Engineering Faculty, Technical University of Košice. Her thesis is focused to drought risk management.

Dorota Simonová works at Slovak Hydrometeorological Institute.

Svedberg's number in diffusion processes

Alfredo Constaín¹, Duvan Mesa², Carlos Peña-Guzmán³ & Paola Acevedo⁴

¹R+D Dept. Hydrocloro Tech Colombia, *alfredo.constain@gmail.com*;

²Faculty of Environmental Engineering, San Totomas University, Bogotá, Colombia, *duvanmesa@usantotomas.edu.co*

³Faculty of Environmental Engineering, Manuela Beltrán University, Bogotá, Colombia, *carlos.guzman@docentes.umb.edu.co*

⁴Faculty of Industrial Engineering, Universidad Cooperativa de Colombia, Bogotá, Colombia, *paola.acevedop@campusucc.edu.co*

Abstract—Since pioneering work on Brownian motion done by T. Svedberg in first years of 1900, the approximate number 1.54 is considered as a mean number of colloidal particles moving randomly in a reticule, but it is actually a pattern property of spatial and time in diffusion processes. This paper presents how the introduction of this number in Poisson's distribution allows to describe particle dynamics not only in the so-called "diffusive period" (after Complete Mixing condition), but also in early period of plume evolution (Convective Period) in stream transport processes. An experimental proof of this statement is discussed to show how last period is Gaussian too, against current picture of mass transport.

Keywords—Mass transport in fluids; Tracer dynamics; Svedberg's number

I. INTRODUCTION

It is a well-known subject from statistics the close relationship between normal (Gaussian) and Poisson probability distribution, especially when the independence of events (among them and from time) is a main consideration of a phenomenon. Equation (1) is the definition of Poisson probability of count $m=0, 1, 2, \dots$, m particles with an average of a [1]–[3].

$$p_m = \frac{a^m}{m!} e^{-a} \quad (1)$$

The main aim of this article is analyze the behavior in diffusion processes and its relation with Poisson probability distribution, especially the derived from some calculations done by T. Svedberg in earlier XX century regarding Brownian motion. Poisson's distribution has a special rank in Physics whereas it describes the well-known behavior of massive systems in which fluctuations vanish when number of considered particles is increased (Large Number Laws). This due that in this distribution variance equals square root of

average, and the relative error of observations decreases when their number increases. Finally, these considerations are applied to trace dispersion-diffusion events in streams.

II. SVEDBERG'S EXPERIMENT.

Considering tracer particles as a diluted gas in a fluid, it is valid to model its evolution as a Poisson's process where the probability of count tracer particles (among fluid particles) is very small. Then, the probability of count them independently is proportional to a very small observing times (differential). So the probability of count one tracer particle in certain conditions is proportional to this differential and the probability of count two or more tracer particles is proportional to a second order differential. An experiment of this case study was developed by T. Svedberg using colloidal particles of gold solved in a unit volume; in the experiment they count the number of particles per unit time. The average number of gold particles measure was approximately 1.54. Table 1 shows the experiment data and probability calculations [4].

Table 1 Svedberg’s probability results.

No. Of particles m	Cases	Relative frequency	Binomial Prob.	Poisson Prob.
0	112	0.216	0.212	0.214
1	168	0.325	0.328	0.330
2	130	0.251	0.253	0.254
3	69	0.133	0.130	0.131
4	32	0.062	0.050	0.050
5	5	0.010	0.016	0.016
6	1	0.002	0.004	0.004
7	1	0.002	0.001	0.001

$$a = \frac{0 \cdot 112 + 1 \cdot 168 + 2 \cdot 130 + 3 \cdot 69 + 4 \cdot 32 + 5 \cdot 5 + 6 \cdot 1 + 7 \cdot 1}{518} \approx 1.54 \quad (2)$$

Although the number of observations done by Svedberg were limited, they were sufficient to show their statistical Poissonian nature, following Large Number laws accordingly with convergence of relative frequencies of experiment with current theoretical probability models.

III. DIFFUSION PHENOMENA AS A SVEDBERG EFFECT

Now, it is interesting to see the very nature of a. From expression (2) it may be understood that this average value is a fraction relating succeeded outcomes (i.e.: one or more particles counted) to all outcomes (i.e: whatever result). As was pointed out by mathematician and philosopher R. Von Mises [4], Brownian motion description of Svedberg’s experiment may be put as fraction of observation times.

When it is considered a Gaussian process there are two kinds of reference situations: One, related with inflection points (one standard deviation σ , toward both sides from centre) and another with the whole curve Fig.1.

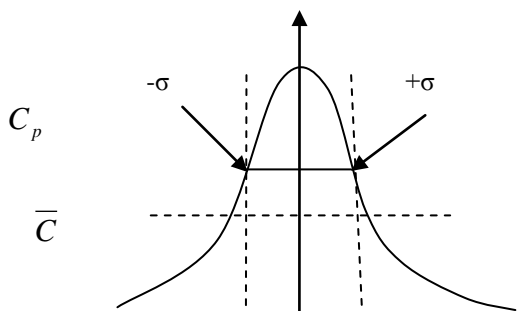
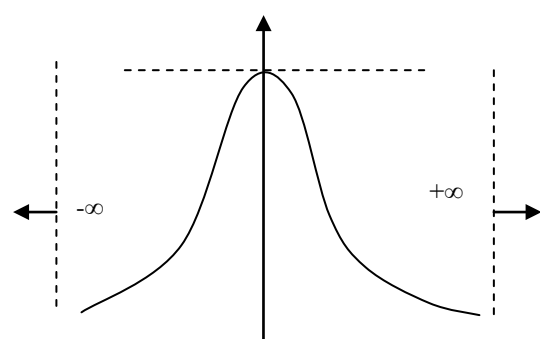


Fig. 1. Reference points: Inflection and whole curve.



First

case (concentrated one) may be related to succeeded outcomes while second one (extended one) may be related to all outcomes. To apply this in a definition both situations are described in terms of “observation times” as follows. First it is defined as an observation time for variance situation using proper integration times and an average concentration (which is a key concentration that may be related properly to this restricted observation case).

$$\theta_{\sigma} = \frac{\int_{-\sigma}^{\sigma} c(t) dt}{C} \quad (3)$$

Second, it is defined an observation time for the whole curve using infinite limits in integration and peak concentration (the other key concentration).

$$\theta_{Whole} = \frac{\int_{-\infty}^{\infty} c(t) dt}{C_p} \quad (4)$$

Then, as was stated and reordering

$$a = \frac{\theta_{\sigma}}{\theta_{Whole}} = \frac{\frac{\int_{-\sigma_{\tau}}^{\sigma_{\tau}} c(t) dt}{\bar{C}}}{\frac{\int_{-\infty}^{\infty} c(t) dt}{C_p}} = \frac{\int_{-\sigma_{\tau}}^{\sigma_{\tau}} c(t) dt}{\int_{-\infty}^{\infty} c(t) dt} \frac{C_p}{\bar{C}} \quad (5)$$

It is easy to see than for Gaussian tracer curve it holds that:

$$\frac{\int_{-\sigma_{\tau}}^{\sigma_{\tau}} c(t) dt}{\int_{-\infty}^{\infty} c(t) dt} \approx 0.68 \quad (6)$$

And using error function may be demonstrated that:

$$\frac{\bar{C}}{C_p} \approx 0.441 \quad (7)$$

Then, congruent with prior Svedberg's results:

$$a = \frac{0.68}{0.441} \approx 1.54 \quad (8)$$

Finally, using definition of Poisson's distribution relating whole and variance times

$$t = \tau \left(1 + a + \frac{a^2}{2!} + \dots \right) = \tau e^{1.54} \quad (9)$$

Then,

$$\frac{\tau}{t} = \beta = e^{-1.54} \approx 0.215 \quad (10)$$

So, $a \approx 1.54$ Svedberg's number has a strong signification: It is not only a particular result in Brownian colloidal gold particles dynamic but also is a general pattern derived from observation times in diffusion processes. The relationship described in Equation(10) is valid in every case as will be discussed following.

IV. GAUSSIAN NATURE OF NON-FICKIAN DIFFUSION PHENOMENA

Current mass transport theories state that Non-Fickian (skewed) curves are not Gaussian based on the conjecture that long tails observed in experimental field tests are a real, permanent external effect (dead zone storage effect) which adds a kind of bias to non-perturbed symmetrical curve. However, no one of these theories give a specific model of acting interactions which give satisfactory mathematical explanation of skewness (most of them use instead, probabilistic adjustment as Monte Carlo models). Rather, despite asymmetric bias shape of all tracer curves, Gaussian (bell shaped) nature is evident. Then, how to solve this contradiction? There is a way to hold Gaussian nature for Non-Fickian curves, accepting that this skewness is a virtual effect (not real), due to a velocity composition (mechanical relativity principle). A simple example helps to view this case as in Fig 2. An observer fixed at border (Eulerian) will view a ball moving from the top of boat with a parabolic trajectory as result of velocity composition (acceleration and stream velocity) while moving observer (Lagrangian) will view only acceleration of ball and then a linear trajectory.

Applying this concept to tracer plume motion, Eulerian observer (at border of flow) will see an asymmetrical tracer curve as a result of addition (and subtraction) of stream velocity and diffusion velocity of solute. By the other hand, a Lagrangian observer (travelling over peak of tracer curve with stream velocity) will not compose stream velocity because this not exist for him (her), the observer will see only two opposite, equal module, diffusive velocities, given a symmetrical curve. So, skewness of tracer curves is a motion dependent parameter.

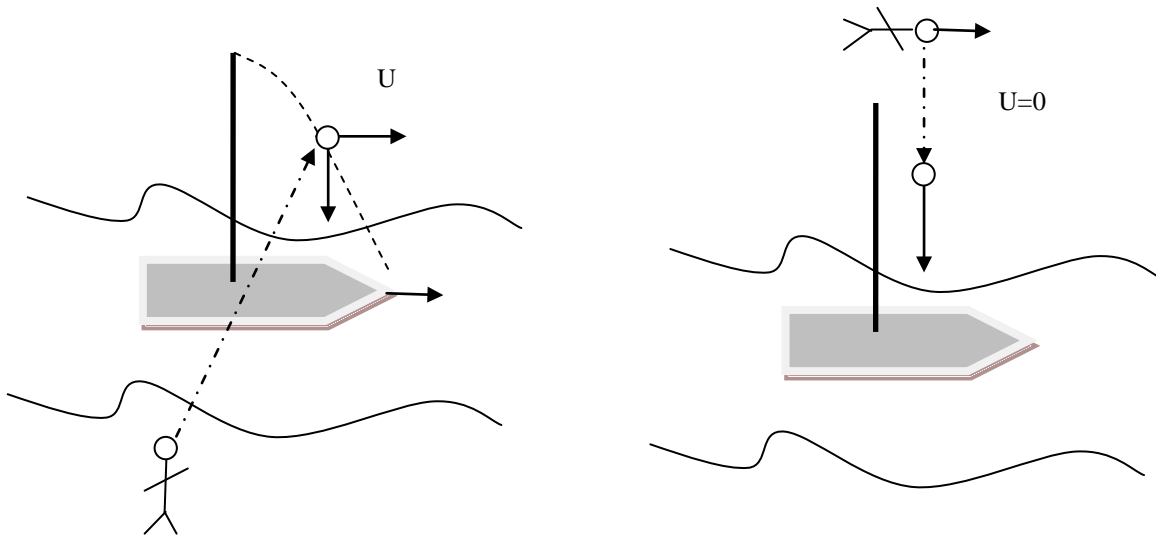


Fig. 2. Composition velocity depending of state of motion of observers, (left) Lagrangian observer (moving with boat) and (right) Eulerian observer (fixed at the border)

V. MODIFIED FICK'S EQUATION TO APPLY VELOCITY COMPOSITION IN TRACER MOTION IN STREAMS.

If there is a composition of velocities that modifies the apparent shape of tracer curves in flows, it is convenient to apply the Galilean transformation of coordinates, in the following form:

$$z' = z \quad (11)$$

$$y' = y$$

(12)

$$x' = x - U \times t \quad (13)$$

The prime coordinates are moving system viewed from border. Then Eulerian (at border) observer will see the following Fick's equation. M is mass, A is cross section of flow, E is the longitudinal dispersion coefficient:

$$C(x, t) = \frac{M}{A\sqrt{4\pi Et}} e^{-\frac{(x-Ut)^2}{4Et}} \quad (14)$$

A graphical representation example of Equation (14) is shown in Fig.3 which has X fixed and t as variable. It should be noted that there is certain skewness due to Galilean composition that is involved as transformation is used (13)

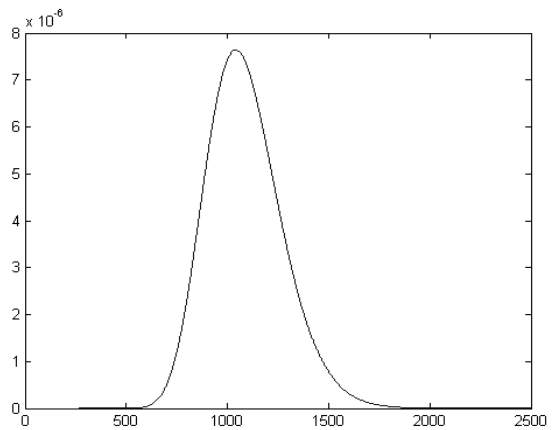


Fig. 3. Eulerian tracer curve with expected asymmetrical shape.

For the La Grangian (moving) observer we can simply use Equation (14) fixing time t and changing continuously distance X . Furthermore, we can put moving distance coordinate X' and varying time. Fig 4. The result obtained is the same independent of the procedure used.

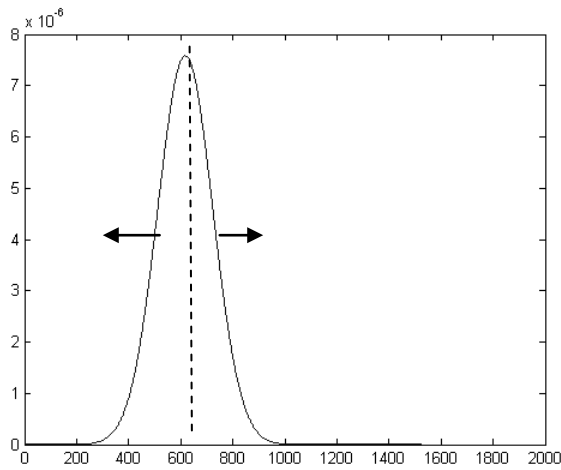


Fig. 4. La Grangian tracer curve with expected symmetrical shape expressed from border distance in an instant.

It may seem that this explanation solves the Non-Fickian problem interpretation for tracer curves in terms of kinematic composition of velocities, however a careful examination of these theoretical curves with the corresponding experimental ones, shows that a peak concentration and skewness do not completely agree to real data. The reason for this difference is that if Equation (14) should represent accurately diffusion-dispersion along the entire trench, E cannot be a constant value; rather it should be a time function in either case, from border or moving with plume, as well. This requirement addresses the fact that the only way to represent two coordinate motion (longitudinal and transverse) using a one-dimensional equation as Equation (14) is using transport coefficient as time functions. (Fick's definition) Fi

A way to introduce this kind of functions is to consider a definition of $E(t)$ in the form:

$$E = k(t) U^2 t \quad (15)$$

It is important to realize that $k(t)$ should be a thermodynamic function that reflects either longitudinal or transverse irreversible evolution of plume. Then, the function will indicate when the transverse diffusion vanishes. A way to find this time dependent coefficient is defining a function that links diffusion and stream velocities [5]-[9]:

$$\phi = \frac{V_{diff}}{U} \quad (16)$$

Also defining a one-dimensional Brownian displacement for diffusion-dispersion:

$$\Delta = \sqrt{2E\tau} \quad (17)$$

Here Δ is a characteristic displacement measured from inflection points in Gaussian curve, and τ is also a characteristic time for this displacement. So, diffusion velocity may be defined in the following way:

$$V_{diff} = \frac{\Delta}{\tau} \quad (18)$$

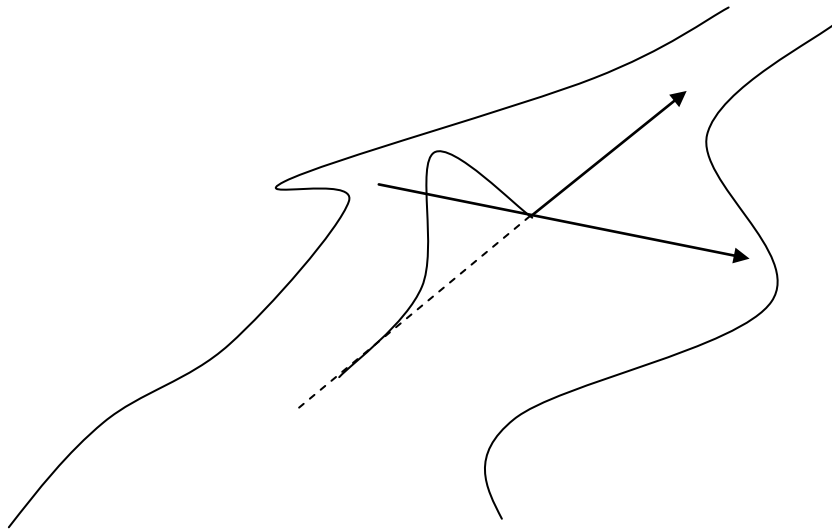


Fig. 5. Longitudinal dispersion and transverse Diffusion require time dependent transport coefficients in X equations. Placing these equations together it is obtained.

$$U = \frac{1}{\phi} \sqrt{\frac{2E}{\tau}} \quad (19)$$

This is a non-uniform flow velocity equation with the same squared-root structure that Chezy's equation. Clearing E , and using Svedberg's relationship, $\beta \approx 0.215$:

$$E = \frac{\phi^2 U^2 \beta t}{2} \quad (20)$$

Then, $k(t)$ is:

$$k(t) = \frac{\phi^2 \beta}{2} \quad (21)$$

This equation shows the thermodynamic nature of phenomenon and also the Poisson's character of diffusion along the entire trench. Now it is possible to define a modified Fick's equation that represents accurately the real tracer curves in every instant. C_0 is background concentration

$$C(x, t) = \frac{M}{Q \times \phi \times t \times \sqrt{2\pi\beta}} e^{-\frac{(x-Ut)^2}{2\beta\phi^2 U^2 t^2}} + C_0 \quad (22)$$

This new definition involves the discharge value of the stream. An example of its utilization is shown in Fig.6.

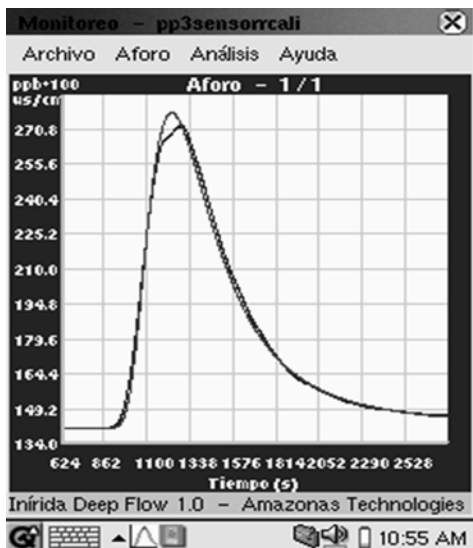


Fig. 6. Modelation of a real tracer Non-Fickian curve using Equation (22).

In order to measure this, the author used a special hardware-software tool named **INIRIDA DEEP FLOW (IDF)** which allows real-time operations. This device has: A.-A hand computer B.-A digital interface C.-Probes and interconnection cables.

Now it is possible to define the Non-Fickian curves as Gaussian in nature whereas skewed shapes are reproduced using equations based on Poisson's distribution that is totally random, and converges with Normal distribution accordingly with Central limit theorem. Key values in these definitions are the Svedberg's number, $\alpha \approx 1.54$ and Poisson's relationship $\beta \approx 0.215$ linking diverse time scenarios. Following task is testing experimentally this view.

VI. AN EXPERIMENTAL TEST TO GAUSSIAN NATURE OF NON-FICKIAN TRACER CURVES.

Using common salt as a tracer in a small mountain stream in Colombia, it is presented and discussed a field journey with screens of IDF fluvial tool. In this case the aim is to show how for the entire trench of stream, modelations using Fick's modified Equation (22) which is based on Poisson's distribution and uses Svedberg's number are close to experimental tracer curves, and then this nature is clearly shown. The stream is one of 42 l/s of discharge and a mean velocity of 0.110 m/s. Trench total distance is 110 m. Experimenters done twelve pouring of 200 g each of NaCl ionic tracer, with measurement points every 10 m. Photos of these duties and stream characteristics are enclosed in next Fig.7. We start with nearest pouring point. Also screens of all measurements with modelations are presented. Broken curves are experimental ones. Smooth ones are theoretical.

The IDF tool allows making simultaneous measurements with common salt and Rhodamine WT tracers. Also this hardware-software tool has subroutines as: A) Clean the high frequency noise in experimental curves. B) Calculate discharge also using current mass conservation equation. B) Shows thermodynamic function value that indicates if "Complete mixing" condition is reached.

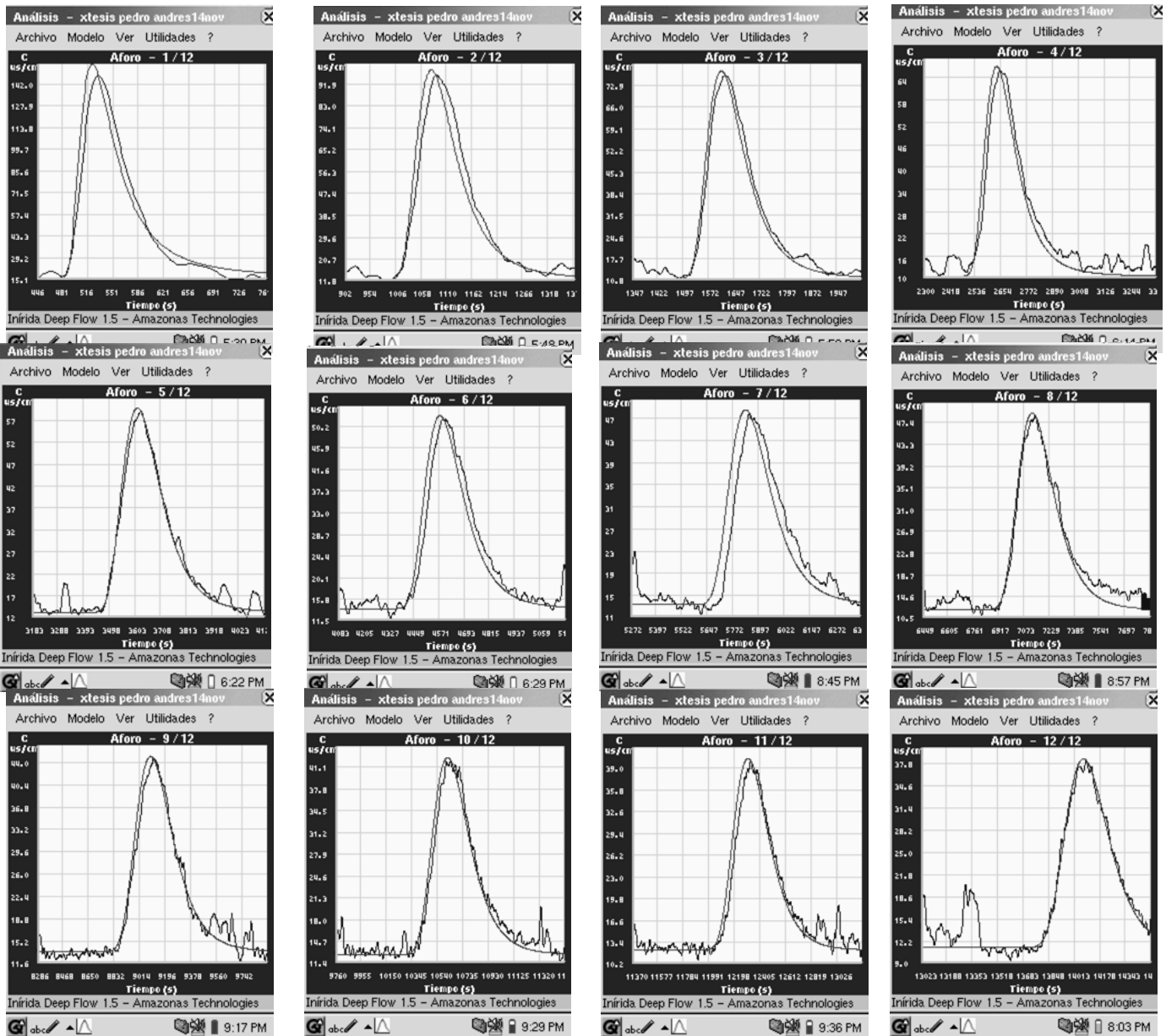


Fig. 7. Stream aspects and Modelation of real tracer Non-Fickian curves with Gaussian models

VII. REMARKS AND CONCLUSIONS

In this paper Poisson and Svedberg relationships were developed to be applied in a tracer mass transport theory. These concepts support the hypothesis that these curves are Gaussian in every instant, against current concept in which a dead zone storage effect involves a certain force that changes this nature.

The authors discuss an alternate view of mass transport using Galilean composition principle to interpret Non-Fickian effect in tracer curves simply as a kinematic effect. This means that mechanisms of plume formation do not respond only to local fluid conditions but also to general physical principles as those that guide several observers' descriptions of reality.

It is apparent that one-dimensional equations require time dependant transport coefficients to describe dispersion-diffusion processes occurring in two-dimension frame. It is a necessary consequence of Fick's definition itself in which spatial (in one or several axis) variations are defined by time variations.

A field journey in a small mountain stream in Colombia is described. Twelve experimental ionic modelations based on these relationships were documented herein. Despite some low frequency noise spikes and some small out-of-phase model curves show right skewness and pick of concentration; these results support the hypothesis that Gaussian nature of tracer curves is present in every moment of plume evolution, despite its skewness.

A hardware-software tool allows real time measurements and modelations. This device gives numerical values of velocity and discharge of streams and also information about "Complete mixing" condition of tracer using a thermodynamic relationship.

ACKNOWLEDGMENT

The Authors has been supported in his researches by Colombian government small companies' agency (FOMIPYME), by Salle University in Bogotá Colombia and by Dr. Edgard Holguin, Universidad de los Andes (Bogota, Colombia) former researcher. Also Amazonas Technologies company in Cali. Colombia.

REFERENCES

- [1] Pugachev V. Introduction to Probability theory. Nauka, Moscow, 1973..
- [2] Moroney M.. Facts from figures. Penguin Books Ltd., Harmondsworth, Middlesex, England, 1968.
- [3] Borel É. Les Probabilités et la Vie. , Presses Universitaires de France, Paris. 1971.
- [4] MisesR.,Probability, statistics, and truth, Dover Publications, 1957.
- [5] Constain A., Carvajal A. & Carvajal J. Applications of a non uniform flow velocity equation in streams. River Flow, 2002 Belgium. AA Balkema Publishers- Netherlands, 135-142.
- [6] Constain A., Carvajal A. & Carvajal J. Accurate discharge measurement using tracers. Flucom 7, 2007 USA.
- [7] Constain A., Carvajal A. & Carvajal J. A thermodynamic method to measure mixing length for conservative tracers in flows. River Flow, 2008b Turkey.
- [8] Constain A., Carvajal, a. & Carvajal J. Recalculation of Frenkel formula through dispersion parameters. Flucom 9, 2009 Russia.
- [9] Constain A., Carvajal A. & Carvajal J. A Non uniform flow velocity equation and its applications to mass transport in natural streams. TRACER 5 International Conference on tracer and tracing method, 2008a Brasil.

Wet scrubber for cleaning of syngas from biomass gasification

Marek Balas, Martin Lisy, Zdenek Skala, Jiri Pospisil

Abstract—This paper deals with gas wet scrubbing which cleans the impurities in the gas so that the gas may be used in combustion engines. Gas is contaminated and has high temperature (500-800°C) as it leaves atmospheric fluid gasifier. Research focuses mostly on tar elimination and dust removal.

Keywords— biomass, gasification, gas cleaning, wet scrubber

I. INTRODUCTION

GASIFICATION is a very old technology, historic records about its use date back to first half of the 19th century. Mass use of this technology began during World War II when automobiles combusted wood gas. Renewed interest in the technology continued at the turn of 1980s and in the early 1990s. Current research in the area of gasification is fuelled by need to replace fossil fuels with renewable energy sources due to expected unavailability of the fossil fuels in the future and increased impact of greenhouse effect.

Gas generated by gasification contains several impurities which impede its direct use. There are several methods to modify actual gas quality so that it complies with requirements for final gas quality. Primary methods, which positively affect gasification process itself, and secondary methods, which clean the produced gas, are researched. Both of these methods have their pros and cons. Unless their principles, boundary conditions, particulars and restrictions of use are sufficiently described, the methods cannot be compared.

This paper deals with gas wet scrubbing which cleans the impurities in the gas so that the gas may be used in combustion engines. Gas is contaminated and has high temperature (500-800°C) as it leaves atmospheric fluid gasifier. Research focuses mostly on tar elimination and dust removal.

Core of our work lies in research of tar elimination, which is a mixture of higher hydrocarbons and their compounds. Water and organic liquid may be both applied in tar elimination from gas. Boiling point (volatility), availability, and price of organic liquid are major criteria for selection of a proper material. In past, scrubbing oil was often applied for the purposes of extensive research in the area of coal gasification and production of town gas. Biodiesel and/or rapeseed oil methyl ester (RME) are alternatively widely used nowadays. Both

liquids were assessed; however, since RME comes from renewable sources of energy and seems to be more environmentally friendly, most of the paper deals with RME technologies.

Scrubbing of gas generated by biomass gasification (or a different organic material) has its own specifics. Gas contains very fine little wettable dust (ash, unburned residues, and soot), tar (mixture of higher hydrocarbons and their compounds) and water vapour. Tar condensates in a wide temperature range from ca. 180 to 300°C and in temperatures below zero. As the tar condensates, it creates adhesive liquid coating on cool surfaces which, together with dust, forms deposits that are very difficult to remove. If the temperature drops below condensation point, fine tar mist is formed; this mist cannot be removed from gas by common separators. Condensation temperature and tar in gas are bound by phase equilibrium.

Different mechanisms apply when water and organic liquid are used in gas scrubbing since the tar has different solubility. This concerns condensation and subsequent capture of aerosol droplets in water applications, and absorption and diffusion in organic liquid applications. Both these mechanisms are described in the paper, and comparison of tar concentrations for various temperatures of scrubbing liquid before and after the gas scrubbing is given. Temperature range for both liquids during experiments overlaps only partially (water: 0-40°C, RME: 30-85°C). Temperature range was selected so that both types of liquid may be later practically applied. In case of scrubbing using organic liquid, the process will be conducted below water condensation point so that amount of waste water polluted with PAH and its derivatives is minimized.

In addition to studying efficiency of the scrubbing, we also analysed other properties of scrubbing liquids and important technology aspects. This includes particular transport and thermodynamic properties (heat capacity, viscosity, and vapour tension), disposal and regeneration of waste liquid, risks of liquid treatment, its availability, and price.

II. GAS IMPURITIES

Potential of gas generated by biomass gasification for subsequent production of electrical energy is restricted by difficulties related to purification of this gas. Gas impurities cause several operating problems to facilities. Corrosion, fouling of supply routes and tarring of engines and turbines work areas may lead to severe accidents. Impurities may be

M. Balas is with the Brno University of Technology, Brno, Czech Republic. (corresponding author to provide phone: +420 541142582; e-mail: balas.m@fme.vutbr.cz).

classified as:

- Dust (solid particulate matter)
- Alkali compounds
- Nitrogen compounds
- Tar
- Light hydrocarbons (methane, ethane)
- Heavy hydrocarbons

Chlorine, fluorine, and silicon may also be dangerous for certain pieces of equipment. Silicon is monitored in combustion engines especially as it has negative impact on quality of lubrication oil.

A. Solid particulate matter

Solid particles in raw gas leaving the gasifier comprise inorganic fuel residues (ash), non-reacted biomass in the form of charred material (the so called coalite), and inert material of gasifier bed. Soot is also present in the dust. Gas with high concentrations of solid particles is typical of gasifiers with bubbling and circulating fluidized bed (turbulent conditions inside the reactor). Thermal treatment of biomass may form aerosol that has negative impact on human health and causes greenhouse effect.

Together with tar, it fouls pipe walls and causes abrasion as well as fouling of equipment modifying and using the gas.

Cyclone separators, barrier filters, electrostatic separators, and wet scrubbers are used and/or tested for elimination of solid particles.

B. Alkali compounds

Biomass is low in dust. Certain components of dust may cause several operation problems, and include alkali metals, i.e. potassium (K) and sodium (Na). These are present in stalk culm plants. Salts of potassium and sodium evaporate below 700 °C; they are easily meltable and form deposits of ash on cooler surfaces of equipment (below 650 °C). Deposits concern mostly heat exchangers, combustion engines and gas turbines positioned beyond generator because unless alkali compounds are removed from the gas, they pass through the whole system, and condensate and deposit beyond the filtering devices. Another issue is a high-temperature corrosion of metal materials, which may be caused by alkali salts, especially if vanadium catalyses the corrosion (cogasification of biomass and waste).

Deposition of alkali salts is usually treated by cooling the gas and eliminating fine particles where salts condensate at temperatures below 600 °C. These technologies are highly efficient, e.g. electrostatic and bag filters, or wet scrubbers.

C. Nitrogen compounds

Most of nitrogen in the produced gas is in the form of N₂, and its concentration depends on type of the gasifying medium. Nitrogen also forms compounds where ammonia (NH₃) is the main nitrogen component in the raw gas from biomass gasification. NH₃ is created by conversion of protein and other nitrogen-containing biomass components. Fuel rich in protein (such as animal waste) are therefore a source of high

amounts of ammonia. Cyanide (HCN) is a less significant compound.

Elimination of nitrogen compounds may be performed via standard catalytic methods for NO_x reduction. It is even better to use a catalyst for destruction of NH₃ prior to combustion or wet scrubbing, provided gas temperatures are low enough. Nitrogen compounds may cause various operation problems in the scrubbers due to high solubility in water since their elimination from the water is very difficult (water is saturated with HCN and NH₃ and is not capable of collecting them anymore).

D. Sulphure

Considering the reducing environment in the gasification reactor, sulphure in the raw gas is in the form of H₂S (93-96 %); carbon disulphide CS₂, COS and SO_x concentrations are minimum. These compounds are formed from sulphure in the fuel. In general, concentrations of these compounds in biomass are very low (hundredth and tenth of weight %) and thus H₂S concentrations are commonly below limits of traceability. Yet, elimination of sulphure from the gas is highly desirable for majority of gas applications because it may cause various operation complications. Sulphure together with chlorine, fluorine, and alkali salts is corrosive for steel constructions. Sulphure is also potentially hazardous for certain types of catalysts, even in low concentrations (ppm). Technology of methanol production from syngas employs catalysts which may be deactivated (poisoned) by sulphure. Particular tar elimination catalysts are also sensitive to sulphure. Therefore it is important to thoroughly eliminate sulphure from the gas.

Wet scrubbing using additives (very costly), reactions of suitable sorbents or adsorption on metal catalysts (see chapter 6.7.3) are field-tested technologies, readily available.

E. Chlorine

Concentrations of chlorine in biofuel are rather low. Despite this fact, chlorine may cause formation of HCl and persistent organic compounds substances (PCDD, PCDF) which are created by reactions of carbon and chlorine, and catalysed by copper oxides. HCl is the most common form of chlorine in the gas.

Wet scrubber may eliminate certain chlorine compounds, especially HCl.

F. Tar

Tar is a by-product of pyrolysis (main source is a volatile combustible). Definitions of tar differ and there had not been a unified scientific view on what constitutes tar, what its composition is, and how to analyse it. Energy Research Centre of the Netherlands (ECN) has researched tar for a long time and initiated a change in studying tar, its components, properties, tar collecting, and analyses. ECN published the so called Tar Protocol whose definition and methods are recognized both in Europe and in the world [1]. Tar designates a group of organic substances with various

structures and chemical properties with boiling point higher than boiling point of benzene (80.1 °C). [2]

Concentrations of tar in gas from biomass gasification ranges from 1 to 15 g.m⁻³ (in rare cases up to 75 g.m⁻³) depending on a type of gasifier, temperature in the gasifier bed during gasification, temperature and retention time of gas in freeboard, and fuel properties (granulometry, moisture, etc.). [3][4][5]

Tar in gas is in the form of vapours or persistent aerosols. Tar condensates in lower temperatures. Tar, condensed on cool surfaces, creates tar deposits and, together with solid particles, fouls pipe and other equipment. Initiation of tar condensation is related to concentrations of tar in the gas and its composition. If temperatures are below 400 °C, tar components may be dehydrated and start to create charred materials and coke. Not all tar components are dangerous and undesired, certain compounds may have positive impact on gas lower heating value and cause no operational difficulties. Despite this fact, tar is considered to be an underbelly of thermal treatment of biomass. Therefore, if the gas from biomass is to be further used, tar has to be removed.

III. DECREASE IN CONCENTRATIONS OF TAR FROM GAS

There are generally two types of methods to decrease tar concentrations in gas: primary and secondary methods. Secondary methods further distinguish between dry and wet procedures.

A. Primary methods

Primary methods concern procedures performed inside the reactor. This is a desired practice because it has a potential to increase a total efficiency of energy conversion; concentrations of tar in produced gas are reduced and subsequent tar disposal is eliminated. In general, two procedures are applied:

Thermal destruction – pyrolysis process takes place with temperatures above ca. 1200 °C, no catalysts needed [4]. There is no minimum temperature defined for efficient destruction which depends on type of tar produced in reactor. Gasifiers with counter-current arrangement and sliding bed create primary tar and sufficient temperature for thermal destruction is 900 °C. Partial combustion of produced gas usually increases temperature; however, this process is accompanied by decrease in lower heating value by 25-30 %. Use of plasma also increases temperature but this is more suitable for waste disposal where electrical energy necessary for plasma creation is a by-product. Both these procedures are expensive and therefore thermal destruction is not a very promising method of elimination of tar from gas produced in biomass gasification.

Catalytic destruction – various materials, such olivenite, silica sand and other minerals and metals, are added into reactor fluidized bed as catalysts to enhance cracking. Dolomite, thanks to its availability, price and properties, seems to be the most promising catalyst. Relatively high temperatures and turbulent streaming produces intensive reactions in the fluidized bed; however, catalyst is scratched and becomes

deactive. On the other hand, there is insufficient contact between catalyst and tar in fixed bed reactors, and tar destruction is often incomplete.

B. Secondary methods

Secondary methods for decrease in tar concentrations are applied outside of the reactor:

Barrier filters – fixed layer of loose material, e.g. wood chips, sawdust, cork, sand. Filters remove especially dust (tar elimination is less significant). Also, there has to be a continuous renewal of filtration material so that high pressure drop due to filtration cake is avoided. Used material has to be either regenerated, combusted or disposed.

Catalysts – dolomites, zeolites, calcites, and silicates are commonly used for tar destruction as well as metal catalysts based on Ni, Mo, Co, Pt, Ru, and other metals. Majority of metal catalysts is highly sensitive to sulphure deactivation and their life is rather short. Tar elimination using dolomite achieved 95-99 % efficiency in laboratory conditions, with temperature ranging from 750 to 900 °C. Obvious disadvantage is the need to reheat the gas (temperature of gas leaving a reactor is mostly below 800 °C) to temperatures above 900 °C. Temperature distribution also has to be even throughout the whole reactor. Catalyst may be heated internally by gas combustion (decrease in lower heating value will be smaller than decrease for thermal destruction); catalyst may be heated with external sources of heat. Both types of heating lower the efficiency of the equipment. Dolomite may be further deactivated due to carbonate forming on the catalyst surface, and it is also sensitive to scratching (due turbulences in a bed – slightly bubbling fluidized bed).

Wet scrubbers – droplets of separated matter and scrubbing liquid precipitate in the scrubber, and thus decrease tar concentrations. Formation of tar droplets has to be preceded by cooling of the gas to temperatures below 100 °C (usually from filtration temperature of ca. 250 °C - separates solid particles). Exhaust temperature of gas is required to range from 35 to 60 °C. Scrubber must comprise a cooler, fine tar mist separator, and occasionally a solid particle separator, at the same time. High concentrations of solid particles may have a negative impact on efficiency of the process of tar elimination. In addition to condensation and precipitation of particles, other physical phenomena may be used for tar elimination, e.g. diffusion, solubility, and absorption. Therefore, we should focus on properties of scrubbing liquid that not only collects the relevant particles but also cleans the gas. This issue is discussed further in the text. Disadvantage of gas scrubbing systems is their decreased efficiency, which may be influenced by applying organic liquids. High-capacity sensible heat of the gas passes into a scrubbing liquid but cannot be utilized due to low output temperature of the liquid. Unless a different liquid is used, polluted water is produced and has to be pre-treated before entering the sewage system.

IV. COMPARISON OF SCRUBBING LIQUIDS

Elimination of tar from gas using a wet scrubber technique

differs for water and for RME. Although the scrubber may remove dust from the gas, dust should be removed prior to entering the scrubber as it may cause several difficulties in operation of the equipment.

A. Scrubber using organic liquid

Several organic liquids dissolve tar compounds very easily. The two substances may be mutually miscible. Scrubber using organic liquid separates tar by absorption and the process is driven by differences in actual and equilibrium concentrations. Temperatures of scrubbing should be higher than condensation point of water contained in the gas because properly selected scrubbing liquid provides satisfactory results even for high temperatures (e.g. 70-90 °C) and the scrubbing liquid should be easily regenerated. Process of tar elimination from the gas using organic liquid may be divided into several stages:

- Direct gas-to-liquid contact cooling – gas inlet temperature should be higher than initial condensation temperature of tar so that fouling of connection pipes and equipment located prior to absorber is prevented. Certain amount of tar is to be absorbed by scrubbing liquid during a cooling phase. Tar vapors may be oversaturated and aerosol formed due to sudden temperature drop; this does not occur on large-scale basis, though. Outlet gas temperature should not be lower than water condensation point so that scrubbing liquid is not spoiled.

- Tar absorption and tar mist separation – mass transfer by diffusion, driven by concentration differences, occurs when gas gets in contact with liquid under relatively stabilized temperatures (gas may be further cooled in second stage of tar elimination). Mass flow dominates over mechanical actions in aerosol separation. Scrubber for mass transfer is preferred in a second stage of tar elimination. Efficient droplet separator should be arranged beyond the scrubber to avoid scrubbing liquid or coagulated aerosol droplets leaving the scrubber.

- Cooling and treatment of gas – temperature of gas leaving the scrubber is too high and cannot be lead directly into combustion engine; therefore the gas has to be further cooled. Gas is not saturated with tar vapours due to absorption of tar by scrubbing liquid and may be further cooled to a certain level without the risk of condensate formation. Or another stage of gas cleaning may be alternatively located beyond the scrubber, e.g. for elimination of hydrogen sulphide, hydrogen chloride or nitrogen compounds .

B. Scrubbing using water

Water absorbs PAH only to a certain degree. It saturates quickly and tar starts to form a separate liquid phase – sub-micron type of aerosol (tar mist). This dispersion has to be separated so that the gas is pure enough. Tar separation in water-scrubber consists of following steps:

- Direct gas-to-liquid contact cooling – gas inlet temperature should be higher than initial condensation temperature of tar so that fouling of connection pipes and equipment located prior to absorber is prevented. Minority of

tar may be absorbed by water during the cooling stage; tar vapours may be oversaturated and aerosol formed due to sudden temperature drop; water condensates in low temperatures, too.

- Tar mist separation - expected dispersity of tar mist reaches 0.1 to 2 μm , according to literature. Tar droplets may be separated using certain types of scrubbers or other separators, see below. Their use is limited by a potential of micron and submicron particles to be separated.

- Gas heating – gas leaves the equipment saturated with tar, it is therefore recommended to slightly increase its temperature to prevent further condensation. Final outlet temperature has to be lower than maximum allowed temperature of the gas at the engine entrance.

Gas may be cooled to low temperatures using organic liquids, e.g. scrubbing oil. Outlet tar concentrations may be much lower, too. Disadvantage of this solution is the mixing of condensing water and organic substances. Used liquid is then hard to regenerate. If water is the cooling medium, NH_3 , H_2S and HCl may be absorbed from the gas, too. However, absorption process is limited by water saturation, and successful separation of these gases is conditioned by regeneration of the scrubbing liquid.

Efficient droplet separator should be positioned beyond every scrubber so that final effect of the method is not spoiled by droplets driven by scrubbing liquid and aerosol .

V. METHODOLOGY OF MEASUREMENT AT BIOFLUID 100 GASIFICATION FLUID GENERATOR

Research was performed at Biofluid 100 stand (see Fig. 1) which is equipment with stationary fluidized bed.



Fig. 1 Experimental equipment Biofluid 100

Simplified scheme of experimental equipment is presented at Fig. 2. Fuel is supplied from fuel storage tank equipped with

shovel and is introduced via dosing screw with frequency convertor into reactor. Primary supply of blower compressed air is lead into reactor under the bed, secondary and tertiary supplies are located at two high-rise levels. Produced energogas is stripped of its solid particulate matter in cyclone. Output gas is combusted in burner equipped with stabilization burner for natural gas and individual air supply. Ashes from reactor can be removed from tank located beneath bed. Power based heater for primary air supply is placed behind blower so that impact of air preheating may be monitored. In recent years, filters for research of efficiency of various methods of gas cleaning were attached to basic part of stand.

Reactor parameters:

- Capacity (in produced gas) 100 kW_t
- Fuel demand (consumption, requirement) 150 kW_t
- Wood consumption 40 kg.h⁻¹
- Air flow rate 50 m³.h⁻¹

Basic characteristics of operation at fluid generator are described in following respect:

- Operation of fluid generator – after ignition, fluid generator is operated in combustion mode so that its heating is quick. After achieving required gasification temperatures, secondary and tertiary air is supplied into generator and thus produced gas is immediately combusted and consequently heats up the generator. Air supplies are then shut off and generator is introduced into stable mode for specific and preset gasification temperature. Stable mode is achieved when amount of dosed fuel is not altered, amount of gasified air is even and temperature swings in middle section of gasification generator are stable within narrow range given by gasification temperature.

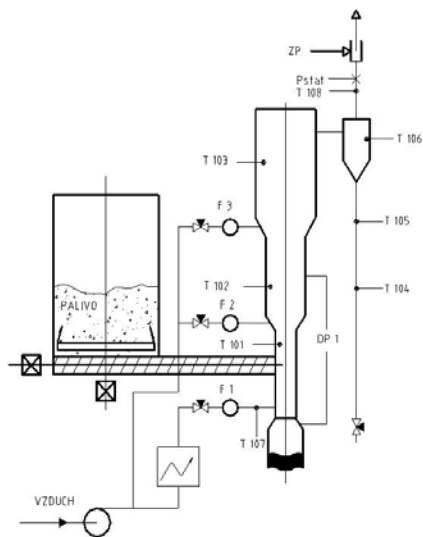


Fig. 2 Scheme of Biofluid gasifier

- Data entry of gasification process – monitored data are continuously recorded by computer in time interval of 10 seconds for each measurement. Following values are monitored:

- Frequency of convertor of dosing screw so that mass flow rate is determined;
- Temperature in various parts of equipment which is measured by thermocouples; position of thermocouples is given in detail in scheme at Fig. 2. There are 3 thermocouples along generator top, 1 thermocouple in cyclone and 2 thermocouples in in semi-coke pipe, 1 thermocouple in output gas pipe and 1 thermocouple measures temperature of primary air supply.
- Pressure difference between upper and lower sections of fluid generator (fluid bed);
- Pressure difference at orifice plate so that gas flow rate is determined;
- Pressure of the generated gas at the generator outlet and at the fuel storage tank.

Other values such as temperature and air moisture, primary air flow rate and its temperature have to be recorded manually.

Aim of the research was to determine concentrations of tar eliminated from the generated gas. Tar samples were collected using a methodology of Tar Protocol [6] and evaluated by weight spectrometer of a gas chromatograph.

VI. RESULTS AND DISCUSSION

Several experiments were performed to assess theoretical requirements of gasification. Results are given in the graph below.

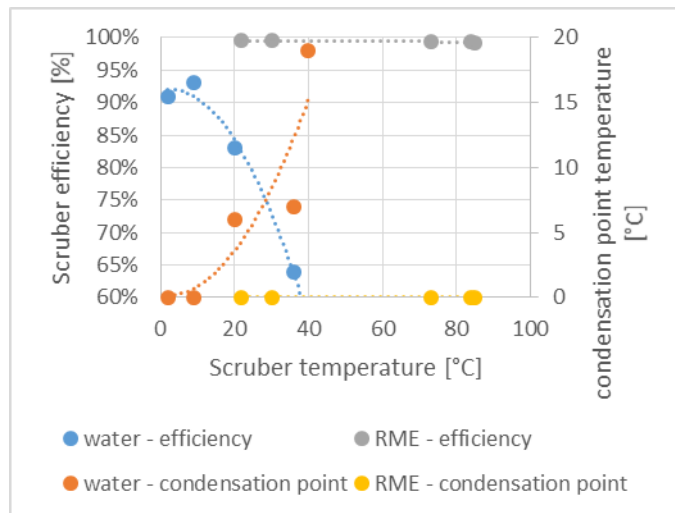


Fig. 3 Graph dependency of scrubber efficiency and condensation point temperature on temperature

- Graph shows a strong dependence of scrubber efficiency on scrubbing water temperature and thus also on condensation point of tar after scrubber. If RME is used as a scrubbing liquid, this dependence is not obvious. This may be attributed to the fact that efficiency of tar absorption by RME is very high and no dependence can be observed.
- Paper deals with elimination of tar from gas generated by biomass gasification. Tar is especially dangerous due to

formation of thick condensate. Engine manufacturers do not provide limit concentrations of tar but they do require there are no condensates in the suction area. Problems related to corrosion (H_2S , HCl , and NH_4Cl) and fouling (alkali compounds, tar, dust, NH_4Cl) may arise during cooling of gas from gasifier outlet temperature (ca. 700 °C) to engine inlet temperature (10-60 °C). It is recommended to eliminate dust at high temperatures (ca. 180-300 °C, depending on tar concentration and composition) and then lead the gas into the scrubber; this procedure helps prevent formation of sticky deposits (mixtures of tar and dust).

- Sudden cooling of gas creates fine persistent aerosol: tar mist. Size of aerosol droplets ranges from 0.1 to 2 μm . If gas saturated with vapour cools slowly, small amount of droplets nuclei are formed which develop into small droplets, as the gas continues to cool. If the gas is cooled suddenly, lot of droplet nuclei are formed and later form small droplets. If the diffused droplets are very small, mist is stable. Efficient elimination of aerosol or prevention of its formation is a key factor in gas scrubbing.

- Combustion engines require gas free from mist with temperature sufficiently exceeding condensation point of the tar. Temperature of cool walls and external pressure in suction must be considered.

- There are vast differences between water scrubbing and organic liquid scrubbing.

A. WATER

- Solubility of most tar components in water is low (except for heterocyclic compounds). Absorption by pure water eliminates heterocyclic compounds and highest PAH, especially. Polycyclic hydrocarbons with two to three rings remain in the gas and their concentrations allow for subsequent condensation. Separate liquid phase is either driven by water or leaves with gas in the form of aerosol. Water supplied to real-life equipment is assumed to be partially saturated with tar. Tar scrubbing is therefore based on elimination of aerosol.

- Disadvantage of gas scrubbing using water is a transfer of applicable heat of the gas into low-potential production of environmentally unfriendly waste water; another disadvantage is the need to have a source of cool water or equipment for its production. During summer, facilities may utilize spray tower, sprinkled cooler or chiller. Chiller is very expensive.

- Method of scrubbing using water is relatively cheap.

B. ORGANIC LIQUID

- Most of the tar components are fully soluble in the organic liquid. Ability of organic liquids to collect tar is therefore high, and the equilibrium concentrations corresponding with the selected temperature are much lower than equilibrium concentrations of tar condensation. Elimination of tar using organic liquid is based above all on diffusion, and therefore it is necessary to use an efficient mass exchanger. Similar to the technology of water scrubbing, the gas must be cooled. Gas output temperature should not drop below 75-80 °C (depending on gas moisture) so that scrubbing

liquid is not impaired by the condensing water, and that no condensation of water disrupts the heat and mass flows in the scrubber.

- The advantage of organic scrubbing is high efficiency and ability to reduce tar condensation point well below the scrubbing temperature. Other positive aspects include: virtually waste-free facility and the ability to use gas heat for cooling of scrubbing liquid.

- Disadvantage of scrubbing using organic liquid is especially the high cost of scrubbing liquid, which must be constantly replenished due to evaporation.

- Type of organic liquid should be selected with respect to price, in accordance with Ewell classification and vapour pressure. Considering the need to minimize the liquid loss, scrubbing liquid pressure at operating temperature should be as low as possible.

- For economic reasons, it is desirable that the tar concentrations, or concentrations of other impurities in the gas, are minimized within the scope of primary methods (as a part of optimization). This reduces consumption of scrubbing liquid and requirements for gas scrubber efficiency.

- Organic dust dispersed in the generated gas is difficult to wet with water and contains a large proportion of micron and submicron particles. Its removal in water scrubber is therefore very difficult. Alternatively, direct water cooler and electroseparator may be used. Elimination of dust using organic liquid is, from the physical point of view, relatively simple, and it is therefore possible to combine the process with tar scrubbing. It is necessary to be careful and take measures to prevent the formation of sticky deposits in the scrubber and find solution to liquid regeneration problems. Elimination of dust using textile filter seems to be a much easier solution for both tar elimination methods.

ACKNOWLEDGEMENT

"This work is an output of research and scientific activities of NETME Centre, regional R&D centre built with the financial support from the Operational Programme Research and Development for Innovations within the project NETME Centre (New Technologies for Mechanical Engineering), Reg. No. CZ.1.05/2.1.00/01.0002 and, in the follow-up sustainability stage, supported through NETME CENTRE PLUS (LO1202) by financial means from the Ministry of Education, Youth and Sports under the „National Sustainability Programme I“. "If you are using *Word*, use either the Microsoft Equation Editor or the *MathType* add-on (<http://www.mathtype.com>) for equations in your paper (Insert | Object | Create New | Microsoft Equation *or* MathType Equation). "Float over text" should *not* be selected.

REFERENCES

- [1] Simell, P. at al Provisional protocol for the sampling and analysis of tar and particulates in the gas from large-scale biomass gasifiers. Version 1998, Biomass and Bioenergy, Volume 18, Issue 1, January 2000, Pages 19-38, ISSN 0961-9534, DOI: 10.1016/S0961-9534(99)00064-1.

(<http://www.sciencedirect.com/science/article/B6V22-3Y0J95P-3/2/bb9078796862ce621fac3f15ac3c8187>)

- [2] Neft, J. P. A. et al. Guideline for Sampling and Analysis of Tar and Particles in Biomass Producer Gases. Energy project ERK6-Ct199-2002 www.tarweb.net
- [3] Kurkela, E., Ståhlberg, P. Air Gasification of Peat Fluidized-bed Reactor. I. Carbon Conversion, gas yields and tar formation. Fuel Processing Technology 31, 1992, 1-21
- [4] Coll, R., Salvado, J., Farriol, X., Montané, D. Steam Reforming Model Compounds of Biomass Gasification Tars: Conversion at Different Operating Conditions and Tendency towards Coke Formation. Fuel Processing Technology 74, 19-31, 2001, Elsevier
- [5] Kurkela, E., Ståhlberg, P., Laatikainen, J., Simell, P. Development of Simplified IGCC-Processes for Biofuels: Supporting Gasification Research at VTT. Bioresource Technology 46 (1993) No.1-2, p.
- [6] Good, J., Ventress, L., Knoef H.: Sampling and analysis of tar and particles in biomass producer gases, [on-line] http://www.tarweb.net/results/pdf/Technical-Report-version-3_8-final.pdf

The effect of regulatory uncertainty on water-right prices: The case of the Loa Basin in the Antofagasta Region of Chile

Oscar Cristi, Carlos Díaz, Gonzalo Edwards and Eric Edwards

Abstract— This paper analyzes institutional arrangements that impose barriers to voluntary water transfers in the Loa Basin, in northern Chile, and their effect on the willingness of mining firms to purchase freshwater rights in the market. We argue that the restrictions help explain why mining companies prefer desalination to acquiring additional water rights in the market, despite the high relative price of desalination. We use data from the Antofagasta Region, in Northern Chile, to provide evidence to support this assessment. We focus on restrictions imposed by the Chilean Water Authority (Dirección General de Aguas: DGA) via a new dataset on the frequency transfers are approved. The restrictions on trade are based on regulations granting the Water Authority broad powers in regulating changes in water-diversion location and in the nature or type of water use. We find mining firms are utilizing desalinated water at significant price premiums, even after adjusting for the institutional uncertainty of freshwater use, and we speculate that other institutional and resource-specific factors contribute to this decision.

Keywords— Desalination, Water Markets, Water Regulation, Water Rights.

I. INTRODUCTION

GROWING pressure on fresh water resources has led countries to increasingly rely on water markets to allow water to move from low to high value uses [1], [2]. This is the case in the western United States, Chile, Australia, South Africa and New Zealand. Moreover, other Latin American countries have been discussing policy reforms moving towards markets [3], [4]. Despite optimism that water markets would provide an effective mechanism for rectifying inefficient water allocations, the impact of water markets on water reallocation has been slow. This is the case despite significantly higher marginal values in urban, industrial and mining uses, as compared to irrigated agriculture, where most of the water rights are presently concentrated [5]. Institutional

Oscar Cristi is Professor of Economics, Universidad de San Sebastián, Santiago, Chile (e-mail: oscar.cristi@uss.cl).

Carlos Díaz is Professor of Business Administration, Pontificia Universidad Católica de Chile, Santiago, Chile (e-mail: cdiazv@uc.cl).

Gonzalo Edwards is Professor of Economics, Pontificia Universidad Católica de Chile, Santiago, Chile (e-mail: gedwards@uc.cl).

Eric Edwards is Assistant Professor of Applied Economics at Utah State University (e-mail: eric.charles.edwards@gmail.com).

arrangements that impose barriers to voluntary water transfers help explain this anomaly [6]. These arrangements have been developed to protect the environment and the interests of third parties from adverse impacts that may result from trade. The latter includes conflicts with the exercise of other water rights, threats to public safety, and harms to public welfare [6].

Examples of the arrangements that deter transactions are the need to get approval from the Chilean Water Authority when either the location or nature of the use is changed with the transaction; and when the regulator restricts the amount to be consumed by the new owner, not to the amount of rights held by the original owner, but to the amount actually consumed by him/her [6]. Regulatory restrictions that limit trades to particular parties or to and from particular types of users should be clearly visible in the average prices paid for inter-sector trades. After accounting for the priority of rights and the quality of water delivered, a smoothly operating water market without restrictions on trade should see prices stabilize across sectors. Northern Chile offers an example where active water markets have moved water from low-value agriculture to the mining sector. It also offers an example where market prices for water from freshwater sources appear much different from the prices paid by mining firms for desalinated water.

In this paper, we analyze institutional arrangements that impose barriers to voluntary water transfers in the Loa Basin, in northern Chile, and their impact on water prices in the market. We focus on restrictions imposed by the Chilean Water Authority. These restrictions affect the probability of getting final approval on the use of purchased water rights in another location, and thus reduce the willingness of buyers to pay for a water right. Use is approved only after a period of delay while the regulator judges whether the change should be granted, which also reduces the price of the right. Because these restrictions are not equally applied to all sectors, with mining facing the higher number of restrictions, these arrangements are a partial explanation for water-right price differences among uses.

We hypothesize that these restrictions help explain why mining companies, instead of acquiring additional water rights in the market, use desalinated water, in spite of its high relative price. We use water price data for the Antofagasta Region in northern Chile, along with data from the regulatory approval

process in the same region, to find the price of water after accounting for uncertainty and delay. We then compare these prices to the cost of desalination, finding that this regulatory action explains most of the use of high-cost desalination in the region.

II. BACKGROUND

This study will focus on the Loa Basin in northern Chile's Second Region, also known as the Antofagasta Region. Northern Chile represents over one-fourth of world copper production and is a relevant player in many other minerals. It has a growing urban population, is the home of indigenous populations with traditional agriculture, and is the site of valued ecosystems. It is an extremely arid area with the annual average precipitation ranging from 4 mm in Calama (elevation 2,260m) to 146 mm in Lequena (elevation 4,000m). Mining is the main economic activity in the region, with 65% of the regional GDP. Copper is the primary mineral resource. Agriculture represents less than 1% of regional GDP and produces only for the local market. The importance of the approximately 2,000 hectares of irrigated land lies in its link to traditional agriculture and to indigenous communities in the area.

Freshwater in the Antofagasta Region originates high in the mountains on the eastern border between Chile and Bolivia and percolates into an aquifer system. This system encompasses the Loa River and its two main tributaries, the Salado and the San Salvador, as well as at least two non-connected groundwater aquifers [7]. These aquifers are linked to surface water, primarily fed by the aquifers, although some percolation occurs from surface to groundwater sources [8]. Although primarily fed by groundwater, surface water availability is still variable due to the relationship between precipitation, water table level, and surface flow. For this reason, the availability of groundwater is considered much less variable than that of surface water. Current evidence is not conclusive as to whether water is being extracted at higher or lower rates than aquifer recharge [9].

Water Rights and the Market

Water rights in Chile, once granted, are fully protected as private property under Article 19 of the Chilean Constitution. Under the 1981 Water Code, water rights are completely separated from land ownership, being subject to the general system of real estate title registration, to be freely bought, sold, mortgaged, and transferred, like other forms of real property. In the Antofagasta region, groundwater rights granted between 1990 and 2012 total 1.06 million m³/day (prepared by the authors with information from DGA). Surface water rights, many of which were granted prior to 1990, total 0.55 million m³/day [10], [11]. Because much of the available water (surface water and groundwater) has been already granted as water rights, new water requirements need to be satisfied through the market or by the development of new water sources such as desalinated water.

As Table I shows, consumption in Region II is less than

total rights granted in spite of very high water scarcity. The reason behind the low relative consumption lies, at least partially, in institutional factors. As an example, mining companies use only 48% of the water rights they hold [12] due to restrictions on the use of water.

Economic Sector	Consumption (m ³ /day)	Percentage
Agriculture & Livestock	285,811	25%
Urban use	94,608	8%
Industry	164,678	15%
Mining	419,472	37%
Energy	128,995	11%
Other	29,117	3%
Total	1,122,682	100%

Sources: DGA [12]. The source for mining is DGA [13].

Regulation of the Water Market

Water-right trading in the Antofagasta Region has been affected by the DGA, which has established restrictions to changes in the location of ground and surface water extractions. These restrictions impose uncertainty on mining purchases of freshwater, because these firms must typically change the location of extraction. Restrictions to changes in groundwater-diversion location seek to avoid possible damage to groundwater-fed wetlands and surface water availability at specific locations. Restrictions on surface water diversion are pursued to reduce third-party effects of trade, such as negative externalities on water quality. As an example, a change in the location of water diversion from the Salado (Salty) River to some downstream location on the Loa River, after the place in which the Loa and the Salado meet, may affect the quality of water for some water users.

Other restrictions to market activity come from environmental concerns. Industries that acquire water to develop new non agricultural projects need to carry out an environmental impact assessment. In the Antofagasta Region, mining is the main industry and there are cases where a mining company has bought water rights, not being able to use them after the environmental agency rejected the project. As an example, the mining company Quadra Minino bought underground water in 2008 in the Pampa Llalqui, 30 kilometers from Calama, for around US\$ 40 million, but has not been able to use it for environmental reasons.

These constraints in the Antofagasta Region create market segmentation with most surface water transactions taking place within a canal, where changes in the point of extraction do not need DGA approval.

III. MODEL

We assume the market for freshwater rights is competitive, and water is available at a price of P_{WR} . Mining firms can purchase water at this price, but in order to use the water they must pass a regulatory review. The review is passed, $I=1$, with a probability of p , and takes some amount of time, T , to be conducted. The review is not passed, $I=0$, with probability $1-p$, taking the same amount of time T . If the review is passed, the mining firm uses the rights. If the review is not passed, the rights can be sold at a fraction, α , of the purchase price.

As an alternative to freshwater, mining firms have the option of using desalinated water. The unit price of desalinated water, P_{DW} , is based on a number of parameters: size of desalination plant, size of pumping infrastructure, expected plant life, distance of mine from ocean, elevation of mine above sea level, cost of electricity, and interest rate. If a mine can obtain desalinated water at P_{DW} , the value of a water right to the mining firm, V_{WR} , is as follows:

$$V_{WR} = \begin{cases} \frac{P_{DW}}{(1+r)^T}, & I = 1 \\ \frac{\alpha P_{WR}}{(1+r)^T}, & I = 0 \end{cases} \quad (1)$$

If $I=1$, the right is as valuable as the desalinated water, but with a time delay T . If $I=0$, the right is only worth its salvage value, after time T . To the mining firm, the expected value of freshwater is:

$$E[V_{WR}] = p \cdot \frac{P_{DW}}{(1+r)^T} + (1-p) \cdot \frac{\alpha \cdot P_{WR}}{(1+r)^T} \quad (2)$$

A risk neutral mining firm will then buy freshwater when:

$$P_{WR} \leq E[V_{WR}] \quad (3)$$

Substituting the expected value of a water right from equation 2 and doing some algebra, we arrive at the condition for a firm purchasing a freshwater right:

$$P_{WR} \leq \frac{p}{(1+r)^T - \alpha(1-p)} P_{DW} \quad (4)$$

If P_{DW} and P_{WR} are such that the condition in equation 4 is not met, we expect the firm to use desalinated water. If firms use both fresh and desalinated water, we would expect equality to hold. We use data from Chile's Region II to explore the implications of this formula further in the forthcoming sections.

IV. DATA

A. Water Market Data

The market in the Rio Loa Basin is one in which farmers, indigenous communities, water utilities and mining companies

trade water rights. In the analysis that follows, we use data on 102 surface water and 24 groundwater-right transactions occurring in the period from January 2005 to December 2009, recorded in the official Property Registers (Conservadores de Bienes Raíces) of Loa and Taltal. The 126 registers is the outcome of filtering a wider data set on 447 registers of the Property Registers of Loa and Taltal. The filters were: 1) The register is not due to a market transaction (such as inheritance, mergers). 2) The transaction includes other goods together with the water right (typically land). 3) The water right does not belong to the Loa Basin. 4) The transaction is for a water flow of less than 4.3 m³/day. 5) The use of the water right is not permanent and/or continuous through time. 6) There is no information on the water flow or the water flow unit is missing. 7) There is a family relationship between the buyer and the seller. 8) The transaction took place before 2005. 9) The transaction price is missing. 10) The reported price is clearly wrong (one case).

The final sample of 126 registers represents a total amount of 11,335.9 m³/day of surface water with an average of 111.1 m³/day per transaction, and a total amount of 52,249.5 m³/day of groundwater with an average of 2,177.1 m³/day per transaction.

Weighted average prices were US\$ 0.1841 and US\$ 0.9017 per cubic meter, for surface and groundwater respectively. It must be said that original prices were in UF's per liter per second. This is a perpetual right. The UF or Unidad de Fomento is a non-circulating currency in Chile, which adjusts for inflation. Prices were translated into dollars per cubic meter, using the December 2011 average UF and dollar values, and a 7% rate of interest.

These differences in prices have two components: explained differences, based on different probabilities of regulator approval and length of delay, and unobserved causes, one of which is perceived reliability of groundwater versus surface water. We discuss these differences later in the paper. As another theoretically possible unobserved cause, we should mention that prices for surface and groundwater rights differ in their exact transaction dates within the period.

As Table II shows, prices for both types of rights are highly dispersed.

	Surface Water		Groundwater	
	US\$/m ³ /day	US\$/m ³	US\$/m ³ /day	US\$/m ³
Number of observations	102	102	24	24
Weighted average	959.93	0.1841	4,701.66	0.9017
Weighted st. dev.	492.12	0.0944	6,051.64	1.606

Note: Water-right prices in dollars per m³/day have been converted into dollars per m³ using a 7% discount rate and considering 365 days per year.

B. Regulator Approval Data

Restrictions to changes in the location of water extractions

can affect the time the DGA takes to resolve each application, and the likelihood of receiving a positive answer from the DGA. Public data from the *Catastro Público de Aguas* of the DGA indicate that during the period 1988 to 2012, the DGA approved 18% and 76% of the applications for changes on extraction location of surface and groundwater, respectively, in terms of volume. The average time for the DGA's approvals on these applications is 1.66 years in the case of groundwater, and 2.49 years in the case of surface water. Table III summarizes the data for those applications. Although we report averages for resolution time of each category individually, we fail to reject the hypothesis that the means of the approved applications is different from applications that were turned down. For the calculations we assume the length of time is that given for the 'Total Applications.'

	Surface Water			Groundwater		
	Number	m ³ /day	Time to resolution (days)	Number	m ³ /day	Time to resolution (days)
Total Applications	29	45,765	947	73	309,795	537
Approved by DGA	11	8,158	908	42	236,207	606
Denied by DGA	11	19,072	841	27	63,220	315
Withdrawn	6	18,064	1,214	3	7,776	1,560
Pending	1	472		1	2,592	

Source: Prepared with information from *Catastro Público de Aguas*, DGA.

C. Desalination Cost Data

Table IV shows current and expected production of desalinated water for the period 2010-2019. Expected production of desalinated seawater for year 2019 reaches 472,090 m³/day, and it represents approximately 25% of the total amount of water flows granted through permanent and continuous-use consumptive water rights in the Second Region.

Firm	2010	2013	2016	2019
Escondida Mining Co., Coloso Plant (a)	45,360	45,360	45,360	45,360
Escondida Mining Co., Coloso Plant Enlargement			55,296	276,480
Aguas Antofagasta, La Chimba (b)	51,840	51,840	51,840	51,840
Aguas Antofagasta, Southern Desalination Plant (b)		86,400	86,400	86,400
Antofagasta Minerals, Esperanza (b)	4,320	4,320	4,320	4,320
Quadra Mining Co., Sierra Gorda Project ©		5,443	5,443	5,443
Michilla Mining Co. (d)	2,246	2,246	2,246	2,246
TOTAL	103,766	195,610	250,906	472,090

Sources: (a) Cochilco [14]; (b) information provided by Aguas Antofagasta; (c) Quadra [15]; (d) Cochilco [16].

Desalination costs depend on several factors including technology used, plant capacity, site characteristics, water quality standards, regulatory requirements, construction and financial costs, and the variable costs associated with labor, chemicals, maintenance and energy. Table V summarizes costs reported in the literature for a variety of reverse-osmosis desalination projects. Plant capital and water production costs decrease significantly as a function of capacity. The unit cost of seawater desalination is more variable for smaller plants.

	Size of Plant (m ³ /day)	Total Costs (US\$/m ³)
Karagianis and Soldato [17]	15,000-60,000	0.48-1.62
	100,000-320,000	0.45-0.66
Wittholz, O'Neill, Colby and Lewis [18]	50,000	0.70
	275,000	0.50
	500,000	0.45

Table VI shows investment and operating desalination costs by reverse osmosis in the northern part of Chile. Operating costs represent on the order of 55% of total costs, while electricity is by far the most important of the operating costs, assumed to represent 80% of such costs at present. Case A assumes an investment of US\$ 70 million, a useful life of 20 years and no residual value [16]. Case B corresponds to a plant developed by Aguas Antofagasta in the southern part of Antofagasta named "Planta Desaladora Sur Antofagasta." It assumes an investment of US\$ 120 million, a useful life of 20 years and no residual value. To estimate the capital costs involved, a rate of discount of 7% was assumed. This is the rate of discount used to determine urban-water prices in Chile. Electricity consumption was estimated at 3,4KWh/ m³ [13]. The cost of the KWh was calculated by the authors using the average marginal cost of electricity in the northern part of Chile for 2011 (US\$/KWh 0.092) and the capacity cost used in April 2011 for calculating the regulated price for consumers (US\$/KWh 0.0137). The plant capacity factor was assumed at 90%.

	Size of Plant (m ³ /day)	Fixed Costs (US\$/m ³)	Electricity Costs (US\$/m ³)	Other Variable Costs (US\$/m ³)	Total Costs (US\$/m ³)
Case A	45,360	0.40	0.36	0.09	0.85
Case B	86,400	0.36	0.36	0.09	0.81

In the case of the mining industry in northern Chile, pumping to reach the mines is a major component of total cost. Total cost for desalinated water is a function of the geographical and altitude of the location in which desalinated water is used. As Table VII shows for a project at an altitude of 3,150m and a plant size of 45,360 m³/day, the pumping costs of \$2.91 increase the production cost of desalinated water from US\$ 0.85 per m³ to approximately US\$ 3.76 per m³ (pumping capital costs are US\$ 1.25 per m³ and operating

costs are US\$ 1.65 per m³). Energy is again the most important of the operating costs of pumping, assumed to represent 90% of such costs. For a plant size of 10,368 m³/day and an altitude of 900m, the total cost of desalination, pumping included, is estimated at US\$ 2.47 per m³.

	Size of Plant (m ³ /day)	Fixed Costs (US\$/m ³)	Variable Costs (US\$/m ³)	Total Costs (US\$/m ³)
Case 1: Pumping from 0 to 3,150 m.a.s.l.	45,360	1.65	2.10	3.76
Case 2: Pumping from 0 to 900 m.a.s.l.	10,368	1.55	0.92	2.47

V. ANALYSIS

From the prior section, it is clear that desalination costs for mines at altitude are much higher than observed water trading prices. We argue that for mining firms, water-right prices are related to desalinated water costs, including pumping, through an observable mechanism, namely the probability of the approval of purchased water rights by the water regulator. In this section we use the data and model discussed in the previous two sections to create estimates of where the use of freshwater should make sense for mining companies as a function of elevation, based on assumptions about other aspects of the desalination decision, then compare these estimates with observed mining firm decisions about desalinated water.

The weighted average price of groundwater, US\$ 0.9017 per cubic meter as shown in Table II, is slightly higher than the cost of desalination at sea level. When pumping to higher elevations is considered, observed groundwater right prices are a fraction of the cost of desalination, which can be as high as \$3.76 at an elevation of 3,150m. (cf. Table VII). If the approval of the change in water diversion location were certain, with no delay in the process, then mining firms would purchase groundwater rights when they were the same price or less than desalinated water. Because the price of desalination is high, we would expect that all mines, in this case, would choose to purchase groundwater rights because the groundwater is located near the mines, thus avoiding desalination and pumping costs.

If the approval is not guaranteed and/or it is not automatic without delay, then the observed price of a groundwater right is not the correct price for comparison. Instead, we must modify the observed water prices using equation 4 to account for the uncertainty the mining firm faces when purchasing a groundwater right. Table VIII provides the parameters to determine the equivalent groundwater price for the two cases discussed previously as well as for the case of sea level desalination. The final row of the table provides the equivalent groundwater price, the right hand side of the inequality in equation 4, which is the price at which a groundwater right would need to be available for a mining company to consider purchasing it.

	Sea Level	Case 1 (900 m.a.s.l.)	Case 2 (3,150 m.a.s.l.)
Regulator approval probability (p)	76.25%	76.25%	76.25%
Interest rate (r)	7%	7%	7%
Time to decision (T, in years)	1.47	1.47	1.47
Price of desalinated water (P _{d,w})	\$0.83	\$2.47	3.76
Salvage value percentage (alpha)	20%	20%	20%
Equivalent groundwater price (RHS of inequality in (3))	\$0.60	\$1.78	\$2.71

Note: The parameter p was obtained from dividing approved applications (in cubic meters) by total applications, in Table III.

The weighted average price for a groundwater right in the region is \$0.9017 per cubic meter, the left side of the inequality in equation 4. We see that in the case of water at sea level, it is not sensible for a mining firm to purchase groundwater rights, as the desalination alternative is cheaper after accounting for uncertainty and delay. The mining firm would not pay more than sixty cents for a groundwater right to a cubic meter. Case 2 seems a clear case where the purchase of groundwater rights is justified. However, while we can definitively say the purchase of groundwater rights is not justified in the sea level case, because the uncertain asset is also more expensive, we cannot make the claim that it is unjustifiable to use desalinated water at high altitudes, because we do not know the risk preferences of the mining firms. That is, it may be worth it to the mining firm to pay more for desalinated water to guarantee its availability, rather than to buy groundwater rights whose expected value is cheaper but water flow not guaranteed.

Surface Water Rights

The weighted average price of surface water, US\$ 0.1841 per cubic meter, is much less than that of groundwater, US\$ 0.9017 per cubic meter. This price difference is explained by both observed and unobserved factors. The observed factors involve the regulatory decision on the transfer of the use of the water right. Surface water transfers were only approved 18% of the time, whereas groundwater transfers were approved approximately 76% of the time. This regulatory decision also took longer for surface water approvals, 2.59 years, versus 1.47 years in the case of groundwater. We know groundwater is more reliable than surface water as well, independent of the regulatory framework. Thus, the price of surface water also reflects the natural system reliability issues associated with its use. Table IX provides the parameters used to calculate the equivalent surface water right price for the three scenarios previously discussed. The final row of the table provides the right hand side of the inequality in equation 4 for surface water—the price a surface water right must not exceed to be considered for purchase by a mining company.

	Sea Level	Case 1 (900 m.a.s.l.)	Case 2 (3,150 m.a.s.l.)
Regulator approval probability (p)	17.83%	17.83%	17.83%
Interest rate (r)	7%	7%	7%
Time to decision (T, in years)	2.59	2.59	2.59
Price of desalinated water (P_{dw})	\$0.83	2.47	3.76
Salvage value percentage (alpha)	20%	20%	20%
Equivalent surface water price (RHS of inequality in (3))	\$0.14	\$0.43	\$0.65

Note: The parameter p was obtained from dividing approved applications (in cubic meters) by total applications, in Table III.

We see that the average price of a surface water right (\$0.1841 per cubic meter) is less than half the price at which surface water is competitive with desalinated water at 900m. This means that if the desalinated water is not to be used at sea level, then there would be gains in buying freshwater rights instead.

VI. DISCUSSION

This paper illustrates the impact of regulation on prices, volumes traded and the allocation of water-related rents in an environment where water rights are allocated and protected by law, even where there exists a market where the rights can be traded. In the Loa Basin, where regulations from DGA restrict water-diversion changes, mining firms use desalinated water at a higher cost compared with fresh water because of uncertainty among prospective buyers about approval of their use of the rights. This hinders the exchange of water rights and has prevented farmers and indigenous communities—who own water rights—from capturing the scarcity rents through trade.

Thus, even in a setting where we expect secure rights and efficient markets, the typical problems of water markets abound. Reference [119] describes the process of water transfers saying: "... underlying decisions regarding resource allocation are taken through an on-going dance involving water users, environmental and other non-ownership interests, legislatures, state water agencies, and others." As [20] pointed out almost two decades ago, these arrangements cause uncertainty in water-transfer completion because regulators could decide not to approve the water transfer, court challenges could appear based on regulations or environmental concerns, and the threat of regulatory or court challenge could dissuade water buyers from continuing the pursuit of water transfers.

Data on water right transactions performed between January 2005 and December 2009, together with available information on the cost of desalinating sea water and pumping it to different elevations above sea level, show that the cost of desalinating and transporting one cubic meter of seawater to 3,150m is 20.4 times the price of surface water and 4.2 times the price of groundwater. These differentials may be used to proxy the magnitude of the effects of regulations limiting the transfer of water rights across geographic zones, and potentially, the lost economic rents by farmers and indigenous

communities.

Today, mining companies are both using desalinated water and building desalination plants for use at altitudes much higher than the model presented here would predict. This means that observable variables, approval probabilities and time to completion, only go so far in explaining price differences. One possible explanation is the fact that approvals to changes on extraction location have become harder to obtain, due to increased environmental concerns. Increasingly, restrictions to transfer water away from the point of diversion are imposed not only by the DGA, but also by the Environmental Authority. Accordingly, the probability of obtaining approval for the transfer today is even lower than indicated from the data presented in this paper.

Another possible explanation is that mining companies are willing to pay a high premium to eliminate risk. Desalination, once the initial investment is made, is a more secure supply of water than natural sources, leading mining companies to be willing to pay a higher price for the water. Water is not a homogeneous commodity in this case, as the risk profile of the water becomes an important feature in determining its price.

REFERENCES

- [1] Rosengrant, Mark W. and Hans Binswanger (1994): "Markets in tradable water rights: Potential for efficiency gains in developing country water resource allocation." *World Development*. 22: 1631-1625.
- [2] World Bank (1993): "Water Resource Management: A World Bank Policy Paper". Washington, D.C. World Bank, Washington, D.C. 20433 U.S.A. ISBN 0-8213-2636.
- [3] Bauer, Carl J. (2004): "Siren Song: Chilean Water Law As Model For International Reform." Washington DC: Resources for the Future.
- [4] Cristi, Oscar (2010): "Risk Analysis and Water Market Activity: The influence of heterogeneous risk preferences on water market activity: an application to the Paloma System of the Limarí Water Basin, Chile" 2010. VDM Verlag, Dr. Muller Aktiengesellschaft & Co. KG.
- [5] Brewer, Jedidiah, Robert Glennon, Alan Ker and Gary D. Libecap. (2007). "Water Markets in the West: Prices, Trading, and Contractual Forms," NBER Working Papers 13002, National Bureau of Economic Research, Inc.
- [6] Eden, Susanna, Robert Glennon, Alan Ker, Gary Libecap, Sharon Megdal and Taylor Shipman. (2008). "Agricultural Water to Municipal Use: The legal and institutional context for voluntary transactions in Arizona" *The Water Report, December 15. Envirotech Publications*. http://ag.arizona.edu/azwater/files/ag_to_muni_article.pdf.
- [7] Houston, J and Hart, D. (2004). "Theoretical head decay in closed basin aquifers: an insight into fossil groundwater and recharge events in the Andes of northern Chile." *Quart J. Eng. Geol. Hydrogeol.*, 37: 131 – 139.
- [8] Houston, J. (2006): "Variability of precipitation in the Atacama Desert: its causes and hydrological impact." *International Journal of Climatology*, 26(15), 2181-2198.
- [9] Grosjean, M. and Veit, H. (2005). Water Resources in the Arid Mountains of the Atacama Desert (Northern Chile): Past Climate Changes and Modern Conflicts. U.M. Huber et al. (eds), *Global Change and Mountain Regions*, pp. 93-104.
- [10] Dirección General de Aguas (2003) Evaluación de los Recursos Hídricos Sectores Calama y Llalqui, Cuenca del Río Loa, Informe Técnico S.I.T. 85: 1-114.
- [11] Dirección General De Aguas (2005) Evaluación de los Recursos Hídricos Superficiales en La Cuenca del Río Loa S.I.T. 192: 1-38.
- [12] Dirección General de Aguas (2007): "Estimaciones de Demanda de Agua y Proyecciones Futuras. Zona I Norte. Regiones I A IV. S.I.T. N° 122. Santiago, Enero Del 2007.

- [13] Dirección General de Aguas (2008): “Derechos, Extracciones y Tasas Unitarias de Consumo de Agua del Sector Minero, Regiones Centro-Norte de Chile” S.I.T. N° 146, Santiago, Marzo.
- [14] Comisión Chilena del Cobre (COCHILCO). (2009) “Gestión Del Recurso Hídrico Y La Minería En Chile: Proyección Consumo De Agua En La Minería del cobre 2009-2020.” http://www.cochilco.cl/productos/pdf/2009/proyecciones_consumo_agua_AZ_RB.pdf
- [15] Minera Quadra Chile Ltda: Environmental Assessment report for "Proyecto Sierra Gorda", URL: https://www.eseia.cl/archivos/089_215_3109_Cap_02_Descripcion_Proyecto_Rev0.pdf.
- [16] Comisión Chilena del Cobre (COCHILCO) (2008): “Good practices and water efficiency in the Mining Industry.” http://www.cochilco.cl/english/productos/doc/best_practices_and_the_efficient_use_of_water.pdf
- [17] Karagiannis, Ioannis C. and Petros G. Soldatos (2008): Water desalination cost literature: review and assessment. *Desalination*, 223, pp. 448-456. Published by Elsevier.
- [18] Wittholz, Michelle K.; Brian K. O'Neill; Chris B. Colby and David Lewis (2008): “Estimating the cost of desalination plants using a cost database.” *Desalination*, Volume 229, Issues 1-3, pp. 10-20, September.
- [19] Slaughter, R. A. (2009): “A Transactions Cost Approach to the Theoretical Foundations of Water Markets.” *JAWRA Journal of the American Water Resources Association*, 45: 331–342. doi: 10.1111/j.1752-1688.2008.00294.x.
- [20] Lund, Jay R. (1993): “Transaction Risk versus Transaction Costs in Water Transfers.” *Water Resources Research*, Vol. 29, No. 9, pp. 3103-3107, September.

Accounting aspects of risk management and improvement of the entrepreneurial venture enterprise

Nenad R. Lalić*, Srdjan M. Lalić**, Dragan Milovanović ***, Biljana Kovačević ****

*Professor, University of East Sarajevo, Faculty of Economics Brčko, Bosnia and Hercegovina

** Ph. D., University of East Sarajevo, Faculty of Business Economics Bijeljina, Bosnia and Hercegovina

*** assistant master, University of Banja Luka, Faculty of Economics, Bosnia and Hercegovina

**** assistant master, University of East Sarajevo, Faculty of Business Economics Bijeljina, Bosnia and Hercegovina

Abstract—The economic crisis has affected many of the world capital markets and we are faced with its effects were relatively prepared for the next one, conducted numerous studies in the field of risk management in the past decade. This research has made major news in the field of risk management, especially in the modeling of market risk. Investor on the basis of risk analysis balance between yield and the potential risk.

This paper is about analyzes of the situation in the capital of Bosnia and Hercegovina, it's analyzed the risk and the state in the management of the same. Since there is no system for dealing with risk management, many companies have suffered financial losses in the global market.

The aim of this paper, through mathematical analysis of different method values, elaborate features and the importance of its applications in the capital market of Bosnia and Hercegovina. There were used scientific methods of deduction, comparative analysis and analysis of good practices. The processed data will be used for technical and scientific discussion on the importance of applying the method risk values as a function of risk management, as well as the basis for improving existing analytical framework.

Keywords—accounting, risk management, business performance, the discount rate, risk analysis, leverage;

I. INTRODUCTION

Globalization has brought some changes throughout society. These changes are also reflected in the economy, especially on the trade. Trade is exposed to numerous risks. Risk is determined by economic adverse event that may affect trade.

Risk is inevitable and he can not be avoided, however, it can be controlled. It is in human nature to tend to protect all adverse events that adversely affect it to a minimum, so with the trade. There are numerous methods of hedging.

Risk management is a process with a clear goal, which is to assist investors in understanding and evaluating the risks and when to take steps in order to achieve success. Risk management seeks to reduce the risks to which the investor is exposed.

Risk is inevitable and can not be avoided, but it can and must be managed. There are numerous examples in which financial institutions have come into difficulties in business because they are in the situation that led to not adequately deal with the risks and didn't manage them. Information about the risk management are closely linked with other information on which to make the right decisions. There are many organizations involved in risk management and outcome of these studies is to define international standards for risk management AS / NZ 4360:2004 and ISO 31000:2009. International standard ISO 31000:2009 is the first international standard for risk management in the world and appears in 2010.

It is important to note that the risk management process that includes a series of steps that allow for initial and continuous assessment of potential risks and hazards, all with the aim to provide business and to achieve goals. Risk management is a business function that, first of all, identify risk, then assess and manages it, to keep it controlled at the end, which means that the system manages the risks with which are exposed to business.

II. TYPOLOGY AND INCLUDING RISKS IN BUSINESS ENTERPRISE REVIEW STAGE

Risk is determined by economic adverse event that may affect trade. There are many risks involved in the sale and they arise in connection with the goods and finance. In order to effect on risk quickly and efficiently, it is necessary to know and its causes.

The risks may be:
Commodity risk,
Financial risks;

Commodity risk in trading:	Financial risks in the store:
Risks delivery Transport risks, Inventory risk, Risk taking The risk of quality Price risk, etc...	Credit risk Liquid risk Transfer risk Exchange rate risk Currency risk

The buyer is faced with the risk of supply in the case of the supplier / manufacturer fails to deliver the agreed / bought goods or he delivers it outside of the agreed time frame. With this supplier is not only threatening the sale, but also has a negative impact on the creditworthiness of the business enterprise, because its customers can be satisfied.

Incoterms rules regulates the issue of transport risks in international trade. The transport risk is the loss that may be caused to the goods which are the subject of trade. This risk is determined by many factors: the type of transport, distance, type and quantity of goods and the like.

If a customer, for whatever reason, refuse to accept the goods it comes to the risk of taking the goods. In this case, the seller faces with loss on various grounds (damage to the delivered goods, the cost of returning the goods, storage costs, etc.)..

Unnecessary holding excess and obsolete goods leads to a variety of losses. This is due to inventory risk. This risk can be successfully removed if the trade system applies just-in-time inventory control, especially when it comes to perishable goods or foodstuffs which are used in everyday life.

We are witnesses today that many speculate about quality. Each goods should be specified in accordance to quality, therefor today, imitation goods are sold as "genuine" goods, and the buyer is unaware. Consumers are faced with the risk of quality. Today there are various certificates of quality and they guarantee that the purchased goods are of adequate quality. The buyer may retain the goods even when he is not satisfied with the quality, with some discounts, then, may return the goods or complete substitute for other / similar goods to the value returned, or returned goods supplier / manufacturer and to receive payments of cash back.

Each commodity has its price, and accordingly to that, there is a risk of price too. The price is determined by supply and demand, and of this risk can be protected by a good knowledge of the conditions and situations that prevail in the market of goods traded.

The risk of theft is expressed, whether by employees or customers. The risk of theft by employees is reduced by introducing a collective responsibility for the merchandise. While the risk of theft by consumers / customers minimizes the

retail stores at the outlet so that every commodity has special codes that trigger an audible signal when attempting theft.

Credit risk arises if the accounts receivable can not be, for whatever reason, charged on the agreed time, with or without interest. This minimizes the risk of export credit insurance.

"Liquidity risk" arises if customers are insolvent or unable to settle claims due to vendors for goods or services agreed. This risk can be avoided by using short-term loans.

If the company decides to credit, there is a possibility to deal with interest rate risk due to the variable rate loan. Reducing credit risk, leads to reducing the financial risk.

Foreign exchange risk is the uncertainty of the domestic currency against the value of foreign currency due to changes in exchange rates. If you want to avoid exchange rate risk at the same time it is necessary to establish foreign liabilities and foreign claims in the same amount of the same maturity and the same foreign currency, there will be a loss to one side to compensate for gain on the other. Recently, using financial derivatives (forwards, futures, options and swaps) in order to protect the exchange risk, but also for speculative purposes.

Foreign exchange risk is the uncertainty of the domestic currency against the value of foreign currency due to changes in exchange rates. If you want to avoid exchange rate risk at the same time it is necessary to establish foreign liabilities and foreign claims in the same amount of the same maturity and the same foreign currency, there will be a loss to one side to compensate for gain on the other. Recently, using financial derivatives (forwards, futures, options and swaps) in order to protect the exchange risk, but also for speculative purposes.

Currency risk is the risk of international trade and it occurs if there is a change of the national currency against the other (foreign) currency. Devaluation is fall of value in value of the local currency against foreign, stimulates exports, but it discourages imports. Revaluation is an increase in the value of the national currency against the side, there is an increase in imports from abroad and a reduction in exports. Devaluation is a common phenomenon in relation to revaluation. Currency risk can be protected by using: contractual gold clauses, clauses of hard currency and the like.

Some states, for certain reasons, prohibit or restrict the transfer of funds from the country's importers exporters in countries which leads to unable to execute a payment order, irrespective of liquidity and the willingness of importers. The best protection against this risk is to avoid doing business with partenirima imposed certain restrictions.

Other - non-financial risks:

Catastrophic risks;
Political risks;

Catastrophic risks:	Political risks:
Fire	War
Flood	Revolution
Earthquake	Expropriation
Other natural phenomena	Nationalization and similar events

Catastrophic risks are the risks of "force majeure" and no man can affect on them. Basically the objective character and the best protection are actually preventive measures, mainly insurance with an insurance company. Catastrophic risks can destroy warehouse and retail supplies of goods.

Political risks are caused by undesirable social phenomena and events, there can be: macro-and micro-political. Macro-political risk covers all operations of foreign firms in the country, while the micro-political risk applies to a particular foreign company or a group of foreign companies.

According to the degree of risk, Bosnia and Herzegovina is a high-risk country for overseas business partners, which means that not a lot people will decide to invest into the development of our country.

Retail companies of Bosnia and Herzegovina are poorly developed, we can say that they are in the initial stage of development. With privatization of commercial companies it comes to the development of financial markets. Accounting in process privatization provides appropriate data to determine the credit worthiness of the trading company, customer profitability and valuation of commercial enterprises subject to privatization. Through an objective and realistic determination of these data there is shown also importance of accounting in the process of privatization of commercial enterprises. Operations in financial markets characterized by business risk.

Risks can be classified differently, depending on which segment of the company are related. Business risk (business risk) is the risk related to the financial performance of the company. Risks that appear in the company, appear in the work, business and enterprise development, and leadership and management of the company. Business risk is comprised of numerous internal and external risks in business, and are presented in Table 1 .

Table 1: Internal and external business risks

Ord. number	Internal business risks	Ord. number	External business risk
1	The risk of the company	1	Economic risk
2	The risk structure of corporate assets	2	Market risk
3	The risk of staff	3	The risk of execution of the sales contract

4	Commodity risk	4	Transport risk
5	The risk of resource use	5	Export risk
6	The risk of capital investment	6	Political and social risk
7	The risk of success		
8	The risk of innovation		

Source: Deželjin, D., Deželjin, J., Dujanić, M., Tadin, H., Vujic V., *Business management challenges, risk, pleasure, M.E.R.CONSLT, Zagreb, 2002 .. 173 page .*

Business risks that arise within the business enterprise is called internal business risks, including the following risks:

1. The risk of the enterprise is a special risk that is consisted of threat to the organization of companies that do not comply with the requirements of business and its needs. This risk depends on the size of the company, as well as the mutual harmonization of certain parts and functions of the company. The risk of the company may include: the risk of quality organizations, risk resilience, risk-sidedness of the risk of instability of the risk, size and location of the company.

2. The risk structure of corporate assets is expressed quantitatively and qualitatively, and the data used is obtained by analyzing business and enterprise balance. The risk structure of corporate assets may include: quantitative risk again include: the risk of profitability, liquidity, excessive (too small) stocks, the risk of disruption of production, then a qualitative risk, rigidity, volatility risk, the risk structure of corporate assets including: quantitative and qualitative risk of financial resources.

3. The risk of staff refers to the risk that the company is damaged due to inadequate staffing structures, professional incompetence and others. The risk of personnel includes: qualitative and quantitative human risk, staffing levels and risk management personnel.

4. Commodity risk is one in the area of determining the quantity, quality and value of the goods. The risk is all the greater if the company has a wide assortment of.

5. The risk of the use of resources stems from the danger that some resources are not exploited, or they are used contrary to the technical rules or some interrelated and complementary resources are not sufficient quantitatively and qualitatively consistent.

6. Risk of capital investment is related to any investment in the development of the company.

7. The risk of success is tied to the profitability of the company and is a danger that, for whatever reason it does not achieve the expected rate of return on invested capital.

8. The risk of innovation comes from the danger that innovation is not given, or that its application does not achieve the expected result.

External business risks are those whose source outside the company, and include a variety of types shown in Table 29.

Generally speaking: the company makes their business decisions based on information of which depends on the risk, that means, in this case, the uncertainty of the expected economic results. In order to minimize risk and maximize the performance of the company, designed a model of leverage.

Depending on the form of results and economic factors, it is possible to distinguish;¹

1. business risk and operating leverage,
2. financial risk and financial leverage,
3. total risk and combined leverage.

Business risk is the uncertainty of achieving operating profit as a return on total business assets. In most cases, the size of business profits depends on sales volume, product range, sales prices, variable and fixed costs. Operating leverage expresses the efficiency of business operations with fixed costs. The effect of business leverage is determined by factors over business leverage.

Factor for business leverage = % change Operating profit / % change in sales volume = marginal profit / operating profit.

Factor for business leverage ratio shows the percentage changes of business profits generated on the basis of the percentage changes in sales volume.

Financial risk is the risk of achieving gross profit on its own result. Financial risk is measured by the factor of financial leverage.

Factor of financial leverage = Operating profit / (operating income – interest).

For how long will increase the net profit of the company, it depends on the source of funding, by that it means, from the size of the debt and the absolute difference between the interest rate and the rate of return on total assets employed business. Total risk arises from the uncertainty of the gross income and hence net income and return on equity, taking into account the business and financial risks. Combined leverage is the result of accumulation of operating and financial leverage, and is expressed through factors combined leverage.

*Combined leverage factor = factor * factor business leverage financial leverage*

Factor combined leverage is much more reliable and comprehensive, as it includes both the business and financial risks in business. Significantly, the previous relation can greatly assist the company during the removal of a number of business and financial risks in business.

Risk business environment is determined by political, economic and social conditions in the country and the region, affecting the operations and performance of the companies in B'n'H. In addition to political risk depends on its relations with the neighboring countries and the world, the risk depends on the impact of the transition to a market economy.

Business risk society involves risks of everyday activities related to the future survival of the company, maintaining and improving its competitive position and business stability. Business risk is determined by the operating environment of society, the characteristics of industries, as well as its own business policies and decisions.

The company, which is exposed to credit risk has obligations under the loans granted at fixed and variable interest rates that are tied to Euribor. Also, in the economic literature, there is also the risk of force majeure (force majeure). This term implies the events that have a negative impact on the business of the issuer, such as:

- War, invasion, the effects of outside enemies, acts of terrorism in the Serbian Republic of Bosnia and Herzegovina;
- Epidemic which affected citizens;
- Cases such as earthquakes, tornadoes, hurricanes, floods, fires, except for the predictable and conventional climate and natural phenomena that cause damage or destruction;
- Significant delay in work as a result of court orders, prohibitions or similar accounts that have received third-party
- Collective labor disputes, strikes or acts of protesters, unless affecting the relations between a company and its employees.

III. RISK ANALYSIS IN FUNCTION OF WORK MANAGEMENT IN THE ENTREPRENEURIAL VENTURE ENTERPRISE

Operational risks are an integral part of every business venture, something that can not be avoided. The paper will cover the risks related to the ability to obtain funding in the capital markets, and business risks that result from business. Furthermore, the risk can be defined as the deviation of the actual from the expected return [Van Horne, J., Wachowicz, J., Fundamentals of Financial Management, Mate, Zagreb, 2002, p. 91].²

² Van Horne, J.; Wachowicz, J., Fundamentals of Financial Management, Mate, Zagreb, 2002, str. 91.

¹ Bojovic P., Business Finance, Cigoja, Belgrade, 2006, page 69 .

Also, the risk can be seen as the probability of suffering loss, damage or injury. However, they should be seen as an opportunity, and when any significant entrepreneurial decision should balance the relationship between profit and loss, and try to find ways to reduce the risk to a tolerable minimum. In short, it is necessary to manage the risk. Profit, according to the American economist Frank X. Find arises as a residual income that remains available after deducting all contractual obligations of the company's income.³ It is a reward for bearing the costs of uncertainty. Modern corporations are specialized to market decision-making under uncertainty and risk.⁴ In order to diversify risk and minimize the need is strategic foresight and planning. Managers differ in the ability to predict, and the capital market provides the investors with foresight and strategic planning, benefit most.

The modern view of the risk perceived risk as an opportunity where a company can achieve the planned level of growth and development. The objective of the risk management function is to provide analytical support to the process of decision making, based on which will determine the possible dangers and ways to respond to possible unforeseen problems. It is the implementation of a number of techniques and models of operational risk management, risk control, risk management and governance process itself. In the context of the problems that we process at work, the risk is seen in many aspects. One of these aspects are the risks during the implementation of the IPO. **Some of the main risks are:**

1. **The risk of not collecting sufficient funds to finance investment projects in the company;**
2. **Risk that it will not reach a statutory% realization of shares in the initial public offering;**
3. **Risk potcjenjenosti price action during the implementation of the IPO;**
4. **Risk taking company (dilution of ownership);**
5. **Risks related to further increase the cost of issue of shares, which may arise as a result of procedural steps.**

There are also business risks (*business risk*) related to the likelihood of achieving the business results of the company, which, in most cases, expressed as the financial performance of the company.

From a theoretical point of view, the risk (risk) has four basic

3 Vukmirovic, N., Modern Entrepreneurship - the science and art of business success, Faculty of Economics, Banja Luka, 2006, page 32.

4 Vukmirovic, N., Modern Entrepreneurship - Science and art of business success, economic Engineering, Banja Luka, 2006, page 33.

meanings:⁵

1. *The general meaning*, refers to the risk of an event that was not expected and made into a damage or loss;
2. *In business life companies*, whether it is caused by bad decisions, or man, or some unforeseen event;
3. *In the area of corporate finance*, involves a risk of causing damage or loss of financial operations;
4. *Insurance against performing* which does certain professional insurance company.

IV. ACCOUNTED COVERAGE OF EXPOSURE OF ASSET COMPANY RISK⁶

Asset classification is the process by which an item of assets attributable risk category as determined probability that the debtor's obligations to be serviced and long settled in accordance with the agreement. Asset classification provides a basis for determining the appropriate level of reserves for possible losses due to exposure to credit risk. These provisions, together with the general reserves for unidentified risks and capital are the basis for determining the ability of banks to absorb losses. Policy on the provision for credit risk exposure ranges from strictly regulated according to the discretion of the banking system. In our country, the policy prescribed by the Banking Agency of RS (RS) and FBA (*for banks headquartered in Federation of B'n'H*).

Banking Agency of the Republic of Serbian states the following levels of provision for credit losses of banks⁷.

<i>Asset Quality</i>		<i>% of provision</i>
Category	Good assets	2%
Category	Special mention	5 - 15%
Category	Substandard	16 - 40%
Category	Doubtful	41- 60%
Category	Loss	100%

Category A - Good assets

In this category of commercial bank can classify items of assets that are not subject to criticism as follows:

- Items of assets or loans that are fully secured by first-class collateral and regardless of any other outstanding debts, debts or other parts of adverse

5 Deželjin, D.; Deželjin, J.; Dujanić, M.; Tadin, H.; Vujic V., Entrepreneurial management: challenges, risk, pleasure, M.E.R.CONSULT, Zagreb, 2002, page 172.

6 Vukmirović, N., *Special Accounting*, Faculty of Economics, Banja Luka.

7 Decision on minimum standards for credit risk management and assets classification <http://www.abrs.ba/>

credit factors of the user;

- Items of assets for which there is no detected problems and obstacles that would hinder or prevent the payment of principal and interest on the maturity date, where it is not expected that the bank will pay users for any potential liability.

Category B - Special mention

In this category of commercial bank is required to classify items of assets whose collection is ensured quality collateral, and also have potential weaknesses that, if they are not monitored, and they don't check and timely correct, they can deteriorate and weaken the creditworthiness and solvency of banks in the future and include :

- Items that are not sufficiently addressed, monitored, controlled and corrected by the credit of the bank employees ie. that do not have a complete and high-quality credit file with all the evidence of the feasibility and quality of the loan;
- Items which are not adequately and professionally structured by deadline, documentation or other conditions.

In this category the bank shall include all items for which the borrower-customer is late with payments or delayed, according to a bank or independent from banks to other parties, officially or unofficially, but no later than 90 days from the date initially agreed deadline and the deadlines .

Category C - Substandard:

In this category of commercial bank is required to classify items of assets that are not supported by the successful ongoing operations and a solid ability to pay by the user and include the following:

- Claims against the debtor-beneficiary whose current cash flows are not sufficient to cover maturing debt (liabilities);
- Claims against the debtor in which the cycle of the assets (property) in cash exceeding the deadlines for repayment of the debt; and
- Claims by users who are insolvent.

The Bank is required to include this category with all items for which the user is late with a payment or delayed, according to a bank or independent from banks to other parties, officially or unofficially, for more than 90 and less than 180 days after the initial contractual term or contracted deadlines.

Category D – Doubtful

In this category of commercial bank is required to classify items of assets that have all the weaknesses that contains assets classified as category C-Substandard, with insurance billing

commercial bank has no collateral. These weaknesses make full payment of claims is very problematic, the big question and the high probability of loss to the bank, but because of certain specific factors that could still lead to raising the quality of these assets, its classification in category E-loss can be delayed until the objective has been established its definitive status.

The Bank shall in this category include all items for which the user is late with a payment or delayed, according to a bank or independent from banks to other parties, officially or unofficially, for more than 180 and less than 270 days after the initial contractual term or contracted terms, except the time when the bank has already initiated legal action for the realization of collateral and already has a safe arguments and documentary evidence that is reasonably expected an orderly, timely and full realization of collateral.

Category E - Loss

In this category bank is required to classify items of assets which are considered uncollectible and for those that further retention in the categories of recoverable assets is not warranted. Classification in this category does not mean that the assets can not possibly subsequently improve quality or that it can not possibly be saved, at least partially, but to delay its complete write-off is no longer justified. These items of assets are essentially worthless likely (*irrecoverable*) assets, even if its partial recovery in the future and possible.

The Bank is required to include in this category all items for which the user is late with a payment or delayed, according to a bank or independent from banks to other parties, officially or unofficially, for more than 270 days after the initial contractual term or contractual terms, unless the bank has proven foreclosure in progress.

V. ANALYSIS AND BUDGET RATE RISK INVESTMENT IN COMPANIES IN BOSNIA AND HERZEGOVINA

To the investor decided to invest in shares in the capital market of Bosnia and Herzegovina, it is the assessment of the risk of the company. There are several ways in which you can determine the state shares of the company whose shares it intends to buy. If we compare the market price of shares of the company that it intends to buy the actual value of the shares of the company, may apply the discounted cash flow method, on of the ways of calculation of the discount rate is a method of building.

According to the method of building, the discount rate is calculated as the sum of the following three components⁸:

8 Bojovic, P., *Business Finance*, Cigoja, Belgrade, 2006, page 137

- Real rate of return on investment without risk,
- Risk premium for investing in the country,
- Risk premium for investing in the company.

Interest rates on government bonds in Bosnia and Herzegovina is about 3% annually. In this regard, according to this method, the real rate of return on investment with no risk of Bosnia and Herzegovina is 3%⁹ [Privatization Directorate]. If we assume that the risk premium for investing in the country, based on the assessment of specific risk is 6%¹⁰ [Privatization Directorate]. We will analyze the levels of risk of investing in a company at a hypothetical example of "Swallow". Table 2 shows the calculation of the rate of risk of investing in a company "Swallow".¹¹

Table 2. Calculation of at-risk investment in the company "Swallow"

	The scale of the investment risk in the enterprise in%			
	0	1	2	3
Key man				
Organization Structure				
Compact management team			+	
Strategic planning			+	
Production program				+
Specialized knowledge of an expert			+	
				+
Weighted	0			
Sum	12	0	6	6
Number of parameters	5			
Specific risk	2,4%			
Size enterprises				
Number of Employees		+		
The value of business assets		+		
Rating competition		+		
Weighted	0	3	0	0
Sum	3			
Number of	3			

9 Directorate for Privatization

10 Directorate for Privatization

11 Adapted from: Leko, V., Vlahovic, A., Acquaintances, V., in 1997., Valuation-methodology and examples, Belgrade, Institute of Economics, Belgrade, page167.

parameters				
Specific risk	1%			
Financial structure				
Fixed/Assets/ Equity		+		
Fixed assets and inventory/ long-term capital		+		
Equity/ Total Capital			+	
Contributory profit/ revenue			+	
Financial expenses /Income		+		
Weighted	0	3	4	0
Sum	7			
Number of parameters	5			
Specific risk	1,4%			
Product/ geographic diversification				
Contribution of product revenue		+		
The existence of long-term contracts			+	
The share of foreign investments in income			+	
Access to the EU market	+			
Weighted	0	1	4	0
Sum	5			
Number of parameters	4			
Specific risk	1,25%			
The importance of the product to customers				
The existence of long-term contracts				+
The size and position of the dominant customers				+
Concentration of customers				+
Diversification of customers			+	
Weighted	0	0	2	9
Sum	11			
Number of parameters	4			
Specific risk	2,7%			

The ability to predict				
Age enterprises				+
The stability of operating results				+
Discontinuities in business			+	
Changing economic environment sectors				+
Weighted	0	0	2	9
Sum	11			
Number of parameters	4			
Specific risk	2,7%			
Total at-risk companies in %	11,45%			

When you add up all the previous components, will receive the discount rate in the amount of 20.45%. This means that good risk management provides a great warranty in the business activities and administrative functions of individual sectors to the senior management team at the end of the administration of the organization.

The potential benefits of risk management are¹²;

1. Supports strategic and business planning
2. Support efficient use of resources
3. Promote continuous improvement
4. Reduces shocks and unwelcome surprises
5. To quickly use new features
6. Improving communication between management and other parts of the organization
7. Encourages investors
8. Helps focus the internal audit programs

VI. CONCLUSION

We live in uncertain and turbulent times that are characterized by a high degree of risk. Risk can not be avoided, but it can be in control. In the business world, companies may be exposed to a wide variety of risks, which occurs as a result of the performance of specific economic activities. To influence the risk, it is necessary first of all to define. Properly defined risk gives the possibility to have influence by certain methods.

Risks can greatly endanger the market and the financial position of commercial enterprises in the domestic and international market. So that a company should determine the acceptable risk limits. For these reasons, managers tend to adverse events that adversely affect trade to a minimum.

Foreign projects are riskier than domestic projects, because the discount rate is higher, the diversification of foreign investment projects operating on the level of the discount rate in the sense that it reduces.

Entrepreneurs should have the information and to have a positive relationship with them, because the only way to achieve good results. Besides entrepreneurs, information should be available to consumers.

REFERENCES

- [1] Bodie, Z., Kane, A., J., Marcus, 2009th, *Fundamentals of investment*, Belgrade, Datastatus.
- [2] Bodie, Z., Kane, A., Marcus J., 2006th, *I started investing*, Zagreb, Mate.
- [3] Bojovic, P., 2006th, *Business Finance*, Belgrade, Cigoja.
- [4] Brzaković, T., 2007a. *Capital market and investment strategy*, Belgrade, Čugura
- [4] Van Horne, J., Wachowicz, J., 2002nd, *Fundamentals of Financial Management*, Zagreb, Mate.
- [5] Leko, V., Vlahovic, A., Acquaintances, V., in 1997., *Valuation-methodology and examples*, Belgrade, Institute of Economics, Belgrade.
- [6] Đurićin, D., Potter, D., 2007a., *Management by projects*, Belgrade, CID Faculty of Economics, Belgrade.
- [7] Eric, D. 2003., *Financial markets and instruments*, Belgrade, Cigoja.
- [8] Ivanisevic M. 2008th, *Business Finance*, Belgrade, Faculty of Economics, Belgrade.
- [9] Jim Kelleher, 2010th, *Equity Valuation for Analysts & Investors A Unique Stock Valuation Tool for Financial Statement Analysis and Model-Building*, The McGraw-Hill Companies.
- [10] Mikerević, D., 2009th, *Financial Management*, Banja Luka, Faculty of Economics, Banja Luka.
- [11] Peterlin, J., Mladenovic, M., *Financial instruments and financial risk management*, Pim, Banja Luka, 2007a.
- [12] Scott A. Hoover, 2006th, *Stock Valuation An Essential Guide to Wall Street's Most Popular Valuation Models*, The McGraw-Hill Companies.
- [13] Frederic S. Mishkin, Stanley G. Eakins, 2006th, *Monetary Economics*, Banking and Financial Markets, Belgrade, Datastatus.
- [14] Soskic, D. Zivkovic, B., 2006th, *financial markets and institutions*, Belgrade, CID Faculty of Economics, Belgrade.
- Soskic, D., 2006th, *securities-portfolio management and mutual funds*, Belgrade, CID Faculty of Economics, Belgrade.

12 [<http://www.investopedia.com>]

The Comparison of Wood Chips and Cocoa Shells Combustion

Michal Spilacek, Martin Lisy, Marek Balas, Zdenek Skala

Abstract— This article compares the combustion of the different biomass types in a multi-stage combustor. The two biomass specimen are wood chips and cocoa shells. For the testing purposes, the wood chips represents an easily accessible and combustible biomass type with low emissions and the cocoa shells are an unusual specimen that needs to be examined closely. The comparison contains the combustion process, emissions and the operational problems. The monitored emissions are carbon dioxide, carbon monoxide, nitrogen dioxide and particulates, all monitored at the highest achieved efficiency. For the operational problems, the most notable one is the possibility of slugging of the combustion device while combusting the cocoa shells. Co-combustion of the two fuels is not included.

Keywords— cocoa, combustion, biomass, comparison.

I. INTRODUCTION

Energy requirements are ever-changing and in pursuit for lower emissions and emissions of greenhouse gasses it is necessary to seek more and more considerate ways of combustion. That is on the side of more efficient combustion devices [1] and on the side of used fuels [9, 10] as well. For these reasons looking for new fuels has become an important part of combustion research and what was used to be considered waste is now considered an adequate fuel with recognizable potential. One such fuel is a waste from cocoa beans processing – cocoa shells. This fuels seems to be very suitable for combustion and for this reason it is necessary to

This work is an output of cooperation between Research and Development Project of Ministry of Industry and Trade: FR-TI4/353 “Intensification and optimization of gasifying units and combustion chambers for very sodden waste biomass”, and NETME Centre, regional R&D centre built with the financial support from the financial support from the Operational Programme Research and Development for Innovations within the project NETME Centre (New Technologies for Mechanical Engineering), Reg. No. CZ.1.05/2.1.00/01.0002 and, in the follow-up sustainability stage, supported through NETME CENTRE PLUS (LO1202) by financial means from the Ministry of Education, Youth and Sports under the “National Sustainability Programme I”.

M. Spilacek is with the Energy Institute, Brno University of Technology, Technická 2896/2, 616 69 Brno, Czech Republic (phone: +420 54114 2583; e-mail: spilacek@fme.vutbr.cz).

M. Lisy is with the Energy Institute, Brno University of Technology, Technická 2896/2, 616 69 Brno, Czech Republic (e-mail: lisy@fme.vutbr.cz).

M. Balas is with the Energy Institute, Brno University of Technology, Technická 2896/2, 616 69 Brno, Czech Republic (e-mail: balas.m@fme.vutbr.cz).

Z. Skala is with the Energy Institute, Brno University of Technology, Technická 2896/2, 616 69 Brno, Czech Republic (e-mail: skala@fme.vutbr.cz).

pay attention to it a found more about its behavior during combustion.

II. PROPERTIES OF BIOMASS

A. General information

General characteristics of biomass is a very complicated a problematic [2], as biomass fuels from the same species can have different composition depending on location and harvest time. Generally, biomass residues like shells, husks and straw usually contain a higher volume of ashes [3]. Moisture content and higher heating value is not easily predictable, but the volume of ashes, these values should be lower compared to wood chips.

B. Used fuel

In the table below can be seen the results from analysis of three fuel. The cocoa shells, sawdust and woodchips. The ash content of the cocoa shells is by far the highest, resulting in the lowest overall content of combustibles. The moisture content is almost the same as in the wood chips. In a direct contrast with the low content of combustibles is the highest higher heating value of all thee samples.

Tab. 1 Properties of compared fuels

Parameter	Fuel [†]		
	Cocoa	Sawdust	Wood chips
Moisture	7.15	9.88	7.35
Ash [mass %]	9.85	0.48	1.55
Combustibles [mass %]	83.00	89.64	91.11
HHV [kJ/kg]	18.08	13.47	17.54
LHV [kJ/kg]	16.85	12.13	16.17
C [mass %]	42.98	47.29	47.09
H [mass %]	4.85	5.05	5.46
N [mass %]	2.64	0.16	0.38
O [mass %]	32.32	37.00	37.97
S [mass %]	0.20	0.15	0.20

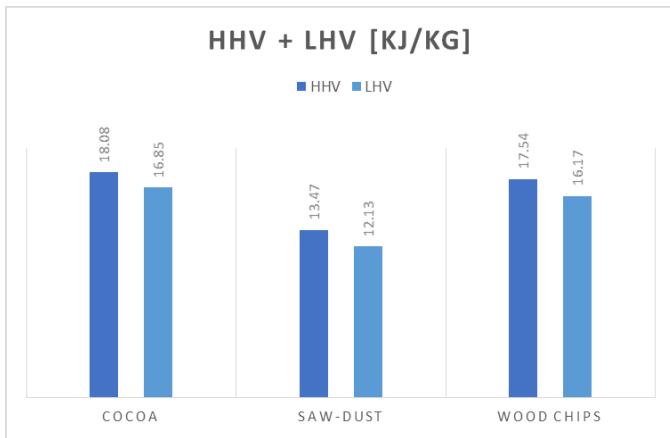


Fig. 1 Comparison of higher heating values and lower heating values

This might be a result of different composition of the respective part of the plant, as all biomass is basically composed of lignin, hemicellulose and cellulose and every part of a plant has different ratio of these three and other components [4]. For the cocoa shells it seems that the constituent with the highest higher heating value is dominant. The same can be said for wood chips. The lower results for sawdust in this case implicate that bark is the main carrier of heating value and cocoa shells should have a similar composition as bark. Because bark has a higher volume of lignin than wood, lignin should be the main cause of the results.

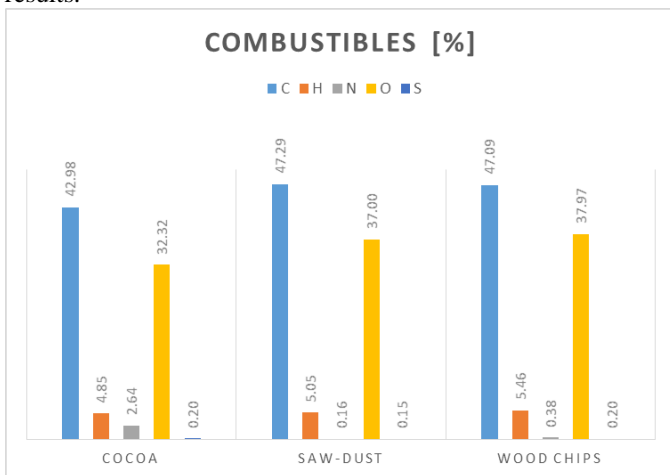


Fig. 2 Comparison of combustibles

Another important characteristic is the content of possible emission producing elements like nitrogen and sulfur. The sulfur content in biomass is generally very low compared to coal and the resulting emissions are low [3]. The cocoa shells are no exception. But the content of nitrogen is considerably higher and because nitrogen emissions are highly dependent on combustion temperature, which in the case of biomass are relatively low, the main source of nitrogen emissions is the nitrogen contained in fuel [1]-[6] and this may cause higher than allowed emissions. This will be observed later in this article.

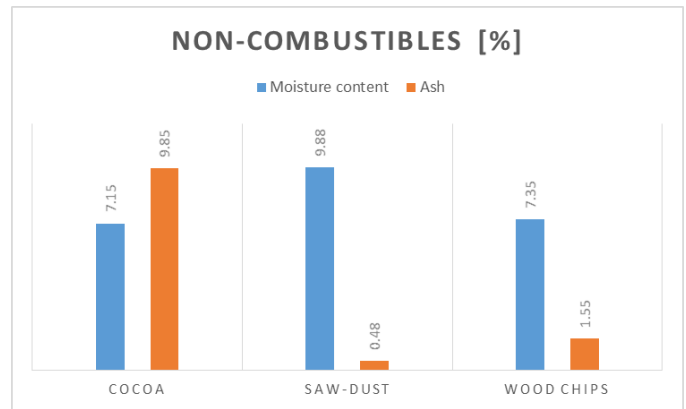


Fig. 3 Comparison of non-combustibles

III. MEASUREMENT

A. Experimental device

The experimental device used for combustion of the biomass samples is a modified combustion unit specialized for measurement and extensive control of the combustion process. It consists of these main parts: Gasification chamber, Water heater, fuel feeder, air preheater and measurement and regulation unit.

1) Gasification chamber

The Gasification chamber is meant for better control of the combustion process by a better resolution of the main biomass combustion stages (drying, pyrolysis, combustion of volatiles, and combustion of char), mainly the pyrolysis. To observe the process, three thermocouples are placed evenly over the length of the chamber and one pressure gauge is measuring the underpressure in the chamber. To achieve better control over the combustion of volatiles and char, combustion air is distributed in three parts: primary, secondary and tertiary air. A better view of the chamber is provided by Fig. 4.

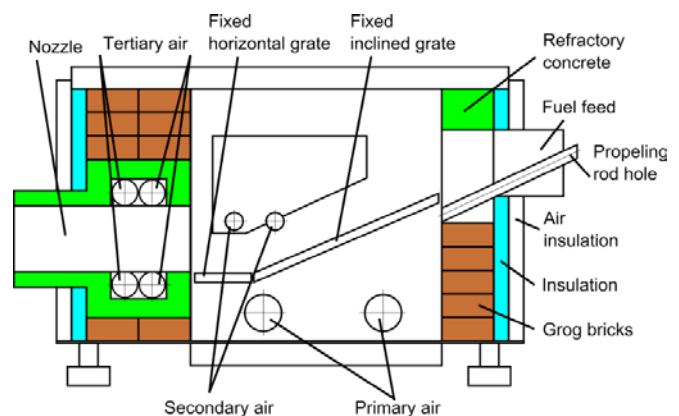


Fig. 4 Gasification chamber

2) Water heater

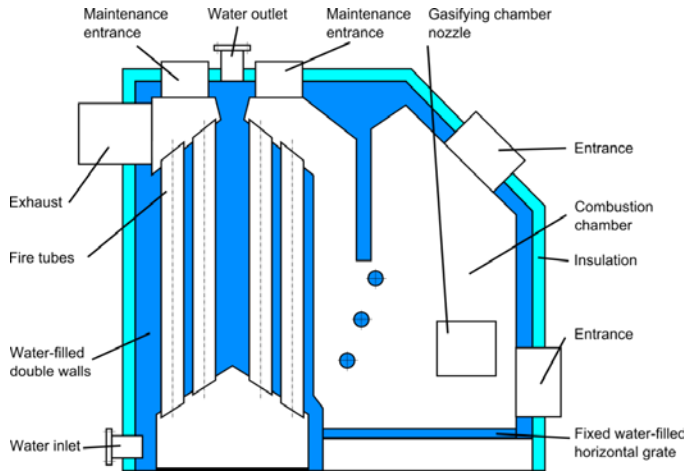


Fig. 5 Water heater

After the combustion products leave the gasification chamber they enter the water heater. Here they are cooled down and transfer their heat in water. The water heater is a standard grate combustion unit for wood, but in our case no wood is placed inside and all heat is brought by the combustion products from the gasification chamber. The nominal power output is 110 kW. For our purposes it is equipped with three thermocouples. A cross-section of the water heater is shown in Fig. 5.

3) Other parts

The other parts. For more information about the device, its specifications, other parts (fuel feeder, air preheater, water circuit and measurement and regulation) and function see [7].

B. Readings

1) Combustion

Even with the characteristics of moisture content and higher heating value similar to the woodchips, combustion of cocoa shells yielded high temperatures “easily”. These were about 300 °C higher then when combusting wood chips (Fig. 6 and Fig. 7). The mentioned figures are showing temperature and power output progress over time.

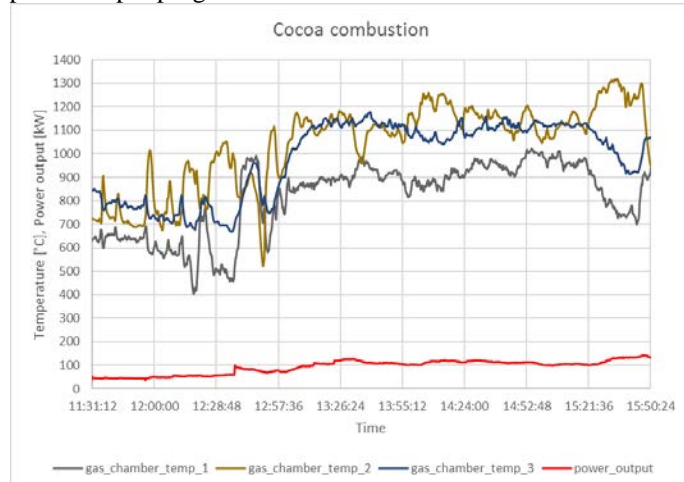


Fig. 6 Cocoa combustion

While woodchips were able to reach nominal output of 110 kW without reaching melting point of ashes that usually are over 900 °C [8]. In our case the temperatures are almost reaching 1000 °C and no signs of melting were observed.

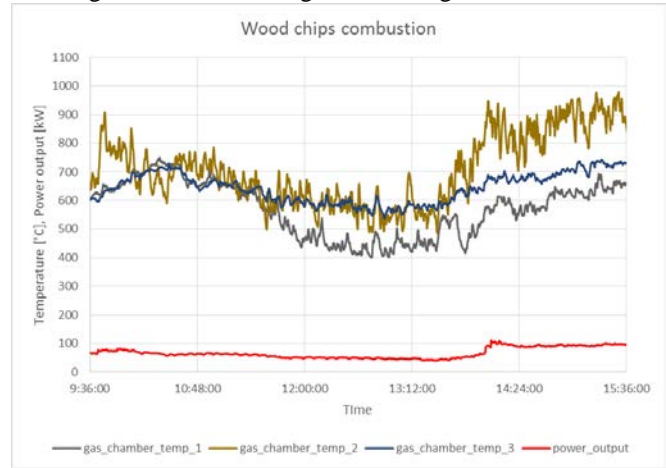


Fig. 7: Wood chips combustion

Cocoa shells, on the other hand, reached the temperature of 1200 °C and for some time over 1300 °C and the melting point of ashes was reached, creating an uniform and thick cover of hard, almost glass-like porous material on the grate of the gasification chamber. That cover lately caused a considerable damage on said grate that needed a welding repair to continue working.

2) Emissions

Having in mind the high temperatures and content of nitrogen in the fuel, the emissions from the combustion must be observed more closely. The results can be seen in Fig. 8. They show results from a 30 minutes long measurement after reaching a stable combustion that is characterized by the oxygen concentration around 11 % in the flue gas. The peaks in CO emissions are most probably caused by avalanching of the fuel and the consequent incomplete combustion. The levels of SO₂ are very small, but the level of NO are mostly between 1000 – 1400 mg/m³. That can be considered a fairly high number.

3) Ash coating

Another observed issue, that may cause problems, is a creation of a grey coating on heat exchanging surfaces made from ash. Analysis of the ash has shown that it is made from a very fine particles. Some of these particles have a size smaller than 1 µm. The particle sizes are in Fig. 9. Such fine coating will reduce heat flux and the efficiency of the device. Also, such fouled device will require a more often cleaning, reducing the effective working time.

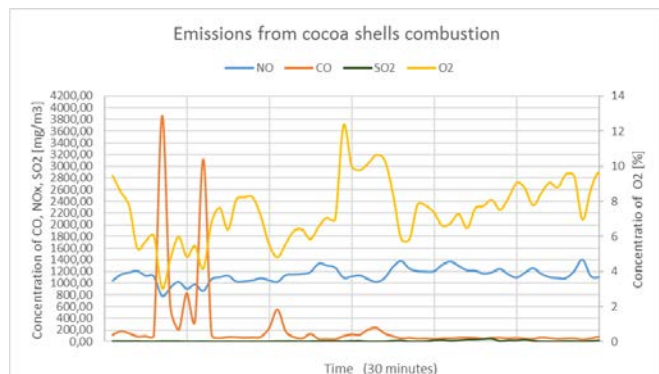


Fig. 8 Emissions from cocoa shells combustion

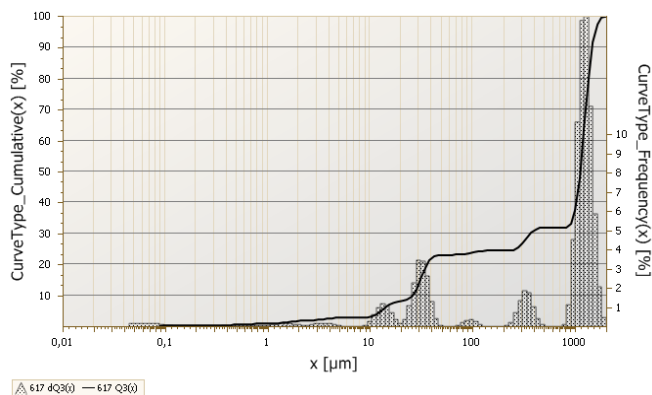


Fig. 9 Fine ash coating

IV. CONCLUSION

After a brief testing of cocoa it seems that this fuel may be considered a suitable biomass for combustion with characteristics comparable with the ones of wood chips. But it has some disadvantages that must be taken in consideration while combustion. First there are “easily” achievable temperatures that are above the melting point of ashes causing slugging. Second, fly ash is composed of very fine particles that create a coating on heat exchanging surfaces. Such coating may result in lowered efficiency of the device and a more frequent need for cleaning. Lastly, higher yield of nitrogen oxides may render the fuel unsuitable for bigger combustion units without a precision emission control system.

REFERENCES

- [1] Law 201/2012 of Czech Republic Legislative
- [2] A. Williams, J.M. Jones, L. Ma, M. Pourkashanian: Pollutants from the combustion of solid biomass fuels, *Progress in Energy and Combustion Science* 38 (2012) 113–137
- [3] A. Demirbas: Combustion characteristics of different biomass fuels, *Progress in Energy and Combustion Science* 30 (2004) 219–230
- [4] Ch. Yin, L. A. Rosendahl, S. K. Kær: Grate-firing of biomass for heat and power production, *Progress in Energy and Combustion Science* 34 (2008) 725–754
- [5] Chemical composition of wood, available on-line 7.4.2014: [http://www.atlasdrevna.hu.cz/makro_exoticke/teorie_chemicke_slozeni_dreva_.html]
- [6] L. D. Smoot, D. T. Pratt: *Pulverized-Coal Combustion and Gasification*, p. 183, ISBN: 0-306-40084-7
- [7] M. Spilacek: Experimental Device for Multi-stage Combustion of Very Wet Biomass, *ANNALS of Faculty Engineering Hunedoara – International Journal of Engineering*, 2014, available on-line: [<http://annals.fih.upt.ro/pdf-full/2014/ANNALS-2014-1-09.pdf>]
- [8] M. Balas: *Cleaning of syngas by metal-based catalysts*, Brno 2010, p. 13
- [9] J. Beniák, J. Ondruška, V. Čáčko: Design process of energy effective shredding machines for biomass treatment. In: *Acta Polytechnica*. - ISSN 1210-2709. - Vol. 52, No. 5 (2012), s. 133–137
- [10] M. Matúš, P. Križan, M. Kováčová, M., J. Beniák, J: The influence of size fraction on the compressibility of pine sawdust and the effectiveness criterion for densification, In: *Acta Polytechnica*. - ISSN 1210-2709. – Vol. 54, No 1 (2014), s. 52–58

Experimental measurement of load and exhaust gas emissions on an outboard engine

Anastasios Karkanis, Charalampos Arapatsakos, Christina Anastasiadou

Abstract—Within the framework of this article, it was built a construction that allows the function of an outboard engine in conditions similar to the factual. An outboard gasoline engine with max power 4HP was placed on the construction. In order to measure the performance of the entire powertrain, a prototype measurement procedure was developed. According to this procedure the measurement of the force is made by a direct connection between the engine's rpm and applied load. During the measurements operating characteristics of the engine, as well as the exhaust gases, were recorded. For the measurement of the emitted pollutants, a laboratory protocol and measurement standards defined by 40 CFR 1045 were used.

Key-Words— Outbord engine, gas emissions, output load.

I. INTRODUCTION

Outboard engines can cover a wide range of needs from recreational craft and small boats to speedboats. The capability vary among the strength of each machine witch starts from max power two PS and can reach up to three hundred and fifty HP. The engine may be two or four stroke, depending on the burning times. These two types of engines come with different pros and cons; however the four strokes have gained popularity due to its technological developments on the last decade. [1]

The outboard engine was invented in the early twenties by Gustave Trouvé and changed permanently the way of travelling at sea. It is a propulsion system for boats, designed to be placed on the vessels' transom and consisting of a self contained unit that includes the engine, a gearbox and a propeller. In addition to movement outboard engines provide steering control of the boat, as they are designed to rotate on their mounting material and thus control the direction of thrust. The direction is controlled by the lower unit that functions as a rudder[2].

The engine operates as follows; initially the fuel is combusted in the cylinder (or cylinders) for power generation. The number of cylinders can vary from one to eight. Thereafter the piston, supplied from the combustion and expansion of the exhaust gases, moves back and forth within the cylinder gradually completing the four or two cycle times. This process is similar to that performed on cars and any classic four or two stroke engine.

This work developed in the Laboratory of Thermodynamics and Thermic machines of Democritus University of Thrace-Greece, under the supervision of Prof. Charalampos Arapatsakos.

Dr C. Arapatsakos is Professor on Democritus University of Thrace-Greece. Tel. 00302541079362, Fax. 00302541079362, email: xarapat@pme.duth.gr

As a result, the piston rod rotates the crankshaft, converting the rectilinear reciprocating motion to rotary. The crankshaft, consequently, rotates the main drive shaft that extends along the lower ridge of the engine. On the bottom of the hinged there is a small gearbox which converts the vertical pivotal movement in a horizontal rotary movement [1,2,3,4].

II. EXHAUST EMISSION LEGISLATION

The legislation for emissions from outboard engines began in 1998. Since the first tests focused on the effects on the undersea environment they concluded that there is no meaningful result. Additionally there where studies that sawed an improvement in the undersea environment, as a result the legislations where delayed. However, the actual need for tests must be concentrated to the air pollutants. The first country, to adopt the exhaust emission legislation for outboard motors were the USA. The US EPA regulations started for 1998 outboard models and aimed at a 75% reduction to 2006 through a progressive scale. Alongside, Europe's regulations for pollutant emissions did not include motor boats until 2003[1,2,3,4].

The directive 94/25/EC establishes the essential requirements for exhaust emissions from marine propulsion engines as showed in Table 1. Propulsion engines must be designed, constructed and assembled in a way that when correctly installed and in normal use, their emissions shall not exceed the limit values laid down in Table 1[5].

Table 1

Type	Carbon monoxide $CO = A + B/P_N^n$			Hydrocarbons $HC = A + B/P_N^n$			Nitrogen oxides NO_x	Particulates PT
	A	B	n	A	B	n		
	Two-stroke spark ignition	150,0	600,0	1,0	30,0	100,0		
Four-stroke spark ignition	150,0	600,0	1,0	6,0	50,0	0,75	15,0	Not applicable
Compression ignition	5,0	0	0	1,5	2,0	0,5	9,8	1,0

Table 1 The exhaust emissions of the marine propulsion engine[5]

Where A, B and n are constants in accordance with table, P_N is the rated engine power in KW and the

exhaust emissions are measured in accordance with the harmonised standard[5].

For engines above 130kW either E3 (IMO) or E5 (recreational marine) duty cycles may be used[5].

The reference fuels to be used for the emissions test for engines fuelled with petrol and diesel shall be as specified in Directive 98/69/EC (Annex IX, Tables 1 and 2) and for those engines fuelled with Liquefied Petroleum Gas as specified in Directive 98/77/EC[5].

The measurement of exhaust emissions in accordance with the harmonized standard EN ISO 8178-1: 1996. It is described in detail the standard according to which the measurement must be fulfilled[6].

Duty Cycles:

Exhaust emission measurements are to be conducted in relevance to the power of the motor in question. ICOMIA 34-88 describes the standard measurement of exhaust gas marine engines and connects directly to ICOMIA 36-88 [Annex IV] standards that determines which loads and speeds should be used. This information is displayed in Table 2[7].

Mode	Engine Speed as Fraction of Rated Speed	Engine Torque as Fraction of Maximum Torque at Rated Speed	Assumed Fraction of Total Time Spent in Mode
1	Idle	0	0.40
2	0.4	0.253	0.25
3	0.6	0.465	0.15
4	0.8	0.716	0.14
5	1.0	1.000	0.06

Table 2 The five modes of the duty cycle[7]

The engine should start operating in the fifth mode in order to enable the determination of the maximum torque of the rated speed. The remaining modes shall be performed in the reduction order of speed and power. When these duty cycles are used the measurement is made separately for each mode. If the measurement is to be consecutive the time that each mode lasted must be noted. The ISO cycles operational modes are associated with transitions of twenty seconds. The entire test sequence must be performed in a specified period of time without interruption.

Duty cycles according to the American standards:

E4 Mode No.	Engine speed ¹	Torque (percent) ²	Weighting factors
1	Maximum test speed	100	0.06
2	80%	71.6	0.14
3	60%	46.5	0.15
4	40%	25.3	0.25
5	Warm idle	0	0.40

Table 3 Duty cycle for discrete mode testing [8]

¹Speed terms are defined in 40 CFR part 1065. Percent speed values are relative to maximum test speed[8].

²Except as noted in §1045.505, the percent torque is relative to maximum torque at maximum test speed [8].

RMC Mode	Time in mode (seconds)	Engine speed ^{1,2}	Torque (percent) ^{2,3}
1a Steady-state	225	Idle	0
1b Transition	20	Linear transition	Linear transition
2a Steady-state	63	Maximum test speed	100
2b Transition	20	Linear transition	Linear transition
3a Steady-state	271	40%	25.3%
3b Transition	20	Linear transition	Linear transition
4a Steady-state	151	80%	71.6%
4b Transition	20	Linear transition	Linear transition
5a Steady-state	161	60%	46.5%
5b Transition	20	Linear transition	Linear transition
6 Steady-state	229	Warm idle	0

Table 4 Duty cycle for ramped modal testing [8]

¹Speed terms are defined in 40 CFR part 1065. Percent speed values are relative to maximum test speed[7].

²Advance from one mode to the next within a 20 second transition phase. During the transition phase, command linear progressions of speed and torque from the speed setting of the current mode to the speed setting and torque setting of the next mode[8].

III. INSTRUMENTATION AND EXPERIMENTAL RESULTS

On a four stroke outboard engine, with 4Hp max output power, measurement of the speed and load took place. The measuring system used is composed of an rpm meter, dynamometer (meter of force), a signal converter, and the data collection unit NI cDAQ-9174 (DAQmx) with the module measurement NI 9205 and a laptop. In order to measure the engine speed, it has been used a rpm meter which it was connected to the the outboard engine and at the same time to the computer for displaying the results with the use of he NI LabVIEW program.

The dynamometer was used to measure the load. Proper circuit connections were made between the signal converter and the the data collection unit NI cDAQ-9174 (DAQmx), so that the signal would be able to be processed from the second. The measurement module which was chosen from the data unit DAQmx modules was the NI 9205 as it is suitable for measuring analog inputs. The signal, coming from the link mentioned above was led to the portable computer and the use of NI LabVIEW made the depiction and later procession of the results possible.

The outboard engine is placed in a tank filled with tab water. The engine is placed and tied on a device which allows its movement, and then fastened to the measuring system mentioned above, aiming to simulate real

conditions of the outboard's use. The measurements that were performed started from the idle position up to the last position of the throttle –position 4- without exceeding the load of 500N. At the same time we started from 1500 rpm increasing by five hundred until we approached 4000 rpm. When we were reducing the speed we were following the same course vice versa, and measuring simultaneously the values of the load. The measurement at each rpm value (with these to remain as constant as possible) lasted about one minute. Maximum rpm value was decided that of 4000 as after that value no change of the load was observed.

This engine is four strokes, gasoline outboard and is used in a small craft or as an auxiliary engine on larger vessels. For the affixing of the outboard a special installation has been constructed. This feature was designed to enable motion during the machine's operation. In other words, to simulate actual operating conditions of the engine as if it was placed on a vessel.

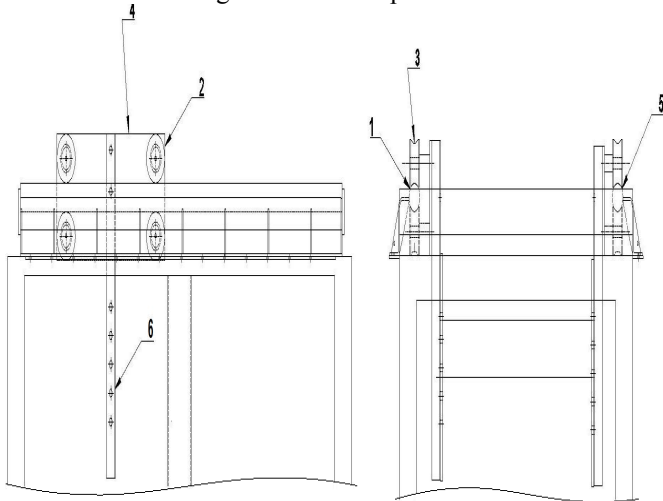


Fig. 1 The stainless steel construction mounted on the tank



Fig. 2. The test measurement unit



Fig 3. The test measurement unit - the engine function
To measure the force of the outboard a digital was made through the traction force exerted on a digital scale. The rpm signal reception was achieved by connecting an inductive rpm sensor between the spark plug and the multiplier. Finally the exhaust gas has been collected by the idle hole of the outboard, where a metal threaded connector M8x1 retaining two $\Phi 6$ tails, was placed. On the first tail, the exhaust sample pipe was plugged and on the other one a k-type thermocouple was connected.

Measurement protocols:

Measurements were performed with two different structures. The first one was a pyramid measuring scale with engines revolutions per 500 rpm. It's purpose was to create a connection between thrust and rpm(Fig 4). The second structure followed the standards of measurements set by the American legislation for marine engines(Fig 5):

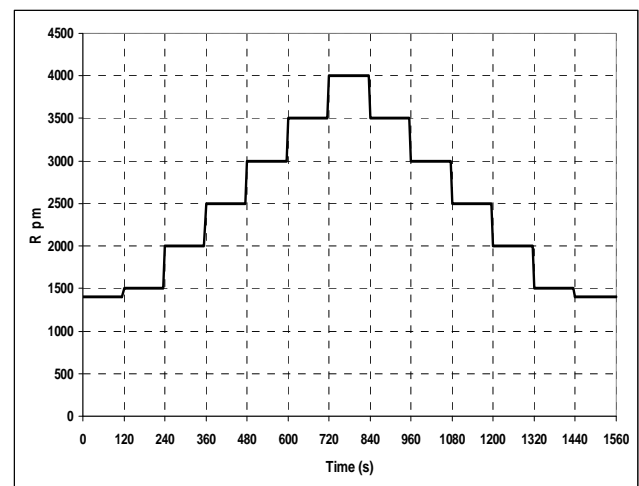


Fig 4. The pyramid of engine rpm

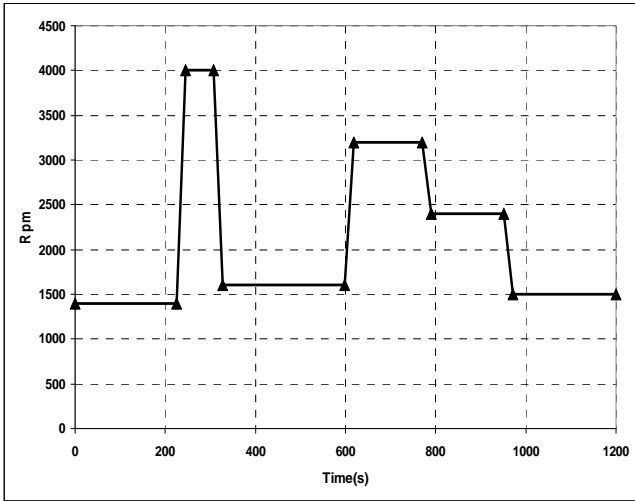


Fig 5. The engine rpm variation according the American legislation

The rpm pyramid protocol:

Rpm	Engine speed	Duration (sec)
Idle	Idle	240
1500	37,5%	240
2000	50%	240
2500	62,5%%	240
3000	75%	240
3500	87,5%	240
4000	100%	120

Table 5. The rpm/engine speed/duration for pyramid structure generation

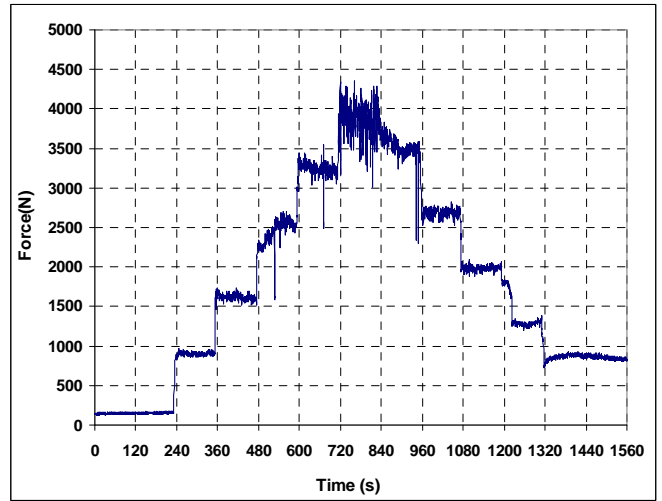


Fig 7. The force variation in relation to the time on the pyramid of engine rpm

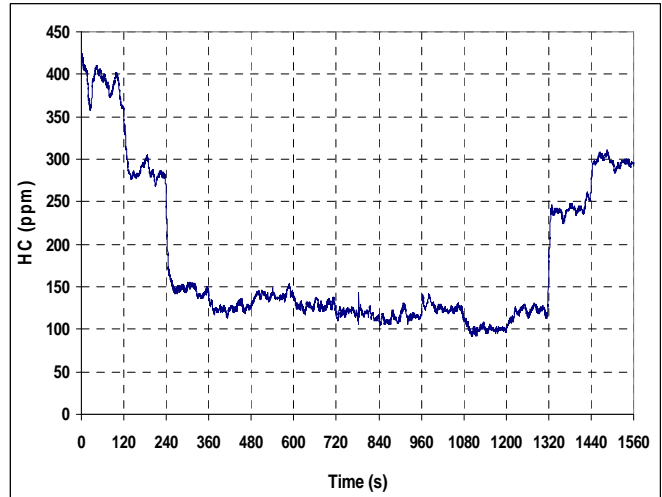


Fig 8. The HC variation

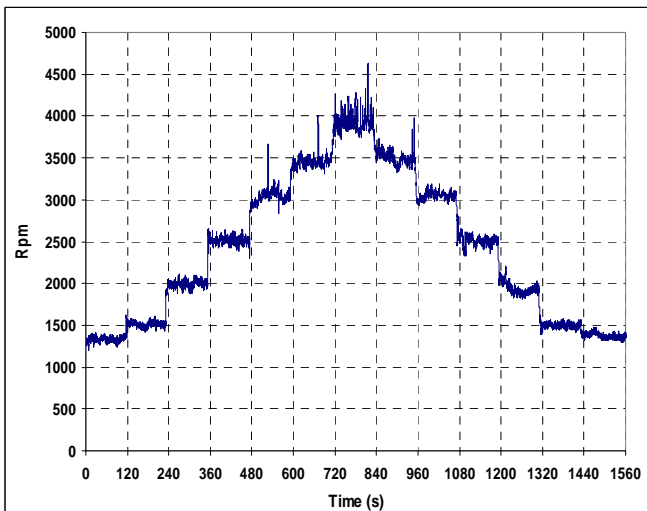


Fig 6. The pyramid of engine rpm in real conditions

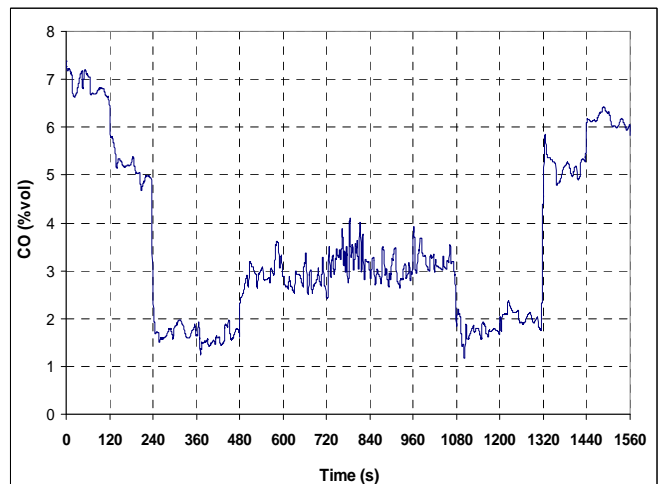


Fig 9. The CO variation

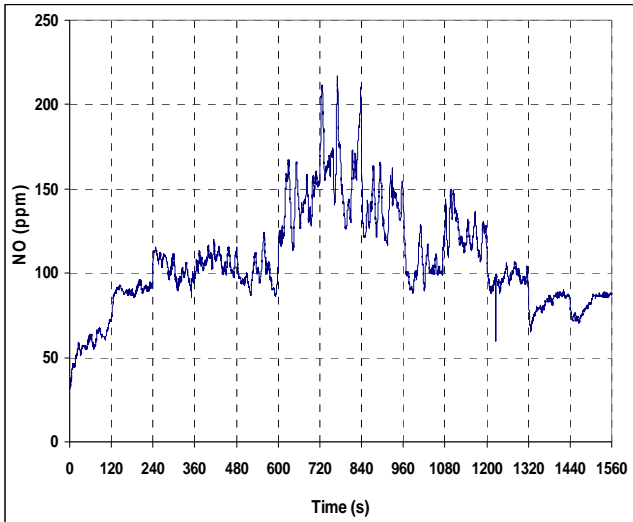


Fig 10. The NO variation

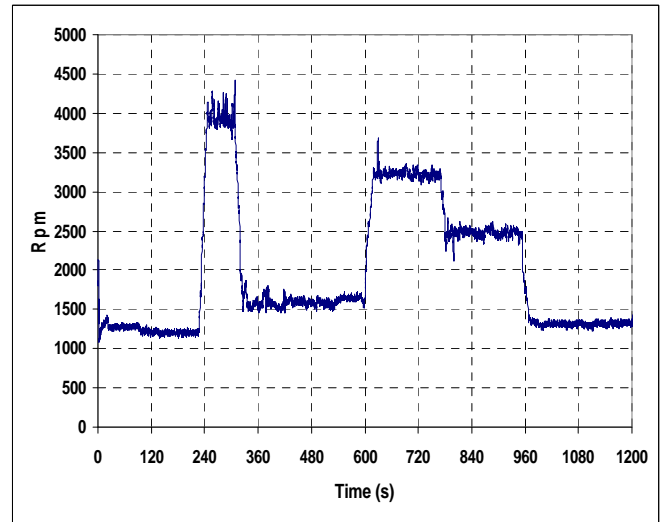


Fig 12. The engine rpm in real conditions

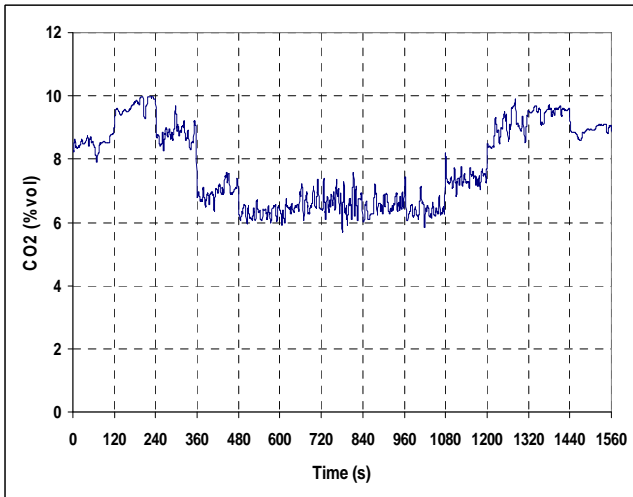


Fig 11. The CO₂ variation

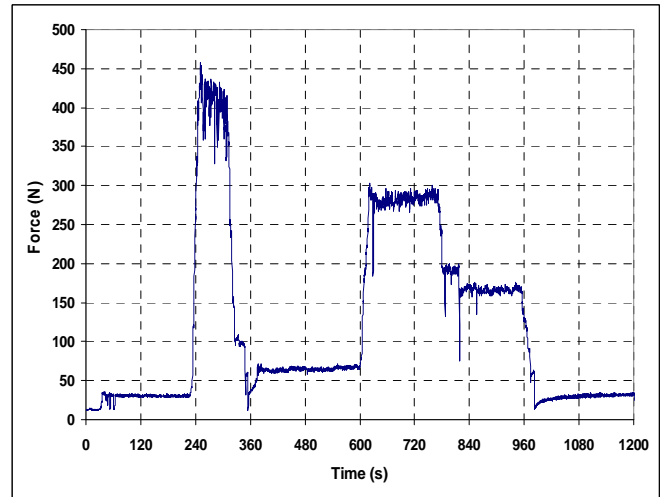


Fig 13. The force variation in relation to the time

American protocol:

Rpm	Engine speed	Duration (sec)
Idle	Idle	474
4000	Max speed	83
1600	40%	291
3200	80%	171
2400	60%	181

Table 6. The rpm/engine speed/duration for American structure generation

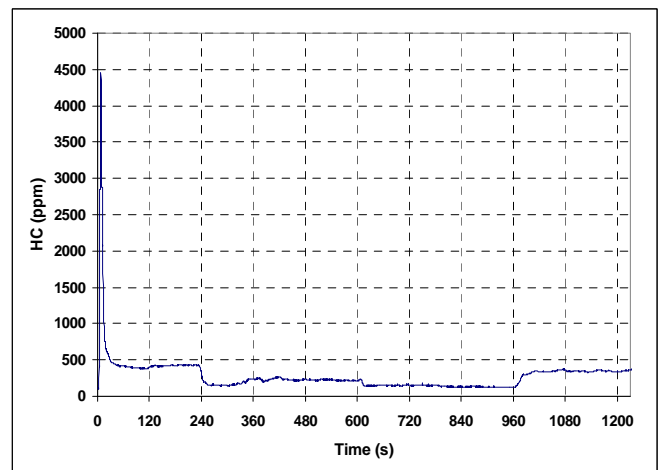


Fig 14. The HC variation

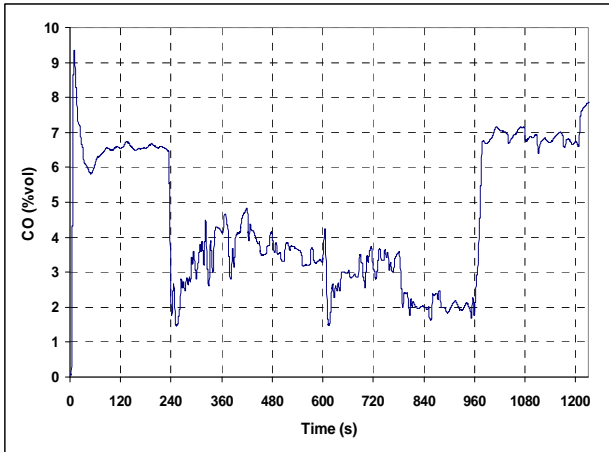


Fig 15. The CO variation

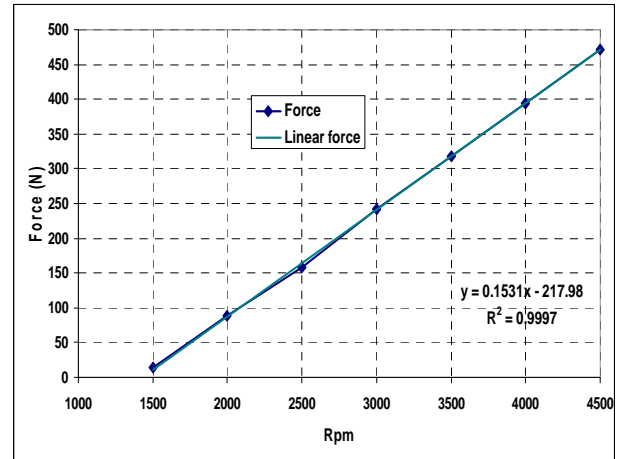


Fig 18. The force variation in relation to the engine rpm

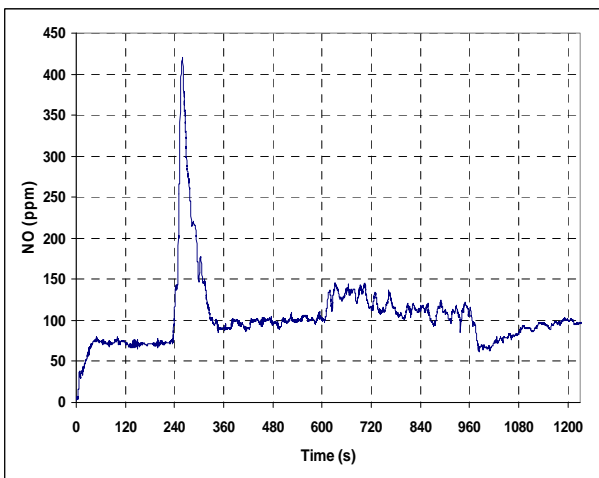


Fig 16. The NO variation

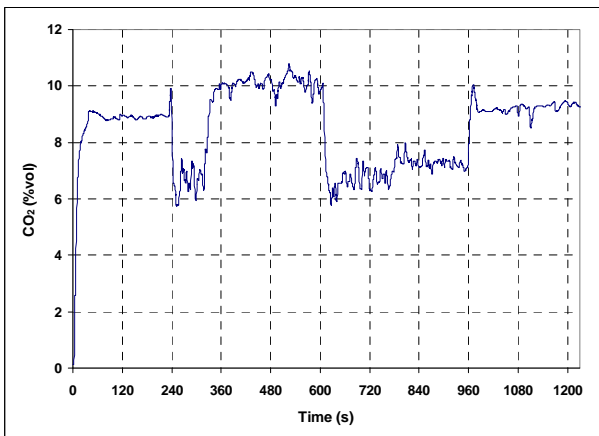


Fig 17. The CO₂ variation

Despite the fact that the maximum speed of the measurement was 4000rpm, the instantaneous value of the load at 4500rpm was measured 472,1945N. The loading of the motor increases linearly with the increase of speed as shown in Fig 18

IV. CONCLUSION

Measuring the outboard's load with the digital scale, proved to be sufficient to determine the applied load to the engine. The results are trustworthy and the measurement represents the actual power of the engine, in addition no further calculations need to be done. Compared to other procedures this is the one recommended as the measuring conditions are ideal and there is minimum deviation from the factual operating conditions. The disadvantage of this particular test can be spotted through the results. As the tank was not big enough, the engine created a wave which lead to great fluctuations, when the speed reached or surpassed 4000rpm. This problem is minor and can be solved by using a bigger tank or by creating a furrow opposite to the propeller. In addition, the wheels' friction caused a thrust variation of 29.43N when moving from high to low rpm. This can be surpassed by affecting the load when this transition occurs, aiming to measure the thrust without price alternation. Finally the exhaust temperature seems to have low value; this is associated with the measurement being performed through the idle hole. If the measurement took place on the main exhaust pipe then the prices should be higher.

REFERENCES

- [1] Stocktaking study on the current status and developments of technology and regulations related to the environmental performance of recreational marine engines: final report, January 10, 2004, Contributors: Rijkboer, R. C.
- [2] http://en.wikipedia.org/wiki/Gustave_Trouv%C3%A9#Inventions, Retrieved 31-5-2014
- [3] <http://www.maritimejournal.com/news101/power-and-propulsion/two-stroke-outboards-still-available-at-seawork>, Retrieved 31-5-2014
- [4] Wordford, Chris. "Outboard Motors", Retrieved 31-5-2014.
- [5] Directive 94/25/EC, <http://eurlex.europa.eu/LexUriServ/LexUriServ.do?uri=CONSLEG:1994L0025:20031120:en:PDF>, Retrieved 31-5-2014.
- [6] ISO 8178-1:2006, http://www.iso.org/iso/home/store/catalogue_ics/catalogue_detail_ics.htm?csnumber=42714, Retrieved 31-5-2014.
- [7] ICONOMIA Standard 34-38, ICONOMIA Standard36-88, <http://www.icomia.com/library/Default.aspx?LibraryDocumentId=945>, Retrieved 31-5-2014.

[8] 40 CFR Part 1045, Appendix II to Part 1045 - Duty Cycles for Propulsion Marine Engines,
<http://www.law.cornell.edu/cfr/text/40/part-1045/appendix-II>,
Retrieved 31-5-2014

The impact of salinity on development the most important Copepoda taxa in Baltic Sea

Lidia Dzierzbicka-Głowacka, Maja Musialik, Anna Lemieszek

Abstract—The thesis discusses the impact of salinity on the development of the most important Copepoda taxa in Baltic Sea: *Pseudocalanus minutus elongatus*, *Temora longicornis*, *Acartia* spp. and *Centropages hamatus*. Geographical distribution of zooplankton in the Baltic Sea has been discussed by taking into consideration both experimental and literature references. For the detailed assessment of the influence exerted by salinity on planktonic copepods, the long-term changes in the biomass of Copepoda and the salinity in the Baltic Sea were analysed between 1959 and 1997. The result of the analysis revealed strong correlation between location of *Pseudocalanus minutus elongatus* in the water column and the salinity level. When comparing the Baltic population of *Pseudocalanus* spp. with the population from the North Sea, considerable differences were observed in the biomass and the number of generations in the annual cycle. *Temora longicornis* is a species for which salinity is important only during the reproduction season by influencing the quantity of eggs produced by females. The literature data revealed a difference in the reproductive abilities between the population from the Baltic and the North Sea. *Acartia* spp. and *Centropages hamatus* are highly concentrated mostly in the surface layer of water, and salinity changes do not influence its development. Fluctuation of *Pseudocalanus minutus elongatus* biomass in the Baltic Sea and limitation of its appearance in the water column are strongly connected with biomass of some (economically important) fish species. Those Copepoda are the main food for the Baltic herring or sprat, so the anomaly of their biomass negatively influences the fish population.

Keywords—Baltic Sea, Copepoda, modelling, salinity.

I. INTRODUCTION

THE Baltic Sea is a specific reservoir of brackish water, in which two environmental factors: salinity and temperature are of major significance for the life of organisms living there. The average salinity of surface waters in the Baltic Sea comes to 7.5 PSU, but there is a considerable variation in salinity of

The partial support for this study was provided by the project Satellite Monitoring of the Baltic Sea Environment – SatBaltyk founded by European Union through European Regional Development Fund contract no. POIG 01.01.02-22-011/09.

Lidia Dzierzbicka-Głowacka is with the Institute of Oceanology, Polish Academy of Sciences, Sopot, Poland (corresponding author to provide phone: (+48 58) 7311912; fax: (+48 58) 5512130; e-mail: dzierzb@iopan.gda.pl).

Maja Musialik is with the Institute of Oceanography, University of Gdansk, Gdynia, Poland (e-mail: m.musialik@ug.edu.pl).

Anna Lemieszek Maja Musialik is with the Maritime Institute in Gdańsk, Poland (e-mail: anna_lemieszek@op.pl).

different areas [26].

In this paper, the attention is focused primarily on the issue how the salinity affects the development of zooplankton in the Baltic Sea. The main species of Copepoda occurring in the Baltic Sea were taken into account. The paper includes mainly the experimental data from various literature sources in order to accurately determine whether there is a correlation between this environmental factor and copepods.

Copepods are included in the pelagic food chain, and hence they play an important role in the transmission of energy between producers and consumers of higher orders, representing, inter alia, food for many pelagic fishes. Extensive knowledge about the impact of salinity on the development of zooplankton in the Baltic Sea will help to predict changes occurring in this specific ecosystem and indicate effects of modification at different trophic levels. Taxa dominant in this water region were taken into account: *Pseudocalanus* spp. and *Temora longicornis*, as well as *Acartia* spp. and *Centropages hamatus*.

II. HYDROLOGY

The Baltic Sea, like other inland seas in humid climate zones, has a positive water balance. The average freshwater surplus amounts to 481 m² [18]. The value of the water balance in the Baltic Sea is determined by a number of factors, including atmospheric precipitation, evaporation, river inflow and exchange of waters through Sund and Belts, as well as the intensity of freezing and ice melting, which depends on the latitude.

Values of the atmospheric precipitation differ between particular regions of the Baltic Sea. They are usually higher in the southern and eastern part of the Baltic Sea, whereas the lowest values are characteristic of the northern regions and the open sea. These values also change seasonally and the lowest precipitation is recorded in spring and winter, whereas the highest values – in summer and autumn months.

Between 1998 and 2003, the fresh water runoff from the rivers into the Baltic Sea decreased from over 17,500m³ to less than 11,000m³. The inflow of fresh water through the rivers increased since 2008. At present the average river runoff into the Baltic Sea ranges from ca. 14,141 mm/year [27].

Baltic water masses are characterized by fluctuations in the salinity, which result from, inter alia, irregular inflows of fresh waters and flows (tides) from the North Sea. This situation occurs mainly in the Danish Straits and estuaries. The Neva

River has the largest catchment area and discharges on average 2,600 m³ of fresh water per year into the Baltic Sea [26]. The Vistula River is the second largest river in terms of the drainage basin size and discharges 954 m³ of water [26].

Stagnation is a phenomenon characteristic of the brackish waters and thus of the Baltic Sea. After a certain time, deposition of heavy, saline water below the halocline leads to oxygen deficit, which can result in extinction of life in this region [23]. Periodic, irregular flows from the North Sea temporarily improve the oxygen conditions in the regions situated within the zone of influence.

The flows depend on the wind field, the pressure over the North Atlantic Ocean and the amount of water in the Baltic Sea [22]. Waters of flow origin sustain the vertical stratification in the sea area and its salinity; the latter decreases from the Danish Straits deep into the Baltic Sea. Waters of Atlantic origin are most apparent in deep parts of western and southern parts of the Baltic Sea. Even minor tides are perceptible in these regions, whereas the farther upstream from the Danish Straits, the influence of tides is getting weaker and only large tides reach the central areas of the Baltic Sea.

Two types of flows (tides) are distinguished: barotropic or baroclinic. Barotropic tides occur during constant, strong westerly winds, preceded with easterly winds. They bring cold, saline waters rich in oxygen into the Baltic Sea. Tides of this type occur mainly in autumn and winter [16]. Baroclinic flows are induced by the baroclinic pressure gradient, as a difference between the salinity outside and inside the Baltic Sea. Those flows are smaller than barotropic ones, the water of which is more deficient in oxygen. They usually occur in summer [9-11],[19]. The last, large flow was observed in August 2003 after 10 years of stagnation [27]. The Baltic Sea received a large amount of saline, cold water (ca. 200 km³) with a temperature of about 1-2°C. The volume of flow waters was so great that they fed and refreshed the water resources in all basins of the Baltic Proper.

III. SEASONAL DYNAMICS OF PSEUDOCALANUS MINUTUS ELONGATUS AND ACARTIA SPP. IN THE SOUTHERN PART OF THE BALTIC SEA (THE GDAŃSK DEEP) – NUMERICAL SIMULATIONS.

Seasonal dynamics of the two main taxa (*Pseudocalanus minutus elongatus* and *Acartia* spp.) in the Southern Baltic was described by Dzierzbicka-Głowacka et al. [5-7] by means of mathematical models. Copepods were presented as organisms with a specific rate of growth, reproduction and mortality.

The main object of the research is not considered from the biomass perspective but from the populational one: mesozooplankton consists of k different age classes for a given taxon with corresponding weights and abundance. The biomass of the studied specimen is the sum of products of its weight and the abundance in subsequent developmental phases $\sum W_i Z_i$. In this case, the population model for one species consists of sixteen state variables with masses W_i and the number of individuals Z_i for each of the eight model stages,

grouped as follows: eggs-N2 – non-feeding stages and eggs; N3–N6 – naupliar stages; C1,C2, C3, C4, C5 – five copepodid stages; C6 – the adult stage. Each of the eight model stages consists of two equations (for each age class-cohort, two state variables represent the mass W_i and the number of individuals Z_i). The model included also parameters describing the physiological processes of selected copepods, in particular developmental phases (growth, production of faecal matter, secretion, the mortality rate, production of eggs). These parameters come from the literature or were described by functional relationships dependent on environmental parameters (temperature, food concentration) based on experimental data available in the literature for the studied sea area. Spatio-temporal distribution of two representative populations: *Pseudocalanus minutus elongatus* and *Acartia* spp., divided into the coastal zone (the Gulf of Gdańsk) and the open sea (the Gdańsk Deep), was investigated using a three-dimensional model of an ecosystem 3D CEMBSv1 [8] combined with the populational model allowing for the influence of salinity on the life functions of organisms.

Due to the fact that *Pseudocalanus minutus elongatus* is an euryhaline organism with a lower tolerance to salinity, 4-5 PSU according to Kinne [15] and 7.5 PSU according to Postel [28], the biomass of this species is largely determined by salinity. In the North Sea, at a temperature of 5°C (~35 PSU), the growth of Copepoda at the naupliar stage is twice as high as in the Gulf of Gdańsk (~8 PSU), whereas the growth of adult individuals – three times higher [4]. In order to estimate the increase of *Pseudocalanus minutus elongatus* biomass in the Gulf of Gdańsk, one should take into account the impact of salinity through the function f_s accepting $S_0=7.5$ PSU as a salinity limit for the development of *P.m. elongatus*, with the assumption that $f_s=1$ for $S=11$ PSU and $f_s=2$ for $S=35$ PSU. However, for *Acartia* spp., the best conditions are: temperature of 3-19°C and salinity of 4-10 PSU Mudrak [20] with salinity threshold of $S_0 \approx 1$ PSU (Figure 1). In the numerical simulations, also the mortality rate and reproduction were included. The mortality rate assumed for *Pseudocalanus minutus elongatus* was ca. 2.5 times higher compared with *Acartia* spp., which is a consequence of lower tolerance to salinity by *Pseudocalanus minutus elongatus*. One complete generation of *Pseudocalanus minutus elongatus* can be observed in the Southern Baltic during one year (from production of eggs to an adult stage), whereas in *Acartia* spp. – from three to five generations in the annual cycle and individual generations overlap with each other. The distributions shown in Figures 2 and 3 present the vertical mean total biomasses, which are the algebraic sum of the vertical mean biomasses of all stages at two stations P1 (the Gdansk Deep) and P2 (at the Gulf of Gdansk) and they reflect mainly the food availability, temperature and salinity. The model results were consistent with experimental data, which came from IMGW (Institute of Meteorology and Water Management) [14] and Mudrak [20]. The concentration of food and temperature are the factors controlling the

development of Copepoda in the Baltic Sea, and salinity is a masking factor mostly for *Pseudocalanus minutus elongatus*. The total biomass of *Acartia* spp. in the Gulf of Gdańsk is significantly higher compared with the Gdańsk Deep (Gdansk Basin). This results from higher concentration of food and higher temperature in the littoral zone, which in the case of *Acartia* spp. have a decisive impact on the development of specimens at each stage of growth. At station P1 (the Gdańsk Deep), the development of *Pseudocalanus minutus elongatus* is shorter than in the Bay of Gdańsk, despite the fact that station P2 is characterised by higher temperatures and higher concentration of food. This results from the parabolic function of temperature, which illustrates the decline of growth at a temperature of above 14°C with the salinity below 11 PSU [8]. The salinity in the upper layer of Gdańsk Bay stays below 8 PSU, which results in the decline of growth up to 20% at higher surface temperatures .

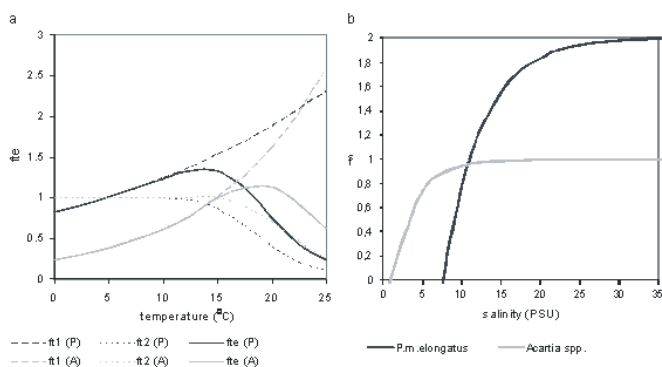


Fig. 1. Diagram of parameters temperature and salinity used in the copepod model for *Pseudocalanus minutus elongatus* (black line) and *Acartia* spp. (grey line) (a) and on salinity (b) [7]

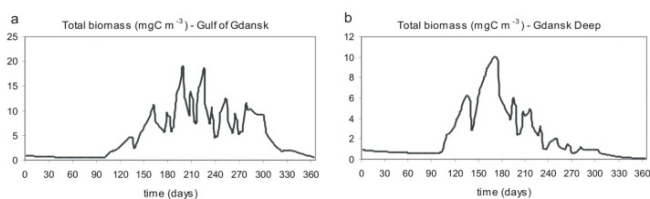


Fig. 2. Total biomass (mg C m^{-3}) of *Acartia* spp. as vertical mean concentrations at the Gulf of Gdańsk (a) and Gdańsk Deep (b) [7]

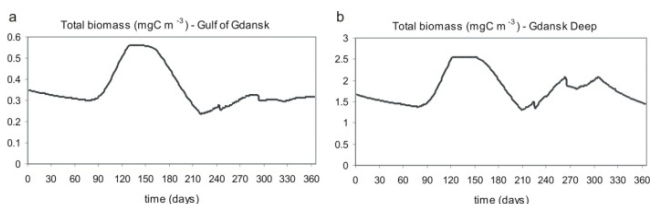


Fig. 3. Total biomass (mg C m^{-3}) of *Pseudocalanus minutus elongatus* as vertical mean concentrations at the Gulf of Gdańsk (a) and Gdańsk Deep (b) [7]

IV. LONG-TERM CHANGES IN THE BIOMASS OF ZOOPLANKTON

In order to obtain more information about the relationship between dominant species of Copepoda in the Baltic Sea and the salinity, the research was conducted, inter alia, in the Baltic Sea Research Institute, Germany. The paper Habitat layer extension and the occurrence of dominant calanoid copepods in the Baltic Sea [28] focuses on the description of the two most important aspects:

The first one concerned the with determination of such a water layer in the vertical profile, where prevailing salinity conditions are potentially favourable to specific species of copepods.

The second one concerned only about the genus *Pseudocalanus*. The objective of this aspect was to identify the potential habitats of this crustacean in the deeper layers of the Baltic Proper, taking into account both the salinity and the content of oxygen dissolved in water.

In order to define the optimal conditions of salinity for *Pseudocalanus* spp., *Acartia* spp. and *Temora longicornis*, organisms at the developmental stage CI – CV were used. The area between the Bay of Kiel and the Gotland Basin was selected as the study area and the place where organisms were collected. The research was conducted on samples in which the concentration of copepods was $>10,000$ specimens per m^{-3} (in this case *Temora longicornis* was excluded from the analysis, because at this density the species occurred only in one case).

Samples for the analysis came from the material collected in 1999 - 2003; 13 samples for *Pseudocalanus* spp. and 20 for *Acartia* spp. *Pseudocalanus* spp. was collected from the water layer beneath the halocline, whereas specimens of *Acartia* spp. were collected entirely from the surface layer at the stations east of the Darss Sill (the Arkona Basin, the Pomeranian Gulf, the Bornholm Basin).

With the abundant phytoplankton ($>10,000$ specimens m^{-3}) *Pseudocalanus* spp. was characterised by high concentration of specimens with the salinity ranging from 8 to 25 PSU, whereas for the genus *Acartia* spp. this range was narrower – from 6 to 8 PSU.

The obtained results in this study [28] identify habitats of two groups of copepods in the Baltic Sea (the first group – *Pseudocalanus* spp., the second group – *Acartia* spp. and *Temora longicornis*), which are separated from each other by the isohaline of 12 PSU. It has been predicted that as long as the salinity, the availability of oxygen and food in this region do not deteriorate, one can expect significant accumulation of Copepoda within the whole water column. Upper layers, up to the halocline will constitute the habitat for *Acartia* spp. and *Temora longicornis*, whereas deeper waters below 12 PSU will provide perfect environment for *Pseudocalanus* spp.

The isohaline of 8 PSU in the upper layer of the sea and the oxycline in the lower, central Gotland Basin limit the habitat of *Pseudocalanus* spp. in this region. Since the beginning of the 1980s, the depth of isohaline 8 PSU has systematically decreased, which consequently led to the reduced concentration of this copepod. This kind of situation was

observed until a significant inflow of saline water in 1993. After a long period of stagnation, the inflow of saline waters improved the oxygen conditions in a reservoir and raised the isohaline 8 PSU up to the smaller depths. The minimum thickness of the habitat layer for *Pseudocalanus* spp. was 1980s and from 2000 to 2002 (Figure 4).

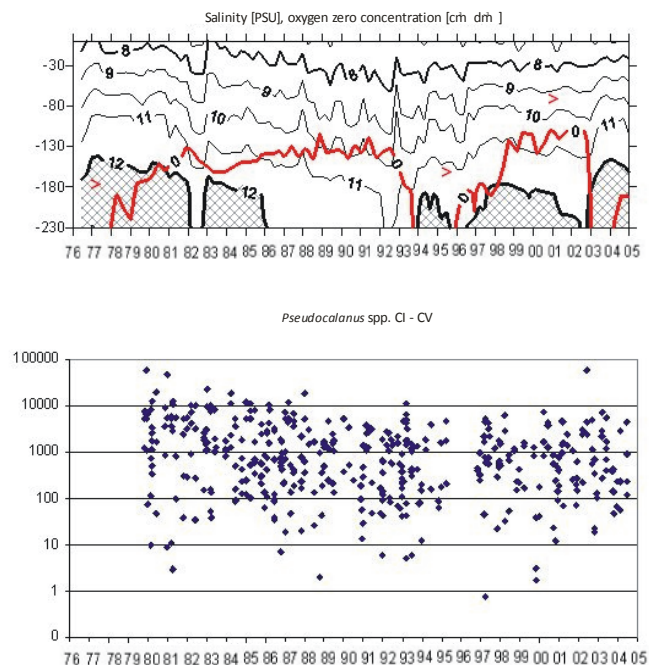


Fig. 4. The salinity profile and the location of oxycline east of Gotland compared with the occurrence of *Pseudocalanus* spp. in this area in 1977-2005 [17]

Similar researches were described in the paper by Möllmann et al. [21]. The objective of their study was to identify the long-term trends in the biomass of the main mesozooplankton species in the central part of the Baltic Sea and to check the hypothesis whether salinity and temperature are the main factors influencing the biomass of the studied organisms.

Data on the biomass of particular mesozooplankton species come from the Latvian database of the Fisheries Research Institute (LATFRI). Samples were collected using the Jedy Net with the mesh size of 160 micrometres and diameter of 0,36 metres. The maximum depth of net hauls was 100 metres. These data come from many studies in 1959-1997.

During laboratory analysis, small sub-samples were collected from each sample for obtaining the species composition. Based on the average value of two sub-samples, the number of specimens per m^3 was calculated, and next the biomass of each species per m^3 . The following organisms were identified in this analysis: *Pseudocalanus elongatus*, *Temora longicornis*, *Acartia* spp. (including *Acartia bifilosa*, *Acartia longiremis* and *Acartia tonsa*), *Centropages hamatus* and taxonomic groups from Cladocera.

Hydrographic analysis of this part of the sea area was also compiled on the basis of data coming from LATFRI. Water for

the analysis was collected with a Nansen sampler with the temperature measured every 5 or 10 metres. Salinity was measured with the use of a salinometer. All the data come from the period of 1961-1997. Average hydrographic values were calculated in the water column of 0-50 metres, as this water layer was mostly inhabited by *Temora longicornis*, *Acartia* spp. and *Centropages hamatus*. For the species *Pseudocalanus elongatus*, data were collected at the depths of 50-100 metres.

All the data were normalized by transformation to natural logarithms. Hydrographic data and biomass were averaged for each station and added up every three months. Further calculations were performed through the analysis of variance a 2-way ANOVA [21].

Biomass of *P. elongatus* at the beginning of 1980 had a certain anomaly in subregion 26. In subareas 25 and 28 at the beginning of the time series, considerable variations in anomalies were observed, which since the 1970s began to take positive values. After a long period of biomass increase, the biomass began to decline drastically since 1993. Biomass of *T. longicornis* was characterised by high variability, without distinct trends. In all subregions, negative anomalies were recorded at the beginning of the 1970s. ICES 26 and 28 were characterised by the highest positive anomalies at the beginning of the 1990s. From 1995 till the end of the research season only negative anomalies were observed, and this was related to a significant decrease in the biomass of *T. longicornis*. Conspicuous changes in the biomass were observed for *Acartia* spp. Negative values were obtained between 1963 and the beginning of 1970. After a short period of growth, a significant drop in the biomass was observed again in 1970. The most characteristic features of *Acartia* spp. were positive anomalies in 1980, observed in subregion 28 until 1990. For *Centropages hamatus*, the values of biomass remained at the positive level until mid-1970. Since 1978 a considerable decline of the biomass occurred in the region of ICES 26 and 28, which lasted to ca. 1980. After 1980 in ICES 26, the biomass of *Centropages hamatus* was increasing and in 1984 reached a positive anomaly. At that time, the biomass of copepods increased also in the region ICES 28, however these values did not reach a positive result and already in 1986 they began to drop in two regions. In 1990 the biomass of this species increased, and then gradually decreased during the last years of the research.

Based on the obtained results and their analysis one can conclude that there are no distinct differences between biomass values in the three subareas for all the studied species of Copepoda. This statement is supported by the results obtained after the statistical analysis a 2-way ANOVA. The analysis revealed that during 5 years significant differences in the biomass were observed for all organisms, but they were not correlated with the study area. And thus an additional analysis 2-way ANOVA was performed, with all the subregions together. Based on the „post hoc” test, the information was obtained that anomalies in the biomass of *Pseudocalanus elongatus* since the late 1980s were lower compared with other

periods. Negative anomalies were also found in the case of *Temora longicornis* in the latter half of 1980 and at the end of 1990. They were considerably lower compared with other periods of time. Anomalies in the biomass of *Acartia* spp. were constantly increasing within the time intervals with a significant positive anomaly starting from 1980. The obtained result for the species *Centropages hamatus* indicated a declining tendency of biomass, with a lap time of a high value at the beginning of the 1990s.

Average salinity in the water column from 0 to 50 metres did not differ significantly in particular seasons. These values were 8.0; 7.6 and 7.5 PSU for regions 25, 26 and 28, respectively. In the deeper layer from 50 to 100 metres, average salinity had the values of 14.6; 9.7 and 9.1 PSU. Non-seasonal anomalies in the salinity have the same interannual distribution in the three study areas, however the region of Bornholm was characterised by obviously high variability. The increased salinity was recorded only after flows, which took place in 1969, 1971 and at the turn of 1975/1976. From 1980 to 1990 a negative trend was observed in all the regions of the Baltic Sea. Deeper layers of the water in the Baltic Sea (50-100 m) were characterised by a more apparent response to saline water inflows. Contrary to the upper layers, positive anomalies were found in 1960.

The results of correlation between the biomass of copepods and hydrographic variables revealed that in spring the biomass of *Temora longicornis* and *Acartia* spp. is positively correlated with temperature in the surface layer of the sea (up to 50 m), whereas for salinity the negative correlation was obtained. This confirms the fact that *Acartia* spp. is classified as a thermophilic organism and the increase in biomass of this copepod follows the increase of temperature. A positive correlation for salinity, both in the surface layer and below 50 metres was obtained for *Pseudocalanus elongatus* throughout the year. For this species, the temperature of the surface layer does not play any significant role. The correlation is apparent only in the deeper layer. A positive relationship between salinity and biomass was also obtained for *Temora longicornis* in summer, autumn and winter. This species is also positively correlated with temperature in the layer up to 50 metres.

V. THE INFLUENCE OF SALINITY AND TEMPERATURE ON REPRODUCTION OF TEMORA LONGICORNIS

The concentration of food in the aquatic environment is the main factor influencing the reproductive capacity of Copepoda [14]. Food can reduce the reproductive parameters, both quantitatively and qualitatively [1]. However, the research was conducted that revealed that other environmental factors, such as temperature or salinity, may influence the reproductive capacity of the species, because they affect the metabolic activity of specimens. In the case of copepods, each of the aforementioned factors indirectly or directly influence the number of eggs produced by females, as well as their vitality at the initial stages of growth. Salinity is a masking factor in the Baltic Sea [24],[13]. This effect is apparent when comparing

the production of eggs of the same copepod species in the North Sea and the Bornholm Basin in the Baltic Sea. Low production of eggs in the Baltic Sea confirms the hypothesis that salinity has a strong influence on the development at an early stage of life [13]. The objective of scientists in the present study was to determine, in a quantitative way, the reproductive process of *Temora longicornis* within a wide range of temperatures and salinity, and to study the interaction between these abiotic factors.

Organisms included in the analysis were collected in May 2005 in the region of Kilonia in the south-western part of the Baltic Sea. The water salinity was 14 PSU, the temperature 10°C. The collected Copepoda were acclimated in a laboratory for 4 days in the water with the same salinity and temperature as the natural environment they live in. The cultures were carried out in the daily system 13:11 with the salinity of 8, 14, 20 and 26 PSU. A control sample was conducted in the following conditions: salinity 14 PSU, temperature 10°C and the daily system 12:12.

Between particular salinity values, there was a clear difference in the number of eggs produced by females. With the salinity of 8 PSU, the result was 1.8-11.0 eggs produced by one female per day. Together with the increasing salinity, also the ability of egg production was increasing. At 14 PSU, 2.7-16.9 eggs were recorded, whereas in water with 20 PSU this number increased to 18.5 eggs female⁻¹ d⁻¹. High productivity was also obtained in the salinity of 26 PSU – 14.1 eggs female⁻¹ d⁻¹ [13]. The egg production (Egg, no. of eggs female⁻¹ d⁻¹) in *Temora longicornis* in the changing environmental conditions of the southern Baltic Sea (Gdansk Deep) by means of modelling is presented by Dzierzbicka-Głowacka et al. [7]. Dzierzbicka-Głowacka et al. [7] speculate that the food-saturated rate of egg matter production is equivalent to the specific growth rate of copepods. The average number of eggs produced per day by one female of *T. longicornis* as a function of growth rate is obtained by multiplying $\exp g_N - 1$ from the growth rate of the naupliar stage equation by $W_{\text{female}} / W_{\text{egg}}$. In this work, the combined effect of food concentration and temperature, as well as salinity as a function of these three parameters on the number of eggs produced per female per day is established for *T. longicornis*. Our study aims to derive a quantitative expression to describe the egg production per day by a female *T. longicornis* from growth rate and experimental data from the south-western Baltic Sea [12].

In the case of the Baltic Sea, egg production of *T. longicornis* is largely dependent on salinity [12] and decreases with diminishing salinity. In Dzierzbicka-Głowacka et al. [7] paper, the egg production is made dependent on salinity by a function f_s including a salinity threshold for egg production of 7 PSU. This means that the egg production rate as a function of three variables – food concentration, temperature and salinity – is given by a non-linear regression: $\text{Egg} = a \exp(b T - f_2) f_s$, where coefficients a and b are functions of the food concentration $Food$ and f_s is a function of salinity S . f_s was defined by exponential function in the shape $f_s = 1 - \exp(-\alpha(S -$

7)), where a coefficient $\alpha = -3$ was adopted numerically including values of *Egg* which were obtained by equations given by [12] that describe the effect of salinity on reproductive success at $T=14^{\circ}\text{C}$ within unlimited feeding conditions.

Our calculations suggest that in the southern Baltic Sea, maximal *Egg* (c. 11 eggs female⁻¹ d⁻¹) coincided with the spring phytoplankton bloom occurring between March and April at 4–6°C at salinities around 7–8 PSU. A second peak in *Egg* (c. 8 eggs female⁻¹ d⁻¹) was obtained in September at surface water temperatures of 15–17°C. Hence, individual egg production rates in the Baltic Sea (Bornholm Basin and Gulf of Gdansk – Dzierzbicka-Głowacka et al. [7] are rather low (c. 3-5 times) in contrast with adjacent waters, i.e. the North Sea and the English Channel, where *Egg* values are moderate or quite high and vary strongly within the investigation area, without reaching maximum values.

VI. DISCUSSION

The researches carried out in the central Baltic Sea in 1959-1997 indicate significant differences in the biomass of mesozooplankton in five-year intervals. Linear correlation revealed that biomass of *Pseudocalanus elongatus* is determined by salinity during all seasons. In fact, after the inflows of saline water coming from the North Sea in 1971 and 1975/1976, the abundance of this copepod increased. But since 1980, when the salinity of the Baltic Sea began to gradually decline due to the lack of saline water inflows [17] with a constant inflow of fresh waters from the land and atmospheric precipitation, the biomass of *Pseudocalanus elongatus* began to decline and the lowest values were recorded in 1993. Strong correlation between the salinity and biomass of this species is characteristic of *Pseudocalanus elongatus*, as a typically marine organism.

In the central Gotland Basin (data coming from Postel [28]), the average biomass of *Pseudocalanus elongatus* obtained from observations in 1980-2004, was compared with a simulation model created on the basis of the data coming from 1977-2005. Since 1979 the count of copepods was decreasing between particular flows, and this reflects the relationship between the occurrence of *Pseudocalanus elongatus* in the Gotland Basin and the prevailing salinity. The results of the observations overlap with the simulation model except for the period between 1997 and 2003. The simulation predicted a high increase in the abundance of *Pseudocalanus elongatus* after a large flow from the North Sea, which took place in 1997 and 2003. The warm years 1997 and 2003, however, led to increased water temperature in the surface layer, thereby to reduced occurrence of this copepod (forms C1-C5 of *Pseudocalanus elongatus* prefer cooler waters).

Slower growth of *Pseudocalanus minutus elongatus* in the Baltic Sea and the reduced reproductive capacity are translated into subsequent characteristics that differentiate the Baltic population from the population of the North Sea. It is about secondary production, which plays an important role in

ecosystems, supplying higher trophic levels with energy. The value of secondary production for *Pseudocalanus minutus elongatus* in the North Sea was 110 mg C m⁻², which was almost 11 times higher than the average values for the production in the Baltic Sea (9.1 mg C m⁻²) [24].

The results of this research indicated that vertical distribution of *Pseudocalanus minutus elongatus* in the pelagic zone of the Baltic Sea is closely connected with the salinity and temperature.

Temora longicornis is a species of a wider range of tolerance to salinity compared with *Pseudocalanus elongatus*, as it can live in waters with the salinity of 8 to 16 PSU [2]. The results concerning the long-term changes in the biomass of this copepod in 1959-1997 do not reveal changes related to salinity. Due to the fact that *Temora longicornis* occurs mostly in the surface layer and its count decreases together with the depth, the salinity of the Baltic Sea should not affect the biological processes of this species, as it does not exceed 16 PSU. The paper by Hostle et al. [12], however, proved the relationship between temperature, salinity and the reproductive capacity of this species. The results of the research by Hostle et al. [12] indicate that in the case of the Baltic Sea, salinity is a masking factor during reproduction of *Temora longicornis*. When comparing the data, one can see the differences between the efficiency of this process in different geographic regions. In the North Sea the quantity of eggs produced by a female of *Temora longicornis* during one day comes to the maximum value of almost 60 at a temperature of 10°C, whereas in the Baltic Sea, the maximum production of eggs takes place at a temperature of 3°C and it comes to just 10 eggs. This discrepancy in the results between the two water regions may be related to physiological capacities of females, due to differences in the size of their body. It is common knowledge that the phenomenon of pauperization concerns many organisms from the Baltic Sea, including copepods.

Positive correlation between the biomass and temperature results from statistical analysis for *Acartia* spp. [21]. No effect of salinity on the growth or decline of this copepod species has been observed. In the initial period of the research, negative anomalies of the biomass were reported. This kind of situation lasted until about 1974. In 1976 – 1993, the biomass of *Acartia* spp. began to increase, which may result from positive anomalies in the temperature during that period, with simultaneous negative anomalies for salinity in the layer of 0-50 metres.

For *Centropages hamatus*, no significant correlations were recorded between the amount of biomass and hydrographic changes in the Baltic Sea in 1959-1997. In the literature this species is described as thermophilous, occurring at a temperature of above 10°C [25]. Inhabiting the upper layer of the Baltic Sea, even despite the positive or negative anomalies in salinity, the species was not exposed to osmotic stress, as it is an euryhaline organism, and its optimum is within the range of 7 PSU.

The research carried out by Möllmann, Kornilovs and

Sidrevics [21] revealed that the biomass of the main Copepoda species in the Baltic Sea in 1959-1997 was partly determined by hydrography of the sea area. The strongest correlation was obtained for *Pseudocalanus elongatus*, which shows strong affinity to higher salinity at a low temperature. Therefore, its occurrence in the Baltic Sea is limited to the water layer near the halocline. Other species are more dependent on temperature.

Reduction of *Pseudocalanus minutus elongatus* biomass in the Baltic Sea, as the major component of food, undoubtedly contributed to the declined growth of the Baltic herring (*Clupea harengus*) since the beginning of the 1980s. For the amount of resources of zooplankton and its composition affects the growth and the survival rate of fishes at early stages of their development [3].

The accurate knowledge about the species composition, dominance of particular taxa, density or biomass combined with abiotic parameters (salinity, temperature, pressure etc.) facilitates the appropriate evaluation of changes taking place in an ecosystem. Such knowledge, combined with simulation models, gives hypothetical forecasts for the future, permits the prediction of negative or positive effects of environment changes.

VII. CONCLUSIONS

Conclusions presented in this study are based on the performed analysis of the literature data:

- Changes in the biomass of *Pseudocalanus elongatus* in the Baltic Sea are strongly correlated with salinity. The highest concentration of this copepod was recorded within the halocline region.
- Salinity of the Baltic Sea does not play any significant role in the long-term changes in the biomass of *Acartia* spp. and *Centropages hamatus*.
- *Temora longicornis* is a species, for which salinity is an important factor in the reproductive processes, influencing the quantity of produced eggs.

REFERENCES

- [1] B.R. Beckman & W.T. Peterson, "Egg production by *Acartia tonsa* in Long Island Sound", *Plankton Res.*, vol. 8, no.5, pp. 917-925, 1986.
- [2] J. Chojnacki, "Biomass estimation of *Temora longicornis* on the basis of geometric method", *Sylogosus*, vol. 58, pp. 534-538, 1986.
- [3] D.H. Cushing, "The long-term relationship between zooplankton and fish", *J. Mar. Sci.*, vol. 52, pp.611-626, 1995.
- [4] L. Dzierzbicka-Głowacka, "Growth and development of copepodite stages of *Pseudocalanus* spp", *J. Plankton Res.*, vol. 26, pp. 49-60, 2004.
- [5] L. Dzierzbicka-Głowacka, L. Bielecka, & S. Mudrak, "Seasonal dynamics of *Pseudocalanus minutus elongatus* and *Acartia* spp. in the southern Baltic Sea (Gdansk Deep) – numerical simulations" *Biogeosciences*, vol. 3, pp. 635–650, 2006.
- [6] L. Dzierzbicka-Głowacka, M. I. Żmijewska, S. Mudrak, J. Jakacki, & A. Lemieszek, "Population modelling of *Acartia* spp. in a water column ecosystem model for the South-Eastern Baltic Sea", *Biogeosciences*, vol. 7, pp. 2247–2259, 2010.
- [7] L. Dzierzbicka-Głowacka, J. Piskozub, J. Jakacki, S. Mudrak, & M.I. Żmijewska, "Spatiotemporal distribution of copepod populations in the Gulf of Gdansk (southern Baltic Sea)", *J. Oceanogr.*, doi. 10.1007/s10872-012-0142-8, 2012.
- [8] L. Dzierzbicka-Głowacka, M. Kalarus, M. Janecki, M. Musialik, S. Mudrak & M.I. Żmijewska, "Population dynamics of *Pseudocalanus minutus elongatus* in the Gulf of Gdansk (southern Baltic Sea) – experimental and numerical results", *J. of Natural History*, vol. 47, Issue 5-12, 2013.
- [9] R. Feistel, G. Nausch, V. Mohrholz, E. Łysiak-Pastuszak, T. Seifert, W. Matthäus, S. Krüger, & I. Hansen, "Warm waters of summer 2002 in the deep Baltic Proper", *Oceanologia*, vol. 45, no. 4, pp. 571–592, 2003b.
- [10] R. Feistel, G. Nausch, T. Heene, J. Piechura & E. Hagen, "Evidence for a warm water inflow into the Baltic Proper in summer 2003", *Oceanologia*, vol. 46, no. 4, pp. 581–598, 2004a.
- [11] R. Feistel, G. Nausch, T. Heene, J. Piechura & E. Hagen, "Evidence for a warm water inflow into the Baltic Proper in summer 2003", *Oceanologia*, vol. 46, no. 4, pp. 581–598, 2004b.
- [12] L. Holste, M. A. St. John, & M. A. Peck, "The effects of temperature and salinity on reproductive success of *Temora longicornis* in the Baltic Sea: a copepod coping with a tough situation", *Marine Biology*, vol. 156, pp. 527–540, 2009.
- [13] A. Ianora, M.G. Mazzocchi, & R. Grottolli, "Seasonal fluctuations in fecundity and hatching success in the planktonic copepod *Centropages typicus*", *J. Plankton Res.*, vol. 14, pp. 1483-1494, 1992.
- [14] IMGW, *Baltyk Południowy. Charakterystyka wybranych elementów środowiska*, Instytut Meteorologii i Gospodarki Wodnej PIB, Warszawa, 2000.
- [15] O. Kinne, "The effects of temperature and salinity on marine and brackish water animals", *Oceanogr. Mar. Biol. Ann. Rev.*, vol. 1, pp. 301–340, 1963.
- [16] W. Matthäus, & H. Franck, "Characteristics of major Baltic inflows: a statistical analysis", *Continental Shelf Res.*, vol. 12, pp. 1375-1992, 1992.
- [17] W. Matthäus, & H. Schinke, "Mean atmospheric circulation patterns associated with major Baltic inflows", *Dt. Hydrogr.*, vol. 46, pp. 321–339, 1994.
- [18] W. Matthäus & H. Schinke, "The influence of river runoff on deep water conditions of the Baltic Sea", *Baltic Sea Research Institute Warnemünde, Kluwer Academic Publishers, Hydrobiologia*, vol. 393, pp. 1–10, 1999.
- [19] V. Mohrholz, J. Dutz, & G. Kraus, "The impacts of exceptionally warm summer inflow events on the environmental conditions in the Bornholm Basin", *J. Mar. Syst.*, vol. 60, pp. 285–301, 2006.
- [20] S. Mudrak, "Short- and long-term variability of zooplankton in coastal Baltic waters: using the Gulf of Gdańsk as an example", PhD Thesis, University of Gdansk, Gdynia, 2004.
- [21] C. Möllmann, G. Kornilovs, & L. Sidrevics, "Long-term dynamics of main zooplankton species in the Baltic Sea", *J. Plankton Res.*, vol. 22, no.11, pp. 2015–2038, 2000.
- [22] R. Osinski, "Simulation of dynamic processes in the Baltic Sea based on ocean-ice coupled model", PhD Thesis, Institute of Oceanology, Polish Academy of Sciences, Sopot, 2008.
- [23] H. Renk, *Produkcja pierwotna południowego Baltyku*, Morski Instytut Rybacki: Gdynia, 2000, 35A, pp. 78
- [24] J. Renz, "Life cycle and population dynamics of the calanoid copepod *Pseudocalanus* spp. in the Baltic Sea and North Sea", PhD Thesis, University Bremen. Bremen, 2006.
- [25] K. Siudziński & R. Maj, *Zooplankton of the Gulf of Gdansk*: Morski Instytut Rybacki, Gdynia, 1977, pp.111.
- [26] L. Håkanson. (2012, December 10). Środowisko Morza Bałtyckiego Charakterystyka fizycznogeograficzna zlewiska Morza Bałtyckiego [Online]. Available: <http://www.wgsw.uw.edu.pl/tmp/BSE-01.pdf>.
- [27] J. Kronsell, & P. Andersson. (2013, Mai 15). Helcom. Total and regional Runoff to the Baltic Sea [Online]. Available: http://www.helcom.fi/BSAP_assessment/ifs/ifs2010/en_GB/Runoff/.
- [28] L. Postel. (2013, December 8). Helcom. Habitat layer extension and the occurrence of dominant calanoid copepods in the Baltic Sea [Online]. Available:http://www.helcom.fi/BSAP_assessment/ifs/archive/ifs2005/en_GB/zooplankton/.

Geochemical Baseline Concentrations of Available Heavy Metals in Mediterranean Agricultural Soils: A Case Study in calcareous soils of Southwest Iberian Peninsula

J. Rato Nunes, J. Ramos-Miras, A. Lopez-Piñeiro, L. Loures, C. Gil, J. Coelho and D. Peña

Abstract— The characterization of the content and sources of trace metals in soils is an instrument in many programs of environmental protection, including the establishment of regional-level standards to detect sites affected by contamination. The objectives of the present study were to study the available levels of Cd, Cr, Cu, Ni, Pb, and Zn in surface horizons of agricultural calcareous soils in a typical European Mediterranean region, to establish the geochemical baseline concentration (GBC), background level (BL), and reference value (RV) of each of these metals, and to investigate their possible correlations with soil properties. To establish the GBC and RV values we used the “standard threshold method”. Topsoil samples (0-20 cm) were collected from 630 sites, and extracted with DTPA to determine their available heavy metal concentrations. The measured total and available concentrations were lower than or close to those reported by other researchers for agricultural soils. The GBC values established were: 0.04 to 0.90 mg kg⁻¹, 0.70 to 2.50 mg kg⁻¹, 0.10 to 6.30 mg kg⁻¹, 0.30 to 7.90 mg kg⁻¹, 0.29 to 4.50 mg kg⁻¹, and 0.18 to 2.50 mg kg⁻¹ for Cd, Cr, Cu, Ni, Pb, and Zn, respectively. Soil properties were found to be correlated with the available heavy metal content, suggesting that the enhanced of mobility of heavy metals are related to anthropic activities. Available GBC determination is a tool that can provide insight into the risk of trace element contamination and transfer to other environmental compartment.

Keywords— available heavy metals, Mediterranean agricultural soils, DTPA, geochemical baseline concentrations, reference values.

J. M. Rato Nunes is with the Polytechnic Institute of Portalegre, C3I and the UIQA – Research Center of Environmental Chemistry. Superior Institute of Agronomy, Portugal.

J.J. Ramos-Miras is with Dept. Edafología y Química Agrícola, Escuela Politécnica Superior, Universidad de Almería, Spain.

A. Lopez-Piñeiro is with UIQA – Research Center of Environmental Chemistry. Superior Institute of Agronomy, Portugal and UIQA – Research Center of Environmental Chemistry. Superior Institute of Agronomy, Portugal

L. Loures is with the Research at the Centre for Spatial and Organizational Dynamics and with the Polytechnic Institute of Portalegre, C3I.

C. Gil is with Dept. Edafología y Química Agrícola, Escuela Politécnica Superior, Universidad de Almería, Spain.

J.P. Coelho is with Instituto Superior de Agronomia, Universidade Técnica de Lisboa, Portugal.

D. Peña is with Área de Edafología y Química Agrícola, Facultad de Ciencias, Universidad de Extremadura

I. INTRODUCTION

THE Mediterranean region has been subject to intense anthropic pressure for millennia, resulting in a vulnerable and often fragile ecosystem [1]. Livestock and crop farming are the main human activities in the area [2]. The excessive use of fertilizers in the region has, in general, led to soil acidification, problems of soil degradation, and a major proportion of contaminant trace metals [3, 4]. Moreover, in the European Mediterranean region, cropping intensity is often inconsistent with the soil's natural potential, with 26% of the soils used for farming being in fact unsuitable for that purpose [5]. The concentration of heavy metals in agricultural soils is related mainly with the parent material of the area [6], although there are few studies on availability and mobility of the heavy metals in agricultural soils.

The characterization of the content and sources of heavy metals in soils is a key element in many programs of environmental protection, including the establishment of regional-level quality standards to detect sites affected by contamination [7, 8].

The accumulation of heavy metals in the soil is considered to be a serious risk at the environmental level [9]. Published results on the levels of heavy metals in soils been based on indirect estimation, small-scale studies, or poorly defined time periods, but often represent the only information available for extensive territories. Also, they are not only hard to extrapolate, but seem unlikely to provide any reliable picture of long-term trends that might be applicable to any large agricultural area under commercial management. For this reason, the present large scale field study represents a major research contribution to determining and quantifying the impact of agriculture on soil available heavy metal content under Mediterranean conditions.

It is widely accepted that determining the total content of heavy metals in a soil is neither sufficient to understand their relative mobility and ecological availability as contaminants nor particularly useful as a tool to estimate potential risks. The toxicity of metals for plants and animals including humans depends not only on their total concentrations, but also on their mobility and reactivity with other components of the

ecosystem [10, 11]. The "bioavailable fraction" is the fraction of the total contaminant in the interstitial water and soil particles that is available to the receptor organism [12]. However, there is still very little direct measurement data or predictions of the available fraction of metals in soils. In Portugal and Spain for instance, there is hardly any information at all on available heavy metals in agricultural soils, and this lack of information is reflected in poorly informed legislation which does not take soil characteristics into account [13, 14].

The initial soil pH and the ability of plant roots to change the pH have been found to be the principal predictors of the exchange of heavy metals, and therefore of their bioavailability [15]. It is generally accepted that anthropogenic heavy metal contamination exists mainly in the form of reactive species on the soil surface, and the concepts of "bioavailability" and "bio-accessibility" were introduced to express the actual effect of the concentration of a contaminant on organisms in the ecosystem [12, 16, 17, 18].

The geochemical baseline concentration (GBC) and background level (BL) of different heavy metals in soils have been studied in various Mediterranean countries [8, 14, 19, 20, 21, 22, 23]. It is widely accepted that the BL and GBC were the best approach to establish the levels of non-contaminated soils. Different approaches have been taken to establishing the GBC of trace elements in Mediterranean soils [8, 14, 24, 25, 26]. Most have centred on the total heavy metal content without considering the bioavailability of the different elements involved [27], even though, according to Baldantoni *et al.* [28], bioavailability constitutes the best indicator of the potential impact of these contaminants.

The present study is aimed at contributing to improved information on available heavy metals in Mediterranean agricultural soils in particular, it being important to bear in mind that there is only limited data available on available heavy metals in Mediterranean soils in general. Given this context, the specific objectives were: (i) to study the levels of available heavy metals in typical agricultural soils of a Mediterranean region; (ii) to establish the available GBC of these metals.

II. MATERIAL AND METHODS

A. Study area and sampling

The study area is located within the administrative townships of Elvas and Campo Maior, at the confluence of the Rivers Caia and Guadiana, near the Portuguese-Spanish border (Figure 1). A total of 630 sites were selected in the "Caia Irrigation Perimeter". At each sample site, 10 topsoil (0–20 cm) subsamples were collected at random and merged to give a composite sample of roughly 2 kg. Later all samples were air dried, crushed and sieved to < 2 mm, and stored.

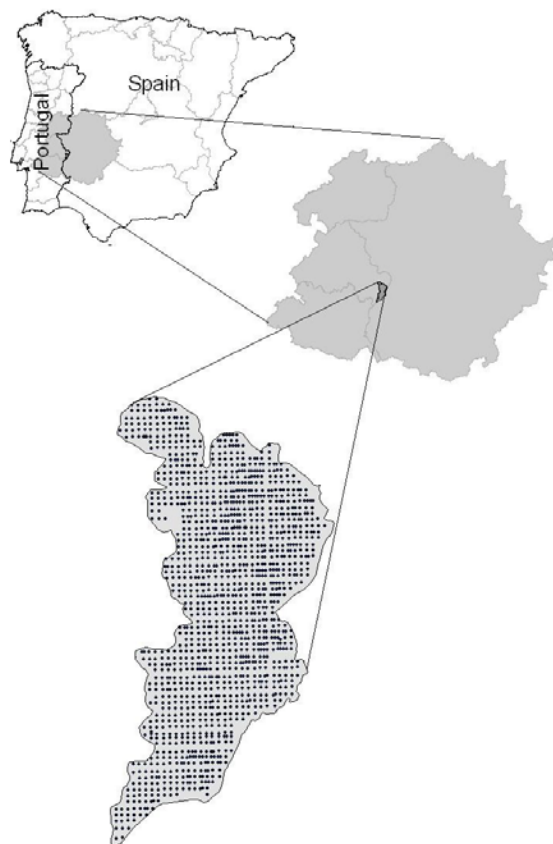


Figure 1 - Localization map of the area studied

The geology of this area consists essentially of Cambrian and Silurian formations, with some small eruptive zones associated with hyper-alkaline and alkaline rocks [29]. The average annual rainfall is approximately 483 mm, most of which coincides with the coolest temperatures from October to March. The maximum average monthly temperature corresponds to July with 24.7°C and the minimum to January with 8.8°C. The Mediterranean region is characterized by its hot dry summers and cool wet winters. The most important crops are: maize (*Zea mays*) for feed-grain production with almost half of the cultivated area (49%), wheat (*Triticum aestivum*) (17%), sunflower (*Helianthus annuus*) (7%), tomato (*Lycopersicon esculento*) (6%), and olive (*Olea europea*) (4%).

B. Analytical methods

The physical and chemical soil analyses were carried out following Roca-Pérez [30] and were determined for each individual soil (data not show). The available heavy metals were determined by the method described by Lindsay and Norvell [31] (extraction with DTPA + CaCl₂ + triethanolamine). According to Hooda and Alloway [32]; Soriano-Disla *et al.* [33] and Hao *et al.* [34], DTPA extraction is the most efficient method of extracting heavy metals from soils, independently of the soil's properties, and hence can be an effective way to assess the availability of heavy metals to plants. We considered this fraction as bioavailable heavy

metals.

Total heavy metals were determined following the method described in EPA 3052 [14]. The concentrations of Cd, Cr, Cu, Ni, Pb, and Zn (total and available) were determined by ICP-OES (IRIS INTREPID II XDL THERMO). Measurements were made in triplicate for each sample to check the precision of the results. To assess both the quality of the methods applied and the assay by atomic absorption spectroscopy, a check was made for matrix interferences using standard addition techniques. No such interferences were observed for the determination of the metals studied. In other hand 30 samples were re-analysed and a paired t-test realized, the results indicated no significant differences in the values [35]. The concentrations of available Cd, Cr, Cu, Ni, Pb, and Zn are indicated as mg kg⁻¹ dry matter. The limit of detection of the method was 0.01 mg kg⁻¹.

identified as data endpoints of the raw data for which the resulting population has a skewness nearest to zero and hence the populations can be segregated (contaminated and non-contaminated soils). The reference value (RV) was taken as the upper limit of the GBC, and was used to determine whether a soil might be contaminated or not [35]. The identification of a specific type of soil as contaminated means that the total contaminant content is higher than would normally be expected in non-contaminated areas [26]. The RV values were used to evaluate the soils' contamination and quality.

III. RESULTS AND DISCUSSION

The main soil characteristics are listed in Table 1. The commonest soil groups in the study area are Fluvisols (42.7%), Luvisols (21.7%), Calcisols (16.1%), Cambisols (6.1%), Vertisols (1.8%), and Regosols (0.6%), as is usual in

Table 1: Mean values, standard deviation, and ranges for general descriptive parameters of Caia soils (n=630)

	SOM (%)	N (%)	Soil Carbonates (%)	pH	CEC cmol.kg ⁻¹	CE ₂₅ dS cm ⁻¹	P ₂ O ₅ (mg/100g)	K ₂ O (mg/100g)
MINV	0.2	0.03	0.1	4.5	3.8	0.01	4.0	18
AM	1.5	0.10	5.5	6.9	15.8	0.11	197	220
MAXV	4.4	0.31	16.4	8.9	71.5	1.00	5920	3268
STD	0.6	0.04	4.2	1.1	10.2	0.11	413	185
GM	1.4	0.09	3.6	6.9	13.5	0.09	120	186

MINV—minimum value.

AM—mean.

MAXV—maximum value.

STD—standard deviation.

GM—geometric mean

The Zn Equivalent Indices (ZnEqT for total heavy metals and ZnEqB for available heavy metals) were used to compare the potential heavy metal toxicity in these soils [8, 13, 14, 36]. They both were calculated as:

$$\text{ZnEq} = [\text{Zn}] + 2[\text{Cu}] + 8[\text{Ni}]$$

where [Zn], [Cu], and [Ni] are the respective soil concentrations of the metal (total and available for ZnEqT and ZnEqB, respectively).

C. Statistical analyses

All statistical analyses were performed using the SPSS version 15.0 software package, calculating the arithmetic mean (AM), range (MINV-MAXV), standard deviation (SD), and geometric mean (GM) as descriptive statistics.

D. Baseline concentrations

To establish the GBC and BL values, the soil sample population was segregated into non-contaminated and contaminated soils on the basis of probability plots applying the "standard threshold method" described by Fleischhauer and Korte [37] and used by several authors.

Following this method a log-normal distribution was assumed, and Q-Q plots were drawn. From these plots the overlap corresponding to different population can be determined from slope changes of the plots. The tipping points formed by the superposition of the two populations were

Mediterranean ecosystems [29]. In general, these are medium-loam and clay-loam soils with a pH close to 7, slightly calcareous, and low levels of soil organic matter (SOM, 1.54%) and total nitrogen (N, 0.1%).

They have intermediate levels of cation exchange capacity (CEC, 15.8 cmolc kg⁻¹), with calcium as the principal exchangeable cation, and a degree of saturation of exchangeable cations of 70%. Their levels of available phosphorus and potassium (P₂O₅ and K₂O, respectively) are high, indicating intensive use of soil fertilizers which is thus suggestive that farming may be incorporating pollutants into the soils [38, 39]. Their saturated soil-paste electrical conductivity is low (EC₂₅, 0.11 dS cm⁻¹), indicating that these soils have no salinity problems.

The total concentrations for the heavy metals in these soils based on the 30 representative top soils of the study area were (mg kg⁻¹): ranges, Cd <d.l.–0.7; Cr 10.8–89, Cu 9.5–489, Ni 5.2–48.6, Pb 7.7–41.9; and Zn 10.1–65.6; mean values ± SD, 0.6 ± 0.1, 48.4 ± 25.5, 16.7 ± 9.1, 23.6 ± 13.6, 19.1 ± 8.9, 29.6 ± 15.1 (mg kg⁻¹) for Cd, Cr, Cu, Ni, Pb, and Zn, respectively (Table 2). According to these data therefore, the order of the heavy metals' total content was Cr>Zn>Ni>Pb>Cu>>Cd. In general, in all the soils these levels are low compared with literature values for Mediterranean agricultural soils [40, 41, 42]. The ZnEqT values (252 ± 135 mg kg⁻¹) were also lower than Gil *et al.* [8] obtained in Mediterranean greenhouse soils, and the present study's heavy metal total concentrations do not surpass the RV established by Inácio *et al.* [20] in Portuguese soils or the GBC values of natural soils in the Mediterranean

region established by Roca-Pérez *et al.* [22].

Table 2: Total concentrations (mg kg⁻¹ dry soil) of trace elements in soil samples (n=30) from Caia area.

	Cd	Cr	Cu	Ni	Pb	Zn	Zn EqT
MINV	<d.l.	10.8	5.4	5.2	7.7	10.1	63
AM	0.6	48.4	16.7	23.6	19.1	29.6	252
MAXV	0.7	89.0	45.0	48.6	41.9	65.6	506
STD	0.1	25.5	9.1	13.6	8.9	15.1	135
GM	0.6	41.1	14.6	19.6	17.1	25.9	214

<d.l. below detection limit

ZnEqT—Zinc equivalent of total heavy metals

Table 3 presents the mean concentrations of available Cd, Cr, Cu, Pb, Ni, and Zn in the soils, with the corresponding values of the standard deviation, range, and geometric mean.

Table 3: Available concentrations (mg kg⁻¹ dry soil) of trace elements in soil samples (n=630) from Caia area with associated statistical parameters.

	Cd	Cr	Cu	Ni	Pb	Zn	Zn EqB
MINV	<d.l.	<d.l.	<d.l.	<d.l.	<d.l.	<d.l.	0.3
AM	0.24	0.85	1.23	1.95	3.16	0.64	19.4
MAXV	1.10	3.30	10.00	6.60	13.00	5.00	130
STD	0.23	0.79	1.15	1.30	2.33	0.58	14.5
GM	0.15	0.50	0.86	1.48	2.25	0.51	14.3

<d.l. below detection limit

Zn EqB—Zinc equivalent of bioavailable heavy metals

The available concentrations of these potentially toxic elements averaged over the 630 representative surface soil samples were (mg kg⁻¹ dry wt, mean ± SD): Cd 0.24 ± 0.23; Cr 0.85 ± 0.79; Cu, 1.23 ± 1.15; Ni, 1.95 ± 1.30; Pb 3.16 ± 2.33, and Zn 0.64 ± 0.58. According to these data, the order of the available content of the metals was Pb>Ni>Cu>Cr>Zn>Cd. The content of the most available heavy metal in this kind of soil, Pb, is known to be essentially anthropogenic [19].

The availability data for Cr, Cu, Pb, and Zn are lower than or close to those reported by different workers in the literature considering the same extractant (Table 4), but the data for Pb are perceptibly higher than those reported by Antolin *et al.* [43] and Buccolieri *et al.* [44]. The only work that determine available Cd is Antolin *et al.* [43] and their data are lower than we found in the study area.

Table 4: Available concentration of Cd, Cr, Cu, Ni, Pb and Zn, extracted with EDTA in different soils (mg kg⁻¹).

	In this work	Bucolieri et al., 2010	Masas et al., 2009	Gisbert et al., 2006	Ramos 2006	Antolin et al., 2005	Walker et al., 2003
Cd	0.24 ± 0.23	n.d.	n.d.	n.d.	n.d.	0.012-0.013	n.d.
Cr	0.85 ± 0.79	n.d.	1.5 ± 0.5	n.d.	n.d.	n.d.	n.d.
Cu	1.23 ± 1.15	5.40 ± 5.67	2.5 ± 1.2	0.9-8.8	15.3 ± 4.3	1.64-1.19	11.3
Ni	1.95 ± 1.30	0.41 ± 0.32	1.3 ± 0.9	n.d.	n.d.	n.d.	n.d.
Pb	3.16 ± 2.33	2.09 ± 1.92	5.8 ± 3.2	22.1-179	n.d.	1.34-1.75	28.2-32.5
Zn	0.64 ± 0.58	3.67 ± 3.27	7.8 ± 9.7	10.5-7.7	2.2 ± 1.2	0.77-2.41	15.2-14.4

MINV-MAXV

AM ± STD

n.d. not determined

Although the levels of available heavy metals vary greatly among different Mediterranean soils, the order of their concentrations in the present study are similar to those found by other workers, implying that the processes operating are similar. The levels of ZnEqB found are lower than those reported by Ramos-Miras *et al.* [36], in greenhouse soils (44.6 ± 43.5 mg kg⁻¹), although they use other extracting agent. This is indicative of the present soils being free of relevant contamination or large scale mobilization of the heavy metals analysed as might have been caused by farming activities, despite the large amounts of fertilizers (available phosphorous and potassium) detected in them.

A. Assessment of soil contamination

Soils constitute a complicated and heterogeneous system [45], so that simple monitoring of their heavy metal concentrations is insufficient guarantee of their environmental quality. Their trace element contents vary widely, so that it is inappropriate to use universal background concentrations as a criterion since the native concentrations of metals in a specific soil may exceed any given listed ranges. It is therefore important to determine the values of the GBC and RV concentrations locally [8, 14, 36, 46, 47]. To estimate the GBC values, the "standard threshold method" was applied [37]. The Q-Q plots are shown in Figure 2. Low values deviate from linearity because they were beneath the detection limit, and were hence assigned the detection limit value as proposed by Tack *et al.* [35]. The threshold was chosen as the point at which the slope of the Q-Q plot changes. Values beneath the threshold point denote the GBC (0.91, 2.52, 6.33, 7.32, 4.60, 2.53 threshold point of Cd, Cr, Cu, Ni, Pb and Zn, respectively). The resulting GBC ranges were (in mg kg⁻¹): 0.04 to 0.90, 0.70 to 2.50, 0.10 to 6.30, 0.30 to 7.30, 0.29 to 4.50, and 0.18 to 2.50 for Cd, Cr, Cu, Ni, Pb, and Zn, respectively. The BL estimated from non-contaminated soils were (in mg kg⁻¹): 0.23, 0.72, 1.22, 2.00, 1.96, and 0.57 for Cd, Cr, Cu, Ni, Pb and Zn, respectively. The method of threshold points allows the differentiation of homogeneous populations using statistical criteria, assuming that populations with higher contents of heavy metals are subject to contamination processes.

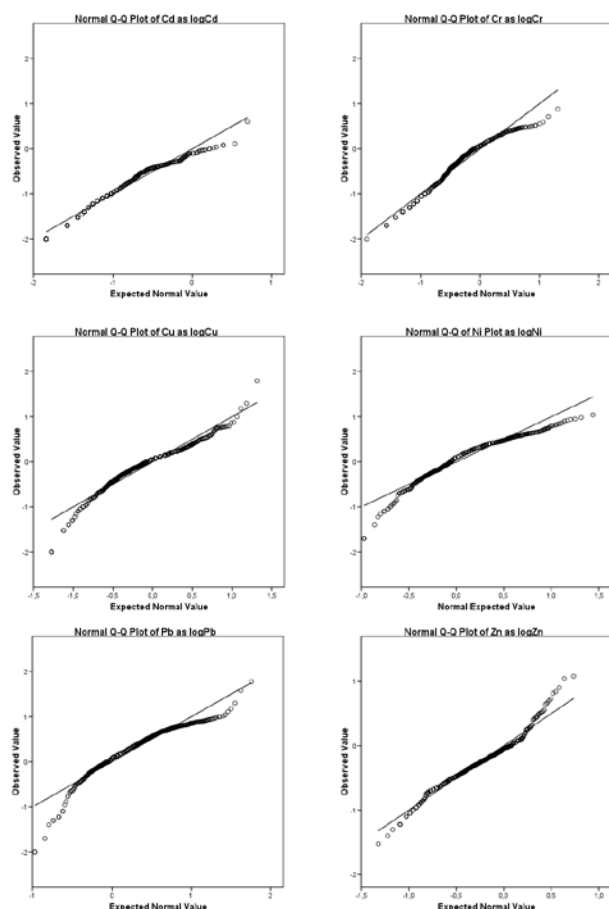


Figure 2 - Normal probability plot of bioavailable Cd, Cr, Cu, Pb, Ni and Zn contents as log[concentration]

There are only two literature studies on the GBC of available heavy metals in soils – Tarvainen and Kallio [27] in natural soils in Finland, and Ramos-Miras *et al.* [36] in agricultural soils. They both used EDTA for extraction, however, so that it is difficult to compare their results with the present findings, even more so given that they did not analyse the same heavy metals. Nevertheless, the present results lie within the limits proposed by those authors.

The upper limit of the GBC could be used as the RV against which to assess soil contamination [26] find that this method is far more effective than others that have been put forward in the specialized literature. Using therefore the upper GBC values as the RVs of the available heavy metals (Cd 0.9; Cr 2.5; Cu 6.3; Ni 7.9; Pb 4.5; and Zn 2.50; all in mg kg⁻¹) with which to determine whether or not a soil is contaminated, we found that 2% for Cd, 6% for Cr, 1% for Cu, 4.5% for Pb, 5% for Ni, and 4% for Zn of the samples were slightly contaminated.

In particular, only 6% of the sample soils had a higher available content of heavy metals than the RV limit (due mainly to Cr, Cu, Ni, and Pb). In sum, these results point to a minimal extension of soil contamination by available heavy metals. Using the 90% percentile value as reference to determine where a soil could be contaminated like Tack *et al.* [35] (Table 5). All of the heavy metals values for 90% percentile were lower than the RV proposed for these soils in this work, except for Pb, who value of 90% is higher than RV. This fact confirm that the contamination for available

heavy metals was minimal except for Pb, who is one of the most mobile [36, 48].

Table 5: Estimated of baseline concentrations of Available heavy metals (mg kg⁻¹ dry soil) based on percentile values of the data considered to be baseline values

Percentile	Cd	Cr	Cu	Pb	Ni	Zn
5%	0.01	0.05	0.14	0.24	0.35	0.14
25%	0.07	0.18	0.53	1.30	0.83	0.32
50%	0.16	0.55	1.00	2.50	1.70	0.50
75%	0.37	1.10	1.60	4.60	2.70	0.72
90%	0.50	1.70	2.37	6.10	3.56	1.00
95%	0.70	2.00	3.30	6.80	3.94	1.20
99%	0.92	2.30	5.70	7.70	4.40	1.90

IV. CONCLUSIONS

The concentrations of total and available heavy metals in these agricultural soils, which are typical of the Mediterranean region, were generally lower than or close to those reported in the literature for other agricultural areas. The GBCs of the available heavy metals were: 0.04 to 0.90 mg kg⁻¹, 0.70 to 2.50 mg kg⁻¹, 0.10 to 6.30 mg kg⁻¹, 0.30 to 7.90 mg kg⁻¹, 0.29 to 4.50 mg kg⁻¹, and 0.18 to 2.50 mg kg⁻¹, for Cd, Cr, Cu, Ni, Pb, and Zn, respectively. The threshold method is a good way to establish GBC values in an initially homogeneous population of soil. Only a small percentage of the 630 soils sampled had high available levels of heavy metals, so that there is no evidence for any extensive heavy metal contamination of these soils.

Given the potential risk to human health represented by available heavy metals, especial effort is called for to determine both the locations of contaminated soils and the sources of their contamination in order to be able to halt the contamination process and avoid larger areas being affected. We must emphasize that the present results are preliminary, and the findings will be more extensively studied in future work.

REFERENCES

- [1] Ramos, M.C., 2006. Metals in vineyard soils of the Penede's area (NE Spain) after compost application. *Journal of Environmental Management* 78, 209-215.
- [2] Kosmas, C.; Danalatos, N. G.; López-Bermúdez, F.; Romero-Díaz, M. A. 2002. The effect of land use on soil erosion and land degradation under Mediterranean conditions. Pages 57–70. In N. A. Geeson, C. J. Brandt, and J. B. Thornes, editors. *Mediterranean desertification: a mosaic of processes and responses*. Wiley, Chichester, UK.
- [3] Zalidis, G., Stamatiadis, S., Takavakoglou, V., Eskridge, K., Misopolinos, N., 2002. Impacts of agricultural practices on soil and water quality in The Mediterranean region and proposed assessment methodology. *Agriculture, Ecosystems & Environment*. 88, 137-146.
- [4] Romic, M., Romic, D., 2003. Heavy metal distribution in agricultural topsoils in urban area. *Environmental Geology* 43, 795-805.
- [5] Borrego, C. 1993. Water, air and soil pollution problems in Portugal. *Science of the Total Environment* 129, 55-70.
- [6] De Tammerman, L., Vanongeval, L., Boon, W., Hoenig, M., 2003. Heavy metal content of arable soils in Northern Belgium. *Water, Air and Soil Pollution* 148, 61-76.
- [7] Rodríguez-Martín, J.A., López-Arias, M., Grau-Corbí, J.M., 2006. Heavy metals contents in agricultural topsoils in the Ebro basin (Spain). Application of the multivariate geochemical methods to study spatial variations. *Environmental Pollution* 144, 1001-1012.
- [8] Gil, C., Ramos-Miras, J., Roca-Perez, L.; Boluda, R., 2010. Determination and assessment of mercury content in calcareous soils. *Chemosphere* 78, 409-415.

- [9] Romaguera, F., Boluda, R., Fornes, F., Abad, M., 2008. Comparison of three sequential extraction procedures for trace element partitioning in three contaminated Mediterranean soils. *Environmental Geochemistry and Health* 30, 171-175.
- [10] Adriano, D.C., 2001. *Trace Elements in Terrestrial Environments: Biochemistry, Bioavailability and risks of metals*, Springer-Verlag, New York.
- [11] Abollino, O., Aceto, M., Malandrino, M., Mentasti, E., Sarzanini, C., Petrella, F., 2002. Heavy metals in agricultural soils from Piedmont, Italy. Distribution, speciation and chemometric data treatment. *Chemosphere* 49, 545-557.
- [12] Vig, K., Megharaj, M., Sethunathan, N., Naidu, R., 2003. Bioavailability and toxicity of cadmium to microorganisms and their activities in soil: a review. *Advances in Environmental Research* 8, 121-135.
- [13] Andreu, V., Boluda, R., 1995. Application of contamination indexes on different farming soils. *Bulletin of Environmental Contamination and Toxicology* 54, 228-236.
- [14] Gil, C., Boluda, R., Ramos, J., 2004. Determination and evaluation of cadmium lead and nickel in greenhouse soils of Almería (Spain). *Chemosphere* 55, 1027-1034.
- [15] Martínez-Alcalá, I., Clemente, R., Bernal, M.P., 2009. Metal Availability and chemical properties in the rhizosphere of *Lupinus albus* L. growing in a high-metal calcareous soil. *Water Air and Soil Pollution* 201, 283-293.
- [16] Meyer, J.S., 2002. The utility of the terms "bioavailability" and "bioavailable fraction" for metals. *Marine Environmental Research* 53, 417-423.
- [17] Peijnenburg, W., Jager, T., 2003. Monitoring approaches to assess bioaccessibility and bioavailability of metals: matrix issues. *Ecotoxicology and Environmental Safety* 56, 63-77.
- [18] Cao, A., Cappai, G., Carucci, A., Lai, T., 2008. Heavy metal bioavailability and chelate mobilization efficiency in an assisted phytoextraction process. *Environmental Geochemistry and Health*. 30, 115-119.
- [19] De Vivo, B., Somma, R., Ayuso, R.A., Calderoni, G., Lima, A., Pagliuca, S., Sava, A., 2001. Pb isotopes and toxic metals in floodplain and stream sediments from the Volturno river basin, Italy. *Environmental Geology* 41, 101-112
- [20] Inácio, M., Pereira, V., Pinto, M., 2008. The Soil Geochemical Atlas of Portugal: Overview and applications. *Journal of Geochemical Exploration* 98, 22-33.
- [21] Albanese, S., De Vivo, B., Lima, A., Cicchella, D., Civitillo, D., Cosenza, A., 2010. Geochemical baselines and risk assessment of the Bagnoli brownfield site coastal sea sediments (Naples, Italy) *Journal of Geochemical Exploration* 105, 19-33.
- [22] Roca-Pérez, L., Gil, C., Cervera, M.L., González, A., J. Ramos-Miras, J., Ponsa, V., Bech, J., Boluda, R., 2010. Selenium and heavy metals content in some Mediterranean soils. *Journal of Geochemical Exploration* 107, 110-116.
- [23] Guillén, M.T., Delgado, J., Albanese, S., Nieto, J.M., Lima, A., De Vivo, B., 2011. Environmental geochemical mapping of Huelva municipality soils (SW Spain) as a tool to determine background and baseline values. *Journal of Geochemical Exploration* 109, 59-69.
- [24] Galán, E., Fernández-Caliani, J.C., González, I., Aparicio, P., Romero, A., 2008. Influence of geological setting on geochemical baselines of trace elements in soils. Application to soils of South-West Spain. *Journal of Geochemical Exploration* 98, 89-106.
- [25] Tume, P., Bech, J., Tume, L., Bech, J., Reverter, F., Longan, L., Cendoya, P., 2008. Concentrations and distributions of Ba, Cr, Sr, V, Al, and Fe in Torrelles soil profiles (Catalonia, Spain). *Journal of Geochemical Exploration* 96, 94-105.
- [26] Díez, M.; Simón, M.; Martín, F.; Dorronsoro, C.; García, I., Van Gestel, C.A.M. 2009. Ambient trace element background concentrations in soils and their use in risk assessment. *Science of the Total Environment*. 407, 4622-4632.
- [27] Tarvainen, T., Kallio, E., 2002. Baselines of certain bioavailable and total heavy metal concentrations in Finland. *Applied. Geochemistry* 17, 975-980.
- [28] Baldantoni D, Leone A., Lovieno P., Morra L., Zaccardelli M., Alfani, A. 2010. Total and available soil trace element concentrations in two Mediterranean agricultural systems treated with municipal waste compost or conventional mineral fertilizers. *Chemosphere* 80, 1006-1013.
- [29] Nunes, J., 2003. *Los suelos del perímetro regable del Caia (Portugal): Tipos, fertilidade, e impacto del riego en sus propiedades químicas*. Tesis Doctoral, Universidad de Extremadura – Facultad de Ciencias, Badajoz.
- [30] Roca-Pérez, L., Pérez-Bermúdez, P., Boluda, R., 2002. Soil characteristics, mineral nutrients, biomass, and cardenolide production in Digitalis obscura wild populations. *Journal of Plant Nutrition* 25, 2015-2026.
- [31] Lindsay WL & Norvell WA 1969. Development of a DTPA micronutrients soil test. *Agronomy Abstracts* 6: 84.
- [32] Hooda, P.S., Alloway, B.J., 1994. The plant availability and DTPA extractability of trace metals in sludge-amended soils. *Science of the Total Environment* 149, 39-51.
- [33] Soriano-Disla, J.M., Gómez, I., Guerrero, C., Jordan, M.M., Navarro-Pedreño, J., 2008. Soil factors related to heavy metal bioavailability after sewage sludge application. *Fresenius Environmental Bulletin* 17, 1839-1845.
- [34] Hao, X.Z., Zhou, D.M., Huang, D.Q., Cang, L., Zhang, H.L., Wang, H., 2009. Heavy Metal Transfer from Soil to Vegetable in Southern Jiangsu Province, China *Pedosphere* 19, 305-311.
- [35] Tack, F.M.G., Vanhaesebroeck, T., Verloo, M.G., Van Rompaey, K., Van Ranst, E., 2005. Mercury baseline levels in Flemish soils (Belgium). *Environmental Pollution* 134, 173-179.
- [36] Ramos-Miras, J.J., Roca-Perez, L., Guzmán-Palomino, M., Boluda, R., Gil C., 2011. Background levels and baseline values of available heavy metals in Mediterranean greenhouse soils (Spain). *Journal of Geochemical Exploration* 110, 186-192
- [37] Fleischhauer, H.L., Korte N., 1990. Formulation of cleanup standards for trace elements with probability plots. *Environmental Management* 14, 95-105.
- [38] Nziguheba, G., Smolders, E. 2008. Inputs of trace elements in agricultural soils via phosphate fertilizers in European countries. *Science of the Total Environment* 390, 53-57.
- [39] Cheraghi, M., Lorestani, B., Merrikhpour, H., 2012. Investigation of the effects of phosphate fertilizer application on the heavy metal content in agricultural soils with different cultivation patterns. *Biological Trace Element Research* 145, 87-92.
- [40] Caridad-Cancela, R., Vidal-Vázquez, E., Vieira, S.R., Abreu, C.A., Paz-González, A., 2005. Assessing the spatial uncertainty of mapping trace elements in cultivated fields. *Communications in Soil Science and Plant Analysis* 36, 253-274.
- [41] Rodríguez-Martín, J.A., López-Arias, M., Grau-Corbí, J.M., 2006. Heavy metals contents in agricultural topsoils in the Ebro basin (Spain). Application of the multivariate geochemical methods to study spatial variations. *Environmental Pollution* 144, 1001-1012.
- [42] Peris, M., Recatalá, L.; Micó, C., Sánchez, R., Sánchez, J., 2007. Heavy metal contents in horticultural crops of a representative area of the European Mediterranean region. *Science of the Total Environment*. 378, 42-48.
- [43] Antolín, M.C.; Pascual, I.; García, C.; Polo, A.; Sánchez-Díaz, M. 2005. Growth, yield and solute content of barley in soils treated with sewage sludge under semiarid Mediterranean conditions. *Field Crops Research* 94, 224-237.
- [44] Buccolieri, A., Buccolieri, G., Dell'Atti, A., Strisciullo, G., Gagliano-Candela, R., 2010. Monitoring of total and bioavailable heavy metals concentration in agricultural soils. *Environmental Monitoring and Assessment* 168, 547-560.
- [45] Chen, H.M., Zheng, C.R., Tu, C., Zhou, D.M., 2001. Studies on loading capacity of agricultural soils for heavy metals and its applications in China. *Applied Geochemistry* 16, 1397-1403.
- [46] Matschullat, J., Ottenstein, R., Reimann, C., 2000. Geochemical background — can we calculate it? *Environmental Geology* 39, 990-1000.
- [47] Horckmans, L., Swennen, R., Deckers, J., Maquil, R., 2005. Local background concentrations of trace elements in soils: a case study in the Grand Duchy of Luxembourg. *Catena* 59, 279-304.
- [48] Massas, I., Ehalotis, C., Kalivas, D., Panagopoulou, G., 2010. Concentrations and availability indicators of soil heavy metals; the case of children's playgrounds in the city of Athens (Greece). *Water, Air, and Soil Pollution* 212, 51-63.

Thermochemical characteristics of the modern gearboxes housing material

Ion Silviu BOROZAN, Veronica ARGEȘANU, Inocențiu MANIU, Raul Miklos KULCSAR, Mihaela JULA

Abstract—The paper consists on the chemical / metallographic analysis of the 7G Tronic automatic gearbox material housing for possible changes in the composition to achieve a more efficient cooling and to improve the housing characteristics.

Keywords—automatic gearbox, 7G Tronic, Magnesium, analysis, diffraction.

I. INTRODUCTION

BECAUSE of the high temperatures in some areas of the automatic gearbox 7G Tronic observed with the thermographic method in which are found the main brakes and couplings, it is recommended that the optimization of the shape of the housing to be made by adding cooling ribs and optimizing the chemical structure of the housing material. This ribs can achieve more efficient cooling in areas where located, because of their geometry, during the running of the vehicle. To identify the metallographic structure of the material and any material failures, we'll use two chemical structural analysis methods (X-ray diffraction and X-ray scanning electron microscopy).

To carry out these studies were collected samples of material from three different areas of the 7 g-Tronic automatic gearbox fig (1):

- area 1-highlighted with red color (corresponding to the portion of the converter and the gearbox, formerly upper area);
- area 2-highlighted with blue color (median-posterior portion corresponding to the gearbox, gross Kevlar coupling);
- area 3-highlighted with green (belonging to the inferior portion of the 7 g-Tronic gearbox, hydraulic control block).

These samples consist of pieces of wool board sized 5 mm long and 2 mm thick.

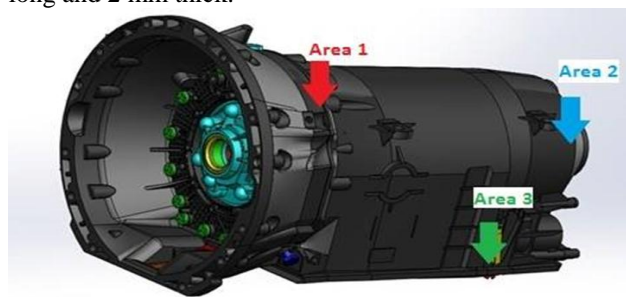


Fig 1. Sample areas

II. STRUCTURAL ANALYSIS BY X-RAY DIFFRACTION

To start with, we achieved diffraction spectra of x-rays in order to be able to notice any difference between the three areas. In Fig (2) are presented X-ray diffraction spectra for three samples.

X-ray diffraction is a nondestructive technique that allows obtaining precise information about the chemical composition and crystalline structure of natural and synthetic materials.

The basic principle of this method is to study the link between the scattering of X-ray and the layout space of the atoms.

X-ray diffraction is a structural analysis method currently used in studying the crystalline structure of mono- or polycrystals, in phase identification and quantitative phase analysis, in phase transformations, and in order to determine the parameters of the network, the internal tensions, or the dimensions of semi-processed [3; 10].

To describe 7G-Tronic's housing material analysis it is being used the X Pert Pro MPD ' (Panalytical), that is a X-ray diffractometer with X-ray tube, with copper anode having the wavelength $\lambda = 0,154$ nm. For all the samples the 2θ angle = 10° - 70° , the pitch is 0.131 seconds, and a random time of 60 min. Spectra have been interpreted and analyzed with Pert Plus Highscore X ' due to the active database.

Structural analysis of 7G-Tronic automatic gearbox casing is represented in fig (3) and fig (4) by highlighting the characteristic spectra of key chemical elements, especially through the length spectrum, Magnesium (Mg), Aluminum (Al), Silicon (Si), Manganese (Mn).



Fig 2. X-ray stress measurements at (RX) Pro MPD Panalytical

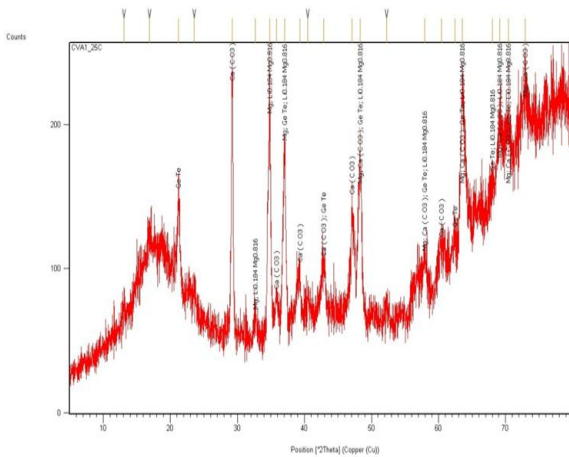


Fig 3. Analysis of diffraction spectra characteristic of the material

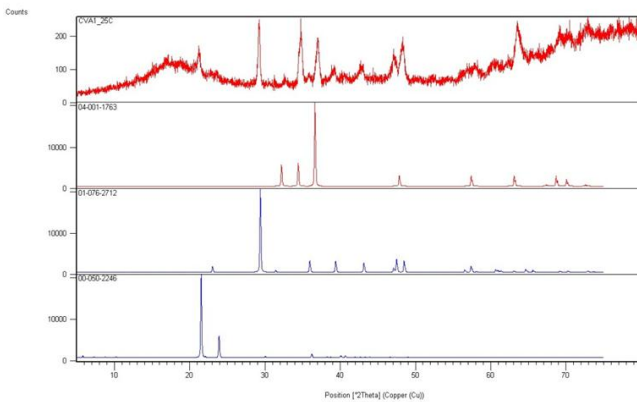


Fig 4 . Analysis of x-ray diffraction of major chemical elements (EDAX)

From the spectra of x-ray diffraction is observed no difference among the three areas, which shows that the homogeneity of the material is the same over the whole surface of the gearbox.

III. STRUCTURAL ANALYSIS BY SCANNING ELECTRON MICROSCOPY

Scanning electronic microscopes are used to study the surface ultra-morphology with the help of secondary electrons or reluctant. This type of microscope enables the examination of materials with a thickness ranging between 1 mm and cm have stayed with irregular surfaces, providing three-dimensional images of objects. Image formation is carried out with the help of secondary electrons or refracted arising from the bombing of the primary electron beam.

Electron beam produced by electron gun is reduced to the Max through two or three electromagnetic lenses thus aiming to achieve an extremely narrow beam with a diameter less than 100 Å, which is designed on the sample. With the help of two deflexiune coils, placed inside the last activated by electromagnetic lenses a current streak of primary electron

beam, such focus is determined to make a zig-zag move over the sample, thus a sweep of the area.

An electron microscope with scanning (SEM) has a direction of inlet light similar to that of an optical microscope. The resolution of an optical system is defined as the minimum distance between two objects that produce images separable and is expressed by the relation:

$$d = \frac{0.61\lambda}{n \sin\theta} \tag{1}$$

where:

λ-the wavelength of light, emission wavelength, in the case of fluorescence

θ- angular semi-aperture of the optical system's lens

n –the index of refraction of the media surrounding the radiating points.

So, as the wavelength of the radiation is less, the resolution is better. In the case of optical microscopy, where it is considered a light wavelength of 200 nm, to obtain a resolution of approximately 2000 Å. in the case of electrons accelerated by a potential difference V, the wavelength of the associated radiations is given by the relations:

$$\lambda = h/[meV \left(1 + \frac{eV}{2mc^2}\right)]^{\frac{1}{2}} \tag{2}$$

Where: h-Planck

m-mass of the electron

e- the electron charge

c-light speed

V- acceleration voltage

At the usual acceleration voltages in electron microscopy there are obtained smaller wavelengths of approximately 104-105 times than the wavelength of light. Therefore, resolution of electronic microscopes is clearly superior to the optical ones, on the order of a few Angstrom the most fine-tuned tools [2; 5; 7; 11].

Characterization of the automatic gearbox housing structure was achieved by means of an electronic microscope streak-Inspect (FEI Company) with EDAX (dissipated energy spectrometer x-rays). Inspect Fig (5) is a scanning electron microscope with easy to use, able to generate and collect all information available from any type of material.



Fig 5 . Electron microscope (SEM) streak-Inspect (FEI Company) + EDAX

Scanning electron microscope is used for qualitative analysis (Imaging) and quantitative (EDAX).

This shows that manufacturing processes (casting) were conducted with a very high precision and perseverance.

Also this analysis regards the structural aspect of the housing material excluding some chemical elements that appear in the diffraction but have a very low amount of quantity and percentage therefore are excluded from the beginning of the final and exact analysis.

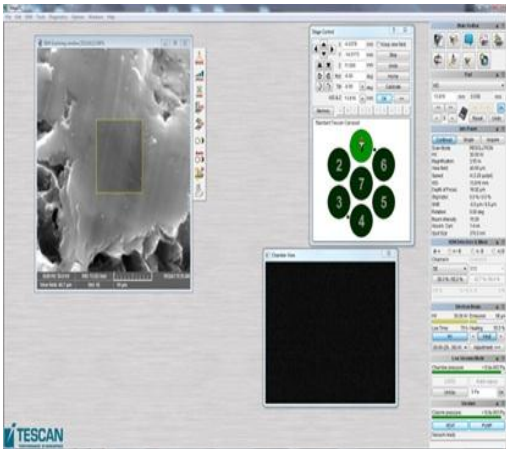


Fig 6. (a)

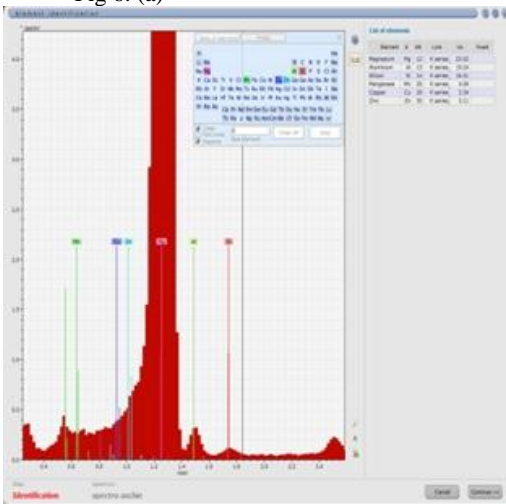


Fig 6. (b)

Screenshot taken following the inspection of samples with scanning electron microscopy qualitative Fig 6 (a) and quantitative (EDAX)

Fig 6 (b)

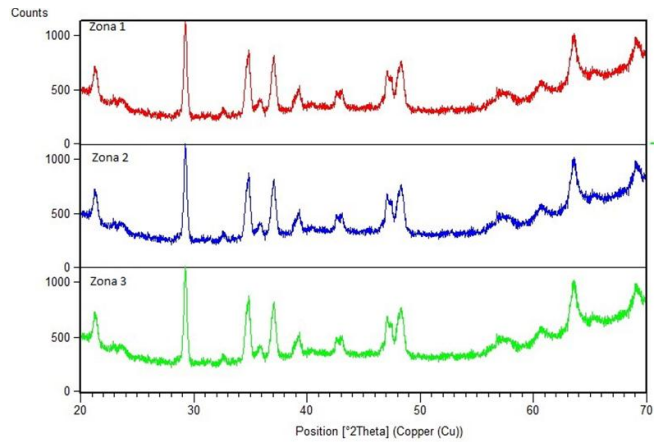


Fig. 7. The spectrum of x-ray diffraction samples: a) area 1, b) area 2, c) area 3

Due to the fact that during operation of the vehicle, one of the parts subjected to tension and major thermal fluctuations is the gearbox, due in particular to oil that has direct contact with the material as well as other external and internal factors is good to achieve thermal stability perspectives.[1; 3; 4; 6]

For this study were taken from zone 1 more test pieces (pieces of-wool Board) which have undergone a heat treatment annealing temperature of 100 ° C and up to a temperature of 500 ° c. The samples were heated with 10 ° C/min, after which they were kept for three hours at the desired temperature. Sample cooling was naturally up to room temperature.

Of the spectrum of x-ray diffraction Fig(7) and Fig (8)observes specific diffraction Maxima mg O2 per compounds identified in the database with the number 01-076-1363, Al2O3 identified in the database with the number 00-001-1305, Mg identified in the database with the number 00-001-1148. He obtained a mixture of Aluminium and magnesium (AlMg) identified in the database with the number 00-011-0571.

The chemical structure of the gearbox casing:

Normal temperature 25 °

c: a Mg-96,67%,-2.40%, And-0.66%, Mn-0.23%

• Temperature 200 °

c: a Mg-83,92% 12,16% O-, Al-3,93%

• Temperature 400 °

c: a Mg-45,74% O-, Al-28,66% 25.6%

• Temperature 500 °

c: a Mg-43,44% 55,27% O-, -0.75%, And-0.54%

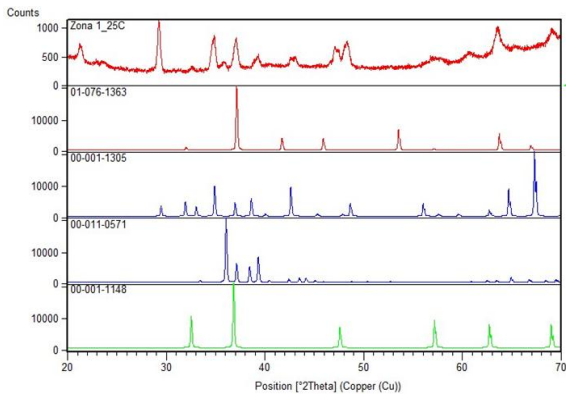


Fig (8) The spectra of x-ray diffraction for zone 1 achieved at room temperature

As shown in Figure 9 It can be seen that in the application of annealing heat treatment at different temperatures is observed the formation of other compounds that affect both the thermal stability as well as the composition of the material. Diffraction Maxima are the same for all the beach temperatures (25-500 ° C).

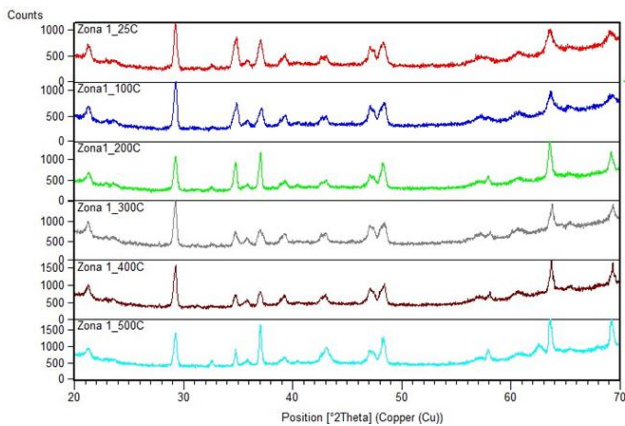


Fig (9) The spectra of x-ray diffraction for zone 1 at different annealing temperatures

In order to have a more precise confirmation of the chemical composition of the samples may have used the electronic scanning microscopy SEM and qualitative form.

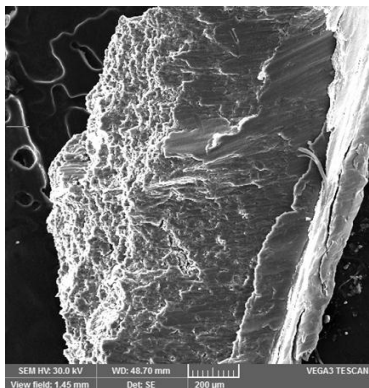


Fig 10 . SEM image of breaking the area 1 sample of housing (75X)

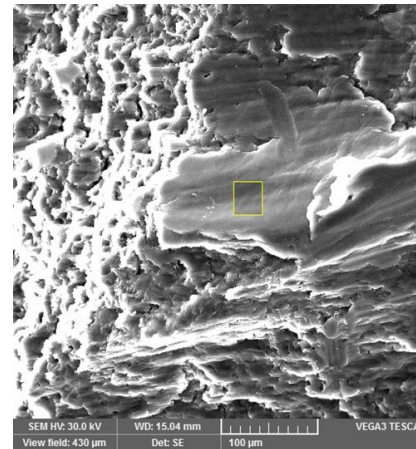


Fig 11 . SEM image of breaking the areal sample of housing (333X)

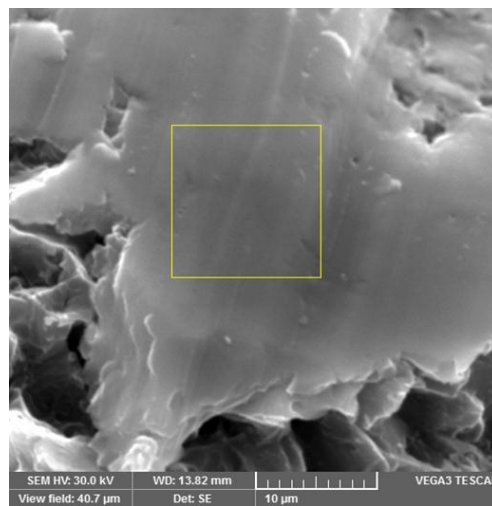


Fig (12) SEM analysis of the spectrum of materials (3300X)

SEM images of an homogenous surface without any other defects in the surface of the material, such as pores, leading to loss of mechanical and chemical properties. The same area is observed in the case of heat-treated at 200 ° c. EDAX images seen just peak caraceristice-magnesium and Aluminium.

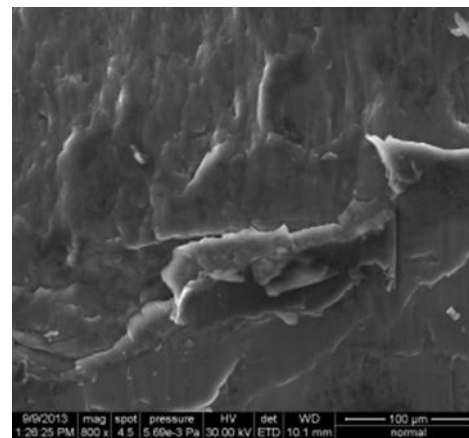


Fig 13 (a)

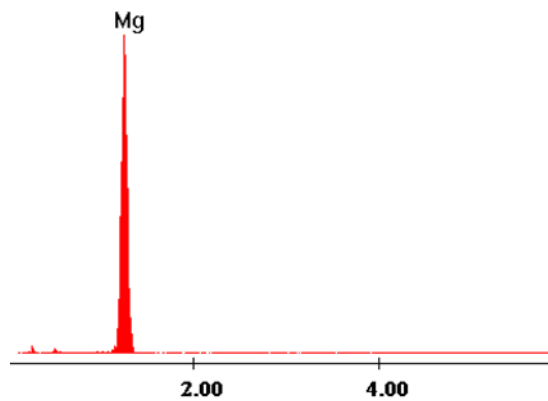


Fig 13 (b)

SEM images, Fig 13 (a) and EDAX Fig 13 (b) at room temperature

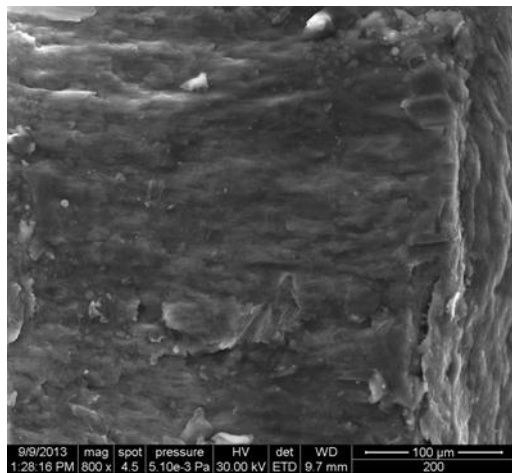


Fig 14 (a)

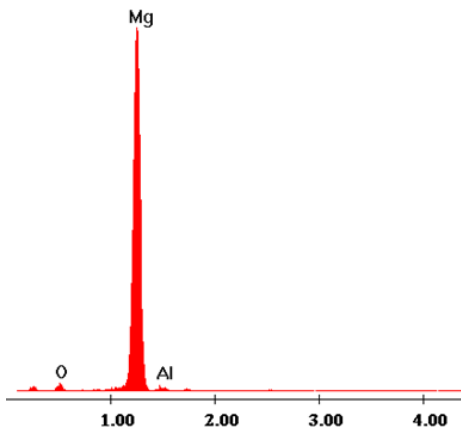


Fig 14 (b)

SEM images, Fig 14 (a) and EDAX Fig 14 (b) at a temperature of 200 °C

Where the sample was calcined at 550 °C, it is observed that the material's surface begins to form porous areas leading to the decomposition of material and its destruction. EDAX analysis is very interesting that in addition to magnesium and aluminum materials may appear Manganese and Silicon. They were detected in x-ray diffraction with less than 1%. This can be put in the account of the fact that silicon and manganese in

material composition, are amorphous and therefore could not be identified very well by x-ray diffraction.

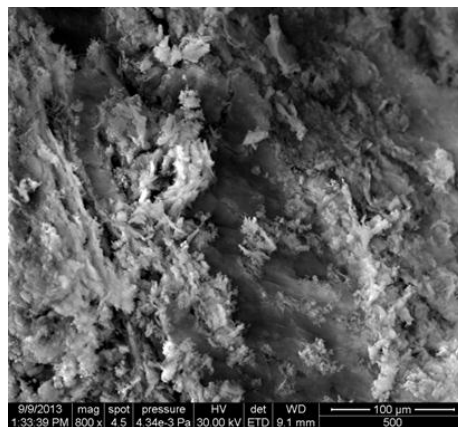


Fig 15 (a)

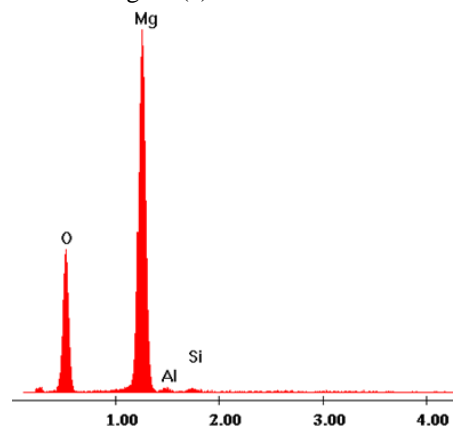


Fig 15 (b)

SEM images, Fig 15 (a) and EDAX, Fig 15 (b) at a temperature of 500 °C

In image analysis can be seen as a homogeneous surface without any defects.

As a result of making qualitative and quantitative analysis of the material of the housing it is noted that this is an Al-Mg alloy that owns Mg in greater proportion of 90%, is observed at the same time a homogeneous structure in the entire housing and the maintenance of this structure and very high temperatures. From the chemical point of view, the casing can optimize by increasing aluminum composition the housing structure, which would result in improving the properties of casting, high corrosion resistance, the introduction of paramagnetic and improving properties of good thermal conductivity properties. If you increase the amount of Silicon improves corrosion resistance. A higher percentage of manganese it might get paramagnetic properties and abrasion resistance slightly higher.

IV. CONCLUSION

Conclusions can be drawn regarding the homogeneity of housing, proving that its structure retains the same chemical composition in all areas. At the same time highlights the characteristics of the material to extreme heating. As an

optimization matter , it is recommended to improve the heat exchange in the high temperature zone by increasing the surface cooling ribs. For a high quality casting conditions and to improve the corrosion resistance it is recommended to possible change the chemical composition of the housing of the automatic gearbox.

REFERENCES

- [1] Argeşanu V., Kulcsar R.,Borozan I., „Automotive mechanical face seal – Tribological Simulation”, Journal of the Balkan Tribological Association 2011, pp 1-12, Vol. 17, No. 1, ISSN 1310-4772, Indexată ISI Thompson Scientific, Factor de impact= 1.104.
- [2] Borozan I., Argeşanu V., Maniu I., Kulcsar R., „The energetic balance of the friction clutches used in automotive”, Recent Researches in Automatic Control, 13th WSEAS International Conference on Automatic, Control, Modelling & Simulation (ACMOS'11), Lanzarote, Canary Islands, Spain, May 27 – 29.2011, ISBN: 978-1-61804-004-6, pp.: 252-256.
- [3] Brown R.E., Future of Magnesium Developments in 21st Century, in: Presentation at Materials Science & Technology Conference, Pittsburgh, PA, USA, October 5e9, 2008.
- [4] Brown Z., A.A. Luo, K. Sadayappan, L.J. Ouimet, J. Zindel, R. Beals, M. Musser, Development of Super Vacuum Die Casting Process for Magnesium Alloys. North American Die Casting Association Transactions, T09-043 (2009).
- [5] DasGupta R., P. Burton, Z. Brown, Microstructure and Mechanical Properties of Squeeze Cast AZ91D Magnesium Alloy. SAE Technical Paper 2005-01-0330, SAE, Warrendale, PA, 2005.
- [6] Greiner J., C. Doerr, H. Nauerz, M. Graeve, The New ‘7G-TRONIC’ of Mercedes-Benz: Innovative Transmission Technology for Better Driving Performance, Comfort, and Fuel Economy. SAE Technical Paper No. 2004-01-0649, SAE International, Warrendale, PA, USA, 2004.
- [7] Luo A. A., P.H. Fu, Y.D. Yu, H.Y. Jiang, L.M. Peng, C.Q. Zhai, A.K. Sachdev, Vacuum-assisted High Pressure Die Casting of AZ91 Magnesium Alloy. North American Die Casting Association Transactions, T08-083 (2008).
- [8] Şerban V.A. „Elemente de Ştiinţa şi Ingineria Materialelor” Editura Politehnica, Timişoara, 1998.
- [9] Şerban V.A. „Elemente de Ştiinţa şi Ingineria Materialelor” Editura Politehnica, Timişoara, 1998.
- [10] *** International Magnesium Association, Magnesium’s Tough Strength Endures Abuse to Protect Portable Electronic Devices, International Magnesium Association, Wauconda, IL, USA, 2008.
- [11] *** International Magnesium Association, Lighter Magnesium Improves Power Tool Performance, International Magnesium Association, Wauconda,IL, USA, 2008.

Managing Value Chain Relationships in Cross-Level Organizations—Compare Cellar-phone Manufacturing and Sport Shoemaking Supply Chain

Chang Jang-Li¹, Lin Yu-Chuan²

¹ Department of Business Management, National Sun Yat-sen University, Taiwan.

² Department of Business Management, National Kaohsiung Normal University, Taiwan

Abstract—Traditional organizational value-chain relationship research focuses on the dyadic, static and unidirectional organizational relationship. The dynamics of cross-level organizational value-chain governance and cooperative and competitive relationships, now a characteristic of supply relationships, are not well understood. Drawing on depth analysis of two different and significant cases we present a model explaining how relationships form and dissipate according to the relational benefits they bring to the downstream brand.

Keywords—value chain relationships in cross-level organizations, competitive and cooperative relationship, smart phone industry, sport shoemaking industry.

I. INTRODUCTION

Value chain relationship management studies that explored the interdependence of upstream and downstream components have identified resource and information sharing hierarchies between components and developed a systemized method for understanding and analyzing this information. The current research had focused on the series of “buyer-seller” relationship as figure 1, that there are the dyadic, unidirectional, and static limited relationships in the vertical value-chain. Recent studies on value chain management in organizations focused on upstream and downstream components in the same level and seldom addressed the uncertainties that influence transactions between cross-level organizations[1]. These studies emphasized the binary relationship between upstream and downstream components. However, few studies on value chain relationship management in organizations have addressed cross-level organizational value chains, such as interactions between downstream brands and key upstream component suppliers that do not involve manufacturers. To maintain the competitive edge, brands forego organizational manufacturers and establish direct interactions with suppliers that have the key resources essential to keep the brands’ survival. In other words, a cross-level organizational relationship exists between

downstream brands and upstream component suppliers in addition to the vertical value chain relationship formed by suppliers, manufacturers, and brands (as Fig. 2).

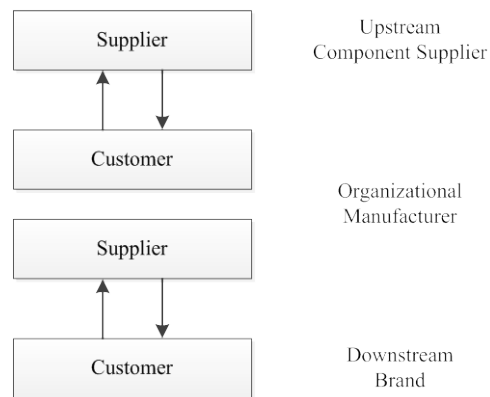


Fig. 1 Traditional value chain relationship

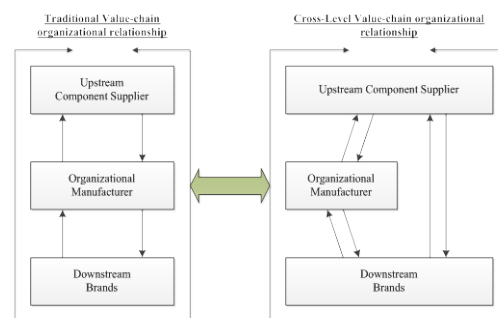


Fig. 2 Cross-level value chain relationship

This study addresses the following issues from two perspectives to address the deficiencies of previous research:

- 1) Following the resource dependent perspective, the downstream brands would forego the organizational manufacturer to build the cross-level relationship with the upstream supplier with critical resource to keep the brands proper, meanwhile that the traditional value would still

exist to keep survival. This research hopes to examine the value-chain relationship governance among the supplier, manufacture and brand when the conventional and cross-level value-chain relationship has been existed simultaneously.

- 2) When downstream brands forgo organizational manufacturers and establish a direct cross-level organizational relationship with upstream component suppliers, organizational manufacturers and upstream supplier would keep the competitive and cooperative relationship to service the downstream brands. The organizational manufactures achieve organizational learning outcomes through the exchange of resources and information. When organizational manufacturers provide more valuable key resources than upstream suppliers to downstream brands, brands sever their cross-level organizational relationships with upstream component suppliers and restore traditional organizational relationships among upstream component suppliers, organizational manufacturers, and downstream brands. This study would use the dynamic competitive and cooperative perspective to thoroughly examine the dynamically competitive and cooperative relationships and cross-level value chain relationship management methods between organizational manufactures upstream component suppliers, when engaging in direct resource transactions.

This study would use the embedding case study method to research the cross-level value-chain relationship governance and competition and cooperation through two different manufacturing supply chain, the cellar-phone manufacturing and sport-shoemaking supplier chain, to review its upstream supplier, organizational manufacture, and downstream brands different embedding units of each manufacturing supplier chain. Hope to use these two different manufacturing fields, it could increase the validity of this study and the finding and result hope to cover the current value-chain research gap.

II. LITERATURE REVIEW

Structural analysis of the interaction and cooperation between organizations can be classified as value chain relationships and network relationship analysis. Network relationship analysis provides several methods of understanding limitations in organizational structure and interactions between organizations to form cross-organization relationships and alliances [2], [3], [4], [5]. Unlike value chain relationship analysis, which emphasizes the interaction of value chains during vertical integration, network relationship analysis emphasizes the horizontal relationship between organizations, especially those in the same industry or community [7]. Granovetter applied a phase embedded concept to explain how societal relationships influence the transactional economic behaviors supported by the system [6]. The concept of value chains can be considered a series of interconnected relationships between component suppliers and brands. Therefore, value chains can be defined as a series of continuous

value relationships generated through sequential, vertical organizational transactions. Analysis of value chain relationships focuses primarily on a systemized understanding of resource allocation and information exchanges between organizations in continuous production activities based on vertical organizational interdependence.

Previous studies on managing value chain relationships in organizations focused on dyadic relationships between vertical organizations, such as between brands and manufacturers and between purchasing and sales. These dyadic relationships are unidirectional. However, research on the interaction between upstream component suppliers, organizational manufacturers, and downstream brands is limited, and even fewer studies examine cross-level organizational value chains. Furthermore, past studies of organizational value relationship management focused more on managing the relationship between brands and manufacturers. Moreover, past analyses of vertical value chain relationships examined the static relationship between brands and manufacturers. There are three main limitations or gaps, dyadic, unidirectional and static relationship, exist in past research on organizational relationships, meanwhile that less attention was provided to cross-level relationship between downstream brands and upstream suppliers also and organizational value chain relationship governance among suppliers, manufacturers, and brands. In this study, we also attempt to identify the dynamically competitive and cooperative relationships between upstream supplier and organizational manufacturers when the cross-level value-chain relationship has been built and organizes the values and key resources provided by the changing environment and time. These dynamic relationship changes would influence the cross-level organizational relationships between downstream brands and upstream suppliers, and change in the vertical organizational relationship formed by upstream brands, organizational manufacturers, and downstream suppliers. One purpose of this study is to design a research model for defining and addressing the three research gaps identified previously.

III. BUILDING A RESEARCH

To facilitate analysis, we investigated the value chain partnership among downstream brand, organizational manufacturer, and upstream component supplier. Figure 3 shows the conventional relationship of the three organizations. When a downstream brand monopolizes a end-user brand market, it can provide an assembly factory steady and sizable orders, as shown in Fig. 3-a. The assembly factory procures all the spare parts, assembles the parts into a finished product, and delivers the products to a designated point. This is the transaction between downstream brands and organizational manufacturers, as shown in Fig. 3-b. The relationship management model of conventional organizational value chains that involve binary bidirectional interaction between manufacturers and brands is shown in Fig. 3-c, where upstream component suppliers provide spare parts to organizational manufacturers, and Fig. 3-d, where organizational

manufacturers deliver finished products to brands.

An organization must obtain resources from the environment and subsist and interact with its surroundings to survive [18]. When an important spare part is a key resource (e.g., production limits, price, or technology) for a product sold by a downstream brand, which cannot obtain the key resource through an organizational manufacturer, the downstream brand should forgo the organizational manufacture to build the cross-level relationship with a key upstream component supplier to fulfill the order. In this case, the resources provided by upstream suppliers to downstream brand is more beneficial for maintaining the survival of upstream component suppliers compared to resources of organizational manufacturers. When upstream component suppliers cooperate with downstream brands, they establish the cross level relationships where they coordinate to assist downstream brands in obtaining key resources. As shown in Fig. 4-e, downstream brands built a cross-level organizational relationship management model with important component suppliers. The conventional system involving upstream component suppliers, organizational manufacturers, and downstream brands was founded on the relationship between upstream component suppliers and organizational manufacturers. Simultaneously, alternative organizational value chain relationship management methods exist for downstream brands and upstream component suppliers, as shown in Fig. 4-g and 4-h. The same is also true for upstream component suppliers. Upstream component suppliers forego organizational manufacturers to initiate cross-level organizational value chain business relationships with downstream brands. Meanwhile, upstream component suppliers maintain a value chain relationship with organizational manufacturers and downstream brands, as shown in Fig. 4-f, 4-i, and 4-j. The following hypothetical model was created from the description:

P1: A cross-level organizational relationship merges when the upstream component supplier gives the downstream brand more efficient access to key resources than the organizational manufacturer.

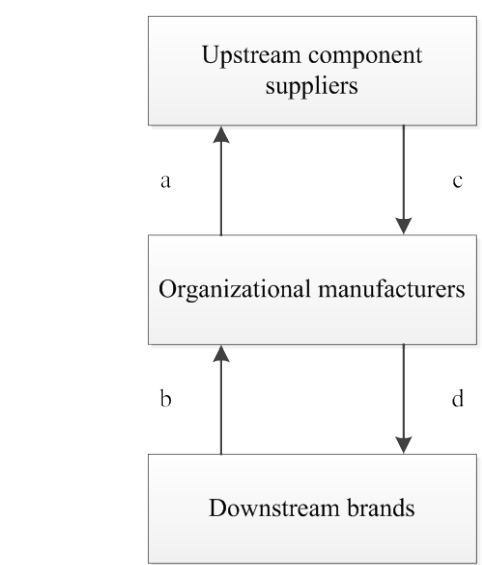


Fig. 3 Conventional value chain relationship management model

Upstream suppliers have two catalogs, one is that upstream supplier does compete with organizational manufacture if they have the similar product line and the other one is that they don't compete in the product line. Organizational manufacture and upstream supplier would have the same downstream customer to serve when the cross-level value-chain relationships have been established. In order to meet the same customer requirement and satisfaction, the organizational manufacture and upstream supplier should cooperate to achieve the downstream brands' goal and requirement. It is the same result, action and reaction if organizational manufacture and upstream supplier are the competitor in the product line or not. This cooperation would continue keeping if the downstream brands still keep the cross-level relationship. Therefore, the relational value-chain relationship governance would be the relational type among upstream supplier, organizational manufacture, and downstream brand, because they have to achieve the same goal .

P2: The value chain relationship governance type would be the relational type among the upstream supplier, organizational manufacture and downstream brand when the cross-level organizational relationship has been established and they need to achieve the same goal.

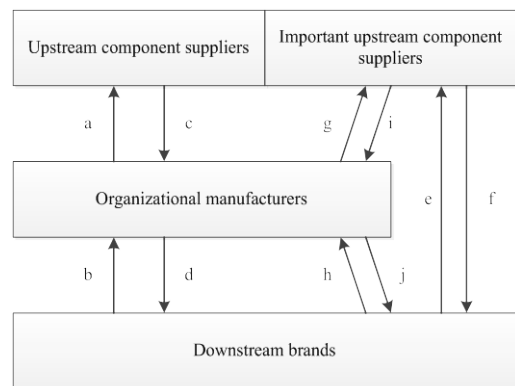


Fig. 4 Sample cross-level organizational value chain management model

In order to seek the competitive advantage, the firm would continue seeking the action and reaction to the competitive during in the field, that it is very important study to review and understand competitive action and reaction [2], [21], [22]. When upstream component suppliers possess resources that are crucial to the survival of downstream brands then upstream component suppliers establish cross-level relationships with downstream brands. During this time organizational manufacturers, in the context of a traditional value chain relationship, interact and learn from both the upstream component suppliers and also the downstream brand. This allows them to identify the skills and competitive advantages of upstream component suppliers and so increase their own key internal resources. By these means the organizational manufacturers re-establishes the ability to efficiently provide valuable and competitive key resources. The benefit of the cross-level interaction decreases and the brand reverts to the conventional network or relational vertical value chain relationship model (see Figure 5).

P3: If the organizational manufacturer capability improves over time to the point where they provide more efficient access to key resource then the downstream brand will reinstate a traditional value-chain relationship.

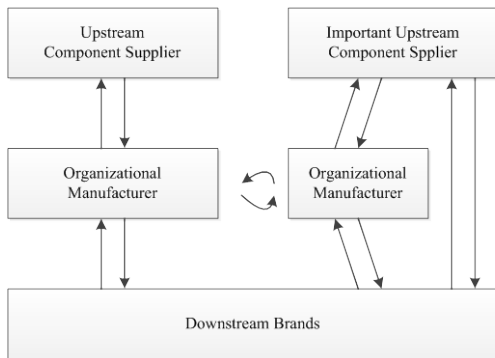


Fig. 5 Conventional and Cross-level value chain relationship management model

IV. RESEARCH METHODS

Because the purpose of this study is to define cross-level interactions and dynamic involvement between integrative vertical value chains and identify the changes that occur, the research is better conducted as a case study [19]. The cross-level value-chain organizations would include three levels, upstream suppliers, organizational manufacturing, and downstream brands in the same vertical value-chain as the different units in the same case. So, we plan to use the embedded multi units and multi case studying method to perform this research.

During the first case study, this study is housed in the cellar-phone manufacturing supplier chain that includes the downstream famous cellar-phone brand client, its organizational assembly house and key upstream suppliers, which are investigated to determine the dynamic value chain management relationship and examine the model designed based on previous studies. For the second case study, the

relationship among a sport shoemaking manufacturer and its famous sport shoe brand client and upstream key supplier is examined. The same method of investigation used for the first case study is employed for the second to verify the theoretical model. Thus, this research project employs an embedded multi-case study approach to derive a conclusion.

In each case interviews were conducted with brand company's supplier management executive and manager, assembly and manufacturing operation executive and supplier manager, and key company agency sales executive form three different perspective viewpoint , cross-level relationship , supplier chain governance and dynamic cooperative and competitive in every supply-chain. (as Fig 6). Collecting data from multiple sources is integral to the case study method. Supporting data was collected from multiple secondary sources including annual reports, newspaper and magazine articles and internal company reports.

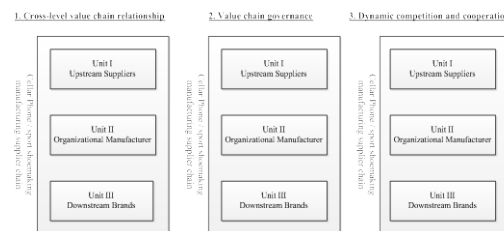


Fig. 6 Research perspectives for cross-level value-chain relationship

V. EXPECTING RESULT

The cross-level organizational value-chain relationship had been implemented on the practically vertical integrated operation for couples of years. But there are few studies and theoretic intents to explain and confirm this practical gap. This study tries to deploy the model to build up the theoretical intents to explain this cross-level interact and organizational value-chain relationship governance and dynamic competitive and cooperative relationship, meanwhile that this study uses the embedded analysis case research method to examine this theoretical model into cellar-phone and sport shoemaking manufacturing supply chain fields. Hope this model that the cross-level interact and organizational vale-chain relation is characteristic of triadic, dynamical competitive and multi-directional intent to cover the research gap of traditional organizational vale-chain relationship governance, that it is characteristic of binary, static, and unidirectional intent.

REFERENCES

- [1] Wathne, Kenneth H. and Jan B. Heide, "Opportunism in Interfirm Relationships: Forms, Outcomes, and Solutions," *Journal of Marketing*, 64(October), pp. 36-51, 2000.
- [2] Granoverter, M., "The strength of weak ties," *American Journal of Sociology*, vol. 78, pp. 1360-80, 1973.
- [3] Burt, R, *Structure Holes*. Cambridge: Harvard University Press, 1992.
- [4] Nohria, N and R. G. Eccles, "Introduction: is a network perspective a useful way to studying organizations?" *Networks and Organizations*, Boston, Harvard University Press, pp. 1-22, 1992.
- [5] Wasserman, S. and K. Faust, *Social Network analysis*. Cambridge: Cambridge University Press, 1994.

- [6] Granovetter, M., "Economic action and social structure: the problem of embeddedness," *American Journal of Sociology*, vol. 91, pp. 481-510, 1995.
- [7] Powell, W. W., "Neither market nor hierarchy: Network forms of organization," *Research in Organizational Behavior*, vol. 12, pp. 295-336, 1990.
- [8] Eisenhardt, Kathleen M., "Control: Organizational and Economic Approaches," *Management Science*, vol. 31, no. 2, pp. 134-49, 1985.
- [9] Heide, Jan B., "Interorganizational Governance in Marketing Channels," *Journal of Marketing*, Vol.58, pp. 71-85, Jan. 1994.
- [10] Ouchi, William G., "A Conceptual Framework for the Design of Organizational Control Mechanism," *Management Science*, vol. 25, no. 9, pp. 833-48, 1979.
- [11] Ouchi, William G., "Markets, Bureaucracies, and Clans," *Administrative Science Quarterly*, vol. 25, n0. 1, pp. 129-41, 1980.
- [12] Williamson, Oliver E., "Credible Commitments: Using Hostages to Support Exchange," *American Economic Review*, vol. 73, pp. 519-40, Sep. 1983.
- [13] MacCaulay, S., "Non-contractual relations in business: A Preliminary study," *American Sociological Review*, vol. 28, no. 1, pp. 55-67, 1963.
- [14] Sako, M., "Supplier development at Honda, Nissan and Toyota: Comparative case studies of organizational capability enhancement," *Industrial and Corporate Change*, vol. 13, no. 2, pp. 281-308, 2004.
- [15] Ritter, T., "A framework for analyzing relationship governance," *Journal of Business & Industrial Marketing*, vol. 22, no. 3, pp. 196-201, 2007.
- [16] Dyer, J. H. and Hatch, N. W., "Using supplier networks to learn faster," *Sloan Management Review*, vol. 45, no. 3, pp.57-63, 2004.
- [17] Swedberg, R., "Markets as Social Structures," In N. J. Smelser & R. Swedberg (Ed.), *Handbook of Economic Sociology*, Princeton University Press, pp. 255-284, 1994.
- [18] Pfeffer J., & Salancik, G. R., *The external control of organizations: A resource dependence perspective*. New York: Harper and Row, 1978.
- [19] Yin, R. K., *Case Study Research: Design and Method*. CA: Sage Publications, 1994.
- [20] MacMillan, Ian C., Mary L. McCaffery and Gilles Van Wijk, "Competitor's responses to easily imitated new products: Exploring commercial banking product introductions," *Strategic Management Journal*, vol. 6, no. 1, pp. 75-86, 1985.
- [21] Smith, K. G., Grimm, C. M., Chen, & Gannon, M. J., "Predictors of response time to competitive strategic actions: Preliminary Theory and Evidence," *J. Business*, vol. 18, pp. 245-258, 1989.
- [22] Ken G. Smith, Curtis M. Grimm, Martin J. Gannon and Ming-Jer Chen, "Organizational Information Processing, Competitive Responses, and Performance in the U.S. Domestic Airline Industry," *The Academy of Management Journal*, vol. 34, no. 1, pp. 60-85, Mar. 1991.

Transformation of soil texture classifications by ensemble modeling

Milan Cisty, Greta Dolakova, Jana Skalova, Peter Minaric

Abstract—This study deals with a description of a soil texture system reclassification by the proposed model on a data set from Slovakia originally labeled by its national classification system. However, the authors of the paper suppose that the methodology proposed could be used more generally and that the information provided is also applicable when dealing with other soil texture classification systems and in other countries. Various theoretical parametric particle size distribution models used for this purpose frequently show different degrees of precision in different soils and under different environments. In this paper the authors are proposing ensemble model in which such particle size distribution models are used as ensemble members. An improvement in soil texture transformation precision from one system to another was proved, and it is documented in the paper that the ensemble model worked better than any of its constituents.

Keywords—soil texture, particle size distribution, ensemble model, random forests.

I. INTRODUCTION

GRAIN size is one of the fundamental physical properties of soil, which is closely related to the quality, quantity and spatial arrangement of soil particles. The classification of soils according to their texture is one of the basic methods used in soil taxonomy. The principle of this classification is to determine the ratio of individual fractions of different sizes.

Through a soil texture description, also known as a particle size distribution (PSD), it is possible to predict various important soil properties (e.g., saturated hydraulic conductivity, the soil water retention curve, available water capacity, thermal conductivity, etc.). So-called pedotransfer functions (PTFs) often serve for this purpose [1], [2], [3].

An example of existing tools that have been developed for the abovementioned tasks is the Rosetta model, which was designed for pedotransfer function evaluations and is based on neural networks [4]. This model works exclusively with the

USDA classification system, so if the available data are not classified in this system, it is often desirable to accomplish a reclassification. Also, in other tasks, it is often necessary to carry out the transformation of textural classifications when data from different sources should be merged and used together.

This present case study deals with a description of a texture system reclassification by the proposed model on a data set from Slovakia originally labeled by national classification system. However, the authors of the paper suppose that the methodology proposed could be used more generally and that the information provided is also applicable when dealing with other soil texture classification systems and in other countries.

Some researchers have already tried to fit the measured PSDs by various continuous parametric curves. When obtaining such a relationship, it is possible to obtain a granular fraction's percentage ratio in the sample under consideration for any size of the particle diameter, which means that it is possible to get the values necessary for accomplishing a translation from one texture classification system to another. To obtain these theoretical parametric PSD curves, several authors have described soil texture by various parametric models (e.g., [5] - [12]) and have conducted comparative studies on various PSD models in order to determine the best model for the soil groups selected for their studies.

The reported findings of the abovementioned works somewhat differ from each other, and there is no generally suitable PSD model available, because it is quite difficult to correctly select the most appropriate type of PSD parametric model and determine its parameters. In some of these models there are also various optional parameters, the selection of which is based on an intuitive know-how. If this is not accomplished correctly, the results of the computations may be biased. Because the transformation of a soil texture system is usually only a prerequisite for solving some subsequent task, this bias is propagated to the subsequent modelling or other work. Therefore, for the sake of achieving more general and precise outputs while developing a continuous description of a grading curve and/or solving tasks dealing with transformations between various soil texture systems, the authors of the present paper are proposing a hybrid approach, which has the potential for obtaining improved results. Although the authors continue recommending the use of the mentioned parametric PSD models in the proposed methodology, the final prediction is made by an ensemble

M. Cisty is with the Slovak University of Technology in Bratislava, Civil Engineering faculty, Radlinskeho 11, 813 65 Slovak Republic (corresponding author, phone: +42159274628; e-mail: milan.cisty@stuba.sk).

G. Dolakova is student of the Slovak University of Technology in Bratislava, Civil Engineering faculty, Radlinskeho 11, 813 65 Slovak Republic (e-mail: gdolakova@gmail.com).

J. Skalova is with the Slovak University of Technology in Bratislava, Civil Engineering faculty, Radlinskeho 11, 813 65 Slovak Republic (e-mail: jana.skalova@stuba.sk).

P. Minaric is with the Slovak University of Technology in Bratislava, Civil Engineering faculty, Radlinskeho 11, 813 65 Slovak Republic (e-mail: peter.minaric@stuba.sk).

learning algorithm based on regression trees, the so-called Random Forest algorithm [13], which is built on top of the outputs of such models, i.e., ensemble members.

II. MATERIALS AND METHODS

A. Classification systems used in this study

Among the various soil texture classification systems, the ones most used in the Slovak Republic are:

- *The Kopecky classification system.* The I. category contains particles (clay) with particle diameters smaller than 0.01 mm; the II. category (dust) is limited to an interval of 0.01 – 0.05 mm; the III. category (powder clay) is 0.05 – 0.1 mm, and the IV. category (sand) contains particles with sizes at intervals of 0.1 – 2.0 mm.
- *USDA classification system,* based on the classification of soils according to the percentage of clay (up to 0.002 mm), silt (0.002 to 0.05 mm) and sand (0.05 to 2 mm) particles. These three fractions are usually called “fine earth.” The upper limit of the average grain size of fine earth is set as 2 mm, which is accepted in most classification systems

A comparison of these two classification systems clearly shows various amounts of fractions in each of them and the discordant limits for each fraction. For example, the fraction of clay particles in the USDA classification system ranges up to a value of 0.002 mm, while the Kopecky classification sets this limit at 0.01 mm. While solving various tasks for which it is necessary to have pedological data in the USDA classification (e.g., the mentioned example with the application of the Rosetta model), datasets using the Kopecky classification system are not compatible, which can be a problem. As we have already mentioned, there are many different texture classification systems in the world, so similar situations could arise more often, and the methodology which the authors would like to propose in this paper may be generally useful.

B. Description of the data sets used

Two data sets were used in this paper:

1. Data A - data for which we have the whole texture curve (grading curve) from which it is possible to calculate the PSD values for both the Kopecky and USDA classifications
2. Data B – data with only texture grain intervals under the Kopecky classification available
3. Data C – a relatively large data set containing data with only the USDA classification available and no data on the water retention characteristics.

Data set A

The samples were taken from the Zahorska Lowland. The number of samples was 43; they were air-dried and sieved; textural and other analyses were performed. After these analyses were accomplished the data set contained the following parameters: four grain categories according to the Kopecky textural classification, reduced bulk density ρ_d , and the points of the drying branches of the water retention curve

(WRC) for the pressure head values of -2.5, -56, -209, -558, -976, -3060 and -15,300 cm. The last variables were estimated using overpressure equipment. Additionally, the samples also contained the volume of humus in the soil, the value of the saturated hydraulic conductivity K , and the geographic coordinates of the individual samples. Data set A was recently obtained, and for each sample a complete grading curve from which the readings of the percentages of the Kopecky and USDA classifications were made is also available. Since textural information for both classifications (Kopecky, USDA) is available in this data set, these data were used to create and verify a model that serves for converting the soil textural description from the Kopecky classification to the USDA classification system.

Data set B

This data set contains data obtained from a previous, which was conducted in the area of the Zahorska Lowland in Slovakia [14]. A total of 140 soil samples was taken from various localities in this area, but unfortunately the exact geographic location was not recorded when the samples were taken.

The soil samples were evaluated by similar laboratory methods as in the previous dataset. The points of the drying branches of the WRC for the pressure head values of -2.5, -56, -209, -558, -976, -3060 and -15,300 cm were estimated using the overpressure equipment. The dry bulk density, particle density, porosity and saturated hydraulic conductivity were measured on the soil samples as well.

As they were in a sufficiently large quantity these data, served for the derivation of the pedotransfer functions (PTFs) by the utilization of the data-driven model. Their textural description is only in the Kopecky classification.

Purpose of this work was to have the design data in the USDA classification as an input to the PTFs, so it was necessary to accomplish the transformation between the two PSD systems before the PTF specifications by the data-driven model. Pedotransfer functions derived in this way were planned to be used for a spatial evaluation of a so-called plant-available soil water range, which could be expressed as the difference between the field capacity and the wilting point. This spatial evaluation on the Zahorska Lowland would be carried out with a third and larger data set (suitable for spatial interpolation) that contains data with only the USDA classification available and no data on the water retention characteristics (that is why the pedotransfer function evaluated needs to have the USDA classification system as an input). By these last remarks the authors only want to demonstrate the purpose of the transformation of the data between the different classification systems in this particular task, although this analysis of the available soil water range is not included in the present article.

C. Particle size distribution models and their fitting

The nine models involved in this study were evaluated and compared in order to derive the particle-size distribution functions. The models were developed by utilizing an optimization procedure in order to choose the most suitable one. All the models are listed in Table I.

The models chosen are the Fredlund models with three and

other parts. One of the possible solutions of this problem is the application of the ensemble methodology, which uses the best features of various parametric models for achieving more general results from fitting the data to the actual values measured.

The goal of the ensemble methodology is to combine the outputs of several models in order to improve the

TABLE I. PSD MODELS USED IN THIS STUDY

Name	Model	Parameters
Fredlund (FR3)	$F(d) = \frac{1}{\ln \left[\exp(1) + \left(\frac{a}{d} \right)^b \right]} \left\{ 1 - \frac{\ln \left(1 + \frac{d_f}{d} \right)}{\ln \left(1 + \frac{d_f}{d_m} \right)} \right\}^{-\gamma}$	$a, b, c,$ $d_f=0.001\text{mm},$ $d_m=0.0001\text{mm}$
Fredlund (FR4)	$F(d) = \frac{1}{\ln \left[\exp(1) + \left(\frac{a}{d} \right)^b \right]} \left\{ 1 - \frac{\ln \left(1 + \frac{d_f}{d} \right)}{\ln \left(1 + \frac{d_f}{d_m} \right)} \right\}^{-\gamma}$	$a, b, c, d_f,$ $d_m=0.0001\text{mm}$
Weibull (WB3)	$F(d) = c + (1 - c) \{ 1 - \exp(-aD^b) \}$ where $D = (d - d_{\min}) / (d_{\max} - d_{\min})$	$a, b, c,$ $d_{\min}=0.002\text{mm}$ $d_{\max}=2\text{mm}$
Andersson (AND4)	$F(d) = a + \text{barctg} \left[c \log \left(\frac{d}{e} \right) \right]$	a, b, c, e
Van Genuchten (VG3)	$F(d) = \left[1 + \left(\frac{a}{d} \right)^b \right]^{-c}$, where b and c are independent to each other	a, b, c
Gompertz (GP2)	$F(d) = \exp(-\exp[-a(d-b)])$	a, b
Gompertz (GP4)	$F(d) = c + e \exp(-\exp[-a(d-b)])$	a, b, c, e
Logarithmic (LG)	$F(d) = a \ln d + b$	a, b
Exponential (EXP)	$F(d) = cd^{-b}$	c, b

four parameters (FR3, FR4), the Weibull model with three parameters (WB3), the Andersson model, which contains four parameters (AND4), the van Genuchten models with two and three parameters (VG2, VG3), the Gompertz models (GP2, GP4), exponential (EXP) and logarithmic (LG), which were previously applied in various works, e.g., in [15] or [16].

All the listed models were used for determining the PSD functions by the optimization using method proposed by Byrd [26] which allows box constraints, that is each variable can be given a lower and/or upper bound. The initial value must satisfy the constraints. This uses a limited-memory modification of the quasi-Newton method. The purpose of this optimization was to predict the points of the grain curve for each model as closely as possible to the observed data.

D. Description and tuning of the Random Forest model

The usual process for finding the “best” model for obtaining a proper theoretical parametric PSD curve is applying more methods, e.g. the models from Table I., comparing their results with the observed data, and finally choosing the best performing model. However, there is usually no best parametric model which is superior under all circumstances. Various parametric models frequently show different degrees of precision in different soils and under different environments, so the application of a single parametric model often leads to a functional relationship that could be more precise in one part of a texture domain, but less suitable in

generalizability / robustness that could be obtained from any of the constituent models. The nine parametric models described hereinbefore were used for obtaining the chosen parametric PSD curves in the present study. The outputs of these parametric models are inputs for the ensemble model, namely, a data-driven model based on the Random Forests algorithm. Details and a mathematically based explanation of this model could be found in [17].

1) Optimization of the model

Data-driven models must be optimized to obtain reliable results that are as precise as possible. The optimization of the model mainly means finding the optimal model parameters. A random Forest has three tunable parameters: *n_{tree}* (the number of trees to grow), *m_{try}* (the number of variables randomly sampled as candidates at each tree split), and *nodesize* (the minimum size of the terminal nodes), which has the main influence on the final precision of the model. As the means used for optimally setting these parameters, two concepts are applied in this work: grid search and repeated cross-validation.

The grid search is designed in the optimization process to choose the values for each parameter of the model from a grid of predefined values. The grid search involves running the model with the parameters actually chosen in the current iteration, in which the model tries to learn the dependencies between the inputs and outputs.

This precision is evaluated as an average value from more

runs of the so-called cross-validation process. The cross-validation is a type of validation process by which the proper parameters of a model are searched, and the performance of the model is evaluated. Different types of validations exist, and the so-called “repeated cross-validation” is used in the present paper [17].

The use of cross-validation in the optimization process improves the selection of the parameters in comparison with other methods (e.g., a method based on only a single division of the data into the training and validation groups). The resulting model is likely to be more general and stable because more data variations are introduced into the training (calibration) process. Moreover, it is a necessity for small amounts of training data, which is the usual case when required measurements are too expensive or demanding for manual labor.

This modelling concept involves two purposes in this study: 1) finding the best parameters of the Random Forest algorithm, and 2) estimating of the precision of the proposed model, which could be expected for future data.

III. RESULTS

A. Fitting of the parametric particle size distribution functions (PSD)

In previous works, while finding the percentages of unknown fractions in a soil sample, interpolation problems were mainly solved [17]. In this work it is necessary to solve the extrapolation problem on the left tail of a PSD distribution. Actually, while dealing with the transformation of a soil texture classification from the Kopecky system to the USDA classification, the fitting of the data to a theoretical PSD model is only necessary for the subsequent computation of just one point of the PSD, i.e., a soil particle diameter of 0.002 mm. Other USDA fractions could be derived from the Kopecky classification system by basic arithmetic operations.

The results of fitting various PSD functions to the soil texture data measured is evaluated by the statistical coefficients, which serve for an evaluation of the model's fitting, are available in Table II. The statistics used are mean error (ME), mean absolute error (MAE), mean squared error (MSE), root mean square error (RMSE), percent bias between simulated and observed values (PBIAS%) and the Pearson correlation coefficient (r).

As can be seen in Table II, some models are not suitable for extrapolation problems regarding PSD fitting, so they were excluded from the final modeling. By extrapolation, we mean a situation when it is necessary to predict the soil particle content below the minimum input limit. This inappropriateness for extrapolation is especially clear for the Weibull model. This is true not only in the case study presented, but also could be considered as a general result. Besides the empirical results, which were obtained by the computational experiment accomplished in this work and evaluated in Table II, an important issue for this model is that parameter d_{\min} should be set to represent the minimal diameters of the soil particles, which are assumed to be present in the sample. However, in the case of the left tail extrapolation, this is the unknown information which one is searching for, so it cannot be correctly set in advance. The second model which was excluded from the final modelling was the LG model, because negative values of the clay content were computed by this model for some samples. This means that the results of the eight models finally served as inputs to the ensemble modelling.

Fig. 1 shows an evaluation of the best models for various soils by their absolute errors. As can be seen, there is no single best model which could be preferred, either for a whole set of data samples or for samples of various soil types. Moreover, according to the statistical values in Table I, evaluations of the results by various statistical coefficients differ: e.g., the EXP is evaluated as the best model by the correlation coefficient (r), but the FR4 model is evaluated as the best model by the RMSE. Various goodness of fit statistics evaluate different aspects of fitting, e.g., the emphasis of one is more from a perspective of variances, and other statistics capture the bias better. An error due to bias is taken as the difference between the expected prediction of the model and the correct value which one is trying to predict. The error due to a variance is taken as the variability of a model's prediction for a given data point. E.g., although the best correlation coefficient is for the EXP model, its prediction has multiplicative errors, which are not evident if one is only using an evaluation by the correlation coefficient.

Typically, the goal is to find an optimal trade-off between the bias and variance. In this paper the authors propose a methodology inspired by the idea of ensemble learning, in which the Random Forests (RF) algorithm is built on the top of

TABLE II. GOODNESS OF FIT MEASURES FOR THE PSD MODELS

	AND4	EXP	FR3	FR4	GP2	GP4	LE	LG	VG2	VG3	WB3
ME	-0.023	0.044	-0.004	-0.0002	0.069	0.055	0.044	-0.064	-0.138	-0.043	-0.105
MAE	0.055	0.058	0.036	0.033	0.070	0.061	0.058	0.088	0.139	0.050	0.137
MSE	0.010	0.006	0.002	0.002	0.007	0.006	0.006	0.010	0.034	0.007	0.037
RMSE	0.100	0.076	0.047	0.042	0.081	0.074	0.076	0.099	0.185	0.081	0.192
PBIAS%	-12.8	24.2	-2.4	-0.1	38.0	30.2	24.2	-35.1	-75.7	-23.7	-57.9
r	0.790	0.967	0.907	0.926	0.966	0.944	0.967	0.964	0.261	0.784	-0.477

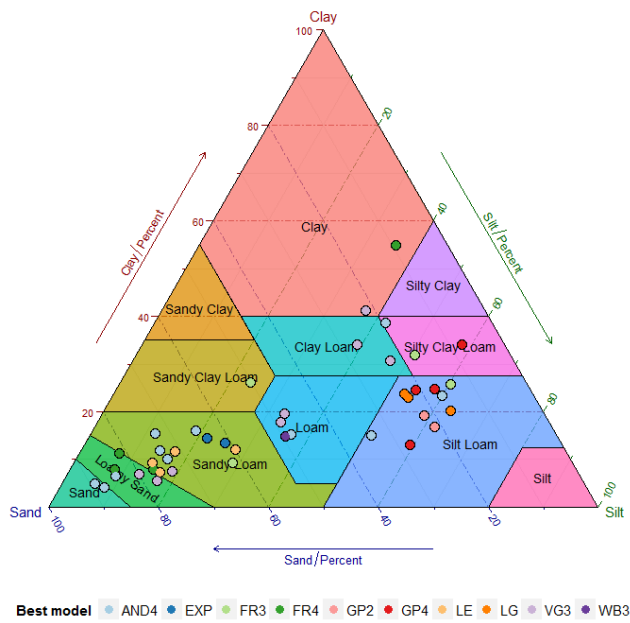


Fig. 1 Evaluation of the PSD fittings for various USDA soil types

the predictions computed by various parametric PSD models (they are inputs to the RF), and the optimal final result is obtained from this ensemble.

B. Fitting of the Random Forests algorithm

While producing the final model for fitting the PSD, there are two basic tasks which are necessary to deal with: 1) to find the optimal model (e.g., the optimal parameters of the RF algorithm which are suitable for the task to be solved) and 2) to evaluate the model’s expected performance. Predicted values of the USDA clay fractions from the nine PSD models derived from the data set A were applied as inputs for the model’s calibration or so-called training. This data set is used because in the training phase of data-driven modelling, it is necessary to know not only the input data (Kopecky grain fractions), but also the outputs measured (USDA clay fractions). The model developed can then serve for the computation of the unknown outputs for the other data sets under the condition that it has similar statistical properties (data set B in our case, where the USDA clay fraction is unknown).

The authors used the repeated cross-validation approach. This approach involves randomly dividing the set of observations into k groups, or folds, of approximately equal sizes. The first fold is treated as a validation set, and the method is fit on the remaining k-1 folds. Moreover, the partitioning of the dataset into folds is repeated n times, as described in the methodology section of this paper. Principally, through the know-how of the data mining community as expressed in various books and papers, (e.g., [17]), 5-fold cross-validation was used with two repetitions. The resulting Random Forests model is based on the best parameters obtained from the cross-validation evaluations. The expected precision of the model by some statistics is calculated by using the computed and observed data from the folds held

out in each iteration of the cross-validation. This procedure is repeated five times with two repetitions; each time, a different group of observations is treated as a validation set. This process results in k*n estimates of the test statistics. The cross-validation estimate of expected precision of the model is computed by averaging these values.

The fitted RF model has the following parameters: 500 trees, four variables randomly sampled as candidates at each tree split, and a minimum size of 5 for the terminal nodes. As has already been stated in the methodology part, the purpose of the cross-validation was not only to find these optimal parameters, but also to evaluate the precision of the proposed model, which could be expected for future data. This precision was evaluated on the test data from each cross-validation iteration as described hereinbefore. The precision by regression coefficient r was evaluated for the ensemble model of the soil texture transformation from the Kopecky to the USDA classification as 0.971 and the RMSE as 0.0343. When these values are compared with the results of the individual models from which the ensemble model consists (Table II.), it can be seen that no model achieved such precision, so the usefulness of the ensemble approach was verified in this study.

In the RF model its author also included the ability to measure the importance or influence of each variable in the model [13]. The importance of each member of the proposed ensemble model (e.g., the importance of parametric PSD models) is scaled from zero to 100 and displayed in Fig. 2. With this evaluation it is possible to see which model is more important and useful for the final prediction. The most important is the exponential model and the Gompertz model with two parameters. This result allows us to assume that in the context of ensemble modelling, the correlation coefficient is a more important for model selection than the other statistical measures which evaluate errors (such as MSE, RMSE, etc.), because these error coefficients are better, for instance, for both Fredlund models (see Table II.). This is true only in the context of ensemble modelling; otherwise the Fredlund models should be chosen (when one is deciding only between the individual models for the final modeling). It could be explained by the better ability of the ensemble to repair systematic errors (the bias of the model does not have such a

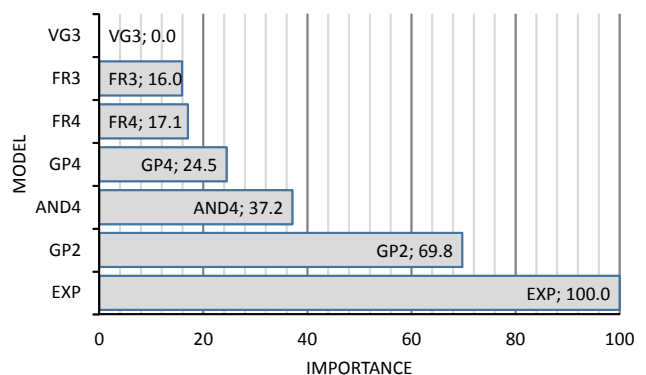


Fig. 2 Importance of individual PSD models in the final Random Forest ensemble

big influence on the correlation coefficient) than the individual inaccuracies. Surprisingly the not very precise Andersson model plays quite an important role in the final ensemble. This is due to the fact that the Andersson model has a small degree of correlation with both of the best models, so that means it is different. An efficient ensemble should be composed of predictors that are not only sufficiently accurate, but are also dissimilar, in the sense that the predictor errors occur in different regions of the input space [18]. Obviously, combining several identical models results in no gain in precision. From the evaluation in Fig. 2, it can be seen that the ensemble mechanism is also capable of excluding a model if it is redundant (the Van Genuchten model with 3 parameters in our case).

IV. CONCLUSION

In this work the authors deal with an investigation of the possible improvement of the grain curve transformation from one classification system to another, namely from the Kopecky texture system, which is used in Slovakia, to the more generally used USDA classification system. Because there are many different texture classification systems in the world by which existing data sets are labelled, similar situations where the necessity to convert data descriptions between various soil texture systems could arise more often and the methodology which the authors have proposed in this paper may be generally useful.

Because various parametric particle size distribution (PSD) models exist which could help with this task, the authors were trying to evaluate whether an ensemble paradigm could bring some improvement to the soil texture transformation task, when existing particle size distribution models are used as ensemble members. An improvement in precision was proved, and it is documented in the paper that the ensemble model worked better than any of its constituents.

ACKNOWLEDGMENT

This work was supported by the Slovak Research and Development Agency under Contract No. APVV-0139-10 and by the Scientific Grant Agency of the Ministry of Education of the Slovak Republic and the Slovak Academy of Sciences, Grant No. 1/1044/11.

REFERENCES

- [1] D. Hillel, *Fundamentals of soil physics*. New York: Academic, 1980.
- [2] Q. Wu, M. Borkovec, H. Sticher, "On particle-size distributions in soils," *Soil Science Society of America Journal*. vol. 57, pp. 883–890, 1993.
- [3] B. Minasny, A. E. Hartemink, "Predicting soil properties in the tropics," *Earth Sci Rev*. vol. 106, pp. 52–62, 2011.
- [4] M. G. Schaap, F. J. Leijl, "Database related accuracy and uncertainty of pedotransfer functions," *Soil Sci*. vol. 163, pp. 765-779, 1998.
- [5] R. Haverkamp and J. Y. Parlange, "Predicting the water-retention curve from particle-size distribution: 1. Sandy soils without organic matter," *Soil Sci*. vol. 142, no. 6, pp. 325-339, 1986.
- [6] K. R. J. Smettem and P.J. Gregory, "The relation between soil water retention and particle size distribution parameters for some predominantly sandy Western Australian soils," *Aust. J. Soil Res*. vol. 34, no. 5, pp. 695-708, 1996.
- [7] Wu, L., J.A. Vomocil, and S.W. Childs (1990), Pore size, particle size, aggregate size, and water retention, *Soil Sci. Soc. Am. J.* 54, 4, 952-956, DOI: 10.2136/sssaj1990.03615995005400040002x.
- [8] A. Kravchenko and R. Zhang, "Estimating the soil water retention from particle-size distributions: A fractal approach," *Soil Sci*. vol. 163, no. 3, pp. 171-179, 1998.
- [9] M. D. Fredlund, D. G. Fredlund and G. W. Wilson, "An equation to represent grain-size distribution," *Can. Geotech. J.* vol. 37, no. 4, pp. 817-827, 2000.
- [10] A. Nemes, J. H. M. Wosten, A. Lilly, J. H. O Voshaar, "Evaluation of different procedures to interpolate particle-size distributions to achieve compatibility within soil databases," *Geoderma*. vol. 90, pp. 187–202, 1999.
- [11] S. Hwang, "Effect of texture on the performance of soil particle-size distribution models," *Geoderma*. vol. 123, no. 3-4, pp. 363-371, 2004.
- [12] Y. D. Botula, W. M. Cornelis, G. Baert, P. Mafuka, E. Van Ranst, "Particle size distribution models for soils of the humid tropics," *J Soils Sediments*. vol. 13, pp. 686–698, 2013.
- [13] L. Breiman, "Random forests," *Machine learning*. vol. 45, no. 1, pp. 5-32, 2001.
- [14] J. Skalova, V. Stekauerova, *Pedotransfer functions and their application in modeling soil water regime*. Bratislava: STU in Bratislava, 2011, pp. 101.
- [15] Y. D. Botula, W. M. Cornelis, G. Baert, E. Van Ranst, "Evaluation of pedotransfer functions for predicting water retention of soils in Lower Congo (D.R. Congo)," *Agr Water Manage*. vol. 111, pp. 1–10, 2012.
- [16] P. Zhao, M. Shao, R. Horton, "Performance of Soil Particle-Size Distribution Models for Describing Deposited Soils Adjacent to Constructed Dams in the China Loess Plateau," *Acta Geophysica, Versita*. pp. 124-138, 2011.
- [17] M. Kuhn and K. Johnson, *Applied predictive modeling*. New York: Springer, 2013.
- [18] L. I. Kuncheva, C. J. Whitaker, "Measures of diversity in classifier ensembles and their relationship with the ensemble accuracy," *Machine Learning*. vol. 51, no. 2, pp. 181–207, 2003.

The altitude of the Pannonian Basin flat bottom where the city of Novi Sad is situated ranges from 76 m.a.s.l. to 82 m.a.s.l. The right Danube banks are at the altitude ranging from 77 m.a.s.l. to 180 m.a.s.l.

B. Climate

Novi Sad is located in the middle moderate climate zone. The average annual precipitation is cca 609 mm as measured at state weather station Rimski Šančevi.

C. The existing sewer system of Novi Sad

The sewer system within the area of Novi Sad is a general (combined) sewer system with the common wastewater (sanitary, industry) and stormwater drainage. The system has been designed to receive the rainfall runoff with the return periods of two and three years depending on the city area it serves. The system is divided in two subcatchments: the south city subcatchment and the north city subcatchment ending in main pump stations GC II and GC I, respectively.

The north city subcatchment encompasses the area of about 930 ha. The receiving water of the total flow rate is the Danube immediately downstream of the GC II. The south city subcatchment covers the area of about 1060 ha. The receiving water of the total flow rate is the Danube immediately downstream of the pump station GC I.

Stormwater and wastewater at the main pump stations GC I and GC II are discharged into the river by gravity at the Danube water level lower than +240 cm whereas the water is pumped into the Danube at the higher river levels. Figure 2 illustrates the existing sewer system in the city of Novi Sad where the force mains are shown in bold.

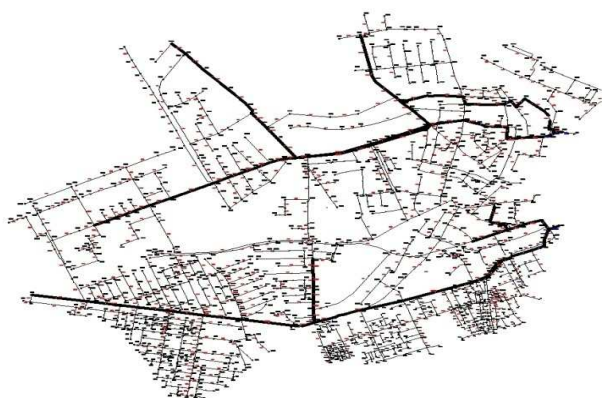


Figure 2. The sewer system in the city of Novi Sad (force mains in bold)

D. Application of EPA SWMM 5.0 in the hydraulic calculation

EPA stormwater management modelling (SWMM) is a dynamic model of the rainfall-runoff simulation for a single storm event or a long (continuous) wastewater quantity-quality simulation from urban areas in particular. The SWMM works based on the sum of drainage areas receiving rainfall and generating runoff carrying pollutants. In the part of SWMM regarding the hydraulic calculation the runoff is transported through a system of pipelines, conduits, retention/treatment facilities, pumps and control structures. The quantity and

quality of the wastewater from each drainage area as well as the flow, level and velocity of the wastewater and the water quality in each pipeline and conduit are monitored in SWMM during the simulation comprised of many time steps.

Hydrological features of the subcatchments studied are defined by the following set of input parameters in SWMM:

- 1) Area – the area enclosed within the subcatchment boundary;
- 2) Width – the surface flow which depends on the gutter inlets distribution. The mean spacing between the inlets represents the width and should not exceed 30 m;
- 3) Slope – the inclination of the drainage area and it is the same for pervious and impervious surfaces;
- 4) Imperviousness – the ratio of impervious surfaces on the catchment such as rooftops, roads with no infiltration;
- 5) Roughness coefficient – this represents the resistance or the friction applied to the surface flow. Since Manning's equation is used in SWMM this coefficient is the same as Manning's roughness coefficient n ;
- 6) Detention ponds – correspond to the capacity which has to be reached prior to the runoff occurrence.

Three different methods for the calculation of losses due to the infiltration on the catchment pervious areas are available in SWMM. They include the Horton, Green-Ampt and Curve Number models. The Horton model has long been applied in dynamic simulations. The Green-Ampt model is rather a physical model whereas the curve number (CN) model is used in simplified discharge models. The Horton model is used in the work.

The software enables the use of the hydraulic calculation under different flow conditions, unsteady flow in open channels and overloading in pipelines. It enables the application of different flow coefficients across the subcatchments and rainfall hyetographs for the subcatchment under consideration. Unsteady flow in open channels represents the flow where the water level and flow rate change in time, $Q = Q(x, t)$, $z = z(x, t)$. The flow in open channels is spatial, 3D, but one-dimensional analysis is used for practical reasons. The intersection mean velocity is used as a referential value instead of the velocity at each intersection point, the distribution of streamlines is quasi-parallel and the head distribution is hydrostatic. The Saint Venant equations describe the flow.

E. Setting of the impervious surfaces per the city areas

Imperviousness represents the ratio of the subcatchment covered with surfaces such as rooftops, roads, pavements or car parks from which stormwater is discharged into the sewer system. This is usually the most sensitive parameter in the hydrological description of a catchment. The ratio of impervious surface ranges from 5% with undeveloped land up to 95% with high density development. The ratio of impervious surfaces in Novi Sad has been calculated for each individual area of the city. The impervious surfaces have been calculated for the following areas of the city: Liman, Telep, Novo Naselje, Detelinara, Banatić, Podbara, Salajka, Centar and Grbavica. The percentage of impervious surfaces per the city areas is specified in Table 1. Rooftops, roads, pavements are defined as impervious surfaces whereas the remaining surfaces are green pervious surfaces from which no runoff

flows into the sewer system. The ratio of the impervious surface and the total area of a subcatchment is the runoff coefficient. In addition, the parks and cemeteries from which there is no runoff have been separated. This results in a more real model of impervious surfaces in the city.

Table 1. Percentage of impervious surfaces per the city areas[3]

City area	Percentage of impervious surfaces (%)
Banatic	30
Novo Naselje	35
Telep	30
Liman	30
Detelinara	31
Salajka	26
Podbara	39
Centar	60
Grbavica	50

Georeferential layouts – KAT-KOM layouts used to calculate the total impervious surfaces per the city areas were first put into AutoCAD which then generated the impervious and green surfaces. Figure 3 illustrates pervious and impervious surfaces in the Centre of Novi Sad with roofed surfaces in red, pavements in gray and green surfaces in green.

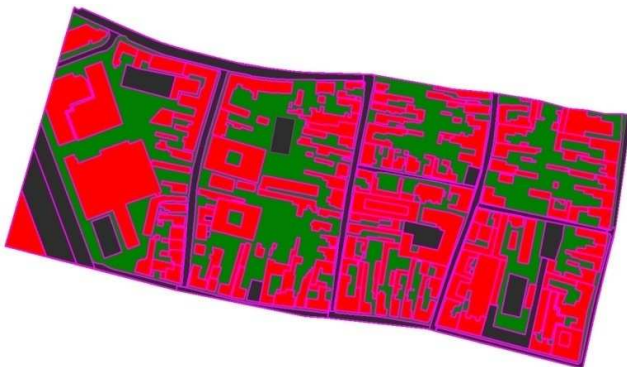


Figure 3. Impervious surfaces in the Centre of Novi Sad (the impervious surface of 60%)

The calculated mean (average) ratio of impervious surfaces for the entire Novi Sad catchment is 35%.

F. Determination of design storms

Stormwater drainage system is dimensioned according to the design storm. The statistic analysis of storms was made at the nearest weather station Rimski Šančevi (Figure 4) to determine design storms. The storm intensity on ITP curves represents average storm intensities in their duration.

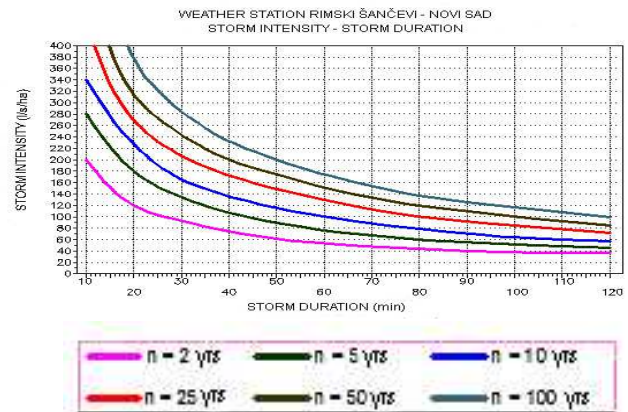


Figure 4. Storm intensity – storm duration – return period [1]

According to Serbian standard SRPS EN 752-4 regarding sewer systems outside buildings hydraulic calculation of the sewer system in the central urban areas is made such that the system overloading and pressurized flow in the pipelines are not allowed where the system is designed for the 5-year storm for the central urban area and the 3-year storm for residential areas. The sewer system is designed to receive runoff from storms with the return period of three and five years (Figure 5). The central city area is dimensioned for the 5-year storm whereas the residential areas (Telep, Novo Naselje, Detelinara) are dimensioned for the 3-year storm. This is the first hydraulic requirement [1].

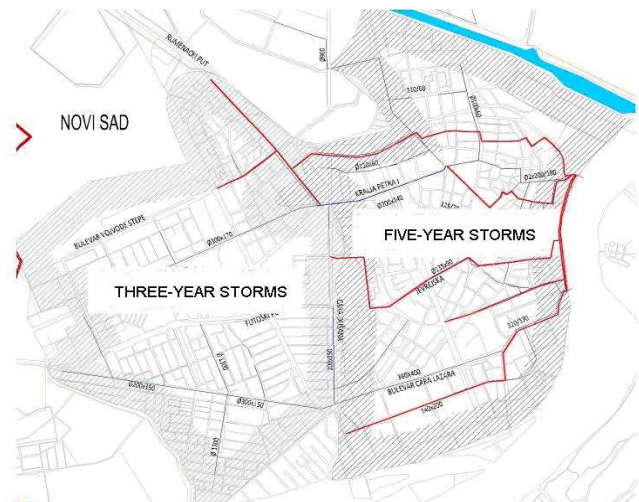


Figure 5. Three- and five-year storms design

G. Determination of the design stormwater runoff from non-public areas

Stormwater management from non-public areas is analyzed in this section and the design stormwater runoff recommended as a function of the subcatchment size. Non-public areas include the areas outside streets or boulevards that is, city block interior courtyards, single lots, trade and industrial facilities, public buildings (hospitals, military barracks, schools, universities, ...).

The average designed ratio of impervious surfaces for the entire city catchment is 35%. The sewer system has been

designed for the stormwater drainage from these surfaces. The construction of some large buildings such as shopping malls in certain city areas will significantly increase impervious surfaces. It is assumed that impervious surfaces will increase to 90% after the construction [2]. Maximum allowed runoff rates from these surfaces into the public sewer system of Novi Sad depend on the subcatchment size. Maximum runoff rates from the subcatchment of 1 ha into the sewer system are shown in Figure 6.

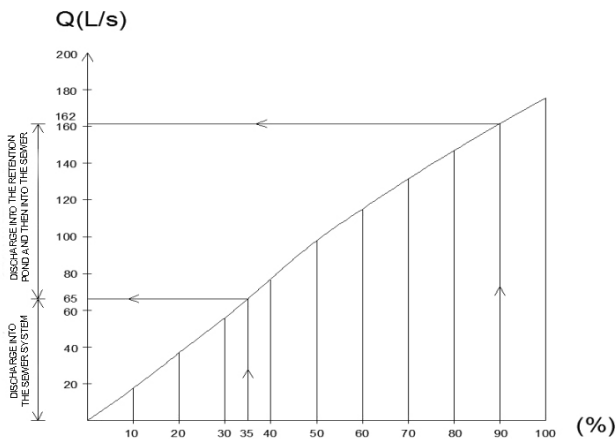


Figure 6. Runoff rates depending on the ratio of imperviousness for the area of 1 ha

It can be seen in Figure 6 that the maximum runoff rate with the imperviousness of 35% is 65 L/s. Maximum runoff rates with the imperviousness of 35% calculated for the subcatchments of 2 ha, 5 ha and 10 ha are 132 L/s, 256 L/s and 358 L/s, respectively.

The analysis of runoff from impervious areas of various sizes indicates that the runoff rates range from 36 L/s for the subcatchment of 10 ha to 65 L/s for the subcatchment of 1 ha. It is recommended for the allowed runoff rate – flow Q_{dir} discharged directly into the sewer system to range between 30 and 65 L/s/ha depending on the subcatchment size.

H. Analysis of the relevant water consumption

It is determined based on the document 'Demographic Development of the City of Novi Sad, Vojvodina Spatial Information Centre, Novi Sad, 2009' that 230 000 people live in the city area oriented to the GCI and GCII subcatchments [5]. In the city there are 20 000 students who live here but are not registered. Wastewater from the local communities of Futog and Veternik with the population of 42 000 is discharged into the sewer system of Novi Sad [5]. The total population on the city catchment is 290 000 [5]. It is estimated that 140 000 people live in the north city subcatchment based on the housing study made for the Novi Sad General Development Plan where the information on the population in the city areas is provided.

The average specific water consumption per capita of 250 L/per capita a day is determined based on the analysis of the public water supply consumption. This specific consumption also includes the average consumption in public buildings, sport facilities, restaurants, hotels, schools and commercial and

non-commercial usage. It can be taken based on the consumption structure that 90% of the total used water is discharged into the sewer system.

Thus the total daily mean wastewater discharge from homes and businesses to the city outfalls is 290 000 people x 250 L/per capita x 0.9 = 65250 m³/day.

The total daily mean discharge of wastewater from the north city subcatchment is 140 000 people x 250 L/per capita x 0.9 = 31500 m³/day.

The total length of the north city subcatchment drainage system is about 200 km. Provided the infiltration of 0.25 L/s/km² per sewer the total daily infiltration is 200 km x 0.25 L/s/km² = 50 L/s that is, 4320 m³/day.

The total calculated mean daily flow from the north city subcatchment is 31500 m³/day (households and industry + 4320 m³/day (infiltration) = 35820 m³/day i.e. 414 L/s.

The results of the wastewater discharge rate measurement in a single day at the GC II pump station outfall are shown in Figure 7. It can be concluded based on the measurements that the mean daily discharge rate from the north city subcatchment is 407 L/s.

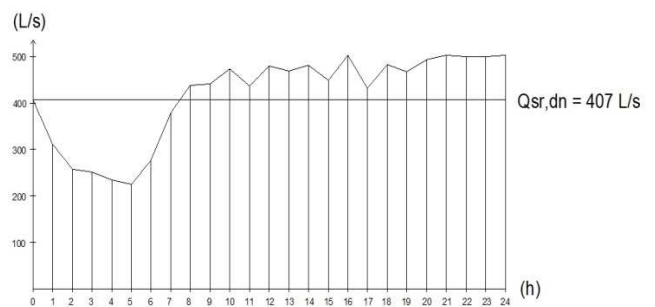


Figure 7. Pump station GC II daily discharge rate.

III. RESULTS AND DISCUSSION

A. Hydraulic calculation analysis by the existing model

The existing model includes the model of force mains of diameters larger than 600 mm. The area of Novi Sad under consideration encompasses the area of 1985 ha [6]. This area includes parks and cemeteries. The design ratio of impervious surface is 35%. The total length of the sewer system is 71.3 km. The model consists of 414 nodes and 418 sections (Figure 8). Manning's roughness coefficient of 0.014 m^{-1/3}/s is used in the calculation [2]. The hydraulic calculation with the software package EPA SWMM 5.0 for 3- and 5-year storms has shown neither manhole overflowing nor pressurized flow in the sewer system.

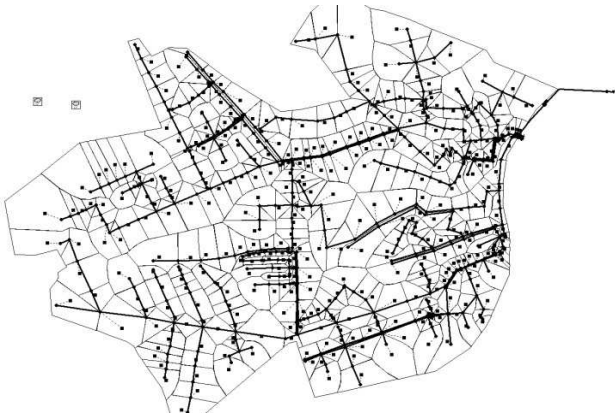


Figure 8. The existing Novi Sad sewer system model

Longitudinal profiles of the force mains in the north and south city subcatchments with maximum water elevation are shown in Figures 9 and 10, and it can be concluded that there is neither manhole overflowing nor pressurized flow in these mains. The force mains are filled up to 70% at maximum.

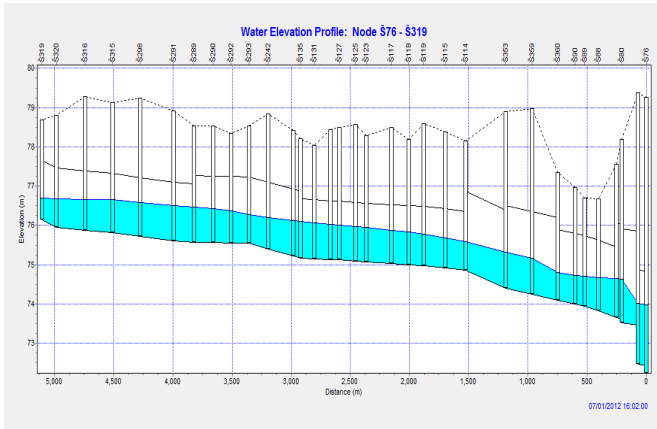


Figure 9. Longitudinal profile of the north city subcatchment force main with maximum water elevation

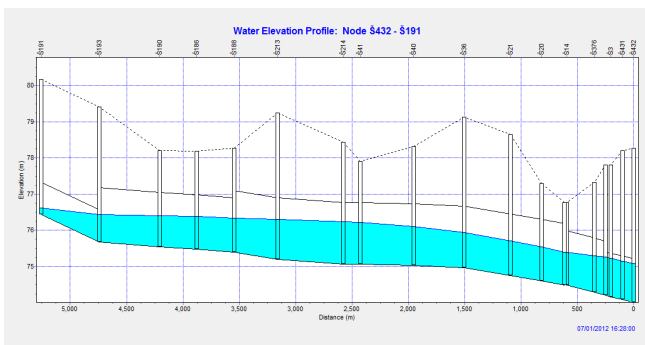


Figure 10. Longitudinal profile of the south city subcatchment force main with maximum water elevation

Inflow hydrographs at the main pump station GC II and GC I outfalls for 3- and 5-year storms are shown in Figures 11 and 12. The hydrographs indicate maximum discharge rate at the pump stations GC II and GC I of 7215 L/s and 6620 l/s, respectively.



Figure 11. Inflow hydrograph for the pump station GC II outfall for 3- and 5-year storms

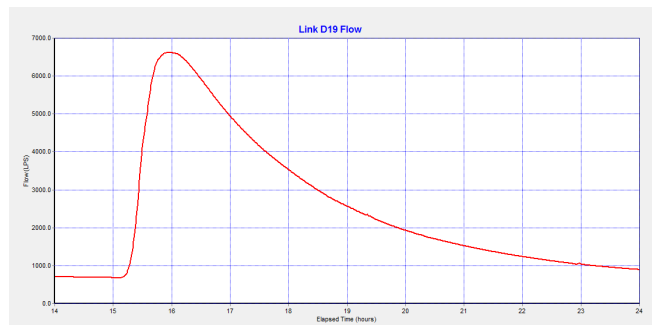


Figure 12. Inflow hydrograph for the pump station GC I outfall for 3- and 5-year storms

B. Analysis of the hydraulic calculation in the upgraded model of the sewer system for 3- and 5-year storms and the constant impervious ratio of 35%

The study catchment of Novi Sad including green surfaces (parks and cemeteries) encompasses the area of 1985 ha. The green areas cover 73 ha. The sewer system with added pipelines of diameters larger than 300 mm is simulated in the upgraded model. The model is more complex and it consists of 1323 nodes and 1325 sections. (Figure 13). There are 382 and 941 nodes in the north and south city subcatchments, respectively. The total length of the input sewer system is 155 km. Manning's roughness coefficient is set at 0.014 m^{-1/3}/s.

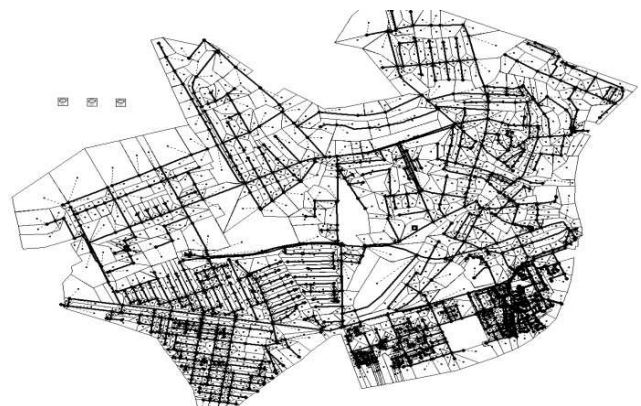


Figure 13. The upgraded model of Novi Sad sewer system

Longitudinal profiles of the force mains in the north and south city subcatchments with maximum water elevation are shown in Figures 14 and 15. It can be concluded that there is

neither manhole overflowing nor pressurized flow in these mains. The force mains are filled up to 80% at maximum.

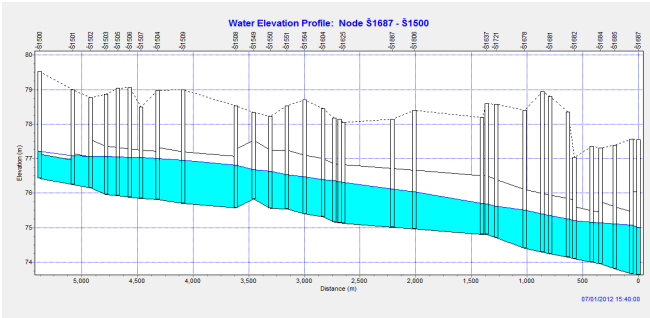


Figure 14. Longitudinal profile of the north city subcatchment force main with maximum water elevation

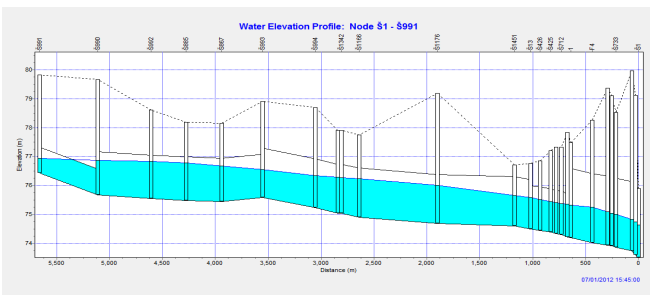


Figure 15. Longitudinal profile of the south city subcatchment force main with maximum water elevation

Inflow hydrographs at the main pump station GC II and GC I outfalls for 3- and 5-year storms are shown in Figures 16 and 17. The hydrographs indicate maximum discharge rates at the pump stations GC II and GC I of 8380 L/s and 7155 l/s, respectively.

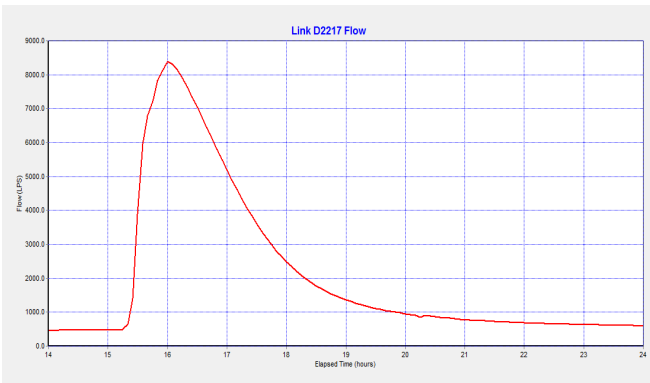


Figure 16. Inflow hydrograph for the pump station GC II outfall for 3- and 5-year storms

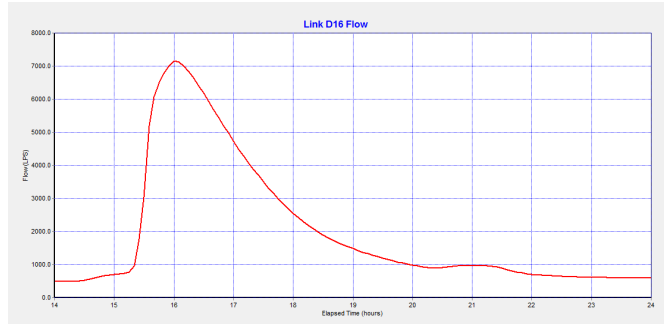


Figure 17. Inflow hydrograph for the pump station GC I outfall for 3- and 5-year storms

C. Analysis of the hydraulic calculation in the upgraded model for the imperviousness calculated per areas for 3- and 5-year storms

Longitudinal profiles of the force mains in the north and south city subcatchments with maximum water elevation are shown in Figures 18 and 19. It can be concluded that there is neither manhole overflowing nor pressurized flow in these mains. The force mains are filled up to 80% at maximum.

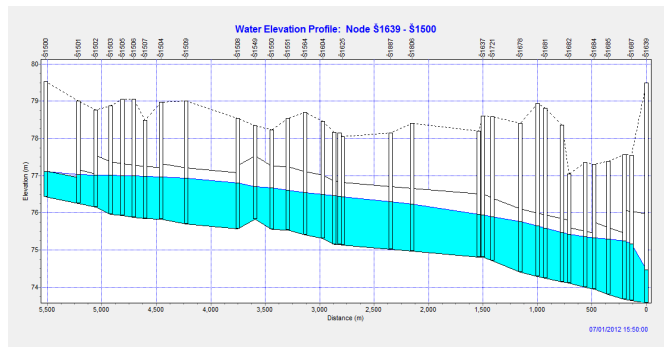


Figure 18. Longitudinal profile of the north city subcatchment force main with maximum water elevation

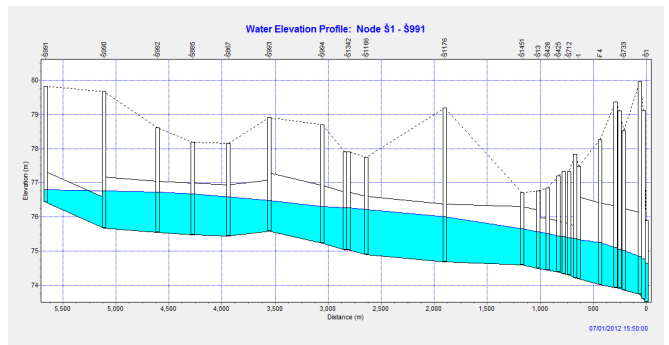


Figure 19. Longitudinal profile of the south city subcatchment force main with maximum water elevation

Inflow hydrographs at the main pump station GC II and GC I outfalls for 3- and 5-year storms are shown in Figures 20 and 21. Maximum discharge rates at the pump stations GC II and GC I are 9417 L/s and 7190 l/s, respectively.

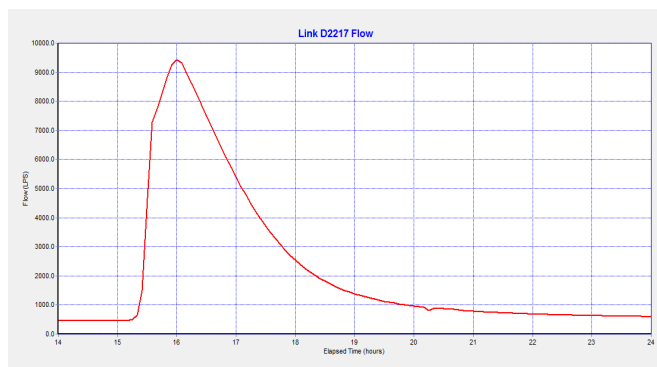


Figure 20. Inflow hydrograph for the pump station GC II outfall for 3- and 5-year storms

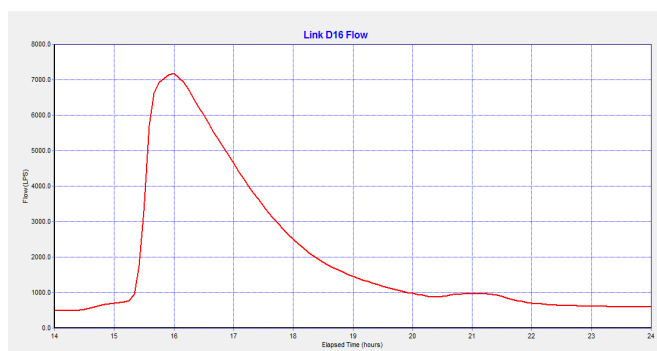


Figure 21. Inflow hydrograph for the pump station GC I outfall for 3- and 5-year storms

IV. CONCLUSION

The following can be concluded based on the analysis results and calculations:

1) The existing model has been hydraulically analyzed. There are 414 nodes (manholes) and 418 sections (sewers). The total length of the sewer system is about 71 km. The combined sewer system has been designed for 5- (the central city area) and 3-year (the residential area) storms. The impervious rate of 35% has been taken into account. The hydraulic calculation has indicated that there is no pressurized flow in the sewer system. The force mains are filled up to 70% at maximum. The sewer system can be considered well designed based on the results since the requirement for no manhole overflowing and pressurized flowing during 3- and 5-year storms has been met.

2) The upgraded sewer system model has been hydraulically calculated. The upgraded sewer system model provides a more real and complete understanding of the city sewer system. There are 1323 nodes and 1325 sections in the upgraded sewer system model. The total length of the sewer system is about 155 km. The system is designed for 3- and 5-year storms. The impervious ratio of 35% is taken into account. The upgraded model hydraulic analysis has shown neither manhole overflowing nor pressurized flowing. The force mains are filled up to 80% at maximum. It can be concluded that the system has been well designed. Runoff inflow hydrographs at the outfalls in the existing model and the upgraded model show different maximum discharge rates. In the existing model discharge rates at the outfalls are smaller but the discharge time is longer. This is due to the sparse existing network and

section connections to large drainage areas. Drainage areas in the upgraded model are smaller due to more sections and the water flows into the sewers faster than in the existing model. Maximum discharge rates at the outfalls are larger in the upgraded system. The total stormwater volume discharged in the upgraded model approximates that in the existing model.

3) The hydraulic simulation has been run for the case with the impervious ratio calculated for each city area instead of the impervious ratio of 35%. The average calculated imperviousness for the entire city is 35% but it varies across the city areas ranging from 23% in Salajka to 60% in the city centre. The hydraulic calculation has shown neither manhole overflowing nor pressurized flowing in the system. The mains are filled up to 80%. The system has been well designed. Maximum inflow rate at the pump station GC II is by cca 1000 L/s larger in the case with the calculated imperviousness than in the model with the imperviousness of 35% for the entire city area whereas it is approximately the same as that at the pump station GC I. The larger maximum inflow rate in the case with the calculated imperviousness is due to the fact that the part of the north city subcatchment is the city centre located downstream and 60% impervious, which is significantly more than the existing 35%. The south city subcatchment is about 35% impervious and the inflow rate at the pump station GC I is approximately the same.

ACKNOWLEDGMENT

This work is supported by Ministry of Education and Science, Republic of Serbia (Grant No. TR 37003, TR 37018).

REFERENCES

- [1] M. Stipic at all., 2011, *Novi Sad sewerage system development programme revision*, Novi Sad, Serbia
- [2] M. Stipic at all., 2012, *Redesign of the Existing Combined Sewer System (CSS) od Novi Sad*, 9th International Conference on Urban Drainage Modelling, Belgrade, Serbia
- [3] F. Stipic, *The analysis of stormwater runoff and overflow from the Novi Sad catchment-Master's Thesis*, Faculty of Technical Sciences, University of Novi Sad, Serbia, 2014.
- [4] Serbian standards SRPS EN 752-4:2007. Sewer systems beyond the objects-part 4: *Hydraulic calculation and aspects of the environmental protection*.
- [5] *Demographic development of Novi Sad*, Center for spatial planning of Vojvodina, Novi Sad, Serbia, 2009.
- [6] JP Zavod za urbanizam Novi Sad, *Study of hydrotechnical systems*, Novi Sad, Serbia, 2009.

Fate of metribuzin affected by de-oiled two phase olive mill waste amendment in an olive grove soil

D. Peña, A. López-Piñeiro, A. Albarrán, D. Becerra, J. Sánchez-Llerena, J. Rato-Nunes

Abstract—In order to investigate the impact of de-oiled two-phase olive mill waste (DW) amendments to soil on the sorption-desorption, degradation, and leaching of the herbicide metribuzin, field and laboratory experiments were conducted on a representative olive grove soil. The soil was amended in the laboratory with DW at the rates of 2.5%, 5% and 10%, and in the field with 27 and 54 Mg ha⁻¹ of DW for nine years. Significant increases in metribuzin sorption were observed in the laboratory and field-amended soils, mainly promoted by an increase in humic acid content. The addition of DW transformed naturally under field conditions decreased the half-lives of the metribuzin, ranging from 20.0 d for the unamended soil to 3.93 d at the greater application rate. In contrast, the application of fresh DW (in laboratory) increased the persistence of metribuzin until 45.0 d at the greater application rate, attributable mainly to the inhibitory effect of this amendment on microbial activity. Both amendments (fresh and field-aged DW) significantly reduced the amount of metribuzin leached. This study has shown that in olive grove soils DW amendment may be an effective management practice for controlling ground water contamination by metribuzin.

Keywords—Dehydrogenase activity, De-oiled two-phase olive mill waste, Leaching, Metribuzin.

I. INTRODUCTION

METRIBUZIN (4-amino-6-tert-butyl-3-methylthio-1,2,4-triazin-5-one), is a triazine herbicide applied in pre-emergence and post-emergence on intensive vegetable crops, including potatoes, tomatoes and wheat. Its herbicide efficiency and its relatively low toxicity are such that it is widely used around the world [1], however metribuzin has

D. Peña is with Área de Edafología y Química Agrícola, Facultad de Ciencias, Universidad de Extremadura, Avda de Elvas s/n, 06071, Badajoz, Spain (corresponding author to provide phone: +34924289355; dpenaaba@alumnos.unex.es).

A. López-Piñeiro is with Área de Edafología y Química Agrícola, Facultad de Ciencias, Universidad de Extremadura, Avda de Elvas s/n, 06071, Badajoz, Spain (pineiro@unex.es).

A. Albarrán is with Área de Producción Vegetal, Escuela de Ingenierías Agrarias, Universidad de Extremadura, Ctra. de Cáceres s/n, 06071, Badajoz, Spain (angliso@unex.es).

D. Becerra is with Área de Producción Vegetal, Escuela de Ingenierías Agrarias, Universidad de Extremadura, Ctra. de Cáceres s/n, 06071, Badajoz, Spain (dbecerra@alumnos.unex.es).

J. Sánchez-Llerena is with Área de Edafología y Química Agrícola, Facultad de Ciencias, Universidad de Extremadura, Avda de Elvas s/n, 06071, Badajoz, Spain (jsanchezllerena@gmail.com).

J.M. Rato-Nunes is with C3I, Polytechnic Institute of Portalegre, Portugal (ratonunes@esaelvas.pt).

been detected in ground and surface waters [1]-[3]. It is therefore necessary to develop effective management practices to control water contamination by metribuzin.

Agronomic practices as addition of organic amendments could be involved in the pesticide transfer to sources of water [4]. Usually, with increase in the total organic carbon (TOC) the sorption of herbicides on soil particles increases, and thus their mobility in the soil profile could be decreased [5], [6]. Alternatives, such as animal manure or green covers, are usually expensive or impractical, therefore the application of different residues rich in organic matter to agricultural soils is becoming increasingly advised [7].

Actually, the most usually used procedure in olive oil extraction is a continuous centrifuge two-phases process that generates a liquid phase (olive oil) and organic slurry known as two-phase olive mill waste (OW). After drying, the OW is generally subjected to a subsequent extraction with hexane to recover the remaining oil still present, leading to the formation of a solid residue known as de-oiled two-phase olive mill waste (DW). In the Mediterranean countries, more than 30 10⁶ m³ of both wastes are produced during the harvest season, [8] meaning a major problem for the industry. The use of OW and DW as organic amendments have been proposed to effective strategy in the control of herbicide leaching in Mediterranean agricultural soils with low organic matter content [9], [10]. However, application of raw (OW and DW) can lead to an important amount of water soluble organic carbon (WSOC) which may enhance the herbicide mobility on soil profile [11], [12]. Therefore, the effect of the organic amendment on behaviour of herbicide depends on the type of amendment and the dosage, as well as on the herbicide's properties and on type of soil [13], [14]. Moreover, the evolution and transformation of organic matter may also modify the further interactions of pesticides with the amended soils [15], so that it would be of great interest to know the effect of aging, preferably under field conditions, on herbicide behaviour.

Although, metribuzin is widely used and represents a potent source of water pollution, only a very few studies have investigated the effects of organic amendment on behaviour of metribuzin [4], [16], [17], and only one study have investigated the impact of OW on sorption, leaching and persistence of metribuzin [10]. Besides, to the best of our knowledge, there have been no published studies evaluating metribuzin's fate in DW-amended soils. Such information

would be useful from the environmental perspective of pesticide management in soils receiving this waste.

The aim of the present study was therefore to investigate the effect of fresh and aged DW on the sorption-desorption, persistence, and leaching of the herbicide metribuzin in an olive grove soil.

II. MATERIALS AND METHODS

A. Soil and Organic Amendment

The soil used in this study (0-30 cm depth) was selected from Alentejo (south-eastern Portugal) and representative of Mediterranean agricultural soils dedicated to olive grove (*Olea europaea* L.). The soil classified as Cutanic Luvisol [18] consisted of 29.7% clay, 21.1% silt, and 49.2% sand.

The fresh DW was obtained from the UCASUL oil industry located in Beja (Portugal). It had the following properties: pH 5.30, 516 g kg⁻¹ TOC, 74.3 g kg⁻¹ WSOC, 5.40% moisture content, and 5.30 dS m⁻¹ electrical conductivity.

To investigate the effect of DW on metribuzin's behaviour the amendment was added to the unamended soil in the laboratory at 2.5%, 5% and 10% dosages by weight. The samples of the amended soils so obtained were labelled as DW2.5, DW5 and DW10. To evaluate the "aging" effects of DW organic matter evolution and transformation on metribuzin's behaviour under field conditions, amended soil samples (0-30 cm depth) were also collected from a field experiment 15 months after the last DW addition to the same soil mentioned above. The soil had received addition of this waste for nine years. The two amendment treatments selected for study consisted of 27 Mg DW ha⁻¹ yr⁻¹ (equivalent to 0.56% yr⁻¹, SADW5) and 54 Mg DW ha⁻¹ yr⁻¹ (equivalent to 1.12% yr⁻¹, SADW10), dry weight equivalents. Therefore, after nine years of repeated field DW application, the total amount of DW received by the field-amended soil is similar to the amounts received by the laboratory amended.

B. Analysis of the soils and DW

Soil texture was determined by sedimentation using the pipette method. TOC, was determined by dichromate oxidation [19]. WSOC was extracted with de-ionized water at 3:1 (water to soil) and 100:1 (water to DW) ratios. Humic and fulvic acids (HA and FA, respectively) were extracted by a solution of 0.1 M Na₄P₂O₇ + NaOH using a ratio of extractant to sample of 10:1, and to precipitate HA the supernatant was acidified to pH 2 with H₂SO₄. Water content of the DW was calculated from weight loss after oven drying to constant weight at 105 °C. Electrical conductivity (EC) was measured in a saturation extract for soil [20] and 1:10 (w/v) DW water mixtures. The humification index (HI) was calculated as ((HA/TOC) x 100). The pH was measured in 1:1 (w/v) soil/water and 1:5 (w/v) DW water mixtures using a combination electrode. Physicochemical characteristics of the unamended and amended soils are given in Table I.

C. Sorption-desorption experiment

Triplicate soil samples (5 g) were equilibrated with 10 mL

of initial metribuzin solutions (5, 10, 20, 40 and 50 µM) by shaking mechanically at 20 ± 2 °C for 24 h. Concentrations in the supernatants were determined by high performance liquid chromatography (HPLC). The amount of metribuzin sorbed (C_s) was calculated from the difference between the initial (C_i) and equilibrium (C_e) solution concentrations.

Following the adsorption experiment, the desorption of metribuzin from the soils was measured by successive dilution from the 50 µM initial concentration points. The 5 mL of supernatant removed for sorption analysis was replaced with the same volume of metribuzin free water. The samples were re-suspended, shaken for 24 h, and centrifuged, and the equilibrium concentration in the supernatant was determined. The herbicide sorption and desorption results were fitted by the Freundlich model (1),

$$C_s = K_f C_e^{1/n_f} \quad (1)$$

where C_s (µM kg⁻¹) is the amount of herbicide sorbed at the equilibrium concentration C_e (µM L⁻¹), and K_f (µM^{1-1/n} kg⁻¹ L^{1/n}) and n_f are the Freundlich coefficient and linearity parameter, respectively. The K_d values (partition coefficients) were calculated from the fit of the experimental sorption isotherms (2),

$$C_s = K_d C_e \quad (2)$$

at 10 µM initial metribuzin concentration. Hysteresis coefficients, H, for the sorption-desorption isotherms were calculated as (3),

$$H = n_a / n_d \quad (3)$$

where n_a and n_d are the Freundlich constants obtained from the sorption and desorption isotherms, respectively.

D. Persistence studies

Triplicate unamended and amended soil samples (500 g) were spiked with 8 mL of an ethanol solution of metribuzin to give a concentration of 1 mg metribuzin kg⁻¹ of dry soil. The soils were sampled periodically, and finally frozen until assay. For the assay, 5 g of soil samples were extracted with 10 mL of methanol by shaking mechanically on an end-over-end shaker at 20 ± 2 °C for 24 h followed by centrifugation, and the metribuzin concentration in the extracts was determined by HPLC. Metribuzin dissipation curves in soils were fitted to first-order kinetics (4) and the half-lives (t_{1/2}) were calculated.

$$C = C_o e^{-kt} \quad (4)$$

where C is the herbicide concentration at time t (days), C_o is the initial herbicide concentration, and k (day⁻¹) is the degradation constant. Dehydrogenase (DH) activity was determined in unamended and amended soil samples from the persistence studies [21].

Table I. Selected characteristics of the unamended and amended soils.

Properties	TOC (g kg ⁻¹)	WSOC (mg kg ⁻¹)	HA (g kg ⁻¹)	FA (g kg ⁻¹)	IH	EC (dS m ⁻¹)	pH
S	9.86a	69.0a	1.02a	0.960a	10.3c	0.426a	7.80de
SDW2.5	24.9b	3149d	1.64b	2.75d	6.57a	3.78d	7.08c
SDW5	39.0c	5372e	2.40c	4.75e	6.15a	6.57e	6.54b
SDW10	58.6d	10297f	4.13e	7.58f	7.05a	10.64f	5.96a
SADW5	20.4b	444b	2.27c	1.23b	11.14c	0.940b	7.97e
SADW10	34.2c	686c	2.92d	1.67c	8.55b	1.56c	7.69d

E. Column leaching tests

Leaching experiments were carried out using disturbed-soil columns (30 cm length x 5 cm i.d.) constructed of PVC. The experiment was performed with triplicates of the unamended and amended soil samples. The soil columns were saturated with 0.01 M CaCl₂, allowed to drain for 24 h, and then the amount of metribuzin corresponding to an application rate of 1.0 kg ha⁻¹ dissolved in water was applied to the top of the columns. Each day the columns were leached with 0.01M CaCl₂ at a rate of 50 mL day⁻¹ until no herbicide was detected in the leachates. Leachates containing the herbicide were collected daily, filtered, and assayed by HPLC. At the end of the leaching experiment, the columns were sectioned into 5-cm deep portions to determine the residual amount of metribuzin at the different depths of the soil column.

III. RESULTS AND DISCUSSION

A. Sorption studies

The values of correlation coefficient (Table II) for all treatment were very high ($R^2 > 0.935$), indicating that the Freundlich adsorption equation satisfactorily explained the results obtained for metribuzin sorption. The DW amendment had a significant influence on the sorption of metribuzin (Table II). The n_f value of unamended soils was 0.647, indicating a L-type isotherms [22], suggesting a decrease in specific sorption sites when concentrations of herbicide in solution increased. However, the n_f values of amended soils were near unity (Table II), indicating a C-type [22], suggesting that metribuzin sorption in these soils were not affected by its concentration in solution and involved a simple partitioning mechanism [4]. The K_d values of the amended soils were greater than of unamended soil, although the magnitudes were different between treatments. In the case of DW was application in laboratory, in particular for 5% and 10% of DW addition, the K_d values increased with reference to unamended soil by factors of 3.6 and 5.2, respectively, while, in the case of field treatments (SADW5 and SADW10) the increases were by factors of 4.8 and 6.8, respectively (Table II). These results showed that TOC may not be the only factor determining metribuzin sorption from the DW amendments, and that the sorption of metribuzin increases with the degree of humification. Indeed, K_d was positively and significantly ($p < 0.05$) correlated with HA ($r = 0.780$) and was higher than obtained with TOC ($r = 0.584$), confirming that the organic

matter transformed into humic substances was quite important in metribuzin sorption. The highest values of K_{oc} for field soils amended (Table II), also suggesting that the TOC is not the most important determinant of metribuzin sorption. This is consistent with results published by [10] who found that the sorption of metribuzin increases with the degree of humification.

The hysteresis coefficients (H) indicated that adsorbed metribuzin was more readily desorbed in the amended soils than unamended soil (Table II). This result could be explained because of high amount of WSOC present in amended treatments. Previous studies have reported low hysteresis coefficients in OW and DW amended soils for herbicides as S-metolachlor, metribuzin and simazine [9], [10] and [13], respectively.

B. Degradation studies

The dissipation rates of metribuzin in unamended and amended soils are shown in Fig. 1.A. The experimental data in all treatments fit first-order kinetics well, with $R^2 > 0.903$ (Table II). The addition of DW in soil had a significant influence ($p < 0.05$) on the $t_{1/2}$ of metribuzin, but the effect was different between laboratory and field treatments (Table II). The application of fresh DW in the laboratory trials increased the $t_{1/2}$ of metribuzin, consistent with a greater decreased in microbial activity in these soils as reflected in the lower values of their DA (Table II, Fig. 1.B). These findings are consistent with those of previous reports indicating that olive mill waste can depress soil microbial activity because of the action of toxic compounds such as phenols [23]. Different results were observed in the treatments with incorporations of DW transformed naturally under field conditions in which there were significant decreases in the $t_{1/2}$ of metribuzin, although the field DW-amended soils presented the highest K_d values (Table II).

The microbial activity of the soils amended with aged DW, whose DH values were similar to those of the laboratory DW-amended soils, could not be an explanation for the shorter $t_{1/2}$ of metribuzin (Table II, Fig. 1B). It is possible that the soil microorganisms in the field OW amended soils may have used the pesticide preferentially as a carbon and energy source instead of the labile fraction of soil organic matter [10], which was significantly reduced in these soils which had the highest humification index (Table I). These results were according with showed by [10] who suggesting that the transformation of the organic matter of the OW due to maturation processes (the

ageing effect) is likely to have been responsible for the shorter persistence of the herbicide metribuzin.

Table II. Effects of de-oiled two-phase olive mill waste addition on sorption-desorption, half-live ($t_{1/2}$) in dissipation studies, and percentage leached and extracted from the soils for metribuzin.

	n_f	k_d	k_{OC}	R^2	H	$t_{1/2}$ (days)	R^2	Leached (%)	Extracted (%)
S	0.647a	0.492a	49.7a	0.936	19.8d	20.0b	0.918	59.3c	33.0ab
SDW2.5	0.883b	1.29b	51.8a	0.994	24.4e	24.0bc	0.909	34.9a	38.9bc
SDW5	0.809b	1.75c	44.9a	0.996	8.48c	29.4c	0.969	45.9b	42.4bc
SDW10	0.866b	2.56e	43.7a	0.957	5.52a	45.1d	0.957	35.4a	34.7abc
SADW5	0.898b	2.36d	115c	0.986	7.01b	7.27a	0.975	43.8b	28.0a
SADW10	0.878b	3.37f	98.5b	0.981	5.89a	3.93a	0.904	36.3a	44.1c

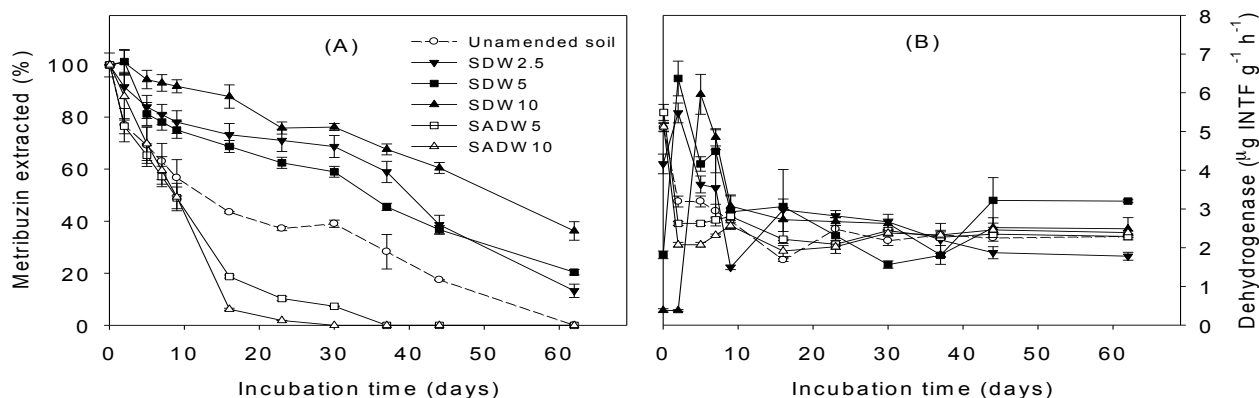


Figure 1. Effects of fresh, composted, and aged olive mill waste on metribuzin dissipation (A) and dehydrogenase activity (B). Error bars represent one standard error of the mean.

Similar conclusions have been reported for herbicide as diuron, terbuthylazine and MCPA, [24], [25], [11], respectively, in different amended soils with residues of the olive-oil extraction process.

C. Leaching studies

In unamended soil the value of total metribuzin leached was 59.3% (Table II). This result shows the high risk of groundwater contamination represented by metribuzin in this soil, consistent with its low sorption capacity. However, the application of DW significantly decreased the amount of metribuzin leached from the soil columns in all treatments (laboratory and field, Table II). In particular, the amounts of metribuzin in the leachates relative to the unamended soil were reduced by about 1.66 and 1.63 for SDW10 and SADW10, respectively.

The increase in sorption may explain the greater reduction of this herbicide in the leachate of the DW-amended soils (Table II). The amount of metribuzin leached was significantly ($p < 0.05$) negatively correlated with K_d ($r = 0.686$) and HA ($r = 0.655$), indicating that the metribuzin leaching in DW-amended soils at least partially depends on the organic matter transformed into humic substances.

Similar correlations were found by [10] for metribuzin in OW-amended soils. Also, [16] showed that animal manure was quite effective in reducing the downward mobility of metribuzin in packed soil columns of a sandy loam soil. The amount of metribuzin extracted from soils columns ranged

between 28.0 and 44.1% (Table II). The application of DW, except SADW5 treatment, led to an increase in the amount of herbicide recovered, results are consistent with those described above for sorption and persistence.

IV. CONCLUSIONS

The application of de-oiled two-phase olive mill waste to olive grove soil greatly influenced sorption, degradation and leaching of the herbicide metribuzin. Amendment with fresh and field-aged de-oiled two-phase olive mill waste led to an increase in metribuzin sorption capacity, and a decrease in the amount of herbicide leached. This suggested that, independently of the degree of organic matter humification, application of de-oiled two-phase olive mill waste may help reduce metribuzin leaching, and therefore may be an effective management practice for controlling metribuzin leaching. Whereas the fresh de-oiled two-phase olive mill waste amendment increased the persistence of metribuzin, the field-aged treatments decreased the herbicide's half-life, thereby contributing to its disappearance from the environment, but also potentially decreasing the herbicide's activity. The positive effect of de-oiled two-phase olive mill waste could be especially significant in semiarid Mediterranean areas, whose agricultural soils are very poor in organic matter and are at a high risk of groundwater contamination by intensive annual pesticide applications.

ACKNOWLEDGMENT

This research was supported by the Spanish Ministries of Education and Science (Project AGL2007-655771-C02-02) and Science and Innovation (AGL2010-21421-C02-02). David Peña and Daniel Becerra are the recipients of a grant from the Consejería of Economía, Comercio e Innovación of the Junta of Extremadura.

REFERENCES

- [1] O. Oukali-Haouchine, E. Barriuso, Y. Mayata, and M. Moussaoui, "Factors affecting metribuzin retention in Algerian soils and assessment of the risks of contamination," *Environ. Monit. Assess.*, vol. 185, no. 5, pp. 4107-4115, May 2013.
- [2] V. Pot, P. Benoit, M.L. Menn, O.M. Eklo, T. Sveistrup, and J. Kværner, "Metribuzin transport in undisturbed soil cores under controlled water potential conditions: experiments and modelling to evaluate the risk of leaching in a sandy loam soil profile," *Pest. Manag. Sci.*, vol. 67, no. 4, pp. 397-407, April 2011.
- [3] M.J. Cerejeira et al, "Pesticides in Portuguese surface and ground waters," *Water Res.*, vol. 37, no. 5, pp. 1055-1063, March 2003.
- [4] N. Singh, "Biocompost from sugar distillery effluent: effect on metribuzin degradation, sorption and mobility," *Pest. Manag. Sci.*, vol. 64, no. 10, pp. 1057-1062, October 2008.
- [5] E.R. Graber, C. Sluszny, and Z. Gerstl, "Influence of sludge amendment on transport and sorption ideality of s-triazines in soil columns," *Environ. Toxicol. Chem.*, vol. 16, no. 12, pp. 2463-2469, December 1997.
- [6] N. Singh, "Organic manure and urea effect on metolachlor transport through packed soil columns," *J. Environ. Qual.*, vol. 32, no. 5, pp. 1743-1749, September 2003.
- [7] L. Delgado-Moreno, and A. Peña, "Sorption/desorption behaviour of sulfonylurea herbicides as affected by the addition of fresh and composted olive cake to soil," *Weed Res.*, vol. 48, no. 5, pp. 461-469, October 2008.
- [8] A.C. Barbera, C. Maucieri, C., V. Cavallaro, A. Ioppolo, and G. Spagna, "Effects of spreading olive mill wastewater on soil properties and crops, a review", *Agr. Water Manage.*, vol. 119, pp. 43-53, March 2013.
- [9] D. Peña, A. Albarrán, A. López-Piñeiro, J.M. Rato-Nunes, J. Sánchez-Llerena, and D. Becerra, "Impact of oiled and de-oiled olive mill waste amendments on the sorption, leaching, and persistence of S-metolachlor in a calcareous clay soil," *J. Environ. Sci. Heal. B*, vol. 48, no. 9, pp. 767-775, September 2013.
- [10] A. López-Piñeiro, D. Peña, A. Albarrán, D. Becerra, and J. Sánchez-Llerena, "Sorption, leaching and persistence of metribuzin in Mediterranean soils amended with olive mill waste of different degrees of organic matter maturity" *J. Environ. Manag.*, vol. 122, no. 5, pp. 76-84, June 2013.
- [11] A. López-Piñeiro, D. Peña, A. Albarrán, J. Sánchez-Llerena, and D. Becerra, "Behavior of MCPA in four intensive cropping soils amended with fresh, composted, and aged olive mill waste", *J. Contam. Hydrol.*, vol. 152, pp. 137-146, 2013.
- [12] A. Cabrera, L. Cox, K.A. Spokas, R. Celis, M.C. Hermosín, J. Cornejo, and W.C. Koskinen, "Comparative sorption and leaching study of the herbicides fluometuron and 4-chloro-2-methylphenoxyacetic acid (MCPA) in a soil amended with biochars and other sorbents", *J. Agric. Food Chem.*, vol. 59, no. 23, pp.12550-12560, October 2011.
- [13] A. Albarrán, R. Celis, M.C. Hermosín, A. López-Piñeiro, and J. Cornejo, "Behaviour of simazine in soil amended with the final residue of the olive-oil extraction process", *Chemosphere* vol. 54, no. 6, pp. 717-724, February 2004.
- [14] A.G. Ahangar, R.J. Smernik, R.S. Kookana, and D.J. Chittleborough, "Separating the effects of organic matter-mineral interactions and organic matter chemistry on the sorption of diuron and phenanthrene", *Chemosphere*, vol. 72, no. 6, pp. 886-890, June 2008.
- [15] E. Morillo, C. Maqueda, R. Reinoso, and T. Undabeytia, "Effect of two organic amendments on norflurazon retention and release by soils of different characteristics", *Environ. Sci. Technol.*, vol. 36, no. 20, pp.4319-4325, October 2002
- [16] K. Majumdar, and N. Singh, "Effect of soil amendments on sorption and mobility of metribuzin in soils", *Chemosphere*, vol. 66, no. 4, pp. 630-637, January 2007.
- [17] N. Singh, Raunaq, and S.B. Singh, "Reduced downward mobility of metribuzin in fly ash-amended soils", *J. Environ. Sci. Heal. B*, vol. 48, no. 7, pp. 587-592, July 2013.
- [18] ISSS-ISRIC-FAO, "World reference base for soil resources", Draft. Wageningen: Roma; 1994.
- [19] D.W. Nelson, and L.E. Sommers, "Total carbon, organic carbon and organic matter", in *Methods of soil analysis*; D.L. Sparks, Ed. Part 3, SSSA, Madison, WI, 1996, pp. 961-1010.
- [20] United States Salinity Laboratory Staff, "Diagnosis and Improvement of Saline and Alkali Soils", in *US Department of Agriculture, US Salinity Laboratory Staff, Ed. Handbook n°60*; Washington, DC, 1954; pp. 7-16.
- [21] C. García, T. Hernandez, C. Costa, B. Ceccanti, G. Masciandaro, and C. Ciardi, "A study of biochemical parameters of composted and fresh municipal wastes", *Bioresour. Technol.*, vol. 44, no. 1, pp.17-23. 1993.
- [22] C.H. Giles, J.H. McEwan, S.N. Nakwa, and D. Smith, "Studies in adsorption. Part XI. A system of classification of solution adsorption isotherms, and its use in diagnosis of adsorption mechanisms and in measurement of specific surface areas of solids". *J. Chem. Soc.* Vol. 3, no. 1, pp. 3973-3993. 1960
- [23] I. Sampedro, M. Giubilei, T. Cajthaml, E. Federici, F. Federici, M. Petruccioli, and A D'annibale, "Short-term impact of dry olive mill residue addition to soil on the resident microbiota", *Bioresour. Technol.*, Vol. 100, no. 23, pp. 6098-6106. December 2009.
- [24] A. López-Piñeiro, D. Cabrera, A. Albarrán, and D. Peña, "Cumulative and residual effects of de-oiled two-phase olive mill waste application to soil on diuron sorption, leaching, degradation, and persistence", *Chemosphere*, vol. 78, no. 2, pp. 139-146, January, 2010.
- [25] A. López-Piñeiro, D. Cabrera, A. Albarrán, and D. Peña, "Influence of two-phase olive mill waste application to soil on terbuthylazine behaviour and persistence under controlled and field conditions", *J. Soils Sediments*, vol. 11 no. 5, pp. 771-782, July, 2011.

Assessment of Surface Water Quality for Sustainable Water Management in Samut Songkram Province, Thailand

Tatsanawalai Utarasakul , Sivapan Choo-in, Chaisri Tharasawatpipat , Srisuwan Kasemsawat and Sathaporn Monprapussorn

Abstract—This research aimed to analyze surface water quality in Samut Songkram Province, Thailand in order to propose sustainable management plan. Water samples were collected from 217 sampling sites during 3 seasons from December 2011 to August 2012. The results of this study reveal that prominent parameters such as temperature, pH, Dissolved Oxygen (DO), Biochemical Oxygen Demand (BOD), Nitrogen compounds in Nitrate and Ammonia and Fecal Coliforms Bacteria were lower than the standard (Class III) of Pollution Control Department, Ministry of Natural Resources and Environment. However, the concentration of heavy metals including lead, cadmium, copper and zinc compounds were higher than the standard. In addition, total value of Total Dissolved Solid (TDS) and turbidity were also higher but cannot be compared with any standard due to a lack of national standard for those parameters.

Appropriate guidelines and management of surface water quality for sustainable water management including: (1) strongly support mitigations plan to reduce water pollution from point source (2) provide collective management of waste water before discharging into water bodies and support campaign for the Corporate social responsibility (CSR), and (3) set up the water quality monitoring stations in each district. Last but not least, the government should prepare an integrated water quality management plans with building a collaborative teams among local government administrations, private sectors and academic institutes.

Keywords— surface water quality, sustainable water management and Samut Songkram.

Dr. Tatsanawalai Utarasakul is with the Environmental Science Program, Faculty of Science and Technology, Suan Sunandha Rajabhat University, Bangkok, Thailand (e-mail: tatsanawalai.ut@ssru.ac.th).

Sivapan Choo-in is with the Environmental Science Program, Faculty of Science and Technology, Suan Sunandha Rajabhat University, Bangkok, Thailand (e-mail: sivapan.ch@ssru.ac.th).

Chaisri Tharasawatpipat is with the Environmental Science Program, Faculty of Science and Technology, Suan Sunandha Rajabhat University, Bangkok, Thailand.

Srisuwan Kasemsawat is with the Environmental Science Program, Faculty of Science and Technology, Suan Sunandha Rajabhat University, Bangkok, Thailand.

Sathaporn Monprapussorn is with Department of Geography, Faculty of Social Sciences, Srinakharinwirot University, Bangkok, Thailand.

I. INTRODUCTION

SAMUT Songkram province is a small province, located at central of Thailand near the mouth of Mae Klong River. With regard to provincial strategic development, this province has been dedicated to ecotourism and hospitality. Currently in many areas, massive landscape has been changed from residential area to ecotourism purpose, especially area close to Mae Klong River and canal branches. Increasing a number of home stays, floating market and fireflies watching in many areas have directly impacts on local livelihood. The plan also promoted public participation strategy in configuring suitable service standard and carrying capacity with the balancing purpose between the use of natural resources and tourism activity.

As a result of SWOT analysis, the strengths of the province include magnificent natural resources and environment, diversity of careers, stock for marine and agricultural products, high quality of human resources and local lifestyle conservation. The weaknesses include degradation of natural resources and environment, threat of water pollution from neighborhood and improper water resources management [3].

In addition, ecotourism has been identified as having a potential in provincial development strategy because it comprises of many canals which are suitable for ecotourism activities. Besides, Mae Klong River was categorized into level three standard by Pollution Control Department, Ministry of Natural Resources and Environment [2]. It serves as one of the major rivers that obtain water from various sources and are suitable for agriculture, household consumption but need to be sterilized for quality improvement. In 2009, monitoring result shown that the degradation of water resource nearby police station in Amphawa area is very high and only useful for transportation purpose due to the release of wastewater from surrounding tributary canals.

In 2010, Department of Environmental Science, Suan Sunandha Rajabhat University has conducted environmental research in Amphawa area, Samut Songkram Province as

identified by university strategic plan and found that water quality in Amphawa canal is still supplies of good water quality except some parameters such as nitrate, ammonia and lead quantity that are higher than standard [1]. Regarding to Tha Ka, Bangkae and Kvae Om canals, only cadmium and lead quantities are higher than surface water quality standard [4]. The reasons behind the degradation come from the discharge of wastewater from nearby upstream provinces, lack of potable water sources and lack of quality analysis for domestic consumption. Some communities might be at risk because they brought water from canals and underground water sources directly without monitoring the impact of water on their health.

As a consequence, this research aimed to study water quality in Samut Songkram Province by investigating raw water for household consumption and also study the relationship between water quality and seasonal variability. Geographic information system has been used as a tool to handle and to analyze water resources data in order to propose sustainable water resources management in Samut Songkram Province..

II. MATERIALS AND METHODS

A. Study Area

Surface water were collected and analyzed in three areas of Samut Songkram Province namely; Muang, Amphawa and Bang Khon Thee Districts as shown in Figure1.

- 1) Muang area has 69 sampling sites (7 from three canals, 1 from river and 61 from small tributary canals)
- 2) Amphawa area has 72 sampling sites (9 from canals, 2 from river and 61 from small tributary canals)
- 3) Bang Khon Thee area has 68 sampling sites (6 from canals, 3 from river and 59 from small tributary canals)

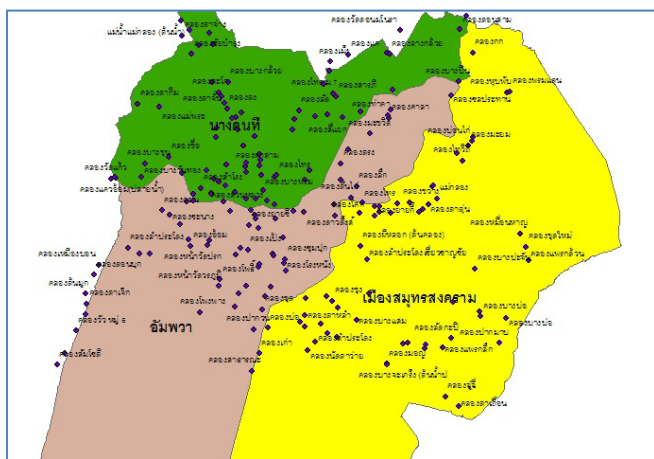


Figure. 1 Sampling sites in Samut Songkram Province

B. Research equipments

- 1) Water sampling and water depth meter
- 2) Sampling and preservation container
- 3) pH meters “HANNA HI 98217 and HORIBA D-54 models

- 4) Turbidity meter Lovibond TurbiCheck
- 5) Dissolved oxygen meter HORIBA OM-51
- 6) Salinity meter
- 7) Global positioning system GARMIN Etrex 20
- 8) Atomic absorption spectrophotometer GBC Avanta ver 2.02
- 9) Spectrophotometer
- 10) Ammonia distillation apparatus
- 11) BOD incubator
- 12) Cadmium column
- 13) Weight balance
- 14) Humidity incubator
- 15) Thermometer
- 16) Laboratory glassware
- 17) Chemicals for analyzing water quality

C. Methodology

A survey research has been conducted in Samut Songkram Province as the following:

- 1) Survey and study water quality for household consumption in canals by sampling seasons (three seasons)
- 2) Analyze water quality by using methods and parameters as shown in Table 1
- 3) Statistical analysis of variance to water quality by using T-test

TABLE I

PARAMETERS AND METHODS USED IN WATER QUALITY ANALYSIS

N o.	Parameters	Method of analysis	Place of analysis	
			Field	Laborator
1	Turbidity	Turbidity meter	√	√
2	Total dissolved solids	Filtration paper		
3	Salinity	Salinity meter	√	
4	pH	pH meter	√	
5	Nitrogen in Nitrite form	Colorimetric method		√
6	Nitrogen in Nitrate form	Cadmium reduction method		√
7	Nitrogen in Ammonia form	Distillation Titrate method		√
8	Sulfate	Iodometric method		√
9	Chloride	DPD Colorimetric method		√
10	Hardness	Titrate with EDTA		√
11	Dissolved Oxygen	Azide modification or DO meter	√	√
12	BOD	Azide modification or DO meter at 20 degree celcius for 5 days		√
13	Lead	Atomic absorption- Direct aspiration		√
14	Cadmium	Atomic absorption- Direct aspiration		√
15	Fecal Coliform	Multiple tube fermentation technique		√

III. RESULTS AND DISCUSSION

A. Surface water quality

Surface water quality was measured from 217 sampling sites from 3 seasons as shown in Table 2. Prominent results can be concluded as the following:

Range of water temperature from canals in Amphawa, Bang Khon Thee and Muang Districts are 21.9-39.0°C (average 30.0°C), 25.0- 52.0°C (average 30.0°C) and 21.9-39.0°C (average 32.6 °C), respectively. All values meet the surface water quality standard type III of PCD.

Range of pH for canal water in Amphawa, Bang Khon Thee and Muang Districts are 6.1-8.8 (average 7.9), 6.8-8.6 (average 7.69) and 5.4-8.7 (average 7.45), respectively. All of pH values are also meet the standard of surface water quality type III mentioned by PCD that a range of pH should be 5-9.

Total dissolved solids (TDS) values in Amphawa, Bang Khon Thee and Muang Districts are 16-54,082 mg/l (average 528 mg/l), 58-400,180 mg/l (average 4,435 mg/l) and 31-29,200 mg/l (average 3,762 mg/l), respectively. However, TDS values cannot be compared with PCD standard because TDS did not appear in type III standard of surface water quality. From this study, tributaries canals in Bang Khon Thee District have the highest TDS values.

TABLE II

SURFACE WATER QUALITY IN SAMUT SONGKRAM PROVINCE

Parameters	Values	Location			Seasons		
		Muang	Amphawa	Bang Khon Thee	Winter	Summer	Rainy
Temperature (°C)	Range	27.0-42.0	21.9-39.0	25.0-52.0	24.0-37.0	28.0-52.0	21.9-34.0
	Average	32.6	30.0	30.6	30.1	34.2	29.0
TDS (mg/l)	Range	31-29,200	16-54,082	58-400,180	16-400,180	52-57,186	31-29,200
	Average	3762	529	4,435	3285	3580	1934
pH	Range	5.4-8.7	6.1-8.8	6.8-8.6	5.4-8.8	6.1-8.7	6.5-8.3
	Average	7.4	7.6	7.7	7.7	7.6	7.4
DO (mg/l)	Range	1.15-7.47	0.76-8.90	0.62-9.50	0.62-9.50	1.17-8.9	0.76-8.8
	Average	3.20	4.27	4.63	4.16	3.91	4.04
BOD(mg/l)	Range	1.1-7.5	0.0-7.6	0-8.7	0-6.7	0.1-8.7	0-7.5
	Average	3.2	2.2	2.0	1.9	3.4	2.1
Turbidity (NTU)	Range	2.07-93.70	2.19-65.20	0.91-78.70	3.69-196.0	0.91-93.70	2.07-78.7
	Average	27.72	15.46	16.04	19.43	24.57	17.61
Nitrate (µg/l)	Range	0.00-668.00	0.00-256.36	0.00-848.36	0.00-9.14	0.00-133.55	0.05-848.36
	Average	30.79	9.38	40.03	0.31	11.33	65.86
Pb (mg/l)	Range	0.118-4.168	0.026-3.916	0.038-5.223	0.232-5.223	2.259-4.168	0.026-0.603
	Average	2.157	1.220	1.685	1.663	3.155	0.228
Cd (mg/l)	Range	0.000-5.545	0.000-3.526	0.004-5.244	0.471-2.792	0.000-5.244	0.004-0.062
	Average	1.743	0.026	2.007	1.206	3.969	0.020

A range of turbidity values from canal water in Amphawa, Bang Khon Thee and Muang Districts are 2.19-65.2 NTU (average 15.46 NTU), 0.91 – 78.70 NTU (average 16.04 NTU) and 2.07 – 93.70 NTU (average 27.72 NTU),

respectively. However, there is currently no surface water quality standard for turbidity.

Dissolved oxygen (DO) content from canal water in Amphawa, Bang Khon Thee and Muang Districts are 0.76-0.89 mg/l (average 4.27 mg/l), 0.62-9.5 mg/l (average 4.63 mg/l) and 1.15-7.47 mg/l (average 3.20mg/l), respectively. Seasonal comparison has also been measured and found that DO contents are 0.62 – 9.50 mg/l (average 4.16 mg/l) in winter, 1.17-8.9 mg/l (average 3.91mg/l) in summer and 0.76-8.8 mg/l (average 4.04 mg/l) in rainy season. Refer to the level of dissolved oxygen in all areas, it is compliance with specific standard that DO content should not below 4 mg/l.

Range of Biochemical oxygen demand (BOD) from canals in Amphawa, Bang Khon Thee and Muang Districts are 0.0-7.6 mg/l (average 2.2 mg/l), 0.0-8.7 mg/l (average 2.0 mg/l) and 1.15-7.47 mg/l (average 3.20mg/l), respectively. Refer to surface water quality standard type three, Amphawa and Bang Khon Thee Districts compliance with. While, BOD content in Muang area is higher than the standard, but still more within type four standard (less than 4 mg/l).

Nitrogen content in nitrate form for Amphawa, Bang Khon Thee and Muang Districts are 0.0-256.36 µg/l (average 9.38µg/l), 0.00 – 848.36 µg/l (average 40.03µg/l) and 0.00 – 668.00 µg/l (average 30.79µg/l), respectively. Refer to surface water quality standard, all areas have nitrogen content below 5 µg/l and the quality in term of nitrogen content is acceptable.

Lead content in canal water for Amphawa, Bang Khon Thee and Muang Districts are 0.026-3.916 mg/l (average 1.220mg/l), 0.038 – 5.223 mg/l (average 1.658mg/l) and 0.118 – 4.168 mg/l (average 2.517mg/l), respectively. According to surface water quality standard, lead content in the water should not higher than 0.05 mg/l and therefore average water quality from all areas are over the standard (type III).

Cadmium content in canal water for Amphawa, Bang Khon Thee and Muang areas are 0.000 - 3.526 mg/l (average 0.260±0.685 mg/l), 0.004 – 5.224 mg/l (average 2.007 ± 2.002 mg/l) and 0.000 – 5.545 mg/l (average 1.743 ± 1.491 mg/l) respectively. In according to surface water quality standard, cadmium content in the water should not greater than 0.05 mg/l and therefore not acceptable based on type III standard.

When considering results of the studies, Lead content was found at range 0.026 to 5.223 mg/l with the average 1.69 mg/l. In comparison with the standard (less than 0.05 mg/l), lead content is therefore much higher than standard. Range of Cadmium content was found from 0-5.545 mg/l with the average 1.39mg/l. In comparison with the standard (less than 0.05 mg/l), cadmium content is therefore much higher than the standard. For the range of Iron content was found from 0-8.18 mg/l with the average 0.29mg/l, but no specific water quality standard for iron content.

Range of Zinc value was found from 0-6.941 mg/l with the average 3.55mg/l. In comparison with the standard (less than 1.00 mg/l), zinc content is therefore much higher than standard. Copper value was found from 0-6.91 mg/l with the

average 0.45mg/l. When compare with the standard (less than 0.1 mg/l), copper content is therefore slightly higher than standard.

The reason behind high concentration of heavy metals comes from pre-treatment process of samplings before sending to analysis. The samplings were first digested by conc. nitric acid before analyzing with Atomic Absorption Spectrophotometer (AAS). The measured metal concentrations are not only a content in the water, but also include metal content in dissolved sediments load.

Graph of major parameters of water quality in Samut Songkram also represented in Figure 2.

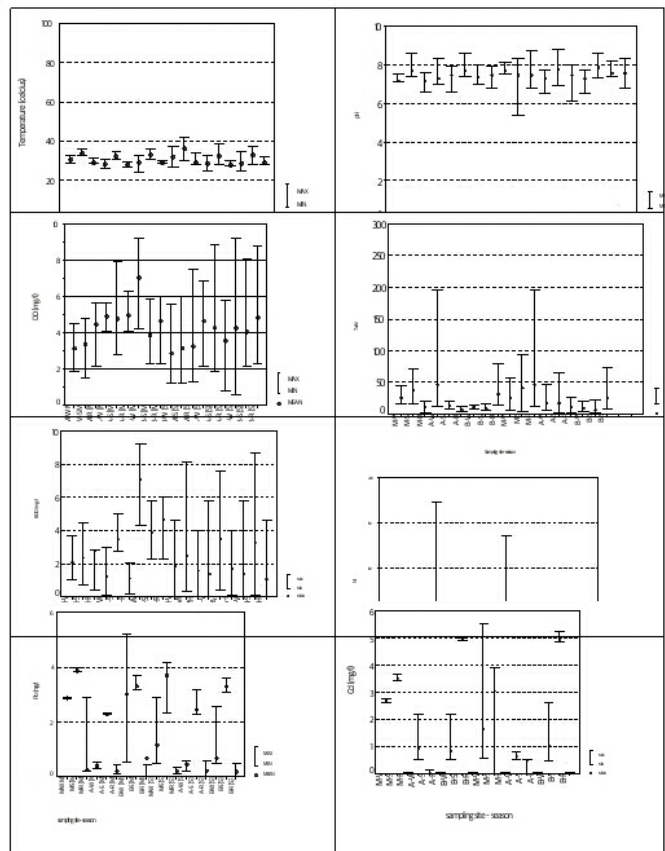


Figure. 2 Graphs illustrate average water quality of the prominent parameters in each season.

B. Analysis of seasonal variations of surface water quality

TABLE III

STATISTICAL ANALYSIS BETWEEN SEASONAL VARIATIONS AND SURFACE WATER QUALITY BY PAIRED – SAMPLES T-TEST

Parameters	Season	Statistical Significant		
		Winter	Summer	Rainy
Temperature (°C) N = 198	winter	-	0.000	0.000
	summer	0.000	-	0.000
	rainy	0.000	0.000	-
pH N=200	winter	-	0.005	0.000
	summer	0.005	-	0.000
	rainy	0.000	0.000	-

Parameters	Season	Statistical Significant		
		Winter	Summer	Rainy
TDS (mg/l) N = 196	winter	-	0.008	0.006
	summer	0.008	-	0.064
	rainy	0.006	0.064	-
Turbidity N=168	winter	-	0.072	0.010
	summer	0.072	-	0.000
	rainy	0.010	0.000	-
Nitrate N = 193	winter	-	0.000	0.000
	summer	-	-	0.000
	rainy	0.000	0.000	-
DO N = 204	winter	-	0.149	0.489
	summer	0.149	-	0.256
	rainy	0.489	0.149	-
BOD N= 201	winter	-	0.000	0.339
	summer	0.000	-	0.000
	rainy	0.339	0.000	-
Pb N= 42	winter	-	0.000	0.000
	summer	0.000	-	0.000
	rainy	0.000	0.000	-
Cd N = 86	winter	-	0.000	0.000
	summer	0.000	-	0.000
	rainy	0.000	0.000	-

Remarks: 0.05 level of significance

Paired sample T-test analysis have been conducted in order to find out the difference of water quality and seasonal variations. Results revealed that pH and temperature are different statistically significant at 0.05 level of significance.

Seasonal variations of Total dissolved solids (TDS) between winter and summer, winter and rainy have statistical difference ($\alpha = 0.008$ and $\alpha = 0.006$). However, no statistical difference between summer and rainy seasons ($\alpha = 0.064$)

Seasonal variations of Biochemical demand (BOD) between summer and rainy season have statistical difference ($\alpha = 0.000$ and $\alpha = 0.000$). However, no statistical difference between winter and rainy seasons ($\alpha = 0.339$) Seasonal variations of nitrogen in nitrate form, lead, and cadmium have statistical difference as well.

Whereas, no statistical difference between seasonal and dissolved oxygen

IV. CONCLUSION

From the investigation of surface water quality in Mae Klong River, main and tributaries canals which flow through three districts in Samut Songkram Province, were found that water quality meet the standard type III of surface water quality as issued by National Environmental Quality Act B.E. 1992. A framework of water quality management for domestic consumption in Sumut Sonkram Province is categorized by water quality and water utilization as the following;

A. Surface water quality management plan

The results of impurity in form of BOD and Nitrate which are represent as an indicator of organic content and nutrient for plant growth revealed that surface water quality in three districts of Samut Songkram Province consists of organic contaminations. A level of nutrient present in surface water needed by plant growth meet the standard type III of surface

water quality standard and is suitable in withdrawing for agricultural purposes.

Regarding to the effect of pollutants on water quality, streams quality was largely affected by local people who live at riverside, canal and tributary canal. Pollutants come from various sources such as homestays and resorts, restaurants, orchards, small business. Concentrations of heavy metals were higher than surface water quality standard. For example, Pb, Cd and Zn are major pollutants for consumption. Thus, it needs to be effectively purified before consumption.

When focusing on hydraulic factors like sediment flow also considerate, two provinces namely; Kanchanaburi and Rachaburi, located in upstream watershed, can largely contribute in discharging wastewater into Mae Klong River and directly pass to downstream before flowing to Gulf of Thailand. All stakeholders such as central and local government agencies, industries and local people should concern this issue and take effective attention in order to find out suitable framework, plan and management system.

The surface water management framework for sustainable utilization and consumption include wastewater reduction practice at upstream sources; establish local gathering team to handle wastewater before discharge to water bodies; take corporate social responsibility (CSR) paradigm into practice; set up water quality monitoring stations in each area. Finally, government should establish integrated water resource management plan by collaborating with local people both in short term and long term period.

ACKNOWLEDGMENT

This research was supported by National Research Council of Thailand and Suan Sunandha Rajabhat University. Special thanks also extended to the Samut Songkram Province Staff, and students of SSRU who helped and supported this project.

REFERENCES

- [1] Chantama, P. and Tae-ouang, P. *Changing of water quality from Amphawa Floating Market, Samut Songkram Province*. Suan Sunandha Rajabhat University.2010: 120 p.
- [2] Pollution Control Department. Surface Water Quality. Retrieved September 28, 2012. Available from: <http://www.pcd.go.th>
- [3] Samut Songkram Province. *Samut Songkram Development Plan: 2010-2013*. Retrieved September 20, 2010. Available from <http://www.samutsongkhram.go.th/index1.htm>
- [4] Sukorn, W. and Srihuatone, P. *Factors related with Fireflies population in orchard areas of Amphawa, Samut Songkram*. Suan Sunandha Rajabhat University.2010: 150 p.

The effect of roof material on rain water quality parameters in conditions of Slovak Republic

Mohamed Ahmidat , Daniela Kaposztasova, Gabriel Markovic, Zuzana Vranayova

Abstract—We need to change the thinking of the society which will be in balance with nature and magnitude of the problems arising from the advent of climate change, increasing urbanization and raising of the sea levels. Problems with torrential rains and drought only confirm the need for evolving new technologies, approaches and solutions in building services, as a proposal for green alternatives for the transition to a sustainable society. This article describes the simulation of roofing material influence on the quality and quantity of rainfall water in the area of Kosice-City. It offers deep analysis of the factors valid for quality of harvested rainwater from university building's roof and also the analysis of simulation of two model with ceramic roofing tile and organic coated metal roofing.

Keywords—rainwater harvesting, rainwater harvested from surface runoff, quality of water, roofing material, model

I. INTRODUCTION

WATER is essential for all dimensions of life. Over the past few decades, use of water has increased, and in many places water availability is falling to crisis levels. More than eighty countries, with forty percent of the world's population, are already facing water shortages, while by year 2020 the world's population will double. The costs of water infrastructure have risen dramatically. The quality of water in rivers and underground has deteriorated, due to pollution by waste and contaminants from cities, industry and agriculture. These and other aspects lead us to do something to save this blue gold and use the rainwater. Progressive management of wastewater is in Slovakia relatively new topic. Due to recurrent floods we need more efficient handling of rainfall. The objective is to dispose of the water as close as possible to its origin, to what is necessary to adopt a comprehensive legislative framework and on the basis of experiments in

This work was supported by the VEGA 1/0450/12 Energy balance research on rainwater management in the cities of the future.

The APVV - SK-CZ-2013-0188 Talk about the Water – An Essential Dimension of Sustainable Society of the 21. century

Ing. Mohamad Ahmidat, Technical University of Košice, Faculty of Civil Engineering, Institute of Architectural Engineering, Vysokoškolská 4, 042 00 Košice, mail: mohamed.ahmidat@tuke.sk

Ing. Gabriel Markovič, PhD., Technical University of Košice, Faculty of Civil Engineering, Institute of Architectural Engineering, Vysokoškolská 4, 042 00 Košice, mail: gabriel.markovic@tuke.sk

Ing. Daniela Kaposztasová, PhD., Technical University of Košice, Faculty of Civil Engineering, Institute of Architectural Engineering, Vysokoškolská 4, 042 00 Košice, mail: daniela.ocipova@tuke.sk

doc. Ing. Zuzana Vranayová, PhD., Technical University of Košice, Faculty of Civil Engineering, Institute of Architectural Engineering, Vysokoškolská 4, 042 00, Košice, e-mail: zuzana.vranayova@tuke.sk.

laboratory and real-world design methodology to derive applicable management systems. Massive use of waste water for non-potable purposes in buildings also promotes the conservation of natural resources, water, and thus the overall sustainability in water management. The step forward is to introduce strategic areas for energy conservation in the technology of green buildings (Figure1) [1,15,14]. We are aimed at the water sources and their reuse.

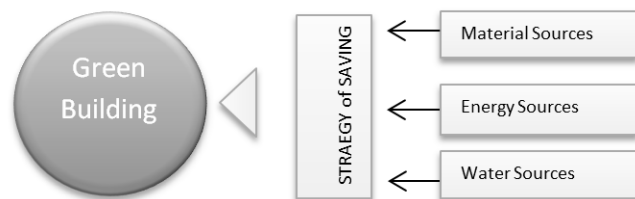


Fig. 1 Strategic areas for energy conservation in the technology of green buildings [16]

In the past, rainwater harvested from surface runoff - RHSR in Slovakia was used mainly for irrigation of gardens. These days, systems for collecting RHSR are built mainly in buildings like supermarkets, stadiums, etc. where RHSR is used for toilets flushing. Only negligible numbers of Slovak families use RHSR for household needs (washing, flushing, etc.). RHSR can become widely used in everyday life in the near future once systems for RHSR collecting are installed to houses, schools or office buildings. For RHSR use in households it is essential that collected water complies with both health and hygienic requirements and also meets quality requirements [2].

The aim of our research was to identify factors that affect the quality of rainwater, such as surrounding environment in which the system of rainwater harvested from surface runoff (RHSR) is located also impact of rain periods (rainfall periods or periods without precipitation) and roofing material on the quality of rainwater harvested from surface runoff.

II. MATERIALS AND METHODS

Main goal of the research is to obtain information about rainwater collected from roofs of various roofing materials and, based on this information to identify roofing material which appears to be the most suitable material for the monitored area of Košice. The study was conducted in two places directly at campus of the Technical University of

Košice as shown in Figure 2. Quality of water is measured in two model tanks, one located on a roof of university library, second on a real roof of PK6 Building (258 m far from the library building). Campus of the Technical University in Košice is located in the city of Košice - North and falls under the precipitation station SHMÚ Košice - City.

Assessment of individual quality indicators of RHSR follows the Regulation of the Slovak Republic (NV SR) No. 269/2010 Z. z., effective May 25th, 2010, laying down the requirements for achieving good water status results



Fig. 2 Locations of research points at the campus of the Technical University in Košice (TUKE)

From our previous studies [3,4] we used the measured data from the rain gauge on the roof of University library (Figure 3).



Fig. 3 rain gauge on the roof of University library [8]

Totals of rainfall represent the theoretical amount of rainfall in mm, falling on surface of interest. Totals of rainfall depend on specific locations. The average of yearly totals of rainfall is about 770 mm/year in Slovakia [12,13,14].

Data obtained from our precipitation station and precipitation stations SHMU are comparable, so we can take them as a guide, because we know that one of the main principles of stormwater management is to use the data as closest to the place of reuse.

Drinking water quality is evaluated according to basic indicators :

- microbiological and biological indicators (coliform bacteria, thermotolerant coliform bacteria and faecal

streptococci),

- physico - chemical parameters (pH, conductivity, levels of heavy metals and chemicals that could harm human health),
- sensorial characteristics (taste, odor, color) [2].

Factors affecting the quality of RHSR are:

- environment in which the system for SWR operates (proximity of roads, traffic density, proximity of the manufacturing and construction industries, heavy industry, housing sector, agriculture),
- meteorological conditions (temperature, amount of rainfall periods and dry periods, course of fronts), SWR system (material used, its sustainability, filtration),
- human factors (proper sizing, regular maintenance, information about the operation of system as a whole and also about individual components) [3].

In the next two paragraphs we will describe our measurement location and goals.

A. Location 1- PK6 building

PK6 Building (Figure 4) is a computer center of the Faculty of Electrical Engineering and Informatics (FEI) at TUKE. System for monitoring of RHSR quality from PK6 Building consists of the following components:

- Roof - roof material: Ceberit – fibrecement small-area coating with smooth surface.
- Gutters – material: steel.
- Two concrete infiltration shafts with a diameter of 1000 mm.
- Monitoring devices placed in shafts (flowmeter - runoff of rainwater from the roof, water level sensor - water level in shaft, Levellogger - groundwater sensor, Barologger - atmospheric pressure, multi-parameter sensor of water quality (pH, conductivity))[9].

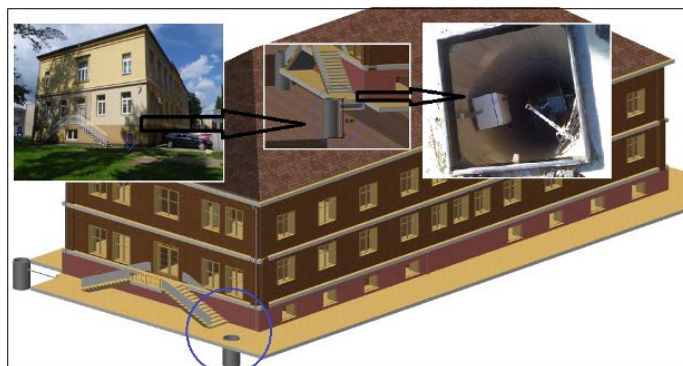


Fig. 4 PK6 Building – location of shafts A

Choice of roofing material for the RHSR collecting system depends on:

- material surface structures (roughness, porosity and surface topography),
- mechanical material properties (hardness, firmness),
- resistance to climatic conditions and to environment pollution in particular region. Combination of these factors ensures smooth operation of the system for collecting RHSR, it prolongs its lifetime and minimizes maintenance.

Appropriately selected roofing material ensures adequate water quantity and quality [7,8,9] Measuring of qualitative parameters began in late 2011 using multi-parameter water sensor, type YSI 600 XL, placed in a concrete shaft. Conductivity and pH measurements took place continuously.

B. Location 2- university library roof - models

There are 2 equivalent models located on the roof of the University library with different roof materials (ceramic, organic coated metal roof) (Figure 5). Roofing material of the model was chosen according to the most commonly used roofing materials in Slovakia as well as for the suitability of their use for harvesting of RHSR.



Fig. 5 Location of models on the roof of university library building.



Fig.6 First flush device

Measurement and analysis of the quality of stormwater in these models began in June 2012 on ceramic roofing material and in October 2013 on the roofing organic coated metal roof. For the analysis purposes, stormwater samples are taken from two places, i.e. from the place of „first flush" (Figure 6) and from the 300 liter plastic tank collecting RHSR (Figure 7).



Fig.7 Samples from water tanks collecting RHSR

The analysis of the quality of rainwater is made on the spot by means of a multi-parameter water quality sensor HANNA HI 991301. Control measurements are performed in laboratory using a pH and conductivity meter WTW pH / cond 340i.

III. RESULTS AND DISCUSSION.

A. Results from experiments in PK6 building

Study in Brazil described [5] that prolonged periods of drought provide the rain water drained roof surfaces, an increase in the values of parameters such as turbidity and color, conductivity, dissolved solids and alkalinity.

Results of qualitative indicators of RHSR collected from a models. The PH and conductivity was explored. Box – plot graph on Figure 8 shows pH values of RHSR collected from PK6 Building during 2013. According to (NV SR) No. 269/2010 Z. z.. pH values should range from 6 to 8.5. pH values vary in particular months. Lower tolerance limit of pH 6 is exceeded during summer months from May to September.

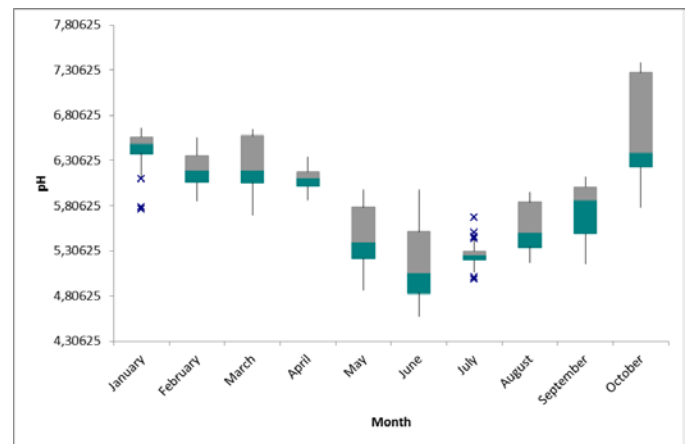


Fig.8 pH values of rainwater from PK6 Building during 2013

Another indicator of quality of the water collected from PK6 building is conductivity. Conductivity is an approximate level of concentration of electrolytes in water. Conductivity limit for drinking water, according to (NV SR) No. 269/2010 Z. z., equals 100 mS/m which is about 1000 mg/l.

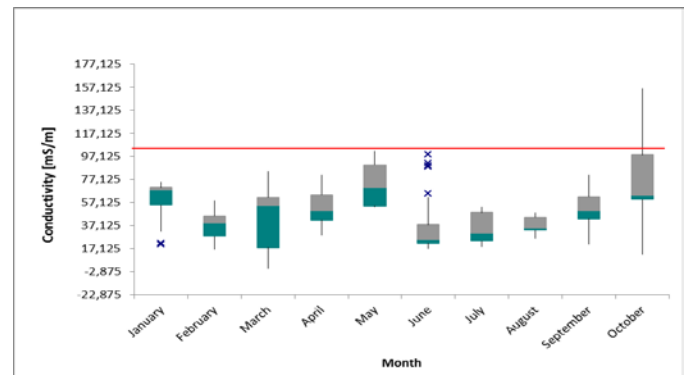


Fig.9 Conductivity values of rainwater from PK6 Building during 2013 [11]

However, optimally, drinking water should contain less soluble compounds, only about 200-400 mg/l (about 25-50

mS/m). Conductivity, similarly to pH, is measured continuously by means of a multi-parameter sensor. Conductivity values of rainwater during 2013 are displayed in box-plot graph on Figure 9. From graph below we can see that the average conductivity value for particular month varies, in most cases it is within normal limits (red line) and in the months from April to August average conductivity value are optimal (blue line). Critical month is October where limits are exceeded.

B. Results from experiments - university roof models

Monitoring of the quality of RHSR from the model with ceramic roof tiles started in June 2012. **Two parameters were evaluated, pH and conductivity.** Water sample was taken always on the 3rd, 15th and 30th day of month from 300 liter plastic water tank.

1. Roof material: ceramic roof tiles

These were obtained by sampling and subsequent chemical analysis of water samples. pH values of water in tank during 2013 are outlined in box-plot graph on Figure 10. In 2013, average pH value equaled 7.5, maximum pH was 8.6 and minimum value reached 6.89. According to (NV SR) No. 269/2010 Z. z., pH value should range from 6 to 8.5.

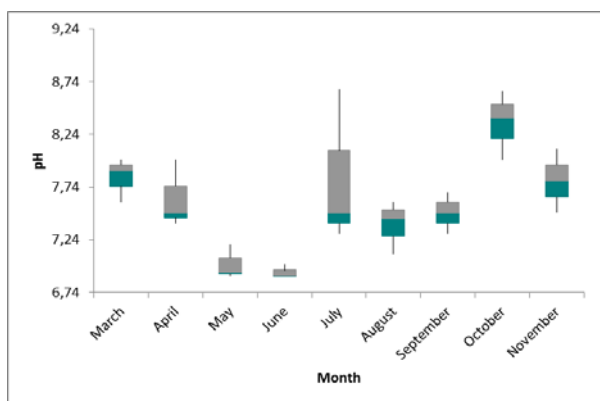


Fig. 10 pH values measured in 2013 - model with ceramic roofing

In May 2013, “first flush“ system was attached to the model with ceramic roofing. Figure 11 below shows a comparison of pH values of water from the system of “first flush“ and of water from tank. Samples were taken on the same day and at the same time from the tank and from the “first flush“ system. Water from the “first flush“ is generally more acidic than RHSR from the tank, i.e. pH differs in 0.45 on average.

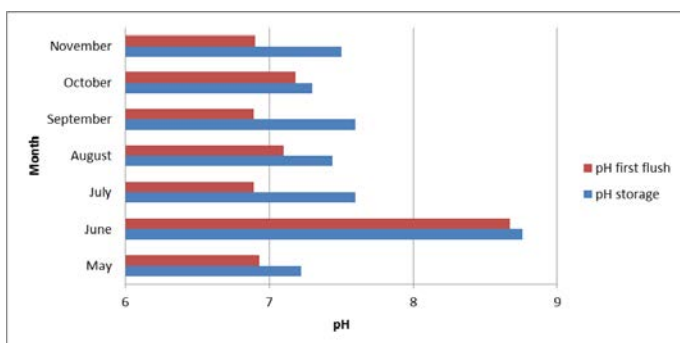


Fig. 11 Comparison of pH values of water from “first flush“ system and from tank in the model with ceramic roofing

Water conductivity values during 2013 are shown in box – plot graph on Figure 12. In 2013, conductivity values are optimal, not exceeding 50 mS/m.

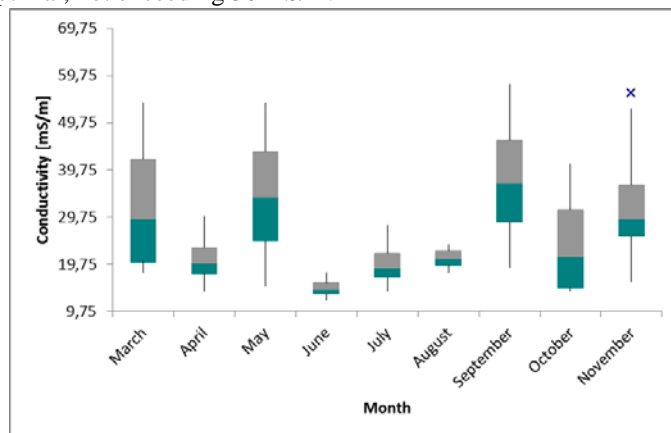


Fig. 12 Conductivity values measured in 2013 - model with ceramic roofing

2. Roof material: organic coated metal roof

Measuring of qualitative indicators for the model with organic coated metal roof began in October 2013. Water samples were collected from the “first flush“ and from the tank. Samples were taken at the 3rd, 15th and 30th day in month and after large precipitation events. Figure 13 shows pH values during the monitored periods in 2013 displayed in box – plot graph. Average pH value recorded was 8, maximum pH was 8.6 and minimum 7.6.

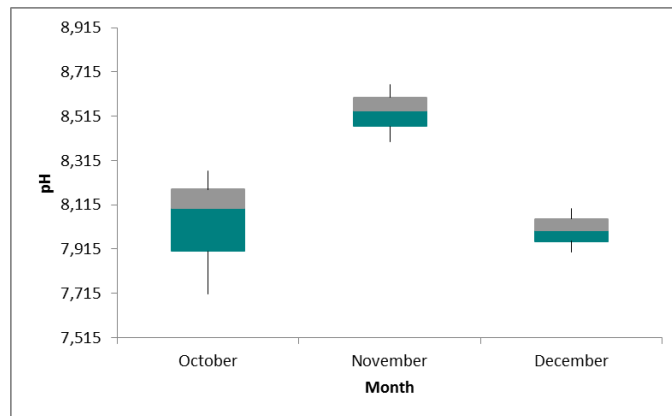


Fig. 13 pH values of rainwater from the model with organic coated metal roofing during the monitored period in 2013

Figure 14 below serves as a comparison of pH values of water collected from the “first flush“ system and pH of water collected from the tank. Generally, water from the “first flush“ is more acidic than SWR taken from the tank, on average the difference is 0.1.

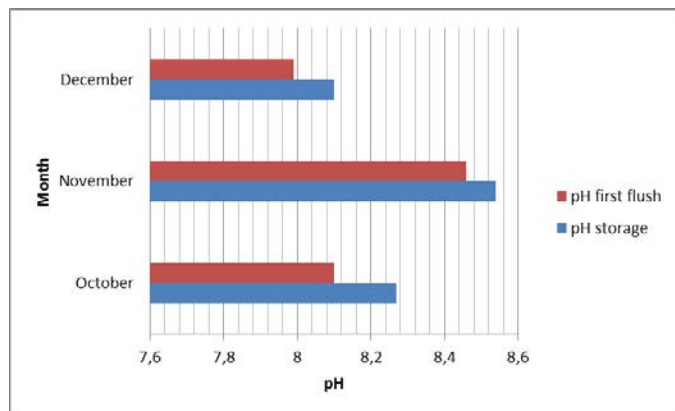


Fig. 14 Comparison of pH values of water taken from the “first flush” and from the tank for the model with organic coated metal roofing

Water conductivity values during the monitored period in 2013 are shown in box graph on Fig. 21. During the 2013 monitored period, conductivity values were optimal and did not exceed 50 mS/m. Average conductivity value was 17 mS/m, maximum value reached 42 mS/m and minimum was 3 mS/m.

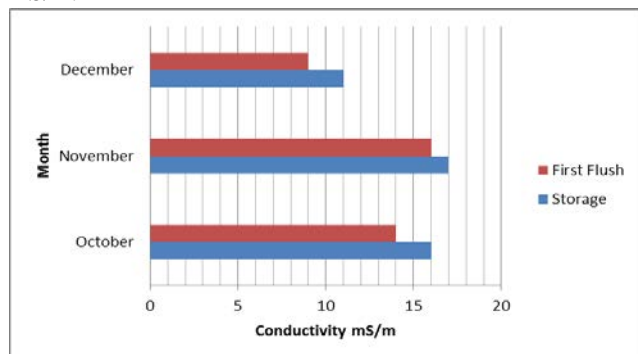


Fig. 15 Comparison of water conductivity values of “first flush” water and of water from the tank for the model with organic coated metal roofing

On Figure 15 we can see a comparison of water conductivity values of water from the “first flush” and of water from the tank. Conductivity of water taken from the “first flush” is lower than of water taken from the tank, on average it is 1 mS/m, so the difference is negligible.

IV. CONCLUSION

One of the methods of effective use of potable water sources used more frequently nowadays, not only in industrial but also in developing countries, is rainwater harvesting from surface runoff [1,11,4]. The basic element of environment affecting the quality of RHSR is atmosphere. Polluted atmosphere is an important factor that degrades the quality of materials and affects the occurrence of acid rain. Each material gives different response depending on the material composition and other characteristics. Most of the materials exposed to atmosphere show sensitivity to the effect of sulfur compounds, chloride aerosols and acidity of atmospheric precipitation [4,5,6]. In this study, the results obtained through the research on the roofing materials demonstrated that organic coated metal roofing appear to be the most advantageous roofs for the collection of RHSR in the given area of Košice. Qualitative

parameters of RHSR from ceramic roofings comply with the requirements on drinking water. Incorporation of “first flush” system into RHSR collecting system has significant effects on the final quality of RHSR. RHSR from “first flush” is more acidic and with higher concentration of pollutants. RHSR from model tanks meet high quality requirements on drinking water. RHSR from real building PK6 with fibrecement roof coating is, on the basis of selected indicators, suitable for irrigation and, after treatment and disinfection, also for drinking.

REFERENCES

- [1] D. Očipová, Z. Vranayová, Z. Karellová, TZB-info. - The potential use of rainwater from surface runoff, Topinfo s.r.o., 20. December 2010. [Date 19. January 2011.] [Online] <http://voda.tzb-info.cz/vlastnosti-a-zdroje-vody/7024-potencial-vyuzivania-zraskovej-vody-z-povrchoveho-odtoku>.
- [2] Regulation n. 354/2006 Z. z. Slovak Government Regulation laying for requirements on water intended for human consumption and quality control of water intended for human consumption
- [3] M. Ahmidat, Analysis of environment for the design of effective and efficient system for collecting rain water from surface runoff. PhD seminar ÚBP. Košice : Faculty of civil engineering, 2011.
- [4] SAŽP Banská Bystrica, Centre for Environmental regionalization Košice. Report on the state of the environment in the Kosice region 2002. Košice : SAŽP, 2002.
- [5] A. Fargašová, Enviro-edu. Metal pollution in Slovakia. [Online] 1. January 2009. [Date: 11. January 2011.] http://www.enviro-edu.sk/database/environmentalne_problemy/zncistenie_kovmi_na_slovensku/Enviro-edu_4013_Zncistenie_kovmi_na_Slovensku.pdf.
- [6] D. Knotková, K. Kreislerová, I. Skorepová, Map of corrosion rate of zinc for the Czech Republic. Krompachy : 10. Conference of hot-dip galvanizing, 2004.
- [7] M.I. Yaziz, et al., Variations in rainwater quality from roof catchments. Water Resources. 1989, Vol. 23, 6, pp. 761-765.
- [8] M. Ahmidat, a Z. Vranayová, Effective use of roofs for stormwater capturing. Water and voda . Štrbské pleso: ELSEWA s.r.o, 2010. ISBN 978-80-89385.who.int. [Online] 2013. [Date: 1. January 2014.] http://www.who.int/water_sanitation_health/gdwqrevision/rainwater.pdf
- [9] Z. Vranayová, TZB-info, Is an effective use of rainwater runoff? [Online] 11. April 2005. [Date: 25. March 2010.] <http://www.tzb-info.cz/2445-je-efektivne-vyuzitie-zraskovych-vod-z-povrchoveho-odtoku-i>.
- [10] A Master Framework for UWCS Sustainability (April, 2013), Available: <http://www.trust-i.net>
- [11] Technical documentation Fiedler-magr – Manual M4016.
- [12] G. Markovič, Z. Vranayová, Infiltration as a means of surface water drainage, Košice : TU - 2013. - 137 s.. - ISBN 978-80-553-1541-6. .
- [13] P. Hlavínek, “ Rainwater management in urban areas,” ARDEC s.r.o., ISBN 80-86020-55-X, 2007.
- [14] P.J. Coombes, G. Kuczera, J. Argue, J.D. Kalma, “An evaluation of the benefits of source control measures at the regional scale,” Urban Water, vol. 4 (4), 2002a, pp. 307-320.
- [15] V.G. Mitchell, R.G. Mein, T.A. McMahon, “Evaluating the resource potential of stormwater and wastewater an Australian perspective,” Australian Journal of Water Resources, vol. 2(1), 1997, pp. 19–22.
- [16] B. Bielek, J. Hires, D. Lukasik, M. Bielek, Development of Technology in Architecture for Sustainable Society, STU BA, monograph, ISBN 978-80-887-3838-5, 2013
- [17] M. Zeleňáková, P. Purcz, I. Gargar, H. Hlavatá, “ Research of Monthly Precipitation Trends in Libya and Slovakia,” Proceedings of the 2014 International Conference on Environmental Science and Geoscience (ESG '14) p.46, March 15-17, 2014, Venice, Italy
- [18] A. Bucur, J. L.López-Bonilla, , “An Approach to the Quality of Drinking Water as a Matter of Multicriterial Decision, Recent advances in energy, environment, ecosystems and development (EEED '13), p.43, July 16-19, 2013, Rhodes island, Greece
- [19] H. Raclavská, J. Drozdova, S. Hartmann, “ Municipal Waste Water Toxicity Evaluation with Vibrio Fisheri, “Recent advances in

environment, energy, ecosystems and development (EEEAD 2013),
p.226, September 28-30, 2013, Venice, Italy

Ahmidat Mohamed is PhD student at the Faculty of Civil Engineering, Technical University in Kosice. He is specialised in Water supply and drainage systems. Recently he has been concentrated on the field of rainwater harvesting and rainwater infiltration systems.

Gabriel Markovič is researcher at the Faculty of Civil Engineering, Technical University in Kosice. He is specialised in Water supply and drainage systems. Recently he has been concentrated on the field of rainwater harvesting and rainwater infiltration systems.

Daniela Kaposztasova is lecturer at the Faculty of Civil Engineering, Technical University in Kosice. She is specialised in Water supply and drainage systems. Recently she has been concentrated on the field of hot water distribution systems and rainwater reuse.

Zuzana Vranayova is the professor at the Civil Engineering Faculty, Technical University in Kosice, Department of Building Services. She is conducting various researches on her major field of study of water supply and drainage system in buildings. She is also actively involved in governmental and academic institutions and committees related to her field of study as chief coordinator and board member. She is a vice dean for education

Socio-hydrological vulnerability: A new science through remote Sensing and GIS

Mukesh Singh Boori, Vit Voženílek

Abstract—Socio-hydrological vulnerability is a new area of research that integrates people and their activities into water science. This type of research is important in water scarce areas such as arid and semi-arid areas on the globe. The main objective of this type of research is to develop a socio-hydrological vulnerability index in semi-arid region by combining remote sensing, bio-geophysical and social data. In general, vulnerability is expressed as a function of the exposure, sensitivity and adaptive capacity of a region to natural disasters and climate change effects. The heart of water security is the ability of water systems to meet changing human and environmental needs. Socio-hydrological vulnerability research ensures that decisions made about our water resources incorporate a range of values and perspectives about the meaning, value and use of water. Presently scientists bring an interest in human values, markets, social organizations and political institutions to the traditional focus of water science on climate, social and hydrology. It is a reality that natural disasters (such as drought and floods) results in sets of socio-hydrological impacts starting with crop-yield failure, unemployment, erosion of assets, income decrease, poor nutrition and decreasing risk absorptive capacity, thereby increasing the vulnerability of the community. In addition, it is demonstrated that the severity of these social impacts is experienced differently and depends one hand on socio-hydrological characteristics and on other hand on people's exposure and characteristics, which are respectively named bio-geophysical, hydrology and social vulnerability. Mapping socio-hydrological vulnerability patterns across space and time helps to identify socially and bio-geophysical vulnerable areas and assists with climate change adaptation strategies in areas to projected socio-hydrological vulnerability.

Keywords— Remote Sensing, GIS, Socio-hydrological vulnerability.

I. A NEW SCIENTIFIC APPROACH

Natural disasters and climate change is a global phenomenon which can be adopted and mitigated only through the unified action of the people across the globe. The issue surrounding climate change and its impacts human health, patterns and the intensity of the precipitation, water and the food supplies, energy supplies and the viability of the natural system will be affected as the earth's climate continues to change [1]. Many of these changes are the irreversible and

will shape generations to come. It is therefore vital to engage and mobilize today's young minds to create innovative and the multidisciplinary answers to the many potential problems, to bring them together and promote productive and the informative discussion and to share each other's thoughts, foster ideas and the establish connections can also be the best seen as interactions and the learning between generations each learning from the one another [2]. This type of research work consider semi-arid region, which is experiencing a reduction of water availability due to changes in the climate [3] as well as increase in human water demand for urban supply, irrigation, and other purposes. As such, these regions are broadly representative of water-scarce regions globally those are facing increasing threats to water security [4].

One of the most important impacts of natural disasters and climate change occurs in water resources availability. Surface water and groundwater recharge may be directly affected by change in rainfall and increase in air temperature that causes higher evapotranspiration rates [5]. A direct consequence of changes in stream flow regime is the impact on water supplies. This is expected to lead to decreased water quantity available for different uses, especially to guarantee food supply for population in the arid and semi-arid tropics [6]. Natural disasters and climate change may also affect the function and operation of existing water infrastructure as well as water management practices [7]. Conversely, adaptive water management through forward-looking planning and operation of infrastructure coupled with flexible demand management represent important strategies to face climate change and variability [8]. Social impacts refer to all changes in the way *people* live, work, related and organize. (Inter-organizational Committee on Guidelines and Principles for SIA 1998) More concrete, social impacts concern poverty, loss of life, health effects, loss of community cohesion, loss of time, changing attitudes, impoverished neighborhood, etc... But social impacts are difficult to quantify in monetary terms and are often not estimated ex-ante [9]. However, several studies, like the wide impact-survey in Scotland and the survey on natural disasters experience in Belgium, have concluded that natural disaster victims experience intangible impacts as being even more severe than tangible impacts [10].

Understanding the concept of socio-hydrological vulnerability, its extent, mapping, formulating vulnerability functions enabling risk impact assessments and the gravity of its dynamics at the levels of significance are needed before natural disasters management planning can be put into action[11]. These exercises will aid in recognizing, prioritizing, planning and channeling the resources to improve

Mukesh Singh Boori, was with NOAA/NASA. Now he is with the Dept. of Geo-informatics, Section of Earth Science, Palacky University Olomouc, Czech Republic – Europe. (Ph.:+420585634519(O); +420732287744(M); +420585639196(R); Email: mukesh.boori@upol.cz).

Vit Voženílek is with the Palacky University Olomouc, 17. listopadu 50, 771 46 Olomouc, Czech Republic. (e-mail: vit.vozenilek@upol.cz).

the capacity to adapt [12]. Furthermore, the existing constraints in financing the adaptation apply equally to all regions. So prioritizing, the regions need special attention and one should take into account the socio-hydrological vulnerability and impacts caused by climate change and natural disasters (drought and flood).

Socio-hydrological vulnerability research will give a brief of the existing approaches that focus on socio-hydrology and impact assessment aid to characterize and identify regions, sectors and communities which are at risk for socio-hydrological vulnerability currently and in the future [13]. It will also discuss the limitation, constraints and pre-requisites in these approaches and highlights the importance of micro level information to have a more realistic understanding of impact and socio-hydrological vulnerability through illustration. Socio-hydrological vulnerability will provide a guiding framework for devising action plans to improve adaptive capacity among vulnerable populations. For this type of research, the socio-hydrological vulnerability index incorporated not only the frequency and intensity of hazard events such as floods, drought conditions, and natural disasters, but also the gradual changes in mean temperature and precipitation. Socio-hydrological vulnerability research will estimate the natural resources of the study area and will be effective for evaluating natural resource mapping and their proper management for future utilization. This type of research work will entails the maximum utilization of existing natural resources to reduce regional imbalances, promote sustainable development and at the same time ensure the protection of fragile eco-environment [14].

II. EMBRYONIC VIGOROUS IMPORTANCE FOR HUMAN-WATER SYSTEM

The main aim of socio-hydrological vulnerability research must be detect the spatial and temporal patterns of socio-hydrological vulnerability due to land use/cover, hydrology and socio-economic changes and to get a deeper insight in the mechanisms of these changes and to contribute to the ongoing debate about the causes and consequences or actual regional condition in arid and semi-arid regions by:

- (i) Build relationships with stakeholder communities to develop a common understanding of their values and what they identify as threats to water security,
- (ii) Collecting reliable data on vegetation degradation, deforestation rates, encroachment of agricultural land, silt deposition in river, flooding, droughts and patterns in the different landscape settings,
- (iii) Understand divergent perspectives on the definition of socio-hydrological vulnerability and the major driving forces for future insecurity,
- (iv) Create a spatial and non-spatial temporal data base of geo-environmental units, soil, slop, surface water bodies, drainage system and non-spatial like demographic data, occupation data and data related to amenities and general facilities, land and power availability (socio-hydrology) etc.

- (v) Assess the social and natural science questions deemed important by stakeholder communities and draw on local knowledge to inform the research,
- (vi) Identify problem and demands of the inhabitants and also distinguish and prioritize the factors that influence development of systems related to socio-hydrological vulnerability,
- (vii) Study societal response to water stress and to economic and policy instruments for socio-hydrological vulnerability,
- (viii) Determine the sustainability of these systems through indicators of economic, social and hydrology,
- (ix) Inform policy options to address water uncertainty and impediments to effective water governance,
- (x) Analyzing the drivers and mechanisms of land cover change with ecosystem and there effect on socio-hydrological vulnerability,
- (xi) Socio-hydrological vulnerability distribution and its dynamic change and cause of its levels,
- (xii) The development of future land use scenario's based on typical pathways of changes.

The focus of socio-hydrology is on observing, understanding and predicting future trajectories of co-evolution of coupled human-water systems. In this sense, one could say that socio-hydrology is the fundamental science. Could we predict this? What will be the role of hydrology in any changes in the landscape including societal changes, and in return, what will be the impact of the societal changes on water cycle dynamics? Should such predictions be the business of hydrologists or social scientists? [15].

III. SOCIO-HYDROLOGY: THE WAY FOR WORLD

Arid and semi-arid regions such as North America, Northeast Brazil, Sahel Africa, Central-eastern Iran, North-west India and Central Australia are interesting because of the change in vegetation cover from dense vegetation to very little or no vegetation as desert area. In these areas living standard are highly variable due to different types of socio-economic activities. There are different types of soil, vegetation cover, climate and relief along its extension. In these areas, many families live in the interior without access to water for drinking, cooking and hygiene. These families live far from the systems of water supply. During periods of severe droughts, these populations are supplied with water by tanker trucks and, in some cases, collecting water from springs and small reservoirs in daily journeys, generally made by women and children. In addition to this, wells and cisterns are the more common water collection and storage systems in these regions [15].

NASA climate and land cover datasets are useful to advance the climate change portion of the socio-hydrological vulnerability assessment. Specifically, changes in temperature and precipitation can measure using monthly NASA's Modern-Era Retrospective Analysis for Research and Applications (MERRA) and Tropical Rainfall Measuring Mission (TRMM) 3B43 datasets, respectively. The satellite data can compare with the weather station data from the

Department of Hydrology and Meteorology in these regions. The socio-economic data can obtain from the Statistics departments to measure the social vulnerability of the population. Historical records of climatic disaster events can acquire from Disaster Information offices to measure exposure to climatic disasters. Land cover maps such as Landsat 7 can useful to identify high-density urban areas prone to the urban heat island effect, and areas prone to landslides and natural disasters.



Fig.1 Arid and semi-arid region on globe.

The datasets should obtain and reviewed with literature review for quality and completeness. Indicators should define as a variable that quantifies and characterizes the level of vulnerability or resilience in these areas. The index must be a consequently composite of the indicators that summarizes overall vulnerability to natural disasters, social factors, hydrological and climate impacts. This type of research work must be focus on data analysis and model building in order to develop the socio-hydrological vulnerability index by following stapes:

- *Literature study and compilation of past and present-day land cover maps for Socio-hydrological vulnerability evaluation using visible and microwave remote sensing multi-temporal and multispectral satellite imagery.*
- *Collection of socio-economic, population, environmental and hydrological data for socio-hydrological vulnerability estimation. Also comprehension of the mechanism of socio-hydrological vulnerability – influencing parameters, special attention on biomass, hydrology and social communities.*
- *Identification of the main socio-economic, biogeophysical and socio-hydrological drivers for land use change with ecosystem and there effect on socio-hydrological vulnerability.*
- *And in last develop future socio-hydrological vulnaribility scenarios and evaluation of possible management strategies.*

Medium and high resolution multispectral satellite imagery (ASTER, AMSR-E, LANDSAT, IRS and SPOT) must be used to compile land cover maps for these areas. The developed spectral signatures should be used to identify upland fields,

forest, scrubland, rangeland, surface water body, potential ground water zone, and degraded areas [16]. For calculating socio-hydrological vulnerability, at least fifteen factors such as elevation, slope, accumulated temperature, flood index, drought index, land use, vegetation, soil, geology, geomorphology, water-soil erosion, socio-economic activities, population density etc. must be use. Reference data for ground calibration and validation would be collect by means of GPS-measurements in representative landscape types. Additional land cover data from available aerial photographs and topographic maps are useful to calibrate and validate the classification procedures in small test areas. These results will allow analyzing the spatial and temporal patterns of land cover and socio-hydrological vulnerability change in these regions.

Table 1 Possible components and indicators which, useful for the vulnerability index.

Component	Indicator
Exposure	Deaths per 100,000 inhabitants (climate-related disasters)
	Losses per GDP in % (climate-related disasters)
	Number of droughts
	Number of floods
Sensitivity	Number of storms
	Land cover
	Forest cover
	Rain-fed agriculture
Adaptive capacity	Cereal yield (crop production)
	Water access (rural)
	Water access (urban)
	Paved roads
	Governance
	Population growth rate
	Population below poverty line
	Vulnerable employment
Rural population	

A balanced weight approach [17] must be used in this index, assuming that each component contributes equally to the index, regardless of the number of indicators under each component. To do this, the component score must be divided by the number of indicators. The weight scheme can be adjust to reflect the perceived importance of specific factors. The application of subjective weighting on the one hand give us some indication of how the relative importance of different factors might vary with context and can also tell us how sensitive socio-hydrological vulnerability ratings will to perception of vulnerability in the expert community. Alos follow on following basic factors, which are affect on study area vulnerability:

- A) Natural impact:
 1. Climatic impact: drought index, rain fall, wind, temperature,
 2. Topographic impact: slope, elevation,

3. Physical impact: geology, geomorphology, soil, vegetation, land use/cover, hydrology,
- B) Environmental impact: hazards, surface and ground water, water-soil erosion, atmospheric composition, biogeography and biodiversity,
- C) Human impact: road density, population density, socio-economic characteristics.

Indicators must be select based on the statistical analysis. Multiple indicators should select to represent each of the three major components of socio-hydrological vulnerability (exposure, sensitivity and adaptive capacity). If no statistically significant relationship could be ascertained between a candidate indicator and socio-hydrology, the indicator must remove from consideration. The indicators should also taste for autocorrelation. Further, selected indicators use to calculate the socio-hydrological vulnerability index as outlined below. The results of the calculation will map on a Geographic Information System (ArcMap) to determine the geographical distribution of socio-hydrological vulnerability; the results should subsequently compare with statistical results at the global level.

Each indicator should measure on a different scale (or different units), so it's necessary to standardize them. In order to carry out the conversion, the values should index and represent as a percentage of the maximum for that indicator:

$$\text{Indicator}_{\text{standardised}} = \frac{\text{Indicator}_{\text{value}}}{\text{Indicator}_{\text{maximum}}}$$

Subsequently the indicator values add to obtain the value of the component:

$$\text{Component value} = \frac{\text{Indicator}_1 + \text{Indicator}_2 + \dots + \text{Indicator}_n}{n}$$

Where n is the number of indicators for a particular component.

Component value should similarly normalize, such that the maximum value for each should 1. The resulting normalize values would then multiply to obtain the index score:

$$\text{Vulnerability score} = \text{Exposure}_{\text{value}} \times \text{Adaptive capacity}_{\text{value}}$$

The index score should also normalize with 1 being the maximum value. The results of the calculation should use to express relative socio-hydrological vulnerability. Values associated with the model would divide into five different categories using the quintile method, with each range cumulatively representing 20% of the maximum vulnerability.

IV. CONCLUSION

The relevance of natural disasters such as droughts, floods and its impacts is well recognized. Socio-hydrological

vulnerability studies have shown that the tropics of South America, Africa, Asia and Australia could experience a significant change in the frequency of occurrence and the intensity of natural disasters [10] and they have a multidimensional effect on humanity in terms of several socio-economic parameters like agriculture, human health, sea level rise, scarcity of labor, disease prevalence, etc. Natural disasters are expected to impact livelihood and their occurrence will further aggravate poverty levels and sustainability of livelihood means in the years to come. The adversities resulting from natural disasters emphasize the importance of strategies needed to cope with the impacts. Unless well-thought strategies are implemented, they can result in a far reaching consequence and cause severe impacts on societies and livelihood especially among the natural resource dependent communities [18]. Managing socio-hydrological vulnerability and enhancing resilience against natural disasters are the major pressing issues particularly among the developing tropical countries of the continents. However, the impacts, socio-hydrological vulnerability and capacity to adapt to these changes differ with time and space [19]. For the same reason, international and national organizations, viz., United Nations Frame work Convention on Climate Change (UNFCCC), World Meteorological Organization (WMO), United Nations Convention to Combat Desertification (UNCCD), etc., are partnered to formalize plans to minimize the impacts.

REFERENCES

- [1] Boori, M.S., Vozenilek, V. (2014), Land use/cover, vulnerability index and exposer intensity. *Journal of Environments*. Vol. 1(1): 01 – 07.
- [2] Boori, M.S., Vozenilek, V. (2014), Remote sensing and GIS for Socio-hydrological vulnerability. *Journal of Geology and Geosciences (JGG)*, ISSN 2329-6755. Vol. 3(3): 01 – 04, [Doi: 10.4172/2329-6755.1000e115](https://doi.org/10.4172/2329-6755.1000e115)
- [3] Boori, M.S., Vozenilek, V., Burian, J. (2014), Land-cover disturbances due to tourism. Proceedings of the Fifth International Conference on Innovations in Bio-Inspired Computing and Applications IBICA 2014. Springer International Publishing, Pages 63-72.
- [4] Brus, J., Boori, M.S., Vozenilek, V. (2013). Detection and visualizations of ecotones – important landscape pattern under uncertainty. *Journal of Earth Science and Climate Change (JESCC)*, ISSN 2157-7617. Vol. 4(3): 01 – 04, [Doi: 10.4172/2169-0316.1000e108](https://doi.org/10.4172/2169-0316.1000e108)
- [5] Boori, M.S., & Ferraro, R.R. (2013), Microwave polarization and gradient ratio (MPGR) for global land surface phenology. *Journal of Geology and Geosciences (JGG)*, ISSN 2329-6755. Vol. 2(2): 01 – 10, [Doi: 10.4172/2329-6755.1000114](https://doi.org/10.4172/2329-6755.1000114)
- [6] Voženílek, V., Morkesová, P., & Vondráková, A. (2014), Cognitive aspects of map symbology in the world school atlases. *Procedia - Social and Behavioral Sciences, Volume 112, Pages 1121-1136*.
- [7] Boori, M.S., & Ferraro, R.R. (2012), Northern Hemisphere snow variation with season and elevation using GIS and AMSR-E data. *Journal of Earth Science*

- and *Climate Change (JESCC)*, ISSN 2157-7617. Vol. S12: 001, Special Issue 2012: 01 – 06, Doi:[10.4172/2157-7617.S12-001](https://doi.org/10.4172/2157-7617.S12-001)
- [8] Boori, M.S., Amaro, V.E., & Targino, A. (2012), Coastal risk assessment and adaptation of the impact of sea-level rise, climate change and hazards: A RS and GIS based approach in Apodi-Mossoro estuary, Northeast Brazil. *International Journal of Geomatics and Geosciences (IJGGS)*, ISSN 0976-4380. Vol. 2(3): 815 – 832.
- [9] Boori, M.S. (2011), [Avaliação de impacto ambiental e gestão dos recursos natuarias no estuário Apodi Mossoró, nordeste do Brasil](#). Library thesis from Federal University of Rio Grande do Norte, Brazil.
- [10] Boori, M.S., & Amaro, V.E. (2011), Natural and eco-environmental vulnerability assessment through multi-temporal satellite data sets in Apodi valley region, Northeast Brazil. *Journal of Geography and Regional Planning (JGRP)*, ISSN 2070-1845. Vol. 4(4): 216 – 230.
- [11] Boori, M.S., & Amaro, V.E. (2011), A remote sensing and GIS based approach for climate change and adaptation due to sea-level rise and hazards in Apodi-Mossoro estuary, Northeast Brazil. *International Journal of Plant, Animal and Environmental Sciences (IJPAES)*, ISSN: 0976-4550. Vol. 1(1): 14–25.
- [12] Evers, M.; Jonoski, A.; Maksimovic, C.; Lange, L.; Ochoa, S.; Cortés, J.; Almoradie, A.; Dinkneh, A. (2012). Enhancing stakeholders` role by collaborative modelling for urban flood risk reduction. *Nat. Hazards Earth Syst. Sci.*, 12, 2821-2842, 2012.
- [13] Boori, M.S., & Amaro, V.E. (2011), A remote sensing approach for vulnerability and environmental change in Apodi valley region, Northeast Brazil. *World Academy of Science, Engineering and Technology (WASET)*, *International Science Index 50, International journal of Environmental, Earth Science and Engineering*, ISSN 1307-6892. Vol. 5(2): 01-11.
- [14] Boori, M.S. (2010), Coastal vulnerability, adaptation and risk assessment due to environmental change in Apodi-Mossoro estuary, Northeast Brazil. *International Journal of Geomatics and Geosciences (IJGGS)*, ISSN 0976-4380. Vol. 1(3): 620 – 638.
- [15] Boori, M.S., Amaro, V.E., & Vital, H. (2010), Coastal ecological sensitivity and risk assessment: A case study of sea level change in Apodi River (Atlantic Ocean), Northeast Brazil. *World Academy of Science, Engineering and Technology (WASET)*, *International Science Index 47, International journal of Environmental, Earth Science and Engineering*, ISSN 1307-6892. Vol. 4(11): 44-53.
- [16] Nevtipilova, V., Pastwa, J., Boori, M.S., Vozenilek, V. (2014), Testing artificial neural network (ANN) for spatial interpolation. *International Journal of Geology and Geosciences (JGG)*, ISSN 2329-6755. Vol. 3(2): 01 – 09, Doi:[10.4172/2329-6755.1000145](https://doi.org/10.4172/2329-6755.1000145)
- [17] Boori, M.S., & Amaro, V.E. (2010), Detecting and understanding drivers of natural and eco-environmental vulnerability due to hydro geophysical parameters, ecosystem and land use change through multispectral satellite data sets in Apodi estuarine, Northeast Brazil. *International Journal of Environmental Sciences (IJES)*, ISSN 0976-4402. Vol. 1(4): 543–557.
- [18] Boori, M.S., & Amaro, V.E. (2010), Land use change detection for environmental management: using multi-temporal, satellite data in Apodi Valley of northeastern Brazil. *Applied GIS International Journal*, ISSN 1832-5505. Vol. 6(2): 1-15.
- [19] Voženílek, V., Michalík, J., Vondráková, A., & Brychtová, A. (2014), Mapping and visualisation of activities in special education. *Procedia - Social and Behavioral Sciences*, Volume 112, Pages 1106-1120.

Prof. Dr. Mukesh S. Boori (Asst. Prof.) involve in European Union Project as well as Visiting Assistant Professor in Palacky University Olomouc, Czech Republic since 04/2013 and University of Leicester (Honorary Fellow 2014) funded by European Union. He joined JECRC University India since 01/2013. He was Scientist in Satellite Climate Studies Branch (NOAA/NASA), selected by National Research Council (NRC), Central Govt. of USA, Washington DC, USA. At the same time he completed his Postdoc from University of Maryland, USA (10/2012). He has done PhD (*EIA & Management of Natural Resources*) from Federal University – RN (UFRN), Natal –RN Brazil (08/2011), funded by Brazil-Italy Govt. fellowship. He has done Predoc (*Earth & Environmental Science*) from Katholieke University Leuven, Belgium (08/2008), selected by Ministry of Human Resource Development (MHRD) New Delhi, India and funded by Govt. of Belgium. He has done MSc (*Remote sensing & GIS*) from MDS University Ajmer (2004) and BSc (*Bio-group*) from University of Rajasthan, Jaipur, India (2002). In early career, he was scientist in JSAC/ISRO (2006-2007) and before that Lecturer (PG) at MDS University Ajmer (2005-2007Sessions). He received international awards/fellowships from UK, USA, Brazil, Italy, Indonesia, Belgium, Czech Republic and India. He known Six Language and visit four Continents for Awards, Meetings, Trainings, Field Trips and Conferences. He is an active Organizing Committee Member in Earth & Space Science Conferences, Co-Chaired a session and gave Conference Opening Ceremony Speech (08/2012) at Chicago, USA. He is editor and member of more than 10 International Scientific Societies/Journals/Committees, related to Earth & Space Science, which include organize conferences. His prime research interest is “EIA and Management of Natural Resources through Remote Sensing & GIS Technology”. He has more than 35 International Publications including Books as a first author on Vulnerability, Risk Assessment and Climate Change.

Research interest: Remote Sensing & GIS, Vulnerability & Risk Assessment, Digital Image Processing, Thermal & Microwave remote sensing, Earth Observation, Land Use/Cover Change Trajectories, Geoscience/Geo-informatics, Bio-Geography, Biodiversity, Hydrology, Climate Change, Environmental Impact Assessment, Management of Natural Resources, Land Resources Management, Sustainable Development & Disaster Management, Remote Sensing Applications in: Forest, Agriculture, Ecosystem, Ecology, Urban & Desert Study.

Improvement of Power Management System in Electro-Solar Vehicle

Hemza SAIDI¹, Abdelhamid MUDOUN²

^{1,3}Electrical Engineering Department, Mohamed Boudiaf University of Science and Technology, Oran, Algeria, e-mail: hamzaing2008@yahoo.fr, ah_midoun@hotmail.com

ABSTRACT

Electric vehicles are ultimately a real answer to current problems related to environmental pollution and noise in cities. In line with current public issues, the electric vehicle is quiet. In addition, it is considered as environmentally friendly since it does not emit CO₂. This paper tries to answer the question 'does solar energy able to compensate fossil energy in the means of land transport?', and highlight a new approach to improve energy management in a solar car. The global objectives of the energy management system are to guarantee the general power balance, and to get the maximal amount of braking energy. Electric vehicle is a complex assembly that includes various parts like mechanical, electrical, control, pneumatic, electrochemical and management etc... A fully autonomous vehicle in real dimensions was built to implement the new strategy and management control using Matlab/Simulink and electronics compounds.

A prototype electric vehicle was built having reached speed of 100km/h and an autonomy range of 60km with a minimum number of PV module and on-board batteries

Keywords-Solar Car, battery management systems, electric vehicle, hybrid power systems, MPPT, traction power supplies.

1. INTRODUCTION

Algeria is among the firsts countries producing oil and gas. And that doesn't prevent the government to implement a policy for the development of Renewable Energies (RE) and adopt gradually mix energy. The objective is to attain 40% of its electricity production from renewable energy source, by 2030, according to its international commitments, to protect the planet.

In this context, efforts to improve air quality in heavily populated urban communities- by reducing vehicular emissions – have rekindled interest in the development of electric vehicle technology. To our knowledge until now no electric vehicle is used in Algeria. Fabricate a solar vehicle presents a tremendous engineering challenge requiring the design and the integration of various aspects of the vehicle as the electric engine, suspensions, the body, the drive train, the fuel system, the electrical systems, and the climate control-chain. All these aspects are time-consuming and costly. The access to energy, the environmental and climate problems, and the need to solve

the mobility problems in the cities are all fields in which electric, hybrid and fuel cells vehicles offer a large attractive prototype and necessary solutions.

This paper addresses the design considerations involved in the electric vehicle conversion which includes: removal of internal combustion engine and related parts, choice of electric vehicle components, installation of electric vehicle accessory system and design of battery chargers with specific applications to electric vehicles. As the battery is the most important part in an electric vehicle therefore the energy density and the power density are the first battery's parameters to be considered. The power density of proton exchange membrane fuel cells (PEMFC) is significantly higher and it is able to work at ambient temperature. Most of the car companies develop big efforts to integrate the PEM fuel cells in a small part of the car body.

Many solutions regarding friendly alternate vehicles are raised, and the questions regarding practical development of these vehicles owing to their high initial technology development cost. The specialty of these vehicles is they are zero emission vehicles. (Jaegul Lee et al) propose dynamic state, empirical model of energy and power as the state variables derived from electrical behaviour of a lead acid battery system [5].

The empirical model describes the relationship between the total, usable and loss of power and energy under dynamic load conditions. Juan W. Dixon, Micah Ortúzar and Eduardo Wiechmann did work on regenerative braking for an electric vehicle using ultra capacitors [6/7]. (Vidyadhar Gulhane, et al), conclude that the main problems are the poor battery performance, under developed control circuit and inadequate capacity of electric motor to match with the road situation [7].

For the lead-acid batteries used in this work, the energy density is too low to meet the energy requirements when vehicles accelerate, decelerate and brake frequently.

Section II of this paper presents the design environment of the vehicle. **Section III** is devoted to the design of the system. **Sections IV** and **V** present the control and energy management strategy used in the Electro-solar vehicle. Finally, **Section VI** presents a set of simulation results and comments.

Note: During manufacturing, we were constrained to change many parts in the study according to the available

means, and that leads to limit the performance. We have to indicate the lack of tools which are necessary to the achievement of our project we need.

2. DESIGN ENVIRONMENT

The urban drive cycle was used as input to represent the road load. Signals of power were passed through the modules. In a mechanical module, the power was the production of torque and rotation speed fig 1. In the electrical module, the power was the production of voltage and current. The reverse simulation showed if the power was transmitted through vehicle module, traction motor module, energy management and control module and battery module. The forward simulation showed if the power was transmitted through the opposite direction.

The road slope torque T is defined by:

$$T_w = \frac{P}{2} \cdot c_w \cdot A \cdot v^2 \quad (1)$$

$$T_R = k_R \cdot m \cdot g \cdot \cos \alpha \quad (2)$$

$$T_A = k_m \cdot m \cdot a \quad (3)$$

$$T_G = m \cdot g \cdot \sin \alpha \quad (4)$$

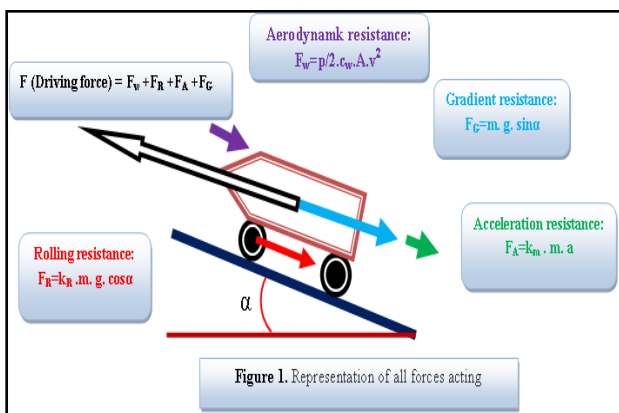
$$T = T_w + T_R + T_A + T_G \quad (5)$$

Where; T_w is aerodynamic torque, T_R : rolling torque, T_A acceleration torque and T_G gradient torque.

Torque evaluation Evaluation of the power flow occurring into a vehicle is in strong relation with his mass and a total couple will be expressed as:

$$C_t = T_A + T_{permanent} \quad (6)$$

Where; m is a vehicle mass, C_t total torque, T_A



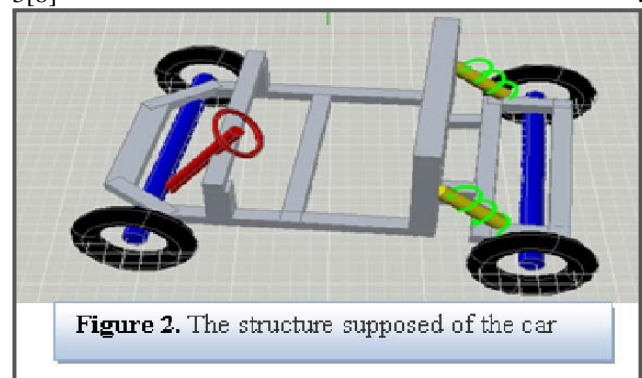
acceleration torque, $T_{permanent}$ permanent torque.

3. SYSTEM DESIGN

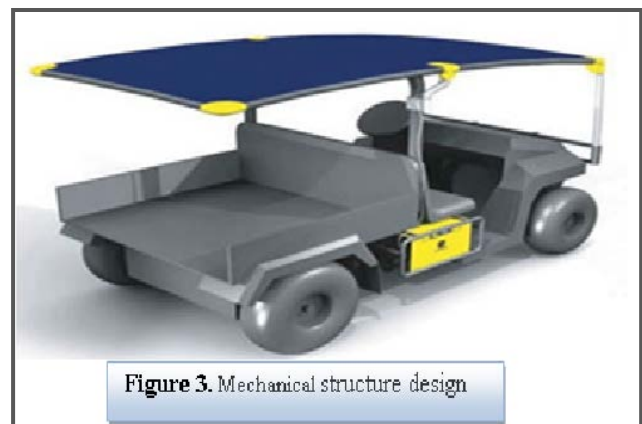
The structure of an electro-solar vehicle is a strong evaluating manner because of the more or less rapid but

steady evolution of the components technology and performance. As electric vehicles, the different parts are an emerging industry, it is necessary to set time constraints and objectives to be achieved at the level of performance cars, like to improve the acceleration performance of the vehicle. There have been remarkable developments in the area of solar cells and in the development of ultra light weight solar charging battery powered cars. The photovoltaic array could provide a large current in a short time, delivering extra energy to meet the energy requirement when it is needed. In addition, the electronics itself is an important constraint in terms of the shape of the car.

AutoCAD software is used to design the vehicle shape in order to choose the best frame vehicle shape and determining the weak points of the vehicle fig 2, fig 3[8]



The front consists of a suspension system coupled with the



vehicle steering system. The suspensions will be considered "double wishbone": they will consist in two triangles, each of them is bound by two hinges one to the frame and the other ball to knuckle. These suspensions are similar to McPherson, often fitted to luxury vehicles or competition one, as they allow an infinite number of settings positions. The study has been divided into four parts:

- First, the double wishbone system have been designed and studied taking into account the expected load for four people,

then the tendering system management will be discussed, after the complete system will be designed to meet final

desired vehicle in terms of safety, functioning, robustness and cost, improvement will be forwarded to the end. The windshield should be made out of a substance with safety in brain.

4. MECHANICAL STRUCTURE DESIGN

This part allowed us to design our vehicle according to standards and technical regulations for Solar Electro Vehicles and the alternative energy imposed by FIA [9] and the equipment available in the market fig4, 5,6,7,8.



Figure 4. The structure of the car industry



Figure 5. The first car manufacturer



Figure 6. The second car manufacturer



Figure 7. Structure of the third car manufacturer



Figure 8. The third car manufacturer

5. ELECTRICAL DESIGN AND CONTROL

In this section all the vehicle elements involved in the energy management will be studied. Management strategies and algorithms will allow us to achieve out a control board, where it will make all the simulations needed for each party. And that, in order to have a reference for comparing the results obtained before and after test operations.

5.1 Solar Cells

The electronic part of this project consist to the objective of the electronic part is the contribution to the optimization of the powering of propulsive parts of the car from batteries powered by photovoltaic panels. Obviously, the major constraint that influenced the treatment of this part came from the settlement of the Solar Challenge of the City; the only source of energy powering the car is solar via battery.

Lead acid batteries called "starters" used in Electro-Solar Vehicle are not well suited to solar energy. In fact, they can be compared to "sprin-ters" to provide common significant start in a very short time (load and rapid discharge). "Solar" battery in turn, rather "Running" will be sought over time to common much lower and the technology is not quite the same (exchange surface

electrolyte / upper electrodes, in particular). Power resources performance at all levels of power; also it will be able to provide the full operation of the battery and motor. We will describe more fully the various bodies in the remainder of this work.

5.2 Influence of Temperature on Cell Efficiency

If the battery is charged directly instead of powering other devices, it is the battery voltage which requires the operation point of the PV panel. The I_{cc} current varies directly with the light radiation (the relationship is proportional) fig 9, the voltage remaining relatively constant. This is interesting, especially for the care of a battery, the temperature also has a significant influence on the characteristics of this panel .When the temperature rises, the voltage decreases and therefore the power too.

Note: that the variation is greater than that provided by simple variation of the exponential. Indeed, the term short circuit current is strongly temperature dependent. The curves in figures 4 and 5 show the drift characteristics this PV panel of crystalline silicon as a function of the temperature.

We see that we move more from an optimal power at 25°C at a deceased power for a temperature 45°C. It is therefore compelled to take into account the temperature of use of the photovoltaic cell in order to apply a reduction coefficient of the optimum at 25°C. Paradoxically, this disadvantage, in very hot climates, becomes an advantage in countries with temperate climate and high brightness fig 10.

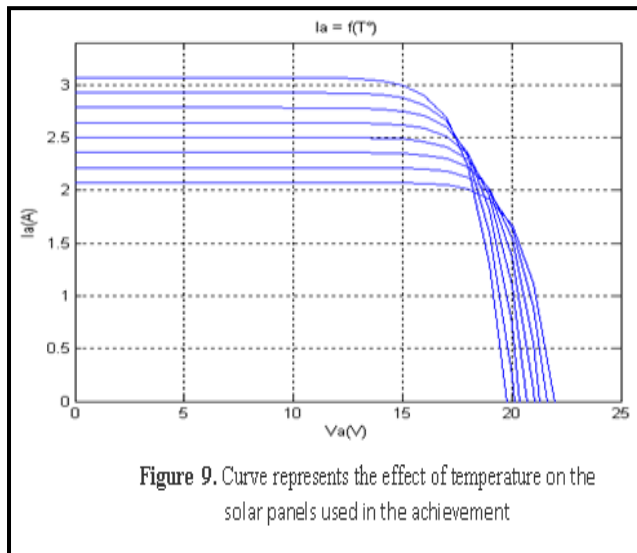


Figure 9. Curve represents the effect of temperature on the solar panels used in the achievement

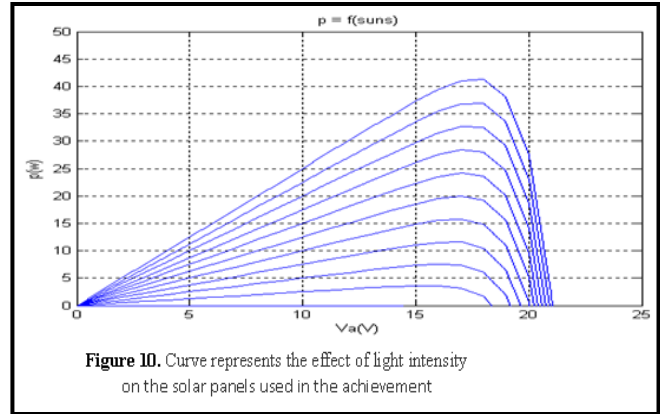


Figure 10. Curve represents the effect of light intensity on the solar panels used in the achievement

5.3 THE SYSTEM DESIGN

Real dimensions of the system are more complex, since there are many additional parameters to consider and many technology choices available. Each step of the design should always seek the best solution and must be performed by considering it with the other steps.

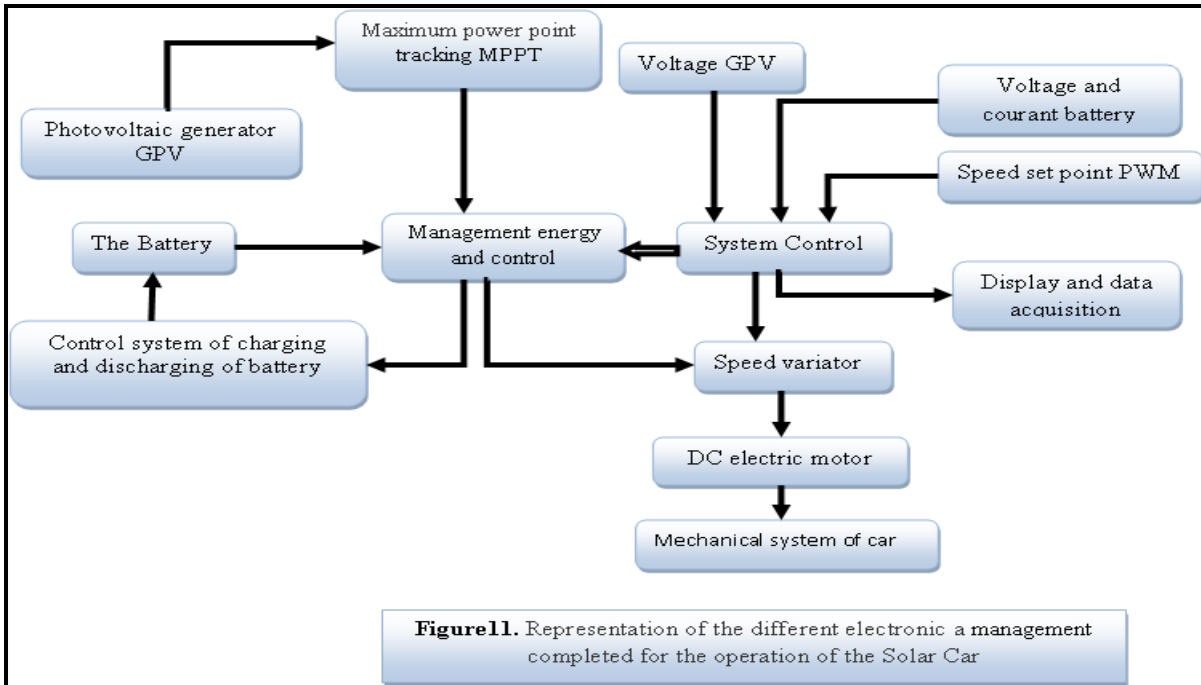
The sizing procedure of the system could be listed as following: Step 1: Identifying the needs: voltage, power and duration of use of equipment ... Step 2: Estimation of solar energy recoverable depending on the location; Step 3: Set the PV module: operating voltage, technology used, total power;

Step 4: Define the capacity and the choice of the battery;

Step 5: Selection of the charge controller; Step 6: Wiring diagram: sections of the cables,...

6. PART ELECTRONICS (PRACTICAL)

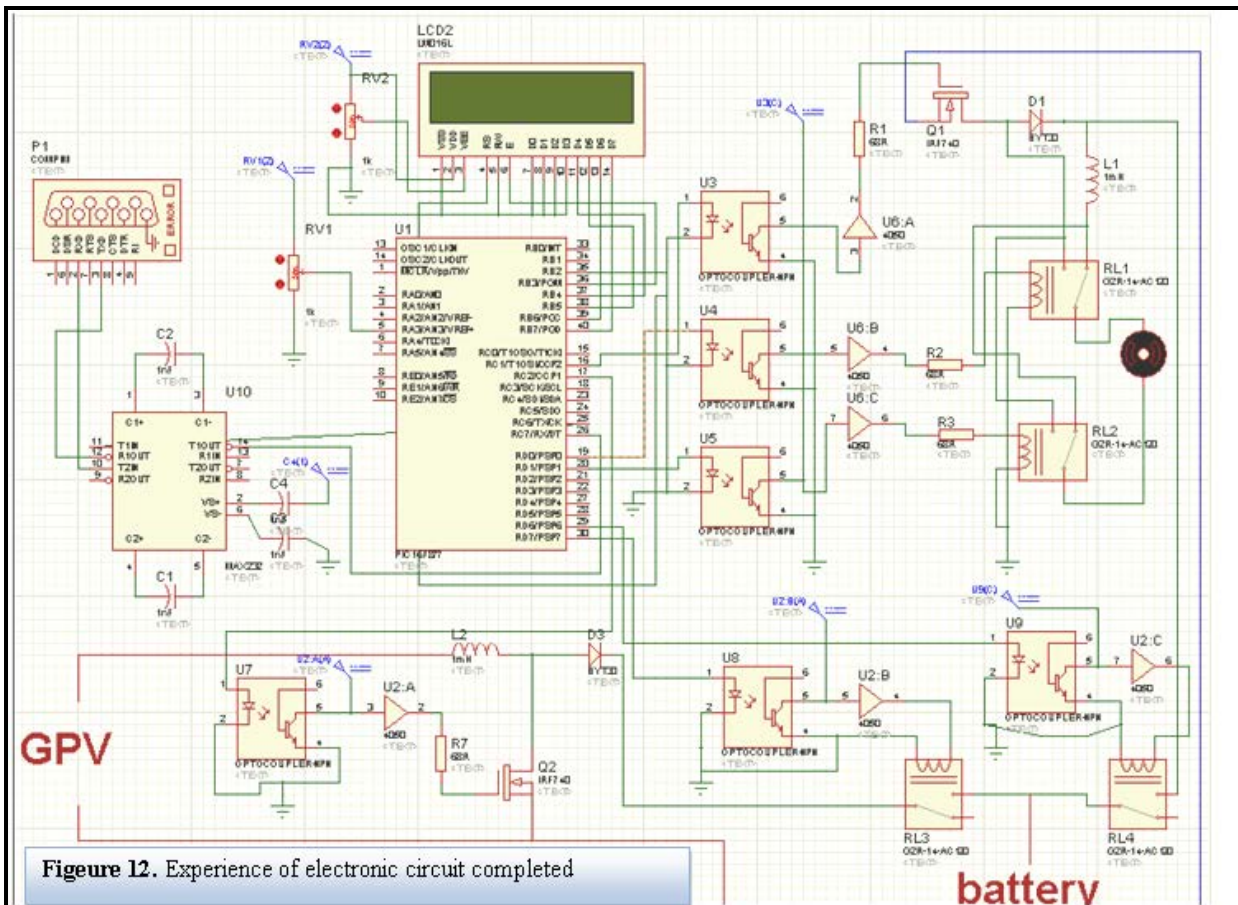
To ensure the effective operation and control of our vehicle, we used all our resources and knowledge. Like all parts of the vehicle fig 11.



6.1

Practical Realization of the Electronics

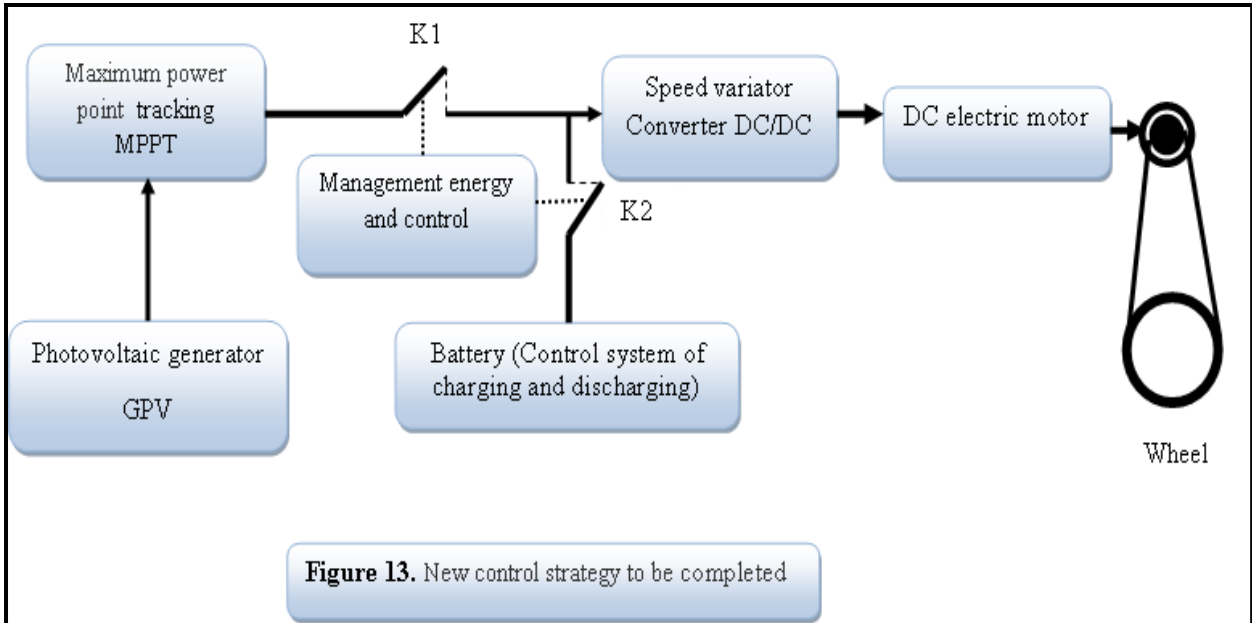
For the implementation, we took into account the synoptic chosen for the desired operation; the failure of one affects all (fig 12).



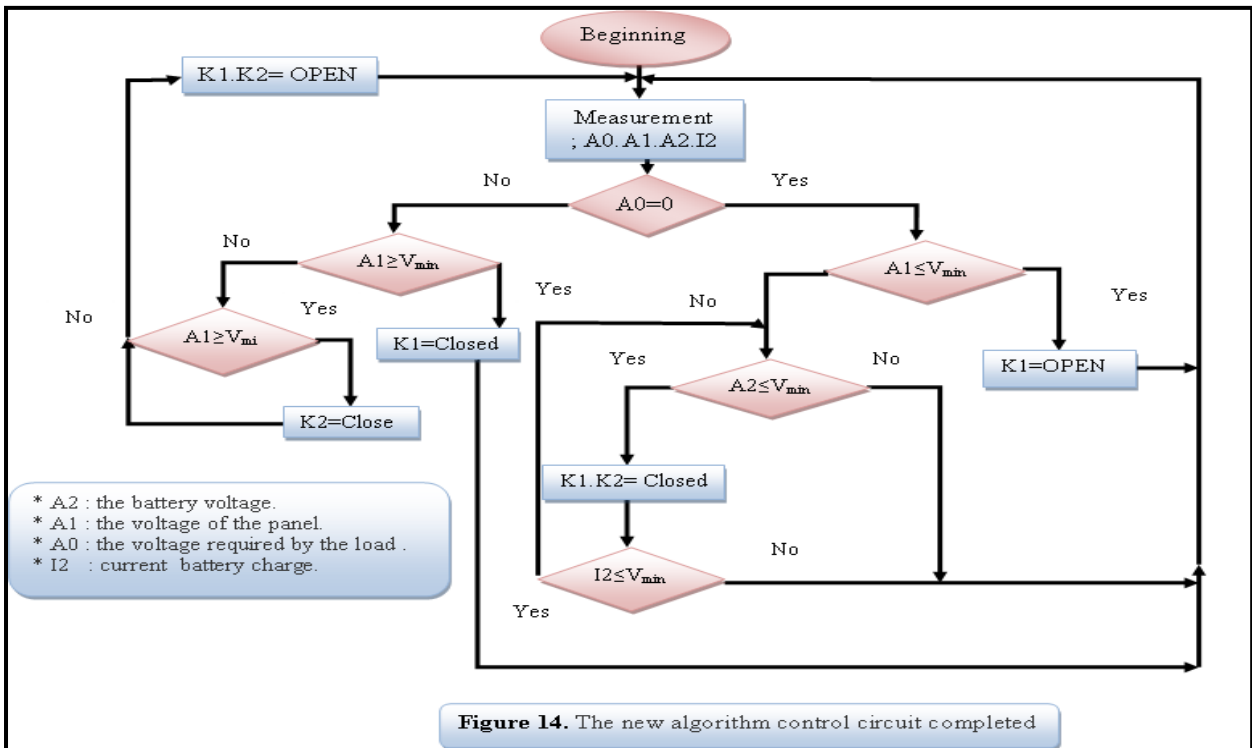
6.2 Operation of Circuit

The vehicle starts with battery mode to provide the current required, after that it rocks to mode panels. Research is going on to develop Brushless DC motor (BLDC motors)

as a prime mover for electric vehicles. These motors possess higher efficiency, lower weight and compact size as compared to others motors fig 13.



The Energy Manager provides load regulation and proper function of the vehicle. The operation manager is described as follows fig 14:



For the proper function of the manager is providing the following algorithm:

- The parameter A2 is the battery voltage;
- The parameter A1 is the voltage of the panel;
- The parameter A0 is the voltage required by the load parameter I2 current battery charge.

6.3 Energy Management of Charge

The energy management strategy aims to fulfill predetermined requirements with no knowledge of future driving conditions. The first step to design the energy management strategy is to define the global strategy

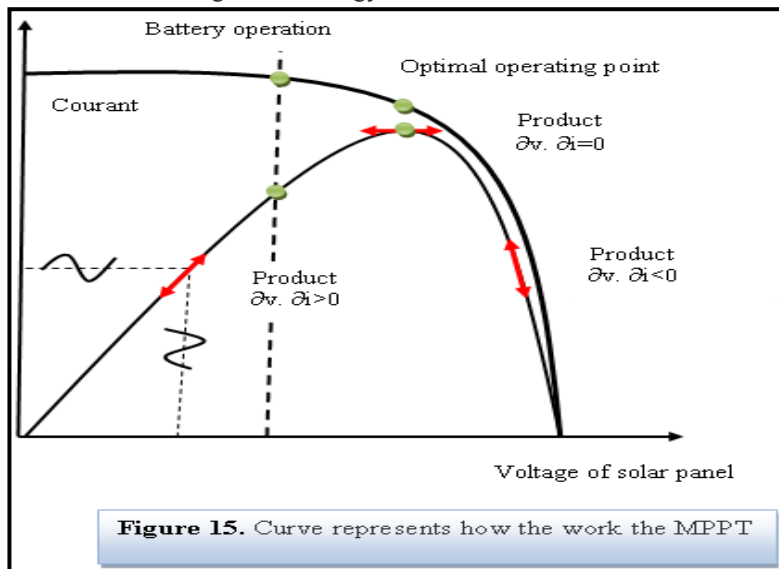
regarding the characteristics and constraints of the vehicle and the hybrid source

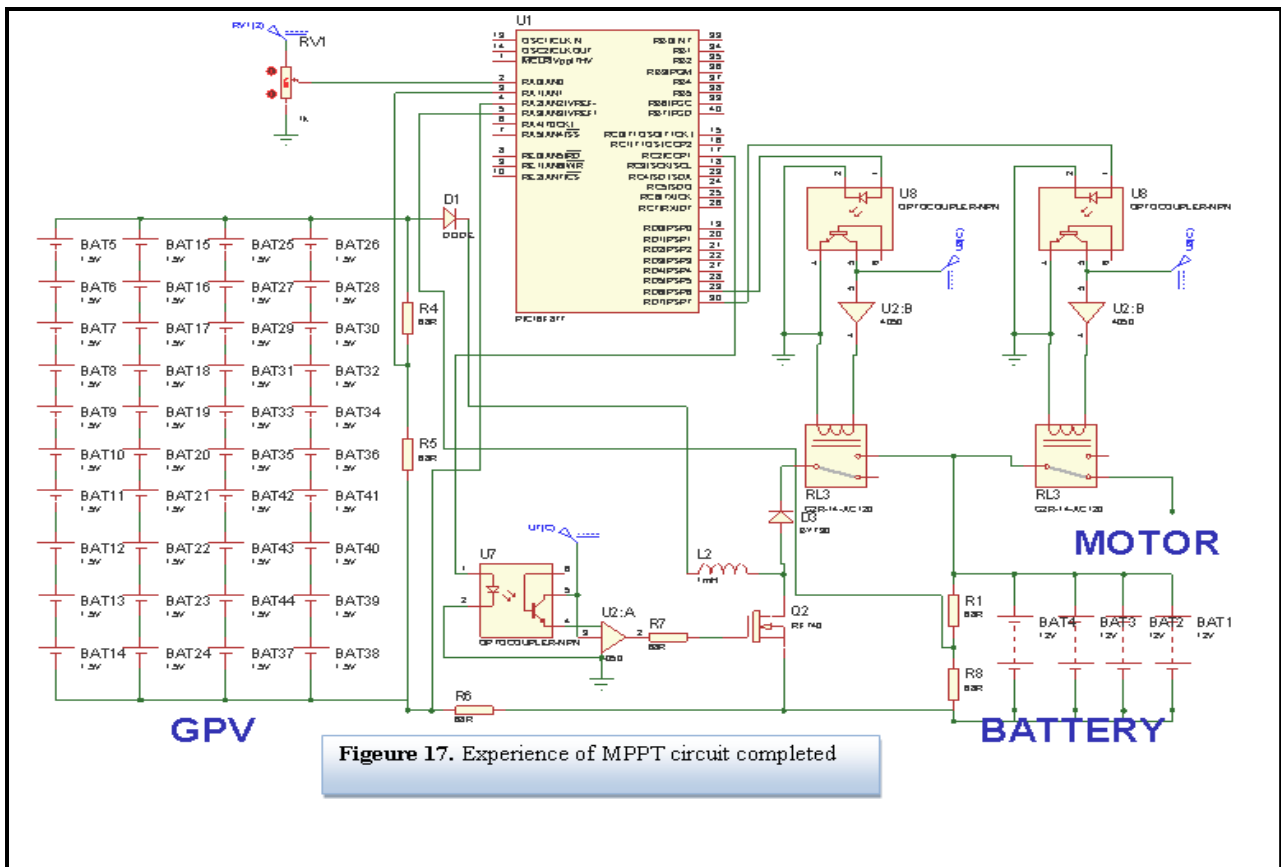
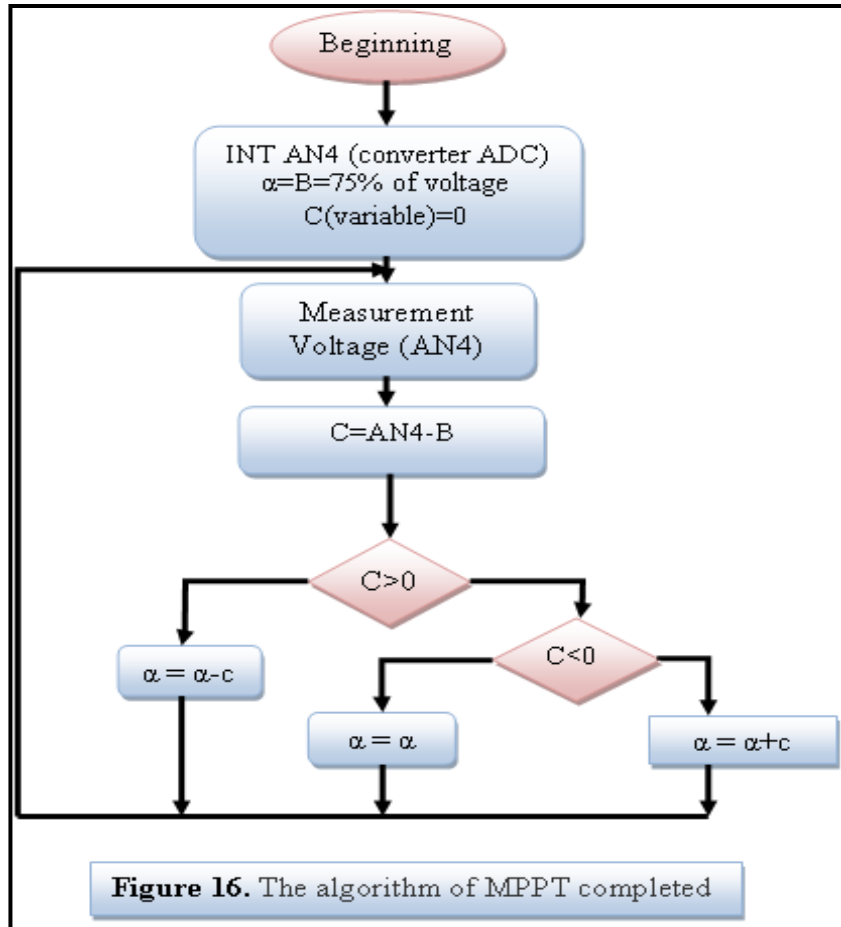
6.4 Mppt

The principle is simple, as we see on the next curve of the characteristic of power, depending on where one is on the curve fig 15, a small voltage change

($dV > 0$) implies either a positive or dI negative, and that's playing on these intensity variations that we will seek to achieve the maximum power point.

For this I have choose the following algorithm for achievement fig 16.





7. EMULATETHE WORK OFTHE CAR

In order to study the operation of the car four modes have been considered:

7.1 Case 1 no batteries

we have undertaken this study to see if we can use solar panels as the only source of energy fig 18 as we studied the effect of light intensity on the speed. Andin order to show the influence of light on speed fig 19, we have re-

simulated, and this time by using the intensity of light fig 20 constantly changing so the results were expected, where speedis directly related to the strong lighting consequently there was lack of control of the car. Consequently, we reached

the conclusion that we cannot use solar panels as the only source of energy, because to get the speed and capacity required to the work of the car, we need more surfaces of solar panels, which not available in this kind of use.

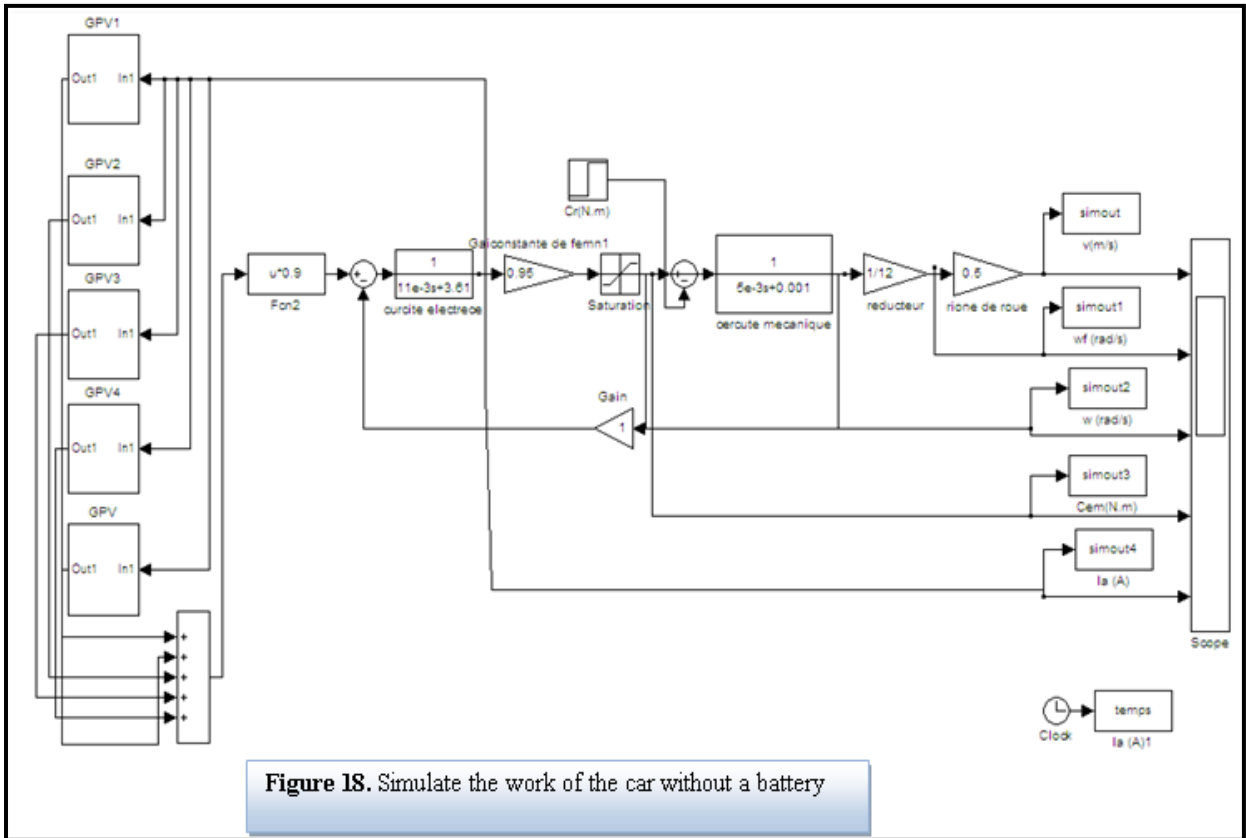


Figure 18. Simulate the work of the car without a battery

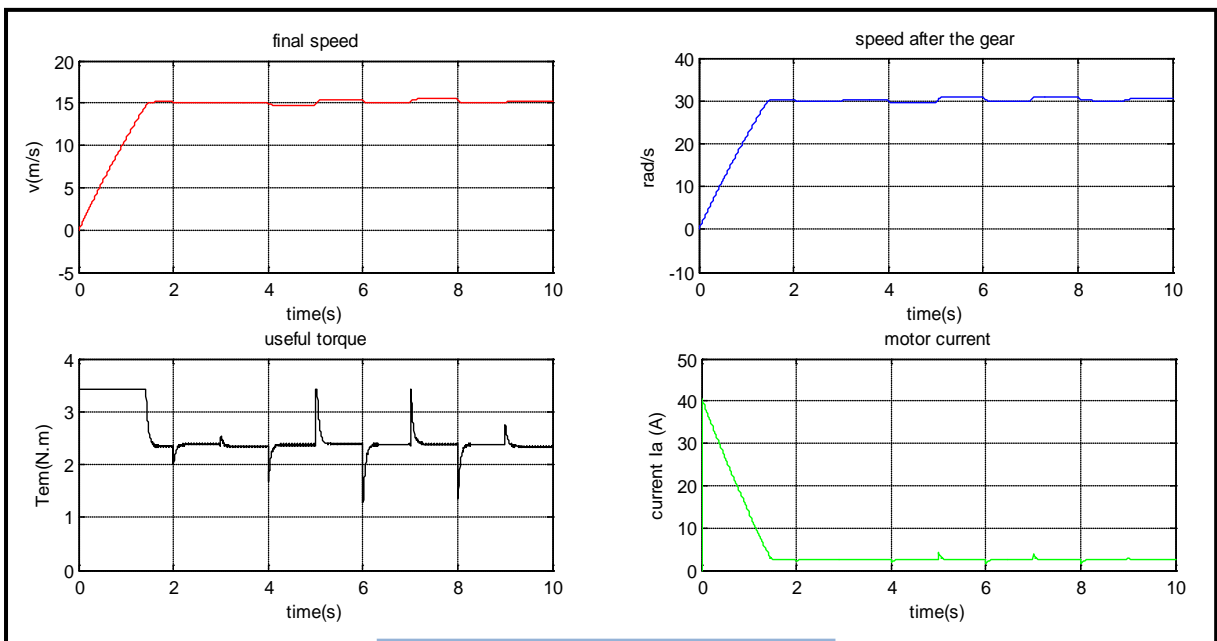


Figure 19 : Case no batteries

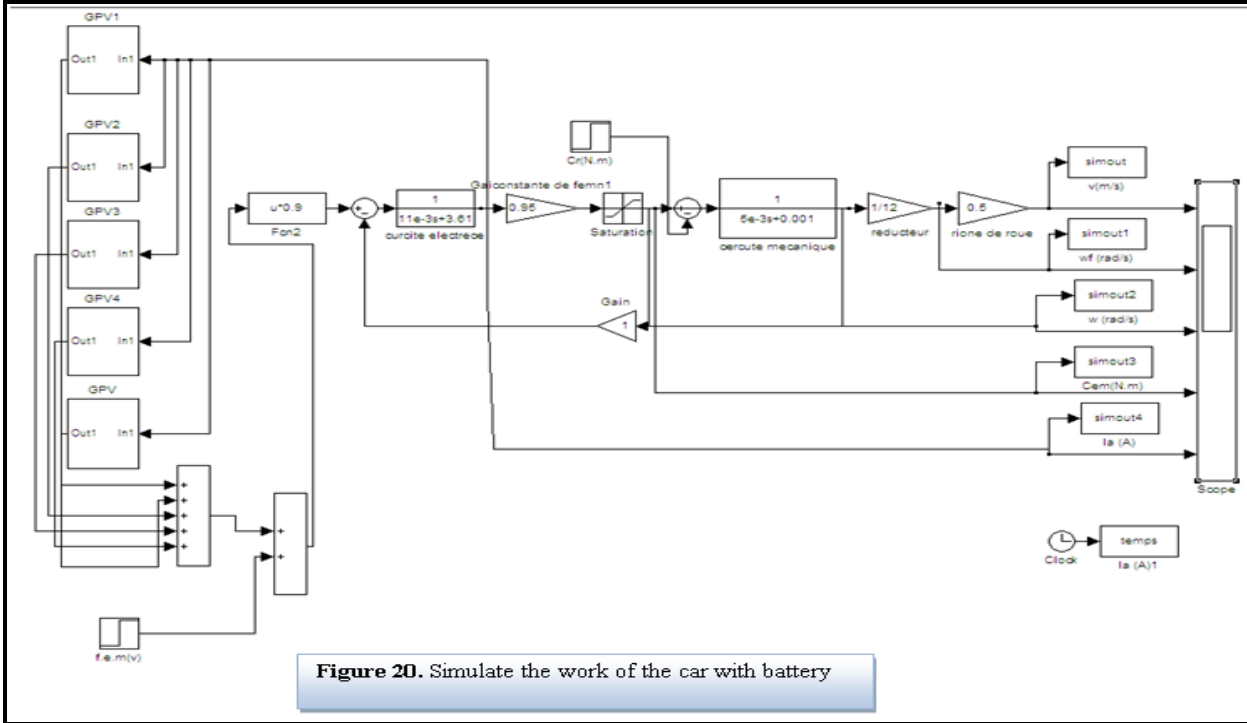


Figure 20. Simulate the work of the car with battery

7.2 Case 2 using the batteries

To solve the problem of changing the speed with changing the climate, we added another source of energy which the batteries fig 21.

Results were that the speed is not related to the climate, to confirm that we did the same simulations again and this time with all the possibilities of function of the car at the same time fig 22.

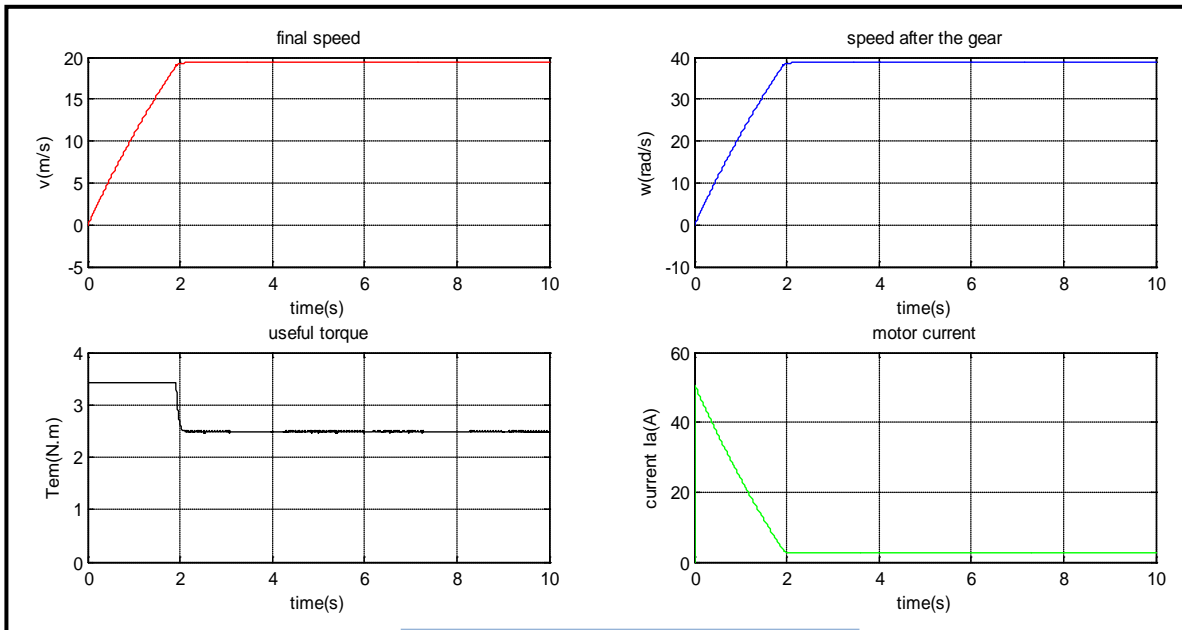


Figure21 : Case no batteries

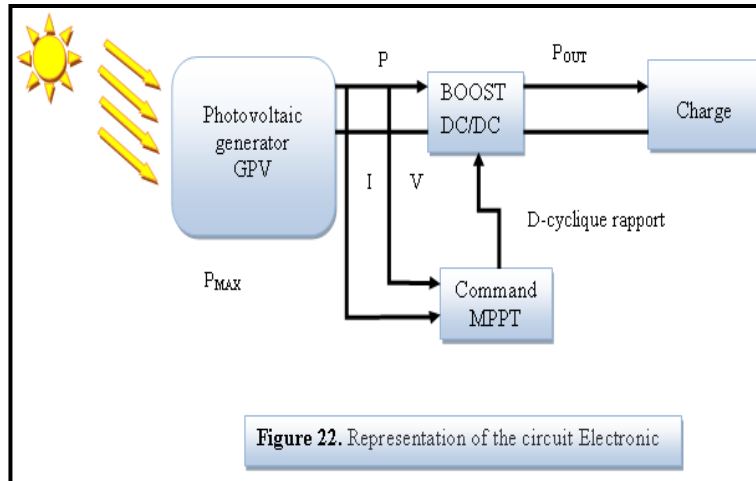


Figure 22. Representation of the circuit Electronic

We noticed that when the car works with batteries it becomes more stable, that the current flowing to the engines is directly related to required speed fig 23.

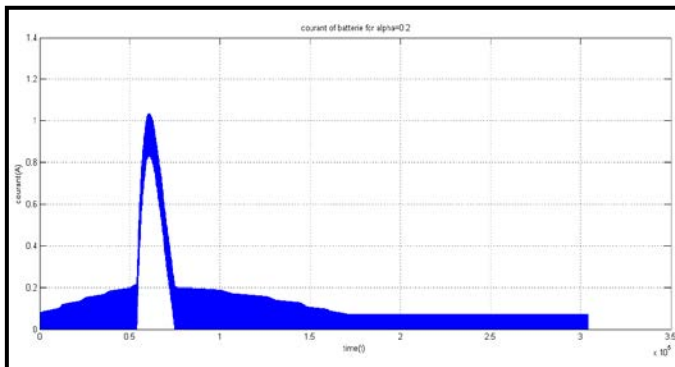


Figure23.Simulationsshow

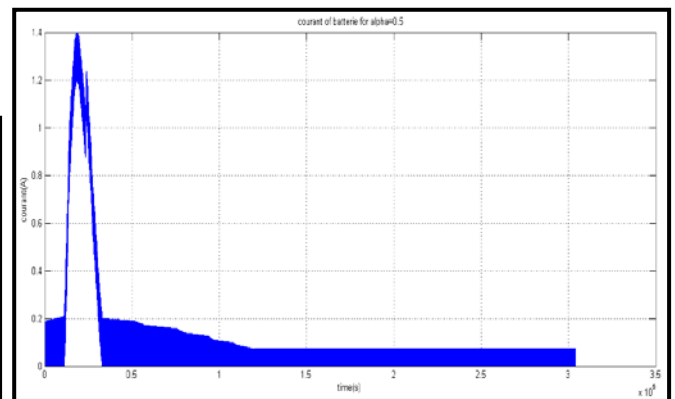


Figure24.Simulationsshowthe courant of the battery for alpha=0.5

7.3 In the case of solar panels and batteries

the situation was more stable, but cannot use this case in the application, because of the difference between the power panels and batteries, according to the total weight, size and maximum speed.

7.4 In the case of solar panels alone

we noticed that the work of the car is related to the factors outside the control, so it cannot be used in practice.

8. SIMULATION OF THE BATTERY CHARGE

This simulation is done by Matlab. We observed the voltage, current, changes in alpha (we took account of all the parameters of the assembly). Simulate the assembly is fig 24:

Notes

we noticed that in all cases the time required to charge the batteries is longer than the duration of the day light fig 25, 26, 27, this stresses that we cannot charge the batteries using the solar panels, and this according to the movement of the car and the charging time, space and the type of solar panels and its output, in relation to each case. In fact there must be another source to charge the batteries and there must be many batteries working in alternation.

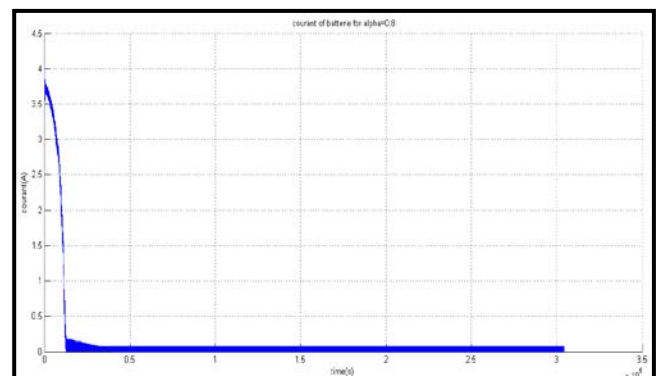


Figure25.Simulationsshowthe courant ofthe batteryfor alpha=0.8

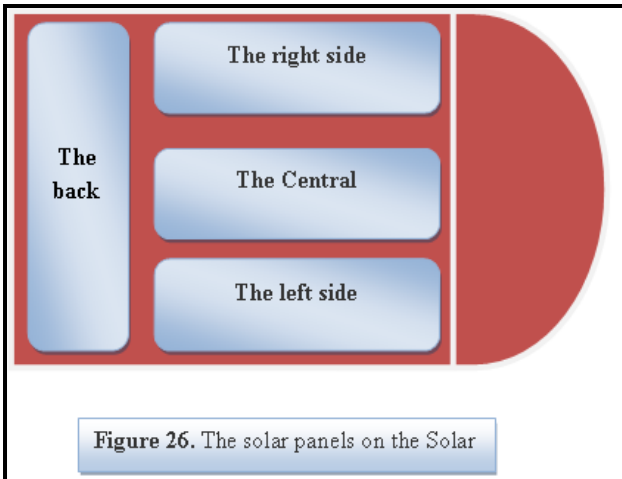


Figure 26. The solar panels on the Solar

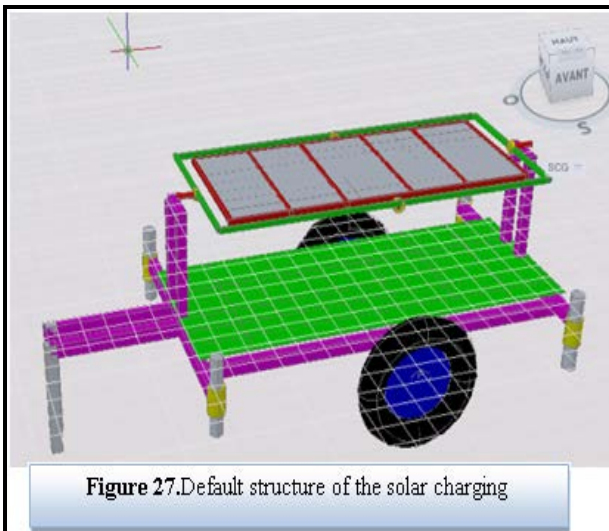


Figure 27. Default structure of the solar charging

9. CLASSIFICATION OF THE VEHICLE ACCORDING TO THE INTERNATIONAL STANDARDS OF THE INTERNATIONAL FEDERATION FOR CARS

We classified our vehicle according to technical criteria for solar power ed vehicles in categories 1 and 4 in the weight class 1 and 8 in the categories of solar electric

propulsion vehicles, and meets the technical regulations of the fourth

10. COMPARISONS WITH OTHER DIRECTORS

If we would like to compare our car with others solar cars, it will better to know even if our car work fully with solar energy. If we look at the cars in the table we note that:

-Engine capacity is greater than the capacity which generate the solar panels, comparing with spacepanels allowed 8 m² (meters square), and the type of panels used.

-In addition to that, the place and the type of the panels does not allow us to use the whole space to produce greater power for energy, because we always have a part which does not produce energy. In the other hand, the solar rays are not perpendicular on the panels, and that decrease its efficiency.

-As well as the battery's type and its capacity; indeed we conclude that the cars are electric -use the batteries to work, the evidence is the total weight and speed and the impossibility to charge the batteries using solar panels only.

-In all cases the time required to charge the batteries is longer than the duration of the day light, this stresses that we cannot charge the batteries using the solar panels, and this according to the movement of the car and the charging time.

Consequently they are not considered as solar cars. And we consider that our results are positive.

11. PROPOSED SOLUTIONS

in order to solve the problems we have the following * the separation of the solar panels from the car and put it in a fixed place fig 29, and make the car work with batteries which, in turn, are charged using solar panels.

For industrialization Follow the following chart fig 30.

This is the unit manufacturer fig 31, 32.

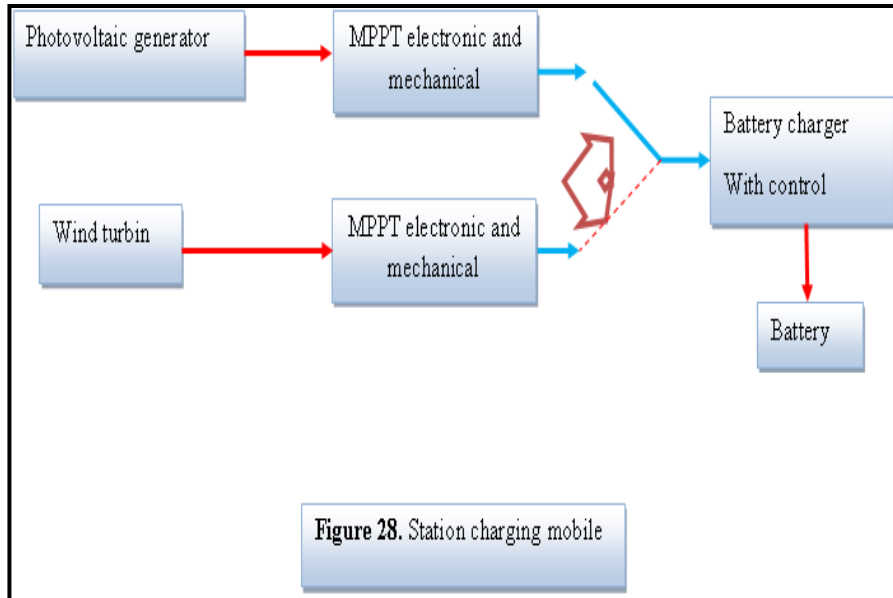
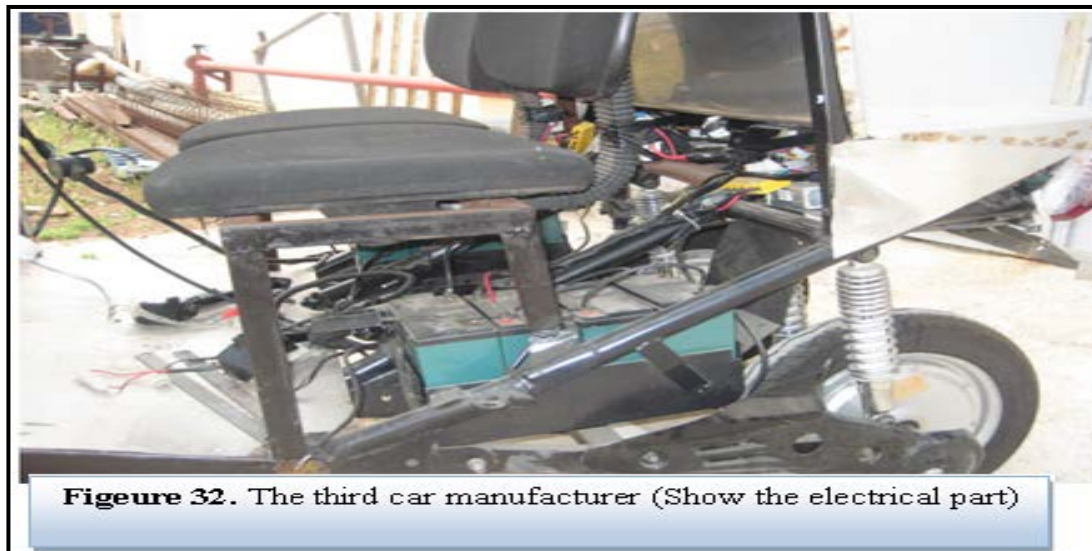
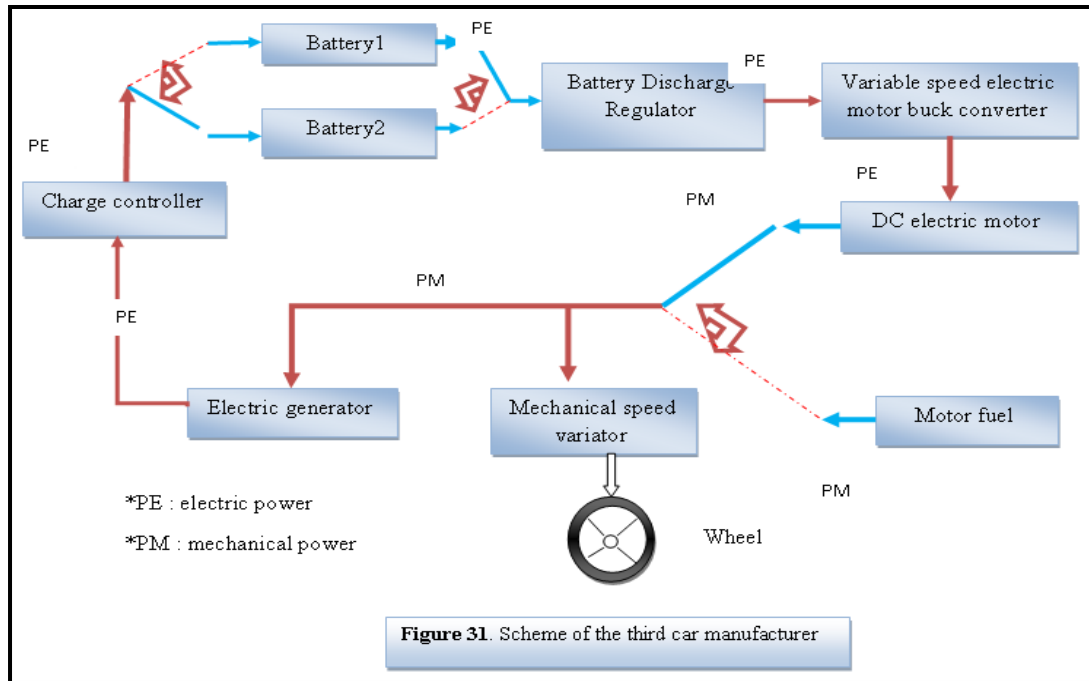


Figure 29. Solar charging unit manufacturer (The front face)



Figure 30. Solar charging unit manufacturer (Back flip)



*As for the time of loading, we've run out of the batteries which are replaced by others charged with solar panels and let the empty to be charged fig 33. The following plans show the mechanism used fig 34.

*We are in the process of experiments in order to replace the batteries by a generator working with the free energy.

12. CONCLUSION

These works aim to design and construct a solar vehicle. This type of engine can be used in open cities (industrial, tourism, golf courses ...). The objective of this work is to achieve a fully autonomous vehicle that is powered by a solar power system equipped with a secondary battery. Our motivations for this project were numerous, but most important was that it is a laboratory for our first confrontation against the design and implementation of such a vehicle.

The implementation of this work needs to study the mechanical and electronic parts; the results obtained are the means for their integration and observation the correlation between them to start up our vehicle. The constraints of this project were numerous. First, it is not easy to build a solar car with little experience; we have established ourselves to achieve a light vehicle and energy optimization. This work was divided into an electronic part and a mechanical part. To do this, we presented the theory, technical problems; the solutions which we thought to solve them, and especially the solutions that we have chosen. But this view was also intended to be reusable, so that our work and our research conserve in the coming years and bring the team to EPES why not win a challenge sun.

A sleek, professional electric vehicle conversion will provide satisfying, economical, and environmentally-friendly transportation.

REFERENCES

- [1] H.C. Lovatt , V.S. Ramsden , B.C. Mecrow “Design of an in-Wheel Motor for a Solar-Powered Electric Vehicle”. IEE Proc-Electr. Power Appl., Vol. 145, No. 5, September 1998, pp 402-408.
- [2] CARICCHI, F., CRESCIMBINI, F., HONORATI, O., DINAPOLI, A., and SANTINI, E.: “Compact wheel direct drive for EVS”, IEEE Ind. Appl. Mag., 1996, pp. 25-32
- [3]. G. Guo Dong , G. Yu Han, L. Chee Ken , “studies of electric motors for light-weight electric vehicle”. Proceeding of Malaysian Universities Transportation Research Forum and Conferences 2010 (MUTRFC2010), 21 December 2010, Universiti Tenaga Nasional. ISBN 978-967-5770-08-1 pp.135-148
- [4] J.Connors, “Telemetric development in solar vehicles with synplify pro software,” The Syndicated, vol. 5, no. 1, pp. 1,3–5, 2005.
- [5] K.D.Huang, S.-C. Tzeng, W.-P. Ma, and M.-F. Wu, “Intelligent solarpowered automobile-ventilation system,” Applied Energy, vol. 80, pp.141–154, 2005.
- [6] A. Riisnaes, C. Allen and P. Winkler. ““Dakota Sun” The Next Generation Solar Powered Racing Vehicle”. IEEEAES Systems Magazine, November 1996. Pp.3-6.
- [7] N. Mutoh, Senior Member, IEEE, and T.Inoue “A Control Method to Charge Series-Connected Ultraelectric Double-Layer Capacitors Suitable for Photovoltaic Generation Systems Combining MPPT Control Method”. IEEE TRANSACTIONS ON INDUSTRIAL ELECTRONICS, VOL. 54, NO. 1, FEBRUARY 2007. Pp.374-383.
- [8] <http://www.google.fr/imgres?imgurl=http://webecoist.momtastic.com/wp-content/uploads/2008/11/10-solar-powered-golf-cart->
- [9] Règlement Technique Energie Alternative / Alternative Energy Technical Regulations. FIA Sport / Technical Department. 11.12.2006
- [10] Techniques d'ingénieur (Conversion photovoltaïque de la cellule aux systems par Stéphan ASTIER)

Novel data-mining methodologies for detecting drug-drug interactions: A review of pharmacovigilance literature

I. Heba, A. Amany, S. E. Ahmed, and S. Amr

Abstract— Pharmacovigilance (PhV) is an important clinical activity with strong implications for population health and conducting clinical research. The overarching goal of PhV is the timely detection of adverse drug events (ADEs) that are novel in their clinical nature, severity, and/or frequency. Until recently, the core of PhV is based on the systematic collection of valid safety data through spontaneous reporting systems (SRSs) that can be rigorously analyzed, interpreted, and acted upon as part of patient care. Data mining algorithms have been developed for the quantitative signal detection of ADEs from such databases. Drug-drug interactions (DDIs) constitute an important problem in the development of new drugs and postmarketing PhV which contribute to 6 - 30% of all ADEs. This article, therefore, reviews studies in which novel mining approaches and/or nontraditional data sources have been proposed for signaling DDIs. The authors provide a focused review of recent methodological innovations and alternative data sources used to support DDIs detection in the postmarketing period. We do not aim to elaborately examine all relevant work. Instead, we presented a synopsis of basic concepts, then following by the involved data-mining algorithms (DMAs) covering the computation of their statistical models, contributions, and major findings from published literature with respect to DDIs. Regarding data mining methodologies, the review is organized according to data source axis. Finally, the authors presented some of the challenges related to the currently used mining algorithms and suggestions for further research for drug interactions (DIs) surveillance are offered.

Keywords —pharmacovigilance, data mining, signal detection, disproportionality analysis, spontaneous reporting system, drug-drug interactions, Electronic Health Record, adverse event

I. Heba is a biomedical informatics researcher with the Department of Information Systems, Faculty of Computers and Information, Helwan University, Egypt (phone: +2 02 23648046; fax: +2 02 23684194; e-mail: pharma_heba@hotmail.com).

A. Amany is a lecturer, Department of Information Systems, Faculty of Computers and Information, Helwan University, Egypt (e-mail: amanyabdo_80@yahoo.com).

S. E. Ahmed is a Chairman, Department of Information Systems, Faculty of Computers and Information, Helwan University, Egypt (e-mail: profase2000@yahoo.com).

S. Amr is a lecturer, the National Organization for Drug Control and Research (NODCAR). He is also the head of the Egyptian pharmacovigilance Center (EPVC), Egyptian Drug Authority (e-mail: amr.saad@Eda.mohealth.gov.eg).

INTRODUCTION

The application domain: pharmacovigilance

Pharmacovigilance (PhV), also known as drug safety surveillance, it has been defined by the World Health Organization (WHO) as “the science and activities relating to the detection, assessment, understanding and prevention of drug-related problems” [1] PhV can be divided into two stages: (1) premarketing surveillance – information regarding adverse drug reactions (ADRs) is collected from pre-clinical screening and phases I to III clinical trials; [2] and (2) postmarketing surveillance – data accumulated in the postapproval stage and throughout a drug’s market life. Although the premarketing controlled randomized clinical trials (RCTs) are considered a hallmark of demonstrating the efficacy of a drug, they may not detect all safety issues related to a particular drug before its use in clinical practice. As they have well recognized limitations, represented in the limited number of study subjects included in the trials (compared with the size of patient populations that may be exposed to the drug once on the market), the limited duration of exposure to the drug per study subject (particularly in case of a drug intended for long-term use), limited or no data for potentially higher risk patient sub-populations that are often excluded from RCTs (e.g., patients with organ impairment, pediatric and geriatric patients, and women of childbearing age who may be treated during pregnancy and lactation), ethnicity restrictions in RCTs of chemotherapeutics [3]. Moreover, premarketing RCTs are not powered to detect rare (incidence of 1 in 10,000) or long-term (latency of > 6 months) adverse drug events [4]. In other means, the efficacy data of a drug is generally more robust and well-established based on premarketing RCTs, while less is known concerning safety profiles [4]. These limitations make it necessary that the marketing authorization holder of a drug and regulatory authority continue to collect, analyze, and interpret data relevant to patient safety that become available after the drug is introduced to market.

Interaction between drug substances is a major cause of morbidity worldwide and a leading source of treatment inefficacy. Drug-drug interactions (DDIs) may account for up to 30% of unexpected adverse drug events [5]. However, premarketing clinical trials focus on establishing the safety and efficacy of single drugs, and don’t typically investigate DDIs [6]. In premarketing trials, patients with multiple drug use are usually excluded. Even when DDIs are suspected DDIs are

suspected, sample sizes and cohort biases limit the ability to discover rare adverse effects [7]. Unfortunately, the interactions between drugs are difficult to study, and there are few predictive methods for discovery novel DDIs. Adverse drug reactions (ADRs) may occur when drug combinations target shared metabolic and pharmacological pathways altering the efficacy and safety profile of the drugs. In other means, the co-administration may alter significantly the safety and efficacy profile of a drug. Drugs may also interact with proteins that are not their primary therapeutic target. Unpredictable adverse events, due to DDIs, can be identified only through postmarketing surveillance and signal detection [8]. Depending on the seriousness of the DDI, different measures are carried out ranging from the introduction of warnings in drug labels to the withdrawal of drugs from the market. As an example, mibefradil, a calcium channel blocker approved by the FDA [9] in June 1997, was shortly withdrawn from the market due to dangerous and even fatal interactions with at least 25 other drugs, including common antibiotics, antihistamines, and cancer drugs, that prolong the QT interval [10]. In contrast, US FDA issued a warning in August 2008 about the possibility of developing major hemorrhagic events through the treatment combination of agrylin with aspirin [11]. In recognition of the challenge of postmarketing surveillance of interaction profiles between different drugs [5] and involvement in patient safety, research into application of data mining approaches on heterogeneous data sources, for DDIs discovery and prediction, have been adopted in recent years.

Data sources of PhV in support of signal detection

Several unique data sources are available for postmarketing PhV. Spontaneous reporting systems (SRSs) have served as the core data collection system for post-marketing drug safety surveillance since 1960s. These are passive systems composed of reports of suspected ADEs collected from health-care professionals, consumers, and pharmaceutical companies, and maintained largely by regulatory and health agencies. Among the prominent SRSs are; the FDA adverse events reporting System (FAERS) [12], the VigiBase co-managed by the World Health Organization (WHO) and the Uppsala Monitoring Centre, Uppsala (UMC), Sweden, which maintains the WHO Global Individual Case Safety Report Database, VigiBase [13], and EudraVigilance managed by the European medicines evaluation agency (EMA) which involving adverse event (AE) reports for medicinal products authorized in the European Economic Area (EEA) EMA [14]. In addition, there are other databases associated with spontaneous reporting such as, the vaccine adverse event reporting systems (VAERS) that is a US program for vaccine safety, co-managed by the Centers for Disease Control and Prevention (CDC) and the Food and Drug Administration (FDA) [15]. These databases are designed to support post-marketing safety surveillance program for drug and therapeutic biologic products. SRSs' structures adhere to the international safety reporting guidance issued by the International Conference on Harmonisation, ICH E2B [16]. Moreover, company safety databases that may allow for earlier detection of safety signals particularly for new products, as they are not subjected to the

delays associated with the public databases SRSs capture information on the drug(s) suspected to cause the adverse drug event (ADE). SRSs provide information on concomitant drugs, indications, suspected events, and limited demographic information in a structured format directly amenable to data mining.

Although the SRSs play a vital role in supporting regulatory decisions for a long list of marketed drugs [17], those passive systems have well recognized limitations, such as missing or incomplete or unspecified data overreporting (adverse events known to be linked to certain drugs are more likely to be reported than other adverse events), duplication of reporting, limited demographic information (age and sex), date of report, fail to provide information about a denominator (i.e., the number of individuals consuming a particular drug) due to SRSs only contain reports of adverse effects, and misattribution causal ADEs links due to unmeasured confounding factors (e.g., disease-related AE, interacting drug(s)).

Other type of data sources for supporting post-marketing surveillance are pharmacoepidemiology databases such as: prescription event monitoring (PEM) in New Zealand [18], the medicine monitoring unit (Memo), general practice research databases (GPRD) in the UK [19] and PHARMO record linkage system in Netherlands. Pharmacoepidemiology is defined by WHO as: "the study of the use and effects/side-effects of drugs in large numbers of people with the purpose of supporting the rational and cost-effective use of drugs in the population thereby improving health outcomes" [20].

These databases have strengths including; 1) Large numbers of patients could provide sufficient power for the analysis; 2) The population could be linked to the corresponding medical, pharmacy and demographic information for a more complete analysis. 3) The detailed information could be followed for a long periods of time. The information in these databases includes demographics, medical diagnosis, treatment, hospitalizations etc., along with date and location of events. There are also options of free text, referral to hospital, all prescriptions (including date, formulation strength, quantity, indication for treatment for new drugs etc.). These databases have enabled researchers to investigate a wide range of hypotheses including PhV [21]. Their creation provides a great opportunity for active surveillance. The active surveillance has the potential to monitor safety signals prospectively when a new drug is marketed for detecting new AEs [22]. Limitations of using these databases in PhV include the following; first, although the availability of a substantial amount of comprehensive information in both structured and unstructured form, only a very small amount of structured data can be accessed by pharmacovigilance applications; Second, data integration from disparate clinical settings is extremely challenging, and the quality of integration can profoundly affects the outcome of pharmacovigilance research; third, real time surveillance is difficult due to the fact that the integration process usually lags behind [23].

For that said; the researchers recently have begun to focus on data sources that have not traditionally been used for PhV. Each of these sources offers promising prospects that may augment existing PhV approaches. Here we discuss some of these information sources.

Text mining of electronic health records (EHRs) could be very useful for detection of safety signal by applying natural language processing (NLP) systems such as MedLEE, BioMedLEE, SemRep, and MetaMap to identify, extract and encode information within EHR systems [24]-[27]. Information from these EHRs is often derived from a defined population with comprehensive, non-specific, capture of clinical important events, these data sources. An EHR is a type of longitudinal observational database (LOD) providing electronic record of patient health information generated by one or more encounters in any care delivery setting. This record includes both structured data, such as laboratory test results, and unstructured data such as narrative reports. As an example, the interaction of beta-blockers and warfarin could affect the risk of hemorrhage in CHF patients was found by using prescription and lab test data in the EHR [28]. The biggest advantage of using EHR systems for pharmacovigilance is the ability to perform active and real time surveillance. However, the majority of the records consist of unstructured narratives, such as discharge summaries, progress reports, or nursing notes which representing the main limitation to be accessed directly by pharmacovigilance applications.

Publically available chemical and biological knowledge bases such as STITCH (search tool for interactions of chemicals), and DDI DrugBank database [29], [30] provide the researchers the chance to create predictive models for potential DDIs. Such databases contain information on molecular structure, protein binding sites, biological pathways of drug action and metabolism, chemical structural similarities between drugs, and linkages between chemical substructures and specific toxicities. Leveraging this type of knowledge provide merits such as possibility to predict toxicological effects in the preclinical drug design stage in aim of decreasing late-stage attrition of new drugs due to toxicity [31]. Additionally, better predictive models can be created by linking chemical and biological knowledge with knowledge on post-marketed drug interaction adverse effects (DIAEs) or enriching subsets of drug interactions generated by other sources likely to be interested for further clinical studies [32].

Although screening the medical/ scientific literature by pharmaceutical companies on adverse reactions related to drugs they commercialize has become mandatory in European countries according to council regulation (EEC 2309/93) volume 9 of Eudralex (i.e., literature research is one of the required steps for standard management procedure in PhV centres), few studies have been conducted by drug safety researchers on mining biomedical literature for extracting new discoveries from the large amounts of biomedical knowledge available [33], [34]. Data mining algorithms (DMAs) in PhV have focused on coded and structured data and therefore miss important clinical data that is relevant to PhV. The biomedical

literature contains ADE-related information based on observations (e.g., case reports) and clinical studies. Analysis of biomedical literature for safety signal detection is challenging and labor intensive due to unstructured nature. Therefore, natural-language processing (NLP) techniques recently developed for extracting ADE-related information or direct/indirect drug interactions have gained large popularity[35]- [37].

The concept of “signal detection” in Pharmacovigilance

In pharmacovigilance, these methods are dedicated to hypothesis generation”, also called “signal detection/generation”, where signal being defined by WHO Uppsala Monitoring Centre (UMC) as: “reported information on a possible causal relationship between an adverse event (AE) and a drug, of which the relationship is unknown or incompletely documented previously” [1]. The term “signal” is primarily used to refer to marketed products. The signal may be a new issue never before seen with a drug, or it may be the worsening or changing of a known AE or problem (e.g., a previously unaffected patient group is experiencing this problem or it is now fatal in those it attacks, whereas before it was not or the incidence has increased, etc.).

The major aim of PhV is the timely detection of either new adverse drug reactions (ADRs) or a change of the frequency and/ or severity of ADRs that are already known to be associated with the drugs involved (i.e., signal detection). The whole process of risk/benefit evaluation depends on effective detection of signals. Signals may be “qualitative” (based on case by case analysis of observations by clinicians, case reports in the literature) or “quantitative” (based on data mining of observational databases, assessment of epidemiologic data, or clinical trials data). The detection of signals requires clinical assessment assisted by epidemiological and statistical analyses.

Despite its inherent limitations, analysis of spontaneous reporting systems (SRSs) for suspected ADRs is a valuable tool in the detection of previously unknown ADRs [38]. Hypothesis generation of new possible adverse effects from such data is referred to as signal detection. The aims of data mining for quantitative signal detection are: to flag potential new signals that might be missed; to earlier identify AEs and decrease person- time expended per AE; to confirm signals that had been clinically first identified; to prioritise resources for signal detection when combined with more traditional methods; to probably distinguish a specific adverse drug effect of a molecule, not shared by its whole therapeutic family; to focus clinical review on the most likely candidates; to detect more complex associations in the data, which are hard to detect by manual review, in particular, drug– drug interactions and to aid prioritisation of potential signals. Safety data mining algorithms (DMAs) have shown high potentialities in the quantitative analysis of the very large PhV spontaneous reporting databases [39] - [43]. Data mining has become a powerful tool for knowledge discovery in biomedical informatics, and particularly useful for hypothesis generation in PhV.

Methodologies for signal detection within spontaneous reporting systems: basic concepts

Disproportionality analysis (DPA) methods for post-marketing drug safety surveillance, which are detailed in several publications, comprise the most widely used analytic methods for signal detection in SRSs [44], [45]. Also, DPAs are the most often data mining methods been described in PhV literature. They are based on measures of disproportionality that require comparisons of observed to expected proportions of drug-adverse event combinations (DECs). Disproportionality analysis (DPA) methodologies are generally be classified into two categories: frequentist and Bayesian. Both approaches use the entries of 2×2 contingency table (see Table I) to derive a statistical association / disproportionality measure. 2×2 contingency table is usually computed for each drug–event pair in the SRS. At the first level, each report generates n “D \times AE associations”, n being the number of drugs notifying one AE. At the aggregated level (the whole database being taken into account), the observed number of cases of each DEC is compared with the estimation of the expected number of cases. As the expected number of cases is calculated using data from the database only, these methods are also named “numerator dependent”. A safety signal is to be generated when there is a discrepancy between the observed number of a DEC within the database and the expected number of cases. In other words, these methods are using the “background noise” summarized in the marginal counts of 2×2 contingency table. Several methods are proposed to estimate the magnitude of the disproportion measure and its confidence interval. DPAs include Proportional Reporting Ratio (PRR) [46], [47], Reporting Odds Ratio (ROR) [45], Information Component (IC) [48], [49], and Multi-item Gamma Poisson Shrinker (GPS or MGPS) [50] are widely used, and currently employed by the Medicines and Healthcare products Regulatory Agency (MHRA), UK, the Netherlands Pharmacovigilance Centre Lareb, the World Health Organization (WHO), and the US FDA, respectively. Although the methodology of the aforementioned algorithms differs, they all share to what extent the number of observed cases differs from the number of expected cases. All of these algorithms calculate signal scores, i.e., the values for PRR, ROR, IC, and EBGM, to assess whether a drug is significantly associated with an adverse event or not.

Classical or frequentist approaches

Frequentist approaches of DPAs involve ROR and PRR. The common feature of these approaches is that they rely solely on information contained in the 2×2 table (table I) corresponding to the drug-event combination (DEC) of interest [51]. A limitation in such a binary approach (i.e. dividing ADRs into two classes: exposed versus non-exposed, as discussed in further detail below) is that with very small observed counts, if the expected count is small, the statistics will fail to screen out such associations, some of which may be false positives [51].

Table 1: Formal 2×2 contingency table

	Suspected event	All other events	Total
Suspected drug	a	b	a + b
All other drugs	c	d	c + d
Total	a + c	b + d	a + b + c + d

The ROR has been described in the PhV literature as an approach for disproportionality analysis of spontaneous data [52], [53]. The ROR was first established in the Netherlands Pharmacovigilance Foundation Lareb [45]. The ROR like traditional odds ratio; it is an estimate of incidence rate ratio, calculating the odds of the AE in those exposed to particular drug divided by the odds of the AE occurring in those not exposed to that drug [54]. The computation of the ROR is based upon the 2×2 table (see Table I). In practice, $ROR - 1.96 \text{ Standard Error (SE)} > 1$ with $p - \text{value} \leq 0.05$ are often used as the criteria to identify signals [55]. The ROR with 95% confidence interval (CI) is computed through the following formulae [56];

$$ROR = \frac{A/B}{C/D} = \frac{AD}{BC} \quad (1)$$

$$95\% \text{ CI} = e^{\ln(ROR) \pm 1.96 \sqrt{\frac{1}{A} + \frac{1}{B} + \frac{1}{C} + \frac{1}{D}}} \quad (2)$$

The PRR, as another metric of frequentist DPAs, was first used by Evans et al. in 2000 to demonstrate the risk of uveitis associated with the use of rifabutin [47], [57]. The PRR measures the strength of association between the suspected ADRs and the suspected drugs, behaving in a similar way to the relative risk (RR) [58]. The higher the value of the PRR is, the stronger the strength of the signal appears to be. The PhV literature suggests two common signal generation criteria for PRR method. The first one is a composite criterion requiring that the number of co-occurrences/observed cases (**a**) is at least equal to 3, PRR measure is at least equal to 2, and chi-squared measure (corresponding to a $p - \text{value of} \leq 0.05$) for this association is at least equal to 4 respectively: $a \geq 3$ and $PRR \geq 2$ and $\chi^2 \geq 4$ [59]. The second is that the lower bound of its 95% confidence interval has to exceed one: $PRR_{0.025} > 1$ [60]. The computation of PRR is same as the RR estimated in epidemiology and can be calculated using the 2×2 contingency table. PRR with 95% confidence interval (CI) can be calculated through the following formulae [61].

$$PRR = \frac{A/(A + C)}{B/(B + D)} = \frac{A(B + D)}{B(A + C)} \quad (3)$$

$$95\% \text{ CI} = e^{\ln(PRR) \pm 1.96 \sqrt{\frac{1}{A} - \frac{1}{A+C} + \frac{1}{B} + \frac{1}{B+D}}} \quad (4)$$

These approaches are easy to understand and more computationally efficient than Bayesian based approaches. However they show limitations involving; some have argued that, for small counts of a specific DEC, frequentist approaches are more liable to extreme values and therefore generating more false positives and also this type of approach

does not adjust the counts for exposure to the various drug combinations and thus does not provide an appropriate statistical context for studying drug interaction [61].

Bayesian approaches

There are currently two major Bayesian techniques used for data mining in pharmacovigilance, the Information Component (IC) [48] and the multi-item Gamma-Poisson shrinker (GPS/MGPS) [50]. Bayesian approaches, based on 2×2 table, calculate an observed to expected ratio in which a database of adverse event reports is mined for the occurrence of significantly unexpected itemsets for relevant drug-AE or drug-drug-AE combination and/or syndromes. Both approaches calculate a Bayesian version of the relative reporting ratio (RRR) or O/E , along with a range of plausible values. For each itemset in the database, a RRR is defined as the observed count ' O ' for that itemset divided by the expected count ' E ' (for drug i and event j) as in the following formula [62];

$$RRR = \frac{\text{observed count 'O'}}{\text{expected count 'E'}} = \frac{N_{ij}}{E_{ij}} = \frac{a(a+b+c+d)}{(a+c)(a+b)} \quad (5)$$

The expected frequency would be the frequency expected under fully independent model, in which the likelihood of a given AE in a report is independent of drug(s) appear in the report. Bayesian approaches are based on Bayes' law to estimate the probability (posterior probability) that the AE occurs given the use of suspect drug by "shrinking" the measure toward the baseline of no association. This shrinkage to the null results in a reduction in spurious associations that have insufficient data to support them. Hence, Bayesian approaches show superiority to frequentist approaches when the available information is extremely limited.

Among the Bayesian approaches is BCPNN that was first adapted to drug safety signal detection by the WHO collaborative centre on pharmacovigilance (WHO-UMC) for International Drug Monitoring, Sweden [48]. Since 1998, WHO has implemented the IC using a Bayesian confidence propagation neural network (BCPNN) for screening international pharmacovigilance database (VigiBase) as part of the routine signal detection process [48], [49], [63], [64]. The BCPNN constructs a null 2×2 table for each AE in the database to achieve a desired null $O/E = 1$. A measure of disproportionality, called the Information Component (IC), and its credibility/ confidence interval is calculated for each drug-adverse reaction combination in the dataset. The IC is defined for a specific drug adverse reaction combination as [49], [65];

$$IC = \log_2 \left[\frac{\text{observed count} + 1/2}{\text{expected count} + 1/2} \right] \quad (6)$$

A signal for drug-ADR pair is detected if the lower limit of the 95% confidence interval ($IC_{0.25}$) exceeds zero. Positive values for $IC_{0.25}$ are highlighted for clinical review.

Another Bayesian approach is the multi-item gamma Poisson shrinker (MGPS) and its predecessor GPS which described by DuMouchel, also named "Dumouchel method" [42], [50]. MGPS is the DMA currently used by some drug regularity

authorities such as US FDA to interrogate signals of drug-AE associations in its SRS database, named as MedWatch [66]. Bayes computes a measure known as the empirical Bayes geometric mean (EBGM). EBGM, which is based on the whole database, is defined as a centrality measure of the posterior distribution of the true RRR in the population; also it is computed by the exponential of expectation value of logarithm of RRR under the posterior probability distributions for a true RRR, which can be represented as following [50], [67];

$$EBGM_{ij} = 2^{\log(RRR)} = 2^{E \log 2_{ij}} \quad (7)$$

MGPS computes an adjusted value of the observed-to-expected reporting ratio (RRR), corrected for temporal trends and for confounding by a particular stratum (e.g. age, sex) [68]. The posterior probability distribution supports the calculation of lower and upper 95% confidence limits (EB05, EB95) for the RRR. The EB05 metric, a lower one-sided 95% confidence limit of the EBGM, is used for signal detection when the EB05 is greater than or equal to the threshold value 2.0 [69]. Typically, the EB05 measure corresponds to the lower 5th percentile of the posterior distribution of RRR; meaning that there is a 95% probability that the true RRR exceeds the EB05.

Performance evaluation of DPAs most used in PhV

Although the comparative performance of DPAs, which are DMAs widely used in routine PhV, is beyond the objectives of this article, the authors believed that it is useful to be touched. Table II shows a comparison among the most frequently used disproportionality algorithms in PhV. Although several studies have been compared DPAs that are routinely applied to the SRSs, those studies mainly have focused on sensitivity. Shortcomings of these studies may be represented in; some have been conducted on a gold standard of limited size, most have focused on fixed thresholds for signal detection, some covered a limited time interval of study, and some examine a narrow spectrum of drug- AE combinations [70]- [72]. Also there are a paucity of studies comparing DPAs' performance in the context of trade-off between sensitivity and specificity [68]. The comparative performance of these methods can be summarized as follows:

- In general, frequentist forms of DPAs (e.g., ROR, PRR) seem to be more sensitive via highlighting a greater number of DECs than Bayesian forms of DPAs (e.g., IC, (M)GPS), while MGPS method has been shown to be the most conservative among DPAs [73];
- Bayesian approaches have showed superiority to frequentist approaches when the available information is extremely limited [45], [74];
- Some of the DECs obtained with frequentist DPAs may be false positives that can be attributed to confounding, thus requiring additional triage criteria for practical implementation, or further investigation by other methods [43];

- For DECAs which are highlighted by both frequentist and Bayesian DPAs, frequentist DPAs tend to do so earlier [75];
- ROR measure performs better than other DPAs from the standpoint of early and timely signal detection [76];
- Both ROR and PRR disproportionality metrics show near equivalence of performance and no obvious advantage of using the ROR over the PRR, in addition; LR-based approaches outperform DPA-based approaches across all levels of sensitivity/specificity [43], [77], [78].

In summary, no single method seems superior as this is highly situation-dependent due to heterogeneity in implementation choices, such as threshold election /titration and the triage logic for signals investigation.

Need for multivariate association approaches

While bivariate/two dimensional (2D) disproportionality analyses (DPA) represent the bulk of daily routine of PhV, higher dimensional associations are important for patient well-being. Although bivariate associations have shown to be adjunct for many of safety analyses, the reduction of ADE analysis to 2D dimensionality may result in missing clinically crucial information. Some studies showed that DDIs may account for up to 30% of all adverse drug events (ADEs) [5] and close to 50% in hospital patients [79]. Multivariate associations may involve detection of DDIs (e.g. drug₁- drug₂ – adverse event/(s)) or drug- induced syndromes in which a constellation of signs and symptoms (e.g. drug-event₁ –event₂ –event₃) exists.

Among the information may be hidden in 2×2 table is confounding factors, also known as covariates or effect modifiers. The term “confounding” refers to a situation when one finds a spurious association or misses a true association between an exposure (i.e. drug) variable and an outcome variable (i.e. disease or adverse event) as a result of a third factor or group of factors referred to as confounding variable(s)” [80]. In other means, confounding may lead to safety signals of spurious associations, if not accounted for. Confounding may be addressed either through design stage of the experiment before data collection (e.g. randomization, matching) or in the analysis stage when the data already been collected (as in case of SRSs). Confounders may be the key to realize potential risk factors or high risk subgroups even in simple 2D associations between a drug and AE. There are several types of confounders, a simpler type, such as confounding by age, gender, and year, have been effectively handled by stratification and Mantel – Haenszel type adjustments where the overall expected count is the sum of the expected counts for each stratum, and is compared to the observed count [81], [82]. However adjustment of confounding by a large number of potential confounders can lead to the missing of signals in the application of data mining [83], [84]. Another limitation, stratification according to age, sex or other variables is not yet relevant; as the number of cases per associations is already low and thus many DECAs may

be unable to reach statistical significance. Additionally; there are other types of confounding involving DDIs, and confounding by co-reporting pairs of drugs, known as “innocent bystander” in which the reported event is associated with the indication for treatment. Adjustments of such confounding types by Mantel – Haenszel methods are not effective [82]. Multiple logistic- regression (LR) is more appropriate approach for such types where large numbers of covariates present. The LR may allow the estimation of a drug– event association by adjusting for the presence of potential confounders; hence it can be applied in the domain of PhV [84].

Methodologies to interrogate drug interactions (DIs) signals in spontaneous reporting databases

Newer approaches have been designed to facilitate identification of higher-order or multivariate associations that represent more complex safety phenomena such as drug–drug interactions (DDIs). In general, the detection of potential DDIs is based on the concept: when a suspected AE is reported more frequently in the combination of two drugs compared with the situation when reported in the absence of other, the drugs combination may indicate the existence of DDI. The currently proposed approaches for quantitative signal detection of DDIs in SRSs include frequentist, Bayesian, and regression approaches as discussed later in further detail.

DPA extensions

DPA extensions to search for mostly three-dimensional associations corresponding to DDIs have been proposed both in **MGPS**, and **IC** measures in which observed-to-expected ratios are calculated in a similar manner but based on three elements (*drug₁ – drug₂ – AE*) [85], [86]. As an example, MGPS has been investigated by Almenoff et al. for AE profiles of combinations between the calcium channel blocker verapamil and three classes of cardiovascular drugs with well-established safety profiles [85]. The authors have identified significant drug associations based on EBGm values for the two drugs and their lower limit of 90% CI being greater than the upper limit of the 90% CI estimate for each of the two drugs. The results suggest that MGPS as a disproportionality analysis is a promising tool for predicting safety profiles of potential drug interactions and safety problems in polytherapy situations.

Multivariate logistic regression (LR)

The LR is a type of predictive modeling that is used to relate a dependent variable with a set of independent variables which has been proposed by Van Puijenbroek [67], [87], [88]. This approach can be used to assess the effect of age, sex and co-

Table II characteristics of most commonly used signal detection algorithms

	Frequentist methods	Bayesian methods
Algorithms	Proportional Reporting Ratio (PRR), Reporting Odds Ratio (ROR)	Information Component (IC), Multi-item Gamma Poisson Shrinker (GPS or MGPS)
Description	ROR: a method to compute a measure similar to odds ratio to quantify the strength of association between a drug and event PRR: a method to compute a measure similar to relative risk to quantify the strength of association between a drug and event	IC: a method to compute logarithmic measure of relative reporting ratio (RRR). MGPS: a method to compute an adjusted value of the Observed-to-expected reporting ratio called empirical Bayes geometric mean (EBGM)
Published signal score thresholds	$ROR - 1.96 SE > 1$ with $p - value \leq 0.05$ $a \geq 3, PRR \geq 2,$ $\chi^2 \geq 4$ and $PRR_{0.025} > 1$	$IC_{025} > 0$ $EB_{05} \geq 2$
Regularity users	Netherlands Pharmacovigilance Foundation Lareb European Medicinal Agency (EMA) - EudraVigilance	WHO-UMC collaborative centre for International Drug Monitoring, Sweden - VigiBase US Food and Drug Administration (FDA) - FAERS
Advantages	More sensitive Easy to understand Easily applicable Adjustments for temporal trends and covariates in logistic regression analyses Earlier signal detection	More specific Configured for detecting higher-order associations (e.g. drug interactions, medical syndromes)
Limitations	Lower specificity leading to false positive signals that may require additional triage criteria	Lower sensitivity leading to false negative associations Showing superiority to be more conservative

morbidity on signal generation. In other mean, LR provides the appropriate statistical context for studying multiple covariates including drug interactions. The LR requires the predictors (drugs and other covariates such as sex and age) first to be selected in advance to be included in the regression model.

It computes RORs by dividing all records in the database into cases and non-cases according to different AEs, all records in cases defined as patients who reported ADRs of interest, while 'noncases' consisted of all other reports.

There have been two publications applying LR for the retrospective detection of DDIs using a SRS database [89], [90]. The first publication by Van Puijenbroek et al. demonstrated potential association between delay of

withdrawal bleeding during concomitant use of oral contraceptives (OCs) and antifungal itraconazole (I) using the Netherlands PhV foundation Lareb which maintains SRS in Netherlands [89]. This interaction had previously only been suggested by case reports after receiving 19 reports of delayed withdrawal bleeding in women receiving OCs; in 10 of these reports OCs and itraconazole (I) were used concomitantly. The analysis of this interaction is based on the concept that target ADR is reported more often on the combination of two drugs compared with the situation where either of these drugs has been used in the absence of the other one. RORs were adjusted for source of reporting (physician or pharmacist), year of reporting, and age. In constructing the logistic model, drug OC, drug (I) as well as the concomitant use of OC and (I) were coded, respectively, by the system according to AE of delay of withdrawal bleeding and the model would then look like:

$$\log(\text{odds}) = \beta_0 + \beta_2 A + \beta_3 S + \beta_4 Y + \beta_5 I + \beta_6 OC + \beta_7 OC * I \quad (8)$$

Where A= age, S= source, Y = reporting year, I = itraconazole, OC = oral contraceptive, $OC * I$ = the concomitant use of both drugs.

The second publication by the same authors assessed the statistical interaction between the use of diuretics and nonsteroidal anti-inflammatory drugs (NSAID), and showed significantly higher use in combination, suggesting decreasing in the efficacy of diuretics resulting in worsening of congestive heart failure (CHF) associated with their combination [90]. The authors calculated RORs and examined the effects of pairs of NSAIDs and diuretics using a logistic regression model with AE case reports of Netherlands PhV foundation LAREB (as in the following formula);

$$\log(\text{odds}) = \beta_0 + \beta_1 N + \beta_2 D + \beta_3 N \times D + \beta_{n-x} C_{n-x} \quad (9)$$

Where N = NSAIDs, D = diuretics, C_{n-x} = different covariates, i.e. age, source, and reporting year. The analysis showed that the use of diuretics or NSAIDs itself was not statistically significantly associated with an increased risk for onset or worsening of symptoms of CHF. However, the odds ratio of the statistical interaction term NSAIDs \times diuretics, was statistically significantly elevated (adjusted ROR 2.0; 95% CI 1.1 to 3.7).

Mining SRS databases by LR approach show some key limitations such as; building predictive model for a single AE and ignoring dependencies/ associations between AEs (like in syndromes), performing regression analyses to very- large-dimensions of predictors (> 10,000 drugs in SRSs), i.e. confounding by comedication by using all drugs in an SRS as regression predictors for an event, represent computational as well a theoretical barrier. However, new extension of logistic regression to very-large-dimensional data, known as Bayesian logistic regression (BLR), can carry out regression analyses with millions of predictors [91]. Caster et al. conducted a study on the WHO SRS (VigiBase) using the BLR algorithm to address confounding caused by co-medication and "masking effect" in which an increase in background reporting of a specific event can attenuate disproportionately values of true association to values of no association [92]. The authors

showed that BLR corrected several real examples of false-positive DECs due to confounding by comedication and also true DECs that were masked by media focus on the withdrawal of a drug causing rhabdomyolysis. In brief, LR/BLR approaches show distinct merits over methods that analyze bivariate associations related to drug safety such as; guarding against masking effects and false signals due to confounding by concomitant drugs, etc.

The Ω Shrinkage measure

The Ω Shrinkage measure was first described by Norén et al. [93] to screen drug interactions (DIs) in SRSs. The authors criticized the logistic regression method in missing some reporting patterns [93] strongly suggestive of potential DIs and they show that the Ω shrinkage measure is a more sophisticated method after conducting a confirmatory study using the WHO database [94]- [96]. The Ω Shrinkage measure calculates an observed-to-expected ratio as a measure of disproportionality and can be calculated according to equation;

$$\log_2 \frac{n_{111} + \alpha}{E_{111} + \alpha} \quad (10)$$

Where E_{111} is the expected value of the incidence of disease suspected to be derived from DI, and α is a tuning parameter, which is set at 0.5 [93] The logarithm of this equation for $\Omega = 0.025$ is a two-sided 95% lower confidence/credibility interval limit which acts as the threshold for generating DI signal when lower bound of its 95% confidence interval exceed zero: $\Omega_{0.025} > 0$ [93].

Qian Yifeng et al. [97] have developed a computerized system aiming to facilitate automated data acquisition, data arrangement and detection of potential DDIs. ADR reports was acquired automatically from the Shanghai ADR SRS which was developed by National Adverse Drug Reaction Monitoring Centre of China. The authors carried out a database-wide screen with three different methods the additive model and multiplicative model, the logistic regression method, and the Ω shrinkage measure method for the detection of possible drug interactions. The three methods were compared according to the detected suspicious DDIs during the database-wide screen. According to results; combinations detected, by at least two methods in average, may reflect the fact that the three methods are highly correlated. The performance of the described system was qualitatively validated by case studies in clinical practice for some of drug interactions detected. After its application in the Shanghai ADR SRS, the authors showed that their system could be a useful tool in detecting and analyzing potential drug interactions for routine surveillance.

Additive and Multiplicative model

The theory of multiplicative and additive models in the context of DDIs signal detection in SRSs has been elaborated by Thakrar et al. by which the detected drug interaction signals could be further identified by statistical test [98]. Referring to

their work, the formulations of the models are based on estimating measure of interaction (coefficient δ) by which the risk associated with drug combination is greater than that predicted for two drugs separately. Risk denote the risk (e.g. incidence rate, odds of developing the event, or percentage of subjects developing a particular event) of an adverse reaction associated with particular drug(s). The formal statistical testing of multiplicative model for interaction coefficient δ is done within the framework of log-linear regression as following:

$$\text{Log}(\text{risk of event}) = \alpha + \beta (\text{drug A}) + \gamma (\text{drug B}) + \delta (\text{drug A and B}) + \text{other covariates} \quad (11)$$

; Where the measure of interaction, the coefficient δ is the PRR associated with the drug combination.

Whilst the formal statistical testing of interaction coefficient of additive model is achieved as follows:

$$\text{Risk of event} = \alpha + \beta (\text{drug A}) + \gamma (\text{drug B}) + \delta (\text{drug A and B}) + \text{other covariates} \quad (12)$$

; Where the measure of interaction, the coefficient δ is the PRR difference associated with drug combination, A and B. The multiplicative model assumed the risk associated with a drug multiplies with the background risk, whilst the additive model assumed the risk associated with a drug adds to the background risk. For multiplicative model, under the assumption that null hypothesis is true (i.e., no interaction), the proportion of an event associated with the drug combination is the same as the product of the proportional risks of individual drugs in the absence of the other ($PRR_{AB} = PRR_A \times PRR_B$) (13). Similarly for the additive model, there is no interaction when the proportion of an event associated with the drug combination is the same as the add of proportional risks of individual drugs ($PRR_{AB} = PRR_A + PRR_B$) (14). DDI signal generated when $PRR_{AB}/PRR_A \times PRR_B > 1$ and $PRR_{AB} - PRR_A - PRR_B > 0$ for multiplicative and additive models respectively and also corresponding $value < 0.05$.

Thakrar et al.'s retrospective study [98] aimed to compare a multiplicative model and an additive model using known interactions of drugs using AE case reports from FDA's AERS. Both models were fitted to four known interactions and to four known non-DDI. The results showed that the additive model has better sensitivity in detecting DI signals and the multiplicative model may further help qualify the strength of the signal detected by the additive model.

Association rule mining

Unsupervised learning techniques have been used as exploratory data analysis to draw inferences of hidden patterns from a dataset. One of these techniques is association rule mining (ARM) [99] which is a well established data-mining technique for discovering interesting relationships hidden in large databases. The technique has been developed in computer science for over a decade and has been used in a variety of fields [100] - [102]. Recently, ARM has been applied in PhV for identification of complex or higher-dimensional drug safety patterns [103].

Apriori algorithm is a type of ARM that partially mitigates the challenge of hard computation of association rules [99]. Its principle is based on considering an item set frequent if its support exceeds the support threshold. An association rule is

an implication expression of the form $X \rightarrow Y$ where x is an item set, Y is an item set and x and y are disjoint. In the case of pharmacovigilance, X denotes a set of drugs and Y denotes a set of AEs. To account for directionality, the general Apriori algorithm works in two steps. The first step searches for item sets that exceed the minimum support, while in the second step, association rules are generated and filtered by selecting “confident” item sets (based on a threshold) from those found in the first step. In other means, an association rule is considered significant if it achieves both minimum support and confidence. The support of an itemset $S(X)$ is the number of records containing X . The support of an association rule $S(X \rightarrow Y)$ is equal to $S(X \cup Y)$. Low support may indicate that a rule has simply occurred by chance. The confidence of a rule $C(X \rightarrow Y)$ is equal to $(S(X \cup Y)) / (S(X))$ (15). Confidence determines how often items in Y appear in records that contain X . Confidence provides an estimate of $(Pr(Y) / (X))$ (16) the conditional probability of Y given X . Although association rules can be filtered by given minimum support and confidence, a variety of measures of “interestingness” have been proposed which can be used to filter these association rules [104]. Multi-item ADE associations are rarely reported in biomedical literature to identify plausible drug-drug interactions.

In a recent study, Harpaz et al. [105] applied an optimized and tailored implementation of the Apriori algorithm to mine a sample of AERS (full set of year 2008) reports with rules at least two drugs and one AE for drug interaction adverse effects (DIAEs) detection. Due to the inappropriateness of standard Apriori scores for PhV applications, the authors used the RRR score instead, with the additional constraint that each rule must have an RRR larger than any of its subsets. The latter constraint was used to exclude spurious associations [106]. The authors showed that ~35% of the DIAE rules corresponded to known associations, thereby demonstrating the potential value of their tailored Apriori algorithm for identifying statistically significant DDIs in SRSs for further investigation.

Methodologies for signaling DDIs using nonstandard data sources or linked multiple data sources

By integrating information from the FDA AERS and several EHRs sources, Tatonetti et al. [107] discovered a potentially new drug interaction between two widely used drugs—the antidepressant paroxetine and the cholesterol-lowering medication pravastatin—that can lead to unexpected increases in blood glucose levels. The finding that motivated their data-mining approach was the observation that side effects are not independent of each other and latent evidence for an (unreported) adverse event can be found by examining other (reported) side effects. By scanning the AERS for pairs of drugs that have matching side-effect profiles when taken together but not when taken individually, the authors created a candidate set of drug–drug interactions. The list of candidates was then narrowed down to the paroxetine–pravastatin interaction by conducting retrospective studies using EHRs from Stanford University Hospital, Vanderbilt University Hospital, and Partners Healthcare. The interaction was

confirmed by a prospective study in an insulin-resistant mouse model.

By linking information from DrugBank database and Human Protein Reference Database (HPRD), Huang J et al. [108] proposed a prediction model of pharmacodynamic DDIs (PD DDIs) using information from heterogeneous data sources which providing information such as drug targets, protein-protein interaction (PPI) network, and side effect similarity. They have predicted 9.626 potential PD DDIs at the accuracy of 82% and the recall of 62%. The proposed model provides opportunities for better understanding the potential molecular mechanisms and physiological effects underlying DDIs. For validation, the authors adopted two independent gold standard positives (GSPs) databases including DrugBank and STITCH [109]. The proposed approach may provide the necessary scientific evidence for the drugs during clinical trials, lead to relabeling drug interaction warning for marketed drugs, and avoiding harmful DDIs or enhancing beneficial drug combination in poly-medication prescriptions.

Villar et al. [110] proposed a model for DDIs based on molecular structure similarity. The authors compiled, from DrugBank database and the Interax Interaction Search engine on the DrugBank website [30], a reference set of drugs and mapped them to two-dimensional molecular fingerprints that represent the presence/ absence of specific structural features. Then, potential drug interactions were generated by screening drug candidates, the 50 most frequently sold drugs in 2009, via comparing their structural fingerprints with the reference set of fingerprints. Highly similar candidates were then retained as the final set of drug candidates. Using this approach, the authors achieved 68% sensitivity and 96% specificity using DrugBank database and Micromedex/Drugdex database as a gold standard reference databases [30]. Moreover, a database of 58 403 new predicted DDIs with structural evidence has been generated which could be useful for further study of possible candidates. This approach can be exploited by regularity authorities in detecting new DDIs that should be contraindicated.

By the same, Villar et al. [111] proposed a predictive method for DDIs on the basis of drug interaction profiles. This method is based on following the concept, if two drugs have similar interaction profile, the drugs with the non intersecting interactions will be DDIs candidates. The authors compiled, from DrugBank database, [112] a reference set of drugs (9.454 well-established DDIs) and mapped them to two-dimensional interaction fingerprints. The model could provide potential 17,230 DDI candidates comparing the interaction profiles of pairs of drugs either in the same or other pharmacological class. For instance, the model detected possible increased effect of antidiabetic Pioglitazone due to its interaction with macrolide antibiotic Clarithromycin.

A recent notable study of the successful detection of novel DDIs through mining of the FDA’s adverse event reporting system (AERS) has been conducted. By linking information from multiple sources (FDA AERS reports through April 2009 and clinical EMR data from Stanford hospital), Nicholas P

Tatonetti et al. [113] proposed a model to predict DDIs in adverse event reports. The authors first constructed profiles to 8 clinically severe adverse event (SAE) classes represented in cholesterol related events, renal impairment, diabetes, liver dysfunction, hepatotoxicity, depression, hypertension, and suicide which were defined through manual expert curation. To construct a predictive model, the authors divided AERS data into two independent sets: reports that listed exactly one drug and reports that listed exactly two drugs. They used the first for training SAE classes computationally and the second for validation. By performing a feature selection and fitting a logistic regression model, the authors identified 171 putative DDIs (for eight adverse event categories). The predictive performance of the model was validated by a hospital's EMR. Through EMR systems, the authors were also able to predict the positive association of paroxetine and pravastatin with increased blood glucose (22.6 mg/dl). The authors claimed that their algorithm may identify hundreds of novel interactions for further study, nevertheless the issue of underreporting in spontaneous reporting systems.

Jon D. Duke et al. [114] describe a novel approach for screening potential drug interactions that increase the risk of myopathy. Myopathy comprises a set of musculoskeletal conditions including muscle pain, weakness, and tissue breakdown (rhabdomyolysis). The authors used biomedical literature mining based on mechanistic properties to predict new DDI signals. Then they validated the resulted drug interactions, which are clinically significant, using a large electronic medical record database (EMR). The authors show that this approach predict five new DDI pairs associated with increased myopathy risk and their associated CYP-mediated metabolism enzymes.

Chung Am Choi et al. [115] examined the potential of using HIRA database as drug interactions (DIs) surveillance database. HIRA is a Korean national health insurance system, consisting of the health information of millions of Korean population including drugs and suspected adverse events (AEs), expressed as diagnoses. ICD-10 codes are used to code all kinds of occurring diagnoses. The authors apply Ω shrinkage measure in HIRA data to the well-known interaction between NSAID and diuretics. A significant disproportionate, correspond to an actual interaction between the two drugs, could be identified with Ω shrinkage measure (0.245) and its 95% lower credibility limit was above zero ($\Omega_{0.95} = 0.247$). This result showed the potential feasibility of HIRA database for DI research.

Closing Remarks, Future Perspectives, and Challenges

In this review, we have shown a portfolio of data-mining approaches and data sources proposed for the analysis and detection of postapproval DDIs. Each approach may renew interest to advance the science of DI surveillance by offering diverse prospects. To our knowledge, this article is the first review of published studies related to screening/detecting signals of DDIs in postmarketing drug safety surveillance programs.

Unfortunately, the interactions between drugs are difficult to study, and there are few predictive methods for discovery novel DDIs. These interactions are not necessarily adverse; sildenafil (Viagra) was developed to treat angina but is now used to treat erectile dysfunction. Some computational algorithms take advantage of these pleiotropic interactions of drugs for predicting off target effects and discovering novel protein targets. Nonetheless, discovering the off target interactions of drugs remains an active area of research.

Potential DDIs are evaluated for experimental drugs pre-clinically during development and then monitored by drug safety surveillance programs after they enter the marketplace. The development of predictive tools, to help study possible DDIs, is of great interest to pharmaceutical companies and regulatory authorities, such as the United States Food and Drug Administration (FDA) [11]. These organizations are interested in better methods to detect and assess drug interactions [116]. It is believed that integration of drug phenotypic, therapeutic, structural, and genomic similarities is promising for disclosing DDIs in drug development and postmarketing surveillance [117]- [119].

New opportunities have emerged to exploit diverse data sources that have not traditionally been used in postmarketing PhV, allowing for active paradigms of DI surveillance and detecting unknown DIs by performing pooled analyses. The purpose of DIs surveillance is to investigate the excess reporting of an event of interest on a combination of two drugs together which is more than reported by each individual drug. Although PhV research is now shifting away from the use of SRSs originating from the relative rarity of reporting DDIs to SRSs, this will not lessen the important value of data mining of SRSs; as SRSs represent the largest collection of population-based clinical data on DIs [120], [121]. The detection of DDIs is much more complicated than the detection of drug-event combinations because of the relatively lower incidence rates and background reporting rates in SRS and in addition, there are still no studies in literature suggesting that any of the proposed DDI detection methods (aforementioned in this article) have been implemented for routine PhV surveillance. Consequently, much effort is needed for developing, implementing and evaluating algorithms for discovering DDIs across disparate data sources for early DDI warnings and routinely DI surveillance.

A central challenge in DI surveillance research is the absence of established guidelines for evaluating the performance of DMAs for DDIs signal detection. Mainly, it is because of absence of gold standard for all possible DI safety profiles for marketed drugs. Consequently, more research is needed to conduct methodological research to evaluate the performance of various analytical methods and to gain better understanding of signaling characteristics of multivariate association measures. We believe that will help in identifying optimal signal-qualifying thresholds in purpose of titrating the threshold of the measure toward a desired level of sensitivity and specificity, and also avoiding costs associated with false-positive and false-negative signals.

In recognition of drug toxicity is a major cause of late-stage product attrition of drug discovery process, early identification about the DI safety profiles of new medicines remains challenging. In Traditional drug discovery, hundreds of new drug molecules are evaluated before a small number of candidates, which mostly relies on scientists' prior knowledge of the therapeutic area, are selected for subsequent laboratory safety testing in cells and animals. In summary, conventional drug development involves the hand-off of drug candidates from medicinal chemists into preclinical testing; followed by a transition to clinical study. Unforeseen DIs can have serious health consequences for patients that probably resulting in serious negative impacts on the whole drug development process. Consequently, there is a need for proposing data mining approaches to explore clinical safety knowledge and derive DIs of new drug candidates in early drug discovery via linking across multiple disciplines; encompassing preclinical, chemical structures, toxicology, drug metabolism, in vitro pharmacology and clinical safety information [122]. We think adopting this strategy in the drug discovery process will add values via providing a way to link clinical safety information to the experimental platforms used in early drug discovery, and enabling the analysis of potential safety issues of drug molecules in the early phases of the drug discovery process resulting in efficient triage of new drug candidates for further testing and elaboration [123].

Last but not least, Data mining does not provide sufficient evidence on causality and they are just adjunctive tool to formulate or strengthen or refine novel hypotheses. In other mean, well-organized clinical reviews remain crucial for further investigation and close surveillance of such safety signals, and data mining approaches should be incorporated into an overall signaling strategy as a first step in a more comprehensive process.

REFERENCES

- [1] Edwards I.R., Aronson J.K. Adverse drug reactions: definitions, diagnosis, and management. *Lancet* 356: 1255-1259, 2000.
- [2] Hartford C.G., Petchel K.S., Mickail H., Perez-Gutthann S., McHale M., Grana J.M., Marquez P. Pharmacovigilance during the pre-approval phases: an evolving pharmaceutical industry model in response to ICH E2E, CIOMS VI, FDA and EMEA/CHMP risk-management guidelines. *Drug Saf*; 29(8):657-73, 2006.
- [3] Sanson-Fisher R.W., Bonevski B., Green L.W., D'Este C. Limitations of the randomized controlled trial in evaluating population-based health interventions. *Am J Prev Med*; 33(2):155-61, 2007.
- [4] Amery W.K. Why there is a need for pharmacovigilance. *Pharmacoepidemiol Drug Saf*; 8(1):61-64, 1999.
- [5] Pirmohamed D., Orme M.L. Drug Interactions of Clinical Importance. In: Davies, D. et al. (Eds.), *Davies's Textbook of adverse Drug Reactions*. London. Chapman & Hall Medical, London, pp. 888-912, 1998.
- [6] Van der Heijden P.G., van Puijenbroek E.P., van Buuren S., van der Hofstede J.W. On the assessment of adverse drug reactions from spontaneous reporting systems: the influence of underreporting on odds ratios. *Stat Med*; 21:2027e44, 2002.
- [7] Olvey E.L., Clauschee S., Malone D.C. Comparison of critical drug-drug interaction listings: the Department of Veterans Affairs medical system and standard reference compendia. *Clin Pharmacol Ther*; 87:48e51, 2010.
- [8] Norén G., Sundberg R., Bate A. A statistical methodology for drug-drug interaction surveillance. *Stat. Med.*; 27:3057-3070, 2008.
- [9] Peter H. Bui, Arnulfo Quesada, Adrian Handforth, and Oliver Hankinson. The Mibefradil Derivative NNC55-0396, a Specific T-Type Calcium Channel Antagonist, Exhibits Less CYP3A4 Inhibition than Mibefradil *Drug Metab. Dispos*; 36:1291-1299, 2008.
- [10] Meinertz T. Mibefradil - a drug which may enhance the propensity for the development of abnormal QT prolongation. *Eur Heart J Suppl* 3: K89-K92, 2001.
- [11] US Food and Drug Administration [online]. Available: <http://www.fda.gov/Drugs/GuidanceComplianceRegulatoryInformation/Surveillance/AdverseDrugEffects/ucm270938.htm>
- [12] The (FAERS): Quarterly Data Files. Available: <http://www.fda.gov/Drugs/GuidanceComplianceRegulatoryInformation/Surveillance/AdverseDrugEffects/ucm082193.htm>
- [13] Lindquist M. VigiBase, the WHO global ICSR database system: basic facts. *Drug Inf J*; 42(5): 409-419, 2008.
- [14] EudraVigilance [online]. Available: http://www.ema.europa.eu/ema/index.jsp?curl=pages/regulation/document_listing/document_listing_000239.jsp
- [15] Vaccine adverse event reporting systems (VAERS). Available: <https://vaers.hhs.gov/index>
- [16] International Conference on Harmonisation, ICH E2B <http://www.ich.org/products/guidelines/efficacy/article/efficacy-guidelines.html>
- [17] Wysowski D.K., Swartz L. Adverse drug event surveillance and drug withdrawals in the United States, 1969-2002: the importance of reporting suspected reactions. *Arch. Intern. Med.* 165, 1363-1369, 2005.
- [18] Coulter DM. "The New Zealand Intensive Medicines Monitoring Programme." *Pharmacoepidemiol Drug Saf* 7(2): 79-90, 1998.
- [19] Wood L., Martinez C. "The general practice research database: role in pharmacovigilance." *Drug Saf* 27(12): 871-881, 2004.
- [20] WHO [online]. Available <http://apps.who.int/medicinedocs/en/d/Js4876e/2.html#Js4876e.2.1>
- [21] Sturkenboom M. "Other database in Europe for the analytic evaluation of drug effects." *Pharmacovigilance* 2nd edition Wiley, chichester, 2007.
- [22] Halpern S.D., Barton T.D. "Epidemiologic studies of adverse effects of anti-retroviral drugs: how well is statistical power reported." *Pharmacoepidemiol Drug Saf* 14(3): 155- 161, 2005.
- [23] Waller P. "Pharmacoepidemiology a tool for public health " *Pharmacoepidemiol Drug Saf* 10(2): 165-172, 2001.
- [24] Aronson A.R. Effective mapping of biomedical text to the UMLS metathesaurus: The MetaMap program. *Proc AMIA Symp*: 17-21, 2001.
- [25] Friedman C., Shagina L., Lussier Y., Hripcsak G. Automated encoding of clinical documents based on natural language processing. *J Am Med Inform Assoc*; 11(5):392-402, 2004.
- [26] Rindflesch T.C., Fiszman M. The interaction of domain knowledge and linguistic structure in natural language processing: Interpreting hypernymic propositions in biomedical text. *J Biomed Inform*; 36(6):462-77, 2003.
- [27] Wang X., Hripcsak G., Markatou M., Friedman C. Drug safety surveillance using de-identified EMR and claims data: issues and challenges. *J Am Med Inform Assoc*; 16(3):328-37, 2009.
- [28] Berlowitz DR, Miller DR, Oliveria SA, Cunningham F, Gomez-Caminero A, Rothendler JA. " Differential associations of beta-blockers with hemorrhagic events for chronic heart failure patients on warfarin." *Pharmacoepidemiol Drug Saf* 15(11): 799-807, 2006.
- [29] Kuhn M., von Mering C., Campillos M., Jensen L.J., Bork P. STITCH: interaction networks of chemicals and proteins. *Nucleic Acids Res* 36: D684-688, 2008.
- [30] DrugBank website. Available: <http://www.drugbank.ca/>
- [31] Vanderwall D.E., et al. Molecular clinical safety intelligence: a system for bridging clinically focused safety knowledge to early-stage drug discovery - the GSK experience. *Drug Discov Today*; 16(15-16):646-53, 2011.
- [32] Vilar S., Uriarte E., Santana L., Tatonetti N.P., Friedman C. Detection of drug-drug interactions by modeling interaction profile fingerprints. *PLoS One.*; 8(3):e58321, 2013.
- [33] Deftereos S.N., Andronis C., Friedla E.J., Persidis A., Persidis A. Drug repurposing and adverse event prediction using high-throughput literature analysis. *Wiley Interdiscip. Rev. Syst. Biol. Med.* 3, 323-334, 2011.

- [34] Shetty, K.D., Dalal S.R. Using information mining of the medical literature to improve drug safety. *J. Am. Med. Inform. Assoc.* 18, 668–674, 2011.
- [35] Botsis T, Nguyen MD, Woo EJ, Markatou M, Ball R. Text mining for the Vaccine Adverse Event Reporting System: medical text classification using informative feature selection. *J Am Med Inform Assoc.*; 18(5):631-8, 2011.
- [36] Gurulingappa H., Mateen-Rajput A., Toldo L. Extraction of potential adverse drug events from medical case reports. *J Biomed Semantics* 20; 3(1):15, 2012.
- [37] Luis Tari, Saadat Anwar, Shanshan Liang, James Cai, Chitta Baral. Discovering drug–drug interactions: a text-mining and reasoning approach based on properties of drug metabolism. Vol. 26 ECCB; pages i547–i553, 2010.
- [38] Rawlins M.D. Spontaneous reporting of adverse drug reactions. II. Uses. *Br J Clin Pharmacol*; 26: 7–11, 1988.
- [39] Bate A., Evans S.J. Quantitative signal detection using spontaneous ADR reporting. *Pharmacoepidemiol Drug Saf*; 18: 427-436, 2009.
- [40] Hauben M., Reich L. Drug-induced pancreatitis: lessons in data mining. *Br J Clin Pharmacol*; 58: 560-562, 2004.
- [41] Almenoff J., Tonning J.M., Gould A.L., et al. Perspectives on the use of data mining in pharmacovigilance. *Drug Saf*; 28: 981-1007, 2005.
- [42] Almenoff J.S., Pattishall E.N., Gibbs T.G., DuMouchel W, Evans SJ and Yuen N. Novel statistical tools for monitoring the safety of marketed drugs. *Clin.Pharmacol. Ther.* 82, 157–166, 2007.
- [43] Hauben M., Bate A. Decision support methods for the detection of adverse events in post-marketing data. *Drug Discov Today*; 14: 343-357, 2009.
- [44] Roux E., Thiessard F., Fourrier A., Bégaud B., Tubert-Bitter P. Evaluation of statistical association measures for the automatic signal generation in pharmacovigilance. *IEEE Tran INF Technol Biomed*; 9:518-27, 2005.
- [45] Van Puijenbroek E.P., Bate A., Leufkens H.G., Lindquist M., Orre R., Egberts A.C. A comparison of measures of disproportionality for signal detection in spontaneous reporting systems for adverse drug reactions. *Pharmacoepidemiol Drug Saf*; 11:3-10, 2002.
- [46] Evans S.J., Waller P.C., and Davis S. Use of proportional reporting ratios (PRRs) for signal generation from spontaneous adverse drug reaction reports. *Pharmacoepidemiol Drug Saf* 10: 483-486, 2001.
- [47] Evans S.J. Pharmacovigilance: a science or fielding emergencies? *Stat Med*; 19:3199-209, 2000.
- [48] A Bate, M Lindquist, I R Edwards, S Olsson, R Orre, A Lansner, R M De Freitas. A Bayesian neural network method for adverse drug reaction signal generation. *Eur J Clin Pharmacol*; 54:315-321, 1998.
- [49] Bate A., Lindquist M., Edwards I.R., Orre R. A data mining approach for signal detection and analysis. *Drug Saf*; 25:393-397, 2002.
- [50] DuMouchel W. Bayesian data mining in large frequency tables, with an application the FDA Spontaneous Reporting System. *Am. Stat.* 53,177–190, 1999.
- [51] Hauben M., Madigan D., Gerrits C.M., Walsh L., Van Puijenbroek EP. The role of data mining in pharmacovigilance. *Expert Opin Drug Saf*; 4(5):929-48, 2005.
- [52] Szarfman A., Machado S.G., O'Neill R.T. Use of screening algorithms and computer systems to efficiently signal higher-than-expected combinations of drugs and events in the US FDA's spontaneous reports database. *Drug Saf.* 25, 381–392, 2002.
- [53] Van der Heijden PGM, van Puijenbroek EP, van Buuren S. On the assessment of adverse drug reactions from spontaneous reporting systems: the influence of under-reporting on odds ratios. *Stat Med*; 21: 2027-44, 2002.
- [54] Almenoff JS, Tonning JM, Gould AL, et al. Perspectives on the Use of Data Mining in Pharmacovigilance. *Drug Saf*; 28:981-1007, 2005.
- [55] Deshpande G., Gogolak V., Sheila W.S. Data mining in drug safety: review of published threshold criteria for defining signals of disproportionate reporting. *Pharmaceut Med*; 24, 37–43, 2010.
- [56] Stricker B.H., Tijssen JGP. Serum sickness-like reactions to cefaclor. *J Clin Epidemiol*; 45:1117-1184, 1992.
- [57] Evans S.J., Waller P.C., Davis S. Use of proportional reporting ratios (PRRs) for signal generation from spontaneous adverse drug reaction reports. *Pharmacoepidemiol Drug Saf*; 10: 483-486, 2001.
- [58] Walter S.D. Choice of effect measure for epidemiological data. *J Clin Epidemiol*; 53(9):931-939, 2000.
- [59] Alsheikh-Ali AA, Abourjaily HM, Karas RH. Risk of adverse events with concomitant use of atorvastatin or simvastatin and glucose-lowering drugs (thiazolidinediones, metformin, sulfonylurea, insulin, and acarbose). *Am J Cardiol*; 89: 1308–10, 2002.
- [60] Deshpande G., Gogolak V., Sheila W.S. Data mining in drug safety: review of published threshold criteria for defining signals of disproportionate reporting. *Pharmaceut Med*; 24, 37–43, 2010.
- [61] Greenland S., Rothman K.J. Introduction to categorical statistics. In: *Modern Epidemiology* (2nd end), Lippincott-Raven: Philadelphia: 231-252, 2001.
- [62] Elisabetta Poluzzi, Emanuel Raschi, Carlo Piccinni, Fabrizio De Ponti. Data Mining Techniques in Pharmacovigilance: Analysis of the Publicly Accessible FDA Adverse Event Reporting System (AERS). 'Computer Science and Engineering', 2012
- [63] Orre R. et al. Bayesian neural networks with confidence estimations applied to data mining. *Comput Stat Data Anal*; 34, 473–493, 2000.
- [64] Stahl M, Lindquist M, Edwards IR, Brown EG. Introducing triage logic as a new strategy for the detection of signals in the WHO Drug Monitoring Database. *Pharmacoepidemiol. Drug Saf*; 13,355–363, 2004.
- [65] Bate A. Bayesian confidence propagation neural network. *Drug Saf*; 30, 623–625, 2007.
- [66] US FDA MedWatch [online]. Available: <http://www.fda.gov/Safety/MedWatch/default.htm>
- [67] DuMouchel W., Pregilbon D. Empirical bayes screening for multi-item associations. Proceedings of the conference on knowledge discovery and data; 26-29; San Diego (CA): ACM Press: 67-76, Aug 2001.
- [68] Harpaz R, DuMouchel W, LePendu P, Bauer-Mehren A, Ryan P, Shah NH. Performance of pharmacovigilance signal-detection algorithms for the FDA adverse event reporting system. *Clin Pharmacol Ther*; 93(6):539-46, 2013.
- [69] Szarfman A, Machado SG, O'Neill RT. Use of screening algorithms and computer systems to efficiently signal higher-than-expected combinations of drugs and events in the US FDA's spontaneous reports database. *Drug Saf*; 25: 381-392, 2002.
- [70] Tamura T, Sakaeda T, Kadoyama K, et al. Omeprazole- and esomeprazole-associated hypomagnesaemia: Data mining of the public version of the FDA Adverse Event Reporting System. *Int J Med Sci*; 9: 322-326, 2012.
- [71] Sakaeda T, Kadoyama K, Okuno Y. Statin-associated muscular and renal adverse events: Data mining of the public version of the FDA Adverse Event Reporting System. *PLoS ONE*; 6: e28124, 2011.
- [72] Sakaeda T, Kadoyama K, Okuno Y. Adverse event profiles of platinum agents: Data mining of the public version of the FDA Adverse Event Reporting System, AERS, and reproducibility of clinical observations. *Int J Med Sci*; 8: 487-491, 2011.
- [73] Toshiyuki Sakaeda, Akiko Tamon, Kaori Kadoyama, Yasushi Okuno. Data Mining of the Public Version of the FDA Adverse Event Reporting System. *Int. J. Med. Sci*; 10(7):796-803, 2013.
- [74] Li C, Xia J, Deng J, Jiang J. A comparison of measures of disproportionality for signal detection on adverse drug reaction spontaneous reporting database of Guangdong province in China. *Pharmacoepidemiol Drug Saf*; 17: 593–600, 2008.
- [75] Hauben M., Reich L. Safety Related Drug-Labeling Changes: Findings from Two Data Mining Algorithms. *Drug Safety*; 27 (10): 735-744, 2004.
- [76] Chen Y, Guo JJ, Steinbuch M, et al. Comparison of sensitivity and timing of early signal detection of four frequently used signal detection methods: An empirical study based on the US FDA Adverse Event Reporting System database. *Pharm Med*; 22: 359-365, 2008.
- [77] Van Puijenbroek EP, Diemont WL, Grootheest K. Application of quantitative signal detection in the Dutch Spontaneous Reporting System for adverse drug reactions. *Drug Saf*; 26:293-301, 2003.
- [78] Waller P., van Puijenbroek E., Egberts A., Evans S. The reporting odds ratio versus the proportional reporting ratio: 'deuce'. *Pharmacoepidemiol Drug Saf*; 13, 525–526; discussion 527, 2004.
- [79] Ramirez E et al. A pharmacovigilance program from laboratory signals for the detection and reporting of serious adverse drug reactions in hospitalized patients. *Clin. Pharmacol. Ther.* 87, 74–86, 2010.
- [80] Jager KJ, Zoccali C, Macleod A, Dekker FW. Confounding: What is it and how do we deal with it? *Kidney Int*; 73(3):256-60.

- [81] Mantel N, Haenszel W (1959). Statistical aspects of the analysis of data from retrospective studies of disease. *J Nat Cancer Inst*; 719–749, 2008.
- [82] Noren GN, Bate A, Orre R, et al. Extending the methods used to screen the WHO drug safety database towards analysis of complex associations and improved accuracy for rare events. *Stat Med*; 25: 3740–3757, 2006.
- [83] Hopstadius J. et al. Impact of stratification on adverse drug reaction surveillance. *Drug Saf*; 31, 1035–1048, 2008.
- [84] Nicholas P. Jewell. *Statistics for Epidemiology*. Texts for statistical sciences, Chapman and Hall, Boca Raton, FL, 2003.
- [85] Almenoff J.S., DuMouchel W., Kindman L.A., Yang X., Ram D. Disproportionality analysis using empirical Bayes data mining: a tool for the evaluation of drug interactions in the post-marketing setting. *Pharmacoepidemiol Drug Saf*; 12, 517–521, 2003.
- [86] Yang X, Fram D. Using disproportionality analysis as a tool to explore drug-drug interactions in AERS database. *Pharmacoepidemiol Drug Safety*; 13: S247, 2004.
- [87] Van Puijtenbroek EP, Egberts AC, Heerdink ER, Leufkens HG. Detecting drug–drug interactions using a database for spontaneous adverse drug reactions: an example with diuretics and non-steroidal anti-inflammatory drugs. *Eur J Clin Pharmacol*; 56: 733–8, 2000.
- [88] Wu X, Barbara D, Ye Y. Screening and interpreting multi-item associations based on log-linear modeling. *Proc KDD*; New York: ACM, 276–85, 2003.
- [89] Van Puijtenbroek EP, Egberts AC, Meyboom RH, Leufkens HG. Signalling possible drug–drug interactions in a spontaneous reporting system: delay of withdrawal bleeding during concomitant use of oral contraceptives and itraconazole. *Br J Clin Pharmacol*; 47: 689–93, 1999.
- [90] Lindquist M, Stahl M, Bate A, Edwards IR, Meyboom RH. A retrospective evaluation of a data mining approach to aid finding new adverse drug reaction signals in the WHO international database. *Drug Saf*; 23: 533–42, 2000.
- [91] Genkin A., Lewis D.D., Madigan D. Large-scale Bayesian logistic regression for text categorization. *Technometrics* 49, 29–304, 2007.
- [92] Caster O., Noren G.N., Madigan D., Bate A. Large-scale regression-based pattern discovery: the example of screening the WHO global drug safety database. *Stat Analy Data Mining*; 3, 197–208, 2010.
- [93] Norén GN, Sundberg R, Bate A, Edwards IR. A statistical methodology for drug–drug interaction surveillance. *Stat Med*; 27(16):3057-70, 2008.
- [94] Skronidal A. Interaction as departure from additivity in case–control studies: a cautionary note. *Am J Epidemiol*; 158: 251–8, 2003.
- [95] Hosmer DW, Lemeshow S. Confidence interval estimation of interaction. *Epidemiology*; 3: 452–6, 1992.
- [96] Qian Y, Ye X, Du W, Ren J, Sun Y, Wang H, Luo B, Gao Q, Wu M, He J. A computerized system for detecting signals due to drug-drug interactions in spontaneous reporting systems. *Br J Clin Pharmacol*; 69(1):67-73, 2010.
- [97] Thakrar BT, Grundschober SB, Doessegger L. Detecting signals of drug–drug interactions in a spontaneous reports database. *Br J Clin Pharmacol*; 64(4):489-95, 2007.
- [98] Agrawal R., Imielinski T, Swami A. Mining association rules between sets of items in large databases. *SIGMOD*, 207–216, 1993.
- [99] Sarawagi S, Thomas S, Agrawal R. Integrating association rule mining with relational database systems: alternatives and implications. *Data Mining Knowledge Discov*; 4(2):89–125, 2000.
- [100] Iskander J, Pool V, Zhou W, English-Bullard R. Data mining in the US using the vaccine adverse event reporting system. *Drug Saf*; 29(5):375–84, 2006.
- [101] Carrino JA, Ohno-Machado L. Development of radiology prediction models using feature analysis. *Acad Radiol*; 12(4):415–21, 2005.
- [102] Rouane H, Toussaint Y, Valtchev P. *Mining Signals in Spontaneous Reports Database Using Concept Analysis*. AIME 2009 (Springer, Berlin, Germany), 2009.
- [103] Tan P, Kumar V, Srivastava J. Selecting the right interestingness measure for association patterns. *Proc Eighth ACM SIGKDD Int Conf Knowledge Discov Data Mining*, 2002.
- [104] Harpaz R1, Haerian K, Chase HS, Friedman C. Statistical Mining of Potential Drug Interaction Adverse Effects in FDA's Spontaneous Reporting System. *AMIA Annu Symp Proc*; 281-5, 2010.
- [105] Rave Harpaz, Herbert S Chase, Carol Friedman. Mining multi-item drug adverse effect associations in spontaneous reporting systems. *BMC Bioinformatics*; 11(Suppl 9):S7, 2010.
- [106] Tatonetti N.P. et al. Detecting drug interactions from adverse-event reports: interaction between paroxetine and pravastatin increases blood glucose levels. *Clin. Pharmacol. Ther.* 90, 133–142, 2011.
- [107] Jialiang Huang, Chaoqun Niu, Christopher D. Green, Lun Yang, Hongkang Mei, Jing-Dong J. Han. Systematic Prediction of Pharmacodynamic Drug-Drug Interactions through Protein-Protein-Interaction Network. *PLoS Comput Biol*; 9(3):e1002998, 2013.
- [108] Kuhn M, von Mering C, Campillos M, Jensen LJ, Bork P. STITCH: interaction networks of chemicals and proteins. *Nucleic Acids Res*; 36: D684–688, 2008.
- [109] Vilar S, Harpaz R, Chase HS, Costanzi S, Rabadan R, Friedman C. Facilitating adverse drug event detection in pharmacovigilance databases using molecular structure similarity: application to rhabdomyolysis. *J. Am. Med. Inform. Assoc.* 18 (suppl. 1), i73–i80, 2011.
- [110] Santiago Vilar, Eugenio Uriarte, Lourdes Santana, Nicholas P. Tatonetti, Carol Friedman. Detection of Drug-Drug Interactions by Modeling Interaction Profile Fingerprint. *PLoS One*; 8(3): e58321, 2013.
- [111] Wishart D.S. et al. DrugBank: a knowledgebase for drugs, drug actions and drug targets. *Nucleic Acids Res.* 36, D901–D906, 2008.
- [112] Nicholas P Tatonetti, Guy Haskin Fernald, Russ B Altman. A novel signal detection algorithm for identifying hidden drug-drug interactions in adverse event reports. *J AM Med Inform Assoc*; 19(1): 79-85, 2012.
- [113] Duke J.D., et al. Literature based drug interaction prediction with clinical assessment using electronic medical records: novel myopathy associated drug interactions. *PLoS Comput Biol*; 8(8):e1002614, 2012.
- [114] Duke J.D. et al. Literature based drug interaction prediction with clinical assessment using electronic medical records: novel myopathy associated drug interactions. *PLoS Comput Biol*; 8(8):e1002614, 2012.
- [115] Choi CA, Chang MJ, Choi HD, Chung WY, Shin WG. Application of a drug–interaction detection method to the Korean National Health Insurance claims database. *Regul Toxicol Pharmacol*; 67(2):294-8, 2013.
- [116] Bjornsson TD, Callaghan JT, Einolf HJ, Fischer V, Gan L, et al. The conduct of in vitro and in vivo drug–drug interaction studies: A Pharmaceutical Research and Manufacturers of America (PhRMA) perspective. *Drug Metabolism and Disposition* 31: 815–832, 2003.
- [117] Greene N. et al. Knowledge-based expert systems for toxicity and metabolism prediction: DEREK, StAR, and METEOR. *SAR & QSAR. Environ. Res.* 10, 299–313, 1999.
- [118] Matthews E.J. et al. Identification of structure–activity relationships for adverse effects of pharmaceuticals in humans: part C: use of QSAR and an expert system for the estimation of the mechanism of action of drug-induced hepatobiliary and urinary tract toxicities. *Regul Tox Pharmacol.* 54, 43–65, 2009.
- [119] Gomba V.K. et al. Assessment of developmental toxicity potential of chemicals by quantitative structure–toxicity relationship models. *Chemosphere* 31, 2499–2510, 1995.
- [120] De Boer A. When to publish measures of disproportionality derived from spontaneous reporting databases? *Br J Clin Pharmacol*; 72: 909-911, 2011.
- [121] Montastruc JL, Sommet A, Bagheri H, et al. Benefits and strengths of the disproportionality analysis for identification of adverse drug reactions in a pharmacovigilance database. *Br J Clin Pharmacol*; 72: 905-908, 2011.
- [122] Schreiber J, et al. Mapping adverse drug reactions in chemical space. *J Med Chem*; 52, 3103–3107, 2009.

- [123] Vanderwall DE, Yuen N, Al-Ansari M, Bailey J, Fram D, Green DV, Pickett S, Vitulli G, Luengo JI, Almenoff JS. Molecular clinical safety intelligence: a system for bridging clinically focused safety knowledge to early-stage drug discovery - the GSK experience. *Drug Discov Today*; 16(15-16):646-53, 2011.

Conversion of 2D medical scan data into 3D printed models

Eva Hnatkova, Petr Kratky and Zdenek Dvorak

Abstract - This work deals with the possibility of using 2D medical image data acquired from computed tomography (CT) and magnetic resonance imaging (MRI) for 3D desing and modeling of implants and other medical applications. In this project the latest medical data processing software Mimics from Materialise was used to generate the 3D models of spinae vertebrae which was converted with CAD software into standard triangulated (STL) files. These highly accurate 3D models of anatomical structures in STL format served to create realistic tissue models using rapid prototyping technology.

Keywords - computed tomography, magnetic resonance, 2D image data, 3D models, medical implants, rapid prototyping.

I. INTRODUCTION

PRODUCTION of anatomical part via rapid prototyping is a modern medical trend. This technology allows the printing of customised implants or the preoperative planning models from medical 2D scans [1-2]. In the past, the production of medical models of individual patient was very difficult, because of the complex geometry of the anatomical parts. Prior to rapid prototyping, medical implants were manufactured using pressing, forging, machining and casting processes. But these processes were expensive and also time-consuming. [3]

Nowadays, there exist special biomedical softwares, for example Mimics developed by Materialise, which can process 2D medical images, coming from computed tomography (CT), magnetic resonance imaging (MRI) or ultrasound, into 3D high accurate models of patient anatomy. Figure 1 shows the medical image segmentation in Mimics software. [4-5]

II. EXPERIMENTAL PART

A. Medical input data

In this project, the real 2D medical images were used as the input data. This data was acquired from a tomograph at Tomas

Eva Hnatkova is with the Department of Production Engineering, Faculty of Technology, Tomas Bata University in Zlín, nám. T. G. Masaryka 5555, 760 01 Zlín, Czech Republic (ehnatkova@ft.utb.cz).

Petr Kratky is with the Department of Production Engineering, Faculty of Technology, Tomas Bata University in Zlín, nám. T. G. Masaryka 5555, 760 01 Zlín, Czech Republic (kratky@ft.utb.cz).

Zdenek Dvorak is with the Department of Production Engineering, Faculty of Technology, Tomas Bata University in Zlín, nám. T. G. Masaryka 5555, 760 01 Zlín, Czech Republic (zdvorak@ft.utb.cz).

Bata regional hospital in Zlín. CT takes pictures of the body in particular slices and provides information on tissues in various locations. The examination outputs are 2D slices saved in stadardized format DICOM. These data could only be displayed as 2D or 3D preview in hospital software (Fig. 2). The previews are not available to any changes and for future work the data have to be adjusted in other software.

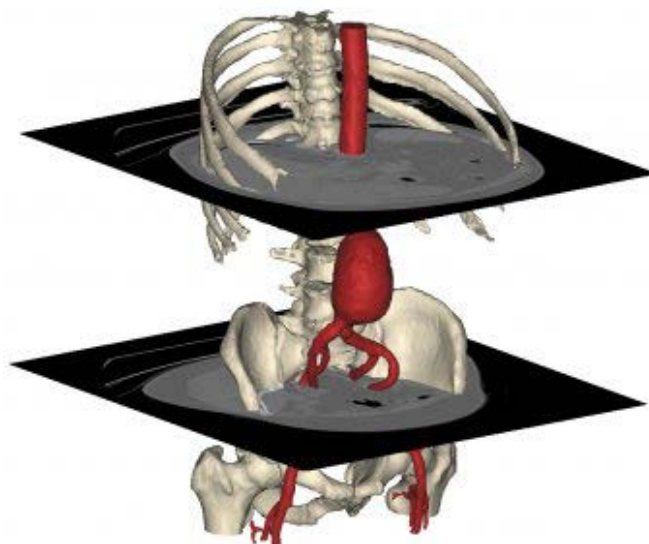


Fig. 1 Medical image segmentation (software Mimics) [6]

B. Preparation of 2D data

Firstly, the 2D image data from the CT had been prepared in Mimics software. The preparation included an upload of DICOM files and selection of analyzed tissue, which would be transferred to 3D model. In this moment, it was possible to get information about patient tissues from the neck to the pelvic. It was required to define the tissue location in any slice, then Mimics software could choose automatically the same tissue type in particular slices and created preview of 3D model.

The created 3D preview gives us information about approximate shape of all vertebrae (Fig. 3), but there are locations with lower density (displayed in dark colour) in particular slices because the vertebrae tissue density is not uniform. These tissues were not included in the selection; therefore, it was necessary to add them to the selection in particular slices. The rest of the directions was calculated. To demonstrate the preparation process, 2 vertebraes were chosen (Fig.4). The rest of the selection was removed away.

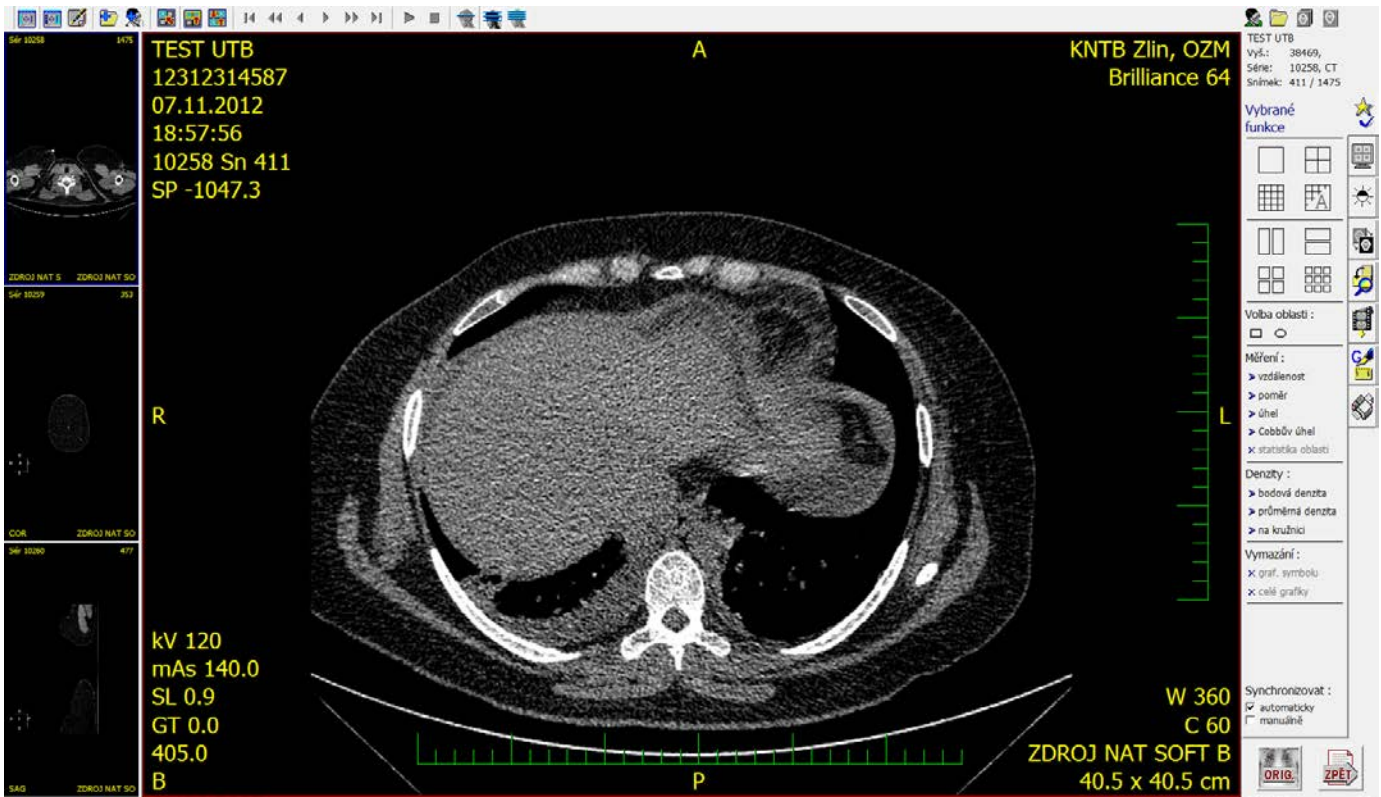


Fig. 2 Two dimensional scan slide after examination (in the hospital software)

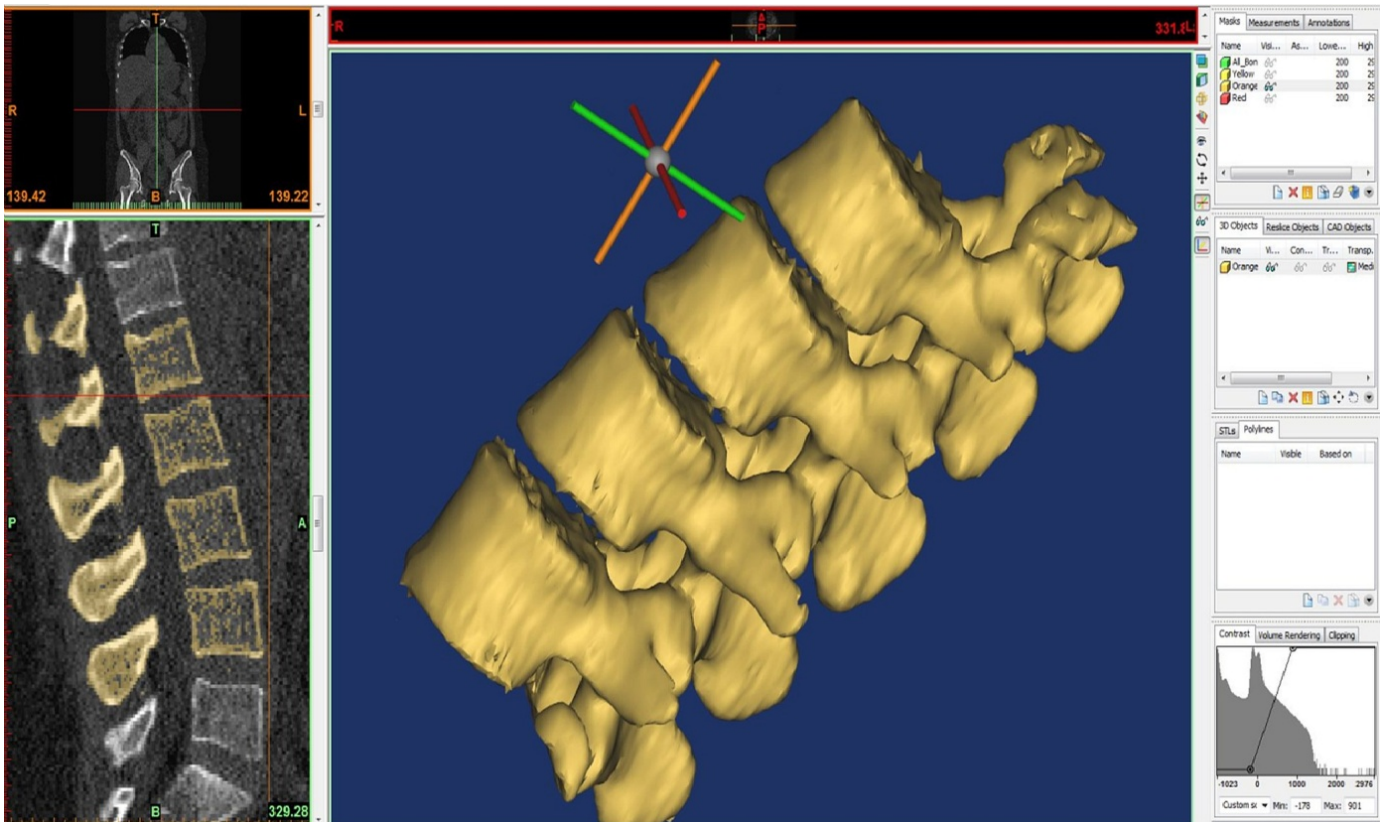


Fig. 3 Three dimensional preview with approximate shape of all vertebrae

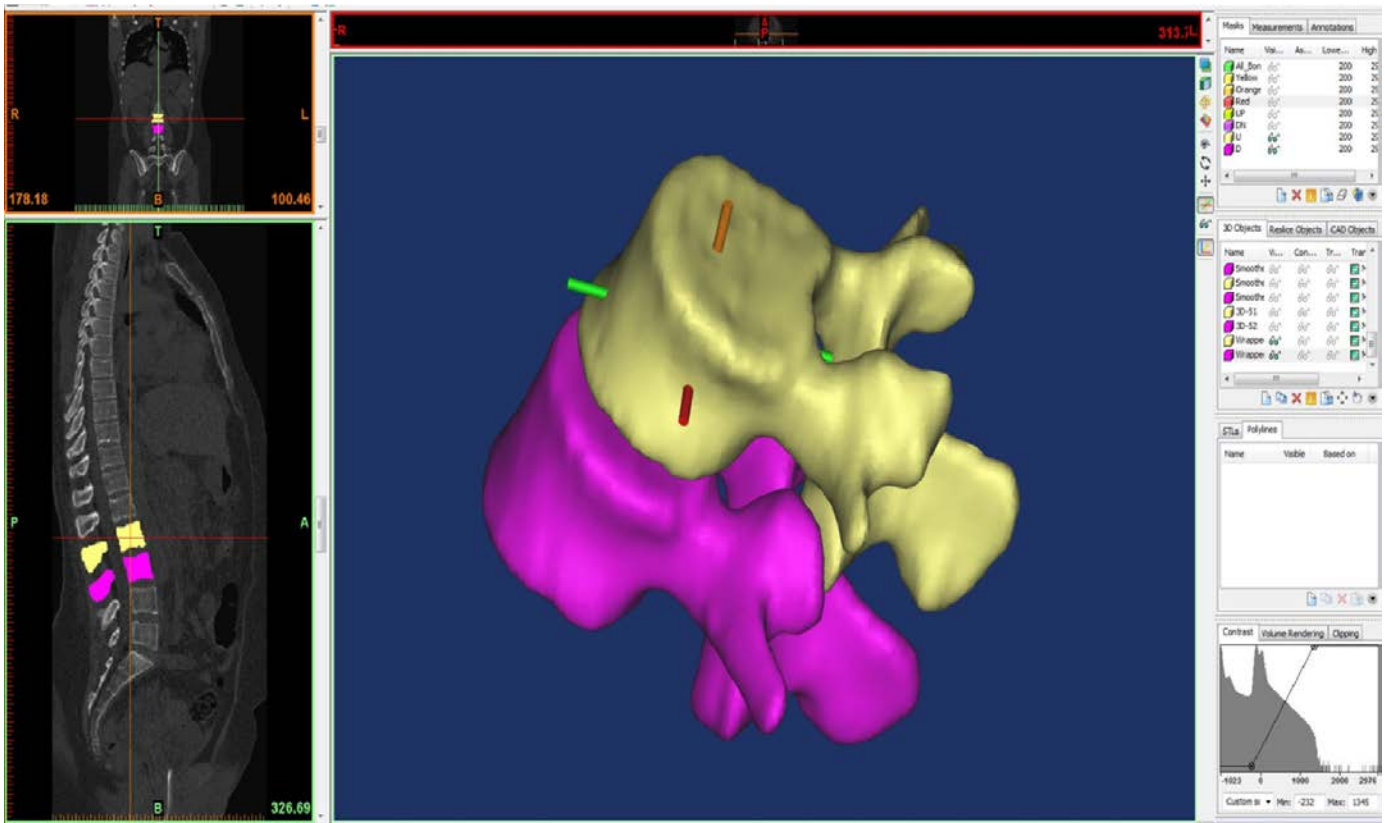


Fig. 4 The correction of chosen vertebrae tissues

C. Processing of 3D models

After corrections of 2D image data in Mimics software, it was possible to generate 3D models to standard STL format. This file format can be processed by any CAD software. In this project, the CAD software from Dassault Systèmes (Catia V5R18) was used (Fig. 5). To continue with printing by Rapid Prototyping it was necessary to move models into zero axis of the system. Other modifications like usual CAD modifications were also possible to use. The process ended by exporting final models to STL format for 3D printing.



Fig. 5 Principle of polyJet method

III. PRINTING OF MODELS VIA RAPID PROTOTYPING

The STL files were postprocessed and printed with a 3D printer (Objet Eden 250), which use the PolyJet method (Fig. 6) based on the jetting photo-sensitive polymer.

In our case, we used “like ABS” material, because the created models have only demonstrative character; there were not any requirements on selected material. The photopolymer was applied from the print head with 96 jets and created the ultra thin layer onto the build tray.

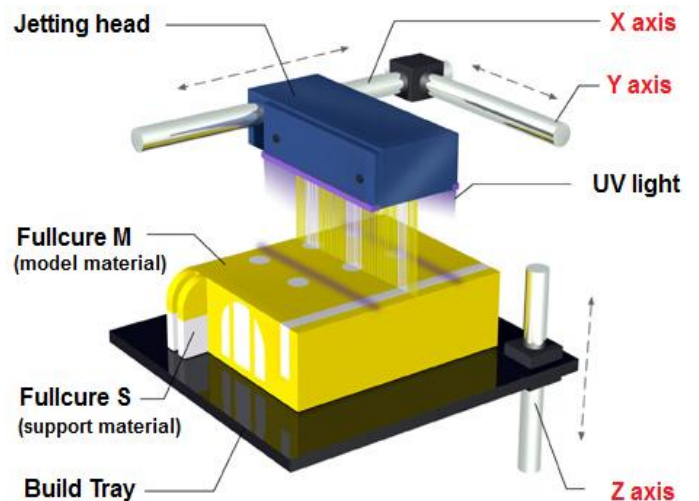


Fig. 6 Principle of polyJet method [7]

Immediately after the building of a layer, the photopolymer was cured by UV lights. The thickness of the layer is 0.016 mm so the final model has a smooth surface with accuracy ranging from 0.05 to 0.1 mm. The support material was based on the gel and it was easy to remove it from the part. Figure 7 shows the real models of spinae vertebrae with support material.



Fig. 7 The 3D models of spinae vertebrae with support material

IV. RESULTS

After removing of support material, we obtained 3D models with two different types of surfaces, one of them is shown in Fig. 7.



Fig. 8 The 3D models of spinae vertebrae with matt surface

V. CONCLUSION

The goal of this project was the modeling and printing of the real 3D anatomical models from the original 2D data. With the advance medical software such as Mimics from Materialise, it is possible to construct three dimensional 3D models of anatomical structures of the human body and by rapid prototyping technology to print them into real parts. In the future, the medical implant technology can continue to improve if we use the biomaterial in 3D printers.

ACKNOWLEDGMENT

Operational Program Research and Development for Innovations co-funded by the ERDF and national budget of Czech Republic, within the framework of project Centre of Polymer Systems (reg. number: CZ.1.05/2.1.00/03.0111) and Operational Program Education for Competitiveness co-funded by the European Social Fund (ESF) and national budget of Czech Republic, within the framework of project Advanced Theoretical and Experimental Studies of Polymer Systems (reg. number: CZ.1.07/2.3.00/20.0104) are acknowledged. This study was also supported by the internal grant of TBU in Zlín IGA/FT/2014/003 funded from the resources of specific university research.

REFERENCES

- [1] J. Wang, V.M. Gharpuray, R.L. Dooley, Automated 3D Reconstruction of 2D Medical Images: Application to Biomedical Modeling, *Proceedings of the 21st Annual Meeting of The American Society of Biomechanics*, Clemson University, South Carolina, USA, 1997
- [2] L. Ciocca, F. De Crescenzo, M. Fantini and R. Scotti, CAD/CAM and rapid prototyped scaffold construction for bone regenerative medicine and surgical transfer of virtual planning: A pilot study, *Computerized Medical Imaging and Graphics*, 33, pp.58–62, 2009
- [3] J. Brennan, *Production of Anatomical Models from CT Scan Data*. Masters Dissertation. De Montfort University, Leicester, United Kingdom, 2010.
- [4] Y. S. Morsi, C. S. Wong and S. S. Patel, Virtual Prototyping of Biomaterials in Medical Applications Conventional manufacturing processes for three-dimensional scaffolds, Book Chapter, 2008, *Virtual Prototyping & Bio Manufacturing in Medical Applications*, pp. 129-148.
- [5] R. Petzold, H. F. Zeilhofer, W. A. Kalender. Rapid prototyping technology in medicine – basics and applications. *Computerized medical imaging and graphics*, 1999
- [6] Materialise develops 3D software for the medical, dental and additive, [Online]. Available at: www.materialise.com
- [7] Polyjet technology [online]. Available at: www.engineershandbook.com/RapidPrototyping/polyjet.htm

Fault Throw and Sealing Thickness Relationship of Middle Cretaceous Muglad Basin, South Sudan

Southeast Basin in JK field study

Dorar Hamdoba Elshaikh and Dr. Zuhar Zahir Bin Tuan Harith

Petroleum Geosciences Department
 University of Technology of Petronas
 Seri Iskandar, Malaysia

dorar15@gmail.com, zuharza@petronas.com.my

Abstract—In this study, the south east Muglad basin, Sudan of JK field area in Middle Cretaceous petroleum system, the fault throw and sealing formation (Aradeiba) are the hydrocarbon successfully trap in the reservoir formation. The observation that had been noted that faults are sealing based on the oil water contact level that even in the absence of the sealing formation (Aradeiba) in the middle and lower parts of Bentiu the oil trapped in the formation due to fault sealing behavior. Also if the fault throw is more than the thickness of the sealing formation the oil trapped successfully but if fault throw is less than sealing formation thickness the trap fail to trap hydrocarbon. From interpreted petro-physical gamma log noticed the sand and shale are inter-bedded. These logs gave a reason for the hydrocarbon distribution in the area of study and explain why in some drilled wells there was no hydrocarbon shows. Observations for Smear Gauge ration (SGR) for wells indicated that 14-20% SGR wells successfully trap hydrocarbon but <14% SGR faults fail to trap oil. Clay Smear Potential (CSP) is lower in oil wells than dry wells.

Keywords—component; Faults, Formation, Lateral Seal, Trap, Reservoir, juxtaposition, Smear, Gouge, Petro-physical, thickness, stratigraphy and Seismic cross-section.

I. INTRODUCTION

Oil exploration in Sudan began in the late fifties but was focused in the offshore areas of the Red Sea. In 1974 Chevron commenced exploration in the interior rift basins, including the Muglad Basin. To date significant hydrocarbon reserves have been discovered, and the country currently produces about 280,000 BOPD. in the southern part of this basin [1], where the

Muglad Basin contains a thick sequence of non-marine sediments, which range in age from Cretaceous to Tertiary. A generalized stratigraphic column shown in (Figure 1), illustrating the sedimentary basin filling and lithology [2] [3]. Showing source (Abu Gabra), reservoir (Bentiu) and sealing (Aradeiba) zones along the column. Figure 2 show study area location

Fault seal behavior of normal faults in most hydrocarbon basins is dependent upon the ratio of sand/shale in the fault zone. Faults with sand-rich gouge tend to leak; faults with shale-rich gouge tend to seal. The estimated sand/shale ratio is the, SHALE GOUGE RATIO (SGR) . The SGR is calculated from the total thickness of sand and shale that has moved past a point along the fault [4].

Petro-physical analysis of the well data was used to define the shale and sand layers [5] in each stratigraphic unit. In combination with detailed juxtapositions and well log data, the Shale Gouge Ratio (SGR) is calculated to provide an estimate of the composition of the fault zone (fault zone % shale). Since the fault displacements are generally greater than the zone thicknesses, the calculated SGR values are good indicator between oil and dry wells. However, the significant area is that of lower values wells fail to trap oil but greater are good trapping faults [6].

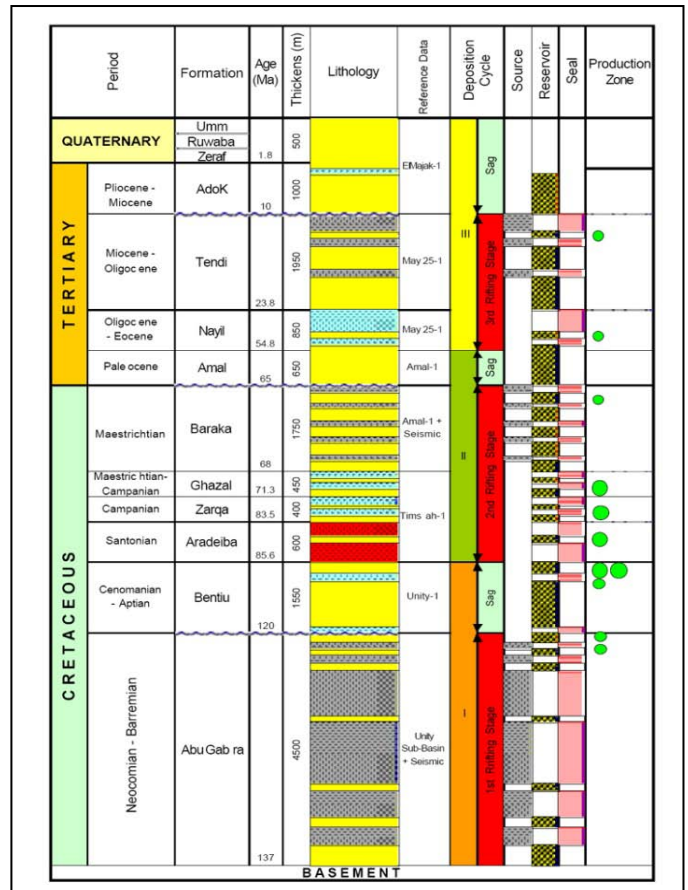


Fig. 1. General Stratigraphic column of Muglad Basin Sudan [1].

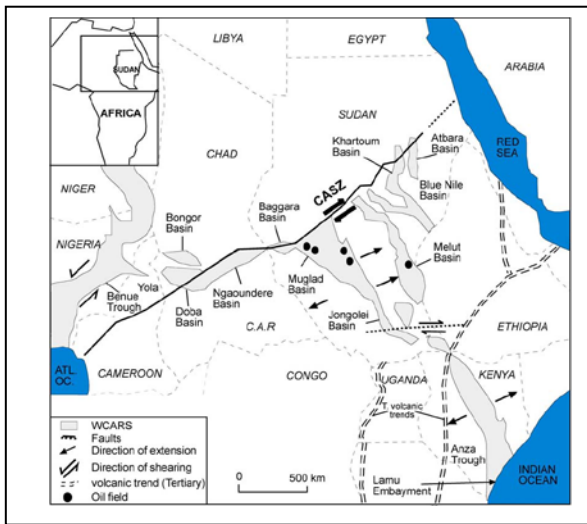


Fig. 2. Muglad Basin location in Sudan Africa region and study area [2].

II. LATERAL SEAL

Lateral seal depends on the thickness and the lithology of the Bentiu shale and the amount of fault throw. The Bentiu Formation is highly variable in thickness (Figure 3) and in sand/shale ratio. Most of the perfect lateral seals are due to direct juxtaposition of Bentiu sandstone reservoir against Aradeiba or Bentiu shale.

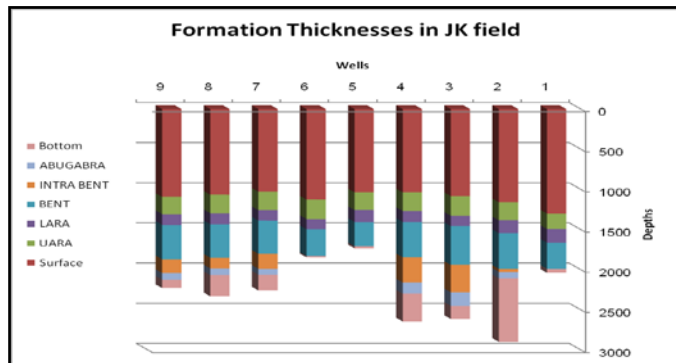


Fig. 3. JK wells with formation thickness from top to bottom.

A. Juxtaposition

Juxtaposition in dictionary[7] is the state of being placed or situated side by side. In reservoir sands are juxtaposed [8, 9] against a low permeability unit (shale) with a high entry pressure. Clay smear is the entrainment of clay or shale into the fault plane, thereby giving the fault itself a high entry pressure [10-12].

B. Fault sealing

If a fault leaks at a sand/sand juxtaposition, hydrocarbon may be trapped only where sand/shale juxtaposition exists. At the leaking sand/sand juxtaposition hydrocarbons [6, 13] are free to migrate up-dip. It is an extremely common type that controls the spill points for many fields. Where spill point is the structurally lowest point in a hydrocarbon trap that can retain hydrocarbons[4, 14].

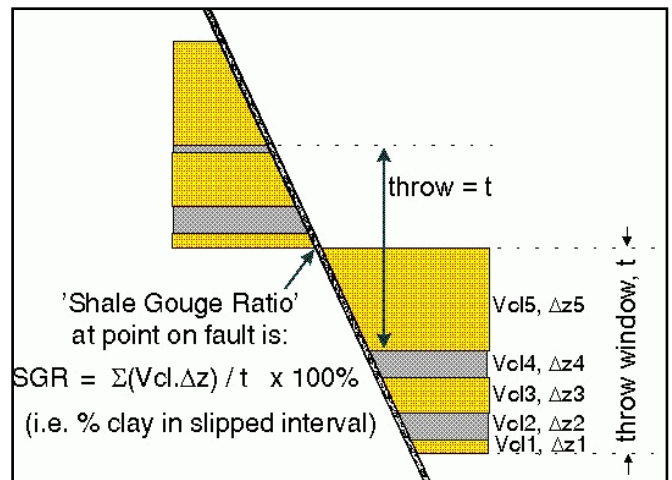


Fig. 4. Shale Gouge Ratio with equation

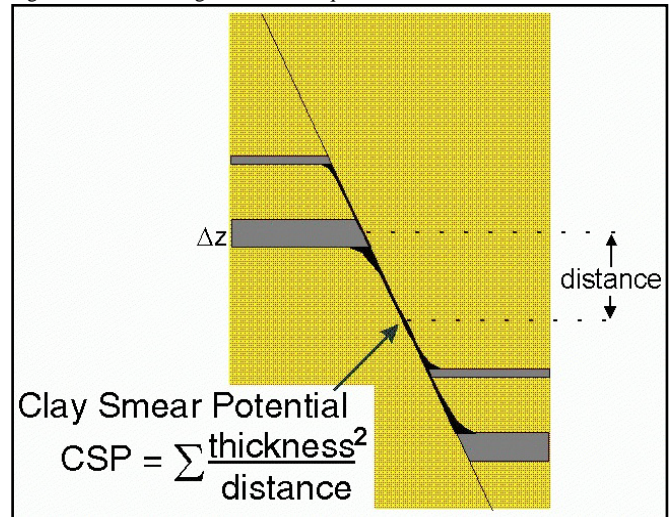


Fig. 5. Clay Smear Potential with equation

III. OBJECTIVE

The main purpose of this study to define following: 1)Analyze the dry wells to understand dry wells in reservoir formation although the good structural trap. 2)Integrating well log data with 3D seismic data to get the fault throw of the structural traps and get information about the lithology using gamma log. To prove that when the fault throw is greater than sealing formation thickness it successfully trap hydrocarbon if it is less the hydrocarbon easily escape from the trap to reservoir formation in the other side of the structure. 3)Calculating SGR and CSP for reservoir fault area and observe result.

IV. METHODOLOGY

Well log petro-physical data used to show sand to sand and sand to shale juxtaposition issue in JK area assuming that fault throw and formation thickness had an effect on hydrocarbon trapping a measurement of fault throw had been conducted and a comparison between formation thicknesses calculated from petro-physical log analysis [1] (Fig.6 and 7).

Using wells petro-physical data specially interpreted gamma log where can be noticed the shale and sand bed in

both seal and reservoir formations[15]. Assuming that both sides of the fault footwall and the hanging wall with gamma log in both sides are placed next to each other and the hanging wall shifted down with the value of the fault throw calculated from seismic section[4].

Although Aradeiba shale in the hanging wall juxtaposes against Bentiu sand laterally, the trap was formed and hydrocarbon accumulated in reservoir as found in all wells except for Well 3 (Fig.6) where fault throw was invalid because it was less than Aradeiba shale thickness the comparison between fault throw measured in Table 1 and Aradeiba thickness from well tops measures in Table 1 confirming the assumption that when fault throw less than Aradeiba (Seal) thickness the fault fail to trap hydrocarbon due to failure in lateral sealing. On the other hand if fault throw is more than seal formation thickness the hydrocarbon is successfully trapped in the reservoir[1] for example (Fig.7) as all other JK wells.

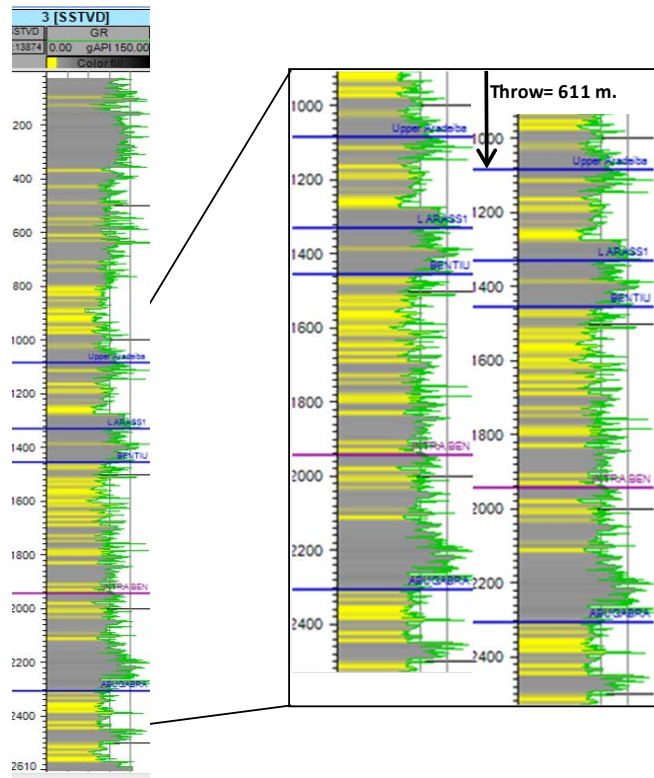


Fig. 6. Well 3 Gamma ray log from top to bottom and zoom out in the seal (Aradeiba) and reservoir (Bentiu) area with the shift of log of fault throw calculated from seismic section.

Juxtaposition play an important role in hydrocarbon trapping in south east Muglad basin. That if sand juxtapose with sand the reservoir fail to trap hydrocarbon and that what happened in well 3 as in Fig.6 the reservoir formation sand juxtapose with the other sand of the fault which cause the escape of hydrocarbon from the formation and the result is drilling a well in a good structure but no lateral sealing for trapping. While the case in the other JK field other wells for

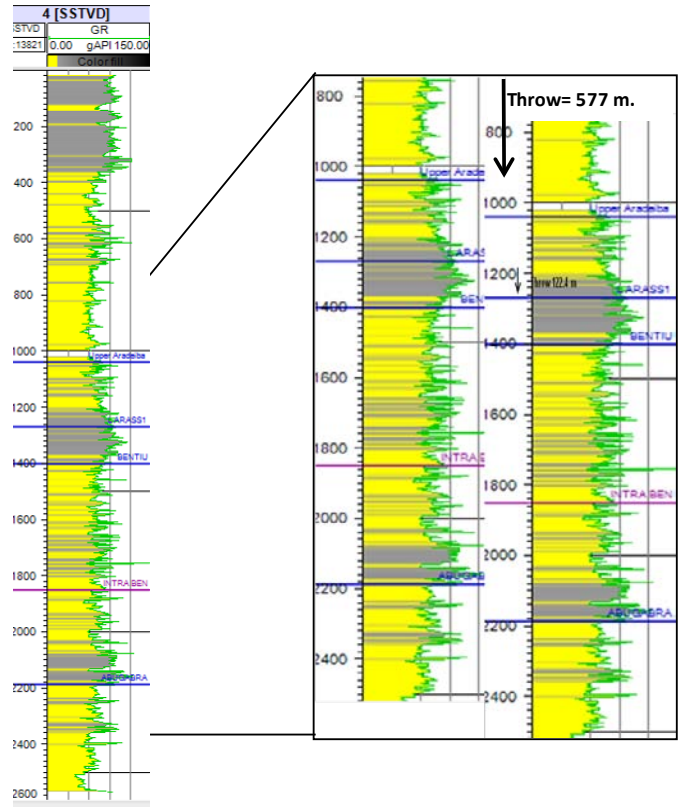


Fig. 7. Well 4 Gamma ray log from top to bottom and zoom out in the seal (Aradeiba) and reservoir (Bentiu) area with the shift of log of fault throw calculated from seismic section.

Example well4 as in Fig.7 the fault throw was greater than sealing formation thickness which bring the sealing formation down to block hydrocarbon from migrating through the porous formation and the reservoir successfully trapped hydrocarbon and successfully have an oil well.

Sealing Thickness and Fault throw				
Well	LARA Thickness	Throw (TWT)	Throw (Depth)	Well result
1	169.99	77.63	205.36	Oil
2	158.60	0	0	Dry
3	128.17	92.88	123.73	Dry
4	136.59	222.47	299.49	Oil
5	148.23	152.65	209.35	Oil
6	127.10	164.58	217.55	Oil
7	137.07	253.36	424.85	Oil
8	136.79	227	383.04	Oil
9	133.47	163.77	278.48	Oil

Table 1 Fault throw measurement made on seismic section from top and bottom of Bentiu formation and throw converted from two way time to meters using depth conversion equation resulted in fault throw in JK field wells.

V. RESULTS

The South East Muglad basin JK field represents a prospective hydrocarbon structure because of trapping and fault sealing mechanism in the area based on the analyzed nine wells results.

The closing ability of the reservoir and the height of oil column were determined by the fault throw and lithologies in both sides of the fault as in Table 1 and Fig.6 and 7 as per assumed. Lateral sealing depends on the thickness and the lithology of the Aradeiba shale and the amount of fault throw (Table 1).

SGR and CSP for JK Wells						
Well	LARA Thickness	Bentiu Thickness	V shale	Throw	SGR	CSP
1	170	326	0.6	496	21%	111
2	159	445	0.0	0	0%	0
3	128	483	0.6	611	13%	63
4	137	440	0.6	577	14%	43
5	148	302	0.6	450	20%	56
6	127	333	0.6	460	17%	54
7	137	412	0.6	549	15%	42
8	137	417	0.6	554	15%	45
9	133	429	0.6	562	14%	47

Table 2 Shale Gouge Ratio and Clay Smear Potential calculated from sealing thickness plus reservoir thickness as throw for both SGR and CSP.

Calculation of Shale Gouge Ration(SGR) and Clay Smear Potential for JK wells resulted in the following observations:

- 1- For dry Well 3 SGR is less than 14% while most of the oil wells SGR is more than 14%.
- 2- For CSP dry Well 3 is above 60 while most of the other wells are below 60 are oil wells.

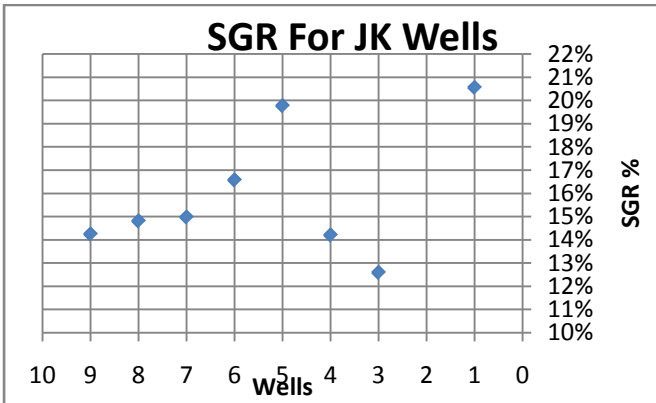


Fig. 8. Shale Gouge Ratio result plot showing that for well 3 the value is less than 14% resulted in dry wells while most of the wells are between 14-21% are oil wells.

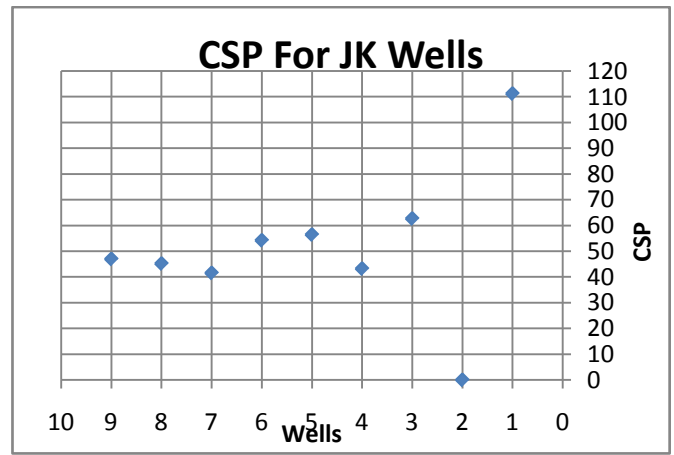


Fig. 9. Clay Smear Potential calculated for all wells resulted in for well 3 is more than 60 the well is dry but for most of the wells the CSP value is less than 60 they are all oil wells.

VI. CONCLUSION

The petroleum system of JK field has a perfect assemblage of source, reservoir and top seal. The Bentiu reservoir rock and Aradeiba regional cap rock formed the major oil-bearing beds.

If the fault throw is greater than sealing formation thickness it usually traps hydrocarbon from migrating and we can find oil in the structure and that was the case for most of JK field wells that had been drilled. For the dry wells it had been noticed that the fault throw was less than the sealing formation thickness so the sand in the reservoir was not juxtaposed with shall and the hydrocarbon escaped from the reservoir and the well that had been drilled in a good structure was found dry.

Observation for the Shale Gouge Ratio in JK wells shows that, if SGR is greater than 14% the fault successfully trap oil, but if less than 14% the well result is dry. For Clay Smear potential it had been observed that, if CSP less than 60 most of the wells results are oil wells if more than 60 the well is dry.

ACKNOWLEDGMENT

Sincere wishes to my family members and all gratitude are to the staff members of the Petroleum Geosciences department. Also, I wish to express my sincere appreciation to the university management and service departments for all the support and services that had been provided to this study to be conducted.

REFERENCES

- [1] M. I. a. S. Yongdi, "Lateral Seal A major exploration risk in the faulted traps of the Cretaceous petroleum system Central Muglad Basin, Sudan," *AAPG, Bulletin*, vol. 88, 2004.
- [2] A. S. M. Abdelhakam E. Mohamed "Stratigraphy and Tectonic Evaluation of the Oil Producing Horizons of Muglad Basin, Sudan," *Journal of Science and Technology*, vol. 9, pp. 1-8, 2008.
- [3] Y. M. Zhang and Q. Gu, "Petroleum System of the Fula Depression at the Muglad Basin in the Central African Fault Zone," *Journal of Earth Science*, vol. 22, pp. 363-370, Jun 2011.
- [4] R. B. Faersth, E. Johnsen, and S. Sperrevik, "Methodology for risking fault seal capacity: Implications of fault zone architecture," *Aapg Bulletin*, vol. 91, pp. 1231-1246, Sep 2007.
- [5] R. B. Faersth, "Shale smear along large faults: continuity of smear and the fault seal capacity," *Journal of the Geological Society*, vol. 163, pp. 741-751, Sep 2006.
- [6] W. R. Bailey, J. Underschultz, D. N. Dewhurst, G. Kovack, S. Mildren, and M. Raven, "Multi-disciplinary approach to fault and top seal appraisal; Pyrenees-Macedon oil and gas fields, Exmouth Sub-basin, Australian Northwest Shelf," *Marine and Petroleum Geology*, vol. 23, pp. 241-259, Feb 2006.
- [7] I. o. E. a. E. E. (IEEE). (2013). *Dictionary.com*, "juxtaposition," in *Dictionary.com Unabridged*. Source location: Random House, Inc. <http://dictionary.reference.com/browse/juxtaposition>. Available: <http://dictionary.reference.com/cite.html?qh=juxtaposition&ia=luna>
- [8] G. Yielding, N. Lykakis, and J. R. Underhill, "The role of stratigraphic juxtaposition for seal integrity in proven CO₂ fault-bound traps of the Southern North Sea," *Petroleum Geoscience*, vol. 17, pp. 193-203, May 2011.
- [9] G. Yielding, "Shale Gouge Ratio – Calibration by Geohistory," *Hydrocarbon Seal Quantification NPF Special Publication*, vol. 11, pp. 1-15, 2002.
- [10] A.-u. R. Farrukh Daud, Gulzeb Nabi Khan, Asad Ilyas, "Fault Seal Analysis, A Tool to reduce the exploration and development risks, a case study from Middle Indus Basin," presented at the PAPG/SPE Annual Technical Conference 2010, Islamabad, 2010.
- [11] J. Wang, "Gudao Oilfield fault seal ability research and development of oil and gas application," *Natural Resources and Sustainable Development II, Pts 1-4*, vol. 524-527, pp. 1435-1438, 2012.
- [12] L. I. Watts, "Theoretical aspects of cap rock and fault seals for single and two phase hydrocarbon columns," *Marine and Petroleum Geology*, vol. 4, pp. 274-307, 1987.
- [13] S. J. Wilkins and S. J. Naruk, "Quantitative analysis of lip-induced dilation with application to fault seal," *Aapg Bulletin*, vol. 91, pp. 97-113, Jan 2007.
- [14] S. M. Clarke, S. D. Burley, and G. D. Williams, "A three-dimensional approach to fault seal analysis: fault-block juxtaposition & argillaceous smear modelling," *Basin Research*, vol. 17, pp. 269-288, Jun 2005.
- [15] G. Akhter, Z. Ahmad, and M. Z. Munir, "Fault seal analysis indicates potential of Paleogene reservoirs in Pakistan," *Oil & Gas Journal*, vol. 108, pp. 34-42, Mar 22 2010.

Environmental impact of masonry and RC frame structures

A. Puskás, J. Virág, L.M. Moga, H. Szilágyi, M. Bindea and Sz.A. Köllő

Abstract—For the realization of current social and public buildings reinforced concrete frame structures with masonry infill walls are frequently used, as well load bearing masonry walls with reinforced concrete tie-beams and pillars. When establishing the appropriate structural solution generally the cost of the realization, the construction time and the architectural impact of the chosen solution are taken into consideration, often neglecting the environmental impact of the chosen solution. The paper presents a study on a three-storey building having the same architecture, realised in two structural solutions. Life cycle analyses are performed for both structural solutions: reinforced concrete frame structure with masonry infill walls and load bearing masonry walls with reinforced concrete tie-beams and pillars. Results based on the material quantities calculated for both situations are compared. Differences appear in all the main LCA indicators taken into consideration: energy, solid emissions in air and water, natural resources consumption and waste generation. Comparing the results the more sustainable structural solution with less environmental impact can be concluded.

Keywords—structural sustainability, masonry walls, reinforced concrete frame, environmental impact.

I. INTRODUCTION

ENGINEERING is traditionally equivalent to numbers, formulas, equations, diagrams and other measurable units, simplifying the evaluation and comparison of different solutions. Sustainability principles defined by the Brundtland

This work expresses the concern of the authors to the sustainability, in general, and to the sustainability of the structural systems used for buildings, specifically. The research is conducted as an internal program of the Department of Structures of the Technical University of Cluj-Napoca.

A. Puskás is with the Department of Structures, Faculty of Civil Engineering, Technical University of Cluj-Napoca, G. Baritiu street no. 25, 400027, Cluj-Napoca, Romania (phone:+40-264-401545, e-mail: attila.puskas@dst.utcluj.ro).

J. Virág is with the Department of Structures, Faculty of Civil Engineering, Technical University of Cluj-Napoca, G. Baritiu street no. 25, 400027, Cluj-Napoca, Romania (e-mail: jacint.virag@dst.utcluj.ro).

L.M. Moga is with the Department of Buildings, Faculty of Civil Engineering, Technical University of Cluj-Napoca, G. Baritiu street no. 25, 400027, Cluj-Napoca, Romania (e-mail: ligia.moga@ccm.utcluj.ro).

H. Szilágyi is with National Institute for Research and Development “Urban-Incere”, 117 Calea Floresti, 400524, Cluj-Napoca, Romania (e-mail: henriette.szilagyi@incerc-cluj.ro).

M. Bindea is with the Department of Structures, Faculty of Civil Engineering, Technical University of Cluj-Napoca, G. Baritiu street no. 25, 400027, Cluj-Napoca, Romania (e-mail: mihai.bindea@dst.utcluj.ro).

Sz.A. Köllő was with Faculty of Civil Engineering, Technical University of Cluj-Napoca, G. Baritiu street no. 25, 400027, Cluj-Napoca, Romania (e-mail: szassza23@yahoo.com).

Commission of the United Nations on March 20, 1987 [1] as part of the notion sustainable development, are representing huge challenge for the structural engineering society: even if the statement of the concept is easy to understand, in practice it brings difficulties in the exercise of the engineering profession. In practice of the structural engineering establishing environmental impact reduction measures of structural systems are unfortunately reduced to choosing of more environmental friendly materials, but how can we conclude the proper structural solution with reduced environmental impact? Since environmental impact of structures is not an absolute science, the better and better structural solutions – environmental impact-wise – can be achieved only by comparing different structural solutions [2].

Sustainability by default lays on three pillars, which are not mutually exclusive but can be mutually reinforcing [3], representing nothing else than the reconciliation – or the compromise - of environmental, social equity and economic demands. In establishing of the structural system for buildings engineers are accustomed to utilize the most appropriate structural codes, norms and standards, as well as the essential requirements stated in the Council Directive 89/108/EEC [4], overtaken also by other specific laws. When focusing on the requirements “hygiene, health and environment” and “energy economy” further dilemmas can be face in lack of specific and practical measuring instruments. Concerns of specialists from all around the world from the field of civil and environmental engineering represents a progress in obtaining more sustainable structures with reduced environmental impact, but no generally valid rules can be found yet for the given scope. The ISO 14000 standard family on environmental management [5] provides theoretical tools to identify and control the environmental impact of companies and organizations and to improve their environmental performance, but in practice there are still huge gaps in the realisation of the structural systems with reduced environmental impact. One of the most efficient methodologies for obtaining a sustainable structural system is the impact assessment of the studied structure using Life Cycle Analysis (LCA), emphasized in studies performed by Danatzko and Sezen [6] and others. The life cycle analysis of structures is considering impact of the whole cradle-to-grave and to cradle again circle of the materials, structures and buildings (Fig. 1), regulated by European framework standards EN 15643-1:2010 [7] and EN 15643-2:2011 [8].

The building has been considered to be placed in a seismic area characterised by the upper limit of the period of the constant spectral acceleration branch $T_c=0.7$ sec and the design ground acceleration $a_g=0.15g$, corresponding to medium ductility area. For permanent and variable loads the same values have been taken into consideration, including live and wind loads.

Since no material quality influence has been aimed the material qualities for the two cases have been considered unchanged. Quantities of materials obtained for the case 1 (reinforced concrete frame structure with masonry infill walls) are presented in Table I to Table IV. Due to technological differences between the studied structural solutions also the formwork quantity shows important variations.

Table I: Concrete quantities in Case 1

Level	Type	No.	Quant. / type [m ³]	Quantity [m ³]
1	Column	24	0.43	10.26
2÷3	Column	48	0.33	15.84
1÷3	Long. beam	12	1.39	16.68
1÷3	Tran. beam	18	1.65	29.70
1÷3	Slab	3	31.05	93.15
TOTAL				165.63

Table II: Rebar quantities in Case 1

Structural element	Quantity [kg]
Longit. beam	2,604.83
Transv. beam	3,852.66
Slab	5,299.46
Column	11,393.48
Total	23,150.43

Table III: Masonry quantities in Case 1

Level	Pos.	Thickness [m]	No. levels	Masonry [m ³]
1	Ext.	0.30	1	61.94
	Int.	0.20	1	55.13
2÷3	Ext.	0.30	2	114.41
	Int.	0.20	2	100.51
TOTAL				331.992

Table IV: Formwork quantities in Case 1

Level	Type	No.	Quant. / type [m ²]	Quantity [m ²]
1	Column	24	5.70	130.10
2÷3	Column	48	4.44	199.72
1÷3	Long. beam	12	11.10	133.20
1÷3	Tran. beam	18	11.28	203.04
1÷3	Slab	3	310.50	940.50
TOTAL				1,606.56

The material quantities for the case 2 are shown in Table V to Table VII.

Table V: Concrete quantities in Case 2

Level	Type	No.	Quant. / type [m ³]	Quantity [m ³]
1	Pillar	24	0.43	10.26
2÷3	Pillar	48	0.33	15.84
1÷3	Tie, long. ext.	6	0.95	5.70
1÷3	Tie, long. int.	6	0.79	4.74
1÷3	Tie, tran. ext.	6	0.72	4.32
1÷3	Tie, tran. int.	12	0.62	7.44
1÷3	Slab	3	40.37	121.10
TOTAL				169.40

Table VI: Rebar quantities in Case 2

Structural element	Quantity [kg]
Pillars	7,144.13
Slabs	5,150.00
Transv. tie beams	3,021.85
Longit. tie beams	2,936.78
Horiz. joint	2,955.12
Total	21,207.88

Table VII: Masonry quantities in Case 2

Level	Pos.	Thickness [m]	No. levels	Masonry [m ³]
1	Ext.	0.30	1	65.85
	Int.	0.25	1	72.98
2÷3	Ext.	0.30	2	122.23
	Int.	0.25	2	133.77
TOTAL				394.83

Table VIII: Formwork quantities in Case 2

Level	Type	No.	Quant. / type [m ²]	Quantity [m ²]
1	Pillar	24	4.275 ÷ 1.425	79.80
2÷3	Pillar	48	3.33 ÷ 1.11	124.32
1÷3	Tie, long.	12	6.48	77.70
1÷3	Tie, trans.	18	4.56	82.08
1÷3	Slab	3	310.50	938.00
TOTAL				1,301.90

Significant variation of the material quantities can be remarked. Due to the already mentioned technological differences in the construction of the structures the formwork quantity decreases for Case 2 with 23.4%. In similar way also the reinforcement quantity decreases for Case 2 with 9.2% with respect to Case 1, mainly due to the column/pillar and beam/tie beam differences. Even if the size of the pillars and tie beams is lower in Case 2 than the size of the columns and

beams in Case 1, due to the excessive imposed minimum thickness of the slab the concrete quantity increases with 2.3% in Case 2 with respect to Case 1. Due to the minimum thickness provision for the load bearing masonry walls also the masonry quantity increases for Case 2 with 18.9% with respect to Case 1.

III. ENVIRONMENTAL IMPACT ASSESSMENT RESULTS

For the environmental impact estimation of the structure the Athena Impact Estimator for Buildings life cycle assessment software has been used [21]. The environmental impact estimation of the structural solutions is made by their embedded material. The analysis of the environmental impact considers the same service conditions for the buildings and the same building life expectancy. The analysis has been done using the previously presented material quantities.

The total energy consumption for the studied cases is presented in Table IX and Fig. 5.

Table IX: Total energy consumption comparison

Structural solution	Total Energy Consumption [MJ]
Case 1	4,558,673.01
Case 2	5,212,523.56

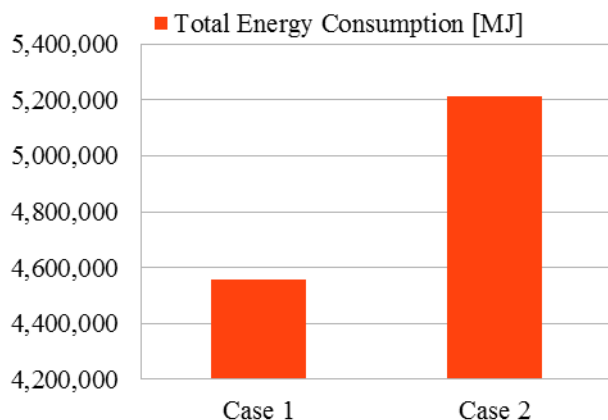


Fig. 5 Comparison of total energy consumption

Table X emphasizes the differences in the solid waste potential of each structural solution. The corresponding graph is shown in Fig. 6.

Table X: Land emissions comparison

Material ID	Case 1	Case 2
Concrete Solid Waste [kg]	8,427.75	8,619.58
Blast Furnace Dust [kg]	246.50	252.11
Other Solid Waste [kg]	21,322.73	25,053.27

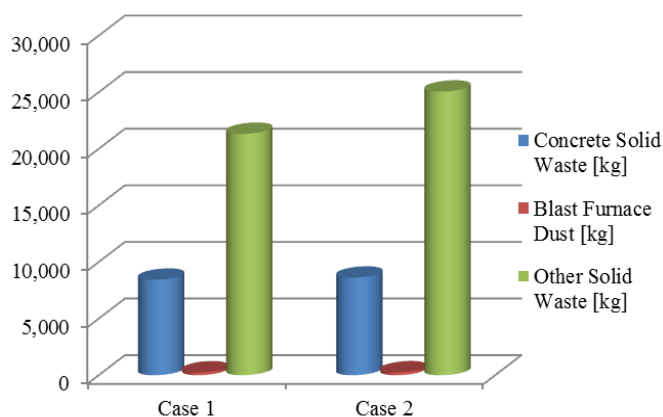


Fig. 5 Land emissions comparison

Quantities of resources used for the studied cases are presented in Table XI. Fig. 6 presents the comparison of the fossil fuel consumption by life cycle stages of the two structural cases.

Table XI: Resource use

Material ID	Case 1	Case 2
Ash kg	241.22	246.71
Carbon dioxide, in air kg	433.78	397.38
Clay & Shale kg	10,900.95	11,149.07
Coal kg	77,857.22	88,169.79
Coarse Aggregate kg	196,172.17	200,637.36
Crude Oil L	12,238.85	13,488.13
Dolomite kg	1,736.96	1,591.21
Ferrous scrap kg	25,750.34	23,589.63
Fine Aggregate kg	144,520.46	147,809.97
Gypsum (Natural) kg	1,694.12	1,732.69
Iron Ore kg	13,316.84	12,225.16
Lignite kg	70.32	64.42
Limestone kg	39,502.54	40,387.65
Natural Gas m3	50,551.85	59,299.90
Sand kg	479.13	490.03
Semi-Cementitious Material kg	5,782.56	5,914.18
Uranium kg	0.57	0.66
Water L	471,366.15	434,424.05

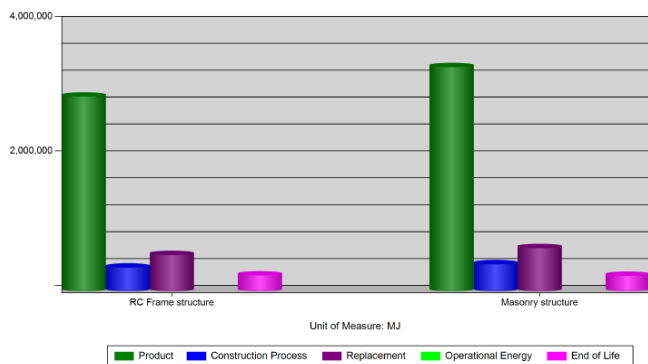


Fig. 6 Land emissions comparison

IV. CONCLUSION

Even if traditionally load bearing masonry walls with reinforced concrete tie-beams and pillars are considered cost efficient with respect to reinforced concrete frame structures with infill walls, the case study leads to unexpected results: for the given building - considering the same placement, architecture, load conditions, material quantities – the environmental impact of the load bearing masonry wall structure is higher than the impact of the reinforced concrete frame building with masonry infill walls. Since economy of the structural solutions has not been studied results on the sustainability of the structural solutions cannot be concluded.

Sustainability of a structural solution – as well as the environmental impact – depends on the location of the studied building due to the high amount of energy needed for all kind of transportation. The presented study presumed standard conditions for the project location hoping to obtain unequivocal results, but unfortunately –due to design standard discrepancies like minimum slab thickness in case of load bearing masonry walls – the obvious and expected results were not achieved.

In order to establish less environmental impact structural solutions use of the presented assessment procedure for similar structures can be recommended, but results have to be read considering also local conditions.

REFERENCES

- [1] Brundtland, H., "Our Common Future", Oxford University Press, 1987.
- [2] Puskas, A., Moga, L.M., "Sustainability of building Relationship between economy and sustainability for a multi-storey reinforced concrete frame structure" WIT Transactions on Ecology and The Environment, Vol. 176, WIT Press, 2013, ISSN 1743-3541, doi:10.2495/ESUS130171
- [3] United Nations General Assembly, 2005 World Summit Outcome, Resolution A/60/1, adopted by the General Assembly on 15 September 2005.
- [4] Council Directive 89/108/EEC, <http://eur-lex.europa.eu/>.
- [5] ISO 14000 standard family, <http://www.iso.org/iso/home/standards/management-standards/iso14000.htm>.
- [6] Danatzko, J.M., Sezen, H., "Sustainable Structural Design Methodologies" Practice Periodical on Structural Design and Construction, Vol. 16, Issue 4, 2011, ISSN 1943-5576, doi: 10.1061/(ASCE)SC.1943-5576.0000095.

- [7] Sustainability of construction works - Sustainability assessment of buildings - Part 1: General framework, EN 15643-1:2010, European Committee for Standardization (CEN), <http://www.cen.eu>.
- [8] Sustainability of construction works - Assessment of buildings - Part 2: Framework for the assessment of environmental performance, EN 15643-2:2011, European Committee for Standardization (CEN), <http://www.cen.eu>.
- [9] Danatzko, J., Sezen, H., Chen, Q., "Sustainable design and energy consumption analysis for structural components" Journal of Green Building: Winter 2013, Vol. 8, No. 1, pp. 120-135., doi: 10.3992/jgb.8.1.120.
- [10] A. Puskas, J. Virag, Cost or energy efficiency? Criteria in design of a reinforced concrete structure of a public building, Proc. of the 8th In. Conf. on Energy & Environment, eds. V. Mladenov, T. Tashev, H. Wang, I. Kralov, S. Stankevich, P. Yildiz & J. Burley, Rhodes Island, pp. 112-117, ISBN: 978-960-474-312-4.
- [11] Naik T. R., Sustainability of Concrete Construction, CBU-2007-02, ASCE Practice Periodical on Structural Design and Construction, Vol. 13, No. 2, pp. 98-103, 2008.
- [12] Struble L., Godfrey J, How sustainable is concrete?, Proc. of the International Workshop on Sustainable Development and Concrete Technology, Ed. K. Wang, Iowa State University, pp. 201-212, 2004
- [13] Eurocode: Basis of structural design, EN 1990/1992
- [14] Eurocode 1: Actions on structures, EN 1991/1992
- [15] Eurocode 2: Design of concrete structures, EN 1992/1992
- [16] Eurocode 6: Design of masonry structures, EN 1996/1992
- [17] Eurocode 8: Design of structures for earthquake resistance, EN 1998/1992
- [18] NP 007-97, Design code for reinforced concrete structures, 1997
- [19] CR6-2013, Design code for masonry structures, 2013
- [20] P100-1/2006, Earthquake resistance design code – Part I - General design rules for buildings, 2006
- [21] Athena Impact Estimator for Buildings 4.5, Athena Sustainable Materials Institute, <http://www.athenasmi.org>

A. Puskás is Assistant Professor at Faculty of Civil Engineering of Technical University of Cluj-Napoca, Romania, since 2007. He received the B.S. and Ph.D. degrees in civil engineering in 1995 and 2012, respectively, from Technical University of Cluj-Napoca, Romania, and M.S. degree in Business Administration from Faculty of Business of Babes-Bolyai University, Cluj-Napoca, Romania, in 2005. In 2013 he graduated a Postgraduate Course in Sustainable Urbanization at Technical University of Cluj-Napoca, Romania and participated in a short course in Sustainability: Principles and Practice at Massachusetts Institute of Technology, Cambridge, United States.

He joined Technical University of Cluj-Napoca, Romania in 2003 as Teaching Assistant. From 2000 he have also worked as Structural Designer, leading or participating in design of several steel, concrete, masonry or wooden structured industrial and public buildings. Since 2005 he is also Technical Director of a privately owned construction company, with extensive activity in industrial and public building design and realization. He has authored more than 30 Journal and Conference papers. His current interests include sustainability of structures and their environmental impact as well as waste recycling in construction industry.

Dr. Puskás is member of The International Federation for Structural Concrete, The American Concrete Institute, Association of Environmental Engineering and Science Professors, Romanian Green Building Council and Association of Structural Designer Civil Engineers.

J. Virág is Teaching Assistant at Faculty of Civil Engineering, Technical University of Cluj-Napoca, Romania since 2005. J. Virág received B.S. Degree in civil engineering in 2004, at Technical University of Cluj-Napoca, where currently he is Ph.D. student. B.S. degree in economics was received from Faculty of Business at Babes-Bolyai University, Cluj-Napoca, Romania, in 2005 and one year later he participated at Ph.D. Course on High Performance Computations for Engineering at the University of Pécs, Hungary.

His current job positions are Lead Structural Designer at Lamina, Cluj-Napoca and Teaching assistant at Technical University of Cluj-Napoca. He is the (co-)author of more than 10 papers concerning masonry and reinforced concrete structures.

Mr. Virág is member of AICPS (Structural Designer Engineers' Association) and AGIR (General Engineers' Association from Romania).

Ligia M. Moga is Associate Professor at Faculty of Civil Engineering of Technical University of Cluj-Napoca, Romania. She received her B.S. diploma in Civil Engineering, from the Technical University of Cluj-Napoca in 2005, an MSc in Civil Engineering "Structural and thermal rehabilitation of buildings" from the Technical University of Cluj-Napoca in 2006. She finished her PhD program in the field of Civil Engineering in 2009 with the thesis "Contributions regarding the thermo energetic optimization of new and existing buildings". Since 2005 she started working at Department of Buildings at Faculty of Civil Engineering, Technical University of Cluj-Napoca. Since October 2012 she is a "Certified Passive House Designer", diploma received from the Passivhaus Institut Darmstadt, Germany. In 2013 she graduated a Postgraduate Course in Sustainable Urbanization at Technical University of Cluj-Napoca, Romania and participated in a short course in Sustainability: Principles and Practice at Massachusetts Institute of Technology, Cambridge, United States. Her teaching activity involves courses, seminars and projects at undergraduate, graduate and postgraduate levels:

She joined the Technical University of Cluj-Napoca after finishing her undergraduate years in 2005 and became Teaching Assistant in 2007 and Assistant Professor in 2011. Her main research fields are: sustainable buildings, energy efficient buildings, environmental impact of buildings, green technologies. Her experience in the mentioned field includes both her academic work and personal work at her company. She was director of a national grant "Methodology, Numeric Method and Automaton Calculus Program- Vitraj- for Defining the Thermal Performance of Windows, Doors and Solar Protection Elements", member in several grants and projects, e.g. "Integrated systems solutions for the rehabilitation of buildings / residential districts", "2006 Action Programme for thermal rehabilitation of 87 blocks of flats", "Thermal Bridges Catalog" and she has authored and co-authored more than 93 papers.

Dr. Moga is a member of International Society of Indoor Air Quality and Climate, The Professional Organisation of Specialists in Building Energetics, Zero Energy Buildings Romanian Association.

H. Szilágyi is Senior Researcher at National Institute for Research and Development "Urban-Incer", Cluj-Napoca Branch, Romania. She is B.Eng. in "Construction materials technology", "BABEȘ-BOLYAI" University Cluj-Napoca, Chemistry and Chemical Engineering Faculty in 1993, B.S. in Oxidic materials science and engineering, "BABEȘ-BOLYAI" University Cluj-Napoca, Chemistry and Chemical Engineering Faculty since 2001. She received: the M.S. degree in „Materials science and technology”, "BABEȘ-BOLYAI" University Cluj-Napoca, Physics Faculty in 2003, and Ph.D. degree in civil engineering from Technical University of Cluj-Napoca, Faculty of Constructions in 2008.

She was employed at Cluj-Napoca Branch of the National Building Research Institute as B.Eng. in 1994, became engineer in 2001, scientific researcher in 2004, scientific researcher grade III in 2007, scientific researcher grade II and branch manager since 2013. She is Associate Lecturer at Technical University, Cluj-Napoca from 2009 to present. She has more than 60 published papers as author or co-author from 2001 to present. Her particular research interests are experimental engineering and building materials, special concrete and waste recycling in construction.

Dr. Szilágyi is member of: CT 321 - Technical Committee for "Concrete and precast concrete" and AFSIC - Association of Proficiency Testing Providers.

M. Bindea is Assistant Professor at Faculty of Civil Engineering of Technical University of Cluj-Napoca, Romania, since 2014. He received the B.S. and Ph.D. degrees in civil engineering in 2004 and 2012, respectively, from Technical University of Cluj-Napoca, Romania. In 2005 he graduated the M.S. in Constructions Rehabilitation at Faculty of Civil Engineering of Technical University of Cluj-Napoca.

Since 2004 he worked as Structural Designer, first in a privately owned company specialized in designing of precast reinforced concrete structures and in recent years in his own company. He designed various structures for residential or administrative buildings and steel structures for industrial and agricultural buildings. He joined Technical University of Cluj-Napoca, Romania in 2009 as Teaching Assistant and he published more than 10 Journal and Conference papers. He published a book on computational and

testing methods in seismic engineering. His current research interests is earthquake engineering including sustainability of precast reinforced concrete structures and their environmental impact with a particular attention to modern solutions for concrete slabs.

Dr. Bindea is member of the Romanian Association of Structural Designer Civil Engineers.

Sz. A. Köllő is Structural Engineer since 2011. Sz. A. Köllő received his B.S. degree in Civil Engineering in 2011 from Technical University of Cluj-Napoca, Romania, and in Railways, Roads and Bridges Engineering in 2013 at the same university. He received his M.S. degree in Structural Engineering in 2013 at the Faculty of Civil Engineering of Technical University of Cluj – Napoca, Romania.

He is working as structural engineer for a privately owned company specialized in structural design and construction of structures. His current research interest is structural optimization.

Mr. Köllő is member of the Romanian Association of Structural Designer Civil Engineers and of the Hungarian Technical Scientific Society of Transylvania.

Long-term water balance changes of the pristine Bela River basin

D. Halmova, P. Miklanek, P. Pekarova

Abstract— Study is devoted to the water balance changes, of the Bela River basin up to the Podbanske gauge, within the two 30-years periods 1940/41–1969/70 and 1975/76–2004/05, to the simulation of the monthly runoff from the Bela River basin and to estimation of individual water balance components in the monthly time step, during the period 1940/41–2004/05.

In the first part, water balance is set up in the monthly and yearly time step, based upon mean monthly discharge data from the gauging station Bela-Podbanske. Also mean monthly precipitation data over the Bela River basin were calculated. Changes of the basin water storage were compared for the two mentioned time periods. The second part of the study is focused on the selected runoff components simulation from the Bela River basin in the monthly time step, during the period 1940/41–2004/05. To assess this aim, we used the BILAN model, which sets individual components of total runoff. The model simulates hydrological processes by simplifying a catchment into series of connected storage reservoirs, where precipitation, air temperature and humidity are inputs and the output is represented by streamflow at in the catchment outlet. The objective of this study was to calibrate the BILAN model for the Bela River basin up to the gauging station Bela: Podbanske, within the period 1940/41–2004/05 and two shorter time periods of 30 years 1940/41–1969/70 and 1975/76–2004/05. We simulated the average monthly values of individual hydrological components during the mentioned periods. We achieved a sufficient agreement between observed and simulated values in regard to input data.

Keywords— Bela River basin, basin water storage change, hydrological balance, rainfall-runoff model, runoff components.

I. INTRODUCTION

HYDROLOGICAL (water) balance reflects the fundamental relationships between elements of the hydrological cycle. Reliable determination of the basic components of water balance (precipitation, runoff, evaporation, water storage) depends primarily on the accuracy of direct measurement of

This work was supported by the Science and Technology Assistance Agency under contract No. APVV-0015-10 during the project implementation of the “Centre of excellence for integrated flood protection of land” (ITMS 26240120004) supported by the Research & Development Operational Programme funded by the ERDF, and KORANET project 052.

D. Halmova is with Institute of Hydrology Slovak Academy of Sciences, Racianska 75, 831 02 Bratislava, Slovakia, (e-mail: halmova@uh.savba.sk).

P. Miklanek is with Institute of Hydrology Slovak Academy of Sciences, Racianska 75, 831 02 Bratislava, Slovakia, (phone: +4212 44259311, Fax: +4212 44259311, e-mail: miklanek@uh.savba.sk).

P. Pekarova is with Institute of Hydrology Slovak Academy of Sciences, Racianska 75, 831 02 Bratislava, Slovakia, (e-mail: pekarova@uh.savba.sk).

the first two components. Evaporation will then be calculated from the first two components of the water balance.

In the '70s an extensive hydrological research, organized by the Slovak Hydrometeorological Institute (SHMI), took place in the representative mountainous Bela River basin (up to Liptovsky Hradok). The aim of the research was the detailed mapping of basic elements of water balance [1]-[2]. Many authors [3]-[10] dealt with the Tatra Mountain hydrology. Hydrological balance of six catchments of the Western and High Tatra mountains was elaborated by Holko et al. [11]-[12] for time period 1989–1998. Its results showed that the use of all existing data and advanced computational methods does not give a satisfactory answer to the doubts which arise when determining the essential elements of the hydrological balance in the different mountain watersheds. Hydrological balance of mountain river basins still remains an unexplained problem.

The Bela River starts with confluence of the Tichy and Koprovy creeks at 976.8 m a.s.l. The total length of the stream is 23.6 km [2]. The Bela River basin area is 244.303 km². From the confluence of the Koprovy creek and Tichy creek Bela River flows south-west and receives seven right and left tributaries. Significant tributaries are Kamenisty creek and Rackovy creek, which have – like the upper Bela River – alpine character (Fig. 1). Bela flows into the River Vah at Liptovsky Hradok at an altitude of 629 m a.s.l. and it is its significant right tributary.



Fig. 1. The Bela River basin, Krivan peak (2494 m. a.s.l.). (Photo Pekarova, May 2014).

The Bela River is the major stream of the Tatras in Slovakia and is considered to be a typical river of the highest part of the Carpathians. In the Bela River basin there occur significant hydrological locations such as lakes and waterfalls. Slovak Hydrometeorological Institute (SHMI) incorporates the catchment area into the international category "representative basin" and river basin is registered under the International Hydrological Programme of UNESCO. The largest anthropogenic modifications, pastures and associated clearing of forests occurred mainly in the 19th century. After the establishment of the Tatra National Park (TANAP) in 1948 grazing has been banned and forests began to be regarded as a beneficial element for flood protection (Pekárová et al., 2009b). The upper part of the Bela River basin up to Podbanske gauge (93.4 km²) is located in the TANAP reserve (protected area), and is not influenced by the human activity (Fig. 2). The vegetation of the Bela basin up to Podbanske water gauge consists by 40% of dwarf pine, 13% cover coniferous forests, 30% is woodland shrub, 16% are natural meadows and the rest are water areas and built-up areas.

In this study we processed the hydrological balance of the upper part of the Bela River up to Podbanske gauge for the time period 1940/1941–2004/2005. We divided this period into two periods of the equal 30 years length.



Fig. 2. The upper Bela River basin up to the Podbanske water gauge (triangle), meteorological stations (MS, cross). Forest boundary (green line), boundary of the disturbed forest during the November 19, 2004, wind-throw (red line).

II. DATA AND METHODS

Water level observations on the Bela River at Podbanske station started in 1924 [13]-[16]. In collaboration with SHMI we examined the historical consumption curve of profile Bela: Podbanske, and for analysis of the hydrological regime we used the mean daily discharge data from the years 1928–2011 (Fig. 3).

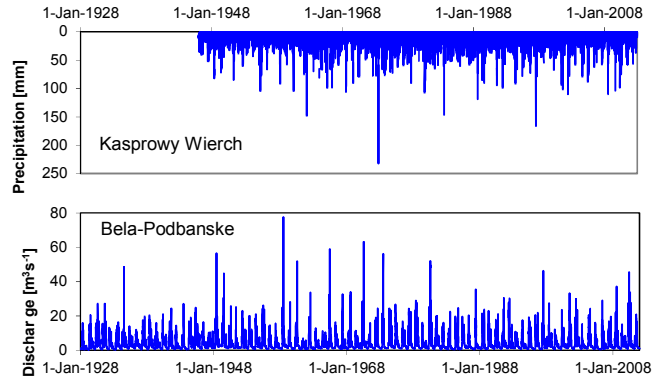


Fig. 3. Daily precipitation on Kasprowy Wierch observatory and daily discharge of the Bela River at Podbanske gauge.



Fig. 4. Kasprowy Wierch observatory and Podbanske MS (Photo Pekarova: October 2013, October 2008).

To calculate the mean monthly areal precipitation totals, we used the monthly precipitation from Podbanske meteorological station since 1930, and from the Polish observatory Kasprowy Wierch since 1938 (Fig. 4). Precipitation (temperature) gradient we calculated from annual precipitation (temperature) from stations in different altitude in the vicinity of the Bela River basin (Strbske Pleso, Podbanske, Liptovsky Hradok, Lomnický štít, and Kasprowy Wierch) (Figs. 5a-b).

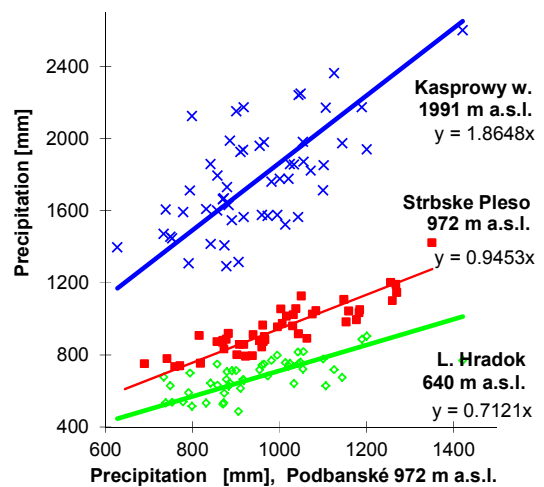


Fig. 5a. Relationship between annual precipitation at Podbanske meteorological station and stations in different altitude.

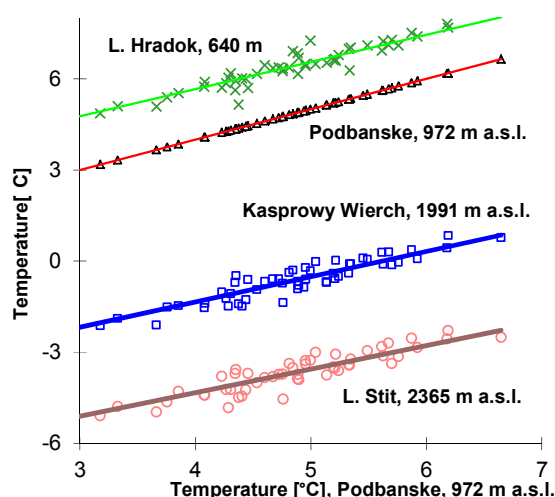


Fig. 5b. Relationship between annual temperature at Podbanske meteorological station and stations in different altitude.

A. Hydrological (Water) Balance

Hydrological balance quantifies the water circulation in a closed system with one concentrated runoff in the final profile of the catchment. The atmospheric precipitation over the basin is the only input to the basin balance. The difference in soil water content at the beginning and at the end of time period can be neglected for a sufficiently long period. In that case, we can identify total annual evapotranspiration with a difference of precipitation and runoff.

The water balance equation in the following form was used:

$$P = R + ET + \Delta S \quad (1)$$

where:

P – annual precipitation depth [mm];

R – annual average runoff [mm];

ET – annual evapotranspiration depth [mm];

ΔS – average total losses that have a higher significance in shorter time intervals Δt . For the long-term water balance this element might be neglected and replaced by $\Delta S = 0$.

For the long-term monthly balance, if we determine the monthly total evapotranspiration in an independent manner, we are able to determine the change in water storage in the basin according to the water balance equation.

B. Monthly evapotranspiration

For the long term monthly water balance calculation it is necessary to know the actual course of the annual evapotranspiration in the study basin. Availability of data on evapotranspiration or evaporation is low. Average monthly and annual potential evapotranspiration values for different stations in Slovakia can be found in tabular and map form, for example in Tomlain [17]. Of course the number of such processed stations is limited. In such areas lying near the station, but at a significantly different altitude, the applicability of such data is limited.

Miklanek [18] dealt with modeling of the average monthly values of potential evapotranspiration. Based on an extensive set of potential evapotranspiration data from several stations at different altitudes he proposed a simple method that allows modeling of the average monthly values of potential evapotranspiration at any altitude, if an estimate of the annual total is known. For the annual potential evapotranspiration approximation Miklanek [18] used equation of normal distribution in the form:

$$ETPR(x) = \frac{1}{\sigma\sqrt{2\pi}} e^{-\left(\frac{(x-x_m)^2}{2\sigma^2}\right)}, \quad (2)$$

where:

$ETPR$ – relative potential evapotranspiration [%],

x – number of month ($x = 1, 2, \dots, 12$),

x_m – time of maximal $ETPR$ expressed in months as a decimal number,

σ – the parameter that influence the shape of the curve.

The values of x_m and σ depend on altitude. Linear relationships were derived for this dependence. Monthly values of potential evapotranspiration, in relative terms, can be calculated on the basis of this linear relationship if we know the locality altitude. The absolute values of potential evapotranspiration in each month can be determined, if we know the annual precipitation total or at least its assessment. In this case, the following equation may be used:

$$ETP(x) = ETPR(x).EP \quad (3)$$

where:

ETP – modeled monthly potential evapotranspiration [mm.month⁻¹];

EP – annual potential evapotranspiration [mm.year⁻¹].

Relative monthly values $ETPR(x)$ were primarily calculated for potential evapotranspiration distribution during the year. But they can be used also for other similar phenomena, such as evaporation from the water surface. In the months with maximum evaporation there occurs also maximum precipitation and water availability should not be a factor modifying the distribution of actual evapotranspiration compared with potential in the Belá basin. This allows to assume that the distribution of potential and actual evapotranspiration will be very similar in the study basins and the relationship can be used also for the distribution of actual evapotranspiration as well as evaporation balance.

C. The Water Balance model BILAN

Over the last decades, hydrological rainfall-runoff models, in a basin scale, have become an important tool in the water management. The user must be able to choose the right model depending on the topic. The biggest problem remains the problem of getting high-quality, sufficiently long series of input data. After proper model selection and calibration, its subsequent use has irreplaceable contribution either in the

water management or in ex post evaluation of specific situations in river basins. Among the conceptual models with lumped parameters there belong, for example monthly water models BILAN, WBMOD, WatBal, or rainfall runoff models. In daily time step there are HBV, SAC SMA Sacramento soil moisture model and HEC-HSM model, for example.

In the study we used the hydrological model BILAN with a monthly time step to assess the individual components of the water balance of the Bela River basin up to station Podbanske. Model belongs to a group of conceptual models with lumped parameters [19]-[20]. The model simplifies catchment areas using three water reservoirs. The structure of the model consists of a system of relations describing the basic principles of water balance of the unsaturated and saturated zones, including the impact of vegetation cover and groundwater.

Measured time series of monthly precipitation, air temperature and potential evapotranspiration, or relative humidity are the inputs into the model BILAN.

The aim of the model is to simulate monthly time series of hydrological variables and apply it to the entire river basin. The model simulates hydrological variables, such as potential evapotranspiration, actual evaporation and infiltration into the zone of aeration, percolation into groundwater aquifers, water storage in snow cover, soil and aquifer [21].

Total runoff of the month consists of three components: base flow, interflow (hypodermic) and direct flow. Direct flow is considered as fast runoff component of total runoff, which does not affect the evaporation, and soil water balance. Hypodermic flow is considered as the water excess in the aeration zone. In winter, during snowmelt, this runoff component also includes direct runoff. The base flow is the slow component of the total runoff, the delay in the basin may be longer than one month. The model in the vertical direction distinguishes three levels, namely the surface, soil zone and groundwater zone. The size of the flows between the reservoirs is determined by the model algorithms, which are controlled by eight free parameters.

III. RESULTS

Long-term mean annual precipitation depths in the Bela River basin (up to Podbanske) is 1728 mm, mean annual runoff depth is 1172 mm and the balance evaporation equals to 555 mm. The highest and lowest runoff at station Bela: Podbanske, for the period of measurements, was 1701 mm (1947/48) and 665 mm (1960/61). The annual runoff coefficient varies from 43 to 87% with the average 68% (Fig. 6). Long-term mean annual temperature at meteorological station Podbanske was 4.99°C, at Kasprowy Wierch observatory it was -0.54°C.

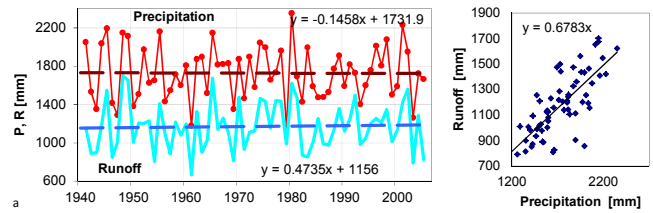


Fig. 6. Relation between annual precipitation and runoff, the Bela River basin, 1940/41–2004/05 .

A. Monthly precipitation and discharge

In terms of monthly precipitation depth in the long-term average (period 1940/41–2004/05), the most precipitation falls in the month of July (238 mm) and minimum in February (96 mm) (Fig. 7). The highest average monthly runoff occurs during snowmelt: average surface flow is 249 mm in May and 194 mm in June. This represents almost 38% of the total annual runoff. In March runoff has the lowest variability and highest runoff fluctuations are recorded in August.

Monthly evaporation values in Podbanske station were calculated from the annual balance of evaporation on the basis of the percentage distribution described above.

Table 1 shows the monthly values of water storage in the Bela River basin for the whole period of water years 1940/1941–2004/2005 (a), and for two sub-periods 1940/1941–1969/1970 (b) and 1975/1976–2004/2005 (c). Water storage (S) in the Bela River basin rises from September to March and accumulated storage of water in the basin is depleted from April to August. Fluctuations of water storage in the basin were 337 mm in average in the 65-years period.

The long-term courses of water balance components are shown in Fig. 8 for two time periods at the station Podbanske. Such water balance allows us to allocate the average monthly change in water storage in the basin, or in the soil and groundwater.

The difference is 14 mm in average annual rainfall in two 30-year periods. A comparison of the balance in the Bela River basin shows that at lower precipitation the runoff was higher in the period 1975/1976–2004/05 (Fig. 9). Therefore, there was a more rapid depletion of water resources in the Bela River basin.

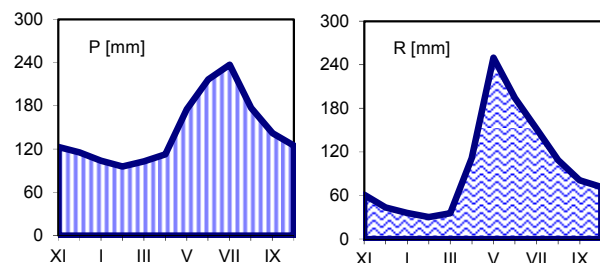


Fig. 7. Monthly precipitation and runoff depths, the Bela River basin, 1940/41–2004/05 .

Table 1: Long – term monthly values of water storage in the Bela River basin for time periods: a) 1940/1941–2004/2005, b) 1940/1941–1969/1970, and c) 1975/1976–2004/2005.

month	a)		b)		c)	
	S=P-R-ET	sum S	S=P-R-ET	sum S	S=P-R-ET	sum S
XI	52.9	53	60.5	61	43.8	44
XII	70.1	123	67.2	128	71.4	115
I	67.2	190	66.7	194	70.3	185
II	62	252	74.8	269	52	237
III	54.4	307	51.7	321	61.3	299
IV	-34.3	272	-51.2	270	-22.9	276
V	-147.1	125	-137.8	132	-161.4	114
VI	-86.4	39	-73.4	59	-103.5	11
VII	-34.9	4	-51	8	-14.7	-4
VIII	-30.9	-27	-25	-17	-28.4	-32
IX	1	-26	-9.4	-27	6.9	-25
X	26	0	26.8	0	25.2	0

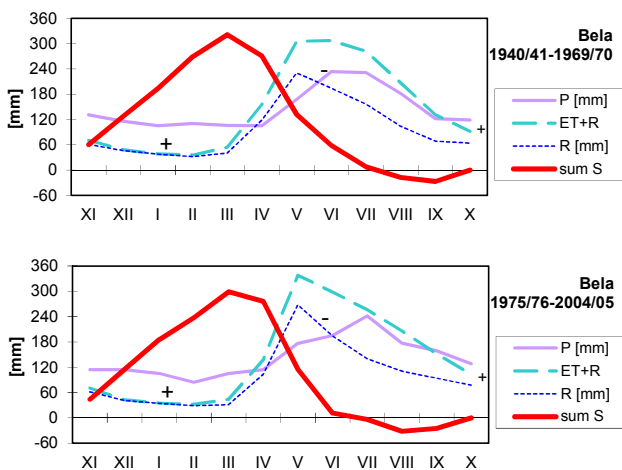


Fig. 8: Water balance components comparison, determined from the long – term monthly means of the Bela River basin up to Podbanske for two 30- years periods 1941/1942–1969/1970, and 1975/1976–2004/2005.

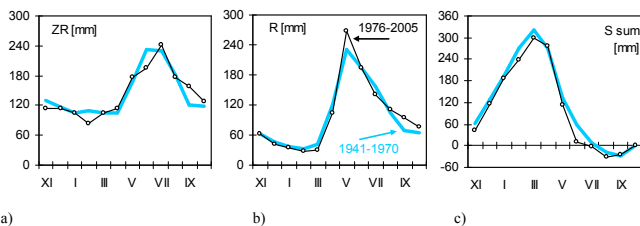


Fig. 9: Water balance components comparison, determined from the long–term monthly means of the Bela River basin up to Podbanske, for two 30- years periods: 1941/1942–1969/1970 (bold line) and 1975/1976–2004/2005 (line with points) a) Long-term monthly precipitation, b) Long-term monthly runoff, c) Basin water storage.

B. Simulation of runoff components and water storage in the Bela River basin

Using the model BILAN we modeled the course of the average monthly values of the individual runoff components in

the Bela River basin according to parameters derived for the entire period 1940/1941–2004/2005. The base flow constitutes 59.32%, interflow 17.95% and direct flow 22.70% of total runoff.

IV. CONCLUSIONS AND DISCUSSION

In the first part, water balance is set up in the monthly and annual time step, based on mean monthly discharge data from the gauging station Bela-Podbanske. Also the mean monthly precipitation data over the Bela River basin were used. Changes of the basin water storage were compared, for the two mentioned time periods.

From water balance of the whole observation period it follows, that the mean annual Bela River basin precipitation depth (up to Podbanske) is 1728 mm, mean annual runoff depth is 1172 mm, and the balance evaporation equals to 555 mm. In the basin precipitation depth calculations, no precipitation corrections were taken into account. From the measured results it follows, that during the 1940/41–2004/05 period, no increase in the mean annual discharge has been observed. The mean annual discharge trend is slightly rising. The monthly water balance comparison for the two different time periods indicates paradoxically, that the slightly lower precipitation within 1975/1976–2004/05, produced higher runoff, particularly in the month of May. This resulted in faster Bela basin water storage depletion and the balance evaporation was lower at higher air temperature.

However, accuracy of the presented water balances depends on several factors. First of all, it depends on the measurements accuracy of precipitation and water levels, accuracy of the river rating curves, and upon processing of the mean daily discharge data. For these reasons, we tried to survey and to evaluate all historical material on the water level observations at the gauging station Bela-Podbanske since 1928 and to eliminate any errors in the evaluation of flow rates. Although the water balance in absolute numbers may actually be different, considering precipitation measurement errors, the relative comparison of the two periods gives a good indication of the ongoing changes in the balance of the individual runoff components in the Bela River basin.

The second part of the study is focused on the selected runoff components simulation from the Bela River basin in the monthly time step, during the period 1940/41–2004/05. To assess this aim, we used BILAN model, which sets individual components of total runoff. The model simulates hydrological processes by simplifying a catchment into series of connected storage reservoirs, where precipitation, air temperature and humidity are inputs and the output is represented by streamflow at the catchment outlet. The objective of this study was to calibrate BILAN model for Bela River basin up to the gauging station Bela-Podbanske, within the period 1940/1941–2004/2005 and two shorter time periods of 30 years 1940/1941–1969/1970 and 1975/1976–2004/2005. We simulated the average monthly values of individual hydrological components during the mentioned periods.

The model describes observed runoff values relatively good. We achieved a sufficient agreement between observed and simulated values in regard to input data. Main non-agreement of simulation is in the area of maxima. Correlation coefficient between observed and simulated runoff is 0.6813. Total runoff was divided into three components: baseflow, interflow and direct runoff. The proportion of the baseflow, interflow and direct runoff of the total runoff is 59.32%, 17.95%, and 22.70%, respectively.

- [20] L. Kasparek, and O. Novicky, "Users guide BILAN," *CD ROM*, 2004, 12 p.
 [21] S. Horacek, O. Rakovec, L. Kasparek, and A. Vizina, "Development model of water balance – BILAN," *Water management technical and economic informations*, Praha, 51, 2009, 2–5.

REFERENCES

- [1] B. Hlubocky, L. Dulovic, M. Matuska, and J. Turcan, "Hydrological regime of Bela representative basin," *Final report* No. 2231, SHMI, Bratislava, 1980, 97 p.
 [2] J. Pacl, "Hydrology of the Tatra National Park," *Proc. of the works of the Tatra National Park*, 15, 1973, 181–238.
 [3] J. Hladny, and J. Pacl, "Analysis of the precipitation-runoff relationships in mountain watersheds," *J. Hydrol. Hydromech.*, 22, 4, 1974, 346–356.
 [4] L. Molnar, and J. Pacl, "The hydrological characteristics of the High Tatra region," *Workshop on Hydrology of Mountainous areas*, IH SAS, 1999, 28 p.
 [5] J. Drako, M. Kupco, J. Turbek, and P. Stastny, "Results of the regime observation of climatic and hydrological phenomena in the Tatras region," *IAHS Publication* no. 190, Wallingford, 1990, 153–164.
 [6] L. Molnar, P. Miklanek, and M. Trizna, "Experimental research of water balance components in the mountainous watershed," *J. Hydrol. Hydromech.*, 39, 5-6, 1991, 448–456.
 [7] Z. Kostka, "Estimation of soil water content in mountain catchment by method of soil profile water balance," *J. Hydrol. Hydromech.*, 40, 5, 1992, 446–458.
 [8] O. Majercakova, and P. Skoda, "Changes in the hydrological regime in the Tatras," *Works and studies* 46, SHMI, Bratislava, 1993, 53 p.
 [9] J. Pacl, "Tatra National Park – Water," *Publ. TANAP*, Tatranska Lomnica, 1994, 66–78.
 [10] J. Parajka, "Estimation of the average basin precipitation for mountain basins in the Western Tatra mountains," *ERB2000-Monitoring and modelling catchment water quantity and quality*, Ghent, Belgium, 2000, 27–29.
 [11] L. Holko, J. Parajka, O. Majercakova, and P. Fasko, "Hydrological balance of selected catchments in the Tatra Mountains region in hydrological years 1989 – 1998," *J. Hydrol. Hydromech.*, 49, 3–4, 2001, 200–222.
 [12] L. Holko, Z. Kostka, and Z. Pecusova, "Snow: Change Scenarios of Selected Components of the Hydrosphere and Biosphere in Vah and Hron River Basin due to Climate Change," VEDA Publ. House, Bratislava, 2005, 105–168.
 [13] P. Pekarova, J. Pekar, and J. Pacl, "Temporal variability of annual discharges of Bela River basin for the period 1901–2000," *Proc. Hydrologic days 2005*, CD, SHMI, Bratislava, 2005.
 [14] P. Pekarova, D. Halmova, P. Miklanek, J. Pekar, P. Skoda, S. Liova, and K. Kucarova, "Homogeneity analysis of the water temperature measurements, Bela River at Podbanske," *Acta Hydrologica Slovaca*, 10, 1, 2009, 140–150.
 [15] P. Pekarova, J. Pacl, S. Liova, P. Miklanek, P. Skoda, and J. Pekar, "Analysis of the maximum annual discharge regime in the high mountain basin of Bela River in Podbanske," *Acta Hydrologica Slovaca*, 10, 2, 2009, 300–311.
 [16] P. Pekarova, P. Miklanek, P. Skoda, J. Pekar, and J. Pacl, "Multi-annual discharge variability and trend analyses of the Bela River (Slovakia) in 1895–2006," *IAHS Publication* 336, Wallingford, 2010, 59–64.
 [17] J. Tomlain, "Evaporation from the soil surface and plants," *Proc. SHMI*, Vol. 33/I, Climatic conditions in Slovakia, selected characteristics, 1991, 163–172.
 [18] P. Miklanek, "Annual course of potential evapotranspiration in different altitudes," *J. Hydrol. Hydromech.*, Vol.43, 4-5, 1995, 275–287.
 [19] L. Kasparek, and O. Novicky, "Background information on BILAN," *CD ROM*, 2004, 9 p.

Short term effect of different management practices on rice production and agronomic behavior in Mediterranean conditions

D. Becerra, J. Sánchez-Llerena, D. Peña, A. López-Piñeiro, A. Albarrán, J. Rato-Nunes and L. Loures

Abstract— Rice is staple food for more than 50% of the world's population. New techniques such as conservation agriculture and aerobic rice can be a very important alternative in semi-arid Mediterranean regions in order to reduce water consumption and improve soil quality. The present work evaluated the viability of aerobic rice management implementation, applying conservation agriculture techniques in soil and climate conditions of Extremadura (Spain), determining the effects of these techniques on rice production and other important agronomic parameters. Grain yield was 46.5% higher under flooded condition than under aerobic condition in conventional tillage treatments. However, in no tillage treatments grain yield was 18.3% higher under aerobic condition. Water productivity was higher under aerobic condition and no tillage practices. Therefore aerobic rice system in Mediterranean conditions could be an effective strategy to save water but the rice production may be lower.

Keywords— Aerobic rice, Conventional tillage, Flooded rice, No tillage.

I. INTRODUCTION

RICE is staple food for more than 50% of the world's population [1], growing up to 80% when considering only Asian population. In the European Union (EU), 475 000 ha are given over rice cultivation, reaching a production of 3.2 millions of tonnes of paddy rice. Spain is one of the largest rice producers in the EU, with 20% of the total European

D. Becerra is with Área de Producción Vegetal, Escuela de Ingenierías Agrarias, Universidad de Extremadura, Ctra. de Cáceres s/n, 06071, Badajoz, Spain (corresponding author to provide phone: +34924289355; e-mail: dbecerra@alumnos.unex.es).

J. Sánchez-Llerena is with Área de Edafología y Química Agrícola, Facultad de Ciencias, Universidad de Extremadura, Avda de Elvas s/n, 06071, Badajoz, Spain (e-mail: jsanchezllerena@gmail.com).

D. Peña is with Área de Edafología y Química Agrícola, Facultad de Ciencias, Universidad de Extremadura, Avda de Elvas s/n, 06071, Badajoz, Spain (e-mail: dpenaaba@alumnos.unex.es).

A. López-Piñeiro is with Área de Edafología y Química Agrícola, Facultad de Ciencias, Universidad de Extremadura, Avda de Elvas s/n, 06071, Badajoz, Spain (e-mail: pineiro@unex.es).

A. Albarrán is with Área de Producción Vegetal, Escuela de Ingenierías Agrarias, Universidad de Extremadura, Ctra. de Cáceres s/n, 06071, Badajoz, Spain (e-mail: angliso@unex.es).

J.M. Rato-Nunes is the C3I, Polytechnic Institute of Portalegre, Portugal (ratonunes@esaelvas.pt).

Luís Loures is with the Centre for Spatial and Organizational Dynamics and the C3I, Polytechnic Institute of Portalegre, Portugal (lcloures@gmail.com)

farmland devoted to rice cultivation. Inside Spain, Extremadura, with an average performance of 7 300 kg ha⁻¹ has been consolidating itself as one of the biggest rice producers regions, with most productive areas gathering around Gadiana river lowlands [2].

Rice crop cultivation in these areas traditionally involves intensive and expensive tillage practices. Furthermore, water consumption in traditional rice production system takes an average of 24 000 m³ ha⁻¹ year⁻¹. In a semi-arid Mediterranean regions, where water resources are strongly limited, flooded irrigation in rice crop is highly endangered due to his lack of sustainability.

From an environmental point of view, modern approaches to rice crop intensification have damaged important natural resources [3]. The development of appropriate management techniques could lead to reduce those negative impacts and increase rice productivity. Research about these management techniques should focus mainly in a rational and sustainable use of two essential resources: soil and water.

Regarding soil management, conservation agriculture is a concept for resource-saving agricultural crop production that strives to achieve acceptable profits which is used to increase soil organic matter, control of erosion and degradation and increase water holding capacity [4].

Regarding water management, new techniques such aerobic rice are being developed all over the world. Aerobic rice production, with alternative methods such as sprinkler irrigation, can be a very important alternative in semi-arid Mediterranean regions [5], however, the development of these systems are still in early stages, and more research is needed in order to implement these techniques correctly [6].

The aim of the present study was to evaluate the viability of aerobic rice management implementation, applying conservation agriculture techniques in soil and climate conditions of Extremadura (Spain), determining the effects of these techniques on rice production and its components.

II. MATERIALS AND METHODS

A. Site description

A field experiment was conducted in 2013 on a Hydragic Anthrosol [7] with 16.96% clay, 35.87% silt, 47.17% sand. The experimental field was located in Extremadura, south western Spain (39° 06' N; 5° 40' W), with Mediterranean

climate (rainfall <480 mm, with hot and dry summers). Historically, the experimental field was cropped with rice using the traditional practices (deep plowing and flooding).

B. Field experiment

For our experiment, the field was divided into 200 m² experimental blocks, and were subjected to four management regimes: 1. Rice cultivation by conventional agricultural techniques in the region, tillage to 30 cm and flooding with continuous water flow (3 plots, “CTF”); 2. Rice cultivation by conventional tillage and sprinkler irrigation (3 plots, “CTS”); 3. Rice cultivation using conservation agriculture techniques and continuous water flow (3 plots “NTF”) and 4. Rice cultivation using conservation agriculture techniques and sprinkler irrigation (3 plots “NTS”). All blocks were cultivated using *Oryza sativa* L. var. Gladio. The physico-chemical properties of soil of the experimental field are presented in Table I.

C. Water consumption monitoring, soil sampling and agronomic parameters determination

The water supply in different treatments was monitored with a water flowmeter. Soil samples were taken by manual auger from each plot from 0-20 cm depth. Three soil subsamples were taken randomly from each of the three replicate plots. All agronomic parameters were determined from a 2 m² sampling area within each plot and productive parameters were corrected to a moisture content of 14% fresh weight.

D. Soil analyses

Texture was determined by sedimentation using the pipette method after organic carbon destruction with H₂O₂ and chemical dispersion using Na₄P₂O₇. Total organic carbon (TOC) content was determined by dichromate oxidation [8]. Water soluble organic carbon (WSOC) was extracted with de-ionized water at 3:1 (water to soil) ratio. Humic acids(HA) and fulvic substances (fulvic acids+humins, FA) were extracted by a solution of 0.1 M Na₄P₂O₇ + NaOH using a ratio extractant to sample of 10:1, and to precipitate humic acid, the supernatant was acidified to pH 2 with H₂SO₄. The WSOC and the TOC associated with each fraction of HA and FA were determined by dichromate oxidation and measurement of the absorbance at 590 nm [9]. Electrical conductivity (EC) was measured in a saturation extract for soil using a combination electrode [10] and pH was measured in 1:1 (w/v) soil/water mixture using combination electrode. Different soil parameters

are shown in Table I.

E. Agronomic parameters

Germination Index (GI) was determined taking into account the number of germinated plants at BBCH 10-BBCH 11 [11] as well as sowing rate and seed weight. Number of panicles per square meter was determined at BBCH 89 using direct observation. Number of tillers per plant was determined indirectly taking into account the number of panicles per square meter and the number of germinated plants. Plant height was measured from soil to last node in the BBCH 89 stadium. Panicle length was determined using representative panicles from each plot, measuring from the last node of the plant to the last grain of the panicle at BBCH 89. The total number of grains per panicle was determined by direct observation, as well as the percentage of filled grains. Specific weight was determined using humidity and specific weight measurer AQ-600, and 1000 grain weight was determined by direct weight of 1000 grain counted by electronic seed counter Swantech-SC2. Grain production was determined by direct weight of all filled grains from each panicle collected in the trial area. Harvest index (HI) was determined as the ratio between grain production and total biomass (grain production + biomass production) and water productivity was determined as the ratio between production and amount of irrigation water applied.

F. Statistical analysis

All analyses were done using IBM SPSS Statistics v 22.0. Data was checked for normality and homogeneity of variances. One way ANOVA was used to analyze soil and agronomic properties, and Duncan’s test was used to analyze the differences of different parameters between treatments.

III. RESULTS AND DISCUSSION

A. Growth parameters

Germination index was significantly (P<0.05) higher under flooded condition (CTF) than aerobic condition (CTS) in the conventional treatments. However in no tillage treatments GI was higher in sprinkler irrigation (NTS) than flooded condition (NTF) (Table II). Germination may be deficient after flooding rice fields previously sown using conservation agriculture techniques.

A higher (P<0.05) number of tillers per plant was observed in no tillage with flooded irrigation soil (NTF) than the rest of treatments. Significantly higher number of tillers per square meter was observed by other authors [12] under flooded conditions as compared to aerobic condition. CTS treatment presented the lowest value for these parameters.

Plant height was significantly (P<0.05) higher under flooded and direct seeding condition (NTF) than conventional tillage conditions (CTS and CTF) (Table II). A significant reduction in plant height under aerobic situation compared to flooded irrigation may be due to limitation in cell elongation resulting in reduction of intermodal length, which in turn had

Table I. Soil characteristics of the field (0-20 cm depth).

Parameters	NTS	NTF	CTS	CTF
TOC (g kg ⁻¹)	7.68	8.22	7.03	8.60
WSOC (mg kg ⁻¹)	112.4	36.24	80.59	64.99
HA (g kg ⁻¹)	1.14	1.10	0.908	0.984
FA (g kg ⁻¹)	0.764	0.575	0.586	0.639
EC (μS cm ⁻¹)	1383	1118	754	1083
pH	5.22	5.44	6.25	5.34

TOC: Total Organic Carbon; WSOC: Water Soluble Organic Carbon; HA: Humic Acid; FA: Fulvic Acid; EC: Electrical conductivity

Table II. Agronomic parameters of rice as influenced by different management practices.

Parameters	NTS	NTF	CTS	CTF	ANOVA
Germination Index (%)	58.72b	46.75a	51.85a	60.68b	**
Panicles m ⁻²	587.3bc	580.0b	379.0a	620.7c	***
Tillers per Plant	0.71b	1.12c	0.25a	0.75b	***
Plant height (cm)	50.28ab	55.29b	45.50a	48.19a	*
Panicle length (cm)	16.11a	18.05b	16.94a	18.19b	**
Grain Panicle ⁻¹	99.55a	98.50a	106.27a	95.38a	NS
Filled grain (%)	81.82b	86.62bc	75.97a	89.93c	**
Specific Weight (g L ⁻¹)	527.5b	532.7b	507.6a	534.7b	**
1000 grains weight (g)	23.00b	22.81ab	21.94a	24.98c	**
Grain Yield (t ha ⁻¹)	8.23c	6.72b	4.78a	8.93d	***
Harvest Index (%)	61.9a	59.2a	57.0a	68.0b	**
Water productivity (g L ⁻¹)	1.05d	0.55b	0.61c	0.27a	***

*, **, *** Significance at 0.05, 0.01 and 0.001 respectively probability level. NS, not significant

lesser plant height [12].

The panicle length is very important, as they allow more grains. Panicle length was significantly ($P < 0.05$) higher under flooded condition than under aerobic condition (Table II) in both management techniques, no tillage and conventional tillage. Reference [12] no observed significant differences under both water management practices in this parameters.

B. Yield parameters and yield

Number of panicles per square meter was lower in the treatments CTS than CTF. On the other hand, under no tillage conditions, there were no significant differences between NTS and NTF. It was also observed by reference [12].

No significant differences were found in the total number of grains per panicle. The percentage of filled grains was significantly ($P < 0.05$) higher under flooded condition than aerobic condition in both tillage practices. Reference [13] no found significant differences between aerobic and flooded rice in the filled grain ratio.

The CTS treatments presented the lowest value of specific weight of the grain. However, no statistical differences were found between the other treatments.

Reference [14] found that grain yield showed significantly positive correlations with aboveground dry matter, number of panicles per square meter, and spikelets per square meter, which are yield components determined before anthesis.

In a study carried out with aerobic rice in China [15] showed that among yield components, the number of productive tillers and percentage of filled grains contributed most to the yield.

1000 grains weight was significantly ($P < 0.05$) higher under flooded condition than aerobic condition in conventional tillage treatments. In no tillage treatments, these values were similar. These results are not in accordance with those shown by reference [12], who observed non-significant differences in 1000 grain weight.

Grain yield was 46.5 % higher under flooded condition than aerobic condition in conventional tillage treatments. However, in no tillage treatments grain yield was 18.3% higher under aerobic condition. Reference [12] found that rice yield under aerobic treatment was 27.5% lower than that recorded under flooded condition. Decrease in the relative yield of aerobic

rice to flooded rice was also reported by other authors [16], [17].

Reference [18] observed significant differences between paddy yields obtained from different irrigation methods. Higher yields were obtained using continuous flooding irrigation instead of sprinkler irrigation. Other authors found that the yield difference between aerobic and flooded rice was attributed to differences in biomass production. Among the yield components, sink size (spikelets per m²) contributed more to the yield gap between aerobic and flooded rice than grain filling percentage and 1000 grain weight [17]. In general, flooded rice produced more panicles with more spikelets per panicle than aerobic rice [17]. Other authors found the high yield under aerobic culture in Japan results mainly from vigorous biomass production [19], with a harvest index that ranges from 0.40 to 0.48 [13].

Harvest index was significantly ($P < 0.05$) higher in CTF treatments than the others. Other authors [12] didn't find significant differences in harvest index between aerobic and flooded condition. Reference [20] observed that the low harvest index of aerobic rice in field experiments in China has been found to correlate with a low percentage of filled grains.

Water productivity was 47.6% higher under aerobic condition than flooded condition in no tillage practices and 55.7% in conventional tillage practices. On the other hand, water productivity was higher under no tillage than conventional tillage. Water use efficiency of aerobic rice compared to other establishment methods has also been studied by reference [21]. Reference [12] also found higher water use efficiency under aerobic condition. According to reference [22] water productivity in continuous flooded rice was typically 0.2-0.4 g grain per kg water in India and 0.3-1.1 g grain per kg water in the Philippines. Water-saving irrigation in its study increases water productivity, up to a maximum of about 1.9 g grain per kg water, but decreases total grain yield.

In a study carried out in Mississippi [23] with center pivot irrigation found grain yield between 8.2-8.31 Mg ha⁻¹ and irrigation water use efficiency between 1.6-2.0 kg m⁻³.

In a study carried out by reference [24] in China, where water-saving irrigation system with alternate wetting and drying systems was studied and compared with conventional irrigation where drainage was in mid-season and flooded at

other times. Intermittent flooding increased grain yield by 7.4% to 11.3%, reduced irrigation water by 24.5% to 29.2%, and increased water productivity (grain yield per cubic meter of irrigation water) by 43.1% to 50.3%. The water-saving irrigation significantly increased harvest index. Increases in grain yield under the water-saving irrigation were mainly attributed to the significant increases in spikelets per panicle and grain weight.

The water productivity (grain yield over water inputs by irrigation and rainfall) with aerobic rice was higher than with flooded rice, suggesting that aerobic rice is an attractive option to “produce more rice with less water” in situations where water is scarce [14].

IV. CONCLUSIONS

In flooded condition rice had higher plant height, panicle length, percentage of filled grain. Water productivity was higher under aerobic conditions. No tillage practices induced higher plant height and water productivity. Grain yield was 46.5% higher under flooded condition than aerobic condition in conventional tillage treatments. However, in no tillage treatments grain yield was 18.3% higher under aerobic condition. Harvest index was higher under flooded condition than aerobic condition in conventional tillage. Therefore aerobic rice system to short term in Mediterranean condition could be an effective strategy to save water increasing its productivity up to 47.6% under aerobic conditions.

ACKNOWLEDGMENT

This research was supported by the Extremadura Regional Government, and the Spanish Ministry of Science and Innovation (AGL2010-21421-C02-02). D. Becerra and D. Peña are the recipients of a grant from the Consejería de Economía, Comercio e Innovación of the Junta of Extremadura.

REFERENCES

- [1] FAO, “Rice is life”, Food and Agriculture Organization of the United Nations, Rome, Italy, 2004.
- [2] MAGRAMA. 2013. Cultivos herbáceos e industriales: el arroz. [Online]. Available: <http://www.magrama.gob.es/es/agricultura/temas/produccion-s-agricolas/cultivos-herbaceos/arroz>.
- [3] FAO, “Concerns about rice production practices”, Food and Agriculture Organization of the United Nations, Rome, Italy, 2003.
- [4] R. López-Garrido “Laboreo de conservación: Efectos a corto y largo plazo sobre la calidad del suelo y el desarrollo de los cultivos”, PhD., Dept. of Cristalografía, Mineralogía y Química Agrícola, Sevilla Univ., Sevilla, Spain, 2010.
- [5] A. Spanu, G. Pruneddu, and M. Deidda, “Primi risultati sulla coltivazione del riso (*Oryza sativa*) irrigato per aspersione”, *Rev. Agron.*, vol. 23, no. 4, pp. 378-384, October 1989.
- [6] R.E. Namara, I. Hussain, D. Bossio, and S. Verma, “Innovative land and water management approaches in Asia: productivity impacts, adoption prospects and poverty outreach”, *Irrig. Drain.*, vol. 56, no. 2-3, pp. 335-348, April 2007.
- [7] FAO, “Guidelines for soil description”, Food and Agriculture Organization of the United Nations, Rome, Italy, 2006.
- [8] D.W. Nelson, and L.E. Sommers, “Total carbon, organic carbon and organic matter”, in *Methods of soil analysis*, D.L. Sparks, Ed. Part 3, SSAA, Madison, WI, 1996, pp. 961-1010.
- [9] J.R. Sims, and V.A. Haby, “Simplified colorimetric determination of soil organic matter”, *Soil Sci.*, vol. 112, no. 2, pp. 137-141, 1971.
- [10] United State Salinity Laboratory Staff, “Diagnosis and Improvement of

- Saline and Alkali Soils”, in *US Department of Agriculture*, US Salinity Laboratory Staff, Ed. Handbook n°60, Washington, DC, 1954, pp. 7-16.
- [11] P.D. Lancashire, H. Bleiholder, P. Langelüddecke, R. Stauss, T. Van den Boom, E. Weber, and A. Witzten-Berger, “An uniform decimal code for growth stages of crops and weeds”, *Ann. Appl. Biol.*, vol. 119, no. 3, pp. 561-601, December 1991.
- [12] D.P. Patel, A. Das, G.C. Munda, P.K. Ghosh, J.S. Bordoloi, and M. Kumar, “Evaluation of yield and physiological attributes of high-yielding rice varieties under aerobic and flood-irrigated management practices in mild-hills ecosystem”, *Agr. Water Manage.*, vol. 97, pp. 1269-1276, March 2010.
- [13] Y. Kato, M. Okami, and K. Katsura, “Yield potential and water use efficiency of aerobic rice (*Oryza sativa* L.) in Japan”, *Field Crops Res.*, vol. 113, no. 3, pp. 328-334, September 2009.
- [14] L. Zhang, S. Lin, B.A.M. Bouman, C. Xue, F. Wei, H. Tao, X. Yang, H. Wang, D. Zhao, and K. Dittert, “Response of aerobic rice growth and grain yield to N fertilizer at two contrasting sites near Beijing, China”, *Field Crop Res.*, vol. 114, no. 1, pp. 45-53, October 2009.
- [15] F. Wei, H. Tao, S. Lin, B.A.M. Bouman, L. Zhang, P. Wang, and K. Dittert, “Rate and duration of grain filling of aerobic rice HD297 and their influence on grain yield under different growing conditions”, *ScienceAsia*, vol. 37, no. 1, pp. 98-104, May 2011.
- [16] B.A.M. Bouman, S. Peng, A.R. Castaneda, and R.M. Visperas, “Yield and water use of irrigated tropical aerobic rice systems”, *Agri. Water Manage.*, vol. 74, no. 2, pp. 87-105, June 2005.
- [17] S. Peng, B. Bouman, R.M. Visperas, A. Castaneda, L. Nie, and H.K. Park, “Comparison between aerobic and flooded rice in the tropics: agronomic performance in an eight season experiment”, *Field Crop Res.*, vol. 96, no. 2-3, pp. 252-259, April 2006.
- [18] N. Beser, “Effects of various planting and irrigation methods on yield and yield components and quality characters of rice (*Oryza Sativa* L.) at the Thrace region”, Directorate of Trakia Agricultural Research Institute, Ministry of Food, Agriculture and Livestock, Republic of Turkey, Trakya, Turkey, 1996.
- [19] K. Katsura, M. Okami, H. Mizunuma, and Y. Kato, “Radiation-use efficiency, N accumulation and biomass production of high-yielding rice in aerobic culture”, *Field Crops Res.*, vol. 117, no. 1, pp. 81-89, May 2010.
- [20] B.A.M. Bouman, X. Yang, H. Wang, Z. Wang, J. Zhao, and B. Chen, “Performance of aerobic rice varieties under irrigated condition in north China”, *Field Crop Res.*, vol. 97, no. 1, pp. 53-65, May 2006.
- [21] S. Singh, J.K. Ladha, R.K. Gupta, L. Bhusan, and A.N. Rao, “Weed management in aerobic rice systems under varying establishment methods”, *Crop Prot.*, vol. 27, no. 3-5, pp. 660-671, March 2008.
- [22] B.A.M. Bouman, and T.P. Toung, “Field water management to save water and increase its productivity in irrigated lowland rice”, *Agri. Water Manage.*, vol. 49, no. 1, pp. 11-30, July 2001.
- [23] E.D. Vories, W.E. Stevens, P.L. Tacker, T.W. Griffin, and P.A. Counce, “Rice production with center pivot irrigation”, *Appl. Eng. Agric.*, vol. 29, no. 1, pp. 51-60, 2013.
- [24] J. Yang, K. Liu, Z. Wang, Y. Du, and J. Zhang, “Water-saving and High-Yield Irrigation for Lowland rice by controlling limiting values of soil water potential”, *J. Integr. Plant. Biol.*, vol. 49, no. 10, pp. 1445-1454, October 2007.

Engine Performance and Economic Impact Study of Gasoline-Like Tyre Pyrolysis Oil in Thailand

C. Wongkhorsub, N. Chindaprasert, S. Peanprasit

Abstract—The purpose of this paper is to study the comparing performance and efficiency of small gasoline engine using gasoline blended with Gasoline-like tyre pyrolysis oil (GTPO) in difference blended ratios. The comparisons of economic impact of using the blended oils are also investigate. The Blended GTPOs are compared with gasoline produced in Thailand by testing in gasoline engine (Honda GX140, four stoke, multi-purpose one cylinder, 144 CC). The testing is done by comparing performance of fuel which are torque, engine break power, fuel flow rate, generator output, BSFC (brake specific fuel consumption) based on the 3000 rpm engine rate. The result of the experiment shows that the torque output of the 100% blended GTPO is 94.2% lower compare to the normal gasoline, the BSFC of the 100% blended GTPO is 1.3% higher than normal gasoline but the thermal efficiency of the 100% blended GTPO is 1.86% higher than normal gasoline. Therefore, it is found that the 100% GTPO can be used to replace the normal gasoline in small engine but the best blended GTPO use in the engine is 25% blended ratio as the engine run smoothly in long term without wax and tars in the engine.

Index Terms—Pyrolysis, Gasoline-Like Tyre Pyrolysis Oil, Engine Performance, Energy Cost.

I. INTRODUCTION

The fast depletion of petroleum fuel and the environmental issues have led to an intensive search for alternate fuels for internal combustion engines. One of the methods to derive alternate fuels is the conversion of waste substances to energy. Biomass based fuels like methanol, ethanol etc. are some of the examples in which waste to energy is adopted, and these are used as alternate fuels for the internal combustion engines. On the other hand, due to the increase in automotive vehicle population, the disposal of waste automobile tyres has become essential. In Thailand, it is found that there are about 56.7-170 millions tyres has been discarded per year or approximately 1.7 million tons per year [1].

Different alternatives for tyre recycling, such as retreading, reclaiming, incineration, grinding, etc., have been used. However, all these methods have significant drawbacks and limitations. Pyrolysis can be considered as a non-conventional method for tyre recycling, which is currently receiving renewed attention. In the pyrolysis process mainly the rubber polymers are heated and decomposed to low molecular weight products, like liquid or

gases, which can be useful as fuels or chemicals source. In the past, several laboratory, pilot plant and even commercial attempts have been made to establish economic units for pyrolysis of tyres[2]. Tyre pyrolysis has been investigated for more than 20 years. The process converts waste tyre into potentially recyclable materials such as flammable gas, pyrolysis oil and carbon black [3]. Composition of the oil depends on reactor design and operating condition. Tyre pyrolysis oil plant has been established around the world in order to produce the substitute liquid fuel for heating purpose as found that the tyre pyrolysis oil have a high gross calorific value (GCV) of around 41-44 MJ/kg [4]. Desulfurization process is needed for tyre pyrolysis oil as the high concentration of sulfur in pyrolysis oil leads the emission of SO₂ and sulfate particular matter. The main purpose of the commercial scale of the pyrolysis oil is used as a replacement of bunker oil. Therefore, the tyre pyrolysis plant is not widely established due to the product usage and economic of scale. However, the attempt of developing tyre pyrolysis oil has been made by applying some catalysts for the purpose of product yield distribution and quality of the oil[5], distilling the tyre pyrolysis oil to become diesel-like tyre pyrolysis[6][7].

The use of the tyre pyrolysis oil has been research in diesel engine and found the potential of using the diesel-like tyre pyrolysis to replace the diesel oil in small diesel engine [8][9]. However, one of the by-product of distilling the pyrolysis oil is naphtha oil. It is used primarily as feedstock for producing gasoline. Thus, the researcher is investigating the potential of using the naphtha or the gasoline-like tyre pyrolysis oil in small gasoline engine in order to be an alternative fuel for the small scale agriculture engine.

This paper presents the engine performances with energy output in kilowatt-hour applying blended various compositions of gasoline-like tyre pyrolysis oil (GTPO) and diesel oil in agriculture gasoline engine. The gasoline-like tyre pyrolysis oil was researched by distilled the tyre pyrolysis oil between 50-200°C so as to obtain the gasoline-like tyre pyrolysis oil. The economic analysis is investigated in terms of cost of fuel compare with energy output in kilowatt-hour applying blended various percentage of the GTPO and gasoline in small gasoline engine in order to predict the behavior of cost in each blended oil.

II. TYRE PYROLYSIS

A. Gasoline-like Tyre Pyrolysis Oil(GTPO)

Pyrolysis process is a chemical and thermal process that reacts to decompose organic material under oxygen-free conditions. The products of pyrolysis include oils, gases and char. For tyre pyrolysis oil, it has been researched that the tyre

Manuscript received April 5, 2014. This work was supported in part by Thailand Institute of Scientific and Technological Research and the Department of Mechanical Engineering, Faculty of Engineering, Rajamangala University of Technology Phra Nakhon, Thailand

C. Wongkhorsub, N. Chindaprasert, and S. Peanprasit are with the Department of Mechanical Engineering, Faculty of Engineering, Rajamangala University of Technology Phra Nakhon, Thailand (e-mail: chonlakarn.w@rmutp.ac.th, nataporn.c@rmutp.ac.th)

pyrolysis oil is a complex mixture of organic compounds of 5-20 carbons with high proportion of aromatics [10].

The process of tyre pyrolysis is started from collecting the waste tyre and shred it to small pieces to be suitable to feed in to the pyrolysis reactor. In general, product yields from pyrolysis are varied with temperature. The oil production yield of tyre pyrolysis process has a maximum at 350°C and decomposes rapidly above 400°C [11]. The pyrolysis oil used in this research is processed from a batch pyrolysis reactor with desulfurization process. The tyre pyrolysis oil sample was prepared using a commercial tyre pyrolysis plant in Thailand. The average product yield of tyre pyrolysis process is distinguished into 3 types of product as shown in Fig.1.

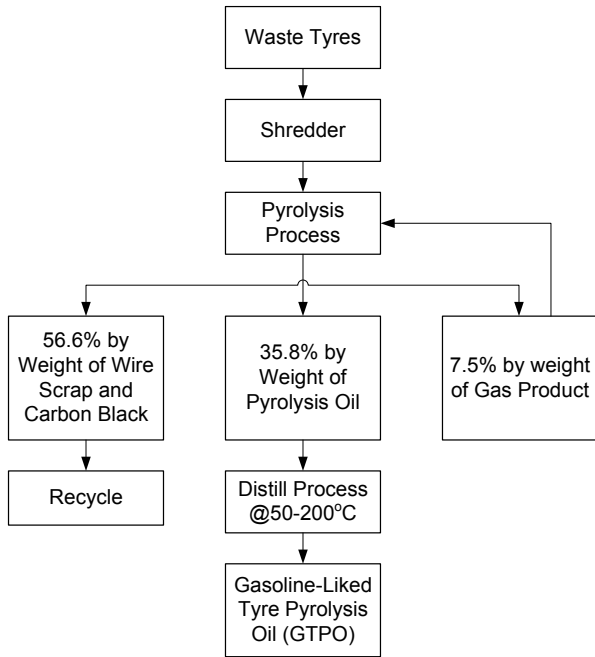


Fig. 1. Process and Average Product Yield of Tyre Pyrolysis Process.

The sample oil was distilled by flash distillation method at temperatures between 50-200°C respect to the distill temperature of light to heavy naphtha (C6-C14) without reforming process and additives.

B. GTPO Blending and Properties

The GTPO from pyrolysis and distill process is blended with the commercial Gasoline in Thailand in the variation of GTPO 10%, 25%, 50%, 100% by volume. The basic properties of the blended oil in ratio variation were analyzed and compared to gasoline by the laboratory of Energy Technology Department, Thailand Institute of Scientific and Technological Research, as shown in Table 1.

TABLE I: THE PROPERTIES OF THE GTPO BLENDED WITH GASOLINE

Fuel	LHV (Kcal/kg)	Density	Flash Point °C	C	H	O
100% GTPO	12,162	0.73	25>	82.0	11.4	6.1
50% GTPO	11,784	0.724	25>	82.3	11.6	5.7
25% GTPO	11,542	0.720	25>	82.1	11.8	5.8
10% GTPO	11,425	0.706	25>	83	11.8	5.0
Gasoline	11,361	0.703	25>	84.5	11.8	3.6

III. METHODOLOGY

A. Engine Performance

Engine performance indicates the effects of a oil in the engine. The determination of the engine performance in this experiment are break torque (T), engine break power (P), break specific fuel consumption ($Bsfc$), and break thermal efficiency (η_{th}). These several parameters can be obtained by measuring air and fuel consumption, torque and speed of the engine, and heating value of the oil. The performance parameters can be calculated by equations as followed [12][13].

Break torque (T) is an indicator of the function of break torque in Nm calculated by the moment of engine arm connected to weight scale as:

$$T = Fd \quad (1)$$

Where F is force of engine arm applied to the load in N, and d is the distance of engine arm from center of the rotor to the load.

Engine break power (P) is delivered by engine and absorbed load. It is the product of torque and angular engine speed where P is engine break power in kW, N is angular speed of the engine in rpm as:

$$P = \frac{2\pi NT}{60 \times 1000} \quad (2)$$

Break specific fuel consumption ($Bsfc$) is the comparison of engine to show the efficiency of the engine against with fuel consumption of the engine in g/kW-hr where (\dot{m}_f) is the fuel consumption rate in g/hr as:

$$Bsfc = \frac{\dot{m}_f}{P} \quad (3)$$

The percentage of break thermal efficiency of the engine (η_{th}) is related to engine break power (P) and the total energy input to the engine which is Q_{LHV} lower heating value of fuel in kJ/kg applied to the fuel consumption rate as:

$$\eta_{th} = \frac{P \times 1000}{\dot{m}_f Q_{LHV} \times 3600} \times 100 \quad (4)$$

B. Economic Impact

The economic impact of this research is done under the approach of comparing the energy cost of using the variation of GTPO as a fuel for gasoline engine. However, the energy consumption rate of each fuel are difference therefore, the best indicator that is suitable for all situations to predict the use of oil in terms of economic analysis should be energy cost consumption per power output as:

$$\varphi_E = bsfc \times \left(\frac{Cost_{po}}{\rho_{po}} \right) \quad (5)$$

Where ϕ_E is the cost of energy consumption per power output in Baht/kW-hr, ρ_{PO} is the density of calculating oil. Equation (5) shows the cost of energy compared regarding to the efficiency.

IV. EXPERIMENTAL SET UP

This experimental research is designated to apply the GTPO in small scale Gasoline engine and study the experimental result of using the variation of GTPO as fuels. Therefore, engine specification, schematic of the engine measurement, engine operating condition and experimental results are described in this part.

A multi-purpose agricultural 4-stroke, overhead single cylinder gasoline engine (Honda GX140) is used for the experiment. The engine specifications are shown in Table II.

TABLE II: ENGINE SPECIFICATION

Engine Description	Specification
Engine Brand	Honda GX140
Bore x Stroke	64 mm. x 45 mm.
Swept Volume /Cylinder	144 cc.
Max. Output, HP/rpm	5(3.7) /3600
Max.Torque @2800 rpm	1.0 kg-m
Ignition system	Ignition Coil
Heat Exchanger Sytem	Air Type
Fuel Consumption	0.81 Gallon/Hr.
Weight	14 Kg.

Schematic of the experimental set up is shown in Fig. 2. The engine equipped with measuring elements including weighing device, manometer, orifice plate, tachometer, thermocouple and thermocouple at the exhaust.

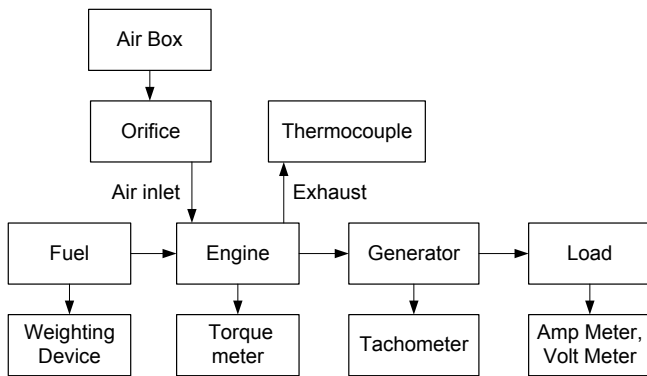


Fig. 2. Schematic of the experimental setup

As the experiment was operate in constant speed, the torque output from the experiment is measured by the breaking force absorbed by the load. The absorbed load is produced by a set of 5x100W light bulbs and 13x500W light bulbs connect in series together in order to vary the absorbed load.

The blended GTPOs with the commercial Gasoline in Thailand in the variation of GTPO 10%, 25% 50% 100% by volume were applied in the experiment. The experiments were conducted by starting engine with the sample fuel. The operating conditions were set at a rated engine speed 3000 rpm.

Loads were applied from 500 W and stepped up until

reached the maximum load. The power output is measured by the watt meter which is lower than the load regarding to the efficiency of the generator. The air box is applied to stabilize the air flow into the engine as the air box volume is 500 times the volume of the engine cylinder. Orifice plate flow meter is applied for air flow measurement. Fuel consumption is measured from the differential of the fuel in time. A chromel-alumel thermocouple was installed to measure the exhaust gas temperature. At the end of the test the engine was run with gasoline fuel for a while to flush out from the engine.

V. EXPERIMENTAL RESULT

The Stoichiometric Air-fuel Ratio of fuel is calculated regarding to the properties of the blended oil in table I are shown in Table III.

TABLE III: STOICHIOMETRIC AIR-FUEL RATIO OF FUEL

Fuel	Gasoline	10%	25%	50%	100%
		GTPO	GTPO	GTPO	GTPO
AF _{Stoich}	13.647	13.435	13.305	13.274	13.161

The stoichiometric air fuel ratio of the variation of the fuels in this experiment shows that the Gasoline obtains the highest number whereas the 100% GTPO is the lowest number. Therefore, this number could predict the trend of fuel consumption rate of each fuel. The more ratio of GTPO causes the high fuel consumption.

The experimental testing shows that the engine performance of variation of GTPO blended fuels are comparable to the gasoline. The trend of engine performance which are torque, break specific fuel consumption and the thermal efficiency of all testing oils including 100% GTPO is in the same direction. It shows that the GTPO is able to use as a replacement of the gasoline in term of engine efficiency. Fig.3. illustrates the relation of the break specific fuel consumption and the engine break power. Fig. 4 illustrates the thermal efficiency of the fuels in various engine break power. The thermal efficiency of the GTPO is higher than the gasoline by reason of the wide range of distillation temperature might cause pre-ignition and knocking.

Though the engine performance of the GTPO is comparable to gasoline, there are some physical limitation that found in the experiment that might affect using the GTPO in long term. It is shown in Fig. 5. that the exhaust temperature of the GTPO is slightly higher than gasoline also, the engine needs to be flushed off with gasoline after the experimental testing of GTPO due to the wax occurred in engine.

The optimum load for using blended GTPO and gasoline in this experiment is at the engine brake power range of medium load, 1,300 - 1,700 W as it performs well in terms of Bsfc and thermal efficiency. The thermal efficiency of gasoline is lower than the blended GTPOs due to the lower heating value as shown in table I.

The result of the experiment shows that the torque output of the 100% blended GTPO is 94.2% lower, the BSFC of the 100% blended GTPO is 1.3% higher than normal gasoline but the thermal efficiency of the 100% blended GTPO is 1.86% higher than normal gasoline in average load.

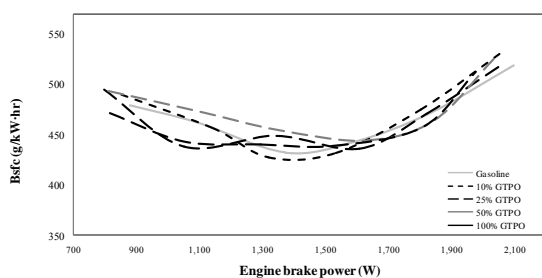


Fig. 3. Variation of brake specific fuel consumption with engine brake power.

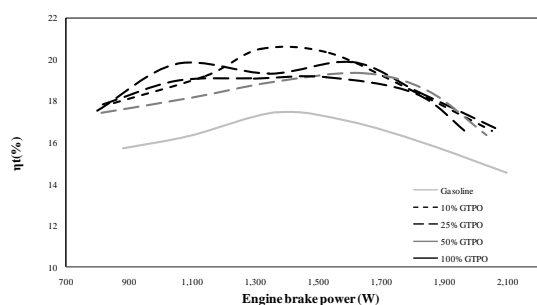


Fig. 4. Variation of thermal efficiency with engine brake power.

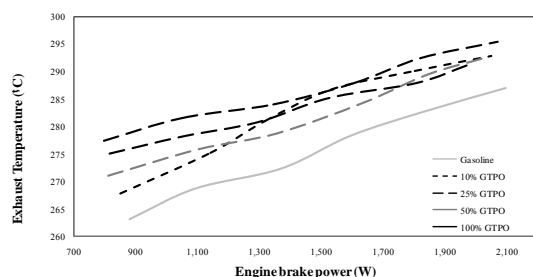


Fig.5. Variation of exhaust temperature with engine brake power.

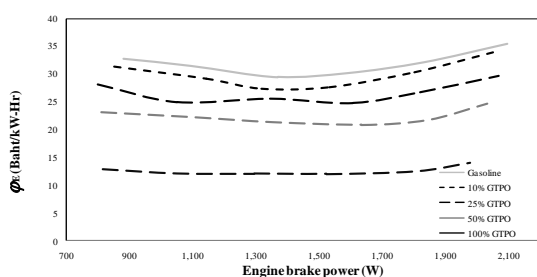


Fig. 6. Variation of the cost of energy consumption per power output with engine brake power.

The torque output of the 25% blended GTPO is 98.2% lower compare to the normal gasoline, the BSFC of the 25% blended GTPO is 0.32% higher than normal gasoline in medium load but the thermal efficiency of the 100% blended GTPO is 0.27% higher than normal gasoline in average load. It shows that the 25% blended GTPO has engine performance similar to the pure gasoline.

As found in the experiment that the GTPO is potentially replacing gasoline, the cost of GTPO is another concerned factor. Since the fuel consumption of the sample fuels are varies, the research use energy cost consumption per power output to indicate the economic impact of the samples. The GTPO cost is 20 Baht per liter whereas the gasoline cost is 48 Baht per liter. The energy consumption cost indicates

that the use of GTPO is economically comparable to gasoline. Though the engine performance of the blended GTPOs is slightly lower than gasoline, the cost of fuel is significantly lower as shown in Fig. 6.

VI. CONCLUSION

Regarding to the engine performance, operating condition and the economic comparison, the potential blended GTPO is 25% blended as the engine performance is similar to normal gasoline but the cost of oil is 16.6% lower than gasoline.

However, the experimental testing of the GTPO compares to gasoline demonstrates that the GTPO is a potentially substitution of the gasoline in terms of engine efficiency. The GTPO in this research has been distilled by flash distillation which might cause the instability effect of the oil. Therefore, the GTPO should be improved by chemical process and distill in commercial scale distillation plant in order to obtain quality GTPO if the purpose of the oil production is for sale in commercial scale. It should be respected that the GTPO is produce from one source of waste. The using GTPO is one of the options to turn waste to energy which not only obtain the energy but also reduce the waste from the area. The environmental value of the product should be added to the economic impact study. The environmental impact in terms of pollution at the exhaust is also another concerning factor as the tyre pyrolysis process requires desulfurization.

ACKNOWLEDGMENT

The authors would like to acknowledge a tire pyrolysis plant to sponsor us the oils. The authors are also grateful for the laboratory support of Energy Technology Department, Thailand Institute of Scientific and Technological Research. The research was conducted by researchers in the pyrolysis research group, in support of Rajamangala University of Technology Phra Nakhon.

REFERENCES

(Periodical style)

- [1] N.A. Dung, R. Klaewkla, S. Wongkasemjit, S. Jitkarnka, "Light olefins and light oil production from catalytic pyrolysis of waste tire" *Journal of Analytical and Applied Pyrolysis*, Volume 86, issue 2, pp. 281-286 November, 2009., ISSN: 0165-2370 DOI: 10.1016/j.jaap.2009.07.006
- [2] G. O. Young, "Synthetic structure of industrial plastics (Book style with paper title and editor)," in *Plastics*, 2nd ed. vol. 3, J. Peters, Ed. New York: McGraw-Hill, pp. 15-64, 1964.
- [3] Miltner, W. Wukovits, T. Pröll, and A. Friedl, "Renewable hydrogen production: a technical evaluation based on process simulation," *Journal of Cleaner Production*, vol 18, pp. 551-562, 2010.
- [4] P. T. Williams, R. P. Bottrill, and A. M. Cunliffe, "Combustion of tire pyrolysis oil," *Trans IChemE*, vol. 76, pp. 291-301, Nov 1998.
- [5] S. Boxiong, W. Chunfei, L. Cai, G. Binbin, W. Rui, "Pyrolysis of waste tyres: The influence of USY catalyst/tyre ratio on products" *Journal of Analytical and Applied Pyrolysis*, Volume 78, Issue 2, pp. 243-249, Mar 2007.
- [6] S. Murugan, M. C. Ramaswamy, and G. Narajan, *The Use of Oil in Diesel Engines*, Waste Management, Vol.28, 2743-2749, 2008.
- [7] C. Wongkhorsub, N. Chindaprasert and S. Peanpravit, *Engine Performance and Economic Impact Study of Diesel-Like Tire Pyrolysis Oil*. 7th International Conference on Renewable Energy Sources (RES'13) ISBN: 978-1-61804-175-3, 267-272, 2013.
- [8] S. Murugan, M. C. Ramaswamy, and G. Narajan, "Performance, emission and combustion studies of a di diesel engine using distilled

- tyre pyrolysis oil-diesel blends,” Fuel Processing Technology, vol. 89, pp. 152-159, 2008.
- [9] C. Wongkhorsub and N. Chindaprasert, A Comparison of the Use of Pyrolysis Oils in Diesel Engine, Energy and Power Engineering Part I, Volume 5, Number 4B, 350-355, July 2013.
- [10] Isabel de Marco Rodriguez, M. F. Laresgoiti, M. A. Cabrero, A. Torres, M. J. Chomon, B. Caballero, “Pyrolysis of scrap tyres”, Fuel Processing Technology, vol. 72, pp. 9-22, 2001.
- [11] Y. M. Chang, “On pyrolysis of waste tire: degradation rate and product yields,” Resources, Conservation and Recycling, vol. 17 pp.125-139, 1996.
- [12] O. Arpa, R. Yumrutas, Z. Argunhan, “Experimental investigation of the effects of diesel-like fuel obtained from waste lubrication oil on engine performance and exhaust emission,” Fuel Process Technology, vol. 91, pp.1241-1249, 2010.
- [13] I. Sezer, “Thermodynamic, performance and emission investigation of a diesel engine running on dimethyl ether and diethyl ether,” International Journal of Thermal Sciences, vol. 50, pp.1594-1603, 2011.



C. Wongkhorsub is a lecturer in Mechanical Engineering Department, Faculty of Engineering, Rajamangala University of Technology Phra Nakhon, Thailand. She received her Ph.D. in Renewable Energy from the University of Nottingham in 2006. Her research focuses on renewable energy related on biomass and thermal system.

Parameters of insolvency proceedings in developed countries and their dependence on economic performance

Luboš Smrčka, Markéta Arltová, Jaroslav Schönfeld, Lee Louda

Abstract – This study deals with the potential relationship between costs and yields of insolvency proceedings for creditors and the performance of an observed economy, which is measured by the GDP per head of population. The authors verified the hypothesis that the costs and yields in insolvency proceedings should be dependent on the extent of development of a given country, and that the extent of economic development can be measured precisely by product per head. This hypothesis can be tested by using mathematical models, whilst several further findings of lesser significance were obtained.

Keywords—Insolvency, GDP, insolvency proceedings, costs of proceedings, bankruptcy, yields for creditors.

I. INTRODUCTION

LOGICALLY speaking, there should be no dependence between the degree of quality by which insolvency proceedings in individual countries run their course and the extent to which this or the other country is developed.¹ In fact, however, it is manifest that countries which have a higher level of gross domestic product per head of population also show higher yields for creditors in insolvency proceedings and, likewise, lower costs.

In our following considerations, we will first focus on the general circumstances of insolvency proceedings and statistical data, which will be utilized so as to compare individual states

The article is processed as one of the outputs of the research project “*Research of insolvency practice in the CR, with the aim of forming proposals for changes in the legislation that would enable increased yields from insolvency proceedings for creditors, which would contribute towards increasing the competitiveness of the Czech economy*”, registered at the Technological Agency of the Czech Republic (TA CR) under the registration number TD020190 and as an output for the grant of the Excellence Grant Agency of the Czech Republic no. P402/12/G097 *DYME-Dynamic Models in the Economy*.

L. Smrčka is an associate professor at the University of Economics, Prague, Faculty of Business Administration (phone: 420- 224-098656; fax: 420- 224 098 649; e-mail: smrckal@vse.cz).

M. Arltová is an associate professor at the University of Economics, Prague, Faculty of Informatics and Statistics (phone: 420- 224-095482, e-mail: arltova@vse.cz)

J. Schönfeld is a professional assistant at the University of Economics, Prague, Faculty of Business Administration, (phone: 420-224-098652; fax: 420-224 098649; e-mail: jaroslav.schonfeld@vse.cz)

L. Louda is an external doctorand at the University of Economics, Prague, Faculty of Business Administration

¹ This text primarily concerns insolvency proceedings with entrepreneurial subjects.

in a realistic way. We will also perform certain operations with the aid of mathematical procedures, i.e. we will carry out regression analyses of gathered data. It will then be possible to evaluate the results gained and draw certain conclusions therefrom.

We generally presume hypothesis, the basis of which is formed on the assumption that the degree to which a specific country, or rather a specific economy, is developed is closely related to the product which the economy generates per population head. Therefore, the degree of economic development can be expressed with the aid of GDP per head of population indicators. Furthermore, the hypothesis in its basic form assumes that the more developed a tested country or economy, the higher the yields will be in the tested country for creditors in insolvency proceedings, and the lower the expenses will be for the actual realization of insolvency proceedings.

This is based on a general assumption, according to which long-successful economic systems and models of individual states achieve such success thanks, among others, to high-quality institutional foundations, the ability to advance rights, the rule of the law and other indisputably positive parameters of the economy as a whole.

II. PROBLEM OF INSOLVENCY PROCEEDINGS AND THE AVAILABLE STATISTICS

A. The problem of insolvency proceedings

The insolvency proceedings is among the fundamental problems of real economic systems, although relatively little attention is devoted thereto.[1] While considerable sums flow through insolvency proceedings in every economic environment, their cost is usually fundamentally dependent on the current economic situation. Insolvency proceedings in times of recession or crisis are especially significant.

The macroeconomic purpose of insolvency proceedings is to ensure that entrepreneurial assets trapped in environments of subjects who are incapable of sensible economic functioning are transferred expediently and with the lowest possible costs to the hands of such subjects that will arrange their renewed involvement in corporate connections and entrepreneurial activity. From the perspective of real economics, these proceedings should ensure that the rights of creditors are quickly and effectively fulfilled and should enable the enforceability of their receivables from the debtor in default or, more precisely, in bankruptcy. This, however, is

not primarily and necessarily an issue of time: What part of the receivable is enforced and at what cost is also at issue. As we see, there is a certain, clear difference between the national-economic and microeconomic point of view. [2]

The unique aspect of insolvency proceedings is that it is a collective procedure enforced by the state (law). As is generally known, the commencement of insolvency proceedings as a collective procedure when enforcing receivables closes the possibility of enforcing receivables individually (i.e. especially through forfeiture proceedings).²

The insolvency proceedings are an extraordinary institute which we can compare to other situations only with difficulty – it nevertheless shares some similarity to the solution of the problem of the common pool. That is, for instance, with quotas, their distribution and apportionment. Similarly to the case of quotas, the participants of insolvency proceedings are faced with a relatively difficult choice – if they abide by all the regulations and prescribed procedures, it will require no small exertion on their part; at the same time, the corresponding profit will not be guaranteed to them and it could easily occur that another participant (who will not suffer as many limitations conditioned by the willingness to abide by the set regulations) will usurp for itself far more from the available or potential gain.

Fishermen who did not respect the limits fixed by quotas will gain higher profits than those who submit thereto. They do, however, risk certain recourse if their contravention of the regulations is discovered. Catching more fish than the quota allows, however, entails contravening the regulations practically repeatedly. A similar situation occurs in insolvency processes, albeit with one or rather two fundamental differences. There are certain assets of the debtor's on which more rights (liabilities) have been issued than can be satisfied thereby (the assets). This means that there are creditors here with greater requirements than can be covered – although if one of them gains an advantage (even if unauthorized), its satisfaction will be higher than that of the other; moreover, the rest will be deprived of part of their satisfaction. Not to mention: this is the first significant difference from the example of the fishermen and one territory. There is also a debtor here who, in uninfluenced insolvency proceedings, will be deprived of all of its assets, i.e. at least of those that could be monetized and utilized to satisfy creditors. The debtor has a logical motivation to attempt to excise these assets from the reach and influence of creditors and thereby ensure supervision over those assets also in the future. In this sense, the classic words of *the prisoner's dilemma* are reminiscent of insolvency proceedings - of course, in the one-round variant, which increases the nervousness of all participants.

We can also refer to insolvency proceedings as the *final judgement*, as we can see from the perspective of history the development towards which insolvency proceedings tend; as far as the future is concerned, however, this does not exist from the debtor's perspective.³ Nor does it exist from the

creditors' perspectives, as what they do not gain now, they never will gain. The fishing quota serves the purpose of the fishing grounds being preserved for forthcoming fishermen. Insolvency proceedings do not have this ambition, nor can they.

When we defined the difference between the macroeconomic and national economic point of view and the point of view from the position of real economics or that of microeconomics, then there is also an aspect that connects these points of view. If the subjects of the real world are confronted by the fact that insolvency proceedings are ineffective and yields for creditors are only marginal, this experience – which amounts to a reality of increased risk – has to be implemented into their commercial calculations. This, however, means that the new risk becomes part of the general price level. This of course means that the general competitive ability of the economy is negatively affected precisely by lack of performance, low efficiency and other negative attributes of insolvency proceedings, whilst the main role will be played by the uncollectibility or difficult collectability of debt.

B. The problem of statistical data

We declared that insolvency proceedings are among the processes of real economics which deserve critical and structured attention, we in fact have only sparse knowledge as to their course and outcomes. It is striking that, even with truly developed economies, no statistical data is available that would give an overview on certain crucial parameters of these proceedings. This concerns especially yields for creditors and also costs incurred for insolvency proceedings.

When we have such information at our disposal, this concerns results of partial investigations of samples of insolvency processes, not on total statistics. [4]– [7] In a certain way, moreover, these samples tend to be aimed, e.g. they specialize on small and medium-sized firms or, by contrast, on relatively large corporations.⁴ Their ability to bear testimony on the general outcome of insolvency processes can therefore be problematic.

In fact, we thus have at our disposal only quite specific data contained in the publication *Doing Business*, which is regularly prepared by a team of professionals from The World Bank and International Finance Corporation. [8]

Although these figures are sometimes labelled as statistical data, this is not true. These are in fact results which we could rather label as a survey of expert opinions. Without even

by the financial rehabilitation method. Reorganization rather than bankruptcy occurs.

⁴ This is not to say that such focus on some more specific groups of insolvency cases would primarily be erroneous or bad. Such a division could, on the contrary, be useful even from the perspective of real economics and the way in which entrepreneurial subjects evaluate information which reaches them. If a business has among its customers small and medium enterprises accounting for a volume of eighty percent of realized deliveries and one corporation of major significance making up twenty percent of the same, separate statistics (or more precisely, a statistical survey) will necessarily be valued more than information "mutually influenced" by two or more highly distinct groups. If such a business had the need to modify its trading habits according to information on usual default among businesses similar to those that are among its clients, specialized information for building such a strategy would serve better.

² This state is generally recognized and accepted, which does not, however, mean that discussion is not occasionally devoted thereto.[3]

³ This is of course a slightly high-flown assertion in view of the fact that in some cases, debtor bankruptcies are settled not only by liquidation, but also

having to elaborate in fine detail as to how the given figures emerge,⁵ it is necessary to describe the whole process to at least some degree. The team compiling the afore-mentioned comparison for evaluation of each of the monitored countries is comprised of a group of specialists whom we could call experts in a given problematic in a given region or directly in a given state. These specialists regularly receive for completion a questionnaire, a part of which is a model case of insolvency proceedings – this case is always the same. The approached experts are then to estimate what results would be gained in a given state in this specific (model) case. The resultant data on the duration of proceedings, their outcomes and costs are thus an estimate of how one case would culminate.

This methodology naturally has its own highly limiting pitfalls. Most importantly, it in fact bears no testimony as to the true insolvency situation in the country which is to be thus described. The model case is in this sense of the word *model* in its international usage, but by no means does it necessarily show the true reality of a tested country. This means that, in a tested country, this model case could be substantially closer to a “standard case” than in another country – for instance, due to the fact that there is a generally worse state of enforceability of rights in one of these countries, and creditors have fewer possibilities to check a debtor’s property. In such countries, it will then mean that debtors enter into insolvency proceedings with a smaller volume of property that could be monetized than in systems in which the possibility of excising property from the company is more complicated.

However, this procedure has one clear and indisputable advantage. It describes the opinions of the professional public as to the true performance of the insolvency system in this or the other state. Let us imagine that we had similarly structured statistics gained from a highly representative sample of insolvency cases in two countries. Practically speaking, we could assume that in places where there is a higher yield, lower cost and perhaps a shorter duration of insolvency proceedings, there is also a better insolvency law and other regulations, better and more educated judges and so forth. Yet this need not necessarily be true – the difference can be given insofar as one of these countries have errors in the laws which are meant to prevent outflow of assets from the business still prior to insolvency; the actual insolvency act and other circumstances could be very good.

The method chosen by the publication *Doing Business*, of course, has the unrepeatability advantage that the exact same case in all monitored countries is assessed. This means that the real performance of the actual insolvency system is assessed. As has already been said, this advantage is nevertheless accompanied by several disadvantages, especially the necessary subjectivity of the witness borne.⁶

⁵ Those interested in more precise information can be referred to the pertinent web page, where the pertinent methodology is described in detail. [9]

⁶ Of course, other circumstances have to be mentioned: the state of asset trade in a given country at a given time. The deeper the running crisis, the lower the asset price will be and the poorer the results – whereas the quality of insolvency law, courts and all other circumstances will not play a role in this regard.

III. REGRESSION ANALYSIS

With the awareness of certain limitations that are connected with data from *Doing Business*, one can also utilize these figures for further research. In compliance of the hypothesis on the relationship between economic performance and the performance of insolvency systems, we therefore began with a search for suitable statistical files which could be analysed together from the perspective of their differences in individual developed countries.

On the economic performance side, we chose GDP per head of population as a comparative datum. These are data drawn from official European Union sources.[10] This comparison was selected for several reasons – firstly, it would be somewhat difficult to work with absolute values of the gross domestic product itself, as these are understandably significantly dependent on the economic volume of the given country, for instance, on the number of inhabitants and others factors. The volume of GDP itself thus need not bear any testimony whatsoever as to the qualitative side of the tested economy; it speaks only of quantitative aspects.

Furthermore, it would make no sense to work with indexes based on international changes, as these data would be incommensurate with the way in which data on insolvency proceedings are given. This is due to the fact experts here define in the above-mentioned manner costs of proceedings as a percent proportion from monetization and, secondly, yields from receivables as a percent proportion from their volume.⁷

This is thus an annual result which is not dependent on the result of the preceding year and does not in itself influence the future result in any way. Comparison with data originating from a time series, in which this datum would stem from previous data, would be nonsensical and could not lead to a reasonable result. We arrived at the conclusion that it is in fact GDP per head of population that determines or, more precisely, describes the economic development of the country, as it is something which we could call the “productivity” of the given economy. As a result, this data to a significant degree informs one on the qualitative level of economy. And finally, comparison using GDP in regular prices converted into euros was selected – regular prices are appropriate: at the given time in the given region, they correspond by their form and expression to receivables enforced in insolvency proceedings.

OECD states were selected as the group of researched countries; 29 of 34 member countries (2014) were included into the research (not all the necessary data is available at the given time in the case of the others).⁸ The selection of OECD states as a comparative sample was given by the relative similarity of the countries in the sense of institutional organization and general economic customs, whilst this group at the same time provides significant differences in the sense

⁷ *Doing Business* itself works with the term “cents on the dollar”, which is understandably the same as a percentage of the entire enforced receivable.

⁸ These states are at issue: Australia, Austria, Belgium, Canada, Czech Republic, Denmark, Finland, France, Germany, Greece, Ireland, Italy, Japan, Korea (South), Mexico, the Netherlands, New Zealand, Poland, Portugal, Slovakia, Spain, Sweden, Switzerland, Turkey, Great Britain, the USA, Hungary, Norway, Iceland.

of the manner in which the GDP per head of population is achieved.⁹

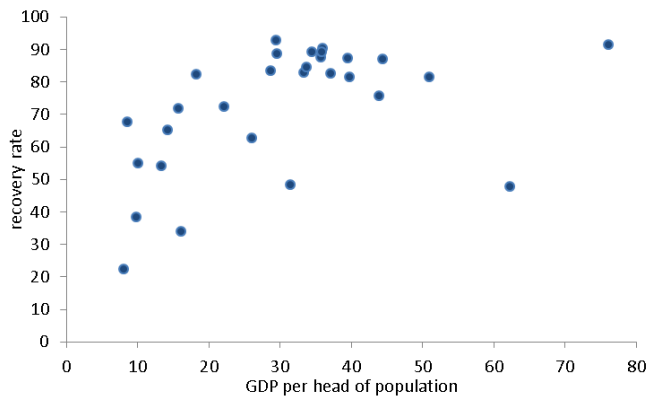


Fig.1 Recovery rate for investors from insolvency proceedings (in percent from investment) and GDP at current market prices per head of population (in EUR thousands) in 2013.

Source: data World Bank, IFC (2013), AMECO (2014)

Fig. 1 does not require particularly broad interpretation. It can be seen at first glance that there is clearly a relationship between economic efficiency, measured by the amount of GDP per head of population, and between the extents to which creditors' receivables in insolvency proceedings are satisfied. Needless to say, even among those states where a low GDP per head of population can be found, we can notice a significant difference in recoverability of investment – after all, countries which are below the line of 10 thousand euros,¹⁰ demonstrate a significant difference in percent of enforced receivables, within a range from 22.3 percent in the case of Turkey to almost 68 percent in the case of Mexico. Nevertheless, it can be observed that the recovery rate grows along the lower axis of Fig.1 towards the right (i.e., towards higher GDP per head of population).

Tab.1 Regression analysis results of recoverability from insolvency proceedings in dependence to GDP at current market prices per head of population in 2013 in OECD countries

Dependent variable: RECOVERY RATE				
Included observations: 29				
Variable	Coefficient	Std. Error	t-Statistic	Prob.
C	54.11412	6.906715	7.835002	0.0000
GDP	0.593861	0.200751	2.958194	0.0064
R-squared	0,244774	Adjusted R-square		0,216803
F-stat.	8,750910	Prob.		0,006364
DW stat.	1,804110			

⁹ Norway reaches about nine times higher a level of gross domestic product per head of population than Mexico or Turkey. For further comparison, it is interesting to note that Mexico, with 18 percent, is among the states with the highest costs for insolvency proceedings (Turkey shows costs of 15 percent of the enforced amount). While Mexican experts, however, state that investors would recover almost 68 percent of their investment (of receivables applied in the scope of insolvency proceedings) in the model case, the situation in Turkey is considerably worse, given that only in the vicinity of twenty percent of the receivable can be expected. We will further investigate especially the case of Mexico.

¹⁰ From the bottom, it is Turkey, Hungary, Poland and Mexico.

Tab.1 Results of regression analysis of recoverability from insolvency proceedings in dependence to GDP at current market prices per head of population. The model can be expressed in the following form:

$$\widehat{recovery\ rate} = 54.11 + 0.59\ gdp$$

from which it follows that if the GDP at current market prices per head of population is higher than one thousand euros, the recoverability of a receivable enforced within the scope of these proceedings is higher by 0.59 of a percentage point. It follows from the regression coefficient (0.59) estimate and from the correlation coefficient ($r = 0.49$) that this is in fact a proportional relationship. All tests were conducted on a five-percent level of significance. [11]

When we want to summarize the result clearly, it then applies that the more developed an economy, the higher the probability of better satisfaction of creditors in insolvency proceedings. The base hypothesis of this study is thus proved, even despite the fact that a more careful scrutiny of Fig.1 reveals an array of placement among individual countries that clearly defy the basic trend, while at least two cases markedly deviate at first glance from an imaginary mean of sorts. The first is the afore-mentioned Mexico, the highest-placed mark in the graph from the column of the first four marks. The second country is Switzerland, which we find as the penultimate towards the right, although very low. More will yet be said about both countries.

Information on the recoverability of investment (the rate of the enforced receivable) is only one side of the coin; the second is necessarily costs for the whole proceedings. As has already been noted, these costs are quantified as percent of the enforced sum, and in the following analytical part we will investigate the relationship of costs and yields to the gross domestic product in OECD countries.

From the following Fig. 2, it is to a certain extent clear that there is a relationship between both quantities, i.e. between costs and the yield from the receivable. This is to a certain extent logical. We can assert that if all other parameters of insolvency proceedings were the same, i.e. if insolvency proceedings in the researched countries ran according to generally identical regulations, and if it at the same time applied that the asset market was in the same state in all the monitored countries and had the same absorptive abilities, then the degree of creditor satisfaction would be decided precisely by costs for proceedings as such, i.e. remuneration of insolvency administrators, court fees, the amount of standard administrator costs and other similar circumstances. Of course, it could also be asserted that costs of proceedings are creditors' costs, as they are always defrayed from the insolvency proceedings' yields. Other solutions do not come into consideration besides this, at least not in any rational insolvency system arrangement.

On the other hand, there cannot be a simple dependence in the relationship between the yield for the creditor and the cost for insolvency proceedings, as the parameters for proceedings in individual countries are never the same, even if only due to the fact that insolvency laws differ significantly; there is variance

even in the definition as to when a debtor is bankrupt, there is varying enforceability of rights and agreements. Debtors are forced to declare or admit bankruptcy in various situations, and creditors too can declare debtors to be debtors in bankruptcy under different regulations. We can thus assert that, in some countries, debtors enter into the insolvency process with a smaller amount of assets than in other countries. This is given by the fact that certain arrangements enable debtors to stall insolvency proceedings and attempt either to control the situation or excise assets from the business or generally out of the reach of the creditors; the pertinent regulations are stricter in other countries.

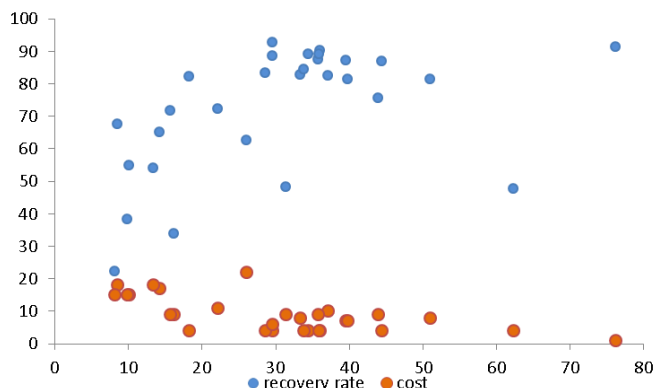


Fig. 2 Recoverability and costs from insolvency proceedings in dependence to GDP at current market prices per head of population in OECD countries in 2013 (costs in percent of property, recoverability in percent from investment, GDP in EUR thousands) Source: data World Bank, IFC (2014), AMECO (2014)

We can observe a great divergence of situations in various national economies, where it often occurs that if laws are set too favourably towards debtors, it has an impact on creditors' possibilities to gain their property. This occurs due to the simple fact that this property is in fact not present anymore, as it has already been expended in attempts to rescue the business, or it has been removed from the creditors' reach. In such a situation, however, costs of proceedings necessarily grow: When little is enforced, labour costs and the administrator's costs will be high in proportion to enforced property. If much has been enforced, the exact opposite applies. Thus, if EUR 900 thousand from EUR one million (i.e. 90 percent of the volume of the receivable) is enforced in a certain country, costs of proceedings at EUR 45,000 represent five percent of the enforced sum. If a mere EUR 279 thousand (27 percent of the entire receivable) is enforced, the same EUR 45,000 changes to 16.6 percent of the enforced sum. This relationship should be borne in mind when evaluating all of the following data.

When examining Fig. 2, we can thus observe once again a relatively clear situation, that a country positioned left in the lower axis, i.e. states with a low productivity of the national economy and lower GDP per head of population, tend to show higher costs, i.e. they are in an area between fifteen to twenty percent on the vertical axis, or on the axis by which costs can be measured. Yet it is illustrative to leave the recovery rate result in this graph also (the results are, of course, the same as

in Fig. 1). We can observe a specularity of relation between recovery rate and costs.¹¹

Tab. 2 Regression analysis results of recoverability from insolvency proceedings in dependence to GDP at current market prices per head of population in 2013 in OECD countries. Source: data World Bank, IFC (2014), AMECO (2014), calculation own

Dependent variable: RECOVERY RATE				
Included observations: 29				
Variable	Coefficient	Std. Error	t-Statistic	Prob.
COST	2.243395	0.548988	4.086421	0.0004
GDP	1.577508	0.165750	9.517395	0.0000
R-squared	0,527554	Adjusted R-square	0,584130	
F-stat.	14,795010	Prob.	0,000336	
DW stat.	1.637552			

Tab. 2 shows results of analysis of recoverability from insolvency proceedings in dependence to GDP at current market prices per head of population. The model can be written in the form:

$$\widehat{recovery\ rate} = 2.24\ cost + 1.58\ gdp$$

Conclusions follow which are in certain respects problematic towards the basic hypothesis of this work. The main problematic conclusion is the statement that increase of insolvency proceeding costs from property by one percentage point increases the recoverability from investment from these proceedings by 2.24 of a percentage point, under the assumption that the GDP at current market prices per head of population is constant. We here arrive at a direct conflict with the hypothesis of the study, according to which increased costs, by contrast, should lead to a reduction of yields. We will return to this problem later.

The second conclusion, however, fully supports the hypothesis. In the model, an increase of GDP at current market

¹¹ In this regard, one has to confront in an honourable manner the case of Switzerland, which we see on the GDP per head of population axis as the second from the right. Some people might want to explain the low yield of less than fifty percent of the receivable, which ranks this country far behind many poorer states, by drawing attention to the well-known high expense of qualified legal services in the Swiss Confederation. This, however, is not an acceptable interpretation, as the costs here monitored are those incurred by the proceedings as such, i.e. costs for monetizing the debtor's property or, for instance, for the services of an insolvency administrator (or otherwise known as the participant of the proceedings who performs technical and other actions throughout the process, directs monetization, draws a record of and supervises the debtor's property and so forth. If one of the creditors hires its solicitors in order to be represented in the proceedings by a qualified person, this expense are not part of this item. In fact, we do not have an adequately plausible interpretation for the position taken by Switzerland according to the evaluation of experts on insolvency proceedings in this country. We consider especially confusing the low costs accompanying the relatively low yield from insolvency proceedings. Swiss law is relatively benevolent towards debtors operating businesses; we are of the opinion, however, that this in itself does not suffice to explain this anomaly.

prices per head of population by EUR one thousand increases recoverability from investment from these proceedings by 1.58 of a percentage point under the assumption that costs of insolvency proceedings from property are constant. Then the hypothesis that creditors attain higher satisfaction in economies with higher performance (which we could also describe as economic systems with a higher quality of the system as a whole) would truly apply.

When we summarize the described model based on data for 29 economies, then both partial regression parameters are positive, so it is in fact a proportional relationship. From the values of the multiple correlation index of 0.73, it follows that the relationship is relatively strong. All tests were conducted on a five-percent level of significance. [11]

It is now necessary to return to the first relationship, which tells us that an increase in insolvency proceeding costs from property by one percentage point increases the investment recoverability from these proceedings by 2.24 of a percentage point, under the assumption that GDP at current market prices per head of population is constant. By closer examination of Fig. 2 and its data foundation, we find that the average costs of insolvency proceedings (not weighted by the size of the economy), reaches a value of 9.2 percent of the value of the enforced property. Average yields (again not weighted) are then 72.9 percent of the receivable. Even a perfunctory glance at all the data reveals that there are two countries in the file which markedly deviate from the notion of the relationship between costs and yields in proportion to the performance of the national economy. We have mentioned both: the first is Switzerland, which, given a high GDP (over EUR 62 thousand) and low costs (4 %), attains a surprisingly small yield for creditors (under 48 %) according to documents from *Doing Business*. The second country is Mexico, which, given a very low GDP at current market prices per head of population (EUR 8.6 thousand) and despite relatively high costs (18 percent) attains a very high yield for creditors (67.6 percent of the enforced receivable). These two states diverge from the general trend, which is precisely shown by Fig. 3.

As we can see on the following image, we could label the general inclination of the data far more frankly after eliminating these two states, which applies especially in the issue of yields. The removal of the two countries from the model strengthens the general impression on the position of the individual states when the trend of growth of yields in dependence to the growth of GDP at current market prices per head of population and at the same time to the reduction of costs of insolvency proceedings. If we wanted to describe the result in a truly colloquial manner, one could say that the new version of the graphic expression of Fig. 3 is substantially neater.

Understandably, the question arises as to why precisely Switzerland and Mexico show such significant divergences from the trend which the remaining 27 countries so clearly confirm.¹²

¹² Emerged doubts could lead many readers towards calculating individual marks in Fig. 2 and Fig. 3, although it will be a considerable problem to calculate a count of 29 or, more precisely, 27 marks of the same colour, i.e. one mark for every researched state. The problem is, however, very simple:

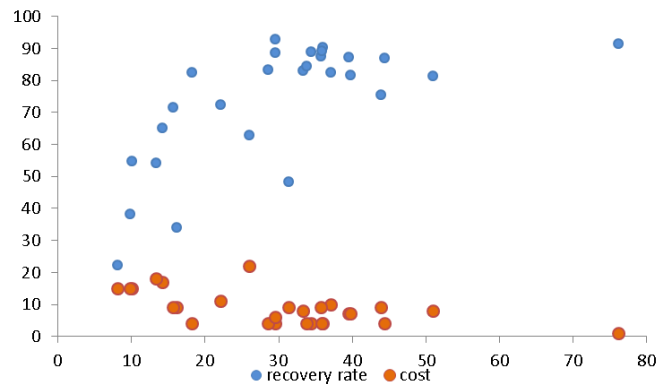


Fig. 3 Recoverability and costs from insolvency proceedings in dependence to GDP at current market prices per head of population in OECD countries in 2013 (costs in percent of property, recoverability in percent from investment, GDP in EUR thousands) Version without Switzerland and Mexico
Source: data World Bank, IFC (2014), AMECO (2014)

One of the possible interpretations could be an error by the respondents of questionnaire on the basis of which *Doing Business* arises. Naturally, it is impossible to ignore the fact that the group of experts who complete the pertinent data for a given country are either too optimistic or, on the contrary, too pessimistic in their opinions. This would, however, necessarily lead to the survey issuing figures that do not correspond with reality. This suspicion is certainly relevant and cannot simply be rejected. In the case of Mexico, the yield from the receivable could truly be a mistake. If the data from *Doing Business* state that creditors gain 67.6 percent of the entire volume of receivables, and insolvency proceedings cost 18 percent of what is enforced, this then means that the entire enforced sum should represent 82.4 percent of registered and recognized receivables. In view of the characteristic of Mexican economy and the institutional maturity of the country, such an assumption can most certainly be cast into doubt.¹³ Every insolvency system is different, laws work differently in every country, as does the enforceability of the law and, most importantly, in numerous countries there are widely divergent regulations as to which trading companies and which entrepreneurs can even enter into the insolvency process as such. To put it more precisely, the following is at issue: In certain states, insolvency proceedings as such are open only to companies that fulfil certain criteria; in principle, the criteria are similar to those fixed by the Czech legal code as a conditioned ticket to reorganization. [12] It is thus primarily necessary to fulfil a certain condition as to size. This then

some marks of countries do indeed overlap very strongly and are visible only when the image is enlarged to the maximum.

¹³ This note is by no means intended as an attempt to in any way lower the level of development in Mexico. Nevertheless, it is truly difficult to conceive that the general enforcement achieved would be higher than in numerous states that are most certainly on a far higher institutional level. For instance, the total monetization of debtor assets in the model case (on which the *Doing Business* survey is based) would reach 78.7 percent of total receivables, 83 percent in Sweden and so forth. If we were to take as decisive the data on Switzerland, the total enforced sum would represent only 49.6 percent of the volume of receivables.

leads to relatively humorous and sometimes, at first glance, incomprehensible situations where (according to statistics) tens of thousands of companies go bankrupt, but in states which are shaken by financial crises, political uncertainty or an extreme level of unemployment, the path of insolvency proceedings is taken by barely a hundred companies annually.

The structure of the “insolvency package” (i.e. the composition of companies that go bankrupt in a given year) is thus to a large extent influenced by the setting of laws. And given that national differences of setting insolvency law are truly great in individual countries, a large “grey area” emerges in every international comparison, in which it is truly difficult to create conditions which would enable serious comparison of individual processes in these states.

Tab. 3 Regression analysis results of recoverability from insolvency proceedings in dependence to GDP at current market prices per head of population in 2013 in OECD countries (without Switzerland and Mexico). *Source: data World Bank, IFC (2014), AMECO (2014), calculation own*

Dependent variable: RECOVERY RATE

Included observations: 27

Variable	Coefficient	Std. Error	t-Statistic	Prob.
C	72.39563	11.32426	6.392967	0.0000
COST	-1.653909	0.634020	-2.608605	0.0154
GDP	0.512255	0.222071	2.306715	0.0300
R-squared	0.565972	Adjusted R-square		0.529803
F-stat.	15.64800	Prob.		0.000045
DW stat.	2.117835			

It can be mentioned that besides the clearly exceptional cases of Switzerland and Mexico, we could nevertheless still find certain cases in the set of 27 states that recede more or less from the relationships defined in the initial hypothesis. This is most certainly the case with France, where, given the high quality of the economy (a GDP of EUR 31.5 thousand per inhabitant) and average costs (9 percent), pay-outs to creditors reach only 48.3 percent of their receivables. Nevertheless, France is relatively well known insofar as their insolvency law is highly problematic [2], [6]: firstly, it favours debtors relatively strongly, and secondly, it prefers “public interest”, which primarily entails preserving employment. Therefore, although France does not exactly conform to the general trend as shown by the results of the analysis, it was left in the sample, as the reasons of difference and low performance of the system are in this case most probably known and are rooted directly in the insolvency legislation itself.

Tab. 3 shows results of analysis of recoverability from insolvency proceedings in dependence to GDP at current market prices per head of population (of course, after reducing the sample from 29 to 27 countries). The model can be written in the form:

$$\widehat{\text{recovery rate}} = 72.39 - 1.65 \text{ cost} + 0.51 \text{ gdp}$$

from which it follows that increase of insolvency proceeding costs from property by one percentage point increases the recoverability from investment from these proceedings by 1.65 of a percentage point, under the assumption that GDP at current market prices per head of population is constant. This revised result, having emerged by analysis of a smaller sample of countries, corresponds precisely to the assumptions that were summarized in the hypothesis upon which this text is based and the research which is the foundation thereof. The second conclusion is similar to that of the sample of 29 countries, but is stronger than in the full sample. A higher GDP at current market prices per head of population by EUR one thousand increases the recoverability from investment by 0.51 of a percentage point, which applies under the assumption that costs from insolvency proceedings from property are constant. Both partial regression parameters are positive, so it is in fact a proportional relationship. From the value of a multiple correlation index of 0.75, it follows that the relationship is relatively strong. [11] All tests were conducted on a five percent level of significance.

IV. CONCLUSIONS

We can form several conclusions on the basis of regression analyses, into which data on insolvency processes provided by *Doing Business* were entered on the one hand, and statistical data on the level of GDP at current market prices per head of population on the other.

The first of these is the assertion that it was possible to confirm the hypothesis according to which the efficiency of insolvency processes is higher in countries which demonstrate a generally higher productivity of the national economy expressed precisely by the data on GDP at current market prices per head of populations. These countries reach a lower level of costs and at the same time, higher satisfaction for creditors. This is shown both by the model described and by viewing Fig. 3, where it is clear that states positioned on the horizontal axis more to the right, i.e. states with higher GDP at current market prices per head of population, usually show a higher utilization percentage of insolvency proceedings for creditors and lower costs for these proceedings.¹⁴

The second conclusion is that in all monitored cases of individual OECD countries, it applies that higher costs for proceedings lead to a reduction of yields for creditors. If we reverse this relationship, we can assert that higher expenses for the insolvency process (i.e. higher remuneration of insolvency administrators, for instance) do not lead to an increase in the quality of insolvency proceedings – at least not in the sense

¹⁴ Here it is understandably necessary to draw attention yet again to the mathematical logic of the whole matter – if debtors in a given country enter insolvency proceedings with relevant property, lower costs of proceedings are logical, as this datum is defined as a percentage of the volume of recorded property at the value of its monetization. Therefore, if costs reach 4 percent, for instance, these could in fact be the same or higher in its absolute value than in a country where costs in percent are optically higher – seven or more percent, for instance.

that this would result in higher efficiency of proceedings expressed by a higher yield. One of the reasons is, once again, the paradox described in note 13.

This conclusion nevertheless has interesting connotations. We can draw numerous further assertions therefrom, which can in fact go directly to the most sensitive areas of insolvency proceedings. If increasing the remuneration of insolvency administrators and a general rise in costs of proceedings do not lead to a higher enforced sum (for instance, thanks to a greater and more structured interest in entrusted cases on the part of the administrator), it would then be possible to reduce these costs without greater effect on the quality of result – at least to a certain extent. This would without doubt lead to greater satisfaction of creditors; moreover, it would not necessarily entail any intervention into the administrator's earnings. Likewise, if the general maximum number of insolvency administrators performing their duties were to become limited there where such a decree exists or would emerge, a generally lower amount of money would suffice to finance the whole system.

The last conclusion is a certain need to interpret correctly the given results in view of the general problem of insolvency proceedings and individual insolvency acts. It seems that the main problem in those states which show the effect of the “connected dish” (i.e. high costs and likewise low yields for creditors) is the elementary fact that the system essentially enables debtors to delay with relative ease the declaration of bankruptcy or hiding of a bankruptcy for so long that their assets are thoroughly insufficient to reasonably cover creditors' receivables. Nevertheless, the data from *Doing Business* primarily do not cover this problem due to the fact that – as has already been said – they are based on expert estimates on the settlement of one specific model case. However, because these experts use as a departure point their experiences with the possibilities of monetizing a debtor's assets, we can assume that their responses also include references to the general situation of insolvency case settlement in a given country.

ACKNOWLEDGMENT

In this connection, we thank Prof. Dr. Tomáš Richter, LL.M., Ph.D. for numerous inputs and suggestions which he provided to the team of authors.

REFERENCES

- [1] Richter, T. (2008): *Insolvenční právo*, ASPI Wolters Kluwer, Praha 2008 27-62.
- [2] S.A.Davydenko, J.R.Franks, “Do Bankruptcy Codes Matter? A Study of Defaults in France, Germany, and the U.K.”, *The Journal of Finance*, vol. LXIII, num. 2, pp. 565–607.
- [3] L. Smrčka, “Filosofické aspekty vztahu insolvenčního a exekučního práva”, *Komorní listy* (in Czech), vol. 1, iss. 4, 2012, Prague, pp. 27 – 33
- [4] O.Knot, O.Vychodil, “What drives the optimal bankruptcy law design?”, *Finance a Úvěr - Czech Journal of Economics and Finance*, 2005, vol. 55, iss. 3, pp. 110-123.
- [5] S.H.Lee, Y.Yamakawa, M.V.Peng, J.B.Barney, “How do bankruptcy laws affects entrepreneurship development around the world?”, *Journal of Business Venturing*, vol. 26, iss. 5, September 2011, pp. 505 – 620
- [6] R.Blazy, B. Chopard, A.Fimayer, J.D.Guigou, “Employment preservation vs. creditors' repayment under bankruptcy law: The French dilemma?”, *International Review of Law and Economics*, vol.: 31 iss: 2, pp. 126-141.
- [7] M.Jacobs, A.K.Karagozoglu, D.N.Layish, “Resolution of Corporate Financial Distress: An Empirical Analysis of Processes and Outcomes”, *Journal of portfolio management*, vol. 38, iss. 2, pp. 117-135.
- [8] World Bank, IFC, *Doing Business 2013*, A co-publication of The World Bank and The International Finance Corporation, Washington DC, 2013, on-line: <http://www.doingbusiness.org>
- [9] World Bank, IFC, *Doing Business 2013 (methodology)*, A co-publication of The World Bank and The International Finance Corporation, Washington DC, 2013, on-line: <http://www.doingbusiness.org/methodology>
- [10] AMECO, *The annual macro-economic database*. Online: http://ec.europa.eu/economy_finance/db_indicators/ameco/index_en.htm
- [11] R.Hindls, S.Hronová, J.Seger, J.Fischer, *Statistika pro ekonomy*. 8. edition Prague: Professional Publishing, 417 pp.
- [12] J.Kotoučová and all., “Zákon o úpadku a způsobech jeho řešení (insolvenční zákon) Komentář”, C.H.Beck, Praha, 2010
- [13] Sieber, P., Hnilica, J. (2011): “Cost – Benefit analýza a riziko v socioekonomickém hodnocení projektů”, *Ekonomický časopis*, vol. 59, iss. 7, pp. 669-683.

Assoc. Prof. Luboš SMRČKA, M.Sc., Ph.D. In 1984, he graduated from the Czech University of Life Sciences in Prague. After 1993, he left the Institute of Experimental Botany at the Czechoslovak Academy of Sciences to start business. He gradually acquired several professional specializations: tax advisor (1993), broker (1996), certified balance accountant, (1998), forensic expert in economy, prices, and valuation specialized in the valuation of securities, RM-S and stock exchange and business valuation (2000, extended in 2003), accounting and tax expert (2001).

In the last 6 years, he has worked as a Lecturer in the Department of Business Economics at the Faculty of Business Administration of the University of Economics in Prague. In 2013, he gained the title of Associate Professor. He focuses primarily on the area of insolvency proceedings, their macroeconomic impacts and issues of insolvency law and the problem of personal finances. Assoc. Prof. Smrčka is the author of numerous books and articles in professional publications.

Assoc. Prof. Markéta Arltová, M.Sc., Ph.D. She studied the field of Economic Statistics at the University of Economics in Prague. In 1999, she defended her doctoral dissertation study in the field of Statistics. At present, she is working as an associate professor at the Department of Statistics and Probability at the University of Economics in Prague. She specializes in the problem connected with the analysis of economic, financial and demographic time series.

Jaroslav Schönfeld, M.Sc. Ph.D. graduated from the University of Economics in Prague in 2007. He works at the Czech Savings Bank, Inc., in the department of restructuring and recovery. Since 2008, he has also been active at the University. He deals with financial management, restructuring, insolvency and pricing. He is the author of the monograph *Modern View on the Valuation of Receivables* (CH Beck 2011) and numerous articles in professional journals.

Lee Louda, M.Sc. studied at the Czech Technical University in Prague – Faculty of Mechanical Engineering in 1992; in 1994, he took a broker's examination and operated actively on the capital markets in the CR until 1999. In 1998-2000, he successfully passed the Institute of Property Valuation at the University of Economics in Prague in the field of securities. In 1999, he passed the insolvency administrator's examination, and in 2010, he passed a special insolvency administrator's examination. In 2013, he commenced doctoral studies at the University of Economics in Prague – Faculty of Business Economics. He focuses mainly on the area of insolvency proceedings in practice, especially financial rehabilitation methods of settling bankruptcy.

HVDC Transmission Corridor - Cost Benefit Analysis

UDREA OANA.*, GHEORGHE LAZAROIU. **, UNGUREANU GABRIELA ***
 *, ***, CNTEE Transelectrica SA, Bucharest, ** University "Politehnica" Bucharest
 * ana.udrea@gmail.com, ** glazaroiu@yahoo.com, *** gabrielaungureanu89@yahoo.com

Abstract – Constructed in 1986, the 750 kV line connecting the Ukrainian and Romanian transmission networks went out of service in the mid-1990s due to damage to the lines. Although the Romanian TSO and the Ukrainian TSO carry plans to restore the line, each has experienced significant development of their transmission networks since the line went out of service. This article identifies the optimal configuration of the corridor to serve the transmission requirements of the system operators in Romania, Ukraine and Moldova. Currently the transmission corridor, which had consisted of a 750kV AC Over Head Line (OHL), is not in operation and is in a state that cannot be easily repaired. The OHL has been damaged so that it could be considered as “non-existent” for each party. The investment scenarios themselves are comprised two voltage levels considered for the corridor: 400 kV and 750 KV. In turn, these voltages can be analyzed in terms of synchronous AC or asynchronous DC connection via a back-to-back station that may be located in either Moldova or Romania.

Keywords: asynchronous, back-to-back, IPS/UPS, RUM

I. INTRODUCTION

Currently the Romanian – Moldovan – Ukrainian (RUM) transmission corridor, which had consisted of a 750kV AC Over Head Line (OHL), is not in operation and is in a state that cannot be easily repaired. The OHL has been damaged so that it could be considered as “non-existent” for each RUM party. The existing route of the old 750 kV transmission line is depicted in Fig.1.

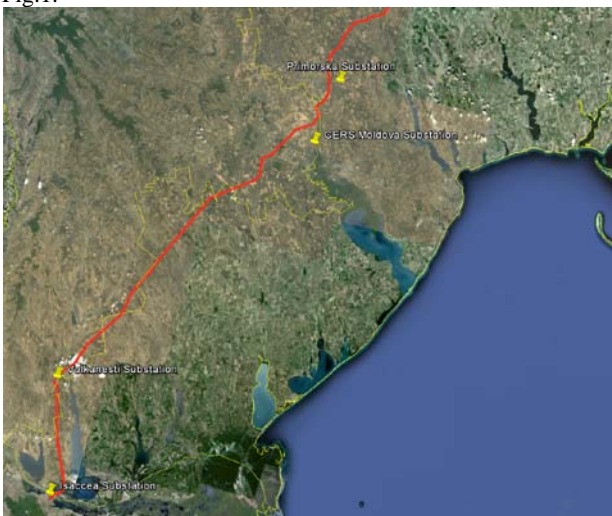


Fig. 1. The route of the old 750 kV transmission line

Although the original transmission corridor is directly between Pivdenoukraisna NPP (Ukraine) and Isaccea (ROM) Substations, Ukraine plans to construct a new 750kV OHL between Pivdenoukraisna NPP and Primorska Substation

(see red dashed line in Fig.2). Hence, the corridor under discussion in this article will cover the existing Right of Way between Primorska (Ukraine)-Isaccea (ROM) substations. This corridor is depicted in Fig.2 (blue dashed line).

The transmission line distances between the substations in the corridor are provided in Table 1. The transmission lengths do not represent fly-over distances but rather the total line lengths assumed in the analysis, which were vetted by the participating TSO.

Table 1. Transmission line distances between the substations.

Expected OHL Distances (km)	From Substation				
	Primorska	CERS Moldova	Vulcanesti	Isaccea	
To Substation	Primorska	-	50	200	260
CERS Moldova	50	-	175	235	
Vulcanesti	200	175	-	60	
Isaccea	260	235	60	-	

The possible connection points (i.e., candidates) in Moldova are: 400 kV CERS Moldova and Vulcanesti Substations. Summary of the substations along the RUM transmission with the corresponding voltage levels are given in Table 2.

Table 2. Summary of the substations along the RUM transmission corridor.

Country	Substation	Abbreviation	Existing EH Voltage Level in Substations		
			750kV	400kV	330kV
Ukraine	Primorska	UKR	✓	✗	✓
Moldova	CERS Moldova	MDV_1	✗	✓	✓
Moldova	Vulcanesti	MDV_2	✗	✓	✗
Romania	Isaccea	ROM	✓	✓	✗

Considering the candidate substations in Moldova and the available voltage levels, three groups of variants are generated as alternatives for the investigations, as presented in Table 3.

Table 3. Substation and voltage level variants to be investigated.

Seasonal Variants	Substation Variants	Voltage Level Variants	Connection Type Variants
Summer Peak Load	UKR - ROM	1 x 750 kV	AC OHL
Summer Min Load	UKR - MDV_1 - ROM	2 x 400 kV	DC B2B (located at ROM)
Winter Peak Load	UKR - MDV_2 - ROM	1 x 400 kV	DC B2B (located at first SS before ROM)
	UKR - MDV_1 - MDV_2 - ROM		

Initial assumption, was to analyze a total of 36 scenarios (Substation Variants (4) x Voltage Level Variants (3) x Seasonal Variants (3) = 36) as given in Table 3. However, the initial analysis indicated a strong dependency of results to “Connection Type Variants”. Hence “Connection Type Variants” are also included in the analysis creating a total of 108 scenarios (108 = 36 x 3 (Connection Type Variants)) to be analyzed.

II. METHODOLOGY

The approach in load flow and N-1 contingency analysis will be to search for the maximum amount of power that can be

transferred safely from/to Ukraine+Moldova to/from Romania, for each combination of Substation and Voltage Level Variants shown in Table 3. Flowchart of this approach (i.e., algorithm) is given in Fig. 3.

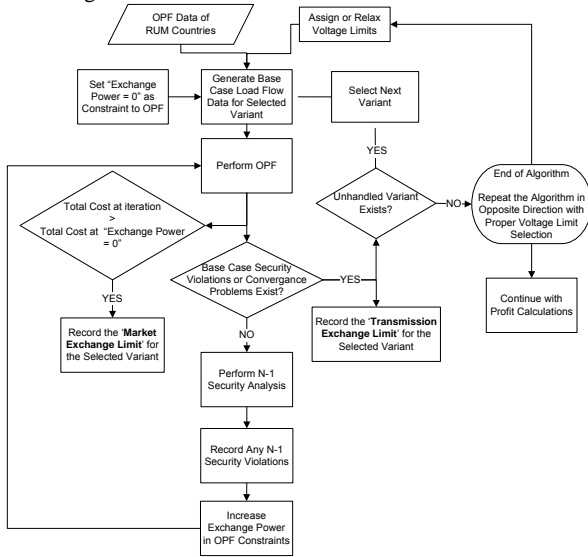


Fig. 2. Flow Chart of the methodology (OPF and N-1 contingency analysis)

The reasoning behind “Assign or Relax Voltage Limits” block can be described as follows: The OPF solution has the ability to assign voltage constraints for individual buses. At the data collection phase, the voltage level limits for each RUM party is collected for high voltage network as given in Table 4.

Table 4. Voltage level limits for analysis.

Country	Voltage Level				
	750kV	500kV	400kV	330kV	220kV
Romania	+/-5%	-	+/-5%	-	+/-10%
Ukraine	+/-5%	+/-5%	+/-5%	+/-10%	+/-10%
Moldova	+/-5%*	-	+/-5%	+10% / -5%	-

Voltage constraints are indeed local problems that can be assumed to be handled by proper operational maneuvers in the short term (e.g., proper selection of generator voltage set points) and relatively easy capacitor/reactor investments in the mid-term. The economical calculations (i.e., cost/benefit analysis) based on the results with voltage constraints might be misleading since such voltage problems can be solved either with reasonable investments in a plausible time frame or with operational maneuvers in real time). Hence, for long term decision making analysis, it is more reasonable to work with OPF results performed ignoring local voltage constraints. Nevertheless, the OPF and contingency analysis are performed and results are recorded for both considering and ignoring the voltage constraints. The effect of voltage constraints on total generation cost and optimum power exchange amounts in Scenario 1 is illustrated in Fig. 4, as an example.

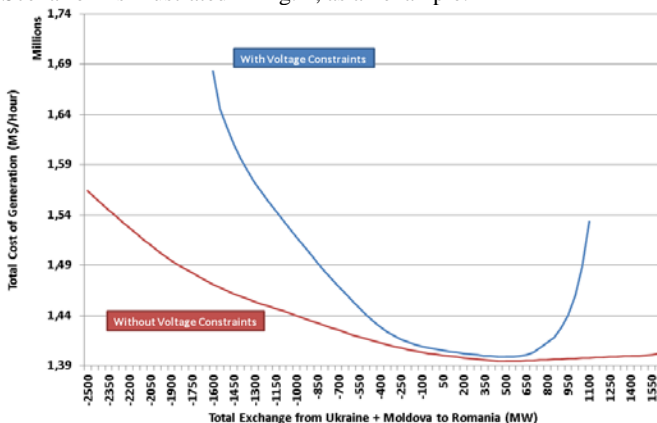


Fig. 4. Total generation cost results of Scenario 1 (with and without voltage constraints).

As illustrated in Fig. 4, the OPF algorithm forces the solution to a higher cost in order to be able to satisfy the voltage constraints. The effect is more observable as the exchange approaches higher values at both directions. However, as the voltage constraints are relaxed, the cost reduces as OPF does not consider voltage constraints. The algorithm of the methodology in Fig. 3 starts from an N-secure case with zero exchanges and iteratively increases the exchange power through the RUM corridor in order to find the optimum power exchange between the parties. The algorithm repeats the followings iteratively:

- Assigns an exchange from/to Ukraine+Moldova to/from Romania as a constraint to OPF,
- Performs an OPF to determine the dispatching,
- Compare total generation cost with zero power exchange case in order to determine the realistic transaction limit due to price difference,
- Creates a load flow scenario based on OPF solution,
- Performs N-1 contingency analysis,
- Records the N-1 security violations of each scenario, if any.
- Power exchange is increased in 50 MW steps.
- The analysis performed with and without voltage constraints and the results are compared.

Trading scenarios between RUM countries, as predicted by each party, are given in Table 5. The trading amounts presented in this table are utilized as “indicative” parameters in the analysis. As described above, the approach in OPF analysis is to search for the “maximum” amount of power that can be transferred N-securely between the RUM countries for each scenario that are shown in Table 3. In other words, the algorithm given in Fig. 3 will give the upper limit (i.e., maximum) for the N-secure power trading among RUM countries. The upper limit for the N-secure power trading could be less or more than the corresponding indicative power transfer amounts that are shown in Table 5 (last column).

Table 5. Trading scenarios initially predicted by RUM parties.

Scenarios	Import from	Export to	Transfer
1	Ukraine and/or Moldova (U&M: Synchronized with IPS/UPS)	Romania (R: Island with IPS/UPS)	200 MW
2	Ukraine and/or Moldova (U&M: Synchronized with IPS/UPS)	Romania (through HVDC B2B) (location of HVDC B2B to be analysed)	500 MW
3	Moldova (through direction of generator Moldavska to Romania)	Romania	480 MW
4	Ukraine and/or Moldova (U&M: Synchronized with IPS/UPS)	ENTSO/E (through Romania) (through HVDC B2B) (location of HVDC B2B to be analysed) (Max export of Moldova = 500 MW)	1500 MW
5	Moldova (through direction of generator Moldavska to Romania)	Romania	480 MW
6	Ukraine and/or Moldova (U&M: Synchronized with ENTSO/E)	ENTSO/E (through Romania) (Max export of Moldova = 500 MW)	1500 MW
7	Ukraine and/or Moldova (U&M: Synchronized with IPS/UPS)	ENTSO/E (through Romania) (through HVDC B2B) (location of HVDC B2B to be analysed) (Max export of Moldova = 500 MW)	1500 MW
8	Ukraine and/or Moldova (U&M: Synchronized with ENTSO/E)	ENTSO/E (through Romania) (Max export of Moldova = 500 MW)	1500 MW
9	Romania Romania (R: Island with IPS/UPS)	Ukraine Moldova (U&M: Synchronized with IPS/UPS)	400 MW 100 MW
10	Romania Romania Romania	ENTSO/E Ukraine Moldova (U&M: Synchronized with ENTSO/E)	1500 MW 400 MW 100 MW
11	Romania Romania Romania	ENTSO/E Ukraine Moldova (To U&M through HVDC B2B) (location of HVDC B2B to be analysed)	1500 MW 400 MW 100 MW

III. COST/BENEFIT ANALYSES

The OPF analyses cover the largest part of the analysis and create a basis for the cost/benefit analysis which is described in this section. In this section, performance indicators for

economic and financial analysis, determination of necessary investments for the corresponding investment scenarios, and calculation of per unit investment and operation and maintenance costs are described.

III.1. PERFORMANCE INDICATORS (IRR, NPV, AND B/C RATIO)

The economic and financial analysis is based on the results of the OPF analysis, which calculates the total savings to region at the optimum power exchange in each loading hour (i.e., winter max, summer max, and summer min). The Cost/benefit analysis was made by comparing the results of the OPF analysis with the investment cost (Inv cost) and operational and maintenance costs (O&M cost) of the candidate investments.

For each scenario, annual cash flow tables for 30 years were determined to conduct the following analyses:

- Internal rate of return (IRR) analysis,
- Net present value (NPV) analysis,
- Benefit/Cost ratio (B/C ratio) analysis.

A 30 year useful life of equipment was assumed for the purposes of the economic/financial calculations. The following parameters (KEPs) were utilized:

- Interest rate of borrowing money for total investment cost
- Loan period
- Discount rate for calculating NPVs

The costs of each investment scenario includes:

- Total investment cost (TIC) at the initial year (USD),
- Annual O&M cost (USD/year).

As described below, annualized savings are considered in the economic and financial analysis. As described in Section 9, sensitivity analyses were performed for the key economic parameters including both AWFs and different generation levels of wind power plants in Romania.

The year 2012 is considered to be the base year in unit costs of the equipment. The annual cash flow table is provided in Table 6.

It should be noted that annual savings can be negative in some investment scenarios that correspond to the most constrained loading conditions (e.g., winter max), even during zero exchange among the countries. This can occur when voltage constraints combine with high technical losses, and higher generation levels of the most costly power plants in the RUM countries than might be dispatched if there was no interconnection between the RUM countries. The total saving is assumed to be zero in such cases because the RUM transmission corridor circuit can be opened to curtail electricity flow in such circumstances.

Table 6. Annual cash flow table of each scenario.

Year	Cost (USD/year)	Saving (USD/year)	Balance (USD/year)
Year 0	Inv cost	0	-(Annual loan payback)
Year 1	Annual O&M cost	Annual Saving	+(Annual Saving)
Year 2	Annual O&M cost	Annual Saving	-(Annual loan payback + O&M cost)
...	+(Cumulative Annual Saving)
Year 30	Annual O&M cost	Annual Saving	-(Annual loan payback + Cumulative O&M cost)
...	+(Cumulative Annual Saving)
...	-(Annual loan payback + Cumulative O&M cost)

In the LF and OPF analysis, the maximum savings in each scenario are determined at three loading hours along the year (i.e., winter max, summer max, and summer min loading hours). The savings at these loading hours are utilized in determining the annual average savings (i.e., annualization of the savings). Annualization of the savings is based on the annualized weighting factors (AWF) of these three loading hours.

The regional system coincident annual hourly load recordings for 2010 were utilized to determine the AWFs. Annual hourly coincident regional load and its distribution along one year are given in Fig. 5 and Fig. 6, respectively. The

following loading hours are indicated in the figures:

- System peak (i.e., winter max)
- System off-peak (i.e., summer min)
- System peak during off-peak season (i.e., summer max)

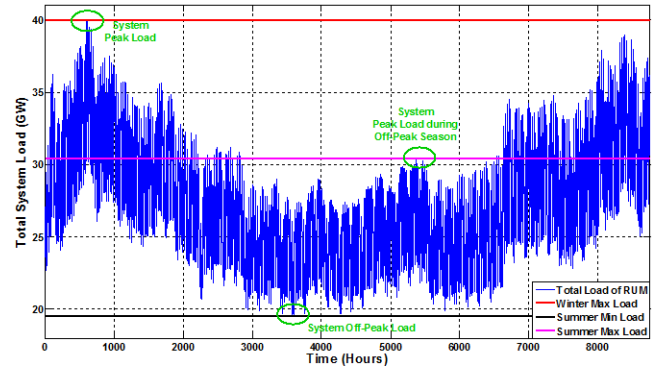


Fig. 5. Annual hourly coincident system load

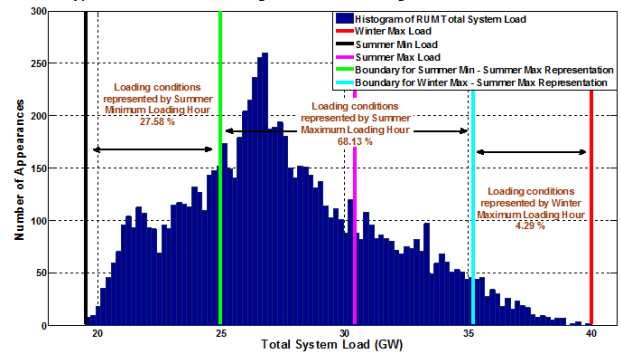


Fig. 5. Distribution of the hourly loads along the year.

AWFs of these three loading hours are indicated in Fig. 6 and summarized in Table 7. Note that, total energy consumed along the year (the area below the blue curve in Fig. 5) is equal to (1):

$$4,29\%*(System\ peak) + 27,58\%*(System\ off-peak) + 68,13\%*(System\ peak\ during\ off-peak\ season) \quad (1)$$

Table 7. AWFs assumed for RUM countries.

Loading condition	Loading hour	AWFs
System peak	Winter max	4,29%
System off-peak	Summer min	27,58%
System peak during off-peak season	Summer max	68,13%

This approach is analyzed below for the following parameter and investment scenario (Case_VC-I_W30%):

- Investment Scenario No: 1
 - 1x400kV Ukraine-MDV_2-ROM (connection through HVDC B2B substation at Romania)
- Wind generation level at Romania: 30%
- Voltage constraints: Ignored
- Loading Scenarios:
 - Scenario 4: System peak (Winter max)
 - Scenario 3: System off-peak (Summer min)
 - Scenario 2: System peak during off-peak season (Summer max)

The savings which are determined by OPF analyses for the three loading scenarios are given in Table 8.

Table 8. Annualization of savings for the Scenarios 2,3 and 4

Loading hour	Savings (USD/h)	Weighting factor (%)	Annualized average saving (USD/h)	Unavailability* of the line along the year (h)	Annual saving (USD/year)
Winter max (Scenario 107)	A = 8.916,25	4,29%	A * 4,29% + B * 27,58% + C * 68,13% = 5.238,68	5% * 8760 h = 438 h	5.238,68 *(8760-438) = 43.596.276,03
Summer min (Scenario 95)	B = 3.635,13	27,58%			
Summer max (Scenario 83)	C = 5.656,25	68,13%			

As illustrated in the table:

- The maximum saving occurs at “system peak” (i.e., winter max).
 - The room for OPF is maximum given high generation levels of cost-ineffective power plants in the region.
- The minimum saving occurs at “system off-peak” (i.e., summer min).
 - The potential for optimization is minimal due to system constraints at minimum loading conditions
 - The availability of cost effective generator capacity in the system is minimum.
- In order to determine the annualized total saving, availability of the line should be estimated (downtime for maintenance and unavailability of the line due to faults must be estimated). An availability of 8322 hours, which corresponds to ≈95% of the hours in a year, is assumed for the economic/financial analysis.
- Annual saving for this investment scenario is calculated as 43.596.276,03 USD/year, as illustrated in Table 8.

This approach was employed in for investment scenarios to in determine the annualized savings for cost/benefit analysis.

IV. HVDC BACK TO BACK TECHNOLOGIES

There are two primary HVDC Back to Back technologies: Line Commutated Converter (LCC) and Voltage Source Converter (VSC). HVDC Back to Back substations based on conventional Line Commutated Converter (LCC) technology depend on the Short Circuit MVA (SCMVA) at the connection point to the grid. The new VSC technology substations can operate independent from the SCMVA at the connection point. Today, both technologies are being deployed

The chronological development of the two HVDC technologies is given in Fig.7.

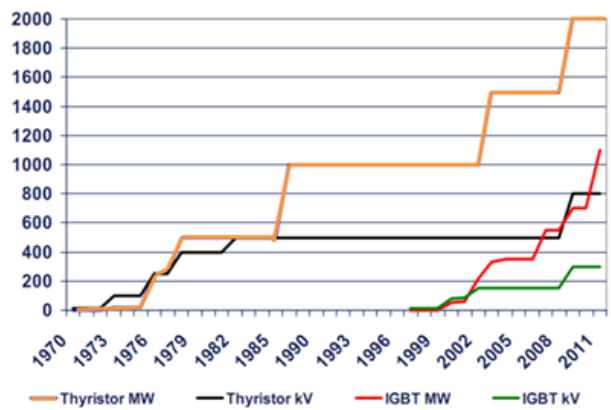


Fig.7. Chronological development in LCC and VSC technologies

While thyristors are utilized in conventional LCCs, (see Fig.8.), VSCs employ IGBTs (see Fig.9.). This make the unit

cost of VSC based technology higher than that of LCC, as illustrated in Table 12.

Table 12. Cost comparison of LCC and VSC technologies (equipment only). [1]

LCC Technology	VSC Technology
0,08 Euro/VA	0,11 Euro/VA

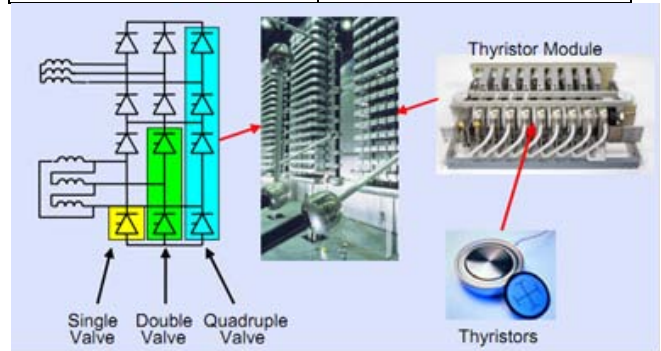


Fig. 8. Line Commutated Converter (LCC).

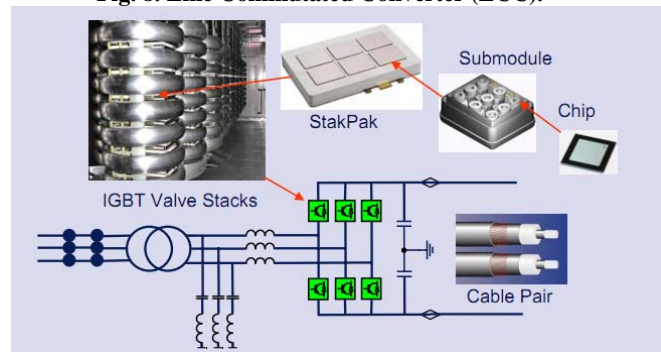


Fig.9. Voltage Source Converter (VSC).

IV.1. REQUIREMENT OF HARMONIC FILTERS

LCC based HVDC Back to Back substations generally require harmonic filters with a capacity of almost 60% of the substation [2]. For example, for a 300 MW block substation, the capacity of the necessary harmonic filters is 300*0.6 = 180 MVar.

IV.2 ESCR CRITERIA

The results of the ESCR calculation results are presented in this section to determine the acceptable level of the LCC technology based HVDC Back to Back substations.

$$ESCR = \frac{SCMVA_{grid} - S_{filter}}{P_{dc}} \quad (2)$$

In this formula, the contribution of the filters to SCMVA is subtracted to consider the true SCMVA of the grid. In this article, HVDC Back to Back connection is modelled by splitting the networks at the point of HVDC connection and introducing POSITIVE and NEGATIVE loads at appropriate sides. The schematic representation of such modelling is illustrated in Fig.7. As seen in the figure, the power flow through HVDC Back to Back substation from Primorska to Isaccea is modelled by splitting the networks and introducing a POSITIVE Load at Primorska side and a NEGATIVE Load at Isaccea side. It should be noted that a NEGATIVE Load is preferred in representing power injection rather than modelling a generator, in order to avoid unrealistic reactive support from the HVDC Back to Back via the generator. Given this representation, the SCMVA contribution of the HVDC Back to Back filters is not considered in the load flow and short circuit analysis. Therefore, the ESCR should be calculated as in (3).

$$ESCR = \frac{SCMVA_{grid}}{P_{dc}} \quad (3)$$

For the secure operation of HVDC Back to Back substation that is based on LCC the

$$ESCR \geq 3 \text{ (base case)} \quad [3] \quad (4)$$

Essentially, the ESCR is different at each connection point of the HVDC Back to Back substations given different topologies. For the sake of security, the minimum value among the SCMVA at each connection point is considered in calculating of the ESCRs. The available HVDC Back to Back substation capacity is calculated assuming that total capacity of the substation is formed by 300 MW blocks, while taking into account the ESCR criteria (4).

IV.3 DETERMINATION OF TOTAL CAPACITY OF HVDC BACK TO BACK SUBSTATION

It is assumed that the HVDC Back to Back substation blocks will be in the order of 300 MW capacities. The following arguments support this approach:

- 300 MW capacity HVDC Back to Back substations are available in the market.
- The order of 300 MW is plausible to match the optimum substation capacity with the optimum power exchange amounts that are determined in LF (Load Flow) and OPF (Optimal Power Flow) analysis.

For example, the approach in determining the total capacity of the HVDC Back to Back substation is presented below (1x400 kV transmission line between Ukraine - Romania through HVDC Back to Back substation in Ukraine):

- Loading condition of the scenario: Summer maximum.
- Wind generation level in Romania: Normal (i.e., generation level of the wind power plants in Dubrudja/ROM region is 30% of the capacity).
- OPF results at base case (i.e., ignoring N-1 contingency):
 - 700 MW (Ukraine => Romania)
- N-1 security exchange technical limit:
 - 1.300 MW (Ukraine => Romania)
 - Since $700 < 1300$, 700 MW power exchange is feasible in the sense of N-1 security concern.
- Voltage collapse power exchange limit:
 - 1.500 MW (Ukraine => Romania)
 - Since $700 < 1.500$, 700 MW power exchange is feasible in the sense of voltage collapse concern.
- Assuming that HVDC Back to Back substation is composed of 300 MW blocks, total number of block to realize 700 MW power exchange is three ($3 \times 300 = 900 > 700$)
 - Total capacity of the HVDC BACK TO BACK substation is 900 MW.
- ESCR criteria:
 - Maximum SCMVA of the grid at the HVDC Back to Back substation is calculated as 2.063 MVA
 - $ESCR = 2.063/900 = 2,29$
 - Since $2,29 < 3$, total capacity of 900 MW is NOT acceptable in the sense of ESCR criteria.
 - If one block among the three blocks is removed, then the total capacity of the substation is $2 \times 300 = 600$ MW
 - $ESCR = 2.063/600 = 3,43 > 3 \Rightarrow$ acceptable

An HVDC Back to Back capacity of 600 MW is proven in

the summer maximum loading conditions. Similar analyses were performed for winter maximum and summer minimum loading conditions, as well. The total capacity of the HVDC Back to Back substation is considered to be the maximum capacity determined among three loading scenarios. This approach is considered in all scenarios that include HVDC Back to Back substation.

VI. CONCLUSIONS

Voltage constraints were local problems that could be resolved through network operations in the short term (e.g., proper selection of generator voltage set points) and relatively inexpensive capacitor/reactor investments in the mid-term. Hence, voltage constraints are ignored in certain cases to determine the maximum volume of power exchange among the countries. The maximum voltage deviation at the key nodes was observed to be +/-20%, which could be resolved by proper compensation through the provision of additional reactors.

The increase in wind generation in Romania dramatically limited the ability of the RUM countries to optimize the regional generation fleet based on the cost of production. In some investment scenarios, the flow of power changed direction from north \rightarrow south to south \rightarrow north when the wind power plant generation in Romania increased from 30% to 70% and it is designated as must run. This occurs when the OPF algorithm forced inefficient high cost generators, first in Romania and then in Moldova and Ukraine, to reduce their generation in favor of must run wind. This process continued until the reduction of generation in Ukraine and Moldova became so much more cost effective than the reduction of generation in Romania that the power flow changed direction. From this point onward, Romania began exporting power in a northward direction to Moldova and Ukraine.

It is important to note that for the investment scenario of a 400 kV connection passing through a HVDC B2B substation, the benefit/cost ratio was > 1 , when Romanian must run wind generation was modeled with a 30% capacity factor.

Connection through the HVDC Back to Back was superior to connection through AC options in almost every investment scenario considered. This was because the HVDC connection reduced technical network constraints to increase power exchange, enlarging the scope for power flows in the sub-region.

In fact, HVDC B2B was the only investment solution which resulted in benefit/cost > 1 when considering the scenario of Romanian must run operating with a 30% capacity factor. And, the technical challenges to synchronizing the current IPS/UPS and ENTSO-E members of the RUM working group would inhibit interconnection via high voltage AC interconnections for the foreseeable future. Therefore, HVDC technology based interconnection of the RUM countries seemed the most rational solution in the short/mid-term.

There was no significant difference revealed in the cost/benefit analyses for the different investment scenarios related to the configuration of the corridor, i.e., either directly from Ukraine to Romania or through Moldova. If the interconnection between RUM countries were realized in intermediate steps, (for example, if the connection between Romania and Moldova were realized before all three countries are interconnected), energy trade between Romania and Moldova could begin before the trading among all three countries by directing a generator in Moldova to operate synchronously with Romania in island mode.

REFERENCES

- [1]. Lazaros P. Lazaridis, "Economic Comparison of HVAC and

HVDC Solutions for Large Offshore Wind Farms under Special Consideration of Reliability”, Master’s Thesis, Royal Institute of Technology Department of Electrical Engineering, Stockholm 2005.

[2]. Dodds, B. Railing, K. Akman, B. Jacobson, T. Worzyk, “HVDC VSC (HVDC light) transmission – operating

experiences,” CIGRE 2010.

[3]. “Feasibility study of the asynchronous interconnection between the power systems of Iran and Turkey”, Interim Report, Professor Francesco Iliceto, Consultant to TEIAS, Rome (Italy), November 2009.

* Siemens PTI Documentation

The ability of water reservoir to assure required water supply under changed climate conditions

D. Halmova, M. Melo, P. Pekarova

Abstract—The assessment of water demand and water management has the ultimate role for solution of this problem in near future. In this paper we study water reservoir ability to assure the required water supply under changed climate conditions. We used data from the coupled general circulation model CCCM2000. Present horizontal resolution of GCMs does not allow making out some regional climate features. We use a statistical method for downscaling of GCMs outputs. We take into account model outputs from four gridpoints near to northern Slovakia. These calculations are studied for time horizon 1951–1980 and for next time horizons 2030 and 2075.

The Liptovska Mara water reservoir operation was calculated by rainfall-runoff balance model WBMOD. The input data series of precipitation, air temperature and the observed reservoir outflows were used to express the expected changes of the total runoff and the required reservoir capacity. Failures in the required water demand in the volume and in the delivery time were evaluated for these changed climate conditions. Presented results, yielding from WBMOD simulations, indicate potential possibilities of the model utilization for reservoir operation. In general, it can be concluded, that the expected climatic change will influence the certainty of the water supply from the reservoirs. This conclusion, of course, pertains only the same water demand realized during the so far historical operation (1951–1980) of the structure.

Keywords— climate change scenario CCCM2000, monthly water balance model WBMOD, water reservoir Liptovska Mara; water supply reliability.

I. INTRODUCTION

IN this contribution we study future ability of northern Slovakia multipurpose water reservoir (WR) Liptovska Mara, to assure the required water demand as defined by downstream water users (hydropower producers, irrigation, industry).

Monthly water balance models were used for runoff forecasting, for proposal of systems and their operation in

This work was supported in part by the Slovak Research and Development Agency under the contract No. APVV-015-10 and results from the project implementation of the “Centre of excellence for integrated flood protection of land” (ITMS 26240120004) supported by the Research & Development Operational Programme funded by the ERDF.

D. Halmova is with Institute of Hydrology Slovak Academy of Sciences, Raciarska 75, 831 02 Bratislava, Slovakia, (e-mail: halmova@uh.savba.sk).

M. Melo is with FMPI Comenius University Bratislava, Mlynska dolina, 842 48 Bratislava, Slovakia (e-mail: marian.melo@fmph.uniba.sk)

P. Pekarova is with Institute of Hydrology Slovak Academy of Sciences, Raciarska 75, 831 02 Bratislava, Slovakia (phone: +4212 44259311, Fax: +4212 44259311, e-mail: pekarova@uh.savba.sk).

water management and for detection of climate change impact on water resources [1]-[5]. For the reservoirs (that operate with the huge volume of water to supply hydropower stations, irrigation systems or downstream nuclear power plants) water balance models with monthly time step, such as the WBMOD model, would be an appropriate tool for the solution of projects dealing with the water supply.

The most physically plausible method for estimation of the regional climate change scenarios is the utilization of climate models [6]. Impacts of climate change upon hydrological processes vary regionally and between climate scenarios, largely following projected changes in precipitation. Demand on water is generally increasing due to population growth and economic development, but it is falling in some countries because of increased efficiency of use. Climate change is unlikely to have a major effect on domestic and industrial water demand, but may substantially affect irrigation withdrawals depending on increase of the evaporation. Higher temperatures, hence higher crop evaporative demand, mean that the general tendency would be towards an increase in the irrigation demands. Water resource management techniques can be applied to adapt to hydrologic effects of the climate change, so as to lessen vulnerabilities [7].

II. WATER RESERVOIR LIPTOVSKA MARA

Water reservoirs Liptovska Mara (on the upper Vah River) and Orava (on the Orava tributary) are two key reservoirs controlling the flows of the Vah River downstream. River Vah is the largest left-side Danube River tributary and the second largest river in Slovakia. The map of Slovakia with the biggest water reservoirs (VN) and map of the WR Liptovska Mara catchment is on Fig. 1. Storage water capacities of WR Liptovska Mara [8] are specified in Table 1.

There are several important water users in the Vah basin: municipal, industrial, agricultural users, extensive hydropower system, and nuclear plants needing water for cooling, and possibly the river navigation transport in future.

Table 1 Water storage capacities of WR Liptovska Mara (according to Slovak civil engineers)

water storage capacity	WR Liptovska Mara [mil.m ³]
Total volume V_c	360.5
Permanent volume V_s	24.96
Retention volume V_r	14.5
Operating volume V_z	320.5

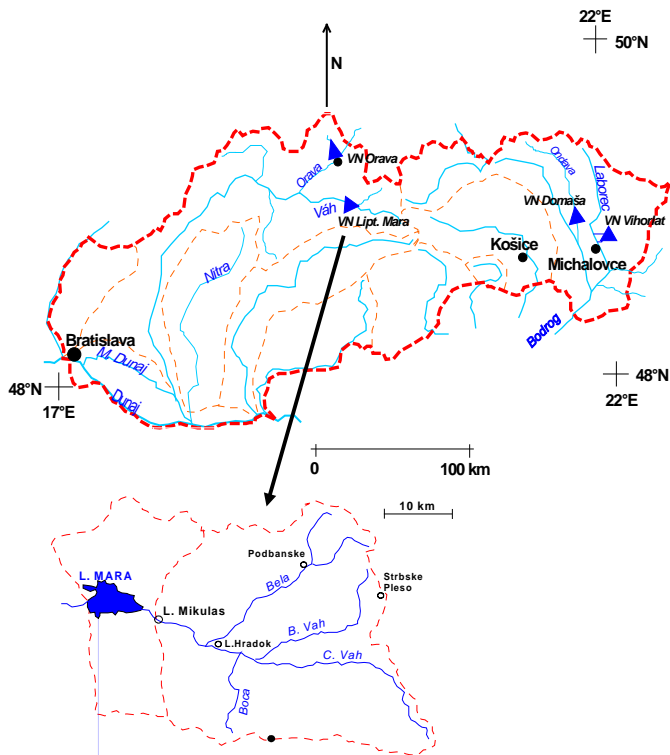


Fig. 1 Map of Slovakia with the biggest water reservoirs (VN) and map of the WR Liptovska Mara catchment

Water reservoirs in Slovakia were built to improve low discharges and further to serve for retention of flood peak discharges, as well as for recreation and sport purposes.

III. CLIMATE SCENARIOS FOR BASIN OF WR LIPTOVSKA MARA

The most important source of information about behavior of climatic system under changed conditions is the climate model. In this contribution we used data from the coupled general circulation model CCCM2000 (with IPCC "IS92a" forcing scenario). CCCM2000 is the second generation coupled global climate model of the Canadian Centre for Climate Modelling and Analysis in Victoria, B.C. Nowadays climate scenarios come out especially from the outcomes of climate models [9]-[11]. Monthly model values of some climatic variables from CCCM2000 in 1900–2100 have been made available.

Present horizontal resolution of the climate models (GCMs) does not allow to make out some regional climate features. Two principally different approaches have been applied for solution of this problem: statistical methods (statistical downscaling) and dynamical methods (dynamical downscaling). Statistical downscaling consists from development of statistical relationships between locally observed climate variables and outputs of global GCM experiments. Dynamical downscaling uses a detailed regional meteorological model nested into the global model system.

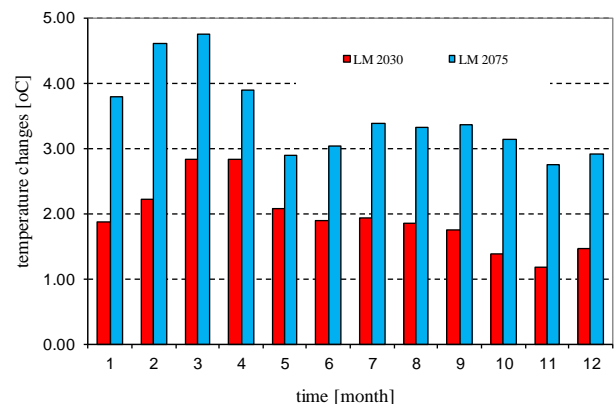
For the regional downscaling the CCCM2000 outputs we selected 4 gridpoints near to Slovakia: gridpoint 1 (southern part of Hungary) – 46.39° N; 18,75° E; 616 m a.s.l., gridpoint

2 (part of the Carpathians in Romania) – 46.39° N; 22.50° E; 554 m a.s.l., gridpoint 3 (southern part of Poland) – 50.10° N; 18.75° E; 531 m a.s.l., gridpoint 4 (south-eastern part of Poland) - 50,10° N; 22.50° E, 566 m a.s.l. It was the statistically based method which was applied in this contribution. As a first step, the interpolation from the GCM gridpoint data round Slovakia to the localities (meteorological stations) of the WR Liptovska Mara (the weights with respect to the distance from a concrete locality) was applied. We made these calculations for „reference“ time horizon 1951–1980, and for next time horizons 2030 (2016–2045) and 2075 (2061–2090). This normal period (1951–1980) was chosen as insignificantly influenced by climate change, because of the IPCC recommendation. Next we have elaborated the scenarios of the air temperature change and the precipitation change, between these periods in form of either differences (in case of air temperature) or quotients (in case of precipitation). We use mean monthly values of both climatic elements.

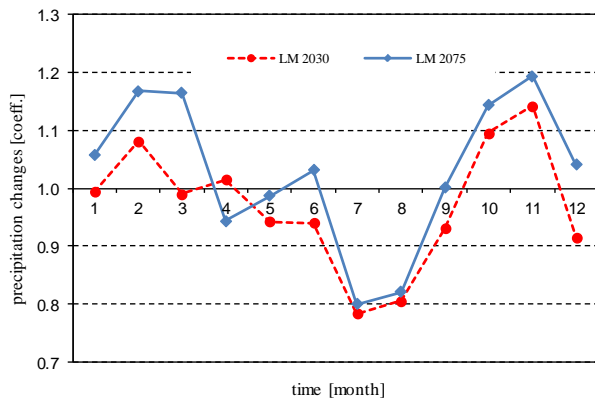
On the base of the Canadian model CCCM2000 output results we can state that temperature will continue to increase in northern Slovakia during the 21st century. The result shows that the air temperature will increase in all months of the year. Increase in annual air temperature means is about 1.9°C in 2016–2045, while in 2061–2090 it is about 3.5°C in comparison to the reference period 1951–1980. Projected precipitation scenarios for northern Slovakia in the 21st century show a decrease in the summer monthly totals (by about 20% in July and August in the period 2061–2090) and on the contrary an increase in the winter monthly totals (by about 20% in November in the period 2061–2090) in comparison to the reference period 1951–1980.

Air temperature and precipitation were modified in each month according to the last climate scenarios, which were calculated by model CCCM2000 and estimated for the Liptovska Mara reservoir catchment, for two time horizons 2030 and 2075, respectively, Fig. 2a, Fig. 2b.

Utilization of climate models is the most physically plausible method for preparation of the regional climate change scenarios [6], [12]. Effect of the climate change upon hydrological processes varies regionally and between climate scenarios, largely following projected changes in precipitation.



a)



b)
 Fig. 2 a) Mean monthly temperature changes in ($^{\circ}\text{C}$) and b) monthly coefficients of precipitation totals changes according to the climate scenario CCCM2000 in two time horizons 2030 and 2075

Demand for water is generally increasing due to population growth and economic development, but it is falling in some countries because of increased efficiency of use. Climate change is unlikely to have a big effect on water demands in general, but may substantially affect irrigation withdrawals, which depend on increase of the evaporation, which is offset or exaggerated by changes of precipitation.

Higher temperatures, hence higher crop evaporative demand, mean that the general tendency would be towards an increase in the irrigation demands. Water resource management techniques can be applied to adapt to hydrologic effects of the climate change, so as to lessen vulnerabilities.

IV. WATER BALANCE MODEL

The WBMOD model as well as other water balance models with monthly time step would be an appropriate tool for the solution of projects dealing with the water supply. Monthly water balance models were used for runoff forecasting, for proposal of systems and their operation in water management, for detection of climate change impact on water resources, etc. [13]-[14], [3], [4], [5].

A. Data

Model WBMOD uses average monthly data of basic water balance components, too. Precipitation is divided into snowfall (in the upper part of the catchment) and rainfall (in the lower part of it). Rainfall is accumulated in soil storage that is reduced by actual evapotranspiration, fast runoff of groundwater and slow runoff of groundwater. The WBMOD model is based on water balance model that was developed at V.U.B.–Vrije Universiteit Brussel-Hydrologie. The applied calculation technique “RESERVOIR”, that was developed by Halmova, balances reservoir overflows or deficits on the basis of the inflow and outflow from water reservoir, and determines required water volume for given inflow, in dependence on water demand characteristics. Input data for the model

WBMOD are:

- catchment area of the WR (km^2),
- average discharge in the gauging station Liptovsky Mikulas ($\text{m}^3 \cdot \text{s}^{-1}$) (Fig.3),
- monthly precipitation totals from selected meteorological stations (mm/month),
- monthly average air temperature from selected meteorological stations ($^{\circ}\text{C}$),
- information about WR: useful storage capacity of reservoir (mil. m^3), outflow from reservoir in monthly time step during the period 1951–1980 ($\text{m}^3 \cdot \text{s}^{-1}$). Chronological series of actual historical outflow from the reservoir was not available. In determining the average monthly outflow from the reservoir for 30-year service period, we relied on the chronological series of discharges in gauging stations under the reservoir (Besenova and Hubova).

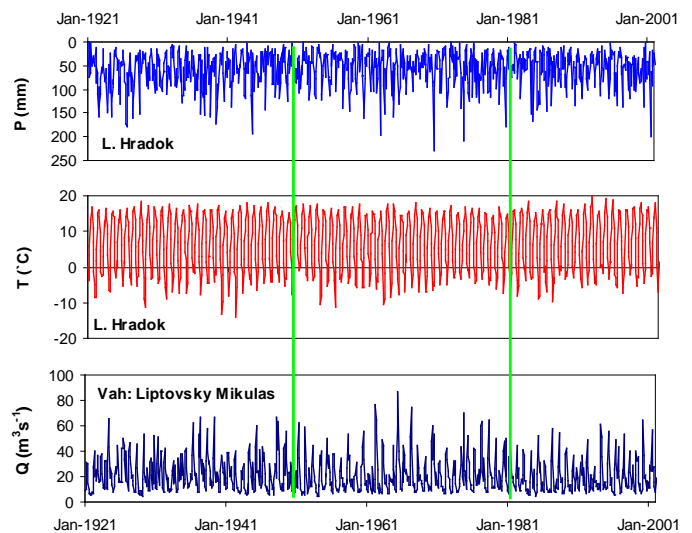


Fig. 3 Examples of the input monthly data to the water balance model WBMOD, P – precipitation, T – temperature, Q – discharge.

B. Model description

Precipitation p_t is divided into the snowfall g_t (in the upper part of the catchment) and rainfall v_t (in the lower part of the catchment). Snowfall is accumulating in storage k_t at the end of the calendar month “t”; storage h_t comes from this storage and contributes to total runoff q_t . Rainfall is accumulated in soil storage m_t at the end of the month “t” too. The storage m_t is reduced by actual evapotranspiration r_t , fast runoff of groundwater f_t and slow runoff of groundwater s_t (Fig. 4).

For the model calibration we used trial- and -error method. Some parameters of the model were changed, but their values had to vary between threshold values recommended by the model authors. In the next step, we tested the ability of water reservoir Liptovska Mara, to ensure the constant outflow of various sizes under the changed climate conditions,. Basically the relationship between the size of constant outflow, its certainty and the necessary storage volume was derived.

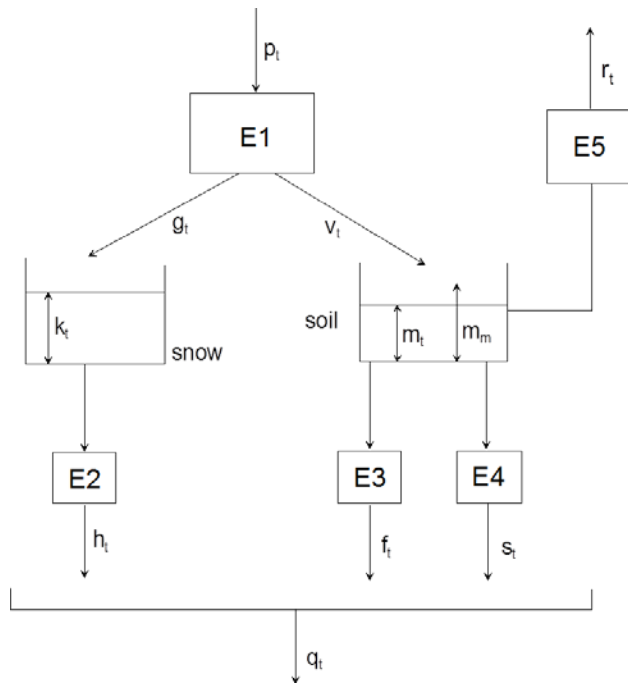


Fig. 4 Structure of the water balance model WBMOD

But the real reservoir operation differs considerably from the scheme oriented to constant outflow, which is typical for drinking water supply reservoir.

The operational rules of the reservoir indicate a considerable variability of the outflow from water reservoir. It was the main reason to test the ensuring of this real outflow (period 1951–1980) from reservoir under the changed climate conditions. Series of changed inflow to water reservoir (according to the climate scenarios), as well as the alternative changes of minimum operational reservoir water level (according to reservoir-storage-elevation curves, Fig. 5 – WR Liptovska Mara), were compared with the real chronological observed series, which represent the historical target.

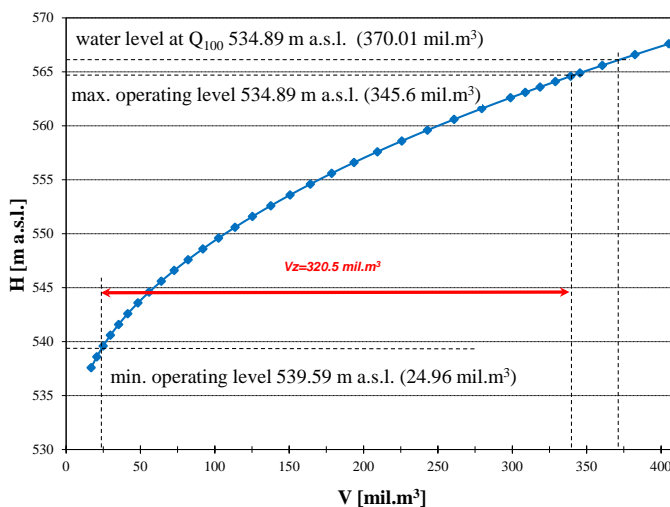


Fig. 5 Liptovska Mara reservoir-storage-elevation curve

Changes of individual alternatives compared with the mentioned target can be expressed by:

- time series of the not supplied water volume during the failures in the required water supply,
- time series of the failures (duration of a period with lower water supply than required),
- total reliability of the supplied water volume (during the period of 30-years) in (mm),
- total reliability of duration with no-failure operation (during the period of 30-years) in (days).

The reservoir inflow changes are introduced in one runoff scenario (according to climate scenario CCCM), and for two time horizons (2030 and 2075). Outputs from the WBMOD model are denoted as “CX” (C means CCCM; A, B, C – alternative model run). Several alternatives of the model runs were executed, for several initial conditions of the reservoir water levels. Only that water storage was used, which behaves between the minimum and maximum operating water level. Initial and boundary conditions (Fig. 5) are quantified in mil.m^3 above the minimum operating level and above the dead storage capacity.

V. RESULTS AND CONCLUSIONS

Calculated reliability represents proportion of water supply in volume (or in duration of non-failure operation), during the 30-years period, under the changed climate conditions, to the real water supply in volume (or in duration of non-failure operation), during the historical period 1951–1980. Calculated reliability of reservoir ability to secure a given water supply (= real water withdrawals from reservoirs during 1951–1980) in volume (water storage) (ZZS) and in duration of non-failure operation (ZZT), for particular alternatives, is listed in Fig. 6 and Fig. 7. Alternatives of the model runs differ also in the minimum accepted summer water level (STMIL). Minimum summer water level limit can be connected with higher risk in supply of the given water volume. From the relationship between reliability of the water supply and minimum summer operating water level it is obvious that there exists the threshold summer water level. Till the summer water level wouldn't rise above this threshold level, reliability of the water supply from water reservoirs wouldn't be considerably reduced.

For the WR Liptovska Mara, total required water supply, during the historical period of 30 years (ZTT= 10950 days) was 20860.4 mm (ZST). In the case of the CA model run and time horizon 2030, total failure in water supply (ZS) is 4716.6 mm and time period with non-ensured water supply (ZT) is 4977 days, Fig. 6. Reliability of the given water supply in the volume (ZZS) is 77.4% $[(20860.4-4716.6)/20860.4=0.774]$, and in duration of non-failure operation (ZZT) is 54.5%, $[(10950-4977)/10950=0.545]$, Fig. 7.

Even the most optimistic calculation alternatives, when the whole reservoir storage (volume between min. and max. operating level) is available for the reservoir management, show considerable decrease of reliability of water supply in

terms of volume and in terms of duration of the non-failure operation after application of scenario CCCM2000. For a time horizon of 2030 reliability of given water supply in volume is less than 85% and reliability in duration of non-failure operation reaches 67.1%; for time horizon 2075 the values are 83.2% and 67.7%, respectively.

At least optimistic calculation alternatives “CA”, where the minimum summer, winter and minimum initial water level in the reservoir reaches maximum values and must be provided, reliability of given water supply decreases to 77.4% (Horizon 2030) and 74.5% (Horizon 2075) in the volume and to 54.5% (in 2030) and 56.0% (2075) in duration of non-failure operation, respectively. Reliability of non-failure operation (ZZT) at alternatives “CD” reaches the highest value, 72.1% and 69.6%. It is obvious that even higher levels of water supply reliability can be achieved by water reservoir management.

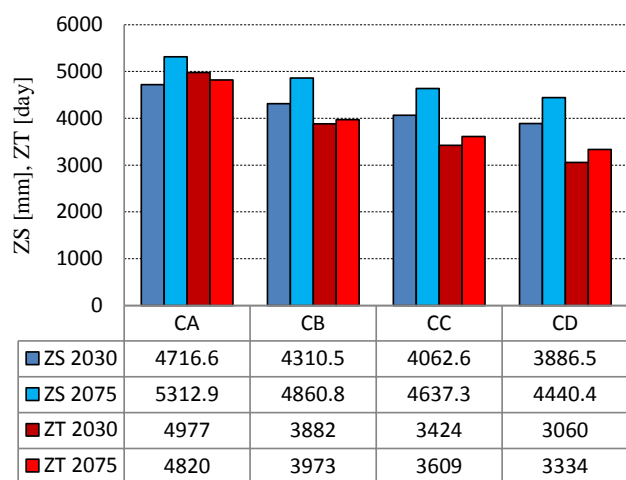


Fig. 6 Total failure in the water supply volume ZS (mm) and total period with the non-ensured water supply ZT (day) during 30-years of simulation.

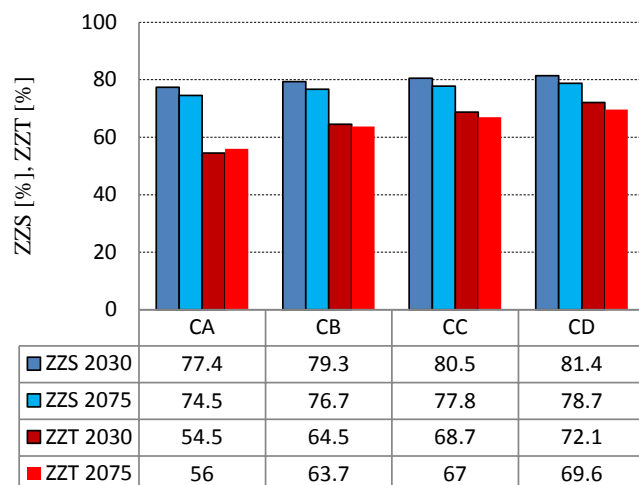


Fig. 7 Reliability of given water supply in the volume (ZZS) and in duration of the non-failure operation (ZZT) for time horizons 2030 and 2075 in %.

Presented conclusions, which result from WBMOD simulations, indicate potential possibility to use the model for reservoir operation, for particular analysis of reservoir utilization for recreation, and development of models for seasonal runoff forecasts. It can be concluded, that in this particular case of the WR Liptovska Mara, the expected climate change scenarios would influence reliability of water supply from the reservoir in a similar way. The developed tool can be of use for alternative hypothetical reservoir operation runs with various variants of the water supply regime defined as a time series, and also for case studies for other similar water reservoirs.

REFERENCES

- [1] P. H. Gleick, “Methods for evaluating the regional hydrologic impacts of global climatic changes,” *J. Hydrol.* 88, 1986, 97–116.
- [2] K. Nachazel, E. Prenosilova, and M. Toman, “Uncertainty of climate changes and their impact on water resources,” (Neurčitost klimatických zmien a jejich dopadů na vodní zdroje). *J. Hydrol. Hydromech.* 43(3), 1995, 173–196.
- [3] J. C. Shaake and C. Liu, “Development and applications of simple water balance models to understand the relationship between climate and water resources,” *New Directions for Surface Water Modelling, IAHS Publ.*, 181, 1989, 343–352.
- [4] G. L. Vandewiele, C. Y. Xu, and NI-LAR-WIN, “Methodology and comparative study of monthly water balance models in Belgium, China and Burma,” *J. Hydrol.*, 134, 1992, 315–347.
- [5] C. Y. Xu, “Modelling the effects of climate change on water resources in Central Sweden,” *Water Resour. Management*, 14, 2000, 177–189.
- [6] M. Lapin and M. Melo, “Methods of climate change scenarios projection in Slovakia and selected results,” *J. Hydrol. Hydromech.*, 52, 4, 2004, 224–238.
- [7] IPCC, *Climate Change, The Scientific Basis*, Contribution of Working Group I to the Third Assessment Report of the Intergovernmental Panel on Climate Change (IPCC). Cambridge Univ. Press, UK, 2001, 944 pp.
- [8] D. Abaffy, M. Lukac, and M. Liska, *Dams in Slovakia*, T.R.T. Medium Bratislava, Slovakia. ISBN 80-88676-03-7, 1995, 103 pp.
- [9] G. M. Flato and G.J. Boer, “Warming asymmetry in climate change simulations,” *Geophysical Research Letters*, 28, 1, 2001, 195–198.
- [10] M. Lapin and M. Melo, “Climate Changes and Variability, Climate Change Scenarios,” (Klimatické zmeny a variabilita klímy, klimatické scenáre) *Životné Prostredie*, 34, 2, 2000, 407–412.
- [11] M. Melo, M. Lapin, and I. Damborska, “Methods for the design of climate change scenario in Slovakia for the 21st century,” *Bulletin of Geography – physical geography series*, 1, 1, 2009, 77–90.
- [12] D. Halmova and M. Melo, “Climate change impact on reservoir water supply reliability,” *IAHS-AISH Publication*, Wallingford, ISSN 0144-7815, 308, 2006, 407–412.
- [13] D. Halmova, “Conflicts between the reservoir water demand and climate changed inflow in case of different Slovak water reservoirs,” Ed. Mari Heinonen, *Proc. of the third International Conference on Climate and Water*, Helsinki, Finnish Environment Institute SYKE, ISBN 978-952-11-2790-8, 2007, 152–157.
- [14] D. Halmova, “Impact of climate change on water supply in northern Slovakia,” *IAHS-AISH Publication*, 340, ISSN 0144-7815, 2010, 236–243.

Backstepping Control Based Three Phase Shunt Active Power Filter

I Ghadbane ,
Laboratory L.G.E.B.

Department of Electrical Engineering, BLida University

E-mail : ghadbanetech@gmail.com

M.T. Benchouia,
Laboratory L.G.E.B.

Department of Electrical Engineering, Biskra University
BP. 145, 07000 Biskra, ALGERIA

E-mail : benchouiat@yahoo.fr

Abstract – This paper presents a simulation study of Backstepping Controller of the DC bus voltage of three phase shunt Active Power Filter (APF). The Backstepping controller is introduced to improve tracking performance characteristics, power quality and minimized consumption of the reactive power. The algorithm used to identify the reference currents is based on the Self Tuning Filter (STF) for application of The method of instantaneous active and reactive power

Keywords – Harmonics, shunt active filter, Backstepping, total harmonic distortion

I. INTRODUCTION

Power electronics devices have been widely used in recent years; while they are convenient in use they cause several power pollutions just like electrical harmonics and low power factor. In high power systems, most electrical devices use three-phase symmetrical power system. But in medium and small power system, single-phase electronic equipments are widely used in domestic, educational and commercial appliances, such as computers, communication equipments and electronic lighting ballasts, etc. These equipments normally have a diode rectifier to convert ac electricity to dc and filter by a huge capacitor.. These equipments behave like nonlinear loads, generating harmonics and cause electromagnetic compatibility problems. For the devices with an alternative input such as: rectifiers, Ac voltage controllers, indirect frequency converters..., the wave shape of the absorptive current of the network is non-sinusoidal. In addition to the fundamental component, this waveform presents harmonic contents which are, in certain cases, very important. These harmonics are propagated from the load towards the network and generate harmonic voltage drops which are added to the fundamental component of the voltage delivered by the network. The result is a form of affected wave, which contains also of harmonic contents; this affected wave can, as mentioned before, cause serious problems of electromagnetic compatibility. Many solutions have been studied in the literature to mitigate the harmonic problems, such as filtering (passive, active, and hybrid) with various topologies (shunt, series or both) [6] Industrial and domestic equipments actually use a large variety of power electronic circuits such as switch mode power converters, adjustable speed drives, rectifiers and dimmers. These ones lead to significant energy savings and productivity benefits. But unfortunately, they also present non-linear impedance to the supply network and therefore generate non-sinusoidal

currents. The outcome of these wide-band current harmonics includes substantially higher losses for the transformers and the power lines, possible over voltages and overheating destroying equipments and disturbances of communication equipments and precision instruments [1]. So, it is necessary to develop techniques to reduce all the harmonics as it is recommended in the IEEE 519-1992. The first approach consists in the design of LC filters. But, passive filters are not well adapted as they do not take into account the time variation of the loads and the network [1], [2]. They can also lead to resonance phenomena. The active power filter (APF) can solve the problems of harmonic and reactive power simultaneously. The theories and applications of active power filters have become more popular and have attracted great attention since two decades ago. Since its introduction some twenty years ago, the Active Power Filter APF presents a good solution for disturbance treatment, particularly for harmonic currents and/or voltages. APF is an up-to-date solution to power quality problems. The shunt APF allows the compensation of current harmonics and unbalance, together with the power factor correction, and can be a much better solution than the conventional approach (capacitors and passive filters)

The performance of the APF is determined by the kind of control used. It is more emphasized when the voltages of electrical network contain harmonics and/or are unbalanced. The identification approach is based on the Phase Locked Loop (PLL), which is not sensitive to the disturbances, specifically to the harmonic and unbalanced voltage [10]. Moreover, the Self Tuning Filter STF is proposed for extracting harmonic currents instead of classical harmonics extraction based on High Pass or Low Pass Filters [4], [5]. The three phase currents/voltages are detected using current/voltage sensors. The inverter currents are controlled by using hysteresis comparators.. The hysteresis control is characterized by its simplicity and its intrinsic speed.. [1][3][7]

II. Shunt Active filter structure

Fig.1 presents the schematic diagram of the three-phase active power filter and the associated control strategy for harmonic mitigation

The power part is composed of an inverter, a filter of coupling R_f L_f and a capacitive element used as source of energy for APF. This element must provide a voltage of quasi-constant value. The fluctuation of this voltage must be weak. The other part is used for commutation control of

the Semiconductor elements of the inverter in power part. By means of control strategies well adapted, it is possible to generate harmonic signals in the output of the inverter, which are used to compensate those present in the distribution network.

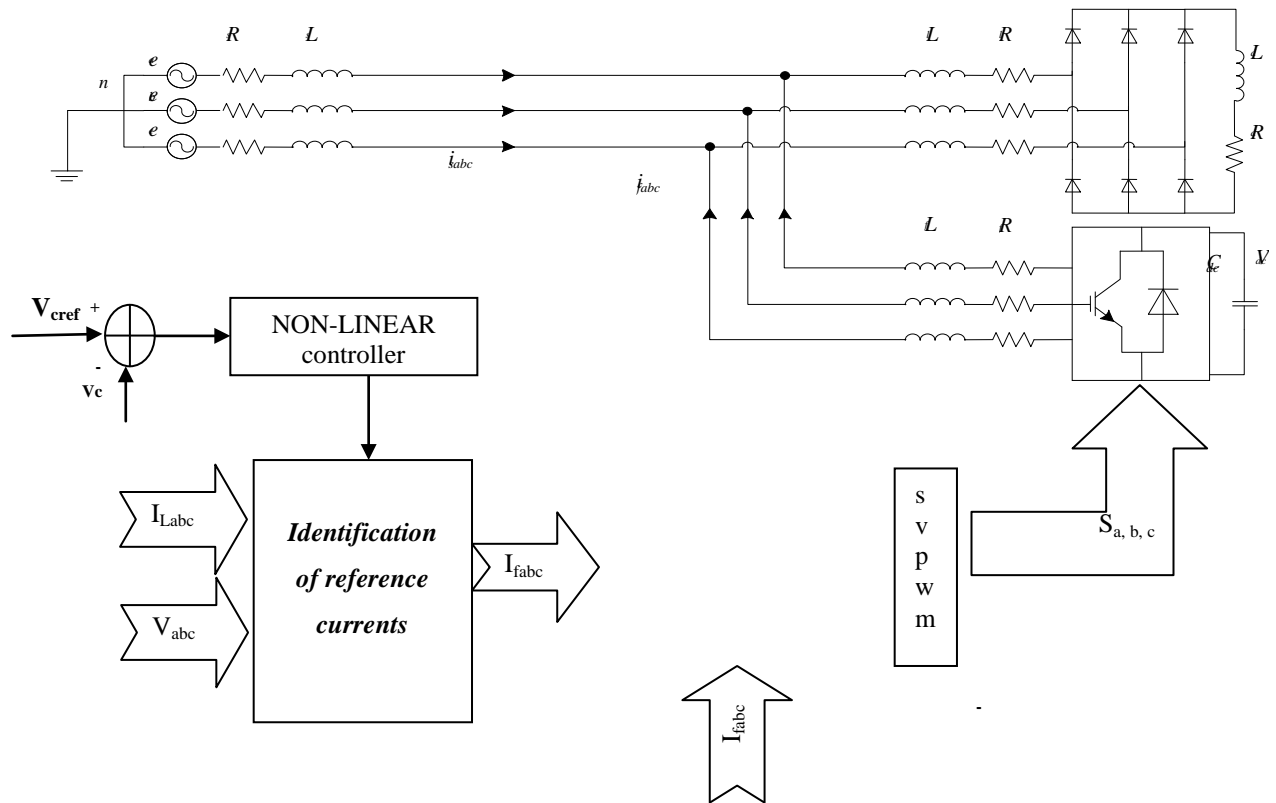


Fig.1 -Network and shunt active filter presentation

III-Harmonic Isolation

Akagi [1] proposed a theory based on instantaneous values in three-phase power systems with or without neutral wire, and is valid for steady-state or transitory operations, as well as for generic voltage and current waveforms called as Instantaneous Power Theory or Active- Reactive (p-q) theory which consists of an algebraic transformation (Clarke transformation) of the three-phase voltages in the a-b-c coordinates to the α - β coordinates, followed by the calculation of the p-q theory instantaneous power components by eliminating the DC component of the instantaneous active power (corresponding to the fundamental component of load current) using a selective Filter STF, so the harmonic components can be identified. Figure 3 shows the modified scheme for the identification of reference currents during simultaneous compensation of harmonic currents and reactive power using the method of instantaneous power by using STF

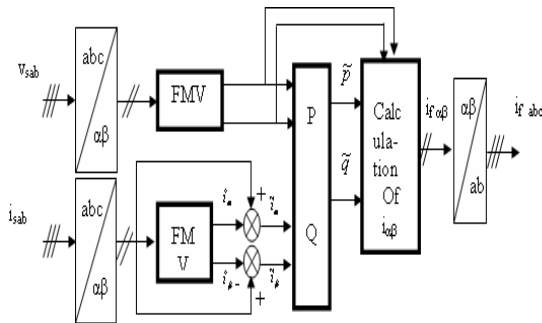


Fig. 2: The method of instantaneous active and reactive power

This method is based on measuring the instantaneous three-phase variables present on the grid with or without zero-sequence components. This method is valid both in steady-state phase. In this control algorithm (Figure 2), measurements of voltages and currents expressed as a three phase (abc) are converted to two-phase system (α - β) is equivalent to using the transform from Concordia leaving the power invariant:

$$\begin{bmatrix} v_\alpha \\ v_\beta \end{bmatrix} = \frac{\sqrt{2}}{\sqrt{3}} \begin{bmatrix} 1 & -1/2 & -1/2 \\ 0 & \sqrt{3}/2 & -\sqrt{3}/2 \end{bmatrix} \begin{bmatrix} v_{sa} \\ v_{sb} \\ v_{sc} \end{bmatrix} \quad (1)$$

$$\begin{bmatrix} i_\alpha \\ i_\beta \end{bmatrix} = \frac{\sqrt{2}}{\sqrt{3}} \begin{bmatrix} 1 & -1/2 & -1/2 \\ 0 & \sqrt{3}/2 & -\sqrt{3}/2 \end{bmatrix} \begin{bmatrix} i_{La} \\ i_{Lb} \\ i_{Lc} \end{bmatrix} \quad (2)$$

In the presence of harmonics, the power is composed of three parts: active (P), reactive (Q) and deformed (D) as shown by the following equation:

$$S = \sqrt{P^2 + Q^2 + D^2} \quad (3)$$

The instantaneous active power, denoted P (t) is defined by the following equation:

$$P(t) = v_{sa}i_{sa} + v_{sb}i_{sb} + v_{sc}i_{sc} \quad (4)$$

Can be written in the stationary reference:

$$P(t) = v_{s\alpha}i_{s\alpha} + v_{s\beta}i_{s\beta} \quad (5)$$

Similarly the instantaneous imaginary power can be written as follows:

$$q(t) = -\frac{1}{\sqrt{3}} [(v_{sa} - v_{sb})i_{lc} + (v_{sb} - v_{sc})i_{la} + (v_{sc} - v_{sa})i_{lb}] = v_{sa}i_{l\beta} - v_{s\beta}i_{l\alpha} \quad (6)$$

Q power a broader meaning than the usual reactive power. In fact, Unlike the reactive power, which considers only the fundamental frequency, the imaginary power takes into account all the harmonic components of current and voltage is why it is given a different name (imaginary power) as a unit with the volt-ampere imaginary (VAI).

The part of the relations (5) and (6), we can establish the following matrix:

$$\begin{bmatrix} P \\ q \end{bmatrix} = \begin{bmatrix} v_{S\alpha} & v_{s\beta} \\ -v_{s\beta} & v_{S\alpha} \end{bmatrix} \begin{bmatrix} i_\alpha \\ i_\beta \end{bmatrix} \quad (7)$$

in the general case, each of the powers p and q has a continuous part and part alternative, which allows us to write the following expression

$$\begin{cases} P = \bar{P} + \tilde{P} \\ q = \bar{q} + \tilde{q} \end{cases} \quad (8)$$

with: \bar{P} Continuous power related to the fundamental component of active power and voltage, \bar{q} Continuous power related to the fundamental component of reactive current and tension, \tilde{p} and \tilde{q} Powers of alternatives related to the sum of the components of disruptive current and voltage.

By inverting the relation (7), we can recalculate the

currents in the coordinate $\alpha \beta$ as shown in Equation

$$\begin{bmatrix} i_\alpha \\ i_\beta \end{bmatrix} = \frac{1}{v_{s\alpha}^2 + v_{s\beta}^2} \begin{bmatrix} v_{s\alpha} & -v_{s\beta} \\ v_{s\beta} & v_{s\alpha} \end{bmatrix} \begin{bmatrix} p \\ q \end{bmatrix} \quad (9)$$

Considering equations (8) and (9), we can separate the current benchmark in the three components, active and reactive at the fundamental frequency and harmonics. This leads to:

Finally, it is easy to obtain the reference currents along the axes abc by the inverse transformation of Concordia

$$\begin{bmatrix} i_\alpha^* \\ i_\beta^* \end{bmatrix} = \frac{1}{v_\alpha^2 + v_\beta^2} \begin{bmatrix} v_\alpha & -v_\beta \\ v_\beta & v_\alpha \end{bmatrix} \begin{bmatrix} \tilde{p} \\ \tilde{q} \end{bmatrix} \quad (10)$$

$$\begin{bmatrix} i_a^* \\ i_b^* \\ i_c^* \end{bmatrix} = \sqrt{\frac{2}{3}} \begin{bmatrix} 1 & 0 \\ -1 & \sqrt{3} \\ 2 & 2 \\ -1 & -\sqrt{3} \\ 2 & 2 \end{bmatrix} \begin{bmatrix} i_\alpha^* \\ i_\beta^* \end{bmatrix} \quad (11)$$

The self tuning filter is the most important part of this control which allows to make insensible the PLL to the disturbances and filtering correctly the currents in $\alpha\beta$ axis. Hong-sok Song [6] had presented in his PhD work how recovered the equivalent transfer function of the integration expressed by The block diagram of the STF tuned at the pulsation ω_c is shown in the figure 5. The transfer function of this filter is:

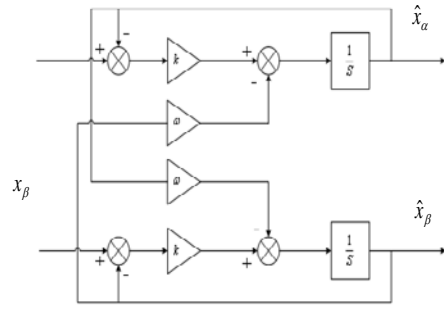
$$H(s) = \frac{\hat{i}_{\alpha\beta}(s)}{i_{\alpha\beta}(s)} = K \frac{(s+K) + j\omega_c}{(s+K)^2 + \omega_c^2} \quad (12)$$

According to the $\alpha\beta$ axes, the expressions linking the components FMV output $\hat{x}_{\alpha\beta}$ to input $x_{\alpha\beta}$ components are:

$$\hat{x}_\alpha = \left(\frac{K}{s} [x_\alpha(s) - \hat{x}_\alpha(s)] - \frac{\omega_c}{s} \hat{x}_\beta(s) \right) \quad (13)$$

$$\hat{x}_\beta = \left(\frac{K}{s} [x_\beta(s) - \hat{x}_\beta(s)] - \frac{\omega_c}{s} \hat{x}_\alpha(s) \right)$$

We obtain the following block diagram for STF:



IV. NON-LINEAR CONTROLLER SYNTHESIS

The dynamic equations of the active filter in the stationary reference are given by:

$$\begin{cases} \frac{dV_{dc}}{dt} = \frac{P_{dc}^*}{C_{dc} V_{dc}} \\ \frac{di_{fa}}{dt} = -\frac{R_f}{L_f} i_{fa} + \frac{V_{fa} - V_{s\alpha}}{L_f} \\ \frac{di_{f\beta}}{dt} = -\frac{R_f}{L_f} i_{f\beta} + \frac{V_{f\beta} - V_{s\beta}}{L_f} \end{cases} \quad (13)$$

In this control strategy, we have three outputs to regulate.

I- subsystem 1

The equation describing this subsystem is :

$$\frac{dV_{dc}}{dt} = \frac{P_{dc}^*}{C_{dc} V_{dc}} \quad (14)$$

The first sub-system of order 1, is characterized by its

state , $x = V_{dc}$ and its control : $u = P_{dc}^*$ We can write

the equation as follows:

$$\dot{x} = f(x) + g(x)u \quad (15)$$

$$f(x) = 0 \quad \text{and} \quad g(x) = \frac{1}{C_{dc} V_{dc}}$$

II-Subsystem 2:

The equation describing this subsystem is:

$$\begin{cases} \frac{di_{fa}}{dt} = -\frac{R_f}{L_f} i_{fa} + \frac{V_{fa} - V_{s\alpha}}{L_f} \\ \frac{di_{f\beta}}{dt} = -\frac{R_f}{L_f} i_{f\beta} + \frac{V_{f\beta} - V_{s\beta}}{L_f} \end{cases} \quad (16)$$

The second sub-system of order 2, is characterized by

its vector state $x = [i_{f\alpha} \ i_{f\beta}]^t$ and vector control is

$u = [v_{f\alpha}^* \ v_{f\beta}^*]^t$ We can write the system of equations

(III.47) under the form:

$$\dot{x} = f(x) + g(x)u$$

When

$$f(x) = \begin{bmatrix} f_1(x) \\ f_2(x) \end{bmatrix} = \begin{bmatrix} -\frac{R_f}{L_f}i_{f\alpha} - \frac{1}{L_f}v_{s\alpha} \\ -\frac{R_f}{L_f}i_{f\beta} - \frac{1}{L_f}v_{s\beta} \end{bmatrix} \text{ and } g(x) = \begin{bmatrix} \frac{1}{L_f} & 0 \\ 0 & \frac{1}{L_f} \end{bmatrix}$$

Now we will apply the state feedback control on models (III.46) and (III.48)

DC voltage controller synthesis

The voltage regulation V_{dc} is provided by the subsystem1. To achieve this object requires we must choose $y=V_{dc}$ as output, then, we seek its relative degree.

$$y = V_{dc} = h(x)$$

$$\nabla h = \frac{\partial h}{\partial x} = \frac{\partial V_{dc}}{\partial V_{dc}} = 1 \tag{18}$$

Its derivative is given by :

$$\dot{y} = \frac{\partial h}{\partial x} \dot{X} = \frac{\partial h}{\partial X} = (f(x) + g(x)u) \tag{19}$$

And as Lie derivatives, we write:

$$\dot{y} = L_f h(X) + L_g h(X)u$$

With :

$$L_f h(X) = 0 \quad , \quad L_g h(X) = \frac{1}{C_{dc} V_{dc}}$$

it follows that:

$$\dot{y} = \frac{1}{C_{dc} V_{dc}} P_{dc}^*$$

$$P_{dc}^* = \frac{1}{L_g h(x)} (-L_f h(x) + v) = C_{dc} V_{dc} v$$

$$v = k_v (V_{dc}^* - V_{dc}) + \frac{d}{dt} V_{dc}^*$$

$$v = k_v (V_{dc}^* - V_{dc})$$

Non-linear current regulator

From the second subsystem, we will construct the command that regulates the currents of the active filter. In the case of the direct control of the active filter without compensation reactive energy. These currents represent the harmonic components of currents pollution

load \tilde{i}_{Ld} and \tilde{i}_{Lq} in the case of direct control with compensation for reactive power, the quadrature component of the active filter reference represents the entire quadrature current (reagent) of the pollution load

$$i_q^* = \tilde{i}_{Lq}$$

Now we will follow the same steps of constructing a non-linear regulator to design a controller active filter current

1st Output :

$$y_1 = h_1(X) \Rightarrow \nabla h_1 = [1 \ 0]$$

Its derivative is:

$$y_1 = f_1(x) + \frac{1}{L_f} V_{fd}^*$$

$$\begin{bmatrix} V_{fd}^* \\ V_{fq}^* \end{bmatrix} = g^{-1}(x) \left[-f(x) + \begin{bmatrix} V_1 \\ V_2 \end{bmatrix} \right]$$

$$\begin{bmatrix} \dot{y}_1 \\ \dot{y}_2 \end{bmatrix} = [V_1 \ V_2]^t$$

$$\begin{cases} V_1 = K_1(i_{fd}^* - i_{fd}) + \frac{d}{dt}i_{fd}^* \\ V_2 = K_2(i_{fq}^* - i_{fq}) + \frac{d}{dt}i_{fq}^* \end{cases}$$

$$v_{fd}^* = L_f \left[\frac{R_f}{L_f} i_{fd} + \omega i_{fq} + \frac{v_{sd}}{L_f} + K_1(i_{fd}^* - i_{fd}) + \frac{d}{dt}i_{fd}^* \right]$$

$$v_{fq}^* = L_f \left[\frac{R_f}{L_f} i_{fq} + \omega i_{fd} + \frac{v_{sq}}{L_f} + K_2(i_{fq}^* - i_{fq}) + \frac{d}{dt}i_{fq}^* \right]$$

III. Control strategy

The control signals needed in semiconductors commutation are carried out from the technique of hysteresis band current control, which is the most suitable for all the applications of current controlled voltage source inverter in active power filters. This method has the advantages of good stability, fast response time and good precision. Fig.3 shows the principle of the hysteresis band current controller for three phase system. The hysteresis band current controller decides the switching pattern of APF. Each violation of this band gives an order of commutation.

This control system is also characterized by a variable frequency of commutation. The hysteresis techniques have also a few undesirable features such as uneven switching frequency that causes acoustic noise and difficulty in designing input filter [1].

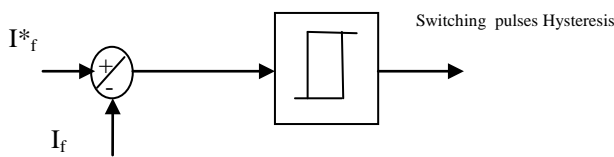


Fig.4 - Hysteresis band current controller

IV . Simulation results and discussions

Some simulation results using model in Matlab-Simulink and SimPower System Blockset are presented. The harmonic current and reactive power compensated by APF implemented in three- phase power systems with the utility power supply voltage of 100V and current source three- phase diode-bridge rectifier with R-L loads as the current compensation object. The design specifications and the circuit parameters used in the simulation are parameters are used for simulation:

$V_s = 50$ V (rms), $R_s = 0.1 \Omega$, $L_s = 0.566$ mH, $R_c = 0.01 \Omega$, $L_c = 1$ mH, $R_{d1} = 26.25 \Omega$ and $R_{d2} = 17 \Omega$, $L_d = 1$ mH, $V_{dr} = 140$ V, $C = 1100 \mu\text{F}$, HB (hysteresis band) = 0.1

To study the performance of the APF, first simulation is done on fixed load (R_L & L_L) and the filter is switched on at 0.12s.

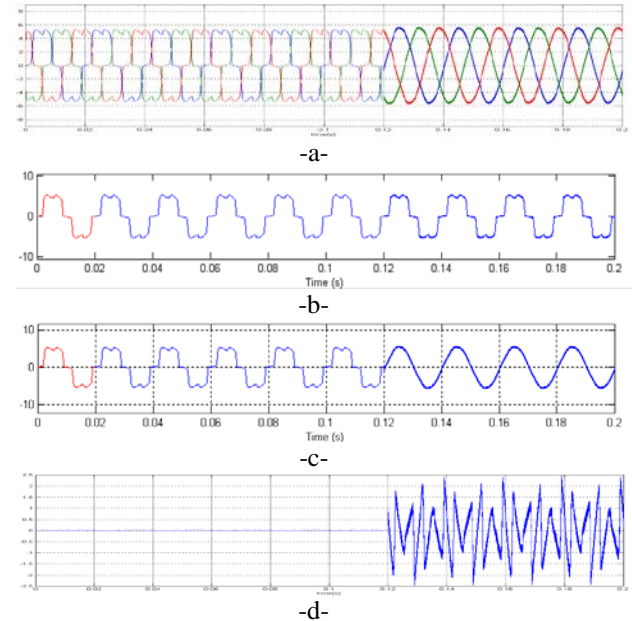


Fig 5 Three phase main current (b) load current; (c) Mains current; (d) compensating current waveform

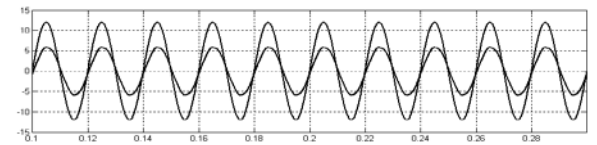


Fig 6. Power factor correction after applying Backstepping APF.

We see that before the connection of the APF, the mains current has a same waveform of the load current. At 0.12s, the APF is connected. mains current will be sinusoidal and exactly in phase with source voltage.

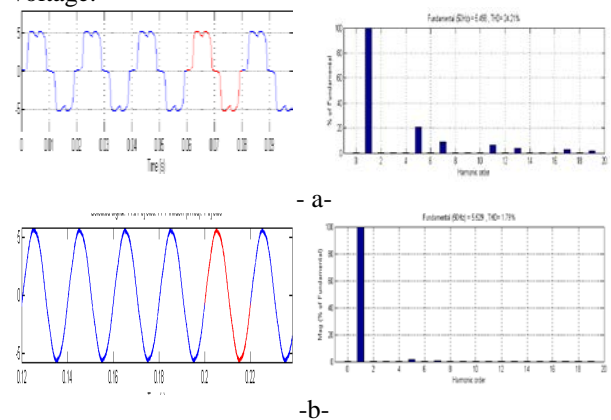


Fig 7 -Mains current waveform and its spectrum, (a) before filtering, (b) after filtering.

Still in Fig.7 a-b; a spectrum analysis shows that I_s current which contained harmonics and a $THD_i = 24.67\%$, will have one spectre at fundamental

frequency, all harmonics disappear and the $THD_i = 1.79\%$.

To observe the regulating process in backstepping control method in transient condition and the dynamics of the proposed APF, the DC side resistance is changed from Rd1 to Rd2 at 0.2s. It is clear from simulation results in Fig.8 that we obtain good transient performance of the source current, DC side capacitor voltage for the backstepping controller and the mains current maintains its sinusoidal waveform.

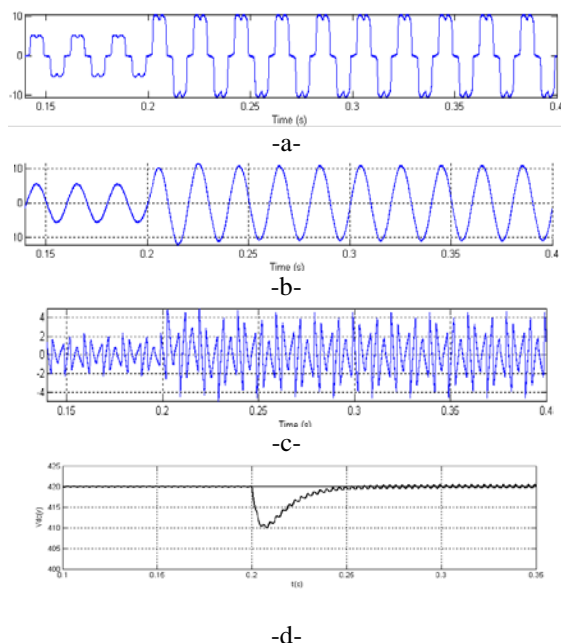


Fig 8 .Load perturbation response of Backstepping controlled shunt APF. (a) load current; (b) Mains current; (c) compensating current waveform (d) dc voltage

VI.Conclusion

In this work, we have shown the effectiveness of the shunt active power filtering especially with the application of backstepping control and with the application of The method of instantaneous active and reactive power The THD of the source current and source voltage after compensation is well below 5%, the harmonics limit imposed by the IEEE-519 standard. Further studies will examine the opportunity of implementing a high frequency output filter with the three- phase inverter. and the power factor was corrected (power supply voltage and current became in phase).

REFERENCES

[1] S.Beaulieu, M. Ouhrouche " real-time modelling and simulation of an active power filter " IASTED International Conference on Power and Energy Systems PES 2007, Clearwater, Florida, U.S.A.
 [2] Mohamed Abdusalam, Philippe Poure and Shahrokh Saadate "Control of Hybrid Active Filter Without Phase Locked Loop in the Feedback and Feedforward Loops" ISIE, IEEE International Symposium on Industrial Electronics, Cambridge, UK, (2008).

[3] Soumia Kerrouche, Fateh Krim "Three -phase Active Power Filter Based on Fuzzy Logic Controller "IJ-STA, Volume 3, N° 1, July 2009, pp. 942-955.
 [4] Hocine Benalla and Hind Djeghloud "Shunt Active Filter Controlled by Fuzzy Logic" J. King Saud Univ., Vol. 18, Eng. Sci. (2), pp. 231-247, Riyadh (1426H/2005)
 [5] C.Sharmeela, M.R.Mohan "Fuzzy Logic Controller Based Three-phase Shunt Active Filter for Line Harmonics Reduction" Journal of Computer Science 3 (2): 76-80, 2007 ISSN 1549-3636
 [6] Mohamed Abdusalam, Philippe Poure and Shahrokh Saadate "Control of Hybrid Active Filter Without Phase Locked Loop in the Feedback et Feedforward Loops"
 [7] Abdelmadjid Chaoui , Jean-Paul Gaubert Fateh Krim , Laurent Rambault "IP Controlled Three-Phase Shunt Active Power Filter for Power Improvement Quality " 1-4244-0136-4/06/ 2006 IEEE.
 [8] Wenjin Dai , Baofu Wang , Youhui Xie " A Novel Fuzzy Logic Controller fro Active power Filter " CIMSA 2009 – International Conference computational intelligence for measurement systems and Applications .
 [9] ANNA witkowska,Mirosław tomera, roman smierczalski " a backstepping approach ship course control " Int J.Appl. Math comput Sci ., 2007, Vol. 17 No 1,73-85 .
 [10] R.R. Joshi, R.A. Gupta and A.K. Wadhvani " adaptive backstepping controller design and implementation for a matrix converter-based im drive system"Journal of Theoretical and Applied Information Technology2007
 [11] K. Hasan, and K. Osman, "Globally Stable Control of Three-Phase Three Wire Shunt Active Power Filters," Elec. Eng., vol. 89, no.5, 2007, pp. 411-418.
 [12] A. Allag, M. Y. Hammoudi, S. M. Mimoune, S. " Adaptive backstepping voltage controller design for an PWM AC-DC converter"international journal of electrical and power engineering 1 (1): 62-69, 2007
 [13] Samir Bouabdallah, and Roland Siegart, "Backstepping and sliding mode techniques applied to an indoor micro quadrotor," Proceeding of IEEE Inter. Con. Rob. Aut, Spain, April 2005, pp. 2259-2264.
 [14] K. Hasan, and K. Osman, "Globally Stable Control of Three-Phase Three Wire Shunt Active Power Filters," Elec. Eng., vol. 89, no. 5, 2007, pp. 411-418
 [15] Helder J. Azevedo, José M. Ferreira, António P. Martins, and Adriano S. Carvalho "Direct current control of an active power filter for harmonic elimination, power factor correction and load unbalancing compensation," Proceedings of the 10th European Conference on Power Electronics and Applications, EPE'03,Toulouse, 2003, pp. 1-10.
 [16] D. Casadi, U. Reggiani, and G. Grandi, "Active power filters based on a single current measurement system," System Proceedings Symposium on Power Electronics, Electrical Drives Advanced Machines Power Quality (SPEEDAM'98), Italy, June 3-5, 1998.
 [17] K. H. Yiauw, and M. S. Khanniche, "A novel three-phase active power filter," Rev. Energ. Ren.: Power Engineering, 2001, pp. 77-84.
 [18] S.Beaulieu, M. Ouhrouche " real-time modelling and simulation of an active power filter" ASTED International Conference on Power and Energy Systems PES 2007, Clearwater, Florida, U

The role of research and development in the Central Region of Romania using fuzzy super FRM model

Moga Monika, Calefariu Gavrilă, Sârbu Flavius Aurelian

Abstract—The aim of the study is to measure resources for R&D (research and development) at the regional level in Romania and obtaining primary data that will be important in making the right decisions to increase the competitiveness and development based on an economic knowledge. Therefore to fulfill the above mentioned aim in this application-oriented paper we decided to use a questionnaire and for the interpretation of the results the Super Fuzzy FRM model, representing the main novelty of our paper. We have to mention that the method is applicable to cases where classical analysis of the multi attribute optimization (Electre, fuzzy classic and value analysis) are difficult to apply, because the number of rows and columns of the matrix can be very large.

Keywords— Questionnaires, research and development, super fuzzy FRM model.

I. INTRODUCTION

R &D (research and development) is the systematic and creative activity initiated to enhance the volume of knowledge, including those on human being, culture and using them for new applications.

The R&D function highlights the importance of research and development for social progress, being an intensive factor that can lead to spectacular leaps in national wealth and the hierarchy of nations as in [1].

The result of research and development is a unique product obtained with great effort and expense, and therefore resource requirements cannot be determined from the beginning.

The importance in the activity of an organization of research and development function is evidenced by the fact that one of the defining features of modern economies is continuing consolidation and proliferation of innovative firms as in [2].

To compensate the lack of detailed statistics in the field

Moga Monika is with the Transilvania University, Faculty of Technological Engineering and Industrial Management, Colina Universitatii nr. 1 corp A, Braşov 500036, Romania.

Calefariu Gavrilă is with Transilvania University, Faculty of Technological Engineering and Industrial Management, Colina Universitatii nr. 1 corp A, Braşov 500036, Romania.

Sârbu Flavius Aurelian is with the Transilvania University, Faculty of Technological Engineering and Industrial Management, Colina Universitatii nr. 1 corp A, Braşov 500036, Romania.

(R&D), a good alternative is considered to carry out a survey that can investigate the current state of R&D at the regional level in Romania by assessing deficits, using a questionnaire and the FRM model.

Considering these aspects we grouped the article into three chapters. In chapter two, we present general aspects related to the method using Super Fuzzy Matrices. Chapter three is entitled generalities about the FRM model, while chapter four presents an overview on the method of Super Fuzzy FRM model used to evaluate the answers received from the respondents of the research.

II. GENERAL ASPECTS RELATED TO USING SUPER FUZZY MATRICES

Proposed by the Polish mathematician Jan Łukasiewicz (inventor of Polish notation) an early type of fuzzy logic has existed since 1920. His system allowed the extension of the truth value of a sentence to all real numbers in the range [0, 1].

A number in this range was interpreted as the possibility that the sentence considered to be true or false. These researches led to the theory of possibility, a technique of reasoning in terms of inaccuracy.

Lotfi Zadeh in 1965 extended the possibility theory into a formal system of mathematical logic, also discussed ways of working with nuanced terms of natural language. This tool of representation and manipulation of nuanced terms is called fuzzy logic. Traditional logic considers that an object can belong to a crowd. Fuzzy logic allows a more flexible interpretation of the concept of belonging. Thus, many items may belong to a crowd within varying degrees as in [3].

For example, if we consider the multitude of young people. A 15 years old child is certainly young, while a 65 years-old-person certainly isn't. But a 35 or 45 years-old-man? In this case, we can say that person belongs to the crowd of 35 years in greater than to 45. Let's say for the example mentioned above, with the linguistic variable young, we have the universe of discourse $X = \{0, 25, 35, 55\}$ and the following membership function: $A = 0/1 + 25/0,9 + 35/0,7 + 55/0$, meaning: a 25-year-old person belongs to the set of young men in a proportion of 90%, a 35 years old in a proportion of 70%,

while a 55 year-old one does not belong to the set (degree of membership is 0). These things are plotted as follows (Fig.1):

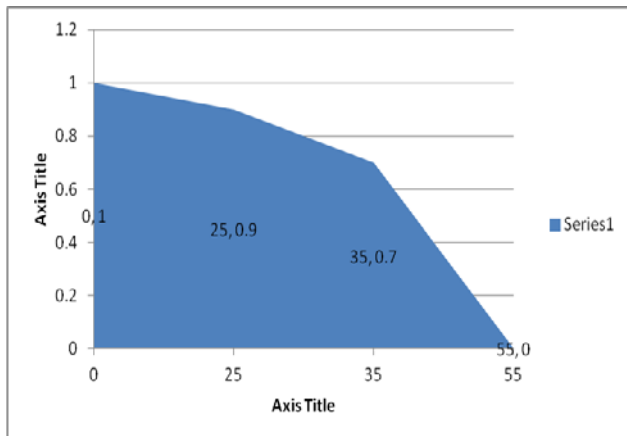


Fig. 1 The plot of the example

On a universe of discourse can be defined several fuzzy subsets. For example, for the universe of ages of people, we can define subsets of young, old or middle aged people. These subsets can intersect (this is highly recommended). The same person will belong to the subset of young people with 70% and to the subset of older people with 30%.

Often, people can not accurately characterize well the numerical information using forms: almost and around 100. In fuzzy set theory, these numbers can be represented as fuzzy subsets of the set of real numbers. A fuzzy number A is a fuzzy set of the set of real numbers, with a convex and continuous membership function and limited support.

III. GENERALITIES ABOUT THE FRM MODEL

To study mainly the problem relating R&D for the first time the three new models (super column fuzzy relational maps, mixed super row fuzzy relational maps and super fuzzy relational maps) have been introduced.

Therefore in the following we describe super column fuzzy relational maps model. Suppose we have some n sets of experts, forming some n distinct category of groups based on education or page or profession end so on. We can describe this model as a multi set of expert's model: we have sets of experts i.e.; not a multi expert model but multi set of expert's model. Thereby we have n sets of experts each set may contain different special features. However the only common factor is that they all agree to work upon the same problem with a same set of attributes as in [4], [5], [6], and [7].

In the following we present what are the domain and the range spaces of this super column fuzzy relational maps model. The domain space is a fuzzy super mixed row vector relating all the n sets of experts who have worked with the model, while the range space of this model has state vectors which are simple row vectors taking its entries from the set {0, 1} as in [6], [7].

Next we define and describe the new row super fuzzy relational maps. We have n sets of attributes related with a problem which is divided into different sets and some n experts view about it and give their opinion. Each of these n-sets, view the problem in a different angle. Therefore at each stage the problem is viewed in a very different way. That is why we construct a single model so that, the hidden pattern is obtained as in [6], [7], [8].

Furthermore we proceed on to describe the super FRM model that comes handy when several sets of experts work with different sets of attributes. We have some problem P at hand and we have n sets of experts $N_1, N_2, N_3, \dots, N_n$ where each N is a set of experts, $i = 1, 2, \dots, n$. We also have some p sets of attributes: we have M_1, \dots, M_p sets of attributes. Suppose we have some experts work on some sets say $M_b, M_k, \dots, M_t, 1 \leq i, k, \dots, t \leq n$. Similarly some other set of experts want to work with $M_s, M_r, M_l, \dots, M_m, 1 \leq s, r, l, m \leq n$ where we may have some of the set of attributes M_i, M_k, \dots, M_t may be coincident with the set of attributes M_s, M_r, \dots, M_m as in [6], [7], [9].

We cannot apply any of the fuzzy models to this. Therefore we use a new model by combining the two models, presented above. We describe the fuzzy super matrix as follows: let the N_i^{th} set of experts give their opinion using the M_j^{th} set of attributes, let P_{ij} denote the connection FRM matrix with the N set of attributes forming the part of the domain space and M_j attributes forming the range space. This is true for $1 \leq i \leq n$ and $1 \leq j \leq p$ as in [6], [7], [10], [11], [12], [13].

To sum up the above mentioned we try to compare the classical Fuzzy model and the FRM model by identifying the main differences between them (Fig.2):

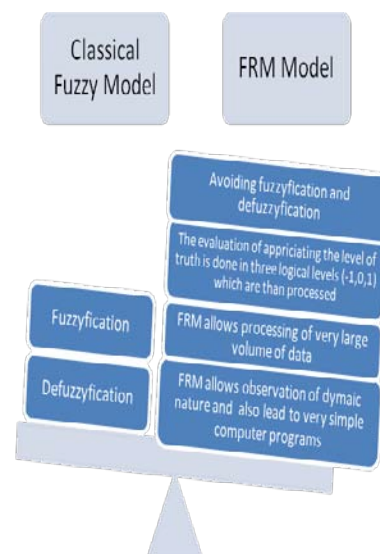


Fig. 2 Comparison between the Classical Fuzzy Model and the FRM Model

Oxidation of 2-Propanol at Low Temperature over Pt/ γ -Al₂O₃ Catalyst

F. Aghazadeh, D.Omidifar, A.Niaei, D.salari

Abstract— An investigation on the kinetics of 2-propanol oxidation over a commercial Pt/ γ -Al₂O₃ catalyst has been performed. Oxidation reactions were carried out in a differential fixed-bed reactor under atmospheric pressure and absence mass transfer resistances (film and pore diffusion resistances). Several kinetic equations derived from mechanistic considerations (Power-rate law, Langmuir–Hinshelwood, Eley-Rideal and Mars-Van Krevelen) have been investigated to account for this fact. Reaction rate constants of models were obtained from the Levenberg–Marquardt algorithm and the genetic algorithm by using Table Curve 3D and Matlab 7.3, respectively.

Keywords— Catalytic oxidation; Kinetics; 2-propanol; Table Curve 3D, Genetic algorithm.

I. INTRODUCTION

Volatile organic compounds are one of the most common pollutants emitted by the chemical process industries, which include most solvents such as thinner, degreasers, cleaners, lubricants, and liquid fuels. VOCs are pollutants because they almost always contribute to ozone formation, and in addition are odorous and toxic. In other words, they react in sunlight with other pollutants such as nitrogen oxides to form ozone and the other compounds (known as photochemical oxidants), which make up photochemical smog (Atkinson and Arey, 2003; Meng et al., 1997; Finlayson-Pitts and Pitts, 1997; Kim et al., 2009). Several techniques for VOCs have been investigated such as thermal incineration, catalytic oxidation, condensation, absorption, bio-filtration, adsorption, and membrane separation (Khan and Ghoshal, 2000). Among these methods, catalytic combustion has advantageous features for VOCs removal, due to complete combustion of dilute fuel proceeds stably at low temperatures (Mazzarino and Barresi, 1993). The main advantages of catalytic combustion compared with other decontamination technologies can be summarized as follows: high efficiency at very low pollutants concentration,

low energy consumption, small size of the depuration unit, and very low production of secondary pollutants (NO_x).

The most common catalysts used for VOC abatement are metals or metal oxides such as Pt, Pd, Rh, and V₂O₅ dispersed on high surface area supports such as Al₂O₃, SiO₂, TiO₂, etc (Arai, 1986; Busby and Trimm, 1979; Cullis and Willatt, 1983; Gonzalez and Nagai, 1985; Patterson and Kembal, 1963; Spivey, 1987; Chantaraviton et al., 2004). Several kinetic models for exploring the mechanism of catalytic incineration of VOCs on the catalyst have been raised and investigated. These models include the power-rate law, Mars-Van Krevelen and Langmuir–Hinshelwood. Power-rate law is a simple expression used to fit the experimental data. The Mars-Van Krevelen and Langmuir–Hinshelwood models are more precise alternatives. The Mars-Van Krevelen model depicts reaction of reactants on the catalyst surface mainly via an oxidation–reduction mechanism; most catalysts with oxidizing activity can be described by this redox mechanism.

On the other hand, the Langmuir–Hinshelwood model depicts reactions in which the adsorbates can only adsorb chemically onto specific sites of the catalyst, each site can only adsorb one molecular (or atom), and the adsorption is limited to a monolayer (Tseng et al., 2005; Hsu and Teng, 2001). The kinetics of deep oxidation of n-hexane and toluene as single components, in their mixture or in mixtures with other types of VOCs over platinum supported catalyst has been studied (Gangwal et al., 1988; Hermia and Vigneron, 1993; Ordóñez et al., 2002), while this effect for 2-propanol oxidation has not been extensively reported. In our pervious study, the effects of different process parameters on the oxidation of 2-propanol over commercial 0.12 wt.% Pt/Al₂O₃ catalyst were investigated at a laboratory-scale (Niaei et al., 2010). The aim of this work is to study the kinetics of the catalytic oxidation of 2-propanol over commercial 0.12wt.% Pt/ γ -Al₂O₃ catalyst. 2-propanol was chosen as sample of oxygen-containing VOC, because it is widely used as a washing agent in semiconductor and precision machinery industries, and large quantities of its waste aqueous solution are generated. For example, the amount of 2-propanol used as a washing agent was 30,000 t in 1997 in Japan and the use of 2-propanol is still increasing (Salari et al., 2012).

This study was carried out by catalytic incineration of 2-propanol over a commercial 0.12wt.% Pt/ γ -Al₂O₃ catalyst in

F.Aghazadeh is with R & D Center, Tabriz Petrochemical Company (e-mail: f.aghazadeh@hotmail.com).

A.Niaei is with Department of Chemical Eng., University of Tabriz.

the isothermal fixed-bed differential reactor. Four kinetic models, i.e. the Power-rate law, Langmuir–Hinshelwood, Eley-Rideal and Mars-Van Krevelen were applied to best fit the experimental results. The effects of the various operating conditions and kinetic behavior of 2-propanol oxidation with catalyst are also determined. The present work can provide valuable information for designing and treating a VOC system.

II. EXPERIMENTAL

Material and Instruments

Volatile organic compounds are one of the most common pollutants emitted by the chemical process industries, which include most solvents such as thinner, degreasers, cleaners, lubricants, and liquid fuels. VOCs are pollutants because they almost always contribute to ozone formation, and in addition are odorous and toxic. In other words, they react in sunlight with other pollutants such as nitrogen oxides to form ozone and the other compounds (known as photochemical oxidants), which make up photochemical smog (Atkinson and Arey, 2003; Meng et al., 1997; Finlayson-Pitts and Pitts, 1997; Kim et al., 2009). Several techniques for VOCs have been investigated such as thermal incineration, catalytic oxidation, condensation, absorption, bio-filtration, adsorption, and membrane separation (Khan and Ghoshal, 2000). Among these methods, catalytic combustion has advantageous features for VOCs removal, due to complete combustion of dilute fuel proceeds stably at low temperatures (Mazzarino and Barresi, 1993). The main advantages of catalytic combustion compared with other decontamination technologies can be summarized as follows: high efficiency at very low pollutants concentration, low energy consumption, small size of the depuration unit, and very low production of secondary pollutants (NO_x).

The most common catalysts used for VOC abatement are metals or metal oxides such as Pt, Pd, Rh, and V₂O₅ dispersed on high surface area supports such as Al₂O₃, SiO₂, TiO₂, etc (Arai, 1986; Busby and Trimm, 1979; Cullis and Willatt, 1983; Gonzalez and Nagai, 1985; Patterson and Kemball, 1963; Spivey, 1987; Chantaraviton et al., 2004). Several kinetic models for exploring the mechanism of catalytic incineration of VOCs on the catalyst have been raised and investigated. These models include the power-rate law, Mars-Van Krevelen and Langmuir–Hinshelwood. Power-rate law is a simple expression used to fit the experimental data. The Mars-Van Krevelen and Langmuir–Hinshelwood models are more precise alternatives. The Mars-Van Krevelen model depicts reaction of reactants on the catalyst surface mainly via an oxidation–reduction mechanism; most catalysts with oxidizing activity can be described by this redox mechanism.

On the other hand, the Langmuir–Hinshelwood model depicts reactions in which the adsorbates can only adsorb chemically onto specific sites of the catalyst, each site can only adsorb one molecular (or atom), and the adsorption is limited to a monolayer (Tseng et al., 2005; Hsu and Teng, 2001). The kinetics of deep oxidation of *n*-hexane and toluene as single components, in their mixture or in mixtures with other types of VOCs over platinum supported catalyst has been studied (Gangwal et al., 1988; Hermia and Vigneron, 1993; Ordonez et al., 2002), while this effect for 2-propanol oxidation has not been extensively reported. In our previous study, the effects of different process parameters on the oxidation of 2-propanol over commercial 0.12 wt.% Pt/Al₂O₃ catalyst were investigated at a laboratory-scale (Niaei et al., 2010). The aim of this work is to study the kinetics of the catalytic oxidation of 2-propanol over commercial 0.12wt.% Pt/ γ -Al₂O₃ catalyst. 2-propanol was chosen as sample of oxygen-containing VOC, because it is widely used as a washing agent in semiconductor and precision machinery industries, and large

quantities of its waste aqueous solution are generated. For example, the amount of 2-propanol used as a washing agent was 30,000 t in 1997 in Japan and the use of 2-propanol is still increasing (Salari et al., 2012).

This study was carried out by catalytic incineration of 2-propanol over a commercial 0.12wt.% Pt/ γ -Al₂O₃ catalyst in the isothermal fixed-bed differential reactor. Four kinetic models, i.e. the Power-rate law, Langmuir–Hinshelwood, Eley-Rideal and Mars-Van Krevelen were applied to best fit the experimental results. The effects of the various operating conditions and kinetic behavior of 2-propanol oxidation with catalyst are also determined. The present work can provide valuable information for designing and treating a VOC system.

III. RESULTS AND DISCUSSION

Physico-chemical characterization

In figure 2 the XRD pattern for the commercial 0.12wt.% Pt/ γ -Al₂O₃ catalyst is shown. The characteristic peaks of γ -Al₂O₃ (2 θ = 35°, 43° and 67°) was observed in spectrum that was in agreement with published literatures (Wang et al., 2008; Hordern, 2004). Since the primary γ -Al₂O₃ peaks were detected in 0.12wt.% Pt/ γ -Al₂O₃ catalyst, as a result it can suggest that the platinum were fairly well dispersed on the γ -Al₂O₃. Figures 3a and 3b show the SEM and TEM analysis of 0.12wt.% Pt/ γ -Al₂O₃ catalyst. It is generally observed that the active phase, Pt, is well dispersed on the γ -Al₂O₃ support.

Kinetic Study for Catalytic Oxidation of 2-Propanol

The overall process of any catalytic reaction is a combination of mass transfer (describing transport of reactants and products to and from the interior of a solid catalyst) and chemical reaction kinetics (describing chemical reaction sequences on the catalyst surface). The overall process is (1) transport of reactants from the bulk fluid through the gas film boundary layer to the surface of the particle, (2) transport of reactants into the catalyst particle by diffusion through the catalyst pores, (3) chemisorption of at least one reactant on the catalyst surface, (4) chemical reaction between chemisorbed species or between a chemisorbed species and a physisorbed or fluid-phase reactant, (5) desorption of reaction products from the catalyst surface, (6) diffusive transport of products through the catalyst pores to the surface of the catalyst particle, and (7) diffusion of products through the exterior gas film to the bulk fluid. In principle, any of these steps, or some combination, can be rate controlling. The rate-controlling step for a given reaction and catalyst can vary depending on temperature, flow rate, gas composition, and catalyst geometry. Any comprehensive analysis of actual catalytic oxidation systems of practical interest must include a quantitative understanding of the relative effects of mass transfer (steps 1, 2, 6, and 7) and surface reaction (steps 3,4, and 5). The discussion herein focuses exclusively on surface reactions. Several kinetic models were tested to describe the kinetics of the complete oxidation of 2-propanol.

Transport effects

Experiments for kinetic's study of 2-propanol oxidation over commercial 0.12wt.% Pt/ γ -Al₂O₃ catalyst must be carried out in the absence of mass and heat transfer control. The effect of internal transport can be evaluated by changing catalyst particle size and external transport of reactants can be evaluated by a set of experiments changing feed gas velocity. Internal mass transfer effects were studied by reacting 4.46×10^{-5} mol.cm⁻³ 2-propanol with commercial 0.12wt.% Pt/ γ -Al₂O₃ catalyst samples of different average particle diameter (from 0.064 to 1.27mm) at temperature of 25°C. It was observed that particle size below 0.286

mm, the 2-propanol conversion did not depend on the catalyst particle diameter (figure 4), reflecting to the absence of internal diffusion limitations. The particle size of 0.137 mm was chosen for the investigation of external mass transfer effects. The external mass transfer effects were checked by obtaining light-off curves working with different total gas flow rates (100-400 cm³/min) and 2-propanol concentration (1.07×10⁻⁵ mol.cm⁻³) at temperature of 25° C, but keeping constant the space time (8615 g.min.mol⁻¹) by varying of catalyst weight (0.05-0.4 gr). Figure 5 shows that external mass transfer is negligible in studied flow rates. The total gas flow rate 200 cm³/min was selected for obtained of kinetics data.

Kinetic Mechanisms for oxidation of 2-propanol

Several kinetic models were tested to describe the kinetics of the complete oxidation of 2-propanol.

Power-Law Kinetic Expression

The Power law model is the simplest approach to describe the dependence of reaction rate on temperature and partial pressures. This very simple type of rate law, although useful for quick comparisons, does not provide any insight into what is occurring at the catalyst surface.

$$(-r_{2\text{-propanol}}) = K_s \cdot P_{2\text{-propanol}}^\alpha \cdot P_O^\beta \quad (1)$$

where $(-r_{2\text{-propanol}})$ is the reaction rate, k_s is the surface reaction rate constant, $P_{2\text{-propanol}}$ and P_O are the partial pressure of 2-propanol and oxygen, respectively, and α and β are reaction orders.

Mechanism-Based Kinetic Expressions

In these kinetic expressions, the controlling steps could be the surface reaction between two adsorbed molecules (Langmuir-Hinshelwood mechanism) or between an adsorbed molecule and a molecule from the gas phase (Eley-Rideal mechanism).

In the Langmuir-Hinshelwood mechanism (L-H) the two gas-phase species of interest are first adsorbed on the surface and then they react which means L-H describes a bimolecular surface reaction between two adsorbed reactant species. The Langmuir-Hinshelwood model (surface reaction between adsorbed 2-propanol and oxygen molecules) is given by equation 2:

$$(-r_{2\text{-propanol}}) = \frac{K_s K_O K_{2\text{-propanol}} P_{2\text{-propanol}} P_O}{(1 + K_O P_O + K_{2\text{-propanol}} P_{2\text{-propanol}})^2} \quad (2)$$

where K_O and $K_{2\text{-propanol}}$ are equilibrium adsorption constants for oxygen and 2-propanol, respectively. As far as the combustion of VOCs on platinum catalysts is concerned, a number of LH rate expressions have been proposed whose mathematical derivation can be found in the literature. Some of the equations provided satisfactory rate data fitting and gave good description of VOCs mixture effects. To our knowledge, there is no previous report on the kinetics of 2-propanol combustion on Pt catalyst.

In the Eley-Rideal mechanism one has reaction between a reactant in the gas phase and a reactant adsorbed on the surface. We considered both chemisorption of oxygen or 2-propanol. The rate expression and their respective controlling mechanisms are as given by equations 3-4.

(I) The Eley-Rideal model (surface reaction between adsorbed oxygen with gas-phase 2-propanol).

$$(-r_{2\text{-propanol}}) = \frac{K_s K_O P_O P_{2\text{-propanol}}}{1 + K_O P_O} \quad (3)$$

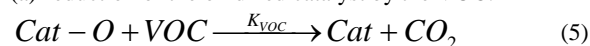
(II) The Eley-Rideal model (surface reaction between adsorbed 2-propanol with gas-phase oxygen).

$$(-r_{2\text{-propanol}}) = \frac{K_s K_{2\text{-propanol}} P_{2\text{-propanol}} P_O}{1 + K_{2\text{-propanol}} P_{2\text{-propanol}}} \quad (4)$$

Two-Stage Redox Model

The two-stage redox model (also so called Mars-Van Krevelen) assumes reaction occurs when reactant molecule interacts with an oxygen-rich portion of the catalyst. A particular portion of the catalyst surface is alternately reduced and oxidized. This model postulates two redox steps:

(a) Reduction of the oxidized catalyst by the VOC:



(b) Oxidation of the catalyst by oxygen from the gas phase:



In steady-state operation, the rates of the oxidation and reduction steps must be equal, considering the overall stoichiometry of the reaction ν .

The Mars-Van Krevelen model is the most frequently reported redox model for catalytic combustion of VOC. According to this model, the reaction rate $(-r_{2\text{-propanol}})$ is expressed by following equation:

$$(-r_{2\text{-propanol}}) = \frac{K_O K_{2\text{-propanol}} P_O P_{2\text{-propanol}}}{K_O P_O + \nu K_{2\text{-propanol}} P_{2\text{-propanol}}} \quad (7)$$

The value of K_O should be independent of the 2-propanol that is oxidized.

To develop a kinetic model, the kinetic studies were carried out under different concentration of 2-propanol and oxygen. The concentration of 2-propanol varied in a range from 5.58×10⁻⁶ to 2.25×10⁻⁵ mol.cm⁻³ and oxygen in a range of 7.77×10⁻⁴ to 1.81×10⁻³ mol.cm⁻³, respectively at temperature of 25°C and total flow of 200 cm³/min over 0.1g commercial 0.12wt.% Pt/ γ -Al₂O₃ catalyst with mean Pt crystallite size of 0.137 mm, is presented in Table. 1. The rates of reaction at various inlet 2-propanol concentrations at this temperature were calculated as follow:

$$-r_{2\text{-propanol}} = \frac{X_{2\text{-propanol}}}{(W / F_{2\text{-propanol}})} \quad (8)$$

where $X_{2\text{-propanol}}$ is the measured 2-propanol conversion at the reactor outlet and $W/F_{2\text{-propanol}}$ the space time referring to the amount of catalyst loaded into the reactor and the inlet 2-propanol molar flow rate.

The orders and reaction constants in rate laws are obtained by both using Levenberg-Marquardt algorithm (Table Curve 3D) and genetic algorithm (Matlab 7.3), respectively. The obtained results from Levenberg-Marquardt algorithm are depicted in figures 6 and 7. The points in the figures 6 and 7 were corresponded to the coordinates of experimental data ($(C_{2\text{-propanol}})_{in}$, C_{oxygen} and r_A). The plates in figure 6 (a,b,c,d and e) were obtained from the Power-Law equation, the Langmuir-Hinshelwood, the Eley-Rideal: (I) Surface reaction between adsorbed oxygen with gas-phase 2-propanol (figure 6(c)) and (II) Surface reaction between adsorbed 2-propanol with gas-phase oxygen (figure 6(d)) and Mars-Van Krevelen models, respectively, with assigned constant coefficients (α , β , K) and

($K_s K_O K_{2\text{-propanol}}$) by Levenberg-Marquardt (LM) learning algorithm. Whatever the observed plates in figure 6 (a,b,c,d and e) to pass adjacency of experimental data, consequently the total sum of

subtractions between distance of the experimental data and the existent plates will be decreased. The decrease of sum of subtractions between experimental data in plate of figure 7 (a,b,c,d and e) indicate best fitting of the experimental data with model and lowest errors in whichever of models.

Two functions were used for fitness function(c) in genetic algorithm:

1) Statically function of NRSS (normalized residual sum of squares). NRSS express to the following equation:

$$c = \text{NRSS} = \sum_{n=1}^N \left(\frac{(-R_{e,n}) - (-R_n)}{R_n} \right)^2 \quad (9)$$

where $(-R_{e,n})$ is the estimated reaction rate, $(-R_n)$ the n th value of the experimentally measured reaction rate, and N the total number of experiments.

2) Geometrical method. This function express to the following equation:

$$c = \sum \text{dis tan ce}(l, ll) / 8 \quad (10)$$

where l are the spots with x, y coordinate equal to $r_{\text{experimental}}$ and ll are the spots with x, y coordinate equal to $r_{\text{calculate}}$, respectively. In genetic algorithm the l spots have constant amounts and the ll spots are variable, since the amount of K, α, β are changeable. Consequently, the genetic algorithm tries to determine the amounts of K, α, β in such manner that the distance of ll spots with l spots and subsequently the fitness function was leaded to minimum amounts. Table 2 summarize the rate models fitting with estimated parameters and regression analyses results of Levenberg–Marquardt algorithm (Table Curve 3D) and genetic algorithm (MATLAB), and also constant amounts of rate equations were obtained from genetic algorithm. As is shown in figures 8 (a-e) the best fitting with lowest error was demonstrated by the power-law model with R^2 of 0.965 in the Levenberg–Marquardt algorithm and 0.98 in the genetic algorithm, respectively.

IV. CONCLUSION

A kinetic study of the catalytic incineration of 2-propanol over a commercial 0.12wt.% Pt/Al₂O₃ catalyst was carried out in a fixed bed catalytic reactor. Four kinetic models, such as the power-rate law, the Langmuir-Hinshelwood, the Eley-Rideal, and the Mars-Van Krevelen were used to best fitting of the experimental data. A direct search namely Levenberg-Marquardt algorithm and a stochastic search algorithm namely genetic algorithm were used to determine the reaction rate constants using Table Curve 3D and MATLAB software, respectively. From mechanism based models, power-rate law present the best fit, suggesting the adsorption of VOC or O₂ has a considerable role in combustion of 2-propanol.

REFERENCES

- Arai, H., Yamada, T., Eguchi, K., Seivama. T., 1986, *Appl. Catal.*, 26, 265.
- Atkinson, R. and Arey, J., 2003, *J. Chem. Rev.*, 103, 4605.
- Busby, J.A., Trimm, D.L., 1979, *J. Catal.*, 60, 430.
- Chantaravitoon, P., Chavadej, S., Schwank, J., 2004, *Chem. Eng. J.*, 97, 161.
- Cullis, C.F., Willatt, B.M., 1983, *J. Catal.*, 83, 267.
- Finlayson-Pitts, B.J., Pitts, J.N., 1997, *Sci.*, 276, 1045.
- Gangwal, S.K., Mullins, M.E., Spivey, J.J., Caffrey, P.R., Tichenor, B.R., 1988, *Appl. Catal.*, 36, 231.
- Gonzalez, R.D., Nagai, M., 1985, *Appl. Catal.*, 18, 57.
- Hermia, J., Vigneron, S., 1993, *Catal. Today*, 17, 349.
- Hordern, B.K., 2004, *Adv. Coll. Int. Sci.*, 110, 19.
- Hsu, L., Teng, H., 2001, *Appl. Catal. B*, 35, 21.

Significant factors of satisfaction of bank customers. Case study from the Czech Republic

J. Belás, A. Chochořáková a L. Gabčová

Abstract— Satisfaction of bank customers is currently at the center of attention of researchers and bankers. It is mainly considered that satisfaction positively affects loyalty of clients and their buying habits. The aim of the article was to quantify and compare the overall level of satisfaction of the Czech banking customers, the most important factors of satisfaction of these customers and number of used banking products in 2014 compared to 2012. Research on the satisfaction of retail customers in the Czech Republic was conducted through a questionnaire survey. Our research confirmed that the Czech Republic remains on a relatively low position with satisfying its bank customers with services provided. The main reason for satisfaction was the ability to use electronic banking. Number of banking products used by the Czech banking clients did not change significantly. It was found that clients in the Czech banking sector suffer from insufficient supply of attractive banking products and relatively low level of interest of bank employees to solve their financial problems.

Keywords— commercial bank, bank customer's satisfaction, satisfaction factors, Cross-selling index

I. INTRODUCTION

THE bank customers satisfaction is currently in the center of attention of researchers and bankers, as it represents an important marketing variable for most of the companies, especially those working in more competitive markets (Munari, Ielasi, Bajetta, 2013; De Matos, Henrique, and De Rosa, 2013).

The satisfaction has a positive influence on customer loyalty (Baumann, Elliott, and Burton, 2012; Mandahachitara and Poolthang, 2011; Fraering, and Minor, 2013; Seiler, Rudolf, and Krume, 2013).

Authors are thankful to the Internal Grant Agency of FaME TBU No. 005/IGA/FaME/2014: Optimization of parameters of the financial performance of the commercial bank, for financial support to carry out this research.

J. B. Author is with Tomas Bata University, Faculty of Management and Economics, Department of Enterprise Economics, Mostní 5139, 760 01 Zlín, Czech Republic (phone: +420576032410; e-mail: belas111@gmail.com)

A. CH. Author is with Tomas Bata University, Faculty of Management and Economics, Department of Enterprise Economics, Mostní 5139, 760 01 Zlín, Czech Republic (e-mail: chochola@gmail.com)

L. G. Author is with Tomas Bata University, Faculty of Management and Economics, Department of Enterprise Economics, Mostní 5139, 760 01 Zlín, Czech Republic (e-mail: gabcova@gmail.com)

Customer satisfaction is an important factor in the performance and competitiveness of banks. (Adolpson, Eklóf, Parmler, 2013; Choudhury, 2013; Keisidou, Sarigiannidis, Maditinos, and Thalassinou, 2013). The high quality of banking services determines further additional purchases of client as well as his loyalty, which means that a satisfied customer provides information about his satisfaction and future bank clients from his own environment: family, friends and colleagues. (De Matos, Henrique, and De Rosa, 2013; Choudhury, 2013).

Banking experience proves that achieving a reasonable rate of customer satisfaction represents a challenge for the bank and it is a permanent process with varied results. Bank customers in many countries show a considerable degree of dissatisfaction and many banks admit that it's necessary to increase the level of customer care.

In this article satisfaction of the Czech bank customers with the services of commercial banks, and its significant attributes were examined, as well as the most important factors of satisfaction, and use of banking products and banks in 2014 compared to 2012.

II. FACTORS DETERMINING SATISFACTION OF BANK CUSTOMER

The achievement of a high degree of banking customer satisfaction represents an important field for banking management.

Customer satisfaction is a complex of various aspects, which operate in a coherent manner and form attitudes of customers to the bank. In the process of forming of customer satisfaction are acting the economic factors, emotional attitudes and habits of consumers. Service quality as perceived by the customers could be defined as the extent of discrepancy between customers' expectations and their perceptions.

Satisfaction can be considered in at least two levels: transaction-specific satisfaction and cumulative satisfaction. The satisfaction of bank customers is also determined by their gender (De Matos, Henrique, and De Rosa, 2013; Karapete, 2011) and age (Baumann, Elliott and Burton, 2012; Tesfom, and Birch, 2011; Frearing and Minor, 2013), which complicates the process of customer relationship management.

A. The quality of banking services and customer satisfaction

According to Chavan and Ahmad (2013) bank business depends very much on the quality of the customer service provided and overall satisfaction of the customer.

Dimensions of service quality are employee behavior, tangibility and information technology. Dimensions of service

convenience are decision convenience, access convenience, transaction convenience, benefit convenience and post-benefit convenience (Kaura, 2013)

The definition of the basic features of independent components of customer satisfaction with the internet banking is (Nochai, and Nochai, 2013): reliability, transaction efficiency, customer support, protection of services, ease of use, performance and content of services.

Mandahachitara and Poolthang (2011) indicate that in terms of the perception of service quality, the most important role belongs to a quality staff and reliability of services. Additional important factors are convenience and service availability. An important role in relationship between a customer and a bank play trust and reliability.

Chavan and Ahmad (2013) have defined eight most important attributes of satisfaction: Paying individual attention to each client, personnel behavior inducing customer trust, attractive bank equipment, zero fees for issuing checks, zero error records, the possibility of online banking, security of transactions, helpful staff and its readiness to answer to customer requirements regardless of occupancy.

Choudhury (2013) indicates that customers distinguish four dimensions of service quality behavior, reliability, tangibles and convenience.

Maddern, Maull, and Smart (2007) state, that the key elements in building customer satisfaction are employee satisfaction and service quality. In this context Gounaris and Boukis (2014) indicate, that the employee job satisfaction influences a customer's perception of quality and customer satisfaction. Customers in business relationships require a high degree of acceptance of their own needs from staff and accurate service delivery (Lages and Piercy, 2012).

B. Satisfaction, Customer Loyalty, Impact on the financial performance of the bank

Many authors agree that customer satisfaction has a strong positive impact on customer loyalty (for example, Seiler, Rudolf, and Krume, 2013) and mediates the impact of service quality on loyalty (Karapete, 2011). Understanding of customer loyalty requires understanding of customer satisfaction first (Fraering, and Minor, 2013).

According to Mandahachitara and Poolthang (2011) customer's loyalty is very important, because getting new customers also brings additional costs (a similar opinion is also shared by Titko, and Lace, 2010) and vice versa with the duration of customer relationship profitability of this relationship grows as well. Effective tool for building true loyalty can be e.g. friendly approach to clients, availability of banking products and services, intensive communication and activities in the field of corporate social responsibility.

Scientific studies that examine the direct impact of customer satisfaction and customer loyalty to shopping habits, respectively, the financial performance of banks are not too numerous. It could be agreed with Choudhury (2013), which states, that the explicit connections between the service quality dimensions and customers' purchase intentions have not been addressed in the services marketing literature so far and a significant gap thus exists. However, there are authors exist who deal with this topic.

According Terpstra, Kuijlen, and Sijtsma (2012) customer satisfaction has a positive effect on future customer revenues when current customer revenues are accounted for. The result supports the theoretical expectation that customer satisfaction influences customer revenues, and as such it also provides an explanation for the relation between average customer satisfaction and financial performance. Loyalty has a significant impact on the financial performance of banks (Keisidou, Sarigiannidis, Maditinos, and Thalassinou, 2013).

Adolpson, Eklöf, and Parmler (2013) indicate in their study that in customer satisfaction changes by one unit causes a change in the average market capitalization of SEK 6.5 billion (the equivalent of 800 million, about 6%) within one year. Improving the financial performance of banks may succeed after approximately one year after the customer satisfaction index increase. It is obvious why customer satisfaction must be strictly a part of a medium- and a long-term strategy of the company.

According to Choudhury (2013) service quality factor reliability is the most important factor for influencing customers' purchase intentions.

In this context, the appropriate examination of the overall satisfaction of bank customers in the context of shopping habits and analyzing the factors that create a feeling of satisfaction among bank customers may be considered.

III. OBJECTIVES, METHODOLOGY AND DATA

The aim of this article was to quantify and compare the overall level of satisfaction of the Czech banking customers, the most important factors of satisfaction of these customers and number of used banking products and banks in 2014 compared to 2012.

Research on the satisfaction of retail customers in the Czech Republic was conducted through a questionnaire survey in 2012 and then in 2014.

In our research, five scientific hypotheses were set. When establishing quantitative criteria estimation techniques were used.

- H 1. The overall level of satisfaction of bank customers in the Czech Republic in 2014 compared to 2012 has not changed and was less than 65%.
- H 2. The intensity of offers of interesting banking services in 2014 compared to 2012 has not changed. Intensity of too frequent offer of attractive banking products was lower than 30%.
- H 3. The rate of concern for bank employees to solve the financial problems of banking clients in 2014 compared to 2012 has not changed. The degree of intensive interest to resolve clients' issues is less than 10%.
- H 4. Czech clients are the mostly satisfied with the availability of banking products and services through electronic banking. More than 60% of Czech clients are satisfied with this factor.
- H 5. The average value of CSI has increased by at least 10% in the last two years. The structure of the used products from 2012 to 2014 remained unchanged.

The structure of the products used since 2012 to 2014 has not changed.

Within the questionnaire survey in 2012, in the Czech Republic a total of 323 respondents was approached, of which 37% were men and 63% were women. Age structure of respondents was as follows: 32% were aged less than 30 years, 50% of them were 30-50 years old and 18% were over 50. The education level of respondents was as follows: 1% had primary education only, 62% had secondary education and 37% were university educated bank customers.

In 2014, there were received responses from 459 respondents, of which 44% were men and 56% were women. The age structure of those respondents was as follows: 39% of respondents were aged under 30 years, 44% were aged from 31 to 50 years and 17% of them were customers over 50. The education level of respondents was as follows: 3% had primary education, 54% had secondary education and 43% were university educated bank customers.

Established scientific assumptions in each table were examined through Pearson statistics. P-value less than 5% leads to the rejection of the null hypothesis. Part of the quantitative analysis is the use of indicators and descriptive statistics such as weighted arithmetical average and the percentage figures.

IV. RESULTS AND DISCUSSION

Table I presented the results of overall satisfaction of the Czech bank customers in 2014 compared to 2012.

Table I Overall satisfaction of bank customers in the Czech Republic (CR)

Are you satisfied with bank products and services provided to you?	CR in 2012 in %	CR in 2014 in %	p-value
1. Yes	62.23	66.23	0.2819
2. No	26.32	16,34	<0.01
3. I don't know	11.45	17.43	0.0275
$\chi^2=14.2141$			
p-value<0.01			

The results of our research confirm the change in the pattern of responses. Significant change in opinion reported in the replies "No" and "I don't know". A large number of respondents who were dissatisfied before are now the undecided. There is no evidence that the situation with satisfied customers has changed and thus it could be assumed that it remained the same (p-value=0.2819). Our data do not provide evidence for the claim that the true proportion of satisfied clients in 2014 is lower than 65% (p-value=0.693). H1 was partially confirmed.

According to the results of our research, the overall satisfaction rate of the Czech customers is at the European average level. These results are comparable with some of the published results of the satisfaction of bank customers (napr. Deloitte, 2012; Belás, Burianová, Cipovová, and Červenka, 2013).

Overall satisfaction of bank customers is significantly determined by the bank employees approach to financial needs of clients. In this context, there was examined the activity of bank employees when offering additional bank products (Table II) and the perceived interest of bank employees in solving the financial problems of bank customers (Table III).

Table II Offer of interesting products from bank employees

How often do you face a situation when the bank employee offers you an interesting product?	CR in 2012 in %	CR in 2014 in %	p-value
1. Often	22.91	29.84	0.0384
2. Rarely	60.99	32.03	<0.01
3. Never	16.10	38.13	<0.01
$\chi^2=71.2200$			
p-value< 0.01			

In comparison to 2012, in the year 2014, the opinions of customers about offering interesting products from bank staff have changed. The numbers of clients who have said that bank employees often offer them attractive banking products has been increased significantly. The number of clients who reported that they seldom receive interesting bank products has decreased significantly and the number of clients who reported that they were never offered any interesting products by their bank has increased substantially. However, the actual intensity of frequent offers in 2014 was not less than 30% (p-value=0.4919). H2 was partially confirmed.

Table III Bank employees interest in solving the financial problems of the client

Do you have a feeling that the bank is interested in solving your financial problems, or just want to sell something to you?	CR in 2012 in %	CR in 2014 in %	p-value
1. Bank is very interested	4.64	4.58	1.0000
2. Bank is sometimes interested	23.84	39.87	<0.01
3. Bank is not interested at all	11.15	3.92	<0.01
4. Bank just wants to sell product and earn more money	43.03	20.70	<0.01
5. Cannot judge	17.34	30.93	<0.01
$\chi^2=74.4420$			
p-value< 0.01			

The values of the test criteria demonstrated a substantial change in the structure of responses of the Czech bank clients. Although the share of respondents who are unable to assess the situation has increased, the table makes it clear that the

situation is progressing positively. There is obviously noted an increase of those clients who feel that the bank is interested in them sometimes, while the proportion of customers who believe that the bank tries only to sell a product or even that it does not care about the customer at all, decreases. The real proportion of clients who believe that their bank is very interested in them is actually lower than 10% (p-value <0.01). Our research has partially confirmed the validity of the H3.

In Table IV are compared the reasons for satisfaction of the Czech banking customers in 2014 compared to 2012.

Table IV Reasons for customer satisfaction in the banking sector of the Czech Republic

What satisfies you the most in the bank? (you can provide up to 3 answers)	CR 2012 in %	CR 2014 in %	p-value
1. quick service in the branch	13.93	11.55	0.3770
2. the possibility of using electronic banking	74.61	78.88	0.1900
3. quality products and services	17.65	17.21	0.9500
4. convenient and friendly service in a branch	17.09	21.13	0.1814
5. availability of the branch	49.54	50.76	0.7910
6. developed network of ATMs	40.25	42.05	0.6670
7. other (account for free, personal Consultant)	0.00	5.44	-

In any of the monitored level of responses there were not identified any significant changes in time. It is still true that more than 60% of clients are satisfied with their electronic banking (p-value<0.01). The results of the research have confirmed the validity of H4.

Our results are comparable to other published results. According to research conducted by Ernst & Young (2012) 78% of banks' clients in the Czech Republic control their bank accounts by using the internet. For comparing it could be stated, that in Slovakia this option was mentioned by 67% of respondents back in 2012. (Belás, Burianová, Cipovová, and Červenka, 2013)

According to Liébana-Cabanillas, Munoz-Leiva and Rejón-Guardia (2013) user satisfaction levels with online banking have increased in recent years, reaching more than 80%. Authors also indicate, that online banking also was favored over other channels that customer have at their disposal (55% selected the online channel as one that satisfied them the most, while 28% chose branches, 13% chose ATMs, and only 2% chose call center and mobile banking as the channel that satisfied them most).

In Table V indicated the number of used banking products in the Czech Republic in 2012 and 2014.

Table V Number of banking products being used

How many	1	2	3	4
----------	---	---	---	---

banking products (current account, consumer credit, mortgage etc.) you are currently using?	product	products	products	products and more
Number of respondents in 2012 in %	26.00	35.91	23.22	14.86
Number of respondents in 2014 in %	27.67	39.21	18.15	14.59
p-value	0.6600	0.3883	0.1299	1.0000
$\chi^2=2.7974$	0.4219			
The average value of CSI*2012=2.27 CSI*2014=2.20				

Note: * CSI (Cross Selling Index – number of products/1 bank client)

Data structure in Table V does not provide evidence that would change the number of products used for the past two years. It also has not confirmed our hypothesis that the average value of CSI has increased by at least 10% in the last two years.

The average value of CSI as per our data is relatively low, indicating that banks in the Czech Republic have quite interesting sales opportunities. The surprising finding was that the CSI for the past period has slightly decreased.

V. CONCLUSION

Satisfaction and loyalty of bank customers represent a significant determinant of future growth of commercial banks' financial performance. In this context it is important that the bank managers devote full attention to creation of those aspects that enhance customer satisfaction and bank customer loyalty.

There exist many options and approaches to boost customer satisfaction and customer loyalty to the bank. Our research has shown that it is important to pay attention to personal communication with clients, to take care about his comfort while implementing banking services and to protect customer's financial interests. It was found that clients in the Czech banking sector suffer from insufficient supply of banking products and relatively low rate of concern of bank employees to solve their financial problems.

Our research, like other researches on this topic, has been somewhat limited by the number of respondents. Nevertheless, it's expected that it may be beneficial for bank managers' inspiration to improve attributes of satisfaction and loyalty of bank employees.

Our future research will focus on the quantification of the effects of satisfaction growth and bank clients' loyalty to increase the financial performance of commercial banks through growth in sales of banking products to satisfied customers.

REFERENCES

- [1] Adolpson, J., Eklóf, J., Parmler, J. (2013). Customer Satisfaction as a Key Performance Indicator in Bank Management. Available from: http://world-finance-conference.com/papers_wfc2/528.pdf [cit. 2013-10-11]
- [2] Baumann, CH., Elliott, G., Burton, S. (2012). Modeling customer satisfaction and loyalty: survey data versus data mining. *Journal of Services Marketing*, 26 (3): 148 – 157.
- [3] Belás, J., Burianová, L., Cipovová, E., Červenka, M. (2013). Customers' satisfaction as the important part of corporate social responsibility's activities in the commercial banking. *Proceedings of the 6th International Scientific Conference Finance and the performance of firms in science, education, and practice*, April 25-26, Zlín, Czech republic.
- [4] Deloitte. (2012). Research. *More than four fifths of Czech people are loyal to the bank*. News release. Prague, 14.6.2012. Available from: http://www.deloitte.com/view/cs_CZ/cz/press/press-releases/9563e3bf3cae7310Vg_nVCM2000001b56f00aRCRD.htm, [cit. 2012-04-10]
- [5] De Matos, C. A., Henrique, J. L., De Rosa, F. (2013). Customer reactions to service failure and recovery in the banking industry: the influence of switching costs. *Journal of service marketing*, 27(7): 526-538.
- [6] Ernst & Young. (2012). *New time of banking. Czech clients want banks more to meet its needs*. News release. Prague, 25.6.2012. Available from: http://www.ey.com/CZ/cs/Newsroom/News-releases/2012_Nova-era-bankovnictvi [cit. 2012-12-10]
- [7] Fraering, M., Minor, M. S. (2013). Beyond Loyalty: Customer Satisfaction, Loyalty and Fortitude. *Journal of Services Marketing*, 27(4): 334 – 344.
- [8] Gounaris, S., Boukis, A. (2013). The role of employee job satisfaction in strengthening customer repurchase intentions. *Journal of Services Marketing*, 27(4): 322 – 333.
- [9] Chavan, J., Ahmad, F. (2013). Factors Affecting On Customer Satisfaction in Retail Banking: An Empirical Study. *International Journal of Business and Management Invention*, vol. 2, no. 1, pp. 55-62.
- [10] Choudhury, K. (2013). Service quality and customers' purchase intentions: an empirical study of the Indian banking sector. *International Journal of Bank marketing*, 31(7): 529 – 543.
- [11] Karapete, O. M. (2011). Service quality, customer satisfaction and loyalty: The moderating role of gender. *Journal of Business Economics and Management*, 12(2): 278 – 300.
- [12] Kaura, V. (2013). Antecedents of customer satisfaction: a study of Indian public and private sector banks. *International Journal of Bank Marketing*, 31(3): 167 – 186.
- [13] Keisidou, E., Sarigiannidis, L., Maditinos, D. I., Thalassinou, E. I. (2013). Customer satisfaction, loyalty and financial performance: A holistic approach of the Greek banking sector. *International Journal of Bank Marketing*, 31(4): 259 – 288.
- [14] Lages, C. R., Piercy, N. F. (2012). Key Drivers of Frontline Employee Generation of Ideas for Customer Service Improvement. *Journal of Service Research*, 15(2): 215 – 230.
- [15] Maddern, H., Maull, R. and Smart, A. (2007). Customer satisfaction and service quality in UK financial services. *International Journal of Operations & Production Management*, 27(9): 999 – 1019.
- [16] Mandahachitara, R., Poolthang, Y. (2011). A model of customer loyalty and corporate social responsibility. *Journal of Service Marketing*, 25(2): 123 – 133.
- [17] Munari, L., Ielasi, F., Bajetta, L. (2013). Customer satisfaction management in Italian banks. *Qualitative Research in Financial Markets*, 5(2): 139 – 160.
- [18] Nochai, R., Nochai, T. (2013). The impact of Internet Banking Service on Customer Satisfaction on Thailand: A Case Study in Bangkok. *International Journal of Humanities nad Management Sciences*, 10(1): 2320 – 2344.
- [19] Seiler, V., Rudolf, M., Krume, T. (2013). The influence of socio-demographic variables on customer satisfaction and loyalty in the private banking industry. *International Journal of Bank Marketing*, 31(4): 235 – 258.
- [20] Terpstra, M., Kuijlen, T., Sijtsma, K. (2012). An empirical study into the influence of customer satisfaction on customer revenues. *The Service Industries Journal*, 32(13): 2129 – 2143.
- [21] Tesfom, G., Birch, N. J. (2011). Do switching barriers in the retail banking industry influence bank customers in different age groups differently? *Journal of service marketing*, 25(5): 371 – 380.
- [22] Titko, J., Lace, N. (2010). Customer Satisfaction and Loyalty in Latvian Retail Banking. *Economics and Management*: 2010.15: 1031 – 1038.

Solute Transfer in Layered Porous Media: An Approach Based on Differential Quadrature Method (DQ)

Meysam Ghamariadyan, Abbas Ghaheri

Abstract—Solute or contaminant transport in porous media can be described by Advection – diffusion equations. In this research, the differential quadrature method (DQM) is employed to solve ADE in solute transport in a double-layered porous medium. This method is applied to two examples with different boundary conditions and the results are compared with analytical solutions. Also, the effect of various parameters on interface conditions are discussed in all examples. Using DQM, provides relatively exact results, while the needed mesh size is much smaller than the traditional approaches which reduces computational time and needed computer storage capacity. Another advantage of this numerical method is that applying the boundary and initial conditions can be performed easier than the other numerical methods.

Keywords—solute transfer, Differential Quadrature method, numerical method, analytical solution.

I. INTRODUCTION

IN a subsurface environment, the characterization of fate and the transfer of solutes is essential for remediation practices specially at last decades. Porous media are seldom homogeneous and the transport properties of these media will vary spatially and sometimes also temporally. Accurate mathematical analyses of transport in heterogeneous media are not easily carried out. However, the formulation and mathematical solution of the transport problem becomes possible if the medium is assumed, somewhat simplistically, to be composed of a series of homogeneous layers. In soil science, composite media have been used for representing stratified soil profiles in which horizons parallel to the soil surface. In order to prevent or make slow the transfer process of a special material, sometimes, this layering in the form of artificial barriers is constructed. Hence, applying the homogeneity assumption for simplifying the problem may lead an inaccurate evaluation of the real case. Solute transport in soils is usually described deterministically by the Advection - Dispersion Equation (ADE), although alternative stochastic approaches also exist [1]. Exact and approximate analytical solutions for transport in layered soils are now available for a limited number of situations. In most cases, Leij et al investigated the solute transfer in layered soil [2]. They addressed mass balance at the interface between the layers by

considering different interface continuity conditions. Leij and van Genuchten presented an analytical solution for the solute transport in a double-layer porous medium with a zero concentration initial condition [2]. Recently, a comprehensive investigation has been conducted by Li et al in which an analytical solution for ADE in a double-layered porous media has been presented [3]. The analytical solutions basically are able to render perception into the governing physical processes, provide useful tools for validating numerical approaches and are rarely applicable to practical problems. Also, finding the simplest and optimal techniques to solve the partial differential equation like ADE has attracted a great importance. A diversity of numerical methods are available now for solving the initial- and/or boundary value problems in physical and engineering science. The frequently used numerical techniques for solving such equations are the standard finite difference method (FDM), finite element method (FEM) and boundary element method (BEM). Usually, above-mentioned methods require a large number of grid points in order to produce a moderately accurate solution and involve complex computer programming algorithms. However, there exist a number of alternative methods such as Differential Quadrature Method which can provide relatively accurate results with inexpensive computation. The method has been applied successfully to solve a wide range of problems, with a diversity of boundary conditions easily and precisely.

After acquiring the correct result as a base in simulations of solute transport which usually is performed by analytical methods, finding the optimal techniques to solve the ADE has attracted a great consideration. One of these effective techniques is the Differential Quadrature Method which in spite of anonymity can provide relatively accurate results depending on the computational efforts. However, there exist a number of alternative methods such as Differential Quadrature Method which can provide relatively accurate results with inexpensive computation. DQM first developed by Bellman and Casti (1971) and has made a noticeable success over the last four decades [4]. The main idea of this method is on the basis of the integral quadrature. Additional developments achieved by Shu et al. based on Polynomial-based differential quadrature (PDQ) as in [5]-[8], Fourier expansion-based differential quadrature (FDQ) as in [9], and Radial basis

function based differential quadrature (RBF-DQ) (Shu et al. 2005, 2007) [10, 11].

In this study, the DQM has used to solve one dimensional ADE on solute transport problem in double-layered porous media. Two problems with different boundary conditions was assumed to provide more insight into the solution of the problem. The DQM results are verified to be in an extremely good agreement with the analytical solution by using a small number of grid points.

II. MATHEMATIC PROBLEM SOLUTION

A porous medium consisting of two homogeneous layers subject to the steady water flow perpendicular to the layer interface is assumed. The transport and flow properties of both layers are the same in time and space as depicted in Fig. 1. The thickness of the layer is set to H , also, $H = h_1 + h_2$. Each layer has its own properties. The z axis is consistent with the constant Darcy velocity. The solute transport in the double layer porous media in one-dimension is well explained by

$$n_{i'}R_{di'} \frac{\partial c_{i'}}{\partial t} = n_{i'}D_{i'}^* \frac{\partial^2 c_{i'}}{\partial z^2} - v \frac{\partial c_{i'}}{\partial z} \quad (i' = 1, 2) \quad (1)$$

Where $n_{i'}$ denotes the porosity, $D_{i'}^*$ stand for constant effective diffusion coefficient, $R_{di'}$ is retardation factor, v denotes the Darcy velocity and $C_{i'}$ provides the solute concentration in layers. It is noteworthy that subscript i' indicates the layer's number. For example $i' = 1$ denotes the inlet layer and $i' = 2$ indicates outlet layer.

Since the apparent velocity in i' th layer is equal to $v/n_{i'}$, Eq. (1) can be written as follows:

$$R_{di'} \frac{\partial c_{i'}}{\partial t} = D_{i'}^* \frac{\partial^2 c_{i'}}{\partial z^2} - v_{si'} \frac{\partial c_{i'}}{\partial z} \quad (i' = 1, 2) \quad (2)$$

In this work the initial condition for all problems are the same and is defined by the following function:

$$c_{i'}(z,t) = c_{i'}(z,0), \quad i' = 1, 2 \quad (3)$$

The additional continuity conditions are considered at the interface between the layers. The Drichlet and Robin conditions are used to make us sure that both concentration and solute flux continuities are satisfied.

The Drichlet and the Robin continuity conditions at the interface can be conveyed as follows, correspondingly:

$$C_1(h_1, t) = C_2(h_1, t) \quad (4)$$

$$\begin{aligned} -n_1 D_1^* \frac{\partial C_1(z, t)}{\partial z} \Big|_{z=h_1} + v C_1(h_1, t) = \\ -n_2 D_2^* \frac{\partial C_2(z, t)}{\partial z} \Big|_{z=h_1} + v C_2(h_1, t) \end{aligned} \quad (5)$$

Equation (5) becomes a Neumann continuity condition after substitution of Equation (4) yielding

$$-n_1 D_1^* \frac{\partial C_1(z, t)}{\partial z} \Big|_{z=h_1} = -n_2 D_2^* \frac{\partial C_2(z, t)}{\partial z} \Big|_{z=h_1} \quad (6)$$

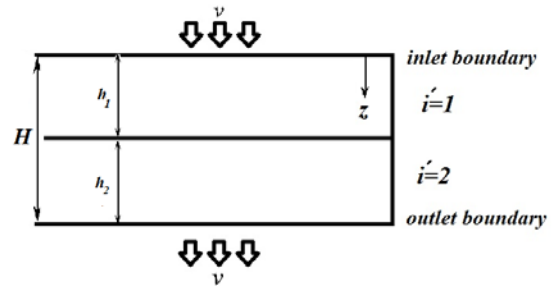


Fig. 1. Schematic representation for solute transport through a double-layered porous medium

But the boundary conditions for the two problems are quite different and will be investigated separately in three types of problems as follows:

A. Problem type 1

Dirichlet or first type inlet and outlet boundary conditions

$$\text{Dirichlet inlet BC: } C_1(0, t) = C_0 \quad (7)$$

$$\text{Neumann outlet BC: } \frac{\partial C_2(z, t)}{\partial z} \Big|_{z=H} = 0$$

Which signifies fixed solute concentration situations.

B. Problem type 2

Dirichlet inlet and Neumann or second type outlet boundary conditions

$$\begin{aligned} \text{Robin's inlet BC: } -n_1 D_1^* \frac{\partial C_1(z, t)}{\partial z} \Big|_{z=0} + v C_1(0, t) = v C_0 \\ \text{Neumann outlet BC: } \frac{\partial C_2(z, t)}{\partial z} \Big|_{z=H} = 0 \end{aligned} \quad (8)$$

That represents fixed solute concentration and zero gradient condition, respectively.

C. Problem type 3

Problem 3: Robin's or third type inlet and Neumann outlet boundary conditions

$$\text{Robin's inlet BC: } -n_1 D^* \left. \frac{\partial c_1(z,t)}{\partial z} \right|_{z=0} + \nu c_1(0,t) = \nu c_0 \tag{9}$$

$$\text{Neumann outlet BC: } \left. \frac{\partial c_2(z,t)}{\partial z} \right|_{z=H} = 0$$

Table 1. Three types of problems with diverse inlet and outlet boundary condition

Problem	Initial condition	Inlet boundary	Outlet boundary
1	$c_1(z,t)=c_1(z,0)=c_0$	$C_1(0,t)=C_0$	$C_2(0,t)=C_H$
2	$c_1(z,t)=c_1(z,0)=c_0$	$C_1(0,t)=C_0$	$\left. \frac{\partial C_2(z,t)}{\partial z} \right _{z=H} = 0$
3	$c_1(z,t)=c_1(z,0)=c_0$	$-n_1 D^* \left. \frac{\partial C_1(z,t)}{\partial z} \right _{z=0} + \nu C_1(0,t) = \nu C_0$	$\left. \frac{\partial C_2(z,t)}{\partial z} \right _{z=H} = 0$

Fixed flux and zero gradient condition as shown in (9).

Where c_0 and c_H stand for constant solute concentrations at the inlet and outlet boundaries, accordingly.

In this paper, the numerical solution for three types of problems subjected to various inlet and outlet boundary conditions are represented (Table 1).

III. DIFFERENTIAL QUADRATURE METHOD

DQM is a numerical method developed to solve both linear and nonlinear partial differential equations. This method was first proposed by Bellman and Casti [4]. Also, many researchers have made important improvements to this method and its applications. For example, to simplify the computational efforts to evaluate weighting coefficients for high order derivatives in DQM, Mingle suggested a linear transformation [13].

Civan and Sliepcevich further extended this method to multi-dimensional problems [14].

In the DQM, a partial derivative of a function with respect to a space variable at a discrete point is approximated as a weighted linear sum of the function values at all discrete points along the corresponding coordinate axes. Its weighting coefficients do not depend to any particular condition and only depend on the grid spacing. Thus, any partial differential equation can be easily reduced to a set of algebraic equations using these coefficients. In this way the n -th-order derivative of the function $f(x)$ at point x_i is calculated by Eq. (10).

$$f^n(x_i) = \sum_{j=1}^N A_{i,j}^n f(x_j) \text{ for } i=1,2,\dots,N \tag{10}$$

Where

$w_{i,j}^n$ = weighting coefficients, $f(x_j)$ = value of the function at point j , $f^n(x_i)$ = the n -th-order derivative value at point x_i .

Calculating the weighting coefficients can be a crucial part of a problem. It influences the accuracy of the results, seriously. The weighting coefficient ($A_{i,j}^n$) can be approximated by a high-order polynomial or by the Fourier series expansion or the harmonic functions as its test functions. In this work Lagrange interpolation basis function is used as the test functions to determine the weighting coefficients [15, 16]:

$$a_{i,j} = \frac{M^{(1)}(x_i)}{(x_i - x_j) M^{(1)}(x_j)}, \text{ for } j \neq i \tag{11}$$

$$a_{i,i} = - \sum_{j=1, j \neq i}^N a_{i,j} \tag{12}$$

$$b_{i,j} = -2a_{i,j} \left(a_{i,i} - \frac{1}{x_i - x_j} \right), \text{ for } j \neq i \tag{13}$$

$$b_{i,i} = - \sum_{j=1, j \neq i}^N b_{i,j} \tag{14}$$

Where $M^{(1)}(x_i) = - \prod_{k=1, k \neq i}^N (x_i - x_k)$, a_{ij} and b_{ij} are the weighted coefficients of first order derivatives and second order derivatives, respectively.

IV. PROBLEM SOLUTION

In this section, application of DQM in discretization and formulation of the governing equations for three chosen to study problems is presented. In the developed model in this study, all spatial derivatives are discretized by DQM and temporal derivatives by first order forward FD scheme. Since the cited problems are transient they can be solved by each of the explicit, implicit and semi implicit Crank-Nicholson schemes.

In the explicit scheme the value of any parameter of time t^{n+1} or $n+1$ -th time step is calculated directly from discretized equations knowing their value in the previous time step n -th or t^n . This method only uses information in time step n for computing parameters in time step $n+1$, so we have to select the small time step Δt ($\Delta t = t^{n+1} - t^n$) to have convergence. **In the implicit scheme** the value of parameters

at time step $n+1$ has been used for discretizing spatial derivatives. Therefore, discretized equations represent a set of algebraic equations that must be solved simultaneously to evaluate new values of the parameters in time step $n+1$. The **semi implicit Crank-Nicholson scheme** is similar to an implicit scheme except that in this way, for solving the problem, the value of parameters in both time step n and $n+1$ is used for discretizing spatial derivatives.

The general form of discretized Eq. (2) can produce Eq. (15) and Eq. (16):

$$R_{di'} \left[\frac{C_{i'}^{n+1} - C_{i'}^n}{\Delta T} \right]_i = \lambda \left[D_{i'}^* \frac{\partial^2 C_{i'}}{\partial Z} - v_{si'} \left(\frac{\partial C_{i'}}{\partial Z} \right) \right]_i^{n+1} + (1-\lambda) \left[D_{i'}^* \frac{\partial^2 C_{i'}}{\partial Z} - v_{si'} \left(\frac{\partial C_{i'}}{\partial Z} \right) \right]_i^n \quad (15)$$

for $i = 1, 2, \dots, N$ and $i' = 1$.

$$R_{di'} \left[\frac{c_{i'}^{n+1} - c_{i'}^n}{\Delta t} \right]_j = \lambda \left[D_{i'}^* \frac{\partial^2 c_{i'}}{\partial z^2} - v_{si'} \left(\frac{\partial c_{i'}}{\partial z} \right) \right]_j^{n+1} + (1-\lambda) \left[D_{i'}^* \frac{\partial^2 c_{i'}}{\partial z^2} - v_{si'} \left(\frac{\partial c_{i'}}{\partial z} \right) \right]_j^n \quad (16)$$

for $j = 1, 2, \dots, M$ and $i' = 2$.

Which Eq.(15), Eq.(16) are applied to the inlet and outlet layer, correspondingly and $\theta=0$, $\theta=1$ and $\theta=0.5$ result in explicit, implicit and semi implicit Crank-Nicholson scheme respectively. In order to establish an equation for water solute concentration calculation, DQ will be used to discretize spatial derivatives in time step n and $n+1$ in Eq. (17) and Eq.(18) for any scheme. The form of spatial discretization is depicted in Fig. 2. The first subscript of C indicates the layer number and the second subscript denotes the grid point number which N, M show that how many grid points are recognized in inlet and outlet layer, respectively.

The general equation then would be:

$$R_{di'} \frac{C_{i',j}^{n+1} - C_{i',j}^n}{\Delta T} = D_{i',j}^* \sum_{k=1}^M b_{i',j,k} \left[\lambda C_{i',k}^{n+1} + (1-\lambda) C_{i',k}^n \right] - v_{si'} \sum_{k=1}^M a_{i',j,k} \left[\lambda C_{i',k}^{n+1} + (1-\lambda) C_{i',k}^n \right] \quad (17)$$

for $j = 1, 3, \dots, M - 1$ and $i' = 2$.

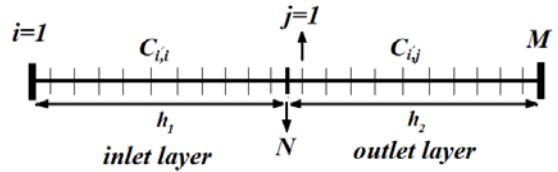


Fig 2. The form of spatial discretization for the double-layered porous medium

Using equations in the form of Equations (17, 18) for each grid, a set of nonlinear equations will be assembled that must be solved simultaneously for each layer.

$$R_{di'} \frac{C_{i',j}^{n+1} - C_{i',j}^n}{\Delta T} = D_{i',j}^* \sum_{k=1}^M b_{i',j,k} \left[\lambda C_{i',k}^{n+1} + (1-\lambda) C_{i',k}^n \right] - v_{si'} \sum_{k=1}^M a_{i',j,k} \left[\lambda C_{i',k}^{n+1} + (1-\lambda) C_{i',k}^n \right] \quad (18)$$

for $j = 1, 3, \dots, M - 1$ and $i' = 2$.

By some simplifications, a set of equations will be acquired in the following:

$$C_{i',i}^{n+1} + \frac{\Delta T}{R_{di'}} (1-\lambda) \sum_{k=1}^N \left[v_{si'} a_{i',i,k} - D_{i',i}^* b_{i',i,k} \right] C_{i',i}^{n+1} = C_{i',i}^n + \frac{\Delta T}{R_{di'}} \lambda \sum_{k=1}^N \left[D_{i',i}^* b_{i',i,k} - v_{si'} a_{i',i,k} \right] C_{i',i}^n \quad (19)$$

for $i = 2, 3, \dots, N - 1$ and $i' = 1$

$$C_{i',j}^{n+1} + \frac{\Delta T}{R_{di'}} (1-\lambda) \sum_{k=1}^M \left[v_{si'} a_{i',j,k} - D_{i',j}^* b_{i',j,k} \right] C_{i',j}^{n+1} = C_{i',j}^n + \frac{\Delta T}{R_{di'}} \lambda \sum_{k=1}^M \left[D_{i',j}^* b_{i',j,k} - v_{si'} a_{i',j,k} \right] C_{i',j}^n \quad (20)$$

for $j = 1, 3, \dots, M - 1$ and $i' = 2$

Using DQM to discretize different type of boundary condition equations, a set of linear equation is created to determine the boundary values of solute concentration in time step $n+1$.

Problem type 1 boundary values:

$$C_{1,1}^{n+1} = C_0, \quad \sum_{k=1}^M A_{M,k} C_{2,k}^{n+1} = 0 \quad (22)$$

Problem type 2 boundary values:

$$C_{1,1}^{n+1} = C_0, \quad \sum_{k=1}^M A_{M,k} C_{2,k}^{n+1} = 0 \quad (22)$$

Problem type 3 boundary values:

$$(v - n_1 D_1^* A_{1,1}) C_{1,1}^{n+1} - n_1 D_1^* \sum_{k=2}^N A_{1,k} C_{1,k}^{n+1} = v C_0$$

$$\sum_{k=1}^M A_{M,k} C_{2,k}^{n+1} = 0 \quad (23)$$

Which are corresponding to Eqs. (7 and 8). To resolve the discretized equations, MATLAB software is used. For this purpose, all the known parameters are placed to the discretized equations. So, the concentration can be obtained from this procedure. The outcomes are examined by analytical results for the model validation.

V. SIMULATION RESULTS

Three types of problems are considered to verify the correctness of the proposed numerical method and also to investigate the influence of various parameters on the transport process in a double-layer porous medium. The numerical results will be compared with the analytical results presented by Li and Cleall and Leij and van Genuchten [2, 3].

In all cases the effect of various parameters on transport process regarding the dimensionless relative parameters $\theta, \varphi, \rho, \delta$ is investigated. These parameters are assumed to provide more insight into the solution of the problem and are obtained as

$$\theta = \frac{h_2}{h_1}, \varphi = \frac{n_2}{n_1}, \rho = \frac{R_{d2}}{R_{d1}}, \delta = \frac{D_2^*}{D_1^*} \quad (24)$$

A. Problem type 1

For the first problem, the two layers are defined to initially have a zero solute concentration. The solute concentration at the inlet boundary is equal to zero and at outlet boundary solute concentration gradient is fixed to zero, which is often considered as appropriate. The effect of various parameters on the interface and the transport process are shown in Figs. 3 to 8 by dimensionless relative parameters $\delta, \rho, \theta, \varphi$ to provide more insight into the solution of the problem. These dimensionless parameters are:

$$\theta = \frac{h_2}{h_1}, \varphi = \frac{n_2}{n_1}, \rho = \frac{R_{d2}}{R_{d1}}, \delta = \frac{D_2^*}{D_1^*} \quad (25)$$

In this investigation each parameter varies, while others are assigned constant values. the effect of the effective dispersion coefficient (D^*) on transport process in the double-layered porous media with constant values of $\rho = \theta = \varphi = 1$, $v = 4 \times 10^{-9} m/s$ and $H = 1m$ at 2 years is depicted in Fig. 3. It is clear from Fig. 3 that the alteration of the relative effective dispersion coefficient (δ), will vary the concentration gradient between the two layers. This shows that

interface condition depends on the effective dispersion coefficient.

The further results represent the effect of retardation factor on solute transport and is provided in Fig. 4 using $\delta = \theta = \varphi = 1$, Darcy velocity = $4 \times 10^{-9} m/s$, thickness

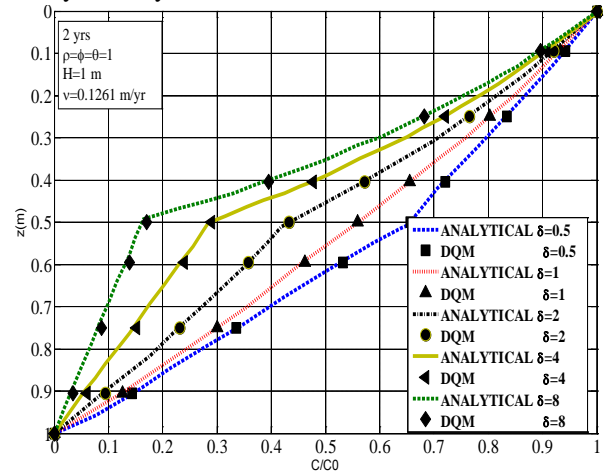


Fig. 3. Calculated Solute concentration profiles for problem 1 with various δ

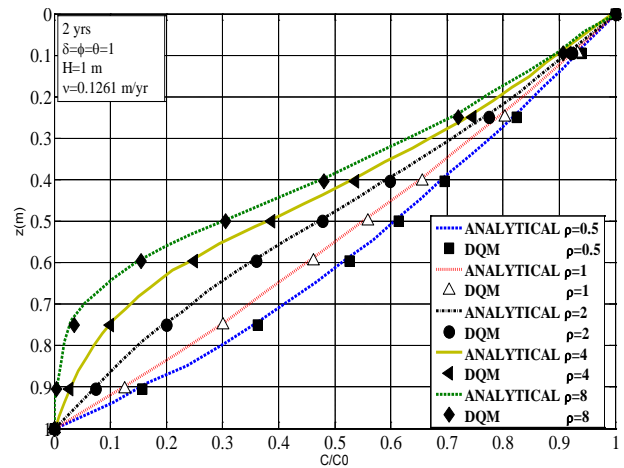


Fig. 4. Calculated Solute concentration profiles for problem 1 with various ρ

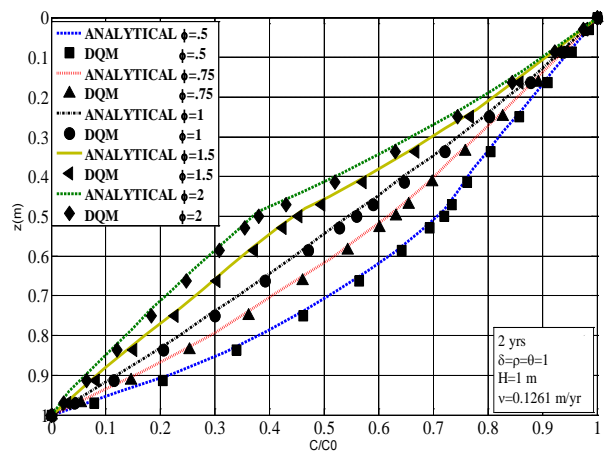


Fig. 5. Calculated Solute concentration profiles for problem 1 with various φ

of the layer is 1m and time is 2 years. After that, φ is assumed to be variable and the rest of the relative variables are assumed fixed ($\rho = \theta = \delta = 1$).

Table 2. RMS values for solute concentration in Fig. 3 in $\delta = 8$

Distance (m)	Analytical result	Mesh size			
		N=5	N= 11	N= 21	N=41
0.2	0.7571	0.7417	0.755	0.7559	0.7575
0.4	0.4037	0.3679	0.3969	0.404	0.404
0.5	0.1693	0.1619	0.1698	0.1702	0.1702
0.6	0.1391	0.1302	0.1368	0.1377	0.1377
0.8	0.0716	0.0665	0.0698	0.0704	0.0704
RMS		0.0183	0.0034	0.0010	0.0009

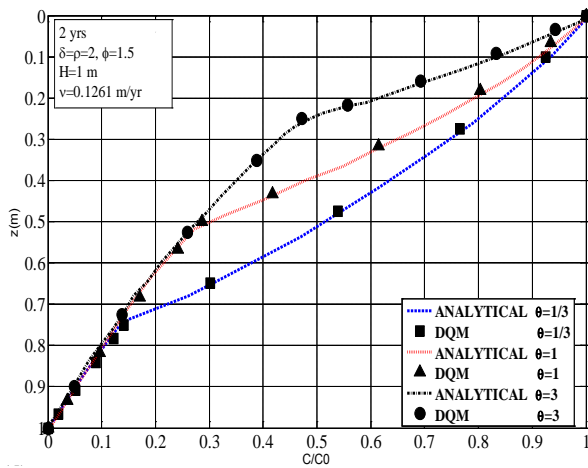


Fig. 6. Calculated Solute concentration profiles for problem 1 with various θ

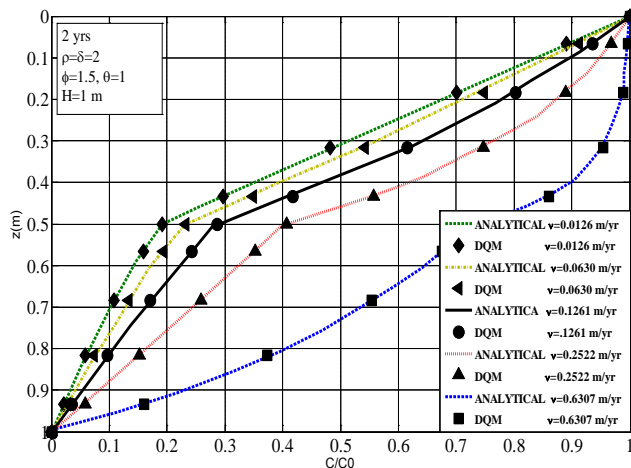


Fig. 7. Calculated Solute concentration profiles for problem 1 with various v

These parameters are kept the same to demonstrate the impact of the porosity of layers on solute transport process (Fig. 5). The impact of the variation of the porosities between the two layers can be clearly seen with a distinct change in the concentration gradient at the interface. To show the impact of

the layer thickness of concentration profile the following values for parameters are used $\rho = \delta = 2$, $H = 1m$ $v = 4 \times 10^{-9} m/s$ and the processing time is considered 2 years.

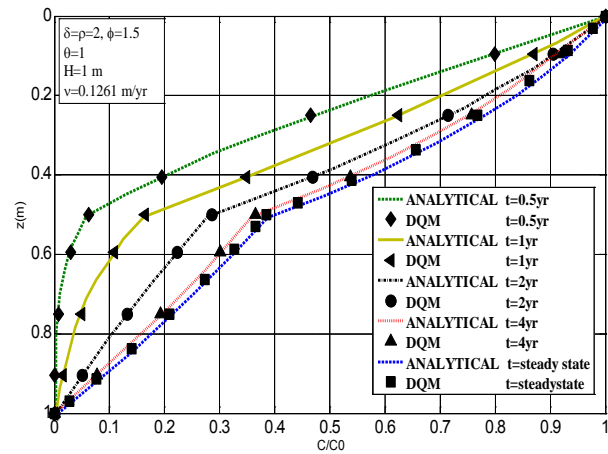


Fig. 8. Calculated Solute concentration profiles for problem 1 at various times

The results are shown in Fig. 6. In Fig. 7 the velocity effect on layers thickness are demonstrated. The solute transport at various times are also investigated using $\rho = \delta = 2$, $\varphi = 1.5$, $\theta = 1$, $H = 1m$ at 0.5, 1, 2, 4 years period while steady state is assumed. Simulation results are provided in Fig. 8.

In the numerical solution, different numbers of grid points were used. Selecting the different number of grid points reveals that mesh sizes can affect the accuracy of the results. To confirm the validity of the results, they are compared with the analytical solution results. Root Mean Square Error (RMS) values for DQ method are calculated for different grid numbers and are given in Table 2 in Fig. 3 with $\delta = 8$ as a case.

From different grid numbers, RMS Error is calculated using Eq. 26 as follows:

$$\Delta h = h_{analytical} - h_{numerical}; RMS = \sqrt{\frac{1}{R} \sum_{i=1}^R |\Delta h_i|^2} \quad (26)$$

Where Δh is the difference between analytical and numerical results for different points and R is the number of data.

The RMS error values for non-uniform mesh size of 5, 11, 21, and 41 using a semi-implicit Crank-Nicholson scheme is compared with analytical solutions as in [3]. The RMS error values can be seen in Table 2 Which indicate there are a good agreement between numerical and analytical results.

Table 2 shows the results for solute concentration at $\delta = 8$ corresponding to Fig. 3. It can be concluded that numerical results obtained from DQM are very close to the analytical

results. Also, when the mesh sizes increase, the RMS error values will reduce.

B. Problem type 2

In this problem it is assumed that the two layers initially have a zero solute concentration and concentration at the inlet boundary is set to C_0 and at outlet boundary solute concentration gradient is equal to zero. Six types of problem similar to prior section are assumed to show the effect of various parameters on contaminant transport under different boundary conditions.

For the four series (depicted in Figs. 9 to 12), one of the dimensionless relative parameters is changed while the rest are kept constant. In these four cases the Darcy velocity is equal to $4 \times 10^{-9} m/s$, the thickness of the porous medium is $H = 1m$ and the time of the process is considered 2 years.

In Fig. 9 effect of the effective dispersion coefficient (D^*) is probed with $\rho = \phi = \theta = 1$. The results show that all curves with different values of $\delta = 0.5, 1, 2, 4, 8$ intersect each other at one point.

In Fig. 10, the impact of retardation factor is investigated considering the different values for ρ while $\delta = \phi = \theta = 1$. In the third case $\delta = \rho = \theta = 1$ is assumed to determine the variation of the porosity on transport process between the two layers. It can be seen that the interface condition is independent of porosity (Fig. 11).

The next case has been depicted in Fig. 12 with $\delta = 2$, $\rho = 0.5$, $\phi = 1.5$ for various values of $\theta = 1, 1/3, 3$ to demonstrate the effect of two layer thickness on solute transport. In the next case, Darcy velocity and its effect on solute transport is investigated. For this purpose, $\delta = 2$, $\rho = 0.5$, $\phi = 1.5$, $\theta = 1$ and $H = 1m$ are assumed. The results have been shown in Fig. 13. The last case with properties equal to prior case except that in this case $v = 4 \times 10^{-9} m/s$ are assumed at different times. The outcomes are depicted in Fig. 14. Normally, selecting the different number of grid points will affect the accuracy of the results. The RMS error values in the case of $\rho = 0.5$ (depicted in Fig. 9) are given in Table 3 (as an example). It can be concluded that the DQM with a rather smaller number of grid points can produce very fine results and negligible RMS error values may occur in DQM results.

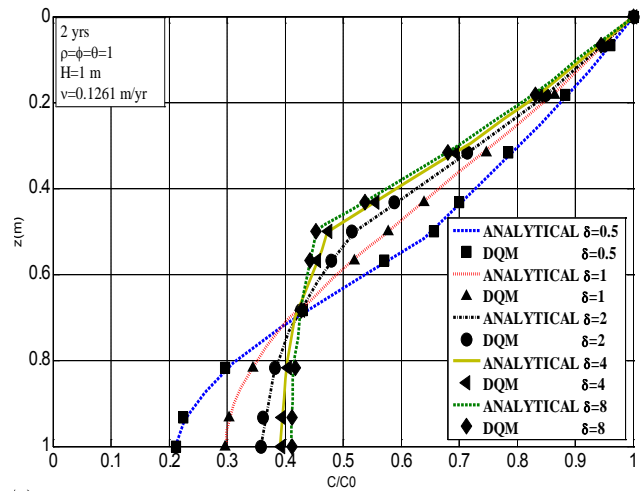


Fig. 9. Calculated Solute concentration profiles for problem 2 with various δ

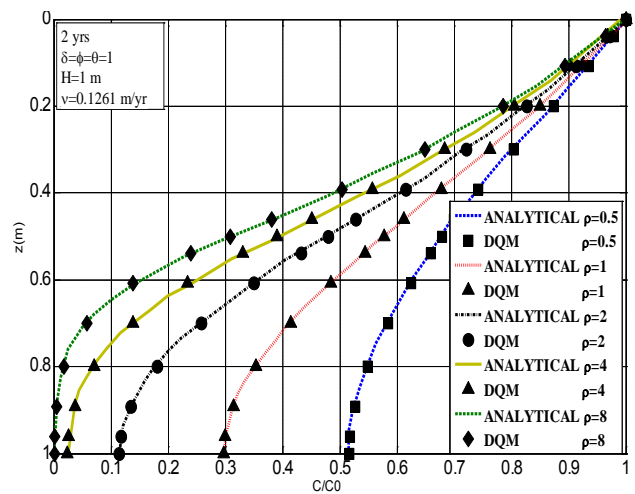


Fig. 10. Calculated Solute concentration profiles for problem 2 with various ρ

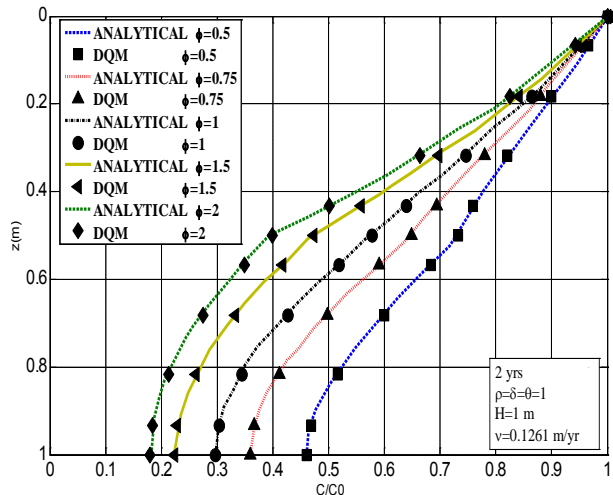


Fig. 11. Calculated Solute concentration profiles for problem 2 with various ϕ

Table 3. RMS values solute concentration in Fig. 10 in $\rho = 0.5$

Distance (m)	Analytical result	Mesh size			
		N=5	N= 11	N= 21	N=41
0.01	0.9370	0.8341	0.9500	0.9358	0.9361
0.06	0.3450	0.4208	0.3427	0.3487	0.3457
0.11	0.0201	0.1364	0.0224	0.0198	0.0198
0.16	0.0025	0.0253	0.0004	0.0006	0.0005
0.19	0.0	0.0004	0.0	0.0044	0.0
RMS		0.0779	0.0060	0.0027	0.001

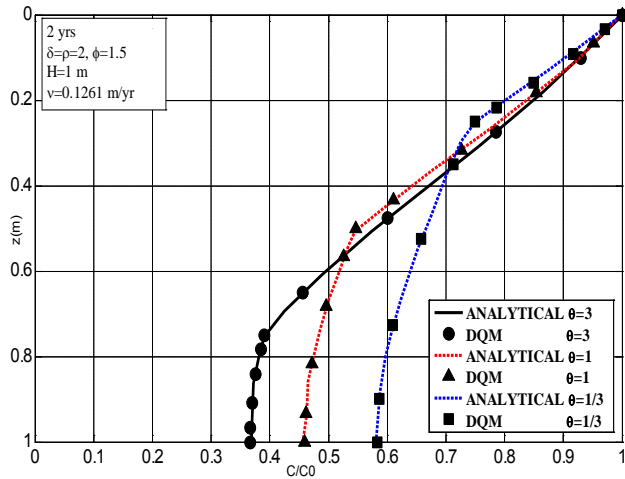


Fig. 12. Calculated Solute concentration profiles for problem 2 with various θ

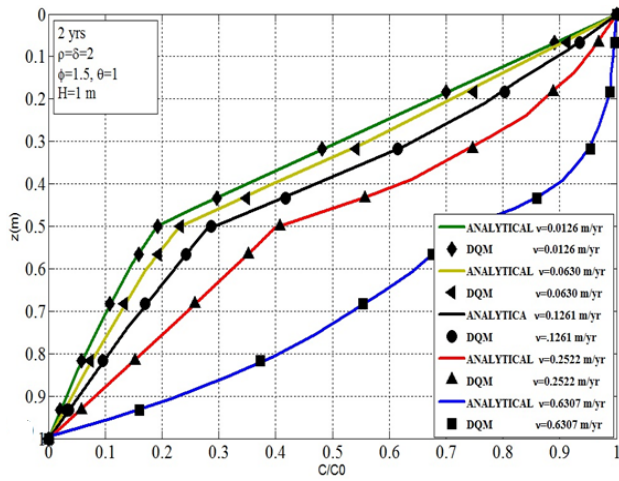


Fig. 13. Calculated Solute concentration profiles for problem 2 with various v

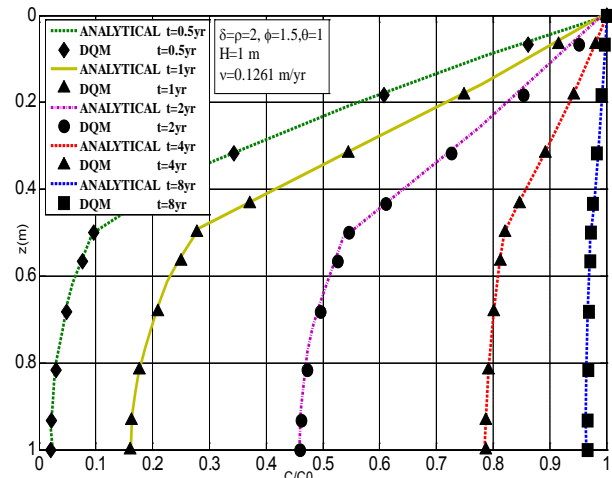


Fig. 14. Calculated Solute concentration profiles for problem 2 at various times

C. Problem type 3

The final problem we studied in this paper is a problem with constant solute flux at the inlet boundary equal to vC_0 and a zero concentration gradient at the outlet boundary as in Eq. (9). The needed parameters to analyze this problem are provided in Table 4.

Table 4. Parameters used in the second problem verification.

Layer	$D^*(m^2/s)$	R_d	n	$h(m)$
Inlet layer	2.315×10^{-8}	1.0	0.4	0.1
Outlet layer	5.787×10^{-8}	1.0	0.25	0.1

In both layers $h = 0.1m$, $R_d = 1$, at inlet layer $D_1^* = 2.315 \times 10^{-8} m/s$ $n_1 = 0.4$ and at outlet layer $n_2 = 0.25$, $D_1^* = 5.787 \times 10^{-8} m/s$ and pore-water velocity $1.1574 \times 10^{-6} m/s$ ($10cm/day$) are assumed. This problem has been probed previously by Leij and van Genuchten and Li and Cleall. The results at various times of 0.2, 0.4, 0.6, 0.8 day are depicted in Fig. 5. The results of the two analytical solutions and DQM show a good match when $t = 0.2$ day but in larger times Leij and van Genuchten as in [3] analytical solution results are less than Li and Cleall work as in [4] and the present work. Indeed, the DQM results are close to the Li and Cleall analytical solution results in Fig 5.

It is seen from Fig 5 that at $t = 0.6$ day and $t = 0.8$ day the solute concentration near the outlet boundary are not correlated with Leij and van Genuchten and Li and Cleall works. In this case, the DQM results are close to Li and Cleall analytical solution.

The RMS error values at $t = 0.2$ day are presented in Tables 5.

Table 5. Leij and van Genuchten and Li and Cleall Analytical and DQM solute concentration represented in Fig. 5 at $t = 0.2$

Distance (m)	Analytical result	Mesh size			
		N=5	N= 11	N= 21	N=41
0.01	0.9370	0.8341	0.9500	0.9358	0.9361
0.06	0.3450	0.4208	0.3427	0.3487	0.3457
0.11	0.0201	0.1364	0.0224	0.0198	0.0198
0.16	0.0025	0.0253	0.0004	0.0006	0.0005
0.19	0.0	0.0004	0.0	0.0044	0.0
RMS		0.0779	0.0060	0.0027	0.001

In this case a good agreement can be seen between Leij and van Genuchten and Li and Cleall analytical solutions. So, the DQM results are compared with Leij and van Genuchten and Li and Cleall analytical solutions simultaneously.

In the case where $t = 0.6$ day (Fig. 5) there is not a good match between the solute concentration for Leij and van Genuchten and Li and Cleall near the outlet boundary. It is seen that the DQM results are in a good agreement with Li and Cleall analytical solution rather than Leij and van Genuchten. Also, negligible errors occur in DQM and Li and Cleall analytical solution.

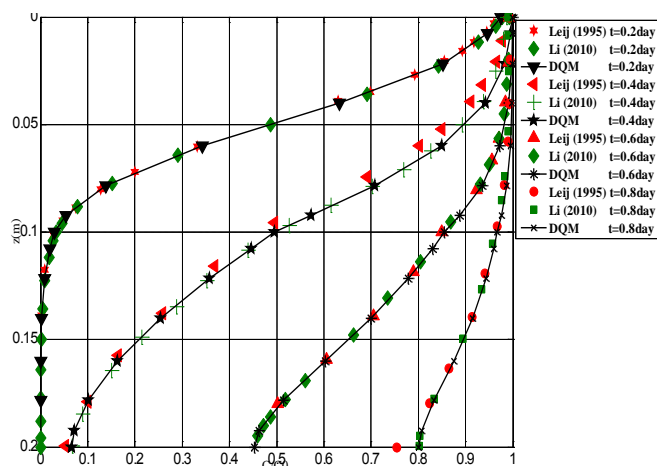


Fig. 5. Solute concentration profiles in problem 3

VI. CONCLUSION

The DQM has been widely used for solving PDE's, recently. However, this method has not been used extensively in solute transport problems and more specifically, in solute transport in layered porous media. In this work, a DQM solution was utilized for solute transport problem in double layered porous media. Three different types of problems were solved and the results were compared with analytical solutions. The comparisons of this work show lower RMS error value, less computational time, rapid convergence than the other numerical methods while a good agreement with the exact results. Furthermore, applying the boundary conditions in

conservative numerical methods (FE, FD, FV) accompanies with many difficulties which is not the case for DQM.

REFERENCES

- [1] W.A. JURY, Simulation of solute transport using a transfer function model". 1982. *Water Resour. Res*
- [2] FJ. Leij, FJ. MT. van Genuchten), Approximate analytical solutions for solute transport in two-layer porous media. *Transport in Porous Media*.1995. 18(1):65–85
- [3] Y. c. Li, P. J. Cleall, Analytical solutions for advective–dispersive solute transport in double-layered finite porous media, *Int. J. Numer. Anal. Meth. Geomech*. 2011. 35:438–460
- [4] R. Bellman, J. Casti, Differential quadrature and long term integration. 1971. *J. Math. Anal. Appl*.
- [5] C. Shu, B. C. Khoo, K. S. Yeo. Numerical solution of incompressible Navier-Stokes equations generalized differential quadrature. 1994. *Finite Element in Analy. Design.*, 18, 83-97.
- [6] C. Shu, B. E. Richards. Application of generalized differential quadrature to solve two-dimensional incompressible Navier-Stokes equations. 1992a. *Int. J. Numer. Methods Fluids.*, 15, 791-798.
- [7] C. Shu, B. E. Richards. Parallel Simulation of Incompressible Viscous Flows by Generalized Differential Quadrature. *Computing Systems in Engineering*. 1992b. 3, 271–281.
- [8] C. Shu, H. Xue. Explicit Computation of Weighting Coefficients in the Harmonic Differential Quadrature. *J. Sound and Vibration*. 1997. 204(6), 549-555.
- [9] C. Shu, Y. T. Chew. Fourier Expansion-Based Differential Quadrature and Its Application to Helmholtz Eigenvalue Problems. 1997. *J. Commun. Numer. Meth. Eng.*, 13(11), 643-653.
- [10] C. Shu, H. Ding, K. S. Yeo. Local radial basis function-based differential quadrature method and its application to solve two-dimensional incompressible Navier–Stokes equations. 2003. *J. Comput. Methods Appl. Mech. Eng.*, 192, 941–954.
- [11] C. Shu, H. Ding, H. Q. Chen, T. G. Wang. An upwind local RBF-DQ method for simulation of inviscid compressible flows. *Comput. Methods Appl. Mech. Eng*. 2005. 194, 2001-2017.
- [12] C. Shu, *Differential Quadrature and its Application in Engineering*. Springer, 2000.
- [13] J. O. Mingle, Computational considerations in nonlinear diffusion. *Inter. J. Numer., Methods Engrg*. 1973. 7, 103-116.
- [14] F. Civan, C. M. Sliepcevich, Differential quadrature for multidimensional problems. *J. Math. Anal. Appl*. 1984. 101, 423-443.
- [15] J. R. Quan, C. T. Chang. New insights in solving distributed system equations by the quadrature method-1. *Comput. Chem. Energy*. 1989. 13, 779–788.
- [16] W. Chen, Y. Yongxi. Calculation and analysis of weighting coefficient matrices in differential quadrature. *Proc., of the 1st Pan-Pacific Conference on Computational Engineering*. 1993. 157-162.



Meysam Ghamari Adyan was born on March 23, 1985. He received the B.S. degree in Civil engineering from Shahid Rajaee university, Tehran, Iran, in 2008 and the M.Sc. degree in Civil Engineering, water engineering from Iran University of science and technology, Tehran, Iran in 2012.

His current research interests include the Fluid dynamics, Solute transport modeling in porous media and Coastal engineering.



Abbas Ghaheri received B.S. degree in Irrigation and Reclamation, University of Tehran, Tehran, Iran and the M.Sc. and Phd degrees in Civil engineering from Colorado State University, USA.

He is currently with the Civil Engineering Department, Faculty of Engineering, Iran University of Science and Technology, Tehran, Iran, as an Associate Professor. His research interests include

Fluid Mechanics, Ground Water Hydrology and Hydraulics and Solution to Ground Water Problems.

Catastrophic Danube flood scenario between Kienstock and Nagymaros using NLN model

V. Bacova Mitkova, P. Pekarova, J. Pekar

Abstract—Hydraulic models used in hydrology are demanding large amounts of the input data. Therefore, utilization of the hydrological models of the wave transformation is one of the alternative solutions for operative real time flood forecasting. This paper presents application of the simple non-linear river model NLN-Danube for the forecasting of the flood event occurred on the Danube River in June 2013. The model NLN-Danube is the hydrologic model aimed on the simulation of discharges in open channels. NLN model simulates flood wave transformation in six river sections: Ybbs–Kienstock–Devin/Bratislava–Medvedov–Iza–Sturovo–Nagymaros. The second part of this paper presents the simulation of the scenario catastrophic flood for the today river conditions, based on the historical Danube flood from the year 1501. This flood was the highest flood described on the Upper Danube River basin during the last 600 years.

Keywords — catastrophic flood scenario, Danube River, nonlinear river routing model.

I. INTRODUCTION

PRACTICAL applications of mathematical models and mathematical methods constantly increase especially in a number of important areas such as hydrology (e.g. flood forecasts in real time, flood protection, planning and design of hydraulic structures, simulation of flood waves). Determination of the flood hazard is an important aspect and difficult task for hydrologic practice.

This development we can see in the growing number of publications, projects and mathematical models focused on hydrological modeling and forecasting. For example in the last years Smith [1] applied data-based mechanistic (DBM) models to forecast flash floods in a small Alpine catchment. Kjeldsen [2] tested the effect of urban land cover on catchment flood response using a lumped rainfall–runoff model, and compared flood events from selected UK catchments with mixed urban

This work was supported in part by the Slovak Research and Development Agency under the contract No. APVV-015-10 and by the MVTS „Flood regime of rivers in the Danube river basin“, and it results from the project implementation of the “Centre of excellence for integrated flood protection of land” (ITMS 26240120004) supported by the Research & Development Operational Programme funded by the ERDF.

V. Bacova Mitkova is with Institute of Hydrology Slovak Academy of Sciences, Bratislava, Slovakia, (e-mail: mitkova@uh.savba.sk).

P. Pekarova is with Institute of Hydrology Slovak Academy of Sciences, Racianska 75, 831 02 Bratislava, Slovakia, (phone: +4212 44259311, Fax: +4212 44259311, e-mail: pekarova@uh.savba.sk).

J. Pekar is with the Faculty of Mathematics, Physics and Informatics, Comenius University, Bratislava, Slovakia (e-mail: pekar@fmph.uniba.sk).

and rural land use. Wu in [3] investigated potential impact of climate change on flood risk for the city of Dayton, which lies at the outlet of the Upper Great Miami River Watershed (Ohio, USA). He used a statistical model based on regression and frequency analysis of random variables to simulate annual mean and peak streamflow from precipitation input. Hydrological model based on the CSC and kinematic wave functions using gauge-adjusted radar rainfall data was applied for flash flood prediction in [4]. Simulation of the June 11, 2010, flood along the Little Missouri River, using a hydrologic model coupled to a hydraulic model was investigated in [5].

Monitoring and evaluation of extreme hydrological phenomena through the different programs, projects and models are also highly actual for the second longest river in Europe – the Danube River – or its tributaries. For example, the floods mapping on the Danube River using radar imaging SAR (Synthetic Aperture Radar) was reported in [6]. Pekarova et al. in [7] presented the history of floods and extreme flood frequency analysis of the upper Danube River at Bratislava. A hydrological modeling framework applied within operational flood forecasting systems on three Danube tributary basins (Traisen, Salzach and Enns) is presented in [8]. Dankers et al. in [9] dealt with simulation of flood risks for the Upper Danube using the hydrologic model LISFLOOD. In [10] Bohm & Wetzel analyzed historical floods on the rivers Lech and Isar. Szolgay [11] used multi-linear discrete cascade model for river flow routing and real time forecasting in river reaches with variable speed. In [12] the model KLN-MULTI was calibrated and used for modeling of several historical flood waves on the Danube River under present hydraulic conditions. Blaskovicova et al. in [13] evaluated trends of the changes of the average annual and maximum annual discharges on the Danube River in Bratislava gauging station.

The Danube River was and still is a symbol of strategic importance and trade. River regime conditions of the Danube River have been continually changing. These changes result from the natural processes (erosion, sedimentation, vegetation cover) or anthropogenic activities (modification of the riverbank, construction of dykes and hydro–power stations). It has significant impact upon the transformation of flood waves in the river channel.

On the basis of the development mentioned above the short-term forecasting of the flows becomes more demanded. From this reason it is necessary to use and to deal with new methods and procedures that better reflect changes in hydrological river

conditions. This process cannot be considered closed. Forecasting models and methods have to be constantly updated to the latest conditions and current situation in the basin. For this purpose simple river model NLN-Danube [14], [15] was constructed. Development of conceptual non-linear reservoir cascade models was one of several approaches to incorporate nonlinearity into hydrological routing models (see [16]-[20]).

The objective of this paper is to present (on the example of extreme flood situation on the Danube River) results needed for flood protection obtained using a relatively simple tool of engineering hydrology. Firstly, short description of the non-linear river model NLN-Danube is presented. Secondly, the model NLN-Danube was used for forecasting of the flood event occurred in June 2013, calibrated on the flood event on the Danube River in August 2002. Forecasting of the June 2013 flood discharges by model NLN-Danube was done on the Danube River reach Kienstock–Sturovo. Finally the simulation of transformation of the potentially catastrophic flood by the model NLN-Danube for present river regime conditions was done.

II. NONLINEAR ROUTING MODEL NLN–DANUBE

A. Model description

Model NLN-Danube [15] goes out from model NONLIN by Svoboda (1993, 2000). Model of each section of the simulated system is based upon the concept of a series of equal non-linear reservoirs, thus belonging to the category of hydrological conceptual non-linear models. Model input (P) represents the input into the first reservoir of the cascade (Figure 1), its output is the input into the second one in series, etc., and the output from the last reservoir is the output (Q) from the model of the section.

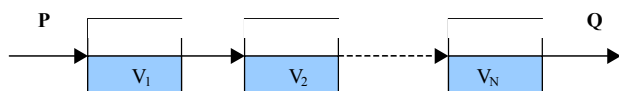


Fig. 1 Scheme of the NLN-Danube model

Movement of the wave through reservoir is defined by discharge (Q) and by volume of reservoir (V) as:

$$Q = BV^{EX} \quad (1)$$

where:

Q - reservoir output;

V - volume of reservoir [m^3];

EX - the nonlinearity parameter;

B - the proportionality parameter.

The flood wave propagation is modeled in equidistant discrete time steps $0, 1, 2, \dots, m$. The difference between two steps is given by parameter ΔT . In time steps i and $i+1$, for known input P_{i+1} and output Q_i , the unknown output Q_{i+1} is determined from the continuity equation within the time interval $i+1$ of the length ΔT as:

$$(P_{i+1} - Q_{i+1})\Delta T = V_{i+1} - V_i, \quad (2)$$

where:

P_{i+1}, Q_{i+1} - the average i/o of the interval $i+1$;

V_{i+1}, V_i - storage at the interval $i+1$ and i .

From equations (1) and (2) we receive:

$$(P_{i+1} - Q_{i+1})\Delta T = \frac{Q_{i+1}^{1/EX} - Q_i^{1/EX}}{B^{1/EX}} \quad (3)$$

The equation (3) defines the non-linear function f of one unknown Q_{i+1} ,

$$f(Q_{i+1}) = (P_{i+1} - Q_{i+1})\Delta T - \frac{Q_{i+1}^{1/EX} - Q_i^{1/EX}}{B^{1/EX}}, \quad (4)$$

which is searched by linearisation (Newton) method

$$Q_{i+1}^{(k+1)} = Q_{i+1}^{(k)} - \frac{f(Q_{i+1}^{(k)})}{f'(Q_{i+1}^{(k)})}, \quad (5)$$

what gives in our case the iteration formula:

$$Q_{i+1}^{(k+1)} = Q_{i+1}^{(k)} + \frac{(P_{i+1} - Q_{i+1}^{(k)})\Delta T - \left[\frac{(Q_{i+1}^{(k)})^{1/EX} - (Q_i)^{1/EX}}{B^{1/EX}} \right]}{\Delta T + (Q_{i+1}^{(k)})^{(1-EX)/EX} \cdot B^{-1/EX} \cdot EX^{-1}} B^{-1/EX} \quad (6)$$

The parameters of the transformation curve shape are expressed by ratio parameter B ,

$$B = \left(\frac{N \cdot \Delta T}{BK} \right)^{EX}, \quad (7)$$

where: N - number of storages in one section of the model;
 BK - "time constant" of an equivalent linear system.

The iteration process (6) is performed with accuracy of 0.001. Parameters of the model calibration are:

BK - time constant of the equivalent linear system [hrs];

ΔT - length of the time step [hrs];

QC - corresponds to the maximum capacity of the main river channel (flow, when water enters the inundation) [$m^3 \cdot s^{-1}$];

EX - the nonlinearity parameter, dimensionless;

N - number of reservoirs in series, dimensionless;

NU, NL - tributaries in section (yes=1, no=0).

B. Model calibration

Model NLN-Danube was calibrated on set of the summer floods occurred during 1991– March 2002 for river reach Kienstock–Nagyvaros (Figure 2). The up stream water gauging station Kienstock was chosen because it is located at a sufficient distance from Bratislava and gives a fair forecast lead time.



Fig. 2 The gauging stations Kienstock-Bratislava-Nagymaros in the Danube River basin

The hourly discharge data of the flood were available from the Slovak Hydrometeorological Institute (SHMI) – Bratislava, gauge Bratislava (Photo 1). Procedure of the calibration of a given river section by trial - error method was evaluated and published in [21]. For evaluation of accuracy of the model simulation the following statistical indicators were used: coefficient of correlation R, mean error ME, mean absolute error MAE, mean absolute percentage error MAPE, standard deviation SD, and maximum absolute error MAX. The MAPE value of 4.8% was obtained for whole river reach between measured and simulated discharges. The mean correlation coefficient value of 0.99 for whole river reach Kienstock–Nagymaros was also calculated. These values show a good agreement between measured and simulated discharges. Figure 3 presents verification of the August 2002 flood wave transformation in each gauging station of the simulated Danube River reach.

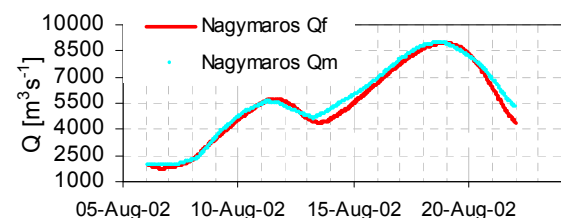
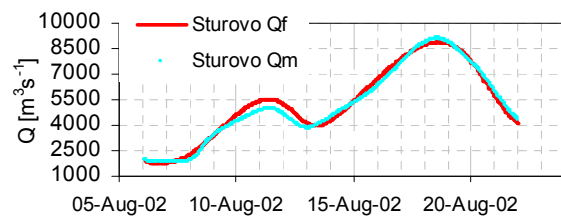
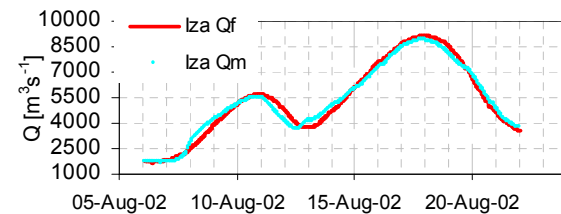
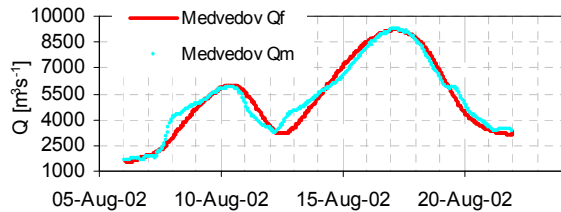
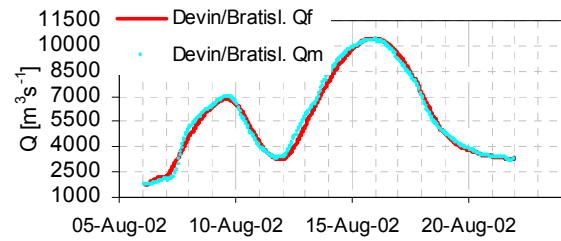


Fig. 3 Verification of the model NLN-Danube on flood occurred in August 2002



Photo 1 Danube River, Bratislava gauge station, 2002 and 2013 floods, (Photo Pekarova, 2.7.2013)

III. FORECASTING OF THE 2013 DANUBE FLOOD

A. Hydrological and meteorological situation

Extreme flooding in Central Europe began after several days of heavy rain in late May and early June 2013. This extreme hydrological situation started on May 29, 2013 based on heavy rains in the upper part of the Danube basin [13]. From the climatologic point of view, May 2013 was one of the three wettest months of May in the past 150-years in this part of the Danube basin.

Heavy precipitation occurred mainly in sub-basins of the rivers Isar, Inn, Traun, Enns, and Ybbs. Bavarian basin, for example, had 120 mm of precipitation in average, the basins of Inn and Salzach had 150 mm of precipitation and the basins of Traun, Enns and Ybbs had 150 mm of precipitation, per four days (May 29–June 2, 2013). The sub-basin of the Danube River between Ybbs and Morava River had 60 mm of precipitation [22]. Blöschl et al. [23] described the June 2013 flood in the Upper Danube basin, and compared it with the 2002, 1954, and 1899 floods. They described local atmospheric and meteorological conditions and runoff generation of the 2013 flood.

Because the heavy precipitation did not hit only the German part of the Danube basin, but also the Austrian part of the Danube basin, water levels started to increase almost simultaneously. The Bavarian Danube and the Inn join at Passau. For example, water level in gauging station Passau-Ilzstadt started to increase already on 30 May from the level of 553 cm to the level of 1102 cm. After the confluence of the Bavarian Danube and Inn the wave traveled downstream the Austrian Danube changing shape and shifting the timing. Recorded flows from Austrian part of Danube were high, caused by heavy precipitation in basins of the rivers Traun, Enns and Ybbs. The culminations at the Austrian gauging stations Ybbs and Kienstock started at the evening on Thursday June 4, 2013.

The Slovak part of the Danube River started to increase on Friday May 31, 2013. Water level increased by 280 cm per 24 hours at Devin gauge. Due to temporary interruption of the rainfall; water level also did not raise temporary. Water levels again started to increase from Sunday June 2, 2013 to Thursday June 6, 2013. The culmination of the Danube River occurred on Thursday June 6, 2013 (at 3:15 p.m.) at Devin gauge station (974 cm , $10\,640 \text{ m}^3\text{s}^{-1}$) and about two hours later at Bratislava (1034 cm , $10\,641 \text{ m}^3\text{s}^{-1}$) [22].

B. Forecasting of the 2013 Danube flood

We continuously forecasted the Danube discharge during the May/June 2013 flood on the Danube River. We used nonlinear river model NLN-Danube, calibrated after the last large Danube flood event in August 2002. The hourly discharges from upstream water gauging station Kienstock were used as input data to the model.

As mentioned above, water gauging station Kienstock gives a fair forecast lead-time for Bratislava. For example, travel time of the peaks of the floods from Kienstock to Bratislava in September 1899 ($10\,870 \text{ m}^3\text{s}^{-1}$ at Bratislava [24]), and in August 2002 ($10\,390 \text{ m}^3\text{s}^{-1}$ at Bratislava) was estimated with values of 45 and 47 hours.

Transformation of forecasted flood wave discharge at current river conditions is illustrated in Figure 4. For each part of the Danube River reach the basic statistical characteristics of forecasted and measured discharges and errors of the forecast for June 2013 flood were calculated. Mean absolute percentage error (MAPE) of the model between forecasted and measured discharges reached the value of 7.6 %. The correlation coefficient between forecasted and measured discharges was calculated with value of 0.978.

The flood wave culmination was forecasted by model NLN-Danube to occur later than it was recorded in reality, at water gauge stations Medvedov and Iza. These differences of the culmination time occurrence in year 2013 are not significant. Therefore we can assume, that there are no significant changes in travel time of the floods with a peak discharge above of $10\,000 \text{ m}^3\text{s}^{-1}$. Travel time of selected historical flood peaks is illustrated in Figure 5.

From Figure 5 it follows, that travel time of the June 2013 flood in river reach Ybbs–Sturovo was similar to travel time of

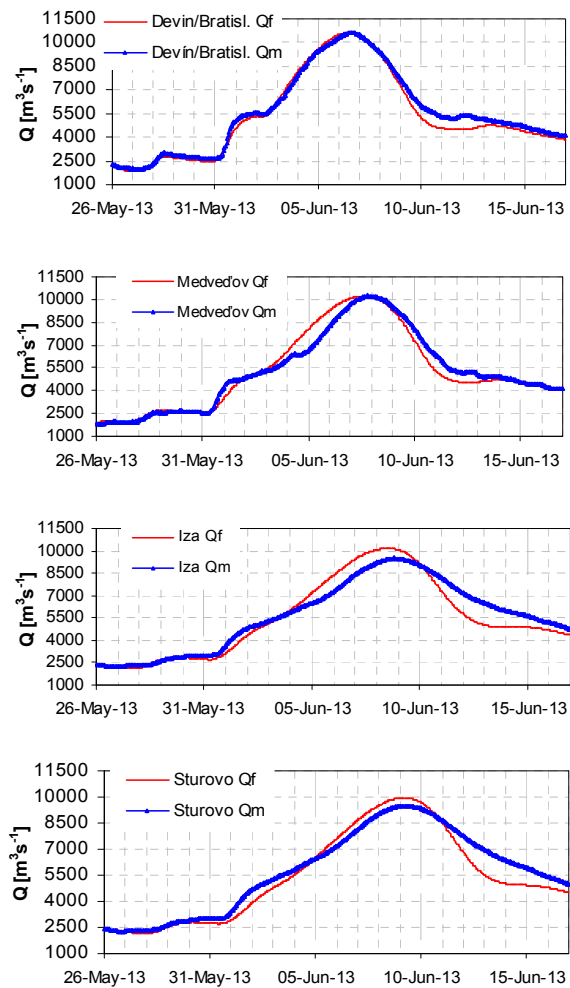


Fig. 4 Forecasting of the June 2013 flood wave transformation by the model NLN-Danube, river reach Kienstock–Sturovo, stations: Devin/Bratislava, Medvedov, Iza, Sturovo. Qm – measured discharge, Qf– forecasted discharge

the flood occurred in August 2002. Moreover, values of the forecasted peak discharges were higher than recorded in stations Medvedov, Iza and Sturovo. This positive result may be caused by the proper manipulation on the water power plant Gabčíkovo or by changes in the river regime conditions of the Danube since 2002 in selected section.

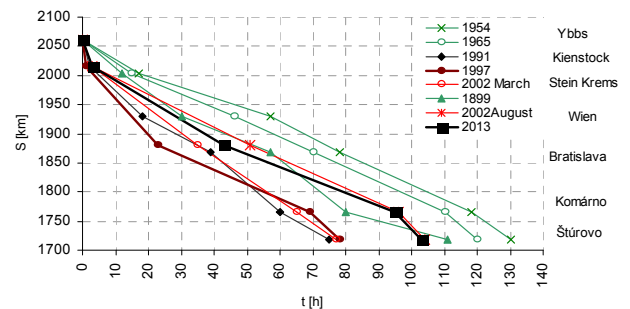


Fig. 5 Travel times of the peak discharges of the selected floods on the Danube River reach Ybbs–Sturovo

C. Recalibration of the model NLN-Danube

Due to results mentioned above, we recalibrated the model NLN-Danube parameters for present river regime conditions on the Danube River. Some basic characteristics and obtained model errors are presented in Table 1 for two stations of the Danube River reach. Mean absolute percentage error (MAPE) was calculated and it reached value of 4.75%. Mean coefficient of correlation reached the value of 0.992 for the whole Kienstock–Sturovo reach of the Danube River.

Table 1 Basic statistical characteristic of simulated and measured discharges and errors of the forecasting – recalibration of the model NLN-Danube parameters including the Danube flood in June 2013

	Devin/Bratislava forecast / measured	Sturovo forecast / measured
Mean [m^3s^{-1}]	5388 / 5601	5636 / 5758
Min [m^3s^{-1}]	1860 / 1968	2290 / 2231
Max [m^3s^{-1}]	10 612 / 10 640	9601 / 9488
Volume [mil m^3]	10 261 / 10 667	10 779 / 10 965
R [-]	0.991	0.993
ME*	213.7	121.2
MAPE*	6.4	4.6

*ME – mean error, MAPE – mean absolute percentage error.

IV. SIMULATION OF CATASTROPHIC FLOOD SCENARIO FOR PRESENT DANUBE RIVER REGIME CONDITIONS

Finally, we used the recalibrated model NLN-Danube for simulation of transformation of the scenario catastrophic flood events.

The peak discharge of the simulated catastrophic flood wave of the value of $14\,000\text{ m}^3\text{s}^{-1}$ was selected. Based on archive records concerning historical floods on the Upper Danube, such catastrophic flood occurred on the Danube River in August 1501 [7]. The peak discharge during 1501 flood was estimated from the peak water level in Vienna. The August 1501 flood has been regarded by hydrologists as the largest flood for the last 600-1000 years on the Upper Danube. The water level of 1070 cm was reached during this flood at Stein-Krems [25], [26]. Moreover, experiences from the regime of summer floods on the Danube River show that flood in August 1501 might be caused by heavy precipitation on the whole Bavarian and Austrian part of the Danube River. The Alpine tributaries are main sources of the water in this area of the Danube River. Their culminations gradually met and contributed to flood wave on the Danube River.

The June 2013 flood was the largest flood recorded and directly measured on the Danube River at Bratislava since 1899 and it had similar meteorological conditions. Therefore, simulation of the catastrophic scenario was based on the hydrograph of the June 2013 flood. Wave transformation of the potentially catastrophic flood between Kienstock and Sturovo is illustrated in Figure 6 for present river regime conditions of the Danube River.

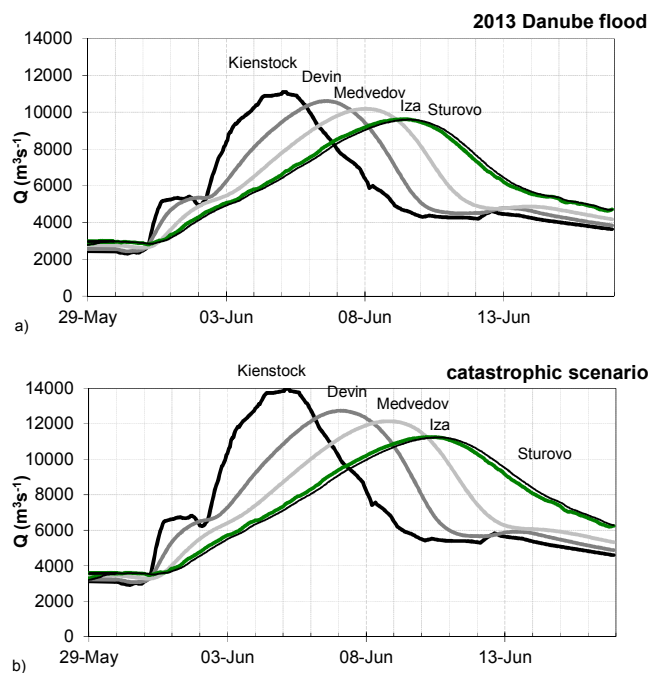


Fig. 6 Transformation of the flood wave:

- simulation of the June 2013 flood between Kienstock and Sturovo for present river conditions on the Danube River
- simulation of the catastrophic flood wave between Kienstock and Sturovo for today river conditions on the Danube River

Simulated peak discharges for individual water gauging stations are presented in Table 2.

Results of this simulation show, that the travel time of the peak catastrophic flood wave could reach value of 50 hours from Kienstock to Devin, with peak discharge on value of $12\,790\text{ m}^3\text{s}^{-1}$ at Devin (it corresponds to water level value of 1 120 cm, for present river conditions of the Danube River).

Table 2 also presents simulated values of peak discharges of the catastrophic flood wave scenario based on the hydrograph of Danube flood in August 2002 between Kienstock and Sturovo given in [12]. Results of the simulation showed the peak travel time value of about 54 hours from Kienstock to Devin with peak discharge value of $12\,430\text{ m}^3\text{s}^{-1}$ (it corresponds to water level value of 1 072 cm, for the Danube River conditions in 2002).

Table 2 Values of peak discharges according to simulation of the catastrophic flood wave scenario on the Danube River by model NLN-Danube

Scenario peak (simulation)	Devin/Bratislava	Iza	Sturovo
Peak₂₀₁₃ [m^3s^{-1}]	10 640	9 497	9 488
Peak ₂₀₀₂ [m^3s^{-1}]	9 240	9 103	8 960
Peak [m^3s^{-1}]*	12 745	11 259	11 233
Peak [m^3s^{-1}]**	12 430	10 930	10 630

* Scenario based on the hydrograph of June 2013 Danube flood.

** Scenario based on the hydrograph of August 2002 Danube flood.

V. CONCLUSIONS

During the June 2013 flood we used nonlinear NLN Danube river model for forecasting of the flood at Bratislava city for 48 hours ahead. After 2013 flood we recalibrated the model, and we used it for catastrophic flood wave simulation for present river conditions on the Danube River. Sufficient accuracy of the model was verified by several statistical criteria. Model NLN-Danube for its relative simplicity and minimal input data requirements is very useful tool.

From our simulations it follows, that the travel time of peaks of the both last big Danube floods (August 2002 and June 2013) was very similar along the Slovak part of the Danube. On the other hand, the peak water levels are continuously rising. Today the peak water levels are higher at the same discharges. While during 1899 flood the water level at Bratislava gauging station reached 970 cm at discharge of the $10870 \text{ m}^3\text{s}^{-1}$, in 2013 the water level reached 1034 cm at discharge of the $10640 \text{ m}^3\text{s}^{-1}$. From the measured water levels and model simulations it follows, that due to man activities along the Austrian and Slovak part of the Danube (construction of dykes) as well as natural raise of sediments and gravel accumulations in the river channel the flood transformation effect continually decreases and the flood thread rises.

REFERENCES

- [1] P. J. Smith, L. Panziera, and K. J. Beven. "Forecasting flash floods using data-based mechanistic models and NORA radar rainfall forecasts". *Hydrol. Sci. J.*, pp. 1-15, Publ. online: Jan 2014, ahead-of-print 2014.
- [2] T. R. Kjeldsen, J. D. Miller, and J. C. Packman, "Modelling design flood hydrographs in catchments with mixed urban and rural land cover", *Hydrology Research*, vol 44, no 6, pp 1040–1057, 2013.
- [3] S. Y. Wu, "Potential impact of climate change on flooding in the Upper Great Miami River Watershed, Ohio, USA a simulation-based approach", *Hydrol. Sci. J.*, vol. 55, no. 8, pp. 1251–1263, 2010.
- [4] S. Rozalis, E. Morin, Y. Yar, and C. Price, "Flash flood prediction using an uncalibrated hydrological model and radar rainfall data in a Mediterranean watershed under changing hydrological conditions", *J. Hydrol.*, vol. 394, pp. 245–255, 2010.
- [5] D. A. Westerman, and B. R. Clark, "Simulation of the June 11, 2010, Flood Along the Little Missouri River near Langley, Arkansas, Using a Hydrologic Model Coupled to a Hydraulic Model", U.S. Geological Survey Scientific Investigations Report no. 5056, p. 35, 2013.
- [6] T.Y. Gan, F. Zunic, and T. Strobl, "Flood mapping of Danube River at Romania using single and multi-date ERS2-SAR images", *International Journal of Applied Earth observation and geoinformation*, vol. 18, p. 69–81, 2012.
- [7] P. Pekarova, D. Halmova, V. Bacova Mitkova, P. Miklanek, J. Pekar, and P. Skoda, "Historic flood marks and flood frequency analysis of the Danube River at Bratislava, Slovakia", *J. Hydrol. Hydromech.*, vol. 61, no. 4, pp. 326–333, 2013
- [8] P. Stanzel, B. Kahl, U. Haberl, M. Hernnegger, and H. P. Nachtnebel, "Continuous hydrological modeling in the context of real time flood forecasting in Alpine Danube tributary catchments", XXIVth Conference of the Danubian Countries. IOP Conf. Ser.: Earth Environ. Sci., vol. 4, 012005, pp. 1–7, 2008.
- [9] R. Dankers, O. B. Christensen, L.Feyen, M. Kalas, and A. De Roo, "Evaluation of very high-resolution climate model data for simulating flood hazards in the Upper Danube basin", *J. Hydrol.*, vol. 347, no. 3–4, pp. 319–331, 2007.
- [10] O. Böhm, and K. F. Wetzel, "Flood history of the Danube tributaries Lech and Isar in the Alpine foreland of Germany", *Hydrol. Sci. J.*, vol. 51, pp. 784–798, 2006.
- [11] J. Szolgay, "Multilinear discrete cascade model for river flow routing and real time forecasting in river reaches with variable speed", *Proceedings of the ESF LESC Exploratory Workshop held at Bologna, Italy*. p. 14, 2003.
- [12] V. Mitkova, P. Pekarova, P. Miklanek, and J. Pekar, "Analysis of flood propagation changes in the Kienstock – Bratislava reach of the Danube River", *Hydrol. Sci. J.*, vol, 50, no.4, pp. 655–668, 2005.
- [13] L. Blaskovicova, Z. Danacova, L. Lovasova, V. Simor, P. Skoda, "Evolution of selected hydrological characteristics of the Danube in Bratislava", *Slovak Hydrometeorological Institute, SHMI Bratislava*, p. 15, 2013 (in Slovak).
- [14] A. Svoboda, "Nonlinear cascade hydrological model NONLIN", HOMS Reference Centre, WMO, Geneva. Component No. J15.2.02, 1993.
- [15] P. Pekarova, J. Pekar, and P. Miklanek, "River model of non-linear cascade NLN-Danube of Danube river between Ybbs and Nagymaros in EXCEL 97", *Acta Hydrologica Slovaca*, vol. 2, no. 2, IH SAS Bratislava, pp. 241–246, 2001 (in Slovak).
- [16] E. M. Laurenson, "A catchment storage model for runoff routing". *J. Hydrol.*, 2, pp. 141-163, 1964.
- [17] T.A. Malone, and I. Cordery, "An assessment of network models in flood forecasting", *New directions of surface water modelling, Proceedings of Baltimore Symposium*, ed. Kavvas, M.L., IAHS publ. no 181, pp. 115–124, 1989.
- [18] C. Corbus, "Contributions to approaching the floods propagation with the help of the theory of the systems", In: *CD Proc. XX1st Conf. of the Danube Countries on Hydrological Forecasting (Bucharest, Romania)*, National Institute of Meteorology and Hydrology, Bucharest, ISBN 973-0-02759-5, 2002.
- [19] N.H. Crawford, R.K. Linsley, "A conceptual model of hydrologic cycle", In *Commission on Subterranean Waters. IAHS Publication No. 63*. IAHS Press: Wallingford; pp. 573–587, 1964.
- [20] V. Mitkova, R. Kubes, J. Szolgay, and P. Pekarova, "Simulation of 1899 and 1954 Danube flood waves transformation in the river reach Kienstock – Bratislava in the present hydraulic conditions", *Acta Hydrologica Slovaca*, vol. 5, no. 1, IH SAS Bratislava, pp. 52–62, 2004 (in Slovak).
- [21] L. Blaskovicova, O. Horvat, K. Hlavcova, S. Kohnova, J. Szolgay J. "Methodology for post-event analysis of flash floods - Svacnický Creek case study". In *Contributions to Geophysics and Geodesy. ISSN 1335-2806*, vol. 41, no. 3, p. 235-250, 2011.
- [22] SHMI, "June 2013 Danube flood", *Slovak Hydrometeorological Institute, SHMI report, Bratislava*, p. 39, 2013.
- [23] G. Blöschl, T. Nester, J. Komma, J. Parajka, and R. A. P. Perdigão, "The June 2013 flood in the Upper Danube basin, and comparisons with the 2002, 1954 and 1899 floods", *Hydrol. Earth Syst. Sci.* vol. 17, no. 7, pp. 9533–9573, 2013.
- [24] H. Angelini, "Danube flood in July 1954", *Bratislava. Hydrological Study. HMI Department of Hydrology, Bratislava, Slovak Republic, 1955* (in Slovak).
- [25] W. Kresser, *Die Hochwaesser der Donau*. Springer Verlag, Wien, Austria, 1957 (in German).
- [26] A. Svoboda, P. Pekarova, and P. Miklanek, *Flood hydrology of Danube between Devin and Nagymaros*, publ. SVH – IH SAS, p. 96, 2000.

Renewable, Non-Renewable Energy Consumption, Economic Growth and CO₂ emission: Evidence for Iran

Soheila Khoshnevis Yazdi¹ Bahman Khanalizadeh²
Nikos Mastorakis³

Abstract—In this study, we employ ARDL approach to provide evidence on the CO₂ emissions, economic growth and coal consumption renewable energy consumption, non-renewable energy consumption and population in Iran using for an extended time period, i.e. from 1975–2011. Furthermore, the causal relationships among the variables are further examined using the Granger causality test. Our empirical results suggest that the variables are cointegrated in the case of Iran. In other words, there is a long-run relationship between CO₂ emissions, economic growth and. Granger causality test reveal a strong evidence of bidirectional causality running from economic growth to CO₂ emissions. Moreover, there is bidirectional causality between economic growth and renewable energy consumption in the short and long run.

Keywords—ARDL.CO₂ emissions, Economic growth, Iran, Non Renewable Energy, Renewable Energy,

I. INTRODUCTION

ENERGY is also an essential factor of production [1]. All production involves the transformation or movement of matter in some way and all such transformations require energy. Some aspects of organized matter that is information might also be considered to be non-reproducible inputs. Energy as a factor of production must be incorporated into machines, workers, and materials in order to be made useful. This provides a biophysical justification for treating capital; labor etc. as factors of production [2].

Energy plays a crucial role in the economic

1. S. Koshnevis Yazdi is with the Department of Economics College of Law, Political Science & Economics Islamic Azad University, South Tehran Branch, Tehran, No.223, North iranshahr St, Tehran, Iran. Also with the Post Doc Project WSEAS Research Department, WSEAS,A.I.Theologou 17-23, Zografou, 15773, Athens, GREECE (corresponding author to provide phone:00989128441103; e-mail: soheila_khoshnevis@yahoo.com).

2.B. Khanalizadeh is faulty the Department of Economics College of Law, Political Science & Economics Islamic Azad University, South Tehran Branch, Tehran, No.223, North iranshahr St, Tehran, Iran. (khanali.bahman@yahoo.com).

3.Nikos Mastorakis is Technical University of Sofia, Department of Industrial Engineering, Sofia Bulgaria (mastor@tu-sofia.bg)

development of a country. It enhances the productivity of factors of production and increases living standards. It is extensively recognized that economic development and energy consumption are interdependent]. Energy demand, supply and pricing impact on the socioeconomic development, the living standards and the overall quality of life of the people [3]. On the other hand, higher level of economic development could induce more energy consumption.

The increasing concern over global warming and growing carbon dioxide (CO₂) emissions in developing countries like India, associations between environmental pollutants and economic activities in developing countries have received more and more attention.

Unfortunately, despite the abundance of research on this topic, the empirical literature has not yet reached a consensus about whether economic growth is the cause or effect of energy consumption, and whether economic growth is the solution or source of environmental pollution problem (known as EKC hypothesis). Thus, further investigation of the relationship between, carbon emissions, and economic growth appears warranted.

II. LITERATURE SURVEY

The causal relationship between co₂ emission and economic growth is a well-studied topic in the energy economics literature. A large number of studies show the causal relationship between both variables; conducted for developing and developed economies. Kraft and Kraft [4] tested for causality between energy consumption and GNP for this country for the 1947-74 periods by utilizing Sims methodology. They concluded unidirectional causality running from GNP to energy consumption.

Energy plays a vital role in economic development. It performs a key for sustainable development. The findings of the previous studies suggested that the results are inconclusive depending on the methods and time period employed.

Alam et al. [5] investigated the causal relationship between energy consumption, CO₂ emissions and income in India. Evidence supported bi-directional causality between energy consumption and CO₂ emissions in the long run. However, there was no causality between

energy consumption and income as well as between CO₂ emissions and income. Thus, the authors conclude that energy conservation policies could be implemented without affecting economic growth. In addition, reducing CO₂ would be less easy in India due to the absence of causality in any direction.

Managi [6] indicated that economic growth and the decrease of environmental degradation are compatible in accordance to the Environmental Kuznets Curve (EKC) hypothesis. It has been proposed that an inverted U-shaped relationship between economic growth and environmental pollution is empirically associated with smaller levels of pollution after some thresh-old income point. On using a simple regression analysis

Li et al. [7] used panel unit root, heterogeneous panel cointegration and dynamic OLS methods to examine the relationship between energy consumption and economic growth for 30 provinces in China. Their results showed that there was a positive long-run relationship between energy consumption, CO₂ emissions and economic growth. They found that a 1% increase in GDP per capita increased the energy consumption and CO₂ emissions by 0.5% and 0.43% respectively.

Richmond and Kaufmann (2006) investigate the EKC for CO₂ using panel data for OECD countries and note that there is limited support for the EKC in the case of OECD countries.

Mallick [8] investigates the link between energy use and economic growth using the Granger causality test on India's annual data for the period of 1970 to 2005. The tests suggest that economic growth fuels increased demand for both crude oil and electricity consumption while the growth in coal consumption drives economic growth. The variance decomposition analysis of Vector Auto regression (VAR) however suggests the possibility of a bidirectional influence between electricity consumption and economic growth.

Sadorsky [9] uses vector auto regression techniques to study the relationship among renewable energy consumption, income, oil prices and CO₂ emissions in the Group of 7 (G7) countries over the period of 1980e2005. The results show that in the long-run, an increase in real GDP per capita and carbon dioxide emissions per capita are found to contribute in increase in G7 renewable energy consumption per capita.

Menyah and Wolde-Rufael [10] uses vector autoregression technique to study the relationship among CO₂, renewable energy, nuclear energy and real output for the US over the period of 1960e2007. They find unidirectional causality running from nuclear energy consumption to CO₂ emissions but no causality is found between renewable energy consumption and CO₂ emissions.

Boopen et al. [11] analyze the relationship between GDP and Carbon dioxide emission for Mauritius over the time period 1975-2007. The results reveal that GDP is

linked with carbon dioxide emission and have a significant negative relationship between them.

Shahbaz et al. [12] examine the relationship between income and energy consumption for Romania by using annual data for the time period 1980e2008. The results suggest a positive association between the real output and energy consumption in Romania. They further identified a strong positive correlation between the nonrenewable energy consumption and the carbon dioxide emissions.

Li et al. [13] examined the relationship between CO₂ emissions, energy consumption and economic development using a panel data of 28 provinces in China. The result confirmed the cointegration relationship among the three variables. Moreover, the study found evidence of bi-directional causality between CO₂ emissions and energy consumption as well as between energy consumption and economic growth. In addition, energy consumption and economic growth caused CO₂ emissions in the long run while CO₂ emissions and economic growth were the long-run causes of energy consumption.

The organization of the remainder of this paper is as follows. The next section briefly describes the empirical methodology employed. Section 4 describes the data and analyzes the main empirical findings. Finally, the summary and the policy implications of our findings are outlined in Section.

III. DATA

This study uses annual time series data for Iran from 1975 to 2011. The period was chosen based on the availability for all the data series. Real GDP per capita (GDP) in constant 2005 US\$, real per capita fixed capital formation population size measured by total of people Iran.

Renewable energy consumption in quadrillion Btu units is measured as wood, waste, geothermal, wind, photovoltaic, and solar thermal energy consumption. Non-renewable energy sources include coal and coal products, oil, and natural gas. Therefore, in this study, non-renewable energy consumption is measured as the aggregate of the consumption of all of these sources in quadrillion Btu units [14].

All data are from the World Development Indicators (WDI) online database [15]. All the variables transformed to natural logarithms for the purpose of the analysis. We have used Microfit 4 and EvIEWS 7.1 to conduct the analysis.

3.2 Model

Following the recent empirical works it is possible to test the long-run relationship between CO₂ emission and economic growth, renewable energy consumption, non-renewable energy consumption and the total population size in a linear logarithmic using the following equation:

$$CO_2_t = f(GDP_t, REC_t, NRECX_t, POP_t) \quad (1)$$

In order to find the long-run relationship between variables, the following linear logarithmic form is proposed:

$$\text{LnCO}_2_t = \alpha_0 + \alpha_1 \text{LnGDP}_t + \alpha_2 \text{LnREC}_t + \alpha_3 \text{LnNREC}_t + \alpha_4 \text{LnPOP}_t \quad (2)$$

Following the recent empirical works it is possible to test the long-run relationship between variables.

IV. . ECONOMETRIC APPROACH

A. Unit Root Test

First, the Augmented Dickey Fuller (ADF) tests are used to check whether each data series is integrated and has a unit root. The ADF test is based on the value of t-statistics for the coefficient of the lagged dependent variable compared with special calculated critical values. If the calculated value is greater than the critical value, then we reject the null hypothesis of a unit root; the unit root does not exist, and our variable is stationary [16].

B. Cointegration Analysis

Engle and Granger [18] provided a totally new method for analyzing time series. It is well known that a time series model can only be built once the included series in the model are stationary. There is a great advantage in finding (long-term) co-integration relationships, as the series need no longer be transformed and, hence, the forecasting power increases substantially.

The existence of long-run equilibrium (stationary) relationships among economic variables is referred to in the literature as cointegration. Engel and Granger pointed out that a linear combination of two or more non-stationary variables may be stationary. If such a stationary combination exists, then the non-stationary time series are said to be co-integrated.

C. Granger Causality Analysis

Cointegration tests are only able to indicate whether the variables are cointegrated and whether a long-run relationship exists between them. To test the direction of causality between CO2 emission, economic growth, renewable energy consumption, non-renewable and population. The Granger [17] approach based on the Vector Error Correction Model (VECM) is employed. Considering each variable in turn as a dependent variable for model.

The residuals obtained from estimating the long-run relationship between the variables in non-renewable and renewable energy use models are used as dynamic error correction terms in the above equations.

The test answers the question of whether x causes y or y causes x. x is said to be Granger caused by y if y helps in the prediction of the present value of x or equivalently if the coefficients on the lagged y's are statistically significant. In the presence of long-run relationship between variables in the model, the lagged Error Correction Term (ECMt-1) was obtained from the long-run cointegration relationship and was included in the

equation as an additional independent variable. The following model was employed to test the causal relationship between the variables Equation 3:

$$\begin{bmatrix} \Delta \text{LnCO}_2_t \\ \Delta \text{LnGDP}_t \\ \Delta \text{LnREC}_t \\ \Delta \text{LnNREC}_t \\ \Delta \text{LnPOP}_t \end{bmatrix} = \begin{bmatrix} c_1 \\ c_2 \\ c_3 \\ c_4 \\ c_5 \end{bmatrix} + \sum_{i=1}^p \begin{bmatrix} \beta_{11i} & \beta_{12i} & \beta_{13i} & \beta_{14i} & \beta_{15i} \\ \beta_{21i} & \beta_{22i} & \beta_{23i} & \beta_{24i} & \beta_{25i} \\ \beta_{31i} & \beta_{32i} & \beta_{33i} & \beta_{34i} & \beta_{35i} \\ \beta_{41i} & \beta_{42i} & \beta_{43i} & \beta_{44i} & \beta_{45i} \\ \beta_{51i} & \beta_{52i} & \beta_{53i} & \beta_{54i} & \beta_{55i} \end{bmatrix} \begin{bmatrix} \Delta \text{LnCO}_2_t \\ \Delta \text{LnGDP}_t \\ \Delta \text{LnREC}_t \\ \Delta \text{LnNREC}_t \\ \Delta \text{LnPOP}_t \end{bmatrix} + \begin{bmatrix} \lambda_1 \\ \lambda_2 \\ \lambda_3 \\ \lambda_4 \\ \lambda_5 \end{bmatrix} \text{ECMt}_{-1} + \begin{bmatrix} \varepsilon_{1t} \\ \varepsilon_{2t} \\ \varepsilon_{3t} \\ \varepsilon_{4t} \\ \varepsilon_{5t} \end{bmatrix} \quad (3)$$

ECMt-1 is the lagged error-correction term. Residual terms are uncorrelated random disturbance term with zero mean and j's are parameters to be estimated. The direction of causality can be detected through the VECM of long-run cointegration. The VECM captures both the short-run and the long-run relationships.

The short-run causality is based on a standard F-test statistics to test jointly the significance of the coefficients of the explanatory variable in their first differences. The long -run causality is based on a standard t-test. Negative and statistically significant values of the coefficients of the error correction terms indicate the existence of long-run causality.

V. RESULTS AND DESCRIPTIVE STATISTICS

In this empirical study we used Augmented Dickey-Fuller Stationary unit root tests to check for the integration order of each variable. We apply unit root tests to ensure that no variable is integrated at I (1) or beyond. We have used the ADF unit root test to check for stationarity. The results in Table 1 indicate that all variables are non-stationary at their level form and stationary at their first differences.

Table 1 Augmented Dickey-Fuller Stationary Test Results

Variable	Constant	Critical Value	Variable	Constant	Critical Value
	No Trend			No Trend	
Ln CO2	-0.159886	-2.945842	Ln CO2	-4.723295	-2.948404
Ln GDP	-0.663392	-2.954021	Ln GDP	-3.720542	-2.954021
Ln REC	-2.665572	-2.945842	Ln REC	-5.703516	-2.948404
Ln NREC	-0.517503	-2.945842	Ln NREC	-5.673434	-2.948404
Ln POP	-9.604951	-2.945842	Ln POP	-3.764502	-3.544284

The number inside brackets denotes the appropriate lag lengths which are chosen using Schwarz Criterion.
* Denotes for 5% significance level

Source: Author's Estimation using Eviews 7.1

The null hypotheses of no cointegration are rejected, implying long-run cointegration relationships amongst the variables. These variables share a common trend and move together over the long run.

All estimated coefficients can be interpreted as long-run elasticities, given that variables are expressed in natural logarithms in table 2.

Table 2 Long-run Estimation Results

Dependent Variable: Ln CO2				
Variable	Coefficient	Std. Error	T-Statistic	Prob
Ln GDP	0.72 **	.14364	4.9746	[0.000]
Ln REC	-.044	.034675	-1.2588	[0.219]
Ln NREC	-0.18 **	.056619	-3.2805	[0.003]
Ln POP	0.97 **	.15992	6.0739	[0.000]
C	-16.34**	2.5635	-6.3735	[0.000]

Note** significant at 5 % level

Source: Author's calculation using Microfit 4

The VECM is set up for investigating short- and long-run causality. The optimum lags are selected relying on minimizing the Akaike Information Criterion (AIC). The maximum lag order two was set. With that maximum lag lengths setting, the

ARDL (2, 0, 0, 0, 0) model is selected using AIC. ARDL (1, 0, 0, 0, 0) represents the ARDL model in which the income and GDP take the lag length 2. The long-run coefficients of GDP, REC, NREC and POP estimated from these techniques have the same magnitude at the 5% significance levels.

For the model indicates that a 1% increase in real GDP increase CO2 emission by approximately 0.72% and a 1% increase in the non-renewable energy consumption decrease real GDP by 0.18%.

The coefficient on population (POP) shows a positive impact on CO2 emission in Iran. The elasticity of CO2 emission with respect to population ratio the long run 0.97, suggesting the contribution of increasing population to CO2 emission is significant during the estimation period.

The long-run estimated coefficient related to renewable energy show that, a 1% increase in renewable energy consumption decrease CO2 emission by 0.44% and is statistically insignificant. Thus, renewable energy cannot play an important role in economic growth.

The results of cointegration in Table 3 show that the F-statistic is not greater than its upper bound critical value. However, we can conclude that cointegration is supported by the significantly negative coefficient obtained for ECM t-1. The error correction mechanism (ECM) is used to check the short-run relationship among the variables. The coefficient of ECM t-1 is statistically significant at 5% level of significance which indicates that speed of adjustment for short-run to research in the long-run

equilibrium is significant. The error correction term is statistically significant and its magnitude is quite higher indicates a faster return to equilibrium in the case of disequilibrium.

This term shows the speed of adjustment process to restore the equilibrium. The relatively high coefficients imply a faster adjustment process. The values of the coefficients of ECM-t1 (-0.70) indicating that the variables will adjust to the long-run equilibrium in about 1.4 period following a short-run shocks.

The coefficient of REC is negative and insignificant. The short-run elasticity of renewable energy with respect to CO2 emission is negative and statistically insignificant. The coefficient value of -0.18 suggests that a 1% non-renewable energy consumption leads to around 0.18% decrease in CO2 emission.

Table 3. Error correction model (ECM) for short-run elasticity ARDL (2,0,0,0,0)selected based on Akaike Information Criterion

Dependent Variable: D(Ln CO2)			
Variable	Coefficient	T-Statistic	Probability
D Ln GDP	0.71	4.9746	[0.000]
D Ln REC	-.044	-1.2588	[0.219]
D Ln NREC	-0.18	-3.2805	[0.003]
D Ln POP	0.97	6.0739	[0.000]
C	-16.34	-6.3735	[0.000]
ECM (- 1)	-0.70	-5.8215	[0.000]
The Short-Run Diagnostic Test Results			
R-Squared	.62735		
Akaike info Criterion	45.7963		
Schwarz Criterion	40.3526		
F-Statistic	7.8562	[.000]	
Durbin-Watson	2.0315		

Note: **shows a percent level of 5%, *shows a percent level of 10%.

Source: Author's calculation using Microfit 4

The coefficient of real GDP and population in short-run are positive and significant. The elasticity of CO2 emission to CO2 emission is 0.71 which suggests that 1% increase in CO2 emission will lead to around 0.71% increase in real GDP in the short-run in Iran.

The existence of a cointegration relationship among the variables, as shown by the cointegration test, indicates

that there is Granger causality in these variables in at least one direction, but it does not show the direction of this causality. Table 4 shows the results of error correction based Granger causality, including weak short-term Granger causality and long-term Granger causality.

Table 4 VECM Granger Causality results

Variable	Short-run					Long-run
	DLn CO2	DLn GDP	DLn REC	DLn NREC	DLn POP	ECM(-1)
DLn CO2	-	24.7466** [0.000]	1.5845 [0.208]	10.7614** [0.001]	36.8924** [0.000]	33.8898** [0.000]
DLn GDP	16.3138** [0.000]	-	2.9523 [0.086]	1.7206 [0.190]	5.4980** [0.019]	25.0021** [0.000]
DLn REC	4.3396** [0.037]	4.8946* [0.027]	-	1.1151 [0.291]	4.5799** [0.032]	11.7392** [0.001]
DLn NREC	2.2962 [0.130]	3.4782 [0.062]	.15178 [0.697]	-	3.5266 [0.060]	4.1298* [0.042]
DLn POP	1.2508 [0.263]	1.7753 [0.183]	.32298 [0.570]	.079691 [0.778]	-	1.2673 [0.260]

$x \rightarrow y$ means x Granger causes y .

Note: **denote the statistical significance at the 5% levels.

Source: Author's calculation using Microfit 4

The results of the causality test based on the VECM. Granger causality tests suggest a bi-directional flow, at 5% significance level, for real per capita GDP and CO2 emission in the Iranian case, in the short-run; and a unidirectional flow, in the direction from non-renewable energy to CO2 emission in the short-run (at 5% level).

The Granger causality test results funding the Also, these findings show that non-renewable energy consumption and economic growth has unidirectional.

There is also bidirectional causal relationship renewable energy consumption and CO2 emission.

VI. CONCLUSION

This study attempts to investigate the relationship between CO2 emissions, economic growth and renewable energy consumption, non-renewable energy consumption and population in Iran using ARDL approach for an extended time period, i.e. from 1975–2011.

The time-series properties of the data were assessed using several unit root tests (ADF). Empirical findings indicate that both series are clearly non-stationary, as and I(1) process.

The analysis shows that CO2 emissions and GDP are cointegrated. This means that there is (possibly bidirectional) causality relationship between the two. Then, cointegration analysis revealed that there is a long-run relationship between GDP and CO2 emissions based on a VEC model after testing for multivariate cointegration between CO2 emissions and per capita GDP.

The short-run dynamics of the variables show that the flow of causality runs from CO2 emissions use to GDP, and there is a long-run bidirectional causal relationship

(or feedback effect) between the two series. So, CO2 emissions and economic growth complement each other such that radical energy conservation measures may significantly hinder economic growth.

This has important policy consequences, as it suggests that energy restrictions do not seem to harm economic growth in Iran. Also, the growth in GDP per capita leads to a similar growth in energy consumption per capita. We find evidence that energy consumption and economic growth move together In Iran.

With respect to this, investment and institutional arrangements should be intensified to speed up the development of renewable energy sectors.

References

- [1]D. I. Stern " Limits to substitution and irreversibility in production and consumption: a neoclassical interpretation of ecological economics", Ecological Economics, vol. 21, pp. 197-215. 1973.Avaliable: http://www.bilkent.edu.tr/~yeldane/Chennai_Yeldan2002.pdf
- [2]D. I. Stern, "Energy and economic growth in the USA: A multivariate approach". Energy Economics, vol. 15, 1 pp. 37–150. 1993.
- [3]A. Iwayemi, "Energy sector development in Africa", African Development Report. 1998.
- [4]J. Kraft, A. Kraft, "On the relationship between energy and GNP". Journal of Energy Development, vol. 3, pp. 401–403. 1978.
- [5]Alam & Butt, "Causality between Energy Consumption and Economic Growth in Pakistan: An Application of Co-Integration and Error Correction Modeling Techniques." Pacific and Asian Journal of Energy, vol. 12, 2, pp 151-165. 2002.
- [6]S. Managi, Are there increasing returns to pollution abatement? Empirical analytics of the Environmental Kuznets Curve in pesticides. Ecological Economics, 2006, 58, 617–636.
- [7] J. Li, H. Song, D. Geng, Causality relationship between coal consumption and GDP: difference of major OECD and non-OECD countries. Appl Energy, 2008; 85: 421–9.
- [8] H.Mallick, "Examining the Linkage between Energy Consumption and Economic Growth in India", The Journal of Developing Areas, vol. 43(1), 2009.
- [9]P. Sadorsky, Renewable energy consumption, CO2 emissions and oil prices in the G7 countries. Energy Econ 2009; 31(3):456e61.
- [10] Menyah K, Wolde-Rufael Y. CO2 emissions, nuclear energy, renewable energy and economic growth in the US. Energy Policy 2010; 38(6):2911e5.
- [11] S. Boopen, S.Vinesh. On the relationship between CO2 emission and economic growth. EDiA Paper No. 776. Online available at: <http://www.csaee.ac.uk/conferences/2011-EDiA/papers/776-Seetanaah.pdf>
- [12]Shahbaz M, Muhammad Z, Kumar TA. Analysis of renewable and nonrenewable energy consumption, real GDP and CO2 emissions: a structural VAR approach in Romania. MPRA Paper 2011No. 34066. Online available <http://mpra.ub.uni-muenchen.de/34066>
- [13] F.i. Li, D. Suocheng, L., Xue, L., Quanxi, Energy consumption-economic growth relationship and carbon dioxide emissions in China. Energy Policy 2011; 2011 (39):568e74.
- [14] EIA. CO2 emissions from fuel combustion: highlights. Washington, DC: US Energy Information Administration, US Department of Energy; 2011.
- [15] World Bank. World development indicators; 2012. <http://www.data.worldbank.org>
- [16] D. Dickey, W. A. Fuller, "Distribution of the Estimates for Autoregressive Time Series with a Unit Root". Journal of the American Statistical Association. Vol. 74, pp. 427-4311. 1979 Available: <http://dx.doi.org/10.2307/2286348>
- [17] C. W.J. Granger ,R. F, Engle Cointegration and error correction: representation, estimation and testing. Econometrica. 1987; 55:251e76.

The assessment of the effectiveness of reforms in various countries

Samson Davoyan and Tatevik Sahakyan

Abstract— The purpose of this article is to suggest a new methodology that will give us an opportunity to create an Index of the Surmount of Post Crisis Challenges (ISPCC) that will include eight indexes which trend will give an opportunity to assess the comparative efficiency of various reforms for different countries (26 countries in transition and 17 developed countries) for 2009-2013. On the purpose of our research we consider more important the following indexes, as their integrity will represent the features of the social-economic development of each country. In our opinion, the analyze of the suggested new index may become the guide for the governments of different countries in terms of choosing the main directions and mechanisms of reforms that will help them to have efficient and well-functioning institutional systems of economies and that is the most essential to become more effective in comparison of other countries in the group.

Keywords— Index, reforms, competitiveness, freedom, challenges, assessment, democracy, comparative, corruption, globalization.

I. INTRODUCTION

THE governments of different countries developed programs to surmount challenges of the last world economic crisis (2008-2009), but those countries implemented the programs with different comparative efficiency. We suppose that the results of those reforms are expressed in various indexes by different international and non-government organizations. [1]. On the purpose of our research we consider more important the following indexes, as their integrity will represent the features of the social-

Samson Davoyan is Doctor of Economic Sciences, professor member of Association of Economists of Armenia, lecturer professor in Russian-Armenian (Slavonic) University, director of Gyumri branch of the Armenian State Economic University (phone: 00374 91434283; e-mail: samsondavoyan2014@gmail.com).

PhD Tatevik Sahakyan, is awarded the Master's degree in Jurisprudence Republic of Armenia International Scientific-Educational Center of NAS (National Academy of Science), PhD student Faculty of Economics, Russian-Armenian (Slavonic) University (phone 00374 98 797919 e-mail: tatevik@comhem.se).

economic development of each country. From this point of view, during the last decades there have been various indexes developed by different international organizations and non-government corporations (Global Innovation index by INSEAD, KOF Index of Globalization by the Economist Intelligence Unit, Human Development Index by UNO, The Corruption Perception Index by Transparency International anti-corruption organization and so on), which are used to assess the institutions of different fields. Based on the new methodology, suggested by us, we have tried to create more integral index based on the following indexes, which trend will give an opportunity to assess the comparative efficiency of various reforms for different countries (26 countries in transition and 17 developed countries). We have splint the countries into 2 main groups. We have highlighted the reforms implemented in 17 developed countries: Austria, Australia, Belgium, Denmark, Finland, France, Germany, Japan, Netherlands, New Zealand, Norway, Portugal, Singapore, Sweden, Switzerland, United Kingdom and United States.

We have also assess the comparative efficiency in 26 countries in transition countries during post-crisis period. These countries are Albania, Armenia, Azerbaijan, Bulgaria, Bosnia and Herzegovina, Croatia, Czech Republic, Estonia, Georgia, Hungary, Kazakhstan, Kyrgyz Republic, Latvia, Lithuania, Macedonia, Moldova, Montenegro, Poland, Romania, Russia, Slovak Republic, Serbia, Slovenia, Ukraine, Vietnam.

The integral index consists of eight indexes for the last 4 years: Global Innovation index for 2010-2013, KOF Index of Globalization for 2010-2013, Democracy Index for 2008, 2010, 2011 and 2012, The Global Competitiveness Index for 2010-2011 and 2013-2014 periods by World Economic Forum, Doing Business for 2011-2014, Corruption Perception for 2010-2013, The Index of Economic Freedom for 2011-2014, The Human Development for 2009-2012.

Our new methodology is based on two regulator-parameters: the changes of the ranks and average of scores of the above mentioned indexes for two periods of time. As a result we have the Index of the Surmount of Post Crisis Challenges (ISPCC).

A.The Global Competitiveness Index (GCI)

The Global Competitiveness Index (GCI) released by the World Economic Forum, which is a comprehensive tool, that

measures the competitiveness of 148 countries, contains 3 sub-indexes: basic requirements, efficiency enhancers, innovation and sophistication factors, that are based on 12 pillars (institutions, infrastructure, macroeconomic environment, health and primary education, higher education and training, etc.) including 119 indicators[2].

B. Doing Business

Doing Business released by the World Bank and International Financial Corporation assesses business activity for 189 countries on the basis of 10 areas of regulation (starting a business, dealing with construction permits, getting credits, paying taxes, etc.) with 36 sub-indexes considering the survey results of organizations in different sectors of economies [3]. The important way to improve the methodology of this index is to consider the influence of the macroeconomic factors on the business environment [4].

C. The Corruption Perception Index

The Corruption Perception Index published by Transparency International anti-corruption organization measures the perceived levels of public-sector corruption for 177 countries based on different assessments and business opinion surveys [5]. The countries, included in the rank of The Corruption Perception Index, are classified on a scale of 0 to 100. The countries, that get 0 are the highly corrupt in judicial system, media, legislative, police, business, public, educational, military areas [6].

D. The Index of Economic Freedom

The Index of Economic Freedom assesses the economic freedom of countries through 10 indicators (Business Freedom, Trade Freedom, Fiscal Freedom, Government spending, Monetary Freedom, Investment Freedom, Financial Freedom, Property Rights, Freedom from Corruption, Labor Freedom) in 185 countries [7]. All ten indicators of the Index are scaled equally. Each of them gets 0 to 100 economic freedom grading scale; countries that get 100 are the freest economies of the world. The Index has been published by The Heritage Foundation and The Wall Street Journal since 1994 [8].

E. The Human Development Index

The Human Development Index is a summary indicator that measures a standard of living, the literacy rate, the life expectancy in order to compare and assess the human potential of different countries [9]. In the viewpoint it is important to mention the research which accounted and analyzed multiple criterias of the standard of life in 17 countries of Eurozone. [10].

F. The Democracy Index

The Democracy Index, compiled by the Economist Intelligence Unit, is the classification of 167 countries by the level of the democracy. The Index includes 60 indicators grouped in five categories: electoral process and pluralism,

civil liberties, functioning of government, political participation, and political culture [11].

G. KOF Index of Globalization

KOF Index of Globalization compiled by the Economist Intelligence Unit. The KOF Index of Globalization measures the three main dimensions of globalization: economic, social and political. In addition to three indices measuring these dimensions, we calculate an overall index of globalization and sub-indices referring to actual economic flows:

economic restrictions

data on information flows

data on personal contact

and data on cultural proximity.

Data are available on a yearly basis for 207 countries over the period 1970 – 2010 [12].

H. The Global Innovation Index (GII)

The GII project was launched by INSEAD in 2007. The core of the GII Report consists of a ranking of world economies' innovation capabilities and results. In 2013, the ranking covered 142 economies, accounting for 94.9% of the world's population and 98.7% of the world's Gross Domestic Product (in US dollars). The GII has established itself as the reference among innovation indices, and has evolved into a valuable benchmarking tool to facilitate public-private dialogue, whereby policymakers, business leaders and other stakeholders can evaluate progress on a continual basis. The GII relies on two subindices: the Innovation Input Sub-Index and the Innovation Output Sub-Index, each built around pillars. Five input pillars capture elements of the national economy that enable innovative activities: (1) Institutions, (2) Human capital and research, (3) Infrastructure, (4) Market sophistication, and (5) Business sophistication. Innovation outputs are the results of innovative activities within the economy. There are two output pillars: (6) Knowledge and technology outputs and (7) Creative outputs. The overall GII score is the simple average of the Input and Output Sub-Indices.

II. PROBLEM SOLUTION

For all represented above indexes we can say, that they are considered to be particular assessment of social-economic development. Besides they often include such indicators, that are not assessed by statistic services and therefore they can only be estimated by experimental method, which is obviously limit wide usage opportunity of these indexes. One of the most important problems is to assess the weight of each component. For the empiric and scientific perspectives there are essential research results in 28 countries of EU for 2001-2011, which is based on the analysis of macroeconomic indicators such as the life expectancy, GDP per capita (PPP), Global competitiveness index, etc [13].

Using above-mentioned indexes, we represent an integral index, that assess social-economic development level for 2009-2013 based on statistic data for eight indexes (KOF Index of Globalization, The Corruption Perception, The Global Competitiveness Index, Doing Business, The Index of Economic Freedom, The Human Development, The Democracy Index). As a result we have the integral assessment of social-economic development for chosen countries.

At the first stage, the values of the indicators normalized in the interval [0;1]. At the second stage, we decide the measurement of the integral indexes. It includes following steps.

Based on the values of the indicators we create $\text{cov}(\tilde{X})$ covariation matrix of $\tilde{X} = (\tilde{x}^{(1)}, \tilde{x}^{(2)}, \dots, \tilde{x}^{(p)})^T$ vector

We create $|\text{cov}(\tilde{X}) - \lambda I_p| = 0$ (1) descriptive equation and the solution result in the matrix with $\lambda_1 \geq \lambda_2 \geq \dots \geq \lambda_p \geq 0$ (2) values

m_0 measurement of the integral indicator is decided from the following requirement:

$$m_0 = \min_{1 \leq m \leq p-1} \left\{ m; \frac{\lambda_1 + \lambda_2 + \dots + \lambda_m}{\lambda_1 + \lambda_2 + \dots + \lambda_p} \geq 0.55 \right\} \quad (3)$$

At the third stage, $\tilde{x}_i^{(1)}, \tilde{x}_i^{(2)}, \dots, \tilde{x}_i^{(p)}$ partial criterias split into groups.

At the fourth stage, we create M_1, M_2, \dots, M_{m_0} groups which include the modified main ingredients of the partial criterias. We can have it after following steps:

create $|\text{cov}(\tilde{X}(M_j))|$ matrix based on the values of $\tilde{x}^{(1)}(M_j), \tilde{x}^{(2)}(M_j), \dots, \tilde{x}^{(p)}(M_j)$ partial criterias included in the $M_j, j = 1, 2, \dots, m_0$ group

decide the maximum $\lambda_1(M_j)$ value of $|\text{cov}(\tilde{X}(M_j))|$ matrix

solving the system of equations decide $\ell(M_j) = (\ell_1(M_j), \ell_2(M_j), \dots, \ell_{p_j}(M_j))^T$ vector of

$|\text{cov}(\tilde{X}(M_j))|$ matrix :

$$(\text{cov}(X(M_j)) - \lambda_1(M_j)I_{p_k})\ell(M_j) = 0 \quad (4)$$

decide the values of $\tilde{y}^{(j)}$ modified main ingredients of the partial criterias in M_j group with the help of the following formula:

$$\tilde{y}^{(j)} = \sum_{q=1}^{p_j} \ell_1^2(M_j) \cdot \tilde{x}^{(q)}, \quad (5)$$

$$i = 1, 2, \dots, n$$

At the fifth stage, we measure \tilde{v}_j scales of $\tilde{y}^{(1)}, \dots, \tilde{y}^{(m_0)}$ integral descriptives based on the relations of the dispersions of the partial criterias in their summary dispersions:

$$\tilde{v}_j = \frac{s_{\tilde{y}_j}^2}{\sum_{k=1}^p s_{\tilde{x}^{(k)}}^2} \quad (6)$$

$$s_{\tilde{x}^{(k)}}^2 = \frac{1}{n} \sum_{i=1}^n (\tilde{y}_i^{(j)} - \bar{y}^{(j)})^2, \quad \bar{y}^{(j)} = \frac{1}{n} \sum_{i=1}^n \tilde{y}_i^{(j)} \quad (7)$$

$$s_{\tilde{x}^{(k)}}^2 = \frac{1}{n} \sum_{i=1}^n (\tilde{x}_i^{(k)} - \bar{x}^{(k)})^2, \quad \bar{x}^{(k)} = \frac{1}{n} \sum_{i=1}^n \tilde{x}_i^{(k)} \quad (8)$$

In order to calculate the Index, \tilde{v}_j scale coefficients are normalized:

$$v_j = \frac{\tilde{v}_j}{\sum_{l=1}^{m_0} \tilde{v}_l} \quad (9)$$

It is obvious that in this case we will have the necessary requirement for the scales:

$$\sum_{j=1}^{m_0} v_j = 1, \quad v_j \geq 0, \quad (j = 1, \dots, m_0) \quad (10)$$

At the sixth stage, we calculate the integral y indicator of development with the help of the following formula:

$$y = \sum_{j=1}^{m_0} v_j \tilde{y}^{(j)} \quad (11)$$

For the calculations we have used MathCad program.

To create ISPCC we calculated the ratio of observed eight indexes. Those ratios were acquired experimentally by 56 both Armenian and foreign experts who are state and non-governmental management workers, as well as economists. In the result of the assessment of the eight indices normalized coefficients were provided and the total sum of their ratios is 1.

Those coefficients are:

α_i^j - the scale of each index,

i and j are indexes

$i=1, 2, \dots, 8$ - the eight indexes,

$j_1=1, 2, \dots, 17$ - developed countries, $j_2=1, 2, \dots, 26$ countries in transition we evaluated. For example,

$\alpha_4^j = 0,13$ - the scale of The Economic Freedom Index in the ISPCC for $j_2=1, 2, \dots, 26$ countries in transition,

$\alpha_4^j = 0,09$ - the scale of The Economic Freedom Index for $j_1=1, 2, \dots, 17$ developed countries, and

$$\sum_{i=1}^8 \alpha_i^j = 1, (12)$$

$$j = \{j_1, j_2, j_3\}$$

With the help of our methodology we first summarized the above-mentioned 8 indexes and attained 1 general index.

$$H_{int.index}^j = \sum_{i=1}^8 \alpha_i^j N_i^j, (13)$$

$H_{int.index}^j$ - the Index of the Surmount of Post Crisis Challenges,

i and j are indexes

$i = 1, 2, \dots, 8$ - the eight indexes. For example, $i = 4$ The Economic Freedom Index,

$j_2 = 1, 2, \dots, 26$ countries in transition we evaluated

$j=1$ - Albania, $j=2$ - Armenia, ... $j=26$ - Vietnam

α_i^j - the scale of each index,

N_i^j - the rank of the j country by i index

For example, Armenia is ranked 4 among 26 countries for 2010-2013 by the Global competitiveness index (considering the change of rank and score), therefore $N_1^2 = 4$

The first stage of creating the index was the rearrangement of the indexes included in analyze. The principle of rearrangement was based on the changes of the ranks and average of scores of the above mentioned indexes for two periods of time. We also normalized the score of

each index to bring them to the same interval and make them more comparable. Then we adjusted the change with scale coefficients substantiated methodologically. Depending on the level of the social-economic development of the country and the comparative efficiency of various reforms we used scale coefficients. For example, for those countries which had more than 7 points of improvements in rank we gave 0,1 for the change of the rank and 0,9 for the average score, for those who had more than 7 points of decrease in rank we gave 0,9 for the change of the rank and 0,1 for the average score [11].

Fig. 1, 2 and Table 1,2 represent ISPC in reports for 2009-2013 compare with the base year (2009) in both 26 countries in transition and 17 developed countries. Fig. 3,4 and Table 3,4 represent ISPC by the new methodology for 2009-2013 compare with the base year (2009). Fig. 5,6 and Table 5,6 represent ISPC in reports and by the new methodology in 26 countries in transition and 17 developed countries for 2009-2013.

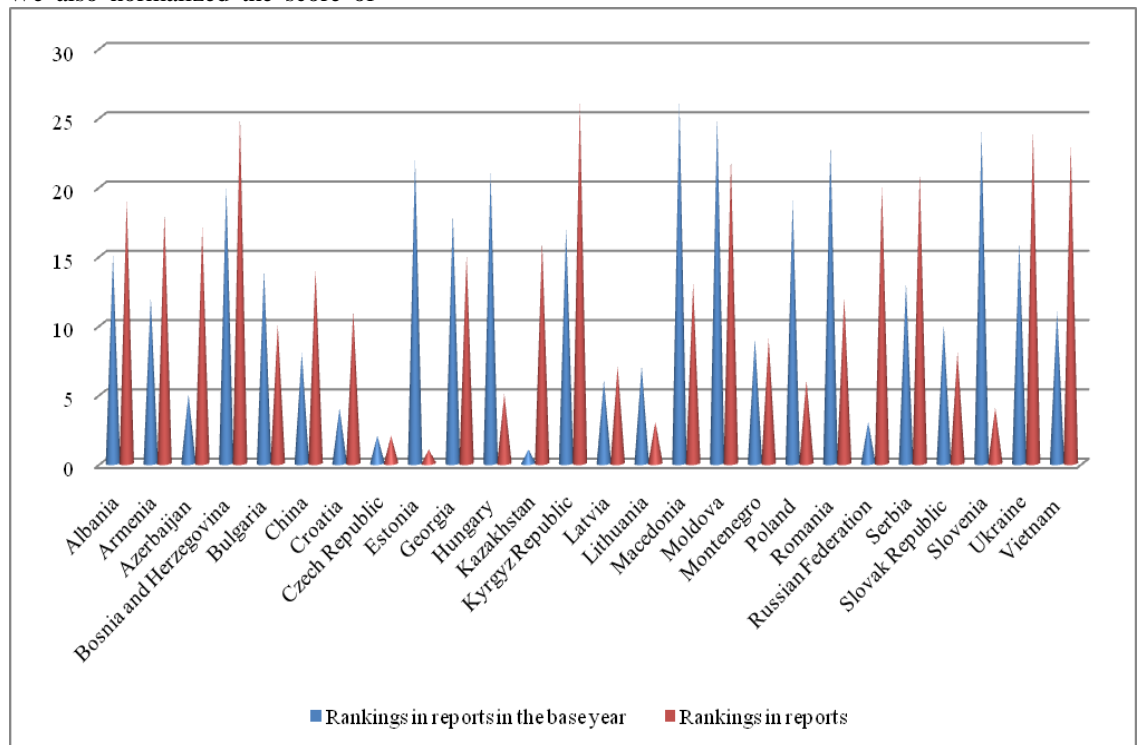


Fig. 1. ISPC in reports for 2009-2013 compared with the base year (2009) in 26 countries in transition.

	Rankings in reports in the base year	Rankings in reports
Albania	15	19
Armenia	12	18
Azerbaijan	5	17
Bosnia and Herzegovina	20	25
Bulgaria	14	10
China	8	14
Croatia	4	11
Czech Republic	2	2
Estonia	22	1
Georgia	18	15
Hungary	21	5
Kazakhstan	1	16
Kyrgyz Republic	17	26
Latvia	6	7
Lithuania	7	3
Macedonia	26	13
Moldova	25	22
Montenegro	9	9
Poland	19	6
Romania	23	12
Russian Federation	3	20
Serbia	13	21
Slovak Republic	10	8
Slovenia	24	4
Ukraine	16	24
Vietnam	11	23

Table 1. ISPC in reports for 2009-2013 compared with the base year (2009) in 26 countries in transition.

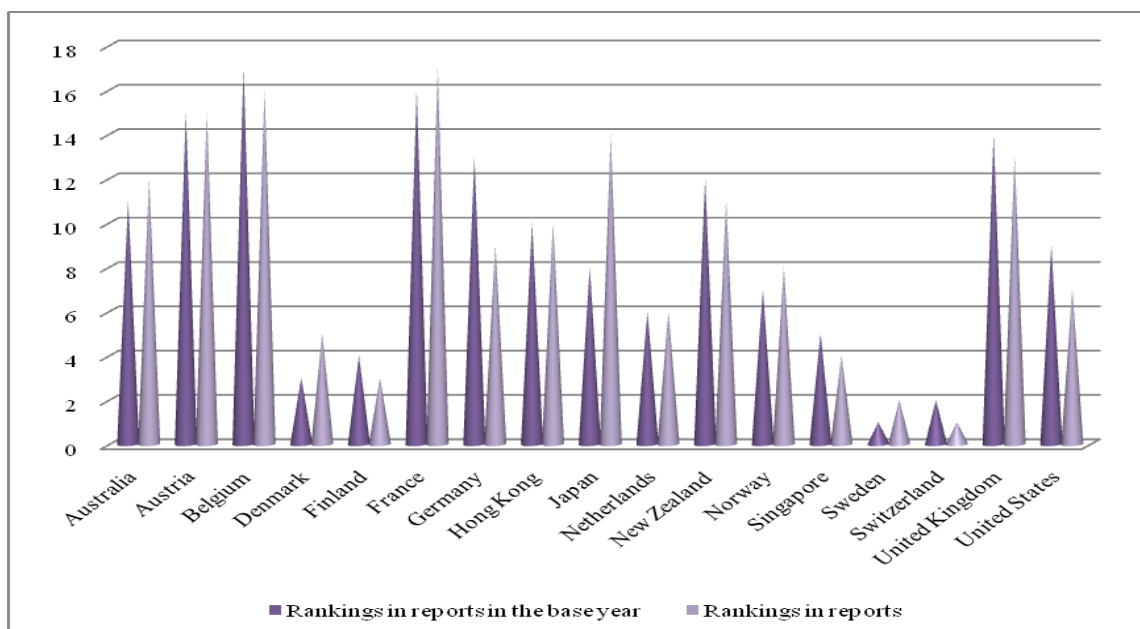


Fig. 2. ISPCCC in reports for 2009-2013 compared with the base year (2009) in 17 developed countries.

	Rankings in reports in the base year	Rankings in reports
Australia	11	12
Austria	15	15
Belgium	17	16
Denmark	3	5
Finland	4	3
France	16	17
Germany	13	9
Hong Kong	10	10
Japan	8	14
Netherlands	6	6
New Zealand	12	11
Norway	7	8
Singapore	5	4
Sweden	1	2
Switzerland	2	1
United Kingdom	14	13
United States	9	7

Table 2. ISPCCC in reports for 2009-2013 compared with the base year (2009) in 17 developed countries.

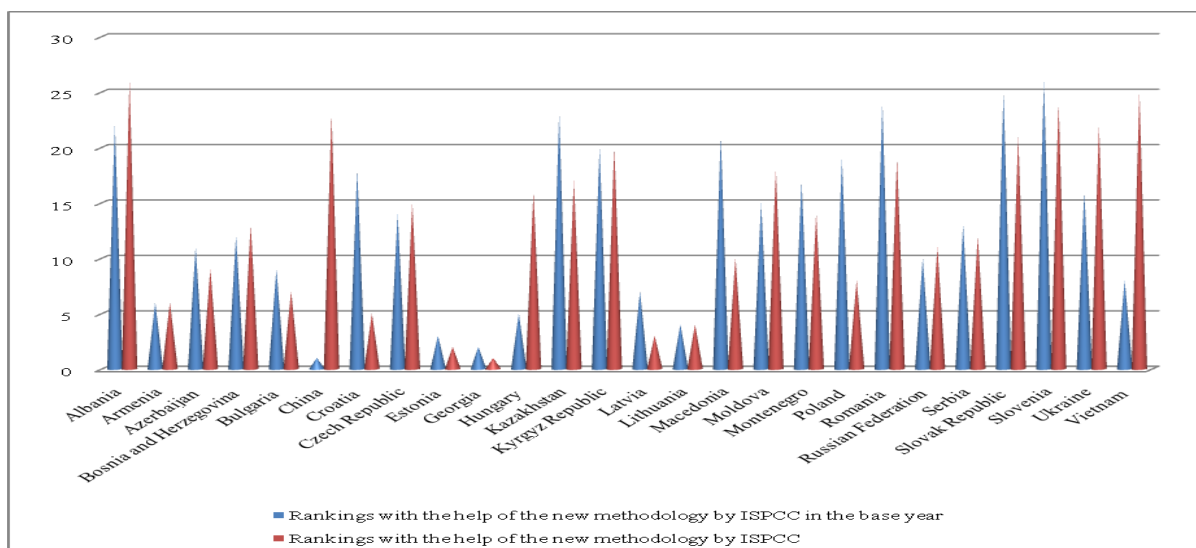


Fig. 3. ISPCCC by the new methodology for 2009-2013 compared with the base year 2009 in 26 countries in transition.

	Rankings with the help of the new methodology by ISPCCC in the base year	Rankings with the help of the new methodology by ISPCCC
Albania	22	26
Armenia	6	6
Azerbaijan	11	9
Bosnia and Herzegovina	12	13
Bulgaria	9	7
China	1	23
Croatia	18	5
Czech Republic	14	15
Estonia	3	2
Georgia	2	1
Hungary	5	16
Kazakhstan	23	17
Kyrgyz Republic	20	20
Latvia	7	3
Lithuania	4	4
Macedonia	21	10
Moldova	15	18
Montenegro	17	14
Poland	19	8
Romania	24	19
Russian Federation	10	11
Serbia	13	12
Slovak Republic	25	21

Slovenia	26	24
Ukraine	16	22
Vietnam	8	25

Table 3. ISPC by the new methodology for 2009-2013 compared with the base year 2009 in 26 countries in transition.

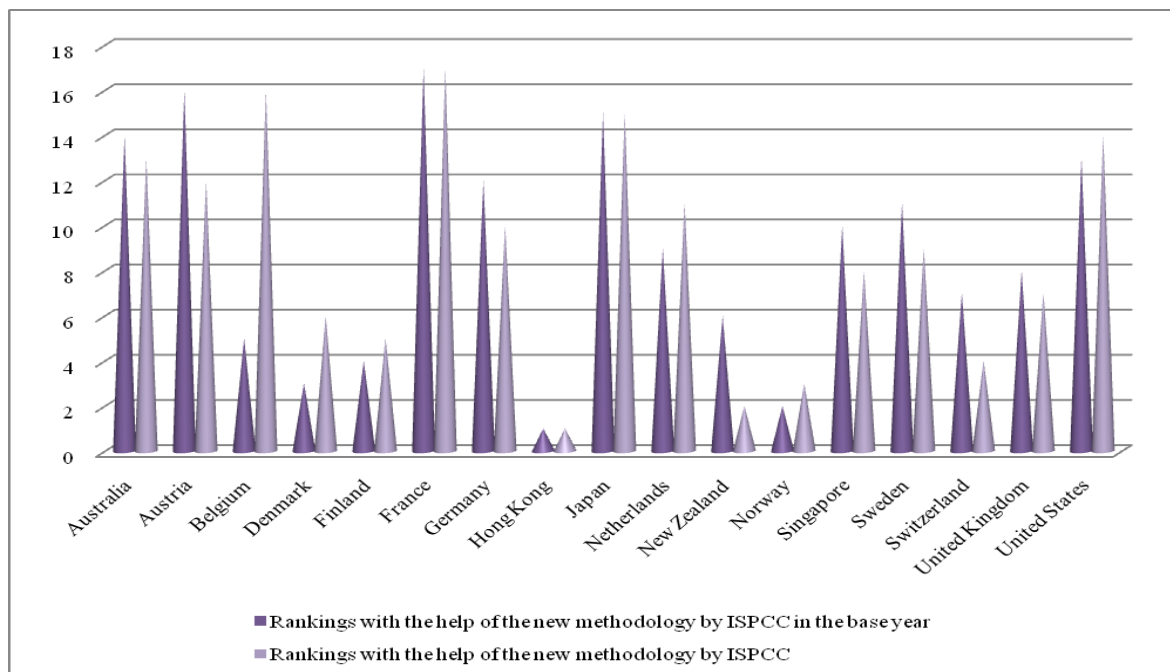


Fig. 4. ISPC by the new methodology for 2009-2013 compared with the base year 2009 in 17 developed countries.

	Rankings with the help of the new methodology by ISPC in the base year	Rankings with the help of the new methodology by ISPC
Australia	14	13
Austria	16	12
Belgium	5	16
Denmark	3	6
Finland	4	5
France	17	17
Germany	12	10
Hong Kong	1	1
Japan	15	15
Netherlands	9	11
New Zealand	6	2
Norway	2	3

Singapore	10	8
Sweden	11	9
Switzerland	7	4
United Kingdom	8	7
United States	13	14

Table 4. ISPCC by the new methodology for 2009-2013 compared with the base year 2009 in 17 developed countries

At the second stage countries were rearranged by the methodology mentioned above. This approach was repeated for each year combining with the previous year. As a result of the first and second stages we had a new range of countries for each index for 2009-2013.

At the third stage we gave scale coefficients to all eight indexes considering the importance and the variety of included indicators, eliminating the usage of the same indicator and finally we had ISPCC of each country for 2009-2013.

Putting the indicators of α_i^j and N_i^j in the equation we will have H_i^j .

$$H_{int.index}^j = \sum_{i=1}^8 \alpha_i^j N_i^j, \text{ For } j_1=1, 2, \dots, 17 \text{ – developed}$$

countries, $j_2=1, 2, \dots, 26$ countries in transition we assess the average of the summary for 4 years.

$$(H_{i_1}^j + H_{i_2}^j + H_{i_3}^j + H_{i_4}^j) / 4$$

For instance, The Economic Freedom Index for Armenia will be:

$$(H_{4_1}^2 + H_{4_2}^2 + H_{4_3}^2 + H_{4_4}^2) / 4$$

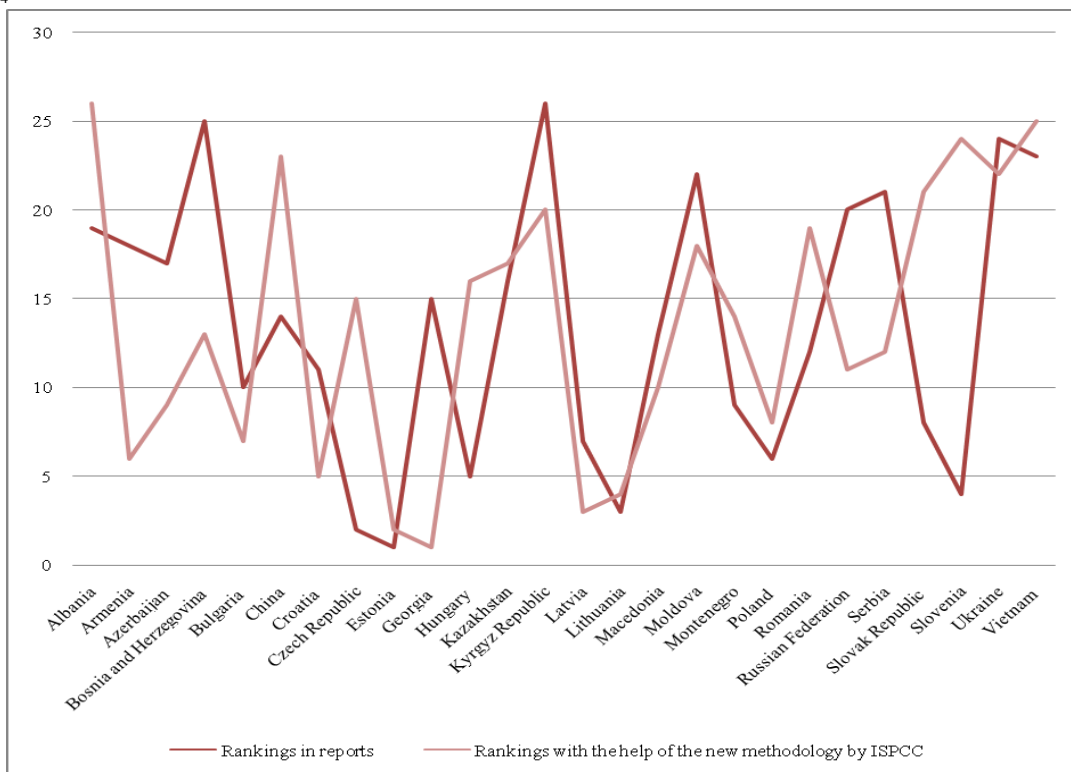


Fig. 5. ISPCC in reports and by the new methodology for 2009-2013 in 26 countries in transition.

	Rankings in reports	Rankings with the help of the new methodology by ISPCC
Albania	19	26
Armenia	18	6
Azerbaijan	17	9
Bosnia and Herzegovina	25	13
Bulgaria	10	7
China	14	23
Croatia	11	5
Czech Republic	2	15
Estonia	1	2
Georgia	15	1
Hungary	5	16
Kazakhstan	16	17
Kyrgyz Republic	26	20
Latvia	7	3
Lithuania	3	4
Macedonia	13	10
Moldova	22	18
Montenegro	9	14
Poland	6	8
Romania	12	19
Russian Federation	20	11
Serbia	21	12
Slovak Republic	8	21
Slovenia	4	24
Ukraine	24	22
Vietnam	23	25

Table 5. ISPCC in reports and by the new methodology for 2009-2013 in 26 countries in transition.

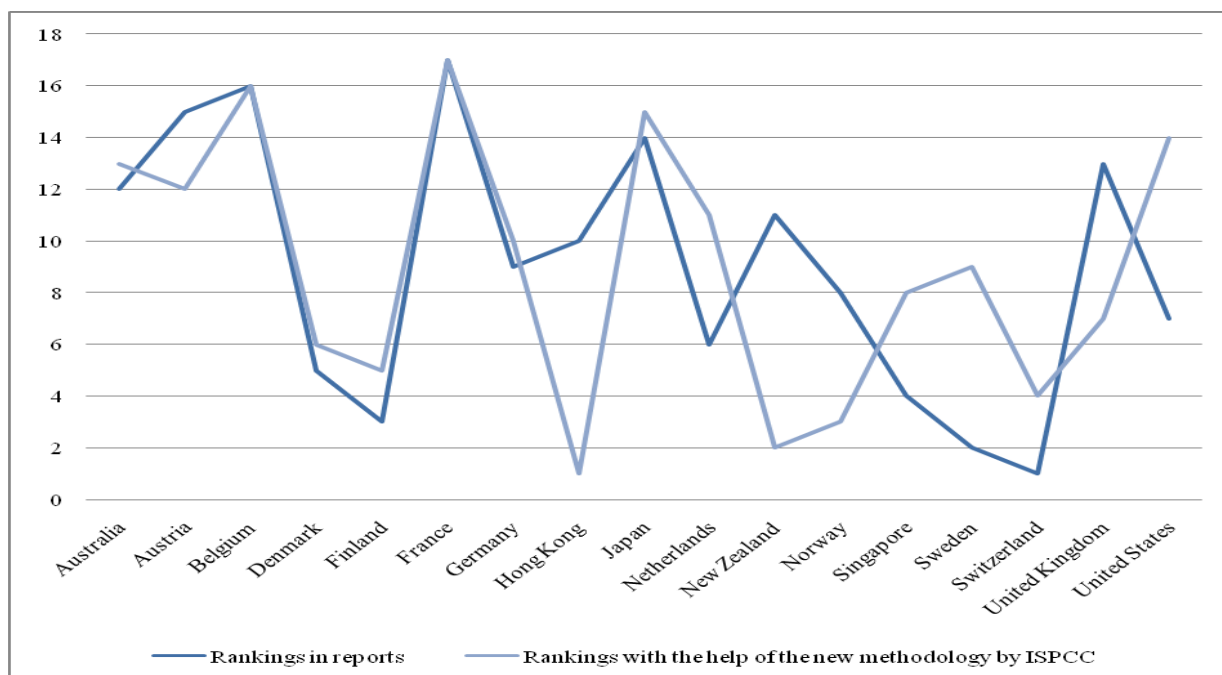


Fig. 6. ISPC in reports and by the new methodology in 17 developed countries for 2009-2013.

	Rankings in reports	Rankings with the help of the new methodology by ISPC
Australia	12	13
Austria	15	12
Belgium	16	16
Denmark	5	6
Finland	3	5
France	17	17
Germany	9	10
Hong Kong	10	1
Japan	14	15
Netherlands	6	11
New Zealand	11	2
Norway	8	3
Singapore	4	8
Sweden	2	9
Switzerland	1	4
United Kingdom	13	7
United States	7	14

Table 6. ISPC in reports and by the new methodology in 17 developed countries for 2009-2013.

According to the suggested methodology, we measure ISPC for 26 countries in transition and 17 developed countries, considering the change of rank and score adjusted with scale coefficients for 2009-2013. The results witness, that the reforms for 2009-2013 have more effectively implemented in Georgia, Estonia, Armenia, Russia, Serbia, Azerbaijan, , and Croatia, but less effectively in Slovak Republic and Slovenia.

CONCLUSION

The trends of the changes of the index of various reforms that we suggest and also the quantitative assessments for two periods can be orientations for the government and non-government institutes that develop and implement reforms in each country, as they, compared to other countries, point those directions in which the comparative efficiency of the reforms in that country is lower than other countries. Therefore, in our later researches we will be able for theoretical and scientific aspects perspectives improve the suggested methodology and give more clear quantitative and qualitative assessments of the various reforms in different countries.

In our opinion, the analyze of the suggested new index may become the guide for the governments of different countries in terms of choosing the main directions and mechanisms of reforms that will help them to have efficient and well-functioning institutional systems of economies and that is the most essential to become more effective in comparison of other countries in the group.

REFERENCES

- [1] Popov V. Shock Therapy versus Gradualism Reconsidered: Lessons from Transition Economies after 15 Years of Reforms. TIGER Working paper No. 82 p. 95, 2006
- [2] The Global Competitiveness Report, The World Economic Forum, weforum.org.
- [3] Doing Business Report, The World Bank, doingbusiness.org.
- [4] Marek Sedlacek, A business strategy and usage of chosen Result indicators as a tool against global crisis impacts on companies in automotive industry, International of economics and statistics, Issue 1, Volume 1, 2013.
- [5] Corruption Perceptions Index 2012: Full Source Description/Transparency International, p. 45, 2012, www.transparency.org.
- [6] Kaufmann, Daniel, "Corruption, Governance and Security: Challenges for the Rich Countries and the World," MPRA Paper 8207, University Library of Munich, Germany, p. 77, 2004.
- [7] Ambassador Terry Miller, Kim R. Holmes, Edwin J. Feulner, "2012 Index of Economic Freedom", The Heritage Foundation and The Wall Street Journal, New York, p. 62, 2012, www.heritage.org.
- [8] Samson Davoyan, Tatevik Sahakyan, The assessment of reforms in different countries by social-economic development integral index, World Academy of Science , Engineering and Technology, Issue 79 Stockholm, July 2013, p. 1324.
- [9] United Nations Organization, UNDP.org
- [10] Jiri Krupka and Romana Provaznikova, Analysis of standard of living models based on multiple criteria decision analysis, International journal of economics and statistics, Volume 2, 2014
- [11] Economist Intelligence Unit, www.eiu.com.
- [12] <http://globalization.kof.ethz.ch/>
- [13] First A. Peter I.Kamyshanov, Second B. Alexander P. Kamyshanov, New paradigm in the regional management, International journal of economics and statistics, Volume 2, 2014.
- [14] Samson Davoyan, The assessment of the reforms in different countries using social-economic development index, Conference on The trends of changes of the world economy and the challenges in Armenia, Gyumri p.6, 2012.

The easiest and least expensive way to control water hammer in irrigation and drainage network of Sivand Dam

Reza Gharekhani, Sayed Abbas Mousavi, Fatemeh Kazemi

Abstract-Water hammer pressure occurs in pipelines of under pressure and it is based on pressure regulation, flow velocity and changes of location, time of fluid motion. In some hydraulic systems under pressure, such as water transmission lines, oil or water distribution systems and piping leading to the turbine, water tunnels, gravity flow and pumping systems, water hammer phenomenon is caused in various risks by creating a fast and damped transient wave, sometimes destructive power of these wave pressures are so, which would bring about serious consequences, burst in pipeline systems and distribution networks, failures and broken valves, control valves and pumps are examples of the impact. In this study for simulation of transmission lines in stable and unstable hydraulic conditions, we use the two software of Bentley Company with the names of WaterGems and Hammer. Results from the model indicated that the phenomenon of water hammer occurs when valves are closing and for harness of this phenomenon we used the simplest way with regarding to the parallelism of the two lines together. Thus, a connection pipe were used that connected with the two main pipes in several points. In this method, during the occurrence of water hammer, every line serves as a repository for other lines.

Keywords-Water hammer effect, Water hammer control, connection pipe, easiest way

INTRODUCTION

Water hammer is the formation of pressure wave as a result of sudden change in liquid velocity in a piping system. The water hammer phenomena usually explained by considering by ideal reservoir pipe-valve system in which the steady flow with velocity V_0 is stopped by an instantaneous valve closure. In other say it occurs when the fluid flow start or stop quickly or is forced to make a rapid change in direction, for example quick closing the valves and stoppage of a pump can create water hammer[4,12]

Background of the Investigations

Joukowsky[6] published the basic theory of water hammer. He achieved acceptable relationship for increase pressure, fluid density, velocity and wave speed changes.

- Reza Gharekhani : Technical head office in irrigation and drainage network of Sivand Dam. E-mail: r_gharekhani@yahoo.com

- Sayed Abbas Mousavi: project manager in irrigation and drainage network of Sivand Dam (pars garma company). E-mail: s.abbasmousavi@yahoo.com

-Fatemeh Kazemi: Technical Expert in Parese banaye shiraz Company.E-mail: fatemeh_128@yahoo.com

$$\Delta H = \frac{a\Delta V}{g}$$

ΔH : Increased pressure on the basis of water head (m)

A : wave velocity (m / s)

ΔV : velocity change of liquid in the pipe line (m / s)

G: acceleration of gravity (m / s ²)

Joukowsky also studied and investigated the emission of waves in the pipeline and their reflections, means the time it takes a wave to go to the boundaries of reflection and return[6].

In 1960s and development of computer industry a new era started in studying and analyzing the phenomenon of water hammer. Stritter and Whily[9] showed that with the aim of computer they can solve very difficult and sophisticate problems and so analyzing of water hammer that in that era was exclusive to the few number of experienced people, proposed for the most of engineers. Parmakian (1950-1963) stated that the aggregation of high pressure waves are dangerous and recommended that for ensuring and having enough safety from danger of the wave it should prevented from vacuum separation in system[8].

In the research by Anton [1] water hammer analysis for control of water in underground mines had been done. Field measurement are comprised with a computer simulation analysis of a transient during power failure to the pump. The result show that the method of characteristic is an acceptable method for water hammer analysis of mine pumping systems.

In the research by Don[5], two procedure for solving the basic transient flow had been comprised . one of them is based on a numerical procedure using the method of characteristics (MOC). Another is referred to the wave characteristics method (WCM). The results show that the MOC and WCM are both capable of accurately solving for transient pressures. The WCM will normally require fewer calculations and faster execution times. Because of the difference in calculation requirements and the comparable accuracy of two techniques, the use of the WCM will be more suitable for analyzing lang pipe network.

Cannizzaro [3] discussed on the failure of the water column in transmission flows and creating a large pressure rise within the pipeline.

In another research, [10] results show that water hammer effect is more in larger and bigger diameter of pipe line. Water hammer effect in the pvc pipe is greater than the water hammer effect in steel pipe. The prevention method of water hammer effect which install the bypass pipe with non return valve had prove that the method is successfully to reduce the water hammer effect in the pipe line. The mean pressure is reducing about 33.33% after installing the prevention method. This method is useful in the household usage as the non return valve is not an expensive method.

Consequences from the water hammer phenomenon

low and high pressures

Non-steady flow can be caused high or low pressures. Excess pressure can damage the pumps, valves and other pipeline equipment or cause fracture in lines. Low pressure causes the release of dissolved air of the fluid and if the pressure reaches the vapor pressure of the fluid leads to intense evaporation. Low pressure inside the pipes (plus the pressure due to external loading) can lead to pipe failure. The vapor cavity-closure can also cause extreme shock pressure that the system will be impaired.

Vibration

Vibration of non-steady flow in pipelines can cause significant effects on pipelines. Intense vibration of non-steady flows results from where that some alternating currents causes agitation of pipeline equipment in frequencies close to their natural frequency. In this case, the stresses and large deformations (with sound) occurs that may impair the system.

Vacuum induction

Rapid condensation and vaporization causing a vacuum induction that it is one of the lasting effects of the non-steady currents. Vapor cavity usually forms when fluid pressure by dynamic or statistic factors is equal to or less than vapor pressure. These holes are expanded by low pressure. When the pressure around these cavities increases over the vapor pressure, the cavities disappears and fall down. This creates noise, vibration and possible damage to the hard surfaces.

Shock waves from collapsing vapor cavities can create pressure fluctuations and causes vibrations in system. Such vibrations can cause screws to loosen, Fatigue of connections, loose or breaking belts and damage to the pipes. If vapor cavities near the hard borders (such as plumbing) fall down, erosion is likely and this causes premature repair or replacement of pipe, valves, pumps, turbines, etc. Vapor induction can reduce system performance such as increased pump head loss reduction,

reducing power generation in turbines and reducing the flow through the valves.

Location and causes of water hammer

The possibility of water hammer phenomenon that its formation mechanism depends on changing in velocity and pressure of flow exists in fluid transfer systems. Water hammer occurs in pipes for water transmission, water distribution networks, oil pipelines or fluid transmission in industries, turbine water flow in pipes or in open streams such as the failure of a dam failure, the a huge wave of water downstream along the path and flows by gravity or pumping flow systems.

The accident occurred due to different causes that the most important are:

- Reduce or increase the velocity and flow with maneuver of control valves in water, oil pipelines and ...
- Reduce or increase the velocity and flow with opening and closing of control valves in water pipe turbines.
- Setup or failure of pumps and turbines.
- When switching or increase and decrease in flow and velocity in gravity flow with using control systems.
- Power failure in pumping systems.
- Existence of changes in flow path, including increasing and decreasing pipe diameter or existence of blind pipes.

Calculation of water hammer (Water Hammer)

One of the important factors for the calculation of water hammer is the calculation of wave velocity. Wave velocity in the pipe is obtained from the relationship based on m/s that is called Olivy relationship:

$$a = \frac{\sqrt{\frac{K}{r}}}{\sqrt{1 + (K/E) * (D/t) * (1 - \frac{m}{2})}}$$

Where μ is Poisson's ratio (dimensionless), D is the pipe diameter (mm), t is the thickness of the pipe wall in terms of (mm), P is the density of water (kg/m³), E is modulus of elasticity of pipe, K is modulus of elasticity of water equal to 19/2 GPa. E values for pipes GRP are 30 to 50 GPa based on the type of material production.

Water hammer in pipes under gravity pressure

Gravity transmission lines are called networks that in which fluid flow from a source with a higher level toward a destination or consumer with lower level due to topography condition of pipeline approach is established by gravity and with the help of gravity.

Factors causes water hammer in the gravity pipelines

Sudden changes and pressure cause distribution of wave in pipelines and the occurrence of water hammer phenomenon. Considering that reservoir level is almost constant in gravity lines therefore it can be concluded that the water hammer in lines is summarized as follows:

- A- Sudden closing of taps on pipeline route
- B- Sudden opening of taps on pipeline route
- C- sudden fracture along the pipeline
- D- Cut or overload the downstream consumers that is associated with an increase or decrease in the current pipeline.

The important point in relation to the gravity network of transmission lines is that separation of water column occurs less during water hammer phenomenon, because between upstream reservoir and nodes or downstream reservoir generally is a line which causes minimum pressure line become steady state in gravity system close to slope hydraulic line. However, where the ground suddenly falls to the lower elevation there is a possibility of water column separation phenomenon.

The effect of pipeline profile and taps in gravity flows on water hammer rate

- Positive pressure due to the maximum height difference of piezometric attenuation flow that obtained from curve difference of maximum difference of piezometric height and profile evaluation of can provide with choosing the pressure bearing of the pipe and Characteristics of suitable work and also, if the pressure is higher than the nominal pressure can control it by safety valves and other safety measures.

- Negative pressures that indicate vacuum induction and water column separation phenomenon cannot be easily controlled like positive pressures. The best and safest way is to inhibit negative pressure is to prevent its occurrence.

- Negative pressures obtain from curve difference of minimum piezometric height and profile evaluation of line. So if in normal condition profile of the line is lower than the curve of minimum piezometric height, damaging effects of negative pressure and vacuum generation and separation of the water column in the line will not create. In design of gravity transmission pipelines whatever the pipeline profile has an upward concave cause that the curve of minimum piezometric pressure locate above the profile of pipeline and possibility of establishment of negative pressures and destructive phenomenon of water hammer is reduced. However, in this case amount of positive pressure on the

pipeline is considerable and only we should select proper nominal pressure of pipes and valves or can be controlled by a suitable buffer device.

- In some of the designs that during the creation of water hammer only enter positive pressures on the pipeline and negative pressure does not occur due to the shape of the line profile, can be used a combination of two types of pipe for the transmission line.

- In gravity pipelines the main parameters determining hammer is the time to open and close TC valves. Therefore for analysis of the equations you should first select an assumed value of the TC, then the equation and the output results are investigated. So the minimum suitable time of closing that during which no serious danger threaten the pipeline and transmission system choose as a closing time of the taps.

Almost in all kinds of taps during closing, amount of creating hammer during closing is about 85 to 90% of low primary tap and the main hammer that causes damage occurs in about 10-15% of distal valve closure. For gravity systems of under pressure 15-10% of the final closing of the valve

should occurs in the time more than $T_r = \frac{2L}{a}$ so

water hammer pressure is reduced considerably[11].

- In plans that the route of the pipeline is so long and the flow discharge capacity is considerable, in order to reduce the time closing the valve operation can be carried out in two stages. So that 85 to 90% of tap sectional area will be operate at first and in a short time that can be calculated and for closing the remaining 10-15% should be done in a relative longer period and so the total time of closing is reduced.

With using valves with electric or hydraulic steering (electric actuator) the opening and closing can be precisely controlled and regulated. In these taps with changing and reducing the operator the opening and closing time of the valves increase. In pilot hydraulic taps we can control and regulate the opening and closing time by creating local pressure drop in the power steering line to the diaphragm and valve components[7].

Existing methods for preventing hammer

In order to avoid sudden shocks in pipes one way of controlling water hammer is selected according to the case arises in the design of water supply pipe networks, pumping stations and turbines.

Basically in prediction of methods of preventing sudden strokes in pipes, pumping stations and water distribution networks, it is necessary to reduce the amount of height changing such as the energy

between tankers and location of taps and pumps, amount of time during wave movement and also changes in velocity. For this purpose the following methods suggested for preventing the hammer:

- Use of safety valves
- The use of check valves (to prevent water from back)
- The use of buffer tanks
- Flue pipes
- Double orifice air valves

What is important is the fact that basically designing water pipelines and networks and the choice of the roughness of the pipe lining and pressure drop should be done with care so to be able to withstand high pressures.

Strategies to anticipate and deal with water hammer in pipelines, irrigation and drainage network project of Sivand Dam

Before choosing one of the techniques for controlling the impact of stroking in the transmission line, the transmission line must be hydraulic modeling and with calculation of the potential stroke, finally the appropriate methods should be presented at the end due to the condition of the project.

Sivand Dam Project of irrigation and drainage network has been designed and implemented as pipe networks. For transmission of water to the first part of the network it has been used from two parallel GRP pipes with a diameter of 1200 mm that receives water from an open reservoir and shall be transferred to the beginning of the network in length of 11800 meters. Because of the height difference between the reservoir and the water outlet area of agricultural land (about 36 meter) pipes went under pressure and it was necessary that investigate the hammer phenomenon and offer a proper method for controlling of that.

It is necessary to precisely modelling part of hydraulic system like pipes, tanks and relief, safety and switching valves for analyzing water transmission line. In this regard, the pipeline is divided into a number of computational reaches and necessary to be considered the pressure values at nodes and flow as input data plan in addition to the physical characteristics. The purpose of the model is to investigate the impact of hydraulic transients in pipelines transporting water results from closing of water taps.

First we stimulate with WaterGems for normal conditions in steady state and then with Hammer for unsteady state of pipeline and results are presented as a graph.

The model boundary conditions

Due to the hydraulic studies conducted, water flow in the basin divider is designed as a free surface and the

output structure is so that the water level is at a constant level of 1611 meters.

Hydraulic modeling in stable condition

It is prepared with entering the transmission line route profile and the placement of nodes and pipes on the hydraulic model of the transmission line in hydraulic stability conditions.

Table 1: Names and computational nodes of main line water transfer project from km 0+000 to 11+800

Label	Elevation (m)	Calculated Hydraulic Grade (m)	Pressure (m H ₂ O)
J-1-A.V	1,609.00	1,610.30	1
J-2-B.O	1,594.97	1,609.51	15
J-3-A.V	1,596.95	1,609.22	12
J-5-B.O&A.V	1,578.97	1,603.78	25
J-6-B.V&A.V	1,576.68	1,602.47	26
J-7	1,576.57	1,601.61	25
J-8-B.O	1,575.34	1,600.63	25
J-9-A.V	1,575.80	1,599.91	24
J-10-A.V	1,576.20	1,599.38	23
J-12-B.O&A.V	1,573.90	1,596.65	23
J-13	1,573.66	1,595.05	21
J-14	1,573.00	1,594.98	22

Table 2 Names and properties of water transmission pipe line project from km 0+000 to 11+800

Label	Length (m)	Pressure Pipe Headloss (m)	Headloss Gradient (m/km)
P-1	147	0.2	1.31
P-2	605	0.8	1.31
P-3	219	0.29	1.31
P-4	2124	2.79	1.31
P-5	2019	2.65	1.31

Label	Length (m)	Pressure Pipe Headloss (m)	Headloss Gradient (m/km)
P-6	999	1.31	1.31
P-7	649	0.85	1.31
P-8	749	0.98	1.31
P-9	549	0.72	1.31
P-10	399	0.53	1.31
P-11	999	1.31	1.31
P-12	1084	1.42	1.31
P-13	1213	1.59	1.31
P-14	53	0.07	1.31

Graph (1) Profiles of main line water transfer project from zero miles to km 11+800

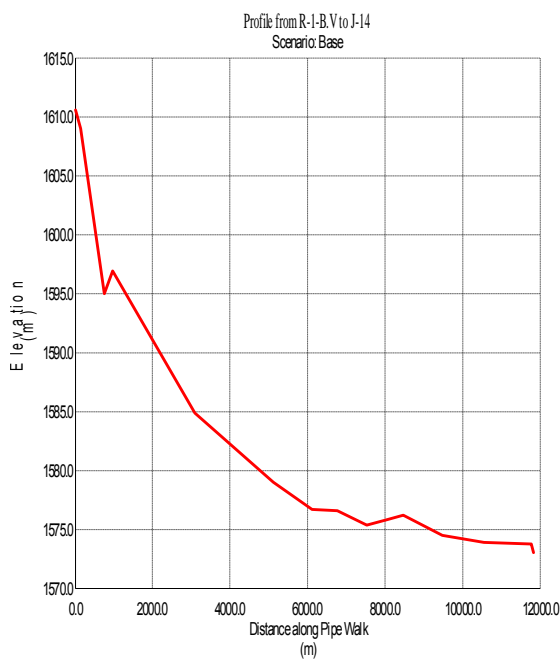


Figure 1 profiles and hydraulic gradient for water transmission line projects in stable hydraulic condition.

With viewing the profile of basin divider from the place of the pipeline to km 11+800, it is observed that static pressure is up to about 5/36 meters of water.

According to the technical report of consulting engineers, shows that the flow rate is about 3.5 cubic meters per second by PN6 GRP pipes with a diameter of 1200 mm shall be transmitted to the network. Dynamic pressure of the flow path is from zero at the beginning of the path to about 3 atm.

calculations and modeling results in unstable hydraulic conditions

inputs to hydraulic hammer model of in HAMMER software

Coefficients and necessary information relating to the characteristics of the pipe and fluid inside the pipe are presented to model the path of unstable modes in Table No. (3)

Table (3) the physical characteristics of GRP pipes

Poisson's Ratio	Young's Modulus		Material
	(GPa)	(109 lbf/ft2)	
0.4	30	1	G.R.P

fluid properties

Pipe material: GRP

Length of the transmission line: 11800 m

Inner diameter: 1200 mm

Wave velocity in the pipe: minimum 400 and maximum of 600 meters per second

Partial pressure of water vapor: 10 - Mtrab

Valves: Butterfly valves with a diameter of 1200 mm and 200 mm diameter air

Water level in the basin divider

Profile Transmission Line

Flow rate for each pipeline 1.75 cubic meter per second

Modeling is done in unstable hydraulic conditions for slow closing of switching valves at the times of 60, 90, 150, 200 and 300 seconds. In Figure (2) to (9) profiles of pipelines and minimum and maximum blow pipes are shown at different times. It is observed with increasing valve closure time in the last 10% hit rate is decreased but

never reach to zero

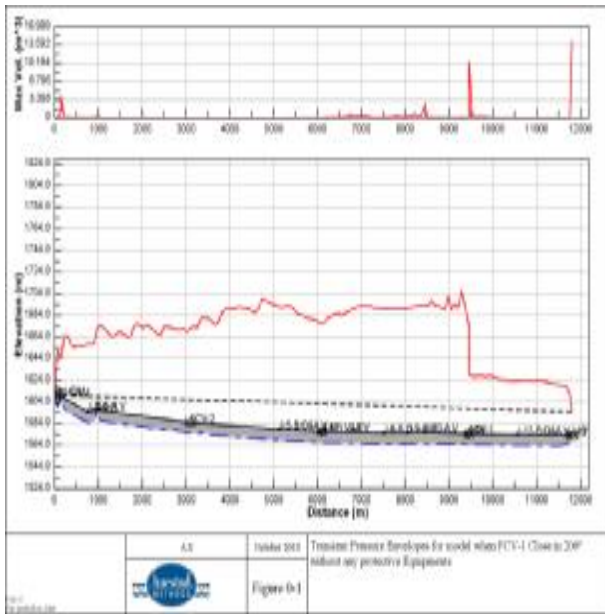


Figure 2: Closing the valve on the wave speed of 600 meters per second for 200 seconds with no impulse control equipment

Figure 2 shows unsteady hydraulic condition when switching valve is closing in about 9+500 km in duration of 200 seconds. It can be seen that without any water hammer control equipment, dynamic pressure of pipeline reaches to about 10 atmospheres before the tap.

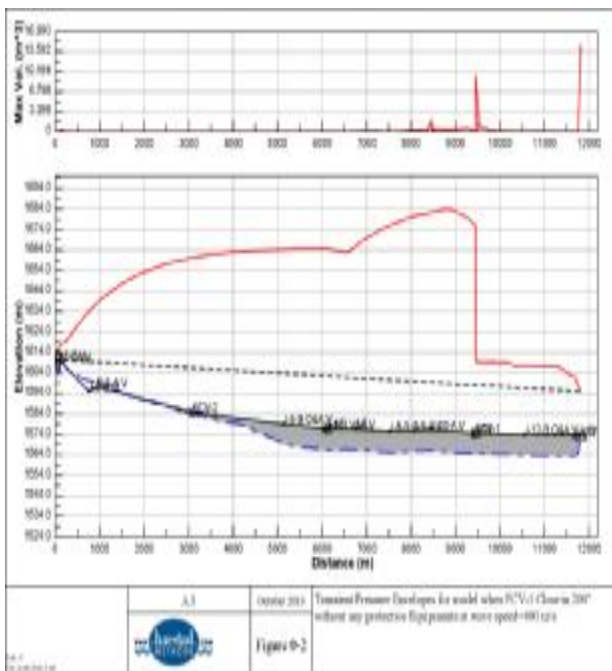


Figure 3: Closing valve for 200 seconds at a speed of 400 meters per second without any impulse control equipment.

Figure (3) shows the increasing pressure result from closing of switching valve in around 9+500 km with wave speed of 400 meters per seconds without any water hammer control equipment. It is observed that with

decreasing the wave speed from 600 to 400 meter per seconds, the amount of potential hit rate decrease about 2 atm.

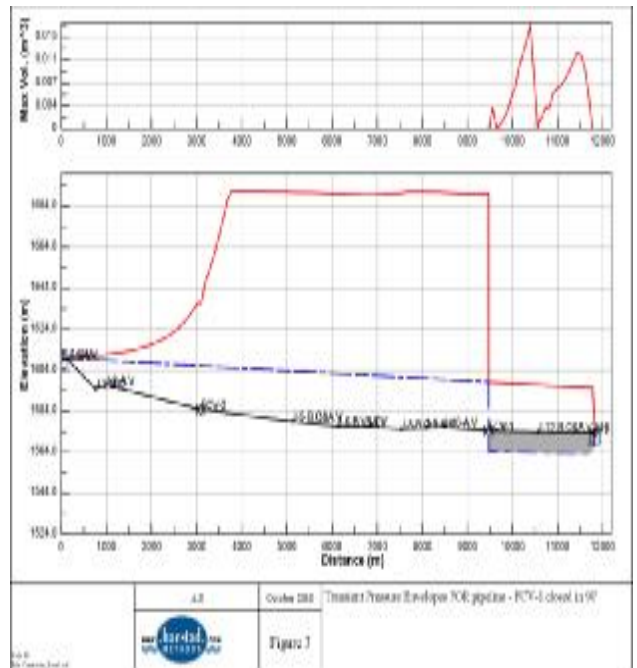


Figure 4: Closing the tap for 90 seconds at a speed of 400 meters per second without any impulse control equipment.

As can be seen in Figure 4, if the switching valve closure time reduced from 200 to 90 seconds, pressure rise due to water hammer occurred slightly than the previous case (200 seconds) but the frontal of positive wave moved at about 4 km further upstream side of the valve.

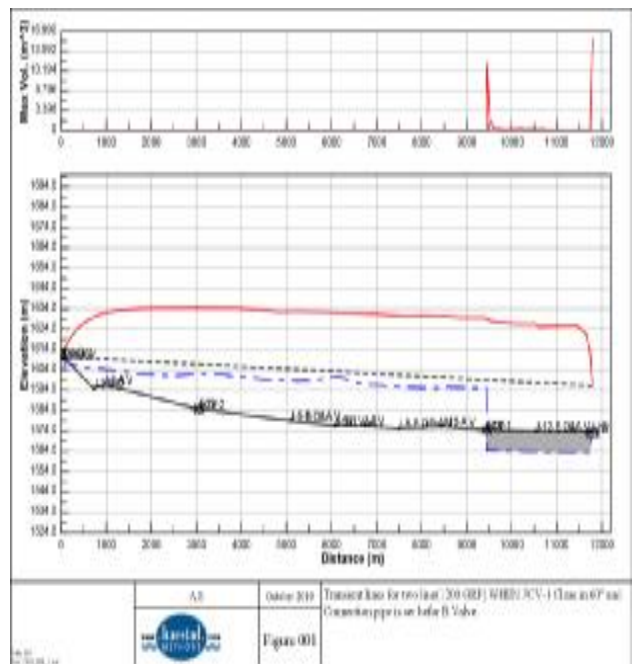


Figure 5: Closing of the tap in 60 seconds by taking a short circuit between two pipes (wave velocity of 600 meters per second)

In figure 5 it is observed in the case of a short circuit between the two pipelines, since the closure time of the valve at about 9+500 km has decreased (from 200 to 60 seconds) than the time when it is not a connection between the two pipes but the increasing pressure of water hammer is reduced considerably or in other words the maximum pressure generated during the worst condition is approximate to working pressure of the pipe (that will not exceed 6 atm.).

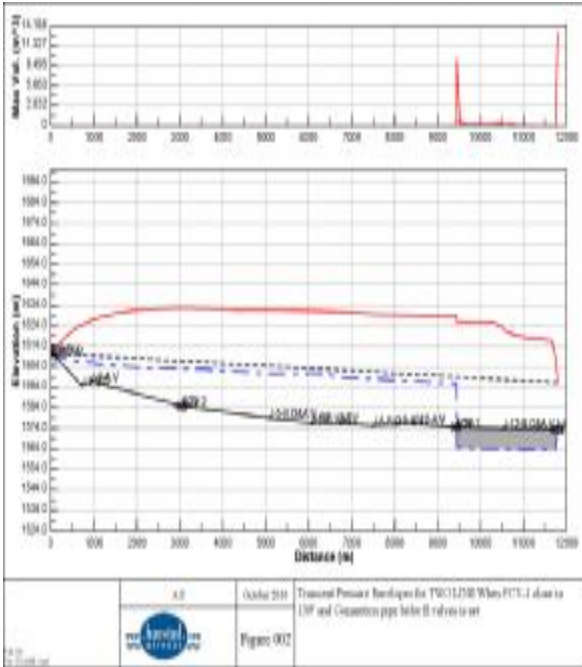


Figure (6): Tap closing in 60 seconds by taking a short circuit between two pipes.

In Figure 6 it can be seen since the valve closure time has increased from 60 to 150 seconds, pressure reduction result from water hammer than the figure 5 is so small.

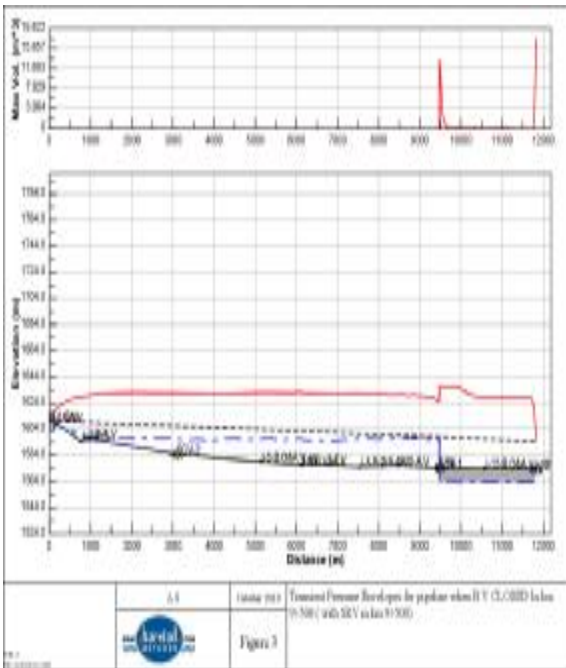


Figure (7): The use of pressure reducing valve in km 9+500 before switching valve

(Wave velocity of 600 meters per second)

Another way to reduce the impact of pressure is to use safety valves.

As it is observed in fig.7 pressure reduction of water hammer in the time of using safety valves is about 1 atm in comparison with fig.6.

But for observing the effect of slowly closure of switching valves in the last 10 to 15%, seven case was modeled, showed that if 90% of the tap close in 200 seconds and the last 10 percent close in 100 seconds reducing the impact in comparison to the second case (Figure 3) is about one to one and a half atmosphere.

But the eight case was modelled for observing the effect results from slowly closure of switching valves in another location of transmission line, showed that if 90 percent of the tap closure (km 3+100) took place in 200 seconds and the other 10 percent took place in 100 seconds, again, there will likely be a hit.

CONCLUSION

Due to the unstable conditions of hydraulic modeling results and comparison of various methods to control the impact from the economic view and the condition to ensure the operation of pipeline the following are discussed:

1 - Almost in all types of valves during closing, the amount of water hammer caused by the closure is approximately 85 to 90 percent of the primary reducing tap and mainly the water hammer causing damage occurs in about 15-10% of distal valve closure. For under pressure gravity systems, 15-10% of the final closing of the valve should be applied in a time more than

$$T_r = \frac{2L}{a}$$

, in order to reduce water hammer pressure.

2 - Using a short circuit(connection pipe) between two pipes that in case of occurrence of strokes, each pipe acts like a reservoir buffer for the pipe and in addition to cost reduction compared to control impulse safety valves or other techniques, the conditions of operation of the transmission line is easy.

3 - One of the oldest method is to install pressure before the valve and so the operator should be trained according to the number of pressure and the maximum pressure should not be increased to a certain value to perform the operation of valve closure. Due to the error of manpower and the possibility of inattention of the owner this method is not recommended.

4 - Using power steering (electric actuator) or hydraulic valves that it can precisely control and regulate the opening and closing time. By changing and reducing the operator rounds, increases the time of opening and closing of the valve. In hydraulic pilot valves with creating local pressure drop in direction of hydraulic steering to the diaphragm and valve components can

control and regulate the opening and closing time of the valve.

5 - The modeling results showed that safety valve control the potential water hammer so good.

6- In total the cost of short circuit(connection pipe) between two pipes is less than the safety valves and power steering, also during the operation of this circuit it gives more flexibility to design and it is recommended to use short circuit between the two pipes in switching valve basin to control the water hammer phenomenon.

REFERENCES

- [1] Anton Bergant., Angus, R. Simpson And Esad Sijahmozic., " Water Hammer Analysis of Pumping Systems For Control of Water in Underground Mines". 4 th International Mine Water Congress, Ljubljana, Slovenia, Yugoslavia. September 1991.
- [2] Allievi, L., " Theory of Water Hammer" Ricardo Garoni, Rome, 1925
- [3] Cannizzaro, D., Pezzigna.G., 2005. "Energy Dissipation in Transient Gaseous Cavitation" Journal of Hydraulic Engineering, ASCE, 131, 724-732.
- [4] C.k. su, and c. camara, " cavitation luminescence in a water hammer: up scaling sonoluminescence". Journal of physics of fluids, vol.15,pp- 1457-1461
- [5] Don J. Wood., " Water Hammer Analysis – Essential And Easy (and Efficient), Journal of Environmental Engineering, vol. 131, No.8, August 1.2005.ASCE, ISSN 0733-9372/2005/8-1123-1131
- [6] Joukowsky, N., " Water Hammer", Proc. Am. Water Works Ass., 1904, v24,pp 338-424
- [7] Magazine NO 517, Vice President of Strategic Planning and Control: guidelines on the selection and design of control equipment and water utility of hammer. pp: 260-290, 2006
- [8] Parmakian, J., 1963. " Water Hammer Analysis". Dover Publications, inc., New York, NY.
- [9] Streeter, V.L. And Wylie, E.B., " Water hammer and surge control".Annual Review of Floud Mechanics, V6, paper 8054, pp 57-73, 1974
- [10] Tan Wee Choon., Lim Kheng Aik., Lim Eng Aik., Thean Him., " Investigation of Water Hammer Effect Through Pipe line System" international journal on Advanced Science Engineering information Technology. Vol. 2(2012) No. 31SSN: 2088-5334
- [11] Taebi, A. And Chamani, M., " Urban Water Distribution Network". University OF Sfahan, Iran, pp: 330- 340, 2000.
- [12] Wood, F.M., "History of Water Hammer" , Dep. Civ. Eng., Queens Univ., Kingston, ont., C.E.Res.Rep. n 65.Apr 1970

Differences between structural, textural and rheological properties of two Cameroonian mineral clays used as cosmetic mask

Orléans Ngomo^{a,b*}, Joseph Marie Sieliechi^a, Jean Bosco Tchatchueng^a, Richard Kamga^a, Aurel Tabacaru^c, Rodica Dinica^d, Mirela Praisler^d

Abstract— This work aims to determine the structural, textural and rheological properties of two clays traditionally used as a beauty mask by women. Clays were sampled at Maroua (MOM) and Douala (DOM) respectively located in the Far North region and Coast of Cameroon. The structure analysis was performed using techniques such as SEM, EDX, FTIR, XRD, and ATG. The determination of the specific surface area was performed by using the adsorption-desorption isotherms of nitrogen. The rheological properties were determined using a rheometer. The results show that the Maroua clays consist mainly of montmorillonite, whereas Douala clays consist primarily of kaolinite. Maroua clays have a surface area of 109.48 m²/g and contain in their structure essential elements such as calcium (1.23%) Magnesium (0.95%) and sodium (0.46%); while Douala clays have a surface area of 55.05 m²/g with the presence within their structure of essential elements such as calcium (0.34%) Magnesium (0.51%) and sodium (0.17%). Rheological analyzes show that Maroua clays has the pseudoplastic character typical montmorillonite while Douala clays has the viscoelastic nature characteristic of kaolinite. Both clays can be used as facial mask with more benefits for montmorillonites.

Keywords— kaolinite, montmorillonite, physico-chemical and textural properties, cosmetic masks

This work was supported in part by the scholarship Program "Eugen Ionescu" AUF for granting a fellowship.

Orléans Ngomo^a Department of Applied Chemistry, National School of Agro-Industrial Sciences, University of Ngaoundere, BP.455 Cameroon. Department of Chemistry, Faculty of Sciences, University of Yaounde I, BP. 812 Cameroon Phone:(0023799614106); e-mail: orleansn@yahoo.fr.

Joseph Marie Sieliechi^a, Department of Applied Chemistry, National School of Agro-Industrial Sciences, University of Ngaoundere, BP.455 Cameroon. e-mail: jsieliechi@yahoo.fr

Jean Bosco Tchatchueng^a, Department of Applied Chemistry, National School of Agro-Industrial Sciences, University of Ngaoundere, BP.455 Cameroon. e-mail: jbotchatchueng@yahoo.fr

Richard Kamga^a Department of Applied Chemistry, National School of Agro-Industrial Sciences, University of Ngaoundere, BP.455 Cameroon. e-mail: richkamga@yahoo.fr.

Aurel Tabacaru^c Department of Chemical Sciences, University degli Stuti di Camerino, Via S. Agostino 1, 62032 Italy. e-mail: aurel.tabacaru@unicam.it
Rodica Dinica^d. Department of Chemistry, Physics and Environment, Faculty of Sciences and Environment, "Dunarea de Jos" University of Galati, 800008, Romania. e-mail: Rodica.Dinica@ugal.ro

Mirela Praisler^d Department of Chemistry, Physics and Environment, Faculty of Sciences and Environment, "Dunarea de Jos" University of Galati, 800008, Romania. e-mail: Mirela.Praisler@ugal.ro

I. INTRODUCTION

Clays are alumino-silicate microcrystallines with leaf structure, originating from the alteration of primary minerals of soil [1]. Clay minerals are not only the "most abundant mineral components of the surface world" [2], but also the minerals showing various applications, in cosmetic, environmental protection and in paper, chemical or food industries for the discoloration and stabilization of vegetable oils [3], [4]. During the last decade, clays beneficial to human health have received great interest [5]-[7]. The most frequently encountered clays are kaolinite, montmorillonite, illite, vermiculite and chlorite [8], [9]. The advantages are : a high sorption capacity , high surface area, water solubility , reactivity with acids, a high refractive index , a large capacity of heat retention , opacity , low hardness , high reflectance and good rheological properties [10].

In this study, the analysis of the structural, textural and rheological properties of clay from Maroua and Douala is made. The morphological analyses were performed by scanning electron microscopy (SEM). The chemical composition was determined by X-ray Dispersive Energy Spectroscopy (XDE) and by X Fluorescence (XF). The different crystalline and superficial phases were studied by using X-ray Diffraction (XRD), Fourier Transform Infrared Spectroscopy (FTIR) and Thermal Gravimetric Analysis (TGA). Textural properties were analyzed by Nitrogen adsorption-desorption and rheological properties are also determined.

II. MATERIAL AND METHODS

A. Material

The two types of clay analyzed in this study originate from the far north and the littoral of Cameroon, in the areas of Maroua and Douala respectively (fig.1). Clay fractions (<2 µm) were separated by sedimentation.

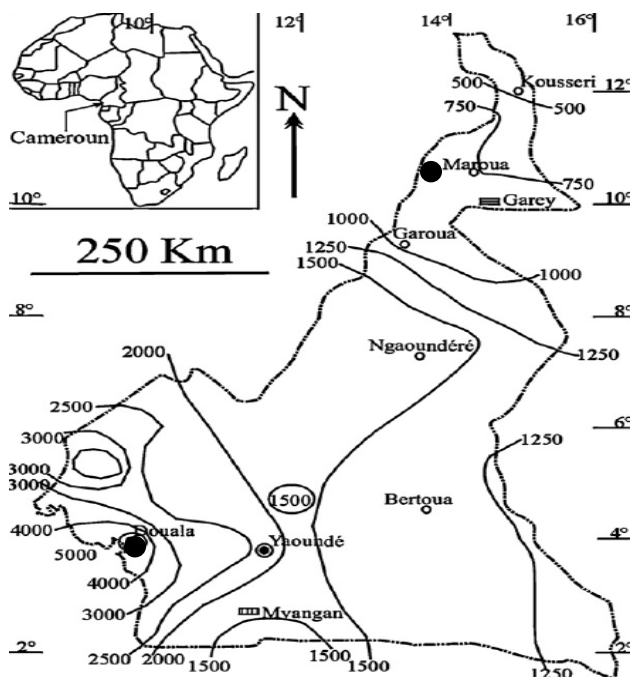


Fig.1. Identification of two sites of clays sample (●)

B. Methods

SEM and XDE observations were carried out with a Beckman Coulter SA 3100 microscope. The chemical analysis of the mineral components (minor and traces) was done, on a AE380 Fluorimeter; XRD data were obtained by using a Siemens X: DRON-3 diffractometer with $CuK\alpha 1$ radiation ($\lambda = 1.4505 \text{ \AA}$), $U=30kV$ and $I=30mA$. The detection limit of a given crystalline phase is estimated around 1% in mass. For the Greene-Kelly test [11], the specimens were exchanged with lithium ions, heated at $400^\circ C$ overnight, and then solvated with glycerol. Infrared spectroscopy were recorded using a Perkin Elmer 100 Fourier Transform Infrared spectrometer ($4000\text{--}650 \text{ cm}^{-1}$) equipped with a detector cooled at $77K$, working in diffuse reflectance mode. The amount of clay was 70 mg dispersed in 370 mg KBr. Nitrogen adsorption-desorption isotherms at $77K$ were recorded on a step-by-step automatic home-built setup. Pressures were measured using 0–10 mbar and 0–1000 mbar Beckman Coulter SA 3100-type pressure sensors provided by Edwards. Prior to adsorption, the samples were out gassed during 18h at $110^\circ C$ and under a residual pressure of 0.3Pa. Nitrogen (purity >99.9995%) that was used for experiments was provided by Alphagaz (Italy). Specific surfaces areas were determined from adsorption data by applying the Brunauer–Emmet–Teller (BET) equation. Micropore volume areas were obtained using the t -plot method. Pore size distributions were calculated based on the desorption branch by using the Barrett–Joyner–Halenda method. The water adsorption capacity was determined using a desiccator and the rheological values are obtained on the Rheological AR 2000 ex with 60mm of stray diameter, by mixing with a ratio water/clay of 3/2 for montmorillonite and 1/1 for kaolinite.

III. RESULTS AND DISCUSSION

A. Morphology and chemical composition

SEM micrographs of clays of $1000\mu m$ size (fig.2) reveal that the structure of Maroua clay presents particles of different shapes and sizes on the compact plaque. This indicates the presence of quartz and amorphous feldspath. The particles of Douala clay have different sizes and look less compact than Maroua clays, showing no agglomeration. This indicates that the two types of clays are different indeed.

The major elements of these two clays were identified by EDX (Fig.3, Table1). Oxygen is the most abundant element; this implies that other elements are found in oxide state. After Oxygen, Silice and Aluminium are most important components for clays which are generally aluminosilicates. Iron is relatively more abundant in Maroua clay, showing that Aluminium was substituted by Iron in the structure of the clay; similar observations were previously made by Nguetnkam et al [12]. The exchangeable cations (Na^+ , K^+ , Ca^{2+} and Mg^{2+}), very important in cosmetics products [13] are more abundant in the Maroua clay than in the Douala samples. The analysis of trace elements by FX (see Table 2) confirms the important proportion of Fe in Maroua clays. The other traces elements are Co, Zr, Rb, Sr, Zn, Mo and Pb.

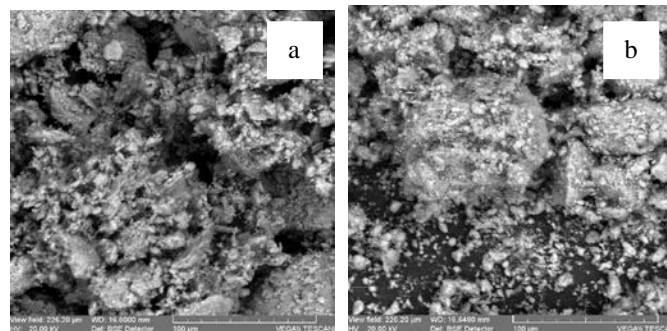


Fig.2. SEM of Maroua (a) and Douala (b) clay samples, size $1000\mu m$.

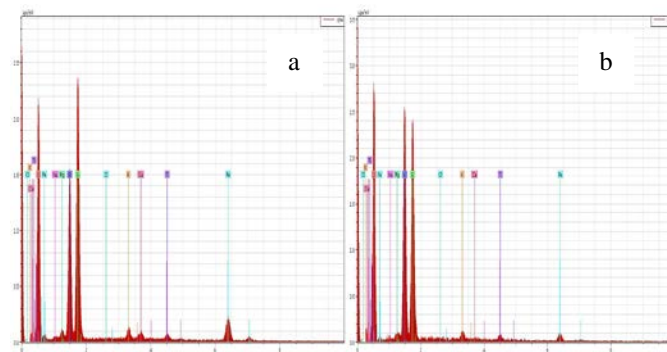


Fig.3. Elemental analysis of Maroua (a) and Douala (b) clay.

Table1. Chemical composition (major elements) of Maroua and Douala clays determined by XDE.

Elements % weight	Si	Al	Fe	Cl	Na
MOM	26,377	15,575	6,948	0,284	0,464
DOM	20,469	18,195	2,570	0,286	0,167

Elements % weight	K	Mg	Ti	Ca	O
MOM	1,651	0,949	1,285	1,233	57,658
DOM	1,039	0,513	1,500	0,341	57,388

Table2. Composition in trace elements of Maroua and Douala clays determined by XF

Elements (ppm)	Fe	Co	Zn	Pb	Rb	Sr	Zr	Mo
MOM	12844	478	37	13	63	53	66	18
DOM	4747	222	146	30	43	44	150	13

B. Structure and superficial phases

The nature of different phases is identified by XRD, as shown in Fig4 for the Maroua and Douala clays. The different elements that were identified are listed in Table 3.

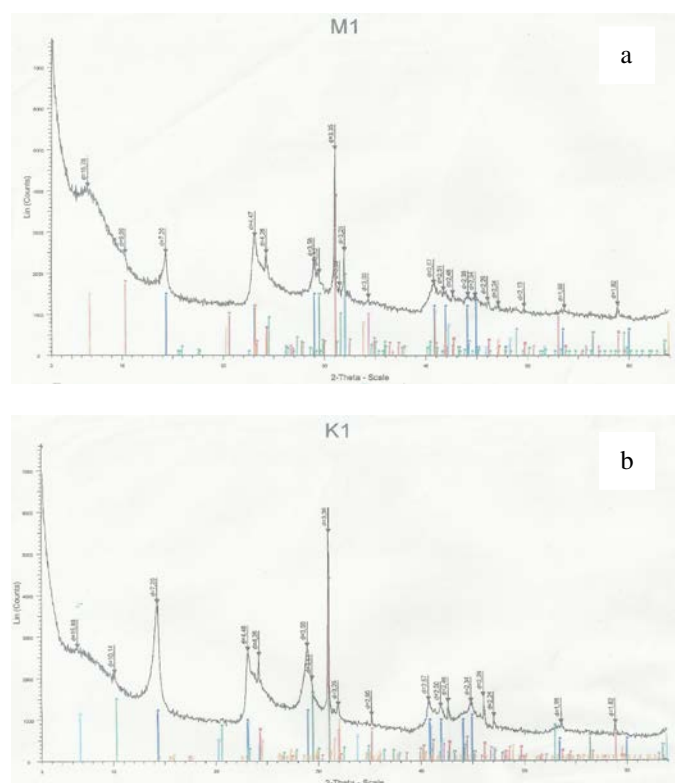


Fig.4. XRD diffractograms of Maroua (a) and Douala (b) clays

Table3. Diffraction results obtained by XRD

Elements	Silice (quartz)	kaolinite
----------	-----------------	-----------

d(A°)	MOM	4.26, 3.35, 4.26	7.20
	DOM	4.26	7.20

Elements	Fe Oxyde	Ti Oxyde	Montmo- rillonite	
d(A°)	MOM	2.57	3.58	15.78
	DOM	2.57	3.58	/

The important number of peak characteristic of quartz on clay from Maroua shows a more amorphous structure.

When the Greene–Kelly test is used on Maroua sample re-expand partly upon contact with glycerol vapor, there is no peak at 19.8 Å, Montmorillonite is the smectite of this mineral clay (not represented here).

The infrared spectra of Maroua and Douala clays are shown in Fig.5. The band interpretation is given in Table 4. The adsorption bands of the two types of samples are similar; many superficial groups have Si and Al, as indicated previously by the EDX observations. The Douala clay shows thinner bands and the band of smectite (around 3400 cm⁻¹) is missing from its spectrum.

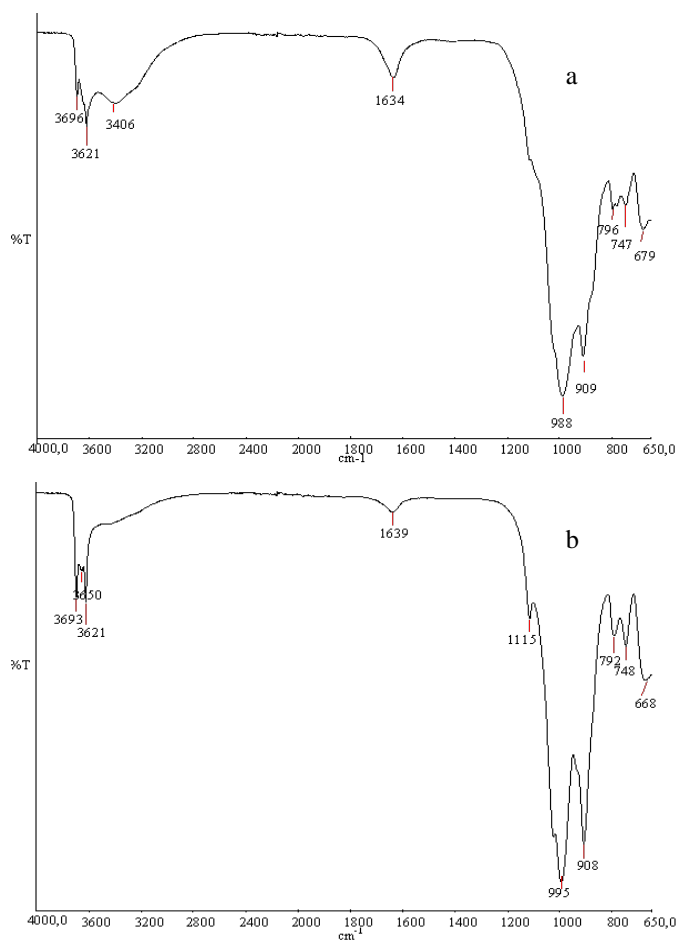


Fig.5. Infrared spectra of Maroua (a) and Douala clays (b)

Table4. Attribution of the infrared spectra bands of Maroua and Douala clays

Wavenumber (cm ⁻¹)		Vibration type	References
MOM	D0M		
3695	3693-3650	γ OH, mainly Al-OH-Al of kaolinite	Nguetkam et al [12], [14]
3621	3621	γ OH of kaolinite and montmorillonite, AlAlOH coupled to AlMgOH	Nguetkam et al [12], Christidis et al [4]
3406	/	γ OH of water and hydroxyde groups involved in the hydrogen links (smectite)	Nguetkam et al [14], Christidis et al [4]
1634	1639	Deformation vibration γ OH of water or Si-O, Si-O-Al	Unuabonah et al[15], Nguetkam et al[12], [14]
/	1115	Peak characteristic to kaolinite	Nguetkam et al[14]
987	995	Si-O of orthosilicates	Nguetkam et al[12], [14]
909	908	Deformation vibration γ OH of Al-OH-Al (smectite / kaolinite)	Wang et al[16] Nguetkam et al[12], [14]
797	792	Deformation vibration Si-O of Quartz	Unuabonah et al[15], Nguetkam et al[12], [14]
747	748	Deformation vibration γ OH of kaolinite	Nguetkam et al[12]
679	668	Si-O-Al (kaolinite and smectite)	Nguetkam et al[12], [14]

The thermoponderal curves of Maroua and Douala clays are presented in Fig.6. We observe on the curve of Maroua clay two loss of weight of about similar importance. The first on 100°C corresponds to absorbed water. The strong slope on the curve indicates that water is absorbed between the leaf like observations on 2/1 clays (swelling clays). The second loss of weight shows between 250-550°C, corresponds to the dehydroxylation of clay. The loss of weight of Douala clays takes place in two steps also. However, the first one less important at 100°C (loss of absorbed water). The weak slope on the curve means that water is on the surface of clay material, meaning that we have 1/1 clay (not swelling clay). The second one is more important occurs between 250-600°C, corresponding to the dehydroxylation of water. Table5. illustrates these losses of weight.

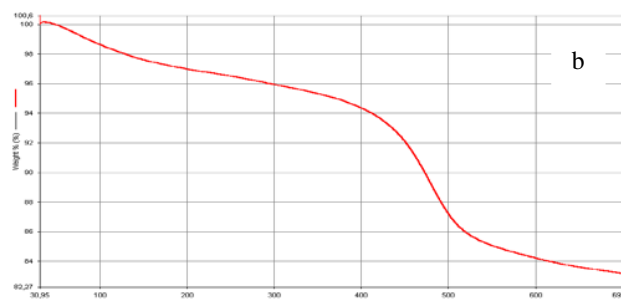
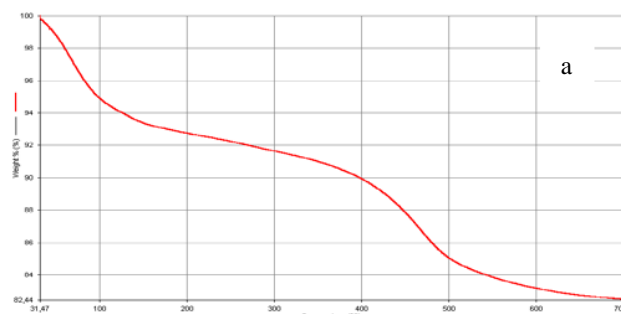


Fig.6. Thermoponderal curves of Maroua (a) and Douala (b) clay

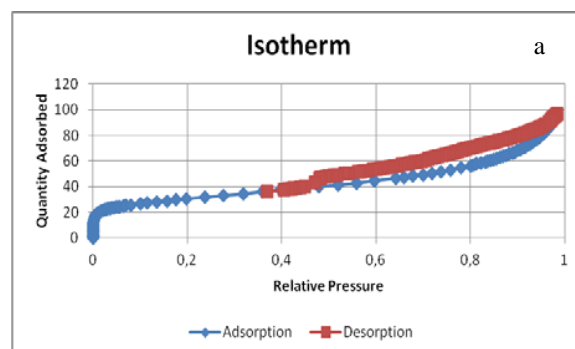
Table5. Relative proportions of weight loss between 30-200°C and 200-600°C as determined by TGA

Weight loss (%)	Temperature variations (°C)	
	30-200	200-600
MOM	39,4	60,6
DOM	19,4	80,6

The different analyses of structure and superficial phase indicate that the Maroua clay is a mixture of kaolinite (type1/1) and montmorillonite (type2/1), while the Douala clay is mainly kaolinite (type1/1).

C. Textural properties of clays

The objective of this part is to define the interstitial spaces between clay platelets and the vacant sites.



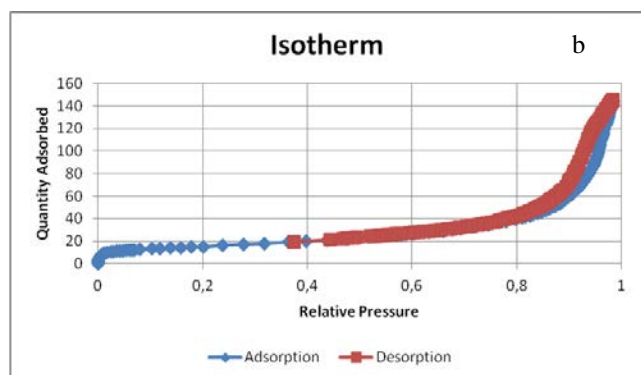


Fig.7. Adsorption/desorption isotherms for Maroua (a) and Douala (b) clay

The nitrogen adsorption–desorption isotherms obtained for the Maroua and Douala clays display very similar shapes (Fig.7). All the isotherms are close in shape to type IV because hysteresis occurs during the desorption branches, according to the IUPAC (International Union of Applied Chemistry) classification. This behavior can be attributed to mesoporous structures [17-19]. However, there are noticeable differences in the shape of their hysteresis loops (Table 6). The specific surface area of Maroua clays is twice that of Douala clay.

Table6. Pore size distribution and specific surface of clays

Pores size distribution (nm)	MOM		DOM	
	Pore volume (ml/g)	Percentage (%)	Pore volume (ml/g)	Percentage (%)
< 6	0,048	37,2	0,014	6,2
6 – 8	0,015	11,7	0,008	3,5
8 – 10	0,011	8,3	0,009	3,9
10 – 12	0,008	6,2	0,012	5,1
12 – 16	0,007	5,6	0,021	9,0
16 – 20	0,006	4,2	0,020	8,8
20 – 80	0,025	19,5	0,130	57,3
> 80	0,010	7,3	0,015	6,3
Total volume(ml/g)	0,130		0,228	
Specific surface (m ² /g)	109,48		55,05	

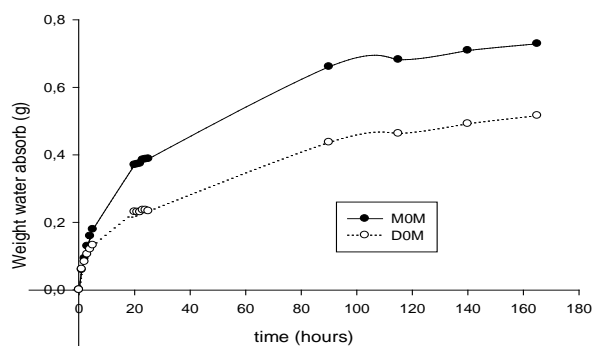


Fig.8. Water adsorption isotherms of Maroua and Douala clay

The water adsorption evaluation (Fig.8) confirms the results of thermoponderal analysis, which shows that the Maroua clays is swelling (type 2/1) and adsorbs too much water, contrary to Douala clays that shows no swelling (type 1/1) property.

D. Rheological properties of clays

The main rheological parameters of suspensions are viscosity, shear rate, yield stress, thixotropy. Fig.9 shows a linear relationship between shear stress and shear rate, and fig. 10 illustrates the relationship between viscosity and shear rate.

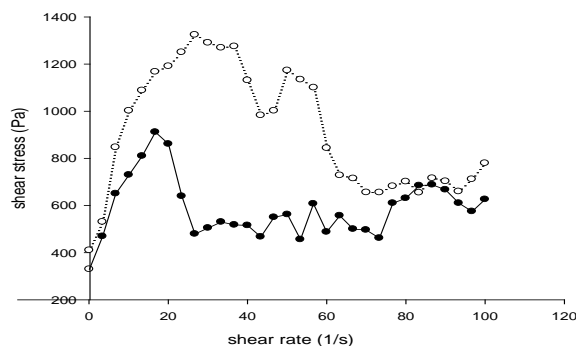


Fig.9. Effect of shear stress on shear rate on clay from Maroua (●) and Douala (○).

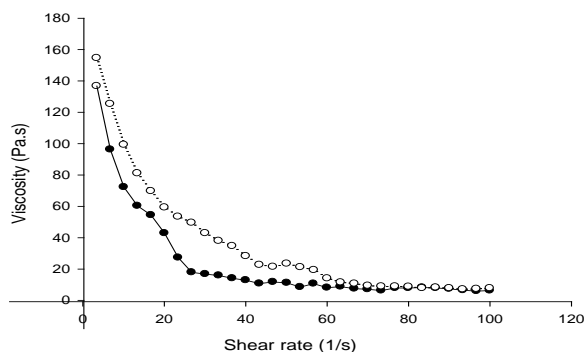


Fig.10. Effect of shear rate on viscosity on clay from Maroua (●) and Douala (○).

According to the graphs below, the two clays behave as viscoplastic suspensions, meaning that, below a certain critical value of stress (the yield point corresponding to the elastic limit defined as a static yield, it marks the beginning of the solid - liquid transition [20], the material behaves as a solid , but flows like a viscous liquid when this stress exceeds. Viscosity depends on the applied stress and decreases with increasing shear rate. We note that the Maroua clay have yield point lowest (about 300Pa) while, Douala clay have greater levels of shear (about 400Pa) (Fig.9). This difference can be explained by the fact that Maroua clay is a swelling clay 2: 1 and adsorb more water, have a high fluidity and low viscosity. It is noted that the evolution of the viscosity versus shear rate is the same for both clays, but it is less important for clays Maroua (fig. 10); this might be due to the more important Calcium quantity [21]. However, the two suspensions formed are thixotropic.

The oscillation dynamic tests are also significant tools to reveal the microscopic structure of viscoelastic materials. In general, the material can respond to this type of deformation through two mechanisms: conventional storage energy and viscous dissipation energy. Quantitatively, these responses can be represented as storage modulus (G') or stored energy per volume unit, and loss modulus (G'') or energy dissipated per unit strain rate per volume unit. The storage modulus is proportional to the extent of the elastic behavior of the system and the loss modulus is proportional to the extent of the viscous behavior of the system. Fig. 11 presents the evolution of the elastic and viscous depending on the frequency modules.

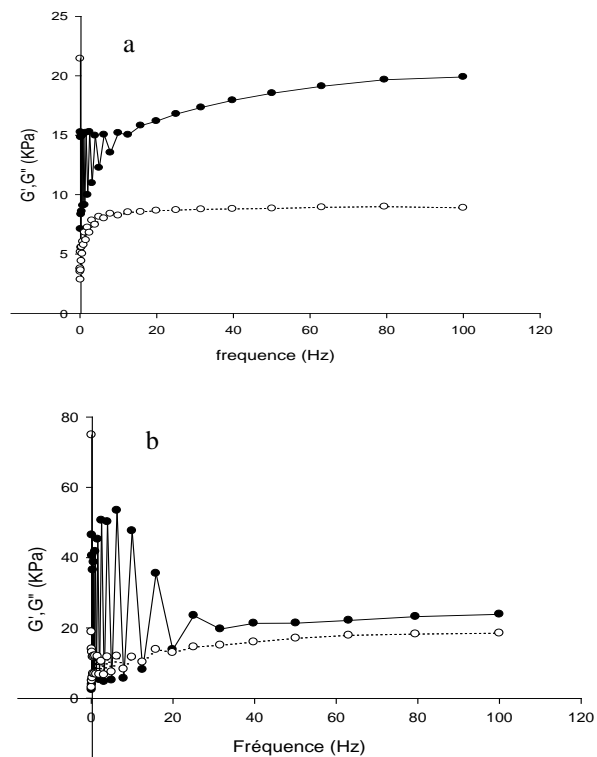


Fig.11. Variation of elastic modulus G' (●) and viscous modulus G'' (○) according to fréquence a)MOM et b) D0M.

We see that Maroua clay is more elastic than viscous, with the storage module most important about 20000 Pa and 25000 Pa for Douala clay, the viscous modulus is 10000 Pa and about 15000 Pa for Douala clay (figure11). Otherwise, the storages and losses modules are comparable, leaving the phase angle delta (phase shift between the imposed stress and displacement, in degrees) around 25 degrees for Maroua clay and 35 degrees for Douala clay (fig.12). This lower angle delta clay Maroua value confirms its greater elasticity compared to Douala. However, the values of the storage and loss modules and phase angle of the two clays are typical for systems of low elasticity [22].

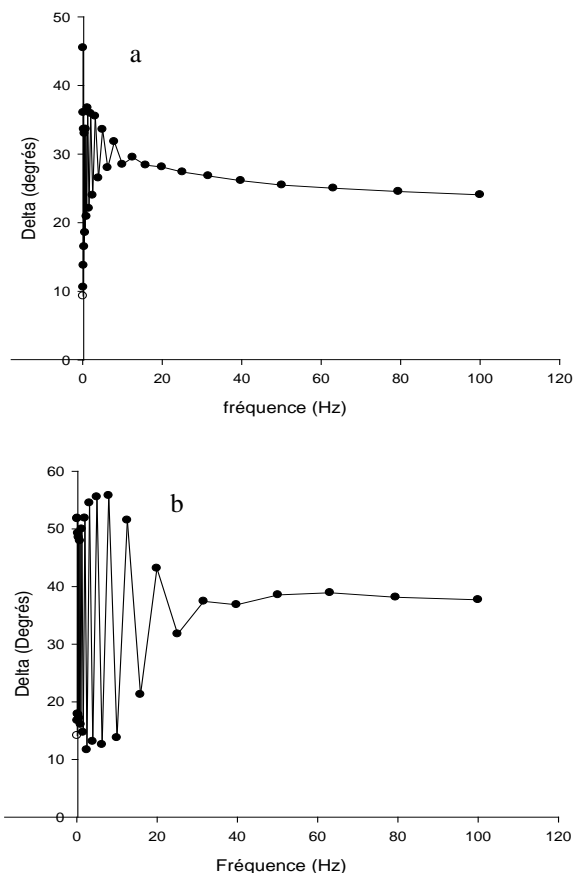


Fig.12. Effect of phase shift between the imposed stress and displacement, and frequency Maroua a) and Douala b)

Gels clays show the characteristics intermediate between liquids and solids with flows generally plastics and high viscosities [23] and hysteresis [24]. This thixotropic behavior is typical to cosmetic products [25].

The paste of clay mineral 2: 1 are typically pseudoplastic with a large usual properties: thixotropy and yield stress (resistance to breaking of the structure) improved stability of the paste [26].

With a high concentration in solids, kaolinites dispersions exhibit a viscoelastic behaviour. This rheological behavior is attributed to pockets closed of deflocculated particles clay, which during shear results of interaction contact and interparticle [27]. The morphology (spherical plane or tubular) greatly affects the viscosity of paste of kaolinite.

IV. CONCLUSION

We have identified notable differences between the Maroua and Douala clays by analyzing their SEM/XDE images, as well as their XF, XRD and FTIR patterns, nitrogen adsorption-desorption isotherms, water adsorption and rheological behavior. We may conclude that the Maroua clay is mainly montmorillonite, few kaolinite and is pseudoplastic. On the other hand, Douala clay is essentially kaolinite and is pseudoplastic. Both of them can be used for cosmetic

application like facial masks, as they are a good support to the skin, ensure expansion of pores and contribute to its moisturizing. Kaolinite has few minerals; it is neutral, sweet and cover very well. montmorillonite absorbs very well and is the best for in-depth cleaning with best thixotropy.

REFERENCES

- [1] H Chamayou and J.P Legros,.. Les argiles. Les bases physiques, chimiques et minéralogiques de la science du sol, Presses universitaires de France (1989).
- [2] B. Velde., Origin and Mineralogy of Clays: Clays and the Environment. 1995 (Springer, Berlin).
- [3] Vicente Rodríguez, M.A., López González, J.D., Bañares Muñoz, M.A., Casado Linarejos, J., Acid activation of a Spanish sepiolite: II. Consideration of kinetics and physicochemical modifications generated. *Clay Minerals* (1995) 30, 315–323.
- [4] G.E, Christidis, P.W. Scott, A.C.Dunham . Acid activation and bleaching capacity of bentonites from the islands of Milos and Chios, Aegean, Greece. *Applied Clay Science* (1997) 12, 329–347.
- [5] Isabel M. Carretero Clay minerals and their beneficial effects upon human health. A review. *Applied Clay Science*. (2002) 21 155–163
- [6] I. M. Carretero, C. S. F. Gomes Tateo F., Clays and human health. In Bergaya, F., Theng, B.K.G., and G. Lagaly, (Eds.), *Handbook of Clay Science, Developments in Clay Science*, (2006) vol. 1 pp. 717–741.
- [7] E. Gamiz, J. Linares, R. Delgado., Assessment of two Spanish bentonites for pharmaceutical uses. *Appl. Clay Sci.* (19926), 359–368.
- [8] V. Chatain, karacterisation of potential mobilisation of arsenic and others inorganic component in soil from aurifer minin site. Doctorat Ph.D. these of chemical Lyon school. (2004) 189p.
- [9] Vivian Zague, Diego De Almeida Silva, Andri Rolim Baby, Telma Mary Kaneko, And Mariav Ali Riar Oblevse Lasc. Clay facial masks:P hysicochemicaslt abilitya t different storage temperatures j. *Cosmet.c i.*, (2007) 58, 45-51
- [10] Isabel M. Carretero, Manuel Pozo. Clay and non-clay minerals in the pharmaceutical and cosmetic industries Part II. Active ingredients *Applied Clay Science* (2010) 47, 171–181.
- [11] Green-Kelly,R,.. The montmorillonite minerals. In: MacKenzie, R.C.(Ed.), *The differential thermal investigation of clays*. Mineralogical Society, London, (1957) pp. 140-164.
- [12] J. P. Nguetnkam, R. Kamga, F. Villiéras, G.E. Ekodeck, A. Razafitianamaharavo, J.Yvon. Assessment of the surface areas of silica and clay in acid-leached clay materials using concepts of adsorption on heterogeneous surfaces. *J. of Colloid and Interface Science* (2005) 289, 104–115.
- [13] Gomes Figueredo Celso de Sousa et Silva Pereira Joao Baptista. Minerals and clay minerals in medical geology. (2007) *Appl. Clay Sc.* 36, 4-21.
- [14] J. P. Nguetnkam., R. Kamga, F.Villiéras, G.E. Ekodeck, J. Yvon. Assessing the bleaching capacity of some Cameroonian clays on vegetable oils. (2008) *Appl. Clay Sci.* 39 113–121.
- [15] Emmanuel I. Unuabonaha, Kayode O. Adebawale, Folasegun A. Dawodu Equilibrium, kinetic and sorber design studies on the adsorption of Aniline blue dye by sodium tetraborate-modified Kaolinite clay adsorbent *Journal of Hazardous Materials* 157 (2008) 397–409.
- [16] Tsing-Hai Wang, Tsung-Ying Liu, Ding-ChiangWu, Ming-Hsu Li , Jiann-Ruey Chen, Shi-Ping Teng, Performance of phosphoric acid activated montmorillonite as buffer materials for radioactive waste repository. *Journal of Hazardous Materials* 173 (2010) 335–342
- [17] Qian Zhongzhong, Hu Guangjun, Zhang Shimin, Yang Mingshu; Preparation and characterization of montmorillonite– silica nanocomposites: A sol– gel approach to modifying clay surfaces. *Physica B* (2008) 403 3231– 3238.
- [18] Srasra E. , Trabelsi-Ayedi M. Textural properties of acid activated glauconite. *Appl. Clay Sci.* (2000). 17, 71–84.
- [19] Kumar P., Jasra R.V., Bhat T.S.G., Evolution of porosity and surface acidity in montmorillonite clay on acid activation, *Ind. Eng. Chem. Res.* (1995)34, 1440–1448.
- [20] Uhlherr, P.H.T., J. Guo, C. Tiu, X.-M. Zhang, J.Z.-Q. Zhou and T.-N. Fang, , The shear-induced solid-liquid transition in yield stress materials with chemically different structures, *J. Non-Newt. Fluid Mech.* (2005) 125, 101-119.
- [21] S. Paumier, P. Monnet and A. Pantet. Etude des propriétés viscoélastiques de suspensions de smectite homoioniques à bi-ioniques (Ca²⁺, Na⁺): influence de la concentration (2-100 g/l). 18ème Congrès Français de Mécanique Grenoble, 27-31 août 2007.
- [22] Sabine Kempe, Metz Hendrik, Bastrop Martin, Hvilsom Annette, Vidor Contri Renata, Mader Karsten. Karacterization of thermosensitive chitosan-based hydrogels by rheology and electron paramagnetic resonance spectroscopy. *European Journal of Pharmaceutics and Biopharmaceutics* (2008) 68; 26–33
- [23] J. Mewis, , C.W. Macosko. Suspension rheology. In: Macosko, C.W. (Ed.), *Rheology: principles, measurements and applications*. VCH Pub, New York, (1994) pp. 425–474.
- [24] Cl.Thirriot , Th.Karalis. Quelques experiences sur la rhéologie des argiles sèches et humides. *Rheologica acta.* (1980) 19, 124-132.
- [25] Peter Herh, Tkachuk Jullian, Wu Spencer, Bernzen Monica and Rudolph Bruce. The rheology of pharmaceutical and cosmetic semisolids. Application Note, American Laboratory, (1998)12-14.
- [26] P.F. Lukham, , S.Rossi, , The colloidal and rheological properties of bentonite suspensions. *Adv. Colloid Interface Sci.* (1999). 82, 43–92.
- [27] C.Viseras, C.Aguzzi, P.Cerezo, A.Lopez-Galindo. Uses of clay minerals in semisolid health care and therapeutic products *Applied Clay Science* (2007) 36. 37–50

Impact of Steering Committee Configuration and Decisions on Project Success in Pakistan

Sabina S. Shirazi

Abstract— In Pakistan, the impact of Steering Committees, when their context is clearly defined, is under-rated. The effect of such committees on project performance, project management and extracting value from project management capabilities is also misunderstood. A quantitative research method was used to carry out analysis of the steering committee factors affecting the output of projects in project-based business environments. The objective of this study is to gather insight from Project managers on project level Steering Committees on how they identify the existence and impact of Steering Committees. The results clearly represent the need to emphasize the importance of the role of Steering Committees (with a special focus on the engineering sector of Pakistan) as they play an integral part in the configuration to the execution of a project. The presence of a Steering Committee in the project management industry in Pakistan is not an entirely new concept. It has existed under different names in Pakistan's work environment for decades. What did not exist was the understanding that their presence and some of their factors could, in fact, bring a positive influence and impact Project Successes significantly. It has been revealed through the this study that Project Success is particularly dependent on the variables identified as Steering Committee Processes and Steering Committee Configuration.

Keywords— Steering Committee, Steering Committee Configuration, Decision Processes, Project Management, Project Success.

I. INTRODUCTION

In Pakistan, the impact of the term Steering Committees is not clearly understood. The purpose and effect of such committees on project performance and their positive impact on project management capabilities is also widely misinterpreted. The role of Steering Committees in setting project management standards has been ignored, in general. Project management practitioners generally relate this function with to the role of a Project Management Office (Kaufman & Korrapati, 2007). In Pakistan, Steering Committees are also referred to by other names such as governing bodies, board of directors, executive committee, and the executive project management team. A Steering Committee, by any other name, is intended to “steer” a project in the correct direction, the requirement being that the committee itself should be structured and conducted properly. In most cases their importance is waived aside because they are often viewed as a Bureaucratic approach to serve the interest of the few top management elements. Whereas this may be the case in some organizations, it is not true for most, as project management

has evolved so as the project management teams' exposure to changing management styles. Compared to the past Pakistani trends, the Steering Committee is now more focused on applying the latest project management styles and hence the concept of a “Steering Committee” is coming into being a more and more reliable way to govern or steer a project keeping in mind that the correct ratio of stakeholders is represented in it. Project sponsors, Project managers and stakeholders have become more and more aware of project management practices and a Steering Committee, Board of directors and any name that may be given to a Steering Committee is becoming more important in the presence of an ongoing project.

A. Rationale of the Study

The rationale of this study is to stress upon the importance of the governing bodies or Steering Committees in any project oriented environment and to recognize the positive role of such bodies through research. The misconception that we have in Pakistan that steering or governing bodies are only used to serve the interest of the top few with no positive influences on the project itself has to be abolished to ensure that a Steering Committee does indeed exist in the best interest of any project.

B. Aim of the Study

The aim of the study is to add to the small database of knowledge that exists in terms of non IT-based, project Steering Committees. In the course of this study very limited data was available as prior research done on non-IT based projects and generally on project management is very limited. The last research published in 2009 by Lechler and Cohen is a very condense research funded by the PMI and an extensive study. This study is aimed at breaking down those variables provided in Thomas G. Lechler and Martin Cohen's study and observe their applicability in Pakistan. The factors taken into account by Lechler and Cohen were more in number than this study. The reason for choosing a very small amount of Independent variables is to explore and gather correct data and research one by one what factors in the Steering Committee have a significant positive effect on Project Success.

C. Research Objective

The research objective of this study is to gather insight from Project Manager on the project level on how they identify the existence of Steering Committees. The Steering Committees have a number of factors to their credit, as per the research by Lechler and Cohen in 2009 which includes Decision

Authority, Committee Configuration, Committee Responsibility, Committee Processes and their impact on Project Success. This research is going to focus on Committee Configuration, Committee Processes and their effect on overall Project Success.

D. Research Question

The research question for this study is does the configuration of a Steering Committee and decision processes significantly impact project success?

E. Delimitations of the Study

The delimitations of the study are the application of this research to engineering project based industries and other project related industries around the globe.

II. LITERATURE REVIEW

A. Concept & Definitions

A Project Steering Committee is recognized as an important structural element in project implementation (Englund & Bucero, 2006). Steering Committees are an essential building block in Managing Projects in an organization. They exist under separate names in separate organizations, some of which may be governing bodies, project valuation Steering Committees, board of directors and Steering Committees. An Effective Steering Committee needs to be small enough to make decisions, but must have all the important stakeholders of the organization/ project represented (Symons, 2003). A Steering Committee is an elite team of representatives from various areas of an organization or project. They are entrusted with the duty of connecting strategies of IT with that of business, by setting project directions, matching corporate concerns with technological potentials, and create commitment to policies (Nolan, R.L., 1982). According to Earl, Steering Committees, chaired by a top executive, typically meet frequently to discuss (IT) direction, approve and prioritize projects, review performances, form or approve policies, establish resource levels, and initiate major plans (Earl, 1989.) Regrettably, successful Steering Committees are not easy to find, and few organizations know what impact these committees play in governing (IT) management (Drury, 1984). In addition, different forms of Steering Committees may be utilized for different reasons (Raghunathan, 1992). Although, configuration and operation of these committees may differ among organizations, their policy-making or direction-setting role in the systems plan typically means that members include executives from several functional areas of the firm. (Doll & Torkzadeh, 1987)

Other than these encouraging effects, committees can also inflict negative consequences on project performances by hindering important execution decisions as well as causing internal conflict in an organization. These influences can be extracted from the general argument centered on dysfunctional management boards (DeVries & Miller, 1984). Mintzberg suggests that linkages formed are vital in building such an informal relationship between management executives

assigned the task of steering a project can help by pass the more bureaucratic responses from Steering Committees (Mintzberg, 1979). This suggests an inverse relationship between linkages and formalization (Doll & Torkzadeh, 1987).

In Pakistan, a Steering Committee, being called by any other name such as a governing body or a board of directors, was known as a committee which gave certain executives the power to take the project in their own chosen direction, be it for project success or personal gain. With the advent of Multinational projects, corporations and more notably “Project Management Practices” the perception of managing a successful project have been altered.

A comprehensive literature search on reference databases (Research papers, PMI Journals and Internet) did not result in the significant number of references that I expected to find addressing the role of Steering Committees in project implementation. The search was then extended to the term “project governance” as was done by Lechler and Cohen in their research in 2009. Again, very few articles were found, most of them are with reference to the IT sector. One reason that the research on Steering Committees is difficult to locate for references is their existence under separate names in various organizations as afore mentioned. The majority of articles that were researched focused on the role of IT related committees in directing IT-related projects (Doll & Torkzadah, 1987, Karimi et al., 2000, Patankar, 2009). The references made by these articles also do not point towards any relevant publications particularly dealing with project Steering Committees except the paper by Lechler & Cohen in 2009 which focuses on a variety of organizations (all non-IT except one).

B. Literature Gaps

The above literature review leads to the conclusion that when it comes to scholarly work, very small database exists regarding the analysis of Steering Committees especially in a database collected in the last five to ten years. Somewhat little scholarly work has been carried out in order to analyze one of the main elements of project management utilized in many organizations.

As afore mentioned, there exists a gap in research with regards to the research conducted on Steering Committees in general and the impact of Steering Committees in the engineering project based sector in particular. Apart from Lechler and Cohen’s research conducted in 2009, there is hardly any research conducted on specifically “Project Steering Committees”, the main focus has been the IT industry thus far.

Lechler and Cohen identified five distinctive components to describe Steering Committees (Lechler & Cohen, 2009). Out of these components, two components will act as independent variables which will further be used to explore the role of a Steering Committee on the dependent variable “Project Success”, in the project based engineering sector of Pakistan. The five components identified by Lechler and Cohen in 2009 are:

- Configuration: This component describes the level of representation of various departments, stakeholders and functional diversity in the committee.

- **Responsibility:** This component elaborates the level of responsibility assumed by a Steering Committee in order to impact project success, cross functional coordination and scope management.

- **Decision Authority:** This component refers to the level of control a Steering Committee exerts over projects and project managers.

- **Organization:** This component describes how Steering Committees organize their work processes, meetings and permanence (ad-hoc vs. permanent).

- **Committee Decision Process:** This component refers to internal committee dynamics and the extent to which the committee controls the project decision- making process.

(Lechler & Cohen, 2009)

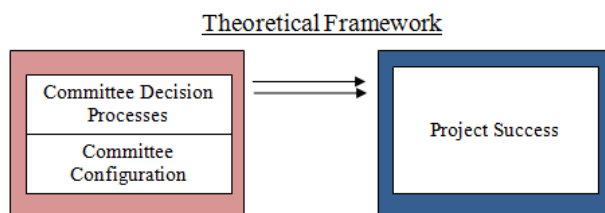
C. Critical Analysis of the Literature

Apart from Mintzberg's research in 1979, the majority of prior research substantiates the positive effect that Steering Committees have on Project Success. It is analyzed that that the predominant image that Steering Committees have given so far is that it consists of executive level people from various parts of an organization who then get together to take important decisions in terms of setting priorities and project direction.

III. THEORETICAL FRAMEWORK

A. Theoretical/Conceptual Framework and Description of Variables

The theoretical framework of the study is given below in graphical shape. This is descriptive study and whole working was carried out around the independent variables' impact on the dependent variable.



B. Proposed Model

The dependent variable in the study is Project Success, whereas independent variables are Committee Decision Processes and Committee Configuration. The relationship between independent and dependent variable is measured with the help of the selected questionnaire. Based on interviews of project managers from a few firms, there are significant evidences that those working in the project based engineering sector in Pakistan are accustomed to the presence of an effective Steering Committee of governing body since the year 2005, especially after the telecom boom took place in the region. This is credit to the multinational work environment and a shift in the project management styles which the Pakistani professionals were exposed to and that they eagerly accepted. It has been observed and through interviewing techniques in this research paper, that project based

professionals are now acknowledging the presence of steering or governing bodies as an entity that not only gives direction to the project but also are quite important for the success of a project. The hypotheses for this study are:

H1: Steering Committee Decision Processes have a significant impact on project success

H2: Steering Committee Configuration has a significant impact on project success

IV. RESEARCH METHODOLOGY

A. Sample Selection

In this research data is collected from various sources including Engineering organizations and interviews. Unfortunately, the strict terminology of "Steering Committee" is not well known to respondents, so all of them were briefed about the subject initially. To gather the data I initially prepared the list of potential respondents through brainstorming and expert judgment techniques. Basing on the convenience sampling technique, questionnaire was to various respondents (Appendix). Convenient sampling was used for the collection of the data by questionnaires. 80% response rate was achieved.

B. Measurement Frame

This study inspects the relationship of the Project Success with the Committee Configuration and Committee Decision Processes in the engineering sector of Pakistan. The questionnaire was developed by Lechler and Cohen in their study in 2009. The sections of the questionnaire that were applied were the ones that relate only to the relevant variables which is the effect of project decision processes and committee configuration on the Project Success.

C. Procedure

This study was supported on primary data. The questionnaire was personally explained to groups which further monitored the respondents in their organizations and professional circles. The questionnaire was distributed among 100 respondents. Only one questionnaire was given to each respondent. Before handing over the questionnaires, questions were explained to the respondents so they could complete the questionnaire and the results could be extracted.

D. Unit of Analysis

The collection of data in any study can be focused on organization, departments, work group and individuals. For this study the main source of information was Project based engineering organizations and concerns. The population frame chosen for this particular research is a number of engineering organizations and companies comprising of performance related engineering projects, the management who answered the questionnaires prefer to remain anonymous.

E. Type of Study

This research is quantitative as well as qualitative as the interview technique was also used in some cases to get a theoretical point of view of the typical project manager. The study can be categorized in to exploratory research, descriptive research and hypothesis testing. Exploratory research is under taken to gain better understand of dimensions of a problem where as descriptive research is use to describe the characteristics of a population. Hypothesis testing is use to explain relationship between different variables.

F. Time Horizon

For this study time horizon was four months. During this period I studied and investigated the impact of Independent variables (Committee Configuration and Committee Decision Processes) on Project Success.

G. Limitations of the Research

This study was conducted in multiple engineering project based organizations. They were then further classified into three types of organizations. Hence, respondents in this study also form three types. On the other hand, this study is only focused on three dimensions or factors of a Steering Committee which are the effects Committee Decision Processes and Committee Configuration on Project Success as a whole whereas there were more factors considered in the original study conducted by Lechler and Cohen conducted in 2009 in their research funded by the PMI (Project Management Institute).

V. DATA ANALYSIS METHODOLOGY

A. Data Collection

Suitable data collection method was used; incomplete and faulty questionnaires were discarded. Problems faced during data collection were that each project manager had to be explained the concept and expectation from the perspective of this research personally. The master training technique was also used in about 10 cases in order to ensure that the questionnaires filled by people who the author was unable to interact with are properly educated by the project manager who acts as a master trainer as well as a liaison between the author and the respondents.

B. Description of Participating Organizations

The participants that responded to the questionnaire were from a variety of engineering project based organizations. Table 1 shows a brief breakdown of types of organizations and number of respondents picked from each organization.

Table 1

Participating Organizations

Sr. No.	Organization Type	Respondents	Remarks
1	New Product	15	The identities of the organizations have been kept anonymous upon request to respect confidentiality and ensure honest responses
	Development		
2	Defense	50	
	Organizations		
3	Telecom Sector	15	
Total		80	

After disregarding incomplete and faulty questionnaires, the number of respondents became 70

C. Data Analysis Techniques

The instrument chosen to be adapted for the data collection is the questionnaire developed by Lechler & Cohen conducted in 2009, also for a similar research on Steering Committees titled Exploring the Role of Steering Committees in Realizing Value from Project Management. The scale used is likert scale on a scale of 5.

The Data analysis software was SPSS, also known as PASW (Predictive Analytic Software) within which Correlation and Regression techniques were used to investigate the impact, strength, direction and significance between Independent Variables (Committee Configuration and Committee Processes) and the Dependent Variable (Project Success).

D. Impact of Committee Configuration and Committee Decision Processes

In this section, it was analyzed how Steering Committees processes can directly impact the implementation and the success/performance of projects. Project managers were requested to respond to the questionnaire keeping in mind their own specific projects and also keeping in mind the main Governing or Steering Committees that they are working with.

- Committee Configurations

Steering Committee Configuration discusses which hierarchical levels or chain of command and which project areas are symbolized in the committee.

- Committee Decision Processes

The decision processes elaborate on project decisions making process and how they were made by the Steering Committee.

- Project Success

The Project Success determines whether the project achieved maximum efficiency, desired outcomes, customer satisfaction and the best economic value for the project.

E. Data Analysis and Reliability Tests

After the completion of data collection and data input, a check was run for any missing values or outliers, having found none, the normality of data was checked and since the skewness was between -1 to +1, the data was found to be normal.

Statistical Package for Social Sciences (SPSS) software was used to apply various statistical tests to the data gathered via questionnaires. Before running more complex tests to analyze the relationship and variance between variables, a pre test was conducted to check the reliability and validity of the instrument. In order to qualify for the reliability the Chronbach's coefficient must be greater than 0.6 (Hair et al., 2006). 0.6 is said to be a safe range for data. Chronbach's Alpha (reliability) for all the variables is more than 0.7. Collected data is reliable. Table 2 shows Chronbach's Alpha' for each research construct. It has been proved through the gathered results that, the constructs are quite reliable and acceptable.

Table 2
Reliability Test- Chronbach's Alpha

Variables	Chronbach's Alpha
Committee Decision Process	.786
Configuration	.921
Project Success	.790

To test our hypotheses, we have conducted Correlation analyses on Committee Decision Process, Committee Configuration as independent variables and Project Success as dependent variable. As the data is normally distributed so the Pearson's correlation two-tailed significance test is applied. This test is used to measure the relationship between independent and dependent variable. The positive correlation validates that the variables are significant at the 0.01 level and all independent variables are strongly correlated with project success. Hence, it verifies one of the research assumptions that Committee Decision Process and Committee Configuration have a significant impact on project success. Correlation was tested following the Chronbach's Alpha reliability test. Table 3 displays the findings of the correlation testing and the relationship of the factors (the correlation results between Committee Decision Process and Committee Configuration).

Table 3
Correlation between Committee Decision Process and Project Success

	Committee Decision Process	Committee Configuration	Project Success
Committee Decision Process	1	.691**	.518**
Committee Configuration		1	.541**
Project Success			1

** . Correlation is significant at the 0.01 level (2-tailed), N=70

The findings are that first of all, there is positive correlation, Committee Decision Process is positively correlated with a value of $r=0.518$ with a significant value of $p<0.5$. Committee Configuration is positively correlated with a value of $r=0.541$ with a significant value of $p<0.05$. The correlation between the two independent variables is also found to be very high.

Followed by correlation, regression analysis was computed to assess overall impact of Committee Configuration and Committee Process on Project Success.

Table 4
Regression Analysis

Model	Model Summary			
	R	R Square	Adjusted R Square	Std. Error of the Estimate
	1	.571 ^a	.326	.306

a. Predictors: (Constant), Configuration, Committee Process

In the findings of the Table 4 it has been ascertained that a statistical value of R-square is 0.326 which means that the relationship among dependent and independent variables is not very strong though being positive, while the Adjusted R Square value shows that the effect of other variables is also not very highly significant.

The regression results show a positive relationship between the dependent and independent variables so hypotheses 1 and 2 are accepted that Committee Decision Processes are also found to have a significant impact on the Project Success. The results of the regression models provide support for the research question: Steering Committee Configuration positively affects the Project Success. Likewise other independent variables namely Committee Decision Processes are also found to have a significant impact on the Project Success. These results provide support our research question that the factors or variables taken into research do, in fact, affect Project Success significantly.

It has been revealed through the above mentioned results that Project Success is greatly dependent on the variables as identified as Steering Committee Processes and Steering Committee Configuration. Better communication among the Steering Committee members also seems to be a contributing factor in Project Successes according to data collected by interview techniques, one reason being consistently quoted as; it improves mutual trust among members regarding decision making and directing a process and further improves the chances of success for project.

VI. DISCUSSION AND RECOMMENDATIONS

The project managers that were our respondents as well as our interviewees signified a strong support from their respective governing body or Steering Committees in project-success focused committee decisions. Conflict is one event that is repeatedly reported as a byproduct of committee meetings by project managers, they do not necessarily mean delayed decision making or a less effective way of taking important steps when in a project based environment. It is encouraging to find that Pakistan has taken to project management approaches quite naturally compared to the resistance to new methods that the professionals used to be stereotyped with previously. A lot of the credit goes to the Project Management

Institute (PMI) for the world wide education of project management based techniques which people have found useful in applied projects as well. Pakistan's engineering sector has rapidly picked up on the new project Management techniques and made it a normal practice. One project manager was asked when she heard the term Steering Committee for the first time and the response was 2006. That was a time when few people who worked in fortune 500 companies recognized the term here in Pakistan. Now, an effective Steering Committee exists under several different names. The point to note is that improved and constant project management awareness inculcated a sense of pride into the same bodies, board and committees which were previously expected to only think of personal gain, now think of a successful project as a matter of greater pride.

VII. CONCLUSION

In conclusion, Steering Committees may be recognized under names other names and terms but the concept of an effective steering process has been evolved successfully. In Pakistan's project related work environment the decision process and configuration of the steering bodies has been found to have a significant impact on overall project success. During the course of my research, few articles on non-IT Steering Committees were found. Hence, it is recommended that further research be conducted on non-IT Steering Committees to add to the existing body of knowledge to assist future researchers who undertake a similar topic.

VIII. REFERENCES

- [1] Doll, W. J., & Torkzadah, G. (1987). The relationship of MIS Steering Committee size of firm and formalization of MIS planning. *Communications of the ACM*, 30, 972-978.
- [2] Englund, R. L., & Bucero, A. (2006). *Project sponsorship, achieving management commitment for Project Success*. New York: Wiley.
- [3] Hair J.F., Black W.C., Babin B.J., Anderson R.E., and Tatham R.L. (2006). *Multivariate data analysis* 6th Edition. Pearson Prentice Hall. New Jersey.
- [4] Kaufman, C., & Korrapati, R. B. (2007). A project management office (PMO) framework for successful implementation of information technology projects. *Proceedings of the Allied Academies International Conference, academy of Information and Management Sciences*, 11(1), 1-7.
- [5] Lechler, T.G., and Cohen, M. (2009). Exploring the Role of Steering Committees in Realizing Value From Project Management, *Project Management Journal*, Vol. 40, No. 1, 42-54.
- [6] Patankar, P.K. (2009). Project management and IT governance. Retrieved from <http://www.slideshare.net/guest7db01d/research-paper-on-project-management-and-it-governance-presentation-942632>
- [7] Symons, C., (2003). IT Governance: Steering Committee Do's and Don'ts, *forrester.com*, retrieved from http://www.forrester.com/rb/Research/it_governance_steering_committee_dos_and_donts/q/id/17511/t/2

[8] Nolan, R.L.(1982). Managing information systems by committee. *Harvard Business Review*, 60, 4, 72-79.

[9] Earl, M.J. (1989). *Management Strategies for Information Technology*. Englewood Cliffs, NJ: Prentice Hall.

Sabina S. Shirazi was born in 1981 in Pakistan. She has a bachelor's degree in Mechanical engineering from University of Engineering and Technology, Taxila, Pakistan, followed by multinational experience in project management and training. She followed up her education and work experience with a research based MS in Project Management from SZABIST Islamabad(2012-2012). She has multiple professional certifications in Telecom, Technical, Ethics, Management (2005 – 2008) from Motorola University. She also has multiple professional certifications from George Washington University- School of Business and ESI in Project Management (April 2007- August 2007).

She currently works in project management, striving to enforce it in the healthcare sector, working for the betterment of the people in the federal capital of Pakistan. Her previous experience includes working as adjunct faculty for management sciences and technology at SZABIST Pakistan. SZABIST ranked among the best Science and Technology and MBA schools in Asia by the CNN-Time publication Asia week. SZABIST is also listed in the CNN Executive Education Schools. SZABIST thus has the unparalleled honor of being the only Pakistani Institute to be recognized internationally by Business Week, Asia week, Asia Inc. and CNN.

Ms. Sabina S. Shirazi's field of interest is project management and its knowledge areas. Her interests also expand into the more generic business and management field of study. She was first inspired by the Project management journal and especially the study conducted by Lechler, T.G., and Cohen, M. (2009), Exploring the Role of Steering Committees in Realizing Value From Project Management which is what she based her current study on. She hopes to contribute significantly to her field in the future.

Assessing environmental impacts of aviation on connected cities via environmental vulnerability studies and fluid dynamics: An Indian case study

Gautham Ramchandran, Jethro Nagawkar, Karthik Ramaswamy and Sat Ghosh

Abstract - As the need for connectivity increases by the day, there is a heavier demand on the aviation industry to cater to the masses required to travel between two cities. This is even more so when the two cities required to be connected are hubs for trade and industrial development. In India, peak annual passenger traffic has increased steeply from 11.02 million in 2010 to 13.52 million in 2012. This calls for an environmental impact assessment (EIA) to be conducted for the two connected cities in question. This study proposes an innovative screening method involving the use of a modified environmental vulnerability index (EVI). The modification suggested is the introduction of aviation related parameters into a pre-existing EVI calculator, as well as extending the use of this calculator to analyze the environmental vulnerabilities of states and cities in addition to countries as has been done previously. Furthermore, the importance given to passenger comfort by passenger airlines these days is addressed, thereby suggesting a need to include the aspect of human comfort in the screening process. This is done through the use of state-of-the-art computational fluid dynamical software and large eddy simulations to estimate forces experienced by differently sized aircraft during in-flight turbulence for various weather conditions. A comparative analysis is presented on how changing the size of the aircraft operating on a particular route in India between the cities of Chennai and Bangalore has better implications for both passenger comfort as well as the environment. It is observed that if commercial airlines incorporated fewer medium-sized aircraft in place of a number of light weight aircraft on a particular route, there is a reduction in the environmental vulnerability of the two connected cities.

Keywords - Aviation, Computational Fluid Dynamics, Environmental Vulnerability, Passenger Comfort

I. INTRODUCTION

THE connectivity between two urban centres is of crucial importance to economies. Chennai and Bangalore are two important cities in Southern India. Bangalore is a software hub and Chennai is a centre for trade and manufacture. Growing industries in both Chennai and Bangalore have demanded

even better connectivity for the two cities. While this demand has not been adequately fulfilled by the roadways and railways, the aviation sector has had to bear the brunt with an increase in frequency of flights. Figs. 1(a-b) show a steep increase in air travel over the past decade in Chennai and Bangalore. There are up to 17 non-stop passenger flights connecting the two cities on a daily basis.

Although, there have been plans of a new high speed road corridor between the two cities, reducing the travel time to three hours, they are still in their rudimentary stages. Until then, the increasing need for more efficient travel will have to be supported by the aviation industry which has undergone massive infrastructural development at both places. The yearly growth in the number of flights operating in this sector could take a heavy toll on the overall environmental health of the two cities. This calls for an environmental impact assessment (EIA) to be conducted to analyse the effect that this increase in the number of passenger flights between the two connected cities has on their environment. This paper seeks to do precisely this, by using a modified version of the environmental vulnerability index (EVI) as a screening tool. It is modified in the sense that factors related to the aviation industry which play key roles in enhancing the environmental vulnerability of the two cities are incorporated into the calculation.

While reducing their environmental impact is one of the prime focuses of airlines all over the world these days, so is passenger comfort. This is primarily due to the large number of people preferring to fly between two cities in order to save time. In India, domestic flights are becoming increasingly affordable to the burgeoning middle class. Although relatively affluent, the Indian upwardly mobile are not necessarily always well informed. Women, children, elderly people and the nouveau riche business community with modest levels of education have no idea about the effects of frequent flying on vulnerable people – pregnant women, people with physical

disabilities, diabetic and heart patients. Unlike the affluent western world, Indian passengers are never briefed about the possibilities of a rough flight – this is mainly true for many of the private airlines who wish to cash in on these well-to-do passengers. It must be borne in mind that India is a monsoon driven country – the south-west monsoon lasts for well over 3 months and is characterized by turbulent weather and concomitant uncomfortable flights. In addition, Chennai bears the brunt of a second monsoon season, the north-east monsoon, which again lasts for approximately 8 to 10 weeks. These clearly defined and well-marked rough periods require special considerations vis-à-vis flight management and citizens' well-being. This has not been done systematically – pilots have access to India Meteorological Department weather charts usually from the Met station at the airport itself. However, technology has moved on – with the advent of state-of-the-art weather forecasting models like the Weather Research and Forecasting Model (WRF) and Large eddy simulation (LES) models, it is possible to predict rough weather on selected routes five days in advance [3]. The large eddy simulation models provide a detailed velocity distribution pattern right from the ground up to the tropopause – they are particularly well-suited to resolve in-cloud turbulence. Monsoon activity is associated with aircrafts having to endure large patches of water-borne towering cumuli and cumulonimbus clouds with updraught velocities of the order of 2.5 ms^{-1} (Fig. 3(b)). Flying times through these turbulent patches can be picked up by sophisticated fluid

dynamical simulations to inform the aviation industry and the population at large. This falls within the remit of an environmental impact assessment (especially through a rigorous screening study) of aviation corridors along some of India's busiest routes.

One way of catering to passenger comfort is to change the type of aircraft used over a sector – this move, however, can play a part in increasing or decreasing the impact on the environment of the two cities. A comparative analysis is put forth in order to better understand the impact on the environment of the two cities by changing the type of aircraft (with respect to size) commonly being flown around this route. In this study, we have applied CFD and large eddy simulations to in-cloud turbulence in order to quantify passenger comfort. This quantified value is then incorporated into the modified EVI as a means of introducing passenger comfort into the EIA screening process. To our knowledge, this direct application of CFD to a screening analysis of an aviation corridor has not been undertaken before.

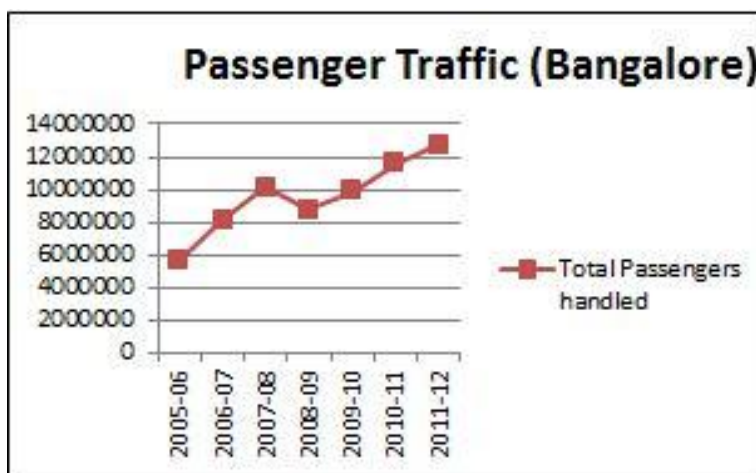


Fig 1(a): Passenger traffic trends in Bangalore (2005-2012);
Sourced and reconstructed from [1]

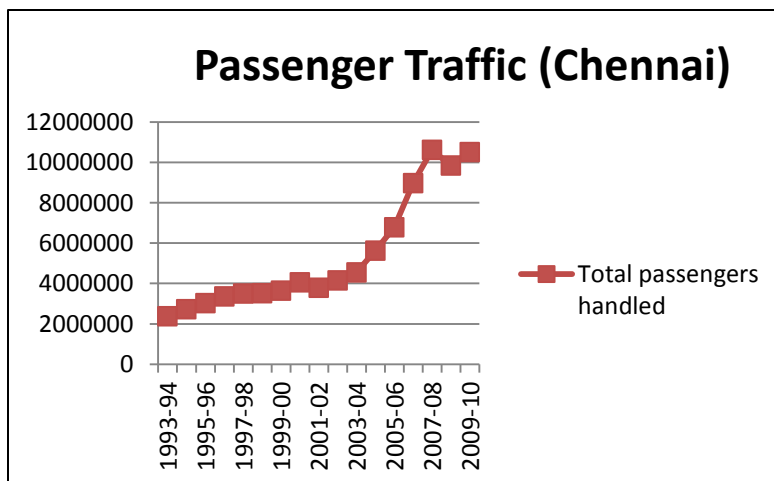


Fig 1(b): Passenger traffic trends in Chennai (1993 to 2010);
Sourced and reconstructed from [2]

II. A DOWNSCALED AND MODIFIED EVI OF CHENNAI AND BANGALORE FROM AN AVIATION PERSPECTIVE

In order to identify and quantify the impact of growth in the aviation sector on the two cities in question, we have modified an existing version of the Environmental Vulnerability Index (EVI) which was formulated under the aegis of the South Pacific Applied Geoscience Commission (SOPAC), the United Nations Environment Program (UNEP), collaborating countries, institutions and experts. We depict how the EVI may be used as a screening tool, as has been done in this case study, for the particular scenario of the effect of aviation on the environmental well-being of the two cities. This screening study may be used as a prelude to a more extensive EIA [4].

The EVI was initially designed in order to quantify the vulnerability of a country to environmental factors. In their technical report, Reference [5] demonstrate the way in which the EVI of a country may be indexed as a consequence of deducing the impact of 50 indicators identified on the environment. Based on the data available from around the world, these indicators have been suitably defined and a scale of 1 to 7 has been proposed for each indicator. These scales depict the degree of vulnerability of a particular country to

that indicator, with 1 being highly resilient and 7 being most vulnerable.

There is a need to apply the EVI to quantify the impact on smaller regions within the country such as *states or cities*. Human interference has largely altered the state of the environment in entire countries, but even more so within independently governed states of those countries. Every state possesses a different environmental vulnerability – this is due to subtle or vast differences in environmental qualities between them as well as variations in policies adopted by each form of state government. Quantifying the EVI of an entire country suppresses these individual regional impacts. For these reasons, a downscaled version of the EVI has been implemented for this study on the cities of Chennai and Bangalore. This is a first approach also. The *raison d'être* of the downscaling procedure is now discussed.

The downscaled EVI calculator is used to quantify the contributions of the aviation industry on the environmental vulnerability of two cities. Out of the 50 indicators considered, aviation plays a major role on 7. Table 1 lists definitions of these indicators and shows corresponding figures for the cities of Chennai and Bangalore. Based on these, scores are ascribed suitably (Table 2).

Table 1: Indicators for EVI study on Chennai and Bangalore

INDICATOR	DEFINITION	COMMENTS
Population Growth	Annual human population growth rate over the last 5 years	Chennai population increased from 6,560,242 in 2001 to 8,696,010 in 2011; growth of 3.3% per year. [6]
		Bangalore population increased from 5,101,000 to 8,425,970 in 2011 [7]; growth of 6.52% per year.
Waste Production	Average annual net amount of generated and imported toxic, hazardous and municipal wastes per km ² land area over the last 5 years	4,500 tonnes of solid waste generated per day [8]; 1,381 tonnes waste generated every year per km ² of land (Chennai metropolitan area being 1,189 km ²).
		2,500 tonnes of solid waste generated per day [9]; 1,232 tonnes of waste generated every year per km ² of land (Bangalore land area is 741 km ²)
Environmental Openness	Total USD freight imports per year over the past 5 years by any means per km ² land area	357,191 freight in tonnes for 2011 [10]; 1502 freight per km ² ; 15.02 USD 1000's km ² for Chennai (Assuming a minimum cost of 10 USD per freight shipment tonne).
		224,949 freight in tonnes for 2011 [10]; 304 freight per km ² ; 3.04 USD 1000's km ² for Bangalore (Assuming a minimum cost of 10 USD per freight shipment tonne).
Tourists	Average annual number of international tourist-days per km ² of land over the last five years	Average of 18 international tourists km ² (area of Tamil Nadu being 130,058 km ²). [11]
		2 international tourists km ² (area of Karnataka being 191,791 km ²). [12]
Habitat Fragmentation	Total length of all roads in the city (km) / land area (km ²)	Total length of roads in Chennai is 2,780 km; land area of Chennai is 1,189 km ² . [13]
		Total length of roads in Bangalore is 2,679 km; land area of Bangalore is 741 km ² . [14]
Vehicles	Number of vehicles per km ² of land area (most recent data)	3.64 million vehicles in Chennai (land area of Chennai is 1,189 km ²). [15]
		4,171,062 vehicles as of October 2012 (land area of Bangalore is 741 km ²). [16]
Human Population Density	Number of humans per km ² of land area	4,681,087 people per 1,189 km ² land. [17]
		9,621,551 people per 741 km ² land area. [18]

Table 2: EVI scores for Chennai and Bangalore based on air traffic rise

	Tourists	Population Growth	Waste Production	Environmental Openness	Habitat Fragmentation	Vehicles	Human Population Density
Bangalore City EVI	1	7	7	5	7	7	7
Chennai City EVI	4	7	6	5	7	7	7
Data years considered	2007,2009	2001 to 2011	2012	2011	2007	2012	2011
Data source (Chennai EVI Calculation)	[11]	[6]	[8]	[10]	[13]	[15]	[17]
Data source (Bangalore EVI Calculation)	[12]	[7]	[9]	[10]	[14]	[16]	[18]

In order to rank these indicators according to the impact that aviation has on them, we identify 6 aviation related parameters which may have a substantial effect on one or more of the indicators. According to the number of aviation parameters affecting a particular EVI indicator (indicated by an 'X'), a

suitable multiplication factor is coupled with the EVI values obtained for that indicator. For instance, from Table 3, since 4 out of 6 aviation parameters affect the EVI indicator "Tourists", we multiply the EVI values obtained for Tourists with the factor 4/6.

Table 3: Ranking scheme for EVI indicators with regard to aviation

	AVIATION PARAMETERS	Fuel consumption	Aircraft Noise	Airport operations	Ticket price affordability	Aircraft emissions	Number of flights for a single route	Multiplication factor
EVI INDICATORS								
Population Growth		X	X	X	X	X	X	6/6
Human population density		X	X	X	X	X		5/6
Tourists		X	X	X		X		4/6
Environmental openness		X	X	X		X	X	5/6
Waste production				X			X	2/6
Habitat Fragmentation				X			X	2/6
Vehicles				X				1/6

The new EVI values obtained are tabulated and the total EVI values are calculated for Chennai and Bangalore and then compared. Table 4 depicts the same.

Table 4: Final modified EVI values for Chennai and Bangalore

Indicators	Chennai EVI	Bangalore EVI	Multiplication factor	Scaled Chennai EVI	Scaled Bangalore EVI
Population Growth	7	7	1	7	7
Human population density	7	7	5/6	5.83	5.83
Tourists	4	1	4/6	2.67	0.67
Environmental openness	5	5	5/6	4.17	4.17
Waste production	6	7	2/6	2	2.33
Habitat Fragmentation	7	7	2/6	2.33	2.33
Vehicles	7	7	1/6	1.17	1.17
Total				25.17	23.50

From this screening study, we can address the issue of reducing the environmental vulnerability of the two cities in a very direct manner simply by reducing the impact of the aviation factors on the EVI indicators. One way this can be done is by operating a larger aircraft on that route, thereby reducing the total number of aircraft being operated by an airline every day for that particular route.

Presently, the aircrafts operated include Boeing 737-800, Boeing 737-900, Aerospatiale/ Alenia ATR 72, Bombardier

Q200 and Airbus A320 with average flying times of 45 to 75 minutes spanning cruise altitudes from 7,500 - 12,000 m. We considered, as an example, a situation in which low cost carriers such as Jetlite and JetKconnect (operated by Jet Airways) replace the lighter ATR 72 flights operating on the Chennai-Bangalore route with the larger Boeing 737s is considered. According to the literature, "large aircraft have lower environmental per passenger km costs than small aircraft" [19]. CO₂ emissions from aviation fuel are estimated to be 3.15 grams per gram of fuel [20]. From this, for 162

seats in a Boeing 737, we calculate the fuel consumed to be 36.6 gms per passenger km whereas it is found to be 63 gms per passenger km for 74 seats in an ATR 72 [21]. By considering the total number of seats in each aircraft, we find that an airline operating 5 ATR 72's from Chennai-Bangalore per day will have the same fuel consumption as that of four Boeing 737s. This also implies a reduction in aircraft noise (by

III. APPLICATION OF FLUID MECHANICAL CALCULATIONS TO ADDRESS HUMAN COMFORT DURING DOMESTIC FLIGHTS

This section deals with incorporating passenger comfort into the screening process discussed in the previous section. Here, the methodology and use of CFD and large eddy simulations in order to estimate in-cloud turbulence for different weather scenarios are discussed.

With the cheaper computational resources and real-time data transmission available today, the use of CFD simulations can help predict the amount of turbulence a pilot might face while flying over cloudy routes, especially during monsoons. By performing simulations such as these, one may calculate the degree of vertical velocity perturbations in the cumuli and cumulonimbus clouds over a particular range of the flight path. With this, we can estimate the incremental aircraft vertical acceleration in units of “g” (ms^{-2}) and find whether these values fall within the moderate or safe turbulence limits for aircrafts. Human comfort being one of the key factors in this screening study, we perform computational fluid dynamics calculations to better understand the discomfort an airline passenger might face on a bad weather day.

virtue of operating fewer aircraft on a given route on any given day), operating costs and ticket prices, which ultimately results in a lower impact on the EVI indicators considered. Hence, we recommend that the impact of replacing smaller aircrafts by larger ones (on relatively short routes, such as the Chennai-Bangalore corridor) must be considered in a full EIA study.

The ANSYS CFX software is used to model flows in simulated environments [22]. This application is used extensively in aerospace and related industries to model fluid flow in different situations. It uses iterative numeric codes to solve fluid mechanical as well as heat and momentum transfer equations (such as Navier-Stokes equations) with specific boundary conditions input by the user. For this study, a 1:33 scale model of an Airbus A320 (Fig 2(a-b)), which is one of the most widely used variants on this corridor, was hybrid meshed using the ANSYS Workbench meshing software. (Meshing is the process of breaking down a volume into differentially small volumes). Navier-Stokes solutions are calculated for each node within the subdomain and the results extrapolated. Solid domain characteristics corresponding to Aluminium (typically used aircraft material) were plugged in [23]. In order for two flows to be similar, they must have the same Reynolds and Euler numbers. In contrast to actual flying conditions (of a velocity of 250 ms^{-1} and pressure equal to 0.8 atm at an altitude of 9000 m), the model airspeed was calculated as 289 ms^{-1} corresponding to a pressure of 1 atm. A k- ω SST model [24], coupled with a high turbulence (10% intensity) profile was used to observe airflow around the model.

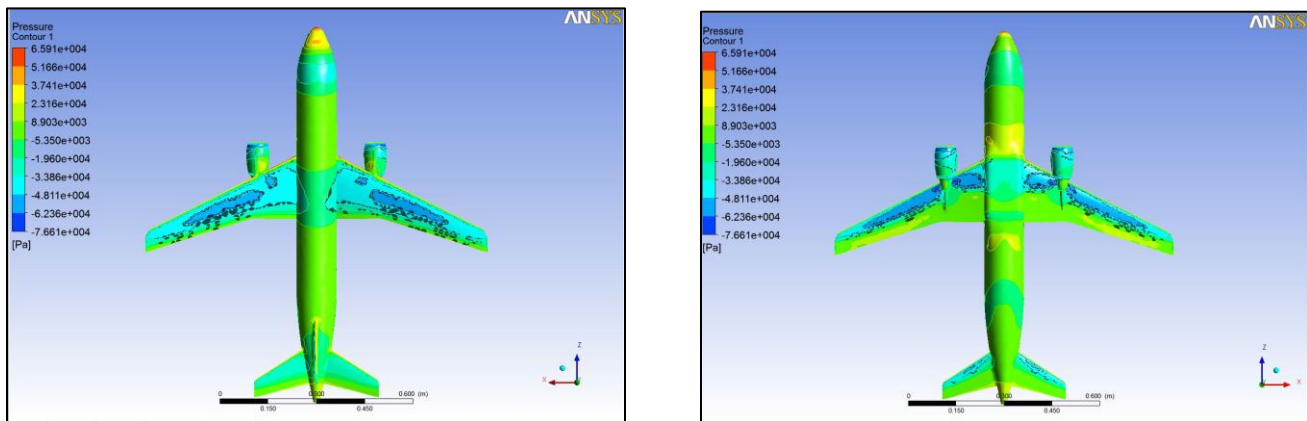


Fig. 2: (a) (Left) Pressure distribution over an Airbus A320 aircraft – Top view; (b) (Right) Pressure distribution over an Airbus A320 aircraft – Bottom view

Air tends to move from regions of high pressure (below the aircraft) to regions of lower pressure (above the aircraft). In the event of an updraught, air rushes towards low pressure areas, reducing the pressure gradient and creating instability

during flight. Figs 2(a-b) shows top and bottom views of pressure distributions for an A320 simulation – one notices regions of high pressure covering the bottom of the wing and the belly of the aircraft. This pressure gradient across the wing

keeps the aircraft in flight. Owing to the presence of an inhomogeneity in pressure distributions below the aircraft, in-cloud turbulence (particularly during approach and landing) acts in tandem with the uneven pressure distributions to sometimes require a sudden increase in engine power (and hence, fuel consumption) during the flight. By utilizing the smaller ATR 72 aircrafts over the Chennai-Bangalore corridor, we cause an adverse response on the EVI indicators because of a higher fuel consumption, higher emissions and

most importantly, by having 5 airplanes in the air as compared to the situation where we only require 4 Boeing 737s. Thus, we strongly recommend the importance of incorporating in-cloud turbulence and passenger comfort to an EIA, especially since the environmental vulnerability of two major port cities are in question.

We have addressed the effects of turbulence on aircraft vertical displacement due to these clumpy, water-laden cumulus clouds frequently encountered on this route.

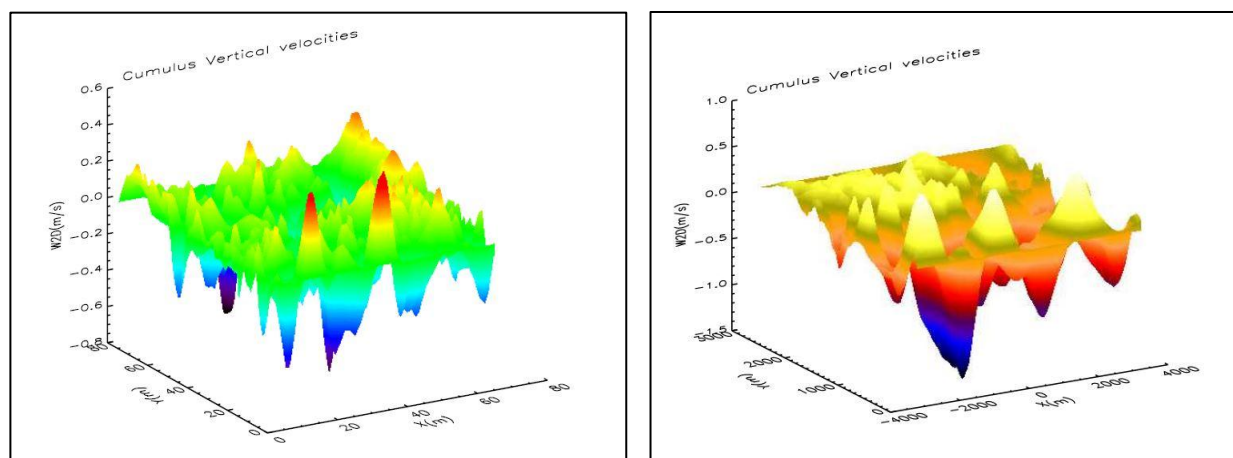


Fig. 3: 3D plot of vertical velocity perturbations in cumulus clouds on (a) Nov. 2011, (b) 31st Oct. 2012 (Cyclone Neelam)

The UK Met office LE model was used [25]. This high-resolution model can simulate a wide range of fluid dynamical problems. It uses periodic boundary conditions and a Boussinesq type approximation set ahead in time and includes parameterizations for sub-grid turbulence, cloud microphysics and radiation. The prognostic variables in the LEM are the three components of the 3D velocity vector (u , v , w), potential temperature perturbations and a number of other scalar variables - usually mixing ratios and number concentrations of water species. Fig. 3 (a) shows the typical variation of the vertical wind velocity perturbations within a cumulus cloud modeled for Chennai city in November 2011, which corresponds to the northeast monsoon period where the cloud covers are generally at their maximum. Additionally, weather data obtained for days wherein in-flight turbulence effects could be drastic (such as those spanning the landfall of cyclone Neelam, as shown in fig. 3(b)) were modeled using the LEM. It was found that the updraught range was much larger, spanning over a distance of 2 km as compared to 20 m on a normal day (Fig. 3). The velocity perturbations were also higher in magnitude (2.5 ms^{-1} as opposed to 1.4 ms^{-1}). As the airplane passes through such clouds, it experiences turbulence. Larger vertical velocity perturbations could contribute to a sudden loss in aircraft lift. An aircraft on this route typically spends 20 minutes (in ascent and descent) in a 45-minute flight in the region where these clouds exist [2000 to 5000 m

[25]. This often causes passenger discomfort leading to nausea, vomiting and minor accidents within the cabin [26]. Cumulus clouds can accumulate up to a height of 6.2 kms over this region [27]. This implies that while all aircraft types could encounter such clouds across their respective flight paths, and more so during landing - where there is a preponderance of low-level clouds over this tropical belt - different aircraft types could have different responses to turbulence.

A sudden pressure change causes the aircraft to lose lift within a short span of time. The degree of downward acceleration exemplifies the effect of turbulence on passenger comfort within the cabin. Reference [28] derived the gust-velocity relationship between an aircraft and a cumulus cloud. It is important to note that the degree of vertical acceleration has a direct dependence on the airplane's Lift-curve slope, gross weight and wing area: characteristics that differ from aircraft to aircraft. The incremental aircraft vertical acceleration was calculated for both weather conditions depicted in Fig. 3, considering data available for two different variants of aircraft - a Boeing 737-800 and an ATR 72. The equation used is given by:

$$\Delta az = (m\rho_0SV_eK / 2W) \times U_{de} \quad (1)$$

where:

$$K = 0.88 \mu g / (5.3 + \mu g) \quad (2)$$

$$\mu g = 2W / (m\rho c g S) \quad (3)$$

The definitions of each term used in these equations are given in Table 5.

Table 5: Parameters used for the calculation of vertical aircraft acceleration

Symbol	Definition	For Boeing 737		Sources	For ATR 72		Sources
		Regular	Stormy		Regular	Stormy	
Δa_z	Incremental aircraft vertical acceleration (in g units ms^{-2})	0.4986	0.89	-	0.608	1.086	-
m	Wing lift curve slope	6.58		[29]	5.966		[30]
ρ_0	Air density at sea level (in kg m^{-3})	1.225		-	1.225		-
S	Wing area (m^2)	124.6		[31]	62.2		[32]
V_e	Equivalent airspeed (ms^{-1})	60.02		[33]	53.35		[34]
W	Aircraft weight (kg)	65,310		[31]	22,350		[32]
U_{de}	Effective gust vertical velocity (ms^{-1})	1.4	2.5	[25]	1.4	2.5	[25]
K	Gust alleviation factor	0.772		-	0.8		-
μg	Airplane mass ratio	37.9		-	53.53		-
c	Aircraft wing chord (m)	4.17		[31]	2.2345		[30]
g	Acceleration due to gravity (ms^{-2})	9.801		-	9.801		-
ρ	Density at flight level (kgm^{-3})	1.007		-	1.007		-

The maximum wind velocities obtained from the Large Eddy simulation were plugged into equation (1) and the values of maximum incremental aircraft vertical accelerations were found to be $0.4986g \text{ ms}^{-2}$ (Boeing 737) and $0.608g \text{ ms}^{-2}$ (ATR 72) for a maximum updraught of 1.4 ms^{-1} (Fig. 3(a)). These values are just within the moderate turbulence limit [35] for the Boeing 737 indicating that the passengers experience a comfortable flight. In the ATR 72 however, they experience moderate turbulence.

For the purpose of drawing a comparison with respect to which aircraft is better suited to fly during extremely turbulent conditions, weather conditions prevailing at the time of Cyclone Neelam were chosen, for which the calculated vertical aircraft acceleration were $0.89g$ (Boeing 737) and $1.086g$ (ATR 72). This indicated that the airplanes face moderate and severe in-flight turbulence respectively. Most

airlines generally cancel flights during cyclones and storms. However, this study was done in order to show that the level of discomfort faced by passengers in an ATR 72 would be well above even severe turbulence limits ($1g$). A Boeing 737 would be able to better negotiate a higher gradient of turbulence than an ATR 72 and this is evident from the study. Only a large eddy simulation is capable of capturing the velocity gradients in a cumulus cloud effectively.

The various aircrafts used by the domestic airlines in the country operating on the Chennai-Bangalore route were identified. From Tables 6 and 7, it may be concluded that all the ATR 72s and Bombardier Q200s used by the airlines Spicejet and Jet Airways may be replaced with aircrafts comparable to the Airbus A320 and the Boeing 737 for direct flights flying from Chennai to Bangalore or vice-versa.

Table 6: Types of aircraft used by airlines operating on the Chennai-Bangalore route (Source: Seatguru 2013)

AIRLINE	AIRCRAFT TYPE	FREQUENCY
Spicejet	Bombardier Q200	6-7 non-stop flights per day
Jet Airways	Boeing 737-800, Boeing 737-900, Aerospatiale/Alenia ATR 72	7-8 non-stop flights per day
Indigo	Airbus A320	1 non-stop flight per day
Air India	Airbus A320	1 non-stop flight per day

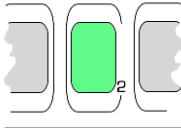
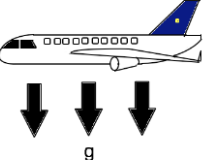
Table 7: Aircraft categorized based on size (weight)

Aircraft Type – I (Medium weight: 60,000 – 70,000 kg)	Aircraft Type – II (Light weight: 15,000 – 25,000 kg)
Boeing 737-800	Bombardier Q200
Boeing 737-900	Aerospatiale/Alenia ATR 72
Airbus A320	

modified EVI values obtained earlier from Table 4. Table 8 depicts the categorization of these factors.

In order to assess the environmental impact benefits of using a heavier aircraft in place of a lighter one on this particular route, we categorize the factors that determine the selection of the aircraft type and assign weights against the

Table 8: Environmental implications on Chennai and Bangalore based on the change in aircraft type

Aircraft Factor	Description	Weight assigned	Type I – Light weight	Type II – Medium weight
CO ₂ emissions (gms per passenger km) ⁽¹⁾ 	High: >50 Low: <50	High: 2 Low: 1	2	1
Incremental aircraft vertical acceleration (“g” units; ms ⁻²) 	(Assuming extreme weather conditions) ⁽²⁾ Moderate: 0.5g to 1g Severe: >1g	Severe: 2 Moderate: 1	2	1
Travel time (minutes) [36] 	Slow: 60 to 80 Fast: <=60	Slow: 2 Fast: 1	2	1

Airport congestion 	In terms of frequency of flights; higher frequency implies more congestion.	High: 2 Low: 1	2	1
Aircraft noise (db(A)) 	High: >70 Low: <70	High: 2 Low: 1	1	2
Total (To be multiplied with the respective scaled EVI values)			9	6

Note:

- (1) Here, the icon for emissions is meant to resemble the symbol “CO₂” integrated into an aircraft window. Iconography such as these lends a sense of visual appeal to the user.
- (2) It was found that even for a jumbo jet such as a Boeing 747 (not used on short routes), the vertical acceleration values were between 0.5g and 0.8g (not shown here) during the Cyclone Neelam (extreme weather). Hence, we consider only “Moderate” and “Severe” criteria and “Normal” levels (<0.5g) are omitted.

We then multiply the final values obtained from Table 8 (i.e. 9 and 6) with the scaled EVI values for Chennai and Bangalore (25.17 and 23.50 respectively) in Table 4 to find the difference in the environmental vulnerability of the two cities due to the use of different aircraft types. We see that the EVI of Chennai is 226.53 when lighter aircrafts are in use whereas it is only 151.02 when a medium weight aircraft is in

operation for this route. Similarly, for Bangalore it is 211.50 when lighter aircraft are operated while the EVI reduces to 141 when medium weight aircrafts are introduced. Hence, this quantitative approach verifies the need for choosing to operate the right aircraft type, also incorporating the social benefit of passenger comfort for passengers frequenting this route.

IV. CONCLUDING REMARKS AND WIDER IMPLICATIONS

A modified, downscaled EVI calculator has been used as a screening tool incorporating aviation related parameters to determine the EVI of the two connected Indian cities, Chennai and Bangalore. In addition, the importance of incorporating passenger comfort into this EIA study is discussed and a methodology is proposed to allow for the introduction of this parameter. This is done by virtue of changing the size of the aircraft used on the given route with regard to in-flight turbulence experienced during regular and abnormal weather conditions. This is done through the use of CFD and large eddy simulations of cumulus clouds present in the path of the flight.

Available EVI calculators today have a tremendous developed country bias and are only developed till date for vulnerable island nations. They yield a score based on empirical formulations alone. This study reveals for the first time that indicators should be country specific and situation specific. It is not enough to give a vulnerability index for a large geographical area – this may well point to the region’s overall vulnerability but fails to assign specific scores on specific themes. We suggest more robust mathematical models be used for identifying indices for the expansion of the aviation industry within the developing world where levels of healthcare and education are not up to the mark. This opens up

a new way of prescribing vulnerability indices for specific, need-based environmental situations.

We have shown how the incremental aircraft vertical accelerations help in predicting overall comfort and vulnerability should not be limited to the physical environment alone. Capturing velocity gradients within monsoon clouds is tricky – when a pilot negotiates these velocity gradients, he has to ensure the minimum levels of in-flight discomfort – this is not done easily. However, advanced computational fluid dynamical techniques are increasingly affordable and must be used suitably for impact assessment. This has been robustly demonstrated in this study concerned with the aviation industry linking Chennai and Bangalore. However, the mathematical framework and the application methodology are transferable over any part of the world. Most importantly, this study showcases the designing of an entirely novel EVI calculator applicable to the aviation industry. Again, a modified version of this new calculator can be used anywhere – it is as easy to use as any other EVI calculator because of its telling visual appeal. Societies are vulnerable now with an expanded scale of action of man’s interaction with the environment, particularly man’s interaction in their working lives as they commute from place to place by road, land and air.

REFERENCES

- [1] Association of Private Airport Operators [Internet]. c2012-2013. Statistics: Bangalore International Airport Limited; [cited 2012 December 8]. Available from: http://www.apaonline.com/?page_id=840.
- [2] Directorate General of Civil Aviation. Yearly Statistics; [cited 2013 December 8]. Available from: <http://www.dgca.nic.in/reports/stat-ind.htm>.
- [3] Michalakes, J., S. Chen, J. Dudhia, L. Hart, J. Klemp, J. Middlecoff, and W. Skamarock. Development of a Next Generation Regional Weather Research and Forecast Model. Developments in Teracomputing. Proceedings of the Ninth ECMWF Workshop on the Use of High Performance Computing in Meteorology (2001). Eds. Walter Zwiefelhofer and Norbert Kreitz. World Scientific, Singapore. pp. 269-276. Available from: <http://www.mmm.ucar.edu/mm5/mpp/ecmwf01.htm>.
- [4] Kværner, J., Swensen, G., and Erikstad, L. 2006. Assessing environmental vulnerability in EIA—The content and context of the vulnerability concept in an alternative approach to standard EIA procedure. *Environ Impact Asses* 26:511-27. <http://dx.doi.org/10.1016/j.eiar.2006.01.003>.
- [5] Kaly, U.L., Pratt, C.R. and Mitchell, J. 2004. The Demonstration Environmental Vulnerability Index (EVI) 2004. SOPAC Technical Report 384. Available from: http://www.vulnerabilityindex.net/EVI_Mechanics.htm.
- [6] Srivathsan, A. 2011 November 29. Chennai 4th in Urban Agglomerations. *The Hindu*. Available from: <http://www.thehindu.com/news/cities/chennai/article2670674.ece>.
- [7] Census of India (a) [Internet]. 2013a. Cities having population 1 lakh and above, Census 2011; [cited 2013 October 28]. Available from: http://www.censusindia.gov.in/2011-prov-results/paper2/data_files/India2/Table_2_PR_Cities_1Lakh_and_Above.pdf
- [8] Chennai Corporation [Internet]. c2008. Solid Waste Management; [cited 2014 February 13]. Available from: <http://www.chennaicorporation.gov.in/departments/solid-waste-management/index.htm>.
- [9] Van Beukering, P., Sehker, M., Gerlagh, R., & Kumar V. 1999. Analysing urban solid waste in developing countries: A perspective of Bangalore, India. CREED Working Paper No. 24.
- [10] Airports Authority of India [Internet]. Traffic Statistics – Freight (International and Domestic); [cited 2012 December 8]. Available from: http://www.aai.aero/traffic_news/mar2k12annex4.pdf.
- [11] TNN. 2010 August 27. Chennai High – City Gets Most Foreign Tourists. *The Times of India*. Available from: http://articles.timesofindia.indiatimes.com/2010-08-27/chennai/28314945_1_tourist-arrivals-foreign-tourists-tamil-nadu-tourism-development.
- [12] Department of Tourism, Govt. of India [Internet]. Share of top 10 states / UT of India in number of foreign tourist visits in 2007; [cited 2014 February 13]. Available from: http://shodhganga.inflibnet.ac.in/bitstream/10603/5261/9/09_chapter%203.pdf.
- [13] Chennai Metropolitan Development Authority [Internet]. Road network; [cited 2013 October 28]. Available from: http://www.cmdachennai.gov.in/Volume1_English_PDF/Vol1_Chapter04_Transport.pdf.
- [14] Karnataka at a glance (GoK) [Internet]. Spread of different types of roads in Karnataka (2011); [cited 2013 October 28]. Available from: http://www.samatolvikas.org/dr_nanjudappa_committee_report/Ch_13_Transport.%20Roads%20etc..pdf.
- [15] Selvaraj, A. 2012 October 12. On the fast-track: Now, every other Chennaiite has a vehicle. *The Times of India*. Available from: http://articles.timesofindia.indiatimes.com/2012-10-12/chennai/34411811_1_public-transport-road-space-chennai-roads.
- [16] Bangalore City Traffic Police [Internet]. c2014. Vehicle Population in Bangalore City; [cited 2014 February 13]. Available from: <http://www.bangaloretrafficpolice.gov.in/index.php>.
- [17] Census of India (b) [Internet]. Population Census 2011; [cited 2013 October 28]. Available from: <http://www.census2011.co.in/>.
- [18] Census of India (c) [Internet]. Karnataka Population Census data 2011; [cited 2013 October 28]. Available from: <http://www.census2011.co.in/census/state/karnataka.html>.
- [19] Peeters P., P. Rietveld, and Y. Schipper, “Deregulation in Europe Aviation and the evolution of hub-and-spoke networks: impacts on the environment”, IN Atzema, O., P. Rietveld, and D. Shefer (eds.) *Regions, land consumption and sustainable growth (2005)*, Edward Elgar Publishing Limited, Cheltenham, UK, ch. 8.
- [20] European CORINAIR manual [Internet]. EMEP Corinair Manual 2011, [cited 2013 October 28]. Available from: <http://reports.eea.europa.eu/EMEP-CORINAIR4/en/B851vs2.4.pdf>.
- [21] Dubois. T. 2009 February 27. ATR 72-600 to fly early this summer. *Aviation International News*. Available from: <http://www.ainonline.com/aviation-news/aviation-international-news/2009-02-27/atr-72-600-fly-early-summer>.
- [22] ANSYS Inc. 2012. ANSYS CFX-Solver Manager User’s Guide. Version 14.5.
- [23] Baker, Timothy, J. 2005. Mesh Generation: Art or Science? *Prog Aerosp Sci*. 41:29-63. doi:10.1086/j.tra.2009.01.001.
- [24] Menter F., R. 1994. Two-equation eddy-viscosity turbulence models for engineering applications. *AIAA Journal* 32:1598-1605.
- [25] Gary, M.E.B., Petch, J., Derbyshire, S.H, Brown, A.R., Lock, A.P. and Swann, H.A. 2001. “Version 2.3 of the Met Office Large Eddy Model. Turbulence and Diffusion Notes.” p. 275-277, Met Office, Exeter, UK.
- [26] Hinninghofen, H. and Enck P. 2006. Passenger well-being in airplanes. *Auton Neurosci* 129:80-85. doi:10.1016/j.autneu.2006.07.018
- [27] Sarkar, S. K. and Kumar, A. 2007. Recent Studies on Cloud and Precipitation Phenomena for Propagation Characteristics over India. *Indian J Radio Space* 36:502-13.
- [28] Pratt, K.G. and Walker, W.G. 1954. A revised gust load formula and a reevaluation of V.G. Data taken on civil transport airplanes from 1933 to 1950. NACA Rep. 1206. Available from: <http://naca.central.cranfield.ac.uk/reports/1954/naca-report-1206.pdf>.

- [29] Rustenburg, John. 1996. Calculation of load factor response of small airplanes to continuous turbulence. FAA Technical centre, FAA research grant – 93-G-051 Small airplane certification directorate.
- [30] Niță, M., F. 2008. Aircraft Design Studies based on the ATR 72. [dissertation]. Hamburg University of Applied Sciences.
- [31] Matthews, Clifford. 2002. Aeronautical Engineer's Data book. Butterworth-Heinemann, Elsevier, Boston, pp. 148-149.
- [32] ATR Aircraft [Internet]. ATR 72-500 Series; [cited 2014 February 13]. Available from: <http://www.atraircraft.com/products/atr-72-500.html>.
- [33] Boeing, Inc [Internet]. c1995-2014. Airport Reference Code and Approach Speeds; [cited 2013 October 28]. Available from: <http://www.boeing.com/boeing/commercial/airports/faq.page>.
- [34] Air Northwest [Internet]. 2003. Aircraft Performance Specifications; [updated 2005 August 5; 2014 cited February 13]. Available from: <http://webpages.charter.net/anw/ANW/performance.html>.
- [35] Dreyling, H. 1973. An airline's experience on turbulence. Proceedings of AGARD Conference, no. 140, 7.1-7.7.
- [36] Seatguru [Internet]. c2001-2014. Find Seat Maps; [cited 2013 November 4]. Available from: <http://www.seatguru.com/findseatmap/findseatmap.php>

Effects of Environmental Factors on Noise Emissions from Pig Housing

M. Šístková, J. Brouček, P. Bartoš, I. Celjak, and A. Dolan

Abstract—The goal of this work was to find effect of the day period, distance, and seasons of the year the noise emissions created in pigs housing. The measurements were performed in building for 1100 heads of fattening pigs with the slatted floor. There were nine measured places designed for the noise load measuring, one place inside the barn, and eight places outside the building. The measurements were performed three times at each season (summer, winter) on five consecutive days. The data were taken in three 30 minutes periods (before feeding, during feeding, and after feeding of pigs). The measurements were realized inside and outside the barn at the same time. Differences among periods and distances were highly significant ($P < 0.001$). Inside the building, the highest noise levels (65.5 ± 1.6 dB, 72.0 ± 1.4 dB, 63.4 ± 0.7 dB, $P < 0.001$) were measured. The highest average levels of noise were recorded (72 ± 1.4 dB, $P < 0.001$) in the time of feeding. There were recorded significantly higher noise levels in summer than winter. We can conclude that the noise in the pigs housing depends significantly on the period of the day, distance from building, and on the season of year.

Keywords— noise, pig, period of day, season.

I. INTRODUCTION

ENVIRONMENTAL noise is widespread in both natural and urban landscapes. Previous studies have

The contribution was created from data measured in the framework of the project QH 72134 Research of principal environmental aspects in breeding of livestock from the point of view of greenhouse gases, smell, dust and noise, supporting the welfare of animals and BAT creation. The work has been supported by the “BAT centrum JU”. This study was possible also through project APVV-0632-10 of the Slovak Research and Development Agency Bratislava.

Marie Šístková is with University of South Bohemia in České Budějovice, Faculty of Agriculture, Studentská 13, 370 05 České Budějovice, Czech Republic (e-mail: sistkova@zf.jcu.cz).

Jan Brouček is with National Agricultural and Food Centre, Research Institute of Animal Production Nitra, 951 41 Lužianky, Slovakia (corresponding author, phone: 00421-944-539672; fax: 00421-37-6546483; e-mail: broucek@vuzv.sk).

Petr Bartoš is with University of South Bohemia in České Budějovice, Faculty of Agriculture, Studentská 13, 370 05 České Budějovice, Faculty of Education, Department of Applied Physics and Technology, Jeronýmova 10, 371 15 České Budějovice, Czech Republic (e-mail: bartos-petr@seznam.cz).

Ivo Celjak is with University of South Bohemia in České Budějovice, Faculty of Agriculture, Studentská 13, 370 05 České Budějovice, Czech Republic (e-mail: celjak@zf.jcu.cz).

Antonín Dolan is with University of South Bohemia in České Budějovice, Faculty of Agriculture, Studentská 13, 370 05 České Budějovice, Czech Republic (e-mail: dolan@zf.jcu.cz).

revealed many negative impacts of noise on organisms, particularly from anthropogenic sources. Human activities may create sounds in providing new noise sources such as traffic, constructions, and ventilation. Noise pollution, as it affects animals and humans, has been a recognized problem for decades, but the effect of noise on farming animals has only recently been considered a potential threat to animal health. Most researchers agree that noise can affect an animal's physiology and behavior, and if it becomes a chronic stress, noise can be injurious to an animal's energy budget, reproductive success and long-term survival [1,2,3,4]. Husbandry procedures cause the loudest sounds, especially if metallic equipment is involved or if the work is performed in a hurried manner. Noise experienced during housing of farm animals can be short-term or chronic. The sources of noise can be technical devices, routine works (opening and closing doors, changing pens, washers, push carts, workers' speech, feed dispensing), basal sound levels caused by mechanical ventilation, animals activities (climbing and chewing on fences), and by their vocalizations [5].

Previous ecological studies focusing on acoustic noises have incorporated urban noise research and architectural science into producing testable hypotheses, for example that on animal signal propagation [6, 5].

Noise is described as unwanted sound, either continuous or intermittent, and can be described in terms including its frequency, intensity, frequency spectrum, and shape of sound pressure through time. Decibel (dB) is unit for measuring the intensity of a sound. It is equal to ten times the logarithm to the base ten of the ratio of the intensity of the sound to be measured to the intensity level of sounds of some reference sound, usually the lowest audible note of the same frequency. Frequency means the number of vibrations per second of the air in which the sound is propagating and it is measured in Hertz (Hz) [7,8,9]. The term "continuous noise" was used to indicate noise that is not intermittent in nature and not characterized by short sound blasts [10]. Noise can be considered to be a stressor if it occurs where animals are located and if it affects their welfare and performance or induces physiological changes. Many studies on domestic animals suggest that some species appear to acclimate to some forms of sound disturbance [11,12]. Some studies have reported such primary and secondary effects as reduced growth. More physiological and behavioral responses have been

described: increased hormonal production, increased heart rate [13].

Propagation phenomena of sound waves in the environment are very complex and a large number of parameters have to be considered [14,15]. The main ones are related to the physical characteristics of the propagation medium (air) on one hand, and to the boundary conditions (natural or artificial grounds, barriers, etc.) on the other hand [16,17,18].

II. MATERIAL AND METHODS

The measurements were performed in building with the fully slatted floor during summer and winter seasons. The pigs at the body weight of 95 kg were kept in pens with the batch system of the management (12 sections, 12 pens in each section, and 8 animals in a pen). The pigs were fed four times a day, at 6 a.m., 10 a.m., 2 p.m. and 6 p.m. The negative pressure ventilation was used; the air was aspirated through the under-grid areas into the vertical shaft led up to three meters above the roof of the object. The building is located about 180 m from the road. The sidewalls contained the cement-fibrous boards (thickness 30 mm) and the glass mineral wool (thickness 60 mm).

Nine places were focused by the digital rangefinder Bosch DLE 50 3 601 K16 000, where the sound intensity was consequently measured. Inside the stable the measuring point was placed in section 7, outside the building the points were placed in the distances of 7 m and 11 m.

The measurements were performed three times in the summer and three times in winter on five consecutive days under almost similar climatic conditions. In every day the data were taken in three half-hour periods – before the feeding, during the feeding and during the resting of the pigs. The ventilation was turned on during measurements. The average daily air temperature and relative humidity in the housing facility were during the individual five days measuring's on summer (24.8 °C, 62.5 %; 23.7 °C, 66.0 %; 24.2 °C, 70.5 %) and winter (19.3 °C 81.0 %; 14.0 °C 70.5 %; 14.5 °C, 81.0 %) period.

The time of duration of all measurements being realized $T = 180$ s. The sound pressure levels were measured by two digital noise meters Voltcraft Plus SL-300, EN 61672 (class of accuracy 2) in dB while using the weight filter A, and the dynamic characteristic „Fast“. The microphone was placed at the camera stand of 1.5 m above the level of terrain and directed on to the stable building (source of noise). During the measurement inside the stable building where the direction of propagation of noise was not identifiable (every animal – potential source of noise, many sources from all directions), the microphone was directed vertically upwards and placed in the middle of the manipulation passage of the section.

The measurement was realized inside and outside the building at the same time (beginning and end of

measurement realized by means of two digital radio transmitters Motorola TLKR T6). Every day before the beginning of the measurements being realized, the calibration of noise meter (the so-called adjusting – adaptation of noise meter to the existing pressure) was realized by the calibrator Voltcraft 326 (IEC 60942, class of accuracy 2). The equivalent level noise pressure $L_{Aeq,T}$ was calculated. The climatic and microclimatic conditions were investigated before every series of measurements by the digital meteorological station Ws-1600 (class of accuracy 2).

The data were analyzed using a General Linear Model ANOVA of the statistical package STATISTIX 9 (Analytical Software, Tallahassee, FL, USA). There were evaluated factors of distance of measuring (1 – 3), period of day (1 = time before feeding; 2 = feeding time; 3 = time after feeding), and season (1 = summer, 2 = winter). The normality of data distribution was evaluated by the Wilk-Shapiro/Rankin Plot procedure. All data conformed to a normal distribution. Significant differences between groups were tested by Comparisons of Mean Ranks. Values are expressed as means \pm SD.

III. RESULTS AND DISCUSSION

The levels of noise depend highly significantly on time of the day (before feeding, during feeding, after feeding). Differences among periods and distances were highly significant (*** $P < 0.001$). Inside the building, the highest noise levels (65.5 ± 1.6 dB, 72.0 ± 1.4 dB, 63.4 ± 0.7 dB, $P < 0.001$) were measured. Significantly lower values were observed outside of barn, however, recorded means did not differ in comparison of distance from sidewalls (47.6 ± 4.5 dB, 47.5 ± 4.4 dB). It does mean that 4 m spacing (as difference between 7 m and 11 m) is for the propagation of noise is negligible. Major proportion of noise was absorbed by the walls of the building.

At the time of feeding (period 2), the highest average levels of noise were recorded (72 ± 1.4 dB, 52.6 ± 3.0 dB, 52.4 ± 2.8 dB, $P < 0.001$). Pigs had very loud vocalization during waiting for the feed, also during eating. They manifested aggressive behavior by pushing against each other by mangers. After feeding (period 3), when almost all pigs were already motionlessly lying, the lowest noise levels were found (63.4 ± 0.7 dB, 44.1 ± 1.9 dB, 44.2 ± 1.9 dB).

Noise values showed in all measurements inside the building (90 measurements) of 66.9 ± 3.9 dB is lower than that stated by [11,19] during housing of pigs with ventilation system. However, McBride et al. [3] recorded at the feeding of fattening pigs the noise level higher than 105 dB. The interpretation of noise assessment in animal housing is difficult as goals and methodology of differ substantially between studies. Whether or not a sound is to be described as noise therefore depends on the subjective notion as to whether listening brings about agreeable or disagreeable feelings. The condition under which a recipient is subjected to

noise is important [11,13]. Animals not only have to accept the noise, but it also emit [10,20].

At the present work, factor of season was found as very important for noise dissemination. During summer were recorded significantly higher noise levels (67.6±3.9 dB vs. 66.3±3.8 dB, 48.7±4.3 dB vs. 46.6±4.4 dB, 48.8±4.3 dB vs. 46.3±4.2 dB). There is some connection between time of day and the season as indicated by the result of calculated interaction between daily period*season (0.0017**).

Effect of season on the noise level has not been proven only in the house (P<0.01) but also outside (P<0.001). Higher noise levels in summer period recorded indoors and outdoors were caused by the need to speed air exchange, running at full ventilation is very noisy. The influence of the noise produced inside barns is often neglected and mainly ventilation systems are installed regardless of the noise creating. Also feeding and manure handling can become a source of noise. Noise produced in intensive animal rearing by ventilation system [20], feeding and excrement removal lines [21,22,23] and by animals themselves is a potential stressor and affects not only animals but also the tending personnel. High sensitivity to noise levels has been observed in pigs with some potential impact on their behaviour.

Numerous studies in the field of urban noise and structural engineering have provided information on permeability of noise from anthropogenic sources [14,24,25]. Our study illustrates potential animal management impacts on the noise environment. Some authors measured noise generated in the animal housing [26,27,28], but there is a lack of sources about noise transmittance from animal barn to outdoors, nobody has probably dealt with this problem except for us. The thickness and composition of the wall can reduce noise emissions from the barn [29,30]. They found that at a noise levels were lowered by crumb rubber concrete panel or wood plate with plasterboard. Generally, the noise emissions from the barn can be reduced by the use of different noise barriers, limitation of ventilation speeds, attaching the fabric layer on the wall or alteration of texture.

At present, the methods in simulation of propagation of the sound to the distance from hundreds of meters up to kilometers are known, and their results are not significantly different from the measured values [16,17], but the most precise method is still the proper measurement. Properties such as thermal conductivity, thermal resistivity, heat transfer, conductance value, sound absorption at different frequency and noise reduction were investigated by [27]. However, information on the performance of crumb rubber concrete on sound properties is limited. The problems arising from sound propagation outdoors may range from relatively simple to very complex, depending upon the nature of the source and distribution of the affected surrounding areas. If the source is composed of many

individual component sources, as would often be the case with an industrial plant, and the surrounding area is extensively affected, then the use of a analysis associated with level prediction is essential and a number of schemes have been designed for the purpose [29,31]. Consequently, the sound intensity in any particular direction is inversely proportional to the increasing surface area of the sphere [32].

IV CONCLUSIONS

The environmental problem of acoustic pollution is gaining increasing importance for our society. Noise levels inside the stable building were influenced primarily by the period of the day, but we did not find high noise levels that would be harmful neither of animals nor of human. In the surroundings of the building, the dependence of noise on season of the year was ascertained. The obtained results should not be overlooked, problem is urgently important for the welfare implications.

REFERENCES

- [1] M. R. Gamble, "Sound and its significance for laboratory animals," *Biological Reviews*, vol. 57, pp. 395–421, 1982.
- [2] O. Norén, "Noise from animal production," in *Animal Production and Environmental Health*, D. Strauch, Ed. New York: Elsevier Science Publishers, 1987, pp. 27-46.
- [3] D. McBride, H. Firth, and G. Herbison, "Noise Exposure and Hearing Loss in Agriculture: A Survey of Farmers and Farm Workers in the Southland Region of New Zealand," *Journal of Occupational and Environmental Medicine*, vol. 45, pp. 1281-1288, 2003.
- [4] J. A. Correa, S. Torrey, N. Devillers, J. P. Laforest, H. W. Gonyou, and L. Faucitano, "Effects of different moving devices at loading on stress response and meat quality in pigs," *Journal of Animal Science*, vol. 88, pp. 4086–4093, 2010.
- [5] A. M. Lauer, A. M. El-Sharkawy, D. L. Kraitchman, and W. A. Edelstein, "MRI Acoustic noise can harm experimental and companion animals," *Journal of Magnetic Resonance Imaging*, vol. 36, pp. 743–747, 2012.
- [6] P. S. Warren, M. Katti, M. Ermann, and A. Brazel, "Urban bioacoustics: it's not just noise," *Animal Behaviour*, vol. 71, pp. 491-502, 2006.
- [7] B. Berglund, T. Lindvall, and D. H. Schwela, *Guidelines for community noise*. Geneva, Switzerland: The World Health Organization, 1999.
- [8] P. A. Kaseeloo and K. O. Tyson, "Synthesis of Noise Effects on Wildlife Populations. Guidelines Research," US Department of Transportation, The Federal Highway Administration (FHWA), National Technical Information Service, Springfield, VA 22161, September 2004, Publication No. FHWA-HEP-06-016.
- [9] L. P. Sánchez-Fernández, L. A. Sánchez-Pérez, and J. J. Carbajal-Hernández, "Wireless monitoring system," in *Recent Advances in Energy, Environment, Ecosystems and Development*. Proc. of the 2013 Intern. Confer. on Energy, Environment, Ecosystems and Development, Venice, Italy, September 28-30, 2013, pp. 83-90.
- [10] D. N. Gladwin, K. M. Mancini, and R. Villella, "Effects of aircraft noise and sonic booms on domestic animals and wildlife: bibliographic abstracts," U.S. Fish Wildl. Serv. National Ecology Research Center, Ft. Collins, CO, 1988, NERC-88/32.
- [11] B. Algers, I. Ekesho, and S. Stromberg, "The impact of continuous noise on animal health," *Acta Veterinaria Scandinavica*, Suppl. 67, pp. 1-26, 1978.
- [12] K. M. Mancini, D. N. Gladwin, R. Villella, and M. G. Cavendish, "Effects of Aircraft Noise and Sonic Booms on Domestic Animals and Wildlife: A Literature Synthesis," U.S. Fish and Wildlife Service National Ecology Research Center, Ft. Collins, CO, 1988, NERC-88/29.

- [13] J. Broucek, "Effects of noise on performance, stress, and behaviour of animals: A review," *Slovak Journal of Animal Science*, vol. 47, pp. 114-120, 2014.
- [14] K. W. Ngai, and C. F. Ng, "Structure-borne noise and vibration of concrete box structure and rail viaduct," *Journal of Sound and Vibration*, vol. 255, pp. 281-297, 2002.
- [15] T. Daddi, F. Testa, S. Tessitore, and F. Iraldo, "Environmental performance improvements and external stakeholder pressures in companies with certified Environmental Management System," in *Recent Advances in Power Systems, Energy, Environment*. Proc. of the 2013 Intern. Confer. on Energy, Environment, Ecosystems and Development, Rhodes Island, Greece, July 16-19, 2013, pp. 93-99.
- [16] B. Günther, K. H. Hansen, and I. Veit, *Technische Akustik – Ausgewählte Kapitel. Grundlagen, aktuelle Probleme und Messtechnik*. D-71268 Renningen: Expert Verlag GmbH, 2008.
- [17] P. Chevret, Ph. Blanc-Benon, and D. Juvé, "A numerical model for sound propagation through a turbulent atmosphere near the ground," *Journal of the Acoustical Society of America*, vol. 100, pp. 3587-3599, 1996.
- [18] Ph. Blanc-Benon, L. Dallois, and D. Juvé, "Long range sound propagation in a turbulent atmosphere within the parabolic approximation," *Acustica united with Acta Acustica*, vol. 87, pp. 659-669, 2001.
- [19] M. C. Bérengier, B. Gauvreau, Ph. Blanc-Benon, and D. Juvé, "Outdoor Sound Propagation: A Short Review on Analytical and Numerical Approaches," *Acta Acustica United with Acustica*, vol. 89, 980-991, 2003.
- [20] J. C. Talling, J. A. Lines, C. M. Wathes, and N. K. Waran, "The acoustic environment of the domestic pig," *Journal of Agricultural Engineering Research*, vol. 71, pp. 1-12, 1998.
- [21] K. Adámek, J. Kolář, P. Půlpán, and M. Pustka, "Noise Reduction at the Fan Outlet," in *Recent Advances in Energy, Environment, Ecosystems and Development*. Proc. of the 2013 Intern. Confer. on Energy, Environment, Ecosystems and Development, Rhodes Island, Greece, July 16-19, 2013, pp. 59-62.
- [22] S. Mihina, V. Kazimirova, T. A. Copland, *Technology for farm animal husbandry*. Nitra: Slovak Agricultural University, 2012.
- [23] J. Venglovsky, N. Sasakova, M. Vargova, O. Ondrasovicova, M. Ondrasovic, R. Hromada, M. Vucemilo, A. Tofant, "Noise in the animal housing environment," in *Proc. XIIIth Intern. Congr. of the Intern. Soc. Anim. Hygiene*, Tartu, Estonia, 2007, pp. 995-999.
- [24] P. Fiala, G. Degrande, and F. Augusztinovicz, "Numerical modelling of groundborne noise and vibration in buildings due to surface rail traffic," *Journal of Sound and Vibration*, vol. 301, pp. 718-738, 2007.
- [25] M. F. M. A., Sadin, N. L. N. Ibrahim, K. Sopian, E. Salleh, "Daylighting rules of thumb and a comparison of different floor depth under overcast and intermediate sky without sun," in *Recent Advances in Power Systems, Energy, Environment*. Proc. of the 2014 Intern. Confer. on Power Systems, Energy, Environment, Interlaken, Switzerland, February 22-24, 2014, pp. 173-177.
- [26] D. Schäffer, V. Marquardt, G. Marx, and E. Borell von, "Lärm in der Nutztierhaltung – eine Übersicht, unter besonderer Berücksichtigung der Schweinehaltung," *Deutsche Tierärztliche Wochenschrift*, vol. 108, pp. 60-66, 2001.
- [27] W. Otten, A. E. Kanitz, B. Puppe, M. Tuchscherer, K. P. Brüssow, G. Nürnberg, and B. Stabenow, "Acute and long term effects of chronic intermittent noise stress on hypothalamic-pituitary-adrenocortical and sympatho-adrenomedullary axis in pigs," *Animal Science*, vol. 78, pp. 271-284, 2004.
- [28] C. A. Weeks, "A review of welfare in cattle, sheep and pig lairages, with emphasis on stocking densities, ventilation and noise," *Animal Welfare*, vol. 17, pp. 275-284, 2008.
- [29] P. Sukontasukkul, "Use of crumb rubber to improve thermal and sound properties of pre-cast concrete panel," *Construction and Building Materials*, vol. 23, pp. 1084-1092, 2009.
- [30] J. Lendelova, J. Plesnik, M. Zitnak, "Effect of Stered using on sound isolation of workspace," in *Rural Buildings in European Regions, Architectural – constructions – technology – safety*, Nitra, 2013, pp. 132-136.
- [31] D. A. Bies, and C. A. Hansen, *Engineering Noise Control: Theory and Practice*, CRC Press, 2009, pp. 232 – 259.
- [32] Z. Chen, and R. C. Maher, "Semi-automatic classification of bird vocalizations using spectral peak tracks," *Journal of Acoustical Society of America*, vol. 120, pp. 2974-2984, 2006.

Decrease the scourge of malnutrition in Sub-Saharan Africa through the implementation of EU financial instruments

Ionel Bostan, Carmen Năstase, Dana Druguș, Alunica Morariu, Ovidiu Bunget

Abstract- Food security is a worldwide problem which entails – in order to be solved or at least alleviated – grassroots efforts made by the states, by international institutions, nongovernmental organizations, etc. Under these circumstances, when the situation has become more difficult due to the global crisis and various other reasons, the European Union plays a special role. We are particularly emphasizing the fact that it has activated several financial instruments that are directed at providing the underprivileged peoples (vulnerable categories) located in certain geographical areas, with the

necessary means to handle the underlying causes of food insecurity. The present paper approaches the most important aspects related to the EU actions directed at improving the availability and accessibility of foodstuff for the beneficiaries (the states) located in sub-Saharan Africa.

Key words - underdevelopment, severe famine, malnutrition, European budgetary resources, audit

I Introduction

Famine and malnutrition have spread worldwide (Figure 1), while underdeveloped countries are highly affected by the increased prices of foodstuff

(2007-2008) and particularly by the recent financial crisis [1], [2]. Almost 1 billion hungry people in the world or 1 in 7 persons (Figure 2).

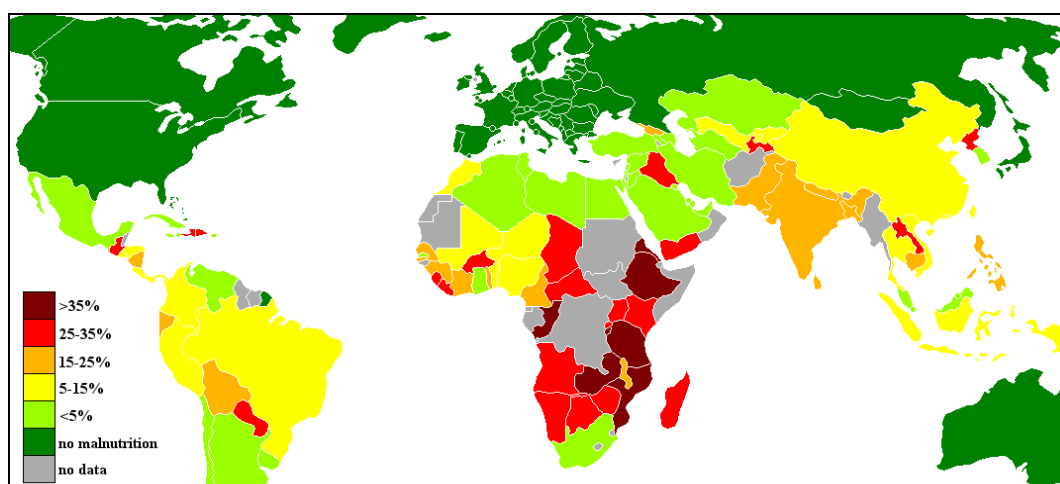


Figure 1. Population hunger/ malnutrition level on different planet zones (% in total population)

(Source: http://commons.wikimedia.org/wiki/File:Global_malnutrition.png)

Ionel Bostan is with "Ștefan cel Mare" University - Suceava (FSEAP), Romania, ionel_bostan@yahoo.com
Carmen Nastase in with "Ștefan cel Mare" University - Suceava (FSEAP), Romania, gprelipcean@yahoo.com
Daniela Drugus is with the Medicine and Pharmacy University, Iasi, Romania (e-mail: drugus_daniela@yahoo.com)

Alunica Morariu is with "Ștefan cel Mare" University - Suceava (FSEAP), Romania morariua@seap.usv.ro
Ovidiu Bunget is with West University - Timisoara (FEAA), Romania, ovidiu.bunget@feaa.uvt.ro

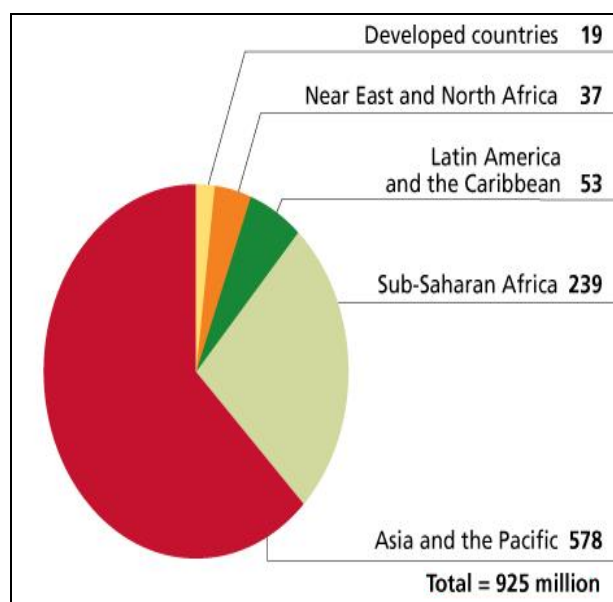


Figure 2. Distribution within the globe zones of population affected by hunger (mill. pers.) (Source: <http://worldinfo.org/2012/01/food-insecurity-preventing-political-famines>)

This issue has raised the interest of several renown authors in the field [3], [4], [5], [6], [8], and, on the other hand, the subject has also become one of the main objectives of certain international institutions/ organizations, among which the European Union (EU). The main focus is to meet the Millennium Development Goals [9], assumed by the EU as well and directed at eradicating poverty and famine.

In such context, the purpose of the present article is to reveal certain coordinates with respect to food insecurity in sub-Saharan Africa and also the concrete manner of action/ counteraction of EU based on Community financial resources. In this instance we are referring to European Development Fund (EDF), as main financing instrument and three other thematic instruments financed by the general budget of EU: (1) the budget line for food security, (2) early warning systems and (3) the storage network.

The data collected and included in our analysis regarding the number of people suffering from hunger for each country, the allocated funds, the level of chronic child malnutrition and many other social or economic indicators, all provided exclusively by prestigious European and international institutions, is emphasizing the accuracy/ the necessary certainty of such a study. Obviously, for all the data and information used we provide the precise references and we indicate the documentation source.

The criteria to be met for a country to benefit from the EU development assistance programmes include: insufficient food resources, the existence of inadequate medical systems, the absence of a competitive educational system, low

standard of living, the presence of unemployment as a social phenomenon, a low GDP, etc.

• *Specific instruments*

The actual implementation of the development cooperation policy entails the deployment of several legal instruments, such as multilateral or bilateral agreements, followed by the “Generalised System of Preferences” [11], which provides preferential EU market access for products originating in developing countries. In terms of finances, an important specific instrument is the EU budget [12], directed at financing external aid projects and programmes in the field of development cooperation, by using the Development Cooperation Instrument (DCI) [13]. This also includes the European Development Fund (EDF) [14] and the loans with preferential interest granted by the [European Investment Bank](#) [15].

In countries where food security has been included in the FED cooperation strategy, specifically those countries with the highest number of malnourished individuals, the development aid granted by the EU is highly relevant to the former’s needs and priorities. Thus, by 2015, the aim is to significantly diminish (by approximately 50%) the number of individuals whose income is lower than a dollar a day – about one billion people - and the number of people affected by famine.

Basically, since 1996, the European Commission has used main instruments [16] for sub-Saharan Africa, directed at financing investments in the field of food security (the topic of the present paper), and the total funds allocated during 2002-2010 amounted to approximately €3.2 billion.

II COORDINATES OF FOOD INSECURITY IN SUB-SAHARAN AFRICA

When considering the concept of food security - “the situation when all people at all times have physical, social and economic access to sufficient, safe and nutritious food that meets their dietary needs and food preferences in order to lead a healthy and active life” [17], and by comparing it to the data reported on the circumstances existing in

sub-Saharan Africa, a major problem is identified in the area.

It actually consists in profound *food insecurity* [16], since about 30% of the population (239 million people in the year 2010) is severely affected by famine.

The countries included in this area and the detailed food security levels for each of these countries are presented in Figure 3.

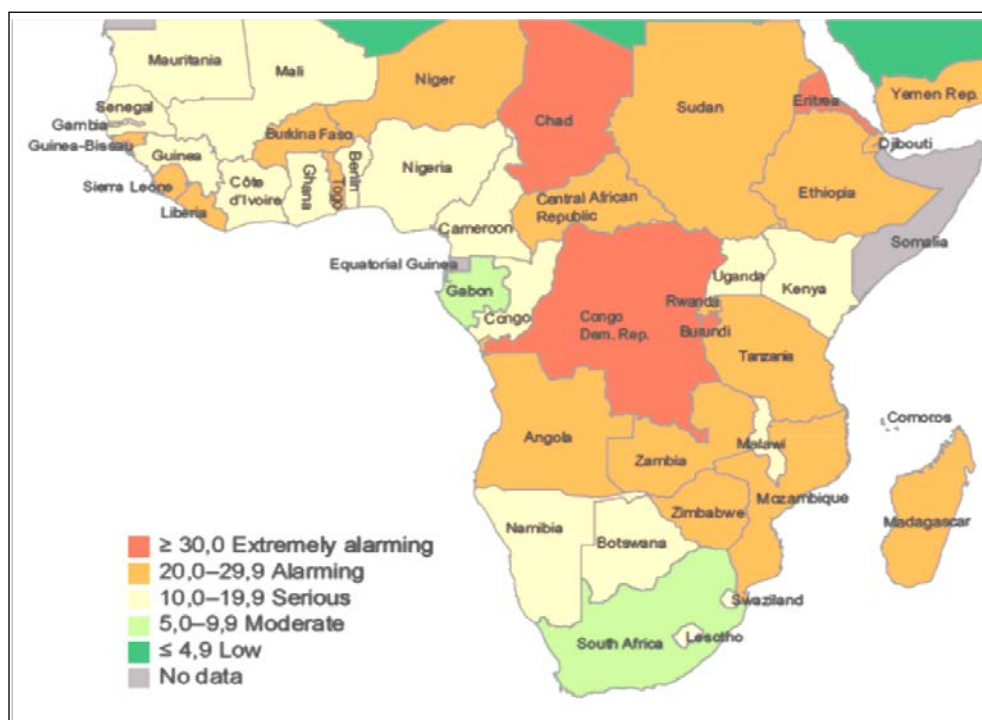


Figure 3. Map of the food security situation in sub-Saharan Africa

(Source: International Food Policy Research Institute, 2012, <http://www.ifpri.org/datasets>)

Note: The figures presented above refer to % of the famine stricken population.

The factors that contribute to the persistence of food insecurity are related to low agricultural productivity, low investment levels and the decreasing aid from donors allocated for agriculture and rural development, low spending power and the inadequate infrastructure for storing, processing and distributing food, etc.

Mention must also be made of the fact that over two thirds of the population inhabit rural areas and live off basic agriculture. Productivity increases at a rate that does not exceed 1-2% per year and is below the annual population growth rate which amounts to 2.2% [18], [19]. The underlying causes are mainly related to the reduced areas of cultivated land, the excessive reliance on rainfall and the insufficient access to or inadequacy of seeds, fertilizers and pesticides.

Overall, one can say that sub-Saharan Africa is undergoing chronic malnutrition,

particularly as far as children are concerned [20], an average of 47% of these – below 5 years of age – suffering from chronic malnutrition, 30% being underweight, while acute protein calorie malnutrition is affecting 9% of these children.

III INTERVENTIONS IN TERMS OF FOOD SECURITY FOR SUB-SAHARAN AFRICA, SUPPORTED BY THE EU FINANCIAL RESOURCES

Since 1996, the EC has used the European Development Fund (EDF) for the area under discussion, followed by another three thematic instruments financed by the EU general budget [16]. These thematic instruments are related to the budget line for food security (directed at financing food aid/short-term actions and long-term financial aid

for the provision of seeds, tools, etc.), as well as to the early warning systems and the storage network.

The Food Security Thematic Programme (2007-2013) is also included here, created according to Regulation No. 1905/2006 establishing a financing instrument for development cooperation (FIDC) [13], as well as the Food Facility which provides a rapid response to the crisis caused by volatile food prices in developing countries [21].

The fund allocation for food security in sub-Saharan Africa for the period 2002-2010

through the four thematic instruments amounts to € 3,177.0 million (Table 1).

In 2011, the EU has allocated humanitarian aid of €158 million, while the member states contributed with €440 million, along with the more than €680 million provided to the region as long-term aid for agriculture, rural development and food security until 2013 [22].

Table 1. The structure of EU funds for food security in sub-Saharan Africa (2002-2010)
(Source: Compiled from ECA, 2012)

Financing instruments	Value (mill. €)	Total weight (%)
9th European Development Fund/ 9th EDF	839.0	26.4
10th European Development Fund/ 9th EDF	1,098.0	34.6
Food Security Thematic Programme/ FSTP	222.0	7.0
Food Facility/ FF	513.0	16.1
Food Security Budget Line/ FSBL	505.0	15.9
Total	3,177.0	x

By the year 2012, approximately 50% of these funds were directed towards the countries mentioned in the table below (Table 2), which have a famine stricken population that amounts to 117.8 million people.

The fund allocations are referring to directed at sustainable results, by providing the local population with the necessary means to act and treat the underlying causes of food insecurity. The latest audit report in the field, developed by the European Court of Auditors [16], reveals that, to a considerable extent, the interventions manage to improve the availability and accessibility of food for beneficiaries, thus leading to the increased income and more diverse agricultural produce. These also significantly support those programmes that provide a safety device for the most vulnerable categories and, these interventions often have reasonable prospects of being sustainable.

In the future, the EU [23] will stay committed to the responsibilities assumed as part of the Millennium Development Goals and to meeting the objective of official development aid of 0.7% of the Gross National Income (GNI) until 2015. In order to reach these objectives [24], the EU has decided to increase the external aid from € 56.8 billion to € 70.0 billion and to extend the use of innovative financial instruments (loans, collateral,

equity capital instruments, etc.) to benefit the recipient countries.

These documents show that the allocated FED funds for a group of 79 states from Africa, the Caribbean and the Pacific area will increase from € 23 billion for six years, to €

30.3 billion for seven years (in 2011 prices) and will continue to be directly provided by EU member states.

Table 2. The main recipients of the aid for development in the field of food security (granted by the EU, 2002-2010) and the relation to the number of famine stricken individuals
(Source: Compiled from ECA, 2012)

Country	Undernourished people		9th EDF (mill. €)	10th EDF (mill. €)	FSBL (mill. €)	Food Facility (mill. €)	FSTP (mill. €)	Other budget lines (mill. €)	Total funding (mill. €) (3+4+5+6+7+8)
	Millions	%							
0	1	2	3	4	5	6	7	8	9
Ethiopia	31.6	41.0	78.0	146.2	36.2	44.6	2.2	3.7	310.9
Malawy	3.9	28.0	76.3	62.0	63.7	18.5	3.3	-	223.8
Niger	2.7	20.0	53.1	39.4	21.8	19.6	-	4.9	138.8
Rwanda	3.1	34.0	64.0	40.0	4.4	15.6	-	12.1	136.2
Burundi	4.7	62.0	74.8	6.1	9.2	14.4	9.1	3.0	116.6
Eritrea	3.0	64.0	7.9	4.9	20.4	13.6	6.3	13.6	66.6
DR Congo	41.9	69.0	34.7	-	26.3	39.8	21.6	2.3	124.8
Zambia	5.2	43.0	16.6	26.6	4.3	15.4	2.0	-	64.9
Mali	1.5	12.0	1.8	20.5	8.0	26.3	0.1	2.0	58.7
Liberia	1.2	33.0	-	22.7	5.7	14.1	8.0	2.7	53.3
Tanzania	13.7	34.0	8.0	5.0	-	31.7	-	-	44.6
Cameroon	3.9	21.0	10.4	18.7	-	2.5	-	1.3	32.9
Swaziland	0.2	18.0	25.7	0.9	-	-	-	3.0	29.6
Gambia	0.3	19.0	-	2.6	-	5.5	-	-	8.1
Lesotho	0.3	14.0	2.0	-	-	5.4	-	-	7.4
Botswana	0.5	25.0	4.0	-	-	-	-	-	4.0
Total	117.8	x	457.2	395.7	200.0	266.9	52.6	48.7	1,421.1

Conclusions

At present, beyond the explanations related to the global crisis, there are several underlying reasons behind the worsening of the world food security. We are here referring to food speculations, climate change, real estate purchases on a global level, the loss of biodiversity, the water resources issue, etc.

Therefore, the present challenges related to hunger and malnutrition require a new vision on food security in general [25]. Thus, all the EU strategies must be analysed and altered, particularly those related to this problem – either

directly or indirectly – and the member states will have to meet their commitments on the global combating of poverty and hunger.

The aid provided by the EU should increasingly rely on sustainable and small scale food production in order to increase the availability of food, since agriculture will continue to be at the core of rural economies in all developing countries.

In terms of food accessibility, a *rights* oriented approach is recommended in the development of the EU cooperation strategies with various countries, while governments should be supported to include the “right to adequate food” in the Constitution of each particular country.

We argue that all this will be possible, in light of what has been written in the “Europe – 2020” Programme [26], and that the EU will remain “a global player that takes its international responsibilities seriously”. These efforts will clearly take place in the broader ongoing efforts to “increase development aid and improve the efficiency of our aid programmes, notably through the efficient division of labour with Member States and by better reflecting development aims in other policies of the European Union”.

References

- [1]. European Commission, **Report - On an EU policy framework to assist developing countries in addressing food security challenges**, Bruxelles, 2011, available from: <http://www.europarl.europa.eu/sides/getDoc.do?type=REPORT&reference=A7-2011-0284&language=EN/>.
- [2]. Robson, M.G., **Food Insecurity: Preventing Political Famines**, School of Environmental and Biological Sciences, Rutgers University, 2012, available from: <http://worldinfo.org/2012/01/food-insecurity-preventing-political-famines/>.
- [3]. **Brown, L.R., Optiuni dificile - Confruntarea cu perspectiva crizei alimentare**, Trad. M. Coliu, Editura Tehnică, Bucharest, 1997.
- [4]. Humă, C., Chiriac, D., **Aspecte globale privind fenomenele de secetă, aridizare și desertificare**, *Calitatea vieții*, (XV)1–2, 2004, available from: <http://www.iccv.ro/oldiccv/romana/revista/rcalvit/pdf/cv2004.1-2.a07.pdf/>.
- [5]. Matshe, I., **Boosting smallholder production for food security: Some approaches and evidence from studies in sub-Saharan Africa**, *Agrekon*, 48(4): 483-511, 2009.
- [6]. Tadesse, T., Haile, M., Senay, G., Wardlow, B.D., Knutson, C.L., **The need for integration of drought monitoring tools for proactive food security management in sub-Saharan Africa**, *Natural Resources Forum*, 32(4): 265-279, 2008.
- [7]. Baro, M., Deubel, T.F., **Persistent hunger: Perspectives on vulnerability, famine, and food security in sub-Saharan Africa**, *Annual Review of Anthropology*, 35: 521-538, 2006.
- [8]. Haile, M., **Weather patterns, food security and humanitarian response in sub-Saharan Africa**, *Philosophical Transactions of the Royal Society - B: Biological Sciences*, 360(1463): 2169-2182, 2005.
- [9]. United Nations, **The Millennium Development Goals Report**, New York, 2009.
- [10]. European Commission, **Communication from the Commission to the European Parliament, the Council, the Economic and Social Committee and the Committee of the Regions - Towards a global partnership for sustainable development**, Bruxelles, 2002, available from: http://europa.eu/legislation_summaries/external_trade/128015_ro.htm/.
- [11]. European Commission, **Taxation and Customs Union**, Bruxelles, 2008, available from: http://ec.europa.eu/taxation_customs/customs/customs_duties/rules_origin/preferential/article_781_en.htm/.
- [12]. Bostan, I., **Drept financiar comunitar**, Tipo-Moldova Publishing, Iasi, 2007.
- [13]. European Commission, **Regulation of The European Parliament and of The Council amending Regulation No. 1905/2006 establishing a financing instrument for development cooperation and Regulation (EC) No. 1889/2006 on establishing a financing instrument for the promotion of democracy and human rights worldwide**, Bruxelles, 2009, available from: <http://eur-lex.europa.eu/LexUriServ/LexUriServ.do?uri=CONSLEG:2006R1905:20091018:RO:PDF/>.
- [14]. European Commission, **European Development Fund**, Bruxelles, 2005, available from: http://europa.eu/legislation_summaries/development/overseas_countries_territories/r12102_en.htm/.
- [15]. **European Investment Bank, Report**, Luxembourg, 2013, available from: http://europa.eu/legislation_summaries/index_ro.htm/.
- [16]. European Court of Auditors, **Special Report No.1 – Effectiveness of European Union development aid for food security in sub-Saharan Africa**, Luxembourg, 2012, available from: <http://eca.europa.eu/portal/pls/portal/docs/1/13300745.PDF/>.
- [17]. Food and Agriculture Organization of The United Nations, **Rome Declaration on World Food Security & World Food Summit Plan of Action**, 1996, available from: <http://www.fao.org/docrep/003/w3613e/w3613e00.htm/>.
- [18]. The World Bank, **Report**, Washington DC., 2011, available from: <http://www.worldbank.org/reference/>.
- [19]. United Nations Population Fund, **Report**, New York, 2011, available from: <http://www.unfpa.org/public/cache/offonce/home/publications;jsessionid=F9B8885CF5591CD77BC638F8D5C86BCB.jahia01/>.
- [20]. Food and Agriculture Organization of The United Nations, **Report**, Rome, 2012, available from: http://www.fao.org/index_en.htm/.
- [21]. European Parliament and of The Council, **Regulation (EC) No 1337/2008 - establishing a facility for rapid response to soaring food prices in developing countries**, Bruxelles, 2008, available from: <http://eur-lex.europa.eu/LexUriServ/LexUriServ.do?uri=OJ:L:2008:354:0062:069:en:PDF/>.
- [22]. European Parliament, **Resolution on famine in East Africa**, Bruxelles, 2011, available from: <http://www.europarl.europa.eu/sides/getDoc.do?pubRef=-//EP//TEXT+MOTION+B7-2011-0492+0+DOC+XML+V0//EN/>.
- [23]. European Commission, **Annual Report on the European Community's Development and External Assistance Policies and their Implementation in 2011**, Bruxelles, 2012, available from: http://ec.europa.eu/europeaid/multimedia/publications/documents/annual-reports/europeaid_annual_report_2012_full_en.pdf/.
- [24]. European Commission, **A Budget For Europe 2020 (I, II)**, Bruxelles, 2011, available from: http://ec.europa.eu/budget/biblio/documents/fin_fw1420/fin_fw1420_en.cfm#doc1/, http://ec.europa.eu/budget/biblio/documents/fin_fw1420/fin_fw1420_en.cfm#doc2/.
- [25]. Zimmer, G., **Report an EU policy framework to assist developing countries in addressing food security challenges - 2010/2100 (INI)**, Committee on Development, Parlamentul European, Bruxelles, 2011, available from: <http://www.europarl.europa.eu/sides/getDoc.do?pubRef=-//EP//TEXT+REPORT+A7-2011-0284+0+DOC+XML+V0//RO/>.
- [26]. European Commission, **Communication from the Commission: Europe 2020 - A strategy for smart, sustainable and inclusive growth**, Bruxelles, 2010, available from: <http://ec.europa.eu/research/era/docs/en/investing-in-research-european-commission-europe-2020-2010.pdf/>.

Performance Measure of Switching Device (MOSFET) in Photo-voltaic System

Kamala J, Janarthanan V, and Santhosh K

College of Engineering Guindy, Anna University, Chennai, Tamil Nadu, India

Abstract — Battery charging circuits utilize switching devices for its control operations. MOSFET is used as switching device in the charge control circuits. This paper analyze the characteristics of Power MOSFET used to charge batteries from solar energy. N channel and P channel MOSFET Device characteristics are investigated for two cases of photo-voltaic system. First case study is done with the device connected between solar panel and battery. Second case study illustrates the performance of device in Buck converter used as photo-voltaic battery charger. Switching losses and efficiency of converter is analyzed for both devices. Results and discussions of this paper are useful for the selection of switching device and the operating frequency.

Index Terms — Buck converter, Power MOSFET, Switching losses, Transfer characteristics.

I. INTRODUCTION

Photo-voltaic energy storage system uses DC-DC converters for maximum energy transfer [1]. DC-DC converters consist of inductance, capacitance and power electronic semi-conductor devices [2]. Inductor and capacitor sizing is decided by switching frequency of power electronic components. Higher frequency leads to smaller values of inductor and capacitor with improved output regulation [3-5]. Power electronic components are designed with low on state resistance, fast switching rate, higher voltage and current carrying capacity [6].

In a battery charging system, source voltage of N-MOSFET is fixed at battery voltage and the drain current varies with battery voltage. Therefore, conventional MPPT algorithm does not deliver maximum current for battery charging [7]. Detailed analysis of MOSFET characteristics in a photo-voltaic system is required to find the switching requirements. Transfer characteristics of the device indicate the required gate drive for switching. It is derived by connecting the power component between solar panel and battery, with various gate voltages, as shown in figure 1. In this case, battery charging is possible only if solar panel voltage is sufficiently greater than battery voltage. N channel and P channel MOSFET transfer characteristics curves are obtained in this paper.

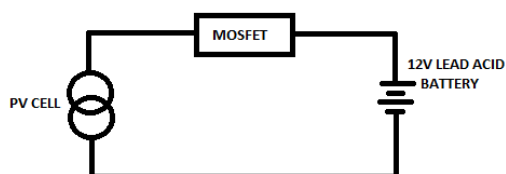


Figure 1 Power MOSFET coupled between PV cell and battery

DC-DC converter is used between solar panel and battery, if battery voltage does not match with solar panel. Efficiency of converter depends on the switching losses of the device. Efficiency of converter is analyzed for various switching frequencies applied to different types of devices. In this case, solar panel is connected to battery through buck converter as shown in figure 2.

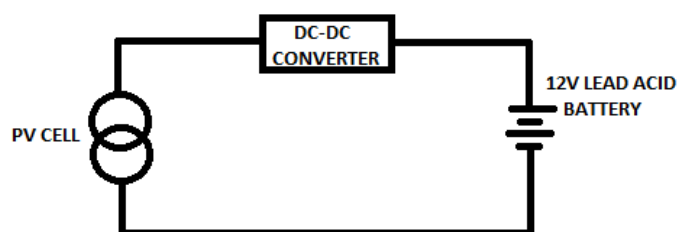


Figure 2 Battery charging through power converter

Photo-voltaic energy storage system with a solar panel of $100W_p$, V_{mp} of 17.5V, and a battery of 12V, 42Ah are considered in the proposed research work. Section II describes overall photo-voltaic charging system and its hardware specifications. Section III discusses the transfer characteristics of power electronic components connected between solar panel and battery. Converter efficiency is analyzed in section IV for various switching frequencies applied to different devices. Section V discusses the results obtained with the experimental set-up. Section VI concludes with the power component requirement and its characteristics applied to battery charging.

II. PHOTO-VOLTAIC BATTERY CHARGING SYSTEM

Specifications of solar panel are given in Table I. Battery charging is achieved either by connecting switch between solar panel and battery as shown in figure 3 or by using DC-DC converter as shown in figure 6.

TABLE I
SPECIFICATIONS OF SOLAR PANEL

Characteristics	Specification
Rated power, P	100W _p
Peak power voltage, V_{mpp}	17.5V
Peak power current, I_{mpp}	5A
Open circuit voltage, V_{oc}	21.4V
Short circuit current, I_{sc}	6A

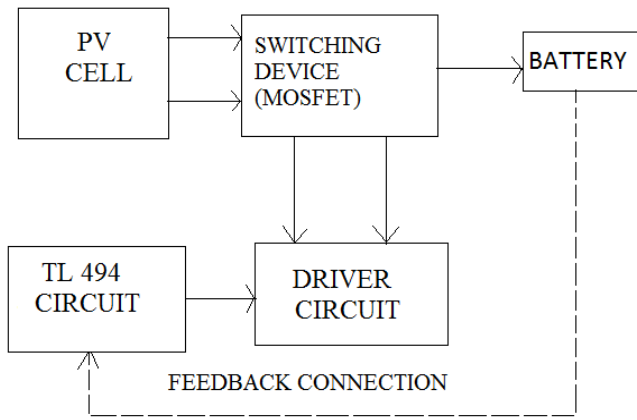


Figure 3 Switch controlled Battery charger

Important parameters of the switching device are given in table II

TABLE II SWITCHING DEVICE PARAMETERS

IRFP150N	IRF9530
$V_{DSS} = 100V$	$V_{DSS} = -100V$
$R_{DS(on)} = 0.036\Omega$	$R_{DS(on)} = 0.3\Omega$
$I_D = 42A$	$I_D = 12A$

Charge pump circuit required for gate of MOSFET is achieved by a driver circuit shown in figure 4. Complementary pair switching transistors 2N2907A and PN2222A are used to improve the drive strength of signal. Opto-isolator TLP250 [10] is used as isolator.

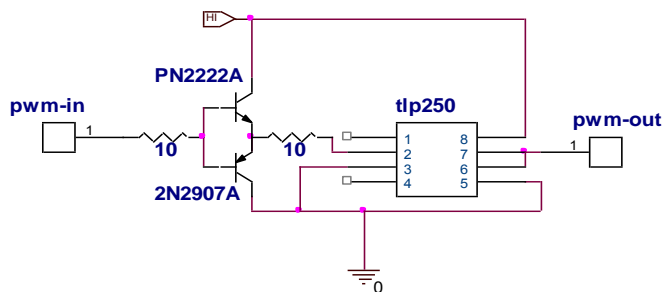


Figure 4 Gate driver circuit

Buck converter capable of handling 500W is designed with the following requirements

- Switching frequency = 5 MHz maximum
- Current ripple < 0.04A
- Voltage ripple < 0.01V
- Charging current = 10A maximum
- Duty cycle = 5% to 95%

Specifications of converter are given as follows and shown in figure 5

- Input voltage : varies between 14V-20V
- Output voltage : fixed by battery voltage
- MOSFET used : IRFP150N / IRF 9530 [8,9]
- Diode used: MBR1545
- Inductance: 100 μ H
- Capacitance: 1000 μ F

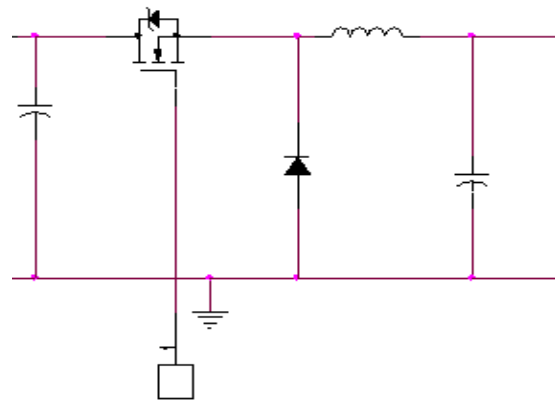


Figure 5 Buck Converter

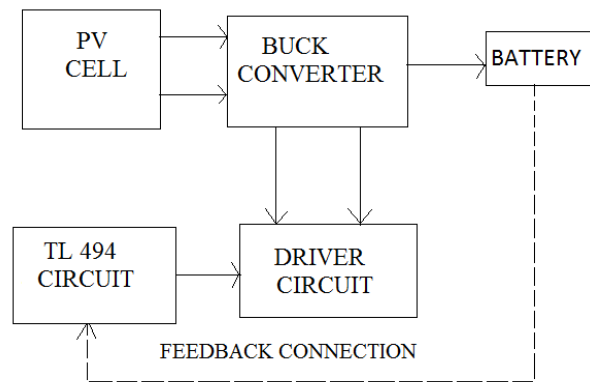


Figure 6 Converter based Battery charger

TL494 [11] pulse width modulator IC is used to generate the PWM signal of converter. Battery voltage is fed back to PWM generator circuit, using potentiometer that can be adjusted to vary the duty cycle of PWM signal. Frequency of PWM signal is varied by varying the resistance of oscillator circuit. Circuit shown in figure 7 uses resistance R13 (potentiometer) to vary frequency and R16 to adjust the duty cycle.

III. MOSFET TRANSFER CHARACTERISTICS COUPLED BETWEEN PV CELL AND BATTERY

HEXFET N channel power MOSFET IRFP150N and P channel device IRF9530 are chosen to study the transfer characteristics. Connection of MOS devices between PV cell and battery is shown in figure 8.

In case of N channel MOSFET, higher gate voltage is required to turn on the device, since the source is at battery potential approximately 12V. Sufficient drain current flows through the device, when gate voltage is greater than 16V. Gate to source voltage required for sufficient drain current is shown in figure 9. Drain current increases with increase in gate to source voltage.

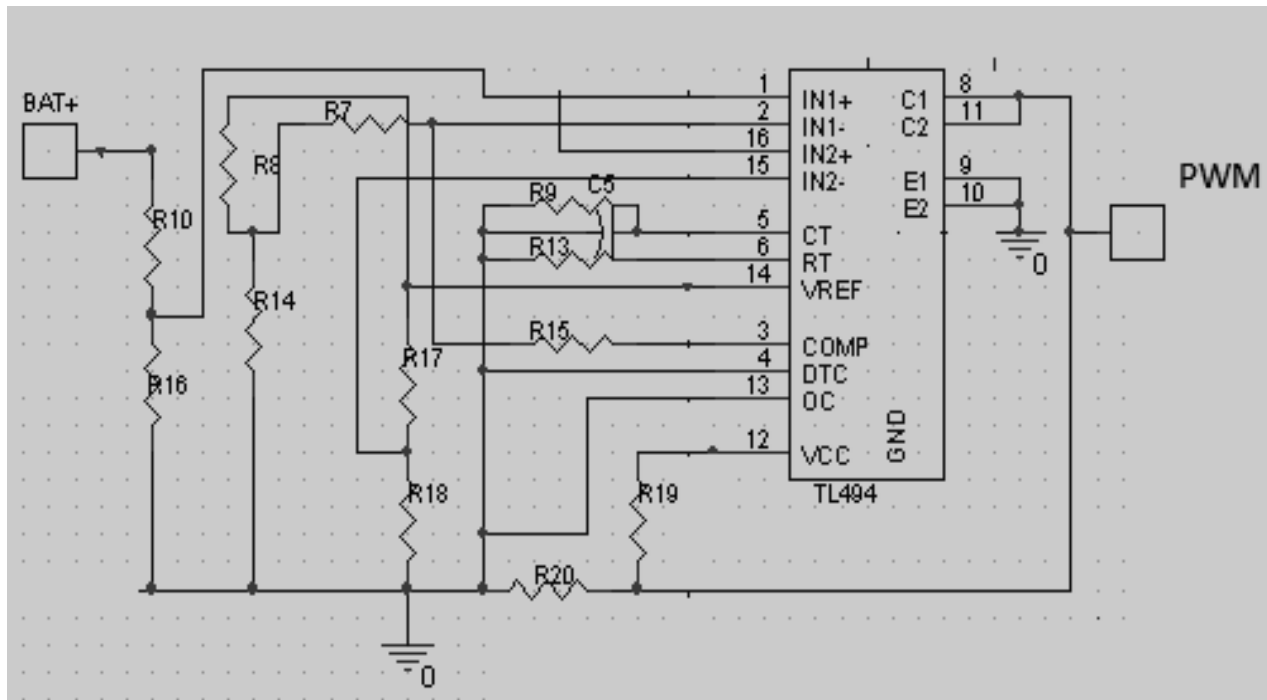


Figure 7 PWM Generation circuit

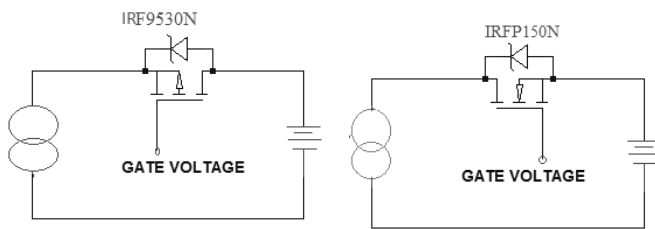


Figure 8 MOS device connected between PV cell and battery

Flow of drain current charges the battery and increases battery voltage with drain to source voltage decreasing from 7V to 0.15V. Maximum drain current is 5.36A with single N channel MOS device and it is increased to 5.41A with two devices in parallel. Parallel connection of devices reduces on-resistance of device and increases drain current.

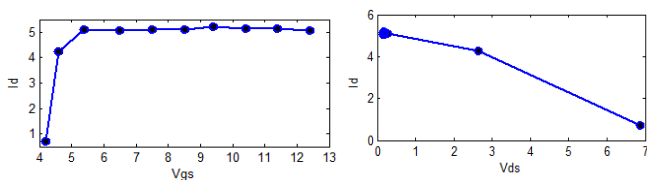


Figure 9 Characteristics of NMOS device

In case of P channel devices, gate voltage need not be higher than source. Gate signal can be derived from the input signal and charge pump circuit is not required. On-resistance of P channel MOS is higher and drain current is comparatively reduced. Maximum drain current for this case is 5.16A with single device and 5.3A with two devices in parallel. Characteristic curves of PMOS device is shown in figure 10.

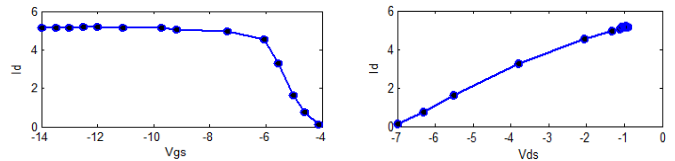


Figure 10 Characteristics of PMOS devices

IV. CONVERTER PERFORMANCE WITH DIFFERENT MOS DEVICES

Conventional MPPT is not effective for battery charging system, since the output voltage is at battery voltage, which is not V_{mp} of PV cell. Faster Charging is achieved with higher current flow. This paper analyzes the efficiency of converter by varying switching frequency for different MOSFET configurations. Input / output measurements of converter is taken for four cases of power electronic component as given below

- Single N channel device
- Two N channel devices in parallel
- Single P channel device
- Two P channel devices in parallel

The efficiency of the Converter is defined in equation 1,

$$Efficiency = \frac{Power\ output}{Total\ Power\ input} \tag{1}$$

Where,

$$\text{Output Power} = \text{Total input power} - \text{Total Power losses} \quad (2)$$

Power losses in the MOSFET is given by

$$\text{Power Losses} = \text{switching power losses} + \text{Conduction losses} \quad (3)$$

Where,

$$P_{sw} = \left(\frac{V_{in} \times I_{out}}{2} \right) \times (T_{rise} + T_{fall}) \times F_{sw} \quad (4)$$

$$P_{con_loss} = I_{out}^2 \times R_{ds(on)} \times \frac{V_{out}}{V_{in}} \quad (5)$$

Based on the experimental results the losses can be estimated for a Single NMOS Device, with following parameters

$$R_{ds(on)} = .036; I_{in} = 4.79; V_{in} = 14.39, \\ I_{out} = 4.89, V_{out} 12.27, F_{sw} = 1000 \text{ Hertz}, \\ T_{rise} = 200us, T_{fall} = 5us$$

$$P_{sw} = \left(\frac{14.39 \times 4.89}{2} \right) \times (200 + 5)us \times 1000 \text{ HZ} \quad (6) \\ P_{sw} = 7.21 \text{ Watts}$$

$$P_{con_loss} = 4.89^2 \times .036 \times \frac{12.27}{14.39} = .734 \text{ Watts}$$

$$P_{efficiency} = \frac{12.27 \times 4.89}{14.39 \times 4.79} = .870 = 87\%$$

Results of this analysis are shown in figure 11.

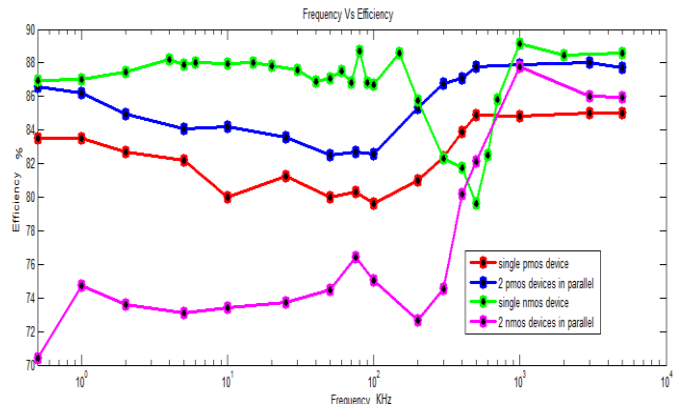


Figure 11 Efficiency of converter with different MOS devices

Efficiency of converter with two NMOS devices is lowered due to higher switching losses of two devices. PMOS devices provide comparable efficiency with simple gate driving circuit.

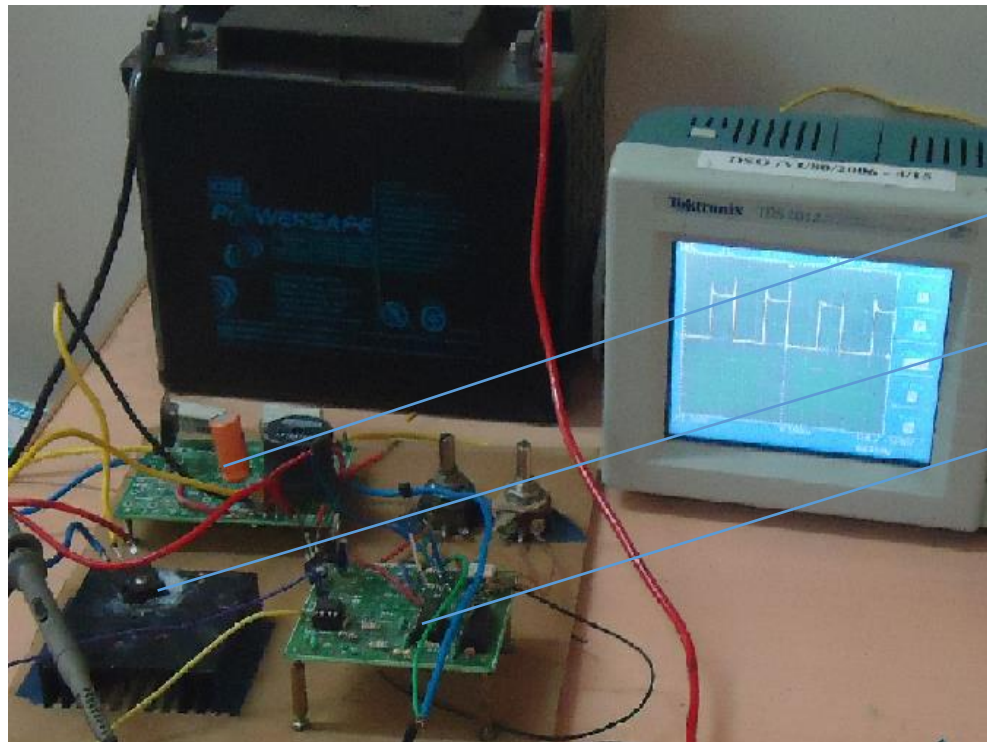


Figure 12 Experimental Set-up

V. EXPERIMENTAL SET UP AND RESULTS

Experimental set-up used to get results is shown in figure 12. Drain current with V_{ds} and PWM signal is shown in figure 13 and 14.

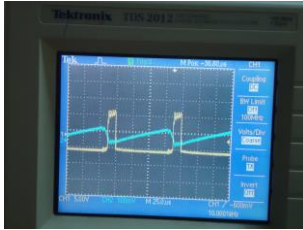


Fig. 13 V_{ds} and I_d

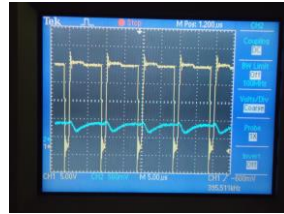


Fig.14 PWM and I_d

VI. CONCLUSION

Power electronic components play vital role in the performance of converters. This paper analyzes various MOSFET configurations with converter. Results show choosing PMOS device with low on-resistance delivers better performance with simple control circuit. N channel MOS devices operate at maximum efficiency with complex driving circuit.

ACKNOWLEDGMENT

Authors of this paper would like to thank for the funding provided by the Centre for Technology Development and Transfer, Research Support Scheme of Anna University, Chennai.

REFERENCES

- [1] B. ChittiBabu, Sriharsha, Ashwin Kumar, NikhilSaroagi and S.R.Samantaray, "Design and Implementation of Low Power Smart PV Energy System for Portable Applications using Synchronous Buck Converter," *International Symposium on Electronic System Design*, 2011.
- [2] Juan Paulo Robles Balestero, Fernando LessaTofoli, Grover Victor Torrico-Bascop'e and FalcondesJos'e Mendes de Seixas, "A DC-DC Converter Based on the Three-StateSwitching Cell for High Current and Voltage Step-Down Applications,"*IEEE transactions on power electronics*, vol. 28, no. 1, january 2013.
- [3] Y. Ren, K. Yao, M. Xu and F. C. Lee, "Analysis of the power delivery path from the 12-V VR to the microprocessor," *IEEE Trans. PowerElectron.*, vol. 19, no. 6, pp. 1507-1514, Nov. 2004.
- [4] L. Huber, K. Hsu, M. M. Jovanovic, D. J. Solley, G. Gurov and R. M.Porter, "1.8-MHz, 48-V resonant VRM: Analysis, design, and performanceevaluation," *IEEE Trans. Power Electron.*, vol. 21, no. 1, pp.79-88, Jan. 2006.
- [5] Drazen Dujic, Gina K. Steinke, , Bellini, Munaf Rahimo Liutauras Storasta, and Juergen K. Steinke, Characterization of 6.5 kV IGBTs for High-Power Medium-Frequency Soft-

Switched Applications, *IEEE Transactions on Power Electronics*, Vol. 29, No. 2, pp. 906-919, , Feb 2011

- [6] K.C. Daly, "Power Electronic Switching Devices" [Online] Available people.physics.anu.edu.au
- [7] Nabil Karami, NazihMoubayed and RachidOutbib, "Analysis of an irradiance adaptativepv based battery floating charger," presented in IEEE Photo-voltaic specialists conference 2011.
- [8] International Rectifer, [Online] Available www.irf.com
- [9] Power MOSFET, [Online] Available www.vishay.com
- [10] Laszlo Balogh, Design and Application Guide for MOSFET Gate Drive Circuits, [Online] Available www.ti.com
- [11] Pulse Width Modulation Control circuits, [Online] Available www.ti.com

Novel Methods for Desulfurization of Petroleum Fractions

H. Hosseini

Abstract— Because of the requirement for low sulfur content of fuel oils, it is necessary to develop alternative methods for desulfurization of petroleum fractions. Due to the disadvantages of HDS technologies such as costs, safety and green environment, new methods have been developed. Among these methods is ultrasound-assisted oxidative desulfurization. Using ultrasound-assisted oxidative desulfurization, compounds such as benzothiophene and dibenzothiophene can be oxidized. As an alternative method is sulfur elimination of heavy petroleum fractions by using of activated carbon in a packed column in batch condition. The removal of sulfur compounds in this case to reach about 99%. The most important property of activated carbon is ability of it for adsorption, which is due to high surface area and pore volume of it.

Keywords— Desulfurization, Petroleum fractions, Activated carbon, Ultrasound-assisted oxidative desulfurization.

I. INTRODUCTION

Presence of sulfur in heavy fuel oils leads to emission of SO_x which endanger public health. In order to control air pollution because of heavy fuel oils combustion, most of the countries released a new regulation requiring the use of low-sulfur fuel oils. It means that the sulfur content of fuel oils used in vehicles be limited to 15 ppm.

Hydrodesulfurization process has been a part of refineries for years, but new rules impose a better technology in this field. During the past years, alternative technologies have been studied by many researchers [1-7], among which ultrasound-assisted oxidative desulfurization has found wide attention.

In the present work, the ultrasound-assisted oxidative desulfurization of Naphtha and Pentane was studied in the Hydrogen peroxide / Acetic acid system. And also, as a alternative technology desulfurization in the activated carbon and molecular sieve packed beds have been studied and the results is compared to ultrasound-assisted oxidative desulfurization.

II. EXPERIMENTAL

Material and Instruments

H.Hosseini is with Department of Chemical Engineering, Abadan Branch, Islamic Azad University, Abadan, Iran (e-mail: h.hosseini@iauabadan.ac.ir).

Naphtha, pentane, acetic acid, hydrogen peroxide, activated carbon in powder and granulated form, molecular sieve, dimethyldisulfide and silica gel were provided from Abadan and Tabriz Petrochemical Companies.

Seven fuel oils with different sulfur contents at 530 ppm, 22 ppm, 17 ppm, 5.8 ppm, 3.5 ppm, 5 ppm and 6.30 ppm have been used for experiments.

An ultrasound apparatus manufactured by Sonics and Materials, Inc. has been used. The sulfur compounds in the feed were analyzed by gas chromatography in Tabriz Petrochemical Company. And also, It is used a pilot plant (length: 1m , width: 10cm) for batch desulfurization of naphtha and pentane.

III. RESULTS AND DISCUSSION

At the first , 100 cc of naphtha with measured sulfur as 22 ppm was placed in ultrasound bath for 10 minutes to which 1cc acetic acid and 1 cc hydrogen peroxide was added. Purity of hydrogen peroxide was read to be 30%. Results from sulphur measurement indicated deletion efficiency to be 60% in 10 minutes which means remained sulfur to be 8.8 ppm.

Tests indicates the best results from desulphurization to obtain in 20-200 KHz frequencies. The best conditions are preferably obtained in 20-50 KHz. The best results are obtained in power range 30-300 W/cm² or 5-100 W/cm² preferably. Generally, sonic analysis of organic contaminants in aqueous solutions in high frequencies (20-850 KHz) would result in higher efficiency than low frequencies (20-80 KHz). Desulfurization rate in low power rates (0.1-0.4 W/cm²) in Naphtha-Hydrogen Peroxide-Acetic acid system decreases with power rate. However if the ultrasonic power is higher than 200 W, we witness desulfurization rate with ultrasonic power increase which is resulted from cavitation. As well ultrasonic power is related to the solution volume. Regular ultrasonic range is 50-200 W while the solution volume ranging from 50 to 60 cc gives the best possible desulfurization. Post ultrasound solution is consisted form aqueous and organic phases. Organic phase includes sulfones obtained from oxidation reactions. We obtained sulfones using liquid-liquid extraction with the aid of dimethyl formamide polar solution. Oxidized naphtha was extracted two times with dimethyl formamide. In the second recovery naphtha was increased for about 10%. Desulfurization efficiency increased with increased solution to naphtha rate and number of extractions.

Practical problem in this method is that in oxidizing desulfurization process with the aid of ultrasound, about 80% of naphthalene alkyls may be lost in liquid-liquid extraction and operational problems appears with increased system dimension in industrial application. For this reason and to lower naphthalene alkyls lose it would be better to use solid absorption system such as alumina or zeolite for solution extraction, instead of dimethyl formamide [2].

The present paper shows that using solid absorbents has no negative effect on the main fuel hydrocarbons and the unit scale is made more practical as the result of very low solid volume used compared with the liquid solution.

Another reason for using such solid absorbent, like Alumina, is their capability in easy reduction with calcinations operation. Meantime sulfones are destructed thermally in this temperature. Using Hydrogen Peroxide-Activated Carbon-Acetic Acid system, percentage of the remaining sulfur would be much lower after desulphurization compared with the usage of Hydrogen Peroxide-Acetic Acid system.

In another test 100 cc naphtha with measured sulfur as 22 ppm was placed in ultrasound bath for 10 minutes to which 1 cc hydrogen peroxide was added. Purity of hydrogen peroxide as read to be 30%. Results from sulfur measurement indicated the omission efficiency to be 20% in 10 minutes.

In the third test 2 cc hydrogen peroxide and 2 cc acetic acid was added to 100 cc of naphtha with measured sulfur as 17 ppm. Hydrogen peroxide purity was 30%. Remainder sulfur was 7 ppm so omission efficiency was 58% in this test.

In the fourth test 5 cc acetic acid was added to 100 cc naphtha with measured sulfur of 28 ppm. Sulfur measurement indicated the omission efficiency to be 7%. Results indicate hydrogen peroxide to have significant role in omission of sulfur.

In the next test 100 cc of pentane with measured sulfur of 3.5 ppm was added to the bed consisted from 10 gr active carbon. Therefore omission efficiency is amounted to 57%.

In the sixth test 100 cc of pentane with measured sulphur as per 3.5 ppm was added to the bed consisted from 20 gr active carbon. Sulfur measurement results after one hour indicated omission efficiency to be about 100% so that the remainder sulfur was ppb. It shows that absorbent rate has significant role in sulfur omission efficiency.

In the seventh test 240 cc pentane with measured sulfur of 5.8 ppm was quickly passed through 50 gr of activated carbon. Results from measuring sulfur indicated the remainder sulphur to be 3.9 ppm with omission efficiency of 32.76%.

In the eighth test 750 gr of granular activated carbon was weighted and added to decanter. 500 cc pentane was passed through activated carbon bed. 300 cc pentane was used for saturation of activated carbon. Pentane sample contained 6.5 ppm of sulfur which was reduced to 1.5 ppm after omission. Therefore omission efficiency was 77%. Benzene was measured by GC to be ppb while no benzene related peak was appeared after omission. Therefore, results indicated that activated carbon is able to omit pentane sulphur intermittently.

Two absorbent beds were selected in the ninth test. One contained 570 gr of activated carbon and the other had 554 gr of molecular sieve. At first 400 cc pentane passed through the

molecular sieve bed. 250 cc of pentane obtained from the first bed (containing molecular sieve) passed through the second bed containing activated carbon, resulted in delivery of 150 cc of pentane. Analysis results indicate that pentane water level was 20 ppm in the zero time (before omission). It was 10 ppm leaving the first bed and reached 5 ppm passing through the second bed. Sulfur rate was 5 ppm in the feed and was finally less than 1 ppm in the second column output (activated carbon bed). In the tenth test 25 gr of activated granular carbon and 25 gr of powder activated carbon were weighted. Then 100 cc pentane was placed near powder activated and granular activated carbon separately for one hour. The sulfur rate was 5 ppm in the feeding. Sulfur rate in the pentane sample adjacent to the powder activated carbon was 1.34 while the rate was reported to be 2.4 ppm in the pentane sample adjacent to granular activated carbon. In the eleventh test 25 gr of granular activated carbon and 25 gr of powder activated carbon were weighted. Then 100 cc pentane was placed near powder activated and granular activated carbon separately for two hours. The sulfur rate was 6.3 ppm in the feeding. Sulfur rate in the pentane sample adjacent to the powder activated carbon was 1.6 while the rate was reported to be 1.8 ppm in the pentane sample adjacent to granular activated carbon. In the twelfth test, pentane omission pilot was made (in length of 1 meter and 10 cm width). Two columns were selected. 1 kg of silica gel of 5x type from Olefin unit and 0.5 kg of Norit granular activated carbon was added to the first and second columns respectively. 5 liters of pentane containing 5 ppm sulfur was passed through the two said beds. Discharge rate was set at 30 ml/min. After omission of the sulfur it reached the ppb. In the thirteenth test 1 kg of silica gel of 5x type from olefin unit was added to the 1st column and 0.5 kg of Norit granule activated carbon was added to the second column. 5 Lit of pentane containing 50 ppm sulphur passed through the said two beds. Discharge rate was set at 100 ml/min. After omission of sulfur it reached 17 ppm.

In the fourteenth test 1 kg of silica gel of olefin 5x type was added to the 1st column and 0.5 kg of powder activated carbon from recovery unit was added to the second column. 5 Lit of pentane containing 5 ppm sulfur passed through the said two beds. Discharge rate was set at 100 ml/min. After omission of sulfur it reached ppm.

In the last test 3 droplets of dimethyldisulfamide was added to 50 cc of pentane. Measured sulfur was reported to be 530 ppm. 50 cc of the sample was added to Jurget balloon 500 and reached to 500 cc. Then the sulfur was measured and reported to be 50 ppm which means the omission to be about 90%. As indicated in fig.1 increased molar rate of hydrogen peroxide to sulfur up to 0.02, discharged sulfur from naphtha would increased too while with higher rate sulfur discharge would be decreased.

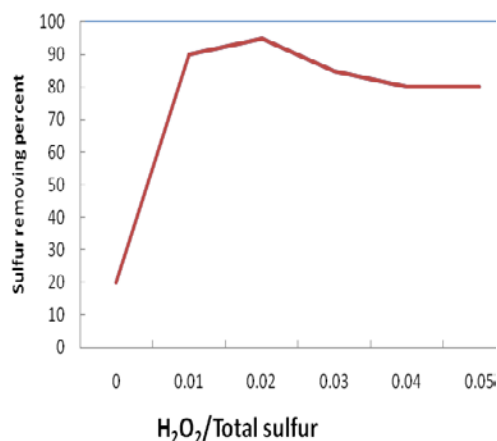


Fig.1. sulfur removing percent *versus* mole fraction changing.

the Selective Oxidation of Sulphur Compounds to Elemental Sulphur, US Patent. No 5,286,697, Feb 1994.

[5] H. Mei, et al., Fuel, vol. 82 (2003), p.405.

[6] T. Aida, Europea Patent 565324, 1993.

[7] S.P. Tu, et al., Journal of Environmental Engineering Science, vol. 1 (2002), p.237.

IV. CONCLUSION

In this research project the ultrasound-assisted oxidative desulfurization was compared to activated carbon packed bed system for removal of sulfur from naphtha and pentane. Primary tests indicate that when using hydrogen peroxide without acetic acid, removed sulfur would be very low (about 20%), but the rate would significantly increase (60%) under similar conditions when using acetic acid. As well further tests indicated that when using activated carbon the highest rate of sulfur omission can be seen (100%) under batch state while when using the system continuously sulfur omission rate would decrease. Ultrasound-assisted oxidative desulfurization method for sulfur omission has main benefit compared to other common methods like HDS. In this method tests can be made in atmospheric pressure and relatively low temperatures. As well no metallic catalyst is necessary in this method for sulfur removal. The present research work indicates that ultrasound method and activated carbon packed bed are suitable alternatives for removal of sulfur from different oil compounds.

REFERENCES

- [1] C. Song, et al., Ultra deep desulfurization by selective adsorption, Catalysis Today, vol. 111 (2006), p.74.
- [2] Z. Wu, et al., Ultrasonics Sonochemistry, vol. 17 (2012), p.1027.
- [3] G.X. Yu, et al., Energy Fuels, vol. 19 (2005), p.447.
- [4] P.J. Brink, Catalyst for the Selective Oxidation of Sulphur Compounds to Elemental Sulphur, Process for Preparing Such a Catalyst and Method for

NEW LAND USE IN RURAL MARGINAL AREAS. RENEWABLE ENERGY VS LANDSCAPE PRESERVATION

Donatella Cialdea, Luigi Mastronardi

L.a.co.s.t.a. Laboratory University of Molise Italy e-mail: a.cialdea@unimol.it; nardi@unimol.it

Abstract—This paper analyzes the evolution of land use in Italy according to “landscape quality aims” in order to provide useful tools for spatial planning choices. It’s focused on the energy infrastructures (systems for wind power and ground-mounted photovoltaic plants) that have the most impact on land in rural marginal areas. The case study is the Region of Molise, in Southern Italy, which is emblematic case because it has a significant number of installations as seen in relationship with the whole national territory. The study proposes a methodology to support Local authorities especially in relation to the definition of landscape quality aims, that the new Regional Landscape Plan must provide.

Keywords—Rural Land, Marginality, Renewable Energy, Landscape, Planning.

I. INTRODUCTION

This paper presents the results of research regarding the new land use in marginal areas, taking care to implement a methodology aimed at the recognition of the scenic and historic values as required by the Strategy Planning.

In European Union, rural areas have undergone a process of transformation rather intense from three points of view: social, economic and environmental [1]-[3].

The literature shows that, in terms of social and economic development, there are *dynamic* and *marginal* areas.

Moreover there is a strong presence of areas in marginal conditions [4], which comes mainly from intrinsic peculiarities of the territory, such as the morphological conditions that involve structural weaknesses in the networks of transportation and communication, disfavoring the settlement and development of productive activities.

These are places away from major urban areas and/or low population density, that have a level of economic and social development not comparable to the territorial context that surrounds them [5], [6].

In Italy, the marginal areas coincide with the zones with rural development problems [7], which include the predominantly rural areas of mountain, hill areas predominantly rural and significantly rural mountain areas (Figure 1).

In these areas, the structural changes and the increasing role of agriculture in recent years have taken on renewable energy profoundly affect land use [8], [9].

Energy infrastructures are relevant for some species and for the aesthetic quality of the landscape [10].

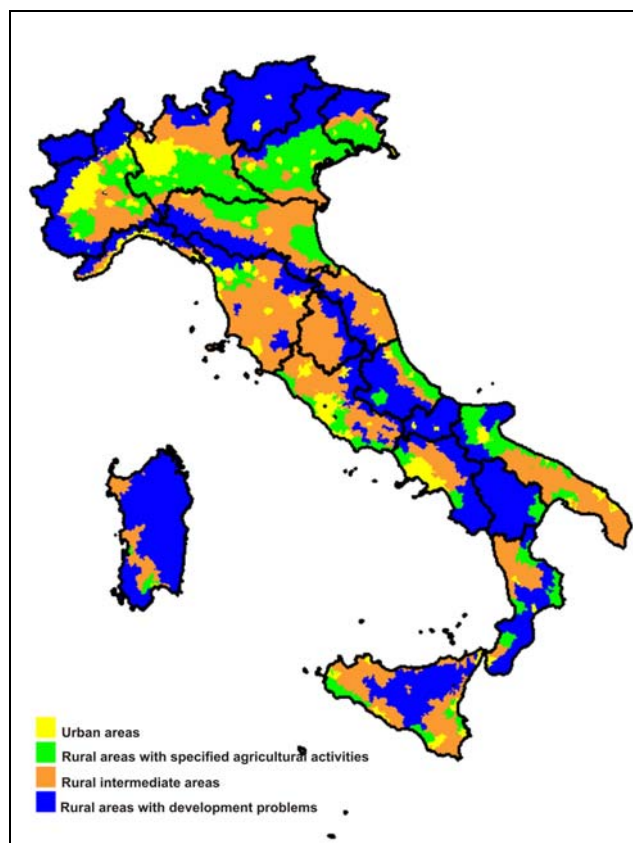


Fig. 1 Rural areas typologies in Italy

Renewable energy supply requires large tracts of land, food production necessitates arable and pasture land with suitable soils, and land is also needed for urban-industrial purposes, transport, resource extraction, reforestation, and recreation, i.e. all of them compete for land.

As a consequence, mankind's growing demands for renewable energy, food, and land cannot be circumvented by any form of adaptation. “These growing demands threaten mankind probably more severely than any other environmental problem. If endeavours for promoting sustainable development disregard these three ecological traps, they will inevitably miss their goals. As a consequence of these growing demands, the remaining unfragmented areas are under an enormous pressure. Therefore, much higher efforts are now required to conserve unfragmented landscapes.” Reference [11]

The impact on the landscape of renewable energy requires an approach designed to make the deployment of systems

compatible with the landscape and with agricultural production. It needs therefore considered the visual impact of the energy infrastructures, caused by the large size of the area occupied and - particularly in agricultural soils - the consequences that the installation of the equipment on the ground could result, if prolonged, on the fertility of the land and, consequently, on their land value [12].

This paper presents the situation of power plants in the Region Molise with reference to the two main types of plants installed in rural areas: wind farms and ground-mounted photovoltaic plants. The invasion of the coastal area by ground-mounted photovoltaic plants and by the large number of wind farms situated along the ridges in the pre-coastal area is very clear, especially in the eastern part of the province of Campobasso, along the ridge located between the Biferno Valley and the Fortore Valley.

II. MATERIAL AND METHODS

Our methodology is intended to fit into the structure of the *New Regional Landscape Plan* – in processing for the Molise Region - through the identification of conservation measures connotative character of the landscape, the determination of the recovery and rehabilitation of areas significantly compromised or degraded, the identification of the measures necessary for the proper insertion of the interventions of land transformation in the landscape, with particular reference to systems for wind power and ground-mounted photovoltaic plants.

In Italy the National Code of Cultural Heritage and Landscape was issued in 2004; following this enactment and its subsequent amendments also the Molise Region must adapt its previous landscape planning and identify the landscape quality aims for each identity-area. Therefore, the landscape planning should not only be interested in the preservation and conservation of the constituent elements of those parts of the territory are deemed exceptional but should be able to define lines of development and landscape quality aims for the entire territory. Objective of the plan will therefore also be the identification of measures for the rehabilitation of areas affected and degraded and the identification of the lines of urban development and construction, on the basis of their compatibility with the landscape values recognized and protected, with particular attention to the protection of rural landscapes and sites inscribed on the world Heritage List of UNESCO.

We therefore developed a method of territory analysis available for the control of the new infrastructures involving rural areas, creating new forms of landscape impact.

Our research on regional territory as embodied in the L.a.co.s.t.a. Laboratory, through the use of GIS software for spatial analysis, wants to reconstruct the main changes in the geography of the rural zone such as changes of the coastal and pre-coastal zone, which remains imprinted on a matrix rural, but suffering from marginalization phenomena.

The analysis of marginality and economic dynamics was carried out in order to focus on the changes which have been

recorded in our sample-area. It wants to investigate major changes due to the settlement of the territory along the coast especially in relation to economic factors. In this regard, the investigated dimensions are the following: I) population; II) agriculture; III) industry and services.

The information sources used for the statistical elaborations are mainly based on data by ISTAT (Central Institute of Statistics) and they are basically census data.

The analytical system concerned, first of all, the construction of "integrated signs", that is the main changes occurred between the first and the last reference year (year 2010), in relation to the investigated phenomena. In this case, the adopted methodologies are the usual ones for the analysis of structural changes and they do not require specific explanations.

The evolution of land use in the Molise Region in order to renewable energy installations is evaluated by taking two representations of the territory fifty years apart. We used data from the vegetation map of the Molise Region drafted after World War II (indicative reference year: 1954) and data from the Corine Land Cover 2006. To do this analysis the keys were standardized and then a comparative vector informative layer was used [13]. In the analysis of the evolution of land use we wanted particularly to highlight the great territorial evolution related to changes in agricultural zones and in urbanized areas.

III. CURRENT NATIONAL AND REGIONAL RULES

As regards the law, we mention the national and regional standards that have evolved in recent years [14], [15]. As is known, the production of electrical energy underwent a great change in the 90's: in fact, the two laws of 1991 opened a new scenario because from that time onwards the power production was no longer just the prerogative of ENEL (National Agency for Electricity), and the Regions were delegated to identify suitable areas within their territory for the exploitation of renewable energy sources. Moreover, the Act recognized the expropriation in the public interest of the land on which to establish installations for the production of renewable energy.

In 1999, to implement Directive 96/92/EC (common rules for the internal electricity market), the Legislative Decree no. 79/99 was issued which promotes the production of electricity from renewable sources. This obliged producers of energy from fossil fuels to introduce green energy into the electricity market by 2001 or, alternatively, as determined by the Ministerial Decree of 11 November 1999, to purchase of "green certificates". The reform of the Title V of the Italian Constitution (Constitutional Law no. 3/2001) assigned legislative power over energy production to the Regions.

Afterwards new Guidelines for the authorization of renewable energy plants were implemented by the National Decree in 2010: they will be analyzed in this paper.

In 2006, the Molise Region adopted the Regional Environmental Energy Plan with the goal of optimizing and encouraging energy conservation, and enhancing green energy sources with particular attention to hydroelectric and wind

power. The Plan highlights the potential of the Molise territory for the production of wind energy and suggests a target scenario for 2015 in which the installation of wind turbines exceeds 1,700 MW. In addition, the plan identifies areas within the river Biferno basin as sites of great interest for wind energy. The 2015 target scenario does not take into account the contribution of PV integrated into buildings, neither does it consider the construction of ground-mounted photovoltaic plants. The Plan also lays down the guidelines for the evaluation of projects and the impacts of wind farms to be implemented by future regional laws.

In 2008, the Molise Region issued its own regional law governing the installation of wind and photovoltaic plants in the area. This law and the subsequent guidelines, identified a number of areas unsuitable for the installation of wind and photovoltaic plants, in particular the areas of regional parks and nature reserves, the "zone 1" of national parks, areas of "protection and integrated conservation" of the Vast Area Landscape Environmental Plans, the SPAs (Special Protection Areas), SCI (Sites of Community Interest) and the area of the Tammaro Valley and the surrounding hills.

Additional changes and additions to the Law of 2009 were made by Regional Law no. 23/2010. This law reinserted the Tammaro Valley and surrounding hills in the list of areas unsuitable to the realization of wind farms and photovoltaic installations, because it is one of the Region's most important archaeological contexts. Subsequently, a Council of Ministers Ruling declared this Regional law to be unconstitutional because of the above-mentioned Legislative Decree no. 387/2003 which states that Regions can proceed with the identification of unsuitable areas, but in accordance with National Guidelines. In fact, according to D.M. of 10th September 2010 (National Guidelines for the authorization of plants powered by renewable sources) unsuitable zones could be identified with regard to specific sites after the completion of a thorough investigation that would identify particularly sensitive or vulnerable areas. Finally, the Molise Region approved final guidelines for a authorization to build and to manage plants producing electricity from renewable sources that reproduces verbatim D.M. of the 10 September 2010.

IV. RESULTS

A. Marginality and Changes in Economic Settlement

The geographical area's marginality comes from a large number of demographic, social and economic causes, but it takes many configurations depending on the methodological approach. From the demographic point of view, the Molise Region is characterized by the presence of small size municipalities with fewer than 5,000 inhabitants (125 out of 136 municipalities), which cover 82% of the total area with the middle of the regional population: 105 towns have less than 2,000 inhabitants and extends over approximately 65% of the region, with almost 30% of the total population, while 88 municipalities that have less than 5,000 inhabitants and

population density of less than 50 inhabitants/km² appear in strong condition of depopulation.

In the "Molise Regional Rural Development Plan" (2007), two different typologies are identified: they are "Urban Centers" and "Rural Areas with Development Problems", which are divided into: a) Hilly Irrigated Areas; b) Hilly Rural Areas; c) Mountain Areas (Figure 2). "Urban Centers" correspond to the most dynamic areas of the region with a good amount of services and good level of well-being; they are attributable to the two capitals of Campobasso and Isernia. "Hilly Irrigated Areas" include the coastal strip and the inland plain: despite their characterization by elements of fragility, they have some characters that are fundamentally different compared to other rural areas with development problems, particularly with regard to their competitiveness of the agricultural activities.

"Hilly Rural Areas" differ from the first one in relation to the reduced incidence of irrigated areas; this situation, also with their geo-morphological conditions, affects their agricultural production and, more generally, on their economic balance. Moreover, they are characterized by strong elements of rurality, associated with lack of infrastructures and services that distinguish them significantly from other hilly areas. "Mountain Areas" correspond to the most marginal and peripheral areas of the region, in which geographic morphological and climatic features, influence in a negative way business decisions and consequently the levels of development of the territory.

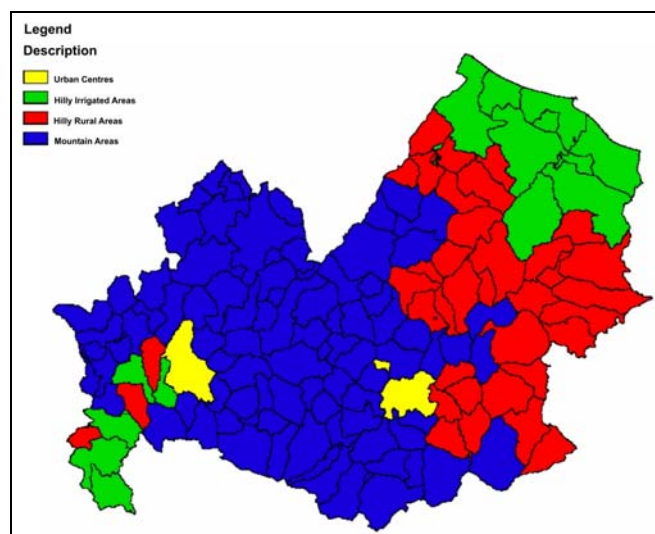


Fig. 2 Land Classification Map of the Molise Region

It is precisely in these areas - identified as predominantly rural from regional investigations - that in recent years were made the most renewable energy installations.

Our attention turns particularly to installations which have a more significant impact on the landscape - and inevitably affect the agricultural activities that take place on it - or wind power and ground-mounted photovoltaic plants (Figure 3).

Our sample area has a clear condition for development and economic diversification with respect to the regional framework.

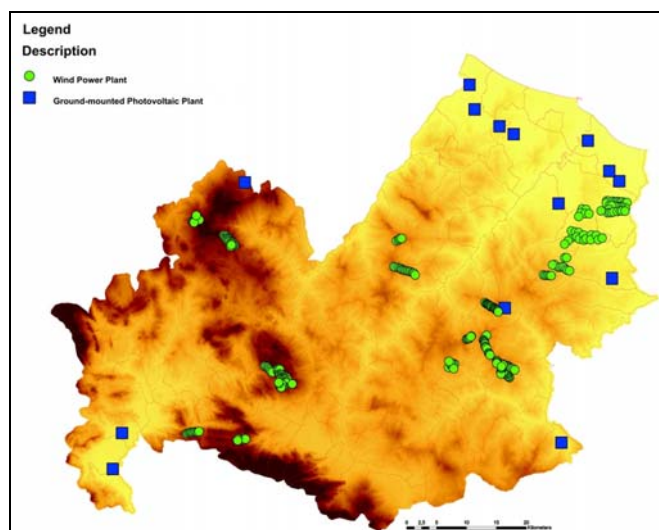


Fig. 3 Wind power and Ground-mounted Photovoltaic Plants in Molise

Industrial activities and services play an important role in the town of Termoli. This condition is significant also in the industrial Map of Italian Localism [16]. In the industrial area of Termoli, that reaches the top of specialization with the participation of the mechanical industry, diversification of production grew up in the direction of agro-food and chemical industries. Starting in '60's, there was a significant increase in local units of industry and services. In 1961 there were just 1,681 local units, while in 2010, local units amount to about 50,000. Really there are significant differences between different National Census. In fact, over the past few decades the increase of local units had a lower intensity compared to the period 1971-1991. The result is, therefore, a framework that emphasizes a clear outsourcing of the production system. Agriculture suffers a drastic restructuring and tends to specialization and intensification. Between 1950 and 2010, the farms number increased slightly, except in Montecilfone, Petacciato and San Giacomo. In contrast, the Total farms Land and the Agricultural Land are greatly reduced in each Municipality, except in Campomarino Montenero di Bisaccia and San Martino in Pensilis. Consequently, the average size corporate decreased significantly. This condition is to be read in relation to the actions of land reclamation.

The land structure does not detect phenomena of sputtering but since the 90s in almost all areas there were a decline in the share of the Agricultural Land of farms with over 50 hectares. Irrigation played a very important role for the development of this area, where rainfall is scarce and poorly distributed over the course of the agricultural year. Irrigation developed in the 80s, thanks to the use of water resources of the Guardialfiera Lake, which has a usable capacity of about 137 million cubic meters of water. In 2010, irrigated areas totals more than 5,000 hectares and affect significantly all the municipalities in the area: it is a phenomenon that must be carefully assessed in terms of farming but also the environmental impact (Forleo et al. 2011). Data relating to farms indicate a widespread presence and extensive use of irrigation. More than half of farms use irrigation for a coverage of more than 70% of their irrigable area. The percentage of irrigated area in the total

Agricultural Land takes significant values in Campomarino, Guglionesi, Petacciato, Portocannone and Termoli. Irrigation affects mainly horticultural crops, industrial plants (sugar beet) and fruit trees. Great importance have dynamics of the production structure of the area: in 2010, the production scenario appears to be more varied than in the 50s. Data reveal, however, a clear decrease of arable land and permanent grassland. In contrast, permanent crops showed a significant increase. Moreover the forest increase appears smaller. The weight of the arable land unchanged, the incidence of meadows and pastures reduced, while there is a significant increase in permanent crops. The so-called "other land" almost disappeared. With particular reference to wine production, it is appropriate to emphasize the special vocation of agriculture in the area and the importance of the production of quality.

The livestock farming is marginal in the context of this area, although in recent years there was a slight increase in the number of farms in Campomarino, San Martino in Pensilis and Petacciato.

The spread of organic farming in the study area is relatively low: farms that adopted organic production amounted to just 108 units (Molise Region, Department of Agriculture 2008). The Total farms Biological Land is 512.35 hectares, while the Agricultural Biological Land covers an area of 291.68 hectares.

At the municipal level, the analysis shows that Petacciato is the Municipality with the majority of biological land, which represents the 44.2% in terms of Agricultural Land and 49.8% in terms of Total farms Land.

In Guglionesi the biological surface amounts to 91.49 hectares and 74.38 hectares of Agricultural Land (25.5% of Agricultural Land and 17.9% of Total farms Land). In Campomarino the Total farms Land and Agricultural biological Land amounted to, respectively, 29.89 and 18.6 hectares. In Termoli, the Total farms Land and the Agricultural Land correspond, respectively, to 6.01 and 3.94 hectares (1.4% of the Total Agricultural Land and 1.2% of the total farms land). The result is a framework that emphasizes a clear process of specialization and intensification of agriculture, which created environmental problems and simplification of the landscape.

B. Changes in Land Use and Renewable Energy Installations

In our sample area, significant remediation of wetlands was made from the late 50s, which have changed the aspect and the land use of most of the coastal and pre-coastal zone (Cialdea 2009). The coastal area is covered by the Landscape Plan No. 1 Coastal Area, for a total of 48,434 hectares, and it is, of course, never returned to any Mountain Community. Moreover, in the last fifty years there were considerable changes in land use (Cialdea et al. 2006, 2007a, b).

First of all, there was a net decrease in areas with shrubs and bushes that it turns into an agricultural area.

Only in few circumstances, where agriculture activities appeared uncomfortable because of the area's topography, agricultural zones were abandoned: consequently these areas

have slowly naturalized (this is the case of the wooded areas along the Teco River, near Petacciato, which before were devoted to agricultural uses). A Campomarino, however, we see the opposite phenomenon: in Ramitelli locality, forest areas disappeared to take place for agricultural use.

Another growing problem is the disappearance of the dune system: on the coast of Molise today do not have that few residual areas, often remained only by chance. This ecosystem degradation began with the early works of reclamation of the Adriatic coast, but in more recent times it had a large increase. In fact, the coastal building development, which was spontaneous, chaotic and deregulated, pushed the anthropic presence more and more close to the shoreline, destroying the sparse vegetation typical of the dunes and leveling the dunes themselves for their own purposes. All along the coast, therefore, there is an increase in number and size of urban areas. This phenomenon is particularly concentrated around the town of Termoli (already in the 90s, there was a consistency of urban areas equal to 10 times that of forty years earlier). The analysis carried out for the definition of the land use (Figure 4) brings out the clear vocation to agricultural production: in particular, land valley and irrigated areas along the hillside are considered as exceptional value, both for their geo-pedological asset and for their cultural attitudes.

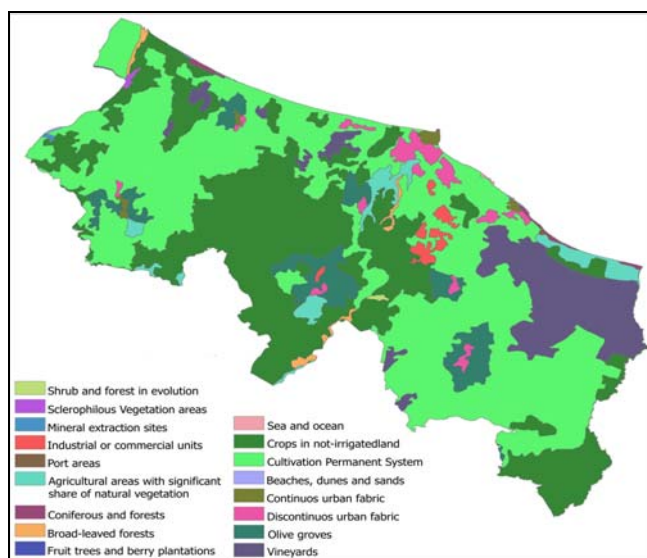


Fig. 4 Land use analysis in the coastal area

Areas along the Biferno and Trigno Rivers, and in general all coastal areas, are considered by the plan of exceptional natural interest: there are, in fact, areas that were then proposed as Sites of Community Importance, reflecting the presence of flora and fauna as important to highlight the need to protect their biodiversity. These are: the dune habitat in Campomarino, rare flora in the coastal area near the Saccione River; the wetland biotope in the district of Salcete in Guglionesi on the left side of the Biferno River; the habitat suitable for aquatic species along the Tamburro River (it is currently the only wetland remaining in the stretch from the Liscione dam to the Biferno's mouth) which is characterized by the presence of holmoak Mediterranean forests. Worth less,

but similarly important elements in this area, are the coastal wetland typical of the Mediterranean basin located near the mouth of the Biferno River- and therefore in an area subject to intense human activity - and the forest named Fantine in Campomarino, currently extremely devastated by the presence of activities, including a dump, but potentially recoverable thanks to the remains of holmoak survivors. Moreover, in the actual Landscape Plan, there are different areas characterized by the visual interest such as peak lines and highly performances. It is necessary to underline the exceptional importance of the so-called headland of Campomarino, that put Campomarino in a panoramic location.

Elements of geological hazard have been identified in Petacciato land slides, in Montenero di Bisaccia and Guglionesi landfall and also in Montenero di Bisaccia along the right side of the Trigno River. In essence, the coastal zone is certainly the part of the region with the major transformations, in the area which is also highly exposed to anthropogenic pressures, especially those linked to the increase in tourism. Of course, also the creation of reservoirs and the abundant mining activity contributed to the actual condition of the landscape feature, particularly in the coastal area, where the already mentioned urbanization occurred rapidly and without effective checks both for the settlement of industrial settlement and for urban increase. Moreover the coastal area could be divided into two sub-areas. The demarcation is essentially signed by the Biferno River. In its right side there is the area with the higher soil fertility and where farming activity is more developed, also as a result of the past land reclamation. In the left side of the Biferno River there are the greater phenomena related to the human activity, to the expansion of the urban area of Termoli and especially to the presence of the industrial area.

The Figure 5 shows the situation in the Coastal Zone of the Region and shows the number of wind farms and ground-mounted photovoltaic plants in each municipality territory. The installations are subdivided in three project typologies:

- Approved projects by Environmental Impact Assessment (EIA): wind or photovoltaic projects for which have been required the EIA act in accordance to the Regional Law no. 21 /200010. The EIA procedure has been positive issue;
- Approved projects only by Screening Act: projects that have been subjected to screening process and for which it isn't necessary the EIA procedure;
- Ongoing projects – EIA in progress: projects that have been subjected to screening process and for which is necessary realize the EIA procedure.

The data refers to the procedures for environmental impact assessment (EIA) and environmental assessment (VA) used for screening wind farms and photovoltaic plants from 2000 to 2014, taken from the Molise Region's institutional website¹¹. Plants already on maps, that are those greater than 1 MW, have not been considered. Most of the cases submitted to the opinion of the Regional Authority, about 90%, are concentrated in three years (2009-2012). In some years (2000 - 2001 - 2003 - 2004 - 2006), no plant was submitted for evaluation by the Molise Region. The data shows that in the coastal areas (Montenero di Bisaccia, Campomarino,

Petacciato) there is a substantial and exclusive concentration of photovoltaic plants, while in the pre-coastal territories there is a higher concentration of wind farms (Acquaviva Collecroce, Santa Croce di Magliano, Bonefro, Ururi, Montecilfone).

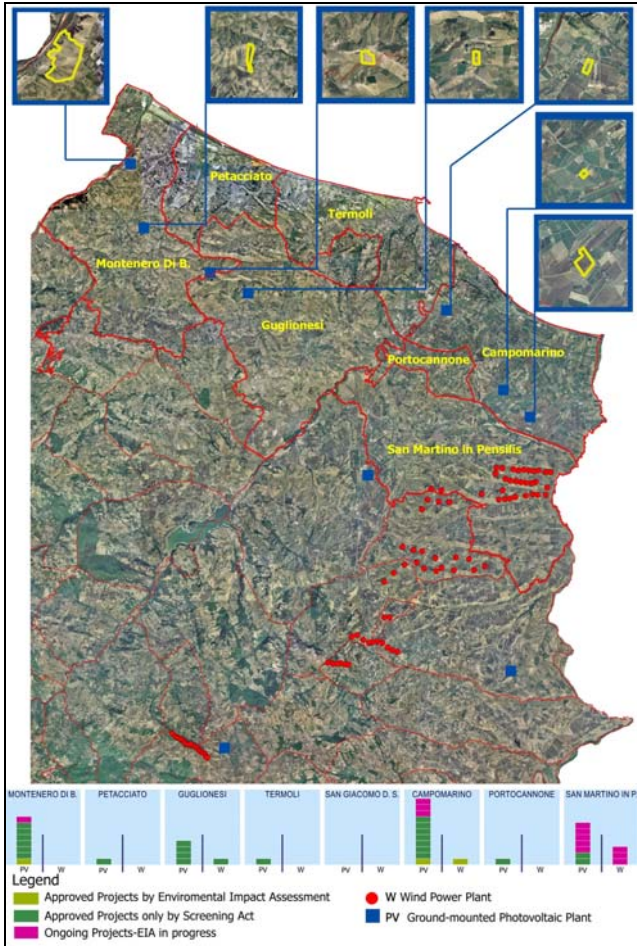


Fig. 5 Wind power and ground-mounted photovoltaic plants in Coastal Zone

Projects submitted to verification in order to determine whether they should undergo environmental impact assessment (commonly called "Screening") represent 97% of all evaluations. The procedure is intended to determine whether the proposed project may have a significant environmental impact and therefore should be subject to further EIA procedures, or not. There are three wind power plants in the Region subject to environmental impact assessment (EIA) localized in Campomarino, Portocannone and San Martino in Pensilis, and two photovoltaic plants localized in Campomarino-Portocannone and Montenero di Bisaccia.

V. CONCLUSION

The aim of this paper was to identify a methodology of territory analysis available for the control of these new infrastructures involving rural areas, creating new forms of landscape impact [17], [18]. Moreover it is important to verify

the current land use. Also we wanted to assess how the current landscape plans, drawn up in the early 90s, provided to safeguard their territories, starting from the identification of their elements of interest. The spirit of the enforcement of the Galasso law, in fact, was to establish the area's transformability by dividing the area of each plans. In fact, as known in the Molise Region the landscape plan did not cover the all regional territory. Therefore, the analysis of the Transformability Map of the Plan no. 1, which covers the coastal area, has highlighted the mode of transformations prescribed by the plan.

The actual Landscape Plans are created from documentation referred to by Art. 6 of the Regional Law no. 24 of December 1, 1989, which regulates the Legislation regarding Territorial Landscape Plans.

Therefore, the project tables containing, among other things, the indications of the degree of landscape and environmental transformability of the area and the methods of protection and enhancement (according to Art. 4 of the same Act) are an integral part of the plans. These indications have been reported for all eight plans drawn up for the Region, in the Transformability Map of the area, scale 1:25,000.

The Map of Coastal Zone, shown in Figure 6, defines the main characteristics of the area analyzed by dividing it into different fields of interest or risk.

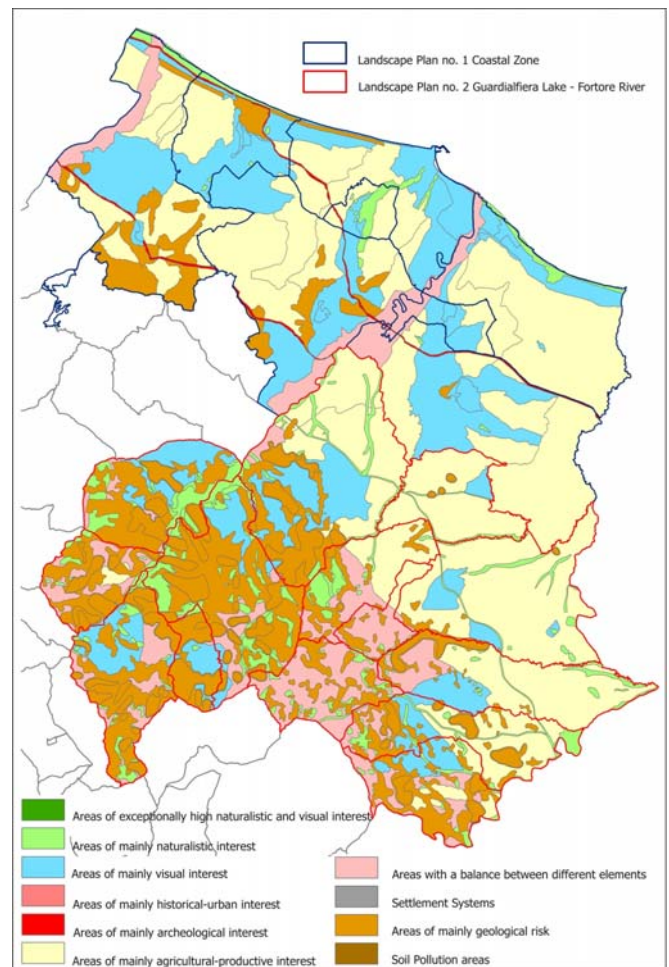


Fig. 6 The Transformability Map of the Coastal Vast Area Landscape Plans

For each of these areas, depending on the prevailing interest, was shown a mode of transformation and the resulting land use regulations through the definition of eligible interventions by identifying the areas to be protected. In order to gain a complete picture of the transformability of the Region, all the Transformability Maps of the eight landscape plans in force have been analyzed. The problem arose in the interpretation of the keys to the plans because, having been drafted by eight different workgroups, they do not present a uniform reading of the territory even though they used the same general guidelines. The keys have been simplified so that they can be standardized.

REFERENCES

- [1] OECD, “The New Rural Paradigm”, Paris: OECD, 2006.
- [2] J.D. van der Ploeg, R. van Broekhuizen, G. Brunori, R. Sonnino, K. Knickel, T. Tisenkopfs, H. Oostindie, “Towards a framework for understanding regional rural development”. In: J.D. van der Ploeg, T.J. Marsden (eds), “Unfolding Webs. The Dynamics of Regional Rural Development”, Assen: Van Gorcum, 2008, pp. 1-28.
- [3] EENRD (2010), Approaches for assessing impacts of the Rural Development Programmes in the context of multiple intervening factors. Available: <http://enrd.ec.europa.eu>.
- [4] J. Murdoch, “Networking rurality: emergent complexity in the countryside”. In: P. Cloke, T. Marsden, P. Mooney (eds.), “The handbook of rural studies”, London: SAGE, 2006, pp. 171-185.
- [5] European Commission, “Rural Development in the EU. Statistical and Economic Information”, Report 2013, Bruxelles, 2013.
- [6] F. Mantino, “Lo Sviluppo Rurale in Europa. Politiche, istituzioni e attori locali dagli anni '70 ad oggi”, Milano: Edagricole, 2008.
- [7] MIPAF (2013), “Zonizzazione delle aree rurali nel PSN”, Roma.
- [8] D. Cialdea, A. Maccarone, “The energy networks landscape. Impacts on rural land in the Molise Region”, *TEMA, Journal of Land Use, Mobility and Environment Special Issue*, June 2014, pp. 223-234.
- [9] D. Cialdea, L. Mastronardi, “Marginality phenomena and new uses on the agricultural land Diachronic and spatial analyses of the Molise coastal area”, *TEMA, Journal of Land Use, Mobility and Environment Special Issue*, June 2014, pp. 235-245.
- [10] EEA-FOEN, “Landscape fragmentation in Europe”, Report 2011, Copenhagen, 2011.
- [11] W. Haber, “Energy, food and land. The ecological traps of humankind”, *Environmental Science and Pollution Research*, Vol. 14, Issue 6, September 2007, pp. 359-365.
- [12] D. Bignami, “E i panni colonizzano i campi”, *Terra e Vita*, Issue 43, Ottobre 2010, pp. 16-21.
- [13] D. Cialdea, A. Maccarone, “Territorial diachronic maps for the Regional Landscape Plan”. In: M. Campagna, A. De Montis, F. Iso la, S. Lai, C. Pira, C. Zoppi (eds), “Planning Support Tools: Policy Analysis, Implementation and Evaluation”, Milano: Franco Angeli, 2010, pp. 386-398.
- [14] D. Cialdea, A. Sollazzo, “Dinamiche evolutive del paesaggio suburbano costiero del Molise”, *Convegno Strumenti, Piani e Progetti per una nuova dimensione “Urbano-Rurale”*. Contributi dell’Ingegneria Agraria. *Imola*, 4-5 Marzo 2010, Paper 8 Sessione Poster. Available: <http://www.iiaruraliaimola2010.unibo.it>.
- [15] D. Cialdea, A. Maccarone, A. Sollazzo (2010), “Wind energy and landscape in Molise. Legislation, Incentives and Problems”, presented at International Conference on Renewable Energies and Power Quality (ICREPQ'10), Granada (Spain), 23rd to 25th March, 2010, Paper n. 493. Available: <http://www.icrepq.com> and CD.
- [16] CENSIS, “Gli effetti di impulso dell’industrializzazione importata: il caso di Termoli”, Rapporto 1982, Milano: Franco Angeli, 1982.
- [17] T. Empler, F. Bianconi, R. Bagagli, “Rappresentazione del paesaggio. Modelli virtuali per la progettazione ambientale e territoriale”, Roma: DeI, 2006.
- [18] F. Steiner, “Costruire il paesaggio. Un approccio ecologico alla pianificazione”, II Ed., New York: McGraw-Hill, 2004.

Economic Analysis of a Pumped Storage Project for Iran Generating System Based on a Dynamic Modeling

A.R. Sohrabi
Tavanir Co.Iran

Abstract-This paper proposes a dynamic model for evaluation of a Pumped Storage Project (PSP) . The optimal expansion policy is determined by considering different alternatives (Types of units: Rodbar PSP(RPSP), Steam Turbine , 2 types of Gas Turbine and a Combined Cycle) . Based on this model dynamic assessment of different alternatives (over a 20 years period and with a target Loss Of Load Probability (LOLP)) provides economic justification for RPSP.

Key words : Pumped Storage - Generating System - Economic Analysis

I. INTRODUCTION

A new Dam construction Program in Rodbar-e-Lorestan area raised a series of questions: mainly is there an economic justification for construction of a PSP in The mentioned area ? If the answer is positive then what capacity is an optimal choice,...?

Two types of assessment is carried out:

1. Dynamic assessment , 2. Static assessment .

In this paper only results of dynamic assessment is presented. Dynamic programming has many advantages over the enumeration scheme, the chief advantage being reduction in the dimensionality of the problem [1] .In dynamic assessment, PSP is evaluated accounting for total generating system . Then it is necessary to determine not only PSP and other candidate units parameters but also parameters of other units within the total generating system . On the other hand an accurate load forecasting for study period (20 years) must be done and necessary constraints as LOLP rate , fuel limitations(natural gas) for thermal units in cold season , limitations on dams seasonal energy , and so on also are taken in to consideration .

Three different categories of units are considered in this assessment : existing , under construction and finally candidate units .

Only candidate units based on optimal procedure will be selected (in type and quantity) by model , excluding RPSP that is unique in each case .

There is no other hydroelectric alternative candidate (Excluding RPSP) this is because these types of units are not selectable as unlimited numbers and existences of these units depend on topology of country and each one must be evaluated separately (like RPSP) .

Nine cases are generated for 9 steps of RPSP capacity (0,250,500,...,2000 Mw) it is because as a final assessment we need also to determine optimal RPSP capacity .

As mentioned before other selectable candidates are defined for model as below:

1. Steam Turbine 325Mw , 2. Base Gas Turbine 130Mw, 3. Peak Gas Turbine 130Mw , 4. Combined Cycle 400Mw .

II. INPUT DATA PREPARATION

The dynamic modeling is performed by using WASP IV (Wien Automatic System Planning)[2], This model consists of six following main modules :

Loadsy – Fixsys -Varsys – Congen – Mersim - Dynpro (Dynamic Programming optimization)

In fact dynamic programming finally performed by last module and almost others act as input data preparation for this block .

In this section all necessary data , mathematical relations and a brief descriptions of calculation procedure is presented in short .

In first step based on the historical load data , peak load values are forecasted for the period of time under study.It is also assumed that Load Duration Curves (LDCs) have the same shape for similar seasons .

A sample of Normalized Load Duration Curve (NLDC) with 31 points for each season is shown in Table 1 . Model uses a fourier approximation for LDC to calculate necessary energy of system in each period .In next step data for fixed generating system consisting of existing , under construction and also for candidate

Table .1 : Sample of NLDC points for Year 2004 period 2: Summer (part of data)

NO	Load	Duration
1	1.0000	0.0000
2	0.9851	0.0077
3	0.9701	0.0158
⋮	⋮	⋮
⋮	⋮	⋮
⋮	⋮	⋮
26	0.6266	0.9181
27	0.6117	0.9410
28	0.5967	0.9594
29	0.5818	0.9747
30	0.5668	0.9881
31	0.5519	1.0000

units are determined .

The data depending on unit type have a wide variety , for example :

Power capacity , Fixed and variable operating and maintenance cost are determined based on Ref [3].

Force Outage Rate (FOR) is calculated based on Ref[4].

Base Load Heat Rate (BLHR) (or Heat rate at minimum operating level) for thermal units can be driven based on following formula:

$$BLHR = \frac{859.8}{e_1} \text{ [kcal/kwh]} \quad (1)$$

And for Full Load Heat Rate (FLHR) we have :

$$FLHR = \frac{859.8}{e_2} \text{ [kcal/kwh]} \quad (2)$$

Then Average Incremental Heat Rate (AIHR) can be calculated as below :

$$AIHR = \frac{FLHR * P_{full} - BLHR * P_{base}}{P_{full} - P_{base}} \quad (3)$$

Table .2 Sample of existing units main data

No	1
Power Plant Name	Tabs
Type	ST
Number of Units	2
MOL[Mw]	225
MGC[Mw]	300
Fuel Type	3
BLHR[kcal/kwh]	2235
AIHR[kcal/kwh]	2271
FOR[%]	17.1
SM[Days/Year]	59
FFC[C/million kcals]	546
FOMC[\$/kw-month]	0.125
VOMC[\$/Mwh]	0.213

Where $e_1, e_2, P_{base}, P_{full}$ respectively are unit efficiencies and power capacities at minimum and maximum operating levels .

See Table.2 for existing and Table.3 for candidate units' data.

following abbreviations are used :

Min Operating Level (MOL),Max Generating Capacity (MGC) , Force Outage Rate (FOR) , Scheduled Maintenance (SM) , Foreign Fuel Cost (FFC) , Fixed O&M Cost (FOMC) , Variable O&M Cost (VOMC) , Depreciable Capital Cost (DCC),Interest During Construction included in capital Cost (IDCC) Construction Time(CT) , Steam(ST),Gas Turbine(GT) , Combined Cycle (CC)

DCC is divided in two parts : 1. Domestic DCC, 2. Foreign DCC.

Transmission line losses and Transfer costs for RPSP also are included in model .

Inflow energy is determined for hydro plants as seasonally . An annual target for LOLP equal 1 day per year is selected . For RPSP we have also following

Table .4
RPSP Data (part of data)

MGC[Mw]	250	500	-----	1750	2000
FOMC[\$/kw-month]	0.39	0.39	-----	0.39	0.39
Cycle Efficiency[%]	80	80	-----	80	80
Max.Feasible energy[Gwh]	137	237	-----	958	1095
Plant Life[Years]	50	50	-----	50	50
DCC: 1.Domestic[\$/Kw]	229	237	-----	256	271
	2.Foreign [\$/Kw]	118	120	-----	127
CT[years]	4	4.5	-----	7	7.5

exclusive parameters :

Cycle efficiency , Pumping capacity and Max feasible energy[5] that are given in Table .4 .

III. DYNAMIC MODELING

Basically this dynamic model is designed to find economically optimal expansion policy for an electric utility system within user specified constrains . Model searches for the optimal scheme by using the forward dynamic programming algorithms . When some of the configuration schemes have been ruled out as infeasible with respect to reliability indices , model search for the minimum cost path in the rest of the schemes from the

Table .3
Candidate units main data

No	1	2	3	4
Candidate Name	S325	G13P	G13B	CC40
Type	ST	GT	GT	CC
MOL[Mw]	163	0.1	65	200
MGC[Mw]	325	130	130	400
Fuel Type	3	4	4	4
BLHR[kcal/kwh]	2330	2507	3140	1857
AIHR[kcal/kwh]	2137	2507	1875	1583
FOR[%]	7.8	6.12	6.12	6.74
SM[Days /Year]	56	40	40	43
FFC[C/million kcals]	546	621	621	621
FOMC[\$/kw-month]	0.3034	0.0892	0.0892	0.1392
VOMC[\$/Mwh]	0.3935	0.8773	0.8773	0.6134
DCC:1.Domestic[\$/Kw], 2.Foreign[\$/Kw]	230.3	137.7	137.7	198.8
	501.2	200.2	200.2	316.2
IDCC [%]	19.21	15	15	30
Plant Life[years]	30	15	15	30
CT[years]	5	2	2	4

Description	Fuel Type:
Heavy Fuel Oil(HFO)	1
Gas Oil	2
5+1	3
5+2	4
Natural Gas(NG)	5

planning start year to the level year . Suppose that there are 100 feasible configuration schemes in the final year of planning . Model finds the minimum cost in the 100 minimum cost paths . The searching process is shown in Fig .1 .

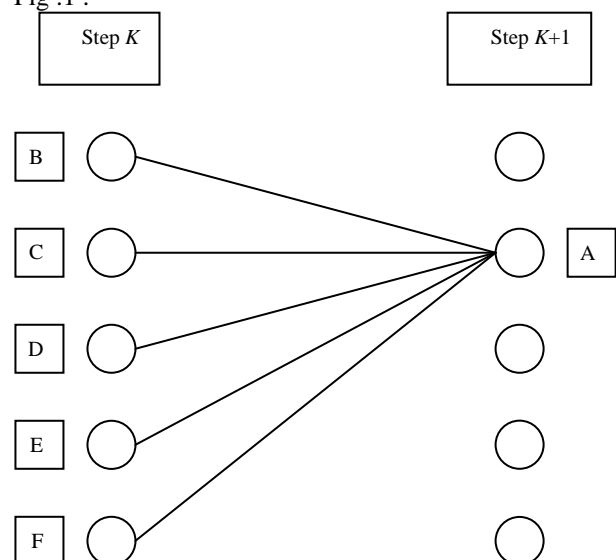


Fig.1 : Solution process of dynamic programming

Some of the feasible schemes in year K and year k+1 are shown in this figure . The cost of every scheme is determined by the minimum cost path from the beginning to the end of the planning year . when calculating the cost from the feasible scheme B in year k to the feasible scheme A in year k+1 , discount conversion should be made on the investment from B to A and the operational cost of A and add on to the cost of B . The same method is used for the other schemes C,D,E,F to A . Thus the minimum cost path to scheme A is found and retained while the other paths to A are waived since the other paths cannot form the optimal scheme according to the basic principles of dynamic programming . When the same principle is applied to all the feasible schemes in the year k+1 and the minimum cost path is found , the computation turns from the year k+1 to the year k+2 . The optimal planning scheme is

Table .5
Final results for case8 (RPS Capacity=1750Mw)
Part I

Year	LOLP %	ST 325 MW	Peak GT 130 MW	CC 400 MW	Base GT 130 MW	RPS 1750 MW
2023	0.27	0	271	171	0	1+
2022	0.27	0	234	154	0	1+
2021	0.26	0	213	134	0	1+
2020	0.27	0	178	120	0	1+
2019	0.26	0	130	112	0	1+
2018	0.27	0	104	100	0	1+
2017	0.27	0	99	81	0	1+
2016	0.26	0	96	64	0	1+
2015	0.27	0	90	48	0	1+
2014	0.27	0	50	42	0	1+
2013	0.26	0	32	32	0	1+
2012	0.27	0	23	20	0	1+
2011	0.26	0	13	9	0	1+
2010	0.26	0	9	5	0	0
2009	0.11	0	0	0	0	0
2008	0.02	0	0	0	0	0
2007	0.01	0	0	0	0	0
2006	3.87	0	0	0	0	0
2005	6.73	0	0	0	0	0
2004	8.23	0	0	0	0	0

(M), Cost of the energy not served (O) , The cost function to be evaluated by WASP can be represented by the following expression[2]:

$$B_j = \sum_{t=1}^T [I_{j,t} - S_{j,t} + F_{j,t} + L_{j,t} + M_{j,t} + O_{j,t}] \tag{4}$$

then the one with the minimum cost in all feasible schemes' minimum cost paths in the final planning year [6] .

Model utilizes probabilistic estimation of system production costs, un served energy cost, and reliability, linear programming technique for determining optimal dispatch policy satisfying exogenous constraints on environmental emissions, fuel availability and electricity generation by some plants, and the dynamic method of optimization for comparing the costs of alternative system expansion policies.

The first step in apply the dynamic programming method is to define the cost objective criteria[7] . Each possible sequence of power units added to the system (expansion plan or expansion policy) meeting the constraints is evaluated by means of a cost function (the objective function) which is composed of :

Capital investment costs (I), Salvage value of investment costs (S), Fuel costs (F), Fuel inventory costs (L), Non-fuel operation and maintenance costs Where:

Bj is the objective function attached to the expansion plan j, t is the time in years (1, 2, ... , T), T is the length of the study period (total number of years), and the bar over the symbols has the meaning of discounted values to a reference date at a given discount rate i. The optimal expansion plan is defined by: Minimum Bj among all j [2] .

IV. MODELING RESULTS AND CONCLUSIONS

A dynamic method has been proposed which can be used to evaluate a PSP. Model is executed for 9 cases . This is because there are 9 steps for RPS capacity . Results for case 8 (Capacity 1750 Mw) are given in Tables 5, 6 .

As shown in Table .5 , firstly (1+) means model is selected RPS in first year of its availability (2011) and for achieving to a target LOLP (1 days per year = 0274%) in an optimal expansion planning many units from two other candidates also are selected (Peak Gas Turbine 13 and combined cycle 9 units in year 2011) and secondly (1+) defines that not only this type of candidate is an economic unit but also model try to select more than one unit but remember that PSP is Unique in each one of cases .

Two other candidates (Steam Turbine , Base Gas Turbine) are rejected by model .

In Table .6 cost main quantities are shown . Table.7 shows all cases Cumulative Costs for last year of study period (2023) .

A comparison has been made between the 9 mentioned cases .With attention to Table.7 and also Fig.2 it can be seen that without RPSP we have Maximum system Cumulative Cost and for capacity of 1750 Mw system Cumulative Cost will be at the lowest level . That means this is optimal capacity for RPSP .

As secondary results these conclusions can be found in model output : Total consumption energy, Load factor, Peak and minimum load, Annual system generated energy based of fuel types and also by Hydro units ,Expected costs of operation & maintenance and Energy Not Served (ENS) ,Capital cash flow summery of candidates .

Table .7
Cumulative System Costs for 9 steps of RPSP Capacity

RPSP Capacity [Mw]	Cumulative System Cost for Year 2023[MillionUS \$]
0	44046.0
250	44031.6
500	44025.5
750	44007.8
1000	44005.9
1250	44003.4
1500	43991.9
1750	43989.5
2000	43995.7

V. ACKNOWLEDGMENTS

The authors gratefully acknowledge The IAEA planning and economic studies section for their useful suggestions .

VII. BIOGRAPHY

Alireza Sohrabi was born in Iran in 1966 , he received his B.Sc degree in Electrical Engineering (Power course) from The Tehran University Faculty of Engineering in 1989 . He joined Iran Ministry of Energy in 1991 , at present he is as production planning engineer in Tavanir Co (affiliated with Ministry of Energy) .

His areas of interest are Power System Planning and Reliability analysis .The author can be contacted at: VallyAsr St , Higher than Vanak Sq ,Rashid Yasami St , Tavanir Blg 4 , production planning Dep ,Tehran , Iran , Tele: 0098-21-27935416 ,Fax: 0098-21-88644968 Email: sohrabi@Tavanir.org.ir

A sensitivity analysis on RPSP economic justification with respect to its DCC shows that RPSP(1750 Mw) uneconomic behavior begins at DCC# 520 [\$/Kw] .

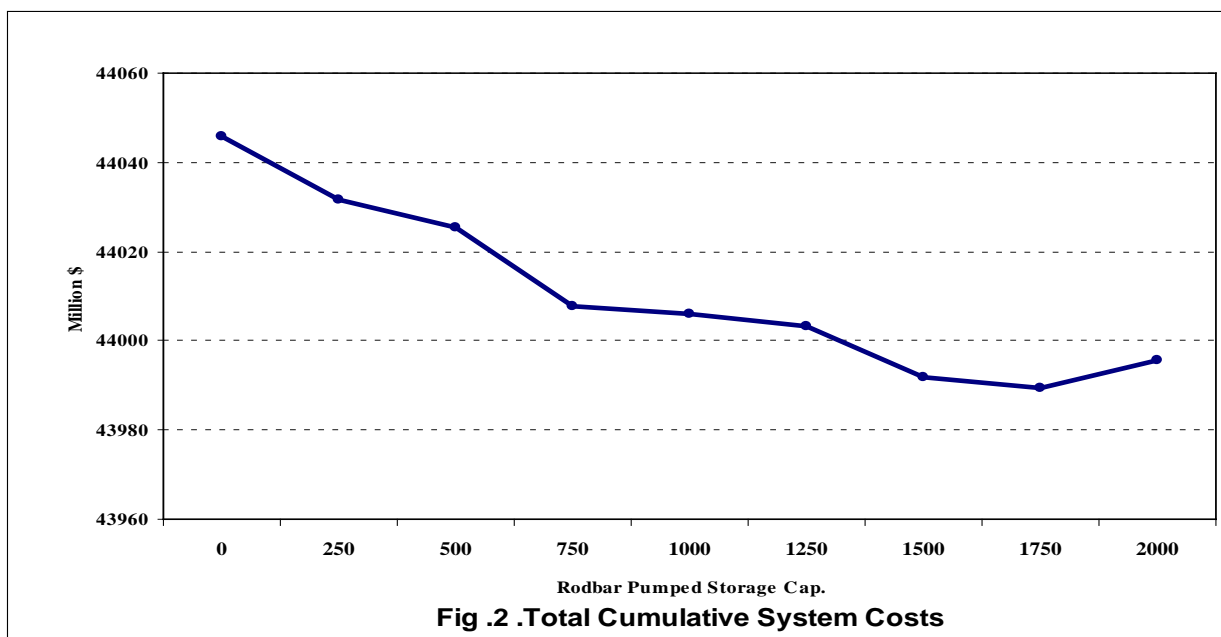
VI. REFERENCES

- [1] Allen J.Wood , Bruce F.Wollenberg ,Power Generation Operation & Control ,John Wiley & Sons,1996,p121
- [2] Wien Automatic System Planning (WASP) Package, Version – IV User's Manual , International Atomic Energy Agency , 2000
- [3] Economic information of Iran power plants, Tavanir production planning Dep , 2004
- [4] IEEE Standard definition for use in Reporting Electric Generating Unit Reliability , Availability, and Productivity , ANSI/IEEE 762 , 1987, p.15
- [5] Technical report for Rodbar Pumped Storage Project, ghodsniroo Consulting engineer Co, 2005
- [6] X.Wang , J.R.McDonald , Modern Power System Planning , McGraw-Hill Book Co., 1994, p.337
- [7] Harry. G . Stoll , Least-Cost electric Utility Planning , john willy & sons inc , 1989 , p516

Table .6
Final results for case8 (RPSP Capacity =1750 Mw)
Part II

Year	Construction costs	Operating Costs	ENS Costs	Total Costs	Cumulative Costs
2023	838.4	1398.7	1.39	1487.0	43989.5
2022	906.9	1431.9	1.03	1607.2	42502.4
2021	874.8	1468.9	0.65	1719.6	40895.3
2020	817.5	1497.7	0.33	1809.8	39175.7
2019	865.2	1520.4	0.33	1894.9	37365.9
2018	1088.5	1554.9	0.66	2064.8	35470.9
2017	1052.6	1592.3	1.16	2141.8	33406.1
2016	1134.2	1635.3	1.75	2290.3	31264.3
2015	1049.1	1682.3	2.31	2415.6	28974.0
2014	1099.1	1694.3	2.43	2460.7	26558.4
2013	1216.0	1726.4	2.04	2593.9	24097.8
2012	1262.0	1753.4	1.21	2702.3	21503.8
2011	856.8	1781.7	1.03	2431.9	18801.6
2010	804.6	1807.8	1.45	2479.7	16369.7
2009	0.0	1838.3	0.73	1839.0	13890.0
2008	0.0	1938.5	0.23	1938.7	12051.0
2007	0.0	1972.7	0.14	1972.9	10112.3
2006	0.0	1964.0	321.41	2285.4	8139.4
2005	0.0	1952.0	809.03	2761.1	5854.0
2004	0.0	1986.4	1106.55	3093.0	3093.0

Cost unit : Million US \$



Authors Index

Acevedo, P.	187	Cristi, O.	202	Kazemi, F.	417
Aghazadeh, F.	375	Daddi, T.	95	Khalyasmaa, A. I.	145
Ahmed, S. E.	301	Davoyan, S.	405	Khanalizadeh, B.	399
Ahmidad, M.	275	Diaz Vela, D. R.	37	Kijärvi, J.	115
Albarrán, A.	265, 336	Díaz, C.	202	Kim, D.	160
Amany, A.	301	Dinica, R.	425	Kokin, S. E.	145
Amr, S.	301	Dmitriev, S. A.	145	Kolakovic, S. R.	29, 151, 173
Anastasiadou, C.	221	Dolakova, G.	252	Kolakovic, S. R.	258, 399
Arapatsakos, C.	130, 221	Dolan, A.	450	Kolakovic, S. S.	29, 151
Argeşanu, V.	241	Drugus, D.	454	Kolakovic, S. S.	173, 258
Arltová, M.	345	Dumitrascu, A.-E.	55	Köllő, S. A.	324
Aurelian, S. F.	371	Dvorak, Z.	315	Kovačević, B.	209
Aylward, N.	121	Dzierzbicka-Głowacka, L.	228	Kratky, P.	315
Bacova Mitkova, V.	393	Edwards, E.	202	Kulcsar, R. M.	241
Balas, M.	195, 217	Edwards, G.	202	Kussaiynov, K.	62
Bartoš, P.	450	Elshaikh, D. H.	319	Kussaiynov, Y.	62
Becerra, D.	169, 265, 336	Frone, D. F.	163	Lalić, N. R.	209
Belás, J.	379	Frone, S.	163	Lalić, S. M.	209
Ben Chaim, M.	92	Gabčová, L.	379	Lazaroiu, G.	353
Benchouia, M. T.	364	Gavrila, C.	371	Lemieszek, A.	228
Bidabad, B.	51	Gendelis, S.	109	Lepadatescu, B.	55
Bin Tuan Harith, Z. Z.	319	Ghadbane, I.	364	Leybovitch, E.	92
Bindea, M.	324	Ghaheer, A.	384	Lin, Y.-C.	247
Boori, M. S.	281	Ghamariadyan, M.	384	Lisy, M.	195, 217
Borozan, I. S.	241	Gharehkhani, R.	417	López-Piñeiro, A.	136, 169, 235
Bostan, I.	454	Ghosh, S.	438	López-Piñeiro, A.	265, 336
Brindusa, C.	21	Gil, C.	235	Louda, L.	345
Brouček, J.	450	Halmova, D.	330, 359	Loures, A.	104, 136
Budinski, L. M.	29, 151	Haq, H. M. K. U.	87	Loures, L.	104, 136, 169
Bulucea, C.	21	Heba, I.	301	Loures, L.	235, 336
Bulucea, C. A.	21	Hiltunen, E.	87, 115	Mäkiranta, A.	115
Bunget, O.	454	Hnatkova, E.	315	Manganelli, B.	46
Cabral, F.	169	Hosseini, H.	465	Maniu, I.	241
Celjak, I.	450	Hudiab, E.	73	Markidou, E.	130
Chang, J.-L.	247	Jakovics, A.	62, 109	Markovic, G.	275
Chindaprasert, N.	340	Janarthanan, V.	460	Marosvölgyi, B.	142
Cho, H.	160	Jeftenic, G. B.	29, 151	Martinkauppi, B.	87
Cho, Y.-S.	160	Jeftenic, G. B.	173, 258	Martinkauppi, J. B.	115
Chochořáková, A.	379	Jula, M.	241	Marusiak, O.	156
Choo-In, S.	270	Kamala, J.	460	Masic, B. T.	29, 151
Cialdea, D.	468	Kambarova, Z.	62	Masic, B. T.	173, 258
Cismaru, D. C.	21	Kamga, R.	425	Mastorakis, N. E.	21, 51, 399
Cisty, M.	252	Kaposztasova, D.	275	Mastronardi, L.	468
Coelho, J.	235	Karkanis, A.	130, 221	Melo, M.	359
Constain, A.	187	Kasemsawat, S.	270	Mesa, D.	187

Miklanek, P.	330	Peña, D.	235, 265, 336	Smrčka, L.	345
Milovanović, D.	209	Peña-Guzmán, C.	187	Sohrabi, A. R.	475
Minaric, P.	252	Pospisil, J.	195	Sofáková, T.	181
Moga, L. M.	324	Praisler, M.	425	Spilacek, M.	217
Moga, M.	371	Purcz, P.	181	Stipic, F. M.	258
Monprapussorn, S.	270	Puskás, A.	324	Stipic, M. B.	258
Morano, P.	46	Pylarinos, D.	67	Szilágyi, H.	324
Morariu, A.	454	Ramaswamy, K.	438	Tabacaru, A.	425
Mousavi, S. A.	417	Ramchandran, G.	438	Tajani, F.	46
Mudoun, A.	286	Ramos-Miras, J.	235	Tchatchueng, J. B.	425
Musialik, M.	228	Rato Nunes, J.	169, 235	Tessitore, S.	95
Nagawkar, J.	438	Rato Nunes, J.	265, 336	Testa, F.	95
Năstase, C.	454	Sahakyan, T.	405	Thalassinakis, E.	67
Navarro, A.	136	Saidi, H.	286	Tharasawatpipat, C.	270
Nedelcu, A.	55	Sakipova, S.	62	Ungureanu, G.	353
Ngomo, O.	425	Sakipova, S.	109	Utarasakul, T.	270
Niaei, A.	375	Salari, D.	375	Virág, J.	324
Nicola, D. A.	21	Salem, A. A.	73	Vityi, A.	142
Nunes, J.	104, 136	Sánchez-Llerena, J.	265, 336	Voženílek, V.	281
Oana, U.	353	Santhosh, K.	460	Vranayova, Z.	275
Omidifar, D.	375	Schönfeld, J.	345	Vujovic, S. R.	29, 151
Ozolins, A.	109	Shirazi, S. S.	432	Vujovic, S. R.	173, 258
Panagopoulos, T.	104	Siderakis, K.	67	Wongkhorsub, C.	340
Pantokratoras, I.	130	Sieliechi, J. M.	425	Yazdi, S. K.	399
Peanprasit, S.	340	Simonová, D.	181	Zeleňáková, M.	181
Pekar, J.	156, 393	Šístková, M.	450	Zou, X.	79
Pekarova, P.	330, 359, 393	Skala, Z.	195, 217		
Pellas, I.	67	Skalova, J.	252		